Lecture Notes in Mechanical Engineering

Francisco Cavas-Martínez
Benoit Eynard
Francisco J. Fernández Cañavate
Daniel G. Fernández-Pacheco
Paz Morer
Vincenzo Nigrelli *Editors*

Advances on Mechanics, Design Engineering and Manufacturing II

Proceedings of the International Joint Conference on Mechanics, Design Engineering & Advanced Manufacturing (JCM 2018)

Springer

Lecture Notes in Mechanical Engineering

Lecture Notes in Mechanical Engineering (LNME) publishes the latest developments in Mechanical Engineering—quickly, informally and with high quality. Original research reported in proceedings and post-proceedings represents the core of LNME. Volumes published in LNME embrace all aspects, subfields and new challenges of mechanical engineering. Topics in the series include:

- Engineering Design
- Machinery and Machine Elements
- Mechanical Structures and Stress Analysis
- Automotive Engineering
- Engine Technology
- Aerospace Technology and Astronautics
- Nanotechnology and Microengineering
- Control, Robotics, Mechatronics
- MEMS
- Theoretical and Applied Mechanics
- Dynamical Systems, Control
- Fluid Mechanics
- Engineering Thermodynamics, Heat and Mass Transfer
- Manufacturing
- Precision Engineering, Instrumentation, Measurement
- Materials Engineering
- Tribology and Surface Technology

To submit a proposal or request further information, please contact the Springer Editor in your country:

China: Li Shen at li.shen@springer.com
India: Dr. Akash Chakraborty at akash.chakraborty@springernature.com
Rest of Asia, Australia, New Zealand: Swati Meherishi at swati.meherishi@springer.com
All other countries: Dr. Leontina Di Cecco at Leontina.dicecco@springer.com
To submit a proposal for a monograph, please check our Springer Tracts in Mechanical Engineering at http://www.springer.com/series/11693 or contact Leontina.dicecco@springer.com

Indexed by SCOPUS. The books of the series are submitted for indexing to Web of Science.

More information about this series at http://www.springer.com/series/11236

Francisco Cavas-Martínez ·
Benoit Eynard · Francisco J. Fernández Cañavate ·
Daniel G. Fernández-Pacheco ·
Paz Morer · Vincenzo Nigrelli
Editors

Advances on Mechanics, Design Engineering and Manufacturing II

Proceedings of the International Joint Conference on Mechanics, Design Engineering & Advanced Manufacturing (JCM 2018)

Springer

Editors
Francisco Cavas-Martínez
Departamento de Expresión Gráfica
Universidad Politécnica de Cartagena
Cartagena, Murcia, Spain

Francisco J. Fernández Cañavate
Departamento de Expresión Gráfica
Universidad Politécnica de Cartagena
Cartagena, Murcia, Spain

Paz Morer
Departamento de Mecánica
Tecnun—Universidad de Navarra
San Sebastián—Donostia, Guipúzcoa, Spain

Benoit Eynard
Département Génie des Systèmes
Mécaniques
Université de Technologie de Compiègne
Compiègne, Oise, France

Daniel G. Fernández-Pacheco
Departamento de Expresión Gráfica
Universidad Politécnica de Cartagena
Cartagena, Murcia, Spain

Vincenzo Nigrelli
Dipartimento di Ingegneria Chimica,
Gestionale, Informatica, Meccanica
Università degli Studi di Palermo
Palermo, Italy

ISSN 2195-4356 ISSN 2195-4364 (electronic)
Lecture Notes in Mechanical Engineering
ISBN 978-3-030-12345-1 ISBN 978-3-030-12346-8 (eBook)
https://doi.org/10.1007/978-3-030-12346-8

Library of Congress Control Number: 2019932621

This Springer imprint is published by the registered company Springer Nature Switzerland AG.
The registered company address is: Gewerbestrasse 11, 6330 Cham, Switzerland

Organization Committee JCM 2018 Members

Conference Chair

Francisco Cavas-Martínez, Universidad Politécnica de Cartagena

Conference Programme Chair

Daniel García Fernández-Pacheco, Universidad Politécnica de Cartagena

Conference Advisory Chairmen

Paz Morer, Universidad de Navarra—Tecnun
Vincenzo Nigrelli, Università degli Studi di Palermo
Benoit Eynard, UT Compiègne

Scientific Committee

Fernando Aguilar Torres, Universidad de Almería
Rita Ambu, Università di Cagliari
Nabil Anwer, Université Paris-Saclay
Alex Ballu, Université de Bordeaux
Richard Bearee, ENSAM Metz
Antonio Bello García, Universidad de Oviedo
Jean-François Boujut, Grenoble INP
Emmanuel Caillaud, Université de Strasbourg

Michele Calì, University of Catania
Francesca Campana, Università di Roma “La Sapienza”
Nicola Cappetti, Università degli Studi di Salerno
Fernando Carvajal Ramírez, Universidad de Almería
Aitor Cazón Martín, Universidad de Navarra—Tecnun
Vincent Cheutet, INSA Lyon
David Corbella, Universidad Politécnica de Madrid
Alain Daidié, INSA Toulouse
Óscar D. de Cózar Macías, Universidad de Málaga
Francesca De Crescenzio, Università di Bologna
Carlos De San Antonio, Universidad Politécnica de Madrid
Maria Gloria del Río Cidoncha, Univesidad de Sevilla
Luca Di Angelo, Università degli Studi dell’Aquila
Joaquín Fernández Sánchez, Universitat Politècnica de Catalunya
Gaspar Fernández San Elías, Universidad de León
Francesco Ferrise, Politecnico di Milano
Xavier Fisher, ESTIA
Cesar García Hernández, Universidad de Zaragoza
Salvatore Gerbino, Università degli Studi del Molise
Valentín Gómez Jáuregui, Universidad de Cantabria
Tommaso Ingrassia, Università degli Studi di Palermo
Samir Lamouri, ENSAM Metz
Julien Le Duigou, Université de technologie de Compiègne
Francesco Leali, Università degli Studi di Modena e Reggio Emilia
Carlos León Robles, Universidad de Granada
Muriel Lombard, Université de Lorraine
Rubén Lostado Lorza, Universidad de La Rioja
Cristina Manchado del Val, Universidad de Cantabria
Antonio Mancuso, Università degli Studi di Palermo
Cristina Martín Doñate, Univesidad de Jaén
Venancio Martínez García, IFKB—Universität Stuttgart
Maria Luisa Martínez Muneta, Universidad Politécnica de Madrid
Massimo Martorelli, Università degli Studi di Napoli “Federico II”
Rikardo Minguez Gabiña, Universidad del País Vasco
Ramón Mirálbes Buil, Universidad de Zaragoza
Anna Eva Morabito, Università del Salento
Alessandro Naddeo, Università degli Studi di Salerno
Frédéric Noël, Grenoble INP
Manuel Paredes, INSA Toulouse
Marcello Pellicciari, Università degli Studi di Modena e Reggio Emilia
Guillemo Peris, Universidad Politécnica de Valencia
Eugenio Pezzuti, Università di Roma “Tor Vergata”
Yann Quinsat, Université Paris-Saclay
Roberto Raffaeli, Università eCampus
Basilio Ramos Barbero, Universidad de Burgos

David Ranz, Universidad de Zaragoza
Roberto Razzoli, Università degli Studi di Genova
Tatiana Reyes, Université de technologie de Troyes
José Ignacio Rojas Sola, Universidad de Jaén
Bertrand Rose, Université de Strasbourg
Jacinto Santamaría Peña, Universidad de La Rioja
José Luis Santolaya, Univesidad de Zaragoza
Félix Sanz-Adan, Universidad de La Rioja
Irene Sentana Gadea, Universidad de Alicante
Gaetano Sequenzia, University of Catania
Domenico Speranza, Università degli Studi di Cassino e del Lazio Meridionale
Miguel Suffo Pino, Universidad de Cádiz
Davide Tumino, Università degli Studi di Enna "Kore"
Mercedes Valiente López, Universidad Politécnica de Madrid

Organizing Committee

Francisco José Fernández Cañavate, Universidad Politécnica de Cartagena
José Nieto Martínez, Universidad Politécnica de Cartagena
Daniel García Fernández-Pacheco, Universidad Politécnica de Cartagena
Francisco Cavas-Martínez, Universidad Politécnica de Cartagena
Dolores Parras Burgos, Universidad Politécnica de Cartagena
Dolores Ojados González, Universidad Politécnica de Cartagena
Tomás López Vivancos, Universidad Politécnica de Cartagena
José Sebastián Velázquez Blázquez, Universidad Politécnica de Cartagena
Francisco Luis Sáez Gutiérrez, Universidad Politécnica de Cartagena

Universidad Politécnica de Cartagena—Departamento de Expresión Gráfica-C/Doctor Fleming S/N, 30202 Cartagena, España

Preface and Acknowledgements

The JCM 2018 Conference originates as the 9th Joint Conference of INGEGRAF (Asociación Española de Ingeniería Gráfica), ADM (Associazione Nazionale Disegno e Metodi dell'Ingegneria Industriale) and S-mart (Systems, Manufacturing, Academics, Resources, Technologies).

JCM 2018 has been organized by Department of Graphical Expression of the Technical University of Cartagena. Cutting-edge topics in product design and manufacturing, innovative design; and computer-aided design were especially encouraged.

The list of topics (and subtopics) covered in the present edition are the following:

- Product Design and Development: Green engineering and eco-design; user centred design; product lifecycle-based design; robust design, reliability and maintenance; modelling and simulation-based design; ergonomics and human factors; global product development.
- Computer-Aided Design and Interactive Design: Virtual approaches for interactive design; virtual prototyping-based design; CAD, CAE, IFC and BIM; image processing and analysis; geomatics engineering: cartography, GIS, geometric modelling and analysis; reverse engineering; virtual and augmented reality.
- Manufacturing and Industrial Process Design: Integrated/Advanced manufacturing; manufacturing process and production management; rapid prototyping; flexible assemblies; remanufacturing; Industry 4.0.
- Graphical Bioengineering: 3D modelling of biological structures; computer-aided methods for pathologic diagnosis; emotional engineering; biomimicry for product design; simulation and visualization of biological systems; life science and design for health care.
- Innovation: Creativity and innovation methods; collaborative engineering; intellectual property management; design and research methods.

- Teaching–Learning: Teaching on graphic expression; theoretical and applied geometry; industrial and graphic design; new approaches in teaching/learning process; project-based education; interactive 3D modelling.

We wish to thank our main organizer/institutions, Higher Technical School of Industrial Engineering from the Technical University of Cartagena, and the rest of the sponsoring/collaborating companies and institutions for their support and grants.

We would also like to express our gratitude to the members of the different committees for their support, collaboration and good work. Thanks to all reviewers for selfless effort reviewing contributions, which positively influence the quality of the final papers presented at the Conference.

Last but not least, thanks to all the participants of JCM 2018.

Cartagena, Spain
November 2018

Francisco Cavas-Martínez
Benoit Eynard
Francisco J. Fernández Cañavate
Daniel G. Fernández-Pacheco
Paz Morer
Vincenzo Nigrelli

Contents

Teaching—Learning

Product Design and Development

Efficiency and Reliability of Gravity Die Casting Models for Simulation Based Design

A. Vergnano[1,2](✉), E. Brambilla[1], and G. Bonfiglioli[1]

[1] Modelleria Brambilla S.p.a., Via del progresso 1, 42015 Correggio, RE, Italy
alberto.vergnano@unimore.it
[2] Department of Engineering "Enzo Ferrari", University of Modena and Reggio Emilia, Via Pietro Vivarelli 10, 41125 Modena, Italy

Abstract. Simulation of Gravity Die Casting (GDC) requires coupling different models for fluid dynamics, heat transfer and solidification, together with material physics properties. Very long calculation times are required since several heating and production cycles have to be run. The simplification of the simulation models is critical to have results in times suitable for the design process. The present work discusses the solidification and heat transfer physics with simplification hypotheses. A simulation approach skipping the pouring model for the heating cycles is introduced. A realistic case study on an engine head GDC is presented to evaluate four possible simulation sequences. The results show that including the heating cycles in the simulation is advisable. The simplified sequences reproduce the temperature field of the die with sufficient accuracy. The proposed simulation approach results in considerable time saving with respect to the actual simulations and even in accuracy improvements.

Keywords: Gravity die casting · Process simulation · Model efficiency · Model reliability · Simulation based design

1 Introduction

Gravity Die Casting (GDC) is an ancient but extremely complex technology, the output quality resulting from the interaction of very many mechanics, physics and chemistry factors [1]. The present research investigates dies for casting of aluminum engine parts, namely engine heads, cylinder blocks and crankcases. Each die is a one-off design but conceived to deliver more than 100,000 quality castings as operating life specification. Moreover, it is very expensive and must be designed, manufactured and delivered to foundries in few months.

A design engineer must conceive the die as a thermal machine. The casting shape determines the die layout and slides, while the pattern size must be scaled to account for thermal expansion of die steel, contraction of solidifying alloy and negligible variation of cores. Moreover, differential heat removal should provide a directional and fast solidification in order to avoid porosities and deliver good material properties regarding Secondary Dendrite Arm Spacing (SDAS) [2].

Nowadays, simulation is a fundamental design tool to handle so many factors [3–5]. However, the models for casting simulations are computationally heavy, since

F. Cavas-Martínez et al. (Eds.): *Advances on Mechanics, Design Engineering and Manufacturing II*, LNME, pp. 3–12, 2019.
https://doi.org/10.1007/978-3-030-12346-8_1

they involve coupled fluid dynamics, heat transfer and metallurgy phenomena equations [6–9]. Moreover, several heating and production cycles must be simulated to reproduce the actual warmed up equipment. In the current design practice, such simulations can require 2 or 3 days run on a workstation with 8 parallel cores and 64 GB RAM. Those long run times make the simulations unsuitable for virtual concepts in the early design stages [10], thus they are used for the final adjustments with a limited number of trials.

The present research focuses on possible simplifications of a GDC process model in order to reduce the simulation run time, improving its role in the decision-making process [11]. Anglada et al. discussed possible simplifications of High Pressure Die Casting (HPDC) simulation [12]. The solidification model usually runs much faster than the pouring one. Considering HPDC, a sequence of heating cycles skipping the pouring model, thus running only the solidification one, is capable to reproduce the temperature field on the actual die. The pouring model is clearly critical in HPDC for cavity filling and air entrapment. On the other hand, GDC involves quite different cycle times. As a rule of thumb, the velocities at the casting gates can be about 0.3–0.5 m/s for GDC and 25–70 m/s for HPDC. HPDC is characterized also by higher heat removal rates, since thinner coating is used and high pressure up to 1200 bar is applied [13].

The pouring model in GDC determines the non-uniform temperature field of the solidifying alloy. The solidification dynamics is critical for GDC, but it is very conditioned by such initial temperature field [14]. On the other hand, the two models must run coupled, since solidification often starts when the pouring phase must still finish. The different involved phenomena require a specific investigation on GDC to determine if the heating cycles can be limited to solidification models or not.

The paper is organized as follows: Sect. 2 introduces the casting model and discusses some solidification physics, especially looking at the heat removal during alloy solidification, Sect. 3 introduces some hypotheses and four possible simulation approaches, compared with a realistic case study, Sect. 4 finally discusses the simulation results, whereas Sect. 5 draws the concluding remarks.

2 Gravity Die Casting Model

A GDC cycle can be modeled including the phases of die preparation, melt alloy pouring, solidification and cooling after eject, as shown in Fig. 1. This section discusses solidification and heat transfer phenomena to explain the hypotheses of the following methodology.

Metal alloys solidify over the range between Liquidus T_{LIQ} and Solidus T_{SOL} temperatures. So, a solidification model must consider a pseudo specific heat of the liquid, solid or two phases solution as function of temperature T as

$$c^* = \begin{cases} c_{SOL}; & T < T_{SOL} \\ f_{SOL} c_{SOL} + (1 - f_{SOL}) \cdot c_{LIQ} - L_F \cdot \partial f_{SOL} / \partial T; & T_{SOL} \le T \le T_{LIQ} \\ c_{LIQ}; & T > T_{LIQ} \end{cases} \quad (1)$$

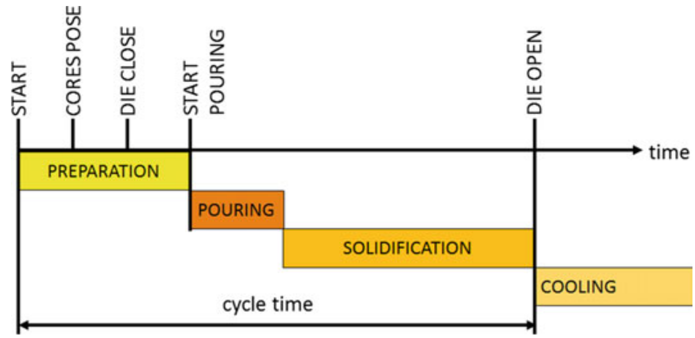

Fig. 1. Phases sequence in a GDC cycle

where c_{SOL} and c_{LIQ} are the specific heats of the solid and liquid phases respectively, f_{SOL} is the solid fraction and L_F is the latent heat of fusion [15, 16]. A qualitative pseudo specific heat relationship on temperature is shown in Fig. 2.

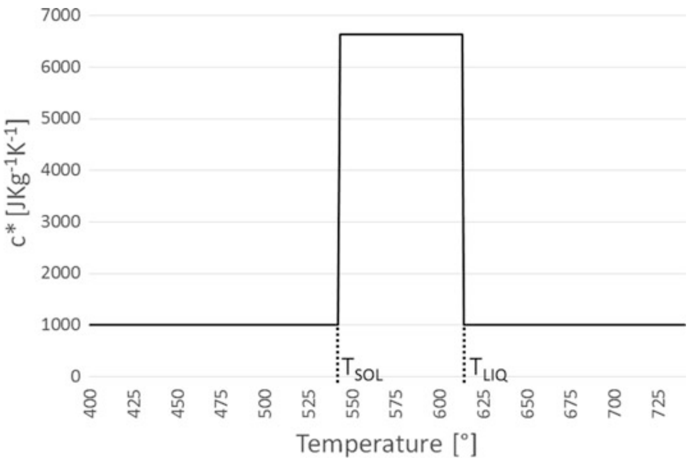

Fig. 2. Qualitative pseudo specific heat for an Al alloy

The heat supplied by a casting element to the adjacent die one is

$$q = \int_{T_I}^{T_F} c^* dT \tag{2}$$

where the initial T_I and final T_F temperatures vary for different casting elements.

The heat transfer between casting and die is difficult to determine, depending on contact pressure, surface finishing, coating thickness and deformation of casting. Those factors can be modeled together as Heat Transfer Coefficient (HTC) between contact surfaces. The HTCs are identified with experimental and inverse optimization procedures [17, 18]. Many factors depend on set up conditions and can be considered constant. However, the casting shrinkage for progressive solidification and cooling may occur in an air gap, determining a drop of the HTC from T_{LIQ} to T_{SOL} [18, 19]. A qualitative temperature dependent HTC is shown in Fig. 3.

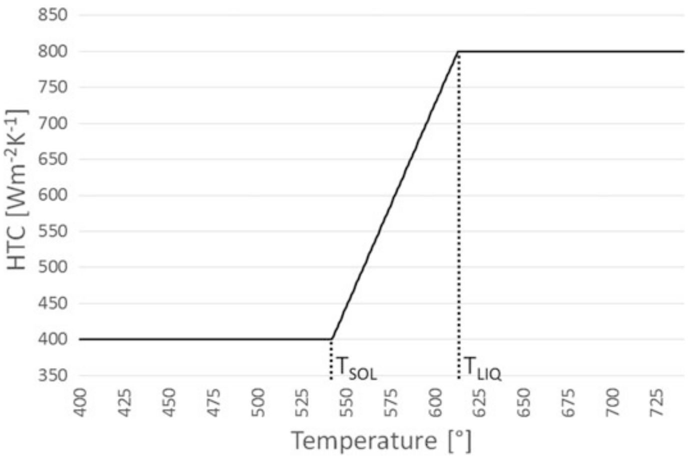

Fig. 3. Qualitative temperature dependent HTC

3 Methodology

3.1 Considerations on Simplification

In a DGC model the alloy is poured at uniform temperature T_P and cools down while flowing into the cavities. The alloy fills each element at a T_I higher, or at most little lower, than T_{LIQ}. Then it continues heating the die till the end of this pouring phase. In the already filled elements the temperature continues decreasing, generally still above T_{LIQ} but even much below T_{LIQ} in some cases. The solidification phase starts from a temperature $T_S < T_I$ as delivered by the pouring simulation and ends at T_F when the die is opened. From (2), q_P is the heat provided in the pouring phase, when cooling from T_I to T_S, while q_S is provided in the solidification phase, when cooling from T_S to T_F.

In the current practice, a sequence of 4–14 heating cycles is sufficient for reproducing the non-uniform temperature field of the warmed-up die. The last production cycle delivers the results the designer is interested in. The die temperature is adjusted at each *i*th cycle and the temperatures $T_{I,i}$, $T_{S,i}$ and $T_{F,i}$ vary as a consequence. However, the pouring phase is skipped for most heating cycles to save a lot of time. It is calculated just for few ones in order to improve the simulation accuracy. If a pouring phase is not calculated in the *i*th cycle, the sequent solidification phase starts from $T_{S,i-1}$ as calculated in the previous $(i–1)th$ cycle. Thus, the temperature decrease from T_P to $T_{S,i-1}$ is not considered and $q_{P,i-1}$ is lost for the simplified cycles. Referring to (2) and to Fig. 2, $q_{P,i-1}$ is a negligible amount if $T_{S,i-1} > T_{LIQ}$. However, for the casting elements with $T_{S,i-1} < T_{LIQ}$, part of the contribution of $-L_F \cdot \partial f_S/\partial T$ of (1) is not considered, which is much more important than $(1-f_{SOL})c_{LIQ}$. So, a cycle skipping the pouring model, thus running only the solidification one, may underestimate the die heating. The temperature dependent HTC even worsen the error. The same $T_S < T_{LIQ}$, thus in the sloped curve of Fig. 3, determines a much lower HTC and limits the transfer of the already reduced available heat.

3.2 Simulation Approaches

The heating cycles must be simplified in order to compute results in times useful for the industry design process [14]. The solidification phase is calculated in all heating and production cycles. Four simulation approaches with calculation or not of pouring in the heating cycles are designed in order to evaluate the hypotheses:

– *H*1-7/*P*8: all the 7 heating and the final 8th production cycles are calculated;
– *P*1: only 1 production cycle is calculated, avoiding heating;
– *H*1/*P*8: calculation of the 1st and 8th cycles only;
– *H-/P*8: calculation of pouring for the 8th cycle only, after 7 heating ones.

The calculation of all phases in all cycles, *H*1-7/*P*8, is assumed as reference for the accuracy with the actual foundry process. It is not feasible in a design process due to the excessive computation times. *P*1 is the simplified approach currently used in the early design phases. The maximum error for the approach *P*1 is considered the 100% possible error for the following evaluations. *H*1/*P*8 is the approach currently used in the detailed design phases for the final adjustments and it is assumed as reference for the simulation time in the evaluations. From 2nd to 7th cycles $T_{S,i}$ is assumed equal to $T_{S,1}$. *H-/P*8 is the suggested approach to keep the results reliability of *H*1-7/*P*8 and *H*1/*P*8 while trying to reduce the computation time as *P*1. With this approach, from 1st to 7th cycles $T_{S,i}$ is assumed constant and equal to T_P.

3.3 Case Study

This paper reports a case study on GDC for an engine head with Magma 5.3.1 software [20]. It was not possible to use an existing CAD model, due to non disclosure agreement with car manufacturers. So, an engine head has been especially modeled for evaluating the previous four approaches. However, it is representative of all the features of actual dies, as cycle timing, geometries, materials, overall masses, top feeders, all cores, die parts, surface coating and thermocouples, as shown in Fig. 4.

Also, cooling channels are provided from the combustion chambers for delivering good material SDAS. The die is conceived to be operated on a tilting machine. The model of the GDC cycle consists of these phases:

1. preparation: 45 s for cleaning, cores pose, die close, die tilting back in the −90° position;
2. pouring: instantaneous pouring cup filling, then 15 s for tilting from −90° to 0°;
3. solidification: 255 s waiting in 0° position, then die open;
4. casting ejection, external cooling.

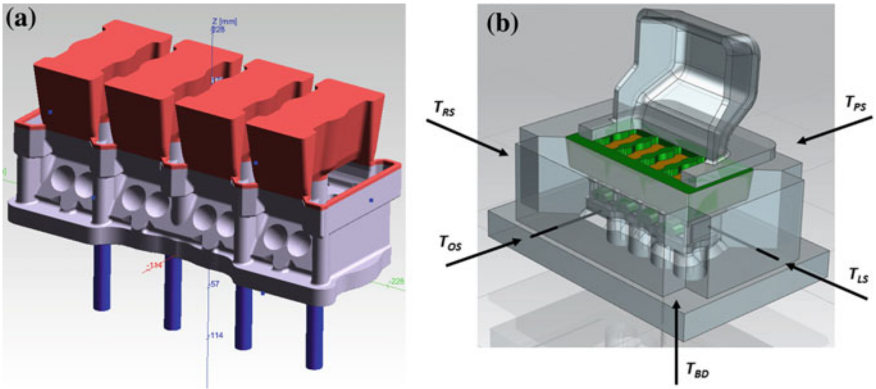

Fig. 4. CAD assemblies of **a** engine head casting, feeder, cooling channels and **b** pouring cup, die parts, cores, thermocouples T_{BD}, T_{OS}, T_{PS}, T_{LS}, T_{RS}

These materials are modeled: AlSi7Mg alloy poured at T_P = 740 °C in the pouring cup, X38CrMoV5 steel for the die at 250 °C initial constant temperature, silica sand for cores at 40 °C initial constant temperature. The AlSi7Mg alloy is characterized by T_{SOL} = 542 °C and T_{LIQ} = 613 °C. The die temperatures are monitored with 5 thermocouples into the die: T_{BD} in the bottom die, T_{OS} and T_{PS} in the opposite and pouring slides, while T_{LS} and T_{RS} in the left and right sides. In order to reduce the computation time, the mesh is quite rough, with only 118,295 cavity cells. Please consider that the actual models are much heavier, with 2,000,000 cells or more. Figure 5 shows the temperature results for the pouring simulation of the 8th cycle at three time-steps. The temperature field is not constant and the next solidification phase will start from a temperature $T_{S,8} < T_{I,8} < T_P$. Moreover, $T_{S,8} < T_{LIQ}$ in some elements.

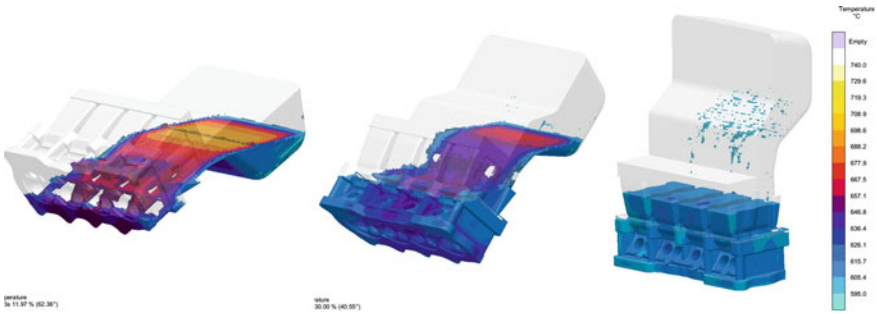

Fig. 5. Temperature results during the pouring phase at 4.6 s, 8.2 s and 15.0 s

4 Results and Discussion

The computation times needed for the different simulation approaches are reported in Table 1. These times have been obtained on a workstation with 8 parallel cores and 64 GB RAM. The complete simulation *H*1-7/*P*8 would increase the computation time by +207%. *P*1 would reduce it by −53%. The suggested approach *H*-/*P*8 would save −35% time.

Table 1. Computation times for different simulation approaches

*H*1-7/*P*8	*P*1	*H*1/*P*8	*H*-/*P*8
3 h 4 m/307%	0 h 28 m/47%	1 h 0 m/100%	39 m/65%

The evolution of the temperatures for all the 8 cycles is reported in Fig. 6 for *H*1-7/*P*8. It can be observed that not including the heating cycles would very reduce the results effectiveness. Clearly, this drawback can be reduced by setting a different initial temperature to each die part, recurring to previous simulations. However, this temperature would be constant from die surface to its internal material. A non-constant temperature field, higher on surface and lower in depth, would be fundamental to reproduce the heat transfer through the HTCs and the heat capacity of the massive steel.

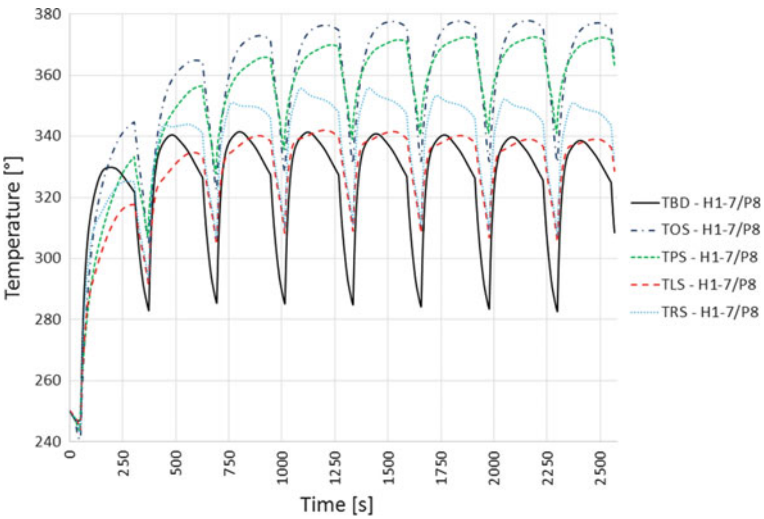

Fig. 6. Evolution of temperatures for the eight cycles in the H1-7/P8 approach, as sampled by the simulated thermocouples T_{BD}, T_{OS}, T_{PS}, T_{LS}, T_{RS}

The evolution of the temperature for the last production cycle is reported in Fig. 7 for all four approaches and five thermocouples. The solid curves describe the reference *H*1-7/*P*8 approach. As expected, *P*1 delivers results too conditioned by the initial temperature. *H*1/*P*8 underestimates die heating in all five thermocouples. *H*-/*P*8

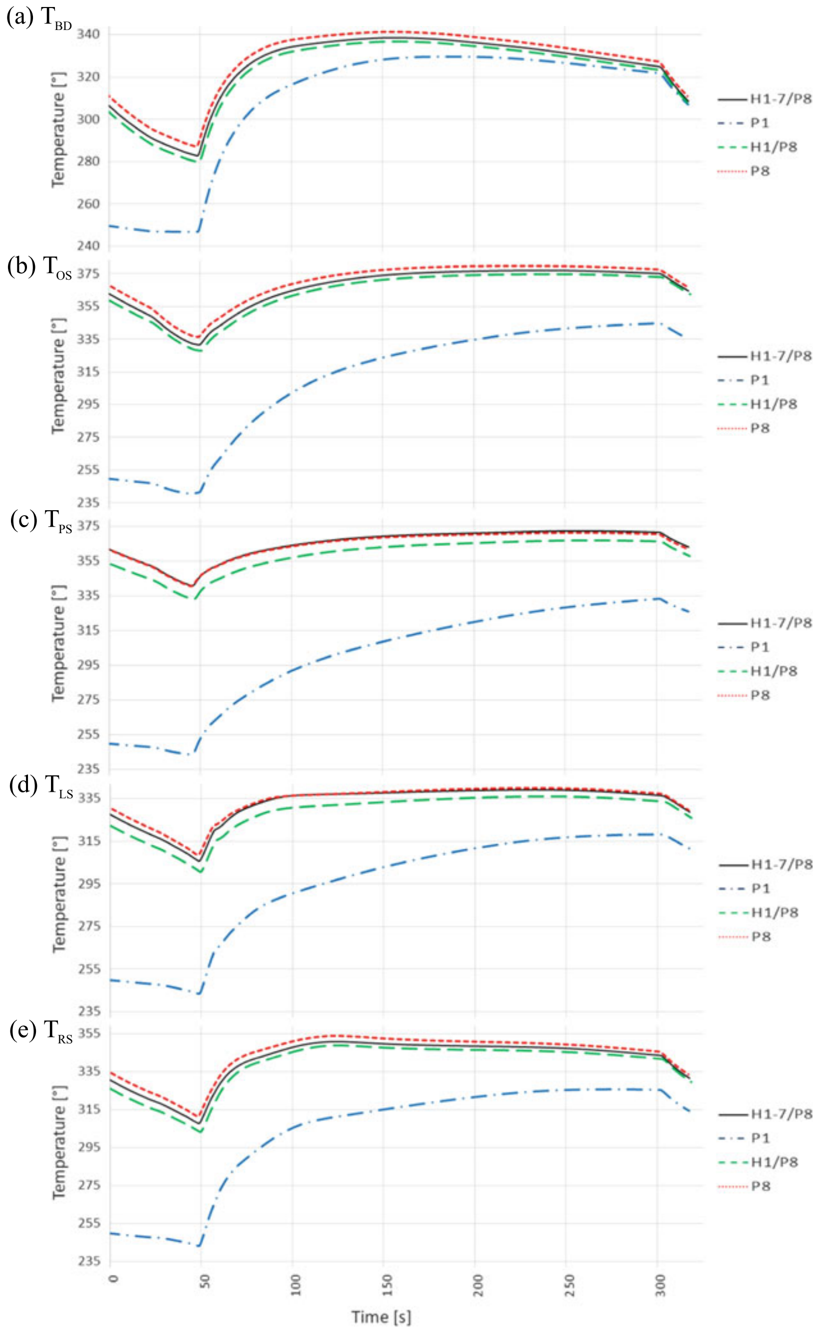

Fig. 7. Evolution of temperatures in the last production cycle for the simulation approaches *H*1-7/*P*8, *P*1, *H*1/*P*8, *P*8, as sampled by the thermocouples **a** T_{BD}, **b** T_{OS}, **c** T_{PS}, **d** T_{LS}, **e** T_{RS}

approach slightly overestimates die heating, except for T_{PS}, where not considering the alloy flow from the pouring cup slightly underestimates the temperature.

The temperature errors, measured at the end of the last preparation phase, just before pouring, are reported in Table 2. The final average considers the absolute value of the errors. The approach *P*1 results in a 72.0% error while *H*1/*P*8 improves the accuracy by 4.9%. *H-*/*P*8 results in a 3.3% error.

Table 2. Temperature errors at the end of the last preparation phase

	*H*1-7/*P*8	*P*1	*H*1/*P*8	*H-*/*P*8
T_{BD}	0°/0%	−35.8°/−36.8%	−2.9°/−3.0%	4.4°/4.5%
T_{OS}	0°/0%	−90.9°/−93.5%	−3.9°/−4.0%	4.9°/5.0%
T_{PS}	0°/0%	−97.2°/−100%	−7.8°/−8.0%	−0.3°/−0.3%
T_{LS}	0°/0%	−62.0°/−63.7%	−4.8°/−4.9%	2.9°/3.0%
T_{RS}	0°/0%	−64.3°/−66.1%	−4.2°/4.3%	3.8°/3.9%
Average	0°/0%	70.0°/72.0%	4.7°/4.9%	3.2°/3.3%

5 Conclusions

In the present paper, a discussion about the physics of aluminum alloy solidification and heat transfer to the die is presented. Four approaches for GDC simulation are defined with different simplification hypotheses. A complex model representative of real cases enables to evaluate the approaches. The complete and simplified simulations confirm the results reported in literature for HPDC [12].

The *H*1-7/*P*8 approach with no simplifications is assumed as reference for the evaluations. It can be estimated that it would require a computation time of about 6–8 days for the actual models in the industry design process, confirming its unfeasibility. The most simplified *P*1 approach is the reference for the maximum error and its simulation confirms that it leads to results too biased by the initial conditions. So, it is advisable to include the heating cycles in the simulation to reproduce the heat removal capability of the die. The simplified *H*1/*P*8 and *H-*/*P*8 approaches are both capable of reproducing the temperature field on the warmed-up die. However, the newly proposed *H-*/*P*8 presents a great reduction of computation time as −35% than *H*1/*P*8. For the proposed case study, *H-*/*P*8 shows even a slight accuracy improvement than *H*1/*P*8.

The calculation of the solidification models only is sufficient for the heating cycles, with the goal of an effective die heating. However, the cycle times for GDC are so different than HPDC that the solidification dynamics is much more influenced by the temperature field resulting from the pouring phase. The pouring simulation becomes critical in GDC for the goal of casting defect calculation.

The reported improvements have been observed in other real case studies for the simulation approaches *P*1, *H*1/*P*8 and *H-*/*P*8 with no opposite results. These dies were designed for engine heads, cylinder blocks, crankcases, pipes and chassis parts. The present research opens new possibilities for using the simulations as design tool in earlier design phases and for optimization algorithms. Future work will compare other simplification approaches. Searching for simulation reliability and design robustness, the results sensitivity to GDC model parameters will be investigated.

References

1. Panseri C (1966) Manuale di Fonderia d'Alluminio, 3rd edn. U. Hoepli, Milan
2. Shabani M, Mazahery A (2011) Prediction of mechanical properties of cast A356 alloy as a function of microstructure and cooling rate. Arch Metall Mater 56(3):671–675
3. Flender E, Sturm J (2010) Thirty years of casting process simulation. Int J Metalcast 4(2):7–23
4. Dabade UA, Bhedasgaonkar RC (2013) Casting defect analysis using design of experiments (DoE) and computer aided casting simulation technique. Procedia CIRP 7:616–621
5. Bonazzi E, Colombini E, Panari D, Vergnano A, Leali F, Veronesi P (2017) Numerical simulation and experimental validation of MIG welding of T-joints of thin aluminum plates for top class vehicles. Metall Mater Trans A Phys Metall Mater Sci Volume 48(1):379–388
6. Barral P, Bermúdez A, Muñiz MC, Otero MV, Quintela P, Salgado P (2003) Numerical simulation of some problems related to aluminium casting. J Mater Process Technol 142 (2):383–399
7. Liu B, Xiong S, Xu Q (2007) Study on macro-and micromodeling of the solidification process of aluminum shape casting. Metall Mater Trans B 38(4):525–532
8. Vijayaram TR, Sulaiman S, Hamouda AMS, Ahmad MHM (2006) Numerical simulation of casting solidification in permanent metallic molds. J Mater Process Technol 178(1–3):29–33
9. Vispute P, Chaudhari D (2017) Utilizing flow simulation in the design phase of a casting die to optimize design parameters and defect analysis. Mater Today Proc 4(8):9256–9263
10. Vergnano A, Berselli G, Pellicciari M (2017) Parametric virtual concepts in the early design of mechanical systems: a case study application. Int J Interact Des Manuf 11(2):331–340
11. Prasad D, Ratna S (2018) Decision support systems in the metal casting industry: an academic review of research articles. Mater Today Proc 5(1):1298–1312
12. Anglada E, Meléndez A, Vicario I, Arratibel E, (2015) Cangas. Simplified models for high pressure die casting simulation. Procedia Eng 132:974–98
13. Ilkhchy AF, Jabbari M, Davami P (2012) Effect of pressure on heat transfer coefficient at the metal/mold interface of A356 aluminum alloy. Int Commun Heat Mass Transfer 39(5):705–712
14. Pathak N, Kumar N, Yadav A, Dutta P (2009) Effects of mould filling on evolution of the solid–liquid interface during solidification. Appl Therm Eng 29(17–18):3669–3678
15. Feng H, Chen L, Xie Z, Ding Z, Sun F (2014) Generalized constructal optimization for solidification heat transfer process of slab continuous casting based on heat loss rate. Energy 66:991–998
16. Santos CA, Fortaleza EL, Ferreira CRF, Spim JA, Garcia A (2015) A solidification heat transfer model and a neural network based algorithm applied to the continuous casting of steel billets and blooms. Modell Simul Mater Sci Eng 13:1071–1087
17. Vasileiou AN, Vosniakos GC, Pantelis DI (2017) On the feasibility of determining the heat transfer coefficient in casting simulations by genetic algorithms. Procedia Manuf 11:509–516
18. Zhang L, Li L, Ju H, Zhu B (2010) Inverse identification of interfacial heat transfer coefficient between the casting and metal mold using neural network. Energy Convers Manag 51(10):1898–1904
19. Griffiths WD (1999) The heat-transfer coefficient during the unidirectional solidification of an Al-Si alloy casting. Metall Mater Trans B 30(3):473–482
20. MAGMASOFT®, https://www.magmasoft.de/en/. Accessed on Feb 02 2017

Integrating Sustainability in Product Development Projects

L. Diago, E. Lacasa, L. Urmente, I. Millán, and J. L. Santolaya(✉)

Department of Design and Manufacturing Engineering, EINA,
University of Zaragoza, C/María de Luna 3, 50018 Saragossa, Spain
jlsanto@unizar.es

Abstract. Sustainable initiatives are increasingly demanded in current production. Methods and tools to take into account environmental impacts in the design of products and services have been evolving in the last decades. In this work, a methodology based on the life cycle sustainability assessment (LCSA) approach is proposed to integrate all sustainability dimensions (environmental, economic and social) in projects of product development. The objective is to provide a practical scheme for companies, which could assist them in their shift towards sustainability. Methodology consists of three different phases: inventory analysis, sustainability assessment and redesign process. In addition, a number of engineering metrics and indicators are used to quantify sustainability issues and to compare different design alternatives. In order to put in practice this methodology the development project of a mobile orthopaedic crane is addressed in this work. Data associated to its manufacturing process are obtained and a product redesign with sustainable criteria is proposed.

Keywords: Sustainability · Design methodology · Product development · Indicators assessment

1 Introduction

The improvement of product sustainability is one of the requirements that are currently being investigated from different fields of engineering [1, 2]. Numerous methods and tools concerning sustainable product development have been proposed throughout the last decades to support companies improve the design and manufacturing of both, existent and new products.

The development of an Eco-design methodology [3, 4] with the aim of reducing the environmental impacts of products was carried out. Eco-design or Design for the Environment (DfE) is a method to address all environmental impacts of a product throughout its complete life cycle, which includes five different phases (Fig. 1): materials extraction, production process, transport and distribution, use and maintenance and final disposition. Other specifications and characteristics of the product like function, cost and appearance should not be comprised.

The study of environmental impacts deals with just one of the sustainability dimensions. However, three dimensions should be considered in sustainability assessment: environmental, economic and social [5]. In order to take into account this

F. Cavas-Martínez et al. (Eds.): *Advances on Mechanics, Design Engineering and Manufacturing II*, LNME, pp. 13–22, 2019.
https://doi.org/10.1007/978-3-030-12346-8_2

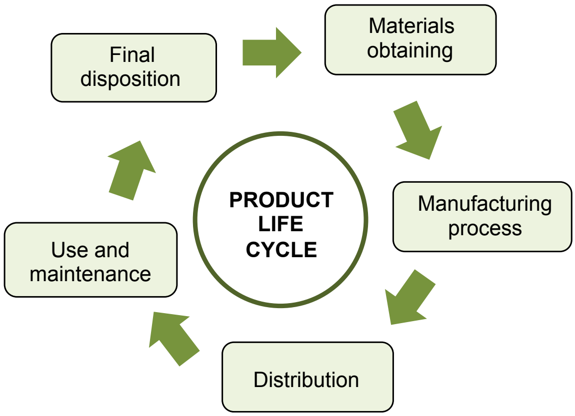

Fig. 1. Phases of the product life cycle

triple dimension, a new framework is being introduced, which is denominated as life cycle sustainability assessment (LCSA) [6, 7]. LCSA aims to evaluate all environmental, social and economic impacts over the entire life cycle of the product and provides guiding principles to design new products or to improve existing ones. Innovation is also stimulated to achieve a more sustainable production.

LCSA combines LCA, LCC and S-LCA techniques. Life Cycle Assessment (LCA) provides information on the environmental effects of a product and, as previously was exposed, its use is well-known. Life cycle costing (LCC) evaluates costs associated to the product throughout its life cycle. Whereas, Social Life Cycle Assessment (S-LCA) is focused on the study of social subjects in order to improve both, performance of organizations and well-being of stakeholders. The socio-economic impacts of the product can be organized in five suggested stakeholder groups [8]: workers, local community, society, consumers and value chain actors. A number of indicators are also proposed by the UNEP's guidelines. Nevertheless, many social subjects are difficult to value quantitatively; so many social indicators are based on qualitative information. In order to integrate sustainability in product development projects, a set of indicators to measure each individual sustainability dimension is required [9]. In addition, appropriate indicators should be selected according to the type of the project and challenges to solve.

Sustainability studies carried out to date [10] are mainly focused on the application of environmental assessment tools to an extensive range of products. Moreover, some studies suggest some design improvements to reduce impacts. This work aims at effectively integrating the three pillars of sustainability in product development projects. A number of metrics and indicators are conveniently selected to measure each sustainability dimension. On the other hand, traditional product specifications are preserved. In the following sections, the methodology applied to assess the product sustainability and results obtained for a case study are exposed. The project of a mobile orthopaedic crane for lifting and transport of patients was addressed.

2 Methodology

The production stage of the product life cycle is established as system boundary. According to LCA methods [11, 12], an approach based on the analysis of the flows exchanged (inputs and outputs) by the industrial facility throughout the production process was applied. As shows Fig. 2, the development of a more sustainable product can be reached in three steps, which are sequenced as follows: (1) Inventory; (2) Sustainability assessment; (3) Product redesign. In the first phase, inputs and outputs due to the production process are identified. Next, engineering metrics and sustainability indicators for each sustainability dimension are assessed. Finally, the product is redesigned integrating sustainability criteria. In order to compare the sustainability performance of both, initial and redesigned product, a new inventory and sustainability assessment should be carried out for the redesign.

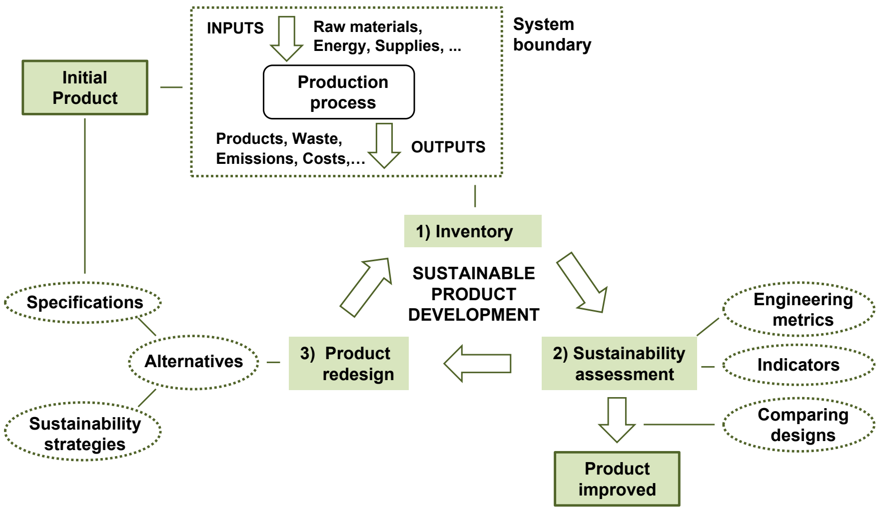

Fig. 2. Steps for a sustainable product development

2.1 Inventory

The functional unit considered appropriate in this work is one manufactured product. Additionally, a high volume of manufactured products is taking into account to value the inputs and outputs associated to the production process. The main flows exchanged by the industry include inputs as raw materials, supplies and energy, and outputs like products, emissions and waste.

All manufacturing operations involved in the production process are analyzed in detail. The resource consumption and the costs associated to the production of each component are valued. In particular, the time to carry out each productive operation and the energy consumed are calculated.

2.2 Sustainability Assessment

In this phase, a set of engineering metrics and indicators are selected to assess the product sustainability in the production stage. Metrics considered appropriate are: product mass, product volume, energy consumption, waste percentage, production costs and average production. These metrics are required to obtain sustainability indicators and are also considered practical in the design of the production process.

In order to assess each sustainability dimension, different indicators are selected. The Global Warming Potential (GWP) and the Eco-indicator 99 (EI99) [13] are proposed to value the environmental dimension. GWP represents total emissions of the greenhouse gases and EI99 is a suitable indicator in design processes because weighs different impact categories into a single score. Probas [14] and MEEuP [15] databases are applied to calculate environmental indicators taking into account the reuse-recycling potential at the final disposition phase of product life cycle.

The value added (VA) and the eco-efficiency (EE) are the indicators selected to assess the economic dimension. VA indicates the net operating profit of the manufacturing company. It is obtained making the difference between sales revenues and production costs. EE is the ratio of the value added and EI99. It combines economic and environmental aspects and quantifies the profit obtained at the expense of environmental impact. Finally, the category of company workers is selected in this study to assess the social dimension of the sustainability and the working hours (average work time) and the hourly wage are the indicators utilized.

2.3 Product Redesign

In order to redesign a product it is necessary to know what your initial specifications are and given that all products consist of different parts or components, the specifications of each component should be also analyzed. Thus, redesign alternatives of each product component are proposed in this phase taking into account the application of different sustainability strategies. One of the most used tools in Eco-design is the Life Cycle Design Strategies Wheel or LiDS wheel [3], in which a set of strategies are proposed to achieve environmental improvements at each stage of the product life cycle. The selection of low-impact materials, reduction of materials and optimization of production techniques are strategies focused on the production process. These strategies are also considered suitable to achieve an improvement at the three sustainability dimensions.

3 Case Study

Methodology was put into practice in the case of a mobile orthopaedic crane. The main components and technical specifications of this product are shown in Fig. 3.

The lifting movement of the upper arm can be achieved through an electric or hydraulic actuator and a set of wheels located at the end of the legs allow the crane to move. Taking into account that the system boundary is the manufacturing process of the components marked from (1) to (6) in Fig. 3, production inventory is obtained.

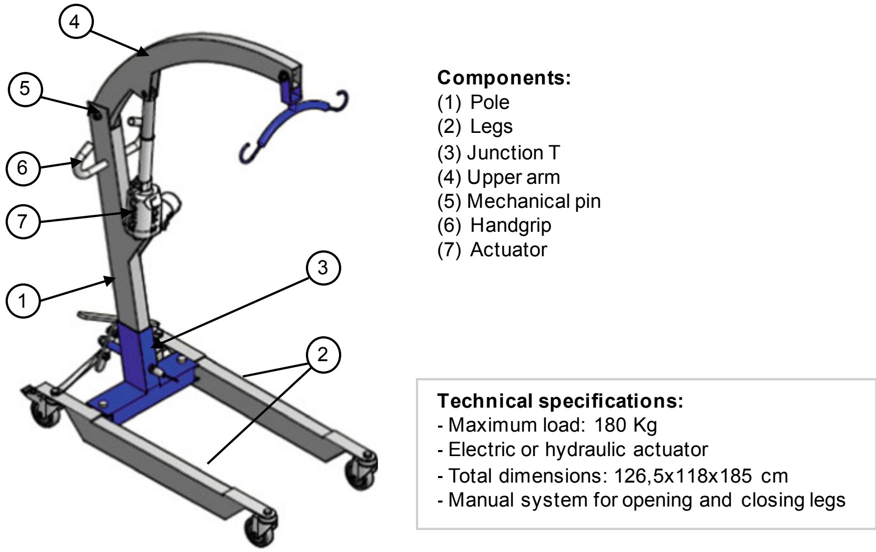

Fig. 3. Mobile orthopaedic crane

Material used is galvanized steel S275JR, which is acquired in sheets, bars and profiles of different sizes. The manufactured components will be transported to another industrial plant where the orthopaedic crane will be finally assembled and tested.

The following data corresponding to the production inventory of one unit of product are indicated in the scheme shown in Fig. 4: processing times and energy consumptions for each productive operation, raw materials needed in the manufacturing process, mass and volume of the final product, amount of material discarded and global energy consumption throughout production process. In addition, revenues as a result of sales and production costs are assessed for each product manufactured. Particularly, costs due to raw materials, labour and energy consumption are obtained.

To note that welding and painting are the operations with higher processing times and energy consumptions. Engineering metrics of the production process are summarized in Table 2. Indicators for each sustainability dimension are also calculated. Metrics and indicators obtained later for the product redesigned are also indicated to facility a comparative study. The mass and volume of the crane components are, respectively, 55.4 kg and 0.25 m^3. A packaging mass of 2.1 kg is already included in the final product mass. The percentage of material removed is 1.6%, which is a small amount of the raw materials acquired. In addition, raw material purchase is the most important factor in production costs (67%). A total energy consumption of 1.8 Mw·s is required to obtain a production of 2.2 ud/h. It is supposed that the company dispose of the necessary resources for the development of the production process and available resources are fully allocated to manufacture this product.

The emissions of greenhouse gases are 581 kg CO_2-eq and the value of EI99 is 16.6 pt (the materials extraction stage is also incorporated in this calculus). A net operating profit of 14 € is obtained for the company and the resulting eco-efficiency is 0.84 €/pt.

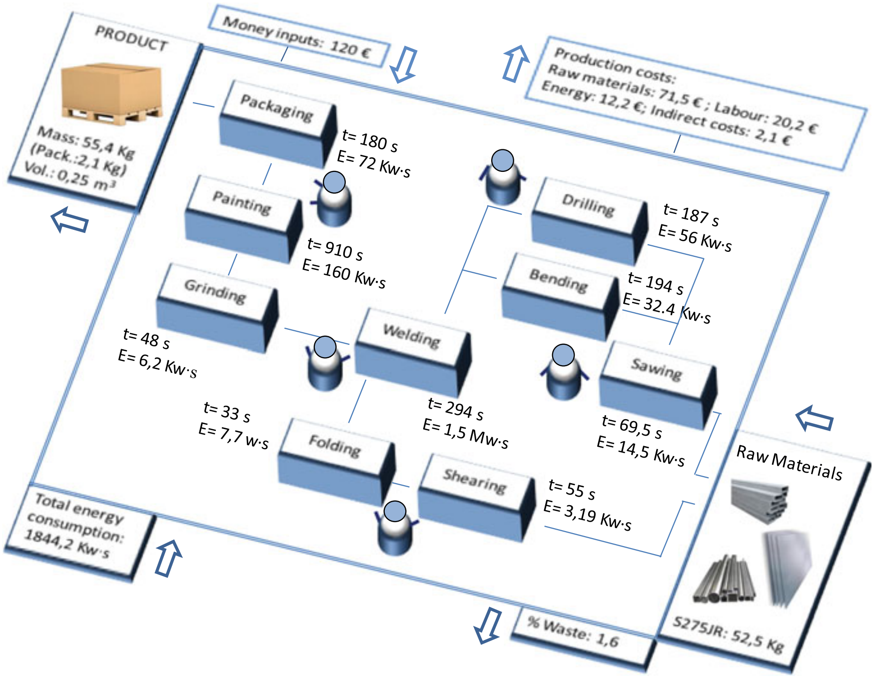

Fig. 4. Manufacturing line and flows exchanged

Regarding social aspects, the average working time and hourly wage are, respectively, 0.4 h and 8.2 €/h.

Next, the redesign of the product is carried out applying two sustainability strategies: the selection of low-impact materials and reduction of materials. Materials as stainless steel (AISI 304 N) and 6066-T4 aluminium alloy are proposed as design alternatives to improve the sustainability of each component. These alternatives are named, respectively, A1, A2 and A3 in Table 1. The following information for the initial design, Di, and the redesign options, is exposed: type and size of raw materials, energy use and quantity of material discarded along the production process, mass of the manufactured component, fulfilment of resistance specifications and EI99.

Mechanical strength and resistance to corrosion are specifications considered in the design of each component. Materials with a working stress (σ) that do not exceed the yield strength (σy) are selected. Type and size of raw material are modified maintaining in all cases a safety factor greater than four. A3 is selected for the redesign of each component because it is the alternative with the lowest environmental impact. It is necessary to take into account that according to EI99 assessment method, 6066-T4 aluminium alloy has higher recyclability coefficient than other materials.

Sustainability is assessed for the crane projected. Inventory of the production process shows that the use of Al6066T4 allow us to avoid the painting process, reduce the time spent in finishing operations and the global manufacturing time (9%) as well

Table 1. Redesign of the orthopaedic crane components

Orthopaedic crane component			Raw materials		Processing		Product	Resistance specification $\sigma < \sigma_y$ (MPa)	EI99 (mPt)
			Material type	Size (mm)	Energy (w·h)	Material rem. (g)	Mass (Kg)		
(1) Pole	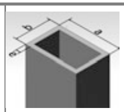	D_i	S275JR	90 × 50 × 5	1.52	15	10.49	51.8 < 275	3152
		A1	AISI	90 × 50 × 4	1.62	13	8.56	61.1 < 330	7204
		A2	304 N	90 × 50 × 4	1.21	12	8.45	61.1 < 275	2539
		A3	S275JR Al 6066T4	90 × 50 × 5	0.38	5	3.68	51.8 < 207	220.8
(2) Legs	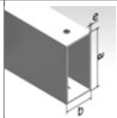	D_i	S275JR	90 × 50 × 4	1.36	13	6.56	35.7 < 275	1971
		A1	AISI	90 × 50 × 3	1.44	11	5.35	46.7 < 330	4502
		A2	304 N	90 × 50 × 3	1.1	11	5.28	46.7 < 275	1586
		A3	S275JR Al 6066T4	90 × 50 × 3	0.34	4	2.30	46.7 < 207	138
(3) Junction T	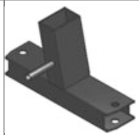	D_i	S275JR	100 × 60 × 5	3.1	18	7.37	53.6 < 275	2213
		A1	AISI	100 × 60 × 4	3.21	15	6.01	63.2 < 330	5054
		A2	304 N	100 × 60 × 4	2.46	14	5.93	63.2 < 275	1781
		A3	S275JR Al 6066T4	100 × 65 × 5	0.77	6	1.54	51.7 < 207	146,1
(4) Upper arm	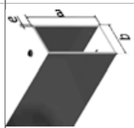	D_i	S275JR	80 × 40 × 4	1.16	10	8.29	49.1 < 275	2490
		A1	AISI	80 × 40 × 3	1.23	8	6.76	57.9 < 330	5689
		A2	304 N	80 × 40 × 3	0.92	8	6.67	57.9 < 275	2004
		A3	S275JR Al 6066T4	8 × x40 × 4	0.29	4	2.90	49.1 < 207	174
(5) Mech. pin	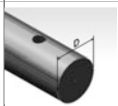	D_i	S275JR	ϕ22	1.1	2.2	0.17	26.2 < 275	51
		A1	AISI	ϕ20	1.2	2	0.14	31.7 < 330	117
		A2	304 N	ϕ20	0.87	2	0.14	31.7 < 275	42
		A3	S275JR Al 6066T4	ϕ20	0.27	2	0.05	31.7 < 207	3

(*continued*)

Table 1. (*continued*)

Orthopaedic crane component			Raw materials		Processing		Product	Resistance specification $\sigma < \sigma_y$ (MPa)	EI99 (mPt)
			Material type	Size (mm)	Energy (w·h)	Material rem. (g)	Mass (Kg)		
(6) Handgrip		D_i	S275JR	ϕ25 × 3	1.7	1.6	0.65	5.2 < 275	195
		A1	AISI	ϕ25 × 2	1.8	1.2	0.53	6.1 < 330	446
		A2	304 N	ϕ25 × 2	1.34	1.2	0.52	6.1 < 275	156
		A3	S275JR 1 6066T4	ϕ25 × 2	0.42	0.6	0.22	6.1 < 207	13

as the costs associated to energy consumption (2.5 €). Nevertheless, raw materials costs increase up to 81.5 € and represents 77% in the total production costs.

Next, engineering metrics and sustainability indicators are evaluated for the new design of orthopaedic crane. These are shown together with those data obtained for the initial design in Table 2. A notable reduction of almost 63% for the product mass is obtained. As a result, an improvement of the distribution stage indicators (i.e. fuel consumption) is expected. In addition, a reduction of 21% is produced in the energy use. Material removed is almost not modified. Production costs increase 1.5 € and the production is raised to 2.4 ud/h.

Table 2. Engineering metrics and sustainability indicators. Initial product and redesign

Engineering metrics	Product mass (Kg)	Product volume (m^3)	Energy (Kw·s)	Waste (%)	Production costs (€)	Production (ud/h)
Initial product	55.4	0.25	1844.2	1.6	106	2.2
Redesign	20.7	0.25	1450.6	1.5	107.5	2.4
Sustainability indicators	GWP_{100} ($KgCO_2eq$)	EI99 (pt)	VA (€)	EE (€/pt)	Working hours (h)	Hourly wage (€/h)
Initial design	58.1	16.6	14	0.84	0.4	8.2
Redesign	46.7	2.8	12.5	4.6	0.36	8.9

Sustainability indicators of both initial and redesigned product can be compared in Fig. 5. We can observe that GWP_{100} decreases 19% and EI99 that collect different impact categories reduces 83%. Additionally, VA decreases 10.5 € and EE significantly improves. It has been supposed that revenues are not changed. On the other hand, the indicators of the social dimension improve 9% due to the production increase. Since a lower environmental impact is achieved, a positive economic profit is kept and social indicators are improved, a more sustainable orthopaedic crane could be developed.

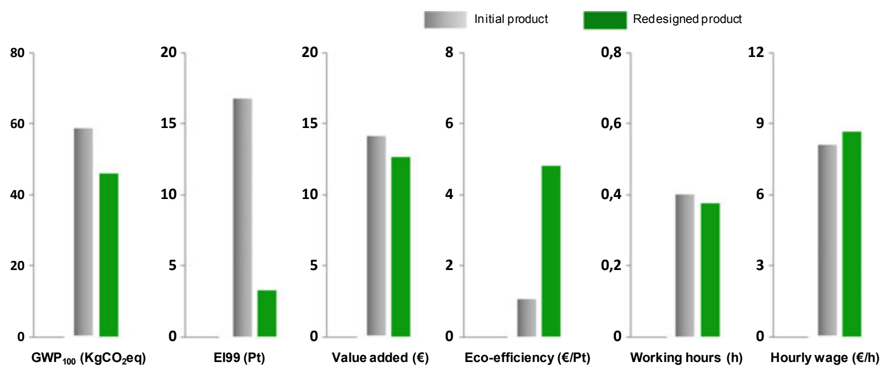

Fig. 5. Comparison between sustainability indicators. Initial product and redesign

4 Conclusions

A methodology to assess and to improve product sustainability is proposed in this work. It is based on the LCSA framework and it is focused on the production stage of the product life cycle. Environmental, economic and social issues are considered simultaneously and are measured using a set of metrics and indicators. Thus, the product sustainability analysis is feasible as well as the presentation of sustainability results to the design decision-makers.

The redesign process of a mobile orthopaedic crane is carried out through methodology applied. Data of materials, manufacturing times, energy consumptions and production costs were firstly obtained to assess the product sustainability. Next, sustainability strategies were applied to project a new crane at the same time that initial specifications of the product were checked. The use of aluminium alloy was found advantageous. As a consequence of the selection of this material, a significant improvement of the sustainability indicators was achieved for the new crane projected.

References

1. Bhamra TA (2004) Ecodesign: the search for new strategies in product development. J Eng Manuf 218(5):557–569
2. Gagnon B, Leduc R, Savard L (2012) From a conventional to a sustainable engineering design process: different shades of sustainability. J Eng Des 23(1):49–74
3. Brezet JC, van Hemel CG (1997) Ecodesign: a promising approach to sustainable production and consumption. UNEP, United Nations Publications, Paris
4. UNCED (1992) Agenda 21, United Nations Conference on Environment and Development. Rio de Janeiro
5. Andriankaja H, Vallet F, Le Duigou J, Eynard B (2015) A method to ecodesign structural parts in the transport sector based on product life cycle management. J Clean Prod 94:165–176
6. Kloepffer W (2008) Life cycle sustainability assessment of products (with comments by Helias A. Udo de Haes, p. 95). Int J Life Cycle Assess 13(2):89–95
7. Finkbeiner M, Schau EM, Lehmann A, Traverso M (2010) Towards life cycle sustainability assessment. Sustainability 2:3309–3322
8. UNEP/SETAC (2009) Guidelines for Social Life Cycle Assessment of Products. United Nations Environment Programme, Paris
9. Azapagic A, Perdan S (2000) Indicators of sustainable development for industry: a general framework. Trans IChemE Process Saf Environ Prot Part B 78(4):243–261
10. Lacasa E, Santolaya JL, Biedermann A (2016) Obtaining sustainable production from the product design analysis. J Clean Prod 139:706–716
11. ISO (2006a). ISO 14040 International standard. In: Environmental management—life cycle assessment—principles and framework. International Organisation, Geneva, Switzerland
12. ISO (2006b) ISO 14040 International standard. In: Environmental management—life cycle assessment—requirements and guidelines. International Organisation, Geneva, Switzerland
13. Goedkoop M, Spriensma R (2000) The Eco-indicator 99. A damage oriented method for Life Cycle Impact Assessment. PRé Consultants B.V., Amersfoort, The Netherlands
14. PROBAS Database http://www.probas.umweltbundesamt.de/php/index.php
15. Kemna R, van Elburg M, Li W, van Holsteijn R (2005) MEEuP Methodology Report

Methodology for a Sustainable Design of Product-Service Systems

I. Millán, E. Lacasa, A. Sánchez, L. Diago, and J. L. Santolaya(✉)

Department of Design and Manufacturing Engineering, EINA,
University of Zaragoza, C/María de Luna 3, 50018 Saragossa, Spain
jlsanto@unizar.es

Abstract. Advances in sustainable product design have been carried out in the last decades both in the development of a suitable methodology and in the application of tools to assess and improve sustainability. Similar progresses for the design of sustainable product-service systems still have limited application and there is need for consistent and robust methods and indictors. This work aims at providing a practical scheme for service based organizations, which could assist them in their shift towards sustainability. A method that makes use of practical metrics and indicators to evaluate the environmental and socio-economic impacts and includes a redesign phase integrating initial specifications and sustainability strategies is proposed. The performance of a nursery school is analyzed. According to methods of sustainable product design, an approach based on the analysis of the flows exchanged throughout the service delivery was developed. Each of the sustainability dimensions were assessed using both, operational metrics and sustainability indicators. A stakeholders' map was elaborated to identify redesign strategies focused on the social demands. In the end, a comparative presentation of both initial and redesigned service indicators is performed to detect if improvements were achieved.

Keywords: Sustainability · Design methodology · Service development · Indicators assessment

1 Introduction

Design for Sustainability (DfS) has progressively expanded from a technical and product-centric focus towards large scale system in which sustainability is understood as a socio-technical challenge [1]. Firstly, DfS was mostly focused on the product level and mainly on the design of products with low environmental impact, usually referred as product Life Cycle Design, Eco-design or Design for the Environment [2, 3]. As a result of the intensive research carried out the last decades, the environmental effects attributable to the production, use and disposal of a product and how to assess them have become clearer and techniques of assessing the environmental impact of products have been developed.

Environmental assessment tools are generally based on a life cycle assessment (LCA) method, which counts, on the one hand, all the energy and material inputs and, on the other hand, the associated emissions and waste outputs at each stage of the

F. Cavas-Martínez et al. (Eds.): *Advances on Mechanics, Design Engineering and Manufacturing II*, LNME, pp. 23–31, 2019.
https://doi.org/10.1007/978-3-030-12346-8_3

product life cycle. Its structure was clearly defined by the harmonization-standardization work by SETAC and ISO [4, 5]. Besides, environmental improvement tools provide guidelines and rules for helping designers to identify potential actions to improve the environmental performance of products, for instance Eco-design Pilot [6] and the Design for Sustainability (D4S) guide [7].

From the end of the 1990s, attention has also been paid to design for eco-efficient Product-Service Systems (PSS), a wider dimension than that of the single product [8]. Eco-efficient services are systems of products and services, which are developed to cause a minimum environmental impact with a maximum added value. In addition, a Product-Service System Design for Sustainability was defined [9]. It consists of the design of the system of products and services that are together able to fulfil a particular customer demand based on the design of innovative interactions of the stakeholders where the economic and competitive interest of the providers continuously seeks both environmentally and socio-ethically beneficial new solutions. A more rigorous interpretation of sustainability is included in this definition since it does not only consist of the environmental impact; it involves three dimensions: environmental (planet), economy (profit) and social well-being (people) [10].

In order to evaluate sustainability in this triple bottom line, guidelines as Sustainability Best Practices Recommendation (sBPR) that cover companies' activities [11] and innovative design methodologies to obtain improved products as the Life Cycle Sustainability Assessment (LCSA) framework [12, 13] are being introduced. LCSA combines LCA, LCC and S-LCA techniques. Life Cycle Assessment (LCA) is focused on the environmental aspects of a product throughout its life cycle and its use is widespread. Life Cycle Costing (LCC) is a compilation and assessment of all costs associated with the life cycle of a product that are directly covered by any or more of the actors in the product life cycle. Whereas, Social Life Cycle Assessment (S-LCA) provides information on social aspects in order to improve performance of organizations and ultimately the well-being of stakeholders. The socio-economic impacts associated with the product' life, are captured in five suggested stakeholder categories [14]: workers, local community, society, consumers and value chain actors. Many social issues are not easy to quantify, so a number of social indicators contain qualitative information.

While Eco-design tools and LCSA approaches could be useful to address the design of sustainable Product-Service Systems, the development of additional methods and tools to carry out the impact assessment and to find improvement strategies, is necessary. LCSA methodology is hardly applied to analyze the sustainability performance in service delivery and a redesign stage including sustainability strategies is not carried out. This work aims at using a methodology to design sustainable services. The performance of a day nursery is analyzed and different metrics and indicators are used to assess the environmental and socio-economic dimensions of the sustainability. In addition, the improvement of the service delivery is addressed. Methodology applied and results obtained for this case study, are shown in the following sections.

2 Methodology

Taking into account that sustainability evaluation is focused on the operational phase, the development of a more sustainable service can be achieved through a sequence of phases organized as follows (Fig. 1): (1) Identification of inputs and outputs associated to the service delivery; (2) Calculus of operational metrics and indicators to assess the three dimensions of sustainability; (3) Service redesign integrating sustainability criteria. Next, a new inventory and sustainability assessment should be carried out for the redesigned service. Finally, the comparative presentation of the sustainability performance of both initial and redesigned service can be performed to detect if service was improved.

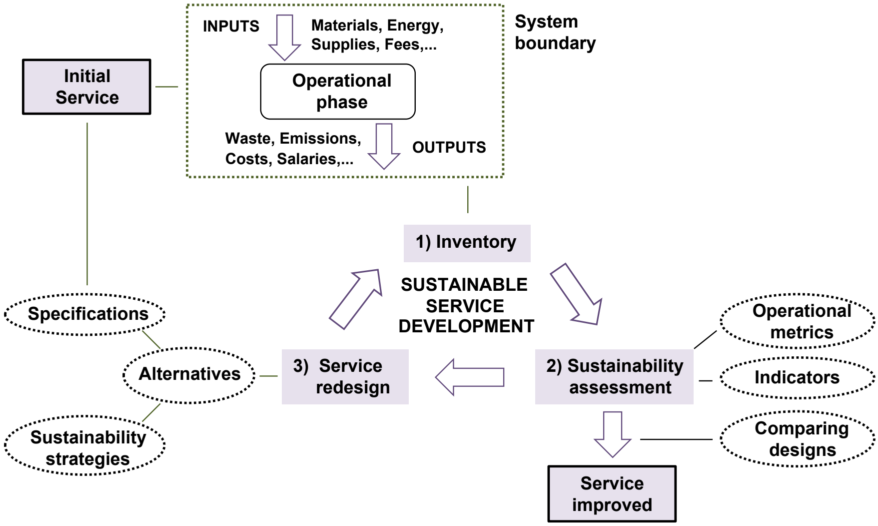

Fig. 1. Phases for a sustainable service development

2.1 Inventory

All existent flows associated to the service delivery are valued in this phase. In view of that the analysis is focused on the operational phase of a nursery school, the elementary flows exchanged include inputs like materials, energy consumption, water consumption, supplies or monthly fees and outputs like waste, emissions, energy costs, salaries, various expenses.

In addition, service development is analyzed carefully to obtain the number of children registered, total number of caregivers and children distribution within the educational centre. The functional unit was defined in such a way that it can account for changes per person per year.

2.2 Sustainability Assessment

To facilitate the application of the principles of sustainable development in practice there is a need to measure the individual sustainability dimensions and to achieving a comprehensive presentation of the results. The use of a set of metrics and indicators for identification of more sustainable practices is proposed. The indicators should be developed at the appropriate level of detail to ensure proper assessment of the situation with regard to each particular challenge. Besides, indicators able to evaluate the most important impact categories by means of easily understandable and user-friendly units, are particularly useful for designers because facilitate the communication of sustainability results to the decision-makers [15].

A number of operational metrics and indicators are selected in this work according to the type of service that is analyzed. The number of children registered in the nursery school, the child-caregiver ratio, the surface area by child, the energy consumption (electricity and gas) and costs due to both, energy use and salaries of caregivers were the metrics selected in this case. I should be noted that these metrics are evaluated for one school year and allow obtaining practical information about the service development.

Different indicators are proposed to assess each of the three dimensions of sustainability. Global Warming Potential (GWP) that represents total emissions of the greenhouse gases and bottled water consumption are selected to assess the environmental dimension. For the economic dimension, the added value (VA) that expresses the net operating profit of the service and the ratio between VA and public subvention are the indicators suggested. Finally, the indicators selected to assess the social dimension are the opening hours and the number of caregivers working in the nursery school, associated to the local community category [14].

2.3 Service Redesign

Designing service activities usually begin with an analytical phase where requirements, specifications and problems are studied along with the anticipated market demands. Since the goal/specification phase is the most crucial as far as service performance and characteristics are concerned, this is where the sustainability issues are considered.

Different methods and tools can be used to the design of eco-efficient services. A number of categories as those named transportation, infrastructure, buildings, staff, tools and support products, consumption goods and main service products are considered to be analyzed in the denominated META-matrix tool [8], which is focused on the environmental dimension. Taking into account that a socio-economic approach of sustainability is also addressed in this work, a stakeholder's map, which is shown in Fig. 2, was elaborated in order to identify service redesign alternatives. Direct users as babies and children, indirect users as parents and tutors, teaching staff and auxiliary services were, respectively, the stakeholders considered for this case study.

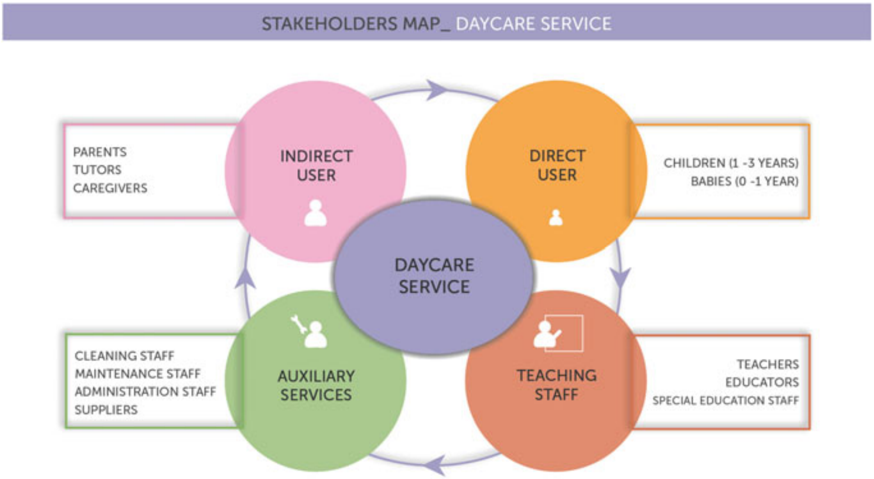

Fig. 2. Stakeholders map. Day-care service

3 Case Study

The service delivered by a public nursery school was addressed. In particular, the study was focused on an educational and care centre for children from 0 to 3 years placed in Alcorisa, which is a municipality of around 3500 habitants located in a sparsely populated region of Spain (little more 9 hab/Km^2).

The building, with a circular cross section, has two floors and six classrooms that can be used according to the demands of each course. The current use includes 4 classrooms: C1 and C2, placed on the first floor and C3 and C4, placed on the ground floor. Children distribution as well as surface area of each classroom (the bathroom surface area is added in each case) is indicated in Fig. 3. C1 is occupied all time; C2 and C3 are occupied only part-time and C4 is used on the morning to care 6 babies up to 1 year old and on the afternoon to care a total of 12 children from 0 to 2 years old. To note that, currently, the nursery school is open a total of 7 h 45’ each day, from Monday to Friday, it is closed 1 h at noon and C2 classroom is only used on the morning.

All metrics and sustainability indicators obtained for the initial service are summarized in Table 1, where can be comparatively analyzed with those obtained later from the service redesigned. It can be observed that a total of 45 children are registered. A maximum number of 15 children per caregiver and a minimum surface of 3.5 m^2/child are calculated for the C1 classroom, which is according to the requirements of the established normative [16]. The annual performance of the nursery school involves, respectively, electricity and gas consumptions of 221.5 and 1924.6 Kw·h per child; the energy cost is 157.3 € and the cost due to salaries of caregivers is 1527 €/child. All data were obtained from bills and interviews with workers.

According to latest International Energy Agency (IEA) highlights report [17], emissions of 585.3 kg CO_2eq per child were obtained. The average consumption of

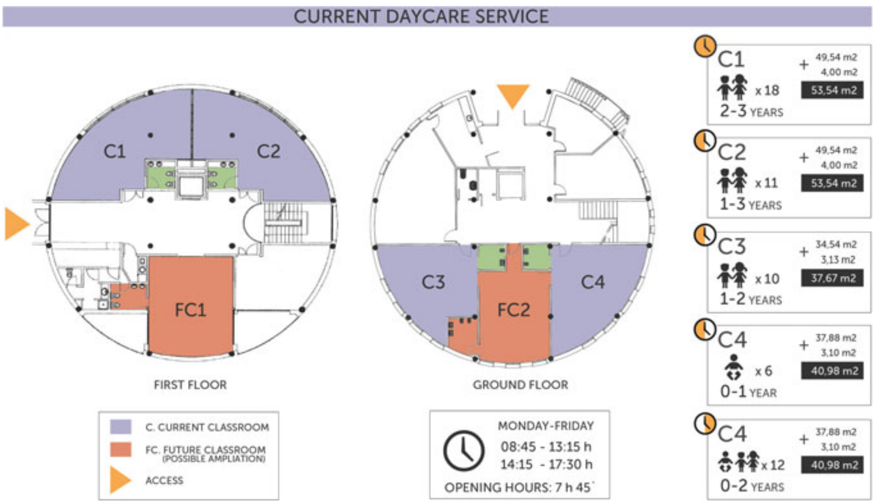

Fig. 3. Children and classrooms distribution. Initial day-care service

Table 1. Operational metrics and sustainability indicators of the initial and redesigned services

Operational metrics	Registered children	Children/caregiver	Elec. cons. (Kw·h)	Gas cons. (Kw·h)	Energy cost (€)	Caregivers cost (€)
Initial design	45	18	221.5	1924.6	157.3	1527
Redesign	53	18	217.9	1893.8	154.7	1502.5
Sustainability indicators	GWP_{100} ($KgCO_2eq$)	Water cons. (l)	VA (€)	VA/Subv (%)	Opening (h/day)	Workers number
Initial design	585.3	110	249.2	20.1	7 h 45.	5
Redesign	577	110	317.1	25.6	9	6

bottled water is 110l. One of the main money inputs in the nursery school is the children's fees (1031.5 €/child), which are relatively low because the service gets a high public subvention. Thus, an annual VA of 249.2 €/child is obtained and 20.1% in the effectiveness of the public subvention are obtained. In addition, the opening hours and the total number of workers of the initial service are indicated in Table 1.

Then, some changes were projected in the service delivery. Alternatives of redesign were proposed taking into account the fulfillment of the requirements and the needs of the stakeholders. With this purpose interviews with parents and teachers were carried out. On the one hand, teachers asked for the need of support staff. Ratios given by the normative are too elevated for them, what suppose a high amount of children per caregiver. On the other hand, parents requested more flexible schedules that allow them to adapt their children care with their working routines. Besides, more than half of them, were interested in the lunch service what involves having the nursery school open at midday.

Consequently, the redesign of the service has focused on these social demands. A new flexible timetable has been proposed, with an increase of 1 h and 15 min every day. The new schedule proposed is from 8 h to 17 h, from Monday to Friday. This adjustment increases the consumptions and costs of the nursery school. Nevertheless, the enrolment is also expected to increase according to the preferences expressed by the parents. A total number of 53 children is estimated due to the implementation of these changes. As shown in Fig. 4, C5 classroom could be now used to care the 8 new children.

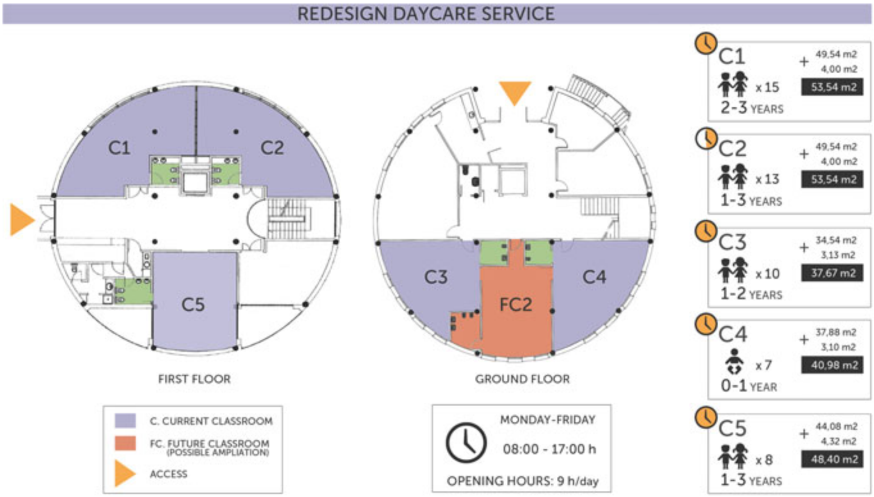

Fig. 4. Children and classrooms distribution. Redesigned day-care service

Inventory and subsequent sustainability assessment were carried out for the redesigned service. Operational metrics and indicators finally obtained are summarized in Table 1. A total of 53 children are registered. Since a new classroom is used, the maximum ratio children per caregiver and the minimum surface area per child are maintained. Even if the projected day-care service increases the opening hours, a slight reduction of 1.5% in electricity and gas consumptions and costs of both, energy and caregivers, is obtained (note that all metrics are expressed per child).

Next, environmental, economic and social indicators are assessed. The emissions of greenhouse gases per child reduce to 577 kg CO_2eq. If children's fees and public subventions are preserved, total revenues increase 17.6% and VA increases 67.9 €. Another option that could be object to study is the reduction of subventions through the increase of the children's fees. Since a new classroom is needed and the opening hours enlarge 1 h 15', the number of workers should be 6 in the redesigned service.

The comparison of the results obtained in the initial and redesigned service (Fig. 5) shows that a reduction of the environmental impact as well as an improvement of the socio-economic indicators is achieved. A reduction of 1.5% in the annual emissions of greenhouse gases per child is obtained while the average consumption of bottled water is not changed. A notable increase of 27.2% is achieved for the economic indicators. On the other hand, the opening hours enlarge 16.1% and the number of workers increase 20%. In this way, the service sustainability is improved according to the indicators that have been studied.

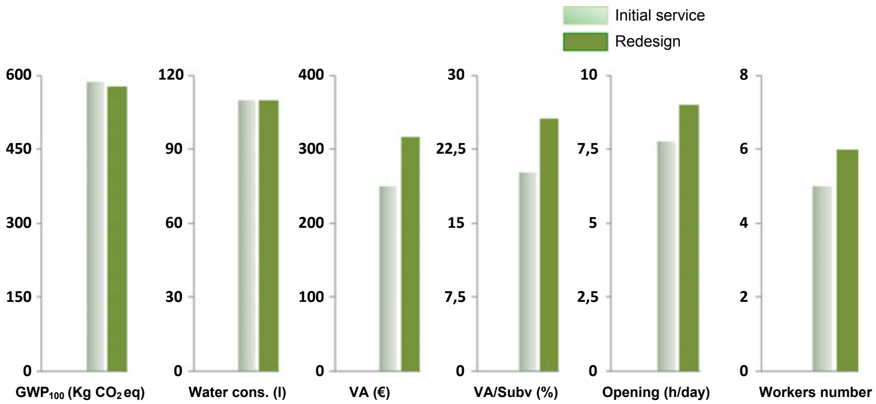

Fig. 5. Day-care service. Sustainability indicators comparison

4 Conclusions

In this work, a methodology to assess and improve sustainability in projects of service design is applied to the case of a day-care service. Economic, environmental and social aspects are simultaneously considered. Each one of the sustainability dimensions are quantified using a set of metrics and indicators that facilitate the analysis and communication of results during the service design decision-making process.

The operational phase of a public nursery school to children from 0 to 3 years is carried out. Inventory was supported by the centre responsible of the education and care of the children. A service redesign was proposed taking into account the fulfillment of the legal requirements and the needs of the stakeholders. In particular, a more flexible timetable, with an increase of 1 h and 15 min every day, was projected in order to allow parents a better adaptation with their working routines. An increase of 8 children and the use of an unoccupied classroom are planned.

An improvement of the indicators for each sustainability dimension was achieved. A reduction of the environmental impact expressed by the global warming and an increase of the added value were measured. Looking at the social dimension, the local employment could be pushed up and the working routines facilitated.

References

1. Ceschin F, Gaziulusoy I (2016) Evolution of design for sustainability: from product design to design for system innovations and transitions. Des Stud 47:118–163
2. Brezet JC, Van Hemel CG (1997) Ecodesign: a promising approach to sustainable production and consumption. UNEP, United Nations Publications, Paris
3. Guinée J, Gorrée M, Heijungs R, Huppes G, Kleijn R, de Koning A et al (2001) Life cycle assessment—an operational guide to the ISO standards. Leiden University, Centre of Environmental Sciences (CML), The Netherlands
4. ISO (2006a) ISO 14040 International Standard. In: Environmental management—life cycle assessment—principles and framework. International Organisation, Geneva, Switzerland
5. ISO (2006b) ISO 14040 International Standard. In: Environmental management—life cycle assessment—requirements and guidelines. International Organisation, Geneva, Switzerland
6. Wimmer W, Züst R (2003) Ecodesign PILOT: product Investigation. Learning and optimization tool for sustainable product development. Kluwer Academic Publishers, Dordrecht
7. Crul M, Diehl JC (2009) Design for sustainability. A step-by-step approach. UNEP, United Nations Publications, Paris
8. Brezet JC, Bijma AS, Ehrenfeld J, Silvester S (2001) The design of eco-efficient services. Design for sustainability program. Delft University of Technology, The Netherlands
9. Vezzoli C, Kohtala C, Srinivasan A (2014) Product-service system design for sustainability. Greenleaf Publishing, Sheffield
10. UNCED (1992) Agenda 21, United Nations Conference on Environment and Development, Rio de Janeiro
11. EPRA (2017) Sustainability Best Practices Recommendations, European Public Real Estate Association. Third version
12. Finkbeiner M, Schau EM, Lehmann A, Traverso M (2010) Towards life cycle sustainability assessment. Sustainability 2:3309–3322
13. Valdivia S, Ugaya CML, Hildenbrand J, Traverso M, Mazijn B, Sonneman GA (2013) UNEP/SETAC approach towards a life cycle sustainability assessment-our contribution to Rio + 20. Int J Life Cycle Assess 18:1673–1685
14. UNEP/SETAC (2009) Guidelines for Social Life Cycle Assessment of Products. United Nations Environment Programme, Paris
15. Adelle C, Pallemaerts M (2009) Sustainable development indicators. An overview of relevant framework programme funded research and identification of further needs in view of EU and international activities, European Communities
16. Order August 25th of 2005. Education. Culture and Sport Department of Aragón
17. International Energy Agency, grid-based emissions factors. www.iea.org/statistics/topics/CO2emissions/. Latest Accessed 27 Feb 2018

Human Factors Assessment for Comfort and Safety in the XCAT Powerboats Rules

S. Abrami[1], F. Cucinotta[2(✉)], E. Guglielmino[2], and F. Sfravara[2]

[1] UIM Technical & Safety Office, Piazza C. Battisti, 25068 Sarezzo, Italy
[2] University of Messina, C.da di Dio, 98166 Messina, Italy
filippo.cucinotta@unime.it

Abstract. In the speed-based competition, with the use of fast vehicles, a fundamental aspect is the safety and comfort of the drivers. In each speed-based competition, the drivers are subjected to vibrations and stresses whose evaluation is fundamental in order to quantify the discomfort of them. The comfort conditions are guaranteed by a deep study of the correct size of the internal spaces, the right posture of the drivers and the right choice of the position of the elements inside the vehicles (damping elements, position of the steering wheel, position of instruments, etc.). Another important aspect is the assessment of the escape spaces in case of accident. To reach these goals, the Governing Body act with the definition and the verification of technical rules. In this work the field of interest is powerboats sport. During the powerboat race, the reached speed and the z-acceleration of the boat lead to several stresses on drivers. Two different approaches have been investigated, a traditional 2D approach and an innovative 3D approach. Results have been discussed.

Keywords: Ergonomics · Human factors · Safety design · Seat comfort

1 Introduction

In racing sports, it is crucial, for safety and comfort reason, to guarantee the correct size of the internal spaces and right position of the drivers. A literature review of the of race driver position and fatigue measurement has been proposed by Owen et al. [1]. In the last years, UIM (*Unione International Motonautique*), powerboat Governing Body, has made an evolution as a very high-tech sport with a great concern for the safety of the pilots. During the racing, the pilots can reach speed over of 200 km/h and this condition can lead to danger situations such as drowning of the pilots and impact effects [2, 3]. As in the history of all motor sports, accidents with powerboats resulted in attention by organisers and boat builders to the importance of safety [4, 5]. In particular, in powerboat sports, that use closed canopy, in order to increase the safety, it is necessary to assess the correct clearances and the escape routes. To reach this goal, sport's officers act with the definition and the verification of technical rules. For this reason, the rules have to be justified by technical motivation and frequently updated.

The first element under study for the comfort of the drivers is the seat. Kamp [6] showed the comfort response of 21 persons sitting on three different car-seats design. In this study, it has been shown the difference between the seats used in racing sport and

F. Cavas-Martínez et al. (Eds.): *Advances on Mechanics, Design Engineering and Manufacturing II*, LNME, pp. 32–40, 2019.
https://doi.org/10.1007/978-3-030-12346-8_4

the ones used in daily cars. This, because all the vibrations during the race caused by the accelerations, principally in z-direction, are transmitted to the buttocks and back of the occupants along the vertebral axis via the back and base of the seat. In the automotive field, many studies concern the evaluation of the fatigue and discomfort of drivers during race. Ebe et al. [7] proposed a qualitative model for the assessment of the discomfort including both static and dynamic conditions. An evaluation of different types of seats has been proposed by El Falou et al. [8] with the assessment of the driver response with the use of surface electrodes. In this case, the vibrations of the car have been produced by a vibrating platform. A new concept design to reduce the vibration effects on drivers has been proposed by Makhsous et al. [9]. Many studies have been conducted in order to decrease the fatal injuries during the racing sports. Until to 2001, the most common cause of injuries in motor sport racing was the fracture of the craniovertebral junction. With the introduction of the HANS system (Head and Neck Support) this type of injury has drastically decreased [10]. The need to define new designs in order to increase the comfort of drivers lead many authors to study virtual solutions. A review of the impact in the use of computer-integrated techniques for the identification of industrial ergonomic factors has been reported by Sharma et al. [11]. One of the most popular software for simulating comfort and ergonomic conditions is Jack, developed at the University of Pennsylvania. Kajaks et al. used this software in order to evaluate the effects of aging on driver visibility [12]. Reed et al. [13] scanned different humans in order to implement them in Jack software. This paper describes the use of 2D and 3D approaches in order to define minimum dimensions of the internal spaces inside the cockpit of a XCAT powerboat for UIM competitions. The 3D approach is conducted thanks to Jack software, with this software has been defined a minimum volumetric distribution of the clear space.

2 Materials and Methods

In this work the field of interest is powerboats sport. During the race of motorboats, the reached velocity and the z-acceleration of the boat lead to several stresses on drivers. Furthermore, a critical aspect in this sport is the escape phase of drivers after an accident. In order to quantify all these aspects the paper proposes an assessment of the spaces with a 2D approach and with the use of a 3D model approach. The 2D approach allows defining the minimum dimensions of the internal spaces inside the cockpit (Fig. 1).

In accordance with European stature at four different male percentiles (5, 50, 80 and 95%) human height and relative proportions of the body parts have been used [14]. The anthropometric data are compatible with the detected measures of the drivers of the XCAT class of the UIM competition. In order to quantify the comfort conditions have been used different posture angles in accordance to the ones defined in racing automotive sport [15, 16]. Thanks to the definition of the posture angles have been defined two different postural quadrilaterals. The first one is relative to the sagittal plane (Fig. 2- top). The vertexes of this quadrilateral are: sitting point (A), head point (B), steering wheel (C) and heel (D). The second one is in transversal plane (Fig. 2- down). In this case the vertexes are: the top of the head, the top of the head rotated of 45°, the

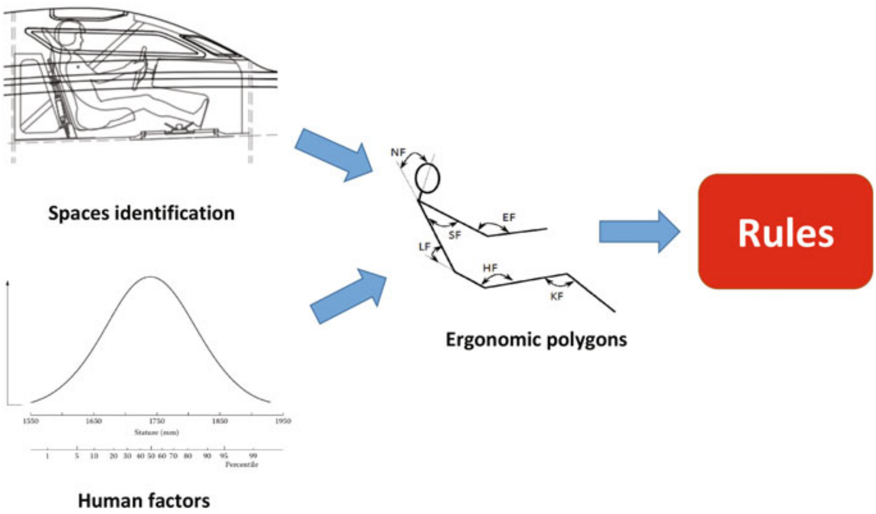

Fig. 1. 2D traditional approach

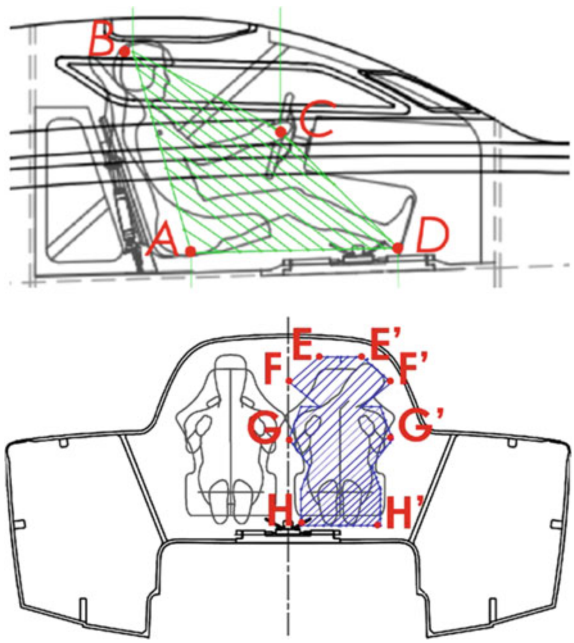

Fig. 2. Sagittal polygon on left, transversal polygon on right

elbow and the maximum encumbrance of the legs. Taking in account the different dimensions of the drivers, the cockpit internal spaces and all driver's equipment (damping system, helmet, seat), have been calculated the minimum height and breadth of the cockpit in order to have the necessary spaces for comfort condition during the race.

The 2D approach has several limits, e.g. it can't take into account the true size of the cockpit, the reachability of the escape routes, including all the movements that the drivers have to do in the transitory stage. For this reason a 3D approach is also proposed. The 3D model allows evaluating these spaces during the escape phase in numerous cases, including the case of capsizing of the boat. In this phase is fundamental to evaluate the encumbrance of the all elements in dynamic mode. Furthermore, a 3D approach allows to evaluate the dynamic effects on the drivers coming from slamming accelerations, collisions, seatbelts and Head and Neck Support (HANS) constraints.

A 3D model has been developed (Fig. 3) on the base of a true XCAT UIM powerboats, several times world champion.

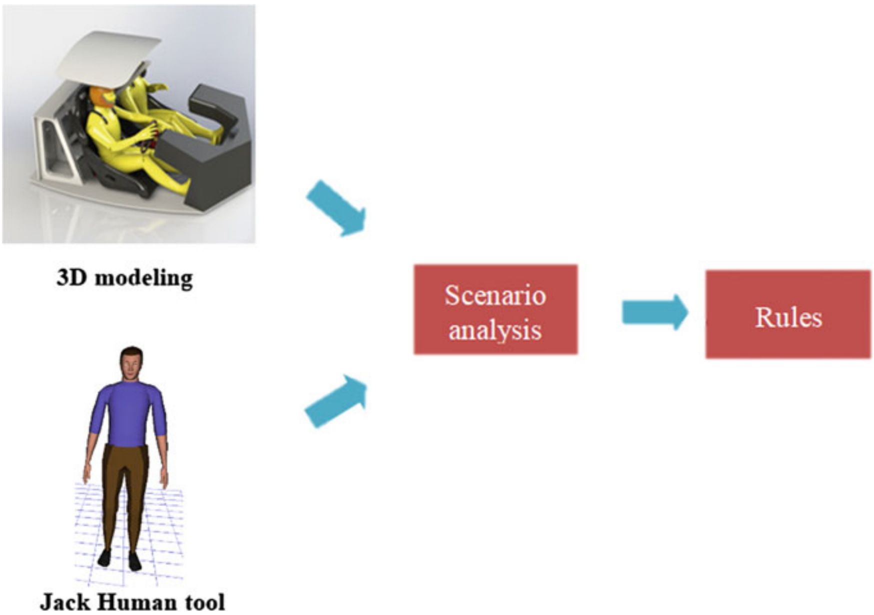

Fig. 3. Virtual 3D model

The implemented anthropometric data comes from Jack, the human simulation system developed at the Center for Human Modeling and Simulation at the University of Pennsylvania in the 1980s & 1990s and now acquired by Siemens.

Jack Human tool allows setting numerous anthropometric variables in function of the human race and the wanted percentile. In particular, the variables are: 1 Stature 2 Abdominal Depth 3 Ankle Height 4 Acromion Height 5 Arm Length 6 Biacromial Breadth 7 Bideltoid Breadth 8 Buttock-Knee Length 9 Elbow Rest Height 10 Elbow-

Fingertip Length 11 Foot Breadth 12 Foot Length 13 Hand Breadth 14 Hand Length 15 Head Breadth 16 Head Height 17 Head Length 18 Hip Breadth 19 Interpupil Distance 20 Shoulder-Elbow Length 21 Sitting-Acromial Height 22 Sitting Eye Height 23 Seated Height 24 Sitting Knee Height 25 Thigh Clearance 26 Thumbtip Reach.

Thanks to 3D model has been defined a minimum volumetric distribution of the clear space. The reach envelope allows to identify the reachability of the controls, for comfort reasons and the hatches in case of accidents (Fig. 4, on left). Furthermore they allows to predict the effectiveness of the restraint systems (i.e. seatbelts and HANS), for example in order to evaluate the permitted movements of the head to find the right compromise between safety and visibility (Fig. 4, on right).

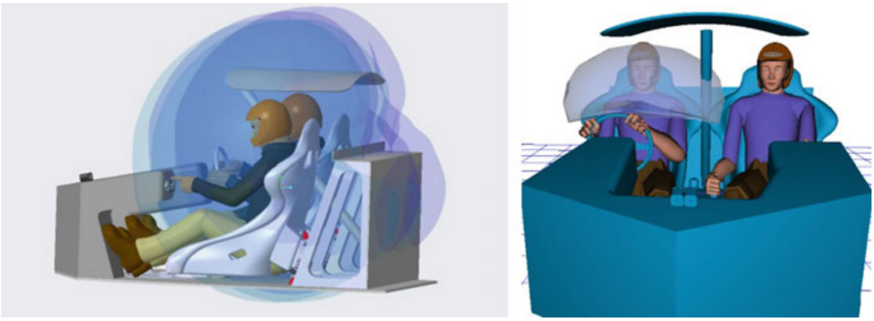

Fig. 4. Reach envelopes of the tip of the fingers, on left, and of the head of the driver using seatbelts, on right

A crucial point is how to quantify the necessary spaces in order to guarantee safe escaping from the bottom of the hull (hatch) or from the top of the cockpit in the shortest possible time. Figure 5, on left, shows a real condition of escaping during a race of motorboats caused by a capsizing accident. In the same Fig. 5, on right, it is shown the corresponding virtual model.

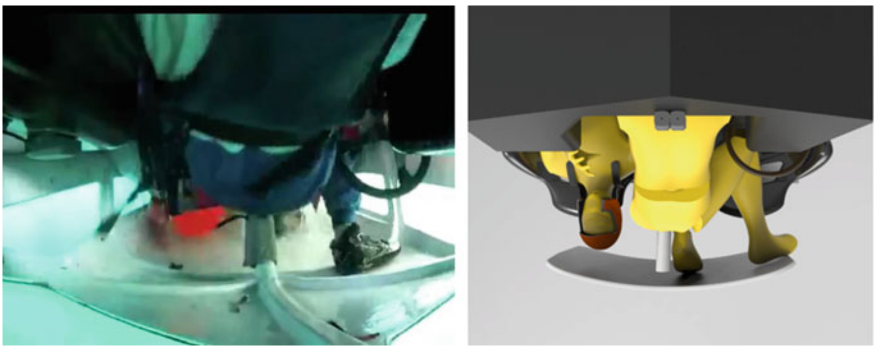

Fig. 5. Escaping condition from the bottom hatch (following a capsizing) in real mode, on left, and virtual mode, on right

The volume that each part of the body can reach during the movements is defined as a reach envelopes. They usually assumes an ellipsoid shape and, in order to evaluate their magnitude, a model based on the span measurement in the 3 directions has been implemented. In this way it is possible to compare the dimensions of the 3D space with numbers that can be easily implemented by the standards in terms of clearance. For the assessment of the head and neck movements, a reference system has been used, as in Fig. 6 (left). The view capability of the pilots is evaluated as the overall envelope of the permitted vision cones by the movements of the neck and head. As a comparison parameter, the maximum envelope angle ϑ has been taken on the plan orthogonal to z-axis as in Fig. 6 (right). The three rotations, defined as lateral bending (χ), around the x-axis, flexion (ψ), around the y-axis and torsion (ζ), around the z-axis, were detected, in their limits, on a real model, as in Fig. 7.

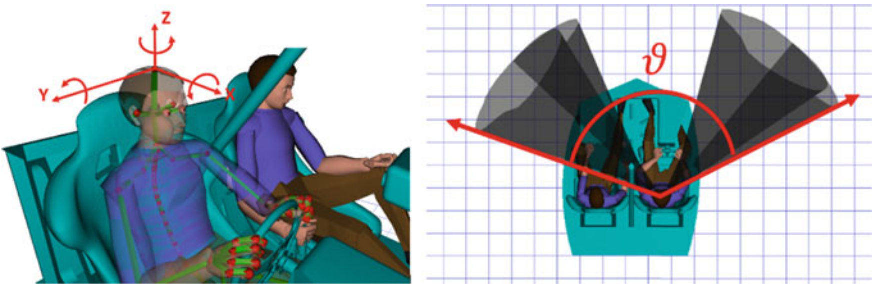

Fig. 6. Reference system, on left, and maximum vision angle, on right

Fig. 7. Three head and neck maximum excursions (with HANS and harness)

3 Results and Discussion

A comparison between the drivers encumbrance, evaluated by means of the 2D polygons, has been carried out. In Table 1, with the significance of the letters H and B as in Fig. 8, the encumbrances, including the regulatory clearances (UIM Official Rulebook 2016), of the cockpit are reported. The sizes have been nondimensionalized on the minimum regulatory ones. Since the clearance at the shoulder, R, is not regulated by rules, it is reported as percentage of regulatory width (1340 mm).

Table 1. Maximum polygons encumbrance, referring to the regulatory cockpit sizes and minimum clearance at the shoulder

Driver's height (percentile of population) (%)	H max (%)	B max (%)	R min (%)	R min
5	86.2	73.7	17.7	237.2
50	91.3	80.6	14.8	198.3
80	93.9	84.2	13.0	174.2
95	96.1	87.9	11.5	154.1

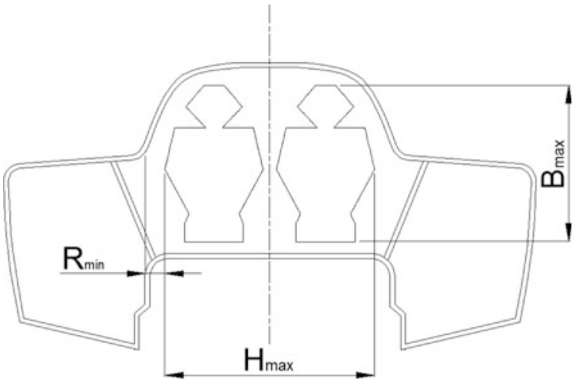

Fig. 8. Definition of the polygons encumbrance and the clearance at the shoulder

Through the 3D analysis of the head reach envelopes, a comparison has been made between three different conditions: without harness (1), with harness only (2) and with harness and HANS (3) (rules condition). The spans are reported in mm in the Table 2.

Table 2. Head envelope spans and vision angle

Condition	X span (mm)	Y span (mm)	Z span (mm)	ϑ (°)
1	369	904	432	325.2
2	197	412	159	239.2
3	159	329	45	127.0

The analysis shows that the use of HANS and harness greatly reduces the movements allowed by the head. In particular, the lateral bending is the most restricted, in comparison to the free pilot condition. Conversely, the visibility of the driver is drastically reduced up to 60%. The range movements, in angles, are reported in Table 3. The back flexion, in both cases, is limited by the headrest.

Table 3. Allowed range head and neck rotation

Rotation	Without HANS (°)	With HANS (°)
χ	−43.5 to +43.5	−20.0 to +20.0
ψ	−8.5 to +71.0	−8.5 to +27.5
ζ	−99.5 to +99.5	−30.0 to +30.0

4 Conclusions

Two different 2D and 3D approaches, for the cockpit size of a UIM XCAT powerboats, have been investigated. The 2D approach, by means of the use for ergonomic polygons, has allowed verifying the effectiveness of the rules clearances. A more complex 3D approach, by the use of Jack manikins into a 3D modelled volume, has permitted to assess the safety and the comfort of the drivers in more detail. The use of reach envelope of the head led to compare three different conditions in terms of maximum encumbrances. In particular, the use at the same time of the HANS and the harness permit a sensible reduction of the head movements, with a substantial safety increasing, but also a significant reduction of the visibility.

Further analyses can make it possible to evaluate the effectiveness of the current rules also in dynamic terms, as e.g. about the body accelerations.

Acknowledgments. The authors wish to thank the Union Internationale Motonautique for providing the information, Sebastiano Pellecchia and Roberto Lo Piano for the precious comments and suggestions and Marcello Raffaele and Fabio Salmeri for the irreplaceable help in 3D modeling and image analysis.

References

1. Owen N, King H, Lamb M (2015) Literature review of race driver fatigue measurement in endurance motorsport. Procedia Eng 112:344–348. https://doi.org/10.1016/j.proeng.2015.07.260
2. Cucinotta F, Guglielmino E, Risitano G, Sfravara F (2016) Assessment of damage evolution in sandwich composite material subjected to repeated impacts by means optical measurements. Procedia Struct Integr 2:3660–3667. https://doi.org/10.1016/j.prostr.2016.06.455
3. Cucinotta F, Paoli A, Risitano G, Sfravara F (2018) Optical measurements and experimental investigations in repeated low-energy impacts in powerboat sandwich composites. Proc Inst Mech Eng Part M J Eng Marit Environ 232:234–244. https://doi.org/10.1177/1475090217720619
4. Van Nueten J (2014) Offshore powerboat rescue, In: Drowning, Springer Berlin Heidelberg, Berlin, Heidelberg, pp 505–508. https://doi.org/10.1007/978-3-642-04253-9_77

5. Cucinotta F, Guglielmino E, Sfravara F (2017) Frequency of ship collisions in the strait of messina through regulatory and environmental constraints assessment. J Navig 1–21. https://doi.org/10.1017/s0373463317000157
6. Kamp I (2012) The influence of car-seat design on its character experience. Appl Ergon 43:329–335. https://doi.org/10.1016/j.apergo.2011.06.008
7. Ebe K, Griffin MJ (2000) Qualitative models of seat discomfort including static and dynamic factors. Ergonomics 43:771–790. https://doi.org/10.1080/001401300404742
8. El Falou W, Duchêne J, Grabisch M, Hewson D, Langeron Y, Lino F (2003) Evaluation of driver discomfort during long-duration car driving. Appl Ergon 34:249–255. https://doi.org/10.1016/S0003-6870(03)00011-5
9. Makhsous M, Hendrix R, Crowther Z, Nam E, Lin F (2005) Reducing whole-body vibration and musculoskeletal injury with a new car seat design. Ergonomics 48:1183–1199. https://doi.org/10.1080/00140130500226903
10. Kaul A, Abbas A, Smith G, Manjila S, Pace J, Steinmetz M (2016) A revolution in preventing fatal craniovertebral junction injuries: lessons learned from the head and neck support device in professional auto racing. J Neurosurg Spine 25:756–761. https://doi.org/10.3171/2015.10.SPINE15337
11. Kumar Sharma H, Singhal P, Sonia P (2018) Computer-assisted industrial ergonomics: a review. pp 37–48. https://doi.org/10.1007/978-981-10-5457-0_4
12. Kajaks T, Vrkljan B, MacDermid J, Godwin A (2016) Using simulation to better understand the effects of aging on driver visibility. Can J Aging/La Rev Can Du Vieil 35:110–116. https://doi.org/10.1017/s0714980816000106
13. Reed MP, Raschke U, Tirumali R, Parkinson MB (2014) Developing and implementing parametric human body shape models in ergonomics software. In: proceedings of the 3rd international digital human modeling conference pp 1–8
14. Pheasant S Haslegrave CM (2005) Bodyspace: anthropometry. Ergonomics and the design of work. Third Edit
15. Schmidt S, Amereller M, Franz M, Kaiser R, Schwirtz A (2014) A literature review on optimum and preferred joint angles in automotive sitting posture. Appl Ergon 45:247–260. https://doi.org/10.1016/j.apergo.2013.04.009
16. Andreoni G, Santambrogio GC, Rabuffetti M, Pedotti A (2002) Method for the analysis of posture and interface pressure of car drivers. Appl Ergon 33:511–522. https://doi.org/10.1016/S0003-6870(02)00069-8

Development of a Low-Cost Wearable Prevention System for Musculoskeletal Disorders Using Inertial Measurement Unit Systems

C. Cao(✉), M. I. Rodríguez-Ferradas, A. Cazón-Martín, and Paz Morer

Department of Mechanical Engineering, University of Navarra-TECNUN, San Sebastián, Spain
ccao@tecnun.es

Abstract. The increasing relevance of occupational injuries and illness related to lean manufacturing strategies in automotive assembly lines brings an increasing interest in this industry by the research and development of new tools and methods for the evaluation and prevention of work-related musculoskeletal disorders (WMSDs). However, few studies have focused on assessing the exposures to the hand region whereas disorder in this region remain at the primary tier of the prevalence ranking. Herein, this paper presents a low-cost, wearable inertial measurement unit (IMU) to measure workplace demands. This technology was selected after analysing an assessment scale composed of seven of the common ergonomic assessment tools and methods. After a brief verification through a laboratory goniometry experiment, eleven joint angles of a volunteer's hand were measured. The results indicated that the mean difference between the values measured by participants and the values obtained directly from the wearable is 2.44°, which has the same accuracy level of the commercial products. The proposed device is scalable enough to be iterated by further improvements, including conductive fabric 3D printing technology.

Keywords: Work-related musculoskeletal disorders · Automotive assembly lines · Measurements assessment · Inertial measurement units · Arduino

1 Introduction

Work-related musculoskeletal disorders (WMSDs), such as Carpal Tunnel Syndrome, Radial Tunnel Syndrome or Tendonitis, are some of the most common injuries in the manufacturing sector that generates pain in the musculoskeletal system [1]. WMSDs led to 3,138,000 lost workdays in the United Kingdom in the period 2015–16 [2] and a total cost of lost productivity of €240 billion or up to 2% of gross domestic product (GDP) in 2015 in the European Union [3]. Repetitive movement, excessive force, enduring awkward postures as well as psychological factors are the main exposures that cause WMSDs [4]. Many studies try to prevent these situations by measuring and

F. Cavas-Martínez et al. (Eds.): *Advances on Mechanics, Design Engineering and Manufacturing II*, LNME, pp. 41–51, 2019.
https://doi.org/10.1007/978-3-030-12346-8_5

estimating workload intensity in order to change the cycle time or replace the layout of an assembly line.

To assess WMSDs risks in a specific workplace, ergonomic experts rely on a variety of methods and techniques which can be generally categorized into: (1) self-report, (2) expert observation and (3) direct measurement that can be combined with biomechanical assessment methods for the later post-processing of the human-motion data collected. With the development of technology and increasing investments, nowadays, ergonomic experts tend to utilize more objective methods to evaluate the ergonomics. However, most of them focus mainly on low-back, upper limb and neck regions while the WMSDs of the hand and the wrist are very hard to measure, or merely treated as a reference group.

Numerous companies and studies in various fields have started some attempts on hand region motion capture by using a variety of advanced techniques. Wang et al. [5] used CyberGlove®, which is supported by a flex sensor as the core technique for presenting a calibration approach for hand motion capture. Sama et al. [6] developed a low-power and low-cost hand motion capture glove by utilising a set of flex sensors, gyroscopes and accelerometers. Kitano et al. [7] presented a wearable finger motion measurement system using 9-axis inertial and geomagnetic sensors that works with the Euler angle system. In fact, it is a challenge for most of the self-made devices and commercial products to balance the cost, the performance and the comfort in a real workplace.

The aim of this paper is to develop a wearable device for tracking worker's finger movements in an automotive assembly plant so as to subsequently analyse if the worker is exposed to WMSDs. An automotive company was selected for the projects since the research team has a long relationship with them and they were concern about workers' safety in the assembly line. Nevertheless, this device can also be adopted by other industrial sectors. Intensive, repetitive and continuous movements, as well as compact workspaces are the fundamental job constraints in the current lean automotive assembly production environment [8]. The design of the wearable should focus on the above facts and the commercial principle of low-cost. Firstly, in order to select the most appropriate measuring technique for the device, seven methods and technologies were evaluated with an assessment scale. These methods included both non-technological and technologically more sophisticated solutions. The assessment scales were later analysed to identify their advantages and disadvantages considered. Finally, an early prototype of the wearable device was introduced for motion capturing of the thumb and index fingers.

2 Methods

Seven of the most prevailing ergonomic methods were evaluated by means of a questionnaire created ad hoc and an open question sheet. The methods were: (1) Assessment of Repetitive Tasks (ART) Tools, (2) Rapid Upper Limb Assessment/Rapid Entire Body Assessment (RULA/REBA), (3) Biomechanical Assessment (BA), (4) Optoelectronic Systems (OES), (5) Electro Goniometer (EG), (6) Accelerometry (AM) and (7) Inertial Measurement Units (IMUs).

The suitability of each method was evaluated through several questions grouped by timing, that is, the evaluation of how good this method is before, during, and after the ergonomic measuring. Questions required a yes/no answer or followed a five-level Likert Scale from negative (1) to positive (5) (Fig. 1). Subsequently, this questionnaire was distributed among three experts. One of the experts is a professional who works for company that are involved in ergonomics in the product design cycle. She is also a lecturer in ergonomics. The second expert is a Ph.D. in mechanical engineering who did this Ph.D. in motion capture field and now works in a research center with these systems. The third expert worked for a research center with motion capture systems and now is lecturer on motion capture systems at and engineering university. All of them were asked to fill out only those questionnaires that they considered themselves experts on. Results are listed in the Table 1.

			RULA / REBA						
	Description		**Rapid Upper Limb Assessment / Rapid Entire Body Assessment**						
Before measuring	**Body Region:** Can you tell use the body regions this method could be applied to?								
	Work attribute: What is the type of work this method can measure? (Yes or No)		Repetitive movements						
			Nonrepetitive movements						
			High loads						
			Low loads						
			Static loads						
			Dynamic loads						
			negative	1	2	3	4	5	positive
	Validity: How good can this method measure ____?	**Movement repetition**	very bad						very good
		Loads supported by body							
		Body angles							
		Velocity of movements							
		Duration of movements							
		Vibration							
		Sudden impacts							
		Muscles activity							
		Lifting							
	Independence: Can this method work alone or need another associated method to optimize it?		much						few
	Numbers: How objective/subjective this method is when analysing the ergonomics?		subjective						objective
	Learning difficulty: How difficult is the learning process to apply this method?		expertise						novice
	Physical space: What is the required room space so as to hold the experiment?		much						few
	Equipments costs: How expensive is the necessary equipment to run ergonomic assessment?		high						low
	Preparation time: How much preparation time does this method need to start the assessment?		much						few
While measuring	**Operating difficulty:** How hard is it to apply this method in reality?		laboratory						workplace
	Test time: How much time does this method need to evaluate the ergonomics?		much						few
	Test-reTest: How similar are the results if you use twice this method to measure?		different						similar
	Inter-rater: How similar are the results if two different testers use this method to measure the same person?		different						similar
	Manual error: How easy is it to make mistakes when applying this method?		easy						hard
	Psychological collaboration: Do workers need the help in psychological aspect from tester during the test?		much						few
	Physical collaboration: Do workers need the help in physical aspect from tester during the test?		much						few
	Safety: How dangerous is the application of this method for the worker?		high						low
After measuring	**Result communication:** How understandable are the results achieved with this method?		low						high
	Correlation: How close are results from this method with results form other method when evaluating the same workplace?		low						high
	Career threat: Can results from this method be a health concern for workers without a previous ergonomic background?		high						low

Fig. 1. Sample of questionnaire (RULA/REBA) for evaluation

Results from ART Tools and RULA/REBA, show that observation methods almost comprehensively cover all the metrics with good validity, accessibility, practicability and cost-effective (Avg. = 3.7), except "Movement velocity", "Vibration" and "Sudden impact" (Avg. = 1.3). Direct measurement systems (OES, EG, AM and IMUs) are the most objective methods to measure (Avg. = 4.4 on "Numbers"). The kinetic validity (Avg. = 3.6 on "Movement repetition", "Body angles", "Velocity of movements", "Vibration" and "Sudden impacts") and the reliability (Avg. = 4.1 on "Test-retest" and "Inter-rater") are also important features of the four methods. Regarding to the order of "Operating difficulty" among direct measurements, EG is the easiest to handle (4.5), then IMUs is the next (3.5), whereas OES and AM are the hardest two

Table 1. Scale results of main WMSD assessment methods

Assessing metrics	Art tools	RULA/REBA	BA	OES	EG	AM	IMUs
Movement repetition	5	5	5	4.5	4.5	4	2.5
Body loads	4	5	5	1	3	1	1
Body angles	4	4	5	4	4	2.3	4
Velocity of movements	2	1	4	4	4	4	3.5
Duration of movements	4	4	3	4.5	4.5	3.3	2
Vibration	1	1	3	3	2.5	4.3	3.5
Sudden impacts	1	2	1	1.5	2	5	4
Muscles activity	3	3	5	2	3	2.3	2
Lifting	5	5	5	2.5	3	1.3	2.5
Independence	5	5	1	4	3	1	3
Numbers	4	4	5	4.5	4	4.7	4.5
Learning difficulty	5	4	1	1.5	3	2.7	3.5
Physical space	5	5	5	1	4.5	4.7	4.5
Equipment costs	5	5	2	1	3.5	3.7	4.5
Preparation time	4	4	1	1.5	3	3.3	3
Operating difficulty	5	5	1	2	4.5	2.3	3.5
Test time	4	4	3	4	4	3.5	4
Test-retest	4	4	5	5	3.5	3.7	4
Inter-rater	4	4	5	4.5	3.5	4.3	4
Manual error	3	3	3	4	3	3.7	3
Psychological collaboration	5	5	4	1.5	4	3.7	2.5
Physical collaboration	5	5	4	3	4.5	4.7	4
Safety	5	5	5	5	4	5	5
Result communication	5	5	5	5	4	4.3	5
Correlation	4	4	3	5	3.5	3.3	4
Career threat	2	2	4	5	4	4	5

Assessment of Repetitive Tasks (ART) Tools
Rapid Upper Limb Assessment/Rapid Entire Body Assessment (RULA/REBA)
Biomechanical Assessment (BA)
Optoelectronic Systems (OES)
Electro Goniometer (EG)
Accelerometry (AM)
Inertial Measurement Units (IMUs)

(2 and 2.3). Additionally, IMUs and EG approximately have the same level on “Manual error” with the other methods. From the interviews with the experts, it is said that although the precision of the captured repetitive movement depends on the capability of different products, the market trends still reveal that nowadays ergonomic experts tend to choose this type of methods to assist or replace expert observation.

However, they evaluate these measuring data (angles, movements) later based on biomechanical or ergonomic database meaning that objectivity would slightly reduce somehow. Then, commercial measurement products are generally with less learning difficulty and more user-friendly, although higher prices are high as well. Thus, based on the overall feedback of the questionnaires and the interviews, we discussed and summarized that the four of the most requested critical feature demands of WMSDs exposure assessment in automotive assembly line are: portability, compactness, precision and the ability to let the user move naturally. The reasons of we choosing IMUs will later be explained in the discussion section.

For the early prototype, only two fingers were tracked. Since mostly human daily hand actions, such as picking and gripping, are done by the thumb and the index finger, those two of the most essential fingers are adopted. According to the experts' responses, the IMUs was the one selected for the prototype. Seven IMUs were attached to each dorsal surfaces of the thumb and index finger phalanges with the help of rubber bands. In particular, the Bosch BNO055 absolute orientation sensor, a 9-DoF IMU with a thumbnail scale (20 × 27 × 4 mm), was selected. It integrates a 14-bit traxial accelerometer, a 16-bit traxial gyroscope, a full performance magnetometer and a 32-bit ARM Cortex-M0 based microcontroller. In addition, this IMU sensor includes a complete calibration algorithm. It is necessary to take approximately one minute to do some calibration movements that are introduced by the Bosch standard calibrating method. An Inter-Integrated Circuit (I2C) multiplexer (TCA9548A, Adafruit) was used to extend the number of IMU sensors and connect to a central controller (Arduino UNO, Arduino.cc). Figure 2 shows several representative gestures that were successfully captured and visualized by the IMUs.

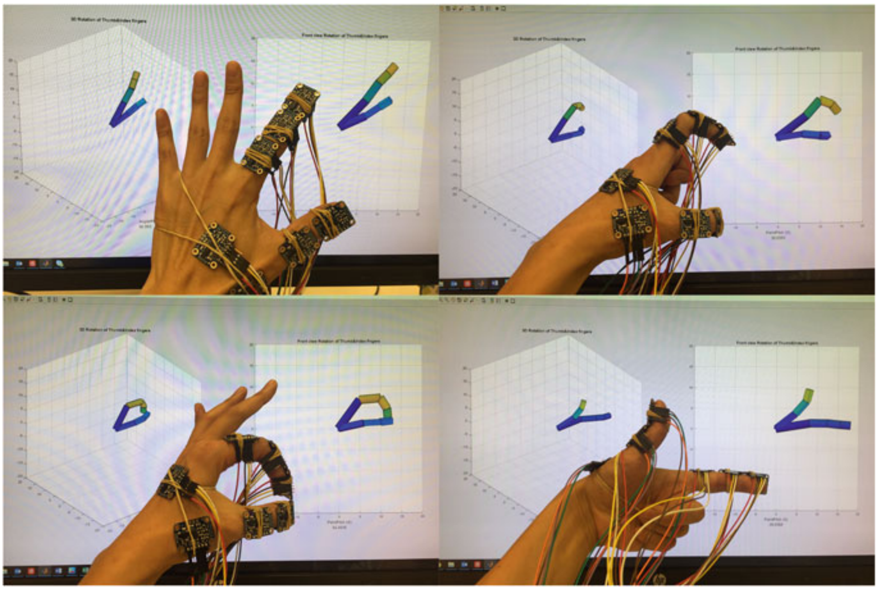

Fig. 2. Thumb & Index finger gesture capturing

The tracking process of the fingers began with the IMU sensors collecting orientation data in the form of unit quaternion vector. Quaternions were selected instead of Euler angles so as to avoid the gimbal lock issue and to optimize later calculation processes. Next, those data are packaged and sent to MATLAB for visualization. In MATLAB, several processes are executed to calculate the coordinates of each finger joint in the local and global reference system. The length of each phalanx is physically measured in advance.

1. Define seven points on the local rigid body coordinate system in quaternion form (w value equals to zero) along forward Y axis in a corresponding real phalanx length.
2. The conjugation of the quaternion is equal to its reciprocal here because of the unit quaternion form data. Hence, rotate each local points with sensor quaternion (representing the rotation) via the quaternion rotation formula sequentially to attain the triple cross product, where each part is multiplied first by its reciprocal quaternion then by the sensor quaternion, which, due to the cross product is not commutative. Thus the local rotated points are obtained correctly. Apart from the carpometacarpal (CMC) joints of each finger, which are located on the original point, the rest of the joints are translationally connected to the previous endpoint of its phalanx.
3. Given a compensation quaternion, representing an offset left-handed rotation angle, which is from magnetic north to the direction orthogonal to the terminal screen, around the upward Z axis given a unit vector, compensate those joints via the same quaternion rotation formula mentioned above. Hereto the local rotated joints are converted to the global coordinate system.
4. Calculate the finger angle between every two normalised segment vectors by the arccosine of the dot product.
5. Use a two-point type 3D cylinder function to model and plot each virtual segment by connecting each proximal joint with the previous distal joint.

To verify the feasibility of this prototype, a laboratory goniometry experiment was designed and conducted. After calibrating IMU sensors, three participants were asked to physically measure those knuckle angles with the help of a universal goniometer while a fourth volunteer wore the IMUs and performed some designed gestures with his hand. Simultaneously, the virtual angles were calculated and displayed in MATLAB. Eleven virtual and physical angles were measured and compared in real time (Fig. 3).

A set of finger goniometry methods in anatomy was adopted. Considering the accuracy and convenience of this experiment, as shown in Fig. 4, active radial abduction and ulnar adduction were measured mainly via the carpometacarpal (CMC) joint of the thumb (Angle No. 2, 3) but also the metacarpophalangeal (MCP) joint of the index finger (Angle No. 4, 5), while active palmar flexion and dorsal extension were measured via the distal interphalangeal (DIP) and the proximal interphalangeal (PIP) of the index finger (Angle No. 7, 8, 10, 11), also the MCP joint of the index finger and the CMC joint of the thumb (Angle No. 1, 6, 9). More specifically, each gestures were maintained by following the goniometry procedures: (1) for measuring each index finger stretch and thumb abduction/adduction, the examiner stabilises the volunteer's finger and maintains the palm in a vertical position along the white

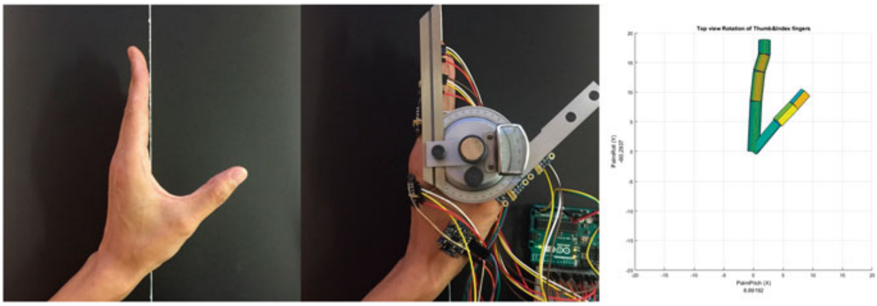

Fig. 3. Thumb abduction angle measuring by goniometer (top) and computer (bottom)

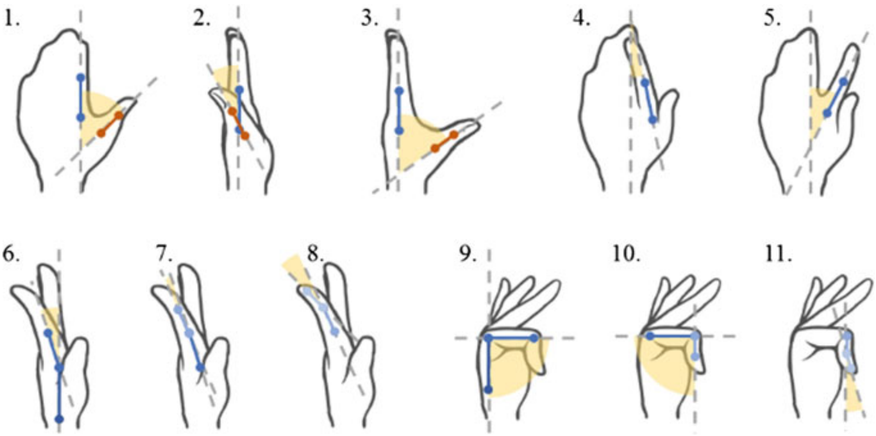

Fig. 4. Measuring gestures of each angle

reference line, then aligns each arm of the goniometer with the dorsal midline of the corresponding phalanx; (2) for measuring each thumb stretch and index finger abduction/adduction, the examiner places the volunteer's index finger along the white reference line, maintains the metacarpal in a neutral position and prevents radial deviation at the wrist, then aligns arms of goniometer with the dorsal midline of the corresponding phalanx [9].

3 Results

The three participants were researchers from an engineering university. Their age range was from 25 to 40 years old, and they were all male. All of them had received basic training with the goniometer. Table 2 represents the angle results of each joint: the thumb carpometacarpal (TCMC) joint; the thumb metacarpophalangeal (TMCP) joint; the index metacarpophalangeal (IMCP) joint; the index proximal interphalangeal (IPIP) and the index distal interphalangeal (IDIP). For each participant the virtual angle results

Table 2. Goniometry experiment results from three participants

		Participant A (°)			Participant B (°)			Participant C (°)		
		Real	Virtual	Dif.	Real	Virtual	Dif.	Real	Virtual	Dif.
1. TCMC	Extension	50.00	50.84	0.84	41.30	43.59	2.29	49.00	50.10	1.10
2. TCMC	Adduction	16.00	15.33	0.67	22.85	25.49	2.64	26.00	20.90	5.10
3. TCMC	Abduction	54.60	56.43	1.83	46.30	45.14	1.16	50.00	56.20	6.20
4. IMCP	Adduction	19.00	17.23	1.77	17.80	15.6	2.20	28.00	23.70	4.30
5. IMCP	Abduction	34.00	34.67	0.67	40.4	41.53	1.13	42.00	41.70	0.30
6. IMCP	Extension	16.00	15.46	0.54	14.3	21.10	6.80	15.00	12.40	2.60
7. IPIP	Extension	6.00	5.94	0.06	6.00	15.19	9.19	3.00	6.50	3.50
8. IDIP	Extension	14.50	14.97	0.47	20.30	18.39	1.91	14.00	15.60	1.60
9. IMCP	Flexion	91.00	91.46	0.46	84.15	80.9	3.25	86.00	81.00	5.00
10. IPIP	Flexion	88.20	79.74	8.46	84.15	82.9	1.25	88.00	89.00	1.00
11. IDIP	Flexion	3.70	6.48	2.78	1.00	4.47	3.47	9.00	5.00	4.00

are correspondingly compared with the manual measuring results. Average differences between the virtual angles and the manual measured angles from the three participants were 1.68°, 3.20° and 3.15°.

To confirm the significance of the results with respect to the angles measured and the participants, an analysis of variance (ANOVA) was held. “Participant” and “Joint” were considered as independent variables, and angle error value as the response variable. The results from the analysis indicated that, “Participant” is not statistically significant (P-value of 0.291). “Joint” was not also statistically significant (P-value of 0.822). These results indicated that neither the “Participant” nor the “Joint” they are measuring are key parameters for the angle error obtained.

4 Discussion

According to the findings of the questionnaire assessment, we point out that the evaluations are relative within their individual knowledge. For example, in terms of the expert observation methods, the metrics of numbers, Test-reTest, Inter-rater, as well as the most of the validity factors have incomprehensible high values. This is because subjects are divided into the expert observation group and the direct measurement group, and they answered without getting a bare idea about the capabilities of the other methods from the other groups. The actual relationship between these two groups has been understood from the interview with experts who have the experience across technologies or methods from both groups. Furthermore, measurement validity, learning difficulty, price and preparation time, those metrics may depend on different tasks, and different features from immensely wide product choices in the current market. Similarly, in the OES for instance, the effective coverage and resolution involve the quantity of camera used, which is related to the demands on real site. We have tried to generalize each metrics as much as possible for a more objective conclusion.

With respect to the selection of the technology, combined with the actual demands of automotive assembly plant workplace, we believe that IMU is the most advisable technique among the present measurements. On the one hand, self-report and expert observation do not meet the requirement of positive observing, objective and accurate results, productivity guarantee, even real time monitoring. As such, selection was focused on direct measurements. On the other hand, noticing that nearly all the facilities in the assembly line are made of metal, OES systems can suffer from "ghost marker" to obstruct the recognition of the camera. Moreover, poor illumination, occlusion, expertise requirement, large operating space, high costs on money and time determine that OES are hardly used on real work site. Likewise, the EG has the problem of size and weight, which will hamper the worker's activities, especially in the intensive and complex assembly environment. Regarding to AM, experts claimed that there is not any single AM measurement currently in the market, because of its critical drift error and poor independence. Additionally, productivity and cost-effectiveness are commonly undervalued in existing ergonomic studies [10]. Throughout the analysis of the State of the Art about direct measurement devices, the IMUs system has become increasingly acceptable, and so has the potential for physical exposure detection of precise movements in the hand region. Meanwhile, the IMUs have the advantage of being applicable to both indoor and outdoor settings [10]. Summing everything up, it can be said that there is not a perfect measurement system, but currently IMUs is the most suitable.

Several points also deserve discussion regarding the validation process with volunteers. Due to the different motives of measuring angle, this paper does not strictly follow the standard joints measurement flow. With the aim of better verification, some specific gestures, such as flexion close to 90° at IMCP and IPIP joints, were required instead of extreme flexion because the angle has to do with the elasticity of the tendon and joint when close to extreme limits, which may cause the instability of actual angle value. It is more important to verify the precision of this device rather than to obtain each finger range of motion. However, there were still some extreme gestures remaining for covering as many situations as possible.

Nonetheless, the observers' errors when using the universal goniometer is the limitation for the reference group. Additional experiment is worth be carried out to make a better comparison with the virtual angles obtained from our prototype, against real angles measured by other advanced direct measurement systems such as OES or flexible EG. Taking into account the accuracy of other prevailing measurements, the Vicon mocap system provided mean accuracy of 89.33% with root mean square error of 5.19° [11], the CyberGlove specification claimed sensor resolution is under 1° with repeatability of ± 3° [12]. Based on the above, we are able to indicate that the value of virtual angles is very close to the real angles, and the precision is at the same level of the mainstream measurement devices and products.

It is worth mentioning that, our whole hardware system so far, including seven sensors for two fingers, costs around 225 EUR in total, purchased from Arduino component supplier. Considering the price of other direct measurement systems, the commercial inertial sensor product such as Xsens MVN, is approximately 12,000 EUR; referring to the OES, the price range is approximately from 5000 EUR of Kinect to

55,000 EUR of Vicon. It was interesting to get a device that would relatively keep in the low-cost level in the market.

For assessing the ergonomic risk and preventing MSDs exposures, capturing motion angle data is only the pre-step for the entire progress. The next technical stage should be to analyse those movements together with force data by using a mathematical model within a software and the help of an expert. To achieve this, various biomechanical analysis software applications are available, such as 3D Static Strength Prediction Program™ (3DSSPP) [13]. Likewise, based on its adaptability, the use of this system can also be extended to assembly lines in the other industrial fields where the worker's safety is a concern.

5 Conclusion

This paper proposes a hand region rotation capture device designed for ergonomic assessment of workers on automotive assembly lines. Through questionnaires filled out by experts, four primary features of portability, compactness, precision and the ability to let the user move naturally for the design of a wearable ergonomics evaluation device were identified. The IMU technique was considered as the cheapest and the most reliable hardware among the abundant variety of direct measurement techniques, thus it was selected for building up an initial hand motion capture prototype. After a series of validation tests with volunteers, the average differences values demonstrate that the virtual wearable angles are very close to the one measured by volunteers. This early research will serve as a base for subsequent studies on the design of user-centred wearable devices for ergonomics evaluation that will focus on reducing deviation factors, integrating conductive 3D printing, improving user experience, and designing the entire compact glove.

References

1. Musculoskeletal disorders and the workplace (2001) Low back and upper extremities—executive summary. Theor Issues Ergon Sci. 2:142–152. https://doi.org/10.1080/14639220110102035
2. Buckley P (2016) Work-related musculoskeletal disorder statistics. Great Britain
3. Bevan S (2015) Economic impact of musculoskeletal disorders (MSDs) on work in Europe. Best Pract Res Clin Rheumatol 29:356–373. https://doi.org/10.1016/j.berh.2015.08.002
4. Costa BR, Vieira ER, da Costa BR, Vieira ER (2010) Risk factors for work-related musculoskeletal disorders: a systematic review of recent longitudinal studies. Am J Ind Med 53:285–323
5. Wang Y, Neff M (2013) Data-driven glove calibration for hand motion capture. In: Proceedings 12th ACM SIGGRAPH/Eurographics Symposium *on* Computer Animation—SCA '13, 15. https://doi.org/10.1145/2485895.2485901
6. Sama M, Pacella V, Farella E, Benini L, Riccó B (2006) 3dID: a low-power, low-cost hand motion capture device. In: Proceedings-Design, Automation Test Europe DATE, 2. https://doi.org/10.1109/date.2004.1269064

7. Kitano K, Member S, Ito A, Tsujiuchi N (2016) Estimation of joint center and measurement of finger motion by inertial sensors. 5668–5671
8. Landsbergis PA, Cahill J, Schnall P (1999) The impact of lean production and related new systems of work organization on worker health. J Occup Health Psychol 4:108–130. https://doi.org/10.1037/1076-8998.4.2.108
9. Cynthia C, Norkin PT, Joyce E, White PT (2009) Measurement of joint motion a guide to goniometry 4th edn. ISBN 978-0803620667
10. Wang D, Dai F, Ning X (2015) Risk Assessment of work-related musculoskeletal disorders in construction: state-of-the-art review. J Constr Eng Manag 141:4015008. https://doi.org/10.1061/(ASCE)CO.1943-7862.0000979
11. Connolly J, Condell J, O'Flynn B, Sanchez JT, Gardiner P (2017) IMU sensor-based electronic goniometric glove (iSEG-Glove) for clinical finger movement analysis. IEEE Sens J 18:1273–1281. https://doi.org/10.1109/JSEN.2017.2776262
12. CyberGloveSystems CyberGlove Systems. Available online: http://www.cyberglovesystems.com/sites/default/files/CyberGloveIII_MoCap_Glove_System_Brochure.pdf
13. The University of Michigan Center for Ergonomics 3D Static Strength Prediction Program. J Occup Environ Med 38:101. https://doi.org/10.1097/00043764-199601000-00028

Fingers' Biomechanical Analysis with Smartphone User Tests

P. Mitrouchev[1(✉)], J. Chen[2], and F. Quaine[3]

[1] Université Grenoble Alpes, CNRS, Grenoble INP, G-SCOP, Grenoble 38000, France
Peter.Mitrouchev@grenoble-inp.fr
[2] CHU Amiens Picardie Site Sud, Salouël 80480, France
[3] Université Grenoble Alpes, CNRS, Grenoble INP, GIPSA-Lab, Grenoble 38000, France

Abstract. With the increase in life expectancy, some new information and communication technologies become poorly adapted to elderly, especially with devices of small size as smartphones for example. In order to predict and improve the accessibility of people with limited forearm motor capacity the paper deals with the study of interaction modalities based on EMG (electromyography) for human-computer interaction, for a more tolerant interaction in the face of vagueness of the gesture. For this purpose series of tests for finger activity estimation were performed according to an appropriated bio-medical protocol (two cases: with and without a strap) while manipulating a smartphone. The EMG signals of the three most involved muscles of the thumb were recorded and analyzed. The results shown that the finger's EMG signals for these muscles are interdependent. It was found that the relationships between positions of touch, for five orders dots disposed on the smart phone screen, and applied force were no linear. The quantitative relationships between force and fingers' displacements have been extracted by using linear regression analysis. Based on the comparison of force-displacement relationships, it is observed that the thumb induces less activating force than the other fingers. It was also found that the relief of the finger muscles involved in the gripping of the smartphone allows to reduce the muscular activity of the thumb and thus to delay the appearance of musculoskeletal disorders.

Keywords: Product design · Human factors · Ergonomics · Muscle–computer interface · Biomechanics · Accessibility · Electromyography

1 Introduction

These last decades, new information and communication technologies have multiplied, making the world more and more "*connected*". Access to information has been greatly facilitated by the emergence of the Internet, and its enabling tools. Smartphones, for instance, are ones of the most effective ways to navigate in this virtual world: their small size and intuitive interface have made them familiar, indispensable and ubiquitous devices. The latter offer a variety of possibilities through an increasingly large touch screen. If the interaction with the phones of yesterday was done mainly by means

F. Cavas-Martínez et al. (Eds.): *Advances on Mechanics, Design Engineering and Manufacturing II*, LNME, pp. 52–61, 2019.
https://doi.org/10.1007/978-3-030-12346-8_6

of a keyboard located under the screen, in today designed phones the whole surfaces of the devices are used thus increasing their functionalities.

However, people with limited hand mobility can experience fatigue-related problems when using such devices [1]. More generally, the long-term effects of everyday use of a smartphone (including young people) are still unknown, but it is reasonable to suppose that illnesses may appear, such as tendinitis [2].

These masse designed devices are mainly based on interaction with gesture or touch: which requires specific gestures especially for elderly [3]. Thus, scientific and technological advances have to be proposed to take this reality into account. To this end a question arises, namely: *How to improve the accessibility for this class of devices*?

Recently new ergonomic solutions were available on the market. The designed ergonomic keyboard "*Word Flow*" from Microsoft was an example. Supposed to do writing easier and faster, it was abandoned last year. The smartphones with classical "*QWERTY*" and "*AZERTY*" keyboards seem not to be obsolete anymore and are still predominant on the market today. For this reason our study concerns the manipulation of these widely used classical devices.

A study of pointing performance of elderly users on smartphones was presented in [1]. Pointing performance was measured by the time taken to complete the *pointing task* and the number of errors during a task. For this purpose authors conducted two experiments. For the first one (three target sizes and two target spacings), they analyzed whether touch screen pointing performance depends on the location of the target. For the second experiment (three types of feedback; auditory, tactile, and audiotactile) the results show that: (i) pointing performance of elderly was significantly influenced by size, spacing, and location of the target, and (ii) the performance was higher in audiotactile feedback condition.

Huawei et al. [4] examined the performance of two scrolling techniques (*flick* and *ring*) for document navigation in touch-based mobile phones, using three input methods (*index finger, pen*, and *thumb*), with specific consideration given to two postures: *sitting* and *walking*. The authors find out that: (i) in both sitting and walking postures, for the three input methods, *flick* resulted in shorter movement time and fewer crossings than *ring*, suggesting *flick* is superior to *ring* for document navigation; (ii) for sitting posture, regarding pen and thumb input, *ring* led to shorter movement time than *flick* for large target distances.

Recently, in [5] authors related age and muscle mobilization during a prolonged reaction-time (*RT*) test. For this purpose they studied the evolution of reaction time with relief of the muscles involved in the gripping of a smartphone by young and older subjects.

Other studies dealt with improving the accessibility of tactile interaction for older users by lowering accuracy requirements to support drag-and-drop interaction [3].

Some studies deal with electromyography (EMG) signal processing, and the flourishing use of smartphones. It was proven that the peak value of EMG signals after root mean square (RMS) processing is an index of fatigue [6] when subjects are performing the task at the same level of force while manipulating daily used devices as smartphones.

In this optic, the speed of motions of the thumb and the intensity of segmental muscular EMG activity of the *abductor pollicis longus* (*APL*) muscle of the hand during an upward writing test were investigated in [7].

The literature review and analysis of the studies, a part of which were presented here above, partially improved accessibility of smartphones touch screen. However, they do not take into account of the vagueness of the gesture thus limiting the performances of the proposed solutions.

In this context, our aims is to show the interdependencies amongst the work done by the thumb and the others fingers while gripping the phone, via the experiments to measure the muscular activity of the thumb.

The rest of the paper is arranged as follows: Sect. 2 presents the materials and the method. The results are presented and discussed in Sect. 3. Finally conclusions and future work are presented in Sect. 4.

2 Materials and Method

The movements of a human limb are possible thanks to a complex network of muscles and tendons, and interaction amongst them. It would be necessary to study the functionality of a lot of muscles to carry out a given complete study. However, studying all the hand muscles while manipulating a smartphone seems to be a very complicated task. Thus, for the sake of accessibility, we studied the behavior of three out of eight more loaded and involved muscles of the hand namely: *adductor pollicis* (*AP*), *abductor pollicis brevis* (APB) and *interossei dorsal muscles* (*DIM*).

2.1 Participants

Seven unpaid, voluntary and healthy subjects (all males, one of them left-handed), aged from 20 to 62 participated in the experiments. All subjects have declared not having: (i) corrected visual impairment; (ii) impairments of haptic sensitivity (sensitivity of touch, numbness of the fingers and loss of finger location perception); (iii) diseases or symptoms which induce hand movement disorders. All subjects declared also being naive to the purpose of the experiment. The study was approved by the Ethics Committees of University Grenoble Alpes (UGA) and all participants gave written informed consent. After a briefing about the experiment, participants filled out a background survey.

2.2 Methodology

Note that due to the relatively low size of the samples this is a pre-study where only healthy subjects have participated in order to evaluate the possibility to use EMG from finger muscles thus allowing to evaluate muscle involvement during smartphone manipulation.

In a first step this study was conducted to evaluate the possibility and the reliability of EMG data to be sensitive to smartphone manipulations. Further studies including subjects, with pathologies related to arthritis and fibromyalgia, are planned in order to better evaluate the results in the use of strapped smartphone.

The methodology consists in: (i) performing experiments to measure the muscular activity of the thumb during two tests for each subject while manipulating a smartphone in both ergonomics cases: with and without strap used; (ii) comparing the data retrieved on each of the tests in order to evaluate the activities of the three more involved muscles of the thumb in these both cases.

During the tests, subjects had to use the thumbs of their predominant hands when touching the smartphone screen. Figure 1, here below, shows partially the test bench for the experiments carried out. Hidden *DIM* muscle electrodes are located behind the hand.

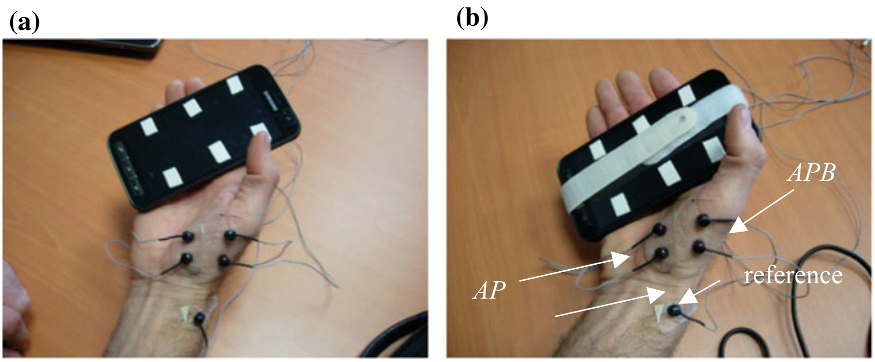

Fig. 1. Positions of the sensors for target dots on the Smartphone: **a** without a strap, **b** with a strap

"The EGM signals of *adductor pollicis* (AP), *abductor pollicis brevis* (APB) and *dorsal interossei muscles* (DIM) were recorded with BIOPAC EL503 Vinyl 1-3/8" electrodes, according to the SENIAM (surface EMG for non-invasive assessment of muscles recommendations) [8] and analyzed with four channel EMG-BIOPAC MP150 system, the fourth channel being the reference one. The smartphone used in the performed experiences was an iPhone 4S. On the touch screen (3.5 in., 88.89 mm) six square visual indicators were spaced from their center regularly (Fig. 1a) to crisscross the entire screen in five different trajectories (layout types) as shown in Fig. 2.

2.3 Experimental Protocol

First, a familiarization session consisting of five trials was dedicated for each participant. Next, after *5* min of recovery, the participants performed the five-order Dot disposals tests. The latter include different layouts such as: semi closed loop (Fig. 2a and b); *S* similar (Fig. 2c); and two opposite cross paths (Fig. 2d and e) that involve sudden movements of the thumb while users perform complex layouts in order to difficult the access to their password, for example.

During the tests, subjects (in sitting position) were asked to only use their predominant thumb finger when touching (pointing) the screen. The first phalange of the

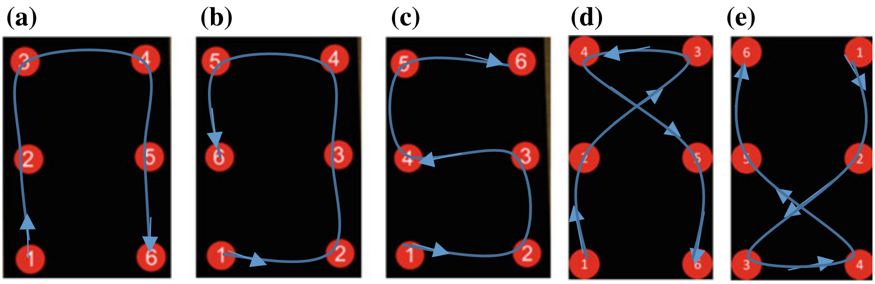

Fig. 2. Five-order Dot disposals (layouts) on the Smart phone screen used in the experiments

little finger was placed on the table and remained in this position throughout the experience.

The procedure of the bio-medical protocol consists in performing two tests of 5 min each.

During the first one, subject held the smartphone in his agile hand, resting elbow and wrist on a fixed support (table). While squeezing the smartphone with his supporting hand, the subject had to touch the six visual markers with the thumb in a specific order (Fig. 2) for 300 s, changing the orders every 60 s.

During the second test, the subjects have to repeat the same movement as in test one. However, a strap passing in the back of the hand and in front of the smartphone screen was attached, as shown in Fig. 1b, so that the muscles involved in the gripping by the fingers were completely relieved. In other words, in this configuration the subject does not need to actively hold the phone while in the first case it must tighten it.

In order to maintain the same speed of action for all subjects, for both tests, a metronome set at 60 bpm (beats per minute) gave the tempo to touch the indicators with a frequency of 1 Hz.

In addition to objective data collected during the experiments, data from a subjective evaluation questionnaire based on ISO 9241 was collected before and after the experiments as well.

2.4 Data Processing and Analysis

Finger involvement during the test is estimated by the treatment of EMG signals emitted by the three more involved muscles of the thumb, while manipulating the Smartphone, in the two cases: without and with a strap. In Fig. 3 the EMG row signals of muscle *AP* (channel 1) for subject *Michel* are presented. However, these signals require treatments in order to be analyzed and compared after then.

For this purpose, first, all raw EMGs signals were simultaneously sampled at 1250 Hz and filtered with Butterworth 2nd order, band-pass 10–5000 Hz and notch-filtered as in [9] using MATLAB software in order to erase the various parasites. Note, that the low frequencies are trained parasites due to external factors such as: cable movement, blood passing in the hand, while the high frequencies represent often the parasitic movements of the hand. Then EMGs signals are RMS (root mean square) processed over a short 2 s period and the maximum RMS values obtained between the

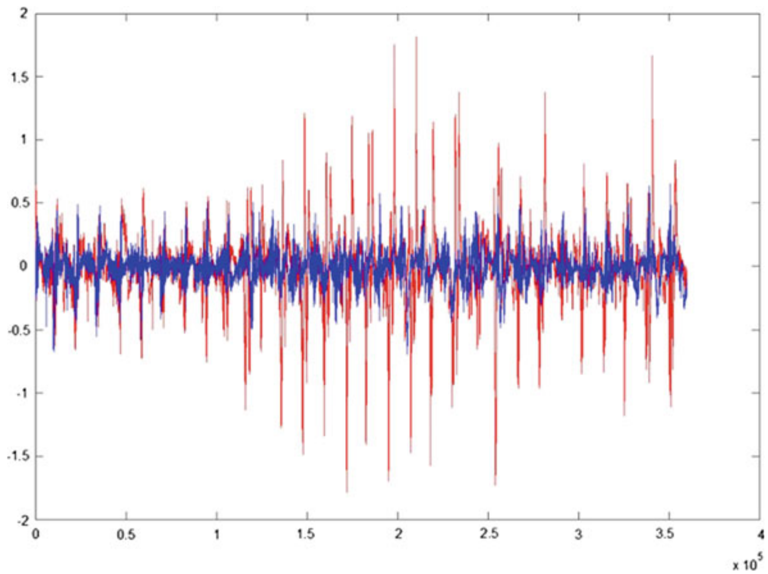

Fig. 3. Raw EGM signals (*AP* muscle) for subject *Michel* (red without a strap, blue with a strap)

different tests are compared. Consequently the absolute values of these signals are taken. Finally these modified signals of the three muscles for each subject are compared in order to find the more leaded one, while manipulating the Smartphone, with and without a strap. Here, it is assumed that the subject is not tired and therefore the EMG/force relationship remains constant.

2.5 Statistical Analysis

First, Shapiro-Wilk method has been applied to verify the normality of the EMG data. Then, a *two-way* Analyses of variance (ANOVA) were performed to test changes on RMS-EMG (i.e. dependent variable) while manipulating the smartphone in both cases: with and without a strap separately for the three muscles. Significance was set a priori $p < 0.001$. All the statistical analyses were performed under the MATLAB Software. The standard error of mean (SEM) of finger's pressing forces of all subjects were calculated as well.

3 Results and Discussion

As previously said, for each subject, after filtering, the RMS values of the EMGs data were compared and averaged (Matlab Software) to get the overall value of the activity by averaging the differences of the three channels in both cases: with and without a strap. Then the average differences for each muscle and for all three muscles on seven subjects were calculated in both cases (without a strap 1 and with a strap 2). The results are presented in Table 1.

Table 1. Average RMS signals values (*Voltage*) for the three muscles of each of the seven subjects (without a strap 1, with a strap 2)

Subject	Muscle AP	Muscle APB	Muscle DIM
Corcel 1	347,177,551	758,794,676	253,623,998
Corcel 2	331,416,386	808,006,639	−594,367,041
Diff in %	−453,979,949	648,554,414	−594,367,041
Average	−191,636,531		
Lionel 1	787,464,349	710,201,037	412,083,936
Lionel 2	456,768,518	451,699,047	139,810,742
Diff in %	−419,950,225	−363,984,247	−660,722,659
Average	−481,552,377		
Luc 1	625,185,035	668,975,272	297,198,872
Luc 2	537,178,183	516,745,813	137,723,244
Diff in %	−140,769,288	−227,556,182	536,595,671
Average	−30,164038		
Jean 1	100,463,538	14,571,706	20,908,563
Jean 2	6,36098922	10,604,789	189,201,241
Diff in %	−366,836,048	−272,237,924	−95,101,655
Average	−244,725,083		
Michel 1	589,589,763	864,893,855	24,830,159
Michel 2	2,66544547	4,15390582	210,543,955
Diff in %	−547,915,256	−519,720,738	−152,063,604
Average	−406,566,533		
Mathieu 1	395,967,805	179,435,117	532,956,626
Mathieu 2	288,711,538	169,567,801	26,993,981
Diff in %	−270,871,185	−54,991,018	−493,505,107
Average	−263,122,439		
Issam 1	402,060,217	818,008,688	335,028,364
Issam 2	402,512,539	804,445,975	324,546,592
Diff in %	011,250,093	−165,801,581	−312,862,215
Average	−155,804,567		
Average/7 subjects			
Total	**−272,117,685**		
Muscle AP	−255,802,144		
Muscle APB	−198,602,118		
Muscle DIM	−36623,457		

As can be seen in Fig. 3, muscle activities are less important while manipulating the strapped phone. This is confirmed also by the values reported in Table 1. It is seen, that the overall muscle activity of the thumb decreased for all the subjects (over 27%). For all of them, the average activity decreased: for *AP* muscle (over 25%), for APB muscle (over 19%) and even significantly for *DIM* muscle (over 36%). However, it seems that this trend is not followed by some muscles because the *APB* activity of *Subject Corcel* and *AP* activity of Subject *Issam* increased. This may be due to a wrong electrode location for these subjects or a specific muscle involvement associated to the great variability in muscle involvement across subjects.

However, it can be assumed that the strap helps the subject significantly if properly used because it keeps the phone without the need for great muscle intervention.

In a second time the muscle activities in the Points 1, 2 … 6 for each orders Dots disposals, (called *Trajectory* 1, *Trajectory* 2, *Trajectory* 3, *Trajectory* 4 and *Trajectory* 5) were compared in order to estimate the difficulty to reach a specific zone of the touch screen. For this purpose, after filtering the row EMG signals with a *BP filter* (20–500 Hz) the RMS values over small periods (2 s) are calculated in order to visualize the contractions of the muscles in these points (Fig. 4a). Finally the RMS value are filtered to smooth the curve (Fig. 4b) where each peak corresponds to a movement of the thumb in the six points for each trajectory for a given muscle.

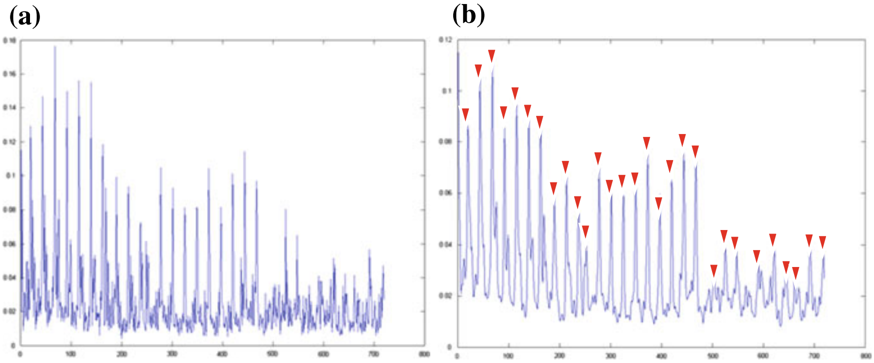

Fig. 4. Subject Corcel *DIM* muscle activity: **a** EMG Rms, **b** filtered EMG Rms

For the right handed subjects the major peaks correspond while touching the bottom left side of the smartphone screen corresponding to the surrounding zone of *Point1*of the four Trajectories (Fig. 2 a, b, c, d) and *Point* 3 of Fig. 2e. While, for the left handed subject the peaks correspond while touching the bottom right side of the smartphone screen corresponding to the surrounding zone of *Point* 6 for *Trajectory* 1 (Fig. 2a), *Point* 2 for *Trajectories* 2 and 3 (Fig. 2b, et Fig. 2c respectively), *Point* 6 for *Trajectory* 4 (Fig. 2d) and *Point* 4 for *Trajectory* 5 (Fig. 2e).

It is also observed, for both right and left hand subjects, that for cross path *Trajectory* 4 (Fig. 2d) the most difficult zone to reach is situated on the top of the screen *Points* 2, 3, 4, 5 (Fig. 2d). On the contrary, the easiest zone to reach is situated on the bottom of the screen for cross path *Trajectory* 5, namely *Points* 2, 3, 4, 5 (Fig. 2e). Thus, the effort to reach these points is more important, which requires most muscle activity.

Finally, in overall *Trajectories* 1, 2, 4 (Fig. 2a, b, d) require more muscular effort. On the contrary *Trajectory* 3 (Fig. 2c) *and Trajectory* 5 (Fig. 2e) requires less effort.

These findings suggest that it can be interesting to investigate on these displacements to create the smartphone's interface most ergonomic possibly.

4 Conclusions

The aim of this study was to investigate the behavior of muscle thumb EMG during manipulation of a Smartphone in two cases: with and without a strap. Through experiments (EMG signal processing) which involve the three more loaded muscles of the thumb finger, subjects' pressing involvement have been recorded and analyzed while touching the smartphone screen for five different trajectories.

The results shown that the finger's EMG signals for the three most involved muscles are interdependent thus increasing the difficulties for a precise finger force analysis.

The experiments shown that the relationships between positions of touch, for these five-order dots disposed on the smart phone screen (layout, trajectories), and EMG level were no linear. They also shown that the EMG decreases significantly while manipulating strapped phone.

The results obtained on the decrease of muscular activity of the thumb with strapped phone are interesting and encouraging. They can contribute to the design of new generation mobile touch screen devices and application button layout. As designers of current smartphones try to include a lot of information and input control in the same display, the latter often include too much information. As a result elderly users with osteoarthritis of the thumb as rhizarthrosis (or trapeziometacarpal) experience pain during and after using such devices.

The experiments suggest that the study have to be deepened in order to determine strap's true utility and if so to optimize its ergonomics. Thus, it is expected that through further study about people interaction with electronic devices, they will fill more comfortable while using these new technologies.

At this stage of the study it may be stated that the use of the strap seems to bring significant help to the thumb for smartphone use by people with limited fingers' mobilities.

Acknowledgments. This project has received funding from the European Union's Horizon 2020 research and innovation program under the Marie Skłodowska-Curie grant agreement No 777720, and has been partially supported by the LabEx PERSYVAL-Lab (ANR-11-LABX-0025-01) (http://www.persyval-lab.org/index.html) funded by the French program "Investissement d' avenir".

Authors would like to thank Mr. Maxime Hanquier and Mr. Lucas Montariol for the realization of the experimental set up and their involvement in the experiments.

References

1. Hwangbo H, Yoon SH. Jin BS, Han YS (2013) A Study of pointing performance of elderly users on smartphones. Int J Hum–Compu Inte 29(9):604–618
2. Bautmans I, Vantieghem S, Gorus E, Grazzini Y-R, Fierens Y, Pool-Goudzwaard A, Mets T (2011) Age-related differences in pre-movement antagonist muscle co-activation and reaction-time performance. Exp Gerontol 46:637–642
3. Genaro Motti L, Vigouroux N, Gorce F (2015) Improving accessibility of tactile interaction for older users: lowering accuracy requirements to support drag-and-drop interaction. Procedia Comput Sci Elsevier 67:366–375
4. Tu H, Ren X, Tian F, Wang F (2014) Evaluation of flick and ring scrolling on touch-based smartphones. Int J Hum-Comput Inter 30(8):643–653
5. Vantieghem S, Gorus E, Lauwers E, Fierens Y, Pool-Goudzwaard A, Bautmans I (2015) Age-related differences in muscle recruitment and reaction-time performance. Exp Gerontol 70 (October):125–130
6. Boyasn S, Guenel, A, Naik Ganesh R (2014) Endurance time prediction using electromyography. In: Applications, challenges, and advancements. Electromyography signal processing: Bd. v. 219–233. IGI Global. ISBN 978-1-4666-6090-8
7. Simard TG, Cerqueira EP (1992) Fine motor control: An EMG study of ability of the thumb in healthy hands of adult subjects. J Electromyograp Kinesiol 2(1):42–52
8. Hermens HJ, Freriks B, Disselhorst-Klug C, Rau G (2000) Development of recommendations for SEMG sensors and sensor placement procedures. J Electromyograp Kinesiol 10(5): 361–374
9. Stins JF, Michielsen ME, Roerdink M, Beek PJ (2009) Sway regularity reflects attentional involvement in postural control: effects of expertise, vision and cognition. Gait Posture 30 (1):106–109

An Impact Testing Machine Development for Helmets According to Several Standards

D. Ranz(✉), R. Miralbes, and D. Sánchez

Departamento de Ingeniería de Diseño y Fabricación, EINA, Universidad de Zaragoza, C/María de Luna s/n, 50018 Saragossa, Spain
dranz@unizar.es

Abstract. The present work has as objective the design and whole mechanical development of an absorption and penetration impact machine. The innovation of this work lies behind the integration of the indispensable characteristics in a single equipment to meet the greatest number of possible tests for different types of helmets; which have to be tested under the greatest possible number of standards. At the beginning of the project, an in-depth study is made of the different types of helmets and their main characteristics, as well as, the tests that are carried out for their certification according to specific standards, contemplating more than 30 international standards. Protective helmets and their corresponding standards are studied in areas as diverse as sporting use, industry, firefighters, motorbikes and for the protection of impacts on children. The search for design smart solutions meeting most amount of studied standards was also addressed for additional requirements, such as a very tight budget and other related with risk prevention. These proposed solutions have been assessed by experimental and/or numerical methods until meet a final solution according to the multidisciplinary requirements. Finally, a testing machine that meets all the requirements for this type of equipment was developed, meeting with a low manufacturing cost and satisfying the extensive standards that regulate the absorption and penetration impact tests of different types of helmets.

Keywords: Impact testing · Helmets · CAE · Multicriteria design

1 Introduction

There are many regulations that, depending on the sector and the geographical area, regulate the tests to be carried out for the certification of protective helmets. This project will focus on the two types of mechanical tests that are usually performed on this type of product: the impact absorption test and the penetration resistance test. The project aims to collect most of the common requirements that these standards require the machines that carry out these certification tests and develop an economic equipment that comply with all of them together.

At the beginning of the project, an in-depth study is made of the different types of helmets and their main characteristics, as well as, the tests that are carried out for their certification according to specific standards, contemplating more than 40 international standards. Protective helmets [1–3] and their corresponding standards [4–35] are

F. Cavas-Martínez et al. (Eds.): *Advances on Mechanics, Design Engineering and Manufacturing II*, LNME, pp. 62–73, 2019.
https://doi.org/10.1007/978-3-030-12346-8_7

studied in areas as diverse as sporting use [9–17, 25–31, 36], industry [19, 20], firefighters [21–23], motorbikes [24, 32, 33, 37, 38] and for the protection of impacts on children [18].

Regarding the composition of the helmets [39, 40], in most typologies have an internal liner of expanded polystyrene (EPS), while the outer material varies, generally using plastics such as acrylonitrile butadiene styrene (ABS) or polycarbonate, and other helmets More demanding, such as firefighting, industrial, or high-end, are manufactured with high density polyethylene (HDPE) or new composite materials. As for the weight of the helmets, it can be seen that sports helmets have a low weight compared to the rest, while other helmets such as motorcycle helmets have higher weights, due to its greater volume of protection [41].

It is the regulations themselves that specify the type of test to be carried out and, in most cases, many of the characteristics and requirements involved during the development of the testing machine. Mainly the UNE standards [4–24], coming from the European regulatory framework and the American Snell regulation [25–33], which is a world benchmark in safety tests on helmets have been analyzed.

The search for design smart solutions meeting most amount of studied standards was also addressed for additional requirements, such as a very tight budget and other related with risk prevention. These proposed solutions have been assessed until meet a final solution according to the multidisciplinary requirements. Throughout the development process is carried out the manufacture of a functional prototype of one of the most decisive components to check and warranty its successful performance, the guidance system. This testing stage was essential to determine if the system is mechanically well resolved and if it complies with the 5% speed tolerance established in the regulations. To do this task, a digital camera has been used to gather up to 240 images per second.

When a final design solution is reached, the representation of these solutions is made by 3D models, making the complete modelling of the machine with the commercial software SolidWorks [42]. In addition, it analyses its optimized structural and impact performance using its finite element simulation module (FEM). Thanks to the Finite Element Analysis, an iterative design is carried out, consequently the different critical components are optimized to improve the results obtained until a reliable and safer design is achieved.

2 Development Methodology

A deep market research was done in order to know the different categories of protective helmets and their associated impact and penetration testing standards. Afterwards, an exhaustive analysis of the different features of each standard was carried out to set up the common requirements, which will be used in the concept design and development stages. Finally, virtual and real prototyping methodologies to check out the compliance with the requirements.

2.1 Helmets Typologies and Standards Analysis

When the protective helmet market is analysed, four different typologies of helmets can be found: sport, industry, firefighter and motorbike helmets (Figs. 1, 2 and 3). Besides, the regulations include another type of protection helmet that has no place in any of the groups mentioned above, and is the standard UNE-EN 1080: Helmets of protection against impacts for children [18].

Fig. 1. Sportive helmets: Equestrian, airborne, cycling and canoeing

Fig. 2. Industry, firefighter and rescue helmets

Fig. 3. Motorbike helmets: Jet, off-road, modular and integral

For each described helmet typology, there is a different standard, with its own requirements depending on the type of impact they may be subject during their use in the environment which they belong. However, European reference standards for each type of helmet normally address to two standards, with its particular requirements, that are those that are intended to be covered with this testing machine: UNE-EN 13087-2:2012 (Protective helmets. Test methods. Part 2: Shock absorption) [5] and UNE-EN 13087-3:2000 (Protective helmets. Test methods. Part 3: Resistance to penetration) [6].

Regarding the test of helmets according to the Snell Foundation, it is necessary to emphasize the uniformity that there is in terms of the tests that are carried out for their respective regulations. The methodology used in these trials is always the same, very similar to the European regulations, and only two factors vary, the drop height and the anvils or punch that are used. While in European regulations there are only two anvils, the plane and the kerbstone, in the Snell regulations six types can be found: Hemispherical, edge, horseshoe, roll bar, plane and the kerbstone. Most of the anvils are restricted by the minimum measures, so most of this tooling can be redesigned to comply with European regulations too. Also note that there is only one conical punch, in this case, unlike UNE standards where there are several types of punches. In addition, in the European regulations we find a test block, consisting of a block of turned wood and at the top a metal insert, which is used for penetration tests. In the Snell standard this type of tooling is not found, and the standard head ISO DIS 6220-1983 is used.

Tables 1 and 2 collect the main requirements for the helmet testing equipment according to some of the most representative standards of different sportive disciplines.

Table 1. UNE protection helmet standards comparative for several sports

	UNE-EN 1077	UNE-EN 1078	UNE-EN 1385	UNE-EN 1384	UNE-EN 966	UNE-EN 12492	UNE-EN 13484
	Ski	Cycling	Canoe	Equestrian	Airborne	Mountain	Sleds
Headforms UNE-EN 960							
Impact absorption test							
Helmet drop method							
Punch drop method							
500 Kg platform (25 mm steel)				60 shore			
Anvil	Flat	Flat/kerb	Flat	Flat/kerb	Flat/kerb		Flat
Punch						Flat and hemisphe.	
Data recording	<60 mm before impact	<60 mm before impact	<60 mm before impact	According standard	<60 mm before impact	<60 mm before impact	<60 mm before impact
Drop height (mm)	1500	1497	500	1500	1500	2000 and 500	1500
Penetration resistance test							
Punch drop							
Hammer drop against punch							
Block/Head	Block			Block	Head	Block	Head
Punch	Conical			Conical	Conical	Conical	Conical
Drop height (mm)	750			500	1000	1000	750

Table 2. Snell standards comparative for several sports

	Snell RS98	Snell B90 A	Snell H2000	Snell L98	Snell/FIA CM2016	SA2015
	Ski	Cycling	Equestrian races	Scooters	Children's Motor Sports	Competi-tions
Headforms ISO DIS 6220-1983			DIT FMVSS 218			
Impact ab-sorption test						
Helmet drop met-hod						
Punch drop met-hod						
500 Kg platform (12 mm steel)	>135 Kg S>0,10 m^2	>135 Kg S>0,10 m^2	>135 Kg S>0,10 m^2	>135 Kg S>0,10 m^2		
Anvil	Flat, he-mispheri-cal and edge	Flat, he-mispheri-cal and kerb	Flat, he-mispherical and horses-hoe	Flat, he-mispheri-cal and edge	Flat, hemisp-herical and edge	Flat, hem-isphe, roll bar, kerb and edge
Punch						
Data recording	40 mm be-fore im-pact	40 mm be-fore im-pact	40 mm befo-re impact	40 mm before impact	30 mm before impact	40 mm be-fore im-pact
Drop height (mm)	100 J (2200 mm for 5kg headform)	100 J (2200 mm for 5kg headform)	145 J (2900 mm for 5kg headform)	80J (1600 mm for 5kg head-form)	3062 mm	3683 mm
Penetration resistance test						
Punch drop						
Hammer drop against punch						
Block/Headform	Head				Head	Head
Punch	Conical				Conical	Conical
Drop height (mm)	1000				2829	2829

Green cells agree with this method, whereas, red cells do not carry out this test method. This analysis method to obtain common requirements has been applied to 30 standards of the named fields.

2.2 Common Requirements and Adopted Solution

The requirements established in the standards for the main functional groups of the machine were unified and collected in the Table 3. Among the different design alternatives, those that optimally satisfied the functional and economic requirements were selected. Some of these solutions have been assessed by experimental and/or numerical

Table 3. System requirements and final solution

System	Requirements	Final solution
Inner Plaform	Weight > 500 kg. Steel and/or concrete. Last 25 mm in steel. Resonance frequency does not affect results	Concrete block with a 25 mm thick anchorage steel plate. Main frame is attached both this block and the floor.
Guidance system	Right impact point. Real speed > 0.95. Theorical speed	Two parallel steel wires with inner tensioner
Headform or punch lifting system	Not specified	Electric hoist. 250 kg. 500 w. With 12 m wire cable (twist-free, Ø 3.0 mm)
Headform or punch fixing system	Quick attachment of headform or punch. Avoid displacement during impact. Rotate the headform	Ball joint fixing by two metal rings wrapping it and fixing by means of a set of bolts
Anvil and headform replacement	Quick attachment and disattachment of tooling. Avoid displacement during impact. Enough strength to support impacts	Connecting flange in the tooling and four threaded holes in the supporting platform.
Speed measurement	Frequency response. 1000-CFC Precision 1%	Double infrared detector
Height measurement	Not specified	Laser measurement device
Acceleration measurement	Range up to 2000 g Maximun weight 50 g Frequency response. 1000-CFC Precision 1%	Uniaxial accelerometer sensor

methods until meet a final solution according to the multidisciplinary requirements (see paragraphs 2.3 and 2.4).

2.3 Prototyping and Testing of Guidance System

Protection helmet testing standards allows to use guidance systems with two or more wires or one or more rails, with the function of guiding the headform/punch support assembly in a vertical drop onto the right place of a test anvil. In this project a two wire guidance system with tensioners was proposed, in order to be cost efficient. Besides, a guidance system and a support assembly were prototyped in order to test its performance and speed tolerance compliance with the standard requirements.

The whole system was set up (Fig. 4) and a digital camera, which can gather more than 240 frames per second, was used to measure the time to impact. The launch is made at 2.40 m high, and the wires have marks to follow the support assembly displacement. This testing stage was essential to determine if the system is mechanically well re-solved and if it complies with the 5% speed tolerance established in the standards. The support assembly spent an average of 155 fps to reach the inner point, so a difference of 1.12% of the impact time was calculated respect of the theoretical value (Table 4).

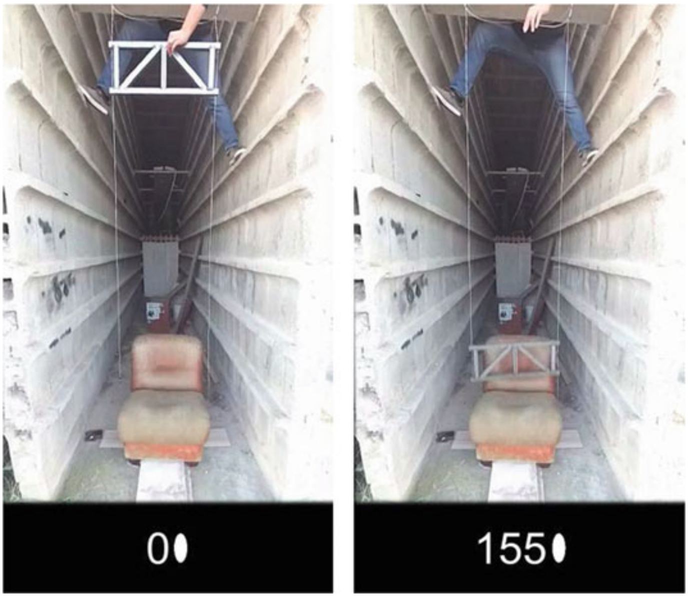

Fig. 4. Guidance system prototype: (Left) beginning of drop; (right) instant of contact (fps)

Table 4. Impact time values

	Theorical	Experimental	Difference (%)
Impact time (s)	0.638659	0.645833	1.12

2.4 Finite Element Analysis

The behavior of systems that are subject to structural requirements during the operation of the machine has been simulated using the finite element software SolidWorks Simulation. Some of the structural load cases have been considered are: the static case of the dead load of the whole system, the drop simulation of the headform/punch support assembly (weight of the attached systems and 10.84 m/sg contact speed were applied) and the buckling simulation of the main frame (with 5.84 m. columns embedded in their bottom side) (Fig. 5). In all cases, beam and shell elements were used with a maximum element size of 50 mm.

This CAE (Computer Aided Engineering) software has allowed to simulate several design solutions and optimize the performance, the weight and the cost of the testing machine.

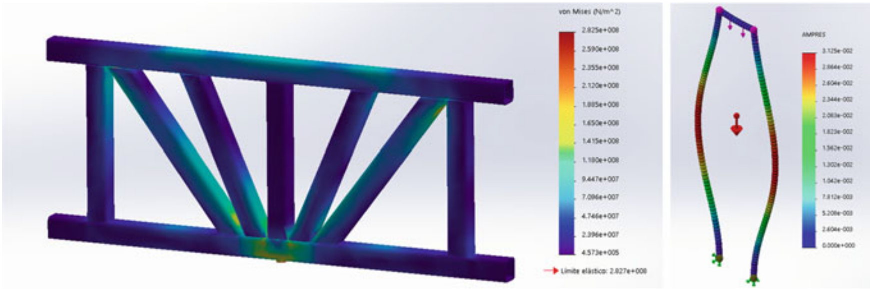

Fig. 5. CAE simulation: Left) Drop of the headform/punch support assembly; right) Buckling

3 Impact Machine Description

Once the final design solution was reached, the representation of these solutions is made by 3D models, making the complete modelling of the machine with the commercial software SolidWorks. This model was use to define a right assembly process and generate the drawings for manufacturing. Figures 6, 7, 8, 9 and 10 show whole model and details of the main functional parts of the testing machine.

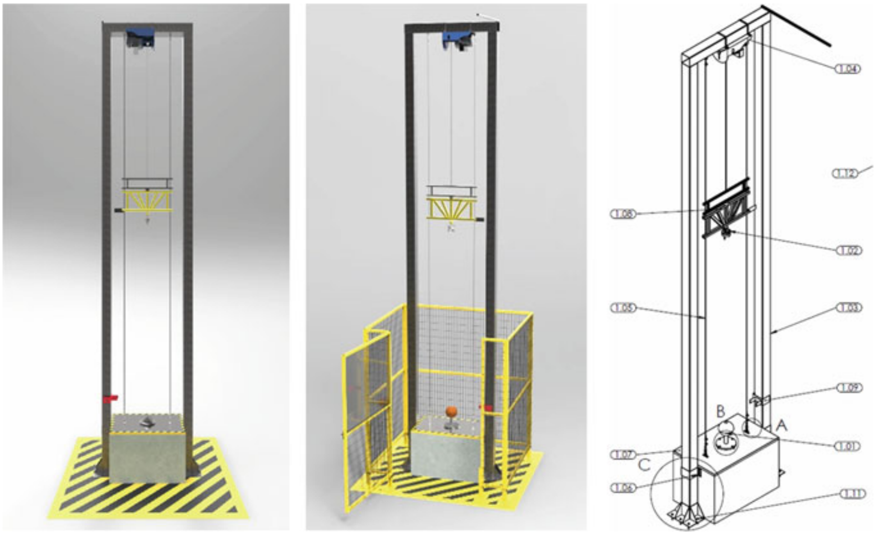

Fig. 6. Front, 3D view (with protection system) and drawing of the impact testing machine

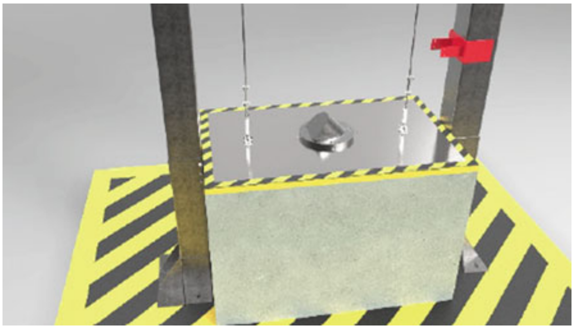

Fig. 7. Equation formatting

Fig. 8. Lifting and positioning system

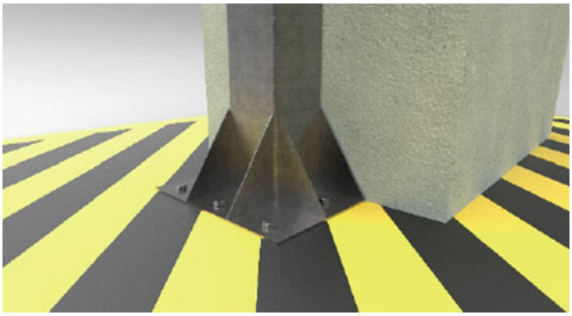

Fig. 9. Floor attachment solution

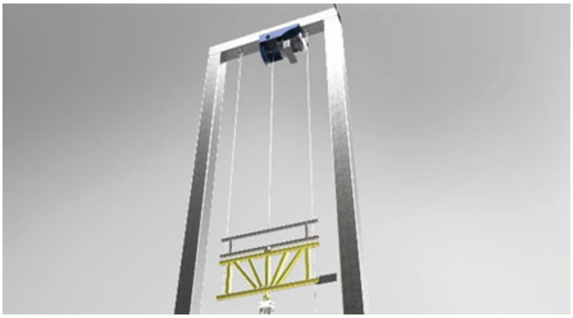

Fig. 10. Guidance and dropping system

4 Conclusions

At the end of this project, a new testing machine that meets all the requirements for this type of equipment was developed, meeting with a low manufacturing cost and satisfying the most of the extensive standards that regulate the absorption and penetration impact tests of different types of helmets.

The machine has been designed with the geometry and necessary systems to cope with the most of protective helmet testing standards. It should be noted an innovative fixing system in order to attach firmly and allow the rotation of the different standardized headform or punch. As well as an anvil and headform support system, which enables their quick replacement and attachment.

References

1. McIntosh A, Suratno B, Haley J, Truong J (2013) Consumer rating and assessment of safety helmets (CRASH). In: 23rd international technical conference on the enhanced safety of vehicles (ESV), Seoul, Korea South
2. J. D. Power and Associates (2005) Motorcycle helmet satisfaction study, Westlake village, California
3. Towner E, Dowswell T, Burkes M, Dickinson H, Towner HM (2003) Bicycle helmets: a review of their effectiveness, a critical rieview of the literature. Road Saf Res Rep 30, Chang C, Ho C, Chang S-Y (2003) Design of a helmet. ME 499/599
4. UNE-EN 960 (2007) Cabezas de ensayo para utilizarse en los ensayos de cascos de protección
5. UNE-EN 13087-2 (2012) Cascos de protección. Métodos de ensayo. Parte 2: Absorción de impactos
6. UNE-EN 13087-3 (2000) Cascos de protección. Métodos de ensayo. Parte 3: Resistencia a la perforación
7. UNE-EN 13087-1 (2000) Cascos de protección. Métodos de ensayo. Parte 1: Condiciones y acondicionamiento
8. UNE-EN 1384 (2013) Cascos para deportes hípicos
9. UNE-EN 966 (2012) Cascos para deportes aéreos

10. UNE-EN 1078 (2012) Cascos para ciclistas y para usuarios de monopatines y patines de ruedas
11. UNE-EN 13781 (2012) Cascos de protección para conductores y pasajeros de motos de nieve y bobsleighs
12. UNE-EN 1385 (2012) Cascos utilizados para la práctica de deportes en canoa, kayak y en rápidos de agua
13. UNE-EN 12492 (2012) Equipos de montañismo. Cascos para montañeros. Requisitos de seguridad y métodos de ensayo
14. UNE-EN 1077 (2008) Cascos para esquiadores alpinos y de snowboards
15. UNE-EN ISO 10256 (2004) Protecciones de cara y cabeza para uso en hockey sobre hielo
16. UNE-EN 13484 (2012) Cascos para los usuarios de trineos
17. UNE-EN 13277-4 (2002) Equipo de protección para artes marciales. Parte 4: Requisitos adicionales y métodos de ensayo para protecciones de la cabeza
18. UNE-EN 1080 (2013) Cascos de protección contra impactos para niños
19. UNE-EN 14052 (2012) Cascos de protección de alto rendimiento para la Industria
20. UNE-EN 397 (2012) Cascos de protección para la industria
21. UNE-EN 443 (2009) Cascos para la lucha contra el fuego en los edificios y otras estructuras
22. UNE-EN 16473 (2014) Cascos de bombero. Cascos para rescate técnico
23. UNE-EN 16471 (2014) Cascos de bombero. Cascos para lucha contra el fuego en espacios abiertos
24. UNE 26428 (1991) Vehículos de carretera. Ciclomotores. Cascos de protección para usuarios
25. Snell $H_2 0$ (2000) Standard for protective headgear for use in harness racing and other equestrian sports
26. Snell RS98 (1998) Standard for protective headgear for use in recreational skiing and snowboarding
27. Snell B90 (1998) Augmentation to the 1990 standard for protective headgear for use in bicycling
28. Snell SA (2015) Standard for protective headgear for use in competitive automotive sports
29. Snell EA (2016) Standard for protective headgear for use in elite automotive Sports
30. Snell K (2015) Standard for protective headgear for use in kart racing
31. Snell E (2016) Standard for protective headgear for use in horseback riding
32. Snell M (2015) 2015 standard for protective headgear for use with motorcycles and other motorized vehicles
33. Snell CM (2016) Snell/FIA standard for protective headgear for use in children's motor sports activities
34. Crash. (25 de 10 de 2017). Obtenido de https://www.crash.org.au/
35. Gadd C (1961) Criteria for injury potential. In: Impact acceleration stress symposium, national research council publication no 977 (págs. 141–144). US: National Academy of Sciences, Washington DC.
36. Towner E, Dowswell T, Burkes M, Dickinson H, Towner J (2002) Bicycle helmets: a review of their effectiveness, a critical rieview of the literature. (D. f. DfT, Ed.) Road Safety Research Report, 30
37. McIntosh A, Suratno B, Haley J, Truong J (2013) Consumer rating and assessment of safety helmets (CRASH). In: 23rd International technical conference on the enhanced safety of vehicles (ESV). Seoul, Korea South
38. SHARP. Helmet Tests (25 de 10 de 2017) Obtenido de https://sharp.dft.gov.uk/

39. Chang C, Ho C, Chang S-Y (200.) Design of a helmet. ME 499/599
40. Shuaeib F, Hamouda A, Hamdan M (2002) Motorcycle Helmet Part II. materials and design issues. J Mater Process Technoly 123:422–431
41. J.D. Power and Associates (25 de May de 2005) Motorcycle helmet satisfaction study. Westlake village, California, USA
42. SolidWorks (30 de 10 de 2017) Obtenido de http://help.solidworks.com/2014/spanish/SolidWorks/sldworks/c_introduction_toplevel_topic.htm

Well Planned Obsolescence and the Eco-Design

J. M. Paricio(✉), J. A. Peña, and R. Miralbes

Department of Design and Manufacturing, University of Zaragoza, C/María de Luna s/n, Saragossa 50018, Spain
joparisa@unizar.es

Abstract. The planned obsolescence was born during the economical crisis that appears as a consequence of the "crack" of 1929. It was planned as a possible solution to the exit of that crisis allowing the increase of the manufacturing productions and the reduction of the unemployment. In the fifties of the twentieth century at the time of the booming of the US consumer society, a substantial part of the producers who provided it, put into practice this planning, supported by the low prices of raw materials and energy. This model was extended to the western world first, and later with the globalization of the economy it continues developing in the rest of the world. This profusely used methodology that has allowed the economic development of Western countries has to be coherent with the sustainability premises that are so necessary today, when the climate change and the overcrowding is a real problem. The successive crises: energy, supply of raw materials and a more sustainability and social consciousness motivated by the effects of the climate change, makes this design methodology inadequate; then, there are more conscious final product users that demand products and services that introduce environmental aspects and specially avoid some practices like the planned obsolescence. Some new design models have appeared and been developed based on the sustainability and the circular economy. The successive conventions and protocols of Vienna, Montreal, Rio, Kyoto and Paris have compromised the governments of the world with the need for control to mitigate the harmful effects. This is why a new model, the eco-design, plays the role of efficiency manager, allowing to weigh certain environmental benefits derived from the replacement of obsolete components, and optimizing product life cycles in a global way. With the use of eco-design and its associated tools, it is possible to integrate the complete life cycle planning with the appropriate model of reuse, including retrofitting, remanufacturing, recycling and if necessary discarding. The benefits derived from an adequate planning of the environmental costs of the product will in the long term also affect the producer, not only through compliance with rules and regulations or through "green" marketing, but also through the return of intangibles. In this paper, the objective is the analysis of how well planned design methodologies can be implemented in the design phases of a product and its final benefits, advantages and disadvantages.

Keywords: Eco-design · Planned obsolescence · Design · Product · Life cycle

F. Cavas-Martínez et al. (Eds.): *Advances on Mechanics, Design Engineering and Manufacturing II*, LNME, pp. 74–84, 2019.
https://doi.org/10.1007/978-3-030-12346-8_8

1 Introduction

Programmed obsolescence is a concept that has been present in our economy for many decades. The companies that produce goods and services have relied on it to increase their sales, at critical moments. After the crisis of 1929, when in the US the stock market downfall was followed by a deep recession, that concept received a significant boost. Even an author theorized with the benefits that obsolescence would bring. In 1932 the intellectual and real estate investor Bernard London postulated that the wheel production-consumption-work should be kept turning at all costs, even at the cost of the products ceased to be used after a certain period [1]. Some companies related to the electrical industry, such as the manufacturers of light bulbs, in an oligopolistic behavior, agreed to reduce the longevity of their product to a typical value of 1000 h, to reduce costs and achieve increases in sales [2].

The concept was used after the World War II 1939-1945. Back in the USA, which had been virtually oblivious to the destruction of the war and the population decline that took place in Europe, there was a re-launch of the economy in a few years that could not be stopped by any hypothetical crisis. The “American Way of Life” led to a lifestyle in which individual progress entailed a significant increase in the consumption of basic and durable goods, with the consequent increase in industrial production. But faced with the risk of saturation of the market and the need to sustain the levels of production, or may also be faced with the temptation to increase profits, the principles that London postulated were resumed and implemented, with adaptations [3].

In this new lifestyle, the inventions that were a luxury a few decades ago, such as the automobile, the refrigerator or the TV receiver, became goods coveted by the general public, and in a short time acquired, either in cash or to credit. But for the machinery to keep turning, it became necessary to introduce motivations for the renewal of these products, so that a new acquisition of them was produced, thus giving way to the mass production of the factories. New forms of obsolescence appeared related to human psychology: it was not enough to get to possess the desired good, in addition that good had to be the last, the best. Although in part the positive response to this approach can be attributed as a very human need for preponderance, to mark a “status”, this effect is also related to the psychological effect of technological advances, applied to products. If the individual unconsciously establishes a correlation between the generation of technological advances and the consequent exit to the market of new products, finally it will find desirable the exit of new products and will even generate a demand for novelties.

The decade of the 1950s and 1960s was a time when this two-way consumerist pressure consecrated the application of the principles of a planned obsolescence that, consciously, manufactured and sold products with the preconceived idea that they were discarded soon. The economic philosophy of unlimited growth was prevalent at the time.

There was a coincidence of diffuse interests between the parties: producers, consumers, banks, governments. Apparently all economic factors gained from this policy: producers could give output to their production, consumers satisfied their needs, real or induced, banks granted consumer credit, governments saw how public revenues from direct and indirect taxes grow. However, subtly, the consequences of this path began to affect everyone.

Obsolete and discarded products became a problem for the environment. At first the traditional methods for disposal of waste, but corrected and increased, served to stop the urgency of the response. The large warehouses of waste required the use of huge extensions, personnel, machinery and other resources for their management. But the growth of production produced disproportionate amounts of waste.

It began to take advantage of waste as raw material in those cases where it was economical. When the raw materials from which the intermediate materials came had little cost, the use of waste was not undertaken, but in cases where for various reasons these raw materials increased their cost, then the use was practical. So the initial reason for the use of the waste was purely economic. A very characteristic example is that of steel scrap. When market saturation was reached, products made of steel that were no longer used came to occupy large areas and were economically reintroduced into the production chain instead of simply leaving them exposed to corrosion. Later, glass was the flag material of this waste reuse [4].

2 Ecology and Environment

Coinciding with this stage of enormous growth of production, there is an expansion of knowledge of our environment. Knowledge about nature and its biodiversity is disseminated. Both the means of transport and the media extend their reach to the entire planet, and an awareness of the vital environment begins to be created. The beginning of space exploration, in particular, by looking at other planets and stars, allows society to realize the smallness and at the same time the importance of our place of residence. We can recognize in this the origin of ecological consciousness.

The manifestation of the ecological conscience starts with inspiring authors, who in their writings transmit their love for nature and thus spread the existence of an alternative, with a way of life closer and more respectful with the environment. Henry David Thoreau in the USA in the 19th century had a huge impact. Robert Baden Powell, at the beginning of the 20th century in England, is an example of an activist who, in addition to spreading ideas, is the creator of an organization, the Boy Scouts, that takes into account the environment. Later, and animated by them, the ecologist movements arise, being the Sierra Club, founded by John Muir in 1892 one of the first. Since a large part of society was so devoid of this awareness, the most motivated people joined groups and undertook awareness and diffusion actions, in a variety of ways. Regardless of the controversies generated at the time, it is undeniable that over the years there has been a change of mentality. What was called progress in the nineteenth century, it is no longer called in the twenty-first century. The smoky chimneys, a sign of development, abundance of products and economic improvement at the beginning of the industrial revolution, which were admitted as minor evil during the 20th century, were already rejected and considered annoying at the end of the 20th century and the beginning of the 21st century [5]. The knowledge of the direct consequences on the health of the human being, the affection in the short and medium term to the biodiversity, and the consequences that in the medium and long term a social carefree behavior could have on the climate, motivated finally the governments and supranational entities begin to implement agreements that result in standards for the control of waste and emissions.

The agreements of Vienna, Montreal, Rio, Kyoto and Paris have successively faced the challenges that for the environment were the dead ends in which the unstoppable and self-sustained development had led to the global society. The levels of periodic reduction of the ozone layer, in an accelerated mismatch, led to agreements for the reduction and progressive elimination of the use of halogenated gases that were used in different processes and products. These gases have a proven effect, and that is why national and supranational bodies were able to reach agreements to reduce them more quickly. In these moments, we are on a path of progressive and accelerated reduction of emissions, which will force important adjustments in numerous fields of our economic structure. If these adjustments are not well implemented, the impact on production, employment and wealth will be very important.

3 Planned Obsolescence and Energy

The planned obsolescence, which is in full application in this period, is compatible with some of the ecological principles, in the end, the objective of the producer is to sell the product repeatedly, it is not so important if the material for its manufacture comes from raw materials or recycling. Therefore, an increase in ecological awareness and an increase in the application of planned obsolescence can be seen simultaneously. In fact, in some areas, the reuse of waste minimizes the costs of raw materials, so it is tempting to accelerate the cycles of use-waste.

So far we have considered the waste from the products when they are no longer usable, as well as the waste that is generated when the product is manufactured. And we can even take care of the waste generated by the product throughout its use. But if we integrate in these considerations the waste and emissions for all the operations and processes related to the product, including the transport, the useful phase, and the recycling and/or disposal, we see that the harmful to the environment amount of pollution and emissions increases a lot.

Modern society requires a huge amount of energy for its development. The origin of this energy, in part at least, comes from non-renewable sources, which consume finite resources of the planet and produce waste usually harmful to the environment. A part of the energy produced is used in the production of goods, their transport, during the use of the goods and finally, when they cease to be useful, to carry out the necessary operations so that their components do not remain as waste, but are reused. or at least do not threaten the environment.

If all the necessary resources are taken into consideration, not only in the form of raw material, but also as energy, some productive processes must be revisited. Remanufacturing using recycled waste saves raw materials, but requires a very significant fraction of the original energy. Since energy is scarce, and in its generation, at least in part, undesirable emissions occur and natural resources are consumed, it is necessary to limit that energy consumption also.

4 Designed to Break

As said before, the application of waste reduction practices such as recycling can have the economic consequence that the production factor suffers the same delusion that first triggered consumerist fever, which is the presence of relatively cheaper raw materials. This situation lends itself to an increase in planned obsolescence, since the rapid and cheap reintroduction of waste in the recycling chain favors a relative decrease in the cost of raw materials, which is partly what produced its appearance.

When what the designer has in mind is that the product has a limited life time, the design changes. The criterion of designing the product with non-durable materials can be applied, but only with a very light use it could meet the life expectancy. This criterion has the disadvantage that the user quickly perceives the intrinsic poor quality of the product, and this can affect sales. Or the criterion of inserting in the design ‘Achilles heels’, predicted failure points, in which, for example, less material than necessary is incorporated and current use will lead to breakage due to fatigue in a statistically predictable period. This second criterion better masks the intention to shorten the life of the product, and even the use of good quality materials for some other parts of the product can serve as an argument for increasing margins. These criteria have to do with the so-called planned obsolescence of operation. When the product fails to work, the user gets it discarded and acquires another one. An example of the aforementioned, referred to the electronic industry, was the massive use of electrolytic capacitors of limited life time, which after the guarantee of the product were decomposed leaving appliances useless [6].

The doctrine of preventive maintenance applied in productive companies has studied these behaviors for decades, since it is cheaper to replace the components at times when the stop does not affect production. It is also performed by security criteria, when the parts to be replaced are of critical type and a failure in them can put at risk the integrity of the rest of the mechanisms or their users. But the doctrine of preventive maintenance also contributes in part to the excessive generation of waste, by replacing parts that actually continue to work. What is justifiable for economical and safety reasons, it is more difficult to justify environmentally.

Indirect induced obsolescence occurs with products that require spare parts, charges and consumables to operate, which are available at the time of acquisition, but after the necessary time they can no longer be obtained through official channels. It becomes very difficult for the user, under these conditions, to continue using the product. Its replacement by another new product, with readily available spare parts and consumables, becomes more practical at the time.

But we must also mention the planned psychological obsolescence, which achieves the same objective by another path. For example, aesthetics. When the product loses some of the aesthetic qualities that made it desirable, such as color, brightness, transparency, texture, etc. the user will also be tempted to discard it even though it still retains its functionalities intact. It can be cited the case of a variety of products that yellow with the passage of time, apparently due to the effect of light on the composition of their coverage. Also as an example of this can be found the case of the metallic type finishes that have certain plastic casings in the electronics industry, and that once the warranty period has passed they begin to detach, revealing the matte plastic found below, which is much less attractive. In the same line it is the obsolescence caused by the reintroduction of the same product to the market, with slight variations, to convince the user that the one in their hands has lost its value (because it is outdated) and should discard it and replace it.

Some of these forms of obsolescence clash with the wishes of the user, who intends the investment made in the good that has been made obsolete be recovered with a longer life of the product. Thus arise alternative uses or unofficial solutions, which companies sometimes tolerate and in others fight.

5 Repair or Discard

If a product suddenly stops working, most users look for a solution that allows them to correct the failure immediately and without disbursement. If the correction is possible, but indicates a malfunction that is expected to recur in the future, the user begins to distance himself from the product and begins to contemplate alternatives. But there are products in which for particular reasons the user is not willing to get rid of them: for practical reasons, the user can believe that the product has not lasted what had to last and can still be taken out; or there may be a sentimental cause, for which you want to keep the product in use; or perhaps the user considers that the product has more value as usable seniority.

The truth is that there is a demand from users to keep the products in use. Even the producers may be interested in brand prestige having official service workshops, where repairs can be carried out under warranty and customer service. But in the case of some products, from the expiration of the guarantees, the costs of the repairs are designed to convince the client that it is better to acquire a product. In some cases it may be the same product that was initially purchased, in others a more modern and usually more expensive version. It is clear that the producer derives more benefit and less annoyance with the sale than with the repair.

In spite of the few economic stimuli that the producer may have to give the most complete service, the user's desire to make the repair finds its way through alternative ways. Apart from the official workshops, alternative workshops that offer similar services arise, but adjusting the costs, since they do not need to enhance the purchase option. If this is combined with the fact that the parts suppliers of the producer use the alternative repair market as a complementary market for their parts, the prestige of the product can be favored by the way the market classifies the product as easily repairable, and so, in a virtuous circle, users are attracted to that particular product instead of those of the competition. In this case, some brands establish parts storage services for repairs, it is the same manufacturer who supplies the components for replacement, thereby obtaining another revenue route and thus fulfilling the possible legal obligations of technical service. It can be disputed whether the quality of the replacement parts stored by the brand is the same as those originally assembled, bearing in mind that the greatest interest is usually in the new sale and not in the lengthening of life.

When the pieces from the official manufacturers are not available, because there are exclusivity contracts or coercive actions of the brand, or because the quality of the available pieces is lower, there is an increase in the value of waste from those specific products. Products that have failed, or specifically their ‘Achilles heel’ has failed, but otherwise contain valid parts, are used as a source to repair another ones in unofficial workshops.

Given the difficulties encountered by users and unofficial workshops to repair, associations have been created that advocate better treatment by manufacturers. The “Right to Repair” movement has arisen in the USA, which advocates the establishment of a “Fair Repair Bill” that requires companies to make available to users and those who carry out repairs the documentation and necessary parts. This movement is strongly opposed by large companies, because it can have an impact on their business model [7]. In Europe, the European Parliament in its session of July 3, 2017 passed a resolution to “Make consumer products more durable and easier to repair” [8].

The European Parliament also included the recommendation to create a voluntary European label that includes information such as durability of the product, ecological design, modulation capacity in accordance with technical progress and the possibility of repair.

Although the recommendations of the European Parliament do not have to be incorporated legislatively into the laws of the Union or of the member states, their issuance sooner or later affects the official regulations. Therefore, they have a lot of value and mark a trend that should be reflected in the future [9].

There are more initiatives that try to promote the principles of the circular economy. The Ellen MacArthur Foundation is working on this promotion through the publishing of documents, organizing circular-economy-centered events, and more initiatives from its founding in 2010. One of this initiatives is the Circular Design Guide [10, 11].

6 Measure Planned Obsolescence and Its Ecological Impact

Although the corporations find economically beneficial the use and abuse of planned obsolescence, the application of the agreements on CO_2 emissions equivalent, which is progressive and leads to great restrictions in the very near future, will force a increase in sustainability policies, with a massive application of eco-labels. The products of low qualification in the system of ecological labeling will be progressively expelled from the market, thanks to the growing awareness of the citizens [12].

But a labeling system, to have meaning, must be based on comparable magnitudes in a simple way. A widely used label is the energy efficiency label, which includes the energy in KWh as well as the amount of CO_2 emitted. These labels vary in complexity, it is different to label an appliance, a consumer electronics product, a vehicle or a building. If we intend to include in the labeling the concepts that the European Parliament marks, such as availability of parts for repair, durability, minimum resistance, the measurement in comparable terms is complicated.

The establishment of metrics on the degree of planned obsolescence and its application in the ecological labels is one of the subjects on which the authors of this work are developing studies at present. The objective is to integrate in the product eco-design process the quantitative measure of the sustainability of each of the design actions that may have an effect on planned obsolescence, so that an effective and simple means is available to foresee the labeling qualification as the design and redesign process occurs and both processes are one. The improvement of the ecological conscience of the citizens together with the adequate labeling of the products, provided with adequate metrics, will affect the market change, both in consumption and production, and will allow the emergence of new activities that are still unknown, as was the case with the new jobs and companies that the development of the information society has brought.

Far from being an obstacle to economic growth, the application of this type of policy is also a good opportunity for the development of productive economic activities that have been depressed as a result of the predominance of waste-oriented manufacturing. For example, activities oriented to repair.

7 Eco-Effective Versus Eco-Eficient

Some authors such as Braungart et al. are committed to overcoming the concept of waste and zero emissions, a motto of the current eco-efficient design paradigm. Such a design is called "From cradle to grave". Faced with the impossibility of reducing negative emissions to zero, they advocate reversing the guilty complex with which the design of the products is modified. And get that as in nature there is no waste, since everything is reused, human products, when they no longer have utility, can continue to be useful for the environment. So that their remains are directly food, support, coverage and promote life instead of attacking it. And so the amount of waste ceases to be a problem to become a beneficial product. So that the toxic components, even in small proportion must be completely absent from the remains. Those technical components that can not be incorporated into the biological cycle must enter a technical cycle, in which there is no degradation of its technical quality, but maintenance, preventing the mixing of various materials such as metal alloys so that the product of waste recovery continues to have high-grade technical utility. This type of design, as opposed to the previous one, is called "From cradle to cradle" [13].

Implementing these strategies has certain consequences: if the waste generated by the products is actually beneficial to the environment, why limit them? What would be the point of thinking about its processing? Its practical application clashes with the harsh reality that creating increasingly useful products generates the problem that they are becoming more complex, made up of a greater number of different materials and less related areas. When their utility phase comes to an end, they become more difficult to convert into pure substances, and are potentially mixtures of low technical quality.

Even with these questions, it will be necessary to take into account in the development of the ecological labels the contribution to sustainability that the products developed with this philosophy carry out [14].

8 Labeling Initiatives

There are several initiatives to carry out the classification and labeling of products, processes, industries, etc.

The EU Ecolabel is a third party certified Type I ISO 14024 aimed to promote products and services which have a reduced environmental impact thus helping European consumers distinguish more environmentally friendly products. It was established in 1992. Over time, the different criteria have been refined and the fields of application of the label have increased. At present, it already contemplates criteria of durability and ease of repair and recycling in some of its fields of application, such as, for example, electronic consumer equipment [15].

Out of the EU, there are many more initiatives, some of them are grouped in the GEN (Global Ecolabeling Network). They follow the standards of the ISO 14024 [16, 17].

It has already been cited, the Cradle to Cradle initiative, which has established a system of certification and labeling of application in all types of materials, products, processes and services, more specific to compliance to the principle "Cradle to cradle" [18].

Those labels have only sense as far as the consumer is conscious of their meaning, and is willing to make use of them as a condition to purchase. But that is a question of education.

9 Conclusions

The planned obsolescence was introduced into the productive environment as a means to guide the market to absorb the enormous transforming productive capacities that the industries acquired as a result of the confluence of the development of mass production and the abundance of raw materials at low cost. It had initial positive consequences, as was the widespread social access to previously restricted consumer products. But the emergence of the social ecological conscience, due to the greater knowledge of our environment, and the evidence of the damage to the environment that our behavior was producing, together with the progressive decrease of resources, motivated the beginning of a change. When the negative consequences of overexploitation of resources were manifested, the planned obsolescence was adapted and took advantage of the development of the recovery and recycling of waste in substitution of dwindling resources. The compatibility of a truly sustainable development, with the excessive consumption of resources and energy needed to maintain the high pace of the increasingly shorter cycles to which the philosophy of planned obsolescence compels, is in doubt.

The planned obsolescence acquires diverse forms, some oriented to the product and others oriented to the behavior of the user. In all of them the objective is to increase the margin of profit for the producer through the reduction of costs and the acceleration of the cycle of use.

Given its widespread application in various fields of production, especially high-tech electronic consumer products, the most conscious users reacted through associations and environmental movements for the authorities to stop the excesses of the industry. The social pressure motivated the appearance of international agreements for the protection of the environment, which include among its contents the reduction of waste and unfavorable emissions. At another level, users are reacting by creating alternative means to keep the products running despite the obstacles that production is intended to impose. In this process, occupation fields were developed that the consumer dynamics had depressed, such as the repair of consumer electronics with the reuse of components.

The social awareness that the problems caused by planned obsolescence motivates, leads to the establishment by the authorities of qualification tools such as ecological labels, to serve as a guide to the user in their criteria of product acquisition. These eco-labels require metrics that include not only the criteria of resource consumption and waste production of the product life cycle, but also those of life-time capabilities, reparability, replacements, and capacity improvement.

Our objective with this work is to lay the foundations for the determination of the metrics that allow in a simple way to relate the degree of planned obsolescence of a product with its qualification by ecological label, so that they are incorporated into the ecodesign process and can be valued to what extent it is a design that meets the criteria sought. At this moment, experiments are being carried out to compare the different methodologies and in this way deduce appropriate measurement systems.

When constructing these metrics, it is necessary to consider especially the designs in which the concept "from cradle to cradle" has been respected with products of residue not already null, but even of a positive character for the environment.

References

1. London B (1933) The new prosperity: permanent employment, wise taxation and equitable distribution of wealth. London B. (ed). New York
2. Krajewski M (2014) The great lightbulb conspiracy. In: IEEE Spectrum vol. 51, issue 10, October pp 56–61. https://doi.org/10.1109/mspec.2014.6905492
3. Cohen L (2004) A consumer's republic: the politics of mass consumption in Post-War America. J Consu Res 31(1):236–239. Oxford University Press. https://doi.org/10.1086/383439
4. Spendlove M (1976) Recycling trends in the United States: a Review. Bureau of Mines, Washington
5. Shefferd V (1991) The shaping of environmentalism in America. University of Washington Press, Seattle and London
6. Bayus B (1998, June) An analysis of product lifetimes in a technologically dynamic industry. Manage Sci 44:6
7. Repair Association Home Page. http://repair.org/. Last Accessed 14 March 2018
8. http://www.europarl.europa.eu/news/en/press-room/20170629IPR78633/making-consumer-products-more-durable-and-easier-to-repair. Last Accessed 14 March 2018
9. Montalvo C et al A Longer lifetime for products: benefits for consumers and companies. http://www.europarl.europa.eu/RegData/etudes/STUD/2016/579000/IPOL_STU(2016)579000_EN.pdf. Last Accessed March 14 2018
10. Ellen MacArthur Foundation. https://www.ellenmacarthurfoundation.org/. Last Accessed 18 May 2018

11. Circular Design Guide. https://www.circulardesignguide.com/. Last Accessed 18 May 2018
12. Luttropp C, Lagersted J (2006) EcoDesign and the ten golden rules: generic advice for merging environmental aspects into product development. J Clean Prod 14(15–16): 1396–1408
13. Braungart M, McDonough W (2002) Cradle to cradle: remaking the way we make things
14. Michael B et al (2006) Cradle-to-cradle design: creating healthy emissions a strategy for eco-effective product and system design, J Cleaner Prod. https://doi.org/10.1016/j.jclepro.2006.08.003
15. Meloni M, Souchet F Sturges, D Circular consumer electronics: an initial exploration. https://www.ellenmacarthurfoundation.org/assets/downloads/Circular-Consumer-Electronics-2704.pdf. Last Accessed 17 May 2018
16. http://ec.europa.eu/environment/ecolabel/index_en.htm last accesed 2018/05/18
17. https://www.globalecolabelling.net. Last Accessed 18 May 2018
18. https://www.c2ccertified.org/. Last Accessed 2018/05/17

Experimental and Numerical Study of the Self-loosening of a Bolted Assembly

V. Rafik[1,2](✉), B. Combes[1], A. Daidié[1], and C. Chirol[2]

[1] Université de Toulouse, Institut Clément Ader, UMR CNRS 5312, INSA/UPS, ISAE/Mines Albi, 3 rue Caroline Aigle, 31400 Toulouse, France
vincent.rafik@airbus.com

[2] Airbus Operations S.A.S, 316 Route de Bayonne, 31060 Toulouse Cedex 9, France

Abstract. The self-loosening of bolted assembly is a phenomenon that has been studied several times in the past. Among the existing solicitations, it has been showed that transverse loading might cause the most severe loosening. Thus, different explanations have been proposed. In spite of their similarity, as they all consider sliding as the root cause, the sliding surface distinguish them one from another. This paper will aim at giving another point of view of the problematic in order to advantage a Zadoks' theory, which highlights the transverse sliding of components. To do so, firstly a double-shear assembly will be modeled. Its specificities are the preload application by screwing the nut, and the use of a self-locking nut. Secondly, some tests will be done in order to valid the built model. Those experiments will also factor the thickness of the assembly in the self-loosening. Thirdly, the analysis of the numerical results and of the experiments, especially the interface surfaces will give us a clue in order to validate the sliding phenomena, which is according to Zadoks, the movement implying the self-loosening of the assembly.

Keywords: Numerical analysis · Bolt · Self-loosening · Experiments

1 Introduction

1.1 Industrial and Scientific Context

When a structure is loaded, its bolted joints also perceive displacement or loading. This solicitation might be the root cause of phenomena which might imply the degradation of the assembly. Some of them are characterized by a loss of the normal load within the bolt. If this loss is too important, then the assembly might not behave as an embedding anymore and the structural integrity might be endangered. In order to increase the life length of bolted joint, a raise of preload is often chosen. Unfortunately, to avoid any plasticity within the bolt, the diameter of the screw needs to be increased, leading to additional mass compared to the initial choice of component. It has been seen that this loss of preload can be caused by the rotation of the nut on the screw [1]. A better understanding of the self-loosening will reduce the weight of the structure without impacting its life length.

F. Cavas-Martínez et al. (Eds.): *Advances on Mechanics, Design Engineering and Manufacturing II*, LNME, pp. 85–94, 2019.
https://doi.org/10.1007/978-3-030-12346-8_9

In order to process to the phenomenological study of the bolted assembly self-loosening, the phenomena implying the loss of preload need to be understood. In the literature, several scientists were interested in this subject [1–13]. However, it is important to distinguish two general aspects of the loss of preload: untightening and unscrewing. On the one hand, untightening implies a loss of preload without any relative movement between the nut and the screw. Creeping or relative dilatation can be one of its root causes. On the other hand, unscrewing is mostly linked to the geometry of the threads as the nut or the screw will rotate whereas the other component will not [6, 9, 10, 12]. The self-loosening, phenomenon studied in this paper, is one of them.

Several scientists worked on this phenomenon. However, the most outstanding works will be presented below.

1.2 State of the Art on Self-loosening

Dinger [2] distinguished 4 different situations of loading which will lead to the self-loosening of the bolted assembly:

- Cross-load: the solicitation is orthogonal to the bolt's axis,
- Axial centered load: the solicitation is coincident with the bolt's axis,
- Axial decentered load: the solicitation is parallel to the bolt's axis but is not coincident.
- Rotational load: the bolt perceives a torque which direction is coincident with its axis.

He concluded that transverse loading is the most severe solicitation in term of self-loosening. Aiming at studying the most critic solicitation, in this paper, we shall only consider cross-loading.

Junker [2] seems to be the first scientist to have studied self-loosening. He designed a specific test bench in order to study the phenomena. Thanks to this device, Junker highlighted the importance of nut or screw head sliding in the phenomena. He also considered that the bending of the screw was the deformation inducing the sliding of these different surfaces. Koch [1] proposed a deeper explanation based on Junker observation and further tests. He considered that self-loosening could be divided into 4 steps, Fig. 1:

- Step 1: the plate sticks to the frame
- Step 2: the plate slips on the frame, the screw starts bending as its nut and head stick to the plate but sliding occurs in the threads,
- Step 3: the screw keeps bending but beyond a certain displacement, either the nut or the head starts to slide on the plate; the loosening seems to occur during this step,
- Step 4: the screw is back to a configuration where the nut and the head stick to the plate.

In addition of having proposed an explanation to the self-loosening, Koch also studied the early stage of the phenomena. As well as Sanclemente or Pai [2, 13], he highlighted the fact that the self-loosening could happen even if the whole surface of the contact didn't slide. Pai named this movement local slip. When the screw is bending, the pressure distributions between the nut, or the screw's head, and the plate

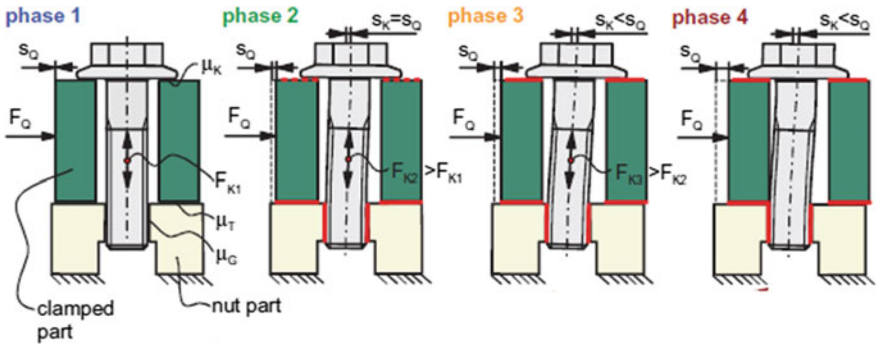

Fig. 1. The 4 phases leading to self-loosening, from [3]

are modified. At some points, this pressure is sufficiently high for the tangential component to overcome the frictional force implying the slippage of the surfaces. At other points it is weak and surfaces will stick together. The possibility of unscrewing under the sole effect of localized slip is still disputed.

Zadoks [8] also studied self-loosening under transverse loading. Unlike Dinger or Koch, he considered that the sliding in the threads wasn't only circumferential and might have other components. He only factored the sliding of the head on the plate in. He took into account the bending of the screw, the deformation of the plate and the influence of the transverse velocity slip. According to him, the transverse sliding will modify the friction force direction lowering the value of the friction torque.

1.3 Aims of the Study

Most of the models built in order to study bolt's self-loosening are considering only the screw as the nut is modeled as a threaded insert [2, 3, 13]. The clamped parts are rarely considered [1, 3, 6, 8, 9, 11, 13]. As the threads are must of the time not modeled, the preload is applied thanks to a bolt load and not thanks to the relative rotation of the nut on the screw [1, 2, 6, 9, 11]. This movement might deform plastically the threads and might impact the behavior of the bolt when the latter is cross-loaded.

In order to build a model which takes into account these remarks, a double lap assembly will be used as it can be seen Fig. 2a. A deformed locking nut and an aeronautical screw, kept still during tightening by an hexagonal hollow at its threaded side, will be considered, the Fig. 2b and c present those components. As the screw is not kept still by its head, it won't perceive any twist during tightening.

The aim of the paper will be to propose an explanation based on Koch and Zadoks theories. Observations made during experiments and analysis of the numerical results and of the contact surfaces will be made in order to determine their sliding direction and amplitude.

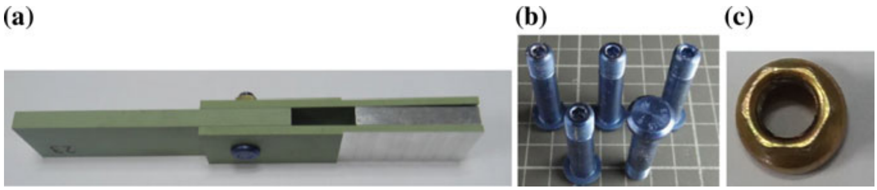

Fig. 2. A double lap assembly **a** an aeronautical screw **b** and a self-locking nut **c**

2 The Numerical Model

2.1 Presentation of the Model

The Abaqus software has been used to model the self-loosening of a cross loaded double-lap assembly as it can be seen Fig. 2. It will be composed of a 9.52 mm diameter' titanium aeronautical screw, whose length, pitch and thread length are respectively 31.31, 1.05 and 10.65 mm, a self-locking steel nut and three aluminum plates: two whose thickness is half of the screw and one whose thickness is equal to that of the screw. A 40 μm clearance exists between the screw rod and the plates.

In order to have reliable results, the threads need to be more finely meshed than the other parts of the bolt. Thus, as it can be seen Fig. 3, two parts will be created in order to model the screw. The average element size of the body is 0.1 mm whereas the threads one is 0.01 mm. A rigid connection between surfaces will embed the parts together. The same method has been used to mesh the nut.

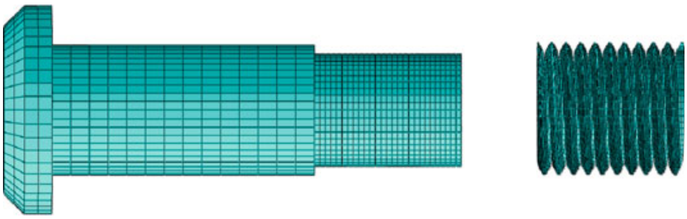

Fig. 3. Meshing of the two parts composing the screw

Three materials have been defined in the model thanks to their Young modulus, Poisson coefficient and kinematic plastic law, defined thanks to two (stress—strain) pairs which define the last point of elastic deformation, (σ_1, ε_1), and the last point before failure, (σ_2, ε_2). The TA6 V titanium will be used for the screw (in blue Fig. 4), the nut will be in A210 V steel (in yellow Fig. 4) and the 2024 aluminum will be used for the plates (in green Fig. 4). The parameters used are summed up in the Table 1.

In order to be closer to a real assembly, several contacts were defined, whose friction coefficients have been measured thanks to some torque—preload tests. The plates are coated with primer, while the threads are lubricated:

- Contact n°1: between the head of the screw and the upper plate, f = 0.27,

Table 1. Definition of the materials

Materials	Young modulus	Poisson coefficients	$(\sigma_1, \varepsilon_1)$	$(\sigma_2, \varepsilon_2)$
TA6 V	114 000 MPa	0.34	(780 MPa, 0.00684)	(860 MPa, 0.10684)
A210 V	210 000 MPa	0.3	(680 MPa, 0.00324)	(800 MPa, 0.12324)
Al2024	73 000 MPa	0.33	(324 MPa, 0.00444)	(469 MPa, 0.19444)

- Contact n°2: between the medium plate and the upper or below plate, f = 0.35,
- Contact n°3: between the below plate and the nut, f = 0.43,
- Contact n°4: between the hole of the plate and the screw, f = 0.35,
- Contact n°5: between the threads of the nut and those of the screw, f = 0.07.

2.2 Numeric Simulation

The penalty method has been chosen to model the normal and tangential behaviors. Four steps have been created to correctly simulate the self-loosening of the assembly:

- Step 1: deformation of the nut in order to self-lock it, Fig. 4a,
- Step 2: tightening of the nut, Fig. 4b,
- Step 3: relaxation of the assembly, Fig. 4c,
- Step 4: cross-load of the assembly, Fig. 4d.

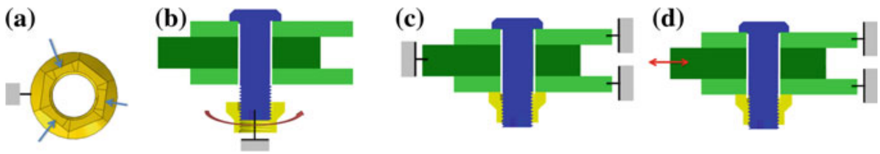

Fig. 4. The four steps of simulation

The Deformation and the Tightening of the Nut

The first step is the deformation of the nut. Three radial forces (Fig. 4a) make the nut oval due to the plastic strain.

The second step of the model is the tightening of the bolt by screwing the nut at a torque of 22 Nm, corresponding to an average preload of 60% of the Ultimate Tensile Strength. As the nut is self-locked, a locking torque needs to be overcome before accosting the plate as it can be seen Fig. 5. Three main parameters will need to be validated: the locking torque, the preload and the tightening torque. These characteristics can be deduced thanks to the evolution of the preload and the tightening torque during this step as it can be seen Fig. 5.

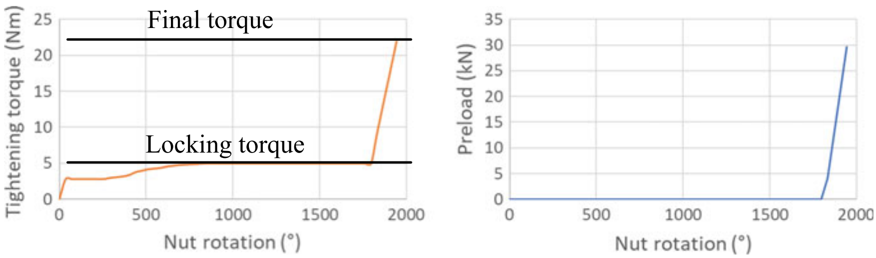

Fig. 5. Evolution of the tightening torque (on the left) and the preload (on the right)

The values of the tightening torque and of the deformation load, used to deform the nut during step 1, have been chosen in order to be in agreement with the Airbus standards for this kind of bolts. The preload has been measured thanks to the evolution of the axial component of the stress in the screw rod. As it can be seen Fig. 6a, the screw is in tension whereas the plates are compressed. However, as it can be seen Fig. 6b and c, the tightening steps create some plastic strain, even in the threads.

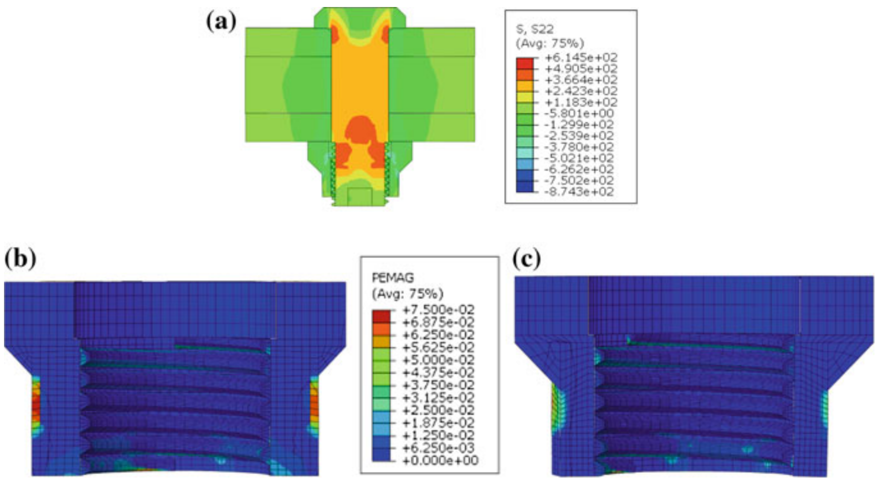

Fig. 6. The axial stress distribution **a** the magnitude of plastic strain at integration point before tightening **b** and after tightening **c**

The Cycling

After a relaxation step, the last simulated step is the cross-load of the assembly. A sinusoidal load of 31kN has been applied to the middle plate. Once the transverse load overcomes the friction between the clamped parts, the medium plate slides on the upper and lower ones. As soon as the medium plate contacts the screw, the latter starts bending. The transverse sliding of the nut can be observed when the transverse load reaches a certain value. The Fig. 7 highlights the evolution of the transverse relative displacement between the nut, or the screw head, and its bearing surface.

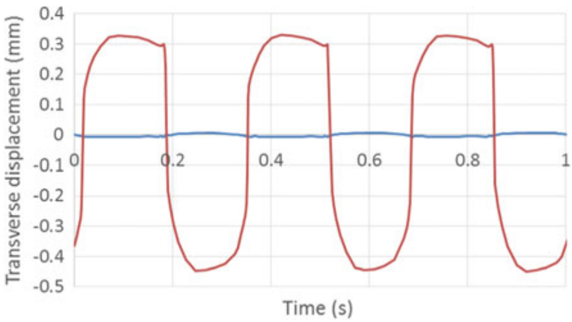

Fig. 7. The transverse sliding of the nut (in red) and the screw (in blue)

According to Zadoks, this movement would also imply the rotation of the nut and thus its loosening. It can be noticed that the curve is not symmetric. In its initial configuration, the bolt might not be centered in the hole of the plate, then the transverse sliding might be different a direction from another. Moreover, due to different friction coefficients, the amplitude of displacement is bigger for the nut than for the screw, and therefore the rotation of the nut should be larger that of for the screw. In order to check this theory, the rotation of the nut and the screw have been drawn Fig. 8. The results are presented for the five first cycles. Assuming that the loosening speed remains the same over the whole step, the loosening angle after 500 cycles should be 73°.

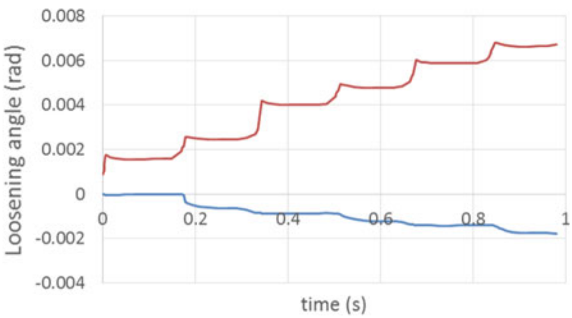

Fig. 8. The loosening angle of the screw (in blue) and the nut (in red)

In order to get results as close as possible of the self-loosening of a real assembly, the value of the cross-load, implying the loosening of the bolt, needs to be determined. Thus, specific tests were done in order to determine the amplitude of rotation of the different components for a specific load after a predefined number of cycles. The latter are presented below.

3 The Experimental Validation

In order to validate the numerical model, some tests are needed. Moreover, they could be used to highlight some specifications linked to the Zadoks explanation. According to him, the loosening of a bolted assembly is only due to the cross-load and to the sliding at the bearing surfaces of either the nut or the screw. Then, the thickness of the clamped plates should not have any influence of the loosening process. In order to verify this theory, three different thicknesses have been tested: 2D, 3D and 4D, D being the diameter of the bolt. Such a test sample can be seen Fig. 2a its geometry is the same than the modeled one. The tightening torque is the same than for the numerical model. The tests are load driven thanks to a 100 kN fatigue test bench, INSTRON 850 l. A sinusoidal shape, with R = −1 and frequency 3 Hz, was chosen for the cross-load. Its amplitude started at 1 kN, and was increased by steps of 2 kN every 500 cycles. We considered that a rotation of 80° was equivalent to a complete loss of preload, as such a rotation has been caused by the tightening torque. The rotation was measured every 500 cycles, and the test was stopped if rotation exceeded 80°.

For each thickness, the bolt starts to loosen for a cross-load around 32 kN as it can be seen Table 2, thus the thickness of the assembly seems not to have any impact on the behavior of the assembly. Moreover, for every test only the nut is rotating and its average amplitude of rotation is 80°, which is equivalent to a complete loss of preload. The rotation at the end of the tests can be seen Table 2, the cross-load at the start of the loosening can also be read. As it can be seen on this Table, the rotation of the nut obtained thanks to the numerical model matches the experimental results. Then the model seems to reproduce the self-loosening of the real assembly.

Table 2. The maximum angular rotation and the cross-load of 3 different thicknesses

Thickness	Cross-load (kN)	Maximum angular rotation (°)	Numerical results (°)
2D	31	83	73
3D	35	78	74
4D	33	85	78

4 Self-loosening Explanation

According to Zadoks theory, the sliding of either the nut or the screw on their bearing surfaces will imply the self-loosening of the bolt. Moreover, as shown before, only the nut is loosening, thus the contacts between this component and the plate will be analyzed. The plates are painted with primer, thus the sliding of the nut might remove the coating where the nut has slid. Moreover, if we take a closer look at the nut, Fig. 9a, a damaged area can be seen.

In order to determine the sliding displacement, the nut gets removed after the test. The marking due the sliding has been analyzed. As the diameter of the nut is known, we can determine the approximate external positions of the nut during the slip, Fig. 9b. A relative displacement of 0.52 mm has been measured between these two positions.

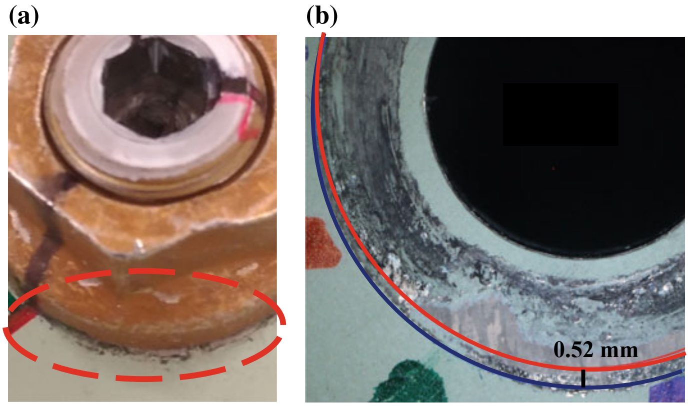

Fig. 9. Damage of the paint under the nut

This sliding is the root cause of loosening according to Zadoks explanation. Thanks to the numerical model developed, this value of transverse sliding has also been measured. Its maximum value is 0.527 mm which matches the experimental measurement.

5 Conclusion

Since the beginning of the seventies, sliding is considered as the root-cause of self-loosening. Junker is the first to have proposed an explanation based on experiments made thanks to a specific test bench. He based his explanation on the sliding movements which are due to the bending of the screw when the assembly is cross-loaded. Zadoks showed that beyond a certain transverse load, the nut or the screw slides on the bearing surface leading to the loosening of the joint.

In order to prove that either the nut or the screw was sliding on the plate, a numerical model was developed. In comparison to existing studies, the specificity of the model was the complete modeling of the threads, the plastic deformation of the nut to self-lock it and the tightening of the joint thanks to the rotation of the nut of the screw. The model has been verified by experiments. In addition to it, the tests also highlighted that the thickness of the assembly has little influence on the behavior of the cross-loaded assembly. An analysis of the surface under the nut showed that the nut slipped on the plate. According to Zadoks theory, this sliding is sufficient to loosen the bolt.

References

1. Dinger G (2016) Design of multi-bolted joints to prevent self-loosening failure. J Mech Eng Sci 230(15):2564–2578. https://doi.org/10.1177/0954406215612813
2. Sanclemente JA, Hess DP (2007) Parametric study of threaded fastener loosening due to cyclic transverse load. Eng Failure Anal 14:239–249

3. Izumi S, Yokoyama T, Iwasaki A, Sakai S (2005) Three-dimensional finite element analysis of tightening and loosening mechanism of threaded fastener. Eng Failure Anal 12:606–615
4. Dominik J, Zmindak M (2012) Spontaneous unfastening and fatigue of Bolted Joints. Manuf Ind Eng 1:41–43
5. Junker G (1968) New criteria for self-loosening of fasteners under vibration.
6. Kasei S (2007) A study of self-loosening of bolted joints due to repetition of small amount of slippage at bearing surface. J Adv Mech Design, Syst Manuf 1:358–67. https://doi.org/10.1299/jamdsm.1.358
7. Zadoks RI, Yu X (1977) An investigation of the self-loosening behavior of bolts under transverse vibration. J Sound Vibration 208:189–209
8. Dinger G (2011) Avoiding self-loosening failure of bolted joints with numerical assessment of local contact state, Eng Failure Anal 18:2188–2200
9. Eccles W, Sherrington I, Arnell RD (2009) Towards an understanding of the loosening characteristics of prevailing torque nuts. J Mech Eng Sci 224:483–494
10. Hatorri T, Yamashita M, Mizuno H, Naruse T (2010) Loosening and sliding behaviour of bolt-nut fastener under transverse loading. EPJ Web of Conference
11. Izumi S, Yokoyama T, Kimura M, Sakai S (2009) Loosening-resistance evaluation of doublé-nut tightening method and spring washer by three-dimensional finite element analysis. Eng Failure Anal 16:1510–1519
12. Jiang Y, Zhang M, Lee CH (2003) A study of early stage self-loosening of bolted joints. J Mech Design 125:518–526
13. Pai NG, Hess DP (2002) Experimental study of loosening of threaded fasteners due to dynamic shear loads. J Sound Vibration 253:585–602

A New Approach for Machine-Tool Architecture Selection at Preliminary Design Stage

M. Lajili, H. Chanal(✉), C. Bouzgarrou, and E. Duc

Université Clermont Auvergne, CNRS, SIGMA Clermont, Institut Pascal, 63000 Clermont–Ferrand, France
Helene.chanal@sigma-clermont.fr

Abstract. Productivity and quality requirements in the aerospace industry involve optimized machine-tools in terms of stiffness, precision, kinematics and dynamics. Many researches aiming at evaluating and optimizing machine-tool performances in the preliminary design stage have been carried-out. This paper presents a new approach for selecting the best appropriate machine-tool architecture, for a given application, based on optimizing conceptual design models. In fact, considered machine-tool structures are modeled with simplified shape parts. The dimensions of these parts are defined as design variables. Afterward, a parametric design optimization is performed for each considered architecture, in order to minimize its total mass under the constraint of a minimal attempted stiffness all over the workspace. After that, several architectures can be compared and classified according to performance indices computed from the mechanical behavior of their corresponding optimized structures. This approach allows restricting the total number of structural arrangements to be detailed further and analyzed more accurately. The paper includes an illustration of the proposed approach through a comparative study between an open-loop and a closed-loop machine-tool architectures.

Keywords: Machine-tool · Stiffness · Preliminary design · Parametric optimization

1 Introduction

The performance requirements of machine-tools dedicated to hard material large parts machining have strongly increased during the last decade due to the expansion of the aerospace industry [1, 2]. Indeed, to boost aeronautical parts performances in terms of weight, corrosion resistance and mechanical ability, titanium alloys are widely used for structural parts [1, 3].

Titanium machining is characterized by low cutting speeds and high cutting forces [4]. High cutting forces coupled with low rotational frequencies of the spindle can produce large deflections and excite natural modes of the machine-tool structure. Thus, static behavior and first natural frequencies have to be controlled during the design stage [5–7].

F. Cavas-Martínez et al. (Eds.): *Advances on Mechanics, Design Engineering and Manufacturing II*, LNME, pp. 95–104, 2019.
https://doi.org/10.1007/978-3-030-12346-8_10

Among the most used performance criteria we find: geometric workspace, dexterity, accuracy, stiffness and the dynamic behavior [8, 9]. Dehong and Kai consider that a static stiffness around 500 N/μm is well desired for heavy cutting machine tools [10]. Thus, methods should be developed to help the designer to evaluate performance indicators of its choice of machine-tool structural arrangement at an early design stage [11].

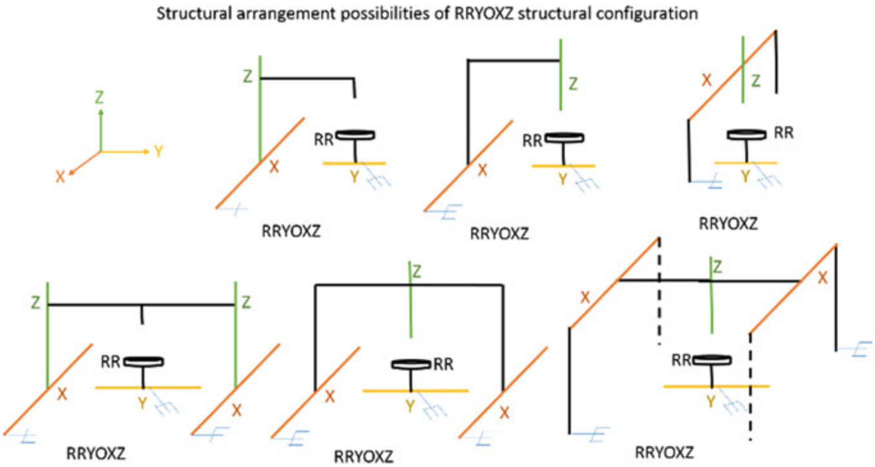

Fig. 1. Several architectures associated with the structural configuration *RRYOXZ*

Conceptual design is a main goal as it ensures designer to check the performance indicators with regard to attempted specifications at an early design stage [11]. Moreover, by performing advanced analysis for different possible architectures, we can observe if a machine-tool structure may be more relevant than another.

A structural configuration indicates axes arrangement of a machine-tool. It can be designated by a configuration code [12, 13]. Several configurations must be considered and analyzed (studied) in order to determine adequates ones for a given machining application. A previous work allowed us to realize a first sorting of 5-axes machine-tool structural configurations for titanium machining [13]. In fact, 2160 machine-tool configurations were analyzed. The classification was done by evaluating structural configurations conformity degree with respect to technical criteria. Indeed, 32 machine-tool configurations, fulfilling all design criteria, were selected.

The above mentioned method made it possible to restrict the number of machine-tool structural configurations for the detailed design phases. However, as could be seen in Fig. 1, *RRYOXZ* configuration can be achieved with different structural arrangements or architectures. Therefore, the design methodology to be elaborated must integrate the selection of the machine-tool architecture.

The approach presented in this paper aims at selecting the most appropriate machine-tool architecture while regarding given machining operations (in our case titanium alloys machining) during preliminary design step. The particularity of our approach is that we consider several possible arrangements of machine-tool mechanical structures. These structures are modeled, analyzed and optimized in terms of mass and stiffness.

Being on preliminary design stage, the machine-tool structure are simplified and modeled with hollow box-shaped parts with shell structural elements. The dimensions of these parts are parametrized and defined as design variables. Design optimization is performed by coupling a constrained optimization algorithm, using a Matlab function, with finite element method (FEM) analysis, in ANSYS, for stiffness evaluations. After that, optimized solutions are compared according to their performances to select the most relevant structure.

In the next sections, we present the parametric design of machine-tool structure, the optimization process is introduced with the stiffness computation method. Finally, we introduce the comparison result of two type of machine tool architecture (closed-loop and open-loop architecture).

2 Parametric Design of Machine-Tool Structure

Parametric modeling of mechanisms is widely used at the early design stage [14]. Performing parametric modeling make it easier to modify structure dimensions, consequently preparing model to be improved and optimized. Danhaive and Mueller combine parametric modeling and interactive optimization in order to obtain efficient and innovative structural design [15]. Maglie relies on parametric design language to achieve automated creation of machine-tool model in particular APDL (Ansys Parametric Design Language) [16].

Koenigsberger presented a structural analysis of machine-tool with a simplified formulation of its structure [17]. In fact, he used beam elements as basic structural components for modeling machine-tool structure (Fig. 2). However, in our case study, we choose to not use beam even if this approach seems to be relevant. Indeed, identified beams sections are larger compared to their lengths due to the important value of the attempted rigidity. Thus, beam theory hypothesis are no longer verified. Therefore this modeling approach is too approximate.

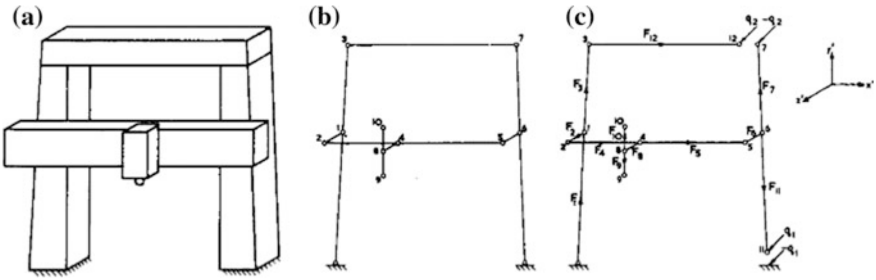

Fig. 2. Lumped model of a milling machine [17]

Kono et al. presented an evaluation of modelling approaches for machine-tool design [18]. Machine-tool components are modeled by parallelepiped shape and obtained results are close to experimental results. In the same context, Li et al. developed an optimization approach to provide an eco-efficient machine-tool bed structure [14]. In the first step of this method, machine bed is modeled simply by a hollow box-shaped structure. Thus, authors choose to use hollow parallelepiped forms to model machine-tool elements.

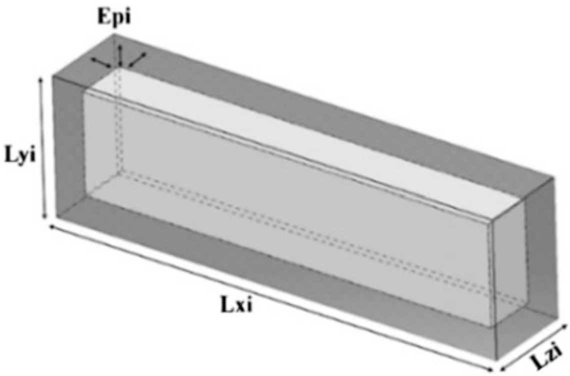

Fig. 3. Parameterized hollow parallelepiped

In this work ANSYS APDL is adopted where model construction uses a script text file. The method consists in sub-structuring machine tool structure. Each elements is modeled by a parameterized hollow parallelepiped as shown in Fig. 3. The parallelepiped parameters are section width, section length and thickness (L_{yi},, L_{zi}, and E_{pi}). Parallelepiped length (L_{xi}) is fixed considering workspace specifications.

In this paper the study is limited to two kind of machine-tool structural arrangements (open-loop and a closed loop machine-tool structure). The two architectures are sub-structured into three principals' components each and parametrically modeled as presented in Fig. 4. Components are clamped to each other by their common surfaces. The first sub-structure is fixed to the ground. The second performs translation along Z axis and the last one can translate along Y axis. Hence, the machines configurations change according to the tool position in the workspace. Translation movement in X direction is performed by the machining table. Thus the workspace of the considered structure is the YZ plane.

Since the aimed machine-tools are designed for aeronautical part machining, their workspace must be large. Thus, milling tool positions along Y and Z axis range from 0 to 2 m. FE models of the structures are implemented in a manner to guarantee always the same workspace independently from components parameters variation. That's why parallelepiped lengths L_{xi} are defined as exposed in Table 1. A steel material is used for the studied machine-tool structure and FE model is meshed by shell elements with a maximal size of 20 cm.

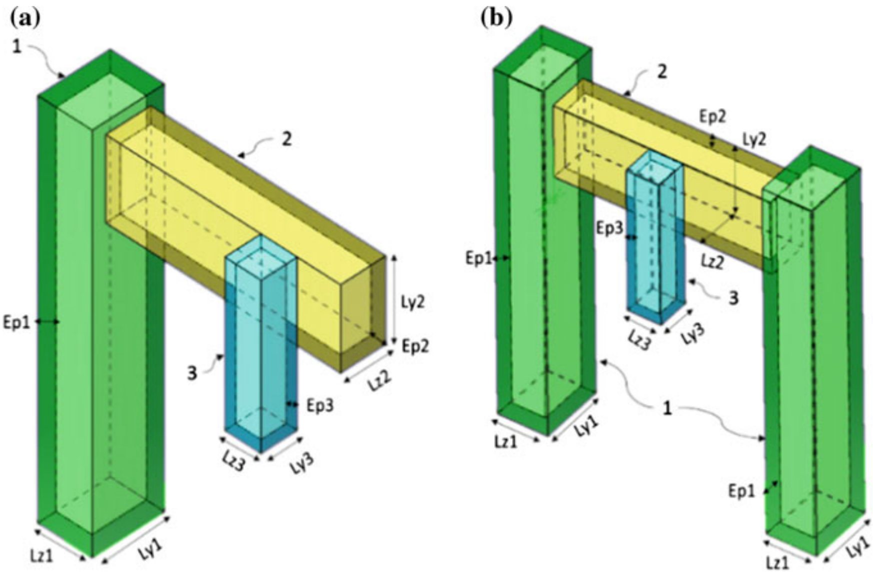

Fig. 4. Parametric model of an open-loop architecture (**a**) and a closed-architecture (**b**)

Table 1. Parallelepiped lengths

Length	L_{x1}	L_{x2}	L_{x3}
Value (m)	3.7	$2.2 + L_{z3}$	1.5

3 Parametric Optimization of Machine-Tool Structure

Parametric optimization consists in varying initial parameterized dimensions of a model in favor of obtaining an optimal design with the allowed resources [19, 20]. Contrarily with topologic optimization and shape optimization, in this type of optimization initial shape and topology are preserved [21]. Pons relies on parametric optimization for the design of ultrasonic motors [22]. He elaborated a parameterized FEM model and observed 5% of error relatively to experimental results.

In order to compare several machine-tool architectures, performance indicators like stiffness at the TCP, the total weight and natural frequencies should be computed. However, to ensure the objectivity of the comparison between machine-tools with different structural arrangements, each mechanical structure must be optimized in terms of mass and stiffness.

To realize the optimization, a Matlab function named ‘fmincon’ is chosen. At each iteration, the objective function is computed and by using ANSYS APDL, structure stiffness is evaluated. The optimization loop continues until a stopping tolerance criteria or minimum is achieved.

3.1 Definition of Objective Function and Constraints

The cost function to be minimized is the total mass of the structure. Design variables are the dimensions of the machine parts modeled by hollow parallelepiped (L_{yi}, L_{zi} and E_{pi}). These variables are collected in a vector denoted by ξ as shown in Eq. (1). Lower and upper bounds of the design variables are given respectively by $\xi_{\min}$ and $\xi_{\max}$.

$$\begin{aligned} \xi &= \left[L_{y1}, L_{z1}, E_{p1}, L_{y2}, L_{z2}, E_{p2}, L_{y3}, L_{z3}, E_{p3}\right] \\ \xi_{\min} &= [0.6, 0.6, 0.02, 0.5, 0.5, 0.02, 0.4, 0.4, 0.05] \\ \xi_{\min} &= [1.5, 1.5, 0.15, 1.4, 1.4, 0.15, 1, 1, 0.15] \end{aligned} \tag{1}$$

The total mass of the structure, denoted by M, is computed by the multiplication of the structure volume V by the material density ρ. The structure volume V is the sum of all hollow parallelepiped volumes forming the structure but without considering common volumes twice. Then, the objective function for considered architectures is expressed in function of design variables ξ and the parallelepiped lengths (L_{x1}, L_{x2}, and L_{x3}) as expressed in (2).

$$M = \rho \times V(\xi, L_{x1}, L_{x2}, L_{x3}) \tag{2}$$

Attempted stiffness is a design constraint. This constraint is fulfilled only if the machine TCP rigidity all over the workspace and along any direction in the 3D space (K) is equal or higher than attempted value. Thus, K must be computed at each optimization iteration and compared with the attempted stiffness. That's why, an under constraint optimization algorithm is used. For a target rigidity of 500 N/μm, the optimization constraint is a nonlinear inequality as indicated in Eq. (3). The machine-tool stiffness computation is explained in next section.

$$K \geq 500 \tag{3}$$

3.2 Machine-Tool Stiffness Computation

Firstly, a static FE ANSYS analysis is performed. Three load cases are applied respectively: a force in each axis x, y and z $\left(\left[F_x, 0, 0\right]^t, \left[0, F_y, 0\right]^t \text{ and } \left[0, 0, F_z\right]^t\right)$ and measured displacements at the TCP is then transferred from ANSYS to Matlab environment. We denote by U_{xi}, U_{yi} and U_{zi} the measured displacements for a force applied in axis i. these measures enable computing compliance and stiffness matrices at the TCP as detailed in Eqs. (4) and (5).

$$[S] = \begin{bmatrix} \frac{U_{xx}}{F_x} & \frac{U_{xy}}{F_x} & \frac{U_{xz}}{F_x} \\ & \frac{U_{yy}}{F_y} & \frac{U_{yz}}{F_y} \\ & & \frac{U_{zz}}{F_z} \end{bmatrix} \tag{4}$$

$$[K] = [S]^{-1} = \begin{bmatrix} K_{xx} & K_{xy} & K_{xz} \\ & K_{yy} & K_{yz} \\ & & K_{zz} \end{bmatrix} \quad (5)$$

Next, the configuration stiffness is computed along any direction in the 3D space considering the eigenvalues of the stiffness matrix. Those eigenvalues represent the stiffness ellipsoid parameters and its minimum value represents the minimal rigidity ensured all over the 3D space directions. This rigidity corresponds to the minimal configuration stiffness K_i.

Afterward, in order to compute machine-tool minimal stiffness *K,* several geometric configurations all over the workspace must be considered. Thus, *Y* and *Z* coordinate of the TCP are discretized. During optimization stage, the range of *Y* and *Z* movement is 2 m by a rough step of 0.5 m, which mean that 25 different configurations are investigated at each iteration (Fig. 5a).

Finally, the machine-tool minimal stiffness *K* could be computed as shown in Eq. (6). The red point at each figure (Fig. 5a and b) represent the minimal stiffness all over the workspace.

$$K = \min_i (K_i) \quad (6)$$

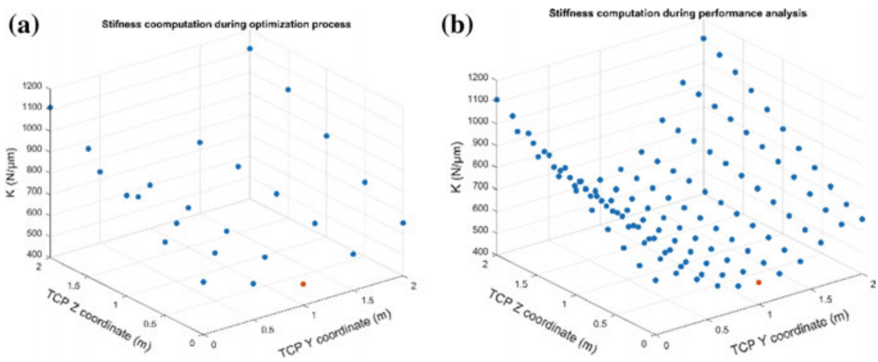

Fig. 5. Closed loop structure stiffness computation during optimization (**a**) and during performance analysis (**b**)

4 Results

The optimization process is realized for different attempted rigidity values (100, 200, 300, 400 and 500 N/µm). Optimized architectures performances are computed by a static and modal analysis overall workspace. As mentioned in Sect. 2, *YZ* plane is considered as the structure workspace independently from *X*. A step of 0.2 m is chosen to discretize *YZ* workspace which means that 121 configurations are investigated (Fig. 5b).

In our approach, the compared structures have the same workspace, and they are optimized to ensure the same stiffness at the TCP. Therefore structure comparison is done regarding total masse, movable masse, and natural frequencies evolution.

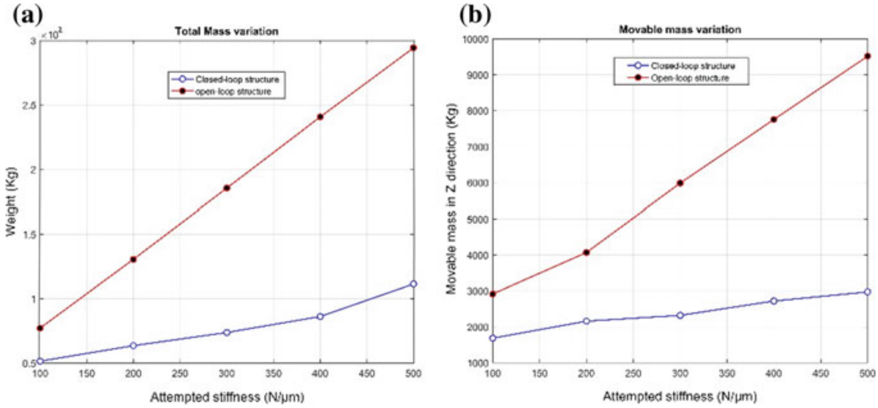

Fig. 6. Comparison of total masse variation (**a**) and movable Z mass (**b**) against attempted rigidity

Comparison of total masse variation of optimized structures shows that closed-loop architecture is significantly lighter in all instances (Fig. 6a).

Movable mass in Z directions varies as could be seen in Fig. 6b. In all cases also, movable mass of closed-loop structure is extremely lower than that of open-loop structure.

Performed modal analysis on optimized structure provides first and second natural frequencies. As long as it changes with structure configuration, the worst configuration case is assumed as a reference for each types of structure. As can be noticed in Fig. 7, first (a) and second (b) natural frequencies of closed-loop model are always higher than frequencies observed on open-loop structure.

Having regard to masse, movable masse and natural frequencies variations, considered closed-loop structure is more relevant for titanium machining operations than open-loop one.

5 Conclusion

In this paper, an approach for machine-tool architecture selection in preliminary design stage has been presented. This approach is based on parametric optimization of several architectures associated with a given structural configuration of the machine-tool. Adopted deign variables are the dimensions of the structural parts with simplified geometry. Optimization has been performed by coupling Matlab constrained

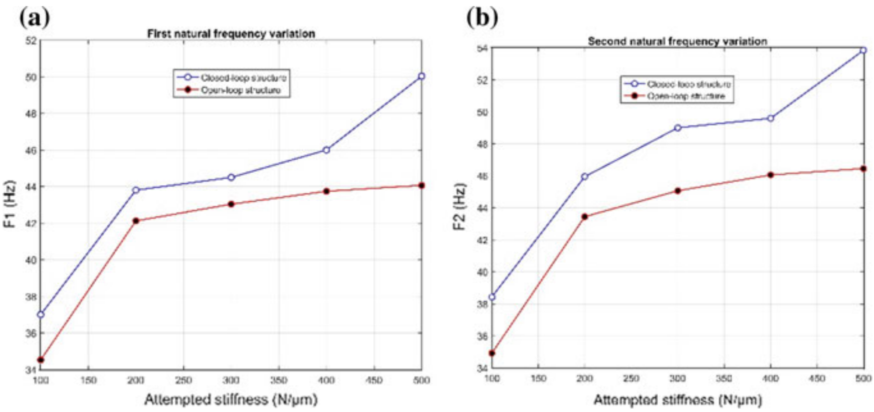

Fig. 7. Comparison of first (**a**) and second (**b**) natural frequencies

optimization algorithm with finite element analysis software (ANSYS). Thus, optimized architectures have been compared referring to performance indicators evaluated with a FEM analysis.

Treated machine-tool examples show the validity and the effectiveness of the developed approach. Investigated performance indicators comparison allowed us to eliminate easily the open-loop structure. Therefore, for the two studied architectures, only the closed-loop one will be analyzed more accurately.

Acknowledgments. This work belongs to the MMaSyF project (2015–2020) funded by the CPER Auvergne-Rhône-Alpes Region for the design and production of a high rigidity machine-tool. This work is co-financed by the European Union. Europe engages in Auvergne with the European Regional Development Fund (FEDER).

L'EUROPE S'ENGAGE en région Auvergne-Rhône-Alpes avec le FEDER

UNION EUROPÉENNE

La Région Auvergne-Rhône-Alpes

References

1. Inagaki I, Tsutomu T, Yoshihisa S, Nozomu A (2014) Application and features of titanium for the aerospace industry. Nippon Steel Sumitomo Met Tech Rep 106:22–27
2. Henriques VAR (2009) Titanium production for aerospace applications. J Aerosp Technol Manag 1(1):7–17
3. Wagner V (2011) Amélioration de la productivité en usinage d'un titane réfractaire : le Ti555.," Université de Toulouse
4. Moussaoui K (2013) Influence de l'usinage sur la durée de vie en fatigue de pièces aéronautiques en alliage de titane. Université Toulouse 3 Paul Sabatier (UT3 Paul Sabatier)
5. Cheng K (2009) Machining dynamics: fundamentals, applications and practices

6. Mori M, Piner Z, Ding K, Hansel A (2008) Virtual evaluation for machine tool design. In: Proceedings of the 9th biennial asme conference on engineering systems design and analysis, 2008, pp 1–5
7. Maj R, Bianchi G (2005) Mechatronic analysis of machine tools. In: SAMTECH Users Conference, pp 1–16
8. Chanal H (2006) Etude de l'emploi des machines outils à structures paeallèle en usinage
9. Bouzgarrou BC (2001) Conception et modélisation d'une machine-outil à architecture hybride pour l'UTGV. Thèse de Doctorat, Institut Français de Mécanique Avancée et Université Blaise Pascal
10. Dehong H, Kai C (2009) Basic concepts and theory. In: Kai C (ed) Machining dynamics fundamentals, applications and practices, pp 7–21
11. Mekid S (2009) Design strategies and machine key-components. In: Introduction to precision machine design and error assessment, Mechanical, pp 129–192
12. Chen F-C (2001) On the structural configuration synthesis and geometry of machining centres. In: Proceedings of the Institution of Mechanical Engineers, Part C vol 215, no. 6, pp 641–652
13. Lajili M, Chanal H, Bouzgarrou BC, Duc E (2017) Methodologie De Choix D'une Architecture De Machine-Outil 5 Axes Pour L' Usinage Du Titane. in *23ème Congrès Français de Mécanique*
14. Li B, Hong J, Wang Z, Wu W, Chen Y (2012) Optimal design of machine tool bed by load bearing topology identification with weight distribution criterion. Procedia CIRP 3 (1):626–631
15. Danhaive RA, Mueller CT (2015, August) Combining parametric modeling and interactive optimization for high-performance and creative structural design. IASS—Annual International Symposia of the IASS Future Vis
16. Maglie P (2012) Parallelization of design and simulation: virtual machine tools in real product development. Mech Eng 19801
17. (Franz) Koenigsberger F, Tlustý J (1970) Machine tool structures
18. Kono D, Lorenzer T, Weikert S, Wegener K (2010) Evaluation of modelling approaches for machine tool design. Precis Eng 34(3):399–407
19. Deneffle R (2017) Définition d'une méthodologie d'allègement de structures sous contrainte de rigidité fonctionnelle, cas d'une machine-outil. Université Clermont Auvergne
20. Ponche R (2013) Méthodologie de conception pour la fabrication additive, application à la projection de poudres
21. Halila F, Fauvin V, Polmard A, Matlab C (2017) Algorithmes d'optimisation topologique pour l'allégement des poutres en PMH de la caisse-en-blanc en utilisant un couplage entre Matlab et Ansys. In: 23ème Congrès Français de Mécanique
22. Pons JL, Rodríguez H, Fernández JF, Villegas M, Seco F (2003) Parametrical optimisation of ultrasonic motors. Sens Actuators A Phys 107(2):169–182

Measurement Device Design: Multipurpose Rain Gauge

M. C. Ladrón-de-Guevara-Muñoz(✉), A. J. Sánchez-Martos,
O. D. de-Cózar-Macías, E. B. Bláquez-Parra, and
I. Ladrón-de-Guevara-López

University of Málaga, c/Dotor Ortiz Ramos s/n, 29010 Málaga, Spain
clguevara@uma.es

Abstract. The need to size large hydraulic infrastructures, exploit extensive agricultural areas or simply arrange water assets for human consumption makes the evaluation of the available water resources essential. Water is a scarce resource that is poorly distributed both, spatially and temporally. Therefore, a set of hydrological networks that allow the evaluation of water quantity and quality is required. In order to achieve this, the first step is to retrieve reliable data on rainfall. To carry out a correct evaluation of water resources, both in the small and large scale, disposing hydrological networks that involve a certain number of measuring devices becomes critical. Despite the great amount of studies that have been developed on measuring devices such as rain gauges, there are still many errors that remain in the measurements and that have not been ruled out yet, thus affecting the accuracy of the measurements. Accordingly, the design of a device that provides an accurate measurement of rainfall and also results affordable, could be the key to a product with great acceptance in the market. This work aims at presenting the design of a measurement device that provides accurate data and can be used in multiple ways: as an ordinary rain gauge, as a rain gauge recorder, or even allowing to carry on both functions simultaneously. Therefore, the design must bring together acceptable requirements regarding precision and economic aspects. As a result of the work developed, the proposed design has led, after a long process, to be patented with previous examination.

Keywords: Rain gauge · Patent · Design · Precipitation · 2-in-1

1 Introduction

For thousands of years, man has tried to quantify rainfall in one way or another. The first recorded measurements were performed in India 400 years BC. In 1639, the benedictine Benedetto Castelli (1548–1643) born in Brescia [1], was the first in Europe to introduce, in a letter addressed to Galileo Galilei (1564–1642), the techniques for rainfall measurement employed to find out how much the water in the Trasimeno lake would increase. Since then, new measuring devices, techniques and procedures have been studied. It is actually not known who the inventor of the rain gauge was for, somehow, direct or indirectly rainfall has been measured since ancient times. Civilizations long BC already tried to store rain for later use, therefore they already had

F. Cavas-Martínez et al. (Eds.): *Advances on Mechanics, Design Engineering and Manufacturing II*, LNME, pp. 105–122, 2019.
https://doi.org/10.1007/978-3-030-12346-8_11

proof of the amount of rainfall occurring. In his work, Strangeways [2] analyzes the different measurement systems in its beginnings (Fig. 1) and Kurtyka [3], on the other hand, makes a chronology that reaches our days and considers the civilizations that began to be interested in precipitations measurement (Fig. 2).

Fig. 1. Korean pluviometer reproduction. London Science Museum

According to WMO (World Meteorological Organization), rainfall can be defined as: “any liquid or solid particle product of the condensation of water vapor fallen from the clouds and deposited on the ground. This includes: rain, hail, snow, frost, dew and haze” [4].

Meanwhile, Maderey Rascón et al. [5] make a classification that may help to understand and have a general perspective of what types of rainfall can occur.

- Properly said precipitation
- Water that reaches the earth’s surface in liquid form (rain)
- Water that arrives in amorphous solid form (hail)
- In crystallized solid form (snow)
- In intermediate form (granulated snow, sleet, etc.)

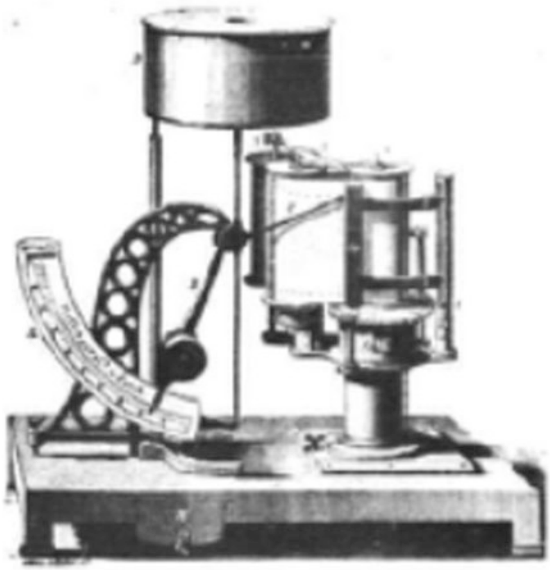

Fig. 2. Hottinger weighing pluviometer. Germany (1871)

– Hidden precipitation
– By condensation (dew)
– By sublimation (frost).

To quantify the total amount of rainfall, the height in millimeters that the water film would reach on a flat horizontal surface is considered. The most elementary way to measure precipitation would be to collect them in any container with straight walls and base and then measure the height with a graduated ruler. The container used to store the fallen precipitation is called 'rain gauge' also known as "Odometer" or "Ombrometer". Rain gauges are included in the so-called non-recorder devices that, unlike the "pluviographs" which belong to the group of so-called recording devices, allow precipitation to be recorded automatically. Precipitation assessment and measurement techniques are known by the name of "Pluviometry".

Usually, the word rain gauge has been used to refer to any device employed to measure rainfall. However, as mentioned previously, there are several kinds of precipitation as well as there are many devices to quantify them. The WMO [4] and [6] includes a classification of the instruments and techniques used to measure precipitation. Note that when referring to precipitation here, it is normally addressed to properly said precipitations such as rain, snow, hail, sleet, etc. In the case of frost, dew, ice, etc., there are other methods for measuring.

2 Brief Description of the Technical Problem

Currently, there are two large groups of rain gauges/pluviographs in the market, generally aimed at different types of users.

On the one hand, there are those devices employed by the public meteorological services and official organisms. In this type of apparatus, the materials, devices and mechanisms are made of higher quality and precision. Consequently, they provide fairly accurate measurements. The price of this kind of equipment is often quite high, hence, its use is rather limited.

On the other hand, there are rain gauges used for small-scale studies by companies within the agricultural or environmental sector, or those used for domestic use by amateurs. These devices incorporate lower quality materials or mechanisms. Subsequently, their price is quite lower and the quality of the measures is affected to a greater extent.

Figures 3 and 4 show examples of professional rain gauges, while Figs. 5 and 6, expose rain gauges generally addressed to particular users or small enterprises.

Fig. 3. Bucket Pluviograph Mod. 15188 (Lambrecht)

Fig. 4. Siphon pluviograph Mod. 1507 (Lambrecht)

Fig. 5. Recorder rain gauge

Fig. 6. Recorder rain gauge. Mod HD 2013 (Delta OHM)

There is a series of systematic errors that affect the measurements quality; in the case of lower quality devices these errors become more latent. Among all these errors, the following are the most important:

- Derived from the location and installation of the rain gauge; inadequate placement and poor installation can greatly affect the measurements. The most significant consequence derived from a bad location are wind effects (the error can go up to 10% for rain and 10–50% for snow). Another consequence, for instance, would be a greater entry of precipitation in the rain gauge mouth due to an inadequate height of the installation.
- *Errors in the readings*; due to errors performed by the observer or defects in the observation instruments (poorly graduated rods or test tubes, liquid spill, etc.).
- *Instrumental errors*; each device has a particular design that affects differently the measurements. These errors may be due to the external shape, the materials used during manufacture, its calibration accuracy, etc.
- *Evaporation*; a common and important mistake especially in hot and dry climate areas. It usually varies between 0 and 4% of the measurement.

- *Moisture or wetness*: water that adheres to the rain gauge walls can cause defects in the measurements depending on the device geometry, materials, etc. In summer, the error can vary between 2 and 15%, and in winter between 1 and 8%.
- *Splashes*; when falling precipitation (especially rain) inside the collector, some splashes may occur that make the precipitation amount measured to be lower than the actual amount that fell. It means an error of 1–2%.
- *Snow blizzards*; if devices are not adequately protected against wind, it can occur that during snow blizzards the gusts and turbulences created by the wind remove the snow from inside the rain gauge. In some cases, this can lead to an error of 50% or more.
- *Small cracks*; in Winter, the contents of the recipient may freeze, resulting in small cracks through which the water can escape.

From the afore mentioned errors, those caused by wind [7], evaporation, wetting, snow blizzards and splashes are the most important since the precipitation measured can differ and be up to 30% lower or more. All these errors can be caused both, by meteorological or instrumental factors.

In order to reduce these errors as much as possible, the WMO has established a set of rules regarding the location [8], installation, and rain gauge testing. Likewise, minimum requirements to be fullfilled by any rain gauge to guarantee the measurement quality and homogeneity have been set up [3, 4].

Figure 7 shows the requirements and goals set for the new design.

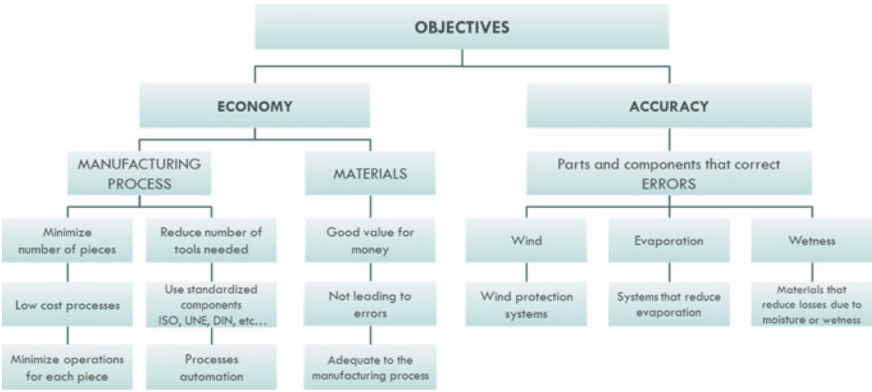

Fig. 7. Chart describing the goals of the new design

3 Methodology

To design and develop the presented rain gauge, the methodology followed has consisted in setting the objectives (Fig. 7), analyzing the techniques and procedures to follow when quantifying rainfall, conducting a market study, and exploring the specifications to agree with WMO. Then, a conceptual design (Fig. 8) is created to finally develop it in full detail (Fig. 9) where different materials are evaluated and simulation tests are performed (Fig. 10) in order to meet acceptable precision and economic requirements.

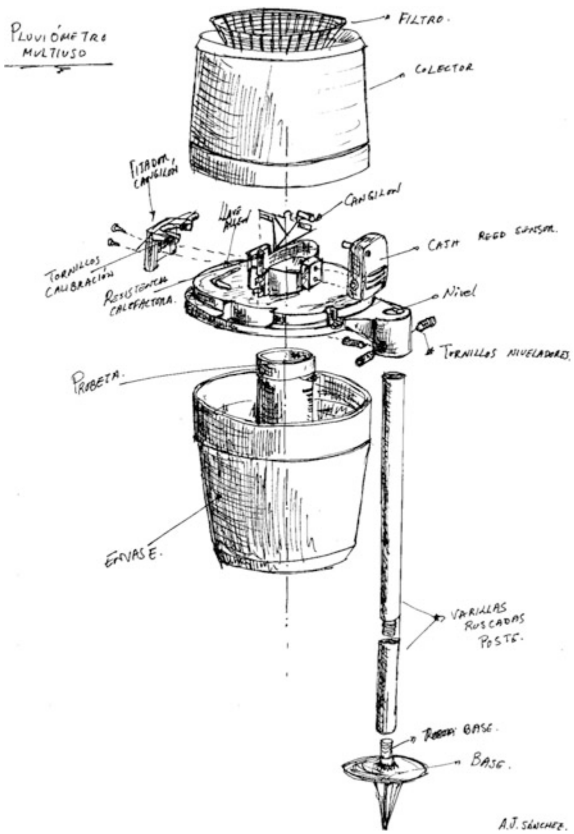

Fig. 8. Conceptual design

4 Description of the Invention

After carrying out an analysis of the techniques, procedures and devices used in the measurement and quantification of atmospheric precipitations, a rain gauge model has been designed with a view to solve the already mentioned problems. A design that is addressed to any kind of user whose components have intended to reduce most common errors in this kind of devices. Through this design, the user has the chance to combine its different components so that it can be used as an ordinary rain gauge (Fig. 11), as a recording rain gauge (pluviograph) (Fig. 12) or both functions at the same time. Besides, the different elements or pieces of the device have been designed aiming at minimizing the errors produced by meteorological factors such as wind and by instrumental factors due to the particular design of the device.

The mechanism used to record rainfall is a precision bucket designed according to Joss-Tognini (Figs. 13 and 14). In this mechanism, a light metal container divided into two compartments is balanced in unstable equilibrium on a horizontal shaft. The bucket

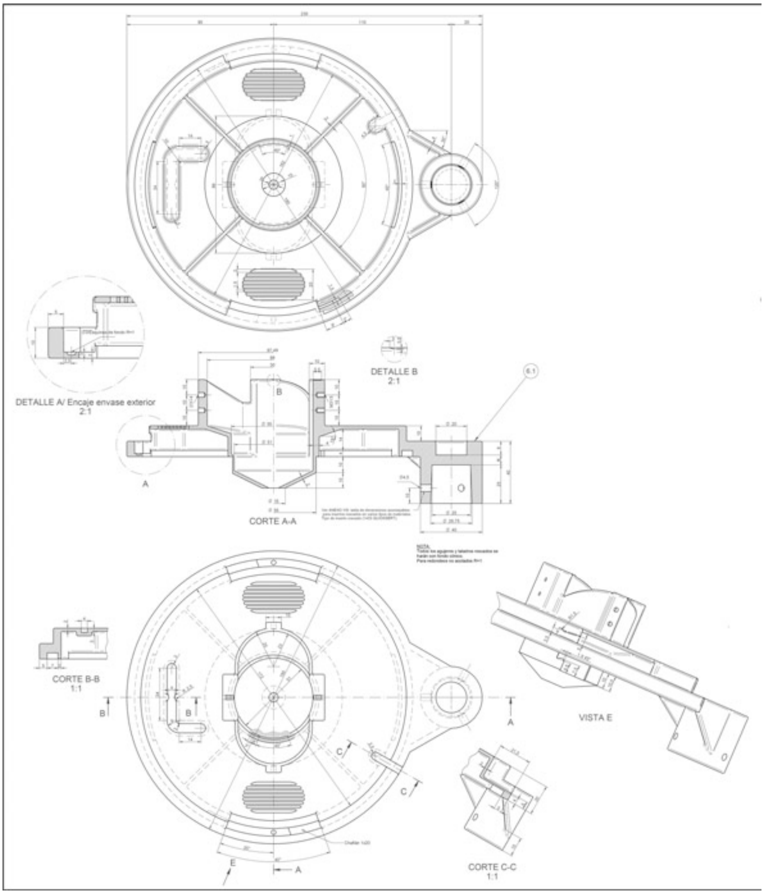

Fig. 9. Detail drawing

normally rests on one of its two stops/ends which prevents it from tipping over completely. Rainwater is conducted from the collector located at its upper part; once a certain amount of water has entered in the bucket, it becomes unstable and turns over, remaining in the other position. The compartments are designed so that when the water is coming out of one of them, it is falling into the other. At the same time, the bucket movement activates a contact relay (Reed sensor) that induces the recording consisting of discontinuous steps; the distance between steps represents the time required to accumulate a certain amount of water.

The design incorporates a bubble level to indicate the perfect leveling of the collector surface (Fig. 15). Three headless screws are responsible for leveling the set. They are distributed at 120° on a conical hole where the pole is inserted. To meet this purpose, an Allen key can be found inside the rain gauge.

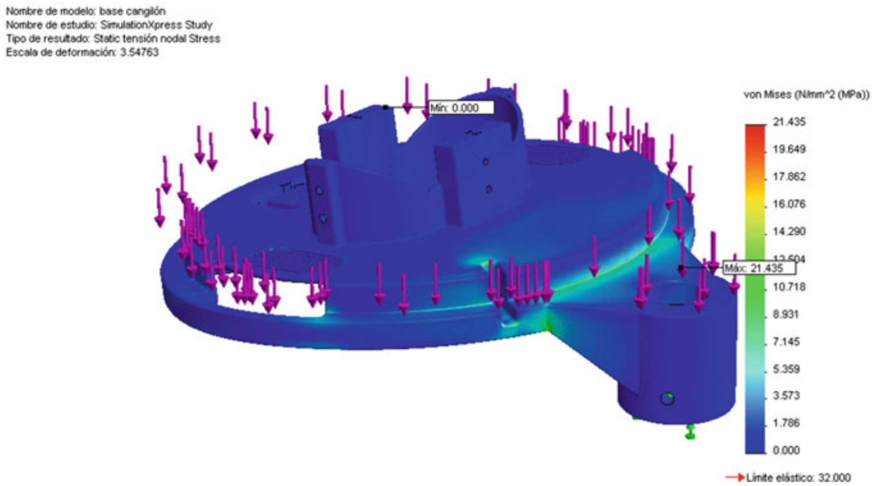

Fig. 10. Simulation tests performed

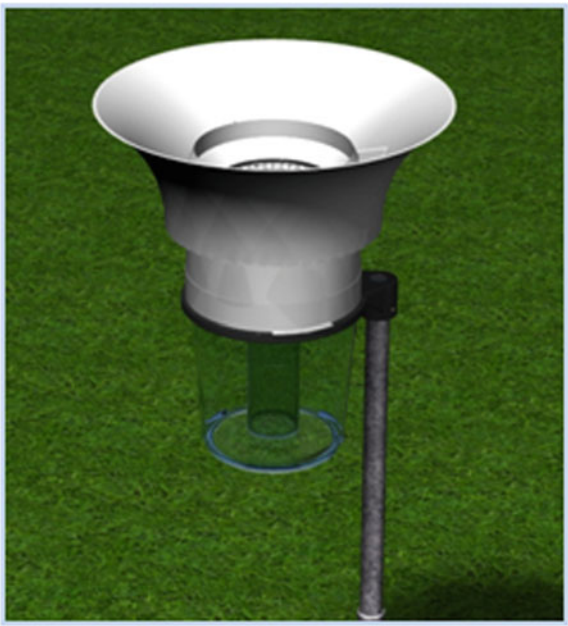

Fig. 11. Ordinary rain gauge

Fig. 12. Recording rain gauge

4.1 Advantages or Benefits Linked to the Invention

The two main advantages achieved by the rain gauge design are the following:

- The user has the possibility to combine the appliance components according to the purpose given, consequently turning it into a recording rain gauge (Fig. 16) and/or into an ordinary rain gauge (Figs. 17 and 18). This novelty helps to reduce manufacturing expenses, since it removes the need to manufacture two types of appliances.
- It is accessible to all kind of users, as its components have been designed employing low cost materials and brief manufacturing processes. In spite of this, the accuracy in the measurements has not been renounced since devices used by professional rain gauges have been incorporated to this model.

In order to reduce the error that affects a greater percentage of rainfall measurements, a collector that incorporates a wind protection element has been designed. Both, the collector and the wind protector are manufactured by plastic injection processes. For this reason, these two parts become one (Fig. 19), thereby reducing manufacturing expenses.

This solution intends to reduce the turbulence created in the collector's mouth that affects the raindrops trajectory and also removes the snow accumulated inside the rain gauge funnel (Fig. 20).

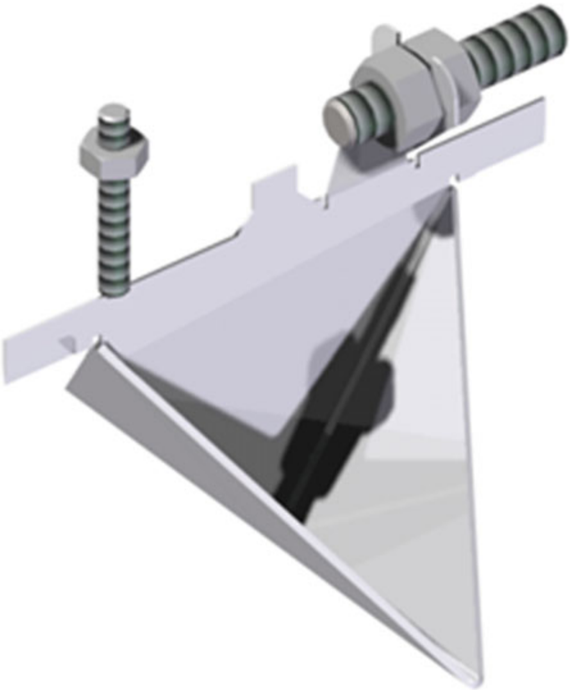

Fig. 13. Precision bucket according to Joss-Tognini

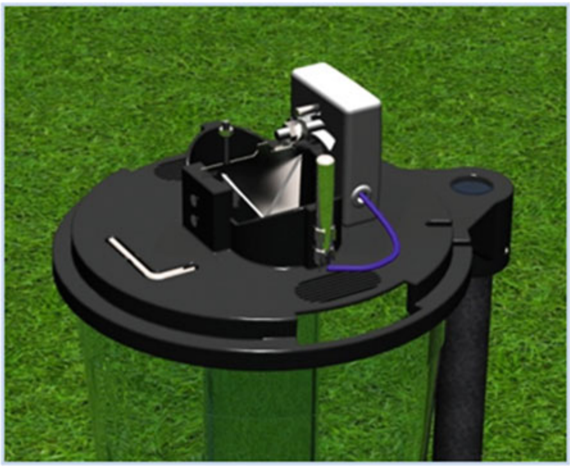

Fig. 14. Bucket assembly detail

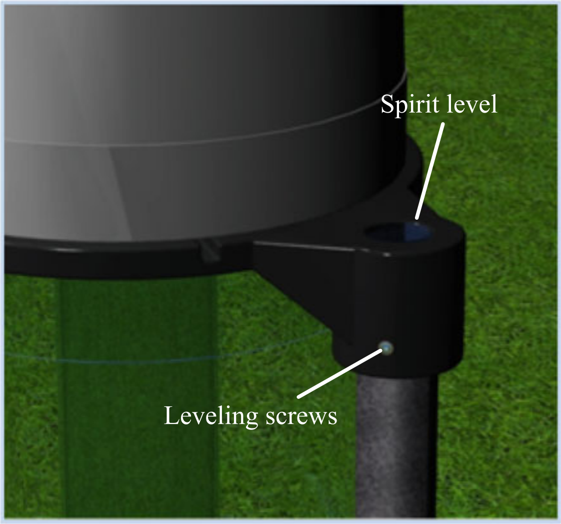

Fig. 15. Bubble level detail

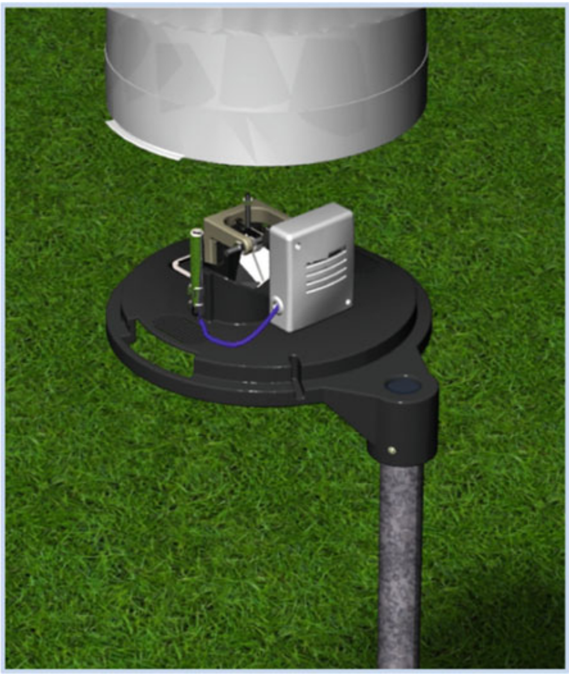

Fig. 16. Recording rain gauge

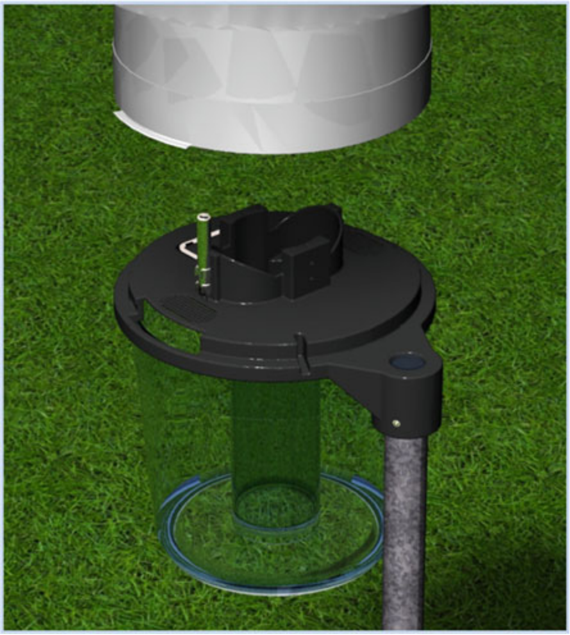

Fig. 17. Ordinary rain gauge

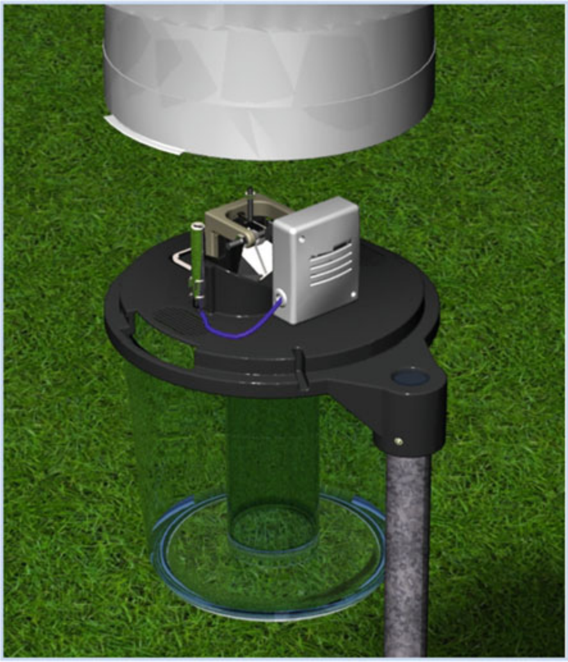

Fig. 18. Ordinary and recording rain gauge

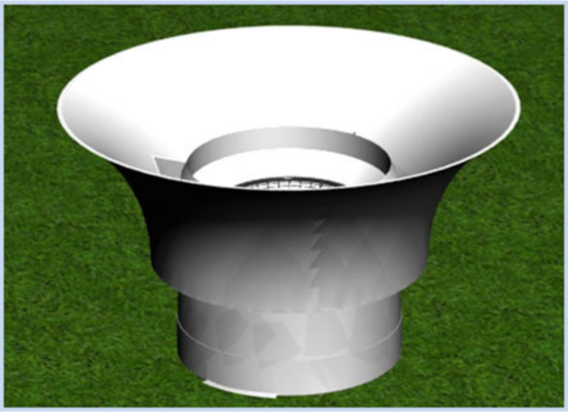

Fig. 19. Collector with wind protection

Fig. 20. Example of wind accumulation at the rain gauge mouth

In addition, a space inside the appliance enables the optional installation of a heater for those users that desire so. The purpose of the heater is to prevent the precipitations from freezing in the collector funnel or inside the device during the winter season.

Another important novelty is the time required to assemble and disassemble the collector, tube and exterior container. All screws and fixation mechanisms have been replaced by strategically distributed grips and tabs in order to insert and attach all elements with a single turn. Therefore, the new design becomes fast and easy to assemble and disassemble.

The tube and the external container transparency allows the readings to be made directly on the rain gauge with no need to transfer the content to an auxiliary metering tube. This also removes errors due to wetting and liquid losses during the transferring operations.

Although the tube capacity reaches 12 l/m^2, a small opening in its upper rear part allows the liquid to flow into the secondary container once the primary is full. This mechanism enables an additional measurement of around 100 l/m^2.

For quick and easy installation on the ground, a support holder has been integrated. Thanks to a set of rods and sleeves (Fig. 21) it can be quickly assembled. Also, a skewer is added in its lower part to easily nail it on the ground.

5 Results

Figure 21 shows an assembly drawing and exploded perspective of the rain gauge, while Fig. 22 exposes a render indicating its main components.

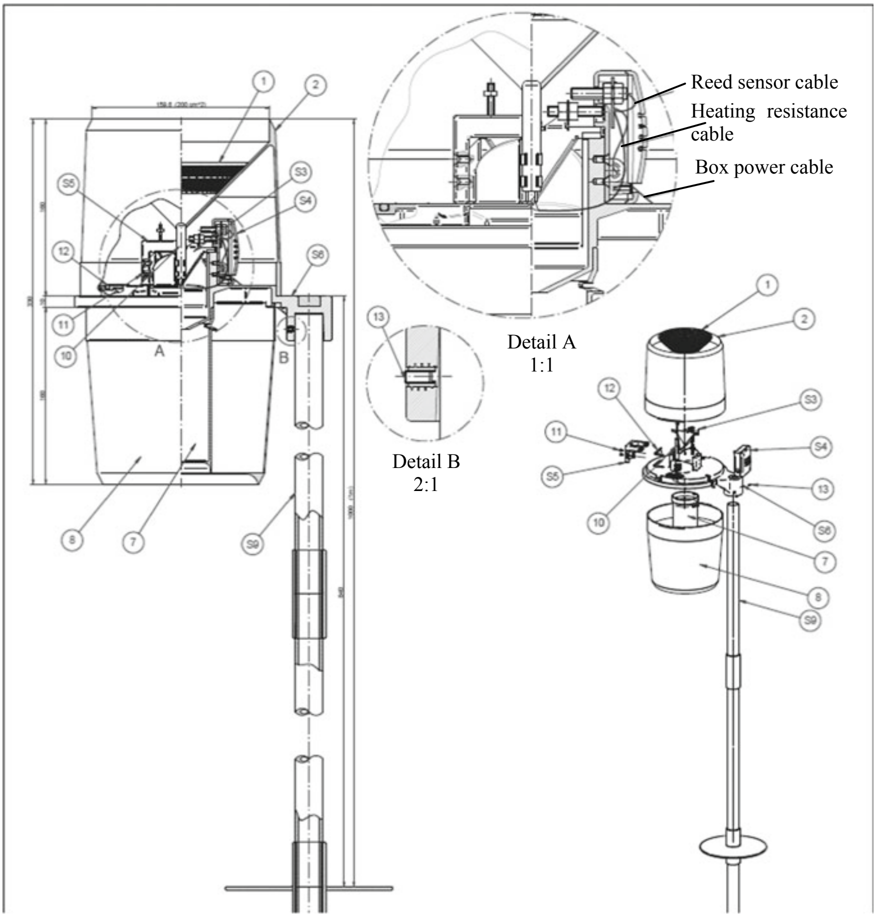

Fig. 21. Assembly drawing

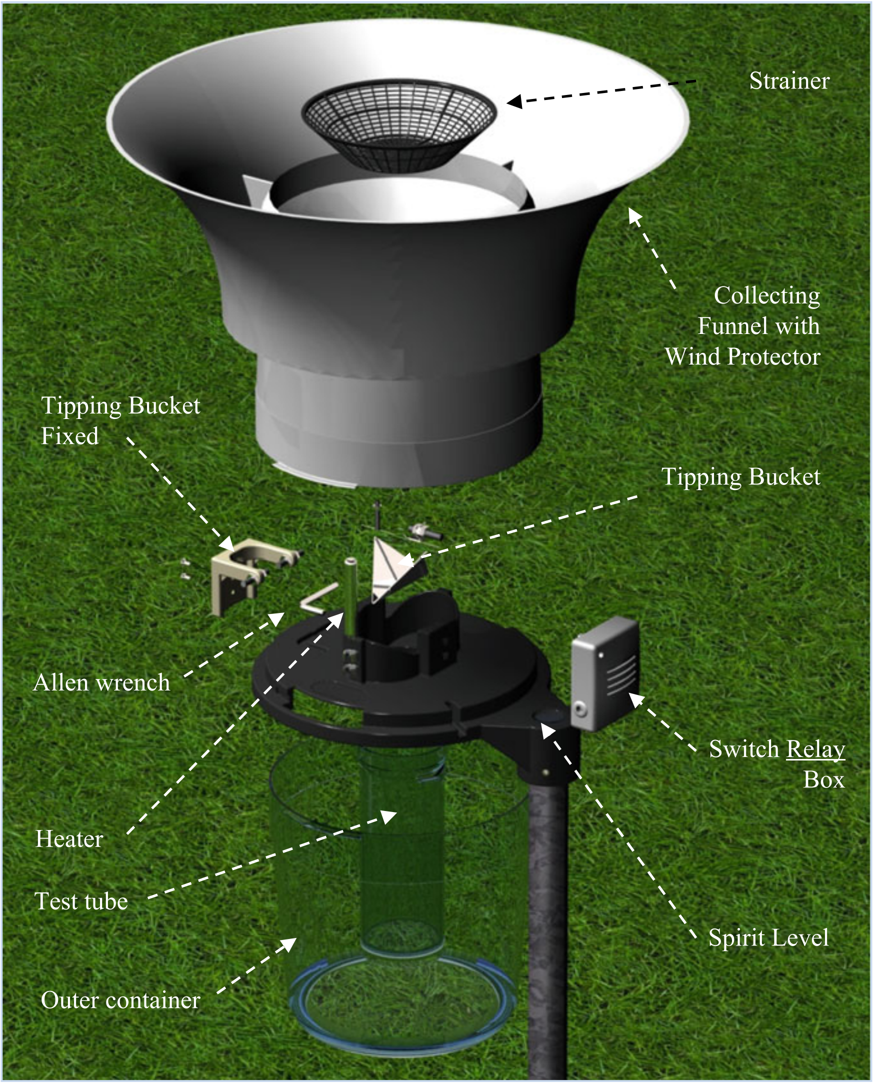

Fig. 22. Render with the main components

6 Conclusions

After collecting the information and by applying engineering and industrial design techniques, a new model for the device aimed at rainfall measurement (whether liquid or solid) has been developed. It consists in a bucket-type rain gauge whose main distinguishing characteristic against other devices already in the market is its versatility since it can be used as an ordinary rain gauge, as a recording rain gauge or, both functions at the same time. Another important attribute or strength of this model is the price: low price versus the accuracy achieved. Moreover, its components can be combined in different ways gaining in adaptability and allowing the user to acquire a quick and easy use device where the utilization of standardized components has been prioritized. For all the above, the proposed design has led to a patent with prior examination, firstly at national level ES2455940 B2 and, at the time, the international level patent can also be applied for with number WO 2013/098437 A2.

References

1. Burzigotti R, Dragoni W, Evangelisti C, Gervasi L (2003) The role of Lake Trasimeno (central Italy) in the history of hydrolgy and water management. In: International Water History Association. IWHA 3rd internacional conference, Alexandrie (Egypt)
2. Stangeways I (2010) A history of rain gauges. Weather J 65(5)
3. Kurtyka JC (1953) Precipitation measurements study. State water survey division, Department of Registration and Education, Illinois
4. WMO (2008). Guide to meteorological instruments and methods of observation, no 8, chapter 6. World Meteorological Organization
5. Maderey Rascón LE, Jiménez Román A (2005) *Principios de hidrogeografía. Estudio del ciclo hidrológico.* (Vol. Nº1). (I. d. México., Ed.) México: Serie textos universitarios
6. WMO (1994) Guide to hydrological practices, vol 168. WMO, Geneva
7. Constantinescu GS, Krajewski WF, Ozdemir CE, Tokyay T (2007) Simulatión of airflow around rain gauges: comparison of LES with RANS models. Adv Water Resour 30:43–58
8. Sánchez San Román FJ (1994) El Ciclo Hidrológico. Univ. Salamanca, Dpto. Geología, Salamanca

Multifunctional Device for Bicycles

P. Lardón-Amat, O. D. de-Cózar-Macías(✉), F. J. Castillo-Rueda, C. Ladrón-de-Guevara-Muñoz, and L. Miravet-Garret

University of Málaga, c/ Dotor Ortiz Ramos s/n, 29018 Málaga, Spain
odecozar@uma.es

Abstract. This paper aims at designing a "Multifunctional device composed of load support and anti-theft lock for standard bicycles". A previous study has been developed in order to justify and validate the final design of the unmet needs of people in their daily lives, with an emphasis on satisfying those that imply specific savings, whether economic, energy or time. As a result, the use of bicycles as a means of transport in Spain is promoted taking as a frame of reference countries such as the Netherlands or France. This means economic and energy savings (by replacing the car) and an improvement in people's health and quality of life. Following the steps of the design methodology, once the need was detected, an information search was carried out in order to identify and prioritize the design specifications that meet the demands of potential customers. For this reason, various sources were used, Cyclelogistics (2013), a European project; a report "Food in Spain" by the Ministry of Agriculture, Food and Environment (2017), and the annual bicycle barometer developed by the DGT (Dirección General de Tráfico, 2017) where the opinion, habits and use that the Spanish people make of the bicycle and the needs and demands they have in relation to it, is known. In addition to meeting the needs of the client, the design must comply with a set of reference regulations both, at the level of security devices and the transport of merchandise at retail. The result of the work has given rise to patent application with prior examination at a national level, in a first phase, and subsequently, at an international level.

Keywords: Product design · Cargo bikes · Anti-theft lock · Patent

1 Introduction

Many researches confirm that the use of bicycle has increased over the last decade at national and international level. The Bike Internacional Day comes on April 19 every year. This day is celebrated with several events in different European and Spanish cities to promote the bike as an alternative daily means of transport [1]. According to the 2014 Eurobarometer of Quality Transport [2] and other relevant publications in this field [3–5], the European average of bicycle use as a daily means of transport is 8%. Spain, with a 3% of daily bicycle use, has not reached those levels yet. Countries like Holland, with 36%; Denmark, with 23%; Hungary, with 22%; Sweden, which meets 17%; Finland, 14%; and Belgium, 13% present a high level of bike use. Statistics are still far from the European level although every year the use of bicycles increases, being 1.6% in 2010. In addition, according to the 2017 Bicycle Barometer elaborated

F. Cavas-Martínez et al. (Eds.): *Advances on Mechanics, Design Engineering and Manufacturing II*, LNME, pp. 123–133, 2019.
https://doi.org/10.1007/978-3-030-12346-8_12

by the Network of Cities for Bicycle (RCxB) [6], in Spain there has been an increase in use compared to 2015.

The barometer confirms that:

- Almost half of Spaniards aged between 12 and 79, that is to say 19 millions, use the bicycle with some frequency and almost a quarter of them use it weekly.
- From the first barometer in 2009, the number of bike users has grown up to 3.5 million.
- In cities the use of bicycles for daily commuting has increased.
- More than 85% of Spanish people agree the environmental pollution reduction must go through the increase of bicycle use.
- Citizens ask to encourage the use of bicycles in companies and schools, more parking lots and appropriate interurban tracks.

The bicycle is increasingly integrated as an alternative way of transport to the motorized one. More and more people are encouraged to use it in their daily lives and it is one of the mainstays in many state plans for sustainable transport [7, 8]. Many public bicycles are being made available in big cities.

Its use has many advantages over other means of transport [6–10]:

- Mobility: it is ecological and it does not pollute, it is fast (in short routes), economical, you can park it very easily and avoid traffic jams.
- Health: the use of a bicycle is healthy. Allowing you to do exercise, improving your physical condition while you move.
- Leisure time: enjoy the trip, fun, take a walk, ….

The research led by the RCxB and the General Directorate of Traffic, which was carried out by GESOP (Cabinet of Social Studies and Public Opinion), reveals that three out of four Spaniards (74.9%) have a bike at home and six out of ten Spaniards have one for personal use. In this sense, it is estimated that there are some 30 million bicycles in Spain.

It also highlights that 16% of bicycle users have suffered at least one theft of their bicycle in the last five years. Several studies have identified that bicycle theft is a problem for cycling communities [8]. In the year 2014, more than 300,000 bikes have been registered as stolen in Germany. However, these figures could be even higher because many cycle thefts are never reported to the police [11]. Internationally, in cities where this mean of transport is well established, the most frequent type of theft per person is that of bicycles, and in 30 cities, it was shown that bicycles are 4 times more likely to be robbed than cars [8].

Likewise, as the materials used for the bike frame are becoming more light-weight thanks to technological breakthrough, the number of bicycle thefts keeps increasing [12]. Thus, anti-theft design is currently an important issue that is being taken seriously by companies. How to make bicycles hard to steal and easy to use is one of the most pressing problems facing this country.

In addition, a study conducted in Montreal found that most robberies occur during the day and not at night [8].

In this sense, most cyclists take some type of prevention to avoid theft, with the lock being the most common prevention measure [12].

Although walking (36.5%) and playing sports (37.7%) are still the main uses of the bicycle, in big cities it also highlights the habitual use of it, especially the most intensive, for daily commuting (54.2%), such as going to work or to the study center.

Among the daily trips considered appropriate to be made by bicycle, the study is focused on the action of "doing the shopping". This is an obviously necessary activity for society and is carried out so frequently that the fact of modifying it can mean a sudden change in the habits of many people. Therefore, it is intended to encourage potential users by designing a product that makes this activity easier and safe in the purchase.

The initial stages of Stuart Pugh's Total Design methodology [13, 14] have been used for product design.

2 Market Research and Design Specifications

During the market research, all aspects that can influence the product design have been considered and some studies [12] have been taken as a reference for product development. Beginning with the cargo bikes, the capacity of load, ease of use, versatility, stability to the rollover, weight, size, aesthetics, etc. have been analysed. As a second item, bags, panniers or baskets of goods transport including their dimensions, restraint systems, resistance, capacity, etc. have been checked. Other aspects under study have been shopping trailers anti-theft devices such as padlocks, articulated pistons and chains. The main objective is to create a standard product, so it is necessary to carry out a detailed analysis of the different types of bicycles. This survey enables the assessment of the dimensions and features of each bike. The design will focus on the dimensional analysis of the most widespread bicycles on the market such as road bikes and their versions with some exceptions, triathlon, mountain bikes and bicycles for walking or City Bikes. The analysis includes the dimensions and geometry of the frame, types of saddle and seat post and dimensions of the wheels, leaving out those less common such as BMX, Bike-Trial, Tandem or Recumbent.

Once the market study including the analysis of the competition and alternative solutions is concluded, defining the relevant aspects about the issue such as those related to the displacement to do the shopping becomes essential. Therefore, the study has focused on the following conditions:

- Quantity or volume of the shopping.
- Distance from home to the shopping establishment/supermarket.
- Time available to do the shopping.
- Orography of the route.
- Lack of infrastructure.

Cyclelogistics [3] defines as "commercial displacement" any displacement that ends in the purchase of one or several articles. Even those trips that involve purchase intention without achieving it are within this definition.

However, a factor that sets the weight and volume of the so-called daily consumption goods is the movements frequency. In addition, the maximum load that the bicycle allows will limit it. The quantity of purchased items and, consequently, their transportation depend on these displacements frequency. The frequency for the purchase of daily supplies has been classified: daily, every 2–3 days, weekly, every 2–3 weeks, monthly and occasionally.

Another important concept to keep in mind is the total distance that must be travelled from home to the purchase establishment/shop, including the round trip. Cyclelogistics defines 7 km as an acceptable distance for cycling. However, this depends largely on individual conditions of each user.

Considering the following starting conditions:

- Weekly purchase frequency.
- Weekly purchase weight per person of 16.8 kg, based on an annual consumption per person between 650 and 700 kg of food products [15].

Once both, the comparative analysis of existing products in the market and the transport and frequency situations have been completed, it is concluded that there is no product that meets the requirements of cargo transport on bikes and anti-theft security simultaneously. That is why a product with this dual functionality is intended.

Firstly, it should be clarified that the main objective of the product is the daily consumer goods transportation, where other types of goods or loads are secondary. Thus, when a user parks the bicycle in a public place to come into the store to make a purchase, the same device that is used for the goods transportation, secures the bike while shopping. Therefore, it is possible to do it without a current anti-theft device. Subsequently, the design product has an added value.

Finally, the following conclusions are drawn taking into account the advantages and drawbacks of bike bags and baskets:

- Cargo transport does not require a specific kind of bicycle. Therefore, the most appropriate design solution is an adaptable device to standard bicycle. It is also sought that the way the device assembles and disassembles must be as simple as possible.
- Regarding the load placement, it should be comfortable for users. Generally, the user transports the load in bags. Consequently, the device design must be developed based on the load placement, avoiding having a platform or container to place the goods.
- The assembled device must not compromise the bicycle usual ride. In addition, when it is loaded it should be as stable as possible.
- The space used is another of the evidences that have an impact on the result. That is why the assembled device must take up little space or not interfere for driving. The fact of not taking up too much space when it is disassembled, in order to be able to store it easily, is also valued.

3 Sketches

The customer requirements and design specifications have been clarified. The methodological process of product design goes to the creative stage from a set of ideas or sketches that attempt to fulfill the aforementioned demands. See Fig. 1.

Fig. 1. Product design sketches

Several designs, such as those, shown in Fig. 1 were rejected for different reasons such as mobility, stability, lack of anti-theft security, etc. Therefore, the idea was developed to achieve the sketch shown in Fig. 2. The transport device adopts the idea of one of the best anti-theft security systems, as it is the U-padlock.

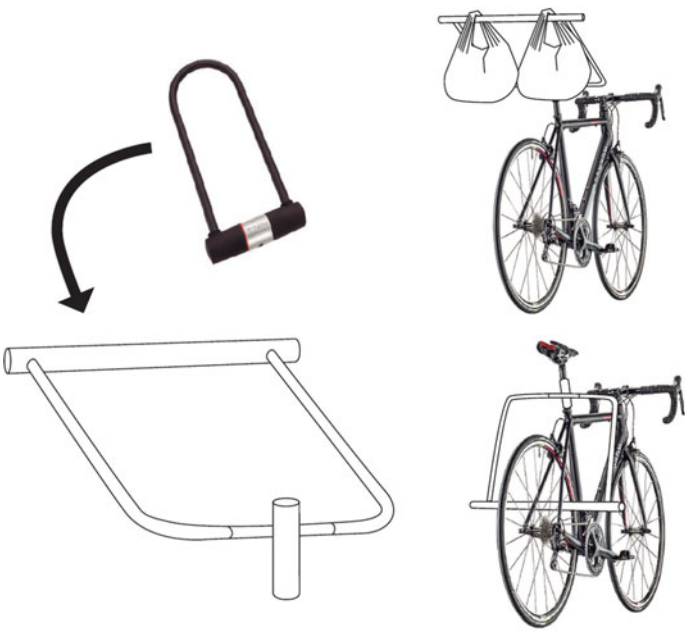

Fig. 2. Transport and anti-theft positions

This design must accomplish the main condition called compatibility, which concerns all the elements involved in it: bicycle, bags and anti-theft mode. That is, the device must allow its use with most types of bicycles, bags and clamping elements.

4 Technical Design

The bicycle is the main component to consider because it contains many parameters that influence compatibility. The bicycle typology is related to the shape of the frame (see Fig. 3), and, above all, to the rear triangle. Compatibility is not ensured on bicycles whose rear triangle does not have the shape and dimensions defined in Fig. 3. For this reason, all bicycles with rear or full suspension which are Mountain Bike variants (In-hard, Freeride, Downhill and Crosscountry) are left out. Apart from those mentioned, Bike Trial, BMX and Recumbent are also excluded.

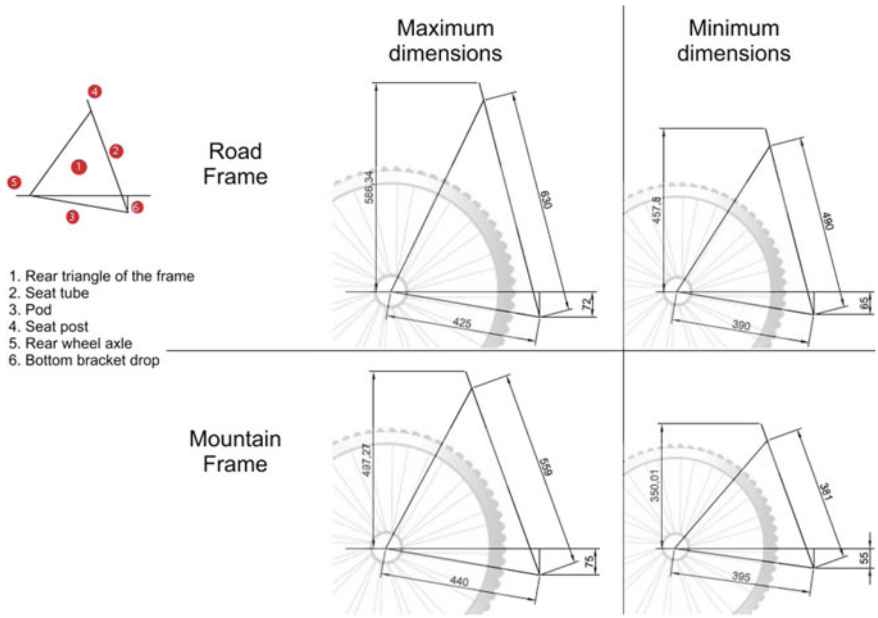

Fig. 3. Maximum and minimum dimensions

As shown in Fig. 3, the device is compatible with the full range of dimensions where the minimum measure is 350 mm. If it is compatible with this minimum measure, it will be compatible with higher dimensions. Therefore, this is the length chosen according to these conditions.

The second condition is also related to the length of the device sidebars. This length should be such that in the transport position, the distance between the bags and the rear wheel avoids contact among them. Thus, one must consider both the dimensions and geometry of the bicycle at the same time that the dimensions and types of existing bags.

Once the analysis presented above had finished, it was verified that the device sidebars length ought to be longer than 517 mm in order to load the maximum length bags without any contact with the rear wheel of the bicycle. This condition conflicts with the previously studied, since a sidebar length of 350 mm is required. For this reason, an alternative solution that combines both conditions was sought.

The solution is to add a second 350 mm termination axis where the removable bar can anchor and set two sidebars distances, one of 350 mm and another of 520 mm. Thus, an appropriate distance for loading the bags (see Fig. 4) is maintained.

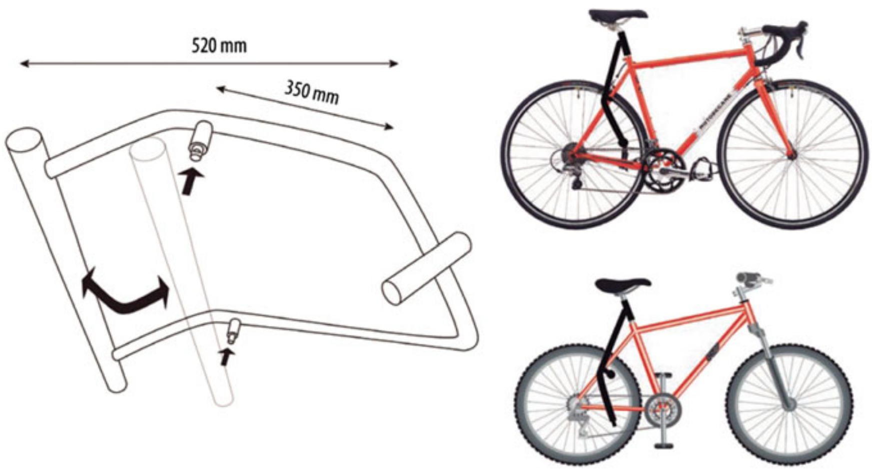

Fig. 4. Removable bar positions

The next step is to set the length of the two crossbars, the removable bar and the bar where the axis is located. The space between the device and the fixed elements to which it will anchor is the main requirement. Secondly, the device must have enough width to transport some hanging bags on the removable bar.

The maximum width of the bicycles rear part analysed is 200 mm. Then, the appropriate distance to fix the device to immobile elements should be added.

The crossbars length has been increased by 150 mm on each side since this distance is enough to join the device into a fixed element (Fig. 5). This gives a total length of 500 mm, which is wide enough to incorporate a large number of bags (depending on type, format and size) hanging on the removable bar.

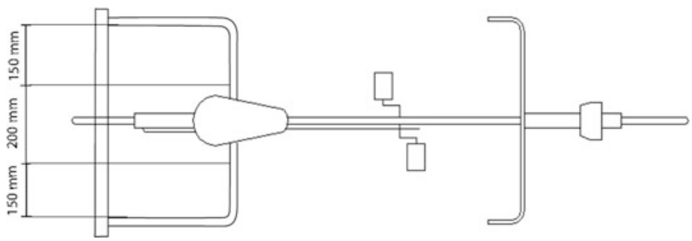

Fig. 5. Range of dimensions for crossbars

By incorporating an axis into its crossbar (Fig. 6), the option of sliding the device through this axis is enabled in order to extend the space available for the fixing element. As a result, the space to secure the bicycle in a fastening element is up to 300 mm in maximum diameter.

Finally, we proceed to specify the diameter of the three bars in the U-shape and the removable bar. The thickness should ensure their resistance to any type of attack, but, in turn, should be thin enough to insert the removable bar between the rear wheel spokes. Furthermore, the resulting weight of the device has to be suitable to move it without too much difficulty.

The removable bar of the device cannot exceed a diameter of 30 mm, otherwise anti-theft mode would not work. The thickness of the main bars should be less than the removable bar in order to anchor the terminations in it.

Dimensional margins have been estimated for both thicknesses, which are between 12 and 18 mm for the main bars, and between 20 and 30 mm for the removable bar.

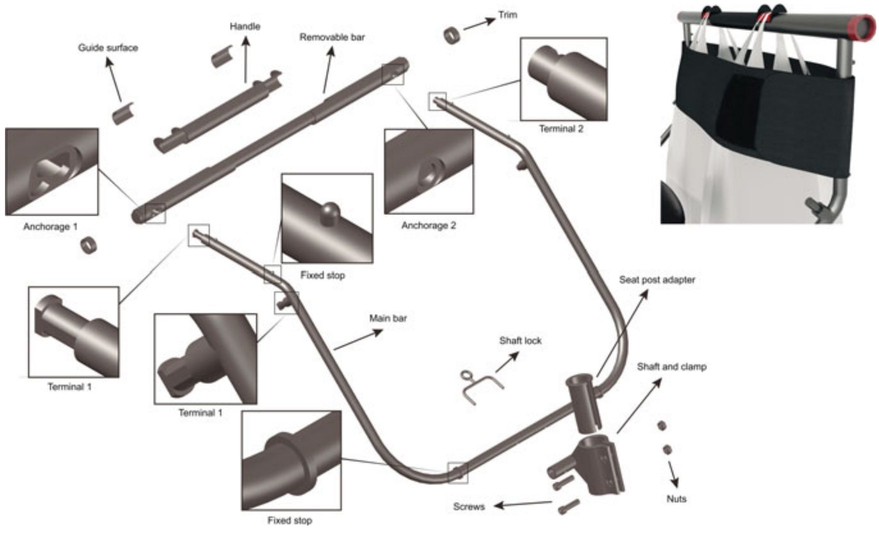

Fig. 6. Device parts

The average density of the steel is 7850 kg/m^3. The approximate weight for the maximum bar diameters (18 and 30 mm) is around 6 kg, which is excessive, while for minimum bar diameters (12 and 20 mm) the desired anti-theft security would not be obtained. That is the reason for choosing the midpoint of both margins (15 and 25 mm) whose weight is 3.91 kg. Part of the device is supported on the seat post, so the actual weight to be hold up during its manipulation becomes 2.47 kg, which would require an approximate force of 24 N to lift the device from the safety position to the transport one.

Finally, Figs. 8 and 9 show two virtual representations of the multifunction design accomplished, such as transport system and anti-thief system. In a viewpoint of load transport, Fig. 8, it can be observed that both the shopping bag and the transport basket can hide the light signals placed in the saddle. Some solutions need to be adopted such as a reflective signal placed on the Velcro strap or in the back of the basket, or using reflective devices for lateral fastening in the rear triangle of the bicycle.

In Fig. 8, it is shown that load lateral displacement is limited by the Velcro tape, by the device sidebars or by the protruding on the removable bar that prevent the lateral glide of the bags handles (Fig. 6). Other solutions could incorporate an elastic mesh (Fig. 7) or, in this case, its own transport basket. Figures 8 and 9 have been realized with 3DStudio Max® software.

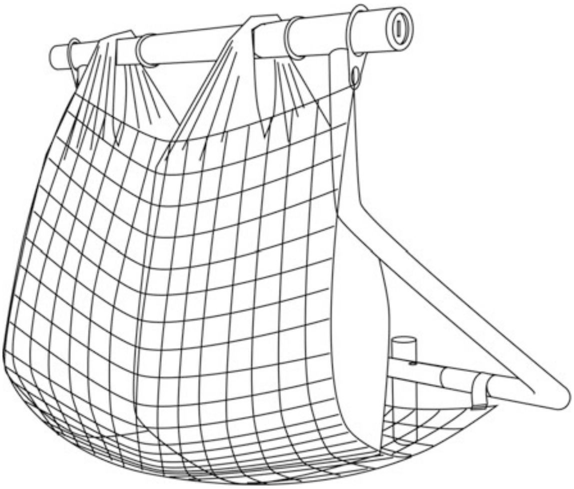

Fig. 7. Elastic mesh

Fig. 8. Transport system

Fig. 9. Anti-thief system

5 Conclusions

In this work, a multifunctional device that helps daily bicycle users has been developed. The dual functionality allows the transport of merchandise of daily consumption products and the anti-theft protection of the bicycle in the destination store. The result of the study has conducted to an invention patent [16] no. ES 2 634 642 B2.

References

1. Woods R, Masthoff J (2017) A comparison of car driving, public transport and cycling experiences in three European cities. Transp Res Part A (103):211–222
2. Directorate-General for Mobility and Transport: Special Eurobarometer 422a. "Quality of Transport". European Union. (2014). ISBN 978-92-79-44436-4. https://doi.org/10.2832/783021
3. Cycle Logistics moving Europe forward. Available online: http://cyclelogistics.eu/. Accessed 18 Jan 2018
4. DGT journal. Available online: http://revista.dgt.es/images/RCxB-Barometro-de-la-Bicicleta-en-Espana-2017-Informe.pdf. Accessed 18 Jan 2018
5. Food in Spain 2017. Available online: http://alimentacionenespaña.es/ae/. Accessed 18 Jan 2018
6. Red de Ciudades por la Bicicleta: Barómetro de la Bicicleta 2017. GESOP, Gabinete de Estudios Sociales y de Opinión Pública S.L. (2017). Available online: http://www.ciudadesporlabicicleta.org. Accessed 18 Jan 2018
7. Lahrmann H, Madsen TKO, Olesen AV (2018) Randomized trials and self-reported accidents as a method to study safety-enhancing measures for cyclists—two case studies. Accid Anal Prev 114:17–24
8. van Lierop D, Grimsrud M, El-Geneidy A (2015) Breaking into bicycle theft: insights from Montreal, Canada. Int J Sustain Transp 9(7):490–501
9. Foley L, Dumuid D, Atkin AJ, Olds T, Ogilvie D (2018) Patterns of health behaviour associated with active travel: a compositional data analysis. Int J Behav Nutr Phys Act 15:26
10. Milani Medeiros R, Duarte F (2013) Policy to promote bicycle use or bicycle to promote politicians? Bicycles in the imagery of urban mobility in Brazil. Urban Plann Transp Res 1 (1):28–39

11. Bochem A, Freeman K, Schwarzmaier M, Alfandi O, Hogrefe D (2016) A privacy-preserving and power-efficient bicycle tracking scheme for theft mitigation. In: 2016 IEEE International Smart Cities Conference (ISC2), Trento, pp 1–4
12. Huang Y, Huang T (2017) A study for prevent theft of the bike design and analysis, 241, 012020. In: 5th Asia Conference on Mechanical and Materials Engineering (ACMME 2017), IOP Publishing
13. Pugh S, Clausing D, Andrade R (1996) Creating innovative products using total design. Addison Wesley Longman
14. Pugh S (1991) Total design: integrated methods for successful product engineering. Addison-Wesley, Wokingham
15. Ministry of Agriculture and Fisheries, Food and Environment (2017) Report on food consumption in Spain 2016, Madrid
16. Lardón Amat P, de Cózar Macías OD, Castillo Rueda FJ, Ladrón de Guevara Muñoz MC, Muñoz Pérez J (2017) Spanish Patent. No. ES 2 634 642 B2. Spanish Patent and Trademark Office

Modeling and Development of a Prosthesis Inspired by the Anthropometry of the Hand

L. Dunai[1(✉)], I. Lengua[1], I. Capcanari[2], and G. Peris-Fajarnés[1]

[1] Centro de Investigación en Tecnologías Gráficas, Universitat Politècnica de València, Camino de vera s/n, 46022 Valencia, Spain
ladu@upv.es
[2] Department of Electronic Systems and Devices, Technical University of Moldova, Street 31 August, No. 78, Bloc 2, 20112 Chişinău, Moldova

Abstract. The present article describes the design, modeling and development of a mechanical hand prosthesis driven by myocardial impulses. The design of the prosthesis is based on the anthropometry of the hand, taking into account the skeletal shape of the phalanges and metacarpals, the connection mechanisms between phalanges, the system of flexor tendons and extension, ligaments and muscles. Through the signals from the muscles, the control system performs the operations of grip, rotation, etc. The control system consists of nano wreck, a motor controller, DC motors and the muscle sensor system.

Keywords: Hand prosthesis · Myoelectric impulses · Modelling · Anthropometry

1 Introduction

Nowadays, the usage of the robotics, EEG and myoelectric signal acquisition devices is common in the development of the prosthetic devices. The main objective of prosthetic devices is to substitute a missing or damaged part of the human body. Over these recent decades, in addition to the previous function, the use of the prosthetic devices has been also expanded to rehabilitation centers in order to facilitate the rehabilitation of the damaged extremities. Damaged extremities, such as lower and upper limbs, are often lost because of trauma, vascular brain diseases or craneoencephalic disease. The prosthetic devices, also known as robots, are designed to strengthen the lower or upper limbs during large training sessions.

The prosthetic devices are dated from Ancient Egypt, around 950-700 years B.C. Their objective was to reinforce the bone structure or helping osseous tears or simply for cosmetic appearance [1]. In Persia, 484 years B.C., solders amputate one of his legs to escape imprisonment and replaced it with a wooden prosthesis [2].

Since the 1960s the improvement of the mobility as well as the increment of the force of the patients became important necessities. Prosthesis was introduced in the military training with the idea of the improvement of the solders force during different programs, such as DARPA, etc. [3, 4].

F. Cavas-Martínez et al. (Eds.): *Advances on Mechanics, Design Engineering and Manufacturing II*, LNME, pp. 134–142, 2019.
https://doi.org/10.1007/978-3-030-12346-8_13

The upper limb prostheses are classified according to:

1. The degree of amputation:
   – Transhumeral
   – Transradial
2. Their integration:
   – Osseointegration
   – Suspension
3. Their function:
   – Cosmetic
   – Body powered
   – Myoelectric.

The osseointegration prostheses are the invasive devices integrated in the human body that are subcutaneous and in contact with the bone. On the other hand, suspension prosthesis are devices that are suspended from the human body via belts, harness, etc.

In the era of new technology, the 3D printing and the advances in computer-aided design (CAD) provide designers and manufacturers great freedom on the product design [5]. These advances [6] have enabled the development of a flexible and more anthropomorphic design of the human prostheses. Besides the anthropometric design of the prosthetic hand/robotic hand, its functionality and the mechanism also play important roles. Most common prosthetic hands are based on tendon simulation working mechanism [7, 8]. Nevertheless, the main movements of the prosthetic device are obtained with actuators, such as electric powered DC motors [9–11], pneumatic [12], ultrasonic [13], hydraulic [14], etc. All previous research has shown that, in order to improve the grasp and extension of the five fingers of the prosthetic hand, a high number of actuators is required.

Considering the advantages and disadvantages of the designs proposed in the existing literature on prosthetic hand [15], this work proposes the design and development of a suspended myoelectric transradial (hand) prosthesis based on DC motors and Arduino board.

2 Human Anatomy

The human hand has a complex anatomic structure. The hand or wrist is composed by 14 phalanges 5 metacarpal bones and the carpus (see Fig. 1). The hand bones are structured as:

1. Fingers
   – Proximal phalanges
   – Media phalanges
   – Distal phalanges

2. Metacarpal bones
3. Carpus bones.

The radiocarpal, carpometacarpal and intercarpal joins are located between the phalanges and bones. The joins contain two Degrees of Freedom (DoF): extension and flexion. The carpus bones realize small movements around instantaneous centers. Since these movements are very small, they are often ignored and it is considered that the hand or wrist have only two DoF [16].

Fig. 1. Hand anatomic structure

Human fingers joins and the concept of transmission mechanism for flexion and extension are presented in Table 1 and Fig. 2a.

Figure 2b, and c, as well as Table 2 are aimed to illustrate the flexion/extension and abduction/adduction movements of the thumb [17].

Table 1. Wrist extension/flexion movement

Element	Description	Abbreviation	Flexion (°)	Extension (°)
0	Metacarpal	MET	–	–
1	Proximal phalanxes	PP	–	–
2	Media phalanxes	MP	–	–
3	Distal phalanxes	DP	–	–
Θ_0	Metatarsophalangeal join	MPJ	90	45
Θ_1	Proximal interphalangeal join	PIPJ	105	5
Θ_2	Distal interphalangeal join	DIPJ	90	10

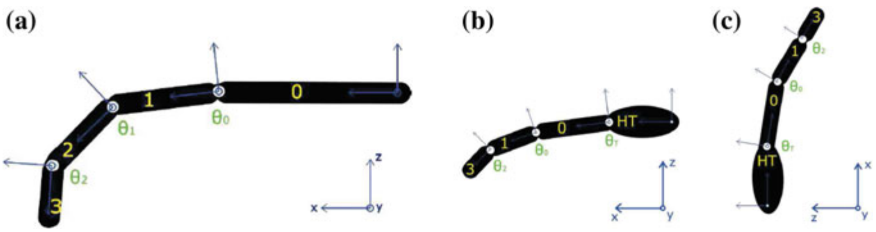

Fig. 2. **a** The wrist extension and flexion. **b** Thumb flexion/extension. **c** Thumb adduction/abduction movements

Table 2. Thumb extension/flexion, adduction and abduction movement

Element	Description	Abbreviation	Flexion (°)	Extension (°)	Adduction (°)	Abduction (°)
0	Metacarpal	MET	–	–	–	–
1	Proximal phalanxes	PP	–	–	–	–
2	Distal phalanxes	DP	–	–	–	–
3	Interphalangeal join	IPJ	90	45	–	–
Θ_0	Metatarsophalangeal join	MCPJ	70	15	–	–
Θ_1	Carpometacarpal join	CMCJ	71	38	71	20
Θ_2	Metacarpal	MET	–	–	–	–

3 Materials and Methods

An Arduino Nano has been used as processing unit; five DC step by step servomotors, one external battery, one muscle Sensor Kit and an Analog-to Digital Converter are the other elements used in the construction of the prosthesis.

For the robotic hand design, the anthropometric measurements of the human hand have been measured. Each phalange has been modelled with a three dimensional drawing tool (Fig. 3). In total, 14 phalanges and 5 metacarpal bones have been

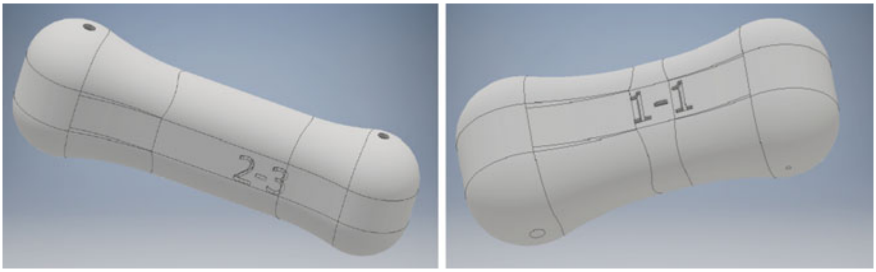

Fig. 3. Modeling of the hand phalanges

modelled, with their measurements, as well as the artificial carpus and the processing unit support.

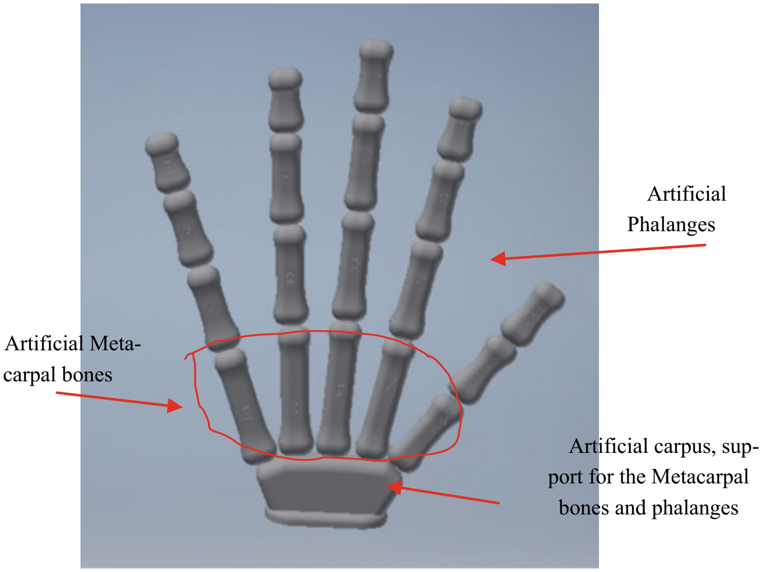

Fig. 4. Integration if the artificial Phalanges, Metacarpal bones on the campus

The processing unit support is composed by five servomotors, the Arduino processing unit and the Analog to Digital Converter, that is fixed to the hand with a harness. The contact with the human hand is made by silicone in order to reduce the friction.

Figure 4 illustrates the integration of the carpus, metacarpal bones and phalanges.

It has to be mentioned that the design of the prosthetic hand is based on the real anthropometric measurements of a young human hand. The idea of the anthropometric measurements is to model and develop an adaptable personalized robotic hand.

The mechanical movement of the prosthetic hand is based on the human biomechanics. The Artificial carpus is a designed with 1 DoF that realizes the movement of rotation. The artificial metacarpal bones are divided in two groups: the group of the fingers is fixed to the carpus. Due to the small degree of movement of the metacarpal bones with the carpus, the movement is considered null. The second group is composed by the thumb metacarpal bone. Its movement consists of the flexion/extension and adduction/abduction movement, which can be seen in Fig. 5.

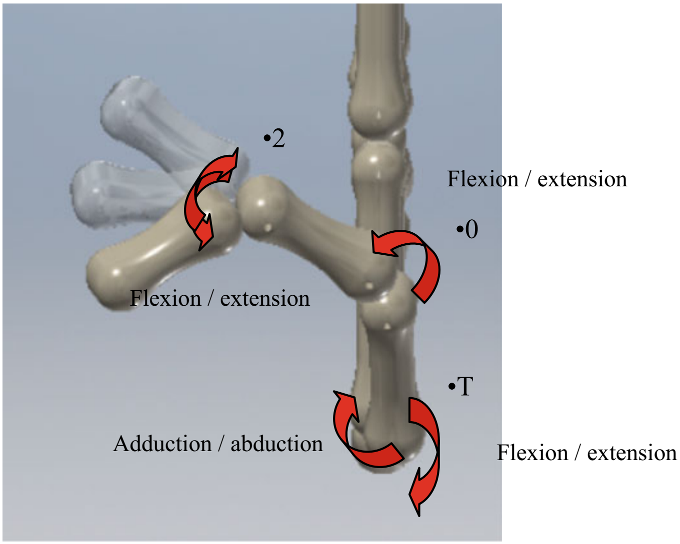

Fig. 5. Phalange movement of the thumb the flexion, extension, adduction and abduction

The main fixing system of the prosthetic hand relies on the tendons and the muscles. The extensor tendons are placed on the dorsal area named opisthenar area (see Fig. 6a, b, c and d).

The flexor tendon is located in the palmar area of the phalanges that realize the flexion of the phalanges and make possible the grasp; it is represented in Fig. 6b.

Once all elements have been designed, they are printed with a 3D printer with different resistance materials. The phalanges and the metacarpal bones, as well as the carpal and principal support are printed in ABS hard material, whereas the tendons and muscles are printed with elastic silicone material, described in Table 3.

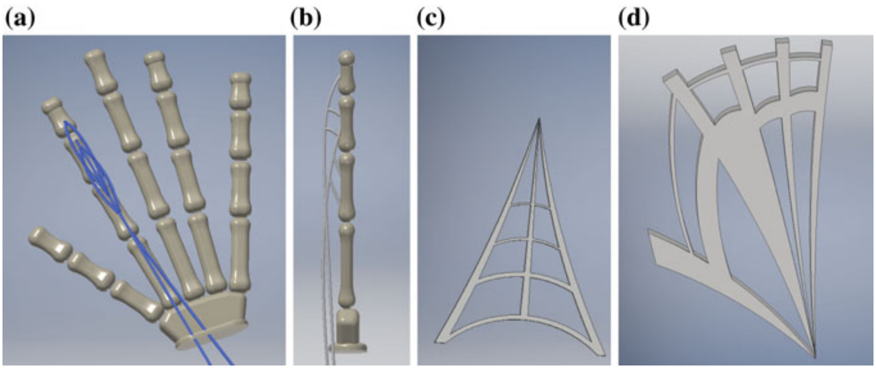

Fig. 6. **a** Example of the extensor tendon. **b** Example of the flexor tendon. **c** Intrinsic muscle modeling. **d** Example of the palmar tendon connection

Table 3. Printing material properties

Abbreviation	Silicone	ABS
Hardness	40	R105
Tensile strength (psi)	850	6.100
Tear strength (ppi)	125	75,400
Density g/cm3	1.07	0.25
Color	Translucent	Beige

Between each phalange, a rubber pad has been inserted in order to avoid the friction (see Fig. 7a). Each pad is designed individually for each connection surface of the robotic hand phalanges. Figure 7b describes the sketches and the developed from silicone fibrous sheath over flexor tendon sheaths.

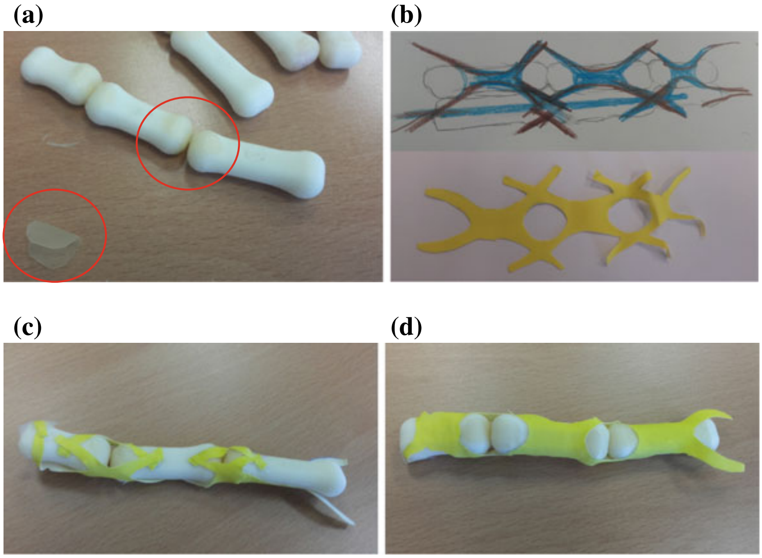

Fig. 7. Silicone elements of the human robotic hand. **a** The silicone pad example, **b** the silicone fibrous sheath, **c** example of the adjustments of the fibrous sheath in the palmar side, and **d** represent the adjustment of the fibrous sheath over flexor tendon sheaths in the dorsal side of the hand

The phalanges are covered with silicone glove.

The grasping is controlled by the Arduino Nano electronics and the pressure sensors placed in the distal phalanges, see Fig. 8.

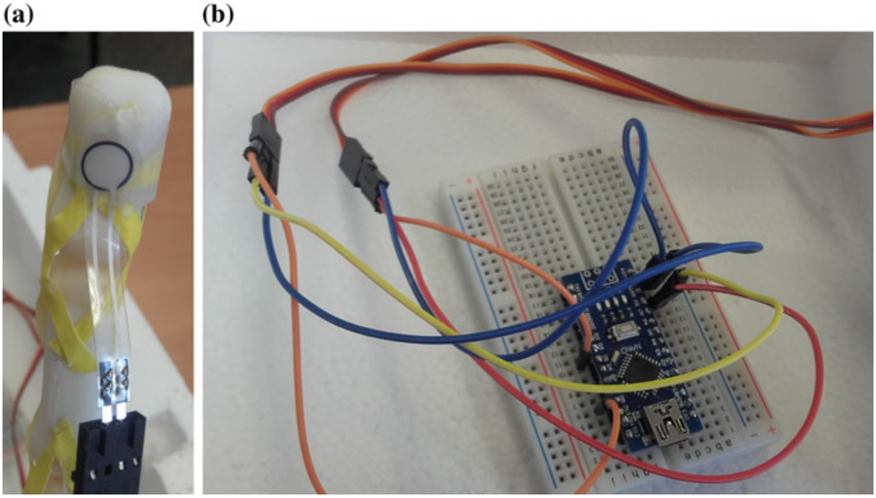

Fig. 8. **a** Pressure sensor inserted in each distal phalanges. **b** Electronic board of the mechanical hand prostesis

4 Conclusions

This paper describes the design and development of an intelligent mechanical hand prosthesis able to realize the grasping and extension of the fingers as well as taking objects thanks to the use of pressure sensors. Based on the human hand anthropometry, the presented robotic hand can be adapted to the user requirements. The phalanges and carpal bones have been carefully measured and designed in order to be able to adapt to different sizes. All elements of the prosthesis as pads between phalanges, the tendons, ligaments and bones have been designed and integrated one by one. The control system is based on Arduino nano board, DC motors, motor controller and the muscle sensor system.

The work presents the experimental prototype. In the future, the work will be improved with temperature sensors, improvement of the design of the adjustable housing to the arm, as well as testing and validation in real environment.

References

1. Espiritu García Molina I, Dunai L, Lengua I (2017) Development of a biomechanical orthotic device. In: Proceedings of 9th international conference on microelectronics and computer science, pp 344–349
2. Thurtston A (2007) Parè and prosthetics: the early history of artificial limbs. ANZ J Surg 77 (2):1114–1119
3. Garcia E, Saler JM (2002) Exoskeleton for human performance augmentation (EHPA): a program summary. J Robot Soc Jpn 2(8):44–48

4. Dollar AM (2008) Lower extremity exoskeletons and active outhouses: challenges and state-of-the-art. IEEE Trans Rob 24(1):144–158
5. Rengier F, Mehndiratta A, Von Tengg-Kobligk H, Zechmann CM, Unterhinninghofen R, Kauczor H-U, Giesel FL (2010) 3D printing based on imaging data: review of medical applications. Int J Comput Assist Radiol Surg 5(4):335–341
6. Schmitz A, Pattacini U, Nori F, Natale L, Metta G, Sandini G (2010) Design, realization and sensorization of the dexterous iCub hand. In: 10th IEEE-RAS International conference on humanoid robots, pp 186–191
7. Melchiorri C, Palli G, Berselli G, Vassura G (2013) Development of the UB Hand IV. IEEE Robotics & Automation Magazine, Sept 2013
8. Grebenstein M, Albu-Schaffer A, Bahls T, Chalon M, Eiberger O, Frieldl W, Gruber R, Haddadin S, Hang U, Haslinger R, Hoppner H, Jorg S, Nickl M, Nothhelfer G, Petit F, Reill J, Seitz N, Wimbock T, Wolf S, Wusthoff T, Hirzinger G (2011) The DLR hand arm system. In : Proceedings of the international conference on robotics and automation, pp 3175–3182
9. Medynski C, Rattary B (2011) Bionic prosthetic design. In: Proceedings of the MEC'11 conference, New Brunswick, Canada, Aug 2011, pp 14–19
10. Belter JT, Segil JL, Dollar AM, Weir RF (2013) Mechanical design and performance specifications of anthropomorphic prosthetic hands: a review. J Rehabil Res Dev 50:599–618
11. Controzzi M, Clemente F, Barone D, Ghionzoli A, Cipriani C (2007) The SSA-MyHand: a dextreous lightweight myoelectric hand prosthesis. IEEE Trans Neural Syst Rehabil Eng 25:459–468
12. Takeda H, Tsujiuchi N, Koizumi T, Kan H, Hirano M, Nakamura Y (2009) Development of prosthetic arm with pneumatic prosthetic hand and tendon-driven wrist. In: 31 Annual international conference of the IEEE EMBS, Mineapolis, Minesota, pp 5048–5051
13. Yamano I, Maeno T (2005) Five-fingered robot hand using ultrasonic motors and elastic elements. In: Proceedings of the IEEE International Conference on Robotics and Automation (ICRA), Barcelona, Spain, pp 2673–2678
14. Kargov A, Werner T, Pylatk C, Schulz S (2008) Development of a miniaturized hydraulic actuation system for artificial hands. Sens Actuators, A 411:548–557
15. Innes E (2013) The 3D printed hand that could change the world. 14 Oct 2013. [Online]. Available: http://www.dailymail.co.uk/health/article-2458572/The-Dextrus-3D-printed-prosthetic-hand-Graduate-creates-600-robotic-limb-change-world.html. Accessed 01 Aug 2015
16. Bruet R, Blanch R, Cani MP (2013) Understanding hands degrees of freedom and natural gesture for 3D interaction on tabletop. In: INTERACT proceedings of the IFIP TC13 conference on human computer interaction, Sept 2013. Springer, Cope Town, South Africa, pp 1–19
17. Barakat MJ, Field J, Taylor J (2003) The range of movement of the thumb. Hand J 8(2): 179–182

Adaptation in the Design of a Weighing Lysimeter for Use in Potato Crops

J. A. Nicolás-Cuevas[1(✉)], D. Parras-Burgos[2], L. Ruíz-Peñalver[3], and J. M. Molina-Martínez[4]

[1] Department of Structures and Construction, Technical University of Cartagena, Cartagena, Spain
juan.nicolas@upct.es
[2] Department of Graphic Expression, Technical University of Cartagena, Cartagena, Spain
[3] Naval Architecture Technology Department, Technical University of Cartagena, Cartagena, Spain
[4] Food Engineering and Agricultural Equipment Department, Technical University of Cartagena, Cartagena, Spain

Abstract. Within the PROLISI research project, several transportable weighing lysimeters have been designed whose technology determines with high precision the water needs of crops. Until now, all the models were focused on a type of crop such as lettuce and brassica, with a root depth of up to 30 cm. Due to the excellent performance of these devices in horticultural crops, the need has developed to cover another type of larger plant, such as the potato, with root depth of up to 50 cm. For this reason, this communication shows the dimensional adaptation of a new portable weighing lysimeter model for this type of solanaceous crop. To ensure proper functioning, several analyses and simulations have been carried out to check the resistance of the main structures and the deformations they undergo. With this model, a prototype has been manufactured and it has already been installed in an agricultural holding, with excellent operating results.

Keywords: Precision agriculture · Lysimeter · Computer-aided design · Structural analysis

1 Introduction

One of the most important challenges of irrigated agriculture is how to efficiently manage irrigation water in order to increase the productivity of a horticultural plantation [1]. To determine the water needs of the crops, it is necessary to obtain crop evapotranspiration (ETc), which can be calculated by using weighing lysimeters [2, 3]. These devices establish a water balance between the water supplied (irrigation and rain) and the water drained in a certain time interval. To do this, the increase or loss of water in the soil is measured by weighing the container in which the soil is located. The most common weighing lysimeters in agriculture are large and require expensive civil works for their installation, so their use is usually limited to research centres [4]. The

F. Cavas-Martínez et al. (Eds.): *Advances on Mechanics, Design Engineering and Manufacturing II*, LNME, pp. 143–151, 2019.
https://doi.org/10.1007/978-3-030-12346-8_14

development of new technologies is making it possible to manufacture weighing lysimeters oriented towards commercial use, allowing for higher operation precision and a reduction in investment and maintenance costs [5–7].

Within the research project "*Irrigation automatic programming system for weighing lysimeter and soil salinity, with remote monitoring of the vegetative state of the crop*" (PROLISI), several transportable weighing lysimeter models have been designed whose most important requirements are easy installation, portability and high precision to quantify evapotranspiration by weight variations in small time intervals. The prototypes designed and installed so far are focused on crops such as lettuce and brassica (a species grown in agriculture and horticulture such as cauliflower, broccoli, etc.), whose root depth reaches approximately 30 cm [8, 9].

Due to the successful functioning of the equipment, it has become necessary to cover another type of crop with a greater root depth ($\leq$ 50 cm), such as Solanaceae, among which the potato is a member. The objective of this communication is to show the adaptation in the design of a weighing lysimeter for this type of crop, whose dimensional characteristics vary considerably with respect to the previous model. In addition, different structural analyses of the most important parts have been carried out, such as the culture vessel and the main structure, determining the stresses and deformations they undergo, thus obtaining the validity of this new design.

2 Materials and Methods

In order to obtain a transportable weighing lysimeter adapted to the potato crop (model LP-5, Fig. 1), the LP-4 model was designed for lettuce and brassica crops. This new lysimeter model has been modified dimensionally to adapt it to this crop that can have a root depth of up to 50 cm. First of all, the culture vessel was adapted to the new dimensions of the plant because it is what harbours the crop portion and, later, the rest of the structures were adapted to these new dimensions.

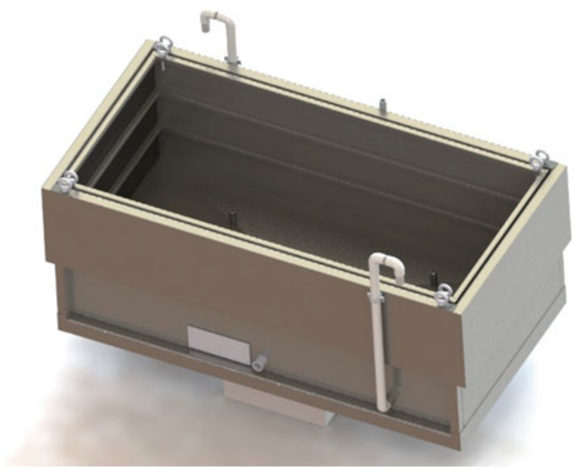

Fig. 1. Perspective view of weighing lysimeter LP-5

In the model LP5, the weighing system of the culture vessel, formed by four load cells, are placed in a different position to counteract the increasing of the charges produced by the new dimensions of the culture vessel. Thus, the resultant forces can be counterbalanced easily so that the section properties of the elements and the thickness of the plates can be maintained.

Since the lysimetric vessel is independent of its environment, the lateral and capillary rise flows are zero, so that the terms of the water balance expression can be determined with precision. To drain and measure the water, which is filtered through the volume of confined soil, a drainage tank is used. In order to know the variations in the water content, the soil mass and the drainage tank, a weighing system is used. Precipitation and irrigation are measured by means of rain gauges and conventional volumetric methods; in this way, the lysimeter provides a direct measure of evapotranspiration in the period considered (Fig. 2).

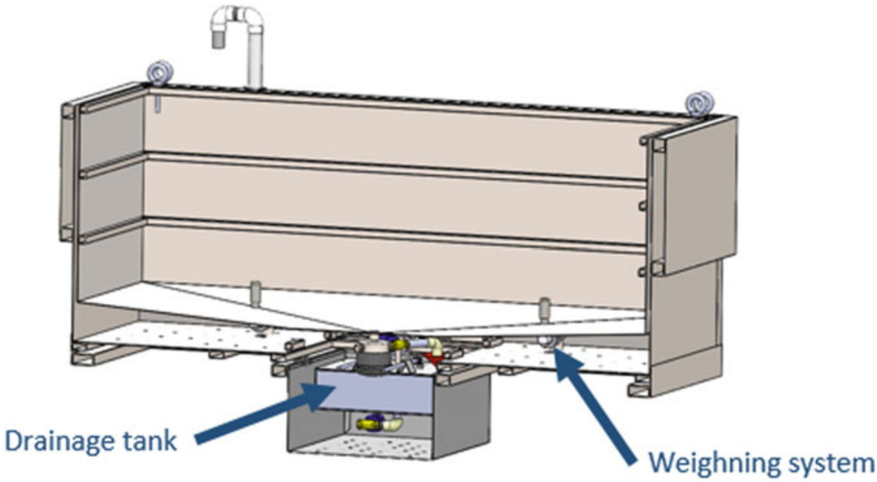

Fig. 2. Section view of model LP-5

All the weighing lysimeter models designed within the PROLISI research project have been modelled with SolidWorks 2016 software, a computer-aided design program for 3D mechanical modelling that allows the modelling of parts and assemblies, obtaining both plans and any other type of information necessary for its production. The structural behaviour of the culture vessel and the main structure have been studied using SolidWorks Simulation.

The following are the most important structures that make up the LP-5 weighing lysimeter:

- **Culture vessel**: what is used to the one that harbours a portion of the crop (Fig. 3). The dimensions of the culture vessel of the model LP-4 are of 1000 × 600 300 mm (length × width × height). For the new model LP-5 the dimensions have been changed to 1544 × 744 × 551 mm. As the dimensional increase is important, several interior reinforcements with 20 × 20 mm profiles were added.

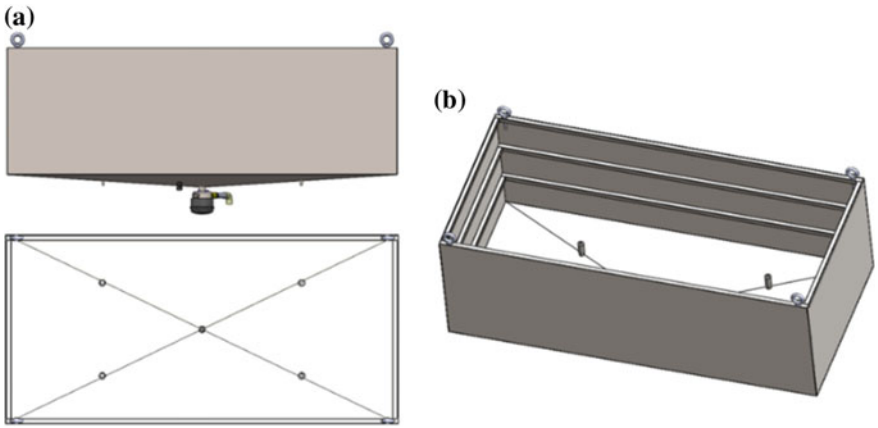

Fig. 3. Culture vessel: **a** front and top view, and **b** perspective view

- **Main structure**: the outer container of the whole system which is in contact with the ground (Fig. 4). It contains the culture vessel, the drainage tank and the weighing system.

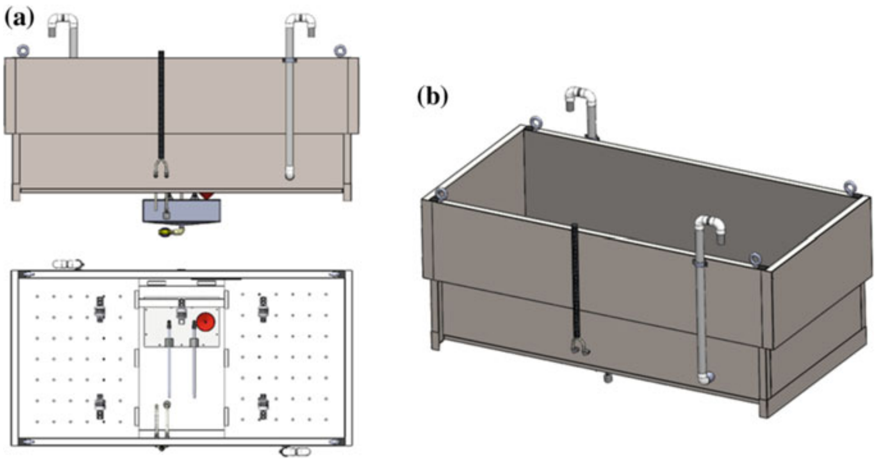

Fig. 4. Main structure: **a** front and top view, and **b** perspective view

- **Structural base**: structure that serves as a support surface for the whole lysimeter, levelling the main structure in case of possible differential settlements (Fig. 5).

To validate the new design, a static analysis has been carried out to simulate the stresses and deformations that occur in the walls of the culture vessel and the main structure under different load conditions. The simple loading cases and the combination

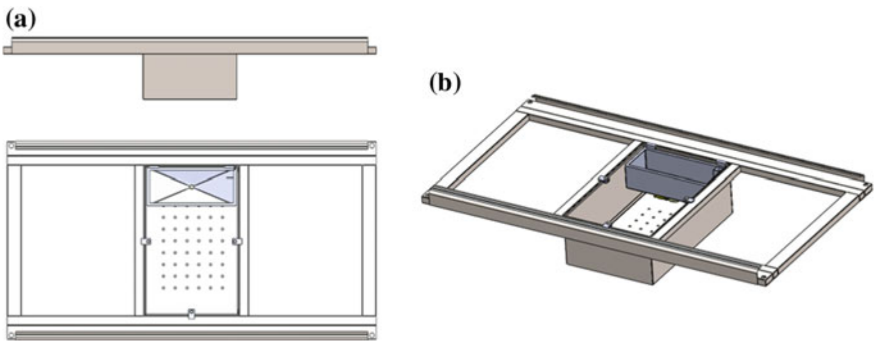

Fig. 5. Structural base: **a** front and top view, and **b** perspective view

loads are indicated in Tables 1 and 2. It has been considered that the ground under the foundation is constituted by a semi-hard clay.

The main structure of the weighing lysimeter is formed by a set of elements that ensure the containment of the ground, separating it from the crop container. The culture vessel houses the reconstituted ground where the plantation develops and rests on a weighing system. The weighing system registers the weight changes of the water flow that enters and leaves the container, allowing the evapotranspiration of the crop to be quantified. In order to ensure a good operation of the lysimeter, the culture vessel and the main structure must be separated, avoiding that the deformations of their elements interfere with each other and modify the measurements of the weighing system.

For the proposed weighing lysimeter, the external dimensions in the plant of the culture container are 1544 × 744 mm, and the internal dimensions of the main structure are 1566 × 768 mm, so that, once placed in their final position, between both containers there is a 12 mm gap before loading.

The structure of the outer container is formed by square tubular profiles 35 × 35 × 2 mm, rectangular tubular profiles 20 × 40 × 2 mm and sheets of thickness 3 mm. The structure of the culture vessel is composed of 20 × 2 mm square tubular profiles and 2 mm thick sheets. The whole unit is designed in AISI 304 stainless steel. To make the finite element model, "BEAM" type elements have been used for the tubular profiles and "SHELL" elements for the sheets.

Table 1. Load cases and load combination considered for the culture vessel

Load case	Load value (N/m^2)	Load distribution
1. Self-weight	–	–
2. Lateral earth pressure	10,000	Triangular
3. Vertical earth pressure	10,469	Uniform
Load combination 1	Load cases 1, 2 and 3	

Table 2. Load cases and load combination considered for the main structure

Load case	Value of the load (N/m^2)	Load distribution
1. Self-weight	–	–
2. Lateral earth pressure	10,000	Triangular
Load combination 1	Load cases 1, 2 and 3	

3 Results and Discussion

For the culture vessel, the highest deformation obtained is 2.64 mm and the equivalent Von Mises stress is 162.7 MPa. On the other hand, the main structure achieves Von Mises equivalent stress and strain of 2.291 mm and 149.3 MPa, respectively. The results of the structural analyses carried out are shown in Tables 3 and 4, and Figs. 6 and 7 show graphical representations of them. In order to carry out the different analyses of the three-dimensional models with SolidWorks Simulation it was necessary to simplify the original models, which has allowed to optimize the mesh size and the computational resources [10].

Table 3. Results of the analysis for the walls of the culture vessel

	Von Mises equivalent stress (MPa)	URES: Resulting displacement (mm)
Load combination 1	162.7	2.64

Table 4. Results of the analysis for the walls of the main structure

	Von Mises equivalent stress (MPa)	URES: Resulting displacement (mm)
Load combination 1	149.3	2.291

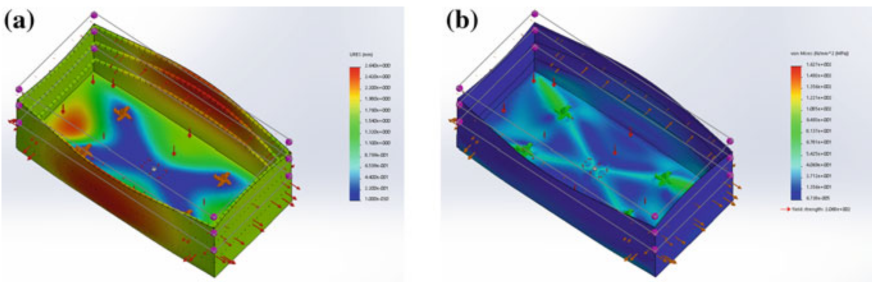

Fig. 6. Three-dimensional view of the results obtained in load combination 1 for the walls of the culture vessel of the low cost weighing lysimeter. **a** Resulting displacement (mm), and **b** Von Mises equivalent stress (MPa)

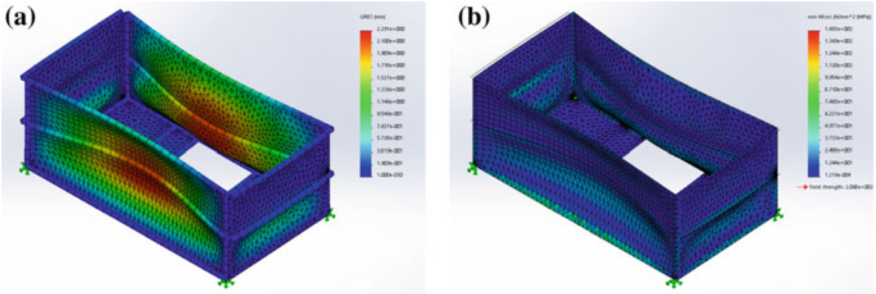

Fig. 7. Three-dimensional view of the results obtained in load combination 1 for the walls of the main structure of the low cost weighing lysimeter. **a** resulting displacement (mm), and **b** Von Mises equivalent stress (MPa)

The static analysis carried out indicates that the maximum deformations that they experience, both the culture vessel and the main structure, do not exceed the separation between them for the load situations considered. For the main structure, in several combinations, the deformations experienced by the sheets exceed half the thickness of itself, so that the principle of small deformations would no longer be valid. The linear theory assumes that there are small displacements, so this method can generate inaccurate results in cases where these assumptions are not valid.

Model LP-4 has overall dimensions of 1090 × 690 × 730 mm. The profiles that make up the main structure are hot rolled steel tubes with square sections of 35 × 35 mm and rectangular ones of 20 × 40 mm. The base structure is formed with steel tubes of 50 × 50 mm. The sheets that cover it are 2 mm thick. The materials used in the whole set are stainless steel AISI 304. For the new model LP-5 all the structures were modified to adapt them to the culture of the potato, reaching a general dimension of 1640 × 840 × 860 mm, maintaining the same type of profiles in all its structures except the base structure that was modified to hollow sections of 40 × 30 mm and 60 × 30 mm, to reduce the height of the set without losing the robustness. As the dimensional increase of the set was important, it needed some extra reinforcement in some of its parts to avoid deformations. Once the validity of the design was obtained with the analyses carried out, a prototype of this model was produced, which is already installed (Fig. 8).

Fig. 8. Prototype LP-5 manufactured and installed on an agricultural holding

4 Conclusions

Efficient management of water resources improves the productivity, stability and quality of crops, thus allowing a rational use of water and energy. The current technological development allows for lysimetric weighing devices with a high precision in the determination of crop evapotranspiration and small dimensions that facilitate installation, transportability and a minimum alteration of the ground. In this communication, the design of a new compact low-cost weighing lysimeter for use in agricultural operations has been presented. This new model is focused on horticultural crops such as Solanaceae, among which the potato is a member, whose root depth reaches 50 cm. To obtain the validity of this new design, different analyses have been done on to the most important parts such as the culture vessel and the main structure. The static analysis performed on these two structures shows Von Mises equivalent stress and strain results of the walls that satisfy the requirements necessary for proper operation. This new lysimeter has already been manufactured and is installed and operating on an agricultural holding.

Acknowledgements. The authors thank the financial support of the Ministry of Economy and Competitiveness (MINECO) and the Regional Development European Fund (FEDER) for the realization of research projects. Reference: AGL2015-66938-C2-1-R.

References

1. López-Urrea R, de Santa Olalla FM, Fabeiro C, Moratalla A (2006) Testing evapotranspiration equations using lysimeter observations in a semiarid climate. Agric Water Manag 85:15–26
2. Hirschi M, Michel D, Lehner I, Seneviratne SI (2017) A site-level comparison of lysimeter and eddy covariance flux measurements of evapotranspiration. Hydrol Earth Syst Sci 21:1809–1825
3. Howell TA, Schneider AD, Jensen ME (1991) Lysimeters for evapotranspiration and environmental measurements. In: History of lysimeter design and use for evapotranspiration measurements. ASCE, pp 1–9
4. Allen RG (2006) *Evapotranspiración del cultivo: Guías para la determinación de los requerimientos de agua de los cultivos*. Food & Agriculture Org.: Vol. 56
5. Egbuikwem PN, Obiechefu GC (2017) In: Evaluation of evapotranspiration models for waterleaf crop using data from lysimeter. ASABE Annual International Meeting, American Society of Agricultural and Biological Engineers, p 1
6. Hertel C, von Unold G (2014) Third-generation lysimeters: scientific engineered monitoring systems. In: Novel measurement and assessment tools for monitoring and management of land and water resources in agricultural landscapes of central Asia. Springer, pp 175–184
7. Meissner R, Rupp H, Seyfarth M (2014) Advanced technologies in lysimetry. In: Novel measurement and assessment tools for monitoring and management of land and water resources in agricultural landscapes of central Asia. Springer, pp 159–173
8. Nicolás JA, Parras D, Ruíz L, Molina JM (2017) In *Análisis estructural del recipiente de cultivo y el cajón exterior de un lisímetro de pesada de bajo coste*, VIII Congreso Ibérico de Ciencias Hortícolas, Coimbra (Portugal), Coimbra (Portugal)

9. Parras D, Nicolás JA, Ruíz L, Molina JM (2018) In *Evolución del diseño de prototipos de lisímetros de pesada enterrados para cultivos hortícolas*, III Symposium Nacional de Ingeniería Hortícola, Lugo (España), Lugo (España)
10. Gómez González S (2010) Solidworks simulation. Alfaomega, Paracuellos del Jarama (Madrid)

Identification of the Main Contributors in the 3D Tolerances Assessment in Mechanical Transmissions

F. Gherardini(✉), D. Panari, and F. Leali

Dipartimento di Ingegneria "Enzo Ferrari", Università degli Studi di Modena e Reggio Emilia, Modena, Italy
francesco.gherardini@unimore.it

Abstract. The management of spatial dimensional variations and 3D tolerance stacks is a key issue to achieve high performance and robust solutions. The state of the art in 3D tolerance analysis addresses two main difficulties: on the one hand, the issue about the dimensioning and tolerancing methods, and the related annotation transfer from 2D drawings to 3D parts. On the other hand, the lack of integration of design methods for 3D tolerance stacks calculation in the design process and, moreover, the restricted application fields in which tolerance methods are applied, as in aerospace or automotive fields. In this scenario, we propose a Computer-Aided Tolerancing (CAT)-based approach, integrated within the embodiment design of the product development and able to support the analysis and the design of 3D tolerance stacks in mechanical assembly, by simulating the 3D effects of both the dimensional and geometrical tolerances. Focusing on a gearbox assembly, the CAT-based approach aims to identify the main contributors (sources) of variation within the tolerance stacks, by means of a statistical and sensitivity analysis. After defining the design inputs (involved parts, tolerances definition, assembly sequence, and required measurements), we follow a bottom-up approach, starting from the part tolerances as set by the designers, up to the assembly tolerances. The CAT software simulates how the tolerances vary within their ranges. Finally, we are able to identify the main contributors to variation, which may require tightening their tolerance values, in order to improve the performance of the gearbox assembly.

Keywords: Computer aided tolerancing · 3D tolerance analysis · Geometric dimensioning and tolerancing · Design method · Gearbox assembly

1 Introduction

Tolerance is one of the most important parameters in product and process design [1]: the 3D tolerance stacks influence the design, the manufacturing, and the assembly phases of industrial products [2–4], so the 3D tolerance management requires specific methods and tools in order to achieve their analysis and assessment [5].

The management of spatial dimensional variations and 3D tolerance stacks is a key issue to achieve high performance and robust solutions in all the industrial fields, in particular in the automotive and aerospace ones. Tolerances are relevant in the design of

F. Cavas-Martínez et al. (Eds.): *Advances on Mechanics, Design Engineering and Manufacturing II*, LNME, pp. 152–161, 2019.
https://doi.org/10.1007/978-3-030-12346-8_15

machines, as mechanical transmissions [1] and hydraulic pumps [6], because affecting their performance; tolerances are strictly connected with manufacturing costs [7], and are a key requirement in robotic manufacturing processes, in order to guarantee high repeatability of tasks, as in the machining of automotive components [8] or in the finishing operation of aerospace parts [9], or in mechanical assembly, as in [10], where the authors aim to identify the most critical tolerances on the welded assembly of a car chassis.

The state of the art in 3D tolerance analysis addresses two main difficulties [2, 4, 11]: the first issue relates to the dimensioning and tolerancing methods, in particular to the annotation transfer from 2D drawings to 3D parts. The simplification of 2D drawings may be achieved by managing tolerances directly in the CAD model, according to ISO [12] and ASME [13] standards, with consequent design time reduction and improvement of the tolerance management.

The second is about the lack of integration of design methods for 3D tolerance stacks calculation in the design process and, moreover, the restricted application fields in which tolerance methods are applied, as in aerospace or automotive fields.

In particular, two main methods for the tolerance stack calculation are used industrially [14]: namely, they are the worst case method and the root sum square method, with a statistical approach. They can be easily implemented and developed by means of a spreadsheet, but one main limitation is the lack of evaluation of 3D effects due to geometrical tolerances (Fig. 1).

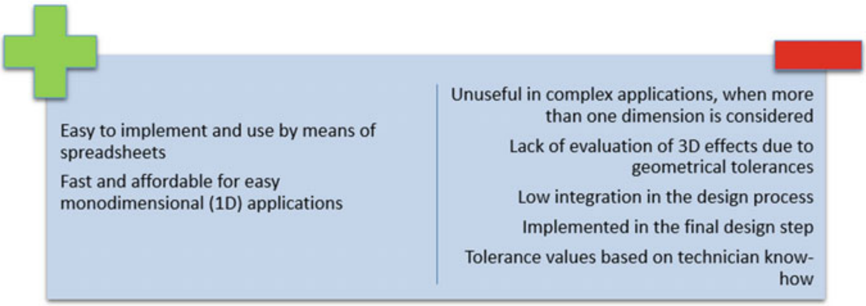

Fig. 1. Pros and cons of traditional tolerance stack calculations

A more efficient method is based on Computer Aided Tolerancing (CAT) software [15–17], which simulates the three-dimensional effects of both the dimensional and geometrical tolerances, but its use is not widespread in industries, with the exception of the automotive and the aerospace fields, other than in the research field. A CAT software simulates the variation of parts and their tolerances [5, 18], mainly by integrating other tools and approaches [10, 11, 19].

The use of a CAT software requires the definition of a model, of its functional analysis, of the functional dimensions and their stacks. It may be based on tolerance analysis or synthesis, and it compares the results with the expected values.

In this scenario, our goal is to develop a method able to support the analysis and the design of 3D tolerance stacks in mechanical assembly, capable of being implemented in industries. Focusing on the selected case study, a gearbox assembly, the method aims to identify the main contributors (sources) of variation within the tolerance stacks in the mechanical transmission field.

The paper is structured as follows. Section 2 describes the CAT-based approach for the tolerance analysis, Sect. 3 presents its application to a case study selected among mechanical transmission, a gearbox assembly, and finally Sect. 4 draws some final remarks.

2 A CAT-Based Approach

In order to face the main difficulties presented in Sect. 1 and to foster the diffusion of CAT analysis in industries, we propose the development of a CAT-based approach integrated early in the design phase (i.e. in the embodiment design phase, as in Fig. 2). The approach aims to manage the spatial dimensional variations of the assembly parts, for assessing and improving the definition of the assembly sequence and the tolerance allocation. It is capable to identify the main contributors (sources) of variation within the tolerance stacks for integrating the tolerance design in the gearbox analysis and their optimization.

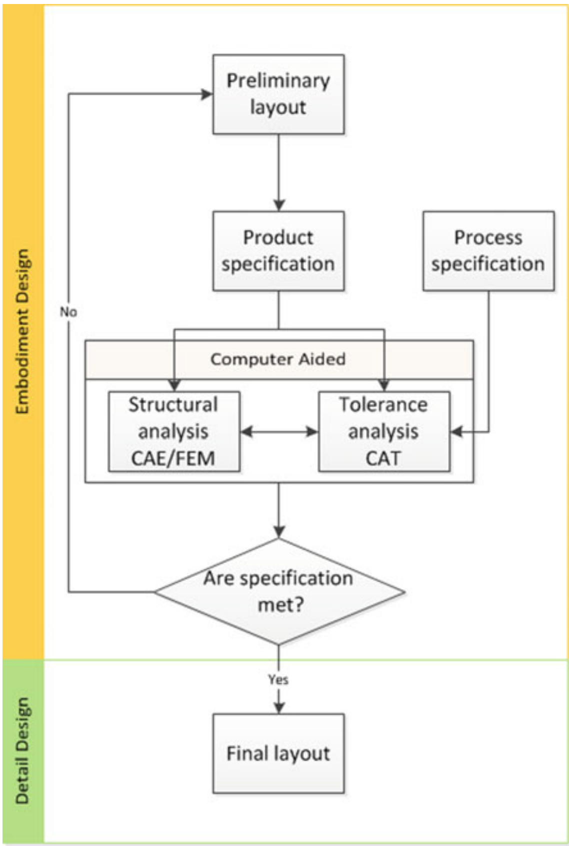

Fig. 2. Integration of CAT analysis into the design process

The approach follows the steps shown in Fig. 3, and detailed in this section. Some key features are:

– It is based on a 3D approach, able to evaluate the 3D effects due to geometrical tolerances.
– It is integrated within the design environment.
– It is implemented in the early design phases.
– It identifies the main contributors in the tolerance stacks, by means of a statistical and sensitivity analysis, and defines the tolerancing schemes.
– It simulates the assembly process.

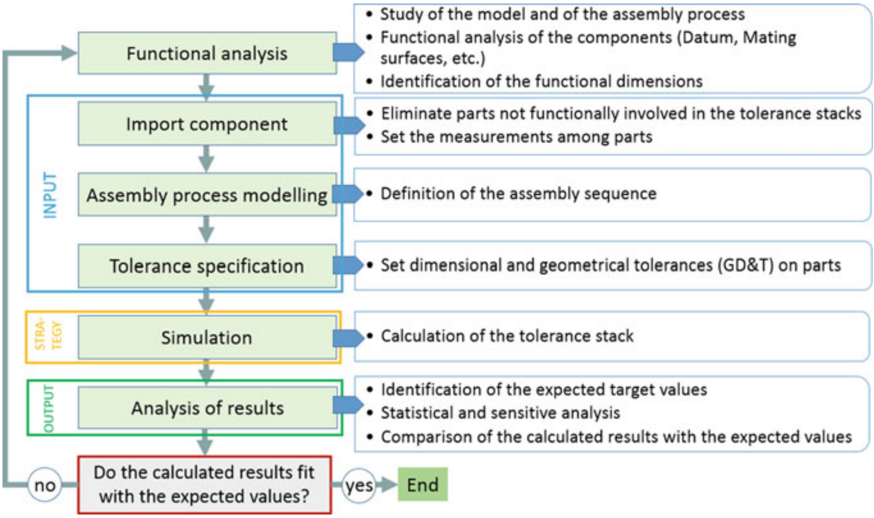

Fig. 3. Steps of the CAT-based approach

(A) The **input definition** follows the listed steps:
  (1) Definition of parts geometry. The first input is to identify the parts geometry. Parts are imported in the CAT software and they may be reduced by eliminating the non-contributing parts in the tolerance stack, as seals, covers, keys, and others mechanical fasteners and components.
  (2) Definition of the assembly sequence, i.e. how a part is positioned and located with respect to another within the assembly.
  (3) Set dimensional and geometrical tolerances (GD&T) on parts. In this specific analysis, GD&T are inputs on the case, contributing to the axial alignment.
  (4) Set the measurements, which are useful to understand the effects of tolerances. The outputs of the simulation will refer to the measures set.

(B) In the **strategy of the simulation**, we follow a bottom-up approach, starting from the part tolerances as set by the designers, up to the assembly tolerances. The bottom-up approach, also called the analytical approach, starts from the part tolerances up to the assembly tolerances, in order to determine if the objective of the model is met.

The designers, by developing "what-if" studies, may determine solutions that include both process and tolerances to keep costs down and quality up.
We use two commercial software, namely 3DCS Variation Analyst (DCS) and Cetol 6σ (Sigmetrix), which are both add-in workbenches integrated in the CAD platform CATIA V5 (Dassault Systemes). The first employs a variational (statistical) approach, based on the Monte Carlo simulation, which simulates the part variations within their tolerance ranges. In each run, each tolerance varies its value according to a randomized value within its tolerance range. Each tolerance may assume different statistical distribution (Gaussian, Weibul, uniform, etc.) in order to simulate different manufacturing conditions. The second CAT software (Cetol 6σ) employs a vector loop approach, based on a series of vectors arranged in a loop to reproduce the effect of the variations on the final assembly, analysed by means of a second-order tolerance analysis (SOTA) method [20].

All the parts are simulated as rigid models, without parts distortion.

(C) The main **outputs** are the statistical and the sensitivity analysis of the tolerances, leading to identify the main contributors to variation, which may require tightening their tolerance values. Conversely, the tolerances of the less critical contributors may be increased. Moreover, the results may lead to evaluate assembly sequences and tolerance alternatives by what-if studies in an iteratively way.

3 Case Study

The case study is a helical-coaxial gearbox. The gearbox is firstly analysed in order to check the current tolerance scheme, which is the input for the further tolerance analysis. The functional measures to be controlled in the tolerance stack analysis are the distance variations along the X and Y directions between the three shafts of the gearbox.

(A) The input phase consists of the following steps:
(1) Definition of parts geometry, by identifying the components involved in the tolerance stack:

- The CAD model of each component is imported in CAT environment.
- The element tree needs to be reduced by eliminating the non-contributing parts in the tolerance stack.
- Finally, the assembly is reduced to 20 parts.

(2) Definition of the entire assembly sequence, i.e. how the gearbox parts are positioned and located in the assembly, with respect to the others. Figure 4 shows the assembly sequence of the output side parts of the gearbox. Some parts, such as the case, may be supposed as fixed.

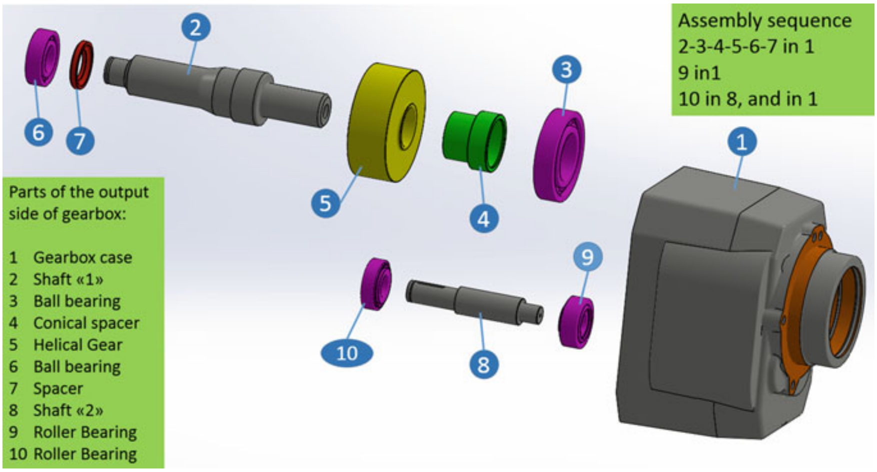

Fig. 4. Parts of the output side of the gearbox and their assembly sequence

(3) In order to set the dimensional and geometrical tolerances (GD&T) on parts, we need to define a Datum Reference Frame (DRF), as shown in Fig. 5 for the gearbox case: then, we allocate the tolerances on its mating features. Similarly, we define a DRF and allocate the tolerances on all the other parts by means of the GD&T annotation, in order to evaluate how each dimensional and geometrical tolerance contributes to the shaft distance variations.

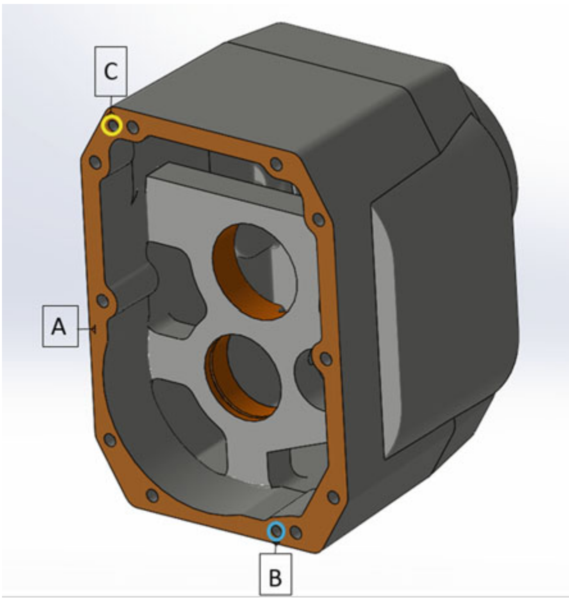

Fig. 5. The datum reference frame defined on the gearbox case

As an example, referring to the gearbox case, we set:

– Dimensional tolerances on the bearing housings.
– Geometrical tolerances, with respect to the DRF: the position of the bearing housing, the parallelism of the axis of the bearing housing, the concentricity of the bearing housings, the position of the pin holes, etc.…

(4) We set four measurements (Fig. 6), which consist of the distances between each pair of the three shafts along the X and Y directions in correspondence of the meshing gears.

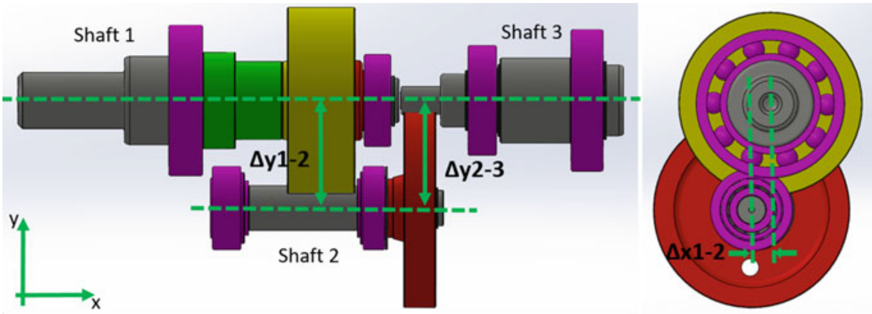

Fig. 6. Measurements of the shaft distances. Left: The vertical distances between shaft 1 and shaft 2, and between shaft 2 and shaft 3. Right: The horizontal distance between shaft 1 and shaft 2 (similarly, on the other side, between shaft 2 and shaft 3)

(B) After the input definition, we define the strategy of the simulation: in this first phase, we follow a bottom-up approach, starting from the part tolerances as set by the designers, up to the assembly tolerances. The simulation is performed with both the CAT software, using both the variational and the vector loop approach, and by considering all the parts as rigid models: the outputs of the two software are fully comparable. Finally, we check the four outputs, which are the four measurements previously described.

Measurement 1 (Δx1 − 2): The statistical analysis (Fig. 7) shows the distribution of the distance along the X axis, its mean value, and its sensitivity analysis, which shows that the main contributors to this measurement are:

– the parallelism tolerance of the axis of the bearing housing 2 (47.86%).
– the run out tolerance of the shaft 1 (19.76%).
– the position tolerance of the bearing housing 1 (13.46%).

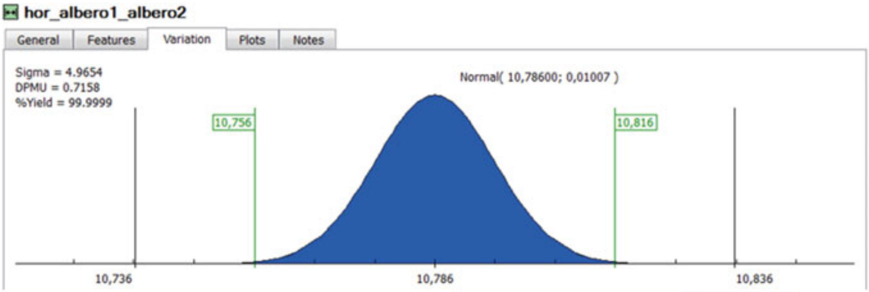

Name	Context	Tolerance	Cpk	Variance Contrib
to sedeCuscineto1	carter;1/sedeCuscinetto2	Ø 0,005	1,00	47,86 %
to A1 - A2	albero;1/Feature3	0,030	1,00	19,76 %
to A|B|C	carter;1/sedeCuscineto1	Ø 0,015	1,00	13,46 %
to A1 - A2	albero2;1/Feature7	0,020	1,00	8,60 %
to A|B|C	carter;1/sedeCuscinetto2	Ø 0,015	1,00	5,48 %
to sedeCuscineto1	carter;1/Feature2	Ø 0,015	1,00	2,36 %
to sedeCuscinetto2	carter;1/Feature6	Ø 0,015	1,00	2,03 %
to diametroInterno	cuscinetto4;1/cuscinetto4;1/diametroEsterno	0,004	1,00	0,16 %

Fig. 7. Tolerance contributors on measurement 1

Similarly, the main contributors on **Measurement 2 (Δy1 − 2)** are:

– the parallelism tolerance of the axis of the bearing housing 2 (47.86%).
– the run out of the shaft 1 (19.76%).
– the position of the bearing housing 1 (13.46%).

Again, the main contributors on **Measurement 3 (Δx2 − 3)** are:

– the position of the bearing housing 1 (27.59%).
– the parallelism of the axis of the bearing housing 2 (24.99%).
– the position of the first parallel pin (18.87%).

Finally, the main contributors on **Measurement 4 (Δy2 − 3)** are:

– the position of the bearing housing 1 (32.03%).
– the parallelism of the axis of the bearing housing 2 (29.01%).
– the perpendicularity of the axis of the first parallel pin (8.55%).

In all the four measurements, the position tolerances of the bearing housing and the parallelism tolerances between their axes are determined as the main contributors to variation. Therefore, when comparing the resulting tolerance ranges on the four measurements with the expect values, two different scenarios may occur:

– If the tolerance ranges are too loose when compared to the expected value, we can tight the tolerance values of the main contributors to variation, in order to improve the performance of the gearbox assembly.
– If the tolerance ranges are too tight when compared to the expected value, we can relax the tolerance values of the main contributors to variation, in order to reduce the manufacturing cost of the parts of the gearbox assembly.

Moreover, we can act on the less critical contributors to variation and increase their tolerance values, without significantly affecting the tolerance stack and the final tolerance value, allowing the use of less expensive manufacturing processes (cost reduction).

According to these outputs and to future "what-if" studies, we will act on the tolerance schemes in order to test design changes by modifying tolerance values on parts and by assessing how their contributions to variation will change, or by modifying the assembly process.

4 Conclusion

In the present work, we propose a CAT-based method for the tolerance analysis of a mechanical assembly. The method is applied to a gearbox assembly, selected as a case study, and proves to be able to:

- identify the main contributors to variation,
- identify the less critical contributors to variation,
- evaluate different assembly sequences and tolerance alternatives by what-if studies.

Focusing on the distance variations between each pair of the three axes of the gearbox shafts, the most critical contributors in the tolerance stacks are determined as the position tolerances of the bearing housings in the gearbox case and the parallelism tolerances between their axes. These results highlight the importance of the tolerance analysis in order to perform actions only on specific tolerances (and not on all the tolerances of a part or an assembly).

This output represents a first step towards the definition of a knowledge-based framework, also called a design archetype, to support designers in the design of gearboxes, which will be integrated in the entire design process. In fact, as future developments, we will implement a top-down approach (tolerance synthesis approach): starting from the assembly tolerances or the functional requirements on the assembly, the tolerances on single parts have to be allocated aiming to achieve the expected tolerance on the assembly.

References

1. Zhang C, Ben Wang H-P (1993) Tolerance analysis and synthesis for cam mechanisms. Int J Prod Res J 31(5):1229–1245
2. Colosimo BM, Senin N (2011) Geometric tolerances—impact on product design, quality inspection and statistical process monitoring. Springer
3. Shah JJ, Yan Y, Zhang B-C (1998) Dimension and tolerance modeling and transfor-mations in feature based design and manufacturing. J Intell Manuf 9(5):475–488
4. Chase KW, Parkinson A (1991) A survey of research in the application of tolerance analysis to the design of mechanical assemblies. Res Eng Design 3(1):23–37
5. Fischer BR (2011) Mechanical tolerance stackup and analysis, 2nd edn. CRC Press
6. Gherardini F, Zardin B, Leali F (2016) A parametric CAD-based method for modelling and simulation of positive displacement machines. J Mech Sci Technol 30(7):3253–3263

7. Etienne A, Dantan JY, Qureshi J, Siadat A (2008) Variation management by functional tolerance allocation and manufacturing process selection. Int J Interact Des Manuf 2(4):207–218
8. Leali F, Pini F, Ansaloni M (2013) Integration of CAM off-line programming in robot high-accuracy machining. In IEEE/SICE international symposium on system in-tegration, Kobe, Japan
9. Leali F, Pellicciari M, Pini F, Vergnano A, Berselli G (2013) A calibration method for the integrated design of finishing robotic workcells in the aerospace industry. In: Neto P, Moreira AP (eds) Robotics in smart manufacturing. Communications in Computer and Information Science, vol 371. Springer, Berlin, Heidelberg
10. Panari D, Renzi C, Vergnano A, Bonazzi E, Leali F (2017) Integrated design method for optimal tolerance stack evaluation for top class automotive chassis. In: advances on mechanics, design engineering and manufacturing. Springer International Publishing, pp 1013–1022
11. Barbero BR, Azcona JP, Pérez JG (2015) A tolerance analysis and optimization methodology. The combined use of 3D CAT, a dimensional hierarchization matrix and an optimization algorithm. Int J Adv Manuf Technol 81(1–4):371–385
12. ISO 16792:2015 (2015) Technical product documentation—Digital product definition data practices
13. ASME Y14.41-2012 (2012) Standard on digital product definition data practices
14. Shen Z, Ameta G, Shah JJ, Davidson JK (2015) A comparative study of tolerance analysis methods. ASME Transa J Comput Inf Sci in Eng V5(3)
15. Bjorke O (1989) Computer aided tolerancing. ASME, New Jersey
16. Anselmetti B, Chavanne R, Yang JX, Anwer N (2010) Quick GPS: a new CAT system for single-part tolerancing. Comput Aided Des 42(9):768–780
17. Söderberg R, Lindkvist L, Carlson J (2006) Virtual geometry assurance for effective product realization. In: 1st Nordic conference on product lifecycle management—NordPLM'06, Göteborg, Sweden
18. Corlew GT, Oakland F (1976) Monte Carlo simulation for setting dimensional tolerances. Machine design, May, 91–95
19. Faerber PJ (1999) Tolerance analysis of assemblies using kinematically-derived sensitivities. ADCATS report no. 99-3
20. Glancy CG, Chase KW (1999) A second order method for assembly tolerance analysis. In: Proceedings of the 1999 ASME design engineering technical conference, September 12–15, 1999, Las Vegas, Nevada, DETC99/DAC-8707

Computer-Aided Design and Interactive Design

A Virtual Kinematic Design of Dental Restorations Using Reverse Engineering

M. Iturrate[1], R. Minguez[1], N. Toledo[1], H. Eguiraun[1], I. De Prado[1], and E. Solaberrieta[2](✉)

[1] University of Basque Country UPV/EHU, Alameda Urquijo sn, 48013 Bilbao, Spain

[2] University of Basque Country UPV/EHU, Europa Plaza 1, 20018 Donostia, Spain

eneko.solaberrieta@ehu.eus

Abstract. In terms of diagnosis, planning and treatment, when a dental patient needs a complex restoration or presents a temporomandibular disorder, it is necessary to reproduce the mandibular movements out from mouth. The best tool for this purpose is the virtual articulator. Virtual articulators enable a design that takes into account the kinematics necessary for the design process of dental restorations and at the same time, avoids possible collisions. The location of the hinge axis constitutes just one step in attempting to reproduce mandibular movement. However, the importance of this step arises from the fact that almost all movements start at the axis and return to it. Therefore, this study focuses on the virtual acquisition of the patient's mandible rotation axis (kinematic axis) using reverse engineering devices.

Keywords: Dental prosthesis design · Dental virtual articulator · Dental CAD/CAM system · Reverse engineering · Kinematic axis

1 Introduction

This project arises out of the need to determine the kinematic axis of dental patients in order to simulate and analyse mandibular movements of the human jaw when designing with a dental virtual articulator. This can be achieved by means of CAD systems and Reverse Engineering tools.

This development has been made at the Product Design Laboratory (PDL, www.ehu.eus/PDL), in the Faculty of Engineering of Bilbao, University of the Basque Country. This Laboratory has focused its investigation on Reverse Engineering and Rapid Prototyping knowledge areas and is currently looking for new fields of application for these new design methods in an effort to promote technological transference with neighbouring companies.

To begin with, the determination of the kinematic axis was carried out through different experiments. The registering process was carried out using the measuring tools and Reverse Engineering tools available at the PDL. These tools are: ATOS I rev.2 GOM 3D scanner (precision: 0,03 mm) and the Reverse Engineering and Computer-Aided Inspection Software the Rapidform XOR.

F. Cavas-Martínez et al. (Eds.): *Advances on Mechanics, Design Engineering and Manufacturing II*, LNME, pp. 165–173, 2019.
https://doi.org/10.1007/978-3-030-12346-8_16

The experiments were carried out in three phases. The first phase was carried out using a mechanical articulator as if it were the patient. Afterwards, the role of the patient was played by a drum and the kinematic axis was determined. And finally, the same procedure was carried out in real patients.

After a thorough analysis of the results obtained with different experiments, the proposed methodology was able to determine the kinematic axis of any patient with different deviations for any patient.

The ultimate aim of this process is to determine the kinematic axis of each patient in order to design dental prostheses that take into account the accurate starting position of excursive movements.

2 Approximation

In current dentistry, the conventional procedure remains common practice. However the presence of the digital workflow (Fig. 1) is rapidly increasing in many fields such as orthodontics, prosthodontics, orthognathic surgery, and so on [1]. This computerized digital procedure provides more control over the planning and treatment process and shortens the time necessary for many of its steps, especially for the designing phase [2, 3].

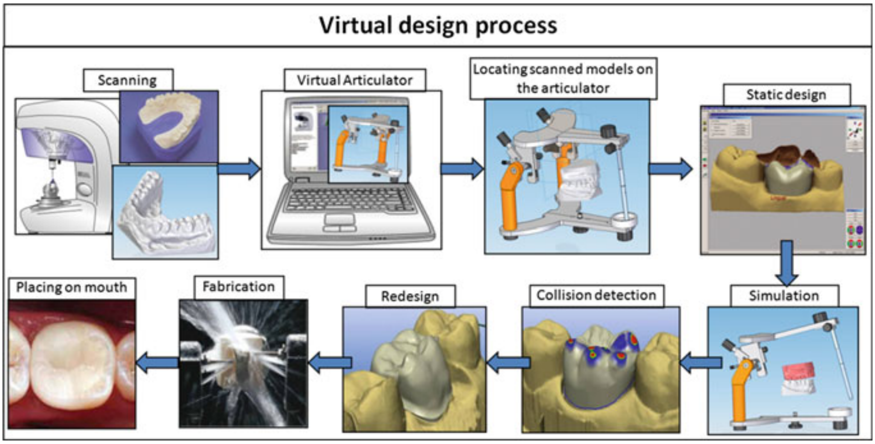

Fig. 1. Digital workflow of the virtual design process

Besides this, some recent developments provide more control and accuracy to the process as well as to the final product design. In dental restoration, the design process is monitored and tailored to the patient's requirements [4].

One of the lacks of this digital workflow is the location of the kinematic axis and consequently the accurate transfer of the models to the articulator. On the conventional procedure an axiograph is used to locate the kinematic axis on the patient and register the mandibular movements [5, 6]. This requires time and besides, the use of such mechanical device involves an inconvenience for the patient. Apart from this, in many cases the same axiograph [7] is used to set the parameters of the semi or fully adjustable articulator.

On the other hand, a literature review shows the importance of the kinematic intercondylar axis [8]. Due to the many purposes for which this axis is useful, it has been intensively studied for a long time. The location of the hinge axis is just one step in attempting to reproduce mandibular movement. However, the importance of this step lies on the fact that almost all movements start at the axis and return to it. The arch of closure determines the hinge axis and every contact position of the teeth is based on this hinge axis. This closure results from the combination of the closing rotation and a gliding path of the axis, after the first 3–5 mm.

Scallhorn [9] found 95% of the axis points located 13 mm anterior to the posterior margin of the tragus on the tragus-canthus line to be within a 5 mm radius of the kinematically located axis. On the other hand, Lauritzen and Bodner [10] said that 33% of a patients true hinge axes are within 5 mm of the patients true axis, although in practice many technicians do not use it because of the required time. Finally, the research carried out by Palik et al. [11] found that the earpiece face-bow related the maxillary cast to the hinge axis only 50% of the time. 92% of the time the arbitrary axis was located anterior to the terminal hinge axis.

Therefore, this study arises out of the need to determine the kinematic axis using reverse engineering. This enables an accurate transfer to the virtual articulator, and hence a kinematic design of dental prostheses.

3 Materials and Methods

As it has been explained in the introduction, the first purpose is to determine the kinematic axis. In order to achieve this, the following methodology is proposed (Fig. 2).

Firstly, the targets are located on the mobile part and fixed to the mandible. It is important that the targets are placed on planar or surfaces with a big curvature. Otherwise, the registering system could have problems. Besides this, at least 3 targets are located on the fixed part. This is necessary in order to have a reference when different sessions are aligned. Even more: in order to ensure a good alignment and obtain a better reference, more targets are used on the fixed part.

Secondly, these targets are registered on 3 or more positions. In order to achieve this, some plastic pieces are introduced in the mouth, this is, these plastic pieces are in a static position at a known distance (Fig. 3). With just 3 positions it is possible to obtain the rotation center for each plane using a method of least squares to determine the circular path. Every time a new position is registered, the corresponding minimum deviation arch is as well calculated.

Each position of the mandible is captured in one session, therefore, different sessions must be aligned or matched into one. With this aim, fixed targets are made to coincide whilst mobile targets remain in different positions.

Afterwards, once the path of different mobile targets is determined, the arch corresponding to each plane is drawn. Since more than 3 points have been obtained, the minimum deviation arch is calculated.

Finally having the centers of these 3 or more arches, the tolerance cylinder and the average axis, which is the kinematic axis of the patient, are determined.

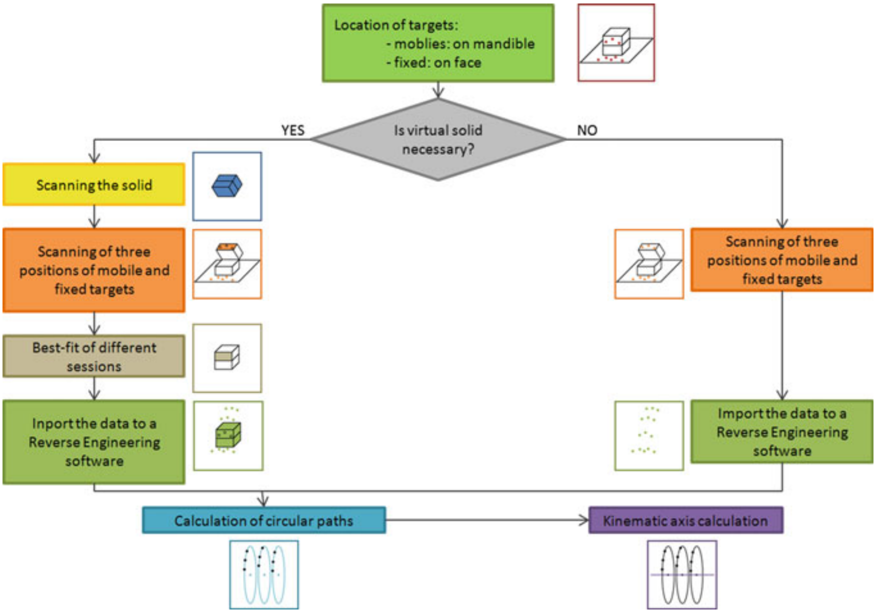

Fig. 2. Proposed methodology to calculate the kinematic axis

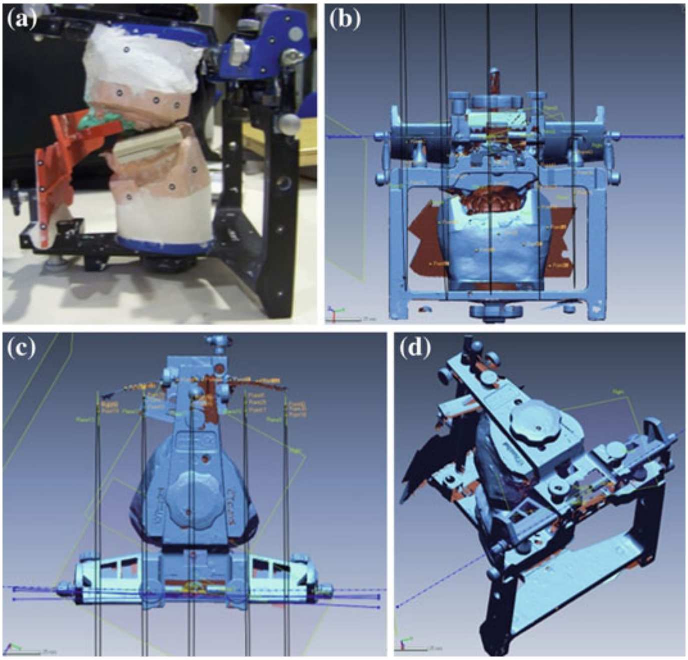

Fig. 3. Experiment with articulator. **a** Position taking a registration. **b** Back view. **c** Top view. **d** The kinematic axis on the virtual articulator

The methodology to determine the kinematic axis has been validated in 3 phases with different experiments. The first experiment type was carried out on a Panadent PSH mechanical articulator. The second phase was carried out using a plastic skull or dum with a mobile jaw and the last phase took place with real patients.

4 Results

On the first phase, different sessions were carried out with 6 different “patient” cases. In this case, as it occurs in most of mechanical articulators, the upper side is the moving part (opposite to human mandible). In this upper mobile part 3 targets were located and the rotation was calculated in 3 different positions. Due to the mechanical articulator was digitized it was able to locate the targets in reference to the virtual articulator. In this case it was possible to calculate the error of each, because the kinematic axis was known on the articulator.

The diameter of rotation in each targets was different, while the axis was the same. However, the value of the relative error (Table 1) was small enough to validate the methodology.

Table 1. Results of the experiments of the first phase

Experiment	Mobile point number	Error (E) [mm]	Diameter (D) [mm]	Relative error (E/D)
1A.I	1	0.35	347.99	0.0010
	2	0.59	366.45	0.0016
	3	0.18	410.25	0.0004
1A.II	1	0.28	363.12	0.0008
	2	0.83	430.76	0.0019
	3	0.67	417.50	0.0016
1B.I	1	1.32	88.63	0.0169
	2	1.32	64.62	0.0204
	3	0.10	150.77	0.0038
1B.II	1	1.32	88.63	0.0169
	2	1.32	64.62	0.0204
	3	0.10	150.77	0.0038
1C.I	1	1.49	159.28	0.0094
	2	1.02	188.13	0.0054
	3	1.75	208.90	0.0084
1C.II	1	0.21	157.82	0.0013
	2	0.18	187.70	0.0010
	3	0.44	207.92	0.0021

The second phase was carried out on a plastic skull or “virtual patient”. The fixed targets were located directly on the face of the skull and the mobile targets were located using an arch fixed to the mandible with alginate. As Fig. 4 shows, different positions of the mobile targets were aligned in the same session and different experiments were carried out with the same patient using different combination of targets.

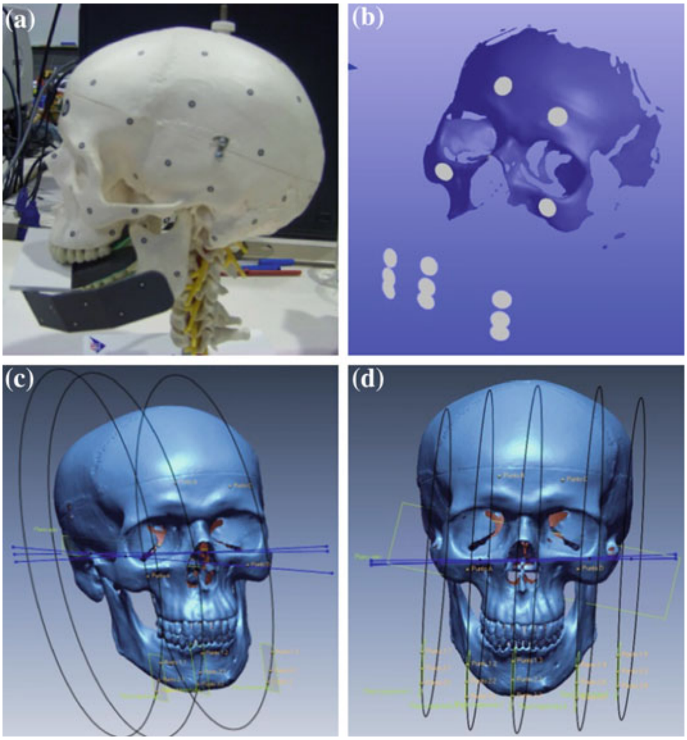

Fig. 4. Experiment with plastic skull. **a** Position taking a registration. **b** Fixed and mobile targets in one session. **c** Using 3 mobile targets. **d** Using 4 mobile targets

Table 2 shows the main result of this experiment; the diameter of the tolerance is determined for each session.

Table 2. Results of the experiments of the second phase

Session	Number of targets	Distance between targets [mm]	Diameter of the tolerance cylinder [mm]
1	3	≈70	1.11
2	4	≈50	0.44
3	5	≈40	0.56
4	6	≈30	0.34
5	5	≈35	0.87
6	4	≈40	1.34

Finally, the methodology was tried with real patients (Fig. 5).

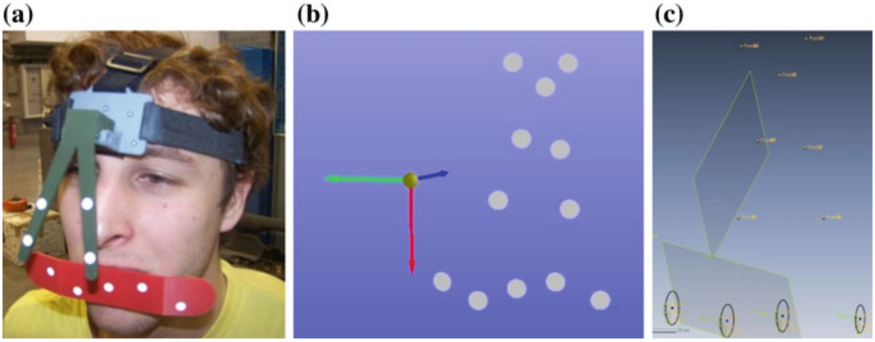

Fig. 5. Experiment with real patient. **a** Taking a registration on a real patient. **b** Fixed and mobile targets in one session. **c** Some results

The results of different phases are quite different (Table 3).

Table 3. Results of the experiments of the third phase

Session	Number of targets	Distance between targets [mm]	Diameter of the tolerance cylinder [mm]
1	3	≈70	2.11
2	4	≈50	1.44
3	5	≈40	1.56
4	6	≈30	0.94
5	7	≈25	1.17

5 Discussion

A literature review remarks the importance of the kinematic axis on dental prostheses design. This is due to the fact that the relationship of the teeth as they come together is determined by the relation of the condyle to the glenoid fossa [10]. The hinge axis governs the arch of closure in every contacting position of the teeth. The rotation of the asymmetrical condyles and the asymmetrical mandible is guided by the form of the surface on the meniscus.

The purpose of an articulator is to reproduce on a mechanical instrument the relations of the teeth as they come together in the mouth. The hinge axis is the key that enables the virtual transfer of the patient to the laboratory bench.

Locating the hinge axis and reproducing the protrusive path (anterior slant and curvature of the condylar path) and lateral paths (Bennett movement) allows all combinations of movements to be made. To locate the hinge axis with a hinge bow, a clutch is mounted on the mandibular teeth. The chin is dropped open with pure hinge motion while a stylus records the position opposite the condyle. No gliding of the condyle should be allowed. The hinge axis must be located in the most posterior superior position of the condyle which is centric relation.

The point of the stylus will reach the stationary point and the patient can be tattooed for future reference. Mounting the cast on the articulator can be accomplished by using the hinge bow as a transfer or face bow. Instead of the ala-tragus plane, the Frankfurt Plane is used to relate the face bow.

This means that an arbitrary marking of the hinge axis may result in inaccurate mounting of casts to an articulator, and occlusal discrepancies may appear if the centric relation record is made with separation between the upper and lower teeth. Therefore, the accurate location of the true hinge axis points is recommended by some authors [12] and any chosen arbitrary location would not reliably represent the true anatomic hinge axis.

Gordon et al. [13] said that locating the kinematic hinge point prior to extensive treatment for edentulous patients' results in a better occlusion and also saves time.

However, these statements were made many years ago and nowadays; there are many different axiographs and jaw movement recording devices [8]. There are different methodologies to register these movements, ultrasonic, LED, etc. and there is a variety of marketed devices used by dental technicians: Freecorder®, Arcusdigma®, Zebris®, Axioquick®, etc. The main disadvantage of these devices is that their use requires a great amount of time as well as a substantial financial investment. What is more, these movements' recorders are not integrated in any dental CAD/CAM systems, so they do not offer a direct connection to virtual articulators.

It should be noted that the accuracy of calculating the mandibular kinematic axis can be improved. After analyzing the results of the various experiments, the conclusion was that these could be factors to consider in order to minimize the deviation:

- Avoiding any movement of the patient while recording data.
- The fact that mandibular movement is not a pure rotation (first 5 mm).
- The scanner accuracy.
- The orientation of the targets.

6 Conclusions

The proposed methodology to determine the kinematic axis has been validated, although some progress should be made to develop a specific device to record at an affordable price the kinematic axis of a real patient.

These experiments have as well proven that these scanners themselves are an effective tool to find the centers of rotation of moving points and, therefore, the rotation axis of a solid element.

Acknowledgements. The authors of this paper thank the Faculty of Engineering of Bilbao for locating the PDL in their facilities and the Country Council of Gipuzkoa and for financing this project (75/18).

References

1. Pieper R (2009) Digital impressions—Easier than ever. Int J Comput Dent 12:47–52
2. Kordass B (2010) Clinical dental CAD/CAM—qualification for tomorrow's networked dentistry. Int J Comput Dent 13:3–6
3. Kurbad A (2011) Impression-free production techniques. Int J Comput Dent 14:59–66
4. Beuer F, Schweiger J, Edelhoff D (2008) Digital dentistry: an overview of recent developments for CAD/CAM generated restorations. Brit Dent J 204(9):505–511
5. Fang JJ, Kuo TH (2008) Modelling of mandibular movement. Comput Biol Med 38:1152–1162
6. Al-Anezi1 T, Khambay1 B, Peng MJ et al (2013) A new method for automatic tracking of facial landmarks in 3D motion captured images (4D). Int J Oral Maxillofac Surg 42:9–18
7. Kucukkeles N, Ozkan H, Ari-Demirkaya A, Cilingirturk AM (2005) Compatibility of mechanical and computerized axiographs: a pilot study. J Prosthet Dent 94(2):190–194
8. Granger ER (1959) Clinical significance of the hinge axis mounting. DCNA 3:205–213
9. Schalhorn RG (1957) A study of the arbitrary center and kinematic center of rotation for facebow mounting. J Prosthet Dent 7:162–169
10. Lauritzen AG, Bodner GH (1961) Variations in location of arbitrary and true hinge axis points. J Prosthet Dent 11:224–229
11. Palik JF, Nelson DR, White JT (1985) Accuracy of an ear piece face-bow. J Prosthet Dent 53:800–804
12. Walker PM (1980) Discrepancies between arbitrary and true hinge axis. J Prosthet Dent 43:279–285
13. Gordon SR, Stoffer WM, Connor SA (1988) Location of the terminal hinge axis and its effect on the second molar cusp position. J Prosthet Dent 60:553–559

Design of an Interactive Web Interface Using Graphics for Simulating and Assessing Visual Impact in Sustainable Building Projects

J. S. Jeong(✉) and A. Ramírez-Gómez

Departamento de Ingeniería Mecánica, Química y Diseño Industrial, Escuela Técnica Superior de Ingeniería y Diseño Industrial, Universidad Politécnica de Madrid, Ronda de Valencia 3, 28012 Madrid, Spain
jinsu.jeong@upm.es

Abstract. Since several decades ago, the technological enrichments and boosts in information organism areas are expended to counterpart various modeling in engineering and other disciplines. Because of its technological improvements, many programs and lineups such as Multi-Criteria Decision Analysis (MCDA), Geographic Information System (GIS), graphic modeling, etc. are required to syndicate and work on the basis of the web and/or internet platform services. These allow designers (engineers, architects, planners, policy authorities, academics, etc.) to simulating and assessing their projects into an interactive web atmosphere supplementary to improved comprehend the dissimilar designs, simulating different states of building process, and brining a new perspective of them. This paper presents the design of an interactive web interface modeling using graphics that, in a case study situation, consenting to gauge and envisage a building projects' visual impact. Here, particularly, GIS and visual theme analysis were employed for that building project indicated. In visual elements theme, GIS model depicted can be graphically exemplified. Consequently, the results can be used to verify visual impact of sustainable and viable building projects in the asynchronous and/or synchronous decision-making progression distinguished space and spatial parts. Accordingly, the generation and authentication of an interactive web interface could be an empirical interface for judging visual impact, eventually accomplishing sustainable and viable design and elaboration of built circumstances.

Keywords: Web graphics · GIS · Computer-aided design · Sustainable and interactive design · Representation techniques

1 Introduction

In the information schemes extents, the technological enlargement and attainment are fitting to the principal contrivance for the Spatial Decision Support System (SDSS) granted [1–3]. The value and usefulness of information propagation for the Decision-Makings (DMs) is reconnoitered by the SDSS, graphic modeling, depiction technique, and the GIS and the MCDA classification and amalgamation [2, 4, 5]. Largely, a web-based GIS classification is a general web-based SDSS classification. That gadgets the

F. Cavas-Martínez et al. (Eds.): *Advances on Mechanics, Design Engineering and Manufacturing II*, LNME, pp. 174–183, 2019.
https://doi.org/10.1007/978-3-030-12346-8_17

GIS evidence and information in the World Wide Web (WWW) upbringing. Occasionally, the GIS gadget and software together with public source are employed, which are merged and assimilated with the MCDA practices [3]. For decision-makers and all-purpose contributors, the web-based GIS classification expedites to make decisions among contributors and, thus, maneuvers meritoriously and conveniently to advance the model classification as an entryway. With diverse and assorted qualifications, interpretations, interests, establishments of their concerns, a bunch of contributor clinches to apprehend the solutions that are community-enhanced in this classification framework. These are convincing due to have a genuine and evenhanded tendency [6–8]. The web MC-SDSS classification is required to be engendered as an interactive web interface, which sketches is insinuated instead of the GIS and MCDA full and specific integration and ArcGIS's Visual Basic for Applications (VBA) and Model View Controller (MVC) color regulation.

This technological enlargement and accomplishment allow designers such as engineers, architects, planners, policy authorities, academics, etc. to simulating and predicting their projects into an interactive web environment supporting to better understand the different designs, simulating different states of building process, and brining a new perspective of them. Currently, several studies have reconnoitered diverse buildings' manifestation to harm their visual impact in different environments and sceneries [7, 9, 10]. The spot-on placement is pondered as one-character along with landscape biological delineations, silhouette and form, constituents, insignias, consistencies, sectioning of volumes. It is also related with the prevailing buildings and assemblages and the conglomerate of the space and spatial bordering the building conjoining the building to the panorama [3, 11]. Particularly, correct optimal choice is the most imperative criteria to amalgamate building projects into scene usually, which is more than on any other prejudiced aspects proposed [3, 7]. In the case of color, it is a noteworthy architectural facet that is exposed to be befitted a foremost evocative piece in the design progression [3, 7, 11]. When appraising and gauging the visual impact of a building, the use of interactive web can assist designers as to encompass visual theme facets. It is the configuration and design progression and is also to display the changes shaped in the different aspects. Besides, it is a very influential communication means that instructs a well-organized method for exhibiting the visual impact, as well as to comprehend and envisage the future scenery for the stakeholders.

In this paper, we design and develop an interactive web interface modeling using graphics as the first-prototype principles study. It can gauge and foresee the building projects' visual impact that a building project could generate in a Spanish case study situation. Accurately, it is related with GIS building placement with visual constituents' theme on the basis of the introductory results obtainable from an ongoing assignment. In visual features theme, a geometrical archetypal can be graphically exemplified in. Hence, we only concentrate on the spot-on location optimal with a building project color assessment that can be employed to assessing and simulating them. The combined full and specific GIS and MCDA classification was utilized herein as a methodology. Particularly, an interactive web interface methodological outline and scaffold is insinuated for a comprehensive and specific GIS and MCDA classification with color adjustment in ArcGIS VBA and MVC implemented and envisaged, presently built in the Internet Information Server (IIS). The interactive web interface with graphics developed in this study could be a new-fangled tactic that will be expediently communal and re-used, and substantiate sustainable and viable building projects' visual impact differentiated space and spatial segments in the asynchronous and/or synchronous decision-making procedure and to extent contributors' sensitivity and perception.

2 Case Study Area

In Extremadura area, man-made building projects' encumbering and compression has predisposed the endeavor, pursuit and sustainability for certain present-day building projects for countless years. This study targets at simulating and assessing visual impact in sustainable and viable building projects in Alange (Spain) as a case study situation. This indication has sufficient values based on ethnic, entertaining, natural, genetic, picturesque, and chronological slant. Alange (Spain) is pinpointed in Badajoz, Extremadura with an around 160 km^2 area. It is located in the epicenter of Extremadura and the southwest of Spain. Thus, it has a particular reservoir with a roughly 35 km^2 neighboring the municipal central (see Fig. 1). Specifically, building projects' gradual increasement has been occurred in this area together with extensive illegitimate constructions, which is the subject of this study. Hence, due to not sustaining contemporary vagaries of building planning and advance, it is necessary to be cogitated new-fangled premeditated prerequisites and goalmouths, that is, for sustainable and cooperative ecosystem and individual reliability.

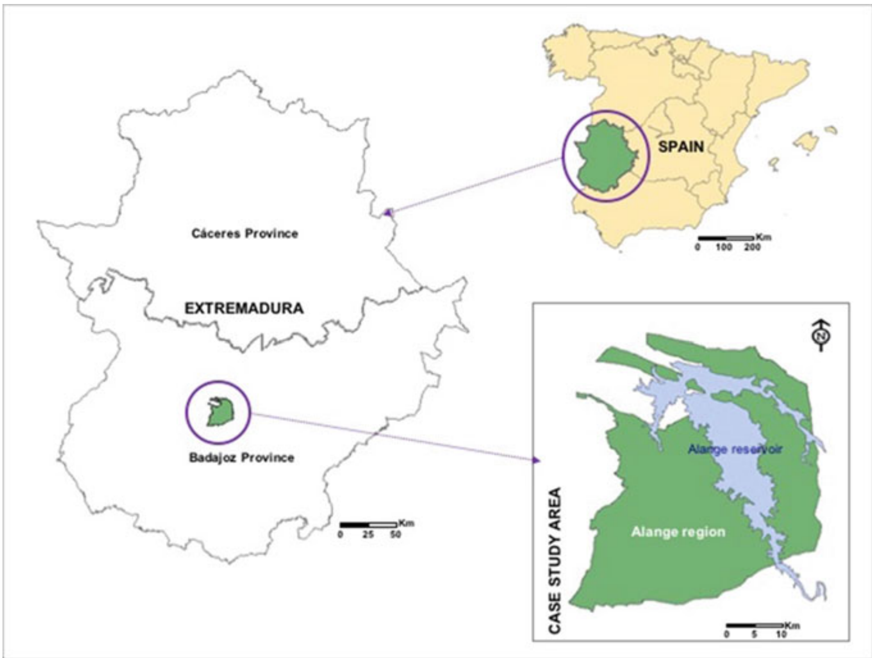

Fig. 1. Alagne, Extremadura, Spain: case study area indicated

3 Methodology

In this section, GIS/MCDA was employed with sixteen criteria with elements specified. They were congregated into four assemblies together with judgement on the basis of pair-wise to get comparative prominence and their numerical tariffs (see Table 1) [3, 7]. Now, Weighted Linear Combination (WLC) employment and the sensitivity assay with contributors scrutinize to check the results of apposite maps and visual impact. Thenceforward, the architecture/outline of an interface web interface modeling with graphics established was a comprehensive and specific GIS and MCDA classification, precisely building placement with GIS and visual components theme. Particularly, in visual elements theme, as shown in Fig. 2, a geometrical map consummates exemplify realistically [12, 13].

Table 1. Pair-wise appraisal to calculate the comparative prominence [3, 7]

More concentration	Definition	Less concentration
1	Identical prominence	1
2	More or less identical to sufficient prominence	1/2
3	More or less sufficient prominence	1/3
4	More or less sufficient to robust prominence	1/4
5	More or less robust prominence	1/5
6	More or less robust to very robust prominence	1/6
7	More or less very robust prominence	1/7
8	More or less very to severely robust prominence	1/8
9	More or less severe prominence	1/9

The gauge/device of a fuzzified Likert parallel interactions with previous considerations can be a fortitude significance, which can acquire certain matrix on criteria means. Consequently, with Triangular Fuzzy Numbers (TFNs), fuzzy marks and admissions can be portrayed in the outlook of its function/occupation as shown in Table 2 [13, 14]. Thus, with Cause and Effect Relationship Diagram (CERD), coefficients of criteria/elements inspiration could be presumed and can be interconnected with aggregate relationship matrix aforementioned.

The interactive web interface with a help of graphics will be a scheme and classification of clients and servers composed and implanted. It is also well-defined such as cooperation and communication, which backing the DM manners of clients and servers [15, 16]. To maneuver the interactive web interface, certain operative necessities are necessary technically like instantaneous attaining and analysis, a few seconds enactment per entreaty, contributor-side function. But it is only with low cost-maintained web browser for contributors through heterogeneous and dissimilar circumstances computed and calculated [8, 17, 18]. Accordingly, technical and practical support necessities are wide-bandwidth internet, software and hardware along with certain tools established. An interactive web interface with a help of graphics insinuates a full and

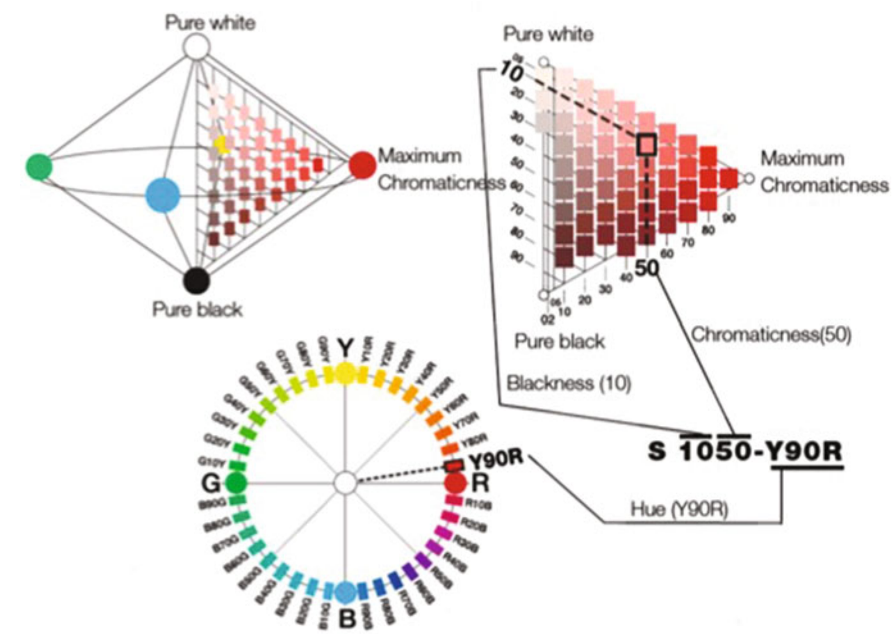

Fig. 2. Geometrical exemplary example from the Natural Color System (NCS) graph. S 1050-Y90R equals to NCS 2edition 50% saturation (S), 10% darkness (B), and 10% yellow + 90% red (H) [12]

Table 2. The gauge of fuzzified Likert equivalent interactions [13]

Linguistic terms	TFNs	Linguistic values
Very high stimulus	(0.75, 1.00, 1.00)	1.00
High stimulus	(0.50, 0.75, 1.00)	0.75
Low stimulus	(0.25, 0.50, 0.75)	0.50
Very low stimulus	(0.00, 0.25, 0.50)	0.25
No stimulus	(0.00, 0.00, 0.25)	0.00

specific GIS and MCDA classification and integration by ArcGIS VBA and MVC prearranged and predetermined. With an algorithm server in a web, the program languages interrelate and cooperate the MCDA classifications computed and calculated. Nevertheless, the interactive web interface is currently resided in the IIS, which is required to test final assignments.

4 Results and Discussion

An interactive web interface methodological agenda and framework with a help of graphics insinuates a full and specific integration GIS and MCDA classification together with the VBA and MVC color adjustment calibrated (see Fig. 3). The prototype interface is characterized by building placement with GIS and visual components theme, which established contributors can access and simulate consecutively [19, 20]. It, in this exercise, resembles to the sequential act of the selection of location for sustainable building projects and their visual components' analysis. For validated contributors, all segment fragments are all-in-one pages in the web. Particularly, contributors ought to register and log-in as to practice interactive web sheets. Within in the up-to-date map credentials, the contributors designate the criteria along with elements tangled into the contribution layer. It specifies data visualization as a convenient interface accredited as decision matrix and delineates its objective (see Fig. 4). The contributors in the objective sagacity choose and upsurge their preference on each criterion with elements, which ought to be augmented or diminished. Likewise, the results' analysis and comparison are conceivable in this study programmed. All sustainable and viable building projects have five diverse groupings to be sorted, that is, no stimulus, very low stimulus, low stimulus, high stimulus and very high stimulus. To stipulate contributors with location and color adjustment information, the web prototype can privilege sustainable building projects' location and visual impact. Particularly, it is theoretically appropriate and correct to be constructed and current buildings built in the suggested situation. Consequently, contributors will know the assignment and commission assigned after ensuring all progressions and activities, and are much better decision-makers to pick location considerations and boundaries.

The proposed interface is a prototype by the inventor for up-to-date realization, but still requests further and extra premeditations and restrictions. At minimum, to practice amalgamated synchronization it is unavoidable to have the internet as to flinch the server and get its outcomes. Like this, in the server interaction decorum, a meticulous method and/or some fluctuations are no longer obtainable. So, the amalgamation established and developed is no more activate. Hitherto, in coding lineups, this can be remunerated as to evade time charges and as to acquire computer competence and enactment.

5 Conclusions

This paper bestows an interactive web interface design and enlargement of using graphics. It allows to gauge and envisage a building project visual impact shaped in a case study venue (Alange), accurately the GIS building assignment and visual components theme together with the introductory results obtainable from an ongoing project. Particularly, with the criteria formerly nominated, contributors can check the diverse building projects' appropriateness constructed and formed. An interactive web interface methodological outline with a help of graphics is insinuated at the full and specific GIS and MCDA classification and the ArcGIS VBA and MVC color amendment. Here, to subtracting MCDA classification, the program languages should

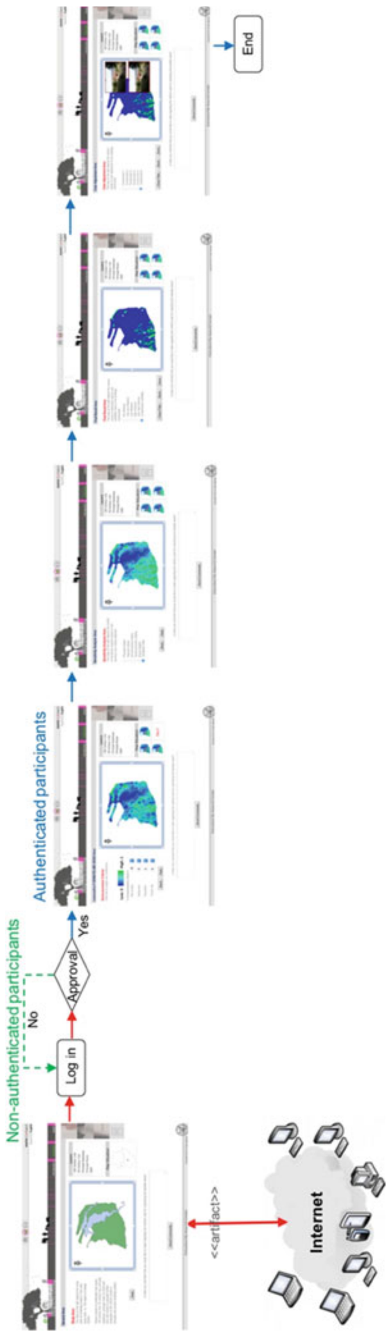

Fig. 3. Interactive web interface disposition with a help of graphics settled

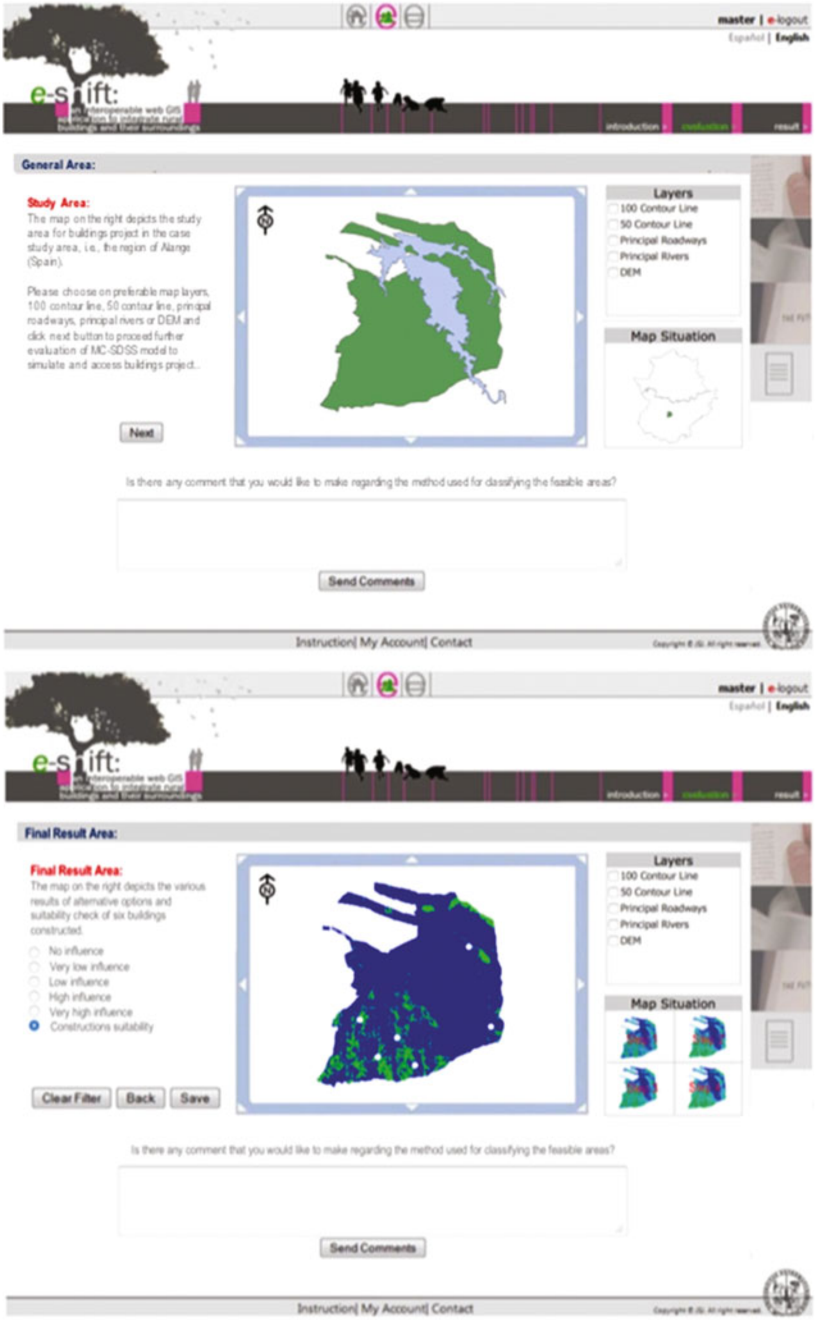

Fig. 4. Screenshots of an interactive web interface with a help of graphics in the ISS

interrelate with an algorithm server in the web and/or internet. Therefore, the results can be employed to substantiate sustainable and viable building projects' visual impact, which can singularize space and spatial parts in the asynchronous and synchronous decision-making progression. The interactive web interface model with a help of graphics established can be an original technique and tactic. Besides, it can be expediently distributed and re-used, and authenticate building projects visual impact to extent contributors' sensitivity. Thus, this prototype model can be the methodological origination and endorsement that employ as an empirical apparatus of visual impact impost, eventually undertaking sustainable and viable design of built circumstances.

Acknowledgements. The Economy and Competitiveness of Spanish Ministry (The Juan de la Cierva-Formación, ref. JDC-2015) supports the work to achieve by the author, which is very grateful for the supports.

References

1. Sharifi MA, Retsios V (2004) Site selection for waste disposal through spatial multiple criteria decision analysis. J Telecommun Inf Technol 3:1–11
2. González-Ramiro A, Gonçalvez G, Sánchez-Ríos A, Jeong JS (2016) Using a VGI and GIS-based multicriteria approach for assessing the potential of rural tourism in Extremadura (Spain). Sustainability 8(11):1144. https://doi.org/10.3390/su8111144
3. Jeong JS, García-Moruno L, Hernández-Blanco J (2012) Integrating buildings into a rural landscape using a multi-criteria spatial decision analysis in GIS-enabled web environment. Biosys Eng 112(2):82–92. https://doi.org/10.1016/j.biosystemseng.2012.03.002
4. Jankowski P, Nyerges T, Smith A, Moore TJ, Horvath E (1997) Spatial group choice: a SDSS tool for collaborative spatial decision-making. Int J Geogr Inf Syst 11(6):577–602. https://doi.org/10.1080/136588197242202
5. Malczewski J (2006) Review article GIS-based multicriteria decision analysis: a survey of the literature. Int J Geogr Inf Sci 20(7):703–726. https://doi.org/10.1080/13658810600661508
6. Jaraíz Cabanillas FJ, Mora Aliseda J, Gutiérrez Gallego JA, Jeong JS (2013) Comparison of regional planning strategies: countywide general plans in USA and territorial plans in Spain. Land Use Policy 30(1):758–773. https://doi.org/10.1016/j.landusepol.2012.06.001
7. Jeong JS, García-Moruno L, Hernández-Blanco J (2013) A site planning approach for rural buildings into a landscape using a spatial multi-criteria decision analysis methodology. Land Use Policy 32:108–118. https://doi.org/10.1016/j.landusepol.2012.09.018
8. Haklay M, Singleton A, Parker C (2008) Web mapping 2.0: the neogeography of the GeoWeb. Geogr Compass 2(6):2011–2039. https://doi.org/10.1111/j.1749-8198.2008.00167.x
9. Jeong JS, García-Moruno L, Hernández-Blanco J, Sánchez-Ríos A (2016) Planning of rural housings in reservoir areas under (mass) tourism based on a fuzzy DEMATEL-GIS/MCDA hybrid and participatory method for Alange, Spain. Habitat Int 57:143–153. https://doi.org/10.1016/j.habitatint.2016.07.008
10. Ruda G (1998) Rural buildings and environment. Landscape Urban Plan 41:93–97. https://doi.org/10.1016/S0169-2046(97)00062-5
11. Smardon RC (1979) Prototype visual assessment manual. State University of New York, Syracuse

12. Natural Color System (2004) Scandinavian color institute AB; Natural Color System. Stockholm, Sweden
13. Jeong JS, Ramírez-Gómez Á (2018) Optimizing the location of a biomass plant with a fuzzy-DEcision-MAking Trial and Evaluation Laboratory (F-DEMATEL) and multi-criteria spatial decision assessment for renewable energy management and long-term sustainability. J Clean Prod 182:509–529. https://doi.org/10.1016/j.jclepro.2017.12.072
14. Jeong JS, Ramírez-Gómez Á (2017) A multicriteria GIS-based assessment to optimize biomass facility sites with parallel environment—a case study in Spain. Energies 10 (12):2095. https://doi.org/10.3390/en10122095
15. Umar A (1997) Object-oriented client/server Internet environments. Prentice Hall Press, Upper Saddle River, NJ
16. Andrienko N, Andrienko G (2001) Intelligent support for geographic data analysis and decision making in the web. J Geogr Inf Decis Anal 5(2):115–128
17. Jeong JS, González-Gómez D, Ramírez-Gómez Á (2017) A web-based scaffolding-learning tool for design students' sustainable spatial planning. Architectural Eng Des Manag 13 (4):262–277. https://doi.org/10.1080/17452007.2017.1300129
18. González-Gómez D, Cañada-Cañada F, Campiglia AD, Espinosa-Mansilla A, Muñoz de la Peña A, Jeong JS (2016) Rapid ultrasensitive chemometrics-fluorescence methodology to quantify fluoroquinolones antibiotics residues in surface water. J Water Chem Technol 38 (5):280–286. https://doi.org/10.3103/S1063455X16050064
19. Gutiérrez Gallego J, Naranjo Gómez JM, Jaraíz-Cabanillas FJ, Ruiz Labrador EE, Jeong JS (2015) A methodology to assess the connectivity caused by a transportation infrastructure: application to the high-speed rail in Extremadura. Case Stud Transp Policy 3(4):392–401. https://doi.org/10.1016/j.cstp.2015.06.003
20. Jeong JS, García-Moruno L, Hernández-Blanco J, Jaraíz-Cabanillas FJ (2014) An operational method to supporting siting decisions for sustainable rural second home planning in ecotourism sites. Land Use Policy 41:550–560. https://doi.org/10.1016/j.landusepol.2014.04.012

Topology Optimization Additive Manufacturing-Oriented for a Biomedical Application

F. Cucinotta[1(✉)], E. Guglielmino[1], G. Longo[2], G. Risitano[1], D. Santonocito[1], and F. Sfravara[1]

[1] University of Messina, C.da di Dio, 98166 Messina, Italy
filippo.cucinotta@unime.it
[2] U.O.C. Ortopedia e Traumatologia A.O, Piazza Santa Maria di Gesù, 95124 Catania, Italy

Abstract. Topological optimization is a fairly innovative numerical technique that makes it possible to reduce the mass of mechanical components. It is an alternative to the optimizations of shape or geometry that allow to highly improve the efficiency of products. The recent development of metal additive manufacturing technologies allows the production of pieces that were not feasible before, permitting the use of topological optimization in many fields. In the biomedical field, for example, the reduction of prosthetic and orthotic materials allows to save weight, to the advantage of comfort, and to minimize the invasiveness of these systems. In this paper, an optimization of a system consisting of a femoral nail and two screws is carried out. The pieces were obtained by 3D scanning of prostheses, so as to obtain the true geometry. The femur is the standard one in literature. Following topological optimization, a new nail, with a mass of 60% of the previous one, was obtained, without limiting the functionality or the reliability of the product. Results and methodological problems are discussed.

Keywords: Additive manufacturing · Topology optimization · Biomedical engineering · Reverse engineering · Femoral nail

1 Introduction

The constraints imposed by the traditional manufacturing processes limit the engineers to the physical realization of products of optimal topology. In many cases, the optimized product is difficult or very expensive to produce with traditional subtractive manufacturing process [1]. In many fields of engineering, the researchers try to find new solutions for a green production of energy [2, 3]. Also in the mechanical field, there is need to optimize the products in order to use the minimum quantity of material. In the last years, reverse engineering and additive manufacturing (AM) have pushed the research towards a new idea of design methodology. Paulic et al. [4] showed the practical aspects in the use of the reverse engineering technique and the successively remanufacturing with AM process of the same product with an improvement in terms of design and efficiency. A state of art of the AM processes and the principal

F. Cavas-Martínez et al. (Eds.): *Advances on Mechanics, Design Engineering and Manufacturing II*, LNME, pp. 184–193, 2019.
https://doi.org/10.1007/978-3-030-12346-8_18

advantages of this technique is proposed by Gardan [5] and [6]. Shapiro et al. [7] showed the potentiality of the application of this new process for the aerospace industry, focusing the attention on seven different main applications in which AM can provide a benefit. Leal et al. [8] proposed a new concept design for body panels in automotive industry. A very deep description of an application of Design for Additive with Selective Laser Melting system is showed by Graziosi et al. [9], in this case the field of application was sport, the principal aim was to optimize an re-shape the cam-system of a compound-bow. The additive manufacturing also allows to manufacture elements with lattice shape [10] and this type of solution could be very useful for applications concerning core-sandwich subjected to repeated impacts [11]. In the medical field, the relative small dimensions of the objects allow to produce them with the use of the AM. Comotti et al. [12] proposed new design rules provided by AM in the prosthetic field of lower limb amputees. Many studies involve new prosthesis solutions in order to minimize the post-surgeon effects on the patient [13]. In all the optimization processes a great effort is produced for the simulation [14] of real working conditions. The authors in this study want to investigate the entire process of optimization, from reverse engineering to final optimization product. The field of interest is the medical one and the application concerns the optimization of the Gamma nail part of an intramedullary trochanteric prosthesis. This prosthesis is useful for the fractures of the trochanteric part of the femur.

The first part of paper describes the geometries involved and the acquisition of the different parts of the prosthesis by means of 3D blue-light scanner. A description of the principal dimensions of these parts and the material used is reported in a second part. The last part describes the static structural simulation with a Finite Element method and the loop of shape optimization in order to reduce the weight of the nail.

2 Geometry, Materials and Method

The flowchart used in this paper is showed in the Fig. 1.

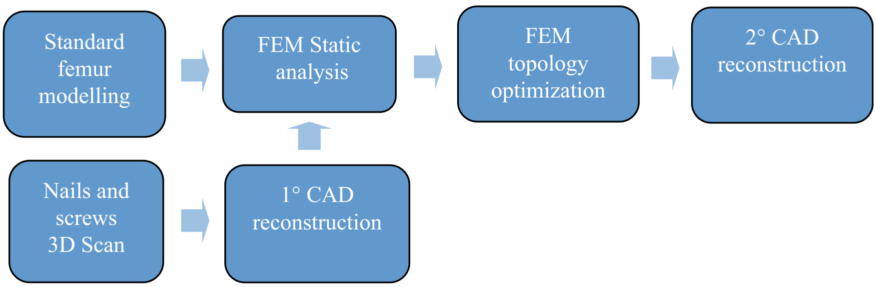

Fig. 1. Flowchart

The femoral bone used in this paper has been modelled thanks to a standard library for this kind of geometry (Fig. 2). The longitudinal direction is the one along the z-axis. In the same figure is possible to see the Fracture line that this kind of prosthesis fixes.

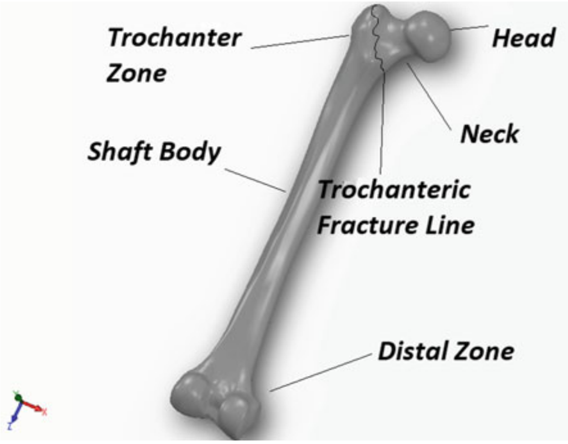

Fig. 2. General geometry of femur in anterior view

The femur modeled is divided in two different parts. The external one defined by the cortical zone and the inner part defined by a spongious zone. In order to simplify the model, the medullary cavity has not been modelled. The cortical bone is the 3D Boolean subtraction of the two parts showed in Fig. 3.

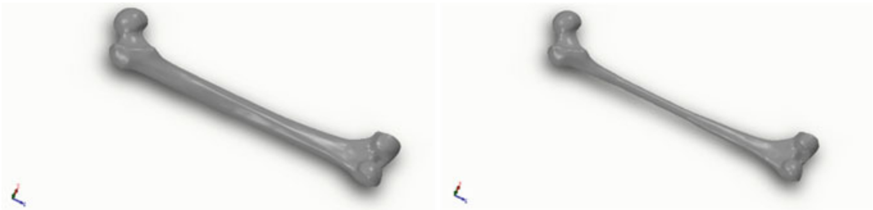

Fig. 3. On left the external surface of the cortical. On right the external surface of the spongious

The principal dimensions of the femur are: the total length, the shaft length, the neck-angle and the femoral head diameter [15]. The total longitudinal length of the femur under investigation is 487 mm. The length of the shaft-part of the femur is 340 mm. The neck angle is 125° and the femur head diameter is 51.2 mm (Fig. 4).

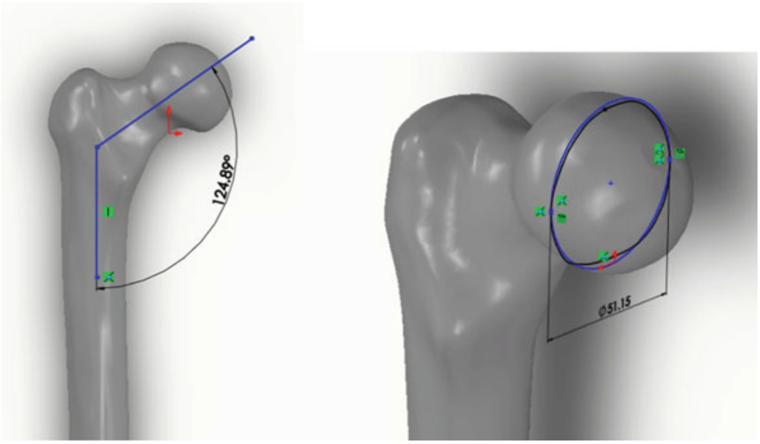

Fig. 4. On left the Neck Angle (125°). On right the Femur Head Diameter (51.2 mm)

The femoral bone is composed of two different materials, cortical and spongious. The behavior and mechanical properties of these two parts have been investigated by many authors. The mechanical properties of the femoral bone are dependent of the apparent density (mass of mineralized bone divided by bulk volume including porous surface). In the papers proposed by Wirtz [16] and Taylor et al. [17] is shown the dependence between Young's Modulus and apparent density in isotropic and orthotropic conditions. Peng et al. [18] showed the difference in the assignments of isotropic mechanical properties or orthotropic mechanical properties. The results have shown that the differences between the two material property assignments are small under two loading conditions (double-leg standing and single-leg standing) [19]. In the case under study, the authors preferred to use the maximum capacity of simulation defining the two parts as orthotropic elements for cortical bone [20] and isotropic elements for spongious bone [21]. The properties used are summarized in Table 1.

Table 1. Principal properties of femoral materials

Materials	E [GPa]		G [GPa]		ν	
Cortical (orthotropic)	E_x	12	G_{xy}	4.53	ν_{xy}	0.376
	E_y	13.4	G_{xz}	5.61	ν_{yz}	0.235
	E_z	20	G_{yz}	6.23	ν_{xz}	0.371
Spongious (isotropic)	1		0.388		0.29	

The second element of the simulation is the system for the treatment of trochanteric fracture (trochanteric nail). It is made by three elements. The principal part is the Gamma nail, it is cannulated, during the surgery, inside the femur bone in order to stabilize the entire structure of the femur. The other two parts are screw elements in order to fix the system with the bone.

In the case proposed by authors, the real geometry of the Trochanteric Nail has been acquired with a 3D Blue-Light scanner system. The reconstruction involves the three principal elements of this part: the Gamma Nail, the Gamma Lag screw and the distal locking screw (Fig. 5).

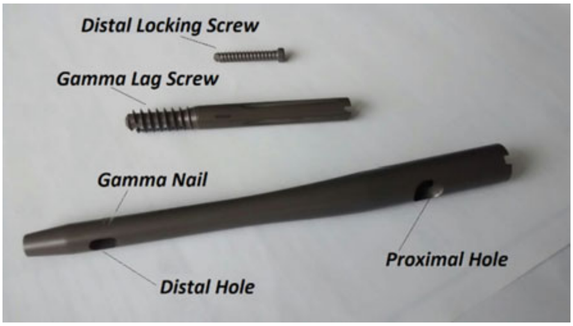

Fig. 5. Elements of the trochanteric nail

The different parts of the trochanteric nail have been modelled after an acquisition with a 3D scanner. Reverse engineering allows to acquire the true CAD geometry of all parts of the nail. This phase involves the use of a 3D scanner with a blue structured light with a precision of one hundredth of a millimeter. The scanner allows obtaining a. stl file. The process involves the use of section curves and a loft procedure for the surface generation and 3D model reconstruction (Fig. 6).

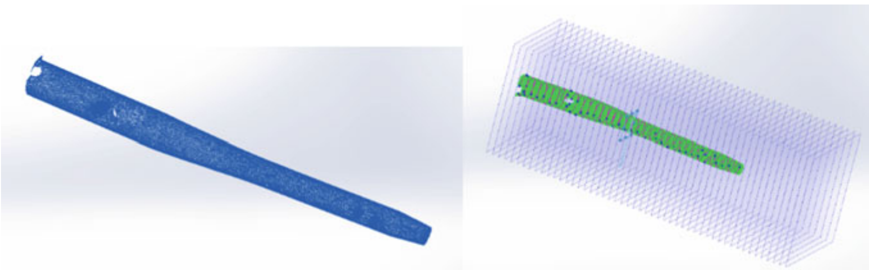

Fig. 6. On left the stl reconstruction with 3D scanner. On right the 3D modeling with section curves

Thanks to this reconstruction, it is possible to obtain all the dimensions of the Trochanteric nail. The total length of the trochanteric nail is 180 mm. The diameter changes along the nail, in the proximal zone it is equal to 15.5 mm, in the distal zone it is equal to 10 mm. The distance between proximal hole and distal hole is about 110 mm. The total length of the Gamma Lag screw is 95 mm and the bigger diameter is 10.5 mm. The length of the threaded zone is 30 mm. The length of the Distal locking screw is 32.5 mm and the diameter is 5 mm. The neck angle between the Gamma Nail and the Gamma Lag screw is 120°.

The material of the nail is titanium alloy with anodized type III (ASTM Grade 3) surface treatment and the principal properties are summarized in Table 2.

Table 2. Nail and screws material properties

Materials	E [GPa]	ν	Yield Strength [MPa]
Titanium grade 3	107	0.33	450

Thanks to the acquisition and reconstruction of the different elements it is possible to assembly the entire system for Finite element simulation.

With all parts modelled, it is possible to define the entire assembled system for the Finite Element simulation (Fig. 7).

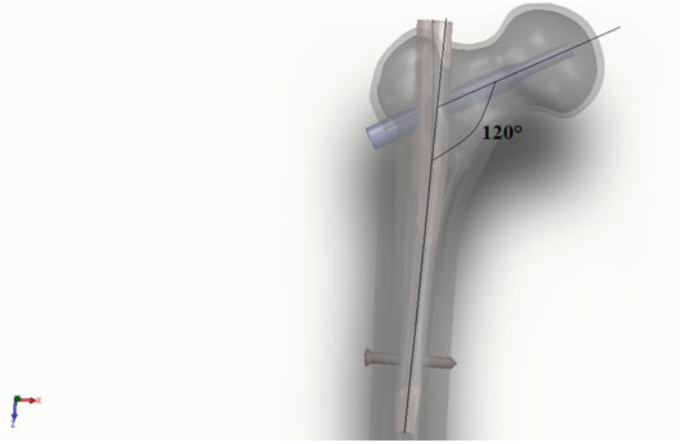

Fig. 7. The entire assembled system

A mixed hexa-tetrahedral mesh has been used with a maximum number of elements equal to 81529.

The reaction of joint and the hip abductor produce the load conditions, as shown by Beaupre [19]. The reaction of joint is along a direction of 24° with respect to the femoral shaft body axis and with a value of 2317 N. The hip abductor reaction is along a direction of 28° with respect to the femoral shaft body axis and with a value of 703 N. The distal zone is completely constrained. In order to simulate the fracture, the bone has been divided, along the fracture line, in two parts. The two surfaces in contact are free to slide without friction.

The optimization has been carried out by means of the Ansys Topology Optimization modulus. As shown by Coutinho et al. [22], a very useful objective function for topology optimization is the minimization of the compliance. The constraint of the optimizer was to retain the 60% of mass. In Fig. 8 are reported the design and exclusion regions of the Gamma Nail. The process required 7 iterations to achieve the convergence conditions.

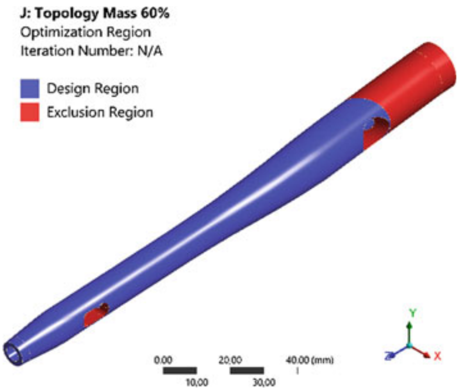

Fig. 8. Design region for topology optimization

3 Results and Discussion

The result of the topological optimization was an effective reduction of 32.3% of Gamma Nail mass, starting from an on original value of 7.83E−2 kg, to a final value of 5.30E−2 kg. In Fig. 9 are shown the retained and removed region of the nail.

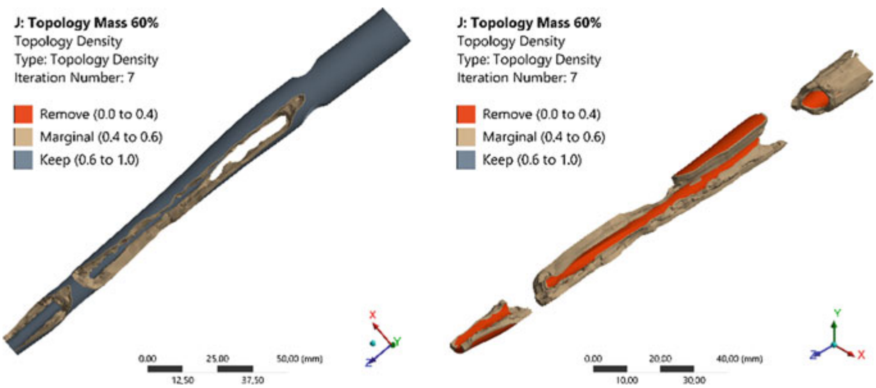

Fig. 9. Retained and removed region of the nail

After the optimization, two different CAD reconstructions of the Gamma Nail have been proposed (Fig. 10), with a mass reduction of 40.2 and 33.7% respectively. The reconstructions allow to obtain again continuous curves and surfaces, overcoming the discretization of the geometry. This phase is important for both manufacturing and setting needs.

The structural assessment of the two optimized geometries have led to equivalent Von Mises stress lower than the original geometry, as reported in Table 3. It is also evident a stress decrease in cortical bone while an increase in spongious bone occurs.

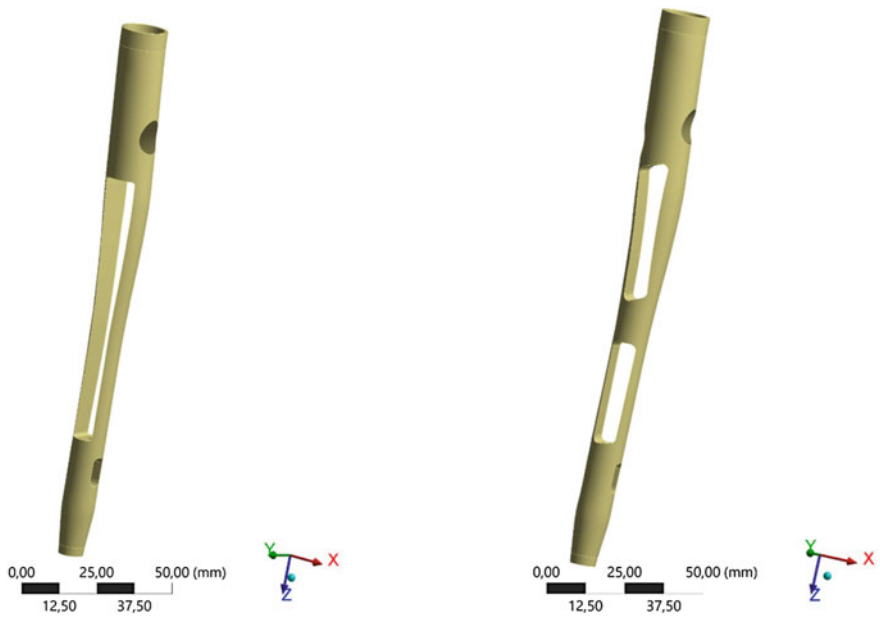

Fig. 10. Two different CAD reconstructions after topology optimization

This is due to the drastic reduction of material and, consequently, to the higher specific energy which each structural material particle is subject to. In Fig. 11 are reported the stress distribution of the two optimized geometries and the original one.

Table 3. Stress range comparison between original and optimized geometries

	Original geometry [MPa]	Optimized geometry 1 [MPa]	Optimized geometry 2 [MPa]
Gamma nail	0.33 ÷ 233.16	0.13 ÷ 119.69	0.10 ÷ 131.23
Cortical bone	0.28 ÷ 56.34	0.24 ÷ 30.33	0.27 ÷ 30.34
Spongious bone	0.02 ÷ 6.55	0.02 ÷ 17.36	0.02 ÷ 17.25

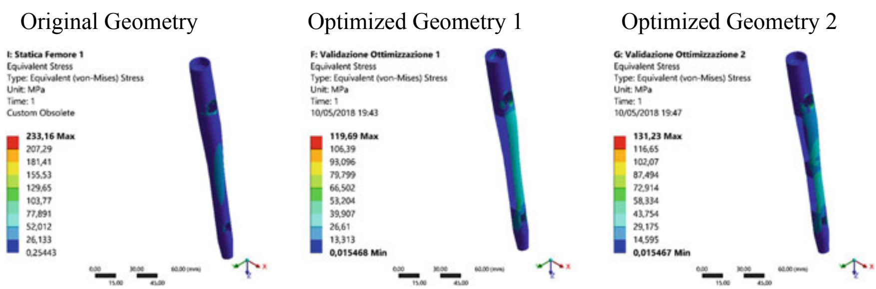

Fig. 11. Stress distribution for the optimized geometries and the original geometry

4 Conclusions

Topological optimization allows to obtain highly efficient products, with great utilization factors. In the paper, a structural compliance analysis has been carried out on a femoral nail. The optimization has led to a consistent mass reduction, up to about 40%, with a little increase of equivalent stress on the nail and without an appreciable change on both the cortical and the spongious tissues.

The material saving allows, not only a less invasive intervention, but also a weight reduction, with an obvious comfort benefit. The optimized topology can be easily manufactured with metal additive manufacturing. Further studies could also be conducted in order to orient the optimization toward osteointegration.

References

1. Berman B (2012) 3-D printing: the new industrial revolution. Bus Horiz 55:155–162
2. Prestipino M, Chiodo V, Maisano S, Zafarana G, Urbani F, Galvagno A (2017) Hydrogen rich syngas production by air-steam gasification of citrus peel residues from citrus juice manufacturing: experimental and simulation activities. Int J Hydrogen Energy 42:26816–26827
3. Chiodo V, Urbani F, Zafarana G, Prestipino M, Galvagno A, Maisano S (2017) Syngas production by catalytic steam gasification of citrus residues. Int J Hydrogen Energy 42:28048–28055
4. Paulic M, Irgolic T, Balic J, Cus F, Cupar A, Brajlih T, Drstvensek I (2014) Reverse engineering of parts with optical scanning and additive manufacturing. Procedia Eng 69:795–803
5. Gardan J (2016) Additive manufacturing technologies: state of the art and trends. Int J Prod Res 54:3118–3132
6. Tamburrino F, Perrotta V, Aversa R, Apicella A (2015) Additive technology and design process : an innovative tool to drive and assist product development. In: XIII international forum Le Vie dei Mercanti, pp. 1742–1747
7. Shapiro AA, Borgonia JP, Chen QN, Dillon RP, McEnerney B, Polit-Casillas R, Soloway L (2016) Additive manufacturing for aerospace flight applications. J Spacecr Rockets 53:952–959
8. Leal R, Barreiros FM, Alves L, Romeiro F, Vasco JC, Santos M, Marto C (2017) Additive manufacturing tooling for the automotive industry. Int J Adv Manuf Technol 92:1671–1676
9. Graziosi S, Rosa F, Casati R, Solarino P, Vedani M, Bordegoni M (2017) Designing for metal additive manufacturing: a case study in the professional sports equipment field. Procedia Manuf 11:1544–1551
10. Graziosi S, Tamburrino F, Bordegoni M (2018) The design process of additively manufactured Meso-Scale Lattice Structures: a review. J Comput Inf Sci, Eng
11. Cucinotta F, Paoli A, Risitano G, Sfravara F (2018) Optical measurements and experimental investigations in repeated low-energy impacts in powerboat sandwich composites. Proc Inst Mech Eng Part M J Eng Marit Environ 232:234–244
12. Comotti C, Regazzoni D, Rizzi C, Vitali A (2017) Additive manufacturing to advance functional design: an application in the medical field. J Comput Inf Sci Eng 17:31006
13. Filardi V (2017) Characterization of an innovative intramedullary nail for diaphyseal fractures of long bones. Med Eng Phys 49:94–102

14. Palomba V, Prestipino M, Galvagno A (2017) Tri-generation for industrial applications: development of a simulation model for a gasification-SOFC based system. Int J Hydrogen Energy 42:27866–27883
15. Yoshioka Y, Siu D, Cooke T (1987) The anatomy and functional axes of the femur. J Bone Jt Surg 69:873–880
16. Wirtz DC, Schiffers N, Pandorf T, Radermacher K, Weichert D, Forst R (2000) Critical evaluation of known bone material properties to realize anisotropic FE-simulation of the proximal femur. J Biomech 33:1325–1330
17. Taylor WR, Roland E, Ploeg H, Hertig D, Klabunde R, Warner MD, Hobatho MC, Rakotomanana L, Clift SE (2002) Determination of orthotropic bone elastic constants using FEA and modal analysis. J Biomech 35:767–773
18. Peng L, Bai J, Zeng X, Zhou Y (2006) Comparison of isotropic and orthotropic material property assignments on femoral finite element models under two loading conditions. Med Eng Phys 28:227–233
19. Beaupre GS, Orr TE (1990) An approach for time-dependent bone modeling and remodeling—application a preliminary remodeling simulation—Beaupré—2005. J Orthop Res 662–670
20. Ashman RB, Cowin SC, Van Buskirk WC, Rice JC (1984) A continuous wave technique for the measurement of the elastic properties of cortical bone. J Biomech 17:349–361
21. Watanabe Y, Shiba N, Matsuo S, Higuchi F, Tagawa Y, Inoue A (2000) Biomechanical study of the resurfacing hip arthroplasty. J Arthroplasty 15:505–511
22. Coutinho KD, Carlos J, Costa A (2011) Compliance minimization using topology optmization. In: Proceedings of COBEM, 21st Brazilian congress of mechanical engineering, Natal, Brazil, p 7

A Reverse-Engineering Approach for the Management of Product Geometrical Variations During Assembly

J. L. Gregorio[1,2], C. Lartigue[1(✉)], F. Thiébaut[1], and H. Falgarone[2]

[1] LURPA ENS Cachan, Université Paris-Sud, Université Paris-Saclay, Cachan 94230, France
+33-1-4740-2986lartigue@lurpa.ens-cachan.fr
[2] Airbus Group Innovations, Suresnes 92152, France

Abstract. One of the major challenges for the aerospace industry is to manage a range of complex products during their manufacturing and assembly process. Digital Mock-Ups (DMU) are nowadays extensively used as supports of information during the aforementioned phases. In this paper we introduce the concept of updated DMU which actually reflects the product being assembled. For this purpose, the nominal product geometry needs to be updated in order to reflect the as-built geometry of the product's components at a given step of its assembly. The geometry of the next components to be assembled, called interface components, are consequently updated in order to adapt to geometrical variations, while the rest of the DMU stays in its original as-designed configuration. A comprehensive method to update the DMU from its as-designed configuration to reflect the actual configuration of the product being assembled is thus proposed. To this end, a framework inspired from the Reverse-Engineering field is developed, then assessed thanks to a simple case study.

Keywords: Reverse-Engineering · Product manufacturing · As-built model · Digital mock-up

1 Introduction

In order to speed-up the manufacturing and assembly processes, physical mock-ups of aeronautical products have been gradually replaced with their digital counterparts, leading to the concept of product virtual representation also known as Digital Mock-Up (DMU). The DMU typically consists in a detailed 3D representation of the product's geometry but also contains information related to manufacturing and assembly processes such as tolerances, machining programs, assembly planning, inspection procedures, and so on. During manufacturing and assembly phases, the DMU stands for the reference geometry of the product. More particularly, the geometry of the elements constituting the DMU is described in the product as-designed configuration, which means the components are without geometrical deviations and in their theoretical position.

F. Cavas-Martínez et al. (Eds.): *Advances on Mechanics, Design Engineering and Manufacturing II*, LNME, pp. 194–202, 2019.
https://doi.org/10.1007/978-3-030-12346-8_19

Tolerancing methods aim to confine product geometrical variations within an admissible interval so that it satisfies the functional requirements expressed in the DMU. Geometrical constraints are thus established between elements to be manufactured or assembled, and specified elements of the initial product. Tolerancing methods are often coupled with Computer Aided Tolerancing Tools [1] relying on the DMU, enabling worst case and/or statistical tolerancing of rigid assemblies. Improvements have been made all along the years in order to provide more realistic tools for aeronautical assemblies [2], which are considered flexible due to large size and low thickness components.

Despite the use of tolerancing methods and tools, the management of product geometrical variations does not allow an accurate prediction of the entire geometry of the actual product at each step of the assembly process. Aeronautical products are typically composed of thousands of parts, often made of composite materials and presenting a high length-to-thickness ratio, which makes geometrical variation estimation very tedious. As a result, unpredicted discrepancies inevitably appear between the actual product and its reference digital model [3, 4]. Consequently, features of already assembled components do not constitute a valid basis to continue the assembly process.

In order to avoid cost-ineffective adjustment operations or the generalized use of jigs, some authors propose to use techniques derived from Reverse-Engineering in order to adapt to discrepancies by manufacturing custom-made components [3, 4]. The geometry of specific interface components is customized so that they perfectly fit within the available space. More particularly, geometrical data are captured in the shop floor assembly station, in order to adjust the interface component CAD model. Interface components are afterwards manufactured then assembled.

In this paper, we introduce the concept of hybrid representation of the updated DMU in order to reflect the actual geometry of a product during its assembly. The updated DMU is composed of as-built components, describing the actual configuration of the product being assembled, interface components and as-designed components. The use of such a DMU allows a more comprehensive management of the product's geometrical variations by establishing bi-directional relations between the physical product and its virtual model, often referred to as digital twin. In a broader scope, some authors show that the establishment of such relations between physical parts and their virtual models would enable a more efficient execution of the product activities all along its lifecycle [5].

Obtaining such an updated DMU, reflecting the actual geometry of the product including its geometrical deviations, is not straightforward and serious difficulties must be overcome. Within the context of Reverse Engineering, only a few papers aim at reconstructing models of existing products in order to underline geometric changes with a preexisting DMU. In most cases, the information—geometrical or linked to the product use—extracted from an eventual preexisting DMU only serves as an initial estimate of the product to be reconstructed [6]. In [7, 8] authors decompose the initial CAD model of the product into a set of tessellated components that can be easily matched to measured data. These components are first recognized in the CAD model, along with their properties and global relations in order to facilitate the matching. Once the matching between tessellated components and measured data is carried out, a registration algorithm is used in order to calculate the as-built pose of the CAD model components, controlling the compliance of the product with respect to corresponding dimensional tolerances. Other authors propose to use CAD templates of mechanical parts [9, 10] containing a set of design features which parameters can be modified thanks to data extracted from the real world (mainly 3D measurements). Such a template-based reverse engineering method consists in exploiting a parametric description of the object in order to retrieve a meaningful digital representation. An extension of the previous method to mechanical products is proposed in [11]. The main advantage of this approach is that it eventually results in a fully editable CAD model which is consistent with the original design intent which mostly makes it suitable for redesign purposes only.

This paper gives a detailed description of our proposition of an updated DMU based on a hybrid representation. Contrary to the as-designed model, the geometry of the updated product reflects product geometrical deviations. Based on this information, the geometry of the components to be assembled is also updated in order to impact the manufacturing and assembly activities based on the DMU. An illustration of our Reverse-Engineering framework for updating the as-designed components to as-built and interface components using data acquired from optical measurements and the available engineering knowledge is also presented.

2 From the As-Designed DMU to the Updated DMU

Our concept of an updated DMU based on a hybrid representation, is illustrated through a simple case study based on a product consisting of four assembled parts: a *flanged box* (Meccano® part n°236), two *triunions* (Meccano® part n°126) and a *perforated strip* (Meccano® part n°4). The as-designed DMU (Fig. 1) is constructed using the CAD software CATIA® V5 and the part's engineering drawings. As it is often the case, and for a better understanding, fixturing parts are not represented in the DMU.

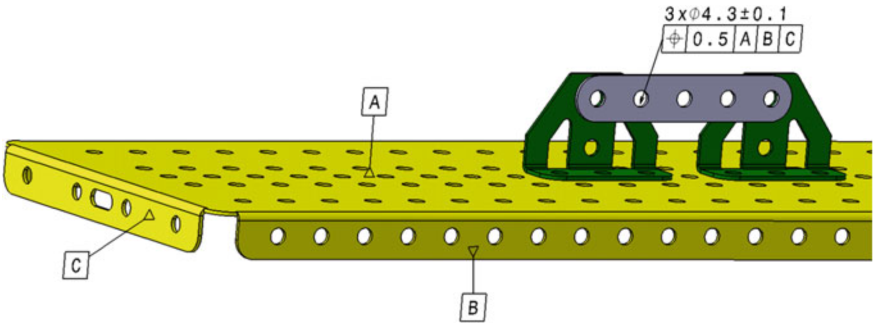

Fig. 1. Partial representation of our case study functional requirements

Global references are defined as a set of three planes, named A, B and C, representing respectively the primary, secondary and tertiary references. Geometrical requirements are defined as a localization tolerance that aims to position a set of three holes regarding to the global references (Fig. 1). Here tolerancing aims to confine the position of each hole axis into the cylindrical region specified by the tolerance value.

In the proposed scenario, the first three parts, i.e. the yellow box and the two green triunions are manufactured then assembled (Fig. 2b). The geometry of the actual product is acquired, and thus updated in the DMU thanks to our method in order to reflect the as-built configuration of the already assembled components. Based on the as-built geometry, the geometry of the last component is updated so that, once assembled, the functional requirements of the final product are met. More particularly, the position of the pattern of holes is updated so that the position of the specified hole axes in the desired tolerance interval.

With the classical manufacturing approach in the aerospace industry [1–4], a specific tolerance is allocated to each functional surface or local reference of the product. In the best case, a statistical or worst case calculation is performed in order to find a tradeoff between the overall production costs induced by these tolerances and the assurance that functional requirements will eventually be met. Very often, these tolerances cannot be directly assessed and the as-designed DMU serves as reference model to transpose geometric constraints between elements to be manufactured and global references into much simpler constraints where only local references are involved. For example, the first fixturing hole axis is assumed to be in the same position than in the as-designed DMU, and the second one is drilled so that the final part remains parallel to reference A. As discrepancies tend to appear between the actual product and the as-designed DMU, this scenario often leads to several mandatory additional adjustment steps in order to guarantee that the final assembled product eventually meets the specified functional requirements (Fig. 1).

The situation of the local references, here the fixturing hole axes (L1 and L2) and the contact plane with the triunions (L3), relatively to the global references, and how it impacts the product's functional requirements is the key concern of our approach. Each local reference is expressed in the frame defined by the global references together with the product's functional requirements. In the as-designed DMU (Fig. 2a), the local references (L1, L2 and L3) are theoretically positioned regarding to global references. This configuration does not account for the actual geometry of the product.

We use a Reverse-Engineering based method to update the product's already assembled components so that they reflect the actual geometrical configuration of the product at a given step of the assembly process (Fig. 2b). The updated as-built components integrate the geometrical variations between the as-designed model and the actual product. As a result, the situation of the local references in the frame defined by global references is known by the user.

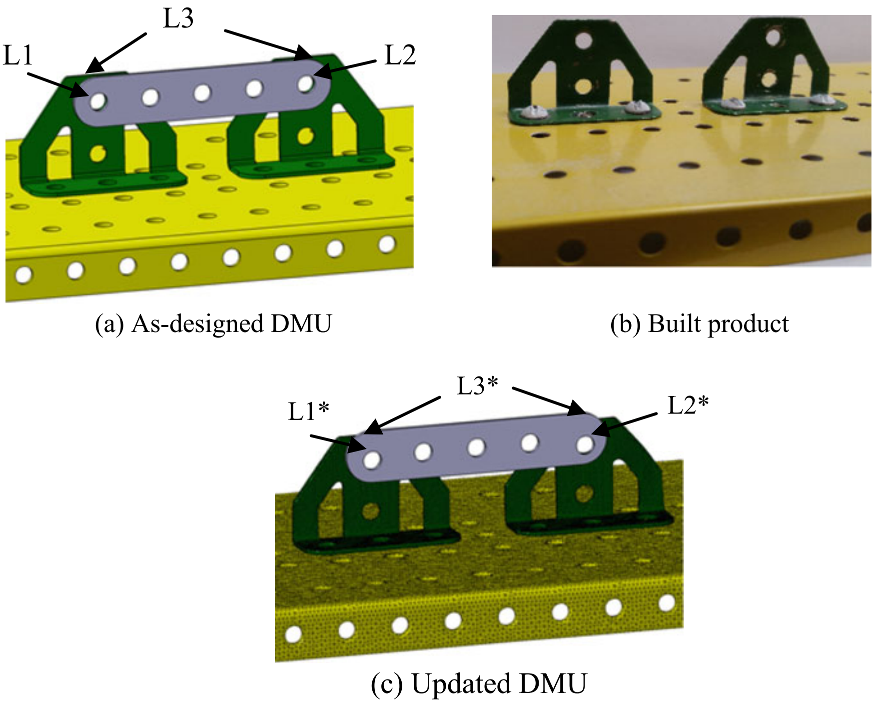

Fig. 2. The product as-designed model (**a**) is updated to reflect the built components at a given assembly step (**b**), following manufacturing and assembling operations are also impacted (**c**)

The newly defined situation of the local references (L1*, L2* and L3*) is used to adapt the geometry of the next component to be assembled, called the interface component, so that the respect of the product's functional requirements is ensured (Fig. 2c). Therefore, following manufacturing and assembly operations, which are based on the interface component's geometry, are impacted.

In the case study, the DMU only contains as-built components and interface components. Nevertheless, we could imagine a scenario where some additional components would be assembled to the interface part. In this scenario, the previously specified hole axes would serve as local references in order to continue the assembly process. As the geometry of the interface part has been updated in order to meet the product specified functional requirements, these local references constitute a valid basis to continue the assembly. Therefore the to-be-assembled component geometry would not require to be updated and the assembly process could be carried on accordingly to the information initially contained in the as-designed DMU. As a result, the updated DMU would contain as-build components, interface components and as-designed components.

In the general concept of updated DMU based on a hybrid representation, as-built components coexist with interface components and as-designed components. As-designed components are components which are already present in the initial as-designed DMU and which have not been assembled yet. As-built components correspond to components that have been manufactured and whose geometry has been acquired and updated in the DMU in order to integrate their geometrical deviations. Interface components correspond to components that have not already been manufactured and assembled and whose design has been updated in order to be assembled to the as-built components so that the product's functional requirements are met.

In the next section an overview of our Reverse-Engineering method is presented. Our method allows the updating of the product's as-designed configuration to as as-built configuration as presented previously (Fig. 2b). The different steps of our method are individually assessed.

3 Illustration of the Proposed Approach

The proposed method aims to update components of an initial as-designed DMU to the as-built configuration which reflect the actual state of a given product.

The first three components are assembled and digitized using a laser plane sensor (Kreon Zephir K2 25) mounted on a CMM. The different steps of our reverse-engineering framework (Fig. 3) are implemented in Python and Matlab® and run on a laptop with a 2.3 GHz CPU and 8 GB of RAM. The as-built DMU is reimported in CATIA® V5.

Data acquired from optical measurements are used as a representation of the real product. These data need to be processed, relying on the as-designed geometry and user's knowledge about the product, in order to retrieve the product's components in the as-built configuration. Our method consists in five steps: data preprocessing, global registration, segmentation, local registration and 3D modelling.

The component surface geometry is acquired using an optical measuring system which delivers a numerical representation of the geometry as a point cloud. The obtained raw point cloud, generally dense, non-homogeneous and highly noisy, is not readily usable for our application, and needs to undergo a data preprocessing step (Fig. 3a).

During the second step (Fig. 3b), the point cloud is registered to the as-designed geometry. In order to establish a meaningful correspondence between the data and the model, engineering knowledge about the product's functional requirements is used. In

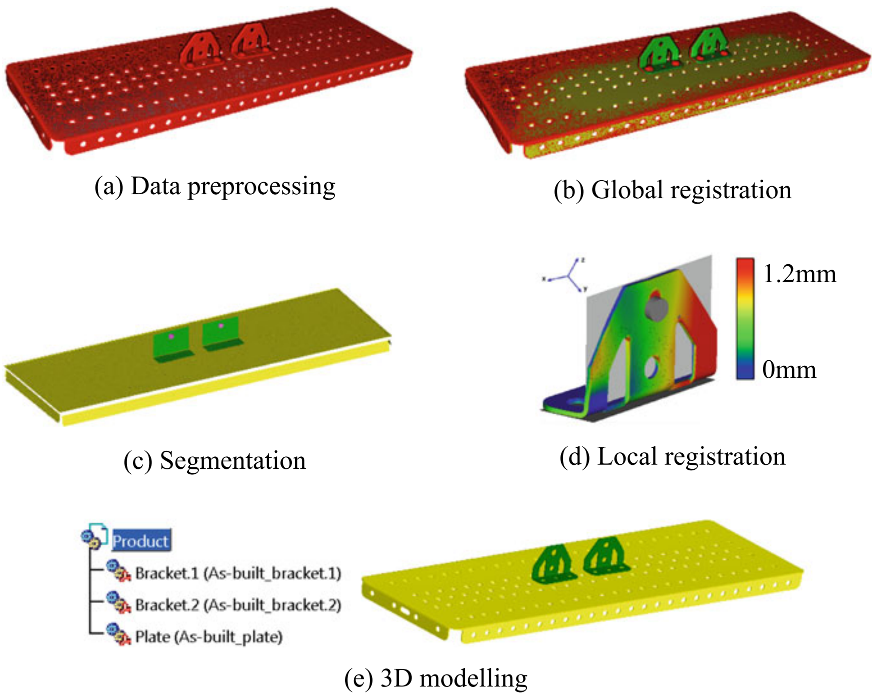

Fig. 3. Illustration of the Reverse-Engineering method on a simple assembly

our case, we use the knowledge about the reference surfaces of our model, i.e. the global references, in order to register the point cloud to our reference frame so that geometrical deviations, extracted during further steps, are also expressed in this reference frame.

During the segmentation step (Fig. 3c), the actual situation of the product's components and elements of interest, i.e. local references, is identified from the point cloud. The first goal specifically aims to divide the point cloud into a set of features representing the assembly components.

Geometrical deviations between the segmented elements and their as-designed equivalents are then characterized, and a step of local registration is next performed in order to integrate these deviations into the initial model (Fig. 3d). The position, the orientation and also the form of the components are adjusted in order to minimize an error metric between the geometry and the measured point cloud.

Finally, the resulting geometry is exported into a commercial CAD software. The global model consistency is checked and adjustments are made in order to guarantee that no gaps or intersections are found in the final as-built geometry (Fig. 3e).

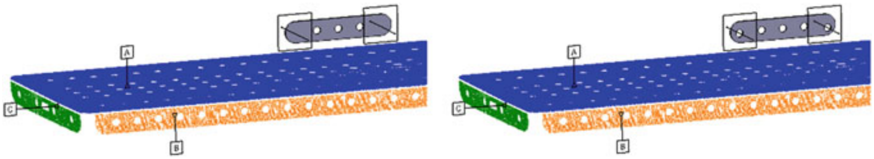

(a) Part before drilling (b) Part after drilling

Fig. 4. Adapting the drilling operation in order to meet functional requirements

Once the component's as-built geometry has been reconstructed, the situation of the local references regarding to the global references can be deduced in order to impact further manufacturing and assembly operations. In the proposed case study, the drilling operation to manufacture the fixturing holes is here impacted (Fig. 4). Indeed, the design of the interface component has been updated so that functional requirements of the assembly are met without the need of adjustment operations. The component is positioned in the global reference frame and features corresponding to local references, here the two fixation hole axes, are updated thanks to the information extracted from the as-built geometry.

4 Results and Discussion

In this paper, we proposed to use a hybrid representation of an updated DMU in order to provide a better management of geometrical variations during assembly. The originality of our approach is that the updated DMU not only reflects the actual geometry of the product, including its geometrical deviations, but also serves to adapt manufacturing and assembly operations so that the final product's functional requirements are met without the need of cost-ineffective adjustment operations.

The Reverse-Engineering method presented in this paper provides theoretical tools necessary to update a given DMU from its as-designed configuration to its hybrid updated configuration. The obtained Digital Mock-up reflects on the one hand the as-built geometry of the product's already assembled components, including geometrical deviations, and on the other hand the geometry of the components to be manufactured and assembled, which is updated in order to adapt to existing geometrical deviations.

However, interfacing as-built components with as-designed components is not straightforward and raises some interesting questions. Interfaces between as-built components and as-designed components involve on the one hand surfaces with geometrical deviations and on the other hand surfaces without geometrical deviations. In this case, deducing the assembly behavior resulting from the contact of these surfaces does not admit a simple solution and would strongly depend on the underlying assembly model.

A solution for a simple test case is proposed in this paper but both theoretical and practical developments will be needed in order to adapt it for industrial aeronautical products.

Based on the results already presented in this paper a roadmap for future developments is established. Future work will primary focus on a better modeling of the product's geometrical behavior and a better interface modeling between as-built and as-designed components. To this end, integrating graph based and skeleton based approaches to our Reverse-Engineering method seems promising.

Acknowledgements. The research work reported here has been carried out in partnership between Airbus Group Innovation and the LURPA—ENS Paris-Saclay.

References

1. Marguet B, Chevassus N, Falgarone H, Bourdet P (2013) Geometrical behavior laws for computer aided tolerancing: anatole a tool for structural assembly tolerance analysis. In: Eighth international seminar on computer-aided tolerancing, Charlotte, NC, pp 301–310
2. Falgarone H, Thiébaut F, Coloos J, Mathieu L (2016) Variation simulation during assembly of non-rigid components. Realistic assembly simulation with ANATOLEFLEX software. Procedia CIRP 43:202–207
3. Fu P (2008) Reverse engineering in the aerospace industry. In: Reverse engineering, Springer, London, pp 157–175
4. Gómez A, Olmos V, Racero J, Ríos J, Arista R, Mas F (2017) Development based on reverse engineering to manufacture aircraft custom-made parts. Int J Mechatron Manuf Syst 10 (1):40–58
5. Schleich B, Anwer N, Mathieu L, Wartzack S (2017) Shaping the digital twin for design and production engineering. CIRP Ann 66(1):141–144
6. Bey A, Chaine R, Marc R, Thibault G, Akkouche S (2011) Reconstruction of consistent 3D CAD models from point cloud data using a priori CAD models. In: ISPRS workshop on laser scanning
7. Bosché F (2010) Automated recognition of 3D CAD model objects in laser scans and calculation of as-built dimensions for dimensional compliance control in construction. Adv Eng Inform 24(1):107–118
8. Erdős G, Nakano T, Váncza J (2014) Adapting CAD models of complex engineering objects to measured point cloud data. CIRP Ann Manuf Technol 63(1):157–160
9. Durupt A, Remy S, Ducellier G, Guyot E (2009) A new reverse engineering process, the combination between the knowledge extraction and the geometrical recognition techniques. In: IEEE international conference on Computers & Industrial Engineering, 2009 (CIE 2009), pp 1367–1372
10. Buonamici F, Carfagni M, Furferi R, Governi L, Lapini A, Volpe Y (2017) Reverse engineering of mechanical parts: a template-based approach. J Comput Des Eng
11. Bruneau M, Durupt A, Vallet L, Roucoules L, Pernot JP (2016) A three-level signature by graph for Reverse Engineering of mechanical assemblies. In: Tools and methods for competitive engineering (Aix-en-Provence: 16: 2016), pp 669–681

Free-State Shape of Aeronautical Components for Assembly Simulation

F. Gringoz[1,2(✉)], F. Thiébaut[1], C. Lartigue[1], and B. Soufflet[2]

[1] LURPA, ENS Cachan, Université Paris-Sud, Université Paris-Saclay, 94235 Cachan, France
florian.gringoz@safrangroup.com

[2] R&T Methods Department, SAFRAN Group, SAFRAN Nacelles, Route Du Pont VIII, Gonfreville-L'Orcher 76700, France

Abstract. This paper deals with a method to extract the free-state shape of aeronautical assembly components from part measurements independently of the assembly configuration of use. Knowledge of the free-state shapes enables to assess the geometrical conformity of an assembly through the assembly simulation using Finite Element Method (FEM). The component is measured, using optical means in a given configuration for which the set-up is well-known. A coarse cleaning is thus applied on the measured data to obtain manipulative data in the CAD model frame. Meanwhile, displacements due to the measuring set-up and to gravity are evaluated from the nominal geometry using FEM. Finally, the free-state shape, as a finite element mesh, is obtained by moving the nominal mesh nodes by a distance equal to the measured defect minus the evaluated displacement. The approach is applied to an aeronautical component.

Keywords: Geometrical deviations · Flexible parts · Optical scanning · Free-state shape

1 Introduction

Within the context of aeronautics assembly structures, the geometry of an assembly is defined through the geometry of its components, described in their nominal configuration, i.e. without form deviations and in their theoretical relative position. In practice, the geometry of manufactured parts differs from its nominal geometry due to manufacturing process variations. Because of these imperfections, the inspection of assembly geometry is a major issue in industry.

During the assembly process, the geometrical conformity of components is verified by measuring the key characteristics (KC) that must respect given specifications to answer the functional requirements of the assembly. The classical method to achieve this purpose is to compare the actual component geometry to its nominal model, most often its CAD model [1, 2]. The actual geometry is generally obtained by surface measurements, and the measured data are compared to the CAD model to determine if the manufactured geometry lies within the tolerance zone. When geometrical deviations out of the admissible tolerance interval are detected on the component, adjustment operations are carried out in order to get closer to the nominal geometry. This

F. Cavas-Martínez et al. (Eds.): *Advances on Mechanics, Design Engineering and Manufacturing II*, LNME, pp. 203–212, 2019.
https://doi.org/10.1007/978-3-030-12346-8_20

procedure turns out to be very expensive. However, in some cases, the assembly of non-conform components could result in assembly conformity. Moreover, an average assembly geometry, differing slightly from the nominal geometry could be just as functional as the geometry initially chosen.

Therefore, analyzing the impact of the geometrical deviations of components on the geometrical functionality of the assembly is a challenging issue due to various difficulties. First, the assembly process generally includes many assembly stages. The output geometry of one stage is the input of the next stage, and thus, the assembly geometry is modified from station to station [3, 4] due to the succession of assembly operations [5]. In addition, the flexibility of aeronautical components makes their inspection arduous because of the deformations induced by the gravity load and by fixturing conditions [6]. The inspection of such components is generally performed when components are in the assembly configuration, at different stages of the assembly process. However, the assembly conditions are not necessarily the same as the conditions of use. Ascione and Polini [6] propose a method to control component geometry using coordinate measuring machines (CMM) in their conditions of use. These conditions are reproduced thanks to modular equipment. Another approach, described by Franciosa et al. [4], consists of coupling a prediction of the defect patterns of a component with a measurement step to find the real causes of these defects at different stages of the assembly process. The previous described methods require the configuration of use to be reproduced, which turns out to be expensive in the context of large aeronautics components.

Some studies propose to use the Finite Element Method (FEM) for assembly inspection. Radvar-Esfahlan and Tahan [7] used FEM simulation that take into account the boundary conditions associated to the measuring configuration of the component geometry. This allows authors to compare the nominal geometry to the measured geometry in the same conditions, even if they are different from the conditions of use. Jaramillo et al. [8] developed an approach which consists in simulating the required deformations to match the reference points before comparing the partial view of the actual geometry restricted to regions that need to be inspected. To evaluate the assembly component geometry from scanned assembly geometries in the context of repair analysis, Yu et al. [9] proposed to assess component geometries through the simulation of a virtual assembly process. Gentilini and Shimada [10] focused on FEM to predict the assembly geometry from measured component geometries through the simulation of the assembly process. Authors note an error between predicted and actual assembly geometries which is probably due to the variations of measuring conditions, which modify the loading conditions (including gravity).

To perform accurate assembly simulations whatever the configuration, the intrinsic geometry of components, called the free-state shape, must be known. The free-state is the shape a component should have in absence of loads [11, 12]. The free-state turns out to be difficult to identify when flexible parts are concerned, which is the case for aeronautical assembly structures, gravity loads and part fixturing indeed induce part deformations.

In this context, a method using finite element simulation to evaluate the geometrical conformity of assemblies is proposed, based on the free-state of components. The geometry of the components is extracted by measuring the components. Then, a FEM enables assembly simulation which is used to assess the assembly conformity. This paper more particularly focuses on the step of geometry extraction from part measurements regardless of the assembly configuration of use. The originality of this method is to extract the free-state geometry of the component based on FEM simulations.

This paper is organized as follows. In Sect. 2, we detail our method to extract the actual free-state shape of a component. A case study is then reported in Sect. 3. Section 4 presents the conclusion and perspectives of this work.

2 Method for Free-State Geometry Identification

The approach, summarized in Fig. 1, is applied to the aeronautical component of an assembly defined by its CAD model.

First, the measurement of useful geometries is only performed in a given configuration, leading to S_{meas}^{conf}. A step of data treatment follows in order to obtain a point cloud that is representative of the geometry in the measuring configuration, giving S_{act}^{conf}. In parallel, a simulation of the component deformation under the gravity and loads (associated to the measuring configuration) is carried out using FEM. Finally, the actual free-state is obtained by comparing both geometries.

$$S_{act}^{conf} = S_{act}^{free} + D_{free}^{conf} \tag{1}$$

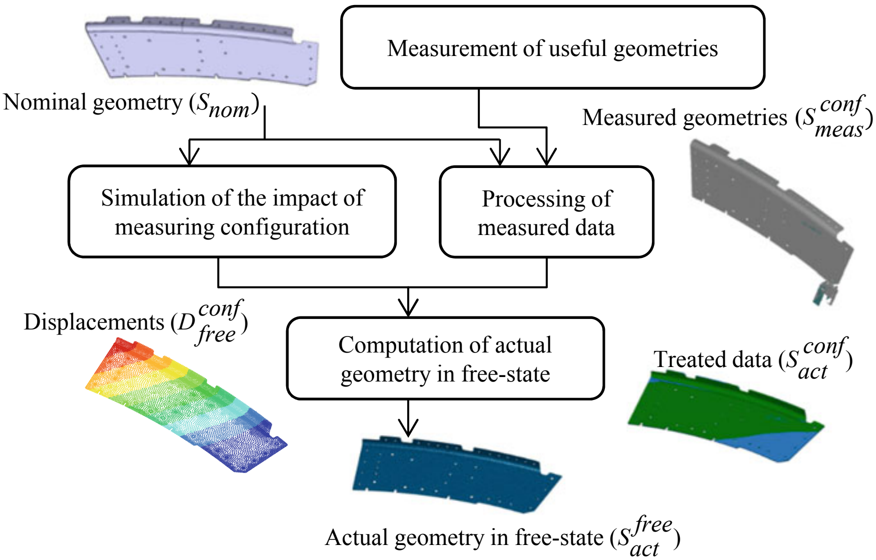

Fig. 1. Method actual free-state geometry identification

This shape, S_{act}^{conf}, is the superposition Eq. (1) of the shape that the component would have in its free-state S_{act}^{free} (free from any loads), and of the deformations induced by the loads associated to the gravity and the measuring configuration, D_{free}^{conf}. The following sections detail how the different terms of the equation are obtained.

2.1 Acquisition of the Component's Actual Shape

The acquisition of the component's actual shape gives the numerical representation of the actual component geometry. This is performed through two stages: measurement of the geometry and processing of the measured data. The first stage yields data that are not directly exploitable, and the second stage makes them usable, thus leading to S_{act}^{conf}.

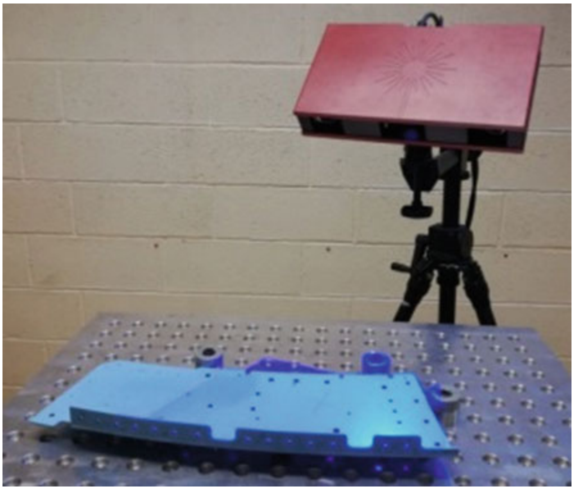

Fig. 2. Stereovision sensor ATOS core

Geometry measurement: For the measurement, the stereovision sensor, ATOS Core, mounted on a tripod, is used (Fig. 2). The measurement noise and the measurement error of this sensor, given by the constructor, are respectively 0.003 mm and −0.019 mm. The system positioning is obtained thanks to a set of targets which define the reference frame.

The measuring set-up plays a major role, as it may ensure part accessibility, but it also defines the boundary conditions that will be used in FE simulations. Therefore, once the measuring set-up is defined, it must be scanned so that its position is completely defined. Then, the component is set in position to be scanned in the same frame. Measuring these two elements in the same frame enables to evaluate the position of the contact points between the measuring set-up and the component. At the end of the measuring stage, the acquired data, expressed in a STL format, represent the measured shape in the given configuration, S_{meas}^{conf}.

Measured data processing: To compute the actual free-state shape of the component, both its actual shape in the given measuring configuration S_{act}^{conf}, and the configuration, must be known. Data treatment thus consists in two main steps. First, points that are not representative of the shape are removed from the measured point cloud (data cleaning). Then, the measured shape is registered to its CAD model. This registration is carried out by matching the common geometrical elements of both shapes. The position of the contact points between the component and the measuring set-up has to be identified for FE simulation. As the measuring set-up is measured in the same frame as the component, the registration previously performed permits to detect the position of the supporting points directly in the CAD frame.

2.2 Displacement Computation by FE Simulation

The measuring configuration induces deformations due to the gravity load and the component's positioning on its measuring set-up. These deformations are evaluated thanks to FE simulation. First, the simplification and the sampling of the CAD model are carried out to obtain a finite element mesh. Due to the thin shape of aeronautic components, shell elements are used for the meshing. Then, the contact between the part surfaces and the set-up are expressed as boundary conditions, whereas gravity is considered as an oriented acceleration. To achieve the simulation, the mechanical behaviour of the component is assumed to be elastic linear. The result of this simulation, carried out in the finite element module of CATIA V5©, is a displacement field, D_{free}^{conf}, which represents the displacement of each node of the mesh in the CAD frame.

2.3 Free-State Shape Computation

The free-state shape computation is expressed by Eq. (1). The first step gives the actual shape in the measuring configuration, S_{act}^{conf}. The second step leads to the displacement field due to the impact of the measuring configuration, D_{free}^{conf} calculated using FE simulation. However, although data are expressed in the same frame, both point clouds are not homogeneous; the measured point cloud is denser than the CAD mesh. In order to homogenize both point clouds, to each node of the nominal mesh, p_i, a corresponding mean point m_i, is computed on the point cloud considering a small neighborhood defined by a cylinder at the vicinity of the node. Furthermore, as the free-state will be the basis for FE simulations [11], it is represented by a finite element mesh.

For this purpose, our approach consists in moving p_i along its normal vector $\overrightarrow{n_i}$ by a distance equal to the projection of the distance between the node p_i and its mean point m_i onto $\overrightarrow{n_i}$, minus the calculated displacement at the node, $\overrightarrow{D_i}$, with $\overrightarrow{D_i}$ the component of D_{free}^{conf} for each node of the mesh. The method is summarized in Fig. 3, using the notations displayed in Table 1.

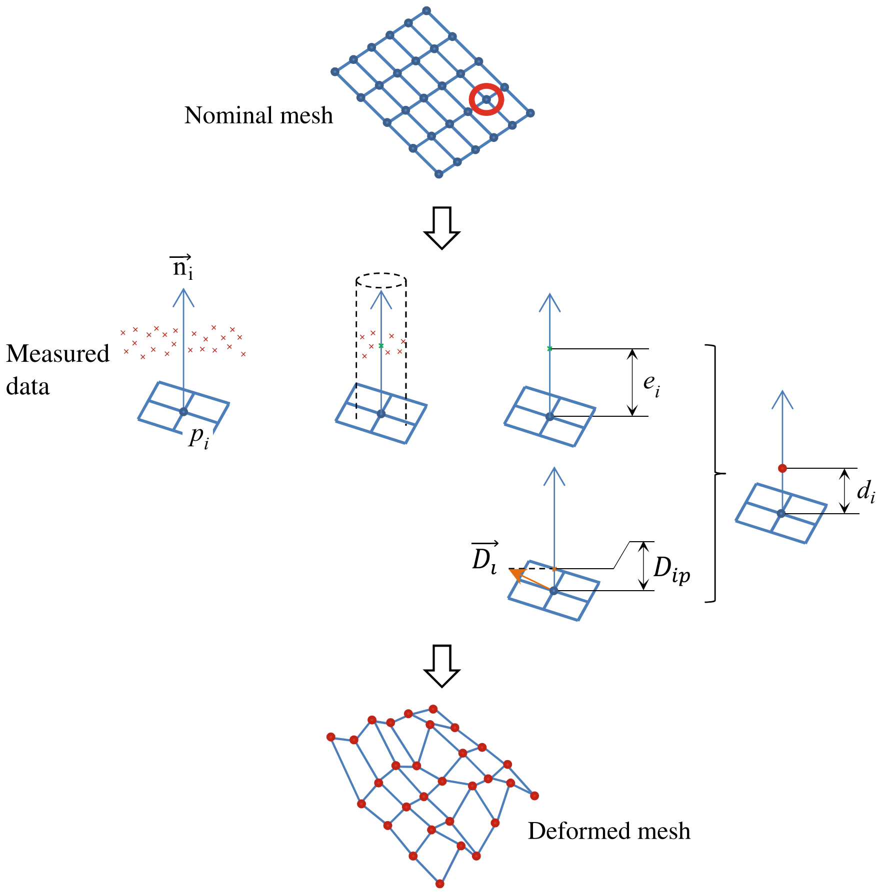

Fig. 3. Deformation of the nominal mesh

Table 1. Notations

p_i	Node of the nominal mesh
$\vec{n_i}$	Computed normal vector of p_i
m_i	Mean point of the neighborhood of p_i
$e_i = \overrightarrow{p_i m_i} \cdot \vec{n_i}$	Distance between p_i and m_i following the direction $\vec{n_i}$
$\vec{D_i}$	Computed displacement thanks to FEM
$D_{ip} = \vec{D_i} \cdot \vec{n_i}$	Computed displacement along $\vec{n_i}$
$d_i = e_i - D_{ip}$	Geometrical deviation

The final result is a finite element mesh which is consistent with finite element software. This mesh is a representation of the actual geometry in the free-state, which enables to simulate various positioning configurations. Our approach is illustrated by an example in the next section.

3 Case Study: A Flexible Aeronautical Component

In this example, the component used is a part of the forward frame of the thrust reverser of the airplane engine nacelle, the front panel (Fig. 4). This component, made of composite material, is very thin, which makes it flexible. Currently, the whole geometry of this component is inspected before assembly, and the geometry of its external skin is inspected after assembly. Predicting the component geometry would be useful to improve the assembly process. In this direction, the use of the actual free-state geometry enables to get rid of the measurement configuration, and thus of the gravity, and is a good support for FE simulations.

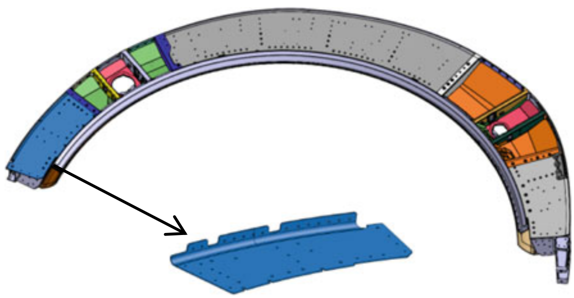

Fig. 4. The Front Panel, a part of the forward frame

The first step of the method is the measurement of the component actual geometry. One face only is measured, as the nominal mesh is a 2D mesh. The component is positioned on an equally geometry constrained set-up, and both the component and the set-up are measured in the same frame (see Fig. 5a). The coarse treatment is then applied, through GOM Inspect software, to the 750,000 measured points. All the points that correspond to the set-up are manually removed from the measured data (Fig. 5b). Finally, the measured data are repositioned in the CAD frame. This alignment is achieved by matching common geometrical elements to both the measured and the nominal geometries. For the case study, the geometrical elements correspond to the front panel which positions holes on the forward frame during assembly. This stage gives an exploitable point cloud of 600,000 points expressed in the CAD frame.

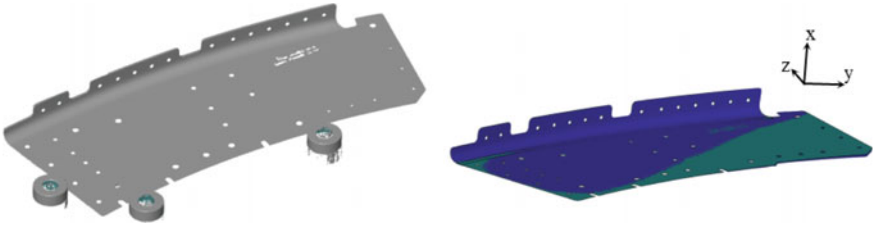

(a) Measured data (b) Treated data

Fig. 5. Acquisition of the component actual shape

In parallel, the displacements induced by gravity and by measuring set-up are computed thanks to FE simulation. The CAD model is simplified as a surface model to build a 2D mesh composed of shell elements with 11,503 elements and 6365 nodes. The implemented material properties are the same than the ones used by the modeling and simulation department for the in service tenue calculation. The contact points are identified from the measured data after their registration on the CAD model. At these points, boundary conditions impose that the displacements along the normal at the contact points be null. There are no additional loads to implement thanks to the use of an equally geometry constrained set-up. The gravity is implemented as an oriented acceleration along the $\vec{x}$ axis (see Fig. 5b). The simulation yields to the displacements of the mesh nodes, which are here relatively small compared to part form defects (see Fig. 6).

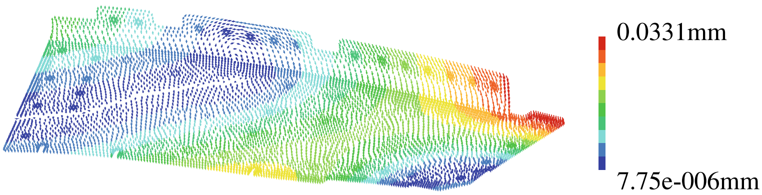

Fig. 6. Displacements

Finally, the free-state shape can be computed according to the method detailed in Sect. 2.3. The mean points in the neighborhood of each node of the finite element mesh are computed, and then projected onto the normal vector at the node. The size of the neighbourhood (cylinder diameter) is defined in function of the size of the mesh. The evaluated displacements at the nodes are substracted from the projected distance between the node and its mean point. Nodes are then moved of the computed distance along its normal. The result is a finite element mesh, which is representative of the actual geometry of the front panel in the free-state, with geometrical deviations (see Fig. 7).

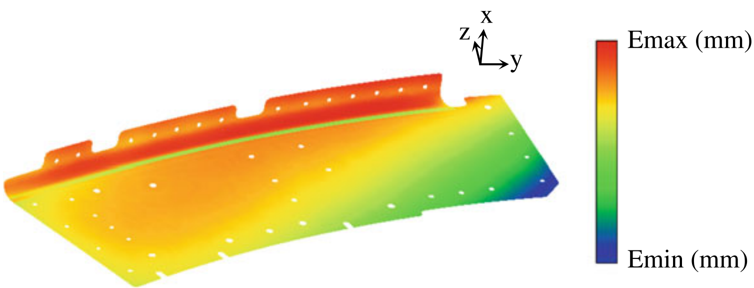

Fig. 7. The actual free-state shape of the front panel

The displacements and the actual free-state shape are shown (see Figs. 6 and 7) to have an idea of the expected results. Values of geometrical deviations cannot be communicated for confidentiality reasons.

4 Conclusion

In this paper, we proposed a method to extract the free-state shape of a component independently of the assembly configuration of use. This method relies on the component geometry measurements. For this purpose, the component is positioned on a set-up that is entirely defined during the measuring stage. When positioned on its set-up, the component is subjected to deformations caused by both the gravity load and the measuring set-up. These deformations, evaluated using FE simulations, are substracted from the measured data to obtain the free-state shape of the component. Finally, the nominal mesh is deformed to obtain the free-state shape of the component as a finite element mesh. Applied to an aeronautical component, the method provides a finite element mesh which is representative of the component's free-state shape that can be used to evaluate the geometry of the component in different configurations or for assembly simulations. If the whole approach seems relevant, each step of the method has now to be assessed. Specific attention will be paid in future work to the evaluation of the mechanical model, by using more than one configuration.

References

1. Bispo EM, Fisher RB (1994) Free-form surface matching for surface inspection
2. Samper S et al (2009) Modeling of 2D and 3D assemblies taking into account form errors of plane surfaces. J Comput Inf Sci Eng 9:041005
3. Hu SJ, Camelio J (2006) Modeling and control of compliant assembly systems. CIRP Ann Manuf Technol 55:19–22
4. Franciosa P et al (2017) Rapid response diagnosis of multi-stage assembly process with compliant non-ideal parts using self-evolving measurement system. Procedia CIRP 60:38–43
5. Liu G et al (2014) Study on analysis and prediction of riveting assembly variation of aircraft fuselage panel. Int J Adv Manuf Technol 75:991–1003
6. Ascione R, Polini W (2010) Measurement of nonrigid freeform surfaces by coordinate measuring machine. Int J Adv Manuf Technol 51:1055–1067
7. Radvar-Esfahlan H, Tahan S-A (2012) Non-rigid geometric metrology using generalized numerical inspection fixtures. Precis Eng 36:1–9
8. Jaramillo A et al (2013) Fast dimensional inspection of deformable parts from partial views. Comput Ind 64:1076–1081
9. Yu A et al (2016) Geometric design model and object scanning mode based virtual assembly and repair analysis. Procedia CIRP 44:144–150
10. Gentilini I, Shimada K (2011) Predicting and evaluated the post-assembly shape of thin-walled components via 3D laser digitization and FEA simulation of the assembly process. Comput Aided Des 43:316–328

11. Thiébaut F et al (2016) Evaluation of the shape deviation of non rigid parts from optical measurements. Int J Adv Manuf Technol 84:9–12
12. Lacroix C (2015) Caractérisation géométrique des assemblages flexibles par la mesure. Phd Thesis. École normale supérieure de Cachan, Cachan, France

Analysis of the Virtual Facebow Transfer by Using a Facebow Fork. An In Vitro Study

E. Solaberrieta[1(✉)], M. Iturrate[2], J. A. Oriozabala[1], X. Amezua[2], L. Barrenetxea[2], and O. Etxaniz[2]

[1] University of Basque Country UPV/EHU, Europa Plaza 1, 20018 Donostia, Spain
eneko.solaberrieta@ehu.eus
[2] University of Basque Country UPV/EHU, Alameda Urquijo sn, 48013 Bilbao, Spain

Abstract. In dentistry, for different reasons, several processes necessary to respond to different patient needs must be performed outside the mouth. This forces to have an "extra ore" model of the patient's masticatory apparatus. For this purpose, the best alternative today is the virtual articulator. For an effective use of the virtual articulator, it is necessary to transfer the patient's data to the virtual environment. This is the base of the virtual facebow technique. There are different virtual methods that meet the function of the facebow, all of which use reverse engineering software. However, the accuracy of these methods is not well-known, and it is therefore clear that this is a matter of analysis before putting it into practice in everyday life. Thus, the aim of this study is to analyze, by means of in vitro tests, the accuracy of one of the virtual methods for transferring the digitized maxillary models to the virtual articulator: the virtual facebow transfer by using a facebow fork.

Keywords: Virtual articulator · Dental CAD/CAM system · Reverse engineering · Virtual facebow transfer

1 Introduction

In dentistry, over the years, different methods and processes have been elaborated to respond to the different patients' needs. For technical and comfort reasons, as well as to be able to predict results, some of these processes must be tested and/or performed outside the patient's mouth [1]. Among these processes can be highlighted those for the production of dental prostheses and restorations, as they require a customized design and manufacturing. These procedures force to have 'extra ore' a mechanical replica of the human masticatory apparatus to be possible to carry them out [1]. This mechanical replica, known as dental articulator, has substantially developed since its origins, becoming increasingly similar to the patients cranio-mandibular static-cinematic situation. Thus, these dental articulators have evolved from being simple hinge-type devices, far apart from the patient's reality, to complex mechanisms that, by transferring different records made to the patient, can be adjusted to simulate a reality very close to their own [2–4].

F. Cavas-Martínez et al. (Eds.): *Advances on Mechanics, Design Engineering and Manufacturing II*, LNME, pp. 213–224, 2019.
https://doi.org/10.1007/978-3-030-12346-8_21

Between the different tools and instruments used to transfer patient data to the dental articulator, the facebow stands out. The facebow is an instrument used to record the spatial relationship of the maxillary arch to some anatomic reference point or points and then transfer this relationship to a dental articulator, in this way, orienting the dental casts in the same relationship to the opening axis of the articulator [5]. Since its inception, this instrument has evolved in parallel with the dental articulator [6–8].

In recent years, dentistry has made a huge impact on technological advances, and the methods used to date have resulted in new processes. This has also had a great impact on the functionality, safety and aesthetics required by patients [1]. As a result, computer technologies, known as Computer Aided Design/Computer Aided Manufacturing (CAD/CAM), are becoming increasingly important in this field of medicine [1, 9].

This is reflected in the fact that, in recent decades, the aforementioned mechanical dental articulators are being replaced or supplemented by a CAD/CAM system [10]. These digital systems have improved design by incorporating new materials and automation and, consequently, reducing the workforce, thereby increasing performance by achieving better quality control [1]. Working in the dental digital workflow, the results have been improved and the cost of these systems has been significantly reduced [10].

However, one of the biggest problems of the virtual environment lies in the patient data transfer. It is precisely from this problem that the virtual facebow arises, which, as its name suggests, is the homologue of the facebow in a virtual environment. There are different virtual methods that meet the function of the facebow [10–13], all of which use reverse engineering software. However, the accuracy of these methods is not well-known, and it is therefore clear that this is a matter of analysis before putting it into practice in everyday life.

Thus, the aim of this study is to analyze, by means of in vitro tests, the accuracy of one of the virtual methods for transferring the digitized maxillary casts to the virtual articulator: virtual facebow transfer by using a facebow fork [10].

2 Material Resources

For the application of the proposed methodology, the following material resources have been required:

- A dum equipped with a maxillary plaster cast.
- A facebow fork consisting of two main parts: front (fork) and back (tray).
- An elastomeric impression material (Aquasil Soft Putty).
- The digitization systems ATOS (composed by the optical scanner ATOS Compact Scan and the software ATOS Professional V7.5), GO (composed by the optical scanner Go! Scan 3D G1 and the software VX Elements) and AGI (composed by a digital camera, in this case the Pentax K-S1, and the software Agisoft Photoscan).
- The reverse engineering software Geomagic Studio.
- The inspection software GOM Inspect.
- The statistical software SPSS.

3 Methodology

The proposed methodology to analyze the accuracy of the aforementioned virtual facebow transfer method can be subdivided in two clear phases. In the first phase, the virtual facebow transfer is applied to the dum used as a patient in this in vitro study and in the second phase, the accuracy of the results obtained is evaluated.

3.1 Phase 1. Virtual Facebow Transfer by Using a Facebow Fork

The following is a step-by-step description of the virtual facebow transfer by using a facebow fork, in a generic way, shading in each of them the adaptations that have been made for this in vitro study:

1. Digitization of the maxillary arch with an intraoral dental scanner (Fig. 1). Considering that this is an in vitro study that starts from a maxillary plaster cast and that the accuracy of the digital maxillary model obtained with an intraoral dental scanner is not the topic of analysis, to avoid errors in this digitization that eclipse the results obtained with the analysed method, the current digitization has been carried out with the high accuracy digitization system ATOS.

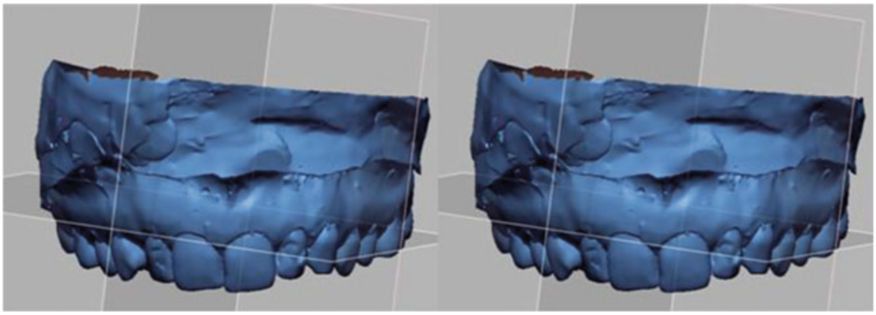

Fig. 1. The digital maxillary model obtained from the digitization of the maxillary cast with the high accuracy digitization system ATOS

2. Sticking three adhesive targets on the patient's head (anatomical points): two near the temporomandibular joints and one above the infraorbital point (Fig. 2).
3. Depositing an elastomeric impression material onto the tray of the facebow fork and introducing this part of the facebow fork into the patient's mouth, squeezing it against the maxillary arch (Fig. 3). The elastomeric impression material used has been the silicone Aquasil Soft Putty, since the durability that it presents avoids the deformation of the impressions.
4. Digitization of the patient's head while holding the facebow fork. This digitization has been carried out with the aforementioned digitization systems ATOS, GO and AGI (Fig. 4). Therefore, in the rest, three cases will be distinguished, one for each device used to approach this step: ATOS_U, GO_U and AGI_U.

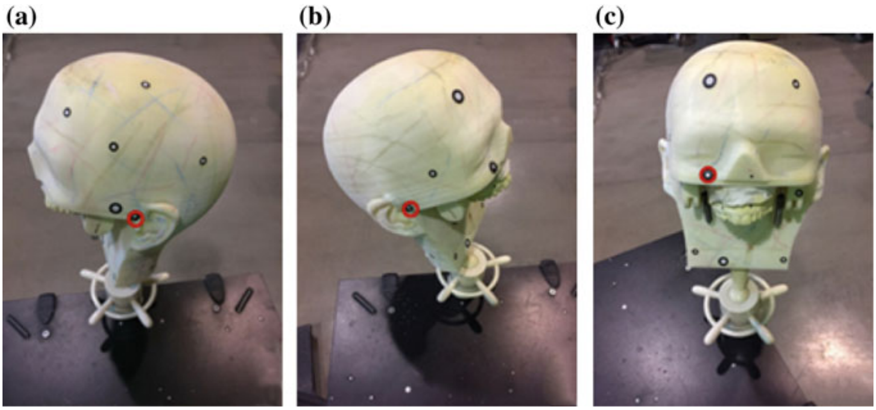

Fig. 2. The three adhesive targets on the patient's head (anatomical points): two near the temporomandibular joints (**a** and **b**) and one above the infraorbital point (**c**)

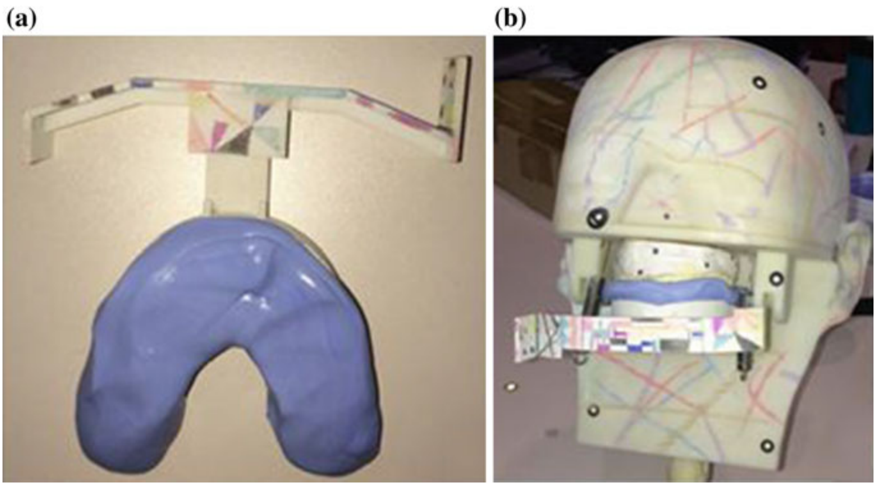

Fig. 3. Depositing an elastomeric impression material onto the tray of the facebow fork (**a**) and introducing this part of the facebow fork into the patient's mouth, squeezing it against the maxillary arch (**b**)

5. Digitization of the impression on the back part of the facebow fork and of the front part of the facebow fork with an intraoral dental scanner. For similar reasons to those mentioned in step 1, this digitization has been carried out with the high accuracy digitization system ATOS (Fig. 5).
6. Alignment of the digital facebow fork model to the digital maxillary model in a reverse engineering software by using the best fit command (Fig. 6). The software used has been Geomagic Studio. Thus, a local alignment has been carried out based exclusively on the surfaces that both digital models have in common: the dental

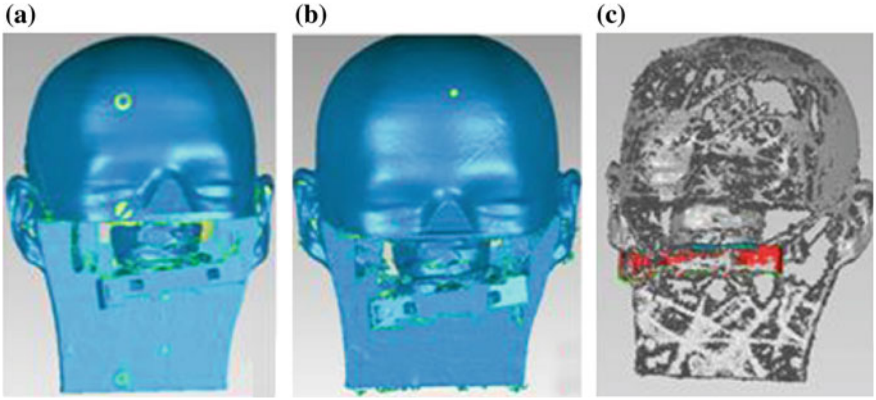

Fig. 4. The digital models obtained from the digitization of the patient's head while holding the facebow fork. Cases ATOS_U (**a**), GO_U (**b**) and AGI_U (**c**)

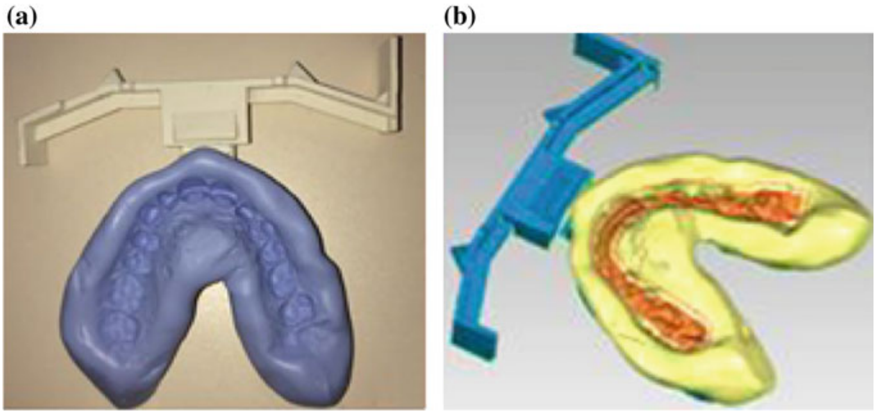

Fig. 5. The digital model obtained (**b**) from the digitization of the impression on the back part of the facebow fork and of the front part of the facebow fork (**a**) with the high accuracy digitization system ATOS

surfaces of the digital maxillary model and its negative formed by the impression on the back part of the digital facebow fork model.

7. Repetition of step 6 to align the digital model obtained in that step to the digital models of the patient's head holding the facebow fork obtained in step 4. In this case, the surfaces selected to perform the corresponding local alignments have been those that belong to the front part of the facebow fork and are visible in both digital models to be aligned. Note that this step has had to be repeated for the cases ATOS_U, GO_U and AGI_U (Fig. 7).

Once these steps have been completed, to culminate the transfer, in practice (but not in this study since it is outside of the field of analysis) it would only remain to define a

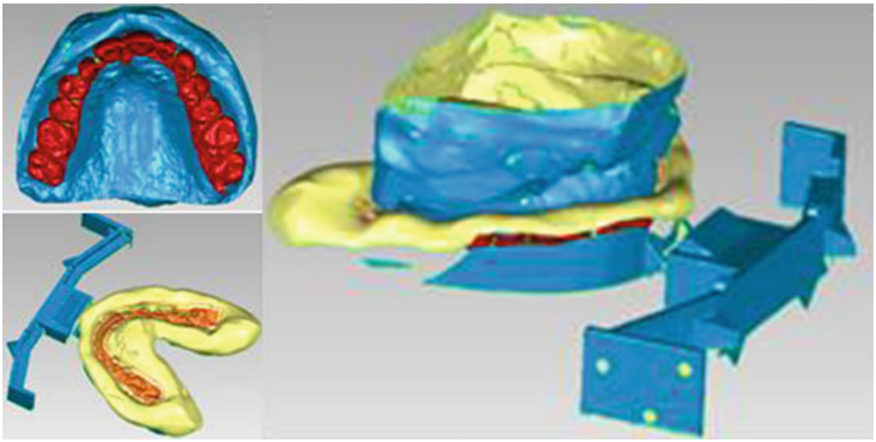

Fig. 6. Result of the alignment of the digital facebow fork model (down to the left) to the digital maxillary model (up to the left). In red the surfaces selected for local alignment

cranial reference system from the three anatomical points defined in step 2, locate the maxillary digital model with respect to this reference system and transfer this model to the virtual articulator software, making the newly defined coordinate system coincide with the virtual articulator's coordinate system.

3.2 Phase 2. Evaluation of the Accuracy of the Results

The following is a step-by-step description of the evaluation of the accuracy of the results obtained with the virtual facebow transfer method described in phase 1:

1. Getting the digital reference model. For this purpose, firstly, the dum has been digitized with the maxillary cast mounted with the high accuracy digitization system ATOS. Subsequently, due to the impossibility of obtaining in the desired way the maxilla of the digital model of the set, this digital model and the digital maxillary model obtained in step 1 of phase 1 have been aligned in the reverse engineering software Geomagic Studio by using the best fit command. For this, only the surfaces that both digital models have in common have been selected: the dental surfaces visible on both digital models. As a result, a single digital model has been obtained (Fig. 8).
2. Alignment of the digital models obtained in the step 7 of the phase 1 to the reference model in a reverse engineering software by using the best fit command (Fig. 9). The software used has been Geomagic Studio. Taking into account that the accuracy of the results obtained with the method described in phase 1 is reflected in the disagreement of the orientation of the digital maxillary model obtained by this method with respect to the orientation of the maxilla of the digital reference model obtained in step 1 of the phase 2, in order to avoid falsifying the results, the surfaces selected to perform the necessary local alignments have been those corresponding to the ears and nose of the dum that can be observed in both digital models to be

(a)

(b)

(c)

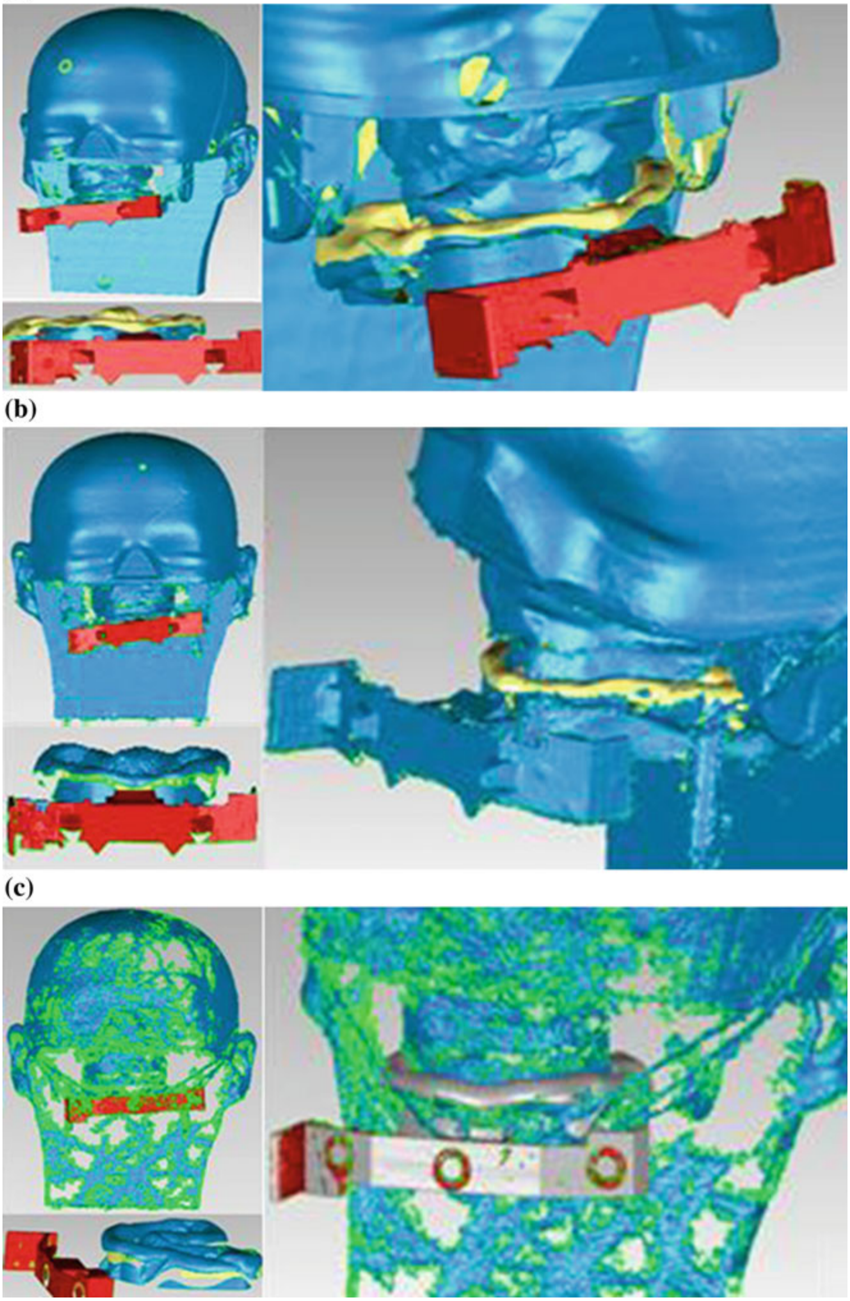

Fig. 7. Results of the alignments of the digital model obtained in step 6 (down to the left) to the digital models of the patient's head holding the facebow fork obtained in step 4 (up to the left). In red the surfaces selected for local alignment. Cases ATOS_U (**a**), GO_U (**b**) and AGI_U (**c**). For clarity, the maxillary digital model has been hidden

Fig. 8. The digital reference model obtained by the alignment of the digital maxillary model (down to the left) to the digital dum's model (up to the left). In red the surfaces selected for local alignment

aligned. Once the task had been completed, only the pairs of aligned maxillary digital models have been saved, deleting the remaining data.

3. Comparison of surfaces in an inspection software. The software used has been GOM Inspect. With this software, the deviations between the dental surfaces of the digital models aligned in the previous step have been measured, i.e. the deviations between the tooth surfaces of the digital maxillary model oriented by the analysed method and the maxilla of the digital reference model. Therefore, these deviations indicate the accuracy of the analysed method: larger deviations indicate less accuracy of the method.

4 Results

After having processed the values of the deviations measured in step 3 of phase 2 with the statistical software SPSS, the values of Table 1 and of the box plot in Fig. 10 have been extracted.

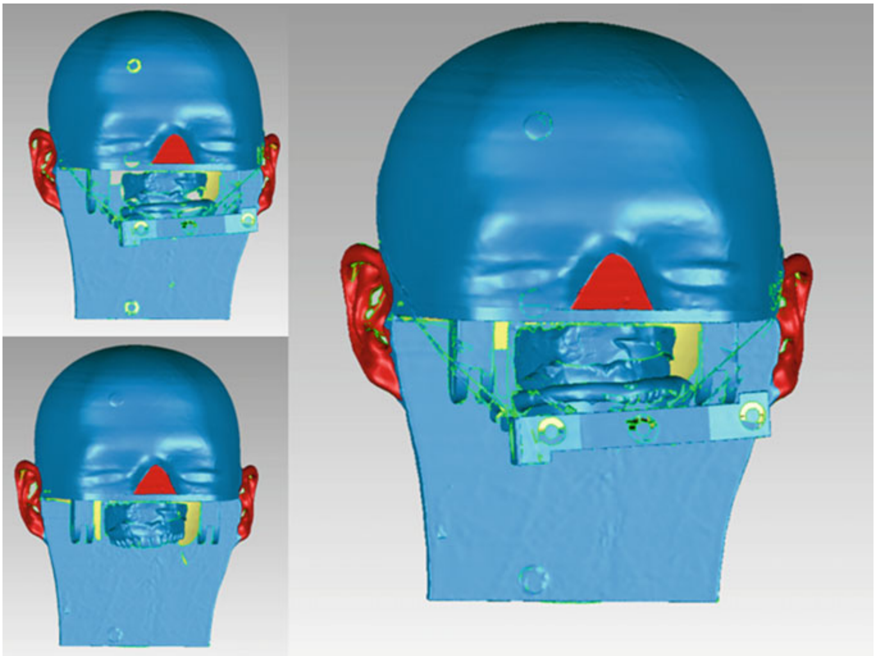

Fig. 9. Result of the alignment of the digital models obtained in the step 7 of the phase 1 (up to the left) to the digital reference model (down to the left). In red the surfaces selected for local alignment. Due to the similarity of this step in all three cases, only the ATOS_U case has been shown

Table 1. Accuracy and trueness of results

Case	Average	Median	Standard deviation	Min.	Max.
ATOS_U	0.5099	0.4809	0.5071	−0.1599	1.2868
GO_U	0.6626	0.6418	0.6598	−0.0778	1.3061
AGI_U	0.9524	1.1941	0.9451	−1.1161	2.0976

Significant values

As mentioned above, the measured deviations reflect the misalignment that the digital maxillary model oriented by the analysed method presents in relation to the maxilla of the digital reference model, which indicates the lack of accuracy of the analysed method. By applying this method with different digitization systems (ATOS, GO and AGI), the sensitivity of this method to the digitization system used can be observed. Therefore as shown in Table 1 (or in the box plot in Fig. 10), the absolute deviations obtained were equal to or less than 1,2868 mm in the case ATOS_U, 1.3061 mm in the case GO_U and 2.0976 mm in the case AGI_U. As for the trueness of the results, a value of 0.5099 ± 0.5071 mm has been obtained in the case ATOS_U, 0.6626 ± 0.6598 mm in the case GO_U and 0.9524 ± 0.9451 mm in the case AGI_U. So the results with greater accuracy and trueness have been obtained using the ATOS digitization system, while the results with less accuracy and trueness have been obtained using the AGI digitization system.

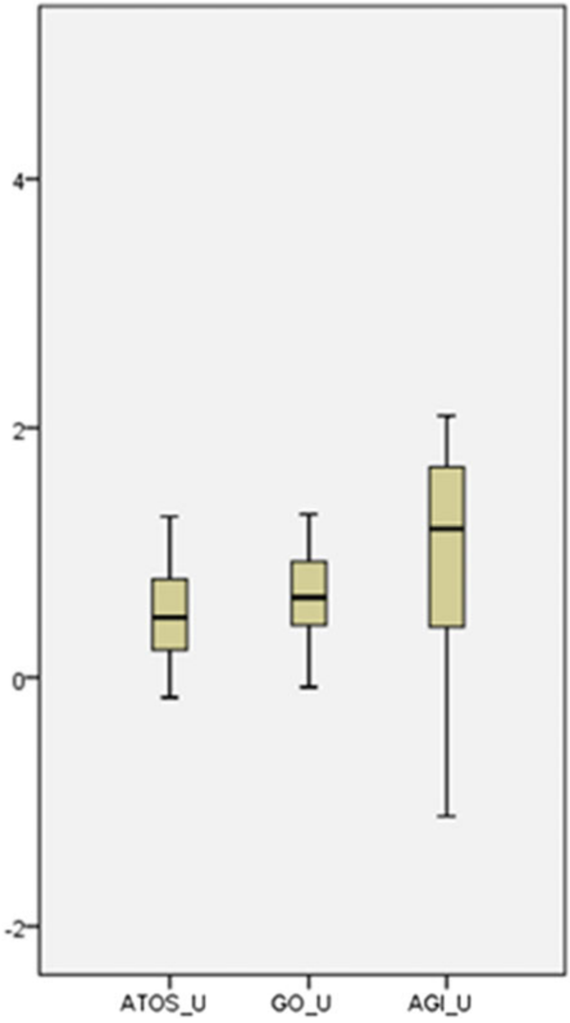

Fig. 10. Accuracy and trueness of results. Box-plot: distribution of the deviation magnitudes in millimetres on the vertical axis and the case to which they refer on the horizontal axis

5 Discussion

The deviations measured to determine the accuracy of the method analysed have different origins. Among them, the most influential are those caused by the numerous best-fit alignments required by the method and those caused by the digitization system used to perform it. The errors caused by the numerous best-fit alignments are reflected in the deviations measured in the case where the most accurate digitization system was used (ATOS_U case), while those caused by the digitization system used are reflected in the deviations measured in the remaining cases (GO_U and AGI_U cases).

Therefore, in contrast to the advantage of allowing the position of the upper dental arch in relation to the patient's facial morphology there are the disadvantages of the numerous alignments by means of the best fit that it requires and its susceptibility to the digitization system used.

However, taking into account that in the cases ATOS_U and GO_U the greater part of the deviations measured have a value less than or equal to 1 mm, it can be stated that the results obtained in this study indicate that this method may be appropriate if a digitizing system with a certain accuracy is used.

6 Conclusions

As evidenced by the results obtained, the accuracy of the analysed virtual facebow transfer method may be appropriate if a digitization system with a certain accuracy is used. This fact highlights the need for further tests to analyse whether this method can be applied with the current digitization systems available for dentistry.

Acknowledgements. The authors of this paper thank the Faculty of Engineering of Bilbao for locating the PDL in their fa-cilities and the Country Council of Gipuzkoa and for financing this project (75/18).

References

1. Solaberrieta E et al (2015) Integración de la ingeniería en la odontología. Dyna 90(1):1–4
2. Mitchell DL, Wilkie ND (1978) Articulators through the years. Part I. Up to 1940. J Prosthet Dent 39(3):330–338
3. Mitchell DL, Wilkie ND (1978) Articulators through the years. Part II. From 1940. J Prosthet Dent 39(4):451–458
4. Starcke EN (2000) The history of articulators: early attempts to reproduce mandibular movement. J Prosthodont 9(1):51–56
5. Driscoll CF et al (2017) The glossary of Prosthodontic terms. J Prosthet Dent 117(5):e1–e105
6. Starcke EN (2000) The history of articulators: the appearance and early history of facebows. J Prosthodont 9(3):161–165
7. Starcke EN (2001) The history of articulators: from facebows to the gnathograph, a brief history of early devices developed for recording condylar movement: Part I. J Prosthodont 10(4):241–248
8. Starcke EN (2002) The history of articulators: from facebows to the gnathograph, a brief history of early devices developed for recording condylar movement: Part II. J Prosthodont 11(1):53–62
9. Beuer F, Schweiger J, Edelhoff D (2008) Digital dentistry: an overview of recent developments for CAD/CAM generated restorations. Br Dent J 204(9):505–511
10. Solaberrieta E, Garmendia A, Minguez R, Brizuela A, Pradies G (2015) Virtual facebow technique. J Prosthet Dent 114(6):751–755
11. Solaberrieta E, Mínguez R, Barrenetxea L, Etxaniz O (2013) Direct transfer of the position of digitized casts to a virtual articulator. J Prosthet Dent 109(6):411–414

12. Solaberrieta E, Otegi JR, Mínguez R, Etxaniz O (2014) Improved digital transfer of the maxillary cast to a virtual articulator. J Prosthet Dent 112(4):921–924
13. Antolín B (2018) Flujo digital con escáner facial en implantología. Gac Dent 300

Methodology for the 3D Reconstruction of Industrials Facilities Using Photogrammetry

R. Miralbes(✉), H. Peña, and J. A. Peña

DIDYF, University of Zaragoza, C/Maria de Luna s/n, 50018 Saragossa, Spain
miralbes@unizar.es

Abstract. There are some areas of project engineering where it is especially necessary to know the spatial distribution of the elements that make up an industrial installation to diverse aims: the planning of future actions in the installation, like expansions, reparations and modifications; the documentation of the current state of an installation; and the construction, supervision and control of execution. It is in these areas where photogrammetry has a high potential to develop. The aim of this article is to establish a methodology that defines the way in which photographs should be made, the main parameters of the camera, the use of markers and targets and so on, so that the 3D reconstruction of industrial facilities is possible, quantifying the error committed. On the other hand, the improvement of smartphone camera lenses and the popularity of their use, as well as the proliferation of fish-eye cameras and action cameras like the GoPro as the main reference, has generalized the use of this type of device, which can be used at a very low cost to make 3D reconstructions using photogrammetry. This article will study, in a comparative way, the following tools: a high-end mobile camera, a fish-eye camera and a high-end single lens reflex (SLR) camera. These methodology and configurations will be tested in diverse industrial areas: a computer room, a warehouse with fluid facilities, a mechanized workshop, a mechanical assembly workshop, a workshop for electrical assemblies and a warehouse with a plastic crusher.

Keywords: Photogrammetry · Industrial facility · 3D reconstruction · Reverse engineering · Project engineering

1 Introduction

One of the main problems that arise when carrying out any type of action in an industrial installation, such as a chemical plant, an assembly line or any other type of existing installation that usually has a certain age, is the lack of technical documentation that spatially defines the installation. This is due to reasons such as the loss of the documentation or the implementation of successive modifications and extensions of the installation through different projects. That is why, usually, when considering any new expansion or modification of the installation, it is mandatory to know the spatial arrangement of the elements of the existing installation.

This aspect is especially important in some types of facilities such as chemical and petrochemical plants where there is a complex network of pipes and ducts, or in the

F. Cavas-Martínez et al. (Eds.): *Advances on Mechanics, Design Engineering and Manufacturing II*, LNME, pp. 225–234, 2019.
https://doi.org/10.1007/978-3-030-12346-8_22

assembly lines of a company where there is a large number of elements such as conveyor belts, rails, etc. In these cases, the arrangement of these elements is not a flat layout, but a three-dimensional arrangement. Therefore, to integrate new elements in the installation, it is necessary to know the three-dimensional location of existing elements. Finally, with this information, it is possible to generate a 3D model to work within to integrate the elements of the new installation.

Currently, to generate the 3D model of an existing installation, as Rashidi [1] indicates, there are some diverse tools that can be complementary to each other that can be used, such as measuring tapes, total stations, ultrasonic measuring devices, laser scanners and other technologies based on the use of images such as for photogrammetry. It should be pointed out that, currently, most of the reconstructions continue to be carried out by measuring tapes and topographic stations, which entails a high temporal cost and a high level of risk during the execution of the measurements. However, it is increasingly common to use new tools such as scanners, mainly those based on Light Detection and Ranging technology (LiDAR), as Qin [2] indicates, or photogrammetry, as can be seen in the work of Abily [3].

Regarding the use of LiDAR technology within the industrial sphere, it is important to mention the work of Cabaleiro [4], applied to the digitization of a 3D structure using these tools, and the work of Conde-Carnero [5], applied to a bridge. In both works it is possible to appreciate the advantages of the application of LiDAR technology, such as speed, danger reduction and the amount of points obtained. However, there are also several problems in the use of these techniques, such as the propagation of errors due to the change of scanner location and the errors due to reflection of the signal or the diameter of the laser that make this technology especially sensitive to atmospheric conditions, to the angle of incidence of the laser and to the level of reflectivity of the materials, as also indicated by García-Gómez [6]. Additionally, the high cost of this type of device may be prohibitive for some applications.

However, the use of photogrammetry can partially solve some of the limitations presented by LiDAR technology, as it only requires an adequate camera and the adequate software, which makes it more economical. Additionally, photogrammetry is not affected by the change in position of the device, although it remains sensitive to the level of reflectivity of the materials and the angle of incidence. It should be noted that, in the case of photogrammetry, the time of work in the field is much less due to the time necessary to perform a scan in comparison with the time needed to take a photograph as well as the time necessary to change the location of the scanner and the geolocation of the scanners in each position. That is why photogrammetry is a tool as attractive as LiDAR technology, as Gasparovic [7] indicates.

After a study of the state-of-the-art referred to the generation of 3D reconstructions based on photogrammetry, there are several related works such as that of Garcia-Leon [8] about open pit mines, the work of Rice [9] about a cement plant or the work of Hou [10] about a petrochemical plant where LiDAR scanner and photogrammetry technologies have been used; in addition, the use of drones for the generation of aerial or in-height photographs was necessary.

Since the point of view of the photogrammetry, the development of digital photography has led to a considerable reduction in the cost of the cameras necessary for photogrammetric reconstruction and an increase in the performance of these cameras.

That is why, nowadays, it may be possible to carry out a photogrammetric reconstruction using a smartphone camera.

Therefore, the objective of this article is to discuss the development of a methodology for the realization of photogrammetric reconstructions in an industrial field, contemplating diverse procedures, types of cameras and lenses. To carry out the 3D reconstruction, Agisoft PhotoScan software, as well as various cameras and methods, have been used, which are discussed below.

Agisoft PhotoScan is specific software that performs photogrammetric processing of digital images enforced with computer vision methods and generates 3D spatial data. So, it can be used in GIS applications, cultural heritage documentation, and visual effects production as well as for 3D reconstruction and indirect measurements of objects of various scales.

Throughout various case studies PhotoScan proves to produce quality and accurate results and has some interest aspects that make it perfect for this purpose like the possibility of the use of markers, the compensation of the fish eye lens, etc.

2 Materials and Methods

2.1 Study of the Influence of the Type of Camera and Lenses

In order to carry out a comparative study of the influence of the camera and the lenses used in a practical way, three different cameras with very different characteristics have been selected, including an action camera like a GoPro, a SLR camera and a high-end mobile camera. The data of the cameras used are presented in Table 1.

Table 1. Main characteristics of the studied photo cameras

Camera	BQ Acuaris 4.5	GoPro silver 4	Nikon D330
Type	Smartphone	Action camera	SLR
Type of lens	Normal	Fish eye	Normal
Sensor dimensions (mm)	4.54 × 3.42	5.37 × 4.33	23.5 × 15.6
Lens opening (f)	2	2.8	3.5 a 5.6
Resolution (MPx)	13	12	24.2 (Used: 13)
Focal length (mm)	3.2	17.2 a 34.4	15.6 a 23.5

The cameras have been selected depending on the type of lens (normal or fish-eye), excluding panoramic types. Based on the recommendations of Kedzierski [11] and Li [12], the use of fish-eye cameras is discouraged due to the high distortion generated by the lens; although, it should be noted that the main photogrammetry programs are able to correct this distortion. The main reasons for selecting the fish-eye camera are its versatility and functionality, its light weight, the large number of accessories it can include (watertight housings, remote shutters, poles, etc.) and the high lens angle, which is practically 180°. The mobile camera has been selected for its versatility, low weight and availability. The SLR camera has been selected as the optimal reference camera and is recommended for the realization of photogrammetric reconstructions.

It should be noted that main photogrammetry programs [13], suggest that photographs should be taken without flash, with the maximum possible resolution of each camera and with the maximum focal length. In this article to try to reduce the influence of the resolution of the camera, in the case of the SLR one it has been used a resolution of 13 MPx, similar to the other cameras.

On the other hand, as regards to the error committed in a photogrammetric reconstruction, as Dai [14] indicates, this depends on the overlap of the photos, the camera itself and the position and angle of the captures. It is usually assumed that this error is between 1 and 4 times the ground sample distance (*GSD*), depending on the overlap, the number of photos, etc. The *GSD* is defined as:

$$GSD = \frac{D_w}{R_w} = \frac{H \cdot S_w}{F_r \cdot R_w} = H \cdot F \tag{1}$$

where D_w is the distance covered by the photograph, R_w is the horizontal resolution of the sensor in pixels, S_w is the width of the camera sensor, H is the maximum distance from the camera to the object/room and F_r is focal length.

Table 2 shows the data of the used cameras and the objectives. As shown, the F factor, which allows comparing cameras, is much lower in the Nikon D330 camera, mainly due to its objective. Therefore, this camera will present the smallest error in the case of taking an image at the same distance.

Table 2. Main parameters of the cameras to determine the error

Camera	Sw (mm)	Fr (mm)	Rw (pixels)	F
Nikon D330	23.5	200	2951 (used 1585)	7.413 E−05
GoPro silver 4	5.37	17.2	1475	0.00021167
BQ Acuaris 4.5	4.54	25	1600	0.0001135

It must be pointed that the reconstruction may depend of the algorithm and of process to take initial pictures so, to avoid this factor, in each reconstruction, for each camera it has been taken the same number of photos and in the same location and orientation using tripod (same height, angle and orientation) and changing in each location the camera.

2.2 Selected Locations

Some different facilities have been selected for the photogrammetric reconstruction: a manufacturing workshop that includes lathes and mills; a small fluid installation that includes tanks, pipes, etc.; a computer room; a warehouse that includes a plastic crusher; a mechanical assembly hall; and an electrical assembly hall. These facilities are quite different due to the aim of the methodology to use various industrial areas, so they include various types of elements such as large machines, pipes and tanks, machine tools and work stations. Figure 1 shows some of the analysed installations. It should be noted that, due to availability, locations smaller than 200 m^2 have been selected, although the methodology used could be applied to larger facilities, generating partial reconstructions by zones in chucks and uniting them using photogrammetry techniques.

Fig. 1. From left to the right: computer room, fluid installation and manufacturing workshop

2.3 Methods to Take the Photos

After conducting a study of the state-of-the-art ways of capturing images, there are hardly any articles related to the methodology to be used in large indoor spaces such as those studied. It should be noted, too, that there are some studies about working outdoors, such as Klein [15] capturing large structures such as bridges, while other authors such as Armesto [16] indicate the methodology to be used in the case of facades and building exteriors. There are a few references about the methodology that can be used for capturing images in large enclosed spaces; one of them is the work of Roh [17], using an object-based approach, and another is the work of Lee [18] for the digitization of fluid installations. It should also be pointed out that the importance of videogrammetry as a future work method, as Brilakis [19] indicates, is not sufficient for the proposed work.

For a good photogrammetry reconstruction, there are some critical aspects to consider. On the one hand, a large overlap between images that common points to align between them, on the other hand some images at a suitable distance so that an admissible error is achieved and finally, a number of suitable images. It should be noted that, in the case of working with a high number of images, a high computational cost is expected because the computer has to compare the different images and then align them by comparing all the pixels of the photos. To avoid this computational cost, it is advisable to generate photos sequentially and to align these photos only by comparing the nearby photos; this reduces the computational cost considerably. To reduce the computational cost, it is also essential to reach a balance between quantity of photos and precision and detail obtained.

For the generation of the photographs, the parallel key method (see Fig. 2) was initially used. This method allows the maximum space available between the camera focus and the area of the environment to be photographed, as one of the main problems is the lack of distance that allows a correct visualization of the area to be photographed. This is a quite common method for the realization of indoor reconstructions, especially for rooms.

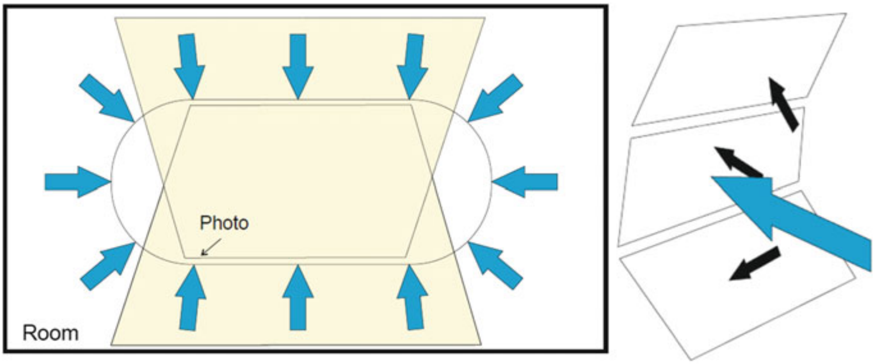

Fig. 2. Left: parallel key method, layout of the capture points of the photographs. Right: triple parallel key method

Based on the keyway method results, this method in areas with a high ceiling height, as in the case of industrial installations, presents serious problems because, due to the lack of an angular opening, especially in the case of the BQ 4.5 camera, the camera is unable to capture the entire height of the industrial warehouse through a single photograph. For this reason, an innovative methodology called ‘triple parallel key’ was developed in which, at each point where a photograph was previously taken, three photographs with different angles were taken (see Fig. 2). So, the operator, from the ground and without the need to subject himself to height hazards, is able to cover the entire height of the industrial building. It should be noted that this method has several disadvantages because when using different photos from the same location, it is difficult to align the vectors of the various photos because the trigger point is in the same position.

Finally, a new methodology was developed, denominated in cross (see Fig. 3) to allow a greater alignment of the photos with each other through the correct crossing of the different photos with an angle between them of 90° and 45° with respect to the walls. This methodology was developed mainly for the digitization of specific lateral zones of an installation instead of a complete installation. It should be noted that, through this methodology, the depth dimension was perfectly cached. It must also be noted that a series of markers was used for the measurement and verification of the error and for the alignment of the photos with each other.

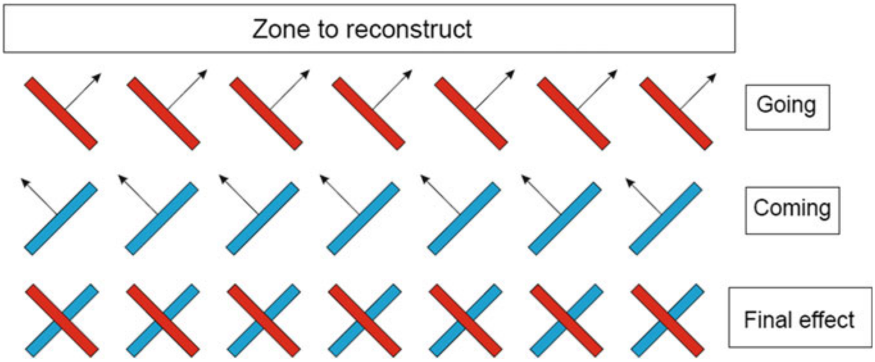

Fig. 3. Methodology in cross for the reconstruction of lateral zones

3 Results and Discussions

After analysing the results obtained with the different cameras, with equal number of photos and the same method of generation, it has been concluded that, even for small spaces, the three analysed cameras are capable of generating adequate reconstructions. In the case of large environments, only the SLR camera allows adequate models to be obtained (see Fig. 4). However, the GoPro camera due to it fish eye lens has not allowed any suitable reconstruction, so its use is discouraged. Another aspect that is important is the camera definition because a higher definition implies a higher number of points in the dense cloud model and a lower error.

Regarding the errors, these were obtained by studying the different installations by means of distance between different points contrasted with those obtained by means of measuring tapes and various manual tools. Figure 5 shows the reconstruction generated for the plastic crusher in which the high quality of the reconstruction can be appreciated. Table 3 shows, for example, the error in the reconstruction of the fluid installation.

Based on the error analysis, it is possible to calculate that for the camera indicated in Table 3 and according to the characteristics of the camera, the error for a shooting distance of 20 m should be between 7 and 21 mm (3–5 times GRD using Eq. 1), but, as shown in Table 3, this error is higher than the previously estimated.

Regarding the various options of alignment, point cloud union, mesh generation, etc., PhotoScan itself allows different qualities (low, medium, high, very high, etc.). By performing a comparative analysis, the obtained results show that there are hardly any variations in the result with the average or superior qualities, while the use of medium and low qualities is undesirable.

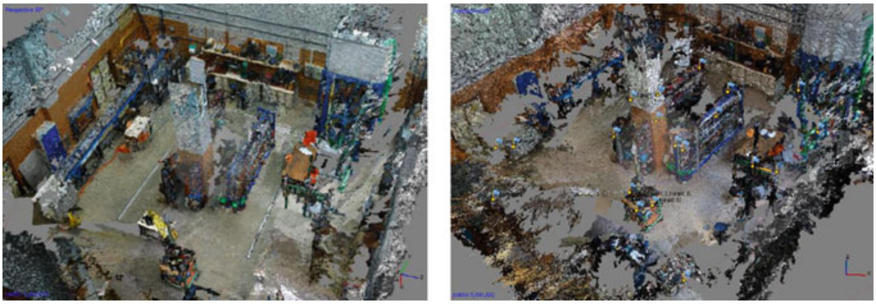

Fig. 4. 3D reconstruction of fluids installation with SLR camera (left) and smartphone BQ 4.5 (right)

Fig. 5. From left to the right: plastic crusher photo with markers, dense cloud points and final 3D model using the SLR camera

Table 3. Study of the error with the GoPro camera (H ≈ 20)

Measuring	Real measurement (mm)	3D model measurement (mm)	Error (mm)	Error (%)
1	3040	3318	−78	2.35
2	2390	2361	29	−1.23
3	1820	1793	27	−1.51
4	1590	1600	−10	0.62
5	1460	1451	9	−0.62
6	1490	1513	−23	1.52
7	860	860	0	0.00
8	925	913	12	−1.31
9	3025	3008	17	−0.57
Total Error			31.2	

Analyzing Fig. 5, it can be seen that the 3D model is not highly accuracy at the top of the machine due to the fact that the photographs are taken from the ground. The final 3D model is not good enough because it has been obtained using the automatic 3D model reconstruction of the PhotoScan but the most suitable method will be manual using other programs like Rhinoceros or 3D magic. With these programs it is possible to obtain a parametric 3D model of the facility that can be integrated in another 3D model with a higher accuracy because it is possible to select the points to use of the dense cloud and to obtain accuracy models and surfaces.

4 Conclusions

The main conclusions obtained from the study are that it is possible to carry out a 3D reconstruction in the industrial environment with any type of camera with the exception of fish-eye cameras that generate enormous distortion. Although the reconstructions generated with the SLR camera are of higher quality and less error, with the same number of photos and the same methodology; the improvement is mainly due to the focal length and the type of lens. It should be noted at this point that, due to functionality, the SLR camera is more appropriate because the focal length and the focus can be optimized.

In relation to the methodologies to be used, it must be indicated that, although an increase in the number of photos generates greater precision and a greater number of points, this aspect is not the most determining factor to increase the quality of the reconstruction; the position and the angle of the shot have greater importance and demonstrate that the parallel key method for applications in general, the triple parallel key method for high spaces and the method in cross for concrete areas (such as a wall or a lateral space) are decisive for a correct reconstruction. The option of including markers in the measurements has been assessed as very positive because their presence allows the division of the photographed set into several digitalisations that can be joined automatically and also allows errors made during digitalisation to be verified.

Finally, the potential use of this method is the possibility to obtain easily and without risks, the 3D model of any existent industrial facility and so, it can be integrated in a expansion project or to verify the dimensions of a location where a new machine must be installed.

References

1. Rashidi A, Maghiar M, Sigari MH (2017) Capturing geometry for labelling and mapping built infrastructure: an overview of technologies. Iran J Sci Technol-Trans Civ Eng 2 (4):415–428
2. Qin R, Tian J, Reinartz P (2016) 3D change detection—approaches and applications. ISPRS J Photogram Remote Sens 122:41–56
3. Abily M, Goulbesville P, Andres L, Duluc CM (2013) Photogrammetric and LiDAR data for high resolution runoff modeling over industrial and urban sites. In: Proceedings of the 35th IAHR World Congress. 2
4. Cabaleiro M, Riveiro B, Caamano JC, Arias P (2016) Non-destructive techniques for the evaluation of structures and infrastructure. Struct Infrastruct Ser 11:303–316
5. Conde-Carnero B, Riveiro B, Arias P, Caamaño JC (2015) Exploitation of geometric data provided by laser scanning to create FEM structural models of bridges. J Perform Constr Facil 30(3)

6. Garcia-Gomez I, Fernandez M, Mesanza A (2011) Laser scanner and point cloud. a horizon applied to the archaeological analysis of buildings. Arqueol Arquit 8:25–44
7. Gasparovic M, Seletkovic A, Berta A, Balenovic I (2017) The evaluation of photogrammetry-based DSM from low-cost UAV by LiDAR-based DSM. Seefor-South-East Eur For 8(2):117–125
8. Garcia-Leon J, Martin AG, Picazo MT, Fernandez J (2017) 3D recording and modelling of mining heritage: the Monserrat Mine, Sierra Minera of Cartagena-La Union, Southeast of Spain. In: Aguilera D, Georgopoulos A, Kersten T, Remondino F, Stathopoulou E (eds) 3D virtual reconstruction and visualization of complex architectures. International Archives of the Photogrammetry Remote Sensing and Spatial Information Sciences, 42(2), pp 325–330
9. Rice AB (2016) Drone technology as applied to the cement industry. In: 2016 IEEE-IAS/PCA Cement Industry Technical Conference. IEEE Ind Applicat Soc; Portland Cement Assoc, Grapevine, pp 13–20
10. Hou L, Wang Y, Wang XY, Maynard N, Cameron IT, Zhang SH, Jiao Y (2014) Combining photogrammetry and augmented reality towards an integrated facility management system for the oil industry. Proc IEEE 102(2):204–220
11. Kedzierski M, Fryskowska A (2009) Application of digital camera with fisheye lens in close range photogrammetry. In: ASPRS 2009 Annual Conference. ASPRS, Maryland
12. Li Z, Chen J, Baltsavias E (2008) Advances in photogrammetry, remote sensing and spatial information sciences: 2008 ISPRS congress book, 1st edn. CRC Press
13. Agisoft PhotoScan User Manual. Professional Edition, Version 1.2
14. Dai F, Feng Y, Hough R (2014) Photogrammetric error sources and impacts on modelling and surveying in construction engineering applications. Vis Eng 2(2):1–14
15. Klein L, Li N, Becerik-Gerber B (2012) Imaged-based verification of as-built documentation of operational buildings. Autom Constr 21:161–171
16. Armesto J, Lubowieckab I, Ordóñeza C, Riala F (2009) FEM modelling of structures based on close range digital photogrammetry. Autom Constr 18(5):559–569
17. Roh S, Aziz Z, Peña-Mora F (2011) An object-based 3D walk-through model for interior construction progress monitoring. Autom Constr 20(1):66–75
18. Lee Y, Son H, Kim C, Kim C (2013) Skeleton-based 3D reconstruction of as-built pipelines from laser-scan data. Autom Constr 35:199–207
19. Brilakis I, Fathi H, Rashidi A (2011) Progressive 3D reconstruction of infrastructure with videogrammetry. Autom Constr 20(7):884–895

Visual Impact Assessment for Offshore Wind Farms Along the Cantabrian Coast

J. López-Uriarte(✉), P. E. Lizcano, C. Manchado,
V. Gómez-Jáuregui, and C. Otero

EGICAD, School of Civil Engineering, Universitiy of Cantabria, Avda. Los Castros s/n, 39005 Santander, Spain
lopezuj@unican.es

Abstract. This paper shows an introduction to a new proposal in the use of quantitative indicators for visual impact assessment over large areas. Implemented in a new software called MarRojo©. It is part of a project named AMBEMAR, which objective is to create a Multi Criteria Decision Support System (DSS) tool to find the optimal siting for offshore wind farms on the Cantabrian coast. The work consists in generating graphical information that allows introducing visual impact criteria in the design stage, and inside AMBEMAR and is essentially oriented to wind energy projects.

Keywords: VIA · GIS · Seascape

1 Introduction

Visual Impact Assessment (VIA) is the analysis of the landscape or seascape changes produced by the construction of a new infrastructure and the resultant effects on visual amenity and people's responses to changes [1]. The measurement of these effects have a high importance because of social and environmental aspects [2]. Typically, the evaluation of these visual effects is carried out for a particular wind farm in a fixed position. When the effects on multiple positions over a large study area have to be measured, the computational time suffers an increment associated to the number of locations to be calculated.

There are other techniques applied to large areas. Usually, they are based on the calculation of the Cumulative Viewshed or Total Viewshed. A Cumulative Viewshed is the result of the viewsheds addition for selected of points, while a Total Viewshed is the result of the viewshed addition for every point in the study area. They have been long used in GIS visibility studies and represented in 2D and 3D [3]. Nowadays, Cumulative Viewshed indicator is widely used [4, 5]. The viewsheds are continuous spatial representation of visibility that indicates whether a viewpoint on a surface can be seen from a particular observer position [6].

F. Cavas-Martínez et al. (Eds.): *Advances on Mechanics, Design Engineering and Manufacturing II*, LNME, pp. 235–241, 2019.
https://doi.org/10.1007/978-3-030-12346-8_23

In our case, instead of calculating the viewsheds for a set of points inland, they are calculated for multiple points of views located on the sea. It allows characterizing directly the impact of a specific sea location. In this approach, it is not needed to consider other viewsheds, which also optimize the required computational time of calculation.

The result is graphically represented with maps, and calculated with a new software tool called MarRojo. In this work, the results concern the Cantabrian coast (Bay of Biscay, North of Spain) because of project requirements.

2 Study Area

The Cantabrian Coast has a seashore with good wind sea conditions. Besides, there are large available zones for locating wind farms, which makes Cantabria a potentially good place for locating offshore wind farms [7].

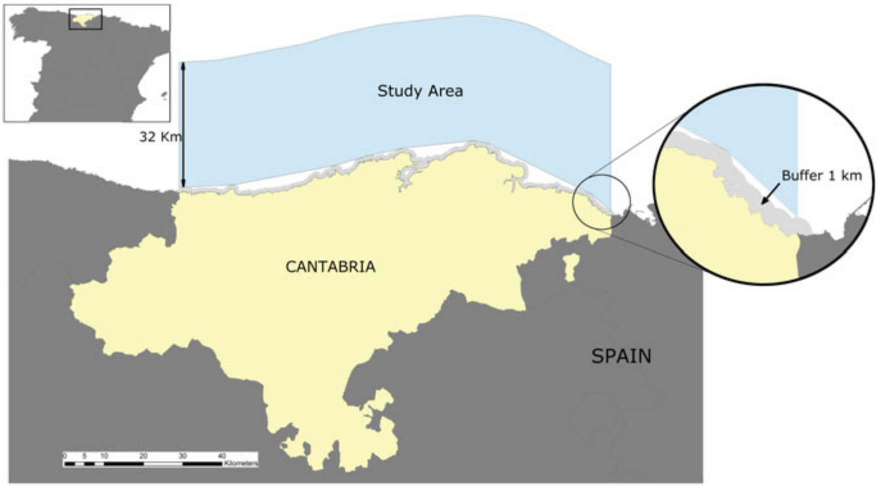

Fig. 1. Study area, represented in blue color

The study area, shown in Fig. 1, has been defined following the next steps: first, one kilometer buffer around shoreline is made; second, this line is manually simplified using the tangent segments between its points placed more to the North; third, a buffer of 32 km up to this line is calculated.

The regulatory framework in the region (PLENERCAN [8, 9]) indicates that a wind farm placed at a distance higher than 30 km has very low visual effects. In this case, the considered affection area for a 200 m high turbine is limited to 35 km. This is based on supplementary considerations taken from the Sottish National Heritage Guide [10], and studies of Manchado et al. [11] and Bishop and Shang [12].

The visual inventory is composed of all elements with information about the landscape, population, culture, planning, land uses, etc. as well as any relevant information for stakeholders.

3 Methodology

Any visibility or VIA index measures quantitatively visual effects over some (or all) elements of the visual inventory. There are diverse kind of indices. Some of them are presented in this paper, such as the land surface area with visibility of a wind turbine, the kilometers of visually affected roads, the area of visually affected nuclei population, the population visually affected, or the magnitude of visual effect (MVE) [13]. MVE is an index obtained by the simple product of population, area of nuclei, and kilometers of roads affected. Other indices, like the ones belonging to the Spanish Method [11], are used in AMBEMAR, but their full description is out of scope of this article.

The calculation of the visual effects requires the use of GIS and computational techniques that allows carrying out all the processes in acceptable time. The following sections describe the necessary steps to take.

Step 1: Viewsheds

The study area is discretized in cells composing a raster model. Each of them in the area defines a possible placement for a wind tower (WT). Consequently, each cell is a potential target point and a viewshed must be calculated for it. Calculation accuracy depends directly on the resolution selected. The higher the resolution considered, the more cells exist and the more accurate is the final output.

Viewsheds must be calculated under the same DTM. In this case, a 25 m resolution has been used. According to this, it is necessary to define a common basis for the raster grid where the pixels of diverse viewsheds can be associated among them, avoiding gaps and overlapping.

Step 2: Visual Inventory

The visual inventory needs to be discretized with the same resolution of the viewshed and its raster grid. This work is carried out for each element of the visual inventory individually.

Step 3: Index Calculation

For each cell of the study area, an index value is calculated. The viewshed for each cell has to be treated with the different elements of the visual inventory. One pixel of an element is considered with visual affection, if this pixel simultaneously has visibility and belongs to the element of visual inventory analyzed. The treatment of this data depends on the nature of the index that is being calculated.

Step 4: Visual Impact Results

All impact values for an index and an element of the visual inventory are sorted and stored in raster format, which makes up the output map.

The step 1 is fulfilled with the software Moyses® [14], and the steps 2, 3 and 4 are carried out by the software MarRojo®. Both of them, Moyses® and MarRojo®, use parallelization techniques in all the steps; this is essential when working at a regional scale. In this order, the use of sequential programming would imply a lot of computing time. For this reason, the use of threading techniques allows dividing the task among the computer cores, decreasing and optimizing the calculation time.

4 Results and Discussion

In this section, some maps with VIA results for the Cantabrian coast are shown. These maps have a cell resolution of 25 m. All the maps are presented with the same color scale: the red color means the highest value of the impact, whereas the blue one means that there is null or no relevant impact.

The chosen resolution has been taken to optimize the computational time needed. For example, time calculation for cell size of 5 m is 25 times greater than 25 m cell (assuming the relation between an increment in data size and time calculation is linear).

Figure 2 shows the visual effects for affected population. Each color represents the amount of people visually affected. The meaning is that the value in a pixel represents the visual effect for a particular VIA index, extended to the whole land territory. Thus, a pixel showing a blue color means that if a WT were placed in this position it would elicit a null or almost null visual effect. Conversely, a red pixel means that a WT placed there would involve a serious damage from a visual impact point of view.

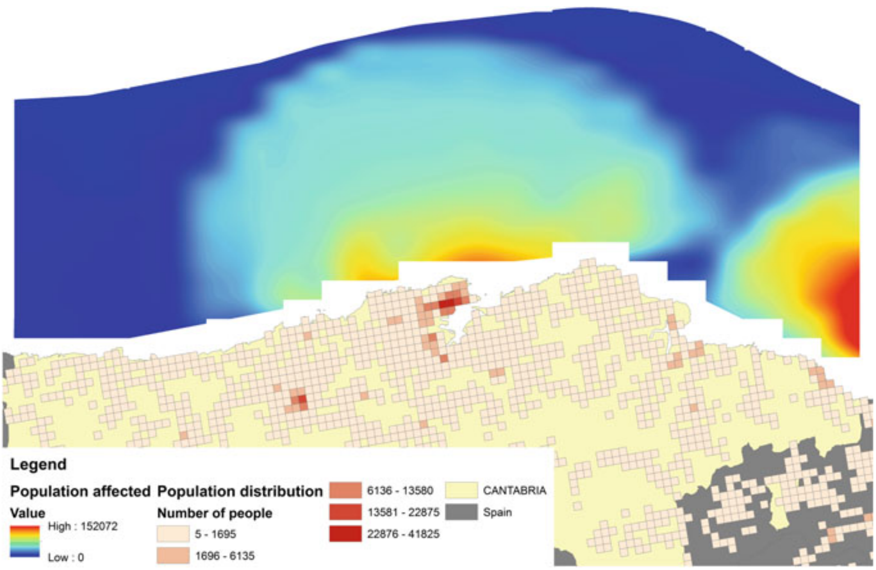

Fig. 2. Affected population in a typical 2D GIS view

In Fig. 3, the same output map is shown as 3D view from a South-West camera point. The zeta elevation represents the value of the VIA index, in the same terms indicated in the paragraph above. It is clear that the zones with the highest impact are around Santander and Bilbao, the most populated cities in the area. Conversely, the West of Cantabria holds extensive rural areas where much less population lives.

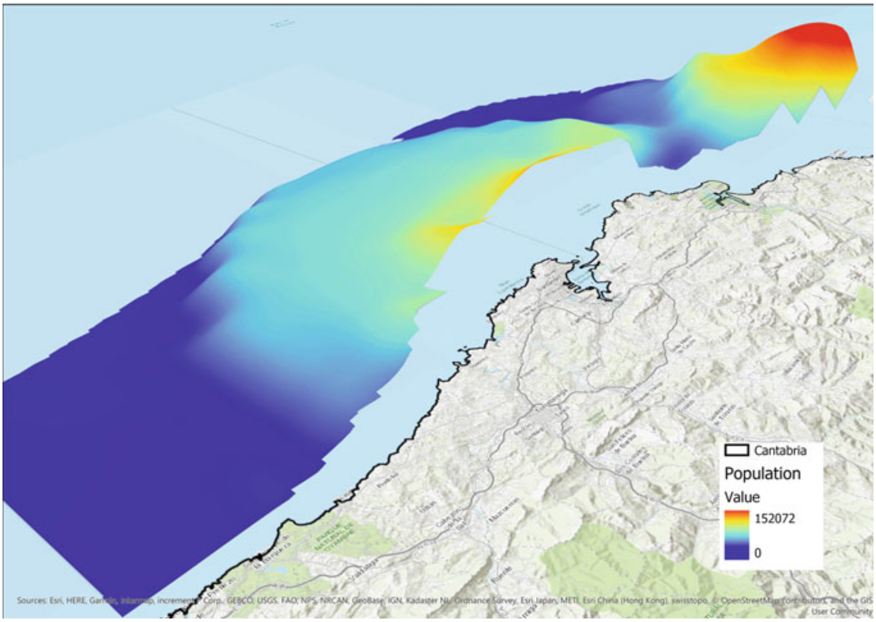

Fig. 3. Affected population in South-West perspective

Figure 4 shows four different outputs associated to other VIA indicators. Figure 4a represents the product of the maps in Figs. 2 and 4b, d, which defines the MVE (composed of area of nuclei, length of roads and population affected) index. Figure 4b represents the visually affected roads in the area of study; Fig. 4c represents the land area with visibility, and Fig. 4d shows the area of visually affected population nuclei.

In Fig. 4a, b and d, the worst areas are around Bilbao and Santander because of the distribution of roads, nuclei population and population. However, Fig. 4c represents a high impact near to Asturias. In the West, the typical landform near to coastline are less mountainous than in the East, where highland landform prevails. It means that visibility increases in these zones since there are more plain zones near to shoreline.

As expected, in all these maps, the minimum values are always far from the coast, while the maximum values are near to the coast. However, there are some areas where the indices show an inversion of this trend, as happens in the coast near to Bilbao. In this case, the visibility of the turbines is lower than in other points further than the seacoast due to the topography of the land near to the shoreline.

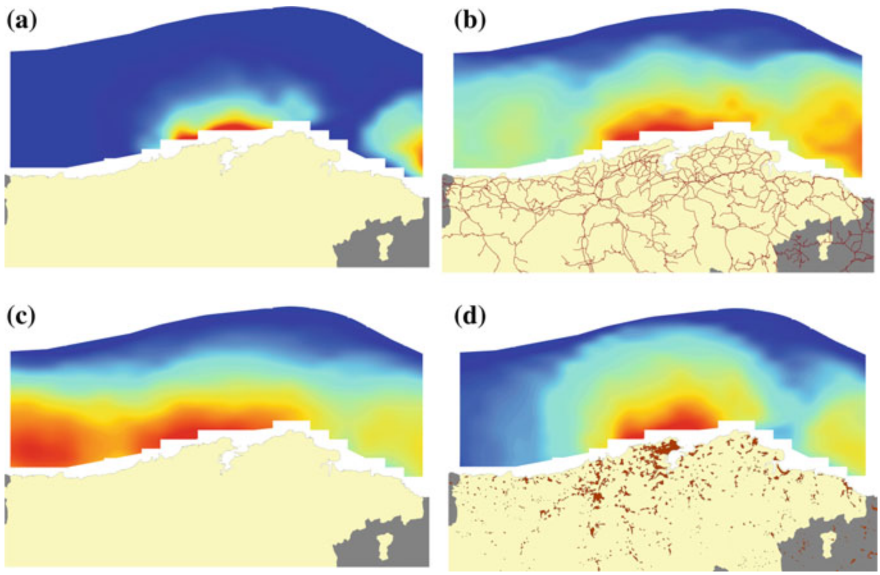

Fig. 4. VIMs for different indices. **a** Magnitude of Visual Effect (MVE). **b** Road Longitude affected. **c** Land surface affected. **d** Area of affected population nuclei

According to these maps (and these indicators), sea zones near to Bilbao and Santander are not suitable to locate a wind farm. This reasoning is carried out only with nuclei, roads and population, but there are other elements in the visual inventory with high landscape values that could give different results.

5 Conclusions

The shown methodology gives rise to a new way to introduce visual impact criteria as a design factor, allowing directly characterizing visual effects according to a specific indicator along the whole study area. Indeed, it is possible for designers (or planners) to query the map and immediately to know its impact value immediately instead of calculating the value each time wind farm position is changed. It reduces a lot the time needed for choosing the location that minimize the visual impacts. The methodology that has been proposed in this paper is applicable to a local or regional scale.

With the method described in this paper, the execution requires excessive time. For this reason, it is currently being improved with the use of interpolation techniques, by calculating indices in some selected pixels, and generating the rest of them by interpolation. Results will be compared with real values obtained with the above methodology.

Acknowledgements. The research work reported here was made possible thanks to the support/funding of the Regional Government of Cantabria. Project AMBEMAR with reference RM16-XX-045—SODERCAN/FEDER.

References

1. Siting and Designing wind farms in the landscape. https://www.nature.scot/siting-and-designing-wind-farms-landscape-version-3a. Last accessed 22 Feb 2018
2. Nadaï A, Labussière O (2009) Wind power planning in France (Aveyron), from state regulation to local planning. Land Use Policy 26:744–754. https://doi.org/10.1016/j.landusepol.2008.10.018
3. Llobera M (2003) Extending GIS-based visual analysis: the concept of visualscapes. Int J Geogr Inf Sci 17:25–48. https://doi.org/10.1080/713811741
4. Depellegrin D (2016) Assesing cumulative visual impacts in coastal areas of the Baltic Sea. Ocean Coast Manag 119:184–198. https://doi.org/10.1016/j.ocecoaman.2015.10.012
5. Griffin R, Chaumont N, Denu D, Guerry A, Kim C, Ruckelshaus M (2015) Incorporating the visibility of coastal energy infrastructure into multi-criteria siting decisions. Mar Policy 62:218–223
6. Möller B (2006) Changing wind-power landscapes: regional assessment of visual impact on land use and population in Northern Jutland, Denmark. Appl Energy 86:477–494. https://doi.org/10.1016/j.apenergy.2005.04.004
7. Análisis del recurso. Atlas eólico de España. http://www.idae.es/publicaciones/analisis-del-recurso-atlas-eolico-de-espana. Last accessed 22 Feb 2018
8. Plan de Sostenibilidad Energética de Cantabria 2014–2020. http://www.dgicc.cantabria.es/documentos/psec-2014-2020/PSEC-2014-2020.pdf. Last accessed 22 Feb 2018
9. Directrices técnicas y ambientales para la regulación del desarrollo de los parques eólicos derivados del plan. http://www.dgicc.cantabria.es/documentos/psec-2014-2020/Directrices-PSEC-2014-2020.pdf. Last accessed 22 Feb 2018
10. Assessing the cumulative impact of onshore wind energy developments. https://www.nature.scot/assessing-cumulative-impact-onshore-wind-energy-developments. Last accessed 22 Feb 2018
11. Manchado C, Gomez-Jauregui V, Otero C (2015) A review on the Spanish Method of visual impact assessment of wind farms: SPM2. Renew Sustain Energy Rev 49:756–767. https://doi.org/10.1016/j.rser.2015.04.067
12. Bishop ID, Shang H (2000) Visual thresholds for detection, recognition and visual impact in landscape settings. J Environ Psychol 20:125–140. https://doi.org/10.1006/jevp.1999.0153
13. Otero C, Manchado C, Gomez-Jauregui V et al (2012) Wind energy development in Cantabria, Spain. Methodological approach, environmental, technological and social issues. Renew Energy 40:137–149 (2012). https://doi.org/10.1016/j.renene.2011.09.008
14. Manchado C, Otero C, Gomez-Jauregui V et al (2013) Visibility analysis and visibility software for the optimization of wind farm design. Renew Energy 60:388–401. https://doi.org/10.1016/j.renene.2013.05.026

Graphic Survey and 3D Virtual Restoration of a 16th Century Watch Tower: Navidad Tower (Cartagena, Spain)

J. García-León(✉), J. Ros-Torres, G. Vázquez Arenas, P. E. Collado Espejo, J. Pérez Navarro, and M. Ramos Martínez

Universidad Politécnica de Cartagena, Paseo Alfonso XIII, nº50, 30203 Cartagena, Spain
josefina.leon@upct.es

Abstract. In 1557, King Philip II started a project consisting in the creation of a network of watch and defence towers for the coast, which would be used to warn neighbouring towns of the frequent pirate attacks. After having examined the area and having planned the number and location of such towers, a great number of these defensive buildings were constructed all along the Mediterranean coastline. Unfortunately, this important historical and architectural heritage of the Mediterranean coastline has lost one of its main characteristics, unity, since many of these towers have disappeared and some of them are neglected. In the Region of Murcia, from the twelve coast towers that were built for watch and defence purposes, eight towers have disappeared. Three towers have been recently restored. From the old watch towers there is only one left, which is almost ruined, and no intervention is planned to guarantee its proper preservation and enhancement: Navidad Tower. That is why this tower has been chosen to be studied and graphically documented. Thus, the research project that is being developed is mainly aimed at depicting the common legacy of all watch and defence towers in the Murcian coastline and documenting the Navidad by laser scanner and photogrammetry in order to obtain the three-dimensional model. This graphic work shall be subsequently supplemented with the carrying out of works for the dissemination of documentation. Likewise, an analysis of towers through the use of Geographic Information Systems.

Keywords: Geomatics engineering · Digital photogrammetry · Defence towers · Heritage restoration

1 Introduction

From 1568 to 1571, the Mediterranean had become a natural border between the Spanish and Turkish empires; so, the Andalusian, Murcian, Valencian and Majorcan coasts were the target of permanent attacks by Turkish-Berber pirates from northern Africa [1].

Against the countless pirate attacks from the Maghreb, in the late 1560s, the Crown had assigned to the Italian military engineer Giovanni Battista Antonelli an ambitious

F. Cavas-Martínez et al. (Eds.): *Advances on Mechanics, Design Engineering and Manufacturing II*, LNME, pp. 242–251, 2019.
https://doi.org/10.1007/978-3-030-12346-8_24

project to fortify and defend the whole Mediterranean coastline, which combined the construction of defence towers with urban fortification [2].

The key feature of this defence network was visibility and coordination between the various towers. Therefore, this network of watch and defence towers would include three types of buildings. The first type would be the coast watch towers, which were the first alert network against enemy attacks. The second type would be made up of fortress-towers, located inland but having visual contact with watch towers along the coast. The third type would be the inland towers, located far from the coast and used to warn and protect more important towns (farming and mining towns) that could also be attacked by North-African pirates [3, 4].

In order to fortify and defend the Murcian coastline, King Philip II entrusted the project to the Italian military engineer and expert in fortifications Vespasiano Gonzaga Colonna. Gonzaga requested the collaboration of Antonelli. Both of them travelled the whole Murcian coastline by land and by sea in order to design and improve the few existing defences. In August 1570, each one of them advised the Crown on how and where the watch and defence towers should be built on the Murcian coast.

Unfortunately, this important historical, architectural and cultural heritage of the Mediterranean coastline has lost one of its main characteristics: unity. Many of these towers have disappeared and some of them are neglected. In the Region of Murcia, from the twelve coast towers that were built for watch and defence purposes, eight towers have disappeared. As regards these towers, the space of three of them was used for the construction of lighthouses (El Estacio, Cabo de Palos or San Antonio and Portman) [5].

Three towers have been recently restored (La Azohía or Santa Elena, Los Caballos [6] and Cope or Santo Cristo). And, from the old watch towers there is only one left, which is almost ruined, and no intervention is planned to guarantee its proper preservation and enhancement: Navidad Tower in Cartagena.

This research is aimed at obtaining the documentation of the Navidad Tower, from the graphic, historical and building point of view, which can serve as a basis for a future restoration project of this tower. This shall be done by means of techniques, such as digital photogrammetry and laser scanning, that are sufficiently developed from the technological point of view and are used to carry out heritage 3D surveys [7–9]. Finally, this work includes the dissemination of documentation, since the awareness of heritage is the best way to appreciate and to preserve it.

2 Materials and Methods

2.1 Constructive Analysis. The Navidad Tower

In his report from August 1570, Vespasiano Gonzaga suggested the construction of these towers with stone blocks or masonry, not with rammed-earth walls, because these are less resistant to weather exposure, salty water or the attack with picks by pirates. Furthermore, he considered that the ground plan of towers had to be hexagonal and not square or round, as suggested by Antonelli. Likewise, the towers had to include, at least, a cistern, an oven, a warehouse for gunpowder and a chimney.

In order to determine how these towers had to be built, the «*Condiciones con que se pregonan y rematan las torres que se hazen en el reyno de Murcia*» were drafted in 1578. This document states that towers must be built with a mixture of lime, sand and concrete and with a hexagonal ground plan measuring fifty-three feet (14.84 m) in diameter, with a reduction of one foot of slope for every five feet, until reaching fifteen feet high, and from that point, they were vertically constructed (Fig. 1). Above the embankment, the wall had to be ten feet thick, 2.80 m approximately. One of the elevations would have the access door, at the height at which the embankment ended. On the right hand, when entering, there would be a spiral staircase leant on the wall, to have access to the first floor and the terraced roof. On the left, not on the stretch of wall opposite the door, but on the following one, there was a chimney. The vaults of both floors (ground and first floors) had to be built of solid brick or concrete slabs. The piece of artillery, the ammunition depot and the room for tower keepers were located on the upper floor. The six corners had to be reinforced with large and properly cut stones, in order to make the building more resistant. Inside, on the ground floor, there had to be an underground cistern to be self-sufficient in drinking water. The estimated time for the construction was three months, approximately. Therefore, the aim was to build large defence towers, visible from a certain distance, resistant and with capacity to house a crew of three guards and a chief, a medium-size piece of artillery, ammunition, weapons and enough provisions to face a siege. However, these towers were seldom equipped with the necessary artillery, weapons and ammunition [1, 10].

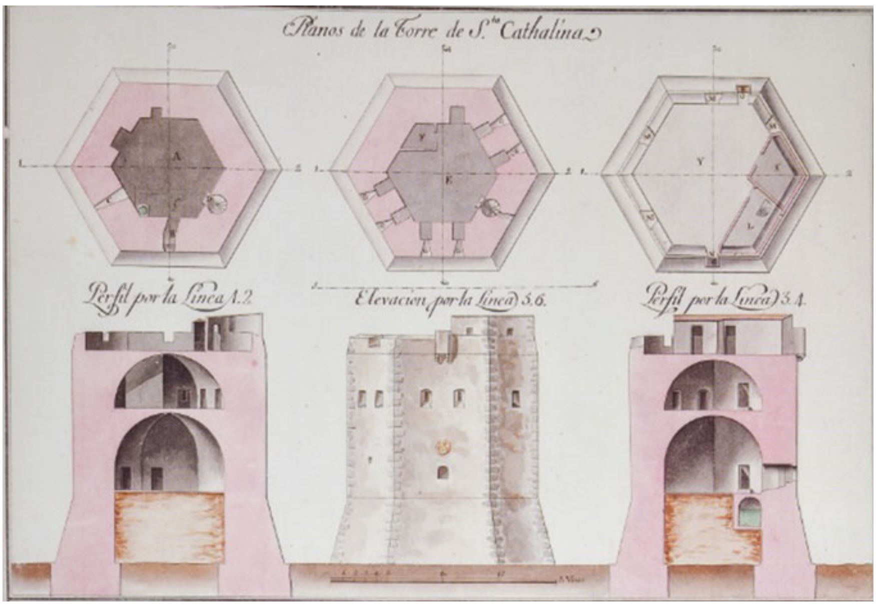

Fig. 1. Cross-section, ground and elevation plan of the Tower of Santa Catalina or Azohía. Copied by Manuel Martínez Nubla (1819) from the original by Juan José Ordovás (1779) [11]

The Navidad Tower was built according to the specifications given for a watch and defence tower on the Murcian coastline. It is located halfway up the hillside and its ground plan is hexagonal, with an internal diameter, between two opposite vertices, of approximately 13.00 m, and of 11.00 m between two of its opposite sides (Fig. 2). The wall thickness ranged from 2.50 to 3.00 m. Its wall stretches were built with masonry and its edges, window jambs and wall structure courses were built with solid brick-work. The same building criterion was applied to edges or corners resulting from the intersection of two sides of the hexagon. This building system was probably used due to the lack of good stonework or the lack of funding, in such a way that the rough stones were used to fill the wall stretches whose edges and corners were carefully defined by the solid brickwork.

Fig. 2. Current image of the Navidad Tower

Bearing in mind the drawings of the towers done in 1799 by the military engineer Juan José Ordovás (Fig. 3), the parts made of red brickwork were executed with facing bricks, with a quite regular and homogeneous layout of stones, as with the masonry area. Nevertheless, a more thorough inspection allows us to determine that, at least, the masonry wall stretches were originally coated with lime mortar, and the brickwork stretches would be probably exposed. Therefore, the tower would originally have a whitish look, where the red colour of bricks stood out at the corners and window jambs.

Nowadays, the state of preservation of the Navidad Tower is quite worrying, since it is abandoned and nearly ruined. Only the stumps of walls and the elevations are preserved up to the height of ground floor gaps (if it ever had two heights, since it apparently just had a ground floor and a terraced roof). The wet and salty environment, together with the wind, rain and cold weather have gradually eroded the solid bricks—especially, at the corners—and the fixing mortar. Nowadays, it is almost hidden behind the Navidad Fort, an impressive defence building constructed according to the Defence Plan of 1860, which has been recently restored. Likewise, it is worth mentioning the difficulty to reach the Tower entrance. This building is located on a highland and with a quite sheer relief. Its hill slopes make it difficult to construct a path allowing visitors to

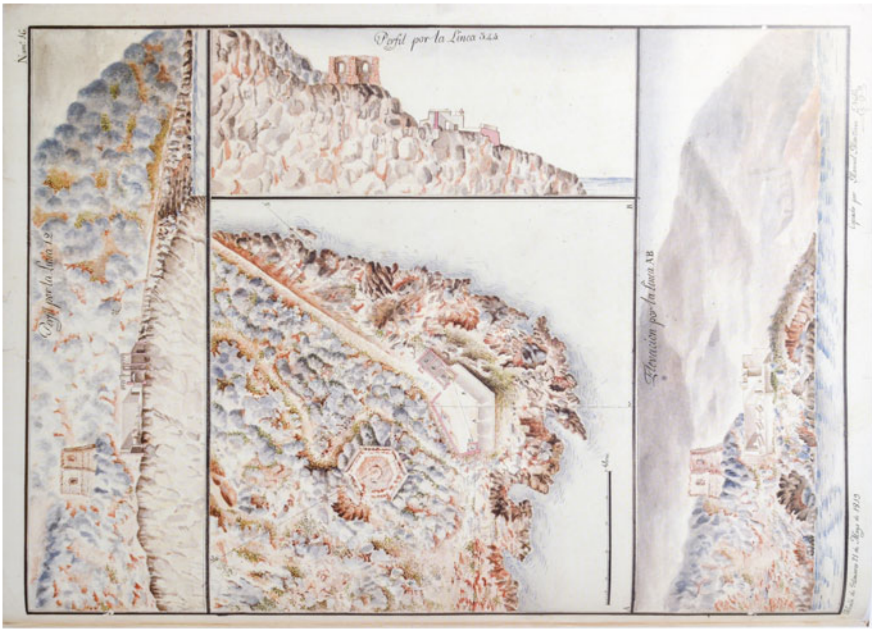

Fig. 3. Cross-section, ground and elevation plan of Navidad Tower and battery and its immediate surroundings. Copied by Manuel Martínez Nubla (1819) from the original by Juan José Ordovás (1779) [11]

have an easy access; consequently, the restoration project for this tower should recover the historical path, which is currently covered with brushwood and partially destroyed.

2.2 Methods Laser Scanner and Photogrammetry

For the graphic documentation of this tower, a field observation has been made with a total station, where a traverse has been observed and, subsequently, data have been collected at some of its vertices through laser scanning (MS50 multi-station) to obtain the point cloud for the tower, by linking this point cloud to classical topography. For the collection of data, a closed traverse has been carried out (Fig. 4a), observed and compensated, made up of 10 vertices surrounding the tower.

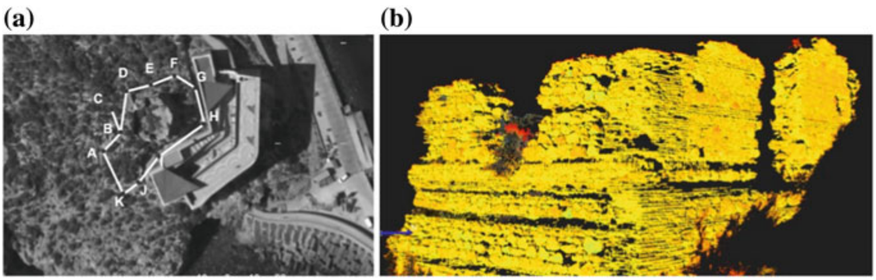

Fig. 4. **a** Ground plan showing all the vertices, from A to K, of the traverse. **b** Point cloud of the Navidad Tower obtained through laser scanning from two of the seven stations

The cloud of points taken in the field from seven stations (A, B, D, F, H, I and K), with a distance between points of 1 cm (Fig. 4), with a minimum and maximum distance, to put a limit to the measured points and establishing the observation window centered on the tower and there have been approximately half a million points of each station.

The point cloud has been dumped into the processing software Leica Infinity and subsequently debugged, by creating a triangle mesh with 3DReshaper. Gaps have been closed and each triangle has been properly placed in the mesh in order to obtain the final model, closed and complete (Fig. 5).

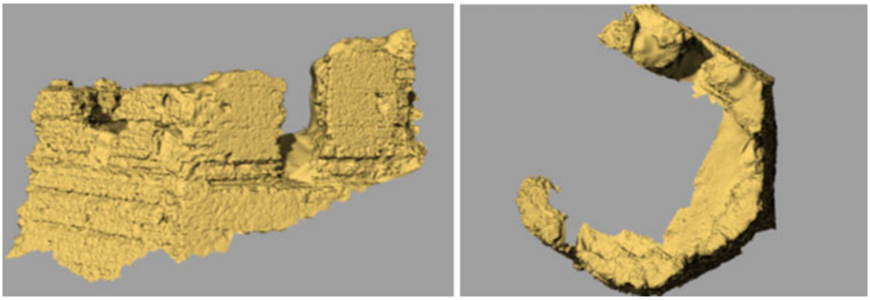

Fig. 5. Model views, obtained following the closure of its triangles

For digital photogrammetry 126 images have been made, which have been oriented with the Agisoft Photoscan program and the texture has been applied with them on the three-dimensional model obtained with the laser scanner and with photogrammetry (Fig. 6). Eight support points measured with total station have been used to solve the absolute orientation and give the model the actual size.

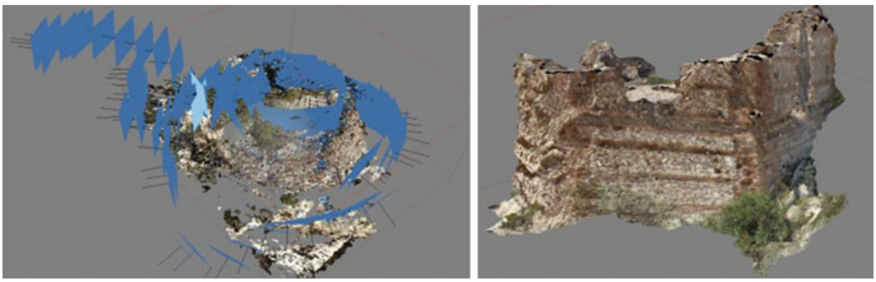

Fig. 6. Model views, above the cloud of points and application of the texture

2.3 Methods Geographical Information Systems

Finally, in 1578, although the King accepted that it was necessary to erect thirty-six towers [8] on the coast of the Kingdom of Murcia, as suggested by Antonelli. From those 36 towers, only twelve were constructed.

We have visited all the towers to verify in situ their state of preservation, how to reach them and their coordinates (Fig. 7). The georeferencing of all the towers has been done with gvSIG, a free GIS, indicating those that are still preserved and those that have disappeared. From North to South: the tower of El Pinatar, La Encañizada, El Estacio, San Antonio or Cabo de Palos, Portmán or San Gil, Navidad, La Azohía or Santa Elena, Almazarrón, Los Caballos, tower of Cope or Santo Cristo, San Pedro de las Águilas and San Juan de los Terreros Blancos [12].

The fundamental importance of these towers is that they formed a unit and their visibility was essential to their proper functioning, since it was basic to warn the rest of the population to send reinforcements in order to defend the tower and to take population to a safe place, given that one of the goals of Berber attacks was to capture and hold people for ransom or for sale as slaves.

Fig. 7. Coast map of the Region of Murcia with the twelve watch towers constructed during the 16th and 17th centuries: black icons represent the missing towers and white icons represent the existing towers

3 Results and Discussions

Once that the whole model has been obtained, as shown in Fig. 8, a section is made to compare it and to check the adjustment of plans and drawings attributed to Antonelli to the plan section. Bearing in mind that the hexagonal ground plan measures 53 ft (Fig. 8a) in diameter and that a Castilian foot measured 0.28 cm approximately, this circumference would be 14.84 m in diameter. According to this comparison, we observe that the remains of the existing walls form a hexagonal ground plan and that each side was slightly longer than the sides shown in the designs attributed to Antonelli, since they would be inscribed into a circumference that was not 14.84 m, but 19.23 m in diameter, as shown in Fig. 8b; therefore, it was built on a ground plan larger than the theoretical hexagonal ground plan of the tower.

Fortresses were repeatedly besieged and were the object of successive restorations, although these did not—in general—alter their plan. Projects were not usually accompanied by the necessary funds, and that is why we can assure that the Navidad Tower was built in the 16th century with a hexagonal ground plan inscribed into a circumference that was 19.23 m in diameter, approximately.

A reconstruction hypothesis of the Navidad tower has been made, presenting it in both elevation and section, (Fig. 9) considering that its height was of one plant based on the plans and sections of said tower, and considering the proven slope.

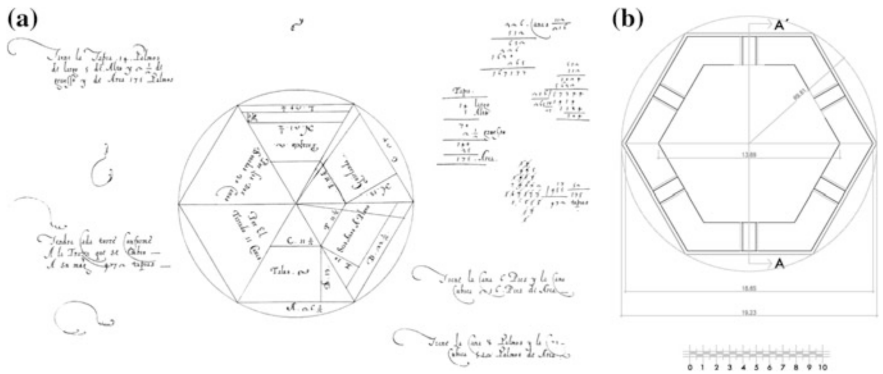

Fig. 8. **a** Hexagonal ground plan of the tower, attributed to Antonelli. Municipal Archive of Towers of the Navy, no number [13]. **b** Hexagonal ground plan of the Navidad Tower with heights and measures in unbroken lines and compared to the plans prepared for similar towers on the Murcian coastline of that period in broken lines

All the historical, graphic and building documentation provided is being used to prepare a restoration project for this tower, which would allow to preserve the building, to visit it and to prevent its collapse. This would prevent the current risk of loss of this historical heritage declared an Asset of Cultural Interest under the category of Monument.

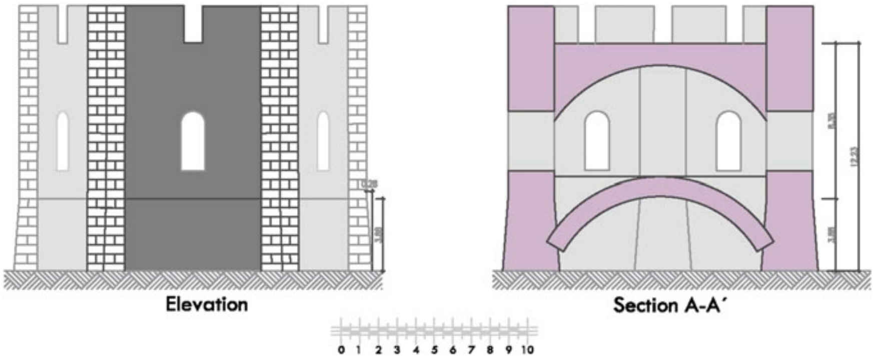

Fig. 9. Elevation and section of the Navidad tower, reconstruction hypothesis

4 Conclusions

We have located and mapped the towers constructed from the 16th to 17th centuries on the Murcian coastline as ordered by Philip II through free GIS. From the 36 towers that were planned, only 12 were built; nowadays, there are only four left: three of them have been recently restored, while the Navidad Tower is nearly ruined and forgotten.

We have prepared the graphic documentation of the remains of Navidad Tower by means of direct measuring methods, classical topography, laser scanning and photogrammetry. We have modelled the point cloud with a triangle mesh and have conducted studies based on this mesh, from which we have obtained the necessary sections to determine the original dimensions of the tower. These dimensions are larger than those specified in the information and descriptions obtained from the filed documents found, and we have verified that it has a hexagonal ground plan, that the thickness of its walls ranged from 2.50 to 3.00 m, that it was built with red brickwork and masonry, and that the project slope coincides with the actual slope. With all this, a reconstruction hypothesis of the single-story tower has been carried out.

This research represents the basis for the preparation of a restoration project for the Tower. The aim of the Christmas Tower is to make these towers become a vehicle for culture. As the recovery, improvement, dissemination and access to these towers will contribute to the enrichment of the coastal zone through the use of culture as the engine of social and economic development.

References

1. Velasco Hernández F (2017) La construcción de torres de defensa en el litoral de Lorca, Mazarrón y Cartagena durante el siglo XVI. In: MURGETANA nº136, Año LXVIII, pp 57–83
2. Gómez Vizcaíno A, Munuera Navarro D (2002) El sistema defensivo de los Austrias. In: Estudio y catalogación de las defensas de Cartagena y su bahía. Dirección General de Cultura, Servicio de Patrimonio Histórico. Murcia, España, pp 122–170

3. Gómez Vizcaíno A (1997) Guía turístico-histórica de los castillos y fortalezas de Cartagena. Aforca DL (eds). Cartagena, España
4. Gómez Vizcaíno JA, Martínez López JA, Munuera Navarro D (2003) Castillos y fortificaciones de la Comarca de Cartagena desde la época púnica hasta nuestros días. Ligia Comunicación. Murcia, España
5. Cámara Muñoz A (1990) Las torres del litoral en el reinado de Felipe II: una arquitectura para la defensa del territorio (I). In: Espacio, Tiempo y Forma. Serie VII. Historia del Arte nº3. UNED, pp 55–86. https://doi.org/10.5944/etfvii.3.1990.2155
6. Collado Espejo PE (2015) Intervención y puesta en valor de la Torre de los Caballos. Un nuevo espacio museístico dedicado a las torres vigía de la costa de Mazarrón. In: Rodríguez-Navarro P (ed) Defensive architecture of the Mediterranean. XV to XVIII centuries, vol I, España. http://dx.doi.org/10.4995/CONGR_2015
7. Peña Velasco C, García León J, Sánchez Allegue P (2017) Documentación, conservación y diffusion de un retablo a través de la geomática: el retablo barroco de la iglesia de San Miguel de Murcia. e-rph: Revista electrónica de Patrimonio histórico 21:67–90. http://dx.doi.org/10.4995/var.2017.5836
8. Rodríguez-Navarro, P. TOVIVA Project: una experiencia en torno al proyecto de defensa de la costa valenciana entre los siglos XVI y XVII. In: González Avilés ÁB (ed) Defensive architecture of the Mediterranean. XV to XVIII centuries, vol VI. UPV, España, pp 345–352
9. Remondino F, Spera MG, Nocerino E, Menna F, Nex F (2014) State of the art in high density image matching. Photogram Rec 29(146):144–166. https://doi.org/10.1111/por.12063
10. Cámara Muñoz A (1991) Las torres del litoral en el reinado de Felipe II: una arquitectura para la defensa del territorio (y II). In: Espacio, Tiempo y Forma. Serie VII. Historia del Arte nº4. UNED, pp 53–94. https://doi.org/10.5944/etfvii.4.1991.2175
11. Martínez López JA, Munuera Navarro D (coord) (2005) Atlas político y militar del Reyno de Murcia firmado por el Capitán de Infantería e Ingeniero Ordinario de los R. Exercitos D. Juan José Ordovás. Año de 1799 (reedición). Edita MIMARQ Arquitectura y Arqueología, Murcia, España, pp 30–45
12. Alonso Navarro S (1990) Libro de los castillos y fortalezas de la Región de Murcia. Asociación Nacional de Amigos de los Castillos, Murcia, España
13. Gil Albarracín A (2017) Coastal Defense in Lorca in the sixteenth and seventeenth centuries. Alberca 15:169–240

Design of a Two Arms Exoskeleton as Haptic Device for Virtual Reality Applications

D. Chakarov[1(✉)], I. Veneva[1], M. Tsveov[1], P. Mitrouchev[2], and P. Venev[3]

[1] Institute of Mechanics, BAS, "Acad. G. Bonchev" Str., Block 4, 1113 Sofia, Bulgaria
mit@imbm.bas.bg
[2] Université Grenoble Alpes, G-SCOP, 38000 Grenoble, France
[3] Technical University, "Sv. Kliment Ohridski" Blvd., No. 8, 1756 Sofia, Bulgaria

Abstract. The work investigates a solution of powered upper arms exoskeleton designed as haptic device for use in VR scenarios. The mechanical structure and the actuation system of the exoskeleton system are presented. To develop a powered upper limbs exoskeleton possessing, natural safety and transparency in the mutual "man-robot" interaction, the hybrid actuation approach is used. The latter includes in each joint parallel actuation of pair pneumatic actuators and a back drivable direct current (DC)-motor. An impedance controller with model feedforward compensations and an algorithm for joint torque control are designed, in order to provide accurate force response from the virtual environment to the operator. For this purpose, computer simulations are carried out to assess the developed exoskeleton capabilities to provide forceful effect on the operator, in the full range of arm joint motions. The experiments demonstrate that by proper selection of the additional DC actuation the desired power feedback can be achieved throughout the exoskeleton's workspace.

Keywords: Exoskeleton arm · Haptic device · Virtual reality · Impedance control · Hybrid actuation

1 Introduction

The importance of exoskeletons such as haptic devices increases when it comes to applications in virtual reality (VR). Through the exoskeleton as a haptic device, the operator feels the forces of interaction generated in the virtual environment (VE). These features of exoskeletons come into play also when operations in a virtual environment are designed for rehabilitation and training [1–3].

When an exoskeleton is intended for rehabilitation [3], it must be able: (i) to create great forces to support, assist and guide the patient's arm; (ii) to follow the human arm without opposition.

F. Cavas-Martínez et al. (Eds.): *Advances on Mechanics, Design Engineering and Manufacturing II*, LNME, pp. 252–262, 2019.
https://doi.org/10.1007/978-3-030-12346-8_25

In order to achieve transparency and natural safety when using exoskeleton as a haptic device, it must be designed with the lowest natural impedance. There are two main approaches to reduce the device's impedance: active and passive approach. Active control is a more widespread approach where impedance compensations have the form of either feedforward [4] or force feedback control [5].

By means of an active impedance control compensation can be achieved in a wide range. However, transparency and safety can be reduced due to disadvantages of active control such as instability of the servo system, sensor noise and poor sensor resolution. The level of safety and transparency can remain high by using a passive impedance, independent of servo system. There are many solutions for implementing passive impedance. All are based on embedding in the structure of passive compliant element [6].

One of the best–known solutions for implementing passive impedance is the pneumatic artificial muscles (PAM) drive [7–9]. The PAM drive is characterized by the highest ratio of power/weight and power/volume compared to other drives. Air muscles have low inertia, natural compliance and damping, so their output impedance is low in a wide frequency range. However, the high natural compliance of the air muscles results in a low dynamic force response, which limits the efficiency of the drive. Other drawbacks of the PAM drive are the limited amount of motion, due to limited muscle contraction, and the limited capacity of the muscle force.

There are a number of solutions to overcome the disadvantages of artificial muscles. Some of them consist in changing the structure of the muscles and/or the air flow. By reducing the dead volume of the muscle and control of the air flow is achieved an increase in stiffness and actuation bandwidth [10]. Other solutions are based on the use of a larger pulley to increase the driving torque [11].

There are also some approaches that rely on control strategies. The hybrid actuation approach [12], for instance, involves parallel operation of a pair of PAM's and a low-inertial DC motor. Artificial muscles perform the low-frequency macro component of the actuation torque, and the DC motor complements the torque error. According to another embodiment of the hybrid actuation [13], the advantages of both actuators: DC motor with harmonic drive and a pair of air muscles are combined. High pressure PAMs provide the basic magnitude of the torque while the harmonic drive actuator ensures the high precision of the torque. In another solution [14] to enhance security, the hybrid actuation approach is expanded by combining PAM's and magnetic brake. The authors show that while hybrid actuation with PAM's and DC motor demonstrates a more rapid dynamic force response, the hybrid drive with PAM's and magnetic brake is more effective in large shift of inertial loads.

In this context, the aim of the work is to find and evaluate an appropriate solution for actuation of upper arms exoskeleton designed as haptic device for use in scenes of VR, providing accurate force feedback and achieving transparency and natural safety in the interaction "human-robot".

In Sect. 2 the mechanical structure and its actuation are presented. The modeling and the control are described in Sect. 3. The simulation and performance evaluations are then shown in Sect. 4. Conclusions and future works are given in Sect. 5.

2 Mechanical Structure and Actuation

The exoskeleton mechanical structure consists of two arms built of five parts (segments), one of which is grounded as shown in Fig. 1a. Each arm includes four active joints, like joints in natural human arm from the shoulder to the elbow.

All segments of the arm have adjustable length thus allowing quick and easy adjustment according to users' size. The human hand is attached to the main segments by means of straps and plastic shells. The prototype of two arm exosceleton is shown in Fig. 1b.

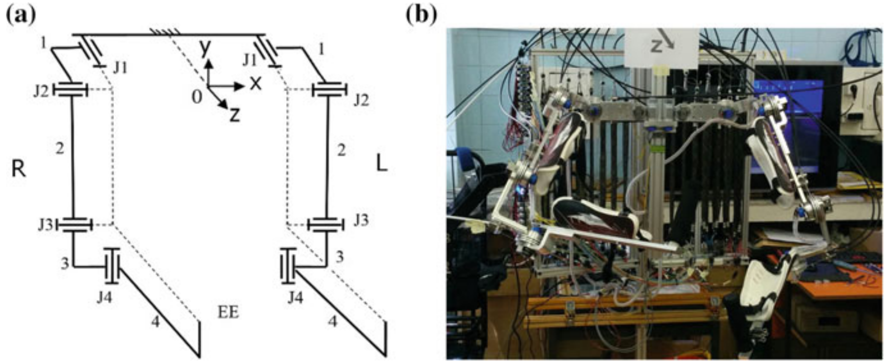

Fig. 1. Two arm exoskeleton: **a** mechanical structure; **b** prototype

Aluminum alloy is used to make the exoskeleton's basic segments. Their masses (Fig. 1a) are M_1 = 0.437 kg, M_2 = 0.594 kg, M_3 = 0.364 kg and M_4 = 0.434 kg. In the initial setup, the exoskeleton arm and forearm lengths were selected 0.286 and 0.370 m respectively. The exoskeleton range of motion is defined by the range of joints (Ji) motion as follows: J1(110°), J2(120°), J3(150°), J4(135°). Thus the exoskeleton meets the requirements of "Activities of daily living" (ADLs) [15].

To develop a powered upper limb exoskeleton possessing natural safety and transparency in the mutual "man-robot" interaction, a PAM-based actuation is developed. To overcome air muscle limitations, the hybrid actuation approach is used. A low-inertia DC-motor is attached in parallel to a pair of PAM actuators. Each PAM actuator in the pair consists of muscles with different number.

Braided pneumatic artificial muscles are self-developed, allowing greater control over the dimensions, forces and overall performance. The actuators represent a bundle of several pneumatic muscles (Fig. 2a). The bundle muscles are fed together with air to a maximum pressure of 500 kPa. Each bundle is equipped with a pressure sensor. The muscles of the bundle are mechanically connected at one end and the other end where they are attached.

The arm segments are actuated by cable transmissions and pulleys located in the joints (Fig. 2b). Each pulley is connected to a pair of PAM actuators *a* and *b*, coupled to a DC-motor (DCM) in parallel (Fig. 2b).

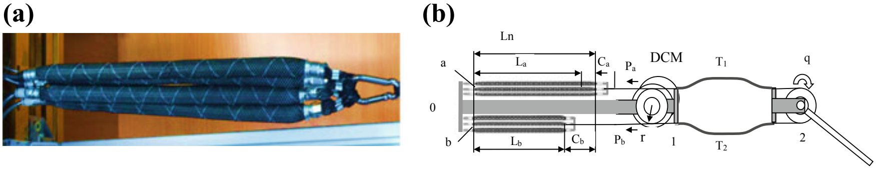

Fig. 2. Actuation system: **a** pneumatic actuator as a bundle of PAMs; **b** scheme for joint motion/torque

The pair of PAM actuators a and b, make an antagonistic interaction similar to the biceps-triceps muscle system. This interaction creates a two-way movement and force on the pulley 1 (Fig. 2b). A back drivable DCM is attached to the pulley 1 in parallel. Second pulley 2 is located in the arm joint. Cable transmissions $T1$ and $T2$ connect pulleys 1 and 2. All actuators are mounted on a stationary structure behind the operator. The number of muscles in each bundle of the pair is selected so, as to provide a nominal torque in the joint over a range of joint motion. Bundles antagonists a and b consist of a different number of muscles denoted by m_{ia} and m_{ib}, $i = 1, \ldots, 4$. The numbers of muscles for the four joints are: $m_{1a} = 7$, $m_{1b} = 3$; $m_{2a} = 6$, $m_{2b} = 3$; $m_{3a} = 4$, $m_{3b} = 2$; $m_{4a} = 4$, $m_{4b} = 3$.

In antagonistic scheme (Fig. 2b), muscles in each bundle are attached to the joint pulley, so that their contraction is determined by the pulley radius $r = 0.0315$ m and the joint position q. To maximize muscle strength, muscles are attached so, as to work with a minimum contraction, *i.e.* in one end position of the joint $q_{\max}$, one bundle has zero contraction and in the other end position of the joint $q_{\min}$, the other bundle has a zero contraction.

Braided PAM become like a pressure-dependent spring with variable stiffness. To describe the PAM used as non-linear quadratic springs, a simplified static model presented in [9] is used. This model is transformed for the case when muscles form bundles [16]. The forces generated by the two PAM bundles "a" and "b" are represented by the equations

$$P_a = (k_{ao} + k_{a1} p_a)(C_{\max} - r(q^{\max} - q))(L_n - r(q^{\max} - q)), \tag{1}$$

$$P_b = (k_{bo} + k_{b1} p_b)(C_{\max} - r(q - q^{\min}))(L_n - r(q - q^{\min})). \tag{2}$$

Above; k_{ao}, k_{bo} and k_{a1}, k_{b1} are empirically derived coefficients, depending on the number m_a, m_b of muscles in the bundle; p_a, p_b are the supply pressures of the bundles; L_n and $C_{\max}$ are nominal length and maximal contraction of the muscles used. The antagonistic action of muscle bundles in each joint creates pneumatic generated torque:

$$Q_p = (P_b - P_a) r, \tag{3}$$

where P_a, P_b represent the antagonistic forces (1) and (2) and r represents the pulley radius.

3 Modelling and Control

According to the kinematic scheme shown in Fig. 1a, a mechanical model of the right exoskeleton arm is build up (see also Sect. 4). As previously said the arm structure is a four DoF mechanism. Thus, it is described with (4 × 1) dimensional vector of joint coordinates $\boldsymbol{q}$.

The model is built when the contact between the operator and the exoskeleton is at the point of end effector (*EE*). In this case, the vector $\boldsymbol{X}$ of *EE* coordinates is (3 × 1) dimensional and Jacobian matrix $\boldsymbol{J}$ is (3 × 4) dimensional.

Impedance controller has been developed [16] as the most appropriate for reflection of the force of the virtual environment on the user (Fig. 3). In the block diagram, feedforward compensations based on a stiffness model and a gravity model are included. Data transfer between exoskeleton and virtual scene takes place through a VR Engine.

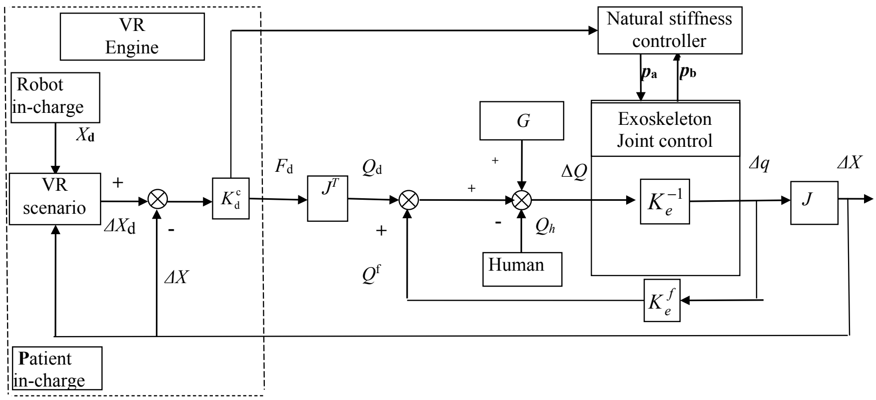

Fig. 3. Block diagram of exoskeleton control

Modelled exoskeleton stiffness in joint-space is indicated in the diagram by $\boldsymbol{K_e^f}$, while the natural exoskeleton stiffness by $\boldsymbol{K_e}$. The role of the natural stiffness controller above is to adjust in Cartesian space the natural exoskeleton stiffness $\boldsymbol{K_e^c}$ to the reference value $\boldsymbol{K_d^c}$. This is achieved by planning the pressures of PAM actuators p_a and p_b such that the natural stiffness to obtain the characteristics of the desired stiffness.

Control force commands in joint space according to block diagram of Fig. 3 are represented by the vector

$$\boldsymbol{\Delta Q} = \boldsymbol{Q_d} + \boldsymbol{Q^f} + \boldsymbol{G} - \boldsymbol{Q_h} \tag{4}$$

where: $\boldsymbol{Q_d}$ denotes the desired force command, $\boldsymbol{Q^f}$ and $\boldsymbol{G}$ denote force commands according to the feedforward compensation models of exoskeleton stiffness and exoskeleton gravitation, and $\boldsymbol{Q_h}$ denotes, in the joint space, the forces that the operator exerts on the exoskeleton end effector. The vector (4) includes the exoskeleton joints torques

$$\Delta \boldsymbol{Q} = [Q_1, \ldots, Q_i, \ldots, Q_4]^T \tag{5}$$

The torque Q_i is a sum of the torques of pneumatic and electric drives Q_{pi} and $Q_{ei.}$

$$Q_i = Q_{pi} + Q_{ei}, \quad i = 1, \ldots, 4 \tag{6}$$

In the block diagram for control of the torques in the exoskeleton joints (Fig. 4) the pressure p_a of one PAM actuator (antagonist) is set by natural stiffness controller to achieve the desired stiffness. The pressure p_b of the other PAM actuator (agonists) determines the pneumatic actuation torque (3). Pressure p_b is calculated according to Eqs. (1)–(3). Both pressures p_a and p_b are monitored by pressure sensors to control the filling and vending valves of each bundle. As the supply pressure has a certain upper limit, the magnitude of the torque (3) is limited.

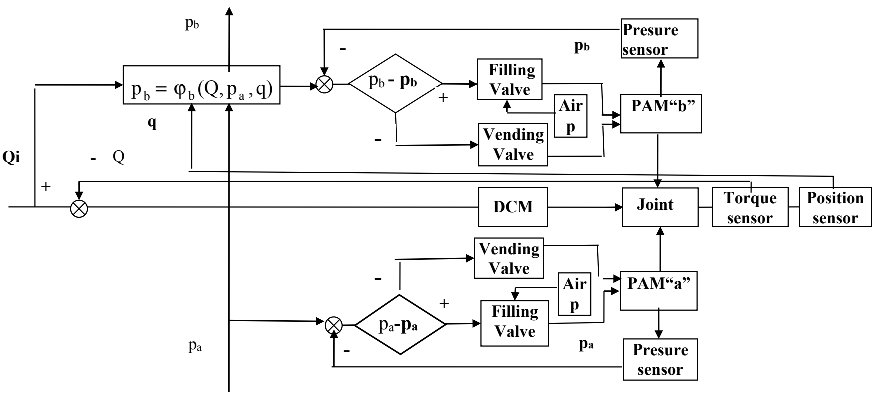

Fig. 4. Block diagram of joint torque control

A torque sensor is mounted in the exoskeleton joint (Fig. 4). The torque tracking error calculated as the difference between the set and the measured torque ($Q_i - Q$) determines the force command of the electric drive. Electric motor (DCM) compensate the torque difference between the set and the resultant torque as it is controlled by an open loop current controller. The role of the additional electric drive is both to compensate the slow dynamic of pneumatic drive and to complement the magnitude of joint torque to the desired value.

4 Simulation and Performance Evaluation

The upper arms exoskeleton designed as haptic device for use in VR scenarios, allows tracking position and orientation thus providing force feedback to human arm. For data transfer between exoskeleton and virtual scene, 3D Unity Virtual Engine is used.

To track the head position and orientation Optical tracker HMD Oculus Rift is used (Fig. 5).

Fig. 5. One arm exoskeleton as a haptic device for a VR application

Simulations of virtual gymnastics scenes were carried out to assess the designed exoskeleton capabilities (Fig. 5). For calculation and evaluation of mechanical parameters a MATLAB application was created.

First experiments are carried out when the exoskeleton is driven only by PAM bundles according to the method described in Sect. 2. For desired *EE* force $\boldsymbol{F_d} = [F_{dx}, F_{dy}, F_{dz}]^T$ in the virtual scene, the joint torques and bundle pressures for all ranges of joint motions are calculated with a step of 20°. The F_{dy} is selected as non-zero component, as its direction corresponds to the gravitational load to achieve maximum load on the joint drives. Only gravitational compensation is considered in this experiment. The natural stiffness controller is not included and the pressures p_a for actuators antagonists are set to zero.

The calculated pressures p_b of the actuators agonists are assessed whether they are within the set limits of 500 kPa. If, in one arm position, all bundle pressures are within the given range, this hand position is recorded and plotted (Fig. 6). By circles, of different sizes and colors, are presented forces of different values achieved in the respective position. Figure 6a shows a solution to achieve a force F_d set with the following values of its components:

$$\boldsymbol{F_d} = [0, 0, 1]^{\mathrm{T}}, \boldsymbol{F_d} = [0, 0, 15]^{\mathrm{T}}, \boldsymbol{F_d} = [0, 0, 30]^{\mathrm{T}}, \boldsymbol{F_d} = [0, 0, 45]^{\mathrm{T}}. \quad (7)$$

Pneumatic actuators being positioning dependent, on different points of the workspace, forces of different magnitude are achieved. In Fig. 6a the circles shown correspond to the highest value of the force achieved in the respective position. The simulations show that setting a high value of the force from VR Engine cannot be achieved in all exoskeleton arm positions. In this case, the force on the operator hand will be different from the force of the virtual system (in magnitude and direction).

Other experiments are carried out to assess the potential for achieving the desired power effect by adding joint torques from parallel electric drives. For example, to achieve the EE force ($F_d = [0, 0, 30]^T N$), torques of electric drive are added according to (6). In this case, through proper selection of the magnitude of the complementary moment, the desired power reflection on the operator's hand can be achieved throughout the workspace as shown in Fig. 6b.

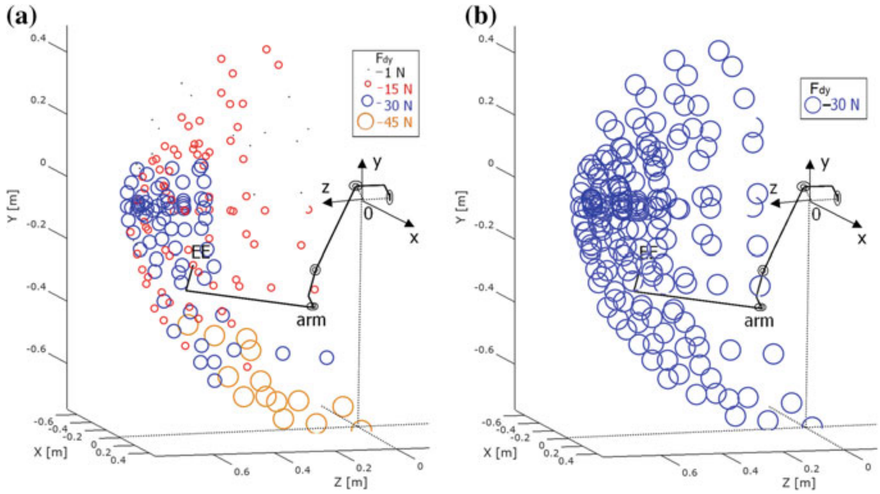

Fig. 6. Graphical representation of force feedback achieved in different arm positions when: **a** only pneumatic drive; **b** pneumatic and electrical drive in parallel

The torque variations in the first two arm joints in this experiment are shown on Fig. 7a, b namely: the desired joint torques Q_1 and Q_2, the torques of the pneumatic drive Q_{p1} and Q_{p2}, as well as the supplementary torques of the electric drive Q_{e1} and Q_{e2}. The maximum values of the complementary torques for the two joints are Q_{e1} = 11.62 Nm, and Q_{e2} = 14.57 Nm. If the desired power of the effector is ($F_d = [0, 0, 15]^T N$), the maximum values of the complementary torques for the two joints are Q_{e1} = 1.04 Nm, and Q_{e2} = 3.52 Nm. At power values ($F_d = [0, 0, 10]^T N$), the complementary moments are $Q_{e1} = 0$, $Q_{e2} = 0$.

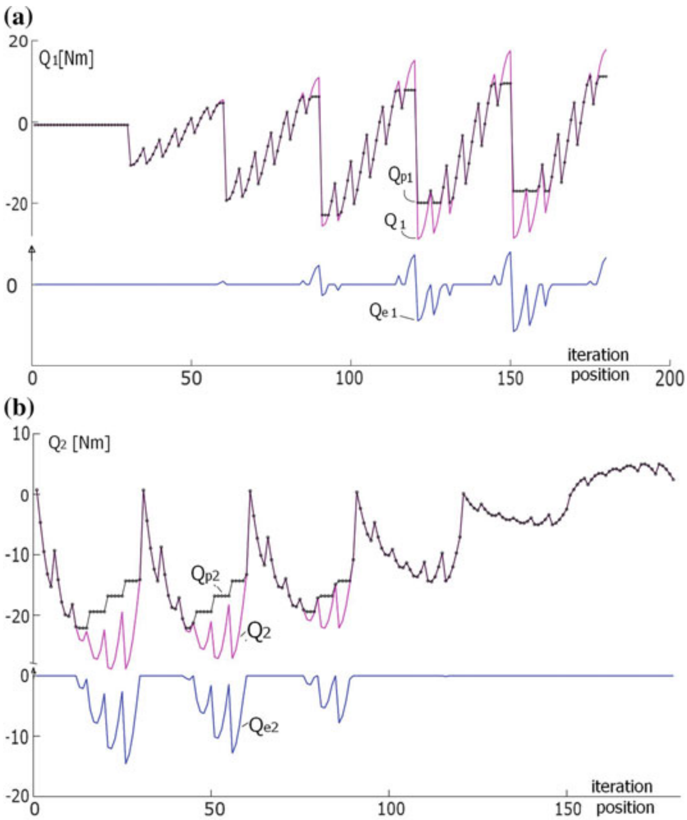

Fig. 7. Variation of the joint torques for generating force feedback F_{dy} = 30 N: **a** in joint 1; **b** in joint 2

5 Conclusion

A design solution of powered upper arms exoskeleton, as haptic device for use in VR scenarios, is presented in the work. To develop a powered upper limbs exoskeleton possessing natural safety and transparency in the mutual "*man-robot*" interaction, the hybrid actuation approach is used, which includes in each joint parallel actuation of a pair of PAM actuators and a back drivable DC-motor. Simulations are carried out to assess the developed exoskeleton capabilities in order to provide forceful effect on the operator, in the full range of arm joint motions. Cases when the exoskeleton is only pneumatically driven and when using pneumatic and electric drive in parallel are discussed. For the first case simulations show that setting of a high value of force from the virtual system cannot be achieved at all points of the exoskeleton's workspace since the pneumatic actuator forces are positioning dependent. For the second case, hybrid actuation approach, experiments demonstrate that by proper selection of the additional DC actuation the desired power feedback can be achieved throughout the entire arms workspace. In this case, the values of the complementary joint torques of the parallel electric drive are not large and DC micromotors can be used mounted directly to the arm joint. Future work is going to involve installation of suitable DC motors and conducting experiments to assess the impact on the operator.

Acknowledgements. This work was funded by the European Commission through FP7 Integrated Project VERE—No. FP7-257695 and by Bulgarian Science Found, Call: 2016, through Project AWERON—DN 07/9, to which the authors would like to express their deepest gratitude.

References

1. Frisoli A, Salsedo F, Bergamasco M, Rossi B, Carboncini MC (2009) A force-feedback exoskeleton for upper-limb rehabilitation in virtual reality. Appl Bion Biomech 6(2): 115–126
2. Guidali M, Duschau-Wicke A, Broggi S, Klamroth-Marganska V, Nef T, Riener R (2011) A robotic system to train activities of daily living in a virtual environment. Med Biol Eng Comput 49:1213–1223. https://doi.org/10.1007/s11517-011-0809-0
3. Jarrasse N, Proietti T, Crocher V, Robertson J, Sahbani A, Morel G, Roby-Brami A (2014) Robotic exoskeletons: a perspective for the rehabilitation of arm coordination in stroke patients. Front Human Neurosci. https://doi.org/10.3389/fnhum.2014.00947
4. Hogan N (1985) Impedance control: an approach to manipulation. ASME J Dyn Syst Meas Contr 107:1–24
5. Bergamasco M, Allotta B, Bosio L, Ferretti L, Perrini G, Prisco GM, Salsedo F, Sartini G (1994) An arm exoskeleton system for teleoperation and virtual environment applications. IEEE Int Conf Robot Automat 2:1449–1454
6. Vanderborght B et al (2013) Variable impedance actuators: a review. Robot Auton Syst 61:1601–1614
7. Chou P, Hannaford B (1996) Measurement and modeling of McKibben pneumatic artificial muscles. IEEE Trans Robot Autom 12(1):1–6
8. Daerden F, Lefeber D (2002) Pneumatic artificial muscles: actuators for robotics and automation. Eur J Mech Environ Eng 47(1):1–11
9. Caldwell DG et al (2007) “Soft” exoskeletons for upper and lower body rehabilitation—design, control and testing. Int J Humanoid Rob 4(3):549–573
10. Davis J, Canderle J, Artrit P, Tsagarakis N, Caldwell DG (2002) Enhanced dynamic performance in pneumatic muscle actuators. In: Proceedings of the IEEE ICRA, Washington, DC, May, pp 2836–2841. https://doi.org/10.1109/robot.2002.1013662
11. Shin D, Yeh X, Khatib O (2011) Variable radius pulley design methodology for pneumatic artifical muscle-based antagonistic actuation systems. In: IEEE/RSJ International Conference on Intelligent Robots and Systems, San Francisco, CA, pp 1830–1835
12. Sardellitti I, Park J, Shin D, Khatib O (2007) Air muscle controller design in the distributed macro-mini (DM^2) actuation approach. In: Proceedings of the 2007 IEEE/RSJ International Conference on Intelligent Robots and Systems, San Diego, CA, pp 1822–1827
13. Aguilar-Sierra H, Yu W, Salazar S, Lopez R (2015) Design and control of hybrid actuation lower limb exoskeleton. Adv Mech Eng 7(6):1–13. https://doi.org/10.1177/1687814015590988
14. Shin D, Yeh X, Khatib O (2014) A new hybrid actuation scheme with artificial pneumatic

muscles and a magnetic particle brake for safe human–robot collaboration. The Int J Robot Res 33(4):507–518. https://doi.org/10.1177/0278364913509858

15. Perry J, Rosen J, Burns S (2007) Upper-limb powered exoskeleton design. IEEE/ASME Trans Mechatron 12(4):408–417
16. Chakarov D, Veneva I, Tsveov M, Zlatanov E (2017) Adjusting the natural stiffness of a pneumatic powered exoskeleton designed as a virtual reality haptic device. Int J Adv Robot Syst 14(6):1–13. https://doi.org/10.1177/1729881417739432

3D Organic Modeling Using Hybrid Techniques with Polygons

C. López(✉), J. A. Peña, and R. Miralbés

Departament of Design and Manufacturing Engineering, University of Zaragoza. EINA, C/María de Luna, 3, 50018 Saragossa, Spain
melopez@unizar.es

Abstract. This work presents a methodology of 3D modeling suitable for the design and manufacture of components with complex forms of organic inspiration. It is applied to a real case of development of a sculptural element related to the corporate image of a company. In the introduction, the boundary conditions of the project and the product to be modeled with the starting specifications are presented. Next, the stages followed for the execution of the project that give justification to the methodology developed are described. The document shows the general flow of activities presenting in each one the particularities and resolved contingencies. The tangible results of the project that includes the variations of the model generated for 3D animation equipped with articulated bones are also exposed. It has been experimentally verified that the proposed modeling methodology allows the integration of components designed by CAD, generates topologies coherent with innovative criteria that they facilitate production through additive manufacturing with related surfaces free of errors. It is, therefore, a hybrid method based on the manipulation of mesh polygons with accessible tools that is suitable for the design and manufacture of bio-inspired products, paleontological reconstructions, prostheses or bio-engineering components. The UV coordinate maps and the designed textures make it possible for the same geometry or simplified versions of the manufactured model to be modified by means of 3D animation techniques with skeletons, to be used in virtual representations and in augmented reality environments, increasingly demanded in the field of Graphic Engineering.

Keywords: Polygonal modeling · 3D mesh optimizing · Retopology · Digital sculpting · Uv.mapping · Organic modeling

1 Introduction

This work is related to the development of a product used for an advertising campaign of a local company. It was a sculpture that represented a human being adjusted to a concept and aesthetic specifications contributed by the client of the project. The main objective was to build the reproduction by additive color manufacturing using ceramic powder injection technology with surface impregnation of inks with CMYK palette [1]. Due to this, there were significant specifications imposed by the resistance of the material used and the tolerances inherent to the manufacturing process [2]. Additionally, the general modeling should adhere to the following technical requirements:

F. Cavas-Martínez et al. (Eds.): *Advances on Mechanics, Design Engineering and Manufacturing II*, LNME, pp. 263–271, 2019.
https://doi.org/10.1007/978-3-030-12346-8_26

- The model had to be built at full size: A human 120 cm high.
- The dimensions of the product exceeded the capacity of the manufacturing bucket by a factor of 1/8. The figure had to be broken down into several parts that could be assembled.
- The productive considerations recommended an obvious reduction of volume of injected material. It was necessary to design hollow components with wall thicknesses according to the printing possibilities and resistance of the prototype.
- The pieces obtained were assembled on axes that provided rigidity and cohesion to the final figure. It was necessary to define and model auxiliary geometric elements that facilitated the assembly on the support system (holes, guides, junction records), confluences, partitions and reinforcements. For the appropriate dimensional interpretation of the auxiliary geometry, CAD would be used.
- The final geometry of each of the pieces to be manufactured would consist of a mesh of triangles free of errors, superficial intersections and connected in a specific format. The print machine used the format .3DS [3] that allows to represent objects in color. This type of file structure has limited size expressed in bytes. Therefore the meshes had to have a variable level of detail, susceptible to reduction, to reduce the volume of information and be able to be printed in color in the available machinery.
- The final prototype had to show the textures of the materials according to the color manufacturing technology. You had to define some projection system associated with the model that was compatible with the print file.

Due to the aforementioned requirements it was necessary to establish a 3D modeling methodology that combined the representation of mechanical forms with others of subjective creation, typical of sculpture. The resulting model would be defined by polygons of variable density and with a 2D image projection system, to represent patterns or color textures. In short, a hybrid method of 3D modeling to design and manufacture non-conventional mechanical components and organic appearance.

Finally, it was considered of interest that given the application context of the product, the 3D models obtained could be used for other purposes and achieve secondary objectives:

- The sculpture could be adapted to smaller formats for more economical reproductions with other 3D printing devices creating alternative products useful for merchandising.
- The mesh of polygons required to shape the sculpture could be used with 3D animation techniques [4] and provide audiovisual content.

2 Description of Modeling Techniques

Figure 1 summarizes the basic methodology activities implemented in the project. The information inputs and the results obtained or expected are included. Describes a logical sequence of modeling activities by using various specific 3D software tools in pipeline process. Next, these activities are reviewed.

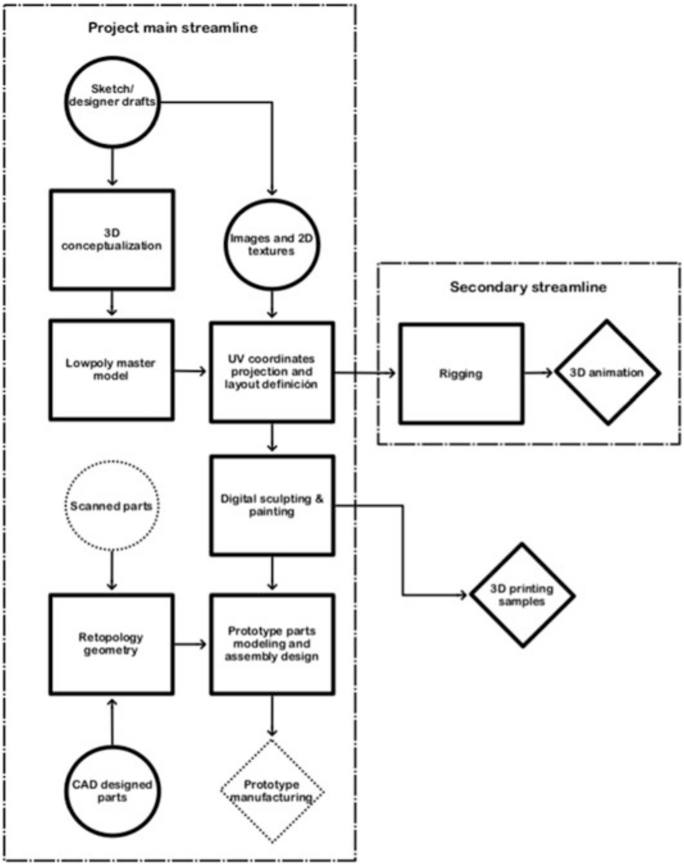

Fig. 1. General diagram of activities

2.1 3D Conceptualization

It is common in projects of product development that the starting point of the activities is a sketch or a conceptual drawing with details of its function, structure and appearance. In the case studied, there was a single image prepared by a graphic designer selected by the client. It represented a human being with an exaggerated anatomy proper to the caricature or the cartoon. The posture and expression of the face provided basic information about his personality and emotional state [5]. The character was dressed in vestments of the late eighteenth century. No details or complementary views were included that would allow having objective data of the back of the model or of certain dimensions or hidden forms in the available view. The illustration did not include any coding of the tone palette used although it contained characteristic details related to the corporate image and colors of the company.

With this starting information, it was considered necessary to redesign the character for its correct interpretation and clarify various details that were ambiguous or non-existent in the original sketch. Consequently, it was decided to develop a new concept directly in 3D [6].

Free-use software and open source Wings 3D 2.5.1 [7] were used in the Project. It is a 3D tool with simple, intuitive commands. By working directly in the space, you avoid the problems of interpretation or detail typical of the sketch and its auxiliary views. It has different polygonal subdivision algorithms, which allows representing smooth surfaces [8, 9]. If it is desired to maintain the hardness of the characteristic curves, characteristic of the concept drawing, it can be done by increasing the local density in the mesh related to them.

The character object of the project was modeled in a neutral position. The "T" position was chosen with hands down and legs closed. The aim was to obtain an anatomical shape with a plane of symmetry that simplifies the work of 3D modeling and, what is more relevant, makes it possible to use the mesh in animation processes. These positions are necessary if you want to give the model a system of articulated bones [10], which was necessary to create variations of pose as reviewed later.

2.2 Establishment of the Master Model

The master model represents the essential polygonal geometry of the product to be manufactured. It will be used as a starting point in all subsequent stages of modeling. Its correct definition is a critical point of the general process.

Figure 2a shows the pattern of the figure related to the project. It is a mesh of quadrangles and triangles similar to the one created in the conceptual stage, after being subjected to a check that takes into account the following aspects:

- *Absence of singularities*: Vertexes originated by the confluence of two edges, polygons of more than four vertices, vertices with excessive confluence of edges, interferences between surfaces or normal inverted polygons that are part of the same shell. These types of problems are common in components imported CAD pieces.
- *Geometric stability of the polygonal subdivision*: The surfaces must maintain the normal ones according to the design criteria in the conceptualization. For example, if the existence of a reference plane or a cylindrical functional surface has been established, they must maintain that condition in the subdivisions executed. It has been verified that the visualization of the model by Phong shading [11] allows to detect these problems.
- *Density of the mesh adjusted to the detail*: The model must have the necessary polygons that correctly define the desired surface. The excess of polygons does not provide information. This aspect is essential for the creation of optimal models of low density compatible for their audiovisual use, animations in real time, virtual or augmented reality.
- *Correct location of isolines of polygons*: This is an aspect of each type of model, shape or anatomy. A harmonic mesh has an explicit topology. It is preferably composed of quadrangles and shows alignment of the edges with respect to certain directions, preferably those of conformation. This circumstance is evident when the surface has been obtained by extrusion. The correct distribution of the isolines facilitates the adequate application of the subdivision algorithms and is essential if they are to model physiological forms related to muscles and joints. They are especially interesting in the face area.

- *Existence of functional edges*: Such is the case of reference or symmetry sections that the model can demand. Another example are the edges of detail increase necessary to effectively represent flexions or partial movements typical of 3D animation that manipulate the meshes as elastic objects. The seams that allow making the mapping layouts obtained in the next stage would also be within this category.

2.3 Preparation of the UV Layouts

The original starting sketch was colored with a variety of graphic resources. It combined flat colors, motifs or patterns, texts and logos. The most convenient solution in this case of heterogeneous graphics, is to provide the 3D model with a UV parametric coordinate projection system [12] that allows to represent them in a convenient way without deformations or discontinuities. Fortunately, the software chosen for the conceptual design and modeling of the 3D pattern was equipped with experimental tools to define the coordinates of projection and editing of the mapping layouts. The integration of this skill in the polygonal modelers is very useful since it allows to adjust the mesh, to obtain the ideal seams. The seams are the border edges that define the "islands" or areas in which any 3D object is divided as it develops in the plane. The islands correspond to logical zones of the model: Surface of the same material, relevant physical parts, front/back views of a component, among other criteria. Once completed it was evaluated using test images (see Fig. 2). They are chess look patterns that show the irregularities of the projection of a sample image and its discontinuities on the seams.

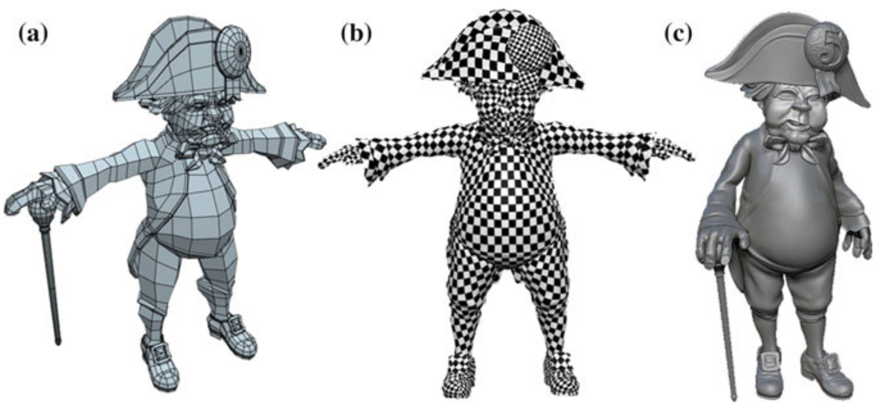

Fig. 2. Examples of meshes. **a** Pattern in low number of polygons in position "T". **b** Pattern model showing the projection of a checkered texture for evaluation of its UV map system. **c** Digital sculpture in high density in a new pose and improvement of details

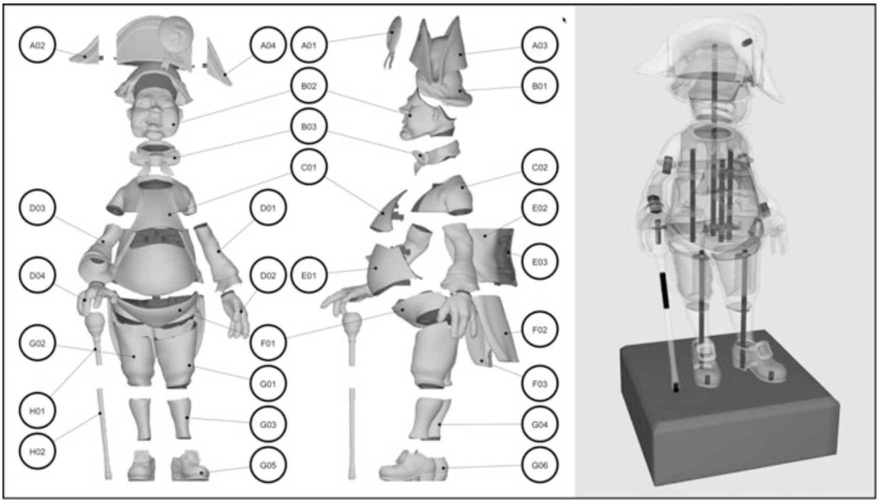

Fig. 3. Set of pieces associated with the life-size figure. and mesh details of the components of the figure at full size. On right, you can see the construction elements some of then designed with CAD

2.4 Sculpture and Digital Painting

The term digital sculpture can be applied to modeling tasks in which tools similar to tools for sculpting or painting are used. In fact, these are local mesh manipulators that allow to modify it and perceive a similar result to make a slit, a protrusion or a weld bead. It allows to represent surface details of the dermis, organic tissues and construction materials, to name a few examples. In order to act in this way the mesh of the model must increase its density. It is verified that an iteration of three subdivisions may be sufficient to operate in low/high relief sculpture. For more precise surface details such as fabric reliefs, grains or cracks of a deteriorated material, one or two more subdivisions may be required. At that point the model can have several million polygons.

In our case we used digital sculpture for:

- Increase the quality of general surface detail.
- Modify the position of the character from the neutral in "T".
- Get the facial expression with wink of an eye and grimace of the mouth.
- Sharpen wrinkles and folds in clothing and hair.

To perform this task, the open source application SCULPTGL [13] was used. This online application is capable of manipulating the models of the previous stage with digital brushes to sculpt, deform and paint the mesh. It respects the original UV layout and can incorporate images as projected textures to represent materials such as those required in the project. It also has algorithms for subdivision control and mesh topology editing tools.

2.5 Design of the Pieces Set Figure

Once the work of modeling the sculpture was completed, we proceeded to design the components that would make up the figure to be built. Its volume should be less than that of the work bucket. They were obtained by sectioning the sculpture using characteristic planes with respect to the vertical direction of the model, trying to maintain a certain continuity in key areas of the sculpture (such as the face). The resulting set is shown in Fig. 3. It was composed of 27 pieces. Assembled it reached a height of 1150 mm. Each piece contained an outer shell corresponding to the sculpted surface and an internal surface designed to provide support with the adjacent pieces and with the tubular structure that provided support. Various constructive solutions were applied:

- Solid pieces with through holes in the lower area of the model subsets G01-05 and the hip part F01 that was an essential component for assembly of the set.
- Hollow pieces, such as arms, head and neck.
- Plate-type pieces, such as the tails of the frock coat, F02-03 or the cockade of the hat. The abdomen and thorax was composed of several pieces of this type assembled around the axes (see Fig. 4).

The CAD elements were imported in .STL format. Its geometry was simplified to quadrangles by post-processing with the application of polygon modeling. The mesh topology was also modified by trying to simplify shapes and reduce the number of vertices with triangles. For each piece, specific internal surfaces were modeled. The same modeling application with polygons of the previous stages was used. The work concluded with the redesign of the UV layouts, respecting the existing configuration for the external zone and taking advantage of the textures designed in the previous stage.

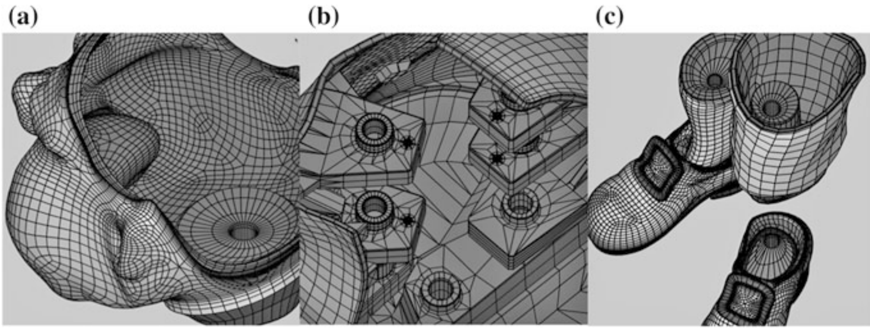

Fig. 4. Mesh details of some pieces that make up the figure. **a** Head showing the hollow interior with CAD records for the guide axis. **b** Area of the thorax in which the different support plates that were designed with CAD. **c** Shoes and legs parts, showing the registration for the guide shaft

3 Final Results of the Modeling Project

Each of the parts was tested using a specific software of the ZPrinter 650 [14] machine, to verify that it could be manufactured. The viability for printing of the patterned meshes was the general characteristic. Despite the formal viability of the process, the final set was not built due to productive considerations related to the cost: The high consumption of ceramic powder (more than 29 kg), the working time of the machine (about 140 h) and the unsatisfactory quality of the pigmentation obtained in the trials. However, a reduced copy of 200 mm was made, which was decomposed into six solid pieces (hat, head, body, legs, right-hand baton and stand) for demonstrative purposes. The pattern was used to make various audiovisual products that are shown in Fig. 5. It was exported in various 3D formats used by mobile devices to visualize augmented reality. A skeleton version was prepared to be animated and to obtain video clips. From the digital sculptures, 3D versions were obtained for their interactive evaluation in HTML and 3D PDF format.

Fig. 5. Version with articulated bones of the model used for animation. On the right display of the model in augmented reality through a mobile device

4 Last Conclusions

- The validity of the methodology has been verified by completing the geometric modeling of a product of non-conventional morphology and the advantages of using polygonal modeling versus 2D drawing in the conceptualization phase of the product.

- Modeling with polygons has also provided very satisfactory results for obtaining error-free components in additive manufacturing. It has been noted the possibility of integrating geometric elements designed with CAD, creating hybrid modeling components that can have UV layouts to represent patterns of complex color.
- The method is compatible with the simultaneous obtaining of virtual prototypes or for augmented reality.
- The technique developed allows for the design of bio-inspired and medium-sized prototype design projects. The use of color printing should be reviewed until the technology improves its chromatic quality. Methods to optimize wall thicknesses and alternatives for the creation of structures that lower manufacturing costs are also being studied.

References

1. Walters P, Huson D, Parraman C, Stanić M (2009) 3D printing in colour: technical evaluation and creative applications. In: Impact 6 International Printmaking Conference, Bristol, September 2009
2. Kitsakis K, Kechagias J, Vaxevanidis N, Giagkopoulos D (2016) Tolerance analysis of 3d-MJM parts according to IT grade. In: 20th Innovative Manufacturing Engineering and Energy Conference (IManEE 2016)
3. McHenry K, Bajcs P (2008) An overview of 3d data content, file formats and viewers. Technical Report: isda08-002 Image Spatial Data Analysis Group National Center for Supercomputing Applications, October 2008
4. Raab R, Gotsman C, Sheffer A (2004) Virtual woodwork: making toys from geometric models. Int J Shape Model 10(1)
5. Isbister K (2006) Better game characters by design. A psychological approach. Elsevier, pp 161–175
6. Wronecki J (2006) Concept modeling with NURBS, polygons, and subdivision surfaces. American Society for Engineering Education
7. WINGS 3D. http://www.wings3d.com
8. Botsch M, Pauly M, Kobbelt L, Alliez P, Lévy B, Bischoff S, Rössl C (2007) Geometric modeling based on polygonal meshes. In: Proceedings SIGGRAPH'07, San Diego, California 5–9 August 2007
9. Cashman TJ (2012) Beyond Catmull–Clark? A survey of advances in subdivision surface methods. J Comput Graph Forum 31(1)
10. Abu Rumman N, Fratarcangeli M (eds) (2017) Skin deformation methods for interactive character animation. In: VISIGRAPP 2016, CCIS 693. Springer International Publishing AG, pp 153–174
11. Nelson M (1989) Smooth appearance for polygonal surfaces. Vis Comput 5:160–173
12. Bennis C, Vézien JM, Iglesias G (1991) Piecewise surface flattening for non-distorted texture mapping. In: Proceedings of the 18th annual conference on Computer graphics and interactive techniques, SIGGRAPH'91, July 1991, pp 237–246
13. SCULPTGL. https://stephaneginier.com
14. MINIMAGICS. http://www.materialise.com/en/software/minimagics

Study of the Cylindrical Symmetry Materials Dependence with the Temperature in a Nonlinear Heat Transfer by Network Method

M. Fernández[1(✉)], J. F. Sanchez-Pérez[2], and F. Del Cerro[1]

[1] Department of Thermal Engines and Machines, Universidad de Murcia, Murcia, Spain
{martina.fernandezg, fcerro}@um.es
[2] Department of Applied Physics, Universidad Politécnica de Cartagena, Cartagena, Spain
juanf.sanchez@upct.es

Abstract. The hollow cylindrical geometry is frequently used in several heat transmission processes, such as: (i) columns in construction, (ii) cylindrical building, (iii) thermal insulation in cylindrical tanks, etc. In these constructions, several stratums usually form environments, one of them are usually the non-thermal conductor stratum (also called insulating stratum), placed in the central zone, while the others usually have other mechanical properties or chemical properties required by the design. Nowadays the insulating of cylindrical tanks is generally a great interest problem in chemical industry and energy industry because most tanks used in the industry enclose dangerous substances fluids, stored to different ranges of temperatures. The model of this cylindrical symmetry is represented by a system of coupled nonlinear equations where the material properties depend on its own temperature, such as density, specific heat and thermal conductivity, so they change when the temperature varies an therefore the behaviour of the material. In the same way, the boundary conditions also depend on the temperature, and it can differentiate between: (i) radiation, (ii) convection, (iii) constant temperature and finally (iv) radiation and convection. In this work, we study the behaviour of temperature in different cylindrical structures, solving the system of coupled nonlinear equations, and varying one of its design parameters, the kind of material, and their boundary conditions. In addition, the obtained solutions will be compared with the assumption of maintaining the material properties constant.

Keywords: Heat transmission · Cylindrical symmetry · Network Simulation Method · Non-linearity

1 Introduction

The hollow cylindrical geometry, shown in Fig. 1, is frequently used in several heat transmission processes, such as: (i) columns in construction, (ii) cylindrical building, (iii) thermal insulation in cylindrical tanks, etc. In these constructions, several stratums

F. Cavas-Martínez et al. (Eds.): *Advances on Mechanics, Design Engineering and Manufacturing II*, LNME, pp. 272–281, 2019.
https://doi.org/10.1007/978-3-030-12346-8_27

usually form environments, one of them are usually the non-thermal conductor stratum (also called insulating stratum), placed in the central zone, while the others usually have other mechanical properties or chemical properties required by the design.

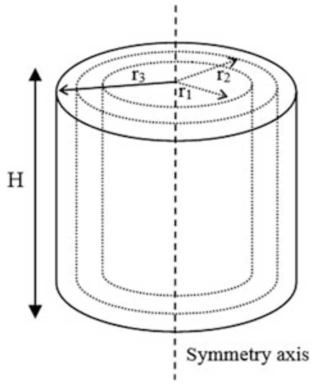

Fig. 1. Cylindrical geometry

From a structural point of view, a tank or column could be considered as a symmetric bidimensional element with two dimensions: radius and height. From a heat transmission point of view, different materials are used to isolate the tank, with the internal or external layers like insulators, depending on whether it is important to maintain a higher temperature inside the tank or vice versa.

Nowadays the insulation of cylindrical tanks is generally a great interest problem in, chemical industry and energy industry because most tanks used in the industry enclose dangerous substances. Fluids stored to different ranges of temperatures, even at high temperature, but at those degrees the materials that these tanks enclose could react in a way that this may be translated in a risk for the external environment. In the case of drinking water tanks, the temperature must be maintained in a range to avoid the growth of microorganisms. In the case of the chemical industry, these tanks should be in a specific range of temperature because of the substance they contain, since a steep rise or sudden drop of its temperature might cause a counterproductive alteration in the optimal conservation conditions of the product. For this reason, the necessity arises to find models, which satisfy the industry requirements and, obviously, will be expected that the industries have this type of tanks with the purpose of guaranteeing the complete safety of the people.

The model for this type of cylindrical symmetry is represented by a system of coupled nonlinear equations where the material properties depend on its own temperature, such as density, specific heat and thermal conductivity, so they change when the temperature varies and therefore the behaviour of the material [1]. In the same way, the boundary conditions also depend on the temperature, and it can differentiate between the following: (i) radiation, (ii) convection, (iii) constant temperature and finally (iv) radiation and convection. When two layers of the tank at different temperatures come into contact, the conduction mechanism is produced. In this case, the heat will flow from the higher temperature object to the less temperature object until to reach the thermal balance (both objects at the same temperature). However, the radiation heat transmission does not need a physical contact between the heat source and the object we want to warm. On the other hand, convection mechanism is produced by means of a fluid that transports heat between zones at different temperatures. The condition of radiation and convection is, obviously, a mixture between both that we just talked about. Finally, a constant temperature condition means that the material we are going to analyse will be at the same temperature all time.

In this work, we study the behaviour of temperature in a cylindrical structure with three different materials, solving the system of coupled nonlinear equations. We analyse a cylinder of five meters of radius and five meters of height, which has adiabatic conditions at top and bottom extreme and radiation plus convection condition at 50 °C at the right one. The left extreme is the cylinder centre and is considered with symmetry. The initial temperature of the cylinder is 25 °C. In addition, the obtained solutions will be compared with the assumption of maintaining the material properties constant. The problem is solved by the Network Simulation Method that provides all the variables involved in the process. This numerical method, accurate and reliable, is explained in detail in several papers and is run on NgSpice, a free electrical circuit simulation software [2, 3].

2 The Governing Equations

For cylindrical geometry, the heat conduction equation is the following

$$\frac{1}{\mathrm{r}}\frac{\partial}{\partial \mathrm{r}}\left(k\mathrm{r}\frac{\partial \mathrm{T}}{\partial \mathrm{r}}\right)+\frac{1}{\mathrm{r}^2}\frac{\partial}{\partial \varphi}\left(k\frac{\partial \mathrm{T}}{\partial \varphi}\right)+\frac{\partial}{\partial \mathrm{z}}\left(k\frac{\partial \mathrm{T}}{\partial \mathrm{z}}\right)=\rho\, c_{\mathrm{e}}\frac{\partial \mathrm{T}}{\partial \mathrm{t}} \tag{1}$$

Where r is the radius (m), φ is the angle (rad), z is the height (m), T is the temperature (K), ρ is the density (kg/m^3), C_e is the specific heat (J/kg K) and finally k is the thermal conductivity (W/mK).

If we consider the thermal diffusivity α (m^2/s) as:

$$\alpha=\frac{k}{Ce} \tag{2}$$

The heat conduction equation in two dimensions will finally be considered as:

$$\frac{1}{r}\frac{\partial}{\partial r}\left(r\frac{\partial T}{\partial r}\right)+\frac{\partial^2 T}{\partial z^2}=\alpha\frac{\partial T}{\partial t} \tag{3}$$

The deduction of this equation could be found in several textbooks, including [2, 4–7].

The dependent equations of temperature for density, expression (4), specific heat capacity, expression (5) and thermal conductivity, expression (6), follows the next type of model, depending on the material and the property we are going to analyse, the coefficients will change.

$$\rho(T) = a + b(T - 298) \tag{4}$$

$$c_e(T) = a + bT + cT^2 \tag{5}$$

$$k(T) = a + bT + cT^2 \tag{6}$$

3 Network Method

The network method uses the analogy between the electrical components and the physical governing equations and has been detailed in several papers and books [8, 9]. For the design of the network model expressions (2)–(6) are used, to which the boundary conditions must be added. Finally, the cylinder is spatially discretized into volume elements and time is a system variable. Moreover, this method has been used as an educational tool, Sánchez-Pérez et al. [10].

4 Results

The problem that we have proposed is a cylinder with the boundary conditions and initials specified in the introduction section. In this work, we study three materials with great differences between their properties: Aluminium A319 (LM4; Al–5Si–3Cu), Copper alloy Cu–Al (Al–bronze) and 316 stainless steel. In all cases 10 h have been simulated with the above conditions to be able to compare the behaviour between the materials.

Table 1 shows the values for the constants of Eqs. (4) and (5) considering the properties of temperature-dependent materials [1].

Table 1. Dependent properties of the temperature

Material	Property									
	Emissivity	Density (kg/m^3)			Thermal conductivity (W/mK)			Specific heat capacity (J/kgK)		
		a	b	c	a	b	c	a	b	c
Al 319	0.09	2753	−223	0	76.64	0.2633	-2×10^{-4}	747.3	0.2	5×10^{-4}
Cu–Al	0.15	7262	−486	0	7.925	0.1375	-6×10^{-5}	353	0.3	-1×10^{-4}
316 stainless Steel	0.28	7950	−501	0	6.31	0.0272	-7×10^{-6}	412	0.2	-2×10^{-5}

Table 2 shows the values for the independent properties of the temperature at 25 °C.

Table 2. Independent properties of the temperature at 298 K

Material	Property			
	Emissivity	Density (kg/m^3)	Thermal conductivity (W/mK)	Specific heat capacity (J/kgK)
Al 319	0.09	2753	137.34	851.3
Cu–Al	0.15	7262	43.57	433.5
316 stainless Steel	0.28	7950	13.79	469.8

Figures 2, 3, 4 and 5 show how the properties we have mentioned vary with the temperature from 25 to 36 °C for the three materials we are going to study.

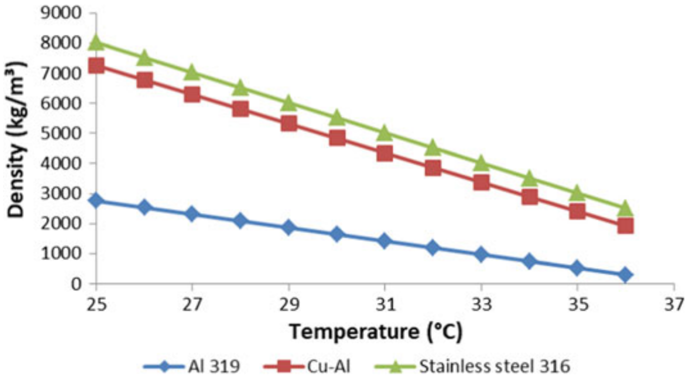

Fig. 2. Density from 25 to 36 °C

In Fig. 2, we can see how the density decreases its value in accordance with the rise of the temperature. It also shows us the differences between the three materials. We can see how Stainless Steel 316 and Cu–Al have a similar range of density while Al 319 has a density less than half of other materials.

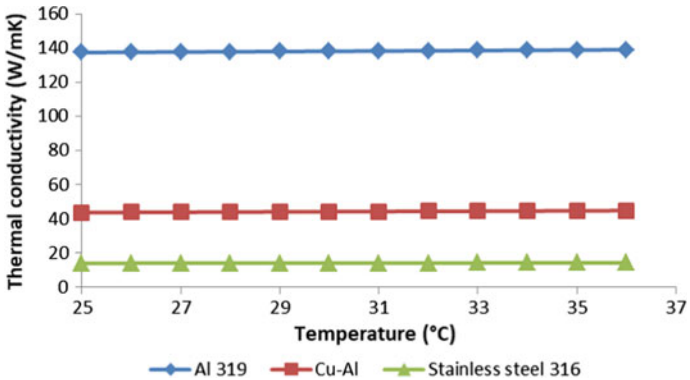

Fig. 3. Thermal conductivity curve from 25 to 36 °C

In Fig. 3, we can see how the thermal conductivity increases its value slightly in accordance with the rise of the temperature. We can see how Stainless Steel 316, which varies approximately between 13.8 and 14 W/mK, and Cu–Al, with a range between 43.6 and 44.7 W/mK, have a similar range while the value of Al 319, varies between 137 and 138 W/mK, is much bigger, about 100 points beyond the others.

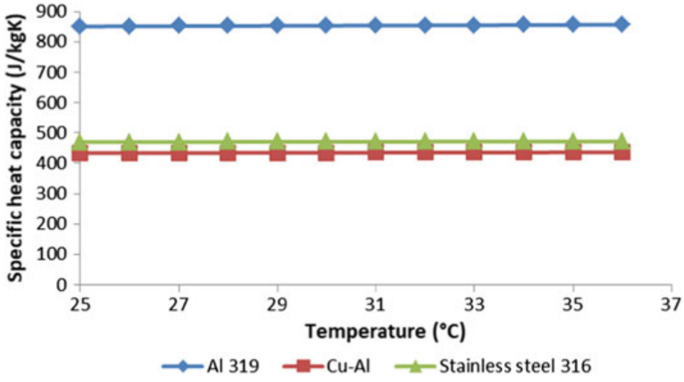

Fig. 4. Specific heat capacity curve from 25 to 36 °C

In Fig. 4, we can see how the thermal conductivity increases its value in accordance with the rise of the temperature. We can see how Stainless Steel 316, which varies approximately between 470 and 472 J/kgK, and Cu–Al, with a range between 433 and 436 J/kgK, have similar values while the value of Al 319, varies between 851 and 857 J/kgK, is much bigger, approximately twice the other values.

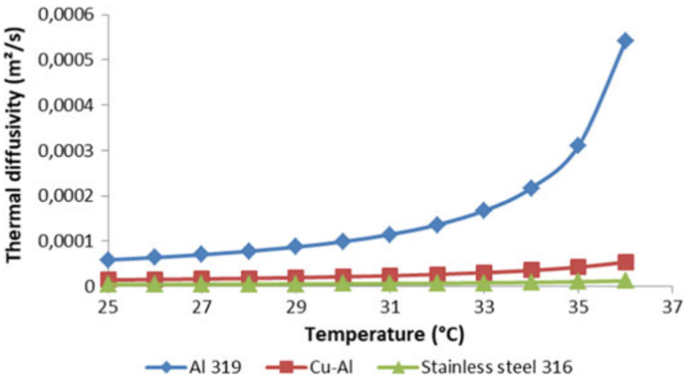

Fig. 5. Thermal diffusivity curve from 25 to 36 °C

In Fig. 5, we can see how the thermal diffusivity increases its value in accordance with the rise of the temperature. We can see how Stainless Steel 316 and Cu–Al have similar values while the value of Al 319 is much higher. For all cases studied the convective heat transfer coefficient is the same for air free convection, h = 10 W/m^2K.

In the following figures we are going to see a section of the cylinder we have simulated. The bottom and the top of the figures show the covers of the cylinder, the right side shows the exterior of the cylinder and finally, the left side represents the cylinder centre and it is considered with symmetry.

Figures 6 and 7 represent the results for the material 316 Stainless Steel. As we can see, there is a difference of approximately 0.1 m for the same temperature between constant and varying properties. In addition, we can see how varying properties reaches 6 °C more than constant properties.

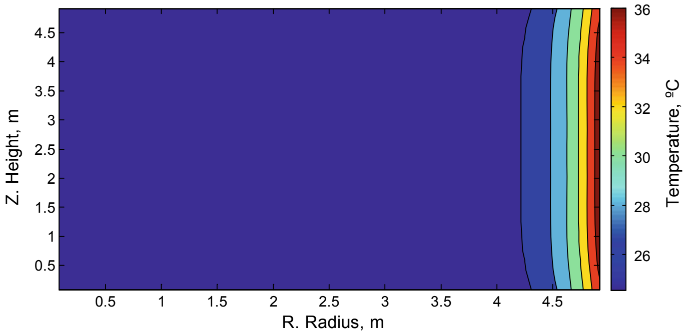

Fig. 6. Results for 316 Stainless Steel with variable properties

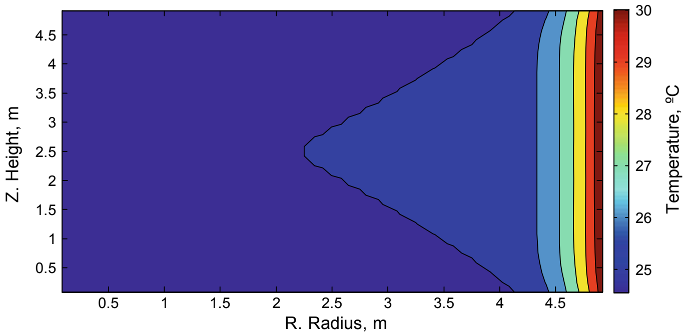

Fig. 7. Results for 316 Stainless Steel constant properties

Figures 8 and 9 represent the results for the material Cu–Al. We can see how the temperature enters into the cylinder in a similar way in both cases, reaching 26 °C at 3.75 m, with variable properties, and 3.92 m, with constant properties. The temperature raises 2 °C more for variable properties.

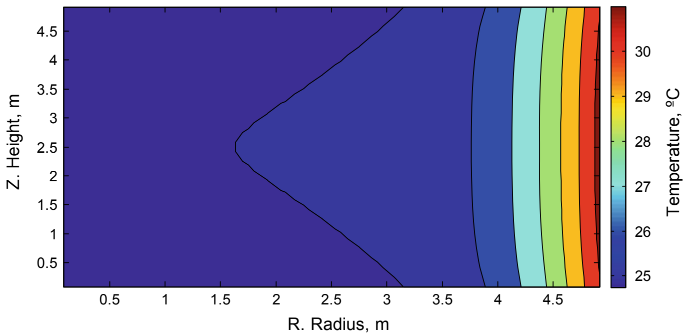

Fig. 8. Results for Cu–Al variable properties

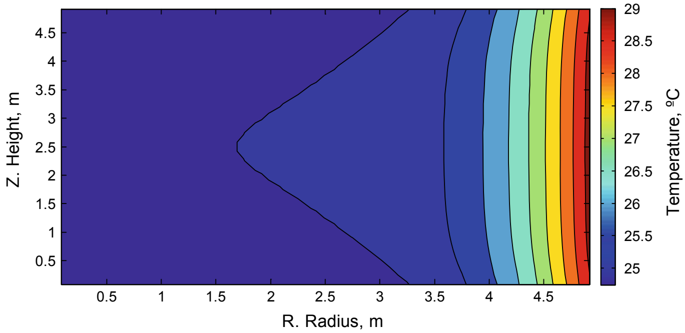

Fig. 9. Results for Cu–Al constant properties

Figures 10 and 11 represent the results for the material Al 319. We can see there is a difference of 0.5 m more or less for the same temperature, penetrating more for variable properties. We can also observe how the variation of the temperature does not affect as much as in the other materials.

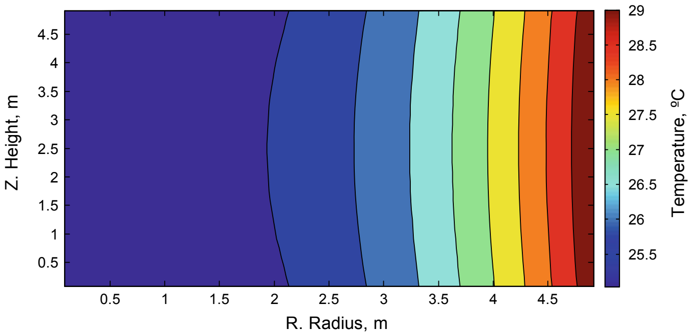

Fig. 10. Results for Al 319 variable properties

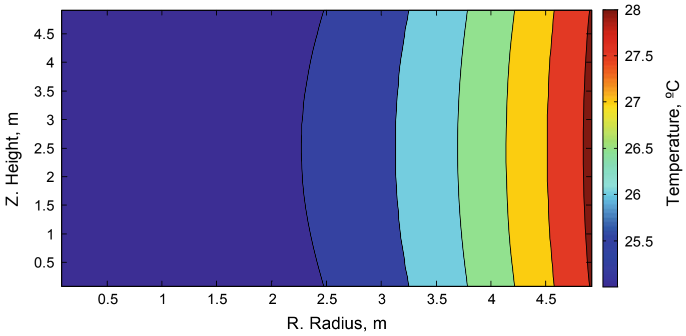

Fig. 11. Results for Al 319 constant properties

Finally, we study the behaviour of the materials for the same case. The material in which the temperature penetrates more is Al 319, followed by Cu–Al and finally Stainless Steel 316 with a difference of 1 m approximately between Al 3619 and Cu–Al and half a meter between Cu–Al and Stainless Steel. The reason for this phenomenon is the thermal diffusivity of these materials. While in Al 319 the thermal diffusivity is higher and has more variation with the increase of the temperature, Cu–Al and Stainless Steel 316 have lower thermal diffusivity. In Cu–Al we can see, in Fig. 5, how this property has an influence of the temperature while in Stainless Steel 316 this variation is negligible. That is, when the dependence of the material thermal diffusivity increases with the temperature, the results difference increases when considering the properties as constants or not, thus increasing the error committed.

The reason why the temperature increases more in Stainless Steel than in Cu–Al or Al 319 is the emissivity. If we observe the Tables 1 and 2, the material which has the highest emissivity is the Stainless Steel 316, allowing it to reach a temperature of 36 °C. Cu–Al and Al 319 has a similar value for the emissivity, reaching similar temperatures in both cases, 31 and 29 °C respectively.

5 Conclusions

After studying the same problem with three different materials, Stainless Steel 316, Cu–Al and Al 319, we can conclude how the temperature influence in the properties (density, thermal conductivity and specific heat capacity) affect the result of our problem, presenting an evident difference between taking these properties like constants or not. That is, when the dependence of the material thermal diffusivity increases with the temperature, the resulting difference increases when considering the properties as constants or not, thus increasing the error committed. It is more evident in Al 319 with a difference in temperature penetration of 0.35 m between considering the properties constant or not, since its properties are the most sensitive to the temperature variation. On the other hand, the reason why the temperature increases more in steel than in the rest of materials, is due to it has a higher emissivity and a lower thermal diffusivity.

References

1. Valencia JJ, Quested PN (2008) Thermophysical properties. ASM Handb 15:468–481
2. Chapman AJ (1984) Heat transfer, 4th edn. Macmillan Publishing Company, New York
3. NgSpice software [online]. (quoted in Mar 2018). Available online: http://ngspice.sourceforge.net/index.html
4. Özisik MN (1993) Heat conduction, 2nd edn. Wiley, New York
5. Bejan A (1995) Convection heat transfer, 2nd edn. Wiley, New York
6. Mills AF (1995) Heat and mass transfer. Richard D. Irwin Inc, Chicago
7. Incropera FP, DeWitt DP (1996) Fundamentals of heat and mass transfer. Wiley, New York
8. González-Fernández CF (2002) Heat transfer and the network simulation method. In: Horno J (ed) Network simulation method. Research Signpost, Trivandrum, pp 33–58
9. Sánchez-Pérez JF, Alhama F, Moreno JA (2012) An efficient and reliable model based on network method to simulate CO_2 corrosion with protective iron carbonate films. Comput Chem Eng 39:57–64
10. Sánchez-Pérez JF, Conesa M, Alhama F (2016) Solving ordinary differential equations by electrical analogy: a multidisciplinary teaching tool. Eur J Phys 37

Exploiting Augmented Reality to Display Technical Information on Industry 4.0 P&ID

A. Boccaccio, G. L. Cascella, M. Fiorentino, M. Gattullo(✉),
V. M. Manghisi, G. Monno, and A. E. Uva

Dipartimento di Meccanica, Matematica e Management, Politecnico di Bari,
Viale Japigia 182, 70126 Bari, Italy
michele.gattullo@poliba.it

Abstract. In this work, we present an Augmented Reality framework for handheld devices that enhance users in the comprehension of plant information traditionally conveyed through printed Piping and Instrumentation Diagrams (P&ID). The proposed framework augments on the P&ID of a plant some virtual interactive graphics (hotspots) referenced to specific components drawn on the P&ID. In this way, it is possible to easily find all the components belonging to the same category (e.g., all the pumps). By tapping, on the tablet screen, on a single hotspot further multimedia information can be displayed: technical data, 3D CAD model of the component, and 360° images of the plant section. The application is connected to the factory database where all the information associated with the plant components is stored. We used, as a case study, the cleaning section of a milling plant. With the tool presented in this work, technicians will be able to find information updated and in less time, so reducing the intervention time and increasing the accuracy of the operations. Furthermore, the cognitive load associated with the task of understanding the plant is highly reduced through the use of virtual information displayed using Augmented Reality.

Keywords: P&ID · Augmented Reality · Technical information · Industry 4.0 · Industrial plant

1 Introduction

One of the biggest impacts of the fourth industrial revolution on industrial companies is the shift from mass production to mass customization of their products. Mass customization mainly implicates the centrality of the consumer, with a revision of the production chain management models as well as the use of innovative technologies (Augmented and Virtual Reality, 3D printers, new materials, and so on). Production lines then will be suitable for rapid change in their configuration to satisfy customer requirements.

In these smart factories, plants will be even more complex, and their configuration will change over time (e.g., in case of maintenance, plant upgrade, and so on). It is important to provide operators that work on the plant always with all the updated information about it. For example, designers that are planning a new production need to

F. Cavas-Martínez et al. (Eds.): *Advances on Mechanics, Design Engineering and Manufacturing II*, LNME, pp. 282–291, 2019.
https://doi.org/10.1007/978-3-030-12346-8_28

know the layout and the interconnections between the components of the plant, maintenance operators need information about the history of maintenance of a machine, new operators need to understand how the plant is made, and so on. Currently, all this information is stored in the P&ID (Piping and Instrumentation Diagram or Process and Instrumentation Diagram). It is a drawing showing the interconnections between the equipment of a process, the system piping and the instrumentation used to control the process itself.

According to Weber [1], P&ID are widely used in the planning and maintenance in the process industry. Common tools for the creation of these graphical plans for hydraulic systems are (amongst others) Autodesk AutoCAD, Microsoft Visio, and Lucidchart. However, the representation through the P&ID of a plant is not the best visualization method, especially for complex plants. A deep knowledge of the plant is necessary to understand the function of each machine quickly. Otherwise, it would take a long time to receive all the information from the scheme. The P&ID does not contain additional information on machinery, such as the description of the machine's functionality or maintenance history. It also requires constant updating because of system modifications.

Many companies use P&ID in paper form, for which the recognition of the various components and their functions is often tied to the know-how of the technicians working in the company. To improve the comprehensibility of P&ID, other works have already been presented in the literature. Many specialists have tried to develop systems that automatically transform the P&ID from a paper to a digital form, including the automatic recognition of the component. Arroyo et al. [2] presented a method based on optical recognition and semantic analysis, which is capable of automatically converting legacy engineering documents, specifically P&ID, into object-oriented plant descriptions and ultimately into qualitative plant simulation models. Tan et al. [3] proposed a novel framework for automated recognition of components in a P&ID of raster form, based on image processing techniques to make a mathematical representation of the scanned image. They further extended this method to acquire also the connectivity among the components [4].

With this tool, technicians can easily understand the components and connections in the plants even if they do not know the coding of the symbols used in the P&ID. However, this tool does not help operators in support of decisions, since it does not provide further information, for example for the planning of maintenance procedures.

In this work, we propose to use Augmented Reality (AR) to help operators in the correct understanding of a plant and to retrieve useful information about the plant (e.g., machines layout, history of maintenance, and so on). AR has been successfully used to support operators in all the phases of the product lifecycle. Nee and Ong [5] provided a review of some studies of AR applications in manufacturing operations, such as product design, robotics, facilities layout planning, maintenance, CNC machining simulation and assembly planning. From the literature, we know that AR allows technicians to reduce intervention times, helps the learning of new technicians, improves safety in the work environment [6–8].

Uva et al. [9] used real technical drawings as a tangible interface for design review. However, they stated that a practical drawback of the system is due to the limits of the optical tracking system, based on fiducial markers printed on the drawing, which is sensitive to camera quality, calibration, illumination. In this work, we used the image-based tracking which is more stable and accurate, and it further does not imply modifications on the original drawing.

Hou et al. [10] made an experimental study to demonstrate that the AR/VR training system that they developed can enhance the quality of training with respect to traditional training paradigms, based on P&ID: it can save the manpower, decrease the travel distance during the work, reduce the learning time, and improve the learning performance. Andaluz et al. [11] developed a VR application to create virtual environments to allow undergraduate students to start familiarizing with physical connections, instrumentation, and equipment as they would be in real process. The virtual environment was created by converting a P&ID into 3D CAD models using AutoCAD Plant 3D. These training systems provide a high level of details for operators that should make step-by-step procedures on the plant. Authoring of these environments require a high effort and they are not easily updatable.

Li et al. [12] made a review of VR/AR prototypes, products and the related training and evaluation paradigms within the research and construction industry in the past two decades. They found that AR has been effectively used for on-the-job training of operators in the conversion of safety information directly from paper-based plans to actual work. It is important to note that the authors underline the concern about what kind of educational methods, theories, and tools could be smoothly embedded into VR/AR systems to improve the performance of training and education.

This concern may be solved with the development and testing of training platforms in different domains, like the one described in this work. We developed a dedicated Augmented Reality framework for efficient visualization of technical plant information, through a handheld device, augmenting the printed P&ID without modifications to the drawing. The proposed framework helps inexperienced operators to understand complex plants in less time and to retrieve technical information more efficiently and engagingly, respect to the traditional manner based on the reading from paper documents. Furthermore, technical information is always up to date thanks to the connection to a database where all the plant's data are stored.

The main features of the application that we developed are the followings:

- Displaying of virtual hotspots in correspondence of plant elements on the P&ID; the hotspots could be of assorted colors to indicate different elements: e.g., pumps, conveyors, filters, and so on.
- Filtering of the hotspots displayed at the same time, grouped either by category (e.g., all the pumps, all the conveyors, and so on) or by subsections of the plant.
- Displaying of technical information of a selected component of the plant; this could be either plate data (e.g., model number, supplier, efficiency, and so on) or history data (for example about maintenance and modifications).
- Displaying of a 3D representation of a selected component; this could be done through a 3D CAD model of the component, if available, a 3D reconstruction of a scan, or finally a 360° picture of the selected section.

2 Materials and Methods

The framework was designed using Unity 3D and Vuforia for the AR behavior. As for the tracking method, we tested both the Vumark tracking by Vuforia and the image-based tracking, using the P&ID image as trackable. The Vumark technique had the following disadvantages. To have a precise tracking, the camera must frame the Vumark, so it was hard to visualize virtual hotspots far from the Vumark on the drawing. To overcome this problem, we used the extended tracking, but there was a drift, so the location of the virtual object was not always correct. Adding Vumark on existing drawings would not be accepted by companies because it removes space for the drawing unless it was not placed in the title block. However, in this case, it was hard to track the rest of the drawing that in most cases are printed on large sheets. For these reasons we decided to use the image-based tracking using the digital version of the drawing as trackable (Fig. 1); an important remark is that all the lines in the drawing should be black in order to achieve the highest tracking quality. Black lines on white sheets are mostly used in technical drawings, according to the drawing standards (UNI EN ISO 128-20:2002), however for P&ID other line colors are often used because many lines may overlap and also to distinguish the fluids flowing.

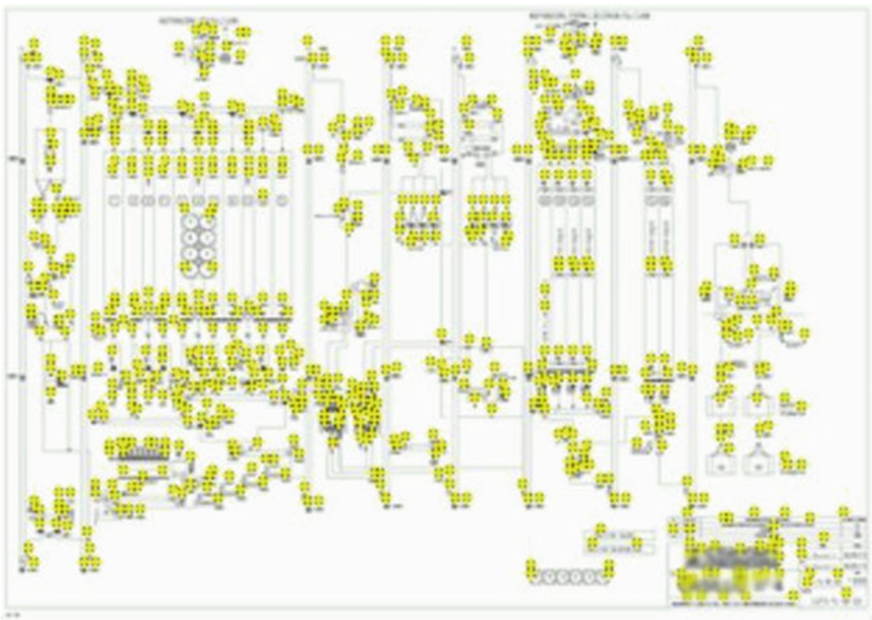

Fig. 1. Feature points used by Vuforia for the tracking

From “AutoCAD plant 3D” [13] we exported a datasheet of the (X, Y) coordinates of the plant components and they were used for the positioning of the virtual hotspots in Unity. We associated a precise color to the hotspots according to their category, as resulting from AutoCAD classification. Then, we made a script to filter the visualization of the components displayed at the same time (Fig. 2). In this way, users would have fewer troubles in the identification of components in the P&ID.

When users tap on the virtual hotspot on the device, that hotspot gets bigger, whereas the others get smaller and become not selectable, and the name of the plant component is displayed. A menu appears on the screen with three selectable buttons. We tested both 2D buttons, i.e., with a fix position on the GUI, and 3D buttons (pie menu) that are registered on the trackable as a generic virtual element (Fig. 3). In the final application, we decided to use the latter because they cause less occlusion of the real world and their usage is more intuitive since they appear just close to the selected

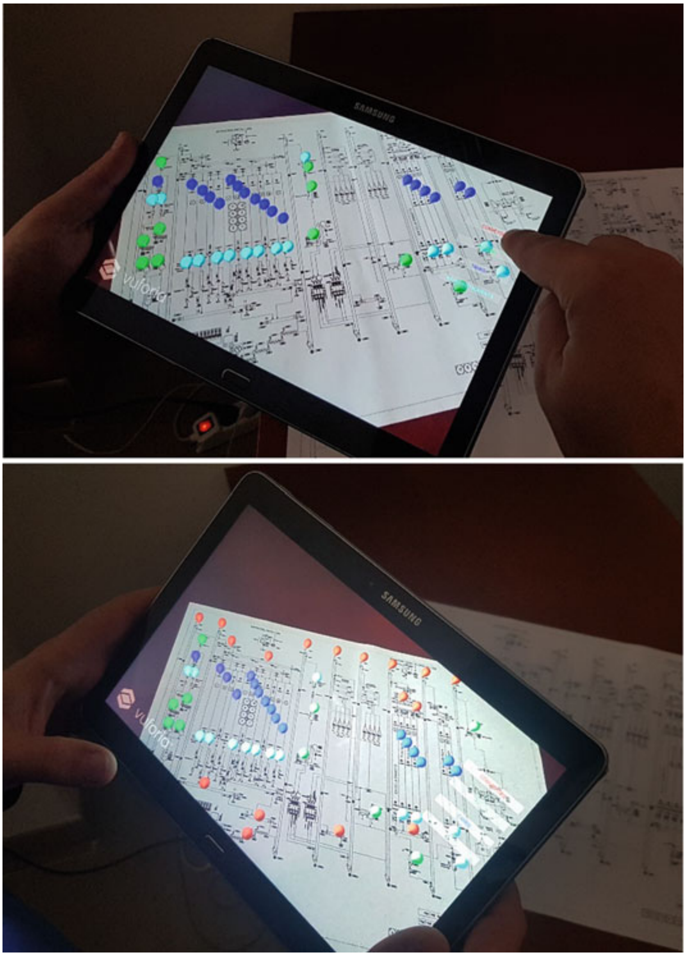

Fig. 2. Example of usage of the application: users can filter the visualization of the hotspots through a menu displayed on the GUI

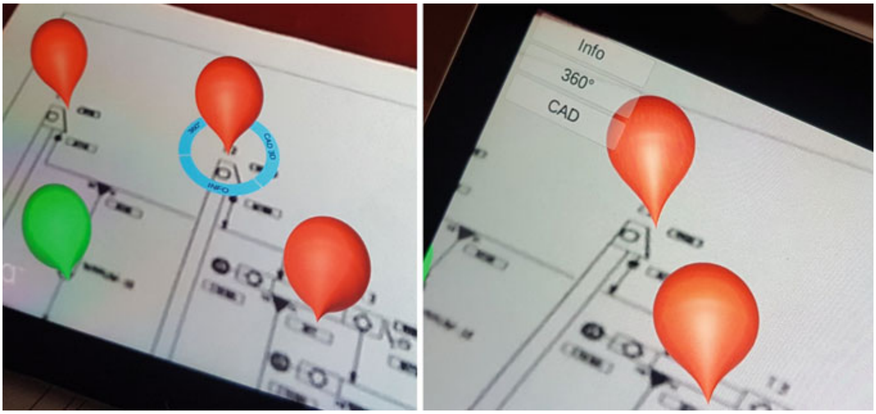

Fig. 3. Comparison of the hotspot menu layout: 3D on the top and 2D on the bottom

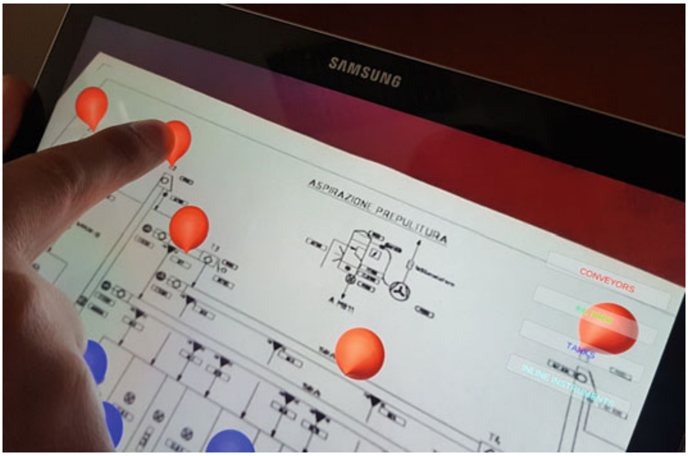

Fig. 4. User tapping on the hotspot to visualize the menu to access technical information

hotspot. When the user clicks on the hotspot, the buttons appear (Fig. 4) while clicking a second time they disappear.

A first button opens a technical chart of the component with all the information retrieved from a database (Fig. 5a). We used an SQLite database automatically generated from AutoCAD Plant 3D. The information can be added either in AutoCAD Plant 3D or in the database since they are synchronized.

A second button opens a navigable 3D CAD model of the selected component to learning how it is made (Fig. 5b). The CAD model could be either a model generated from scratch or a mesh reconstruction of a point cloud deriving from the scanning of the real machine.

Fig. 5. Visualization of additional technical information through a pie menu: a technical chart with information retrieved from a database (**a**), a navigable 3D CAD model (**b**), and a 360° image of a plant section (**c**)

A third button opens a 360° image of the component and its surroundings in the real plant (Fig. 5c). In this way, it is possible to learn how the component is connected to the rest of the plant and its real location within the plant.

3 Results and Discussion

As a case study, we tested the application developed in this work for the following scenario: inexperienced operators are asked to retrieve information on some plant components displayed on the P&ID. We simulated that they were in the plant, i.e., they could not access to personal computers, but only to paper manuals or handheld devices (smartphone, tablet). The P&ID was that of the cleaning section of a milling plant.

The AR application is the one described in Sect. 2, and the displayed hotspots are on conveyors, tanks, filters, and inline instruments. From the menu on the GUI users could display the hotspots of the desired classes, e.g., only conveyors. The pie menu allows the operators to display useful information from a database (e.g., the floor where the selected component is located), a CAD model of the component, and a 360° image of the component within the real plant. The application was tested on the tablet SAMSUNG Galaxy Note 10.1, and the smartphone OnePlus 3.

We made a study with undergraduate students to test the usability of the application and gather useful feedback to improve the application design. The task was that of finding information on five different components indicated on the P&ID.

The main results of the usability study are:

- users found the pie menu not so comfortable, especially when the button to be pressed is behind the hotspot;
- users suggested to leave the user the possibility to rotate the pie menu around the hotspot freely;
- users preferred the smartphone from an ergonomic point of view because it is more comfortable to handle;
- users preferred read information on the tablet because the screen is larger.

The case study developed is just an example of how this application could be used for the training of new operators. However, the application can also be used for other industrial activities. The other potential beneficiaries of this application are:

- Maintainers: they can know the position and all the needed information of the components to be repaired. In this way, maintenance operations would be more accurate and require less time to be accomplished.
- Designers: they can easily make changes to the layout of the plant through the correct understanding of the single components and their connections.
- Security technicians: they can be aided in the updating of the plant security devices through the knowledge of the number, location, and features of the machines.
- Supervisors: they can control the state and the history of all the machines on the plant remotely.
- Visitors: they can be trained on the functioning of the plant through a direct association between the functional information of the drawing and the real form of the components in the plant.

Our work could be integrated with the method developed by Neges et al. [14]. They proposed the synchronization of engineering data, including the P&ID, via a dynamic graph-based model. With the integration of the two frameworks, it would be possible to both visualize and manipulate in real time, the P&ID, and the related technical information. A future step of this research is that of displaying dynamic information like Key Performance Indices of the plant directly from the P&ID. Other future works will involve the optimization of the Graphical User Interface through user studies and the development of the framework on other AR devices.

4 Conclusion

In this work, we present an Augmented Reality framework for the displaying of technical information on plant components attached to the P&ID of the plant. As observed by Nakai et al. [15], sharing plant information is important for making quick decisions and prevent miscommunications. However, they proposed as a communication mean text messages and P&ID, whereas we propose to enhance the P&ID with digital and updatable information displayed in Augmented Reality with a consequent reduced cognitive load for final users, as shown by the literature in the field [7, 8, 16].

The main development issues addressed in this work, supported by a usability study, are:

- Tracking of the printed P&ID: we compared marker based-tracking with image-based tracking, choosing the second one for this application. Contrary to marker-based tracking, dozens of feature points may be found from a single image, which means that the picture can be partly covered up, and the tracking will still work. With the increased computing speeds of the processors in the modern mobile devices, the tracking speed is no longer an issue with image-based tracking, as it was in the past.
- Choice of the device for the visualization in AR: we designed an application for handheld devices since they are readier to use in an industrial context. Users did not show particular preferences for the smartphone or the tablet. In future developments, we will explore the possibility to implement this framework on other AR devices (e.g., Head-Worn displays, projection tables) with a specific study on user interaction.
- Development of a dedicated user interface: we derived the shape of the hotspot from that of web mapping services like Google Maps. We also tested two types of menu buttons, 2D and 3D, to access technical information about a specific component. We decided to use 3D buttons in the form of a pie menu since they cause less occlusion and are more engaging for the final user. However, users did not feel comfortable the pie menu, and they suggested to leave the user the possibility to rotate it freely.

References

1. Weber KH (2016) Engineering verfahrenstechnischer Anlagen: Praxishandbuch mit Checklisten und Beispielen. Springer
2. Arroyo E, Hoernicke M, Rodrguez P, Fay A (2016) Automatic derivation of qualitative plant simulation models from legacy piping and instrumentation diagrams. Comput Chem Eng 92:112–132. https://doi.org/10.1016/j.compchemeng.2016.04.040
3. Tan WC, Chen I-M, Tan HK (2016) Automated identification of components in raster piping and instrumentation diagram with minimal pre-processing. In: 2016 IEEE International Conference on Automation Science and Engineering (CASE). IEEE, pp 1301–1306

4. Tan WC, Chen I-M, Pan SJ, Tan HK (2016) Automated design evaluation on layout of piping and instrumentation diagram using histogram of connectivity. In: 2016 IEEE International Conference on Automation Science and Engineering (CASE). IEEE, pp 1295–1300
5. Nee AY, Ong S-K (2013) Virtual and augmented reality applications in manufacturing. IFAC Proc Vol 46:15–26
6. Zhu J, Ong S, Nee A (2014) A context-aware augmented reality system to assist the maintenance operators. Int J Interact Des Manufact (IJIDeM) 8:293–304. https://doi.org/10.1007/s12008-013-0199-7
7. Fiorentino M, Uva AE, Gattullo M, Debernardis S, Monno G (2014) Augmented reality on large screen for interactive maintenance instructions. Comput Ind 65:270–278
8. Uva AE, Gattullo M, Manghisi VM, Spagnulo D, Cascella GL, Fiorentino M (2018) Evaluating the effectiveness of spatial augmented reality in smart manufacturing: a solution for manual working stations. Int J Adv Manuf Technol 94:509–521
9. Uva AE, Cristiano S, Fiorentino M, Monno G (2010) Distributed design review using tangible augmented technical drawings. Comput Aided Des 42:364–372
10. Hou L, Chi H-L, Tarng W, Chai J, Panuwatwanich K, Wang X (2017) A framework of innovative learning for skill development in complex operational tasks. Autom Constr 83:29–40. https://doi.org/10.1016/j.autcon.2017.07.001
11. Andaluz VH, Castillo-Carrión D, Miranda RJ, Alulema JC (2017) Virtual reality applied to industrial processes. In: International Conference on Augmented Reality, Virtual Reality and Computer Graphics. Springer, pp 59–74
12. Li X, Yi W, Chi H-L, Wang X, Chan AP (2018) A critical review of virtual and augmented reality (VR/AR) applications in construction safety. Autom Constr 86:150–162
13. AutoCAD Plant 3D homepage. https://www.autodesk.com/products/autocad-plant-3d/overview. Last accessed 2 Mar 2018
14. Neges M, Wolf M, Abramovici M (2017) Enabling round-trip engineering between P&I diagrams and augmented reality work instructions in maintenance processes utilizing graph-based modelling. In: International Conference on Intelligent Systems in Production Engineering and Maintenance. Springer, pp 33–42
15. Nakai A, Kajihara Y, Nishimoto K, Suzuki K (2017) Information-sharing system supporting onsite work for chemical plants. J Loss Prev Process Ind 50:15–22
16. Henderson S, Feiner S (2011) Exploring the benefits of augmented reality documentation for maintenance and repair. IEEE Trans Visual Comput Graphics 17:1355–1368

A Design Approach to Support BIM for Existing Structures

P. Cicconi(✉), R. Raffaeli, and A. Borghi

Università degli Studi eCampus, Via Isimbardi 10, 22060 Novedrate, CO, Italy
paolo.cicconi@uniecampus.it

Abstract. Nowadays, Building Information Modeling (BIM) is a common design approach to support the life cycle of projects in the field of Architecture Engineering Construction (AEC). New constructions' projects require a BIM modeling to provide digital information within a 3D digital mockup. The main target is to reduce time and cost related to the elaboration of additional and not integrated documentation. This issue is also common in projects focused on the renovations of existing buildings. In fact, the BIM approach provides tools to improve interoperability between different software to integrate analysis and simulations within the architectural representation. The renovation projects require reverse engineering tools and methods for the 3D modeling of existing structures. One of the issues concerns the digital photogrammetric survey of glass surfaces. This paper proposes a design approach to support BIM phases for already existing structures with a test case focused on a hallway with a continuous glass wall.

Keywords: BIM · Steel-glass buildings · Photo survey · Photo matching

1 Introduction

Building Information Modeling (BIM) is an approach to support the design of structures in the field of Architecture Engineering Construction (AEC) [1]. This modeling approach was born about 30 years ago [2, 3]; one of the first BIM tools was ArchiCAD®, developed by Graphisoft in the 80s. However, today this method is fully developed in only few countries in the world [4], such as Anglo-Saxons nations. United Kingdom is one of the more important countries in the world for the widespread development of BIM modeling in private and public areas [1, 4, 5]. In Europe, different initiatives have been implementing [5] in Italy, Spain, French, and Germany for 5–10 years.

Nowadays, many countries require BIM models in the public procurement agreement for AEC contracts [1, 5]. This approach is not only applied for new constructions, but it is also used for renovation activities in existing buildings and cultural heritage. The necessity to use BIM models in public procurements enhances the use of it in private applications as well. This modeling approach provides many advantages [2, 5] such as a great reduction of printed documents, a good interoperability between different software-tools (such as CAD and FEM solvers), the maintenance scheduling, and the use of an Objected-Oriented model with every attribute and information. Projects of new buildings can be elaborated using BIM software and methods; however, today, many projects of

F. Cavas-Martínez et al. (Eds.): *Advances on Mechanics, Design Engineering and Manufacturing II*, LNME, pp. 292–300, 2019.
https://doi.org/10.1007/978-3-030-12346-8_29

renovation also require BIM models due to the related advantages. Even if a BIM representation can be expensive for already existing structures, the possibility to manage all life cycle [6] is a very interesting issue. The scheduling of maintenance and the possibility to integrate all project information in one file have been increasing the use of BIM in several civil applications. A BIM model is also suitable since the possibility to integrate structural and architectural models with the digital representation of piping and electrical routings (MEP, Mechanical/Electrical/Plumbing).

This paper proposes a design approach to support BIM phases for already existing AEC structures. In particular, the test case shows the interior modeling of a glass hallway. The study case is focused on the former Centro Istruzione IBM, which is a famous Italian building used by IBM as education center for its employees between 1974 and 2003. Nowadays it's the main office of the University eCampus (Fig. 1). This complex building was designed by the Italian architect Bruno Morassutti, who was a student of Frank Lloyd Wright. In 1970s this structure was considered as an icon for modern steel-glass structures.

Fig. 1. The building complex of University eCampus (architect Bruno Morassutti)

The BIM modeling of a 120-m glass hallway has been proposed in this research. In particular, the modeling starts from the photogrammetric survey of the hallway structure that represents a cheap and fast technique to obtain the 3D digital model of buildings for the BIM implementation. The complexity of this specific survey is due to the vertical glass surfaces, which don't allow the automatic meshing to be elaborated using photo matching algorithms.

The remainder of the paper consists of an introduction to the reverse engineering problems for glass facades, a description of the overall approach, and a test case with results and discussions.

2 Glass Facades: Reverse Engineering

Advanced surveying methods, as LiDAR (Light Detection And Ranging) and photogrammetry, can be used to acquire 3D geometries from physical structures, also with integrating approaches between the LiDAR data and the multi-image techniques [7, 8]. Usually, this step is the beginning of a BIM modeling related to a renovation work. However, glass surfaces, such as facades, are difficult to be elaborated using commercial instruments. LIDAR instruments cannot be applied because laser rays cross the glass plate

[9] due to transparency. On the other hand, algorithms for the automatic restitution of a photogrammetric survey present difficulty in the processing due to the glass reflection and transparency. Unfortunately, the modern architectural buildings are characterized by wide glass and reflecting surfaces, that often cover the entire structure of the buildings.

Transparent or reflective surfaces such as glass can be hardly measured with the digital image sensors and with LIDAR as well, because these surfaces can create mismatches and blunders. The reflections of the surrounding objects around a glass facade or surface can even produce ghost structures [10]. For these reasons the glass surfaces of a building façade are usually removed from the images during the matching process. As solution, this paper describes a methodological approach for the modeling of structures with vertical glass surfaces. The proposed test case shows how the combination of 3D modeling and photo matching can support the CAD representation in a BIM project for existing buildings with glass surfaces. The employment of photos in the 3D modeling activity allows the vertical parts of a structure to be easily represented into a CAD system. In fact, technical documents of existing buildings often regard drawings with sheets more focused on 2D layout than vertical structures.

3 Method

A design approach to support BIM phases for already existing buildings is described in Fig. 2. This methodology can be used for the digitalization of structures, which are difficult to be surveyed with automatic tools such as laser scanner of photogrammetry. Glass facades are an example of surfaces which cannot be recognized with automatic survey algorithms and tools. They require a manual modeling of the geometrical domain. However, the modeling phase can be supported by set of photogrammetric images. The modeling from photos is a valid practice [11] in architecture and engineering. Some commercial tools, such as Sketchup®, provide features to rapid modeling volumes and surfaces from photos. However, a methodology approach is necessary to support the complex BIM design of a structure.

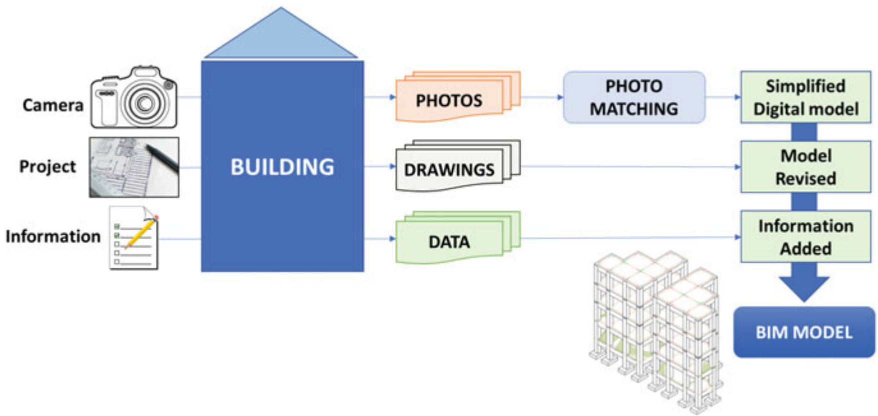

Fig. 2. The BIM modeling for an existing building

The approach, highlighted in Fig. 2, shows a mix of input to support the definition of a BIM model. Drawings and native projects are necessary to define the project layout per each building's level. General and detailed information can be gathered to be added into a BIM model. Information can regard the maintenance booklet, the list of providers, the description of materials and so on. The set of digital photos is a collection of images which can be used as a baseline point for the digital modeling. A simplified 3D digital model can be elaborated from manual or automatic photo matching. This paper proposes a manual recognition of surfaces and edges to be used in a further 3D modeling. The use of photos is important since they show the building in the present form, which can be different from the early project drawings. Therefore, the photogrammetric survey can be considered as a necessary task in the BIM modeling of existing structures. While the survey of the interior design only requires the use of traditional terrestrial cameras, cameras could be mounted on UAV (Unmanned Aerial Vehicle) platforms for the surveying of exterior design. Summarizing, modeling input consists of a set of images, technical drawings, and any information about materials, plants, maintenance, etc. These three levels of information are necessary to define a BIM model.

Figure 3 describes an example of photo matching to support the 3D modeling of a part of an interior building. In particular, Fig. 3 compares the match of a photo with the relative 3D model. The photo matching is proposed as a rapid digitalization approach to reproduce 3D bodies and surfaces into a CAD environment. The interaction between photo matching a technical 2D drawings can improve the accuracy of the resulting model. The interoperability of common BIM tools allows digital model to be imported and exported from and to different CAD platform. In fact, while some CAD tools are very suitable to draw 3D entities inside a conceptual project, other ones are better suited for the information management.

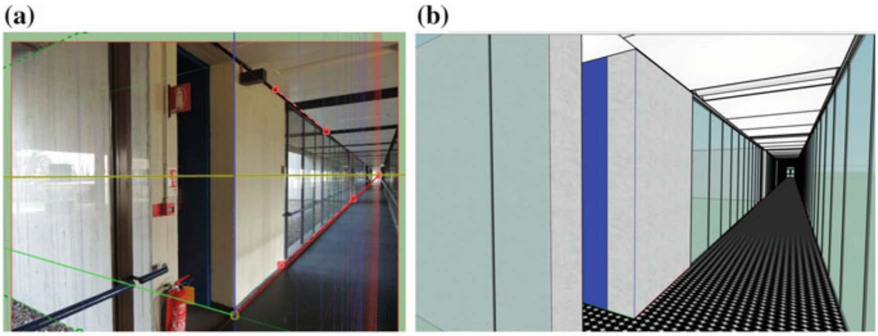

Fig. 3. Photo matching (**a**) and the resultant 3D model (**b**)

The resulting 3D representation is an interpolation between drawings and photo matching. Within the geometrical modeling phase, every necessary information should be added to the digital mockup. In fact, the BIM approach provides that each structure element is classified using an IFC (Industry Foundation Classes) description. The IFC platform is a neutral and open file format, which is has been developed by buildingSMART (also known as the International Alliance for Interoperability, IAI) and standardized by ISO 16739:2013. The IFC format is an object-oriented information which includes construction data such as geometry, manufacturing, materials, providers, and so on. The IFC structure, related to the analyzed digital mockup, encloses the digital representation with every added information.

4 Study Case

This section describes the BIM modeling of a 120-m glass hallway (Fig. 4), which is a part of the ground floor of the eCampus building (Fig. 1), as described into the introduction section.

Fig. 4. Photo of the glass hallway analyzed in the proposed paper

A BIM model related to the highlighted glass hallway has been defined as a test case. The resulting BIM model only concerns one object, which is a 120-m glass hallway related to the ground floor level of the building. However, the representation level consists of three sub-levels such as Floor System, Vertical System, and Ceiling System, as described in Fig. 5, each sub-level concerns a set of Objected-Oriented (O-O) items such as glass panel, downlight block, doors, walls, and so on. These items are components and they are classified with attributes inside the BIM model. First, a BIM component has a geometrical representation which regards the definition of the full 3D features with details about colors and constitutive parts. Then, other attributes regard variables for the resizing of a BIM component and output parameters such as weight and metric information. Finally, the last set of parameters concerns the IFC classification and the construction information related to each component.

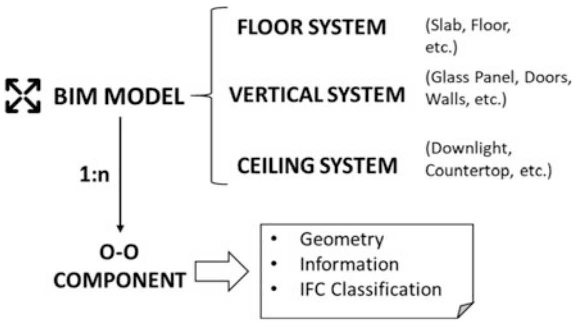

Fig. 5. The structure of the BIM model

The paper shows a BIM model defined using the Sketchup® framework. Even if Sketchup® is not formally a BIM tool, it can be involved in a BIM modeling activity due to its advantages such as rapidly, open libraries, O-O modeling approach, IFC classifier, and so on. A 3D Warehouse, with several libraries of components, allows the interior areas to be represented with a high-level of details if compared with the use of traditional BIM tools. However, customized scripts and plugin must be implemented in Sketchup® to optimize the analysis related to metrics information, cost estimation, and maintenance booklet. Therefore, Ruby scripts have been developed to perform the information management and analysis related to the BIM model proposed.

Figure 6 describes the photo survey, which was carried out for the 3D modeling. About 100 photos have been collected to support the modeling activity. As highlighted in Fig. 7, the technical drawings only describe the information concerning dimensions and layout. Additional information such as glass panels, steel frames, door type, and lighting are missing. All this information can be only added using a BIM-based approach. Therefore, while the 2D drawings have been used to reproduce the structure layout, photos have been used to complete the detailed modeling.

Fig. 6. The technical drawing and a description of the photo survey

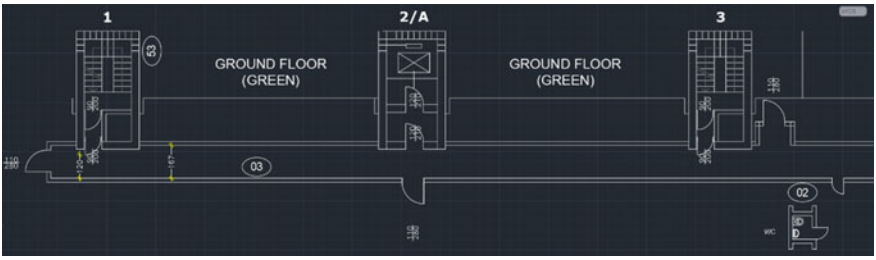

Fig. 7. Detail of technical drawing

As result, a first BIM model has been achieved for the proposes hallway. While Fig. 8 describes the internal area of the proposed hallway, Figs. 9 and 10 show the external representation with the continuous glass façade.

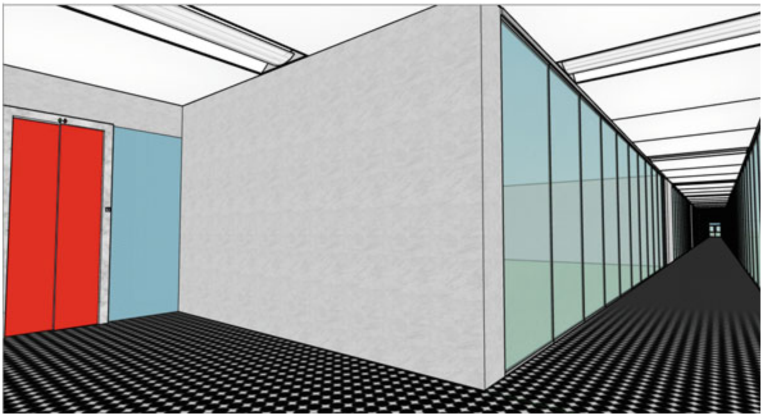

Fig. 8. An internal 3D view of the hallway area

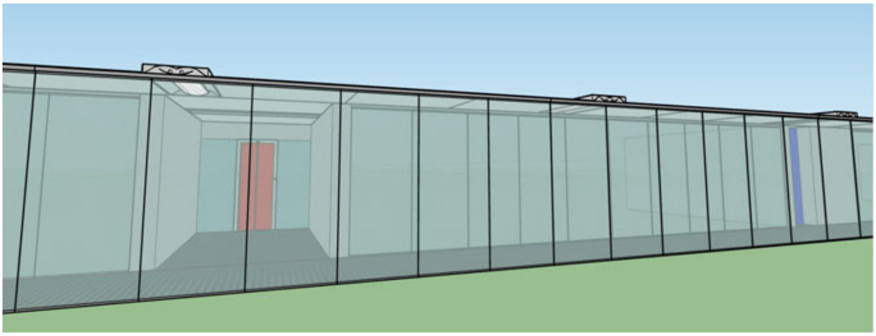

Fig. 9. An external view of the glass hallway with the glass façade

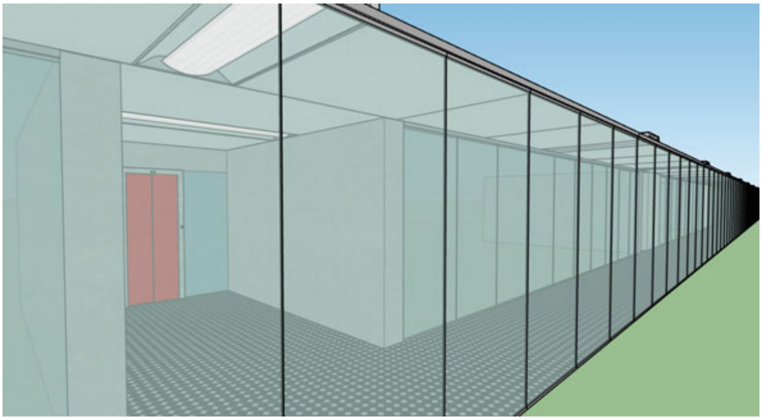

Fig. 10. The model of the glass hallway (120 m)

5 Conclusions

The paper describes a methodological approach to support the BIM modeling for existing structures. As case study, a glass structure has been proposed to show how photo matching can overcome limits related to LIDAR and photogrammetry survey for transparent surfaces. An input mix of photos and technical drawings has been applied to perform the building model of a 120-m glass hallway.

Typical modeling difficulties have been noticed during the design phase. While some of them are related to the differences between the structures and technical drawings, others concern problems in photo matching. In fact, due to the quality of interior photos, sometimes the edge recognition has been difficult to perform for the matching phase. Additionally, a computer with a good-level of performance is required for the modeling of complex structures. However, using a set of low-cost photographic images and software already known by specialists (architects and engineers), like generic CAD tools and Sketchup®, a first BIM of a part of the building has been obtained and this deliverable could be used to drive, for instance, the energetic requalification of the 70s buildings, changing the glass and their frames.

As future development, the authors would like to define a matching algorithm using Ruby programming scripts to support the automatic matching of photos during the 3D modeling phase. This approach could be applied for the exterior modeling of buildings.

Acknowledgements. The authors thank Università degli Studi eCampus for providing them data and information related to the test case proposed in this paper.

References

1. Succar B, Kassem M (2015) Macro-BIM adoption: conceptual structures. Autom Constr 57:64–79. Available at: http://dx.doi.org/10.1016/j.autcon.2015.04.018
2. Ahuja R, Sawhney A, Arif M (2017) Prioritizing BIM capabilities of an organization: an interpretive structural modeling analysis. Proc Eng 196:2–10. Available at: http://dx.doi.org/10.1016/j.proeng.2017.07.166
3. Chuck E (2011) BIM handbook, 2nd edn. Wiley
4. Kassem M, Succar B (2017) Macro BIM adoption: comparative market analysis. Autom Constr 81:286–299. Available at: http://dx.doi.org/10.1016/j.autcon.2017.04.005
5. Ciribini ALC, Mastrolembo Ventura S, Paneroni M (2016) Implementation of an interoperable process to optimise design and construction phases of a residential building: A BIM Pilot Project. Autom Constr 71:62–73. Available at: http://dx.doi.org/10.1016/j.autcon.2016.03.005
6. Matějka P, Tomek A (2017) Ontology of BIM in a construction project life cycle. Proc Eng 196:1080–1087. Available at: http://dx.doi.org/10.1016/j.proeng.2017.08.065
7. Nex F, Rinaudo F. Photogrammetric and LiDAR integration for the cultural heritage metric surveys. Int Arch Photogram Remote Sens Spat Inf Sci XXXVIII(Part 5)
8. Becker S, Haala N (2007) Refinement of building facades by integrated processing of LIDAR and image data. In: Proceedings of PIA07 (Photogrammetric Image Analysis), Munich, Germany, 19–21 September 2007, pp 7–12
9. Paulus S et al (2014) Limits of active laser triangulation as an instrument for high precision plant imaging. Sensors 14(2):2489–2509. Available at: http://dx.doi.org/10.3390/s140202489
10. Ley A, Hänsch R, Hellwich O (2017) Automatic building abstraction from aerial photogrammetry. ISPRS Ann. Photogram Remote Sens Spat Inf Sci IV-2/W4:243–250. https://doi.org/10.5194/isprs-annals-iv-2-w4-243-2017
11. Previtali M, Barazzetti L, Scaioni M (2013) Multi-step and multi-photo matching for accurate 3D reconstruction. ISPRS—Int Arch Photogram Remote Sens Spat Inf Sci XXXVIII-3/W22:103–108. https://doi.org/10.5194/isprsarchives-xxxviii-3-w22-103-2011

A Procedure for Cutting Guides Design in Maxillofacial Surgery: A Case-Study

L. Ulrich[1(✉)], F. Baldassarre[1], F. Marcolin[1], S. Moos[1], S. Tornincasa[1], E. Vezzetti[1], D. Speranza[3], G. Ramieri[2], and E. Zavattero[2]

[1] DIGEP, Politecnico di Torino, C.so Duca degli Abruzzi 24, 10129 Turin, Italy
luca.ulrich@polito.it

[2] Divisione di Chirurgia Maxillofacciale, Dipartimento di Scienze Chirurgiche, Università degli studi di Torino, C.so a. M. Dogliotti 14, 10126 Turin, Italy

[3] Dipartimento di Ingegneria Civile e Meccanica, Università degli studi di Cassino e del Lazio Meridionale, Viale dell'università, Loc. Folcara, 0304 Cassino, FR, Italy

Abstract. Surgical interventions for jaw reconstruction require the design and the production of surgical guides that allow the surgeon to operate quickly and accurately. In some cases, the reconstruction is performed by inserting a prothesis, thus operating exclusively on the jaw, while in other cases the reconstruction is performed by withdrawing and inserting part of the fibula in place of the original jaw bone. This project aims to develop a procedure that allows 3D modeling of the surgical guides necessary for surgical intervention. The idea is to find a surgical guide archetype, a starting shape for the surgeon so that the cutting planes can be oriented without the surgical guide having to be redesigned from scratch for every single patient. The first step of the procedure is the segmentation, performed applying the thresholding operation on the images provided by magnetic resonance MR in order to identify the region of interest (ROI). The second step is the reconstruction of the 3D model, so that a mesh is obtained from 2D images. Subsequently the mesh is post-processed and the cutting plans along which the surgeon will intervene are defined.

Keywords: Surgical guides · 3D modeling · 3D reconstruction · Maxillofacial surgery

1 Introduction

In surgical interventions, as in maxillofacial operations, the bones borders that have to be resected are determined by using a specific tool: the surgical guide [1]. The advantages of using them are to reduce surgical time and, most of all, enhance clinical outcomes.

Surgical guides are usually designed from scratch for each specific patient and this entails a considerable cost in terms of money and time. In particular, in case of urgent interventions, such as the removal of a mandibular tumor [2], the time to obtain a surgical guide may not be sufficient and it is necessary to search for other solutions.

F. Cavas-Martínez et al. (Eds.): *Advances on Mechanics, Design Engineering and Manufacturing II*, LNME, pp. 301–310, 2019.
https://doi.org/10.1007/978-3-030-12346-8_30

Due to these issues, the development of a procedure that leads to the modeling and printing of cutting guides [3] on site would be desirable [4]. Nowadays the cost of 3D printers has greatly decreased [5, 6] and can easily be amortized by medium-large hospital facilities.

The 3D reconstruction process of parts of human body, and in particular bone structures, is a widely dealt with topic in literature and it has been studied in deep in all the steps of the process.

Medical images are segmented to identify regions of interest (ROIs) and this can be done by choosing one of the several methods described in literature, including thresholding [7], clustering [8], edge detection [9] and region based algorithms [10].

The reconstruction step of a 3D model is performed using the marching cubes algorithm [11] implemented in many open-source [12, 13] and paid software [14].

Once the 3D model is obtained, it is possible to develop various applications, which can be helpful mainly during the diagnosis and post-intervention evaluation phase [15–17]. However, 3D modeling is not limited to the sphere of virtual visualization [18]. For several years there is the possibility of printing prostheses of an increasing number of parts of the body such as the arm [19], parts of the skull [20] tissues and organs [21] and to use rapid prototyping techniques for oral and maxillofacial surgery [22] thanks to the improving of accuracy that is growing up day by day [23]. Eventually, the 3D model could be useful in the operating room, after solving the problems linked to the sterilization phase [24].

All the steps listed above compose a procedure that nowadays is performed by different people, an issue that do not conciliate with money and time constraints. This is the reason why maxillofacial surgeons are recently dealing with software able to reconstruct 3D model of mandibula and surgical guides, obtaining interesting results in terms of speed, accuracy and satisfaction [25]. Ganry et al. [26, 27] developed a procedure to standardize the solutions advanced by few independent surgical teams for the mandibular reconstructions with the fibula free flap.

In other works, such as [28–30], the surgical guides were correlated to the pathology, presented, used and the results in terms of clinical outcomes were discussed. But these works did not describe how to obtain 3D reliable and precise information from the CT/MRI slices, how to define the cutting plane positioning and orientation and the modeling procedure of the guides based on a proper 3D geometrical definition of the models features.

In the present literature, there is lack of clear guidelines and a specific protocol for designing surgical guide with an objective methodology is desirable.

This article aims to illustrate a method for modelling surgical guides exploiting GD&T principles [31] in order to obtain a more stable tool defining proper reference system. Stability and proper positioning is a critical issue in this type of interventions due to the presence of soft tissue between the surgical guide and the bone to be resected, especially in low-curvature areas that does not constrain the degrees of freedom of the guide. Thus, a more objective definition of cutting planes positioning is provided. The method will be treated in the next section, the results will be shown in the third paragraph and in the last paragraph conclusions will be drawn.

2 Methods

Before implementing the design process, a bone model has been produced transforming TC Dicom images in a 3D mesh using open-source tools like 3DSlicer or InVesalius. After that the choice of the proper modeling environment has been considered. Some feature-based parametric CAD programs were tested for the purpose, but it resulted that the imported 3D mesh is managed as a single entity on which the common CAD operations like selection, coordinate and normal vector measurement and sectioning don't work properly. So, the testing was oriented toward 3D computer graphic applications that can properly manage mesh models and Blender [32] has been chosen as a case-study platform.

The case-study consists in resecting the lower part of the mandible due to the necrosis that is affecting the tip of the bone. Figure 1 presents a practical example for describing the design methodology and the relevant geometrical features.

The steps required to design the surgical guides are:

1. identification of the cutting plane position and orientation,
2. definition of the tangent plane where to build the guide,
3. definition of the guide block as a solid feature,
4. definition of the guide reference frame for precise positioning during the surgery operation,
5. merge of the two models,
6. formation of the fixing holes and
7. formation of the blade aperture by means of subtract boolean operation.

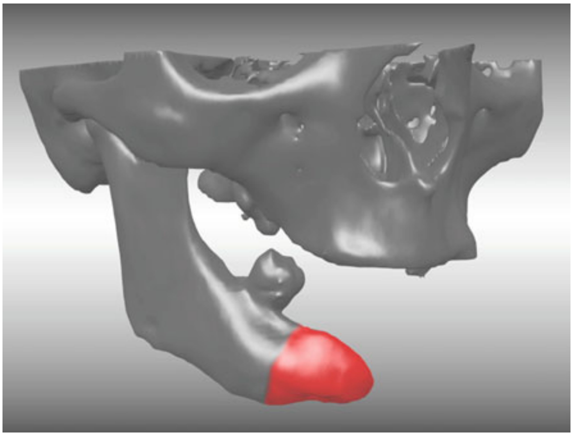

Fig. 1. Patient initial state. It was subjected to a previous surgical intervention where the mandible was resected and substituted with a metallic prosthesis. Due to complications the lower part of the other side mandible (highlighted in red) is going to be resected

In the first step the surgeon is asked to define an initial trial position for the cutting plane. This is done by using the plane manipulators in order to define the centre point O of the plane and the orientation of the plane normal vector $\vec{n}$ (local z axis). The plane normal is then automatically adjusted through the rotation around the x, y axes between a $\pm\Delta$ angle limit, with a fixed angle step set to Δ/th. For each iteration the section area is computed and the configuration giving the smallest area is assumed to be the proper orthogonal section. The resulting section area is described by a contour of connected lines, divided by point entities, as shown in Fig. 2.

The tangent plane is defined by choosing a P point in the section contour. Considering that the data set of the contour contains all the points locations and their connections it is possible to select the points preceding (P_1) and following (P_2) the point P. The orientation of the tangent vector $\vec{t}$ can be defined as the average orientation of the two vectors $\overrightarrow{P_1 - P}$ and $\overrightarrow{P - P_2}$ (which is simply $\overrightarrow{P_1 - P_2}$) then cross-multiplied with $\vec{n}$: $\vec{t} = \vec{n} \times \overrightarrow{P_1 - P_2}$.

The tangent plane is oriented with a rotation around the $\vec{t}$ vector in order to make one of its principal axis parallel to the normal plane $\vec{n}$. The rotation angle is computed as the dot product of the two vectors: $\alpha = \vec{n} \cdot \vec{t}$.

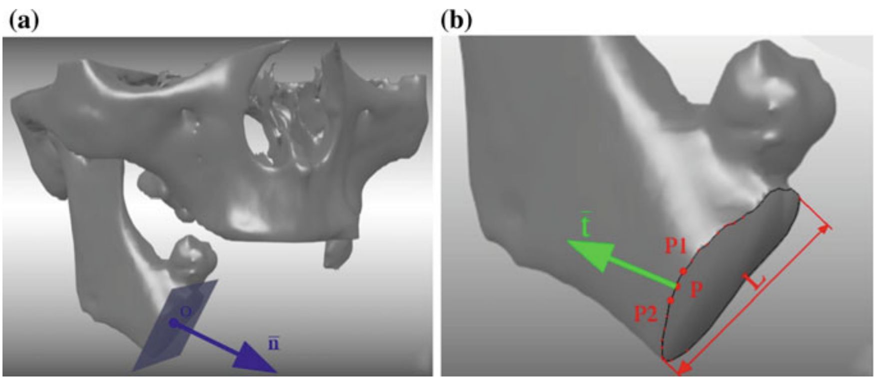

Fig. 2. Normal plane and tangent plane identification

The modeling of the guide block is now possible: upon the tangent plane, that is properly positioned, it is possible to draw the shape of the surgical guide referring to the P point and the local x, y axes for position and orientation. In the example of Fig. 3 a simple parallelepiped has been modeled: a rectangle has been centered on P, aligned with the local coordinates, with the width considering the thickness of the saw plus the thickness of the two walls on both sides and the height considering the height L of the mandible, measured from the section of Fig. 2, plus the thickness of the material above and below the saw.

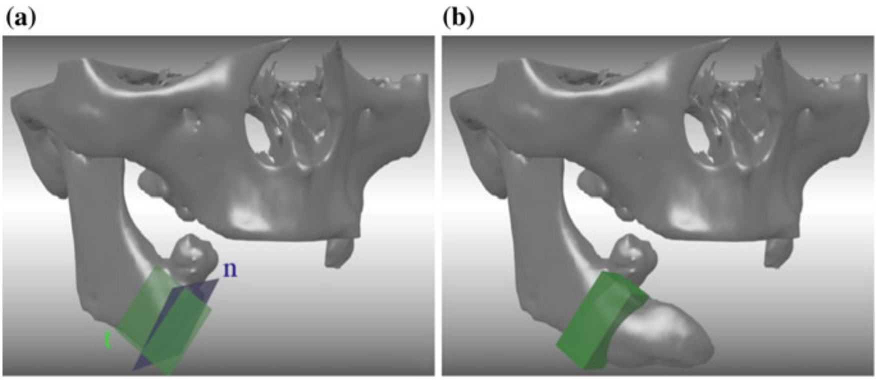

Fig. 3. Properly positioned normal and tangent planes (on the left). Extrusion of the guide block (on the right)

The rectangle is extruded in two directions: away from the mandible, to define the guide height and toward the mandible. The extrusion toward the bone has a depth greater than any gap between the tangent plan and the bone model. Using a boolean operator, the mandible is then subtracted from the guide to shape the guide block with the negative shape of the bone. This allows the proper contact of the surgical guide against the bone. The edges of the block are smoothed with a fillet.

The positioning of the guide on the mandible is another issue. The concave shape impressed on the block in that particular position is quite similar to a cylindrical surface, so it allows the translation of the block along its axis and the rotation around its axis. Depending on the surgeon intentions, two alternatives can be pursued: if the surgeon requires the possibility to adjust minutely the guide position, then the block so obtained requires only to be completed with fixing points. Otherwise, if the surgeon requires a precise and error-proof positioning, a reference frame has to be modeled.

The term “reference frame” is borrowed from GD&T definition of the international standards ISO-16792 (and related norms) or ASME Y14.41. Here the goal is to define a set of geometrical features (planes, axes, points) that can be used to build a coordinate system on which both the part to be measured and the measurement system are aligned and zeroed. Suggestions on how to define a stable, repeatable and exact constraint[1] datum reference by selecting appropriate geometrical entities can be found in Refs. [33, 34].

Figure 4 shows the geometrical entities that are relevant for this work:

1. The principal datum *A* is the lateral surface of the mandible. It is to be approximate to a plane to plane constraint because of its low curvature. This orients the guide in the space and removes three degrees of freedom: the object will be able to translate along two directions tangent to the plane and rotate around its normal.

[1]With an exact constraint all the 6 degrees of freedom of an object in the Cartesian space are locked.

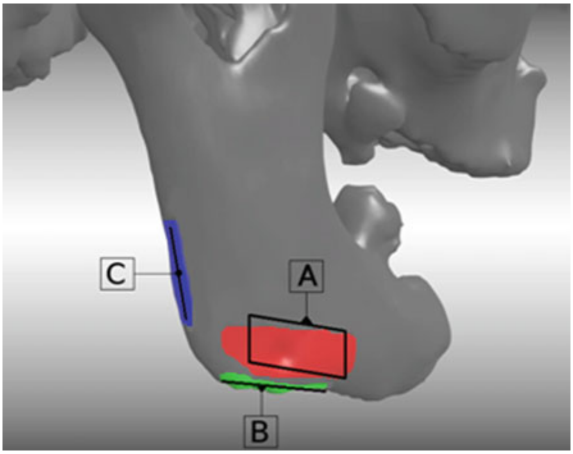

Fig. 4. Rear view of the mandible with the features defining the reference system

2. The secondary datum *B* is the lower border adjacent to the mandible angle. This can be simplified as a line to line contact, removing two further degrees of freedom and locating the object in a precise position in the principal plane. The object will be only able to translate along this axis.
3. The tertiary datum *C* will be a contact point on the rear vertical border adjacent to the mandible angle. This will remove the last degree of freedom, locking the object in a precise position along the secondary axis.

The selected geometrical features can properly orient and locate the surgery guide against the real mandible.

The corresponding surfaces are selected in order to build the reference part of the surgical guide. The surfaces need to be offset from the bone model through the implementation of a scale operation: the scale center is automatically placed in the center of mass of the model, given the distance d of one model point from the origin, the scaled measure will be: $d' = d * s$ with s the scale factor. The wall thickness of the reference body is $th = d' - d = d(s - 1)$. Inverting this, it is possible to obtain the scale factor required to build a wall of a chosen thickness: $s = \frac{th}{d} + 1$.

The so scaled surface presents an offset from the mandible model equal to the thickness of the reference body. It is sufficient to extrude the surface along the principal direction or the normal (mean) vector of the principal datum surface to produce the desired model as shown in Fig. 5.

The last step requires to join the two bodies and then cutting the blade aperture the fixing holes. The tangent plane and its insertion point are used again to draw the rectangle of the blade cutout. This is extruded in both direction and subtracted from the guide. Holes are sketched as circles on the tangent plane, then extruded as cylinders and cut from the guide volume. The final result is shown in Fig. 6

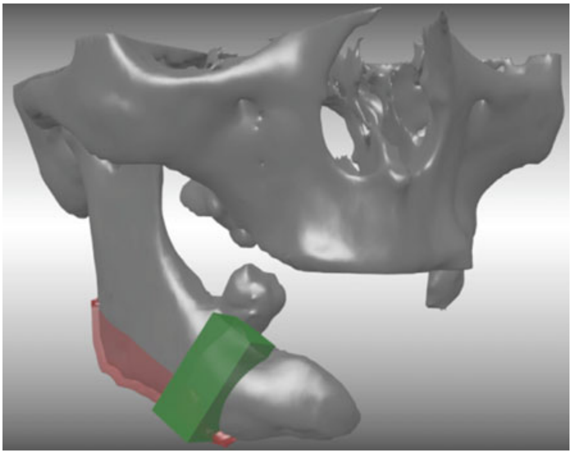

Fig. 5. Scaling and extrusion of the reference part (in red), overlapping the guide block (green)

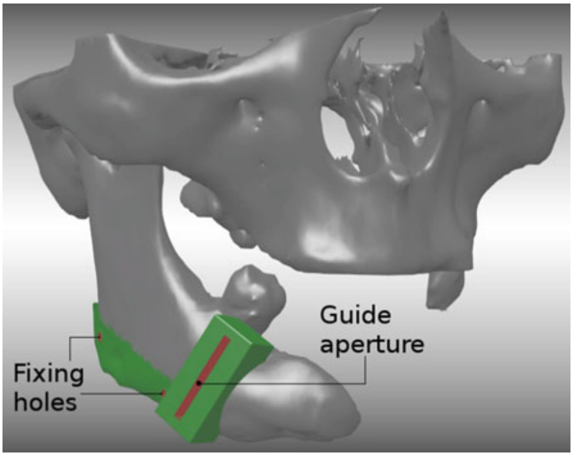

Fig. 6. Final surgical guide. Reference and block parts were joined, fixing holes and blade cutout were added

3 Results and Discussion

Following the procedure described in the previous section a surgical guide for the resection of a mandible affected by necrosis has been modeled in about 4 h. The patient had complications due to a previous prothesis implant intervention, nevertheless the modelling of the surgical guide explained above focused on the remaining right part of the mandible.

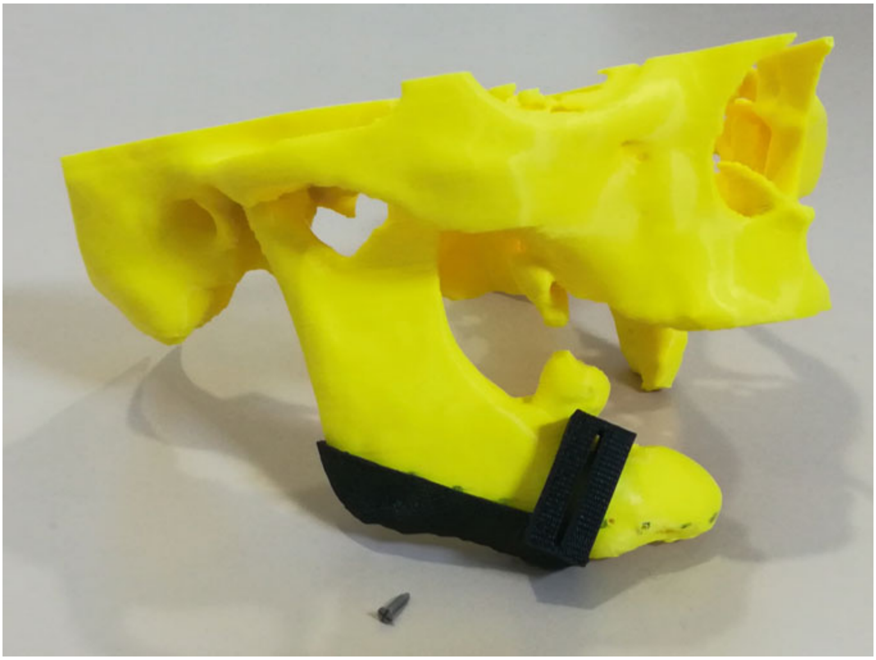

Fig. 7. 3d printed model of the surgical guide

The surgical guide has been obtained conciliating GD&T principles, in order to achieve a better fit between the guide and the bone surface thus a better stability, and the surgeon's need of customize the guide for the specific patient. For this purpose, the cutting plane positioning and orientation refer to the surgeon and the guide is modelled considering his choices and a proper geometrical description. The lack of a proper data structure able to implement feature-based parametric modelling requires to partially or totally erase the geometry and rebuild it if an optimization change is required. So, the procedure is not completely automatic, an issue that will be faced in future work.

However, the surgical guide has been theoretically validated by surgeons and a picture of the 3D printed model is the underlying Fig. 7.

4 Conclusions

This case-study aims to illustrate the design of a surgical guide exploiting geometrical features of the mandible surface and to draw the guidelines for standardize the procedure. The model obtained has been positively evaluated by the medical team, then 3D printed and finally validated by the surgeons. Indeed, it is going to be used on the actual case to perform the resection of the mandible area affected by necrosis.

The future work will be focused on two different directions. Firstly, the procedure will be tested on a more extended set of case studies. Then, it will be simplified automatizing the single steps required for obtaining the 3D model. Finally, a Principal

Component Analysis will be performed to achieve an archetype of surgical guide, a baseline for the modelling process. A Cluster Analysis could be required if morphological differences between various mandibles will result too wide, the overwhelming likelihood due to different patients' categories and pathologies.

Acknowledgements. The research work reported here was carried out thanks to a productive collaboration between the Polytechnic of Turin and the maxillofacial surgery department of Molinette hospital of Turin.

References

1. Yuan X, Xuan M, Tian W, Long J (2016) Application of digital surgical guides in mandibular resection and reconstruction with fibula flaps. Int J Oral Maxillofac Surg 45 (11):1406–1409
2. Tanaka N, Murata A, Yamaguchi A, Kohama G (1999) Clinical features and management of oral and maxillofacial tumors in children. Oral Surg Oral Med Oral Pathol Oral Radiol Endod 88(1):11–15
3. Rengier F, Mehndiratta A, Von Tengg-Kobligk H, Zechmann CM, Unterhinninghofen R, Kauczor HU, Giesel FL (2010) 3D printing based on imaging data: review of medical applications. Int J Comput Assist Radiol Surg 5(4):335–341
4. Louvrier A, Marty P, Barrabé A, Euvrard E, Chatelain B, Weber E, Meyer C (2017) How useful is 3D printing in maxillofacial surgery? J Stomatol Oral Maxillofac Surg 118(4):206–212
5. Canessa E, Fonda C, Zennaro M, Deadline N (2013) Low--cost 3D printing for science, education and sustainable development. Low-Cost 3D Printing 11
6. Dupret-Bories A, Vergez S, Meresse T, Brouillet F, Bertrand G (2017) Contribution of 3D printing to mandibular reconstruction after cancer. Eur Ann Otorhinolaryngol Head Neck Dis
7. Otsu N (1979) A threshold selection method from gray-level histograms. IEEE Trans Syst Man Cybern 9(1):62–66
8. Ng HP, Ong SH, Foong KWC, Goh PS, Nowinski WL (2006) Medical image segmentation using k-means clustering and improved watershed algorithm. In: 2006 IEEE Southwest Symposium on Image Analysis and Interpretation, March 2006, pp 61–65
9. Muthukrishnan R, Radha M (2011) Edge detection techniques for image segmentation. Int J Comput Sci Inf Technol 3(6):259
10. Kamdi S, Krishna RK (2012) Image segmentation and region growing algorithm. Int J Comput Technol Electron Eng (IJCTEE) 2
11. Lorensen WE, Cline HE (1987) Marching cubes: a high resolution 3D surface construction algorithm. In: ACM siggraph computer graphics, vol 21, no 4. ACM, pp 163–169
12. https://www.slicer.org/. Last accessed 4 Mar 2018
13. https://www.cti.gov.br/pt-br/invesalius. Last accessed 4 Mar 2018
14. http://www.osirix-viewer.com/. Last accessed 4 Mar 2018
15. Vezzetti E, Nasi A, Ramieri G, Tornincasa S, Verze L (2005) Methods to measure 3d changes after facial surgery
16. Massè A, Aprato A, Tornincasa S, Vezzetti E, Marcolin F, Ulrich L (2017) Il ruolo della simulazione 3D per gli interventi all'articolazione coxofemorale. Il Progettista Industriale 3
17. Massè A, Giachino M, Vezzetti E, Ulrich L, Aprato A, Palmesino F (2017) The limits and future of collision models

18. Zavattero E, Garzino-Demo P, Fasolis M, Ramieri G (2015) To computer-aided design and manufacturing or not to computer-aided design and manufacturing? Free fibula flap with computer-aided technique for mandibular reconstruction. J Craniofac Surg 26(3):e206–e209
19. Gretsch KF, Lather HD, Peddada KV, Deeken CR, Wall LB, Goldfarb CA (2016) Development of novel 3D-printed robotic prosthetic for transradial amputees. Prosthet Orthot Int 40(3):400–403
20. Ho CMB, Ng SH, Yoon YJ (2015) A review on 3D printed bioimplants. Int J Precis Eng Manuf 16(5):1035–1046
21. Ventola CL (2014) Medical applications for 3D printing: current and projected uses. Pharm Ther 39(10):704
22. Mehra P, Miner J, D'Innocenzo R, Nadershah M (2011) Use of 3-d stereolithographic models in oral and maxillofacial surgery. J Maxillofac Oral Surg 10(1):6–13
23. Chai Y, Li RW, Perriman DM, Chen S, Qin QH, Smith PN (2018) Laser polishing of thermoplastics fabricated using fused deposition modelling. Int J Adv Manuf Technol 1–8
24. Shaheen E, Alhelwani A, Van De Casteele E, Politis C, Jacobs R (2018) Suppl-1, M3: evaluation of dimensional changes of 3D printed models after sterilization: a pilot study. Open Dent J 12:72
25. Ganry L, Hersant B, Bosc R, Leyder P, Quilichini J, Meningaud JP (2018) Study of medical education in 3D surgical modeling by surgeons with free open-source software: example of mandibular reconstruction with fibula free flap and creation of its surgical guides. J Stomatol Oral Maxillofac Surg (2018)
26. Ganry L, Hersant B, Quilichini J, Leyder P, Meningaud JP (2017) Use of the 3D surgical modelling technique with open-source software for mandibular fibula free flap reconstruction and its surgical guides. J Stomatol Oral Maxillofac Surg 118(3):197–202
27. Ganry L, Quilichini J, Bandini CM, Leyder P, Hersant B, Meningaud JP (2017) Three-dimensional surgical modelling with an open-source software protocol: study of precision and reproducibility in mandibular reconstruction with the fibula free flap. Int J Oral Maxillofac Surg 46(8):946–957
28. Caiti G, Dobbe JGG, Strijkers GJ, Strackee SD, Streekstra GJ (2017) Positioning error of custom 3D-printed surgical guides for the radius: influence of fitting location and guide design. Int J Comput Assist Radiol Surg 1–12 (2017)
29. Mihai ID, Mihai R, Vartolomei C, Comaneanu RM, Coman S, Ghergic DL. Study about the precision of surgical guides used in implantology
30. Ruljancich K (2018) Implantology in oral & maxillofacial surgery. The complexity of 'simple' cases. Aust Dent J 63:S27–S34 (2018)
31. Krulikowski A (2012) Fundamentals of geometric dimensioning and tolerancing. Cengage Learning
32. https://www.blender.org/
33. Krulikowski A (1999) Advanced concepts of GD&T: based on ASME Y14. 5M-1994. Effective Training Inc., Wayne
34. Wu Y, Gu Q (2016) The composition principle of the datum reference frame. Proc CIRP 43:226–231

An Integrated Approach for Shape Optimization with Mesh-Morphing

M. Calì[1], S. M. Oliveri[1], M. Evangelos Biancolini[2], and G. Sequenzia[1](✉)

[1] Dipartimento di Ingegneria Elettrica, Elettronica ed Informatica (DIEEI), Università degli Studi di Catania, Viale Andrea Doria 6, 95125 Catania, Italy
gsequenzia@dii.unict.it

[2] Dipartimento di Ingegneria dell'Impresa (DII), Università degli Studi di Roma "Tor Vergata", via del Politecnico 1, 00133 Rome, Italy

Abstract. Although the CAD parameters allow to update easily the geometrical model, the numerical models updating into Finite Elements (FE) software with different mesh result to be often heavy, due to the necessity both to create new mesh and to make usually time consuming and complex CAE calculations for updating the loading conditions. The aim of the present research is to devise a reliable methodology and at the same time to reduce computational burden in the shape optimization studies of mechanical components. In particular, an integrated Multibody (MB) and Mesh-Morphing (MM) approach was developed to perform shape optimization, in order to reduce maximum tensions. Using the *RBF Morph ACT Extension* plugin implemented in the commercial solver FEM ANSYS® Mechanical vers. 18.2 along with the commercial MB software MSC ADAMS® vers. 2017, shape optimizations can be obtained in a very short time, by acting directly at the mesh so updating node positions and mesh elements geometry without bringing different geometrical models of the component into the FE environment. To validate the methodology, a crankshaft for a high performance Internal Combustion Engine (I.C.E.) was chosen, as case study, to optimize the fillet zones between web and pin.

Keywords: FEA · Multibody · Stress analysis · Fillet zones · Crankshaft

1 Introduction

Crankshaft is one of the most characteristic components of an internal combustion engine due to its role in the transmission of motion and the complex issues surrounding its development, which involve important decisions and challenges in terms of structure and vibration [1, 2]. Considering the design of such a component, it appears evident that the crankshaft can not be studied alone, since it is strongly affected by the presence and behaviour of the main bearing, connecting rod and the crankcase [3, 4]. Such a system, considered as a whole and from a dynamic point of view, represents a continuous system containing deformable bodies and should be studied like this in the determination of the equations that constitute its mathematical model [5]. This approach leads to considerable complications in calculation, which can be solved only

F. Cavas-Martínez et al. (Eds.): *Advances on Mechanics, Design Engineering and Manufacturing II*, LNME, pp. 311–322, 2019.
https://doi.org/10.1007/978-3-030-12346-8_31

in a limited number of cases by means of multibody codes. In addition, the differential equations that constitute the mathematical model can rarely be integrated and the problem is even more aggravated by the presence of difficult boundary conditions. The solution of dynamic problems in complex structures by models related to the continuous systems is therefore excluded in most cases of practical interest. The methodology for resolving complex dynamic problems encountered in the design step is usually addressed by building models based on the discretization of continuous systems which also include so-called lumped parameter models and finite element models. From the point of view of the vibration, the inertial and active forces of reciprocal elements exerted on the crankshaft constitute a system of forces the resultant of which is not zero and is variable in time [6]. The decoupling between the axial, torsional and bending behaviour is not possible, if not as a rough approximation, and the vibration modes become complicated. There are several studies in literature, some of which are recently published, aimed at modelling the crankshaft and various elements connected to it, particularly with regard to the simulation of the dynamic behaviour for fatigue analysis [7, 8], to reduce consumption and emissions [9], to improve performance [10, 11] and to reduce manufacturing cost [12].

The modeling and simulation process often involves many iterations of geometric design changes. Geometric parameters are driven automatically via an optimization procedure and the ability to automatically update an existing mesh to conform to a modified geometry is a necessary capability to enable rapid prototyping of many alternate geometric designs [13]. The main mesh update methods are mesh morphing [14, 15], mesh warping [16, 17], or mesh moving [18]. These algorithms first maintain constant mesh topology, while computing new locations for mesh nodes in order to conform to geometry changes.

The aim of the present research is to devise a reliable methodology and at the same time to reduce the computational burden in geometric optimization studies of machine components. An integrated MB and MM approach was developed and applied to optimize the fillet zones in a crankshaft for high performance I.C.E. Using the commercial software MSC ADAMS® vers. 2017 and the plugin *RBF Morph ACT Extension* implemented in the commercial solver FEM ANSYS®. Mechanical vers. 18.2, the dynamic loads, being applied to the crankshaft, were calculated and shape optimization was obtained acting directly on the mesh, so updating the nodes positions and the mesh components geometries, without bringing the geometrical model of the component into FE environment.

2 Method

As previously stated, the proposed methodology has provided the use of two different computational models. The first multibody model with concentrated parameters (lumped parameters model) has allowed the dynamic vibration analysis of the crankshaft to be performed by evaluating the forces which act on bench and crank pins under exercise conditions. The second model, the one with finite elements, has allowed to perform the shape optimization evaluating the stresses and related safety coefficients. In Fig. 1 the workflow of the used methodology is shown.

By following the procedure described in [1], the dynamic boundary conditions acting on the shaft through the multibody simulation carried out with the commercial software MSC ADAMS® vers. 2017 have been evaluated. In particular, the forces acting on bench and crank pins have been analyzed dynamically both at steady and transient speeds considering both the RPM acceleration and deceleration cases. These forces, as illustrated in Fig. 2 for the case of maximum constant speed equal to 8000 rpm, have been verified and compared with those provided by Fiat Chrysler Automobiles (FCA).

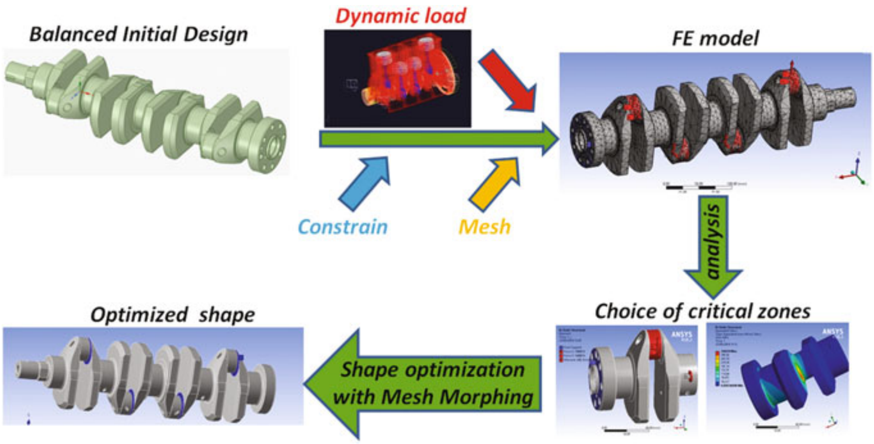

Fig. 1. Work flow of the implemented methodology

By applying the so calculated forces to the FE model, shape optimization was possible using the mesh morphing method. The stages which have occurred in the shape optimization process are briefly described as follows.

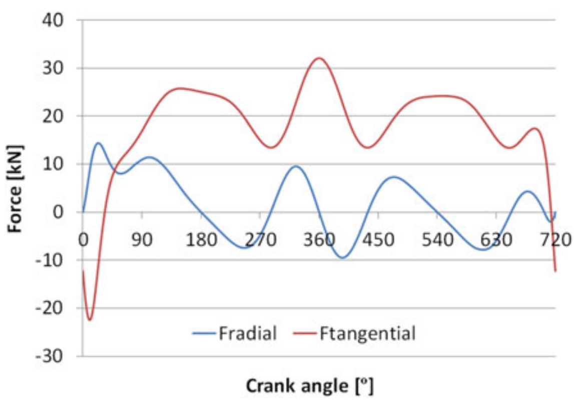

Fig. 2. Loads on crank pins integral with the crank computed with MB

In the first step the status of tension of the shaft has been considered. This analysis has brought forth that the most stressed segment of the shaft is the one of the extremity between the force outlet and the beginning of the consecutive span (Fig. 3a). The maximum tension concentration (according to von Mises) mainly resides in the junction zone between the web and the crank pin (Fig. 3b).

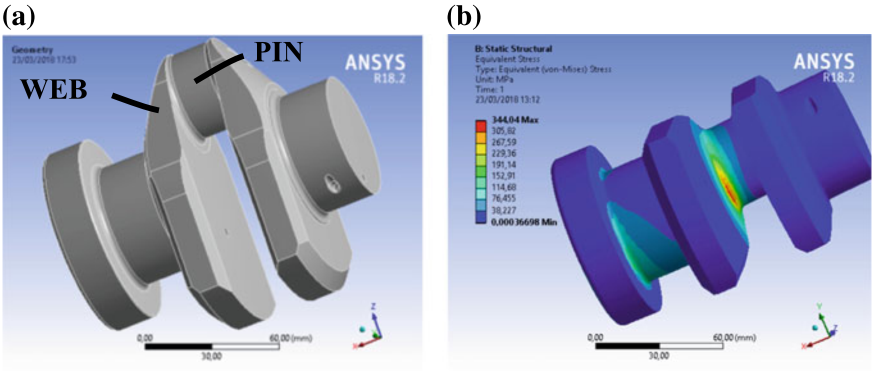

Fig. 3. Most stressed segment in crankshaft: **a** 3D model. **b** von Mises equivalent stress

After locating the most stressed area, the geometry of the critical volume, that is to say the volume where to act by operating the shape optimization minimizing tensions, is defined. By using the mesh morphing method, the parameters of this volume are stated geometrically. Such a plugin is based on the mathematics theory of the Radial Basic Functions (RBF) [19]. The RBF are recognized as belonging to the best mathematics tool for the mesh morphing. It is a powerful and versatile tool which was introduced to solve multidimensional interpolation problems able to interpolate a function defined at discrete points everywhere in the space, keeping the precise value of this at the starting points (origin points).

The choice of the maximum and minimum dimensions of the geometric parameters which characterize such a volume has appeared to be very important for the further phase of discretization (mesh creation) of the component to be optimized. In particular, the mesh optimum dimension (mesh size) in the critical volume (shape optimization area) is strictly linked to the characteristic dimensions of this volume. The present study has enabled to obtain the following empirical formula:

$$ms_{\min} \leq \frac{l_{\min}}{5} \tag{1}$$

This relation has permitted to assign the mesh size in the critical volume (shape optimization area) by allowing the elements to warp in a regular way. Being *ms* the mesh size of the elements in mm and l_{min} the length in mm of the smallest feature among those in the main directions which characterize the geometry of the critical volume.

Having studied in the analyzed case the maximum tension concentration according to von Mises in the junction zone between the web and crank pin, the chosen critical volume has been the one indicated in Fig. 4a, characterized outside by a cylindrical crown with a parabolic section.

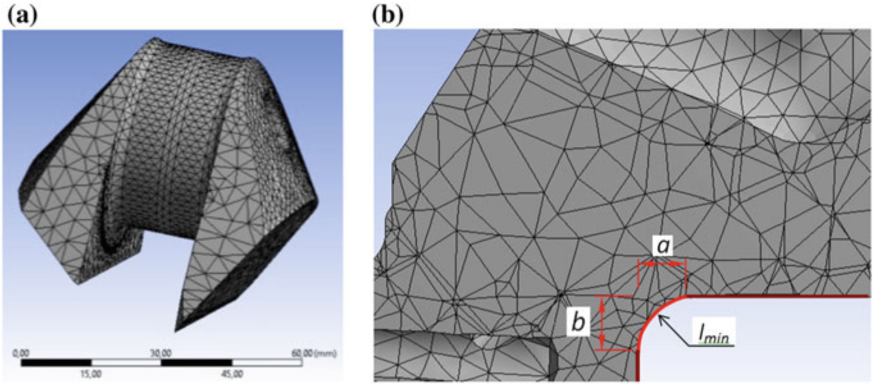

Fig. 4. **a** Critical volume. **b** Geometric parameterization

Being the initial value of l_{min} 6 mm (Fig. 4b), the length ms_{min} is thus:

$$ms_{min} \leq \frac{6}{5} = 1.2 \text{ mm} \tag{2}$$

The geometric parameter definition has been carried out through the a and b parameters as shown in Fig. 4b. In particular, fillet zone has been modelled through a parabolic profile, providing parameters for the position of the tangency point on the generatrix of the crank pin (parameter a) and the position of the tangency point in the radial direction on the web (parameter b). This parabolic profile has allowed to model by means of NURBS the external surface of the critical volume.

Table 1. Range of optimization parameters

Optimization parameter	Initial value	Minimum value	Maximum value
a	3.5	2.5	4
b	3.5	2.5	6

In Table 1 the initial design values of the geometric parameters to be optimize and their variation ranges are indicated.

In Fig. 5a the mesh of the whole segment of the shaft is illustrated; it consists of 118484 node and 70913 Tet 10 element. The min mesh size and max mesh size are 0.18 mm and 1.2 mm respectively. In Fig. 5b, the limits correspondent to the minimum values and to the maximum values of the geometric parameters of the critical volume are indicated with red and blue circles, respectively.

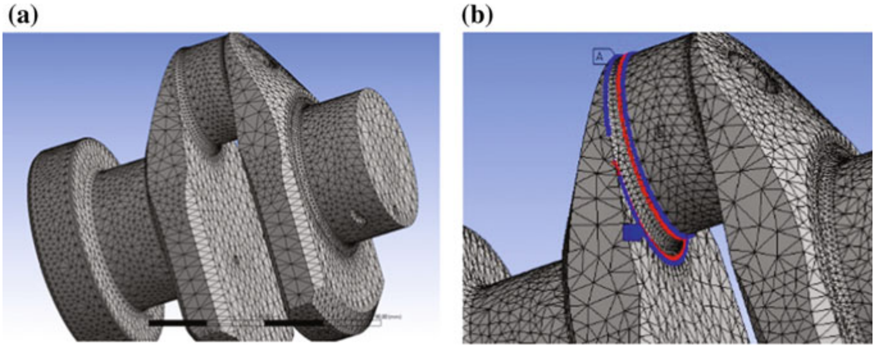

Fig. 5. **a** Segment mesh. **b** Limits of the morphing zone

2.1 FE Model

In the FE model, the external surface marked in blue remained fixed while the surfaces in red loaded with time variable forces evaluated by MB model (Fig. 2). The segment was constrained with a fixed joint in the surface (A) and the force were applied by its radial and tangential components which were distributed on the crank pin (Fig. 6).

The shape optimization was performed on the 3D mesh modelling again the geometric parameters (*a* and *b*) of the fillet zone and propagating the effect in the volume mesh through the set-up of the mesh morphing model (rbf-morph.com), according to the process proposed in [20].

Figure 7 shows the action of the mesh morphing on the external surface of the critical volume; the red points represent the nodes used as origin points in the initial position and the blue points represent a preview of the same points at the deformable position by the mesh morphing referring to the couple of values of the two geometric parameters (a = 3.5; b = 4).

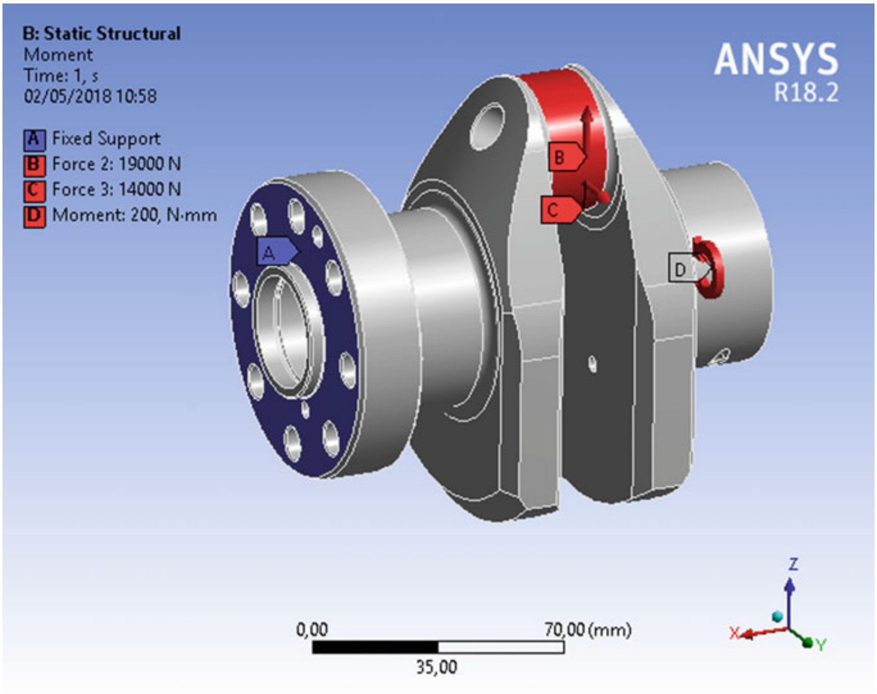

Fig. 6. Load model in the segment

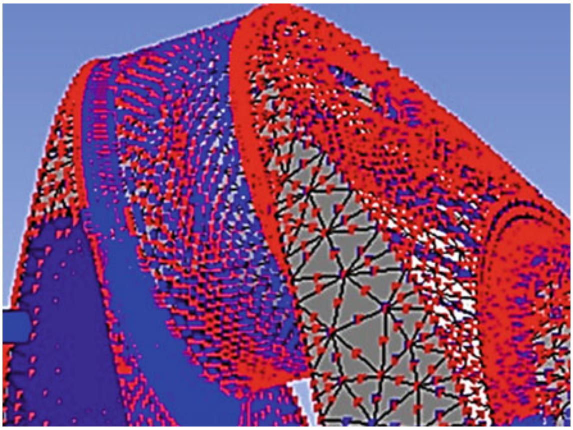

Fig. 7. Surface morphing effect: un-deformed points (red nodes); deformed points (blue nodes)

The volume concerned with the morphing process was controlled by fixed points to define the action of the deformation field and by the parameters procedure of the geometry in fillet zone.

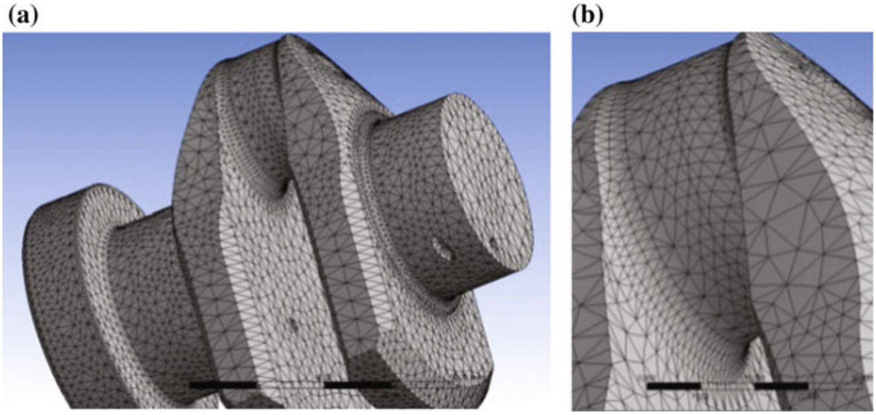

Fig. 8. Post mesh morphing: **a** Mesh in the segment. **b** Mesh in the fillet zone

The updating of the calculation mesh was realized through RBF plugin which brought the points of the junction surface into the wanted position. The points at the border of the domain were kept fixed while the surfaces and the volume mesh inside the domain deformed regularly (Fig. 8). The dimension of the morphing volume was set as to have space enough to deform the mesh (compressing or extending the finite elements). This volume referred to about 2400 nodes of the mesh.

3 Results

The model has been analyzed by studying the von Mises' tensions in a prospective of DOE optimization about the two geometric parameters (*a* and *b*). In particular, the parameters *a* and *b* change inside the range defined in Table 1 with a 0.1 mm increase. The DOE method allows to value continuously the model response in the parametric space (Fig. 9).

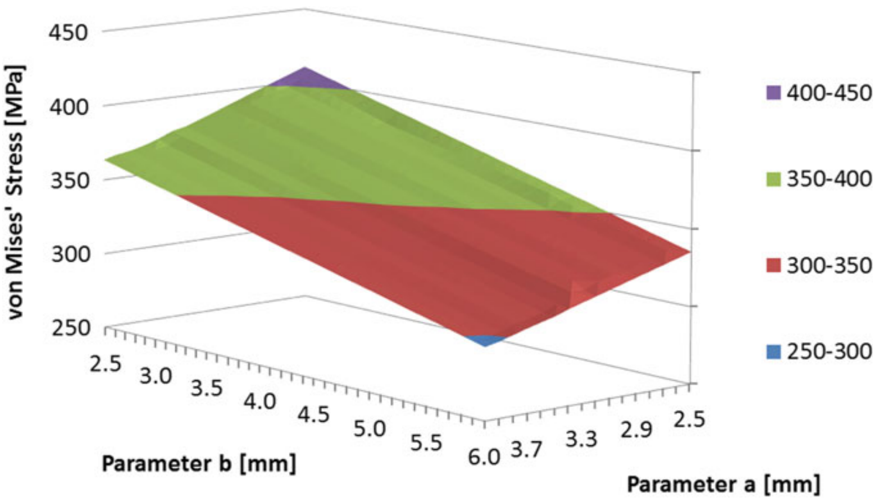

Fig. 9. System response to the two morphing parameters

The maximum equivalent von Mises stress in the fillet zone have the minimum value for a = 4 mm and b = 6 mm. In Figs. 10 and 11 are illustrated the state of maximum equivalent von Mises stress the fillet zone and a detail of the same state in the longitudinal section, before and after the *RBF* optimization respectively.

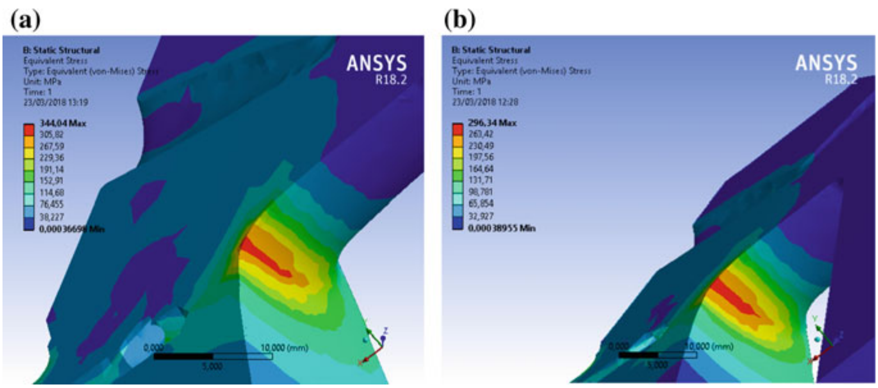

Fig. 10. von Mises stress before (**a**) and after (**b**) the Mesh Morphing optimization

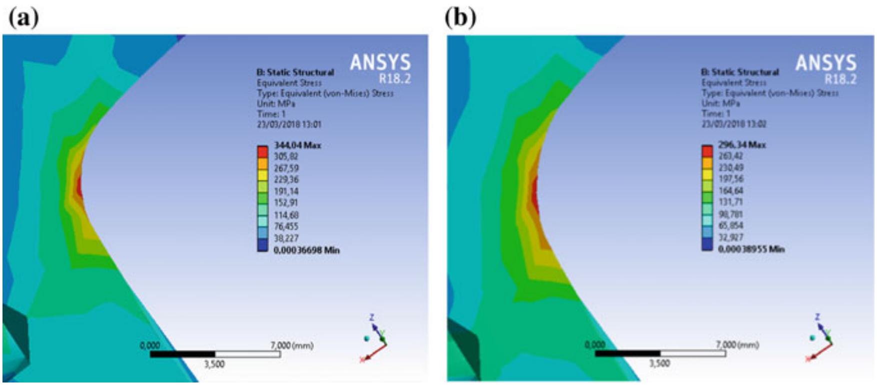

Fig. 11. Detail of the stress state in the longitudinal section before (**a**) and after (**b**) the Mesh-Morphing optimization

4 Discussion

The shape optimization using the *RBF Morph* plugin related to the appropriate selection of geometric parameterization enables to develop the right geometrical shapes that minimize the stress concentration. Adopting a parabolic fillet with an a value of 4 mm and a b value of 6 mm a reduction of −14% of value of the maximum von Mises stresses was obtained in proximity of the junction area with the crankshaft pin.

The plugin used allows a precise evaluation of many geometrical solutions updating geometric model, FE mesh and boundary conditions quickly.

In particular, the use of the parabolic fillet after defining parameters in the tangency points allows to evaluate separately the influence of the parameters a and b on the value of maximum von Mises Stress in the fillet zone. It has come out from this analysis that the increase of both parameters reduces maximum von Mises stress, but the increase of the parameter b results as slightly having more influence on this reduction as shown in Fig. 9. The plugin adopted finally allows the reconstruction through NURBS of the new optimized shape of the component, which can therefore be used immediately in the manufacturing process. The MM method has been applied until now mainly in the CFD field and therefore this work is one of the first applications in the structural field. The capability to optimize geometry, while minimizing stress, appears to be significantly favorable for the development of mechanical components such as the crankshaft.

5 Conclusions

A mesh morphing procedure to help the designer in seeking the best way to optimize the crankshaft shape design has been described. The steps used in the procedure have been illustrated and the choice of the parameters of the optimization and the algorithms outlining in *RBF Morph ACT Extension* plugin have been shown and discussed. The developed procedure has underlined mesh morphing and multibody model being used together as a powerful tool in order to reduce the maximum equivalent von Mises stresses, which is a very important factor usually for sectors such as the automotive industry. In particular, the method has allowed to get a relevant reduction of the value of the maximum tension according to von Mises (−14%) in proximity of the junction area of the crankshaft pin. Finally the proposed method has provided for the reconstruction through NURBS of the new optimized shape of the component, which can therefore be used immediately in the manufacturing process.

Acknowledgements. The research work reported here was made possible by the use of the RBF Morph ACT Extension plugin given by the RBF Morph Srl company. For the technical collaboration and the provided data we thank Eng. Franco Cazzolato, Eng. Giovanni Maiorana and Eng. Gianni Lamonaca of FCA. Finally we thank for the FE simulation with *RBF Morph ACT Extension* the thesis student Daniele Musco.

Funding

The research presented in this paper is part of the AMELiE (Advanced framework for Manufacturing Engineering and product Lifecycle Enhancement) project funded by the Italian Ministry of University and Research (PON03PE_00206_1).

References

1. Cali' M, Oliveri SM, Sequenzia G (2007) Geometric modeling and modal stress formulation for flexible multi-body dynamic analysis of crankshaft. In: 25th conference and exposition on structural dynamics, IMAC-XXV, Orlando, FL, United States
2. Mourelatos ZP (2001) A crankshaft system model for structural dynamic analysis of internal combustion engines. Comput Struct 79(20):2009–2027. https://doi.org/10.1016/S0045-7949(01)00119-5
3. Yar A, Bhatti AI, Ahmed Q (2018) First principle based control oriented model of a gasoline engine including multi-cylinder dynamics. Control Eng Pract 70:63–76. https://doi.org/10.1016/j.conengprac.2017.09.020
4. Oliveri SM, Sequenzia G, Calì M (2009) Flexible multibody model of desmodromic timing system. Mech Based Des Struct Mach 37(1):15–30. https://doi.org/10.1080/15397730802552266
5. Gui C, Sun J, He Z, Li Z (2017) Systematical analysis method for the mechanical behaviors of crankshaft-bearing system. J Tribol 139(2):021702–021702-9. https://doi.org/10.1115/1.4033362
6. Wei L, Wei H, Du H, Duan S (2017) Three-dimensional vibration of the crankshaft of a large marine diesel engine under a mixed thermo-elastic-hydro-dynamic lubrication coupling between flexible crankshaft and engine block. J Eng Gas Turbines Power 1–22. https://doi.org/10.1115/1.4038457
7. He B, Zhou G, Hou S, Zeng L (2017) Virtual prototyping-based fatigue analysis and simulation of crankshaft. Int J Adv Manuf Technol 88(9–12):2631–2650. https://doi.org/10.1007/s00170-016-8941-5
8. Witek L, Sikora M, Stachowicz F, Trzepiecinski T (2017) Stress and failure analysis of the crankshaft of diesel engine. Eng Fail Anal 82:703–712. https://doi.org/10.1016/j.engfailanal.2017.06.001

9. Dinh TQ, Marco J, Greenwood D, Harper L, Corrochano D (2017) Powertrain modelling for engine stop–start dynamics and control of micro/mild hybrid construction machines. Proc Inst Mech Eng Part K: J Multi-body Dyn 231(3):439–456. https://doi.org/10.1177/1464419317709894
10. Ponti F, Ravaglioli V, De Cesare M (2016) Development of a methodology for engine performance investigation through double crankshaft speed measurement. ASME J Eng Gas Turbines Power 138(10):102813–102813-6, https://doi.org/10.1115/1.4033066
11. Calì M, Oliveri SM, Sequenzia G, Fatuzzo G (2017) An effective model for the sliding contact forces in a multibody environment. In: Eynard B, Nigrelli V, Oliveri SM, Peris-Fajarnes G, Rizzuti S (2017) Advances on mechanics, design engineering and manufacturing. Springer International Publishing, pp 675–685. ISSN: 2195-4356
12. Ramnath BV, Elanchezhian C, Jeykrishnan J, Ragavendar R, Rakesh PK, Dhamodar JSM, Danasekar A (2018) Implementation of reverse engineering for crankshaft manufacturing industry. Mater Today: Proc 5(1):994–999. https://doi.org/10.1016/j.matpr.2017.11.175
13. Staten ML, Owen SJ, Shontz SM, Salinger AG, Coffey TS (2011) A comparison of mesh morphing methods for 3D shape optimization. In: Proceedings of the 20th international meshing roundtable. Springer, pp 293–311. https://doi.org/10.1007/978-3-642-24734-7_16
14. Vurputoor R, Mukherjee N, Cabello J, Hancock M (2008) A mesh morphing technique for geometrically dissimilar tessellated surfaces. In: Proceedings of the 16th international meshing roundtable. Springer, pp 315–334. https://doi.org/10.1007/978-3-540-75103-8_18
15. Sigal IA, Hardisty MR, Whyne CM (2008) Mesh-morphing algorithms for specimen-specific finite element modeling. J Biomech 41(7):1381–1389
16. Shontz SM, Vavasis SA (2010) Analysis of and workarounds for element reversal for a finite element-based algorithm for warping triangular and tetrahedral meshes. BIT Numer Math 50 (4):863–884
17. Shontz SM, Vavasis SA (2003) A mesh warping algorithm based on weighted Laplacian smoothing. In: Twelfth international meshing roundtable, Santa Fe, NM, pp 147–158
18. Stein K, Tezduyar T, Benney R (2003) Mesh moving techniques for fluid-structure interactions with large displacements. J Appl Mech 70(1):58–63
19. Buhmann MD (2004) Radial basis functions. Cambridge University Press
20. Biancolini ME (2017) Ridurre le concentrazioni di tensione con il mesh morphing. A&C. ANALISI E CALCOLO, ISSN, pp 1128–3874

Posture Evaluation for Fragment Re-Alignment of Ancient Bronze Statues: The Case Study of the Principe Ellenistico

M. Bici[1(✉)], R. Guachi[1], O. Colacicchi[2], G. D'Ercoli[3], and F. Campana[1]

[1] Dipartimento di Ingegneria Meccanica e Aerospaziale, Sapienza Università di Roma, Via Eudossiana 18, 00184 Rome, Italy
michele.bici@uniroma1.it
[2] Museo Nazionale Romano, Rome, Italy
[3] Istituto Superiore per la Conservazione e il Restauro, Rome, Italy

Abstract. Interventions of ancient bronze statues restoration may last long periods, involving several activities from material and structural analysis to set-up of museum exhibitions, passing through reconstruction of fragments. In this paper, we describe procedures and methods used for evaluation of the current posture of "Principe Ellenistico". In fact, the statue seems to present some inaccuracies, in the fragments assembly, made during the last restoration activity (one of this effect is clearly observed in the spear inclination). The final aims are: (1) evaluation of differences among the postures before and after the last restoration; (2) recognition of the original fragments embedded in a previous restoration; and (3) the study of a possible better positioning of them. Methods applied are related to feature recognition on acquired point clouds, image analysis through control points and algorithms to find centerline of the elements that could need to be repositioned. In the final part, a concept design for a new inner-support is presented, giving the possibility to avoid assembly inaccuracies. Future developments are presented as the prospect of additive manufacturing the support, firstly with a FDM prototype and then through SLM or similar technologies.

Keywords: Cultural heritage · Bronze statue restoration · 3D-reconstruction · Feature recognition · Virtual prototyping

1 Introduction

Traditionally, restoration of ancient bronze statues encompasses several activities like material integrity assessment, reconstruction of fragments, movement and set-up for museum exhibitions. Interventions may occur in long periods, with different experts, in different moments, so that, results and data documentation become relevant.

Nowadays, CAD-CAE methods, as well as rapid prototyping, are used in many cultural heritage applications [1, 2]. Advantages of this usage are relevant in terms of analysis of reconstruction hypotheses, digital reproduction and copy for data archive and enjoyment, improved understanding of stability and strength, anti-seismic or

F. Cavas-Martínez et al. (Eds.): *Advances on Mechanics, Design Engineering and Manufacturing II*, LNME, pp. 323–335, 2019.
https://doi.org/10.1007/978-3-030-12346-8_32

integrity actions related to basement, supports or carriage [3–5]. In [6], a detailed survey about methods and post-processing techniques concerning 3D-reconstruction from digital shape acquisition is presented. Although complex and expensive computations are necessary, digital models for cultural heritage are becoming a well-established approach (see, for examples, [7, 8]). A specific branch of research concerns fragment digitalization and artifact reconstruction. In [9, 10], methods oriented to these targets have been applied for improving measurement of pottery fragments, and for fragments matching and alignment.

The general workflow for these activities starts from feature recognition (mainly regarding central axis and curvature changes on fragments), inserting thickness evaluation and curve matching to solve the “puzzle”, achieving the coincidence between fragments [6, 11]. Apart from pottery, other fields of applications are mosaics and epigraphs that could have been approached as 2D puzzles through image analysis techniques [12] and marble or ceramic statues found in pieces [13]. Image analysis techniques are also applied for other applications. Among them, one of the most relevant is data post processing of ground-penetrating radar, with post-processing similar to DICOM [14], and image processing acquisition and post-processing for paintings [15]. Other ad hoc applications are those related to transcription and recognition of ancient documents [16], restoration of warped documents [17]. From the cultural heritage point of view, the reconstruction of new findings is not the only case which asks for digital model of fragments and their post-processing. They can also help restoration activities that involve a review of solutions found in the past. During centuries, according to technical progresses and aesthetical style, reconstructions were made in different ways, including also artificial remaking of missing fragments. Ancient large bronze statues, especially those found in the 19th Century, may give an example of this problem. Often found in pieces, they were restored and exhibited through reconstruction with artificial parts, ex-novo casted. During the 20th century, disassembly of the pieces was sometimes necessary for the recognition of bronze integrity and its maintenance. Reconstructions were then made empirically with partial substitution of the artificial casted inserts with resin, especially in case of wide fragments. New materials and support systems may have induced reconstruction errors that computer-aided technology may investigate.

In this paper, an application concerning this kind of investigation is provided, working on a bronze statue of the 2nd century B.C., found in Rome in the 19th century, known as the Hellenistic Prince (“Principe Ellenistico”), now conserved in Museo Nazionale Romano. This statue, found in fragments, have been restored two times since the finding, until today. Photographic evidences show different postures among these interventions, so that major investigations about possible reconstructions seem necessary. With this research, we aim to face this specific problem, which have been also approached by other authors in other case-studies [18, 19]. Taking care and highlighting the specificity of the fragments related to the Principe Ellenistico, as derived from digital acquisition, we are going to present the approach used to align the fragments, so that optimal posture hypotheses can be built through algorithms of section lines superimposition, surface best fitting, and image analysis. Finally, experimental evidence of the hypotheses will be given through a conceptual virtual prototype, able to change the arm position, trying to avoid assembly errors, via a guided assembly system. In Sect. 2, the description of the ancient bronze statue is given together with the explanation of the restorers requirements. Section 3 describes the analysis made and the procedure investigated for the posture evaluation and its possible reconstruction, then, in Sect. 4, results and procedures are used to concept a virtual prototype of a new inner-support. Finally, Sect. 5 outlines the major conclusions and future perspectives of the research activity.

2 The Principe Ellenistico and Its Restoration Issues

In this paper, we present the activities made in a collaboration between Department of Mechanical and Aerospace Engineering (DIMA) of “La Sapienza” University of Rome, Museo Nazionale Romano and Istituto Superiore del Restauro, on the statue called “Principe Ellenistico” (Fig. 1a). This bronze, dated from the 2nd century B.C., was found at the end of 19th century during an excavation made in Rome, near the Quirinale Hill (probably in the ancient area of the Costantin’s thermae). It is 2,04 m tall, and it was found in pieces (body, left arm and right leg, the spear is not original). Since its finding, many restorations have been made, together with hypothesis about its meaning and original posture. Only the most recent interventions, from the 80’s of the past century up to now, have been focused on the concept of “preserving”, applying also experimental and numerical investigations.

Restoration and maintenance of bronze statues obviously concern with surface investigation and material integrity, so that, a preliminary assessment via CAE methods has been already done to investigate stress-strain distribution, allowing the evaluation of critical-strength areas, the effect of the support and constraint system on the stability [20].

CAE model derives from the digital acquisition of the statue, which also allows to generate a CAD model suitable to investigate the posture analysis related to the reorientation and reconstruction of the left arm. As shown in Fig. 1b, the arm was found as a fragment, generating needs for correct connections with the thoracic portion. Its reconstruction was made two times: the first one adding a bronze detail (19th century, Fig. 1a), the second one via reconfigurable inner-support plus resin addition (20th century, Fig. 1b).

Resin addition connects four fragments that, considered in pairs, share a common small area that may be seen as a common point (Fig. 2). Fragments are: the statue up to the left shoulder (yellow edge), the arm (green and blue edges) and a triangular part at the armpit (red edge).

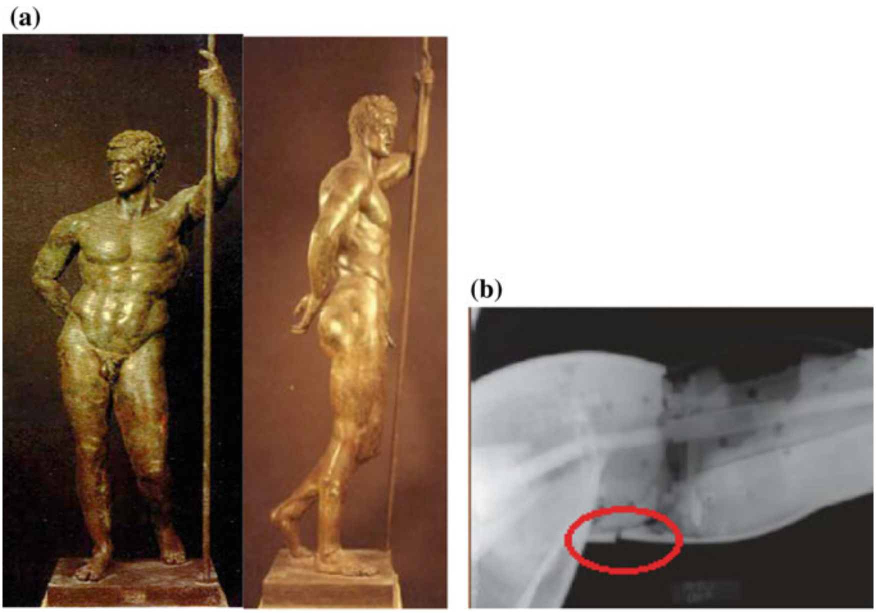

Fig. 1. The Principe Ellenistico: **a** after the XIX Century reconstruction. **b** RX of the actual left arm conjunction

Edges are rough and not always clearly overlapped. As shown in Fig. 2c, yellow-edge fragment and red-edge one are those with better matching. Unfortunately, the red-edge is related to an artificial part casted in the 19th century.

In following restorations, made during the 20th century, the red fragment was left, although the final positioning with the other fragments has resulted with a step among red and blue edges, as shown in the RX of Fig. 1b.

This absence of alignment and different empirical comparisons with photos taken before the last disassembly, give evidence of a different positioning of the left arm, thus of spear and of the whole statue posture. It seems leaning forward, in an unnatural manner. In the next section, some evaluations are made about the entity of this misalignment and a virtual reconstruction is proposed.

The 3D model of the statue has been achieved through a digital acquisition made by a 3D Scanner Artec Eva, able to process up to two million points per second with up to 0.1 mm accuracy. The obtained 3D model has more than 2×10^6 points, suitable to reproduce many of the smaller details, like hair, fingers and muscles and resin-fragment edges. Figure 3 shows a preliminary fragments detection on the 3D model according to the edges highlighted in Fig. 2. It shows also the left arm spine detection, found according to the method explained in next section.

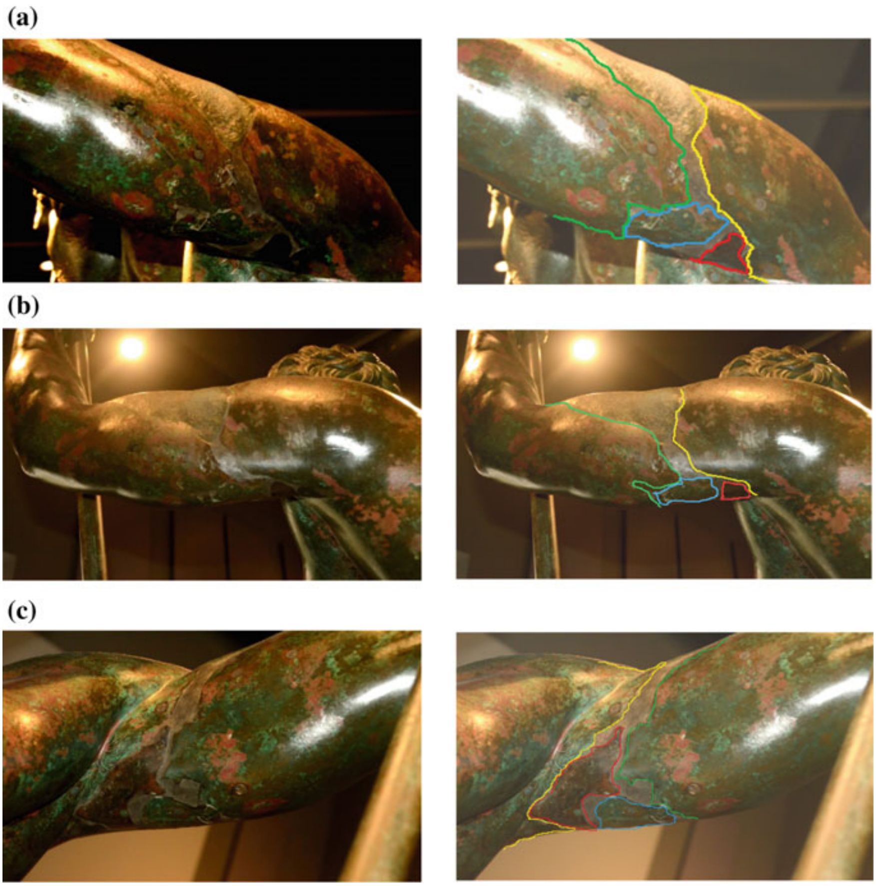

Fig. 2. Highlights of the statue fragments in the left arm

Fig. 3. 3D model of the fragments with left arm spine detection (in white)

3 Developed Procedures and Methods

3.1 Spine Detection

The spine, reported in Fig. 3, has been found through CAD software, selecting the interface zones for yellow and green fragments, considering also the resin made zone (filling surface). In fact, due to the width of the yellow and the green fragments, for the obtainment of the spine and the following developments, the blue and the red fragment are considered united with the green one, assuming that they can be placed consistently after the right relative orientation of yellow and green.

The spine represents the centerline of the considered surfaces and it can also be used for defining the direction of rotation and translation for the repositioning, as explained in Sects. 3.3 and 4.

3.2 Image Analysis to Assess the Change of Posture

The restoration made in the 19th century is documented through few photos like those previously shown in Fig. 1. One of the most impressive differences among postures before and after the restoration of the 20th century is the spear inclination, which increases the effect of leaning down. Spear has been added after restorations and, as resulted by experimental tests and also by simulations, it seems not loaded, so its inclination may be changed after restoration works [20, 21]. Due to the fact that the left arm has "guides" for the spear (on the hand and along the forearm), it is clear that the position of the left arm must be modified to attenuate the inclination issue.

Photos and visual evaluations are obviously affected by the perspective, nevertheless some of them can be mapped onto orthogonal views, through geometric considerations. In particular, an orthogonal view of the statue's 3D-model can be converted into a perspective view, mimic the result of a camera. The applied method adopts this concept, to obtain images of the current posture that are compared with the photos of the old posture, making a correction of the perspective. An orthographic view of the statue 3D model is adopted as Reference Image (RI), while a photo taken before the last restoration is selected as Moving Image (MI).

Image Registration through control points, which are mapped in both RI and MI, can result with a geometrical transformation able to map MI into RI. If the control points are related to areas without changes of posture (mainly yellow-edge fragment) and the MI is reasonably similar to the orthographic view adopted in the RI, the final overlapping must give evidence of the misalignment of the arm.

The Control Point Registration function of Matlab2017, is a basic tool in computer vision, nowadays applied for spatial referencing of photogrammetric maps [22, 23].

In our case, it has been firstly applied on a couple of RI and MI images that are related to a front view of the statue. The adopted Control Point set has 17 points taken outside the left arm fragments. This avoids the selection of control points where change of posture has occurred. Figure 4a shows the control points related to the trunk. The other selected points are positioned on the feet and the vertexes of the basements. On the left, Figure 4a shows the MI, on the right the RI. It has been obtained as a parallel view of the 3D model after a visual rough alignment with perspective according to MI.

Figure 4b shows the pair visualization of the two images after the transformation, while the numerical result is shown in Table 1. In Fig. 4b white areas reveal details without matching. They are located along the left arm and in the rear part of the basement that is not seen in the RI because it is taken from a front view. The good match along the edges of the statue can be seen as proof of the different posture between the assembly of the 19th century and that of the 20th. A preliminary validation of the difference along the left arm has been made through a second Image Registration along a different point of view, which can be seen as equivalent of an axonometric view.

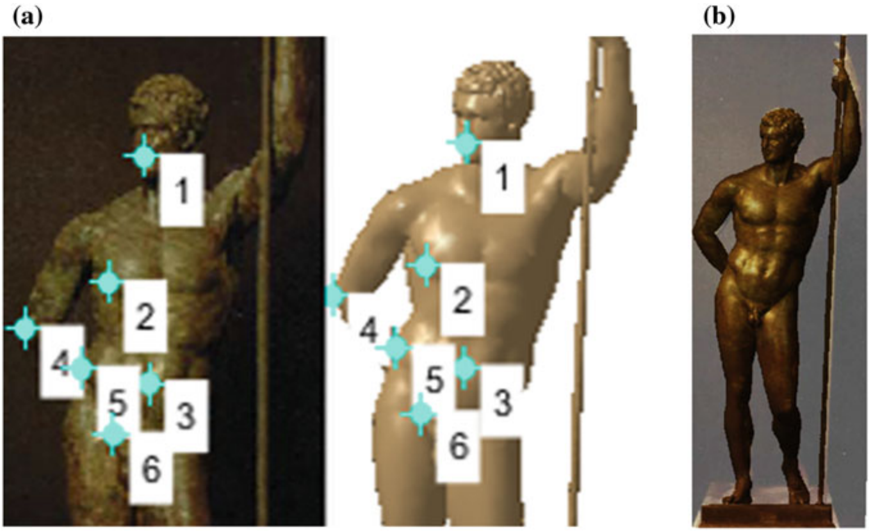

Fig. 4. Image registration front view: **a** control points of MI (left) and RI (right). **b** Results through image overlapping after registration (white areas are that without matching)

Figure 5a summarizes its results in terms of Control Point set, composed of 14 points. We decided to not consider the legs area due to accuracy problems of their point selection in both images. Figure 5b shows the result of registration. In this case, basement, trunk and right leg have good match, while a lack of accuracy is present in the right arm, probably due to a bad selection of the Control Points in a small area of the image. Despite this, white area along left arm is again consistent with an arm rotation that moves the hand and the spear backwards and the armpit high up.

Table 1 reports the rotational matrices, able to map MI into RI, according to the two photographic registrations we have made.

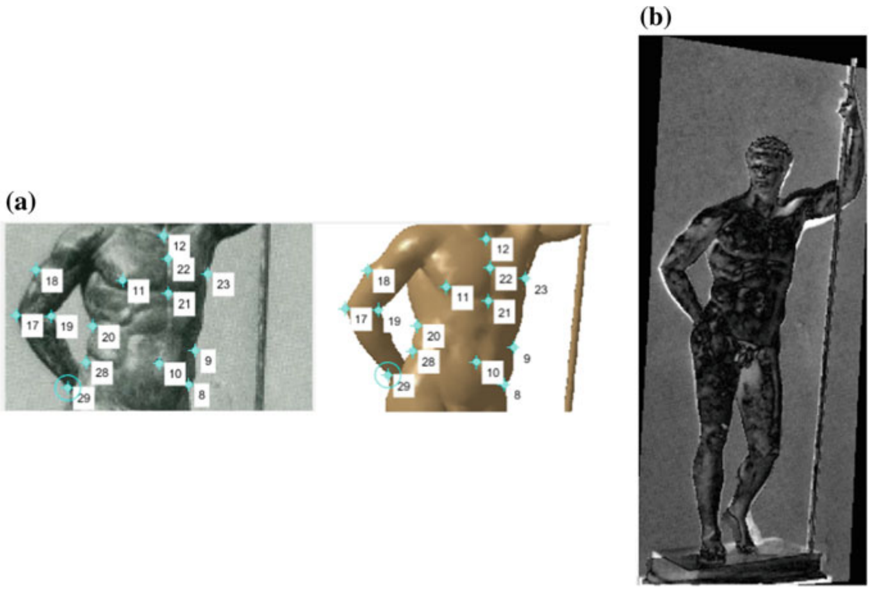

Fig. 5. Image registration axonometric view: **a** control points of MI (left) and RI (right). **b** Results through image overlapping after registration (white areas are that without matching)

3.3 Hypothesis of Fragment Reconstruction

Table 1. Transformation of the image registration according to "perspective" mapping

Front view transformation			Axonometric view transformation		
N1	N2	N3	N1	N2	N3
1.97	0.17	0.00	2.71	0.44	0.00
−0.07	1.90	0.00	−0.14	2.50	0.00
−17.71	−31.05	1.00	39.09	10.20	1.00

According to the results achieved through Image Registration, the two left arm postures have a relative rotation. To estimate its value, the fragments in the 3D model were rotated in the range 2°–5° with a step of 0.5°, so that the left hand allows a vertical insertion of the spear. Rotation has been made assuming the spine articulated inside the end section of the shoulder. In addition, fragments may respect: (a) the invariance of the central spine of the left arm; (b) the match between yellow and other edges.

Figure 6 shows the best solution, achieved through a rotation of 2.5°. It has been detected through visual inspection of the corresponding image alignment.

Figure 7 shows the image analysis of the new posture overlapped to the old photo (MI). In this case, a front view (in perspective) of the new posture has been assumed as reference view for the image mapping (RI).

Fig. 6. Green surface represents the arm fragment in the original positioning, Orange surface represents the rotated fragment

Good agreement between the two views is obtained, since no white areas are clearly visible. It represents a preliminary validation of the hypotheses of a reconstruction

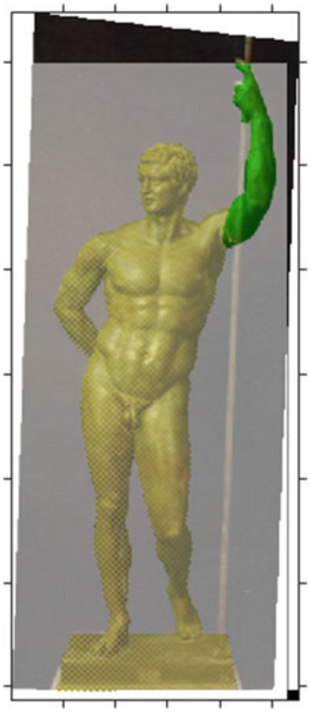

Fig. 7. New posture: results through image overlapping after registration

deviation, after the second restoration, of about 2.5°. The transformation matrix of the final alignment is shown in Table 2.

Finally, after the repositioning of the arm, a filling surface has been made to build the missing area of the bronze. It is made according to an aesthetic evaluation of the shape made by the restorer and to the respect of curvature and tangency continuity on the contour lines of the fragments.

Table 2. Final transformation matrix

Transformation matrix		
N1	N2	N3
1.58	0.16	0.00
−0.05	1.53	0.00
21.31	−48.96	1.00

4 Conceptual Virtual Prototyping of a New Additive Manufactured Inner-Support

After the finding of a more correct orientation of the pieces, the research moved its focus on the design of a new inner-support. In fact, one of the problem highlighted by restorers, is the necessity of avoiding assembly errors, as the one that caused the current wrong orientation of the left arm.

In order to reach this target, we decided to develop a virtual prototype of a support that will be manufactured in additive way. Starting from the acquisition of the inner surfaces of the fragments to be connected, we designed "negative" filling volumes (Fig. 8) capable to be inserted in the shoulder and the arm respectively. As displayed in the Fig. 8, in the shoulder negative, a prismatic guide has been designed and, in the arm negative volume, a cylinder has been added.

Through a prism with a cylindrical guide (Fig. 9), these pieces can be connected. This system allows to isolate the rotation and the translation of the arm in order to correct small errors of alignment, avoiding assembly errors through the possibility of a fine "tuning" of the orientation.

Obviously, this type of connection needs the selection of a roto-translation axis, blocking the other four degrees of freedom. The choice is to assume, as axis, the linear approximation of the spine in the support region. In fact, using the approximated

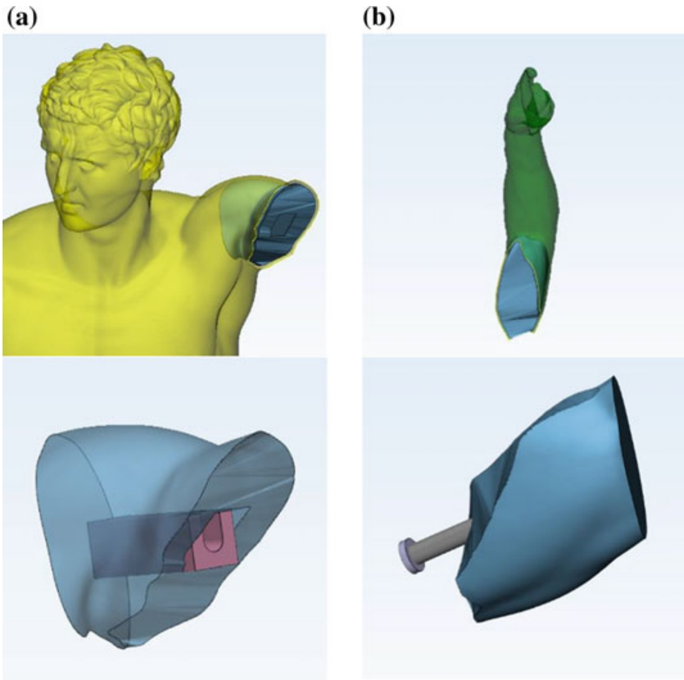

Fig. 8. Filling volumes **a** shoulder negative volume. **b** Arm negative volume

centerline, respect to the rotation in positioning, the displacement of the boundary is minimized, allowing the best alignment.

We want to highlight that the design of assembly system guarantees the possibility of choice the degree of freedom that has to be activated. The restorer can distinctly translate or rotate the arm in order to align it as best as possible, before applying resin for covering.

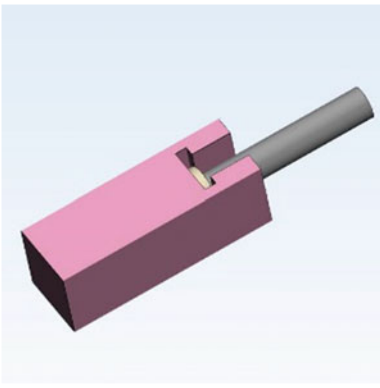

Fig. 9. Assembly system

5 Conclusions and Future Developments

The presented paper provides some evidences of a change in the fragment alignment and reconstruction of an ancient bronze statue. It starts from a subjective evaluation of the misalignment, through photo comparison, and restores experiences, during over 40 years of work on the bronze statue. Evidences are detected through image analysis techniques based on a photo registration algorithm, called Control Point Registration.

The developed procedure applied to the Principe Ellenistico, found in fragments in 19th century, showed that, in a subsequent restoration, the left arm fragment has been wrongly oriented. Through the algorithm, we compared images taken before and after the second (and last) restoration of the statue, obtaining that, to improve the statue posture, the left arm has to be rotated of 2.5°. This could lead to design a new restoration of the statue, finalized to solve this problem.

Although this application was not developed for defining a general procedure, it seems to be useful for restoration analysis of fragmented artifacts whose photographic evidences are available (e.g. restoration after earthquakes). According to this, a future development will be made, to quantify the misalignment, evaluating robustness and accuracy of the algorithm results.

Recently, as explained, a virtual prototype of the inner-support has been conceptually developed, in order to guarantee the possibility of roto-translate the fragment. The new inner-support will be manufactured, (starting from the acquisition of the inner part of the fragments) through additive technologies, firstly as Fused Filament Deposition (FDM) mock-up, to arrive, then, to plan a new restoration intervention, assembling fragments with a metal additive manufactured inner-support (manufactured via Selective Laser Melting (SLM) or other metal powder based technologies), containing the same assembly system of the prototype.

Acknowledgements. Authors want to thank the Ministero dei Beni Culturali e del Turismo – Museo Nazionale Romano, Palazzo Massimo for the kind concession of archival images, for the possibility of making data and photo acquisitions and also for their publication.

References

1. Bruno F, Gallo A, De Filippo F, Muzzupappa M, Davidde Petriaggi B, Caputo P (2013) 3D documentation and monitoring of the experimental cleaning operations in the underwater archaeological site of Baia. (Italy). In: Proceedings of the digital heritage 2013—federating the 19th Int'l VSMM, 10th Eurographics GCH, and 2nd UNESCO. No. 6743719, pp 105–112. https://doi.org/10.1109/digitalheritage.2013.6743719
2. Scopigno R, Cignoni P, Pietroni N, Callieri M, Dellepiane M (2017) Digital fabrication techniques for cultural heritage: a survey. Comput Graph Forum 36:6–21. https://doi.org/10.1111/cgf.12781
3. Accardo G, Amodio D, Bennici A, Cappa P, Santucci G, Torre M (1990) Strain fields on the statue of Marcus Aurelius. Exp Mech 30(4):372–376. https://doi.org/10.1007/BF02321507
4. Fatuzzo G, Sequenzia G, Oliveri SM, Barbagallo R, Calì M (2017) An integrated approach to customize the packaging of heritage artefacts. Lect Notes Mech Eng 167–175

5. Wittich CE, Hutchinson TC (2016) Experimental modal analysis and seismic mitigation of statue-pedestal systems. J Cult Heritage 20:641–648. ISSN 1296-2074
6. Gomes L, Bellon OPR, Silva L (2014) 3D reconstruction methods for digital preservation of cultural heritage: a survey. Pattern Recogn Lett 50:3–14
7. Sansoni G, Docchio F (2005) 3-D optical measurements in the field of cultural heritage: the case of the Vittoria Alata of Brescia. IEEE Trans Instrum Measur 54(1):359–368
8. Barone S, Paoli A, Razionale AV (2012) 3D reconstruction and restoration monitoring of sculptural artworks by a multi-sensor framework. Sensors 12(12):16785–16801 (Switzerland)
9. Di Angelo L, Di Stefano P, Pane C (2017) Automatic dimensional characterisation of pottery. J Cult Heritage 26:118–128
10. Karasik A, Smilansky U (2008) 3D scanning technology as a standard archaeological tool for pottery analysis: practice and theory. J Archaeol Sci 35(5):1148–1168. https://doi.org/10.1016/j.jas.2007.08.008
11. Palmas G, Pietroni N, Cignoni P, Scopigno R (2013) A computer-assisted constraint-based system for assembling fragmented objects. In: Proceedings of the digital heritage 2013—Federating the 19th Int'l VSMM, 10th Eurographics GCH, and 2nd UNESCO memory of the world conferences, plus special sessions from CAA, Arqueologica 2.0 et al., 1, art. no. 6743793, pp 529–536
12. Santachiara M, Gherardini F, Leali F (2018) An augmented reality application for the visualization and the pattern analysis of a roman mosaic. In: International conference Florence Heritech. Florence 16–18 May 2018
13. Benamar FZ, Fauvet E, Hostein A, Laligant O, Truchetet F (2017) Toward a virtual reconstruction of an antique three-dimensional marble puzzle. J Electron Imaging 26(1). https://doi.org/10.1117/1.jei.26.1.011023
14. Goodman D, Piro S (2013) GPR remote sensing in archaeology GPR remote sensing in archaeology. 1–233, Springer, Berlin, Heidelberg. https://doi.org/10.1007/978-3-642-31857-3
15. Barni M, Pelagotti A, Piva A (2005) Image processing for the analysis and conservation of paintings: opportunities and challenges. IEEE Signal Process Mag 22(5):141–144
16. Toselli AH, Leiva LA, Bordes-Cabrera I, Hernández-Tornero C, Bosch V, Vidal E (2018) Transcribing a 17th-century botanical manuscript: longitudinal evaluation of document layout detection and interactive transcription. Digit Sch Humanit 33(1):173–202
17. Brown MS, Seales WB (2004) Image restoration of arbitrarily warped documents. IEEE Trans Pattern Anal Mach Intell 26(10):1295–1306
18. Fatuzzo G, Musumeci G, Oliveri SM, Sequenzia G (2011) The "Guerriero di Castiglione": reconstructing missing elements with integrated non-destructive 3D modelling techniques. J Archaeol Sci 38(12):3533–3540. https://doi.org/10.1016/j.jas.2011.08.016
19. Sá AM, Rodriguez-Echavarria K, Griffin M, Covill D, Kaminski J, Arnold DB (2012) Parametric 3D-fitted frames for packaging heritage artefacts. VAST 105–112
20. Bici M, Campana F, Colacicchi O, D'Ercoli G (2018) CAD-CAE methods to support restoration and museum exhibition of bronze statues: the "Principe Ellenistico". In: International Conference Florence Heritech. Florence, 16–18 May 2018
21. Borri A, Grazini A (2006) Diagnostic analysis of the lesions and stability of Michelangelo's David. J Cult Heritage 7(4):273–285. https://doi.org/10.1016/j.culher.2006.06.004
22. Hartley R, Zisserman A (2003) Multiple view geometry in computer vision. Cambridge University Press, New York
23. Agüera-Vega F, Carvajal-Ramírez F, Martínez-Carricondo P (2017) Assessment of photogrammetric mapping accuracy based on variation ground control points number using unmanned aerial vehicle. Measurement 98:221–227

Review of Industrial Design Optimization by Genetic Algorithms

F. L. Sáez-Gutiérrez[1(✉)], F. J. F. Cañavate[1], and A. Guerrero-González[2]

[1] Graphical Engeniering Department, Technical University of Cartagena, Murcia, Spain
francisco.saez@upct.es
[2] Automation and Systems Engeniering Department, Technical University of Cartagena, Murcia, Spain

Abstract. In engineering, genetic algorithms (GA) have been successfully applied to some cases. The current state of this technique has evolved to allow computer designs from a sketch. Thus, GA generate a solution by optimization. Here the final solution is restricted by the final specifications. While CAD systems employ basic useful parameters to allow users to build the final design, GA utilizes preliminary designs from the beginning. CAD systems use primitives (points, lines and splines), which are controlled by users to build the design. In an evolutionary design system, it is GA that must modify designs to reach the final solution. When GA reach the solution, the design meets the final specifications. For this reason, the representation of an evolutionary design system based on GA must have a good parameter definition. Compared to the configuration design, a preliminary design is more difficult to computerize given its more marked emphasis on creativity. Therefore, the first step is to identify the ways to computerize the process involved in design. A bibliographic review sets the basis of using GA in the industrial design process.

Keywords: Industrial design · Optimization · Genetic algorithm · Computer-aided design

1 Introduction

Nature offers solutions to engineering problems. Nowadays, many engineering solutions mimic those that nature has built through evolution [1]. Evolution is the system that nature uses to adapt to its environment. It is a complex system, but has phases and processes that can be emulated with computation [2]. Genetic evolution is the most widely used tool by nature. Today we better know the processes that control genetics [3], and to the extent that we can emulate it with computational algorithms.

Genetic algorithms (GAs) emulate the process that characterizes genetic evolution using genetic operators [4]. These operators apply to a population from one generation to another. Each generation is evaluated according to the fitness function [5]. In this way, the evolutionary system perfects the solution in each generation.

F. Cavas-Martínez et al. (Eds.): *Advances on Mechanics, Design Engineering and Manufacturing II*, LNME, pp. 336–346, 2019.
https://doi.org/10.1007/978-3-030-12346-8_33

The engineering design process can have different levels of complexity. In industrial design, the desired solution optimizes quality values. However, the design process can involve many parameters that complicate optimization, and the design can contain many non-linear parameters. When the goal function has many local extremes, problems can appear [6]. In these cases, GA can solve the problem [7].

The most widely used optimization methods have problems [8]. The gradient method optimizes only local extremes [9], and the stochastic search method only disturbs the solution of the gradient method [10]. However, GA keep and evolve solutions in a search space.

GAs have been used in many optimization applications. We can see the application of GAs as: image processing [11], numerical optimization [12], programming [13], machine learning [14] or data structures [15]. This optimization method evolves solutions in a search space to obtain the desired result. Using GA as computer tools was introduced by Fraiser [16].

In this bibliographic review, we introduce a GA framework, and then see the relationship between GA and design. Next we see some examples of applying GA in industrial design.

2 Genetic Algorithms: Framework

A GA algorithm contains a search space formed by a population of individuals. Each subject, the so-called specimen, is composed of chromosomes. The so-called genotype forms the information contained in chromosomes. The so-called phenotype is the chromosome appearance. For each subject, the fitness function associates and evaluates an aptitude. From one generation to another, the population is submitted to the so-called genetic operators: crossing, mutation and cloning. Therefore, this process is evolutionary multiobjective optimization (EMO). We can establish a relationship between elements of nature and computation (Table 1).

Table 1. Relationship between nature and evolutionary computation

Nature	Computation
Specimen	Individual solution
Population	Set of solutions
Fitness	Evaluation
Crossover	Binary operator
Mutation	Unitary operator
Cloning	Recover/save operator

GA have the following stages (Fig. 1). First, the initial population is set up. In stage 2, the fitness function evaluates each specimen. If the evaluation is positive, the subject moves to the next generation through cloning. If the evaluation is negative, the subject is selected according to its level of adaptation. In stage 3, genetic operators create new specimens to form the next generation. Stage 2 is repeated until the satisfaction criterion is met.

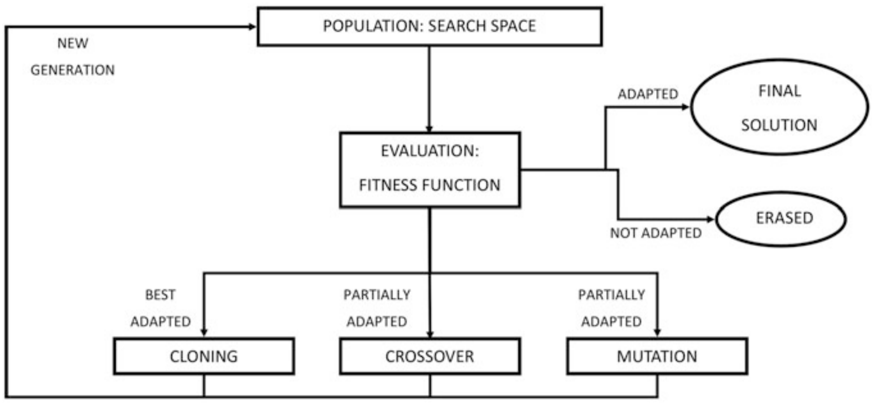

Fig. 1. GA schema

Each specimen represents a solution that needs to evolve from the beginning to reach the final specifications. To build the solutions space, we can use a complex or a simple representation. When we work in design, two problems can appear [17]. On the one hand, if we use a simple representation, GA spends a lot of time searching irrelevant regions. If, on the other hand, chromosomes representation is complex, the next generation can evolve without reaching the point of equilibrium. Zhao et al. [18] has worked in the gene theory to simply the design process.

2.1 Genetic Operators

In each step from one generation to another, GA apply genetic operators. There are three genetic operators: crossing, mutation and cloning. GA performance depends on the choice of crossing and mutation operators [17]. Cloning operator is a save/recover operator. Cloning consists in copying the solutions that adapt well to the final specifications. The crossover operator creates a new specimen from two other individuals. To make the crossover, GA use one crossing point or more by recombining chromosomes to form a new genotype. A recent survey [19] suggests that the geometric crossover operator (or the topological crossover operator) is well-defined when the solution is defined with distance (geometrically). Mutation creates a new specimen by making changes in its genotype. Modifications consist in changing part of the genotype or adding/removing chromosomes.

2.2 Fitness Function

As with nature, the survival of a specimen depends on its adaptation to the environment. In GA, the fitness function evaluates the fitness of each specimen. This fitness function must contain the requirements and specifications desired in the final solution. In this way, the degree each specimen's adaptation represents its distance to the final solution. The fitness function is considered the search core of GA. In design optimization, the fitness function is considerably important. An experimental study [20] establishes that an improved fitness function (IGA) has better convergence than traditional GA.

3 Involving GA in Design

Design generates solutions to cover products and specifications, and must contain information needed to manufacture them. Manufacturing imposes additional restrictions to design. Therefore, design is a task that involves a search to fulfill specifications and requirements. In 1962, a study by Asimov [21] showed the organization while solving a design task without taking into account the role that knowledge plays. It is a huge simplification, but the bases of this model are used in CAD-CAM systems.

Another model that enable knowledge of the design process is the so-called cognitive model [22]. This model can describe the designer's reasoning and decision making in design stages. However, this model is very difficult to translate into computational terms without using a broad simplification [23]. Here the design process is assimilated into parametric design thinking (PDT). PDT englobes the parametric design, the cognitive model and the computer-aided design. In short, the thinking process, involved in design, can be divided into two aspects: creative thinking and the pre-knowledge-based design (e.g. parametric design or configuration design [24]). We can see how GA can be used in these two contexts: creative design and configuration design.

3.1 Creative Design

Computerizing the creative design is a challenging task. In the creative design, there are two research lines: assisting human creativity and solving creative problems. In the former, users evaluate the population. So it is not necessary to define a fitness function. However, this causes a limited iteration speed because users cannot evaluate large populations. Frazer [25] concludes that a computer system´s creativity is attributed to the originator of the method.

A method to expand the search space is to reduce the number of the fitness function's restrictions. In this way, the system can change the initial representation. Then the system can build solutions beyond the optimization problem. The creative problem could have been solved by searching a solution that was not initially represented. This theory has been defended by Boden [26].

Another method is the so-called embryogenesis theory [27]. Here the fitness function evaluates the phenotype. Embryos are used to explore the search space. In this way, search parameters are not fixed.

Other studies have attempted to transform the creative process into an algorithm. Yang et al. [28] proposed dividing the search space into three: design flow space, knowledge inspiration space and solution operating space. In this way, GA acquire a certain level of creativity. Shieh et al. [29] propose three hybrid representations to obtain creative design alternatives. Golberg David [30] explains how to design creative GAs based on human comprehension.

3.2 Configuration Design

While the creative design is based on creative thinking, we can see modeling methods based on the problem's pre-knowledge. The configuration design [31] is based on the selection and assembly of components to build the final solution. The relationship between specifications and configurations is known. Therefore, it is a search to acquire an optimal configuration [32].

We can set a clear analogy between the configuration design and GA: configurable elements are encoded as genes with chromosomes. These elements evolve by GA (Fig. 2).

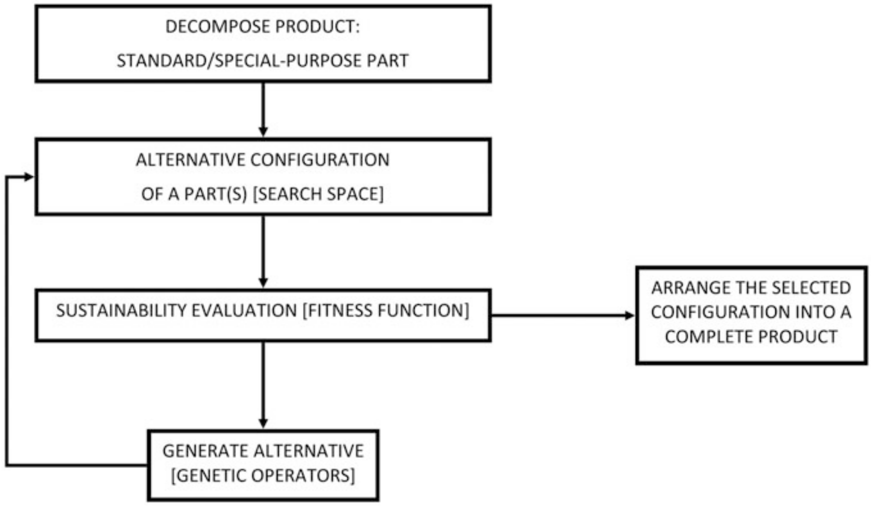

Fig. 2. Relationship between GA and the configuration design

In the configuration design, the configurable elements set the search space. The efficiency of GA is excellent due to the intensive exploring and exploitation that the genetic operators allow. Zou et al. [33] built the airspace grid design with configuration design-based GA. The search space, in this case, is formed by different grid configurations. GA evolve the grid testing alternatives configuration for each grid element. Da et al. [34] evaluated an evolutionary design composed of composite parts with different configurations. Andres-Perez et al. [35] used an enhanced mutation operator to generate different configurations in the search space. Chandrasekaran and Banerjee [36] resorted to a multiobjective evolutionary algorithm to offer an efficient and effective means to obtain a Pareto near-optimal set of solutions.

4 Applications of GA in Industrial Design

The potential use of GA in industrial design is remarkably high as they apply to most engineering fields: mechanical, electrical, aerospace and civil engineering. We analyze their application in three tools used in industrial design:

- Conceptual design
- Parametric design
- Reverse engineering

4.1 Conceptual Design

In conceptual design, either new components are used, or old components are combined in a novel way. There is no fixed method. Goldberg [37] presents a structure with four components: a problem to solve (the design challenge), someone to solve it (the designer), one conceptual design or more, and one method to compare alternative designs. This author presents GA as "a lower limit in the capacity of a designer in the processes of recombination and selection".

In conceptual design, GA are used as the method to compare and to search for alternative designs. This search can be guided by the designer, or the GA guide to the designer, to choose alternatives. Zhu et al. [38] used a GA-based selection method to accomplish an optimum multi-link transmission mechanism design. These authors adopted a polygon model into the iterative optimization process to describe the domination relationships of the individuals on the Pareto front. Mueller and Ochsendorf [39] proposed a computational approach for designing space exploration, which extends existing interactive evolutionary algorithms to enhance the inclusion of designer preferences. Zhang and Mueller [40] used GA to balance conflicting requirements in a conceptual structures design. Skiborowski et al. [41] introduced an interesting hybrid evolutionary-deterministic optimization approach for a conceptual design. They used successively relaxed mixed-integer nonlinear programming (SR-MINLP) to reduce the search time. Another approach to conceptual design optimization is shown by Zhang et al. [42], who followed an improved concurrent subspace optimization strategy (CSSO) and an improved differential evolution (DE) algorithm to solve the system-level and discipline-level optimization problems in conceptual design.

4.2 Parametric Design

In industry the shape of a component is important. Technical specifications and manufacturing costs depend on component shape (weight, torque, strength, etc.). In shape optimization, a parameter value must be found. The dependence function between the objective parameter with the shape variables can be non-linear or discontinuous. GA can assimilate this dependence function. Constraints can be determined by using a differential evolution algorithm in which the parameters are intermediate design variables [43].

The application of GA to parametric design has been successful in different studies. Gunpinar and Gunpinar [44] used GA to change the position of the points in parametric design. Particles are placed at points in the shape space by optimizing the fitness of the particle positions with a permutation GA (Fig. 3). Mostofizadeh et al. [45] performed the parametric design of a row of cylindrical film cooling holes to use GA in the optimization of gas turbines. In this case, the use of parameters improved the artificial neural network (ANN). Dandy et al. [46] compared the use of parameters in two GA: a traditional GA and a modified GA with improved operators. Renzi [47] utilized non-linear constraints to test individuals within each generation with geometric bounds and related parameters in an integrated design environment (IDe). Zhu et al. [38] compared the use of different model parameters in GA by choosing between the deterministic optimal design point and the robust optimal design point. Sekulski [48] selected the genotype by testing phenotype parameters.

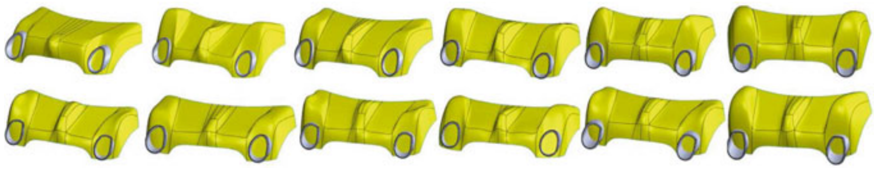

Fig. 3. Car hood models generated by parametric GA [44]

4.3 Reverse Engineering

A reverse engineering process begins by recording existing points by matching the model represented with the physically existing model. The next step is to establish a topology in the unstructured points cloud that reflects the mirror relations between the model and the real object. The rebuilding phase is based on belonging to subsets of the extracted elements.

For all these phases, GA have been investigated by different authors. Zhang et al. [49] applied Euclidean distance to duplicate the position of atoms in a material structure. Brunnstro and Stoddart [50] built mirror relations for points of correspondence in GA. The chromosomes of this model represent a correspondence between two sets of points (model point—real object point). The fitness function reflects the correspondence quality by calculating the distance between a pair of points. Its genetic code is composed of the transformation matrix parameters and the fitness function that minimizes the distance between each pair of points.

5 Results

The bibliographic review has introduced improvements into GA applications in industrial design. We describe the characteristics of different GA examples in several industrial design fields (Table 2). The design tool and case studies show that multiple GA applications are possible with different GA specifications.

We can see priority GA specifications to improve industrial design using GA. These parameters could be: a constrained fitness function, a chromosome substring, a

Table 2. Comparison between the GA applications reported in the literature

Reference	Application	Methodology	GA specs	Results
[39]	Rigid frame 2D model, generation of conceptual designs	Interactive GA	User-guided search space exploration	Lower computational cost than free exploration
[48]	Ship hull structural optimization (2D)	Nonlineal multiobjective optimization	Chromosome substring, constrained control parameters	~30% less generations needed to cover fitness
[38]	Multilink transmission concept design (2D)	Multi-objective optimization design (MOOD)	Ranked genetic operators	~35% total improvement
[47]	Integrated design environment (IDe) (3D modeling)	Integrated GA with numerical simulation	Constrained fitness function	98% iteration time reduction
[45]	Cooling holes CFD (3D)	Integrated artificial neural network-GA (ANN-GA)	Independent search space (database generation)	CFD Improvement
[44]	3D modeling	Particle tracing (PT) algorithm	GA optimizer of the particle position	72% iteration time reduction
[43]	Laminated plates (2D)	Differential evolution (DE)	Constrained genes modified objective reduction	Quick evolution
[49]	Reverse material engineering	GA with particle swarm optimization	Nondominated mutation	Promise tool for computer-driver material design

good selection of genetic operators. In [47], we predict that a constrained fitness function is better than a nondeterministic function. In [43] and [48], we observe that a constrained representation improves evolution. In [38], we discover that modified genetic operators are decisive to accomplish the final design specifications.

6 Conclusions and Future Work

GA can be successfully applied to industrial design. By even considering the creative factor in design, GAs can show the designer additional solutions.

In this bibliographic review, we study the definitions of the elements that compose a GA. We link these elements with the design process, which we see at both the creative and strictly procedural levels. Finally, we describe the characteristics of different GAs examples in several industrial design fields.

With all this, we see how GA have difficulties in creative and conceptual designs. However, we can verify how the fields of parametric design and configurations design have a high potential when applying GA. This is where our path is discovered by developing an optimization method in industrial design.

References

1. Kim SJ, Lee JH (2017) A study on metadata structure and recommenders of biological systems to support bio-inspired design. Eng Appl Artif Intell 57:16–37
2. Guizzo G, Vergilio SR (2018) A pattern-driven solution for designing multi-objective evolutionary algorithms. Nat Comput 1–14
3. Chaturvedi P, Kumar P (2015) Control parameters and mutation based variants of differential evolution algorithm. J Comput Methods Sci Eng 15(4): 783–800
4. Pavai G, Geetha TV (2018) New crossover operators using dominance and co-dominance principles for faster convergence of genetic algorithms. Soft Comput 1–26
5. Hanh LTM, Binh NT, Tung KT (2016) A novel fitness function of metaheuristic algorithms for test data generation for simulink models based on mutation analysis. J Syst Softw 120:17–30
6. Mirjalili S, Lewis A (2015) Novel performance metrics for robust multi-objective optimization algorithms. Swarm Evol Comput 21:1–23
7. Hamdy M, Nguyen AT, Hensen JLM (2016) A performance comparison of multi-objective optimization algorithms for solving nearly-zero-energy-building design problems. Energy Build 121:57–71
8. Qu X et al (2015) Intelligent optimization methods for the design of an overhead travelling crane. Chin J Mech Eng 28(1):187–196 (English Edition)
9. Keshavarzzadeh V, Meidani H, Tortorelli DA (2016) Gradient based design optimization under uncertainty via stochastic expansion methods. Comput Methods Appl Mech Eng 306:47–76
10. Jia G, Taflanidis AA, Beck JL (2015) Non-parametric stochastic subset optimization for design problems with reliability constraints. Struct Multi Optim 52(6):1185–1204
11. Sakthidasan K, Sankaran K, Nagappan NV (2016) Noise free image restoration using hybrid filter with adaptive genetic algorithm. Comput Electr Eng 54:382–392
12. Zang W et al (2018) A cloud model based DNA genetic algorithm for numerical optimization problems. Future Gener Comput Syst 81:465–477
13. Oliveira VPL et al Improved representation and genetic operators for linear genetic programming for automated program repair. Empirical Softw Eng 1–27
14. Wu CC et al (2018) A multi-machine order scheduling with learning using the genetic algorithm and particle swarm optimization. Comput J 61(1):14–31
15. Ting CK et al (2017) Genetic algorithm with a structure-based representation for genetic-fuzzy data mining. Soft Comput 21(11):2871–2882
16. Fraser AS (1957) Simulation of genetic systems by automatic digital computers I. Introduction. Aust J Biol Sci 10(4):484–491
17. Lin CD et al (2015) Using genetic algorithms to design experiments: a review. Q Reliab Eng Int 31(2):155–167

18. Zhao L et al (2016) A gene recombination method for machine tools design based on complex network. Int J Adv Manuf Technol 83(5–8):729–741
19. Pavai G, Geetha TV (2016) A survey on crossover operators. ACM Comput Surv 49(4)
20. Zhu Y, Cai X (2015) Convergence and calculation speed of genetic algorithm in structural engineering optimization. Metall Min Ind 7(8):259–263
21. Asimov M (1962) Introduction to design. Prentice-Hall, Englewood Cliffs, 135 pp
22. MacIntyre H (2015) A design model for cognitive engineering. Int J Technoethics 6(1):21–34
23. Oxman R (2017) Thinking difference: theories and models of parametric design thinking. Des Stud 52:4–39
24. Zhang T et al (2016) Intelligent fixture configuration design based on ontology and knowledge components. Jisuanji Jicheng Zhizao Xitong/Comput Integr Manuf Syst CIMS 22(5):1165–1178
25. Frazer J (2002) Creative design and the generative evolutionary paradigm. In: Creative evolutionary systems. Elsevier, pp 253–274
26. Boden MA (2004) The creative mind: myths and mechanisms. Psychology Press
27. Bentley PJ, Corne DW (2002) An introduction to creative evolutionary systems. In: Creative evolutionary systems. Elsevier, pp 1–75
28. Yang K et al (2016) A model for computer-aided creative design based on cognition and iteration. Proc Inst Mech Eng, Part C: J Mech Eng Sci 230(19):3470–3487
29. Shieh MD, Li Y, Yang CC (2018) Comparison of multi-objective evolutionary algorithms in hybrid Kansei engineering system for product form design. Adv Eng Inform 36:31–42
30. Goldberg David E (2002) The design of innovation, genetic algorithms and evolutionary computation. Kluwer Academic Publishers, USA
31. Levin MS (2016) Modular system design and evaluation, vol 373. Springer
32. McComb C, Cagan J, Kotovsky K (2017) Eliciting configuration design heuristics with hidden Markov models. In: International Conference on Engineering Design
33. Zou X et al (2016) Sectorization and configuration transition in airspace design. Math Probl Eng 2016
34. Da DC et al (2017) Concurrent topological design of composite structures and the underlying multi-phase materials. Comput Struct 179:1–14
35. Andrés-Pérez E et al (2016) Aerodynamic shape design by evolutionary optimization and support vector machines. Springer Tracts Mech Eng 1–24
36. Chandrasekaran S, Banerjee S (2016) Retrofit optimization for resilience enhancement of bridges under Multihazard scenario. J Struct Eng 142(8) (United States)
37. Goldberg DE (1991) Genetic algorithms as a computational theory of conceptual design. In: Applications of artificial intelligence in engineering, vol VI. Springer, pp 3–16
38. Zhu H et al (2016) Research on preference polyhedron model based evolutionary multiobjective optimization method for Multilink transmission mechanism conceptual design. Math Prob Eng 2016
39. Mueller CT, Ochsendorf JA (2015) Combining structural performance and designer preferences in evolutionary design space exploration. Autom Constr 52:70–82
40. Zhang Y, Mueller C (2017) Shear wall layout optimization for conceptual design of tall buildings. Eng Struct 140:225–240
41. Skiborowski M, Rautenberg M, Marquardt W (2015) A hybrid evolutionary-deterministic optimization approach for conceptual design. Ind Eng Chem Res 54(41):10054–10072
42. Zhang XB et al (2016) Multidisciplinary design optimization on conceptual design of aero-engine. Int J Turbo Jet Engines 33(2):195–208
43. Kameyama M, Arai M (2015) Optimal design of symmetrically laminated plates for damping characteristics using lamination parameters. Compos Struct 132:885–897

44. Gunpinar E, Gunpinar S (2018) A shape sampling technique via particle tracing for CAD models. Graph Models 96:11–29
45. Mostofizadeh AR, Adami M, Shahdad MH (2018) Multi-objective optimization of 3D film cooling configuration with thermal barrier coating in a high pressure vane based on CFD-ANN-GA loop. J Braz Soc Mech Sci Eng 40(4)
46. Dandy G, Wilkins A, Rohrlach A (2010) A methodology for comparing evolutionary algorithms for optimising water distribution systems. Water Distrib Syst Anal 2010:786–798
47. Renzi C (2016) A genetic algorithm-based integrated design environment for the preliminary design and optimization of aeronautical piston engine components. Int J Adv Manuf Technol 86(9–12):3365–3381
48. Sekulski Z (2014) Ship hull structural multiobjective optimization by evolutionary algorithm. J Ship Res 58(2):45–69
49. Zhang YY et al (2016) Inverse design of materials by multi-objective differential evolution. Comput Mater Sci 98:51–55
50. Brunnstrom K, Stoddart AJ (1996) Genetic algorithms for free-form surface matching. In: Proceedings of the 13th international conference on pattern recognition

Manufacturing and Industrial Process Design

Defining Scanning Trajectory for on-Machine Inspection Using a Laser-Plane Scanner

D. M. P. Nguyen, Y. Quinsat(✉), and C. Lartigue

LURPA, ENS Paris-Saclay, Université Paris-Sud, Université Paris-Saclay, 61 Avenue Du Président Wilson, 94235 Cachan, France
+33-147-402-213yann.quinsat@ens-paris-saclay.fr

Abstract. Scan path planning for on-machine inspection in a 5-axis machine tool is still a challenge to measure part geometry in a minimum amount of time with a given scanning quality. Indeed, as the laser-plane scanner takes the place of the cutting tool, the time allocated to measurement must be reduced, but not at detrimental of the quality. In this direction, this paper proposes a method for scan path planning in a 5-axis machine tool with the control of scanning overlap. This method is an adaptation of a method dedicated to a robot that has proved its efficiency for part inspection.

Keywords: On-machine inspection · Laser-plane scanner · Overlap · 5-axis machine-tool · Digitization

1 Introduction

Machining process monitoring is an essential challenge for the control of the quality of manufactured parts. To improve process productivity, part inspection procedures are increasingly integrated in the machining process as they allow high speed of inspection, measurement flexibility, and the possibility of 100% inspection [1]. Within this context, on-machine inspection becomes more and more popular as it allows a rapid decision-making with regards to part geometry conformity, and potential machining process corrections [2].

During on-machine inspection, the measurement of the part geometry is performed without removing the part from its set-up when the machining process is stopped. This facilitates the comparison of the machined part to its CAD model. Non-contact measuring techniques are generally used, as they represent a good compromise between data acquisition speed and resolution [3]. As an example, a laser-plane sensor can be integrated in a milling machine tool by taking the place of the cutting tool to measure geometrical deviations of the machining part [2]. In this context, a challenging issue, still unsolved, concerns scanner path planning. Actually, scan path planning methods for part inspection in a 5-axis machine tool are little addressed in the literature. The main difficulty lies in the generation of a set of ordered scanner configurations (positions and orientations) defining the trajectory that answers classical scanning constraints, and is consistent with the description format of a tool trajectory for machining (Fig. 1).

F. Cavas-Martínez et al. (Eds.): *Advances on Mechanics, Design Engineering and Manufacturing II*, LNME, pp. 349–358, 2019.
https://doi.org/10.1007/978-3-030-12346-8_34

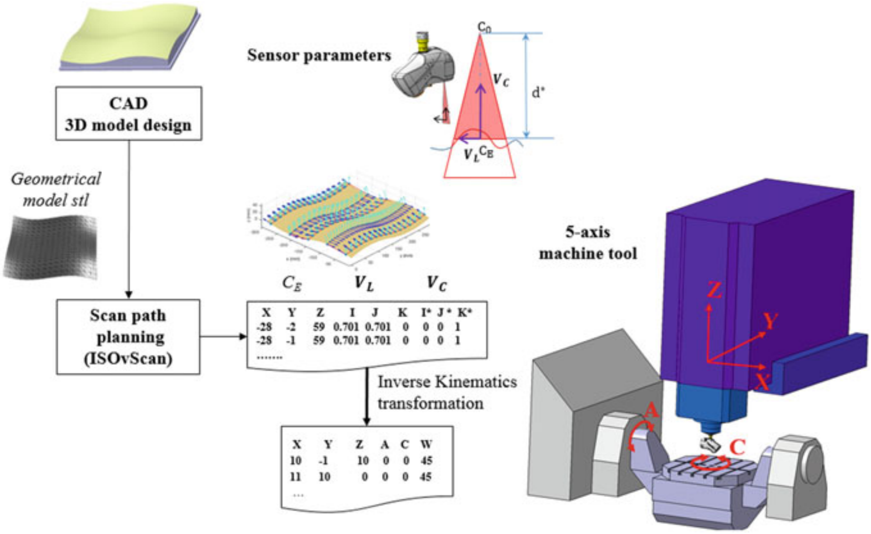

Fig. 1. Parameters defining the scanner path for on-machine inspection

Classical scanning constraints, widely studied in the context of trajectory generation on Coordinate Measuring Machines, are related to visibility and quality criteria [4–7]. For on-machine inspection, the scanner trajectory is the succession of positions and orientations (C_E; $\boldsymbol{V_L}$; $\boldsymbol{V_C}$). The driven point C_E positions the scanning laser line in the field of view, and the couple of vectors ($\boldsymbol{V_L}$; $\boldsymbol{V_C}$) orients the scanner, with $\boldsymbol{V_C}$ the director vector of the light-beam axis, and $\boldsymbol{V_L}$, the director vector of the scanning line. As it takes the place of the tool, the scanner has thus a greater accessibility due to its possible movements: 5 degrees of freedom (dof) plus the spindle rotation for 5-axis machine-tool.

The path planning strategy consists in finding the trajectory of the driven point C_E, and the continuous evolution of the scanner orientations defined by the couple ($\boldsymbol{V_L}$; $\boldsymbol{V_C}$) allowing the scanning of the part. Although this problem has not yet been addressed in the literature, some methods dedicated to part inspection with industrial robots give some interesting insights [8–11]. Most of these methods also rely on visibility and quality criteria.

This paper aims at defining a scanner trajectory well-adapted to on-machine inspection with 5-axis machine tool. In a previous work, we have developed a method that proved to be efficient for scanner path planning on industrial robots that integrates the control of overlap as an additional quality criterion [12]. This approach generates a scanning trajectory dedicated to a structure with 6 dof that must be adapted to 5-axis machine-tool. Indeed, the trajectory expressed in the part frame as a set of coordinates (X, Y, Z, I, J, K, I*, J*, K*) is expressed in the machine-tool frame thanks to the Inverse Kinematics Transformation (IKT). In the case of a RRTTT machine tool, the IKT leads to (X, Y, Z, A, C, W) in the articular space where A and C are the classical angles, and where W allows the spindle indexation. The main difficulty here is that the spindle indexation cannot be continuously controlled between two scanner configurations. It is thus necessary to fix the spindle indexation to a constant value W_{cst} for all the scanner configurations (Fig. 1). The initial trajectory must thus be modified according to two different ways. Priority can be given to quality, with sensor orientation control, or priority is given to measuring time with overlap control.

This paper is organized as follows: the scan path planning method is presented briefly in Sect. 2 and is followed in Sect. 3 by the method for adapting the trajectory to 5-axis scanning on a machine-tool. Finally, some conclusions are drawn in Sect. 4.

2 Scan Path Planning Method—ISOvScan

The originality of the proposed method is the control of the scanning quality, while minimizing measuring time, based on the control of the scanning overlap. In a previous work, the importance of the overlap on the scanning quality has been discussed [12], leading us to develop the Iso-Overlap Scan path method (ISOvScan). This method is based on the stretching of the 3D mesh surface representative of the part to be measured on a 2D parametric surface by the Least-Square Conformal Maps (LSCM) method [13]. The n triangular facets T_j of the 3D surface are transformed into n facets t_j in the 2D space. Then, equidistant paths, each one defined by a set of driven points, are generated in the 2D space, thus transformed in the 3D space by the inverse LSCM. For each driven point, the scanner orientations are finally calculated to satisfy quality constraints. The different steps of the method are briefly detailed in the next sections.

2.1 Generation of the Scanning Driven Points

Driven points are defined in 2D as the intersection between parallel planes and the parametric surface. To control the overlap, parallel planes are equidistant of a value I_{2D}, corresponding to the distance between two successive paths in the 2D space (Fig. 2). As the objective is to control the overlap defined by the distance I_{3D} between two successive paths in the 3D space, a relationship between I_{2D} and I_{3D} is established considering that the ratio of both values is equal to the proportionality coefficient of similar triangles T_j and t_j (Fig. 2) where A_{Tj} and a_{tj}, are the area of the facet, respectively, T_j and t_j.

Each driven point c_{ei} is then transformed into its corresponding point C_{Ei} by the inverse transformation. Once all driven points are calculated, the next step is to determine sensor orientations for each driven point.

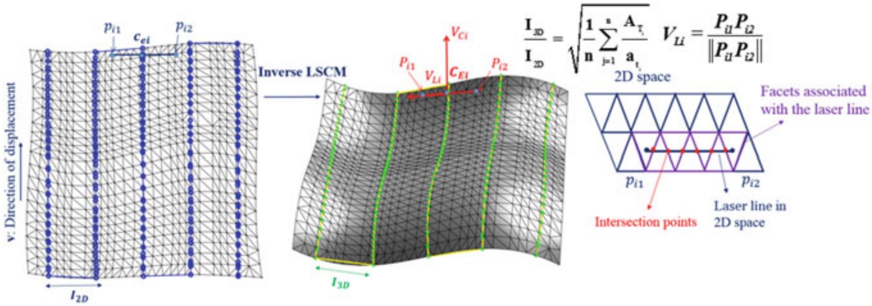

Fig. 2. Calculation of the scan path

2.2 Determination of Scanner Orientation

Scanner orientations are determined in two steps: the vector director of the digitizing line $\boldsymbol{V_L}$ is determined first, and then the light-beam axis $\boldsymbol{V_C}$.

A constant scanning distance is first imposed for all the driven points to ensure that the measured surface at the driven point belongs to the Field Of View (FOV) of the scanner, and to also ensure an expected scanning quality, defined according to the scanner qualification [14].

The width of the laser line, L_{opt} associated to this scanning distance is constant with respect to the scanned surface. In order to maximize the scanned surface, the laser line must be perpendicular to the direction of displacement along the scanner trajectory in the 3D space. The laser-line width l_{opt} in the 2D space is defined from L_{opt} and using the proportionality coefficient: $l_{opt} = L_{opt}\ (I_{3D}/I_{2D})$. At each point c_{ei}, the laser-line is positioned perpendicularly to the path and centered at c_{ei}. The width l_{opt} defines the two end points p_{i1} and p_{i2} of the laser line (Fig. 2). The coordinates of the corresponding points P_{i1} and P_{i2} are calculated using the LSCM inverse transformation. Thus, the director vector of the digitizing line $\boldsymbol{V_{Li}}$ at the driven point C_{Ei} is obtained from the coordinates of P_{i1} and P_{i2}.

The vector of the light-beam axis $\boldsymbol{V_C}$ is determined so that the scanning direction is always perpendicular to the surface. The local normal vector to the surface $\boldsymbol{n_{CEi}}$ at each driven point C_{Ei} is calculated as the mean value of all the normal vectors to the facets related to the laser line at C_{Ei}. Finally, the director vector of the light-beam axis is defined at each driven point by: $\boldsymbol{V_{Ci}} = \boldsymbol{n_{CEi}}$.

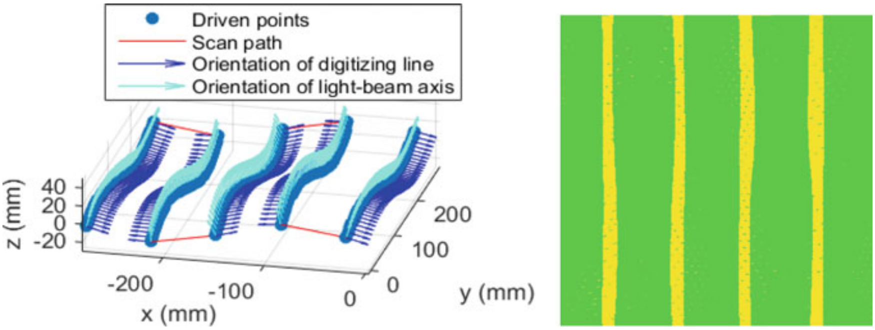

(a) Scan path generated by ISOvScan (b) Scanning simulation

Fig. 3. Generated scan path and scanning simulation

The whole trajectory is thus obtained as a set of positions and orientations (C_{Ei}; $\boldsymbol{V_{Li}}$; $\boldsymbol{V_{Ci}}$). The scan path planning method with overlap control ISOvScan is implemented in Matlab©. This scan path is assessed by a simulator previously developed [15]. Green facets correspond to scanned facets, whereas yellow facets belong to overlap zones (Fig. 3).

3 Adaptation of the Scanning Trajectory to 5-Axis Machine-Tools

Before executing the measurement in the 5-axis machine tool (RRTTT architecture), the scanner configuration (X_{pr}, Y_{pr}, Z_{pr}, I, J, K, I^*, J^*, K^*) corresponding to (C_{Ei}; $\boldsymbol{V_{Li}}$; $\boldsymbol{V_{Ci}}$) and defined in the part frame must be transformed into the articular configuration (X_m, Y_m, Z_m, A, C, W) in the machine frame. This transformation is carried out by IKT. Details of the geometrical modeling of the machine tool, and of the IKT are proposed in the appendix.

The values of the angles A and C are determined from the director vector of light-beam axis $\boldsymbol{V_C}$ (I^*, J^*, K^*) in Eq. (1) where the matrix M is defined in appendix according to the kinematic transformation from the sensor frame to the part frame:

$$\begin{bmatrix} I^* \\ J^* \\ K^* \\ 0 \end{bmatrix}_{(O_{pr},x_{pr},y_{pr},z_{pr})} = M \cdot \begin{bmatrix} 0 \\ 0 \\ 1 \\ 0 \end{bmatrix}_{(O_c,x_c,y_c,z_c)}, \begin{cases} I^* = \sin(C) \cdot \sin(A) \\ J^* = -\cos(C) \cdot \sin(A) \, . \\ K^* = \cos(A) \end{cases} \quad (1)$$

The value of angle W is determined from $\boldsymbol{V_L}(I, J, K)$ and the angles A, C:

$$\begin{bmatrix} I \\ J \\ K \\ 0 \end{bmatrix}_{(O_{pr}, x_{pr}, y_{pr}, z_{pr})} = M \begin{bmatrix} 1 \\ 0 \\ 0 \\ 0 \end{bmatrix}_{(O_c, x_c, y_c, z_c)}, \begin{cases} I = \cos(C) \cdot \cos(W) - \cos(A) \cdot \sin(C) \cdot \sin(W) \\ J = \sin(C) \cdot \cos(W) + \cos(A) \cdot \cos(C) \cdot \sin(W) \\ K = \sin(A) \sin(W) \end{cases}. \quad (2)$$

As mentioned previously, the spindle indexation cannot be continuously controlled between two adjacent scanner configurations. The scanner trajectory must be transformed into (X_m, Y_m, Z_m, A, C, W_{cst}) where W_{cst} represents a constant value of the spindle indexation for all the scanner configurations. In a first approach, the value of W_{cst} is determined by calculating the angle between the mean value of all the director vectors of the digitizing line $\boldsymbol{V_L}$ of the original scan path and the x-axis. The adaptation of the scan trajectory from ISOvScan to a trajectory well-adapted to a machine-tool is carried out in two ways. In the first method, the adapted scan path is computed with priority given to measuring time, with overlap control, and in the second method, priority is given to quality, with sensor orientation control.

In the first case, the adapted scan path respecting the control of overlap is obtained while keeping the director vector of the digitizing line $\boldsymbol{V_L}$ from the original scan path, and by only transforming $\boldsymbol{V_C}$ into the adapted vector $\boldsymbol{V_C}'$. Angles A and C are obtained from Eq. (2) with the original vector $\boldsymbol{V_L}$ and considering a constant value W_{cst}. The adapted vector $\boldsymbol{V_C}'$ is thus simply computed thanks to Eq. (1). Finally, the adapted scan path respecting the control of overlap defined by (C_E; $\boldsymbol{V_L}$; $\boldsymbol{V_C}'$) and the scanning simulation are shown in Fig. 4.

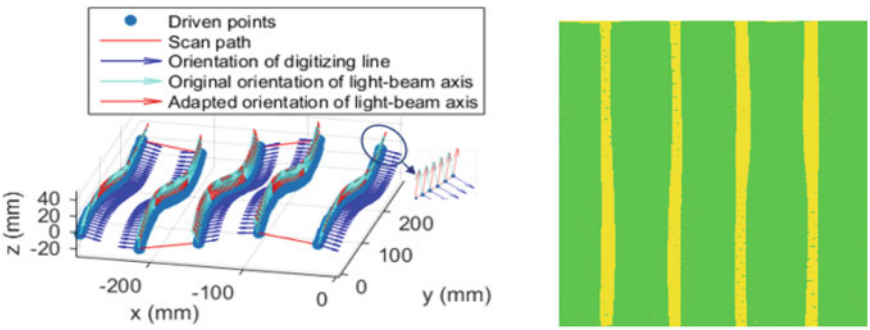

(a) Scan path with priority to the control of overlap (b) Scanning simulation

Fig. 4. Scan path with priority to the overlap control and scanning simulation

In contrast, the adapted scan path with priority to scanning quality is carried out by keeping the director vector of the light-beam axis $\boldsymbol{V_C}$, and by calculating the adapted director vector of the digitizing line $\boldsymbol{V_L}'$. Angles A and C are calculated from the vector $\boldsymbol{V_C}$ by Eq. (1). The adapted vector $\boldsymbol{V_L}'$ is then calculated by (2) with $W = W_{cst}$. The scan path is also assessed by the simulator in Fig. 5. The red color represents the zones that are not scanned by the scanner.

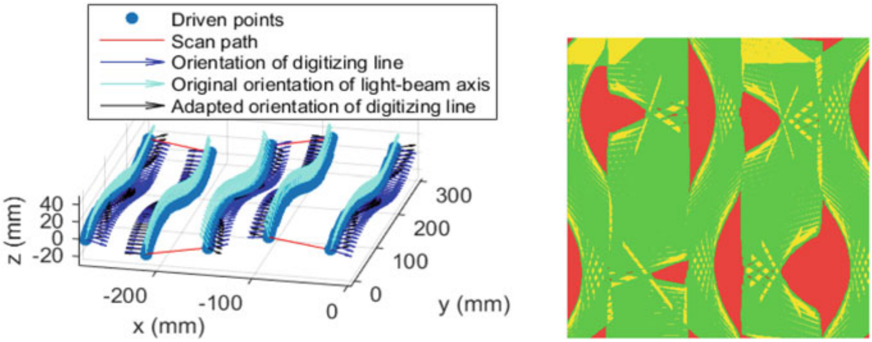

(a) Scan path with priority to the scanning quality (b) Scanning simulation

Fig. 5. Scan path with priority to the scanning quality and scanning simulation

Results and discussion: The results shown in Figs. 4 and 5 bring out the good similarity between the original ISOvScan and the adapted scan path with priority to the control of overlap in terms of scanning quality and overlap zones. The computation of the angle deviation between $\boldsymbol{V_C}'$ and $\boldsymbol{V_C}$ in Fig. 4 has highlighted that this deviation is less than 22°. This ensures that the scanner view angle is still less than the maximum view angle (60° for such a scanner [12]), which is linked to visibility and quality criteria. On the other hand, scanning simulation in Fig. 5 (adapted scan path with priority to the scanning quality) presents many scanning holes (red color zones). Although the director vector of the light-beam axis $\boldsymbol{V_C}$ is unchanged from the original scan path, the large deviations between the adapted director vector of digitizing line $\boldsymbol{V_L}'$ and $\boldsymbol{V_L}$ result in many unscanned zones on the surface. This is likely due to the fact that $\boldsymbol{V_L}$ is calculated from three parameters A, C, W while $\boldsymbol{V_C}$ only depends on two variables A and C.

In our case study, arbitrary choices of both the constant angle W_{cst} and the programming frame associated with the part setup may also influence results. Actually, the part setup is arbitrarily positioned in the machine working space without relation to scanning accessibility. However, these first results suggest that the adapted scan path with priority given to the control of overlap can be used as the suitable scan path for on-machine inspection in the 5-axis machine tool.

4 Conclusion

In this paper, we proposed a method to generate a laser-scanner trajectory suitable to 5-axis scanning in a machine tool. We successfully adapted a previous method that was developed for laser-scanning on a robot, which ensures scanning quality and the control of overlap between two adjacent scanning paths. As the kinematics of the machine-tool does not enable to directly apply the initial scan trajectory it must be adapted by fixing the value of the spindle indexation *W*. For this purpose, two different ways are explored: the value is fixed considering that priority is given to time measurement with overlap control, or priority is given to quality with sensor orientation control. First, results have demonstrated the relevancy of trajectory adaptation, with better results for the adapted scan path which prioritizes overlap control. Nevertheless, only a few experiments have been performed, and the work must be completed by investigating in particular the choice of the constant spindle indexation value, and the influence of the part setup on scanning performance. Future works, highly innovative and already in progress, concern the assessment of our method for on-machine measurement using a laser-plane in the 5-axis machine tool.

Appendix: Modeling of the 5 Axis Milling Machine Structure

The Mikron UCP 710 is a 5-axis milling center with an industrial numerical controller Siemens 840D. The architecture of this machine is CAXYZ for which two rotations are applied to the part, and the tool orientation is fixed in the machine frame (Fig. 6).

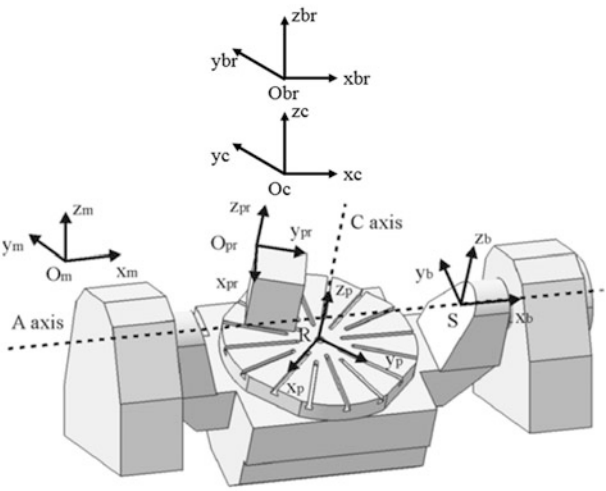

Fig. 6. Definition of different frames [16]

The different frames are defined from the architecture of the machine [16]:

- The spindle frame (O_{br}, x_{br}, y_{br}, z_{br}) is linked to the spindle, the scanner frame (O_C, x_c, y_c, z_c) is linked to the scanner,
- The machine frame (O_m, x_m, y_m, z_m) is linked to the machine structure; its axes are parallel to the XYZ axes; z_m is parallel to the tool axis,
- The tilt frame (S, x_b, y_b, z_b) is linked to the tilt table; x_b is parallel to x_m, S is located on the A axis,
- The table frame (R, x_p, y_p, z_p) is linked to the rotary table; z_p is parallel to z_b, R is defined as the intersection between the C axis and the upper face of the table;

– The programming frame (O_{pr}, x_{pr}, y_{pr}, z_{pr}) is linked to the part, which represents the frame used for scan path planning.

To transform between different frames, we define the matrix that converts a vector expressed in the one frame into another frame:

$$P_{cbr} = \begin{bmatrix} \cos(W) & \sin(W) & 0 & x_{O_cO_{br}} \\ -\sin(W) & \cos(W) & 0 & y_{O_cO_{br}} \\ 0 & 0 & 1 & z_{O_cO_{br}} \\ 0 & 0 & 0 & 1 \end{bmatrix}; P_{brm} = \begin{bmatrix} 1 & 0 & 0 & x_{O_{br}O_m} \\ 0 & 1 & 0 & y_{O_{br}O_m} \\ 0 & 0 & 1 & z_{O_{br}O_m} \\ 0 & 0 & 0 & 1 \end{bmatrix};$$

$$P_{mb} = \begin{bmatrix} 1 & 0 & 0 & x_{O_mS} \\ 0 & \cos(A) & \sin(A) & y_{O_mS} \\ 0 & -\sin(A) & \cos(A) & z_{O_mS} \\ 0 & 0 & 0 & 1 \end{bmatrix}$$

where P_{cbr} is the transformation matrix between the scanner frame and the spindle; P_{brm}, the transformation matrix between the spindle frame and the machine frame and P_{mb}, the transformation matrix between the machine frame and the tilt frame.

$$P_{bp} = \begin{bmatrix} \cos(C) & \sin(C) & 0 & x_{SR} \\ -\sin(C) & \cos(C) & 0 & y_{SR} \\ 0 & 0 & 1 & z_{SR} \\ 0 & 0 & 0 & 1 \end{bmatrix}; P_{ppr} = \begin{bmatrix} 1 & 0 & 0 & x_{RO_{pr}} \\ 0 & 1 & 0 & y_{RO_{pr}} \\ 0 & 0 & 1 & z_{RO_{pr}} \\ 0 & 0 & 0 & 1 \end{bmatrix}$$

where P_{bp} is the transformation matrix between the tilt frame and the rotary table frame and P_{ppr} is the transformation matrix between the rotary table frame and the part frame.

The kinematic transformation matrix M from the sensor to the part is then defined as following: $M = P_{ppr}^{-1} \cdot P_{bp}^{-1} \cdot P_{mb}^{-1} \cdot P_{brm}^{-1} \cdot P_{cbr}^{-1}$.

References

1. Chen FL, Su CT (1996) Vision-based automated inspection system in computer integrated manufacturing. Int J Adv Manuf Technol 11(3):206–213
2. Quinsat Y, Dubreuil L, Lartigue C (2017) A novel approach for in-situ detection of machining defects. Int J Adv Manuf Technol 90(5–8):1625–1638
3. Poulhaon F, Leygue A, Rauch M, Hascoet JY, Chinesta F (2014) Simulation-based adaptative toolpath generation in milling processes. Int J Mach Mach Mater 15(3–4): 263–284
4. Bernard A, Véron M (2000) Visibility theory applied to automatic control of 3D complex parts using plane laser sensors. CIRP Ann Manuf Technol 49(1):113–118
5. Prieto F, Redarce HT, Lepage R, Boulanger P (1999) Range image accuracy improvement by acquisition planning. In: Proceedings of the 12th conference on vision interface, Trois Rivieres, Québec, Canada, pp 18–21
6. Son S, Park H, Lee KH (2002) Automated laser scanning system for reverse engineering and inspection. Int J Mach Tools Manuf 42(8):889–897

7. Mahmud M, Joannic D, Roy M, Isheil A, Fontaine J-F (2011) 3D part inspection path planning of a laser scanner with control on the uncertainty. Comput Aided Des 43(4): 345–355
8. Wu Q, Lu J, Zou W, Xu D (2015) Path planning for surface inspection on a robot-based scanning system. In: IEEE International Conference on Mechatronics and Automation (ICMA), 2015, pp 2284–2289
9. Koutecky T, Palousek D, Brandejs J (2016) Sensor planning system for fringe projection scanning of sheet metal parts. Measurement 94:60–70
10. Larsson S, Kjellander JAP (2008) Path planning for laser scanning with an industrial robot. Robot Auton Syst 56(7):615–624
11. Mineo C, Pierce SG, Nicholson PI, Cooper I (2016) Robotic path planning for non-destructive testing–a custom MATLAB toolbox approach. Robot Comput Integr Manuf 37:1–12
12. Phan NDM, Quinsat Y, Lavernhe S, Lartigue C (2017) Path planning of a laser-scanner with the control of overlap for 3D part inspection. Procedia CIRP 67:392–397
13. Bruno L, Petitjean S, Ray N, Maillot J (2002) Least squares conformal maps for automatic texture atlas generation. ACM Trans Graphics (TOG) 21(3):362–371
14. Mehdi-Souzani C, Quinsat Y, Lartigue C, Bourdet P (2016) A knowledge database of qualified digitizing systems for the selection of the best system according to the application. CIRP J Manufact Sci Technol 13:15–23
15. Phan NDM, Quinsat Y, Lartigue C (2017) Simulation of laser-sensor digitizing for on-machine part inspection. In: Advances on mechanics, design engineering and manufacturing. Springer, pp 301–311
16. Lavernhe S, Tournier C, Lartigue C (2007) Kinematic performances in 5-axis machining. In: Advances in integrated design and manufacturing in mechanical engineering II, pp 489–503

Use of Additive Manufacturing on Models for Sand Casting Process

C. Bermudo(✉), S. Martín-Béjar, F. J. Trujillo, and L. Sevilla

Department of Manufacturing Engineering, University of Malaga, C/ Dr. Ortiz Ramos s/n, E-29071 Malaga, Spain
bgamboa@uma.es

Abstract. Sand casting processes are simple and, generally, require a small initial investment in machines and tools. These characteristics make this manufacturing process very used in the metal industry for the manufacture of small series of any size and complexity, where the dimensional and surface quality requirements are not very demanding. Among the necessary tools, it is worth mentioning the flasks and the patterns as the most important elements. Patterns are usually reusable and manufactured with polymeric materials. However, any change in the design or development of a new product involves the manufacture of new patterns. In case of polymer patterns obtained by injection, these product changes lead to the need of manufacturing new matrix, which deduces into higher costs and time. In this regard, the use of Additive Manufacturing techniques may help to solve these problems. Thereby, a methodology for the design and manufacturing of different patterns by using Fused Deposition Modeling techniques is exposed in this work. The results have been compared with those obtained in injection processes, from a functional and economical point of view. These patterns will be used in the manufacturing of parts for educational purposes. Nevertheless, with the appropriate scale and higher 3D printing resolution, the methodology exposed could be implemented on industrial applications

Keywords: Additive manufacturing · Sand casting · Permanent model · Expendable mold

1 Introduction

Rapid prototyping, developed in the 1980s, is suffering a rapid growth nowadays. Its application can be exported to multiple fields allowing printing parts and models of a wide variety. The main advances of this technology is the time and cost reduction and the potential to create shapes difficult to manufacture by other processes. Entire models or singular parts can be printed in order to facilitate the study or analyze its functionality [1].

Among the rapid prototyping techniques, the use of Additive Manufacturing (AM) in different industries is rapidly increasing, offering new production opportunities and manufacturing possibilities, reducing manufacturing lead times and finally covering customers demand rapidly [2]. Also, the selection of appropriate materials for the AM requirements is critical. These materials require a post-processed acceptability to

F. Cavas-Martínez et al. (Eds.): *Advances on Mechanics, Design Engineering and Manufacturing II*, LNME, pp. 359–369, 2019.
https://doi.org/10.1007/978-3-030-12346-8_35

enhance the geometry, the properties and the necessary performance in service of the printed part. As the technology progress, materials like polymers, metals, ceramics and composites are been considered and studied [3].

Focusing the present work in metal forming processes AM technology is suitable to create dies for traditional forming processes. Its application for mass productions is still not considered due to the time/cost efficiency compared with conventional manufacturing. Also, surface quality lacks on accuracy needed in most cases [4, 5]. Nevertheless, the different 3D printing techniques can offer quality and economic tools for sand casting [5]. AM can be used to generate molds and mold tools directly, reducing time and costs in patterns manufacturing [6, 7].

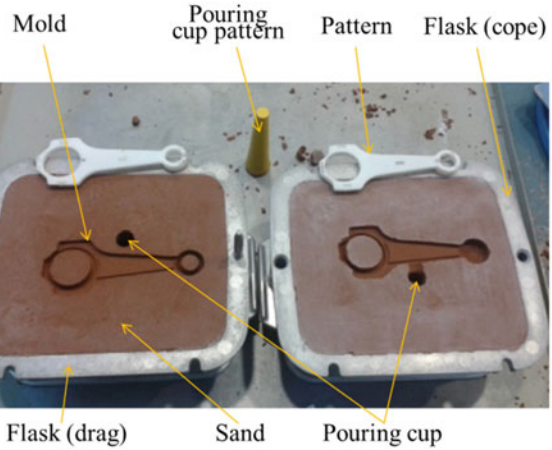

Fig. 1. Sand casting process. Open mold with pattern extracted ready to be closed

As seen in Fig. 1, several elements are needed to obtain a part by a sand casting process: permanent patterns, flasks (cope and drag), gating system (pouring cup, sprue, risers and feeding channels) and cores (only if needed). The aim of this work is to manufacture some of these elements by AM process for educational purposes scaled from real industrial examples, specifically by using a Fused Deposition Modeling (FDM) process. This technique presents reduced material costs, geometric versatility, easy post-processing, redesign and production of new units. Also, is automatable and the equipment is affordable. The equipment that is used for the practical activities that currently take place on the subjects where sand casting processes are taught, in the different Industrial Engineering Degrees at the University of Malaga, can be renewed with the application of the methodology exposed in this work.

The main advantages of FDM versus the conventional procedures (machining, polymer injection molding, etc.) are that allows complex shapes, the pattern can be reprinted as many times as desired and, in addition, it is an economical process [5]. Notwithstanding, there are negative points to take into account: low resolution (finishing operations are needed) and poor mechanical properties, among others [8].

In this work, a methodology for the design and manufacturing of the main elements involved in a sand casting process is exposed. All the necessary calculations for the design of these elements have been carried out. In addition, the patterns (made of ABS) were manufactured by FDM. Finally, the parts (made of a Tin alloy), were manufactured by a sand casting process and the results obtained were analyzed. It is necessary to highlight that the parts obtained for this work are not intended for a direct industrial application but can be scaled for an industrial purpose in further studies, with higher 3D printer resolution.

2 Methodology

There are currently three patterns at the manufacturing engineering workshop which are used for the practical activities: an anvil, a bell and an anchor. They allow to simulate a casting process of three characteristic parts types: one with compact geometry and massive concentration of material (the anvil), which requires a split model for its extraction; another with less material volume, with a thin wall, which requires a natural model (the bell). Finally, the anchor, with small volume of material but a large surface. They present a poor state due, mainly, to many years of use and the nature of the practical activities, which involves the sand compression.

Figure 2 shows the three polymeric patterns. The anchor (Fig. 2a) presents different breaks, the anvil with worn flanges (Fig. 2b) and the bell with a massive crack (Fig. 2c).

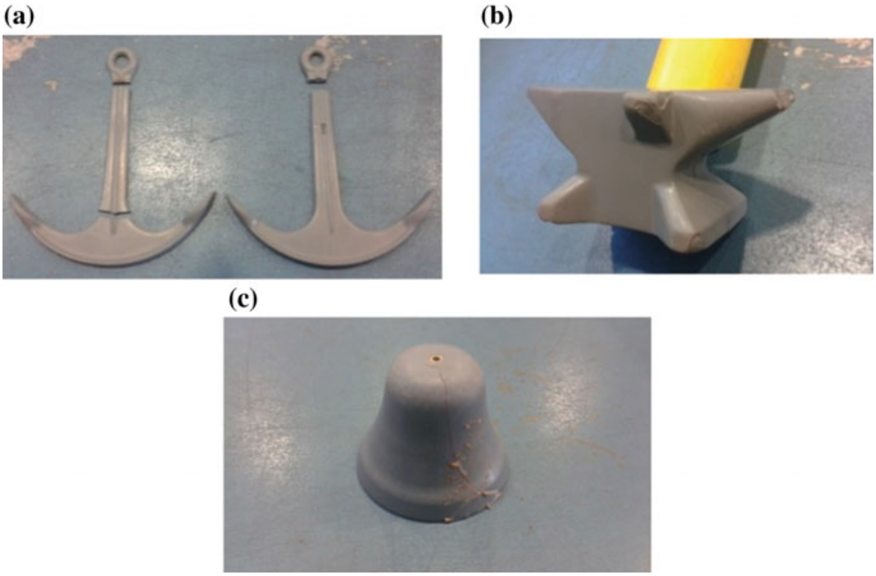

Fig. 2. Current patterns. Anchor (**a**), anvil (**b**) and bell (**c**)

So, the new patterns need to be didactic, cover different types and represent parts that are manufactured with sand casting process in the current industry. At the same time, there are some restrictions to take into account, like volume (*V*) and size. These limits are established by the laboratory material, more specifically the furnace ($V = 1\ dm^3$) and the flask (150 mm long, 200 mm wide and 100 mm high), respectively (Fig. 3).

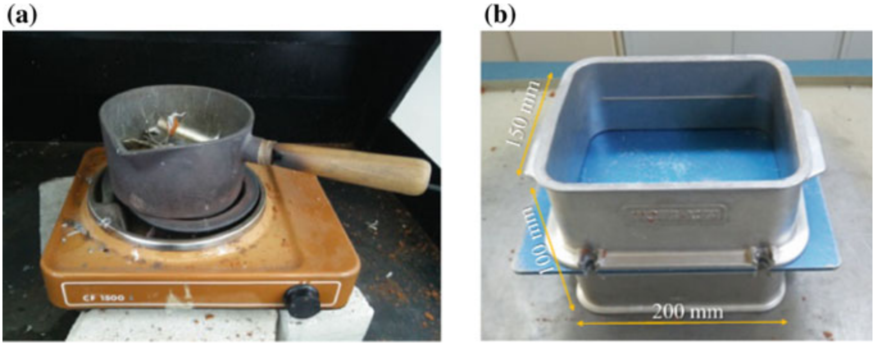

Fig. 3. Furnace (**a**) and current mold (**b**)

The first pattern considered is a scaled connecting rod (Fig. 4a). It replaces the anchor since they have similar characteristics: a flat piece with 2 holes in the demolding direction.

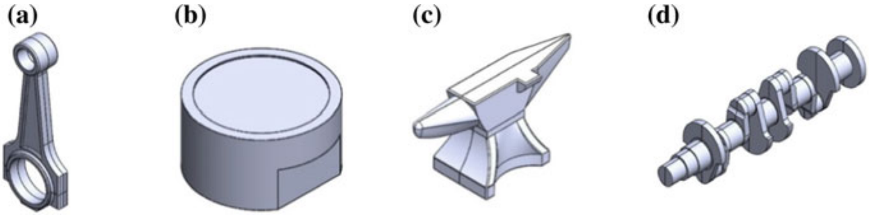

Fig. 4. New patterns. Connecting rod (**a**), piston (**b**), anvil (**c**) and crankshaft (**d**)

The second pattern considered is a piston. This full pattern replaces the bell. The modifications in this case are the elimination of the compression rings and bolt holes, generally located in the flat side areas (Fig. 4b). The casting part will be subjected to other forming processes (machining) to achieve the final shape. The third chosen pattern is an anvil and will obviously replace the previous one. The new shares its design characteristics with its predecessor (Fig. 4c). The last pattern selected is a crankshaft. It stands out for a more intricate design, with abrupt changes of section which may result in several defects (shrinkage cavities, lack of full mold filling, etc.) if the gating system is not correctly design (Fig. 4d).

Many of the defects obtained in casting processes are originated due to a bad gating system design. For its design and calculation, there are diverse analytical methods that can be applied to obtain an optimal sand casting process. Assuring a complete and correct mold filling is essential to avoid part defects. This can be achieved with a proper calculation of the feeding channels and risers, among others [9].

For the design of all the patterns, the SolidWorks 2016 software has been used. It can be especially highlighting the tool "Exit Angle Analysis", a graphical tool that allows to detect easily the pattern faces that needs an exit angle. These angles are useful to make easier the pattern extraction from the sand mold. Figure 5 shows the process with which the exit angle for the crankshaft is provided. Due to the large number of faces perpendicular to the partition line, the software marks in yellow the ones that need an exit angle. All patterns, except the piston, have been divided in 2 parts (cope and drag) and a keyway is designed to make easier their attachment, following the usual sand casting procedure.

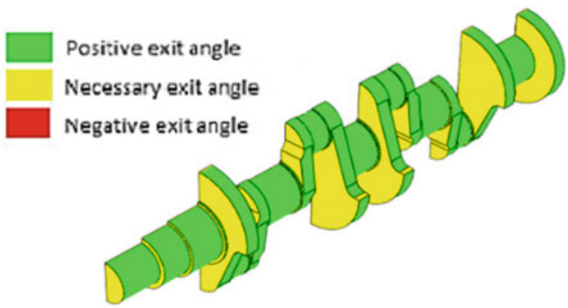

Fig. 5. Exit angle analysis by SolidWorks 2016

To build the optimal part shape, an approximation to the different analytical methods of calculation for the sand casting elements has been made. The gating and feeding system (Fig. 6a) have been calculated with two different methods to ensure the correct filling of the mold (Table 1). The nomogram method [9], following the "British Non-Ferrous Metals Technology Center" guidelines, and the analytical method, implemented in EES software.

A series of considerations must be taken in the design and calculation of the gating system. As the Fig. 6 shows, the system consists of a base for the sprue ($D_{sprue\ base}$), shaped as a cylinder of height ($h_{sprue\ base}$) equal to twice the thickness of the casting channel (e_c) and a diameter equal to twice the lower diameter of the sprue (D_2) (Eqs. 1 and 2). In addition, the area of the runners must be twice the area of the pouring channel (A_{cc}), the sprue has a conical shape and the casting channel will be square base, being its thickness the square root of the pouring channel section (Eq. 3).

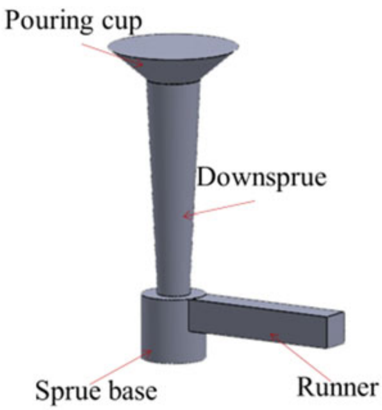

Fig. 6. Gating system

The maximum filling time has been calculated using the Chvorinov equation [4]. This stipulates that the filling time (t_s) will be equal to the solidification time in the thinnest wall of the mold, that is to say the most critical point of the piece (Eq. 4), being $e_{min}/2$ the thinnest section of the piece and C the mold constant. Next, the mass flow rate (Q) has been calculated using the following equation, which represents the total mass between the filling time (Eq. 5).

$$h_{spruebase} = 2 \cdot e_c \tag{1}$$

$$D_{spruebase} = 2 \cdot D_2 \tag{2}$$

$$A_{cc} = e_c^2 \rightarrow e_c = \sqrt{A_{cc}} \tag{3}$$

$$t_s = C \cdot \left(\frac{e_{min}}{2}\right)^2_{min} \tag{4}$$

$$Q = \frac{M_p + M_{sd}}{t_s} \tag{5}$$

For this study, all the volumes have been calculated from known data and unified as a total volume (Eq. 6). The equation achieved will be non-linear third degree. To solve it, mathematical software or the Newton-Raphson method can be applied.

$$V_{total} = V_{sprue} + V_{spruebase} + V_{feedingchanel} \tag{6}$$

Table 1 shows the results for the cast gating system calculated, being D_1 and D_2 the sprue upper and lower diameter, $D_{sprue\ base}$ the sprue base diameter, $h_{sprue\ base}$ the sprue base height and e_c the pouring cup thickness. The riser has been also mathematically calculated, maintaining the shape of the current riser used in the practical activities, a truncated cone shape.

Table 1. Sizing results of the cast gating system. Analytical method

	D_1 (mm)	D_2 (mm)	$D_{sprue\ base}$ (mm)	$h_{sprue\ base}$ (mm)	e_c (mm)
Connecting rod	5.973	2.726	5.453	4.275	2.138
Crankshaft	5.516	2.518	5.035	3.948	1.974
Piston	5.384	2.458	4.915	3.854	1.927
Anvil	8.314	3.795	7.590	5.951	2.975
Generic sprue	25	14.05	12	15	8

The positioning of the riser is important due to its limited radius of action. Its placement is critical. It should be located near the regions that are expected to shrink, either by a sudden section change, a hot spot or another reason [10]. In this case, due to the small size of the parts, it is possible to combine elements and the sprue will act as the riser. Table 2 presents the volume, area and cooling module of the riser available at the workshop at the Engineering Faculty of Malaga University.

In addition, a simulations corresponding to the fillings of the different parts have been carried out with the calculated and generic sprues, applying the SOLIDCast 8.0 software, presenting a better understanding and visualization of the process [11]. Figure 7 shows the simulation for the anvil with a generic riser or sprue (Fig. 7a) and the optimal one (Fig. 7b).

Table 2. Riser volume, area and cooling module

	V (mm^3)	A (mm^3)	$M_{e,\ m} = V/A$
Generic riser 1	26587.04	6138.23	4.33
Generic riser 2	15962.96	5091.16	3.14
Generic riser 3	45880.24	9125.71	5.02

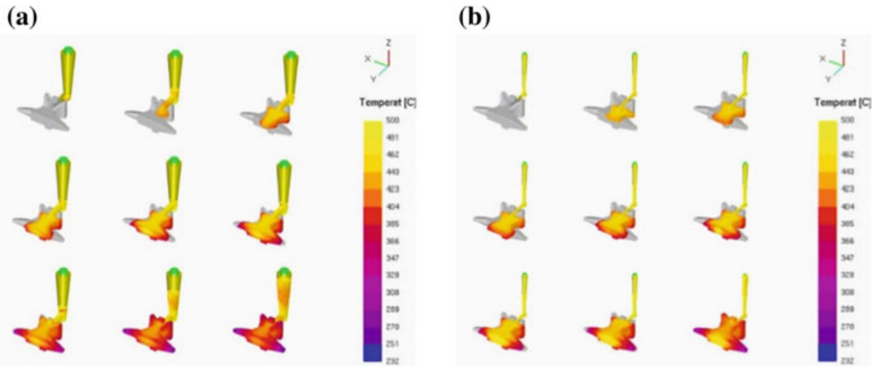

Fig. 7. Filing simulations for a generic sprue (**a**) and an optimal sprue (**b**)

From an industrial point of view, using a generic oversized sprue for all the parts is not practical since it supposes an increase in the material needed and in the energy invested in melting it, causing cost rising. However, in this case study, being a didactic example and small size models is perfectly assumable and a generic sprue has been established.

The manufacturing process of the different selected patterns has been carried out by FDM. The pattern designs are imported (SLF file) to the software CURA in order to obtain the CNC code. Then, the patterns are printed in ABS with a Dimension SST-768 printer [12] (Fig. 8b). It is possible to use this kind of printer due to the escalated size of the patterns. To acquire an optimal pattern, several considerations must be taken into account.

Fig. 8. CNC generation by CURA (**a**) and 3D printer (**b**)

The printing orientation is relevant. The layers of the finished pattern need to be oriented parallel to the partition line to resist the compression efforts during sand compaction and avoid possible fractures in the patter. In addition, due to the low resolution of the 3D printer available, the surface integrity of the patterns usually damages the sand mold when is extracted. Hence, to avoid this problem, a finishing operation has been performed on the patterns surface with sandpaper and a nail file (Fig. 9). The first one allows sanding curved surfaces and reaching corners, while the second is good with straight surfaces and size, presenting a better adaptation to the part thanks to its small size. After, the patterns have been varnished. For this process, transparent spray coating has been used, achieving a homogeneous outer layer on the entire surface. Due to the parts surface finish after casting processes, no other finishing operations are needed.

The aim of both operations is to achieve a smoother and easier surface to avoid deterioration in the mold during the extraction (Fig. 10a). Sanding softens and varnish equalizes and covers the outer layers. Figure 10b shows the correct extraction of one of the patterns after the application of both operations, leaving the mold intact.

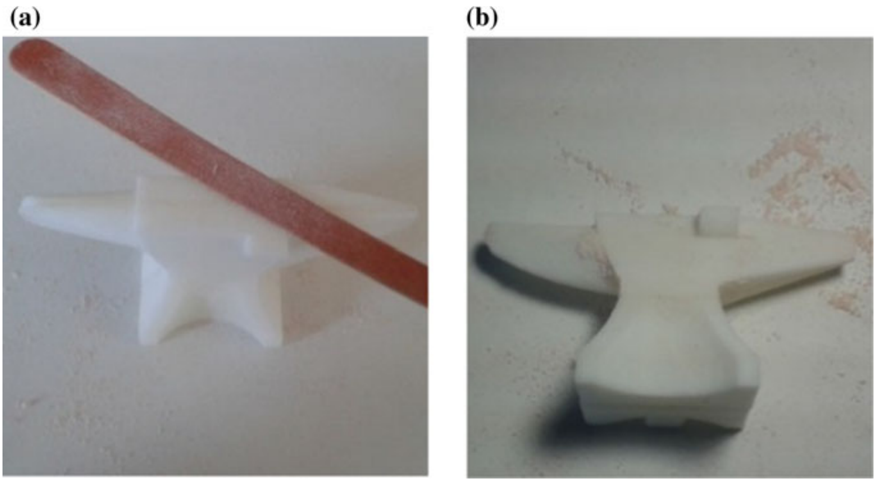

Fig. 9. Pattern finishing operation (**a**) and final pattern (**b**)

The model extraction is the most delicate step in the process, because the sand may break. Because of this, two types of extraction systems have been designed and implemented to make easier the pattern extraction by using a magnetic or a mechanical bending system. The first method is only valid with the connecting rod due to the size of the patterns. A T form handle has been designed for the magnet extraction, with another magnet at its end. For the other patterns, several nuts have been embedded (Fig. 10).

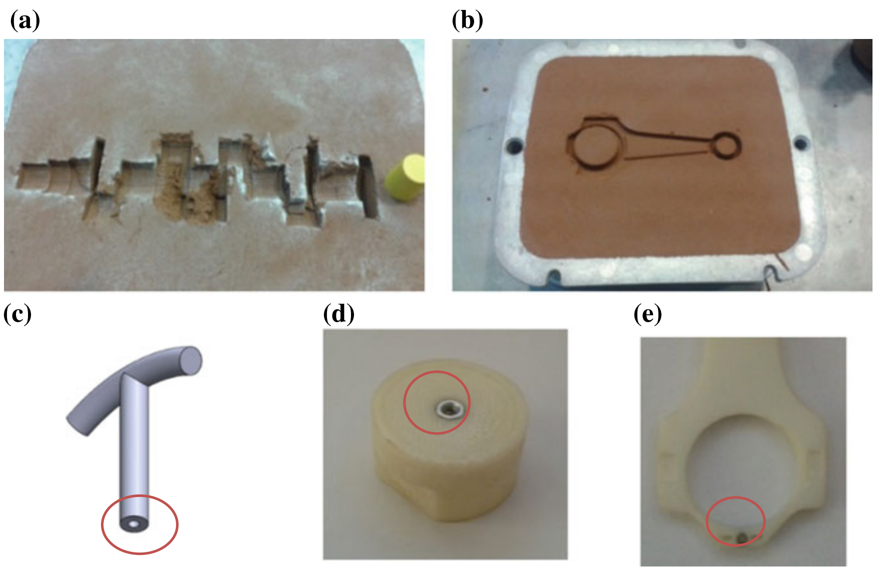

Fig. 10. Sand after extraction of the two pattern before (**a**) and after finishing operations (**b**). Extraction methods. T handle with magnet (**c**), embedded nut (**d**) and embedded magnet (**e**)

3 Results and Discussion

Once the parts have been obtained, several casting tests were carried out to ensure that the casting process was successfully achieved. Finally, the part has been examined for any type of imperfections and cleaned. Figure 11 shows the aspect of the final parts and examples of possible defects. In general, the defects obtained are mainly due to the casting process itself and not to the FDM pattern use. The principal defect attributable to the FDM is the Z resolution, which is partially mitigated with the post-processing. Also, it is a good way to teach students the pros (cheap and simple) and cons (poor dimensional accuracy and high probability of appearance of visible and hidden defects) of this type of process.

Additionally, the total cost of the materials used for this study (printing only one model of each pattern) has been 46.00 € (compared to a complete set: 5.594,40 €). This budget also makes feasible the implementation of additive processes in order to obtain more patterns and any necessary equipment for the sand casting processes.

(a) (b)

Fig. 11. Final parts. Connecting rod (**a**) and superficial defects in piston (**b**)

4 Conclusions

In conclusion, the implementation of FDM as an additive processes fulfills the aims of this work, making additive manufacturing a good alternative to current and more expensive techniques (machining, polymer molding, etc.) for the manufacturing of patterns, used later in a sand casting process. FDM is presented as an easier technique at an affordable cost. This last aspect makes it very interesting from a didactic perspective. In an economical and simpler way, it can be shown to the students, who have previously acquired the necessary theoretical knowledge, how to execute this type of processes, obtaining a functional piece.

In addition, all the calculations for the distribution systems have been analytically developed, obtaining a mathematical code that performs this calculation for new pattern designs, carrying out casting simulations to study and optimize the entire process. Moreover, a post-processing of the patterns after 3D printing is implemented for a correct extraction and is observed that the defects obtained can not be attributable to the patterns' manufacturing method.

Finally, the sand casting equipment available to the students in their practical activities has been increased and complemented, having the possibility to continue increasing the equipment if necessary due to the fast procedure and low costs.

Acknowledgements. The authors thank the University of Malaga—Andalucia Tech Campus of International Excellence for its contribution on this paper.

References

1. Wong KV, Hernandez A (2012) A review of additive manufacturing. ISRN Mech Eng 2012:1–10. https://doi.org/10.5402/2012/208760
2. Attaran M (2017) The rise of 3-D printing: the advantages of additive manufacturing over traditional manufacturing. Bus Horiz 60:677–688. https://doi.org/10.1016/J.BUSHOR.2017.05.011
3. Bourell D, Kruth JP, Leu M, Levy G, Rosen D, Beese AM, Clare A (2017) Materials for additive manufacturing. CIRP Ann 66:659–681. https://doi.org/10.1016/J.CIRP.2017.05.009
4. Hölker-Jäger R, Tekkaya AE (2017) Additive manufacture of tools and dies for metal forming. In: Laser additive manufacturing. Elsevier, pp 439–464. ISBN 9780081004333
5. Upadhyay M, Sivarupan T, El Mansori M (2017) 3D printing for rapid sand casting—a review. J Manuf Process 29:211–220. https://doi.org/10.1016/J.JMAPRO.2017.07.017
6. Hackney P, Wooldridge R (2017) Optimisation of additive manufactured sand printed mould material for aluminium castings. Procedia Manuf 11:457–465. https://doi.org/10.1016/J.PROMFG.2017.07.136
7. Kalpakjian S, Schmid SR (2014) Manufacturing engineering and technology, 7th edn. Pearson, New Jersey, USA. ISBN 978-0133128741
8. Laurenti Gómez JJ, Trujillo Vilches FJ, Martín Béjar S (2017) Design and nanufacturing of a sand casting process equipment, Final year project. Universidad de Malaga, Malaga
9. López Rodríguez J (2011) *Fundamentos de conformación por deformación plástica*; Universidad Politécnica de Cartagena
10. Beeley P, Beeley P (2001) 3—Solidification 2 The feeding of castings. In Foundry technology, pp 100–VIII. ISBN 9780750645676
11. Alberto J, Chacón G, Urra AE (2016) Estudio de la influencia de diferentes diseños de los sistemas de alimentación y compensación en la fundición en arena, Sevilla
12. Hipsher Tool & Die—Indiana tool and die—Indiana Machines—3-D printing. Available online: http://www.hipshertool.com/pages/products-services/3-d-printing.php. Accessed on 23 Jan 2018

Approach to the Management Applied to the Periodical Technical Inspection (PTI) Stations in the Context of Industry 4.0

J. García-Cordonié, P. Izquierdo(✉), J. A. Vilán, A. Segade, E. Casarejos, and M. Lopez

Department of Mechanical Engineering, University of Vigo, Campus as Lagoas-Macosende Vigo, 36210 Vigo, Spain
+34-986-813-781pabloizquierdob@uvigo.es

Abstract. This work is a first approach to the management applied to the Periodical Technical Inspection (PTI) stations in the context of Industry 4.0. Since 1965, PTIs are mandatory in Spain, initially only for public transport and freight trucks, but since the 1980s they are compulsory for all types of vehicles, in order to control vehicles technical performance to avoid traffic accidents. Number of PTI stations and inspection lines have been increased from 1981 to 2017, from about 30 to more than 460 operative stations and from about 70 to more than 1200 inspection lines. This fact makes necessary to implement a new management model in the context of the Industry 4.0 that will lead to the PTI 4.0. The use of cyber physical systems, and the application of smart factory concepts in the inspection processes will allow to incorporate new benefits to the management of PTI stations, in addition to improving their effectiveness and efficiency. Regarding 2016 data, more than 19.5 million of vehicles were inspected in Spain and almost 24 million of defects were detected. Also, the total number of vehicles has increased about a 3.6%, but inspections have been increasing more than 5%. Taking into account the number of items to verify, the use of Industry 4.0 theologies, such as Big Data, is highly recommended. In addition, since 2013, Spanish DGT has launched Telematics' Information Exchange with the objective to get telematics data recording of the PTI results. This make necessary to contemplate concepts based on Industry 4.0 for their management.

Keywords: Periodical technical inspection · Vehicle · Management · Industry 4.0

1 Introduction

This work is focused on the study of the management applied to the Periodical Technical Inspection (PTI) stations in the context of Industry 4.0. This term defines the fourth industrial revolution as a strategic initiative of the German Government adopted as part of the High Technology Strategy Action Plan for 2020 [1]. There is an extensive bibliography that study main principles for industry 4.0, such as [2, 3, 4], and in the

F. Cavas-Martínez et al. (Eds.): *Advances on Mechanics, Design Engineering and Manufacturing II*, LNME, pp. 370–379, 2019.
https://doi.org/10.1007/978-3-030-12346-8_36

current paper, different proposals for applying Industry 4.0 principles to the management of PTI-stations are analyzed.

In the context of the automotive industry, principles of Industry 4.0 are being implemented during last few years [5, 6]. From our point of view, this fact makes necessary to apply the same principles not only to the automotive manufacturing industry, but also to the companies responsible for the vehicle PTI. All those technologies bring along with them an improve not only in relation to cost, but also with quality, and due to that, the aim of PTI: guarantee the appropriate mechanical performance of vehicles during all their useful-life, and in the last case, the traffic safety and the environmental protection. According to several studies, PTI stations avoided 11,000 traffic accidents, about 11,000 injured and 170 fatalities, which represents an economic benefit of 300 M€ [7]. Other studies [8] show similar results. Besides, current legislation about "periodic roadworthiness tests for motor vehicles and their trailers", that is contained in Directive 2014/45/EU [9] that repeals previous Directive 2009/40/EC, established PTI as mandatory.

An approach to PTI 4.0 is analyzed in the current paper, as well as how different technologies could be implemented in PTI in order to improve the stations management, such as Big Data, Cloud Computing, Collaborative Robotics, Augmented Reality and Cybersecurity, in summary, the use of cyber-physical systems (interaction between electronic and physical systems). The use of cyber-physical systems will allow the incorporation of new benefits to the work carried out by the inspectors, in addition to improving their effectiveness and efficiency. This paper describes an approach to the implementation of intelligent factory concepts, this means, the implementation of technologies such as collaborative robotics and augmented reality in the inspection processes to, for example, improving the measurement of the vehicles and the check of tasks during visual inspection.

Moreover, devices interconnection, such as Internet of Things (IoT), applied to PTI stations, can facilitate the information flow. Gathering information about the vehicles (e.g. manufacturer, type approval password, main characteristics, emission levels, etc.) will facilitate the Inspection, but it makes necessary to implement adequate data management and processing systems. In addition, the definition of mobile applications will bring to clients an easier and better interaction before, during and after the inspection: request a service appointment, payment of the service, delivery of documentation, access to the inspection line, information about the inspection, queries, complaints and claims, etc. Likewise, it should take into account the possibilities offered by Cloud Computing and Internet Services: provide new utilities and information to customers, which will be accessible from different electronic devices (computers, tablets, mobile phones, etc.).

In addition, in 2013, Directorate General of Traffic (DGT) of Spain launched the ITICI project (Telematics' Information Exchange with the Industry Departments). This project came with the main objective of getting a real-time update of the data in the vehicle registry, through the telematics recording of the results of the PTI and reforms carried out by the PTI-stations. That makes necessary a better and faster online interconnectivity of the PTI-stations to develop the inspections according to the new reality of Industry 4.0 and that the companies that offer these services have to be adapted to a PTI 4.0.

2 Evolution and Current State of the Periodical Technical Inspection (PTI) in Spain

Periodical Technical Inspection (PTI) starts in Spain in 1965. In the first moment, the inspections were applied only to public transport and freight trucks. Inspection was carried out by the Ministry of Industry (through Provincial Offices). In 1980, due to the increase in the number of vehicles in circulation and the number of traffic accidents, the Administration planned to carry out the inspection of all types of vehicles. In order to carry it out, the exercise of the activity was allowed to the private companies.

The participation of private companies was done under the modality of 'Administration Collaborating Entities' by concession. This participation meant a strong increase in the number of PTI stations and inspection lines in service, such it is shown in Fig. 1, from about 30 in 1981 to about 460 in 2017, and also in the inspection lines: from about 70 to more than 1200 in the same period.

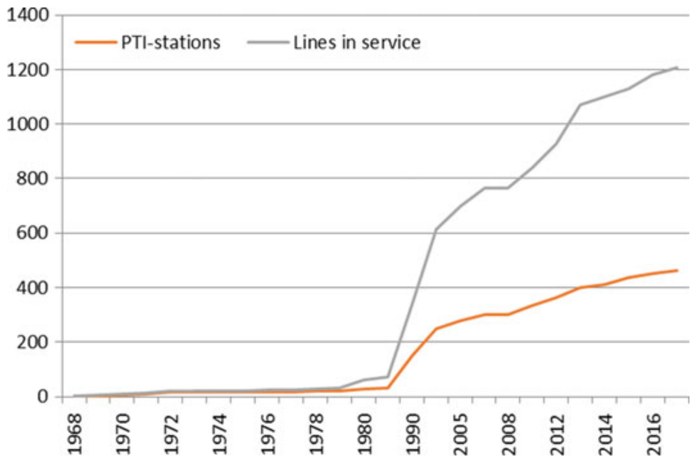

Fig. 1. Evolution of PTI stations and inspection lines in service in Spain (1968–2017). *Source* Own elaboration based on data from PTI Entities Association and Ministry of Industry

During the 1980s, the PTI competence was transferred from the State to the Spanish Autonomous Communities, which received the transferred competencies in industry and, therefore, for vehicle technical inspections. From that moment, the Communities acquired the functions of the organization of the service in their territory and of supervision and control of the operation of the PTI stations. It should be noted that, in terms of tariffs, each Community is able to establish them independently in each territory, since the conditions for providing the service could be different in each one.

In 1982, 30 PTI-station operators, both private and public became the Spanish Association of Collaborating Entities of the Administration in the Technical Inspection of Vehicles (AECA-ITV). This association represents the majority of entities in the sector and it is integrated by practically all the companies that operate the service. The

Association provides updated information on PTI services: stations, lines of operation, registers, 'ok' and 'non-ok' rate, etc. According to the latest published data, in 2017, the number of PTI stations in Spain is about 464 centers and there is a total of 1206 inspection lines. In 1990, the Ministry of Industry, in collaboration with all the Autonomous Communities, published the first Inspection Procedure Manual for ITV Stations. This document includes [10] the different operations to be carried out during the inspection process, indicating the applicable legislation, as well as the interpretation of the defects to be taken into account in each case. According to the database published by AECA-ITV and by the Ministry of Industry [11] from 1992, when the historical records begin, to last year with data, 2016 (pending the publication of the year 2017), the yearly evolution of the inspections has increased, multiplied by 3, but, on average, the number of rejections of this period is about 21%, remaining stable throughout all these years, varying only between 18 and 24% (see Fig. 2).

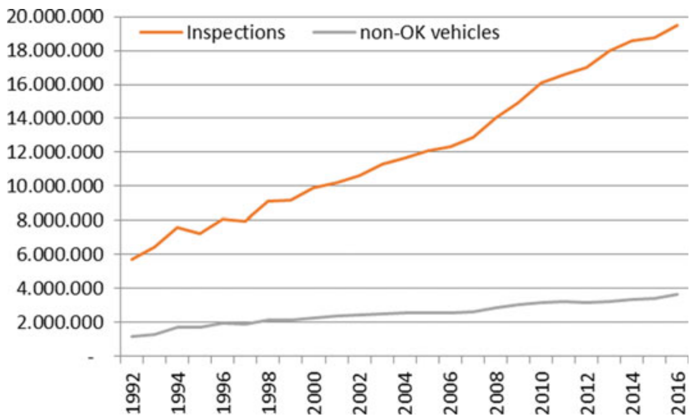

Fig. 2. Evolution of number of technical inspections and rejected vehicles in Spain (1992–2016). *Source* Own elaboration based on data from PTI Entities Association and Ministry of Industry

3 Industry 4.0: Basic Concepts and Application to PTI Stations Management

The term 'Industry 4.0' was originated in Germany as a new Government strategic plan adopted as part of the Action Plan of the High Technology Strategy for 2020, whose objectives are to ensure the future of the country's industry. It was presented at the Technological Fair of Hannover in 2011. This term refers to the 4th industrial revolution characterized by the connectivity between machines and people, that means, Cyber Physical Systems (CPS) in which the physical and virtual worlds converge to achieve greater flexibility in manufacturing and process management. One of the main points of this revolution consists in the integration of products, information and people with high levels of digitalization and connectivity, aiming to achieve a qualitative leap in the procurement of goods and services. It is based fundamentally on three pillars:

Cyber Physical Systems (CPS), *Internet of Things* (IoT) and *smart factories*, with several technologies involved: *Big Data, Cloud Computing*, *Collaborative robotics, Augmented reality* and *Cybersecurity,* which are mentioned below, focusing their applicability on the PTI processes.

3.1 Cyber Physical Systems (CPS)

The Cyber Physical Systems allow the hybridization of the physical and the digital worlds and make possible the interconnection (collaborative work) between objects. It is based on the concept of embedded systems and the integration of both hardware and software into products: vehicles, machinery, equipment, instruments, etc. This concept is useful to PTI stations where the installation of hardware-software in all the equipment allow to get information automatically from them, integrating this information in the inspection processes in an automated way and thus reducing time-operation.

For example, it is possible to digitize the measurements made by the equipment and use them for the automatic qualification of the defects associated with them, while they are transmitted to the station server and presented, to be visualized, on fixed screens installed in the inspection lines and/or portable PDA-type screens handled by the inspectors. In addition, they can register in these devices all other defects that they are detecting, which are also transmitted to the station server for the subsequent generation of the inspection report of each vehicle.

3.2 Internet of Things (IoT)

Internet of Things (IoT) concept was first used in 1999 at the Massachusetts Institute of Technology (MIT). This term refers to the internet connection used on any object, not only usual electronic devices (computers, tablets, mobile phones or televisions). Objects should incorporate a unique identifier (UID) that would allow access to their data and the communication among them. For this reason, the Internet of Things is also called Machine to Machine (M2M) communication, due to the fact that it allows to interconnect objects and devices, and share data between them. One specific application of the IoT, in relation to the automobile industry, is Vehicle-to-Vehicle (V2V) communication technology. The European Commission expressly refers to applications of V2V in one document about the EU's road safety objectives for the 2011–2020 horizon [10] which consists of a standard of communication between vehicles to connect them with 'the cloud' (transmit and receive information in real time), in order to increase the safety of traffic and avoid traffic accidents. The pioneer in the development of these systems has been General Motors, but at the moment, there are also other companies such as Toyota, BMW, Daimler, Honda, Audi and Volvo working on it. Currently, a Car-to-Car (C2C) communication consortium has been set up. This is a European car manufacturers organization that continues to increase the safety and efficiency of road transport using a Cooperative Intelligent Transport Systems (C-ITS), which will allow road users and traffic managers to share information and use it to coordinate their actions, supported by V2V and vehicle-to-internet (V2I) communications.

3.3 Smart Factory

The smart factory consists of the interconnection of machines, processes, systems and people to establish a communication network at an internal level and also linked to the outside. This factory allows sharing information throughout the production process as well as the logistic one, which includes not only manufacturing but also provisioning and distribution. This aims to manage smarter, agilely and efficiently, and optimize it quickly and flexibly to changes in the processes. This concept must be developed and applied in PTI stations to promote a new management concept: PTI 4.0, which we describe in the next section.

4 PTI 4.0: A New Management Model for PTI Stations in the Context of Industry 4.0

During the last years, there has been an impulse of the digitalization in Spain with initiatives such as ‘Connected Industry 4.0’ [11]. This report indicates that digitization, social and specifically industrial, is an opportunity and a challenge that must search for a hyper-connected client. To facilitate the change of the Spanish model to the connected industry 4.0, four main lines of action are defined: digital evolution, training on digitalization, creation of collaborative environments and impulse of digital tools.

4.1 Towards PTI 4.0

In order to respond to the challenges, the technical inspection of vehicles of the future must take up the existing trends in the industry and, therefore, incorporate them into its activities. A new management model must be implemented in the context of the Industry 4.0, leading to the connected PTI 4.0. This will cause an important increase in the competitiveness of the companies, being able to adapt better and faster to the changes, and offering the flexibility in their processes and the personalization of their services that increasingly demand the consumers. The use of cyber physical systems, the application of smart factory concepts and the implementation of technologies such as collaborative robotics and augmented reality in the inspection processes (for example, for vehicle measurement o for checking tasks of visual inspection) will allow to incorporate new benefits to the management of PTI stations, in addition to improving their effectiveness and efficiency. Moreover, the use of some of the possibilities offered by the Internet of Things (IoT) can facilitate gathering information about the inspected vehicles, directly from the vehicle: manufacturer, type-approval password, main characteristics, emission levels…). This also allows an interaction with clients by using mobile devices, both before and after the inspection, and even during it: information requests, payment, documentation delivery, access to the inspection line, information, inquiries, complaints and claims, etc.

Given the huge amount of information generated in PTI stations, the use of Big Data will allow a more appropriate treatment of data in relation to customers: improvement of communication and interaction, strengthening of existing emotional links, realization of commercial actions and, as a consequence of the above, increase of their loyalty to the company which will be considered closer and more transparent and reliable

The management of the information generated by the company contemplating the adoption of concepts and tools based on cybersecurity technology -which, in addition, will be unavoidable to the extent that progress is made towards interconnected PTI-will make it possible to offer greater confidence to the Administration and users of PTI service regarding the use of ICT, the protection of the data handled (guaranteeing, in accordance with the provisions of the UNE-EN ISO/IEC 27001: 2014 [12], the preservation of its confidentiality, integrity and availability, the ability to respond to incidents that may arise and the treatment of existing risks.

In relation to PTI management of Information and communications technology (ICT), it must be taken into account the huge amount of information generated. In the Spanish context, inspections are regulated by the PTI-Station Inspection Procedure Manual [13], issued by the Ministry of Industry, in collaboration with all Autonomous communities and the Spanish Association of Collaborating Entities of the Administration in the Technical Inspection of Vehicles (AECA-ITV). According to this manual, vehicles are classified in five typologies and for each typology, ten specific chapters are developed in the Manual with the instructions about the inspection units (documentation, the number of frames and plates of registration for the first of those indicated) which causes that during a technical inspection more than 100 items have to be checked per vehicle. Ministry publishes a database about PTI in Spain [14]. In 2016, more than 19.5 million of vehicles inspected and less than 19% rejected. Almost 24 million of defect detected more of them minor defects (17 million). Table 1 shows a more exhaustive detail about typology of vehicle and inspections (ok and non-ok).

Beside this, Table 2 shows the yearly evolution of PTI in Spain during last years: from 2014 to 2016. It is clear that the number of inspections is growing, also in relation to the number of vehicles registrations. In fact, even the total number of vehicles increase about a 3.6%, inspections have increased more than 5%. Taking into account the number of items verified in each vehicle during the technical inspection and the number of vehicle, the use of technologies such as Big Data is highly recommended.

Table 1. Database 2016: PTI, OK, non-OK vehicles

	Motorbikes	Touring	Truck	Bus	Trailer	Agric. vehicles	Other	Total
OK	803.921	11.206.227	2.583.608	397.421	64.101	268.541	458.931	15.847.526
Non-OK	165.946	2.369.151	791.106	143.997	20.689	93.203	52.601	3.661.854
Total	969.867	13.575.378	3.374.714	541.418	84.790	361.744	511.532	19.509.380
% Non-OK	17	17	27	24	26	10	28	19

Source MINECO [13]

Table 2. Evolution of number of vehicles and PTI in Spain (2014–2016).

Year	Number of vehicles	PTI	% PTI versus number of vehicles
2014	30.976.047	18.579.016	60.0
2015	31.389.683	18.757.553	60.0
2016	32.106.520	19.509.380	60.7
2014–2016	94.472.250	56.845.949	60.2

Source MINECO [13]

In addition, in 2013, Spanish Directorate General of Traffic (DGT) launched the ITICI project (Telematics' Information Exchange with the Industry Departments). This project is focused on getting a real-time update of the data in the vehicle registry, through the telematics recording of the results of the PTI and reforms carried out by the PTI-stations. That makes necessary a better and faster online interconnectivity of the PTI-stations to develop the inspections according to the new reality of Industry 4.0 and that the companies that offer these services have to be adapted to a PTI 4.0.

Finally, the management of the information generated must contemplate concepts and tools based on cybersecurity, which will be unavoidable insofar towards PTI 4.0 interconnected, making possible to offer confidentiality between the Administration and users.

5 Conclusions

This work is an approach to the management applied to the Periodical Technical Inspection (PTI) stations in the context of Industry 4.0. An extensive review about main principles of the Industry 4.0 is done, in order to study their applicability towards a PTI 4.0. All those technologies bring along with them an improvement not only in relation to cost, but also to quality, and due to that, the aim of PTI: to guarantee the appropriate mechanical performance of vehicles during all their useful-life, and in last case, the traffic safety and the environmental protection.

First, a study of the current state of the PTI in Spain and its evolution since its inception was carried out. PTI starts in Spain in 1965 but in the first moment, only to public transport and freight trucks. Since 1980, due to the increase in the number of vehicles in circulation and the number of traffic accidents, the Administration planned to carry out the inspection of all types of vehicles. It was necessary the participation of private companies to provide the inspection services to all the vehicles and this fact produced a strong increase in the number of PTI stations: from about 30 in 1985 to 500 in 2016, and also in the inspection lines: from 70 to more than 1200.

According to database published by AECA-ITV and by the Ministry of Industry, from 1992 to 2016, the yearly evolution of the inspections is increasing multiplied by 3 (from 6 to 20 million of inspections) but, on average, the number of rejections of this period is about 21%, remaining stable throughout all these years, varying only between 18 and 24%.

During the last years there has been an impulse of the digitalization in Spain. To facilitate the change of the Spanish model to the connected industry 4.0, four main lines of action are defined: digital evolution, training on digitalization, the creation of collaborative environments and impulse of digital tools. In order to respond to the challenges, future vehicles' PTI must take up the existing trends in the industry and, therefore, incorporate them into its activity. A new management model must be implemented in the context of the Industry 4.0 that will lead to the connected PTI 4.0. The use of cyber physical systems, the application of smart factory concepts and the implementation of technologies such as collaborative robotics and augmented reality in the inspection processes (for example, for the checks carried out on tasks of visual inspection) will allow the incorporation of new benefits to the management of PTI stations, in addition to improving their effectiveness and efficiency.

According to the PTI-Station Inspection Procedure Manual, vehicles are classified in five typologies and for each typology, ten specific chapters are developed which causes that during a technical inspection more than 100 items have to be checked per vehicle. According to 2016 data, more than 19.5 million of vehicles were inspected and less than 19% rejected. Almost 24 million of the defects detected, most of them minor defects (17 million). In fact, even the total number of vehicles increase about a 3.6%, inspections have been increasing more than 5%. Taking into account the number of items verified in each vehicle during the technical inspection and the number of vehicles, the use of technologies such as Big Data is highly recommended.

In addition, in 2013, Spanish DGT launched the ITICI project (Telematics' Information Exchange with the Industry Departments). This project come with the main objective of getting a real-time update of the data in the vehicle registry, through the telematics recording of the results of the PTI and reforms carried out by the PTI-stations. In addition to this, the management of the information generated must contemplate concepts and tools based on cybersecurity to make possible to offer confidentiality between the Administration and the users.

References

1. Kagermann H, Wahlste, W, Helbig J (2013) Securing the future of German manufacturing industry: recommendations for implementing the strategic initiative INDUSTRIE 4.0. Final report of the Industrie 4.0 Working Group. Acatech- National Academy of Science and Engineering—Deutsche Akademie der Technikwissenschaften
2. Lasi H, Fettke P, Kemper H-G, Feld T, Hoffmann M (2014) Industry 4.0. Bus Inf Syst Eng 6:239–242. https://doi.org/10.1007/s12599-014-0334-4
3. Hermann M, Pentek T, Otto B (2016) Design principles for Industrie 4.0 scenarios. In: Proceedings of the Annual Hawaii international conference on system sciences. Hawaii, USA. IEEE Computer Society. https://doi.org/10.1109/hicss.2016.488
4. Roblek V, Meško M, Krapež A (2016) A complex view of Industry 4.0, vol 6. SAGE Open, pp 1–11. https://doi.org/10.1177/2158244016653987
5. Gruber FE (2013) Industry 4.0: a best practice project of the automotive industry. In: IFIP TC 5 international conference on digital product and process development systems NEW PROLAMAT. IFIP advances in information and communication technology, vol 411. Dresden, Germany, pp 36–40

6. Santos MY, Oliveira-Sá J, Andrade C, Vale-Lima F, Costa E, Costa C, Martinho B, Galvão J (2017) Big Data system supporting Bosch Braga Industry 4.0 strategy, vol 37. pp 750–760. https://doi.org/10.1016/j.ijinfomgt.2017.07.012
7. San Román García JL, Gauchía Babé A, Díaz López V (2012) Contribution of Periodic Motor Vehicle Inspection (PMVI) to vehicle safety. Fundación Instituto Tecnológico para la Seguridad del Automóvil (FITSA). Instituto de Seguridad de los Vehículos Automóviles (ISVA). Universidad Carlos III, Madrid
8. AUTOFORE (2017) Study on the future options for vehicle roadworthiness enforcement in the European Union. http://citainsp.org/wp-content/uploads/2016/01/PressReleaseEN.pdf. Last Accessed 20 Dec 2017. CITA
9. Directive 2014/45/EU of the European Parliament and of the Council of 3 April 2014 on periodic roadworthiness tests for motor vehicles and their trailers and repealing Directive 2009/40/EC. http://eur-lex.europa.eu/legal-content/EN/TXT/?uri=CELEX:32014L0045. Last Accessed 02 Mar 2018
10. European Commission. COM (2010) 389: Communication from The Commission to The European Parliament, The Council, The European Economic and Social Committee and The Committee of the Regions: Towards a European road safety area: policy orientations on road safety 2011–2020 (2010)
11. Ministry of Industry, Energy and Tourism of Spain. Industria Conectada 4.0: LA TRANSFORMACIÓN DIGITAL DE LA INDUSTRIA ESPAÑOLA (2012). http://www.industriaconectada40.gob.es/Paginas/index.aspx. Last accessed 09 Mar 2018
12. UNE-EN ISO/IEC 27001: 2014 Information technology. Security techniques Information Security Management Systems (ISMS). Requirements
13. PTI-Station Inspection Procedure Manual (Manual de Procedimiento de Inspección de las estaciones-ITV). Ministry of Energy, Tourism and Digital Agend (MINETAD) of Spain. http://www.f2i2.net/documentos/lsi/STO_Vehiculos/ITV/Manual_de_procedimiento_de_inspeccion_de_estaciones_ITV_v722_Feb_2018.pdf. Last accessed 10 Jan 2018
14. PTI Statistics in Spain. Ministry of Economy, Industry and Competitiveness (MINECO). http://www.f2i2.net/legislacionseguridadindustrial/Si_Ambito.aspx?id_am=20100. Last accessed 20 Dec 2017

Influential Parameters in Plunge Milling for Titanium Alloy Ti-6Al-4V

M. Fredj(✉), F. Monies, W. Rubio, and J. Senatore

Institut Clément Ader, Université Toulouse, Paul Sabatier 3, 3 rue Caroline Aigle, 31400 Toulouse, France
montassar-abdelhack.fredj@univ-tlse3.fr

Abstract. Plunge milling is an interesting production mean for machining deep workpieces. It is identified as a process potentially able to afford significant gains in productivity during the roughing phases, especially in the case of workpieces made of hard materials. Within this paper, a study of cutting forces in plunge milling of titanium alloy Ti-6Al-4V is conducted. Several types of inserts provided by manufacturing tools suppliers with various cutting angles, type of chip breaker and nose radius, are exploited along with different cutting parameters. The results show the influence of the geometrical parameters and cutting parameters on the cutting forces, and give various information to establish next the optimal trajectories of the tool during plunge milling operations on titanium alloys, according to the type of workpieces.

Keywords: Plunge milling · Cutting forces · Titanium alloy Ti-6Al-4V

1 Introduction

When working in deep slots and cavities with traditional milling, tool bending and vibrations are usually encountered. These problems are generally solved by reducing cutting parameters. However, using this solution causes a loss of productivity, especially during roughing phases. As a better alternative, plunge milling can be employed [1]. This technique involves a series of successive plunges (axially) into the stock, each time separated by a radial offset as presented in Fig. 1. The benefit of plunge milling is that the cutting forces change from radial to axial, leading to more stability, particularly required when using a long tool assembly and machining difficult-to-cut materials like titanium alloys. Thus, cutting parameters can be increased and less time will be needed to remove the excess material.

Most of the previous works related to cutting forces in plunge milling were conducted on materials other than titanium alloys such as stainless steel [2], magnesium alloys [3], aluminum alloys [4] and they were mainly concentrated on the effect of cutting parameters. On the other hand, plunge milling cutting forces in the case of titanium alloys are little addressed [5] and their analysis didn't take into account the effect of geometrical parameters represented by cutting angles, type of chip breaker, edge radius and nose radius. Therefore, our work focuses on studying the influence of cutting parameters and geometrical parameters on plunge milling operation applied on

F. Cavas-Martínez et al. (Eds.): *Advances on Mechanics, Design Engineering and Manufacturing II*, LNME, pp. 380–390, 2019.
https://doi.org/10.1007/978-3-030-12346-8_37

titanium alloys. The experimental procedure is described in paragraph 2. An analysis of cutting forces in accordance with cutting and geometrical parameters is then carried out in paragraph 3. Finally, a conclusion is given in paragraph 4.

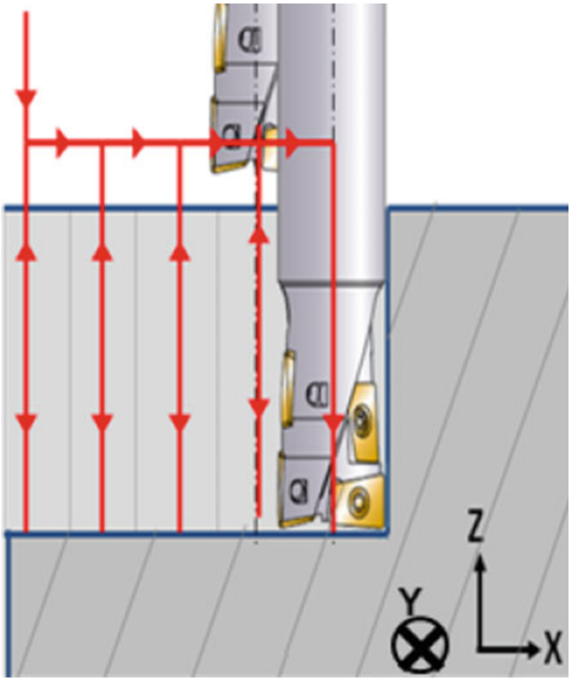

Fig. 1. Plunge milling principle

2 Experimental Protocol

2.1 Material

The studied material Ti-6Al-4V is one of the most commonly used titanium alloys. The composition of this alloy and its properties are presented in Table 1 and Table 2 [6].

Table 1. composition of Ti-6Al-4V

Element	Al	V	N	C	H	Fe	O	Ti
Percentage	6	4	<0.05	<0.1	<0.015	<0.3	<0.2	Balance

Although titanium is as strong as steel, it is about 40% lighter in weight, which, along with its high strength and exceptional corrosion resistance makes it an essential structural metal for aerospace field [7]. However, machinability of titanium alloys is considered as an important issue [8, 9]. In fact, titanium and its alloys have a low

Table 2. Properties of Ti-6Al-4V

Property	Minimum value	Maximum value	Units
Density	4.429	4.512	g/cm^3
Elastic limit	786	910	MPa
Young's modulus	110	119	GPa
Ductility	0.05	0.18	
Thermal conductivity	7.1	7.3	W/m K

modulus of elasticity and a high elastic limit, which causes the problem of spring back during machining. Also, because of the relatively low thermal conductivity of titanium alloys, the intense heat produced during machining is absorbed by the cutting tool which eventually wears more rapidly. Added to that, the feed speed and cutting speed required when machining these metals are generally low, which leads to a low material removal rate. Therefore, an optimum choice of the cutting conditions and tool is essential.

2.2 Cutting Tools

The cutting tools are chosen from the plunge milling products proposed by recognized manufacturing tools suppliers. The first tool is a 32 mm diameter Mitsubishi AJX milling cutter and the second tool is a 33 mm diameter Mitsubishi AQX milling cutter (Fig. 2). Several types of inserts with differences in macro and the micro-geometries are used in order to analyze the influence of those parameters on the process. The cutters are designed for roughing, and the grades of the inserts are adapted for machining titanium alloys.

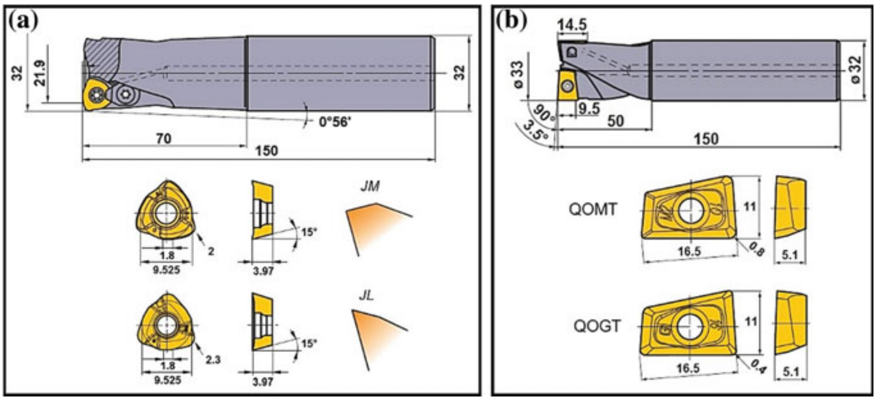

Fig. 2. Cutting tools: Mitsubishi AJX (**a**); Mitsubishi AQX (**b**)

Cutting angles and edge radius of the cutters are obtained with a profile projector and the 3D optical measurement system Alicona (Table 3). Kr is the angle between the main cutting edge of the insert and the tool displacement, $\gamma 1$ and $\gamma 2$ are the effective axial cutting angles ($\gamma 1 = \gamma n1 + \gamma p$ and $\gamma 2 = \gamma n2 + \gamma p$), and fz* is the limit of fz which defines the zone where only $\gamma 1$ is active (Fig. 3).

Table 3. Geometrical parameters of cutting tools

	Mitsubishi—JL	Mitsubishi—JM	Mitsubishi—QOGT	Mitsubishi—QOMT
$r\varepsilon$ (mm)	2.3	2	0.4	0.8
$r\beta$ (μm)	21	27	35	70
Kr °	103	115	86	86
αn °	17	18	12	17
βn °	54	57	59	64
$\gamma n1$ °	5	−19	19	−1.5
$\gamma n2$ °	19	15		9
γf °	−6	−6	0	0
γp °	7	7	6	6
$\gamma 1$ °	12	−12	25	4.5
$\gamma 2$ °	26	22		15
fz*	0.27	0.19		0.22

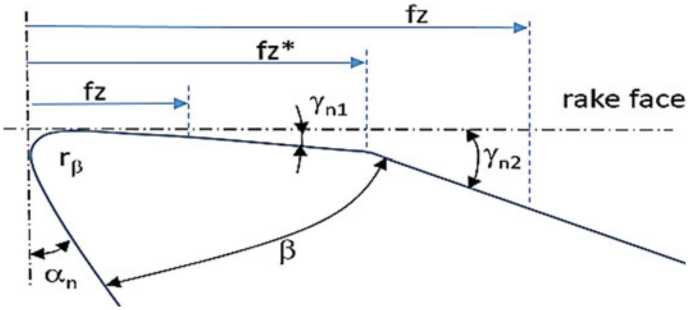

Fig. 3. Geometrical parameters of the insert

2.3 Experimental Procedure

A DMU 85 monoBLOCK 5-axis CNC machine is used to perform full width cut plunge milling tests on titanium alloy Ti-6Al-4V blocks, with lubrication and only one insert. Different values of cutting speed Vc, feed per tooth fz and radial offset ae (Table 4) are used in order to analyze the influence of these parameters on cutting forces. The cutting depth is 10 mm and cutting forces are given by a Kistler six-component force measurement plate 9257B.

Table 4. Cutting parameters

Vc (m/min)	fz (mm)	ae (mm)
50	0.1	2
60	0.15	3
70	0.2	4
80	0.25	5
	0.3	

The measured forces are the three orthogonal components of cutting force Fx, Fy and Fz. These forces are then converted into the rotating reference of the cutter in order to obtain the tangential Ft, radial Fr and axial Fa forces using the Eqs. (1–3) based on the angle of engagement of the insert θ in the chip area and entry angle θ_e (Fig. 4). During tests, one of the cutting parameters is changed for each plunge, in order to evaluate its influence on cutting forces.

$$F_t = F_y \cdot \cos\theta - F_x \cdot \sin\theta \tag{1}$$

$$F_r = F_x \cdot \cos\theta + F_y \cdot \sin\theta \tag{2}$$

$$F_a = F_z \tag{3}$$

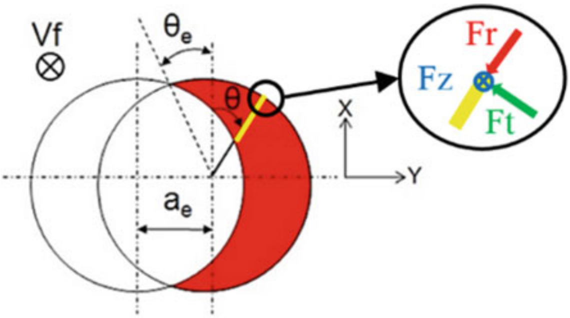

Fig. 4. Chip area for full width cut plunge milling

3 Results and Discussion

The analysis is based on the maximum value of forces. The tangential force and the axial force are maximum in the position θ = 90° (Figs. 4 and 5). Although the radial force reaches its peak before θ = 90°, its value in this position is still close to the maximum. In fact, the highest stress applied on the tool is at the position θ = 90°, due to there is a maximum chip area. Accordingly, all the forces are considered in that position. Mitsubishi AJX tools will be referred as JM and JL and Mitsubishi AQX tools as QOGT and QOMT.

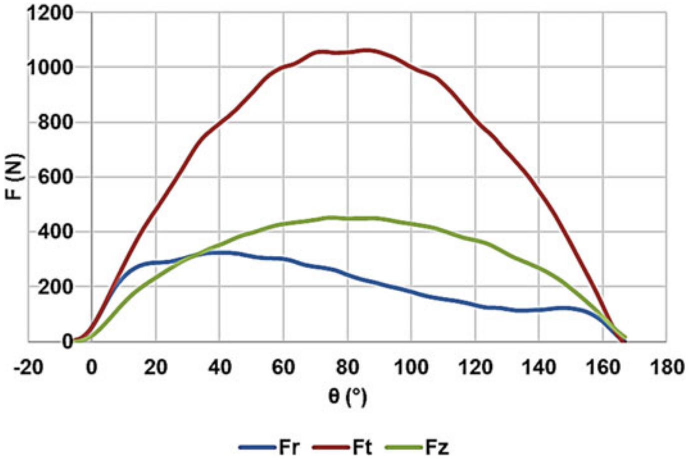

Fig. 5. Test conducted with AQX—QOGT tool using Vc = 60 m/min, fz = 0.2 mm and ae = 5 mm (Low-Pass Filter 150 Hz)

3.1 Influence of Cutting Speed

With a feed per tooth fz = 0.2 mm and a radial offset ae = 3 mm, tests with different values of cutting speed Vc from 50 to 80 m/min are conducted (Fig. 6).

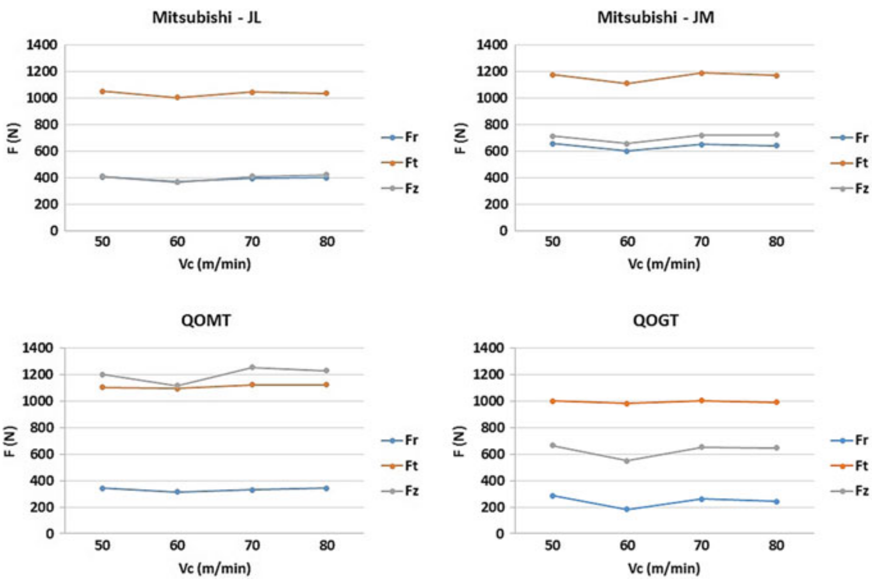

Fig. 6. Influence of cutting speed on cutting forces

For cutting speed Vc = 60 m/min, the cutting forces are minimum and from this value, the cutting speed almost has no effect as we obtain a small increase and then a stabilization. In fact, for that value of cutting speed, the thermal softening is sufficient to cut the material with minimal force and energy. After that, even with greater cutting speed (70 and 80 m/min), a stable cutting process is maintained and the cutting forces almost remain the same. However, cutting speed is considered a very important parameter in terms of the cutting tool life as found in previous works [5, 10].

3.2 Influence of Feed Per Tooth

Tests are carried out with a cutting speed Vc = 60 m/min, a radial offset ae = 3 mm and several values of feed per tooth fz from 0.1 to 0.3 mm (Fig. 7).

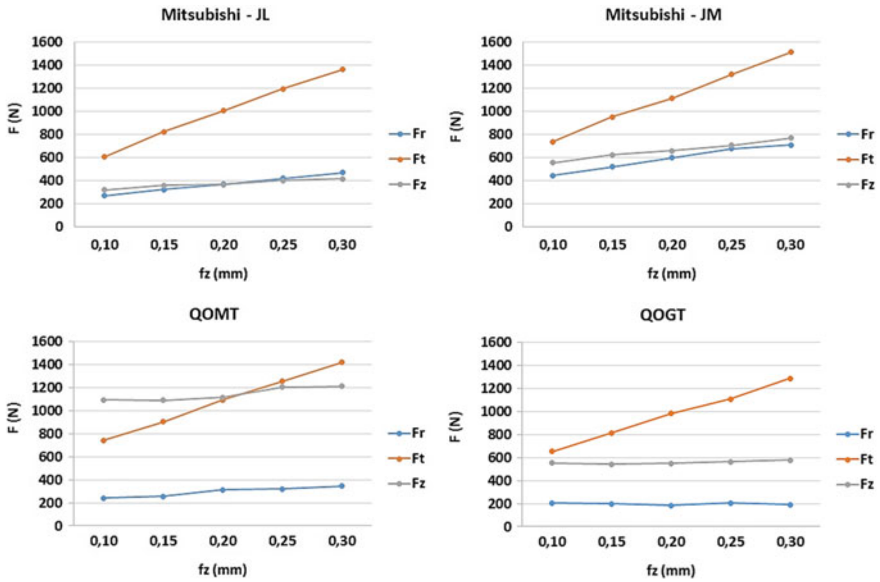

Fig. 7. Influence of feed per tooth on cutting forces

Feed per tooth affects mostly the tangential force which increases almost linearly with this parameter. The dependency of radial and axial forces on the feed per tooth is lower. Indeed, since this parameter represents the height of the maximum cutting section, it indicates the engaged part of the insert nose radius (Fig. 8). When the feed per tooth increases (from fz1 to fz2), that part expands, which induces a raise of both of the forces especially for tools with higher insert nose radius and edge radius.

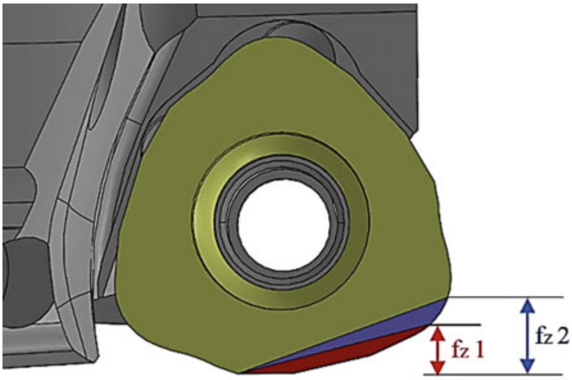

Fig. 8. Dependency of the engaged part of the insert nose radius on feed per tooth (AJX tool)

3.3 Influence of Radial Offset

Different values of radial offset ae from 2 to 5 mm are tested while using a cutting speed Vc = 60 m/min and feed per tooth fz = 0.2 mm (Fig. 9).

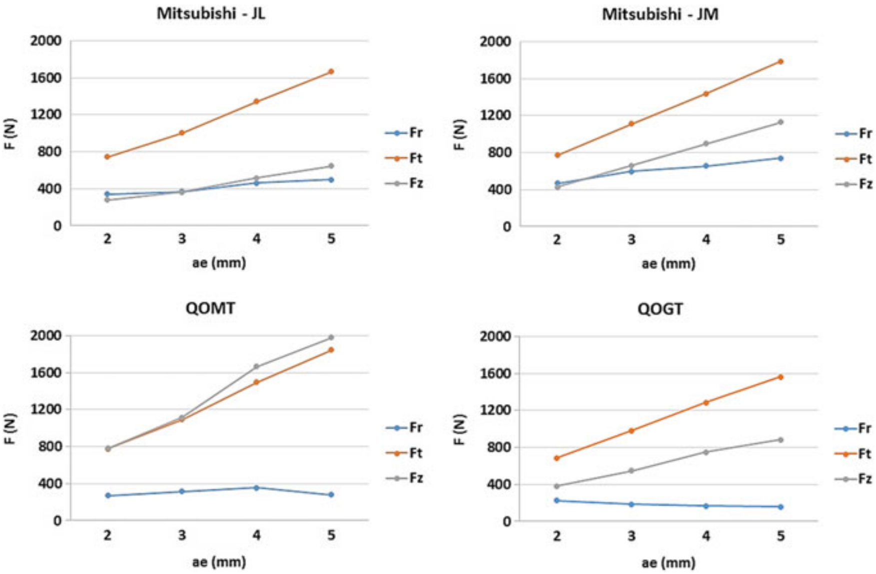

Fig. 9. Influence of radial offset on cutting forces

A quasi-linear increase of the tangential force is obtained when radial offset increases. Besides, a similar behavior is shown by the axial force. The main cause is that when the radial offset increases, the engaged part of the insert becomes larger, resulting in a quasi-linear increase of the axial force. About the radial force, two different behaviors are obtained: for Mitsubishi—JM/JL, a rise of the force is obtained with the increase of radial offset. However, with Mitsubishi AQX, we have a compensation between the components of the force through the main cutting edge, the nose radius and a part of the vertical edge, (Fig. 10) resulting in a little increase and then a decrease of the radial force for QOMT, and a progressive reduction of the effort for QOGT. The two different behaviors are directly related to the cutting edge angle Kr. If this angle is greater than 90°, we have the continuous increase of the radial force. If it is less than 90°, we obtain the compensation between the components of the force.

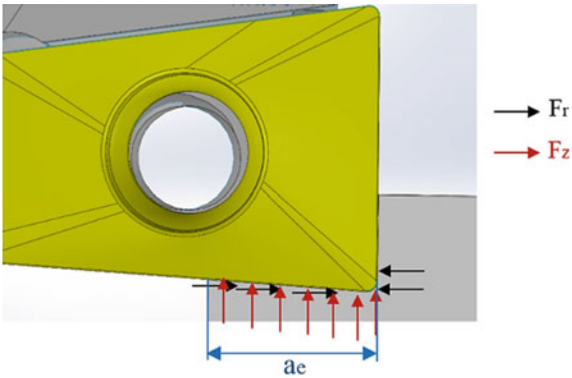

Fig. 10. Representation of radial offset and cutting forces (Mitsubishi AQX tool)

3.4 Influence of Geometrical Parameters

Based on the variation of the maximum forces (Figs. 6, 7 and 9) and the geometrical data of the tools (Table 3), several interpretations are made.

Tangential force is strongly influenced by the axial rake angle as it decreases with the increase of this parameter. In fact, for example with the AJX tool, for feeds per tooth up to fz = 0.25 mm (Fig. 7), the axial rake angle is mainly given by γ1 (JM: −12°, JL: 12°), and the insert JL exhibits then the lowest tangential forces. Edge radius of the insert rβ (QOGT: 35 µm, QOMT: 70 µm) has also an impact on tangential force which is reduced when the tool is sharper, particularly for low feeds per tooth.

Axial force is heavily dependent on the sharpness of cutting edge (rβ) and effective axial cutting angle γ. In fact, the edge radius of QOMT insert is twice as large as that of QOGT insert, and the axial force given by QOMT tool is almost twice that of QOGT tool. In addition to that, the cutting angle γ1 of JM insert is negative (JM: −12°, JL: 12°), resulting in much higher axial force compared to that of JL tool, almost its double.

Radial Forces are heavily influenced by the cutting edge angle Kr, mainly whether it is more or less than 90°. We can see that the tools JL and especially JM (with Kr > 90°) create significant radial forces, which increase when enlarging the engaged part of the insert. But QOGT and QOMT tools generate less radial efforts, which also evolve differently when machining more material (Fig. 9). Besides, radial forces are strongly dependent on nose radius rε too. The laterally engaged part of the insert is greater with using larger nose radius, which engenders higher radial forces. Finally, radial rake angle γf (−6° for JM/JL against 0° for QOGT/QOMT) influences also radial forces, as a negative γf makes the tool blunter and increases the cutting forces.

4 Conclusion

The influence of diverse parameters on plunge milling of titanium alloy Ti-6Al-4V is investigated. Based on the analysis of elementary tests of z-axis milling with different cutting tools, the following conclusions can be drawn:

– Plunge milling provides a minimal radial force, which results in less vibrations and more stability during machining titanium alloys. Besides, radial forces can be minimized by using an insert with a cutting edge angle equal to or less than 90°, a zero radial rake angle, and small edge radius and nose radius.
– On cutting parameters, the radial offset is the most influential on cutting forces. The feed per tooth has a less influence, but considerably important in particular on the tangential and radial forces. While the dependency on cutting speed is relatively low. A good choice of these parameters is essential in order to assure an excellent productivity with acceptable levels of cutting forces.
– The geometrical parameters represented by cutting angles and edge preparation, are very important to have a better behavior of the cutting tool during plunge milling.
– With the inserts JL/JM/QOGT, the tangential force is the highest cutting force. In order to have axial forces of the same order as tangential forces, inserts with high edge radius like QOMT have to be used.
– When using plunge milling for roughing very deep pockets, we can use a tool with a reduced sharpness like AQX – QOMT tool, to have higher axial forces and low radial forces, which results in a better stability during the process.
– The continuation of the study will be related to the wear according to cutting and geometrical parameters, in order to make the best choice of the tool when roughing a specific workpiece made of titanium alloy.

References

1. Cafieri S, Monies F, Mongeau M, Bes C (2016) Plunge milling time optimization via mixed-integer nonlinear programming. Comput Ind Eng 98:434–445. https://doi.org/10.1016/j.cie.2016.06.015
2. Witty M, Bergs T, Schäfer A, Cabral G (2012) Cutting tool geometry for plunge milling—process optimization for a stainless steel. In: 5th CIRP conference on high performance cutting. Procedia CIRP 1, Zurich, Switzerland, pp 506–511
3. Danis I, Monies F, Lagarrigue P, Wojtowcz N (2015) Cutting forces and their modelling in plunge milling of magnesium-rare earth alloys. Int J Adv Manuf Technol 84:1801–1820. https://doi.org/10.1007/s00170-015-7826-3

4. Rafanelli F, Campatelli G, Scippa A (2015) Effects of cutting conditions on forces and force coefficients in plunge milling operations. Adv Mech Eng 7(6):1–9. https://doi.org/10.1177/1687814015589547
5. Sun T, Fu Y, He L, Chen X, Zhang W, Chen W, Su X (2015) Machinability of plunge milling for damage-tolerant titanium alloy TC21. Int J Adv Manuf Technol 85:1315–1323. https://doi.org/10.1007/s00170-015-8022-1
6. AZO Materials, https://www.azom.com/properties.aspx?ArticleID=1547. Last accessed 02 Mar 2018
7. Combres Y (2010) Propriétés du titane et de ses alliages. Techniques de l'ingénieur M4780 1
8. Sun S, Brandt M, Dargusch MS (2009) Characteristics of cutting forces and chip formation in machining of titanium alloys. Int J Mach Tools Manuf 49:561–568. https://doi.org/10.1016/j.ijmachtools.2009.02.008
9. Veiga C, Davim JP, Loureiro AJR (2013) Review on machinability of titanium alloys: the process perspective. Rev Adv Mater Sci 3:148–164
10. Barelli F (2016) Développement d'une méthodologie d'optimisation des conditions d'usinage, application au fraisage de l'alliage de titane ta6v, PhD thesis, Université de Toulouse, France

A Model-Based Approach to Support the Design of Mold Heating for Composites

P. Cicconi[1(✉)], E. Pallotta[1], A. C. Russo[1], R. Raffaeli[2], M. Prist[1], A. Monteriù[1], S. Longhi[1], and M. Germani[1]

[1] Università Politecnica delle Marche, via Brecce Bianche 12, 60131 Ancona, Italy
p.cicconi@staff.univpm.it
[2] Università degli Studi eCampus, Via Isimbardi 10, 22060 Novedrate, CO, Italy

Abstract. Molding is one of the most widely used processing technologies in manufacturing. Among typical molding parameters, the mold temperature is a critical one for the quality of the molding process. A solution to this issue can be the employment of induction heating which, through a high-frequency electromagnetic field, produces eddy currents and a consequent rapid heating of the material into the cavity of the mold. The necessity to maintain the mold walls at the operative temperature makes the induction heating to be one of the most efficient non-contact means of heating. In fact, induction heating is characterized by quickness, efficiency, and energy saving; however, the design and the sizing of an induction heating system is complex due to different parameters involved in the electromagnetic and thermal phenomena. In this context, the paper aims to define a methodology to support engineers in the design and sizing of an induction heating system for molds, taking as case study a mold for composite parts. A model-based approach is proposed to analyze and simulate the mold heating, considering three different levels of modelling: Analytical (0D), Finite-Difference Methods (2D) and Finite Element Methods (3D). The Analytical approach investigates the solution of the physical equations applied to the volume of the material involved. Instead, the Finite-Difference approach (2D) solves the heat transfer problem by discretizing the domain and by solving for temperature at discrete points. Finally, the Finite Element method (3D) solves partial differential equations on a 3D discretized domain.

Keywords: Virtual prototyping · Model-Based simulations · Induction heating · Mold heating · Resin curing · Epoxy-Based carbon fiber prepregs

1 Introduction

Nowadays, different technologies provide solutions for mold heating. A solution is the use of eddy currents with induction systems. Induction heating provides many advantages such as quickness, efficiency, and energy saving [1], if compared with the use of electrical resistances. However, the design and sizing of an induction heating system takes a lot of time due to the complexity of the electromagnetic phenomena [2]. Parameters to be optimized are geometrical dimensions, electrical current, and frequency [3]. The design of a heating system is often a custom application related to the

F. Cavas-Martínez et al. (Eds.): *Advances on Mechanics, Design Engineering and Manufacturing II*, LNME, pp. 391–401, 2019.
https://doi.org/10.1007/978-3-030-12346-8_38

target-objected to be heated [2, 3]. In this context, virtual prototypes and simulations are suitable to estimate energy consumption and validate the resultant temperature profile [4]. In particular, the field of composites manufacturing (epoxy-based carbon fiber prepregs) regards the development of tailored molds for applications such as sports car, racing and aerospace. These applications require high geometrical quality and zero scraps [5]. In addition, this production, which is focused on small batch, requires agile-rapid tools and accurate methods to design and prototype molds.

A virtual prototyping approach is necessary to evaluate the temperature distribution during the polymerization process. In fact, temperature is crucial for the composites manufacturing [6]. The temperature control regulates the chemical polymerization under a defined pressure condition [4, 5]. While the pressure is important to provide no gas-bubbles trapped between the layers of a composite material, the temperature is responsible for the resin curing process. Therefore, the temperature affects the resultant product quality [7]. The necessity to maintain the walls of a mold at the operative temperature, is the motivation on using induction heating in this research. The electromagnetic high-frequency induction is an efficient way for the non-contact heating of magnetic surfaces [2]. Other variothermal-based processes, which use liquid, such as water or oil, have the disadvantage of high cycle times and low productivity [8]. The density of heat flux is very low, and the cooling time is very high. The induction heating enables low cycle times due to the excellent heat flux density, and the possibility to modulate the heating power.

2 Method

The paper describes a methodology to support the engineer during the design, sizing, and simulation of a heating system for molds. A model-based approach is proposed to reproduce the behavior of the related physical system. A model-based simulation is a physical system represented by Object-Oriented (O-O) models, where each model contains information and functions regarding the calculation of performance and system behavior [9]. The model-based approach is an engineering design method applied in several fields such as mechanics, informatics, and electronics [10].

The proposed research approach has been developed considering a test case based on an induction heating system for molds. In particular, a mold for the composites manufacturing has been described in the following test case section. Three different levels of analysis have been considered and discussed to simulate the mold heating. These three levels concern three different domains of geometrical representation: 0D, 2D, and 3D modelling. Figure 1 shows the design workflow to support the molds modelling with virtual prototyping tools in the case of induction heating. Even if the proposed test case is focused on the *Conceptual Design* phase, the approach has been described from the input phase to the detailed design.

The first step regards the input definition, which interests the *Early Planning* phase. The design input is a collection of geometry, material, thermal models, energy consumption and temperature mapping. During the Early Planning phase, the engineer describes the physical model analyzing all involved phenomena and reports them into a graphical representation such as a block diagram.

The second step is the definition of a *Parametric Model*. This model can be performed in three different levels of details from 0D to 3D domain. The resulting model constitutes the *Model-Based Object* (*MBO*) to be performed in the following *Simulation* phase. As stated before, the *Model-Based Object* can be represented with three different levels of domain such as 0D, 2D, and 3D. The approach assigns a simulation level to each level of representation. While a 0D model can be solved using a simple analytical calculation, a 2D model can be computed using a Finite Difference Model (FDM) approach. Finally, a 3D representation is suitable for a Finite Element Method (FEM) analysis.

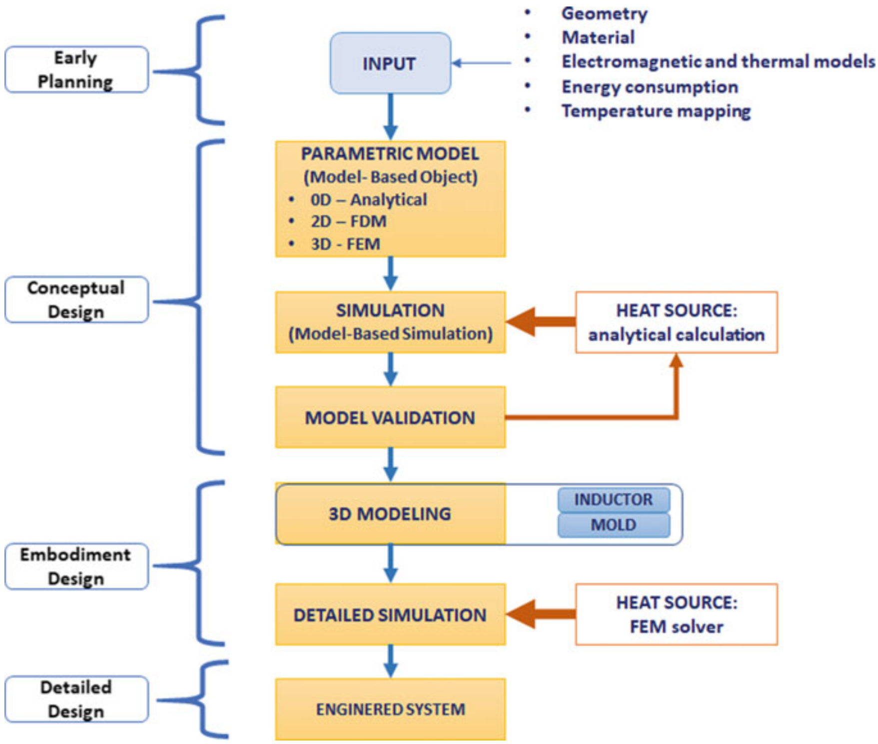

Fig. 1. The proposed design approach

The *Simulation* phase represents the third level of the proposed design workflow. This phase concerns the *Model-Based Simulation* (*MBS*), which is based on the analyzed *MBO*. In this level of *Conceptual Design*, the boundary condition related to the *Heat Source* definition, is evaluated using an analytical calculation. The *Heat Source* condition concerns the induction heating generated from a copper coil (inductor) to a target object to be heated. Therefore, the system efficiency and eddy currents are evaluated considering a 0D analytical approach and solving the Maxwell Functions applied in integral form. The virtual analysis involved in the *MBS* level regards the thermal simulation with a FEM solver to reproduce the temperature distribution on the mold surfaces. On the other hand, the *Embodiment Design* phase concerns the FEM simulation of the electromagnetic phenomena.

The *Model Validation* step is a necessary check analysis to achieve an early feasible study about the performance of the heating system. In particular, in this research, this level concerns the evaluation of the achieved temperature profile and energy consumption. Temperature distribution and energy consumption are compared with the technical specification, highlighted in the *Early Planning* phase as requirements. The design loop iterates until the optimal performance is achieved.

The *Conceptual Design* phase ends with the end of *Model Validation* and the beginning of the *3D Modelling* phase. In fact, this modelling activity regards the definition of a more detailed geometry and the beginning of the *Embodiment Design* phase. This phase also involves virtual analysis; however, the overall simulations are *Detailed Simulations* because the *Heat Source* conditions are calculated using a FEM solver which performs the electromagnetic analysis. Therefore, this simulation level concerns the coupling of two FEM solvers for the analysis of the thermal behavior and the electromagnetic one. Then, the design workflow ends with the *Detailed Design* phase which consists of *Engineered System*.

2.1 Levels of Analysis

As described in Fig. 1, the *Parametric Model* regards the definition of a MBO model which reproduces the behavior of a physical model. In particular, three different levels of modelling are proposed: Analytical (0D), Finite-Difference Methods (2D) and Finite Element Methods (3D). This section describes the three levels of modelling (0D, 2D, 3D) to be used during the Conceptual *Design* phase. Generally, analytical models are more affordable and, therefore, they are used in small-medium enterprises. Even if the designer can use one of them, this paper proposes a comparison between each level of representation. Following, a description has been reported for each level of modelling.

0D: Analytical Analysis

The analytical approach, represented in Fig. 2, considers the solution of the physical equations applied to the volume of the involved material, without analyzing the detailed shapes of the geometry. The approach is 0D-based; therefore, the heat dissipated is calculated considering mass and average area of heat transfer. The heat source is considered as an iterative input calculated at each computing step. The model of the system includes the mass of the mold with its properties (such as heat transfer coefficient, external surfaces, etc.), and the equation of thermal balance between the heat source and the heat dissipated, which will provide the estimation of the average mold temperature. The analytical calculation is applied over an already defined time step. The output is the sizing of the inductor power to achieve a temperature target in a time period. During the phase of *Conceptual Design*, the efficiency of the induction system has been considered as supposed value to be verified in *Detailed Design*.

Generally, the analytical model is a simple representation of a problem because it involves only analytical equations applied to a 0D domain. Analytical solutions are fast and can give an early feedback about the system behavior during the early design phases.

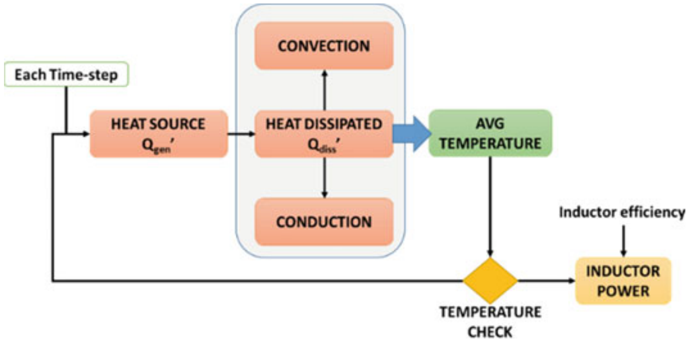

Fig. 2. The workflow of the analytical calculation for a mold heating system

2D: Finite Difference Methods

In the FDM approach, the geometrical volume is divided into a pattern of nodes, called as grid. This paper applied FDM for a 2D-based calculation. The domain regards the 2D section of a mold. However, the same approach also works with 1-D or 3-D domains. Generally, the finite-differences approach is used to solve the heat transfer problem by discretizing the space and solving for temperatures at discrete points called the nodes [11]. In transient problems, temperatures change with time as well as position, and thus the finite difference solution of transient problems requires discretization in time in addition to discretization in space [11]. Therefore, a suitable time step Δt must be selected to repeatedly solve each temperature step until the solution at the desire time is obtained. An example of a 2D discretization of the space by nodes is highlighted in Fig. 3. At each node m, the heat transfer balance can be calculated solving Eq. (1):

$$\sum\nolimits_{all\ sides} \dot{Q}^i + \dot{G}^i_{element} = \rho V_{element} C \frac{T_m^{i+1} - T_m^i}{\Delta t} \tag{1}$$

where the rate of heat transfer Q regards the sum of terms such as conduction, convection, heat flux, radiation etc. The term C is the specific heat of the element (1). The temperature value of m-node is calculated at the $i + 1$ time, considering the values of temperature at the i time for m-node and all sides ($m - 1$, $m + 1$, etc.). The second term of Eq. (1) simplifies as a finite difference approximation the partial derivative dT/dt. Figure 3 shows a rectangular 2D region in which heat conduction is significant in the x and y directions. The heat can be considered as generated in the medium at a rate of $\dot{g}$ per the specific volume in the time.

The following Eq. (2) describes the transient Eq. (1) applied for the case of the conduction heat transfer with heat generated in the medium:

$$k\Delta y \frac{T_{m-1,\mathrm{n}} - 2T_{m,n} + T_{m+1,\mathrm{n}}}{\Delta x^2} + \mathrm{k}\Delta x \frac{T_{m,\mathrm{n}-1} - 2T_{m,n} + T_{m,\mathrm{n}+1}}{\Delta y^2}$$
$$+ g_{\dot{m},n}\Delta x\Delta y = \rho\Delta x\Delta y C \frac{T^{i+1}_{m,n} - T^{i}_{m,n}}{\Delta t} \quad (2)$$

where the term K is the thermal conductivity of the medium assumed to be constant, and ρ is the density of the medium. This equation allows the temperature of node m at the time $i + 1$ to be calculated. The same approach is suitable for the discretization and solution of the steel block where the eddy currents generate the induction heat. A similar approach is described in many research papers for the case of the heat dissipated with the double effect of convection and conduction [2, 3].

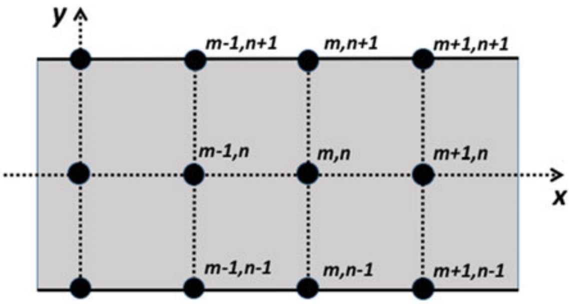

Fig. 3. An example of a 2D discretization of the space by nodes

Focusing on the case of the mold heating, Fig. 3 describes the possible space discretization for a steel mold in a 2D space. The mold is the medium where are applied the boundary conditions such as the heat generated by eddy currents (*Heat Source*), the heat dissipated as convection and the conductive heat transfer (Fig. 4). As stated before, the induction heating is generated as effect of eddy currents in the medium.

A finite difference approach is suitable for the determination of the temperature distribution in a metal mold after a t time. This approach requires the use of a mathematical development framework for solving the FDM equations. Possible convergence problems require the use of small time-step for the computing. Additionally, an accurate solution requires a fine nodes discretization. Therefore, while this approach is suitable and fast for simple geometries, custom solutions with complex geometries require dedicated algorithm to generate the nodes discretization.

3D: Finite Element Method

The third level of representation involves a FEM computing applied to a 3D geometry. The finite element method (FEM) is a numerical technique based on solving partial differential equations. This method subdivides a domain of calculation into smaller parts that are called finite elements. Thus, the problem is divided into a collection of subdomains represented by a set of equations which are then recombined into a global system of equations for the final calculation. The subdivision of a whole domain into simpler parts, has several advantages such as accurate representation of complex geometry and easy representation of a solution. Generally, tetrahedral elements are used to represent a system for a virtual analysis. The discretized domain is called mesh, and a CAD (Computer-Aided Design) tool is necessary to model the geometrical model to be discretized.

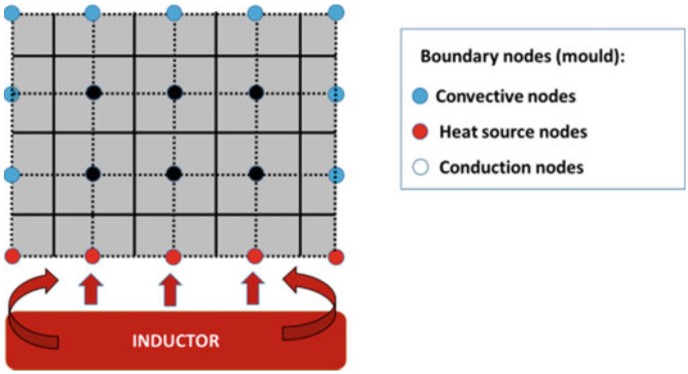

Fig. 4. An example of a 2D finite differences scheme for mold heating

The simulation of a FEM model is focused on a meshed geometry. The meshing requires hardware resources and advanced numerical tools to be generated and solved. Commercial tools provide tools to perform each phase of a FEM calculation such as meshing, pre-processing (boundary conditions definition), processing (FEM computing), post-processing (results analysis). However, this solution method is more expensive in terms of time and cost.

For the analysis of an induction heating system, the application of a FEM approach requires a multi-physics approach for solving the electromagnetic problem and the thermal heat transient. A typical induction heating problem can be solved by an iterative solution of the time harmonic electromagnetic problem and the transient thermal problem. The electromagnetic FEM analysis allows to study the electromagnetic behavior of the structure. As stated before, the FEM calculation involved in *Conceptual Design* is only based on the thermal analysis to reproduce the temperature distribution on the mold surfaces. On the other hand, the *Embodiment Design* phase can include the FEM simulation of the electromagnetic phenomena.

3 Case Study

While the previous section has analyzed the methodological approach considering the design of a heating system for any molding application (Fig. 1), this section describes a test case focused on a mold for the manufacturing of a composites component (epoxy-based carbon fiber prepreg). This component is a part of a lighting system for sport cars. The test case also proposes a comparison between the results achieved using each level of representation (OD, 2D, and 3D). The comparison considers the resultant calculation time and the gap between real and virtual tests.

The mold to be heated consists of three parts: a steel plate (bottom part), an aluminum block (middle part), and a silicone rubber top (upper part). The geometry of the composite component to be produced is shaped between the middle part and the upper one. The molding process is the resin curing. The temperature is a crucial parameter because it affects the polymerization and the curing of the resin. The test case, highlighted in this paper, concerns an epoxy resin curing process where a temperature value of about 130 °C is required on the walls of the mold cavity. This target of temperature depends on the materials involved and it was previously evaluated by experimental testing. The case study shows three levels of virtual prototyping to study the heating effects in terms of temperature achieved on the mold walls.

The proposed heating process consists of four thermal effects: the induction heating on the steel plate, the heat conduction between the steel plate and the aluminum block, the heat conduction between the aluminum block and the silicone rubber top, and the natural heat convection of the mold at room temperature. While the steel plate (bottom part) is a ferromagnetic material and can be heated by eddy currents, the aluminum-block can be only heated through the thermic conduction with the steel plate. In fact, the induction system only transfers energy to the ferromagnetic parts. The inductor consists of a coil, where each wire contributes to generate an electromagnetic field, depending on the current frequency.

The first level of analysis has been based on a 0D modelling. The results achieved by the *Analytical Analysis* shows the necessity to involve a 3000 W induction system for the mold heating. The analytical model (2D) has been performed using MATLAB Simulink® framework (Fig. 5). The main boundary conditions were a total mass of about 20 kg and a heating time of 500 s. The resulting thermal power is 2500 W (2D calculation), which is less than the value calculated by the 0D solution. The achieved temperature value on the walls of the mold cavity is 145 °C. On the other hand, the estimated temperature for the steel plate is 175 °C.

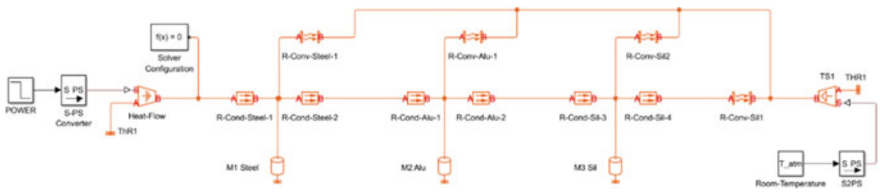

Fig. 5. The thermal model in MATLAB Simulink®

The second level of results has been analyzed using a FDM approach, based on a 2D model. MATLAB Simulink® framework has been also used in this second level of simulations. In particular, two models have been developed: the thermal model and the PID control. Figure 6 shows the thermal gradient on the mold cross section at the simulation time of 500 s. The cross section is related to the middle aluminum block, and it is applied on the middle plane of the cavity. The resulting trend of temperature confirms the results, analyzed using a simple 0D-based *Analytical Analysis*. However, a FDM approach can provide more details about the temperature distribution. Moreover, using a FDM approach is difficult to estimate the temperature distribution on the surface of the cavity. The computation of this FDM approach estimates an induction power of about 2800 W.

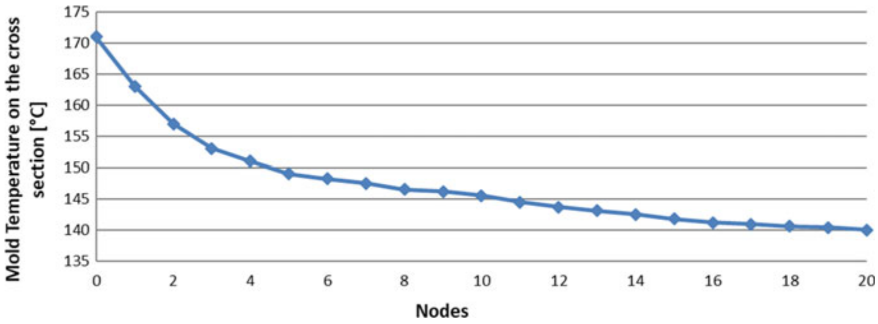

Fig. 6. A report of the temperature behavior on the cross section of the mold

Figure 7 shows a temperature comparison between values simulated in FDM and real values acquired from physical testing. Thermocouple probes were applied on steel plate and aluminum block during the mold heating test. The green line describes the average profile of temperature acquired by 8 probes on the steel plate. The implementation of a PID controller can regulate the power input and evaluate the energy consumption over the operation time.

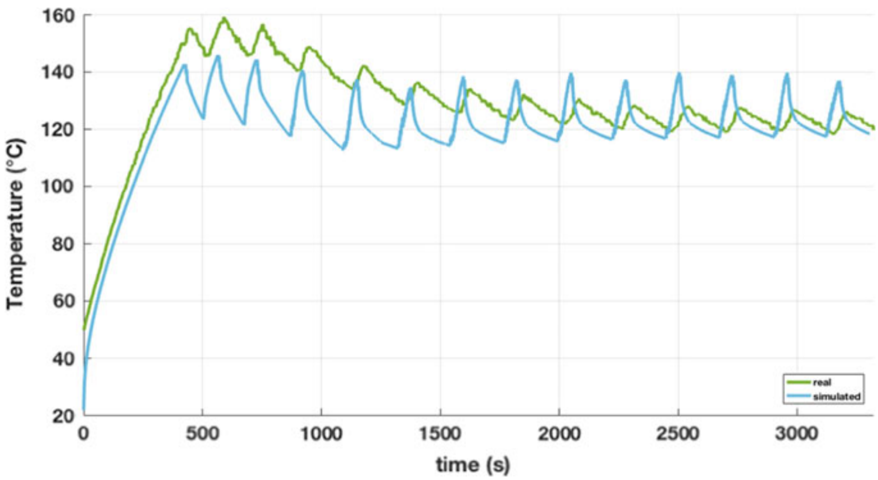

Fig. 7. A comparison between the real (green line) and simulated (blue line) average temperature profile as analyzed on the bottom surface of the steel plate

The third level of simulation regards the use of a FEM model. In this case, a commercial numerical solver has been used to simulate the thermal distribution between the bottom and the middle part of the mold. As a difference with the other analysis, a low-detailed 3D model has been defined in this simulation activity. Figure 8 shows the temperature distribution simulated on the surface of the cavity using the FEM solver. The 3D analysis reports an average temperature on the mold cavity of about 168 °C after a heating time of 500 s. The estimated power for the induction heating is 2900 W considering the resulting data analyzed within this third level of simulation.

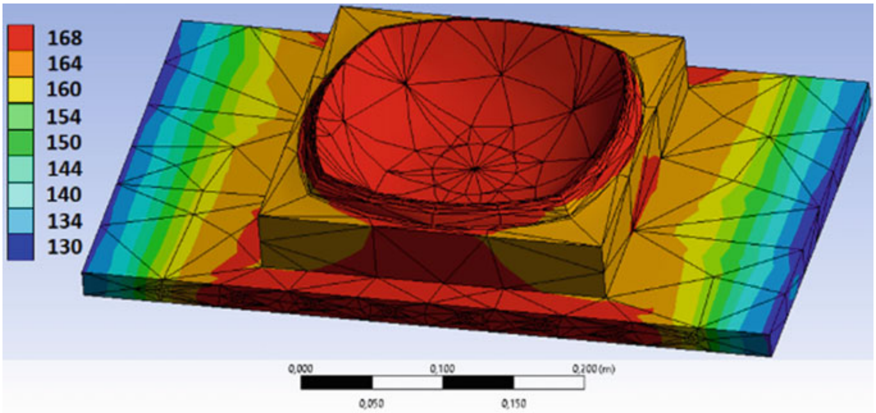

Fig. 8. A FEM simulation report of a mold heating system

4 Conclusions

A methodology to support the engineer in the design and simulation of an induction heating system for molds has been proposed. Three different models (0D, 2D, and 3D) have been described to simulate the behavior of the system. The proposed method is general because it was developed thinking to different molding heating applications. A test case, focused on a mold for a composite component, has been analyzed to show the differences between each levels of analysis (0D, 1D, and 3D). While 0D and 2D cannot evaluate the temperature distribution of the mold cavity, a 3D model can give a stronger feedback to the designer about the thermal distribution. However, despite these limitations and differences, the achieved temperatures result quite similar for each approach. Additionally, a 0D approach is affordable and suitable in the context of small-medium enterprises (SMEs), where a short time computing is a necessary feature. Generally, the employment of an approach setup on model-based simulations concerns the representation of a physical system through an Object-Oriented (O-O) model, which implements analytical and numerical equations for the calculation. The use of a model-based approach can be also suitable in simulations and computing related to a

Cyber Physical System. In this case, 0D and 2D models can be applied in real-time analysis.

The FEM analysis confirms about 25% energy reduction on using an induction heating system instead of a traditional electrical resistance circuit. As a future work, the simulated 2D system will be tested using a Hardware-In-the-Loop approach. In addition, an electromagnetic FEM analysis will be performed and added to the proposed methodological approach.

Acknowledgements. The authors thank Eng. Alessia Nardinocchi, Eng. Carmelo Cera and Eng. Fabio Carucci who provided insight and expertise that greatly assisted the research. The research work reported here was made possible by HP Composites.

References

1. Rudnev V, Loveless D, Cook R (2017) Industrial applications of induction heating. Handb Induction Heating Routledge 3:9–50
2. Prist M, Cicconi P, Ferracuti F, Russo AC, Monteriù A, Pallotta E et al. (2017) Temperature control of an innovative aluminium-steel molds induction preheat process placed on automated laser guided vehicles. In: IEEE international conference on environment and electrical engineering and IEEE industrial and commercial power systems Europe (EEEIC/I & CPS Europe)
3. Cicconi P, Russo AC, Prist M, Ferracuti F, Germani M, Monteriù A (2017) A parametric optimization approach of an induction heating system for energy consumption reduction. In: Volume 2B: 43rd design automation conference. ASME
4. Cicconi P, Russo AC, Germani M, Prist M, Pallotta E, Monteriù A (2017) Cyber-physical system integration for industry 4.0: modelling and simulation of an induction heating process for aluminium-steel molds in footwear soles manufacturing. In: IEEE 3rd international Forum on Research and Technologies for Society and Industry (RTSI), Modena, 11–13 Sept 2007
5. Liu YL (2014) Research on modeling design in composite molding. Appl Mech Mater 608–609:36–40
6. Kang HK, Kang DH, Bang HJ, Hong CS, Kim CG (2002) Cure monitoring of composite laminates using fiber optic sensors. J Korean Soc Aeronaut Space Sci 30(2):59–66
7. Leng JS, Asundi A (2002) Real-time cure monitoring of smart composite materials using extrinsic Fabry-Perot interferometer and fiber Bragg grating sensors. Smart Mater Struct. IOP Publishing 11(2):249–55
8. Shen H et al (2006) Study on temperature field induced in high frequency induction heating. Acta Metall Sin (English Letters) 19(3):190–196
9. Tian F-J, Tian X-T, Geng J-H, Zhang Z-M (2012) Model-based definition process information modeling and application. Jisuanji Jicheng Zhizao Xitong/Comput Integr Manuf Syst, CIMS 18(5):913–919
10. Steimer C, Fischer J, Aurich JC (2017) Model-based design process for the early phases of manufacturing system planning using SysML. Procedia CIRP 60:163–168
11. Cengel YA (2015) Heat and mass transfer: fundamentals and applications, 5th edn. McGraw Hill

New Issues for Workers Safety in the Factory of the Future

P. Martin[1(✉)], B. Daille-Lefèvre[2], J. Marsot[2], X. Godot[1], G. Abba[1], A. Siadat[1], and M. Gomez-Echeverri[1]

[1] Laboratoire de Conception Fabrication Commande—Arts et Métiers ParisTech, Université de Lorraine, 4 rue Augustin Fresnel, 57078 Metz, France
patrick.martin@ensam.eu

[2] Work Equipment Engineering Department, Institut National de Recherche et de Sécurité (INRS), 1 rue du Morvan, 54519 Vandœuvre-Lès-Nancy Cedex, France

Abstract. Human in the factory is one of the main themes of the Factory of the Future; in this context the aim of this paper is to present the new issues for workers safety and integrated design concepts or methodologies which have to be taken into account. New paradigms come into being: the uncertainty of the demand in terms of products as well as production rate, product customization, product/service integration, variability in manufacturing processes and times, reconfiguration of manufacturing machine tools and systems, space organization, auto-organization and planning. Also, new technologies are implemented: robots, "plug and play" devices, virtual/augmented reality, sensors, OPC standards and connected objects. Several tasks are performed by the workers, the robots or both in collaboration. The workers are placed in the center of the Factory of the Future but this concept introduce hazardous events, problems of health and safety (physical or cognitive tasks, fatigue, stress, space and time organization, human-robot interfaces to take into account in the different working situations). So the aim of the paper is to present studies carrying out in order to propose to the machine or manufacturing systems designers as well as production managers structured methods, models and tools to get safe working situations in the frame of the Factory of the Future paradigm.

Keywords: Factory of the future · Manufacturing systems · Human aspects · Safety · Human-robot collaboration

1 Introduction

In the Factory of the Future paradigm, numerous studies highlight the importance of taking into account and integrating human into production systems [1–8]. Analysis of these literature shows that the Factory of the Future presents several angles of approaches:

– Adaptive and smart production systems, production control, organization and planning, data management.

F. Cavas-Martínez et al. (Eds.): *Advances on Mechanics, Design Engineering and Manufacturing II*, LNME, pp. 402–411, 2019.
https://doi.org/10.1007/978-3-030-12346-8_39

- Virtual manufacturing, product –process design, engineering of complex systems, augmented reality, …
- Equipment, robots, reconfigurable machine tools, sensors…
- Advanced manufacturing processes: additive manufacturing, innovative manufacturing processes …
- Human and societal aspects: human centered manufacturing, social assessment, health and safety, sustainable manufacturing, wellbeing….

On the other hand new paradigms come into being:

- The uncertainty of the demand in terms of products as well as production rate.
- Product customization and product/service integration.
- Manufacturing process plans are not fixed, so the manufacturing times cannot be foreseen.
- Reconfiguration of machine tools as manufacturing systems (physical reconfiguration, routing, real time control, etc.).
- Space organization, auto-organization and planning.
- New technologies are implemented: robots, plug and play devices, virtual/augmented reality, sensors, OPC standards, connected objects, big data, artificial intelligence, cloud computing.
- Uses of products as manufacturing equipment are more and more complex.
- Integration of mechanical/electrical/electronical equipment on existing ones.
- Several tasks (physical as well as cognitive) are performed by the workers (preparation, manufacturing, maintenance and machine reconfiguration, storage, assembly, quality control, …), the robots or both in collaboration [9–12] following the production needs.

Workers in the Factory of the Future are exposed to safety problems (accidents) as well as health problems (stress, fatigue, repetitiveness of gestures, prolonged static postures, vibrations, dangerous environments, possibility of anticipating dangerous work situations) [8].

Inside the Factory of the future, the principal risks for health and safety are those identified in the standards [13]. Nevertheless their occurrences, causes and severity, depend directly on the new context and the new work conditions and situations, particularly in terms of equipment design for reconfigurability, human-robot interactions (transport, assembly or product qualification) and the organization of production or workstations (production control, lean-manufacturing, self-organization, margins of manoeuver). This leads to numerous questions about the health and safety of employees:

- How to specify, and then design safe production cells with functional perimeters adapted to their evolving uses for different lifecycle working situations (mounting, setting, exploitation, modification)?
- How to protect workers in constantly changing environment (autonomous platforms, collaborative robots, modular machines)?
- How to safely manage reconfiguration phases?
- What is the impact of collaborative robots and new human-machine interfaces on production activities for workers and supervisors?

- Can we use ever-increasing production data to highlight slight signals announcing dangerous working situations?
- Can the opening of manufacturing systems to the outside world through communication networks compromise workers safety?
- How to ensure the progress of production in a variable and disturbed environment: difference between prescribed and real, transitional phases?
- How to ensure simultaneous responses to performance (productivity, flexibility, quality) and health-safety objectives?

All these questions require acquisition and structuring of new knowledge from an engineering point of view (specification and design methods, simulation tools, risk analysis, definition of preventive measures) as well as human factors in order to integrate flexibility and professional risk prevention to these requirements [11, 14–16]. These works are part of the "Integrated Prevention" approach, which consists of applying as soon as possible safe design principles to future work equipment [17].

Also, the objective of this article is to specify barriers, missing knowledge, tracks of studies and knowledge objects capable of giving to manufacturing systems designers as well as production managers tools to answer to the identified questions. We present the results of the reflection we have undertaken in order to go in depth our future research (objectives, models, methodologies, knowledge …) on workers safety:

– How to specify the use of the manufacturing systems in order to get safety workplace for all its life cycle (assembly, set-up, modification, production, disassembly, …) and for different skills of workers involved (experienced, beginner, maintenance person…)?
– Does actual simulation software for robotized workstation allow forecasting all the working situations?
– What are the relevant parameters to take into account and relevant algorithms to propose in order to develop dedicated simulation software?

2 Equipment Design and Re-configurability

Reconfigurable systems and machines have been studied for several years from a purely technological point of view [18–20]. This reconfiguration can be considered at a machine (modules or tools) (Fig. 1) or cell (machines and product flow) (Fig. 2) level, in terms of physical characteristics, control (PLC, communication network) or command (centralized, coordinated, self-organization).

Design for Safety concept recommends the improvement of knowledge sharing between different actors, with strong involvement of the health and safety expert, and it has been the object of multiple works [21–26]. The analysis of the whole set of methods, techniques and design tools, allows us to make the following remarks [17, 27]:

– There is no proposition of a formalized framework to ensure the identification of key elements and links between use, design and prevention;

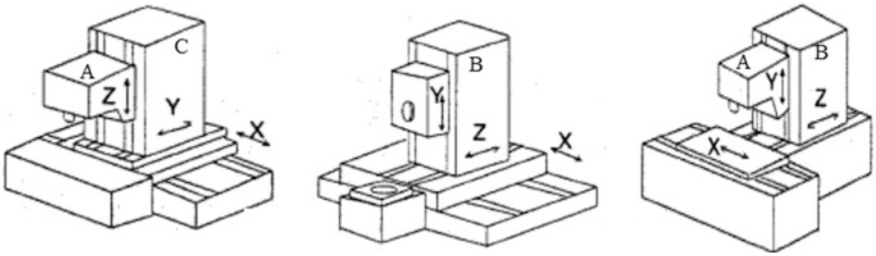

Fig. 1. Machine tool reconfiguration

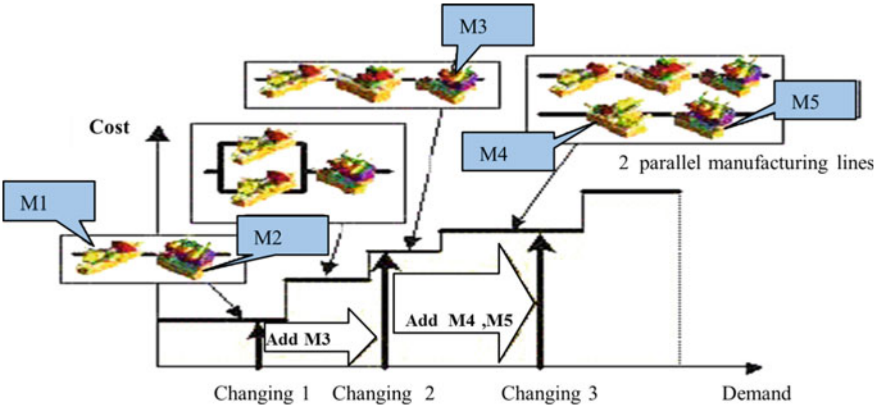

Fig. 2. Product flow reconfiguration

– Consideration of all uses is mainly based on scenarios during validation stages: collaborative project reviews with ergonomists and workers around modeling or prototyping. Although necessary, this articulation of integrated prevention with design process around solely the validation stages is not enough, because it does not guide the designer through the autonomous making decisions process. Risk prevention is therefore treated as a correction task and not as a specification for design.

Moreover, current models of use have limitations towards:

- Functional boundaries specification and evolving usages;
- Management from a health and safety point of view by the combination of possible use scenarios and reconfiguration phases, and this in phases of architectural as well as detailed design.

3 Human and Robot Collaboration

Robots introduction inside production cells with sharing workspaces and tasks is increasingly relevant, the NF EN ISO10218-1: 2011 [28] standard defines four modes for securing collaborative robotic cells:

– Mode 1 or "Controlled nominal safety stop";
– Mode 2 or "Manual guidance": user actions guide the robot. Safety of the worker is mainly based on the utilization of a validation device;
– Mode 3 or "Speed and separation distance control": while the worker is inside the working zone of the robot, it must maintain a certain speed and respect a separation distance with the worker, in order to avoid collisions;
– Mode 4 or "Robot power and force limitation": contact detection and force limitation mechanisms must be integrated into the robot, in the interest of reducing the intensity of potential impacts between human and robot.

In mode 3, the human detection systems required for its implementation are still in the research stage [29–31]. Users prefer to slow down or stop robot movements in case of intrusion in the protected zone (mode 1) or in case of contact (mode 4) rather than trying to modify its trajectory to maintain a separation distance.

Moreover, the Factory of the Future paradigm leads to a more global view of the different approaches (Fig. 3): Resources and tools mobility; Safe collaboration between human and robot; Robots' mobility; Multi-armed robot; Real time perception of tasks and environment; Cognitive contribution dedicated to each operator.

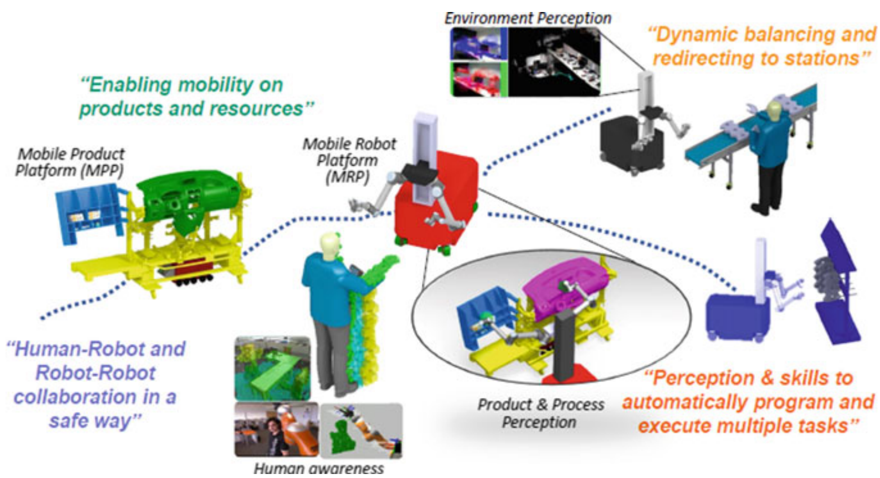

Fig. 3. FOF-NMBP Thomas project [32]

On one hand, simulation is increasingly used to reduce costs and risks related to products and demand variability and quick validation of production objectives in terms of quality or performance; on the other hand, proposed models remain limited. If some software includes modules for viewing and configuring safety zones in nominal operation (paths, speeds and energies managed by the robot control system), it is not guaranteed that these modules make it possible to verify compliance with safety requirements in degraded conditions. Protection measures used to secure a collaborative cell can be of different natures: safety functions specific to robot, protection devices (perimeter, surface, volume). However, they all have as main function to send to the robot a safety order, such as stop completely in the event of a potentially dangerous situation: human intrusion into a protected zone or detection of a malfunction of the robot for example. “Safety distance (S)” is one of the principal criteria to consider when choosing, installing, and setting up protection devices (Fig. 4). This distance ensures that the mobile elements of the robot will not dangerously strike a worker.

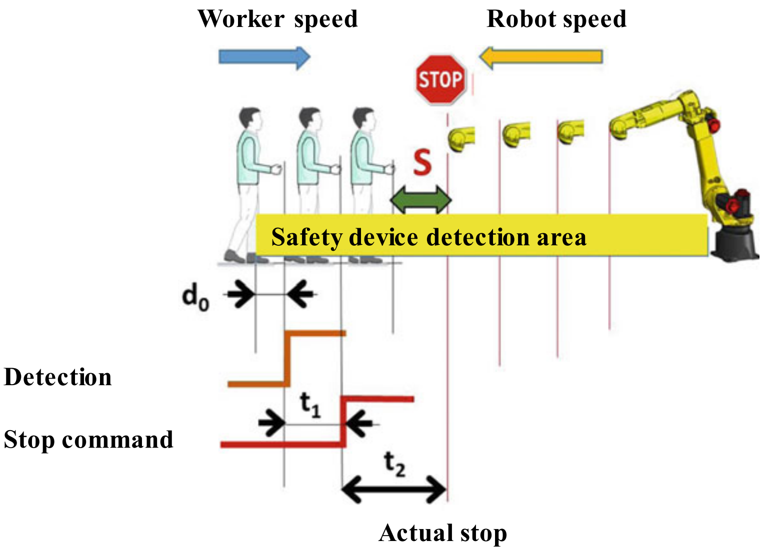

Fig. 4. Safety distance and actual stop

4 Manufacturing System Design and Organization

Given the objectives of productivity and responsiveness, approaches such as Lean Manufacturing or Just in Time, the exploitation of communication systems, the development of connected objects and interfaces (smartphones, tablets, augmented reality) lead to working conditions involving risks such as stress, musculoskeletal disorders and fatigue. Also the concept of leeway “possibility or freedom of a worker to develop different working ways to meet production requirements without adverse health effects” [33] has been introduced by a number of ergonomic researchers and the concept of a production cell with extended responsibility has been proposed. Leeway increases the ability of workers to cope with the variability of work situations; it allows them to absorb the gap between the prescribed work and their actual work. Two levels of margin implementation can be distinguished [34]: leeway in design situations (designer will define a prescriptive framework more flexible and more adapted to the constraints of the future production activity) and those operational ones (improvement of working conditions of the operators once the facilities and the production organization is in place in the workshop).

Following these analyses, key parameters, constraints, and missing knowledge has been identifying in order to go in depth future works and develop specific software. This later will allow carrying out operating scenarios and thus identify the potential risks in terms of health and safety in both design and operation in order to help designers or production managers in decision making. So the modeling of production cell configurations, the spatial organization of the characteristic elements, the operations to be carried out can be undertaken. Concepts and tools as Energy analysis for systematic haZard Identification [17] or hazardous zones [26] combined with tasks planning will be useful. Figure 5 shows an example of hazardous working situation. This virtual representation of working place for each configuration will allow to identify potential risks and to help the designer in the different phases of process design. From the relevant parameters (energy level for example) it is possible to estimate the risk seriousness.

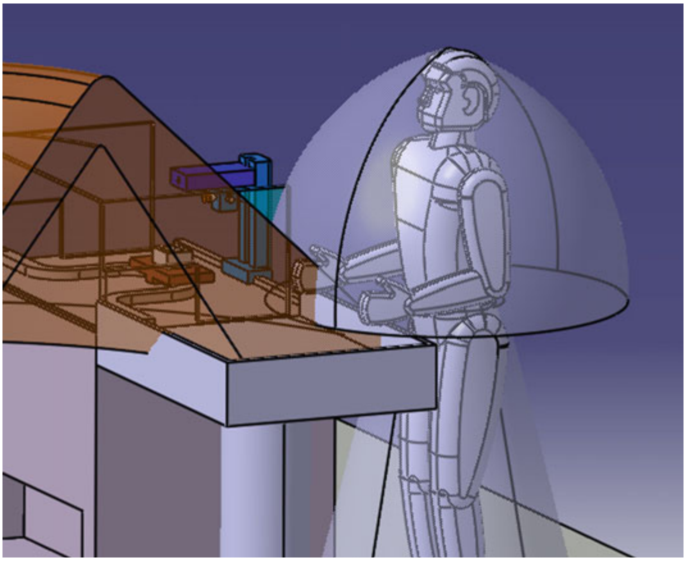

Fig. 5. Hazardous zone model

5 Conclusions

Significant technological leaps are induced by the implementation of the Factory of the Future according to different aspects: reconfiguration of the production system using "plug and produce" bricks, data acquisition and reactivity in real time, exploitation of automated systems, physical and cognitive assistance to humans, virtual twin factory, production organization and high added value processes. Thus the interactions between human and production equipment are modified to meet the objectives of responsiveness, controllability and evolution of the work environment, this leads to new challenges for health and safety at work all along the design and operation cycle of the system through a dynamical mastery (identify, evaluate, act) of the work situation (system/workers/organization).

The consideration of all these elements within configuration models of production cell, spatial organization of characteristic elements, operations scheduling to be carried out, make it possible to create operating scenarios and thus identify potential risks in terms of health-safety at a design and operational level. Key knowledge objects as energy flow, dangerous zone, safety distant, generalized dangerous variables or use specifications new approach and methodology have to be developed from existing tools and knowledge by integrating these new issues, industrial objectives and societal context.

Acknowledgements. This work has been performed in the frame of the dual laboratory between INRS and ENSAM/LCFC (safety design of working situation: functional requirements, equipment design, working place management) which allows to bring the financial and scientific supports.

References

1. Report to the president on ensuring American leadership in advanced manufacturing, Executive office of the President, President's council of advisors on Science and Technology, June 2011; A national strategic plan for advanced manufacturing, Executive Office of the President National and Technology Council, February 2012
2. Factories of the Future (2010) Strategic Multi-annual roadmap. Industrial advisory group FoF, www.effra.eu
3. Consiglio Nazionale delle Rcerche, Flagship Project 2011–2013, "Factory of the Future, National Manufacturing Platform" (Italy)
4. FUTURPROD: les systèmes de production du futur, Atelier de Réflexion Prospective de l'ANR. www.cluster-gospi.fr. Access 16 Jan 2018
5. Pierre Veltz et Thierry Weil: «L'industrie, notre avenir», La Fabrique de l'Industrie, Eyrolles 2015. ISBN: 978-2-212-56115-9
6. «Une industrie européenne plus forte au service de la croissance et de la relance économique», Communication de la commission au parlement européen, au conseil, au comité économique et social européen et au comité des régions, communication sur la politique industrielle {SWD(2012) 299 final}
7. Technologies prioritaires 2020 en mécanique, CETIM 6B13, octobre 2015. ISBN 978-2-36894-079-2

8. Guide pratique de l’usine du futur, enjeux et panorama de solutions, Fédération des Industries Mécaniques, octobre 2015. www.industriedufutur.fim.net. Access 16 Jan 2018
9. INRS—Utilisation des robots d’assistance physique à l’horizon 2030 en France. VEP 1. ISBN 978-2-7389-2217-5, 2015, 261 p
10. Kruger J, Lien TK, Verl A (2009) Cooperation of human and machines in assembly lines. CIRP Ann Manuf Technol 58:628–646
11. Kaivo-Oja J (2015) The future of work and robotics. Seminar of European Agency for Safety and Health at Work. Bilbao, 30 p
12. Literature Review (2009) the human machine interface as an emerging risk—European Agency for Safety and Health at Work, 40 p. ISBN-13: 978-92-9191-300-8
13. NF EN ISO 12100 (2010) Safety of machinery: general principles for design. Risk assessment and risk reduction, CEN, Brussels, 93p
14. Stacey N, Ellwood P, Bradbrook S, Reynolds J, Williams H (2017) Key trends and drivers of change in information and communication technologies and work location foresight on new and emerging risks in OSH working report. European Agency for Safety and Health at Work, 154 p
15. Murashov V, Hearl F, Howard J (2016) Working safely with robot workers: recommendations for the new workplace. J Occup Environ Hyg 13(3):61–71
16. INRS—Modes et méthodes de production en France en 2040: quelles conséquences pour la santé et la sécurité au travail? 72 p. http://www.inrs.fr/dms/inrs/PDF/prospective-2016/synthese-sante-travail2040.pdf
17. De Galvez N, Marsot J, Martin P, Siadat A, Etienne A (2017) A new approach to hazard identification during the design process by analysing energy transfers. Safety Sci Saf Sci 95:1–14
18. Koren Y, Heisel U, Moriwaki T, Jovane F, Ulsoy G, Van Brussel H (1999) Reconfigurable manufacturing systems. Ann CIRP 48(2):527–540
19. Koren Y (2005) Reconfigurable manufacturing and beyond (keynote paper). In: CIRP 3rd international conference on reconfigurable manufacturing, Ann Arbor, Michigan, 11–12 May 2005
20. Garro O, Martin P (1993) Towards new architectures of machine tools. Int J Prod Res 31 (10):2403–2414. ISSN 0020-7543
21. Chinniah Y (2015) Analysis and prevention of serious and fatal accidents related to moving parts of machinery. Saf Sci 75:163–173
22. Fadier E, De la Garza C (2006) Safety design: towards a new philosophy. Saf Sci 44(1):55–73
23. Houssin R, Coulibaly A (2011) An approach to solve contradiction problems for the safety integration in innovative design process. Comput Ind 62(4):398–406
24. Ghemraoui R, Mathieu L, Tricot N (2009) Design method for systematic safety integration. CIRP Ann Manuf Technol 58:161–164
25. Khan F, Rathnayaka S, Ahmed S (2015) Methods and models in process safety and risk management: past, present and future. Process Saf Environ Prot 98:116–147
26. Shahrokhi M, Bernard A (2009) A framework to develop an analysis agent for evaluating human performance in manufacturing systems. CIRP J Manufact Sci Technol 2(1):55–60
27. Sadeghi L, Siadat A, Marsot J, Dantan JY (2016) Design for human safety in manufacturing system: a review of applications of design theories and methodologies and design tools and techniques. J Eng Des 27(12):844–877. https://doi.org/10.1080/09544828.2016.1235262
28. NF EN ISO 10218-1 (2011) Exigences de sécurité pour les robots industriels – Robots et dispositifs robotiques - Partie 1: robots. Paris, AFNOR, 45 p

29. Meguenani A, Padois V, da silva J, Hoarau A, Bidaud P (2016) Energy based control for safe human-robot physical interaction. In: International symposium on experimental robotics (ISER), Tokyo, Japan, 12 p
30. Schleg T, Kroger T, Gaschler A, Khatib O, Zangl H (2013) Virtual whiskers—highly responsive robot collision avoidance. IEEE, 7 p
31. Behrens R, Saenz J, Vogel C, Elkmann N (2015) Upcoming technologies and fundamentals for safeguarding all forms of human robot collaboration. SIAS Königswinter, Germany, p 6
32. Thomas project "Mobile dual arm robotic workers with embedded cognition for hybrid and dynamically reconfigurable manufacturing systems", FoF.NMP-723616. http://www.thomas-project.eu/
33. Durand M, Vézina N, Baril R, Loisel P, Richard MC, Ngomo S, (2008) La marge de manœuvre de travailleurs pendant et après un programme de retour progressif au travail, IRSST: http://www.irsst.qc.ca/media/documents/PubIRSST/R-566.pdf
34. Coutarel F (2004) La prévention des troubles musculo-squelettiques en conception : quelles marges de manœuvre pour le déploiement de l'activité ? Thèse de doctorat en ergonomie, Université Victor Segalen. Bordeaux 2, Editions du Laboratoire d'Ergonomie des Systèmes Complexes

3D Model Representation and Data Exchange for Additive Manufacturing

G. Savio[1,3(✉)], R. Meneghello[2,3], S. Rosso[1,3], and G. Concheri[1,3]

[1] Department of Civil Environmental and Architectural Engineering, University of Padova, Via Venezia, 1, 35131 Padova, Italy
gianpaolo.savio@unipd.it

[2] Department of Management and Engineering, University of Padova, Stradella San Nicola 3, 36100 Vicenza, Italy

[3] Laboratory of Design Tools and Methods in Industrial Engineering, University of Padova, Via Venezia, 1, 35131 Padova, Italy

Abstract. The unique capabilities of additive manufacturing (AM) technologies highlight limits in commercial CAD tools. In this manuscript, after a synthetic description of the main AM technologies based on international standards classification, geometric modeling methods and data exchange file formats available in the literature are presented. Twelve geometric models have been studied to evaluate the effectiveness of the file format, noting the file dimension and the time to open and close the file. As a result, a roadmap in the development of new tools for design in AM is drawn, taking into account the new possibilities offered by AM technologies.

Keywords: Design for additive manufacturing · Data exchange · Geometric modeling · Additive manufacturing

1 Introduction

Additive manufacturing (AM) technologies have unique capabilities, making possible the fabrication of (i) shape with any complexity (in the limits of the design rules, such as minimal wall thickness and escape holes), (ii) parts having desired microstructure (by controlling process parameters), mesostructure (adopting cellular solids) and macrostructure, (iii) pieces having point by point specific materials, (iv) functional mechanisms without the assembly of parts [1].

In order to fulfill these unique capabilities, dedicated design tools and methods are needed, allowing, for instance, mass customization [2], parts consolidation [3], complex free-form and organic shape modeling, voxel and 3D bitmap design [4], cellular solids and topology optimization (multiscale design) [5–9], functionally graded material design (FGM) [10], flow channels [3] and thermal optimization [11]. More broadly it is possible to "maximize product performance in terms of manufacturability, reliability, and cost, through the synthesis of shapes, sizes and material compositions, subject to the capabilities of AM technologies" (adapted from [1]) which is the objective of Design for Additive Manufacturing (DfAM). Few of the mentioned tools

F. Cavas-Martínez et al. (Eds.): *Advances on Mechanics, Design Engineering and Manufacturing II*, LNME, pp. 412–421, 2019.
https://doi.org/10.1007/978-3-030-12346-8_40

are available in commercial CAD software, while others are only described in research projects.

To identify the potential of AM technologies, in this paper, firstly the international standard classification of AM technologies is presented. Then, geometric modeling and analysis approaches able to exploit the AM potential are presented, especially according to the capabilities of complex shape and functionally graded materials modeling. Finally, characteristics and efficiency of file formats for data exchange are discussed, studying 12 test cases. Mesh and NURBS represent effectively and efficiently both boundary and volumetric geometric models, while the implementation tested shows the need to strengthen the data exchange file format supported by international standards.

2 AM Technologies

ISO/ASTM 52900 [12] and ISO 17296-2 [13] provide definitions, classification, and description of the main AM technologies. Seven types of additive processes are identified:

- *vat photopolymerization* in which liquid photopolymer in a vat is selectively cured by light-activated polymerization,
- *material jetting* in which droplets of build material are selectively deposited,
- *binder jetting* in which a liquid bonding agent is selectively deposited to join powder materials,
- *powder bed fusion* in which thermal energy selectively fuses regions of a powder bed,
- *material extrusion* in which material is selectively dispensed through a nozzle or orifice,
- *directed energy deposition* in which focused thermal energy is used to fuse materials by melting as they are being deposited,
- *sheet lamination* in which sheets of material are bonded to form an object.

Due to the limits of commercial CAD/CAM tools, the capabilities of AM technologies are not yet fully exploited. For instance, a number of studies show that it is possible to obtain a continuous variation in material composition, varying gradually the mechanical properties [4, 14, 15], but there are not yet adequate tools to support the relevant design process. Other examples show the ability to embed 3D colors used as a passive wear indicator or embed electronics using metal nanoparticles [16]. Moreover, recent advances in using FGM in parts and AM technologies demonstrate the need of commercial CAD systems for creating heterogeneous objects [17].

3 Geometric Modeling for AM

A number of geometric modeling approaches are available in the literature. These can be classified in 3 main groups (Fig. 1): boundary representation (BRep), volume representation (VRep) and constructive solid geometry (CSG).

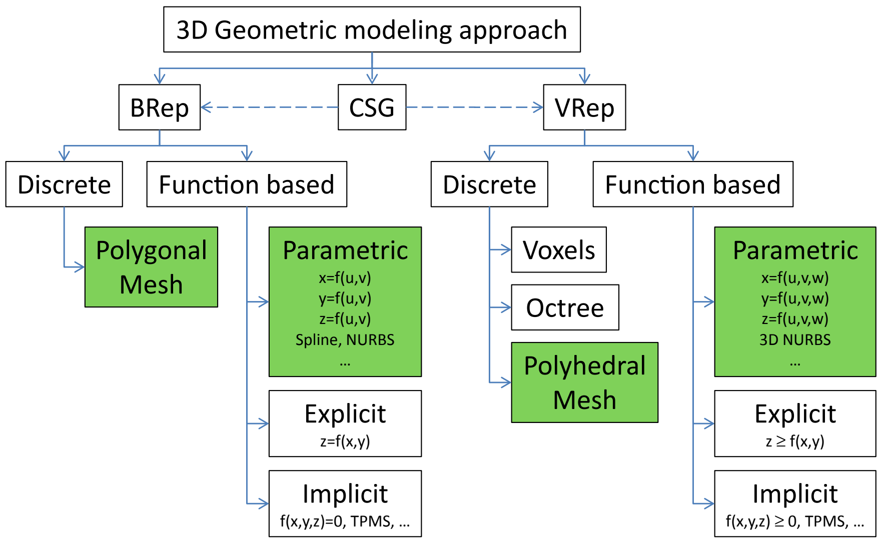

Fig. 1. Geometric modeling approaches

BRep is a method for representing the shape of an object by a collection of connected surfaces describing the skin (i.e. boundary) of the solid and is the basic principle of solid modeling on which all CAD 3D geometric kernels are based since 40 years. In AM this approach is useful when the solid is made by a homogenous material and the skin is the only part that presents variable characteristics such, as colors that can be represented by a texture. A 3D surface can be represented by implicit, explicit or parametric functions, or by polygonal meshes. An equation of form $f(x, y, z) = 0$ is the implicit equation of a surface [18] also known as Function Representation (FRep), widely studied in the literature [19]. Regarding AM, FReps are able to easily design lattice structures [20]; for instance, triply periodic minimal surfaces (TPMS) are periodic implicit surfaces often used in AM for their curvature continuity. On the other hand, FReps are unable to represent and easily transform bounded surfaces. A parametric representation of a surface is given by $S(u, v) = (x(u, v), y(u, v), z(u, v))$, where u and v are independent parameters defined in an arbitrary interval usually normalized to [0, 1] [21]. The parametric surfaces, such as Bézier, Spline and Non Uniform Rational Basis-Splines (NURBS), are supported by numerically stable algorithms and allow more natural design and representation of shapes in a computer than implicit equations [21]. Parametric geometry is easy to express in the form of vector and matrices allowing to use relatively simple techniques to solve very complex analytical geometry problems, providing a common mathematical format for representing any curve and surface, drastically reducing the number and the complexity of subroutines required to solve geometric-modeling problems [22]. It is difficult, instead, to manage very complex shapes such as lattice structures by parametric functions [8]. Mesh models, which represent the surfaces by adjacent closed polygons, can improve the usability of complex shapes especially adopting subdivision surface algorithms [8]. Moreover, the geometric models adopted in AM are usually based on meshes.

When a part is made of heterogeneous materials, BReps are not enough. In this case it is necessary to describe colors or composition point by point, by means of VRep. Recently, voxel (a volumetric pixel) based modeling approach was proposed with a resolution set equal to the native resolution of the AM process [4]. This methodology can be improved by bringing together adjacent voxels with the same properties, making more efficient the spatial-occupancy enumeration (Octree encoding [18]). Alternatively, a more flexible approach based on polyhedral mesh can be adopted in the design of heterogeneous materials taking inspiration from FEA/CAE methodologies. As in the case of BReps, a VRep can be represented by implicit, explicit or parametric functions. Besides the previously mentioned troubles for implicit and explicit functions, it is very difficult to work on different level of inequalities to set the distribution of different materials: it is possible to set a material at each k value of the f (x, y, z) = k, but is quite difficult or impossible to get an adequate match between desired spatial distribution of the materials and f(x, y, z). Instead, parametric functions such as NURBS 3D, show a number of advantages especially in CAD and FEA integration (iso/geometric analysis [23–25]). This approach can be extended in FGM analysis [26]. Moreover, volumetric subdivision can be adopted in both discrete and function based approaches integrating iso-geometric analysis [27]. Additionally, this approach could be integrated into mesh modeling for cellular materials [8], allowing the design and the optimization of lattice structures.

A different approach in geometric modeling is CSG, in which a solid is represented combining a number of primitives, such as prisms and cylinders, by using Boolean operators. Usually, primitive geometries are defined as homogeneous solids and are switched to BRep for visualization, data exchange, and manufacturing. Recent studies show the feasibility of adopting heterogeneous primitives in CSG, redefining the Boolean operations concept [28]. In this case, CSG can be likened to a VRep also called VCSG.

In short, in our opinion, the geometric modeling methodologies highlighted in green in Fig. 1 are the most effective approaches for AM, allowing geometric complexity and an effective and intuitive geometric modeling approach, providing a unified mathematical basis for every shape. Moreover, mesh and NURBS have become the de facto industry standard for the acquisition, representation, design and data exchange of geometric information, supported by many standards.

4 Data Exchange File Format for AM

In AM product development, there is a number of formats for data exchange partially able to cover the different stages of the product development process such as geometric modeling, design, manufacturing, and verification [29–31].

Stl file format is the de facto industry standard for transferring geometric information, but it supports only triangles with face normal, without any other product and manufacturing information (PMI) and color information. When exporting a free-form surface in stl, the geometry is approximated with planar triangles, therefore reducing the model accuracy [32]. Many other file formats can be used in data exchange for additive manufacturing such as ply, Obj, Step, AMF, 3MF, WRLM, JT, slc, each one has its pros and cons. Unlike the other, ply format supports polygonal meshes that are not necessarily triangles.

Step AP 242 (ISO 10303-242 [33]), developed by ISO, is probably the file format that could better cover the whole product development stage, including PMI and annotations, but the implementations tested do not support triangular meshes for now, even if the next version of this standard is introducing a number of features dedicated to AM such as curved triangles (mesh with normal at vertices), building orientation, building volume, support structures. Moreover, in the 3rd edition, Step will include heterogeneous materials, representation of lattice structures and semantic representation of PMI for Additive manufacturing [34].

ISO and ASTM have developed a standard "Specification for additive manufacturing file format (AMF)". The ISO/ASTM 52915 [35] is an XML-based format describing parts by triangles. It supports color, texture mapping, few PMI (currently not tolerances), possibly lattices and FGM. Moreover, ASTM is working on a new specification for AMF supporting voxel information, CSG representations and solid texturing [36].

In 3MF consortium opinion, AMF is widely held to have gone into a standards body too early, having some features not clearly defined and other features missing [37]. AMF inspired the foundations of 3MF, that is an industry consortium working to define a 3D printing format free of royalties, patents and licensing access and implementation.

In order to evaluate the efficiency of different file formats in terms of file dimension and time to open and save a file, 12 geometric models were studied, derived adopting 0, 2 and 4 iterations of the Catmull-Clark subdivision surface algorithm [38] on 4 cases: a regular lattice [8], a random lattice [39, 40], a variable thickness triply periodic surface and an organic model (Fig. 2). Subdivision surface algorithm was used for several reasons: it allows to increase rapidly and consistently the model complexity, it is an interesting approach in designing lattice structures and organic shapes, it can be implemented in graphic card, it is widely used in visualization and rendering, and can potentially can reduce the amount of data in file exchange. Table 1 summarizes the number of vertices and faces for the test cases at different levels of subdivision: the most complex surface is the random lattice after 4 iterations of the Catmull-Clark subdivision scheme.

Table 2 shows the file dimension for each test case in MByte. The number of iterations of the subdivision increases rapidly the file dimension. Moreover in the implementation adopted (Rhinoceros 6 by Robert McNeel & Associates; native file format *.3 dm [41]), AMF uses a large amount of memory, up to 10 GByte, about 10 times the ply format and 20 times the 3MF (a compressed version of AMF consisting of a zip file exists, but requires higher computational time).

Table 3 shows time to open and save the file containing the regular lattice after 4 subdivision iterations. Stl is the fastest to save due to the few information contained, but requests more time to open because the software needs to reconstruct the data structure (stl file format describes each triangle by its vertices coordinates, duplicating the vertex shared by adjacent triangles). In the implementation adopted, 3MF shows the longest time to open and to save.

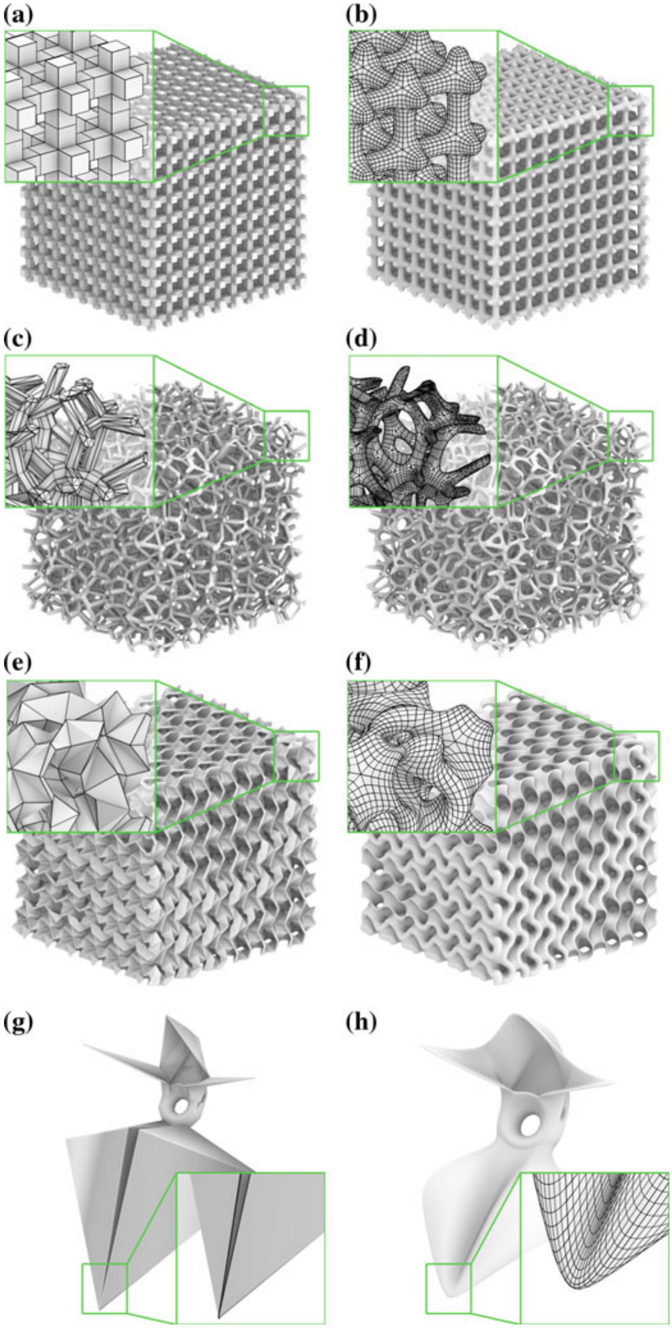

Fig. 2. Test cases adopted for the investigation of data exchange file format: initial (**a**) and subdivided mesh (**b**) of a regular lattice structures based on a cubic cell; initial (**c**) and subdivided mesh (**d**) of a random lattice; initial (**e**) and subdivided mesh (**f**) of a quasi-gyroid lattice with variable thickness; initial (**g**) and subdivided mesh (h) of an organic model

Table 1. Number of vertices and faces of the test cases at different levels of subdivision

	Vertices			Faces		
	0 iter.	2 iter.	4 iter.	0 iter.	2 iter.	4 iter.
Case 1: regular lattice	98,400	390,200	6,294,200	24,600	393,600	6,297,600
Case 2: random lattice	61,014	1,078,360	17,388,040	72,397	1,087,312	17,396,992
Case 3: gyroid lattice	22,679	356,038	5,747,398	22,464	359,424	5,750,784
Case 4: organic model	376	4294	66,174	266	4136	66,176

Table 2. File dimension in MByte of the test cases at different levels of subdivision

	Native			ply			AMF			3MF			stl		
Iter. n.	0	2	4	0	2	4	0	2	4	0	2	4	0	2	4
Case 1	0.9	9.6	177.8	3.1	21.6	387.8	9.4	215.6	3535.7	0.6	9.4	166.4	2.5	39.4	629.8
Case 2	2.0	60.1	1028.6	3.5	63.7	916.0	31.2	603.1	9836.3	1.8	33.2	511.3	6.4	108.7	1739.7
Case 3	0.7	11.1	272.4	1.2	20.7	357.7	10.7	198.6	3232.5	0.6	11.1	171.1	2.3	35.9	575.1
Case 4	0.04	0.37	4.01	0.02	0.21	3.57	0.13	2.24	36.4	0.01	0.12	1.94	0.03	0.41	6.62

Table 3. Time to open and save the file in case 1 after 4 subdivision iteration

	Time to open (s)	Time to save (s)
Native	6.8	27.9
ply	79.0	42.4
AMF	1019.1	336.9
3MF	73.0	63.2
stl	118.7	18.5

5 Conclusion

In this study, geometric modeling approaches for AM technologies were surveyed, identifying the most effective methods, considering the capabilities of AM such as shape complexity and FGM. Mesh and NURBS show the potential to handle the link between shape and function for both boundary and volumetric geometric models.

Moreover, few data exchange file formats were studied, highlighting the pros and cons of their main features. In the implementation tested, file formats supported by international standards show low efficiency. Future development of an adequate file format for data exchange should support volumetric models, complex geometry, exact geometry (tessellation is not fundamental), subdivision surfaces and hierarchical structures along the whole product development, over PMI and color information.

Acknowledgements. This work was partially supported by the University of Padova—Department of Civil, Environmental and Architectural Engineering ICEA (BIRD175287/17, 2017).

References

1. Gibson I, Rosen D, Stucker B (2015) Additive manufacturing technologies. Springer, New York, New York, NY
2. Reeves P, Tuck C, Hague R (2011) Additive manufacturing for mass customization. In: Mass customization, pp 275–289
3. Hopkinson N, Hague RJM, Dickens PM (eds) (2005) Rapid manufacturing. Wiley, Chichester
4. Doubrovski EL, Tsai EY, Dikovsky D, Geraedts JMP, Herr H, Oxman N (2015) Voxel-based fabrication through material property mapping: a design method for bitmap printing. Comput Des 60:3–13
5. Yang S, Tang Y, Zhao YF (2015) A new part consolidation method to embrace the design freedom of additive manufacturing. J Manuf Process 20:444–449
6. Tang Y, Kurtz A, Zhao YF (2015) Bidirectional evolutionary structural optimization (BESO) based design method for lattice structure to be fabricated by additive manufacturing. Comput Des 69:91–101
7. Savio G, Meneghello R, CONCHERI G (2017) Optimization of lattice structures for additive manufacturing technologies. In: Eynard B, Nigrelli V, Oliveri SM, Peris-Fajarnes G, Rizzuti S (eds) Advances on mechanics, design engineering and manufacturing. In Lecture notes in mechanical engineering. Springer, Cham, pp 213–222
8. Savio G, Meneghello R, Concheri G (2018) Geometric modeling of lattice structures for additive manufacturing. Rapid Prototyp J 24:351–360
9. Tamburrino F, Graziosi S, Bordegoni M (2018) The design process of additively manufactured mesoscale lattice structures: a review. J Comput Inf Sci Eng 18:1–16
10. Mahamood R, Akinlabi E, Shukla M, Pityana S (2012) Functionally graded materials: an overview. In: Proceedings of the world congress on engineering 2012, vol III (WCE 2012), London, UK, 4–6 July 2012. pp 1291–1299
11. Challis VJ, Roberts AP, Wilkins AH (2008) Design of three dimensional isotropic microstructures for maximized stiffness and conductivity. Int J Solids Struct 45:4130–4146
12. ASTM (2015) ISO/ASTM52900-15 Standard terminology for additive manufacturing – general principles – terminology, ASTM International, West Conshohocken, PA. https://doi.org/10.1520/ISOASTM52900-15
13. ISO 17296-2:2015 additive manufacturing—general principles—Part 2: overview of process categories and feedstock
14. Garland A, Fadel G (2015) Design and manufacturing functionally gradient material objects with an off the shelf three-dimensional printer: challenges and solutions. J Mech Des 137:111407
15. Grujicic M, Cao G, Fadel GM (2001) Effective materials properties: determination and application in mechanical design and optimization. Proc Inst Mech Eng Part L J Mater Des Appl 215:225–234
16. HP's Jet Fusion 3D Printing Technology: enabling the next industrial revolution. https://higherlogicdownload.s3.amazonaws.com/AUVSI/6322f901-72cc-424f-9550-cee46d4da1d6/UploadedImages/documents/FutureRoboticsForumPresentations/HPJetFusion3D.pdf

17. Bhashyam S, Hoon Shin K, Dutta D (2000) An integrated CAD system for design of heterogeneous objects. Rapid Prototyp J 6:119–135
18. Mortenson ME (1997) Geometric modeling. Wiley (1997)
19. Pasko A, Adzhiev V, Sourin A, Savchenko V (1995) Function representation in geometric modeling: concepts, implementation and applications. Vis Comput 11:429–446
20. Pasko A, Fryazinov O, Vilbrandt T, Fayolle P, Adzhiev V (2011) Procedural function-based modelling of volumetric microstructures. Graph Models 73:165–181
21. Piegl L, Tiller W (1997) The NURBS book. Springer, Berlin, Heidelberg
22. Mortenson ME (1985) Geometric modeling. Wiley
23. Nguyen VP, Kerfriden P, Brino M, Bordas SPA, Bonisoli E (2014) Nitsche's method for two and three dimensional NURBS patch coupling. Comput Mech 53:1163–1182
24. Cottrell JA, Hughes TJR, Bazilevs Y (2009) Isogeometric analysis: toward Integration of CAD and FEA. Wiley, Chichester
25. Tornincasa S, Bonisoli E, Kerfriden P, Brino M (2014) Investigation of crossing and veering phenomena in an isogeometric analysis framework. In: Allemang R (ed) Topics in modal analysis II, vol 8. Springer, Cham, pp 361–376
26. Tran LV, Ferreira AJM, Nguyen-Xuan H (2013) Isogeometric analysis of functionally graded plates using higher-order shear deformation theory. Compos Part B Eng 51:368–383
27. Burkhart D, Hamann B, Umlauf G (2010) Iso-geometric finite element analysis based on Catmull-Clark subdivision solids. Comput Graph Forum 29:1575–1584
28. Fang S, Srinivasan R (1998) Volumetric-CSG—a model-based volume visualization approach. In: Proceedings of sixth international conference in Central Europe on Computer Graphics and Visualization
29. Nassar AR, Reutzel EW (2013) A proposed digital thread for additive manufacturing. Solid Free Fabr 19–43
30. Xiao J, Eynard B, Anwer N, Le Duigou J, Durupt A (2016) Geometric models and standards for additive manufacturing: a preliminary survey. In: Virtual concept 2016 international workshop on major trends in product design, Bordeaux, France, 17–18 March 2016. https://hal.archives-ouvertes.fr/hal-01364825v1
31. Xiao J, Anwer N, Durupt A, Le Duigou J, Eynard B (2017) Standardisation focus on process planning and operations management for additive manufacturing. In: Eynard B, Nigrelli V, Oliveri SM, Peris-Fajarnes G, Rizzuti S (eds) Advances on mechanics, design engineering and manufacturing. In "Lecture notes in mechanical engineering." Springer, Cham, pp 223–232
32. Hällgren S, Pejryd L, Ekengren J (2016) 3D data export for additive manufacturing-improving geometric accuracy. Procedia CIRP 50:518–523
33. ISO 10303-242:2014 Industrial automation systems and integration—product data representation and exchange—Part 242: Application protocol: managed model-based 3D engineering
34. AP 242 Edition 2 capabilities for additive manufacturing interoperability. http://www.ap242.org/additive-manufacturing
35. ASTM (2016) ISO/ASTM52915-16 Standard specification for additive manufacturing file format (AMF) Version 1.2, ASTM International, West Conshohocken, PA. https://doi.org/10.1520/ISOASTM52915-16
36. ASTM WK48549 New specification for AMF support for solid modeling: voxel information, constructive solid geometry representations and solid texturing, ASTM International, West Conshohocken, PA
37. 3MF CONSORTIUM. https://3mf.io
38. Catmull E, Clark J (1978) Recursively generated B-spline surfaces on arbitrary topological meshes. Comput Des 10:350–355

39. Savio G, Rosso S, Meneghello R, Concheri G (2018) Geometric modeling of cellular materials for additive manufacturing in biomedical field: a review. Appl Bionics Biomech 2018:1–14
40. Fantini M, Curto M, De Crescenzio F (2016) A method to design biomimetic scaffolds for bone tissue engineering based on Voronoi lattices. Virtual Phys Prototyp 11:77–90
41. OpenNURBS Initiative. https://www.rhino3d.com/en/opennurbs

Applying High Speed Video to Optimize the Performance of Milling Tools

C. García-Hernández[1(✉)], A. Martínez-Angulo[2], N. Efkolidis[3], P. Ubieto-Artur[1], J. L. Huertas-Talón[1,2], and P. Kyratsis[3]

[1] Department of Design and Manufacturing Engineering, University of Zaragoza —Campus Río Ebro, C/María de Luna, 3-50018 Saragossa, Spain
(+34) 876 555 182garcia-hernandez.cesar@unizar.es
[2] Centro Público Integrado de Formación Profesional Corona de Aragón, C/Corona de Aragón, 35-50009 Saragossa, Spain
[3] Department of Mechanical Engineering and Industrial Design, Technological Educational Institution of Western Macedonia, Kozani, Greece

Abstract. Design and optimization of innovative tools are key aspects for milling metal alloys with a hard machinability, being required for different industrial applications e.g., automobile or aeronautical manufacturing. For this purpose, a correct rupture and evacuation of the generated chips are two crucial aspects, being possible to improve them paying attention to the geometry and materials (particularly those used for coatings) of the milling tools. The influence of these two aspects can be barely registered with conventional video, during a real milling process, while high speed recordings can provide valuable information. In this research project, high speed video was applied to optimize de performance of milling tools, paying special attention to Ti6Al4V, due to its special requirements, as well as to its applicability to the aeronautical industry. The obtained results made possible to compare different versions of the tool geometries, facilitating the evacuation of the chips generated during the milling processes. Thanks to these improvements, the number of unexpected tool breaks, as well as their life were increased and the milled pieces obtained better quality surfaces, in parallel to the reduction of problems caused by chip pressures and collisions.

Keywords: High speed video · Milling · Tool geometry · Tool optimization · Aeronautical alloys

1 Introduction

The applications of metal alloys with a hard machinability are increasing in different industrial environments, thanks to their clear value in sectors like the automobile or aeronautical manufacturing. Comparing mechanical features (density, hardness, etc.) and thermal ones (increasing life of manufactured parts under high temperature conditions) these alloys provide clear advantages compared with conventional materials. For these reasons, although the required milling processes are considerably harder, their convenient applications make essential to develop innovative tools and improving machining processes.

F. Cavas-Martínez et al. (Eds.): *Advances on Mechanics, Design Engineering and Manufacturing II*, LNME, pp. 422–429, 2019.
https://doi.org/10.1007/978-3-030-12346-8_41

Trying to optimize these milling processes, two key aspects must be considered: a correct evacuation of the generated chips and the ideal tool path to be implemented. It is well known that thanks to the optimization of the milling paths, the cutting speed and the tooth feed, it is possible to improve the manufacturing processes, as detailed in the extensive previous literature. Nevertheless, in order to improve the chip rupture and evacuation, efforts should be focused on the optimization of the geometry and materials used to manufacture the milling tools (particularly those applied for coatings). The influence of these two aspects on the rupture and evacuation of the chips can be barely registered with conventional video, while high speed recordings would add valuable information. According to this, high speed video was applied to optimize de performance of milling tools, as it has previously used in other research fields, including experimental biology [1], medical systems [2], surgery [3], physics [4], fluid science [5], biomechanics [6], etc. Not only chip related aspects could be observed and analysed, but also problems related to harmonic vibrations and tool-blade damage were detected.

In fact, the described methodology could be used in order to assess the accuracy of previously developed approaches for modelling different parameters in milling, such as chip thickness or cutting forces [7, 8].

Although different materials were milled, finally, special attention was paid to Ti6Al4V, due to its special requirements, as well as to its applicability to the aeronautical industry. The obtained results made possible to compare different versions of the tool geometries, facilitating the evacuation of the chips generated during the milling processes. Thanks to these improvements, the tool life was increased and the milled pieces obtained better quality surfaces, due to the reduction of problems caused by chip pressures and collisions.

2 Experimental Method

The following sub-sections describe the most important features of the experiments that were developed during this research, including the tools to be optimized, milling equipment, recording set, including its required mechanical protection, and the details of the experimental process.

2.1 Tools to Be Optimized

Three different milling tools were tested in order to optimize their results in a manufacturing process of 42CrMo4 steel parts used in e.g., vertical transportation or aeronautical industries.

The diameter of all the tools for this process was 13.5 mm and had 4 teeth. They were made of tungsten carbide, with the features included in Table 1.

The first tool used in this study is commercially available [9], and its 3D model is shown in Fig. 1, which also includes its geometrical section. The geometry of this initial tool was optimized in order to improve the manufacturing process of the final mechanical pieces, giving a second version of it (Fig. 4) and, finally, a third version (Fig. 6) modified some additional aspects, as described in the following section.

Table 1. Tool material features

Tool base material	
Grain size	Submicron (0.5–0.8 μm)
Binder (% Co)	10%
Hardness	1590 HV10
Coating material	
Material	AlCrN-based
Max. service temp.	1100 °C

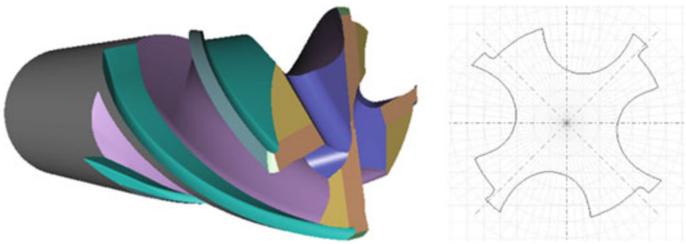

Fig. 1. 3D model and geometrical section of the first tool

2.2 Recording Set Description

The sensor used for the video captures was a 0.52″ × 0.35″ Exmor RS® CMOS, with an aspect ratio 3:2. The optical set was based on a ZEISS® Vario-Sonnar® T* Lens, with a total of 10 elements assembled in 9 groups, being 9 aspheric elements plus AA lens.

A specifically designed case, made of aluminium and polycarbonate, was used and provided with an IR filter, in order to mechanically protect the whole set against metallic chips and liquid coolant (required for the milling processes developed), which was externally controlled by means of an adapted cable-based remote device.

All the videos were directly recorded in MP4 format [10] to a 64 Gb SDXC Memory Card (UHS-I) and processed with different software tools in order to be correctly analysed (Table 2).

Table 2. Recording conditions

Capturing frame rate	1000 frames/s
Frame width	1920
Frame height	1080
Final video length	2 min 31 s
Final video rate	25 frames/s

2.3 Experimental Process

The experimental process was based on the milling of blind slots, in which difficulties on chip evacuation usually can cause unexpected breaks (not only erosion) of tool blades.

Table 3 contains the conditions that were programmed in the milling machine, based on a cutting speed (v_c), a feed of tooth (f_z) and an axial depth (a_p), according to the previously described tools.

Table 3. Blind slots milling conditions

Tool diameter	13.5 mm
Number of teeth	4
v_c	135 m/min
f_z	0.035 mm/tooth
a_p	9 mm
Workpiece material	42CrMo4

The unexpected breaks of the tools were considered to be due to an inadequate material evacuation, causing chip retentions between tool flutes. This was the reason why an exhaustive analysis was required and human vision was not sufficient to develop it. High speed video was apparently a good alternative for this objective, not trying to study the geometry details of the evacuated chips as described in previous research papers [11], but paying attention to the chip ejection and its features e.g., regularity, order and direction.

With the observation and careful analysis of the high speed videos (Fig. 2), it could be concluded that chip evacuation was a serious problem in the milling process of this blind slots. After that, a modified version of the same type of tool was manufactured according to the video analysis, softening the curves in the flute output and decreasing its depth.

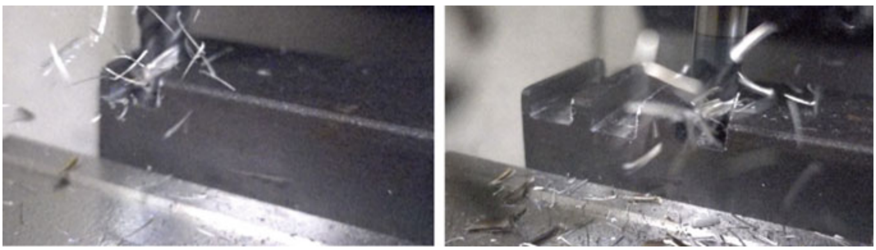

Fig. 2. Two frames from each of the initial high speed video tests

3 Results

The results obtained during the experimental stage, using the three previously described tools, in order to optimize their geometry for manufacturing 42CrMo4 steel parts, are described in this section. These optimized aspects, developed thanks to the observation and analysis of the high speed videos, are also included. Finally, some improvements in the experimental process and their application to the milling of Ti6Al4 V thin wall parts, for aeronautical purposes, are explained in this section.

The optimization process started with the filming of milling processes using two tools with the same features. Two frames of the obtained high-speed videos are shown below (Fig. 2). These videos were carefully observed and analysed with the tool manufacturing experts, paying attention to the shape, dimensions and trajectories of the chips.

After the previous analysis, several changes were applied to the tool geometries, modifying their chip evacuation flutes as compared in Fig. 3.

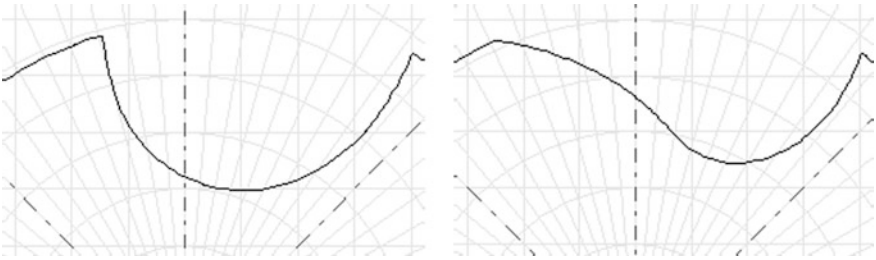

Fig. 3. Chip evacuation slot profiles of the 1st tool (left) versus the 2nd one (right)

The final design of the second tool, after the first optimization process, and its geometrical section are shown in Fig. 4, which can be compared with the original one (Fig. 1), noticing clear differences in the flute shapes.

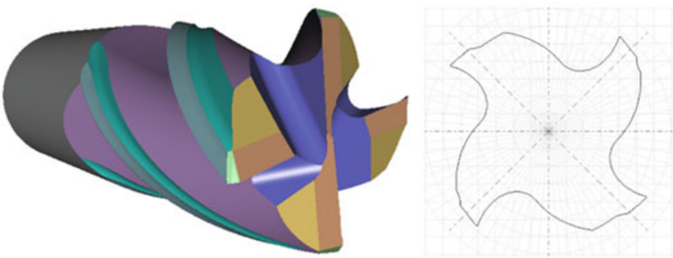

Fig. 4. 3D model and geometrical section of the second version of the tool

Thanks to this optimization process, the number of unexpected tool breaks decreased significantly, according with the final user of the improved tools, and the high-speed video reveals how the chips are thinner and perfectly evacuated, as shown in Fig. 5.

Fig. 5. Sequence of four consecutive video frames, milling with the optimized tool

A last improvement was developed after paying attention to the previously described video and its aspect can be observed in Fig. 6.

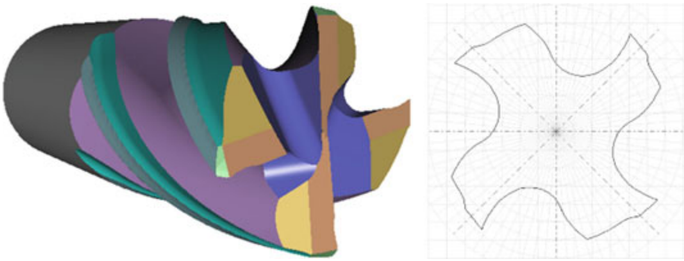

Fig. 6. 3D model and geometrical section of the definitive tool, after final optimization

Finally, new experiments were developed using Ti6Al4V for aeronautical applications, paying special attention to the possibility of capturing the chips in movement so their trajectory angles could be measured. For that purpose, the camera was orthogonally placed in front of the milling tool and, as shown in Fig. 7, a chip was followed frame by frame to graphically describe its trajectory. This made possible to measure α and determine the relation between the chip movement and the helix angle of each flute.

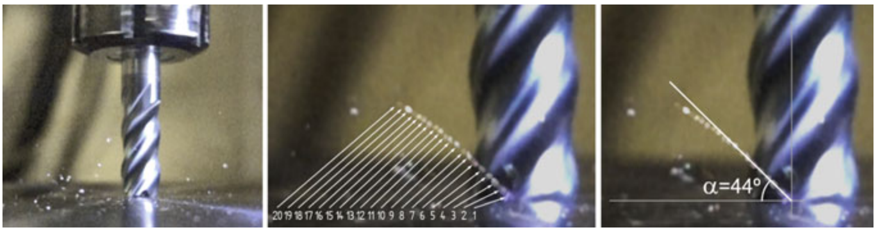

Fig. 7. Trajectory of a chip in a milling process of a Ti6Al4V part

4 Discussion

Although the first videos gave valuable information about aspects like the chip dimensions, evacuation and trajectory, due to the relative position between camera and tool, it was impossible to take reliable measures of e.g., relative angles of the chip trajectories. This was clearly improved in the next stage of this research, with the Ti6Al4V thin-wall parts, as shown in Fig. 7. For that purpose, it was necessary to design and develop a new fastening system for the recording protective case, which was directly attached to the tool holder inside the milling machine.

Due to the visual limitations caused by the use of coolant (Fig. 8), it was considered the application of different methods for cooling the milling processes, which could be based on the projection of CO_2 [12] or refrigerated air [13], although this would modify the chip trajectories.

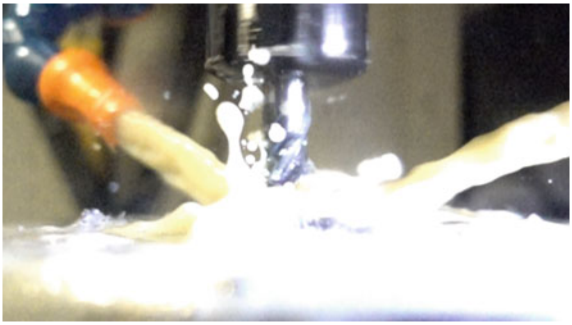

Fig. 8. Video frame showing how coolant makes impossible to capture chip trajectories

Finally, high speed video analysis can be useful to verify the correct direction and angle for the chip trajectories, helping tool designers to optimise their geometries in order to achieve clean chip evacuations, avoiding milling obstruction caused by the accumulation of chips.

5 Conclusions

It was proved that high speed video has clear applications in the tool manufacturing field. Particularly, improvements in the tool geometry can be developed from the observation and careful analysis of the chips, thanks to this implementation.

Tool life can be increased, as previously described. Other features should be explored, such as surface quality, which could also be improved by means of the visualization of superficial chip impacts.

A cost reduction could be noticed thanks to this tool optimizing process, i.e. a reduction of unexpected breaks of the tools was observed, avoiding premature replacements and unnecessary tests.

Industrial processes which involve aeronautical applications can easily be improved thanks to the previously described optimization, reducing production times and increasing sustainability.

Acknowledgments. The research work was possible thanks to the collaboration among researchers from the University of Zaragoza, the CPIFP Corona de Aragón (both from Zaragoza, Spain) and the Western Macedonia University of Applied Sciences (from Kozani, Greece). It was funded by means of the grant JIUZ-2016-TEC-09 (Universidad de Zaragoza and Fundación Ibercaja). Finally, the research team would like to thank the technical staff from the tool manufacturing company Marena SL, for their crucial collaboration in the development and optimization stages.

References

1. Shamur E, Zilka M, Hassner T, China V, Liberzon A, Holzman R (2016) Automated detection of feeding strikes by larval fish using continuous high-speed digital video: a novel method to extract quantitative data from fast, sparse kinematic events. J Exp Biol 219 (11):1608–1617
2. Jeong IC, Finkelstein J (2016) Introducing Contactless Blood Pressure Assessment Using a High Speed Video Camera. J Med Syst 40(4):1–10
3. Volgger V, Schuster ME, Felicio A, Lohscheller J, Al-Muzaini H, Betz CS (2016) Preliminary results regarding The combined use of narrow band imaging and high-speed video laryngoscopy to discriminate laryngeal lesions. Lasers Surg Med 48:41
4. Poonyawatpornkul J, Wattanakasiwich P (2015) High-speed video analysis of a rolling disc in three dimensions. Eur J Phys 36(6):065027
5. Dular M, Petkovšek M (2015) On the mechanisms of cavitation erosion—coupling high speed videos to damage patterns. Exp Thermal Fluid Sci 68:359–370
6. Gutowski C, Darvish K, Liss FE, Ilyas AM, Jones CM (2015) Use of high-speed X ray and video to analyze distal radius fracture pathomechanics. Orthop Clin North Am 46(4):571–576
7. Pleta A, Niaki FA, Mears L (2017) Investigation of chip thickness and force modelling of trochoidal milling. Procedia Manuf 10:612–621
8. Luo S, Dong Z, Jun MB (2017) Chip volume and cutting force calculations in 5-axis CNC machining of free-form surfaces using flat-end mills. Int J Adv Manuf Technol 90(1–4):1145–1154
9. Marena SL Catalogue, http://www.marena.es/catalogo.pdf. Last accessed 1 Mar 2018
10. ISO/IEC Std. 2012, Information technology—Coding of audio-visual objects—Part 12: ISO base media file format, ISO/IEC 14496-12:2012
11. Copenhaver R, Rubeo MA, Guzorek S, Landge S, Smith KS, Ziegert J, Schmitz T (2017) A fundamental investigation of modulated tool Path turning mechanics. Procedia Manuf 10:159–170
12. Huertas JL, Faci E, Ros E (2006) CO_2, la mejor opción. IMHE: Información de máquinas-herramienta, equipos y accesorios, (330), 59–78
13. Zhu L, Cao H, Huang H, Yang X (2017) Exergy analysis and multi-objective optimization of air cooling system for dry machining. Int J Adv Manuf Technol 93(9–12):3175–3188

A Knowledge-Based Augmented Reality Tool for Managing Design Variations

L. Barbieri(✉), E. Marino, and F. Bruno

Department of Mechanical, Energy and Management Engineering (DIMEG), Università della Calabria, 87036 Rende, CS, Italy
loris.barbieri@unical.it

Abstract. In view of the wide scope of challenges concerning Industry 4.0, a variety of enabling digital industrial technologies can support the digitization of the manufacturing sector. Among them, Augmented Reality represents one of the most promising innovation accelerators that will support human workers and bring Smart Factories to a higher level of efficiency. To this end, the paper presents an Augmented Reality tool that provides support at the workplace to easily detect and collect design changes by augmenting virtual 3D models, as defined in the project plan, on the actual design. The proposed tool runs on a consumer smartphone and adopts hybrid tracking techniques to allow workers to formalize and make more efficient the knowledge management of the design changes within the overall design process.

Keywords: Industry 4.0 · Augmented reality · Knowledge-based engineering

1 Introduction

Industry 4.0 names the current upward trend of the industrial automation toward the integration of the modern and efficient product and manufacturing technologies in order to enhance the working conditions and improve the productivity and product quality. The enhancement of the quality and productivity of the companies is tightly dependent by the efficacy of the management and protection of the corporate know-how and its preservation and sharing among the different company's departments, offices, and locations.

To this end, in the last years, many knowledge-based engineering systems and methods [1–4] have been proposed in order to optimally leverage employee-generated know-how, but there is still a number of areas that require the development of custom applications. Among them the oil & gas sector in which the need for a structured method has emerged for the conservation of the design changes and improvements that occur in the production process, and in particular during tubing installations. In fact, the complexity of the piping networks and systems often requires modifications and improvements to be made on-site; a number of design changes that occur especially in the first productions of small-series products made on order. These design changes consist in a series of adjustments and improvements performed by qualified factory workers in order to minimize the number of bendings, reduce overall dimensions,

F. Cavas-Martínez et al. (Eds.): *Advances on Mechanics, Design Engineering and Manufacturing II*, LNME, pp. 430–439, 2019.
https://doi.org/10.1007/978-3-030-12346-8_42

streamline pipe routes, and increase the visibility and manoeuvrability space for easier assembly of the components.

At the moment, this sector lacks structured and reliable methods and tools that allow to keep track and preserve the knowledge about these design changes and improvements. This entails a significant increase of the production cycle's time and causes slowdowns and complications in the maintenance activities because of the project variations.

In view of the wide scope of challenges concerning Industry 4.0, a variety of enabling digital industrial technologies will support the digitization of the manufacturing sector. Among them Augmented Reality (AR) represents one of the most promising innovation accelerators that will support human workers [5] and bring Smart Factories to a higher level of efficiency thanks to the introduction of AR-based systems and applications that can speed up the entire production chain.

On the basis of these considerations, the paper proposes an AR tool that allows to reduce the time and make more efficient the management of the company's know-how. In particular, the AR application can be intuitively and easily adopted by workers at the workplace to take annotations of the design changes made during tubing installations. The AR application runs on a consumer smartphone, equipped with a camera, and augments the 3D model, as established in the design phase of the project, on the visualization of the physical product which can presents design changes because of the operation performed by operators.

2 Related Works

In the last three decades, a plethora of AR-based systems and tools have been proposed to support workers directly at the workplace. Most of these researches focus on the adoption of Augmented Reality as an assistive instrument for providing instructions. Virtual assistance is, in fact, one of nine design elements most representative of the Industry 4.0 [6] that has been declined in a variety of technical and technological AR-based solutions. The first application dates back to 1992 [7] where an HMD device was adopted to show workers drilling distances and positions. Afterward, other HMD [8, 9] and display-based [10, 11] solutions have been proposed to support an industrial process by means of the AR technology. To augment information directly into the worker's field of view various studies have investigated the potentialities offered by projector technologies [12, 13]. Mobile phones [14] and tablet-based systems [15–17] have been used too for providing AR instructions. Thanks to the capability to automate the design of presentations that explain maintenance and repair tasks, some of the abovementioned solutions can be considered knowledge-based AR systems [18].

Although the extensive use of AR for virtual assistance applications, this technology can address almost every aspect of a product life cycle [19–21]. About the adoption of AR for performing discrepancy check between real parts and their associated construction data, only a few systems have been proposed. Furthermore, these systems cannot perform a real-time check [22] because are encapsulated into a CAD viewing software [23], or offer a limited maneuverability and precision because of their dimensions and low-resolution camera [24].

These limitations are overcome by the proposed AR tool because it runs on a handheld device that can be easily adopted by operators at the workplace and adopt hybrid tracking techniques to perform a robust real-time augmented visualization of 3D data on the real parts. The AR tool acquires design knowledge from workers, formalize the acquired information, and collects it into a database. The acquired knowledge is then made available to designers directly into the CAD system in order to review and update 3D models according to the documented discrepancies.

3 AR Tool

The Augmented Reality tool consists of an application developed with the Google Project Tango Development Kit [25]. This software development technology, introduced by Google in 2014, has been preferred to other solutions, such as Vuforia Augmented Reality SDK [26] because it offers hybrid tracking techniques that combine vision-based and sensor-based methods to calculate device's motion and orientation in 3D space in real-time.

In particular, the application takes advantage of both marker-based and natural feature-based techniques, and combine these ones with a sensor fusion technique that uses the various sensors (motion tracking camera, 3D depth sensor, accelerometer, ambient light sensor, barometer, compass, GPS, gyroscope) equipped on the device to remember areas that it has travelled through and localize the user within those areas to up to an accuracy of a few centimeters.

In the last years, Tango technology has been enabled for a small number of consumer smartphones and tablets. In this regard, the proposed AR tool runs on a Lenovo Phab 2 Pro smartphone [27]. This is an Android device equipped with a Qualcomm Snapdragon 652 (1.80 GHz) processor, a 16 MP camera, and integrated depth and motion tracking sensors (accelerometer, digital compass, gyroscope, proximity sensor, ambient light sensor). Since all the computations are carried out on the device itself, there are no other external hardware components required for the data input and processing. The following illustration (Fig. 1) depicts the software architecture of the AR application. It consists of different modules, programmed in 3D Unity, each one dedicated to one or more specific operations.

In particular, the "Marker detection" module has been implemented by means of the Tango SDK in order to perform marker detection, motion tracking, and video overlay for AR functionalities. This module is also responsible for the identification of the information and parameters, settled for each work session, that has to be stored in the database. The "Offset" module has been developed by exploiting the inbuilt functionalities of the 3D Unity engine to edit position, orientation, and scale of the 3D models inserted in the AR scene. The "Color mode" module uses functions to set parent/child relations among 3D models, and applies a script to each model to control its material properties and change, from opaque to transparent, the rendering mode. The last module is dedicated to the creation and editing of 3D annotations. It adopts Raycast and Collision functions to recognize user touch and detect contacts between the ray originated by user touch and 3D models of the scene. 3D notes' position, type, and content are saved into the local database by means of the "Data management" module.

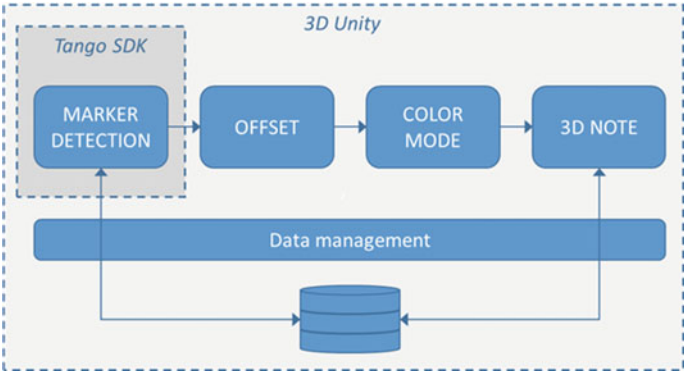

Fig. 1. AR tool's software architecture

This module is responsible for reading and writing database operations, and it allows also the access to an external file system in which the 3D models are stored.

4 Case Study

As abovementioned, the proposed AR tool allows workers to easily identify design changes by superimposing the virtual 3D model, defined in the design stage, on the actual design. Furthermore, this tool allows to formalize and make more efficient the knowledge management of the design changes within the overall design process. In order to provide a better comprehension of the main functionalities provided by the AR tool, this section focuses on a case study consisting of an air handling unit (AHU) on which the user verify the consistency of the actual tube routes with the 3D model geometry originally defined in the project plan.

In order to perform the augmented visualization, the tool employs a visual marker in order to set position and orientation of the virtual 3D model. As a consequence, as depicted in the following figure (Fig. 2), a marker has been placed on the large metal box of the AHU. Then the user can launch the AR application.

When the AR tool starts, the first screen offers to the user a set of options to allow him/her to: create a new session; recall a saved work session; and access to a control panel for setting network connection parameters. The following image (Fig. 2) shows a screenshot of the AR tool when creating a new working session. Most of the screen is dedicated to the live video stream from the camera of the smartphone device, and a menu bar is displayed horizontally across the bottom of the screen. This menu allows the user to interact with the AR tool by selecting, through direct manipulation, from a list of nine buttons. For a proper use of the tool, the command buttons have been placed in the menu according to the logic and chronological sequence of operations that have to be performed by the user.

By clicking on the first button on the left, the device camera records real surrounding, while the application is searching for the predefined marker. When the tool detects and recognizes the marker the virtual model is displayed on the device display

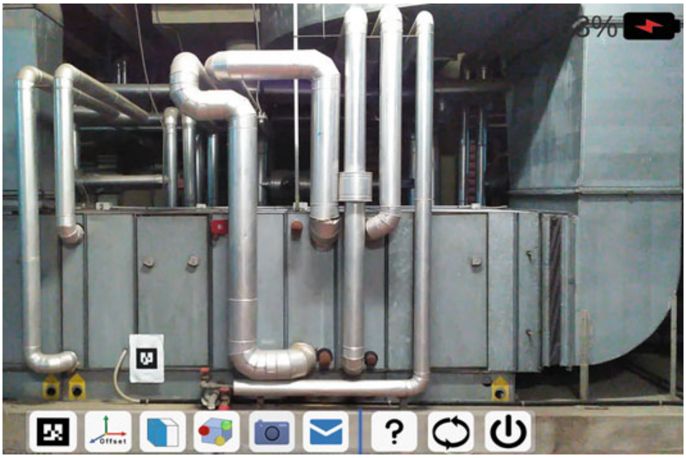

Fig. 2. AHU and marker displayed on the AR tool

with a specific position and orientation (Fig. 3). The next button can be adopted by the user to perform an accurate positioning of the virtual model on the physical AHU. The user can specify new coordinates along the X, Y and Z axes, or proceed through user-defined offsets along one or more axes. This feature becomes very useful when the marker requires being placed in a not easily accessible point or for very large components in which small positioning errors of the marker may entail big alignment inaccuracies of the 3D model.

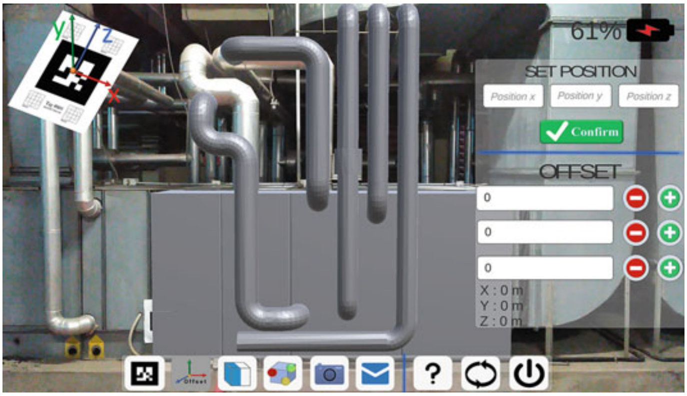

Fig. 3. 3D model augmented on the AHU and menu for fine positioning operations

When the virtual model is correctly augmented on the live camera frame, the user can customize the visual style in order to simplify the detection of design changes. In fact, as depicted in Fig. 3, default setting provides a shaded display of the 3D model in which is not possible to discern the various components of the assembly. In this regard, by selecting the third control button a checkbox menu is displayed on the left side of the display device (Fig. 4). This menu shows a list of the components of the assembly, that for the specific case study consists in two sub-assemblies: the large metal box, that contains fan and filter compartments, heating and cooling elements; and the pipes. The user can select one item at a time in order to: hide the component by clicking on the toggle button; change its color by means of a color palette; set its transparency level through a slider displayed on the right side of the screen.

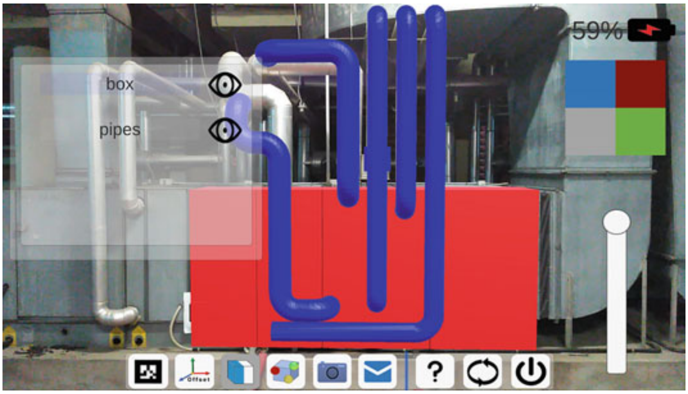

Fig. 4. Menu for the setting of visual style properties of the virtual model

When the user has concluded the customization of the visual style properties of the virtual model, he/she can proceed by adding 3D notes simply by selecting the desired point of the 3D model in which anchor the annotation. For the creation of the 3D annotations, the user has to compile a text field with the content of the design change, the size, and color of a virtual sphere that identifies the placement of the note on the virtual model. The following image (Fig. 5) shows the box and pipe components represented with a different color, in order to clearly differentiate them, and a semi-transparent visualization to easily compare the virtual and the actual pipes and detect design variations between them.

In addition to these main functionalities enabled by means of the first three command buttons of the menu bar, other six buttons facilitate a specific interaction. In particular, the fourth button is a toggle that allows to hide the 3D annotations added by the user. The two following buttons allow the user to take pictures of the design changes and to email the data collected in the work session. 3D notes and screenshots are, in fact, automatically saved and stored in a database that can be reloaded on request by the user. Then users can load annotations taken in previous work sessions in order to check, modify and accept them or simply to continue the tubing installation activities that usually require more than one day of work.

The last three command buttons allow respectively to: display a help user guide on the main functions of the tool; reset the current work session; end the current work session.

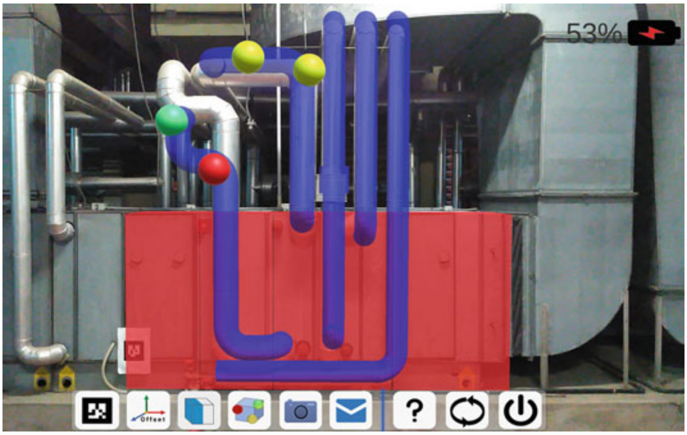

Fig. 5. Augmented 3D model and annotations

As detailed in the previous section, the AR tool requires no external hardware but the Tango-enabled smartphone. Thanks to its compact dimensions it is a handheld device that lends itself well to be used in different industrial contexts. In fact, the user can easily hold the device with one hand and interact with the dominant hand (Fig. 6).

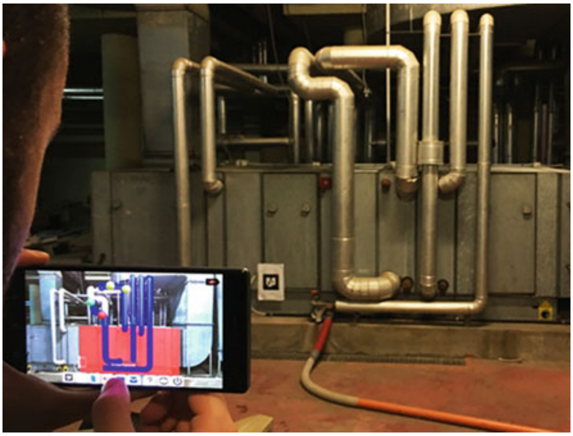

Fig. 6. User while interacting with the AR tool

As abovementioned, the design changes collected with the AR tool can be reloaded to be visualized on the same device, but they can be also imported into a CAD system. In order to formalize the knowledge management, it is fundamental in fact to make these design changes accessible to designers. Figure 7 shows the 3D assembly of the AHU, as defined in the design stage, in which the annotations taken by workers by means of the AR tool have been imported. In this manner, designers are aware of the design changes performed by workers in the production process and have a detailed knowledge of their position and attributes, such as diameter and segment length, bend radius, material, etc.

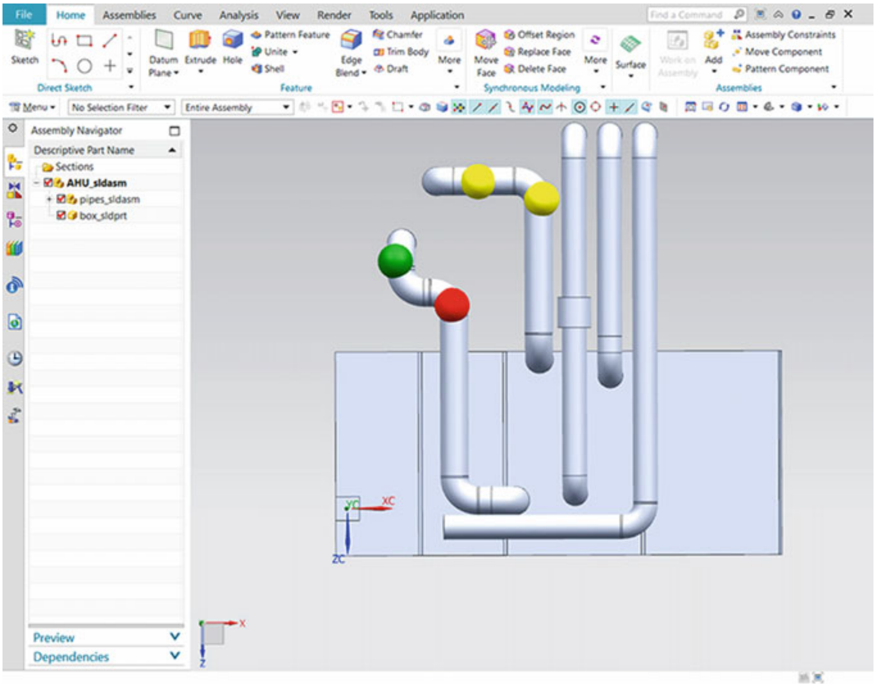

Fig. 7. 3D annotations visualized on the CAD model

5 Conclusions

The paper has presented an AR tool that supports workers to take note of the design change they made in the production process. In particular, the AR tool provides a real-time augmented visualization of 3D model data, as defined in the design stage, onto the physical product framed by the camera. Thanks to the augmented visualization users can easily identify design changes and make annotations directly on the augmented 3D model in order to capture and formalize design knowledge. Furthermore, the AR tool's capability to augment virtual models on the real scenario enables it to be used also for assembly instructions. The virtual model, in fact, could be adopted as a reference to guide operators in the assembly activities.

The AR tool has been specifically developed for the Tango platform that, starting from March 2018, is not supported anymore by Google developers in favor of ARCore development kit [28]. Similarly, Apple has announced ARKit framework [29] that presents the same capabilities of ARCore, but even though these SDKs enable reliable and robust hybrid tracking techniques at the moment they don't make it possible to use makers for deciding ex-ante a fixed point of reference for the virtual models.

References

1. Stjepandić J, Verhagen WJ, Liese H, Bermell-Garcia P (2015) Knowledge-based engineering. In: Concurrent Engineering in the 21st Century, pp 255–286
2. Chandrasegaran SK, Ramani K, Sriram RD, Horváth I, Bernard A, Harik RF, Gao W (2013) The evolution, challenges, and future of knowledge representation in product design systems. Comput Aided Des 45(2):204–228
3. Muzzupappa M, Barbieri L, Bruno F, Cugini U (2010) Methodology and tools to support knowledge management in topology optimization. J Comput Inf Sci Eng 10(4):044503
4. Peng G, Wang H, Zhang H, Zhao Y, Johnson AL (2017) A collaborative system for capturing and reusing in-context design knowledge with an integrated representation model. Adv Eng Inform 33:314–329
5. Industry 4.0 Digitalisation for productivity and growth. European Parliamentary Research Service, Sept 2015
6. Hermann M, Pentek T, Otto B (2016) Design principles for industrie 4.0 scenarios. In: 2016 49th Hawaii international conference on system sciences (HICSS). IEEE, pp 3928–3937
7. Caudell TP, Mizell DW (1992) Augmented reality: an application of heads-up display technology to manual manufacturing processes. In: Proceedings of HICSS'92, vol 2. IEEE, pp 659–669
8. Henderson SJ, Feiner SK (2011) Augmented reality in the psychomotor phase of a procedural task. In: 2011 10th IEEE international symposium on mixed and augmented reality (ISMAR). IEEE, pp 191–200
9. Zheng XS, Foucault C, Matos da Silva P, Dasari S, Yang T, Goose S (2015) Eye-wearable technology for machine maintenance: Effects of display position and hands-free operation. In: Proceedings of the 33rd annual ACM conference on human factors in computing systems. ACM, pp 2125–2134
10. Echtler F, Sturm F, Kindermann K, Klinker G, Stilla J, Trilk J, Najafi H (2004) The intelligent welding gun: augmented reality for experimental vehicle construction. In: Virtual and augmented reality applications in manufacturing. Springer, pp 333–360
11. Fiorentino M, Uva AE, Gattullo M, Debernardis S, Monno G (2014) Augmented reality on large screen for interactive maintenance instructions. Comput Ind 65(2):270–278
12. Korn O, Schmidt A, Hörz T (2013) The potentials of in-situ-projection for augmented workplaces in production: a study with impaired persons. In: CHI'13 extended abstracts on human factors in computing Systems. ACM, pp 979–984
13. Büttner S, Sand O, Röcker C (2015) Extending the design space in industrial manufacturing through mobile projection. In: Proceedings of the 17th international conference on human-computer interaction with mobile devices and services adjunct. ACM, pp 1130–1133
14. Billinghurst M, Hakkarainen M, Woodward C (2008) Augmented assembly using a mobile phone. In: Proceedings of MUM'08. ACM, pp 84–87
15. Gavish N, Gutiérrez T, Webel S, Rodríguez J, Peveri M, Bockholt U, Tecchia F (2013) Evaluating virtual reality and augmented reality training for industrial maintenance and assembly tasks. Interact Learn Environ, pp 1–21
16. Hořejší P (2015) Augmented reality system for virtual training of parts assembly. Procedia Eng 100:699–706

17. Webel S, Bockholt U, Engelke T, Gavish N, Olbrich M, Preusche C (2013) An augmented reality training platform for assembly and maintenance skills. Rob Auton Syst 61(4):398–403
18. Feiner S, Macintyre B, Seligmann D (1993) Knowledge-based augmented reality. Commun ACM 36(7):53–62
19. Nee AY, Ong SK, Chryssolouris G, Mourtzis D (2012) Augmented reality applications in design and manufacturing. CIRP 61(2):657–679
20. Regenbrecht H, Baratoff G, Wilke W (2005) Augmented reality projects in the automotive and aerospace industries. CGA 25(6):48–56
21. Wang X, Ong SK, Nee AYC (2016) A comprehensive survey of augmented reality assembly research. Adv in Manuf 4(1):1–22
22. Nolle S, Klinker G (2006) Augmented reality as a comparison tool in automotive industry. In: Proceedings of the 5th IEEE and ACM international symposium on mixed and augmented reality. IEEE Computer Society, pp 249–250
23. Georgel P, Schroeder P, Navab N (2009) Navigation tools for viewing augmented cad models. IEEE CGA 29(6)
24. Schoenfelder R, Schmalstieg D (2008) Augmented reality for industrial building acceptance. IEEE VR, pp 83–90
25. Project Tango homepage, https://developers.google.com/tango. Last accessed 1 Apr 2018
26. Vuforia homepage, https://www.vuforia.com. Last accessed 1 Apr 2018
27. Lenovo Phab 2 Pro homepage, https://www3.lenovo.com/ee/et/tango. Last accessed 1 Apr 2018
28. ARCore homepage, https://developers.google.com/ar. Last accessed 1 Apr 2018
29. ARKit homepage, https://developer.apple.com/arkit. Last accessed 1 Apr 2018

Check for updates

Investigation of Aluminum Alloy Properties During Helical Roller Burnishing Through Finite Element Simulations and Experiments

L. Kamgaing Souop[1(✉)], A. Daidie[1], Y. Landon[1], J. Senatore[1], and M. Ritou[2]

[1] ICA (Institut Clément Ader), Université de Toulouse, UPS, INSA, ISAE-SUPAERO, MINES-ALBI, CNRS, 3 rue Caroline Aigle, 31400 Toulouse, France
landry-arnaud.kamgaing-souop@univ-tlse3.fr

[2] LS2N (Laboratoire des Sciences du Numérique de Nantes, UMR CNRS 6004), Université de Nantes, 2 avenue du Pr Rouxel, 44475 Carquefou, France

Abstract. Industry is always looking for ways to increase the lifetime of assemblies, especially the fatigue lifetime, from the production phase of fastening holes onwards. Helical roller burnishing is presented here as an innovative mechanical surface treatment. Applied directly after orbital drilling, this technique induces superficial plastic strains that reduce surface roughness and increase hardening and compressive residual stresses. Several studies on 3D finite element models of burnishing have been carried out but they are very time-consuming. In this review, a comparative numerical study of helical burnishing (in terms of calculation time and results on residual stress) between one 3D and two 2D plane strain finite element simulations is performed on 2024-T351 aluminum alloy drilled parts. The impact of the process operating parameters is also investigated. This comparison shows fairly similar results regarding the residual stress profiles but levels are rather different. This could be explained by the complex kinematics of helical roller burnishing, which is strongly three-dimensional. The numerical results of one of the cases studied reveal compressive residual stresses of around −100 and −490 MPa in the radial and circumferential directions of the hole, respectively. Burnishing depth and spindle rotation speed have a great impact on the final residual stress profiles. These simulations are then confronted with experimental results obtained during tests carried out using an orbital drilling unit (ORBIBOT). This demonstrates the interest of the modeling implemented and also points out ways to improve the developed models.

Keywords: Helical roller burnishing · Residual stresses · Hardening · Finite element method · Aluminum alloy

F. Cavas-Martínez et al. (Eds.): *Advances on Mechanics, Design Engineering and Manufacturing II*, LNME, pp. 440–450, 2019.
https://doi.org/10.1007/978-3-030-12346-8_43

1 Introduction

Orbital drilling (or helical milling) is a hole-making process in which a milling tool moves along a helical path while spinning on its axis (Fig. 1a). It has become increasingly popular in hole drilling processes, particularly in the aerospace industry. Compared to conventional drilling, orbital drilling has proved to be particularly advantageous to achieve aeronautical-quality drilling through complex assemblies of metallic materials in a single operation [1–3]. However, this process needs to be improved, mainly in terms of the mechanical properties of the drilled parts. In fact, the enhancement of fatigue lifetime is constantly requested for drilled parts. This is generally achieved by the production of compressive residual stresses and hardening in the surface layers of parts. Several authors [4–8] have shown that burnishing introduces compressive residual stresses, and improves the roughness and the hardening of parts. Delgado et al. also noted that roller burnishing gives a better state of residual stresses and hardening compared to shot peening and laser shock peening [9]. Hassan and Al-Bsharat have shown that burnishing increases the fatigue life of aluminum pieces [10]. As a novel mechanical surface treatment, helical roller burnishing (or orbital roller burnishing) appears to be an excellent solution to the lifetime problem insofar as it can be applied immediately after orbital drilling. The main specificity of this innovative roller burnishing technique lies in the kinematics of the tool. As an orbital drilling tool, the burnisher (which is shaped like a torus) rotates around its own axis and simultaneously describes a helical path around the hole axis (Fig. 1b). But the benefits of helical burnishing need to be investigated in depth. A 3D finite element simulation of conventional roller burnishing has been carried out by Balland et al. and the results (in terms of geometric state of the surface and residual stresses), obtained in a reasonable simulation time, demonstrate the possibility of using this type of modeling as an efficient replacement for 2D plane strain finite element simulation, which is rather limited and approximate [5]. Nevertheless, the simulation time is still considered as huge and the results are in only qualitative agreement. Thus, in this review, a comparative numerical study (in terms of calculation time and results on residual stress) between one 3D and two 2D plane strain finite element simulations is performed first of all. The impact of operating parameters (burnishing depth, spindle rotation speed) is then studied. These simulations are finally confronted with experimental results. All these studies were performed on 2024-T351 aluminum alloy drilled parts using the finite element software ABAQUS®.

2 Finite Element Modeling of Helical Roller Burnishing Process

2.1 Geometry, Material Characterization and Modeling

As mentioned earlier, we first simulated a 3D model on the one hand and two 2D models (which are very time cost effective) on the other. It is important to start by precisely defining the different interactions that occur in the planes involved.

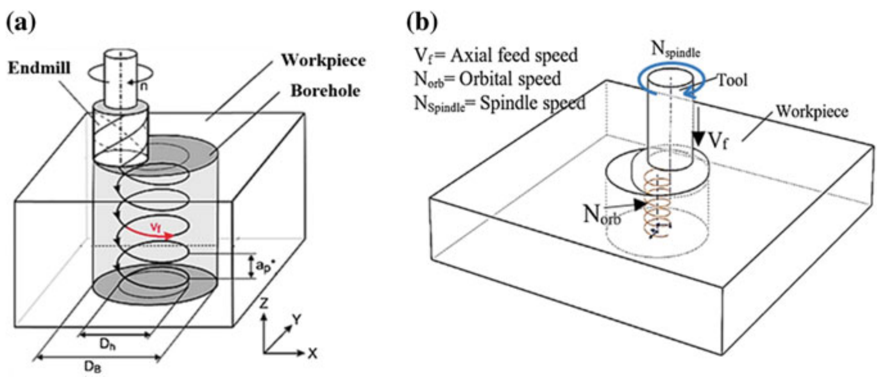

Fig. 1. Schematic drawing of orbital drilling (**a**) and helical roller burnishing process (**b**)

Figure 2a represents the directions of the different forces on a half hole during orbital burnishing. Figures 2b and c show the decomposition of orbital burnishing kinematics and forces in the 2 planes where 2D models were run. The purpose here is to compare the results obtained by the 2D and 3D models and to assess whether they are reliable. The 3D model was used to give the radial, orthoradial and axial residual stresses (σ_R, σ_θ, σ_Z) while the first 2D model gave radial and orthoradial residual stresses (σ_R, σ_θ) and the second 2D model gave axial residual stresses (σ_Z).

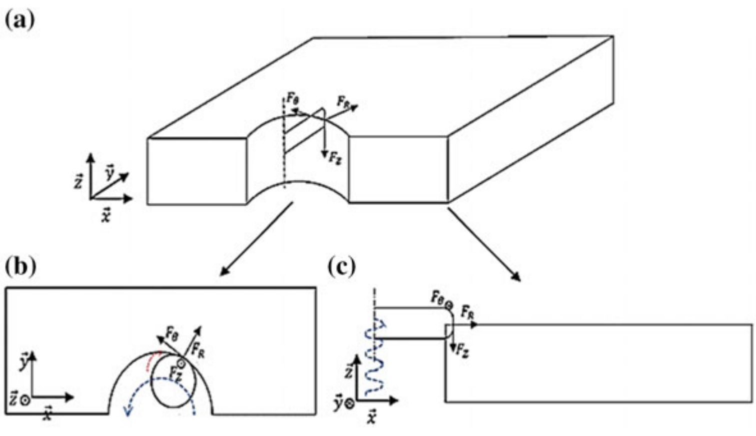

Fig. 2. Decomposition of orbital burnishing kinematics

In order to further reduce computation time, all these simulations were run on a portion of the hole (one eighth). Mathurin has shown that this portion achieves a good compromise between the process studied and the calculation time [15]. The length of the specimen considered was 25.4 mm. It was chosen large enough to minimize edge effects. Its thickness was 1 mm. The hole diameter was 6.35 mm and the radius of the helical path was 0.8 mm. In order to study the impact of the burnishing depth, the different tool diameter values were 4.762, 4.79, 4.81 and 4.83 mm, which gave burnishing depths “e” of 6, 20, 30 and 40 μm respectively. The tool height was 0.6 mm. This study was performed on AA2024-T351 aluminum alloy parts. It was fundamental to determine a robust material for the constitutive model so that the strains could be modelled accurately. The constitutive model used for this material is generally a Johnson-Cook model [11, 12] which is defined by equation (1).

$$\bar{\sigma} = [A + B\overline{\varepsilon p}^n]\left[1 + C\ln\left(\frac{\dot{\varepsilon}}{\dot{\varepsilon}_0}\right)\right]\left[1 - \left(\frac{T - T_0}{T_f - T_0}\right)^m\right]$$

A Yield stress
B Strain factor
C Strain rate factor
n Strain exponent
T_f Melting temperature
T_0 Ambient temperature
m Temperature exponent

However, the parameters of this constitutive model depend on the type of simulation and the experimental operating conditions used to assess them. As we were using severe plastic deformation and high strain rate process modeling, the following parameters were considered (Table 1).

Table 1. Material constants for the Johnson-Cook strain rate dependent yield stress [11]

A (MPa)	B (MPa)	C	n	$\dot{\varepsilon}$ (s^{-1})	T_f (K)
265	426	0.015	0.34	10^3	775

The tool was made of a tungsten carbide material, which had much greater hardness than our specimen (HV_{WC} = 2242 and $HV_{AA2024\text{-}T351}$ = 137). It could, therefore, be represented as a rigid body, which brought two main benefits. Firstly, rigid body modelling allowed the tool to be controlled by a single reference point. Then, strains of the tool were not assessed during analysis. All this helped to reduce calculation time drastically.

Like the constitutive model, contact between parts is another very critical criterion in numerical studies. This parameter governs the modeling of the surface interactions of helical burnishing. The contact model usually used is a Coulomb model [5, 13, 14]. Like Balland et al. [5], we used a master-slave contact algorithm where the friction was taken into account using a penalty method and a value of 0.2.

2.2 Meshing and Boundary Conditions

In order to obtain a suitable balance between results and calculation time, our models were meshed with different types of elements. In fact, it is important to have a very fine mesh near the domain of contact between parts. Thus, C3D8R elements of 0.02 mm dimensions were used in this area. The domain near the specimen edges was meshed with C3D8R elements of $0.12 \times 1.705 \times 1.75\ mm^3$. The intermediate domain was meshed with C3D4 elements to ensure the link between them (Fig. 3a). The specimens in the two 2D models were meshed with CPE4R elements. As the tool was modelled as rigid, there was no need to mesh it.

The part was embedded on the external edge. This condition allowed material flow along the z-axis. Symmetric conditions along the radial axis were applied on the edge where the tool and the part intersected each other at the beginning; the other edge was free. These boundary conditions were established in accordance with Mathurin's findings [15]. He showed that these conditions, although too restrictive, are more realistic than free edge conditions. However, these conditions impose the determination of a region where the results will be observed. Symmetric conditions along the axial axis were also applied on the top and bottom edges of the part. Figure 3b shows all these boundary conditions.

On the tool, we applied the following boundary conditions:

- V3 = 40 mm/min (Axial feed V_{fa})
- N_{orb} = 1000 rpm (Orbital velocity)
- VR3 = 40000 rpm and VR3 = 0 rpm (Spindle velocity N). Two velocity values were selected to study the impact on the results.

In order to reduce calculation time still further, we just simulated 3 passages of the tools at the surface middle plane.

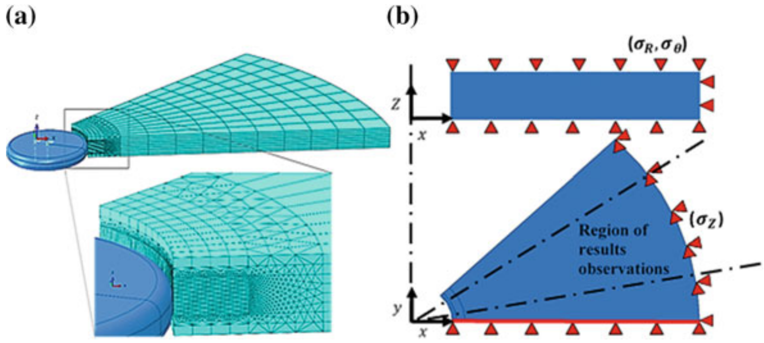

Fig. 3. Helical milling: mesh (**a**) and boundary conditions (**b**)

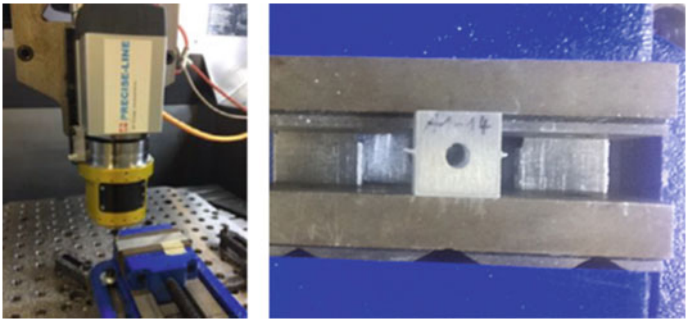

Fig. 4. ORBIBOT orbital drilling unit and specimen

3 Experimental Procedure

The experimental study was done with a CNC machine (DMG DMU85eVo) equipped with an ORBIBOT orbital drilling unit (Fig. 4). Before helical burnishing was executed on the aluminum alloy specimens, they were previously drilled with a 6.35 mm diameter hole. The burnishing depth was 10 µm and the operating conditions were V_{fa} = 40 mm/min, N = 40000 rpm, N_{orb} = 1000 rpm. The orbital rotation was clockwise and the process was conducted without lubrication. The CNC machine was also equipped with a Kistler 9257B measurement system (which measures helical burnishing forces). The software used for data acquisition and processing was WITIS.

4 Results and Discussion

Simulations were run on a computer having 32 GB RAM and an Intel® Xeon® CPU of 1.70 GHz (2 processors). The mean values of simulation calculation time are shown in Table 2.

Table 2. Time calculation for the different models

Model	3D	2D plane strain_1	2D plane strain_2
Calculation time	4 days 10 h 13 min	46 min 17 s	2 h 07 min 18 s

It can be seen that the three-dimensional models need several days while the two-dimensional ones only need a few hours. This could be very helpful regarding the study of different operating conditions (burnishing depth, spindle and orbital velocities, axial feed, etc.).

4.1 Comparison Between 2D and 3D Models

Figure 5 compares residual stresses obtained with our different models for a burnishing depth e = 40 µm and a spindle velocity N = 40000 rpm.

Despite the fact that the stress levels obtained with 3D and 2D models are quite different, the stress state profiles around the hole are nevertheless quite comparable. The differences in stress levels could be explained by the complex kinematics of the tool during orbital burnishing. The hypotheses of plane strains (especially the plane stress hypothesis in the first 2D model) cannot be used despite the fact that the dimensions of the parts are large. In fact, the axial component of the kinematics might not be negligible in comparison with the radial and orthoradial components. An axial speed decrease could reduce the axial force, thus bringing the predictions of these hypotheses closer to observations. Further modeling in this direction should provide more information.

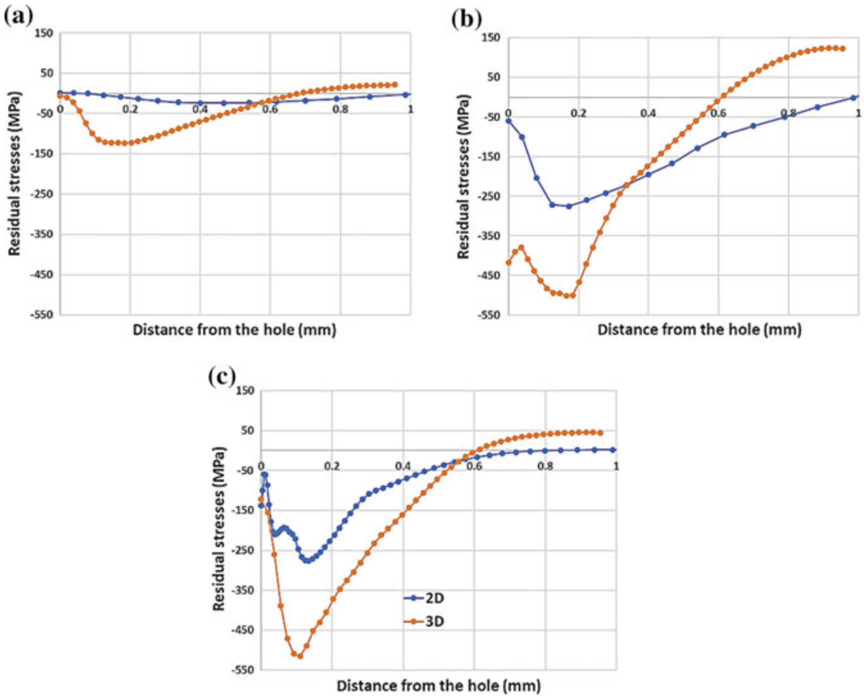

Fig. 5. Comparison of radial (**a**), orthoradial (**b**) and axial (**c**) residual stresses between 3D and 2D models for e = 40 µm and N = 40000 rpm

4.2 Impact of Operating Conditions

– Impact of burnishing depth

Figure 6 shows the residual stresses obtained for different burnishing depths for a spindle velocity N = 40000 rpm.

We observe that the levels of radial residual stresses increase with the burnishing depth. The conclusion seems to be the same for orthoradial and axial residual stresses. Moreover, the position of the compressive peak and the domain in compressive residual state also increase with the burnishing depth. This can be explained by the high strain rates generated with the increase of the burnishing depth: the greater the depth, the greater the pressure and the greater the strains. But the last observation needs to be investigate more thoroughly by refining the meshing of the part. In fact, the curve obtained for e = 40 µm appears to be more accurate (more defined points) because this model mesh was less coarse over a certain distance from the hole.

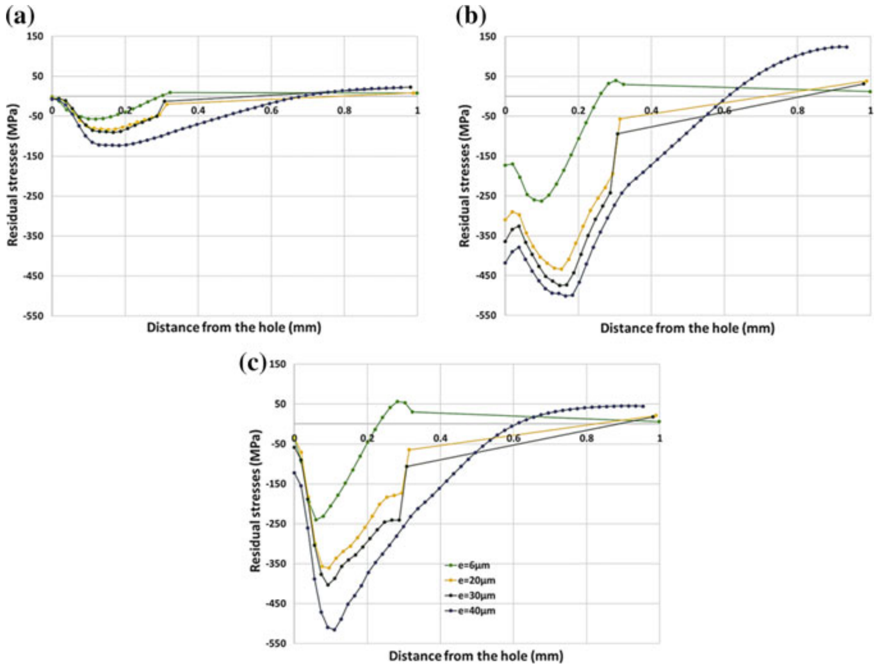

Fig. 6. Impact of burnishing depth on radial (**a**), orthoradial (**b**) and axial (**c**) residual stresses

– Impact of spindle speed

Figure 7 shows the highest compressive residual stresses for 2 spindle velocities (N = 0 rpm and N = 40000 rpm).

The spindle velocity suppression leads to a smaller residual stress, especially in the orthoradial and axial directions. This could be explained by the greater friction of the tool when the spindle velocity is zero (The tool slips intensively on the borehole). This hypothesis could be confirmed by using a kinetic instead of a static friction law in future models.

It would have been preferable to compare all these numerical results with the experimental ones in terms of residual stresses. However, because the residual stress assessment relies on techniques that are rather difficult to set up, we firstly investigated this comparison in terms of global data (burnishing forces).

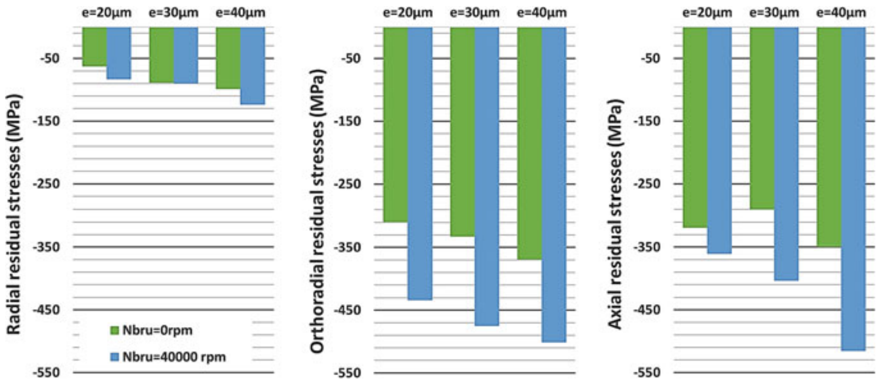

Fig. 7. Impact of spindle velocity on residual stresses

4.3 Burnishing Forces

Figure 8 shows the helical burnishing forces obtained numerically and experimentally (axial forces F_z and normalized transversal forces F_{xy}). Numerical forces are represented only on one tool pass because simulations were not done on the total hole height and circumference.

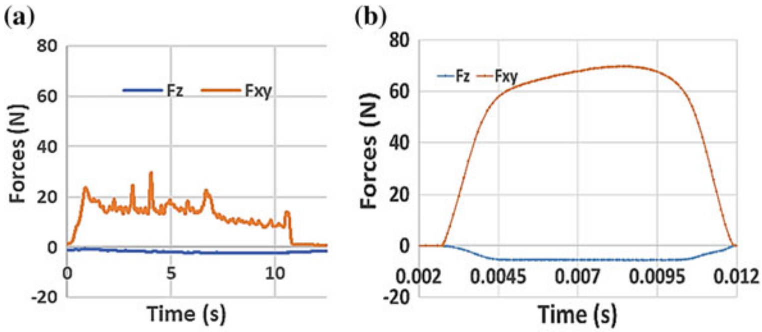

Fig. 8. Helical burnishing forces: experimental (**a**) and numerical (**b**)

We noted a slight overestimation of numerical forces (70 N vs. 25 N). In addition, a considerable amount of material was observed to adhere to the tool during experiments (Built Up Layer). Figure 9 presents the burnisher outlines before and after helical burnishing (height variation Z with position on the burnisher revolution axis l), obtained with an optical profilometer (Alicona InfiniteFocus SL). The Built-Up Layer indicates a large temperature increase and strong friction. This could explain the difference in the levels of forces between experiments and modeling. It would be interesting to refine thermal effects and define a more suitable friction model in future models.

Nevertheless, the experimental residual stress measurements remain the best way to correlate all our numerical results. This operation is planned.

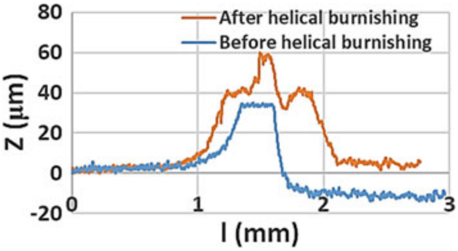

Fig. 9. Burnisher outlines before and after helical burnishing

5 Conclusion

We carried out a numerical study of the helical burnishing process on an AA2024-T351 aluminum alloy specimen. First of all, a comparison was made between two 2D plane strain models and a 3D model. This was done with a view to significantly reducing the calculation time of the simulations. The different geometries and assemblies of our model were implemented in ABAQUS™ software, then a Johnson-Cook constitutive model and a rigid body were used to represent the part and the tool, respectively. The contact model defined between these two parts was a Coulomb model with friction penalty $\mu = 0.2$. The results obtained showed that the 2D models were much more cost-effective than the 3D one (2 h against 4 days). But the levels of residual stresses acquired with the 2D models were lower than those obtained with 3D despite the fact that outlines were comparable. An axial feed reduction might be helpful in strong deformation strain hypotheses. In all cases, these results show that helical burnishing introduces compressive residual stresses into surface layers. We also noted that the operating conditions had a marked impact on the levels and depth of compressive residual stresses. The greater the burnishing depth was, the higher were the levels of compressive residual stresses and the greater were the depths they reached. However, numerical burnishing forces did not agree well with experiments: burnishing without lubrication exhibited thermal and tribological impacts which should be refined in modeling (material conductivity, specific heat, kinetic friction law). To obtain a more accurate contact model and thermal effects, tribological and temperature measurement experiments are planned. It will also be important to investigate the impact of other operating conditions (axial feed, direct or clockwise spindle rotation, etc.). Nevertheless, it is important to compare these numerical studies with experimental measurements of residual stresses obtained by helical burnishing, with a view to validating the models.

Acknowledgments. This work was carried out within the framework of the RODEO project, which received funding from the Clean Sky 2 Joint Undertaking under the European Union's Horizon 2020 research and innovation program, grant agreement No 738219.

The authors are grateful to all the project participants for their support: PRECISE France, MITIS Engineering, KUKA Systems Aerospace France.

References

1. Iyer R, Koshy P, Ng E (2007) Helical milling: an enabling technology for hard machining precision holes in AISI D2 tool steel. Int J Mach Tools Manuf 47(2):205–210
2. Olvera D, de Lacalle LNL, Urbikain G, Lamikiz A, Rodal P, Zamakona I (2012) Hole making using ball helical milling on titanium alloys. Mach Sci Technol 16(2):173–188
3. He G, Li H, Jiang Y, Qin X, Zhang X, Guan Y (2015) Helical milling of CFRP/Ti-6Al-4V stacks with varying machining parameters. Trans Tianjin Univ 21(1):56–63
4. Yen YC, Sartkulvanich P, Altan T (2005) Finite element Modeling of roller burnishing process. CIRP Ann 54(1):237–240
5. Balland P, Tabourot L, Degre F, Moreau V (2013) An investigation of the mechanics of roller burnishing through finite element simulation and experiments. Int J Mach Tools Manuf 65:29–36
6. Wagner L (1999) Mechanical surface treatments on titanium, aluminum and magnesium alloys. Mater Sci Eng, A 263(2):210–216
7. García-Granada AA, Gomez-Gras G, Jerez-Mesa R, Travieso-Rodriguez JA, Reyes G (2017) Ball-burnishing effect on deep residual stress on AISI 1038 and AA2017-T4. Mater Manuf Process 32(11):1279–1289
8. Balland P, Tabourot L, Degre F, Moreau V (2013) Mechanics of the burnishing process. Precis Eng 37(1):129–134
9. Delgado P, Cuesta II, Alegre JM, Díaz A (2016) State of the art of deep rolling. Precis Eng 46:1–10
10. Hassan AM, Al-Bsharat AS (1996) Improvements in some properties of non-ferrous metals by the application of the ball-burnishing process. J Mater Process Technol 59(3):250–256
11. Johnson GR, Cook WH (1983) A constitutive model and data for metals subjected to large strains, high strain rates and high temperatures. Scribd [Online]. Available: https://www.scribd.com/document/81848138/A-Constitutive-Model-and-Data-for-Metals. Accessed 29 Jan 2018
12. 'Verification of Johnson-cook Material Model Constants of Aa2024-t3 for Use in Finite Element Simulation of Friction Stir Welding and Its Utilization in Severe Plastic Deformation | Welding | Continuum Mechanics', *Scribd*. Available: https://www.scribd.com/document/236104784/Verification-of-Johnson-cook-Material-Model-Constants-of-Aa2024-t3-for-Use-in-Finite-Element-Simulation-of-Friction-Stir-Welding-and-Its-Utilization-i. Accessed 29 Jan 2018
13. List G (2004) Etude des mécanismes d'endommagement des outils carbure WC-Co par la caractérisation de l'interface outil copeau: application à l'usinage à sec de l'alliage d'aluminium aéronautique AA2024 T351. ENSAM, Paris
14. John MRS, Wilson AW, Bhardwaj AP, Abraham A, Vinayagam BK (2016) An investigation of ball burnishing process on CNC lathe using finite element analysis. Simul Model Pract Theory 62:88–101
15. Mathurin F (2008) Etude du processus de vissage par vis autoformeuse et élaboration d'une méthode de dimensionnement adaptée. Ph.D. thesis, University of Toulouse awarded by INSA

Topological Optimization of a Structural Naval Component Manufactured in FDM

A. Mancuso[1], G. Pitarresi[1], A. Saporito[1], and D. Tumino[2(✉)]

[1] Università degli Studi di Palermo, DIID, Viale delle Scienze, Palermo 90100, Italy
[2] Università degli Studi di Enna Kore, Cittadella Universitaria, 94100 Enna, Italy
davide.tumino@unikore.it

Abstract. In this paper, a topological optimization procedure has been applied on a real component of the deck of a sailing multi-hull in order to find the internal shape that best save the material used in the manufacturing process without a relevant loss of structural rigidity. The multi-hull boat is a 16 feet length catamaran equipped with an asymmetric foil on both centerboards and with a symmetric foil on both rudders. The task of the analyzed object is to act as a cylindrical support for the screw that drives the rotation of the centerboard. The process adopted to manufacture this object is the Fused Deposition Modeling (FDM) technique, because of its high versatility and its relative low-cost impact. The aim of this work is to verify the applicability of FDM to structural naval component subjected to demanding loads during navigation and, at the same time, to investigate on the robustness of a topology optimization strategy in creating new shapes that recent additive manufacturing are able to create.

Keywords: Topology optimization · CAD modeling · Fused deposition modeling

1 Introduction

Topology Optimization (TO) is a mathematical instrument used during the conceptual design stage and is aimed to reduce the weight of an object by changing the material distribution within a bounding box. This reduction of weight should be obtained with the same mechanical behavior of the component [1]. In association with CFD and FEM methods, shape optimization can be applied to different fields of industrial engineering such as nautical [2, 3] and automotive [4].

One of the most relevant problem of TO is the manufacturability of the components because of irregular boundaries or, sometimes, of non-manifold geometries. With the evolution of technology, such as the Additive Manufacturing (AM) processes, the manufacturability becomes a relatively marginal problem, improving the creativity of the designer and thus the possibility to explore a larger design space in a relative short time and with a reasonable cost [5]. For this reason TO and AM are usually employed together. In literature it is possible to find a wide number of works dealing with the

F. Cavas-Martínez et al. (Eds.): *Advances on Mechanics, Design Engineering and Manufacturing II*, LNME, pp. 451–462, 2019.
https://doi.org/10.1007/978-3-030-12346-8_44

influence of the filament deposition orientation. This is one of the most important aspect of the process because it influences the surface roughness, as studied in [6] where an original model is proposed to take into account of the staircase effect. Other aspects are influenced by the deposition strategy: in [7] the deposition layer and the building path are optimized in order to save time and material resources also considering the contour plurality and concavity as design variables. Effects of manufacturing on the overall final product quality and on costs are discussed in [8], while the Volumetric Error (VE) on a complex shape built with rapid prototyping technologies is studied in [9] starting from the calculation of the VE on geometric primitives. Some other objectives of the optimization building strategy are considered as the minimization of the required post-machining region (RPMR) [10] and of the overhang structures [11]. Another interesting parameter of AM technology is the influence of the tool-path on the final characteristics of the component [12]. Applicability of AM to biomechanical problems is a recent issue that involves several researchers, especially for orthopedic applications [13, 14].

It is common practice in AM components to have an infill structure made by a repetitive pattern. In [15] an analytical method is proposed to obtain the equivalent proprieties of the Representative Unit Cell (RUC). Despite of its novelty, AM is going to become a powerful instrument for a fast and cheap production, not only of aesthetical prototype but also for functional one. For instance, during oceanic regattas, many sailing yachts are equipped with a 3D printer for spare part manufacturing of small and low stressed components such as fan, fittings, etc.

In this work, TO is employed to investigate the behavior of a FDM functional proto-type subjected to relevant loads. For this purpose, an automatic procedure has been set up in ANSYS Workbench environment. Starting from the CAD of the object, a Finite Element model is generated and the TO runs according to a specified objective function. Two parameters have been considered as design variables; the infill density (25%, 35%, 50%) and the layer deposition (xy, yz, xz). A regular honeycomb structure has been considered as infill, whose mechanical characteristics can be evaluated by geometrical considerations.

2 CAD Model Setup

The case study is a component of the deck of a sailing multi-hull that has been designed and manufactured, as prototype version, taking into account of functional and ergonomic issues only. The multi-hull boat is a 16 feet length catamaran equipped with an asymmetric foil on both centerboards and with a symmetric foil on both rudders. The CAD model of the boat is shown in Fig. 1, where the right hull planking is intentionally hidden to exhibit the internal structures. The foil is fixed on each centerboard but its angle of attack can be slightly changed by a system on the deck that rotates the entire centerboard around the transversal axis of the boat. The rotation of the centerboard is obtained with the screw-pulley system in Fig. 2, left: a closed-circuit rope is wound on the pulley that, rotating, drives a screw along the longitudinal x axis of the boat; this movement is transferred to the head of the centerboard and allows its rotation along the transversal y axis of the boat. The screw needs two cylindrical bushes at its ends and, under typical conditions, is subjected to the longitudinal force along x caused by the hydraulic resistance of the foil.

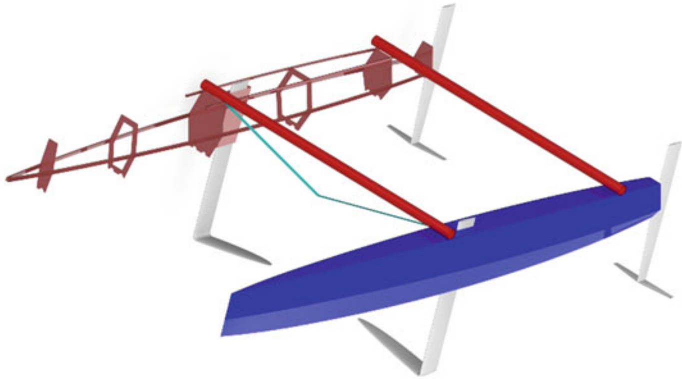

Fig. 1. CAD model of the multihull catamaran

The process adopted to manufacture the prototype is the Fused Deposition Modeling (FDM), because of its high versatility and its relative low-cost impact. The block has been 3D modelled in CREO and then printed in FDM with a 3D printer da Vinci 1.0A by XYZ Printing. The preliminar shape of Fig. 2 left comes from constraints due to the geometry of the trunk and the deck layout.

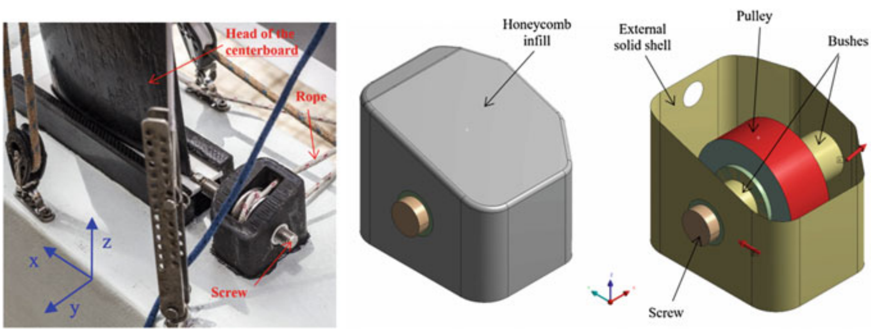

Fig. 2. A prototype of the 3D printed support mounted on the deck (left), the assembled CAD model (middle) and a view of the external ABS shell with the pulley, the screw and the bushes (right)

The object is printed with an ABS filament, considering an external 1 mm thick shell of solid ABS and an internal honeycomb infill. In Fig. 2 right the external ABS shell is shown, while the internal infill has been hidden to see the screw, the pulley and the two bushes. The printed block is assumed to be fixed at its lower base while the screw is subjected to an almost axial force along the positive x axis (caused mainly by the hydrodynamic resistance on the foil and by spurious minor transversal loads) and the pulley is loaded with a force along the *y* axis (caused by the rope). A torsional moment is also applied to the object by means of a couple of equal and opposite forces in the *y* direction applied on the bushes. Loads are then: P_{fx} = 5000 N, P_{fy} = 2500 N on the forward bush and P_{ay} = −2500 N on the aft bush. These values are the results of a work-in-progress experimental test activity that is focused on the strength of such a component. Nevertheless, details of this activity are not the sake of the present paper and for this reason they will be omitted.

An equivalent orthotropic elastic behavior [15] has been assigned to the honeycomb, coming from the Cartesian plane selected as deposition layer. With this approach, it is not necessary to model the geometry of the honeycomb but a continuous solid with an equivalent elastic behavior can be adopted. The unit cell of the equivalent material is $3l$ wide and $\sqrt{3}l$ high, see Fig. 3, left. Elastic characteristics of the homogenized material are functions of the bulk material and of the geometry of the honeycomb infill, in particular of the thickness of the filament *t* and the length of the honeycomb side *l*. If the axis 1 is the direction normal to the deposition plane of the printer and 2 and 3 are the axes shown in Fig. 3 left, the equivalent mechanical characteristics are expressed by the following formulae [15]:

$$E_1 = \frac{2}{\sqrt{3}}\frac{t}{l}E_s; E_2 = E_3 = \frac{4}{\sqrt{3}}\left(\frac{t}{l}\right)^3 E_s \tag{1}$$

$$G_{12} = G_{13} = \frac{1}{\sqrt{3}}\frac{t}{l}G_s; G_{23} = \frac{\sqrt{3}}{2}\left(\frac{t}{l}\right)^3 E_s \tag{2}$$

$$v_{12} = v_{13} = 0.15; v_{23} = 0.33 \tag{3}$$

Where E_s = 2700 MPa is the Young modulus of the bulk ABS.

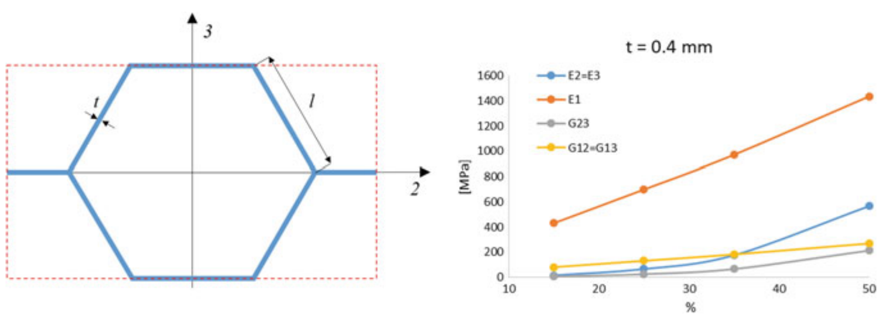

Fig. 3. The unit cell of the homogenized equivalent material (left) and the influence of infill density on its mechanical characteristics (right)

Assuming that the thickness *t* = 0,4 mm is a fixed characteristic of the printer nozzle, different values of the infill density can be obtained by changing the length *l* of the honeycomb side. All the over mentioned mechanical moduli increase with the infill density, as shown in Fig. 3, right.

3 Numerical Procedure

A numerical procedure has been setup in ANSYS Workbench environment, using CAD modeling, FEM and Topology Optimization modules, sharing each other the obtained results. The block scheme used in this study can be observed in Fig. 4. The initial bulk CAD is modelled and transferred to the FEM module, varying the deposition layer and the infill density. A preliminary Static Structural analysis is performed on each configuration and the results are used for the Topology Optimization module to modify the shape of the object. Finally, on the optimized volumes, a Static Structural analysis is carried out to verify the feasibility and the mechanical consistency of the results.

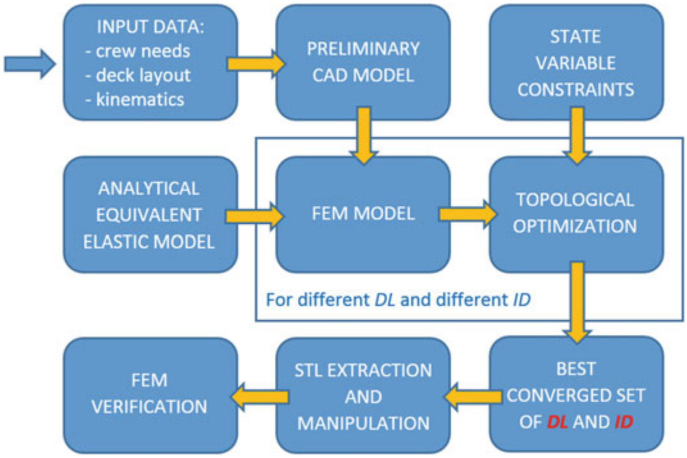

Fig. 4. Block scheme of the numerical procedure (*DL*: Deposition Layer; *ID*: Infill Density)

3.1 Static Structural Analysis

For the following simulations, three values of the infill density are considered: 25, 35 and 50%, following from these honeycomb edge length: 1.85, 1.33 and 0.9 mm respectively. Three different layers of deposition are assumed: *xy*, *yz* and *xz* (see Fig. 2 left) which are named as Dep_xy, Dep_yz and Dep_xz. According to Eqs. 1, 2 and 3, the resulting elastic moduli and Poisson coefficients are listed in Table 1.

For each configuration of the infill density and deposition layer, a Static Structural analysis has been performed in Ansys Workbench. The object has been meshed with regular hexagonal solid elements with a typical side of 2 mm. In Fig. 5, results are shown, as an example, in terms of equivalent Von-Mises stress distribution on the object with the 50% infill density and for the three deposition layer cases.

Table 1. Elastic moduli and poisson coefficient with different infill densities

Deposition	Dep_xy			Dep_yz			Dep_xz		
Infill density (%)	25	35	50	25	35	50	25	35	50
E_x (MPa)	65	176	568	699	972	1437	65	176	568
E_y (MPa)	65	176	568	65	176	568	699	972	1437
E_z (MPa)	699	972	1437	65	176	568	65	176	568
ν_{xy}	0.33	0.33	0.33	0.15	0.15	0.15	0.15	0.15	0.15
ν_{yz}	0.15	0.15	0.15	0.33	0.33	0.33	0.15	0.15	0.15
ν_{xz}	0.15	0.15	0.15	0.15	0.15	0.15	0.33	0.33	0.33
G_{xy} (MPa)	25	66	213	131	182	269	131	182	269
G_{yz} (MPa)	131	182	269	25	66	213	131	182	269
G_{xz} (MPa)	131	182	269	131	182	269	25	66	213

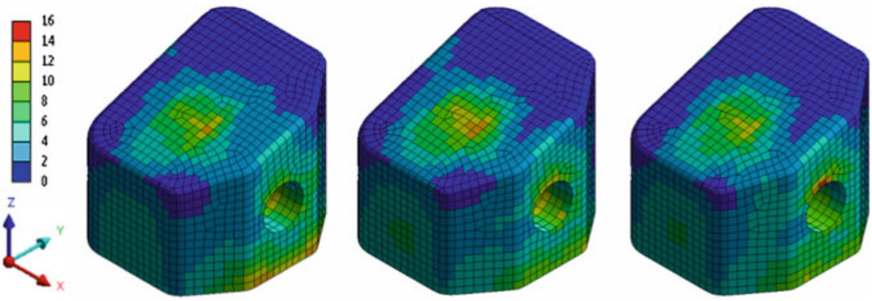

Fig. 5. Equivalent Von-Mises stress [MPa] distribution with 50% infill density: Dep_xy (left), Dep_yz (middle) and Dep_xz (right)

Furthermore, two parameters have been calculated to quantify the mechanical response of the object to the applied loads; these are the longitudinal rigidity K_L and the torsional rigidity K_T, calculated as follows:

$$K_L = \frac{P_{fx}}{d_{fx}}; K_T = \frac{P_{fy} \cdot b^2}{d_{fy} - d_{ay}} \tag{4}$$

where d_{fx} and d_{fy} are the displacement of the forward bush in the x and the y direction, d_{ay} is the displacement of the aft bush in the y direction and b is the distance between the centers of the forward and the aft bush. The stiffness values are shown in Fig. 6 as a function of the infill density and of the deposition layer. Looking at Fig. 6, left, it is observed that, at a fixed value of infill density, the longitudinal stiffness is maximum in the case of Dep_xy, then of Dep_yz and is minimum in the case Dep_xz. For a specific deposition layer, the longitudinal stiffness always increases with the infill density. The torsional stiffness is reported in Fig. 6, right, where the Dep_yz looks as the weakest among the three cases, for each value of the infill density. When the deposition layer is fixed, the torsional stiffness always increases with the infill density.

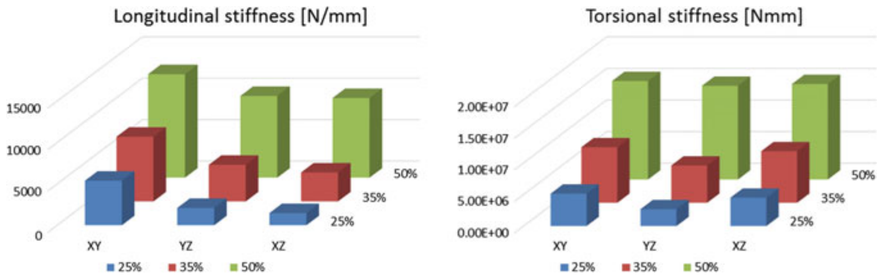

Fig. 6. Longitudinal stiffness (left) and Torsional stiffness (right) in function of infill density and deposition layer orientation

3.2 Topology Optimization Analysis

Once the solution of the Static Structural is obtained, a Topology Optimization module has been linked in order to reduce the total volume of the object and to maximize its rigidity. This tool works with an Evolutionary Structural Optimization (ESO) approach and uses a Solid Isotropic Material with Penalization (SIMP) method to delete the unstrained elements during the iterative process. ESO and SIMP are two of the most common topology optimization methods [16]. The optimization region is limited to the infill and the surfaces in contact with the bushes are excluded from the optimization process. The objective function of the procedure mixes, with equal weights, the minimization of the compliance and the minimization of the volume.

Some state variables have been constrained during the procedure in order to limit excessive longitudinal displacements and/or rotations of the screw when the loads are applied. A maximum displacement of 1 mm for d_{fx} and a maximum rotation of 1.5° (corresponding to a maximum of 0.3 mm for d_{fy} and −0.6 mm for d_{ay}) are assumed. In Fig. 7 the values that these state variables assume at the end of the optimization process are reported. It can be noted that only in the case Dep_xy the three state variables are within the limits for all the infill densities; in particular, as far as the density increases, the state variables decrease. In the other cases (Dep_yz and Dep_xz) only the infill at 50% fulfills the constrains to the state variables; for the infill density of 25 and 35%, at least one state variables exceeds the corresponding limit value.

In Table 2, final values of volume and mass of all the configurations are summarized. It must be remarked that values with the asterisk are obtained from unconverged analyses. For these results, the final volume is almost the same as the initial one, that is, the optimizer could not remove a relevant amount of unstrained elements because the global stiffness of the object was too low already in the bulk version.

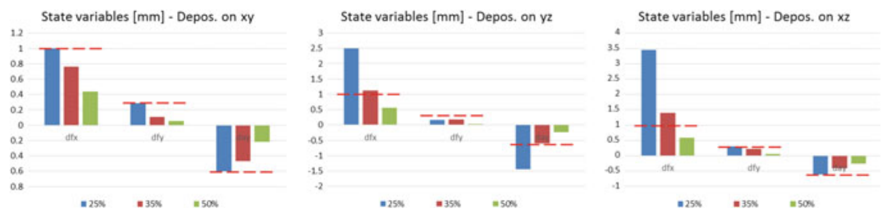

Fig. 7. State variables at the end of the optimization process

Table 2. Volume and mass as a function of different infill densities

Deposition	xy			yz			xz		
Infill density (%)	25	35	50	25	35	50	25	35	50
Final volume (%)	68.4	60.3	67	96.5*	99.5*	68.4	94*	95.7*	68.4
Final mass (g)	27.4	36.3	53.8	38.8*	60*	55	37.8*	57.7*	55
Initial mass (g)	40.1	60.2	80.3	40.1	60.2	80.3	40.1	60.2	80.3

It is interesting to compare the increment of the stiffness calculated after the topology optimization, related to the final mass of the object. A specific stiffness K' has been defined as:

$$K' = \frac{K}{mass}, \tag{5}$$

and its relative increment can be calculated as:

$$\Delta K'_L = 100 \frac{(K'_L)_{final} - (K'_L)_{initial}}{(K'_L)_{initial}} ; \Delta K'_T = 100 \frac{(K'_T)_{final} - (K'_T)_{initial}}{(K'_T)_{initial}} \tag{6}$$

This parameter quantifies the efficiency of the optimization process. In fact, an ESO process has to give inevitably a reduction of the absolute stiffness of the optimized object, if the optimized (eroded) structure is compared to the original (bulk) one, but the goal of the numerical procedure is to reduce as much as possible the volume of the structure without an excessive loss in rigidity. Under these conditions, a null variation of $\Delta K'$ means that the original and the optimized structure have the same stiffness associated to their mass while an increment of $\Delta K'$ proves that the optimization process has returned a more efficient configuration.

Figure 8, left shows that Dep_xy takes advantage of the optimization for all the infill densities simulated, with a $\Delta K'$ between the 35% and the 40% and a consistent $\Delta K'_T$ = 52% for the case of 50% of infill density. Figure 8, middle and right, on the contrary, show a different behavior, where Dep_yz has a decrease of $\Delta K'$ for the 25%

and the 35% infill densities, while Dep_xz has a small increase of $\Delta K'$ for the 25% of infill density, and a decrease of $\Delta K'_T$ equal to −13% for the 35% of infill density.

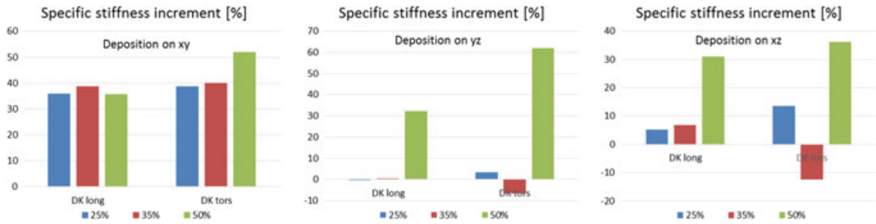

Fig. 8. Specific stiffness increment for Dep_xy (left), Dep_yz (middle) and Dep_xz (right)

Then, in Fig. 9, the optimized volumes have been reported for the infill density 35%. For this density, as well as for the 25%, only the Dep_xy reaches the convergence and a relevant number of element is removed (about the 40%, as reported in Table 2), as Fig. 9 left shows. The other two cases, in Fig. 9 middle and right, exhibit a marginal reduction in the number of element, that is, the initial bulk configurations were too flexible to fulfil the limits on the state variables.

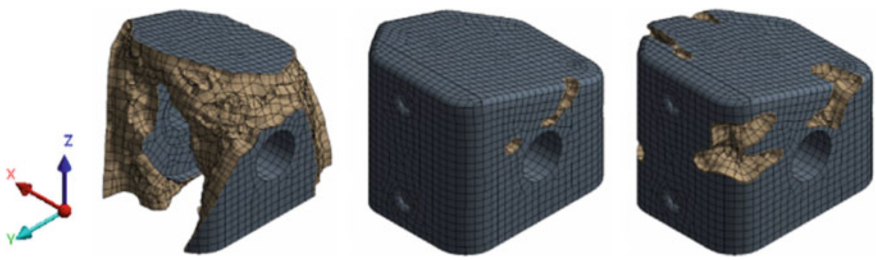

Fig. 9. The final shape of the optimized object for the 35% of infill density for Dep_xy (left), Dep_yz (middle) and Dep_xz (right)

It is worth noting, also, that the final volume obtained for the Dep_xy has a functional utility when the pulley has to be placed inside the support. In the preliminary version of the object shown in Fig. 2 left, the opening required to place the pulley is located at the top of the object, and the pulley is supposed to enter along the z direction. From a structural point of view, this empirical solution could lead to an excessive weakness of the object. The topology optimization, on the contrary, ensures that the solution in Fig. 9 left has an enhanced specific stiffness, fulfils the displacement limits and is compatible with the assembly issues.

3.3 Static Structural Verification

Last step of the present procedure is the final verification of the stress state in the optimized volumes subjected to the design loads. This analysis is limited to the Dep_xy case that, due to the above considerations, resulted the best among the three deposition configurations. To verify the optimized volume, an STL file is extracted, based on the mesh of the original bulk geometry. Some singularities appear on the surfaces where elements have been eroded (in brown in Fig. 9) because very small facets are created by the optimization module. To give a more regular aspect on these surfaces, a wrapping patch has been applied to the optimized STL, in order to obtain a regular tessellation, deleting spikes and small cavities. Von-Mises stress maps are given in Fig. 10 for different infill densities. Comparing Fig. 10 with Fig. 5 left, it can be observed that the optimized objects have a stress level very similar to the one calculated for the original object but in a smaller volume, sign of a more efficient stress distribution.

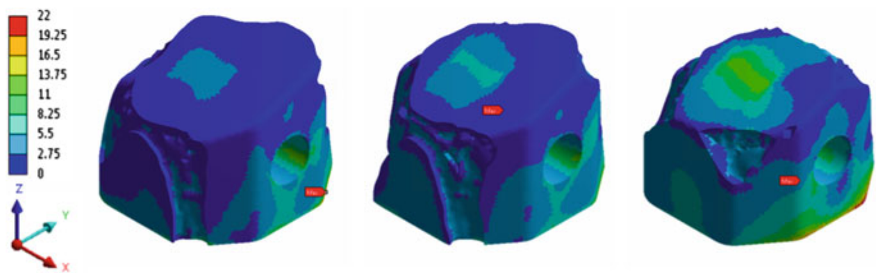

Fig. 10. Equivalent Von-Mises stress (MPa) maps on the optimized volume of Dep_xy for different infill density: 25% (left), 35% middle and 50% (right)

4 Conclusions

In this paper, an integrated numerical procedure has been setup involving CAD, FEM and Topology Optimization activities. This procedure is applied to a registry system mounted on the deck of a sailing catamaran and manufactured by means of FDM techniques. The study has revealed that the choice of the deposition layer plays a relevant role in the efficiency of an object printed in FDM especially when honeycomb structures are used to fill the internal volume. The topology optimization returned an enhanced shape of the analyzed object in terms of specific stiffness, function of the deposition layer and of the infill density. Moreover, shapes obtained at the end of the optimization process suggest different mounting procedures of the components inside the registry than the ones assumed in a preliminary prototype version.

Acknowledgments. This activity is the result of a research program named “The use of rapid prototyping techniques in yachting” where the University of Palermo and the University of Enna

Kore are involved in. The authors also wish to thank ANSYS Inc. and HBM Italia for their support in supplying software and hardware equipments. Finally, a special thank goes to the Zyz Sailing Team of Palermo that makes available the boat LED and its crew for the test at sea.

References

1. Rezaie R, Badrossamay M, Ghaie A, Moosavi H (2013) Topology optimization for fused deposition modeling process. In: Lauwers B, Kruth J-P (eds) The Seventeenth CIRP Conference on Electro Physical and Chemical Machining (ISEM), Procedia CIRP 6:521–526. https://doi.org/10.1016/j.procir.2013.03.098
2. Cirello A, Cucinotta F, Ingrassia T, Nigrelli V, Sfravara F (in press) Fluid-structure interaction of downwind sails: a new computational method. J Mar Sci Technol. https://doi.org/10.1007/s00773-018-0533-7
3. Mancuso A, Pitarresi G, Tumino D (in press) Using FEM simulation to predict structural performances of a sailing dinghy. Int J Interact Des Manufs
4. Cappello F, Ingrassia T, Mancuso A, Nigrelli V (2005) Methodical redesign of a semitrailer. WIT Trans Built Environ 80:359–369
5. Mirzendehdel AM, Rankouhi B, Suresh K (2018) Strength-based topology optimization for anisotropic parts. Addit Manuf 19:104–113. https://doi.org/10.1016/j.addma.2017.11.007
6. Di Angelo L, Di Stefano P, Marzola A (2017) Surface quality prediction in FDM additive manufacturing. Int J Adv Manuf Technol 93(9–12):3655–3662. https://doi.org/10.1007/s00170-017-0763-6
7. Ahsan AMMN, Habib MA, Khoda B (2015) Resource based process planning for additive manufacturing. Comput Aided Des 69:112–125. https://doi.org/10.1016/j.cad.2015.03.006
8. Thrimurthulu K, Pandey PM, Reddy NV (2004) Optimum part deposition orientation in fused deposition modeling. Mach Tools Manuf 44(6):585–594. https://doi.org/10.1016/j.ijmachtools.2003.12.004
9. Rattanawong W, Masood SH, Iovenitti P (2001) A volumetric approach to part-build orientations in rapid prototyping. J Mater Process Technol 119(1–3):348–353. https://doi.org/10.1016/S0924-0136(01)00924-4
10. Ahna D, Kimb H, Lee S (2007) Fabrication direction optimization to minimize post-machining in layer manufacturing. Int J Mach Tools Manuf 47(3):593–606. https://doi.org/10.1016/j.ijmachtools.2006.05.004
11. Zwier MP, Wits WW (2016) Design for additive manufacturing: automated build orientation selection and optimization. In: Alexopoulos A (ed) 5th CIRP Global Web Conference Research and Innovation for Future Production, Procedia CIRP 55:128–133. https://doi.org/10.1016/j.procir.2016.08.040
12. Ahsan N, Khoda B (2016) AM optimization framework for part and process attributes through geometric analysis. Addit Manuf 11:85–96. https://doi.org/10.1016/j.addma.2016.05.013
13. Mirulla AI, Bragonzoni L, Zaffagnini S, Bontempi M, Nigrelli V, Ingrassia T (in press) Virtual simulation of an osseointegrated trans-humeral prosthesis: A falling scenario. Injury. https://doi.org/10.1016/j.injury.2018.03.004
14. Ingrassia T, Nalbone L, Nigrelli V, Ricotta V, Pisciotta D (in press) Biomechanical analysis of the humeral tray positioning in reverse shoulder arthroplasty design. Int J Interact Des Manuf. https://doi.org/10.1007/s12008-017-0418-8

15. He X, Liao Y, Liang X (2013) Mechanical properties Analysis on honeycomb sandwich structure considering flexural rigidity of face sheets. Adv Mater Res 705:216–222. https://doi.org/10.4028/www.scientific.net/AMR.705.216
16. Da DC, Cui XY, Long K, Li GY (2017) Concurrent topological design of composite structures and the underlying multi-phase materials. Comput Struct 179:1–14. https://doi.org/10.1016/j.compstruc.2016.10.006

The Influence of Build Orientation on the Flatness Error in Artifact Produced by Direct Metal Laser Sintering (DMLS) Process

S. Rizzuti, L. De Napoli(✉), and S. Ventra

University of Calabria—DIMEG, Ponte Pietro Bucci 46/C, Arcavacata, 87036 Rende, CS, Italy
luigi.denapoli@unical.it

Abstract. Additive Manufacturing (AM) involves a set of production processes in which a layer-based material deposition approach to build parts is applied. These technologies are now extensively used in the industry in many cases as the main manufacturing process for making components with high shape complexity. The dimensional and geometric accuracy of the parts manufactured by means of AM are mostly determined by the specific type of additive process employed and the related process parameters. The part orientation in the build space is an important process parameter that has an influence on the stair-step effect and on the need of support structures and the subsequent post-processing refinements. In addition, the position of the part in the build volume may have an influence on the shape. These factors concur to the surface finish and to the dimensional and shape accuracy. In this paper, the flatness error on several surfaces, built on a test artefact ad hoc conceived, has been measured by means of a CMM-based setup in order to quantify the variation of the error in relation to: the orientation of the surfaces with respect to the platform, and the position of the part in the build volume of the AM machine. The test part has been produced by Direct Metal Laser Sintering (DMLS) process using the EOS Stainless Steel GP1. The test artifact has been designed with five flat surfaces at different angles with respect to the building platform. Two specimens were built in the same DMLS session with different position and alignment. The influence of the surface slope on the flatness error has been investigated. Flatness, 3D Roughness and orientation errors (parallelism, inclination, perpendicularity) have been measured and compared between both specimens.

Keywords: Flatness · 3D surface roughness · Additive manufacturing · Orientation error

1 Introduction

ASTM has defined additive manufacturing (AM) as "a process of joining materials to make objects from 3D model data, usually layer upon layer, as opposed to subtractive manufacturing methodologies. Synonyms: additive fabrication, additive processes,

F. Cavas-Martínez et al. (Eds.): *Advances on Mechanics, Design Engineering and Manufacturing II*, LNME, pp. 463–472, 2019.
https://doi.org/10.1007/978-3-030-12346-8_45

additive techniques, additive layer manufacturing, layer manufacturing, and freeform fabrication” [1].

Generally, AM includes a wide range of technologies that allow to translate virtual solid data into a physical part, usually in STL format, decomposing it into a series of finitely thick cross sections, which are fed into an AM machine that adds up material (that could be of various type, depending on the technology) layer by layer to fabricate the physical part [2]. Such kind of technology influences many aspects of the traditional manufacturing process and the relations among all stakeholders must be rearranged and updated [3]. One of the first approaches towards AM processes was essentially a powder deposition method using an energy beam, patented in the early seventies. Also following this approach, in the last decades, metallic additive manufacturing systems were among the most developed [4]. Metal-based AM processes, primarily laser-based powder bed fusion, are extremely interesting in sectors as aerospace, medical devices and defence, because of the significant lead-time reduction, weight reduction, part count reduction, high level of geometric complexity [5].

Since the metal additive manufacturing industry moves towards industrial production, the need for standardization of AM processes has been received by ISO and ASTM that decided to cooperate jointly in order to characterize all aspects of such technology [6, 7].

The accuracy of the process is generally investigated by measurements performed on test artefact ad hoc conceived. This allows to benchmarking among different AM machine or compare different configuration of process parameters [8–12].

In addition, design rules must be further pointed out in order to take into account the peculiarity of such technology during the conceiving of component shape. It is necessary to emphasize which functional surfaces must be reworked and which can be left as obtained by AM process.

The present work verifies and underlines the need for new guidelines in product design and new strategies in geometric control and verification.

In this context, the paper presents the results obtained in a survey conceived to investigate the assessment of the positioning in the build chamber in order to keep in control geometric features of a product. The test artefact was not conceived to assess the machine performances, nonetheless suggests some considerations about the AM process used.

2 Geometric Dimensioning and Tolerancing in Metal-Based Additive Manufacturing Process

GD&T is a language to communicate acceptable 3D variations of geometric elements in a part from design to manufacturing and inspection. Tolerance specification is the specification of the type and value of tolerances based on the GD&T standards (ISO 1101 [13] or ASME Y14.5 [14]). GD&T is based on mathematical representations of the variation of geometric elements and manufacturing knowledge bases. GD&T is also a way of specifying design intent to prevent misrepresentation during production processes. The final tolerance assignment to each geometric feature is a tradeoff between tight tolerances, which usually result in better performance of the assembly, and relaxed tolerances, which result in lower cost to manufacture the individual parts but also in a lower probability of proper assembly and/or function. In the last years, the continuous growing of AM technologies has introduced the need to rethink the procedures for synthesis and control of tolerances [15]. In the present paper we focus mostly on flatness tolerance [16, 17]. Further, searching for the relationship between the part build orientation and flatness error [18], some evidences are emerged on the measurement methodology and on the angularity specification with respect to the related datum.

3 Design of the Experiment. General Definition of Parameters

The test artefact has been produced by the Direct Metal Laser Sintering (DMLS) process using the EOS Stainless Steel GP1, a kind of steel characterized by having good corrosion resistance and mechanical properties, widely used in a variety of engineering applications. The test artifact has been fabricated with the following process parameters: 40 µm—layer thickness; 900 mm/s—scan speed; 0.1 mm—hatch spacing; 195 W—laser power; 54.2 J/mm^3—energy density. The printing settings are those suggested by the manufacturer with a little tuning on the basis of previous works. The influence of such parameters on an object made by AM is well illustrated in [19].

Two items of an artefact were built, putting their solid models orthogonal each other and positioned at two sides on the working table. The building volume was 150 × 64 × 40 mm^3 (see Fig. 1). The building time was of about 18 h.

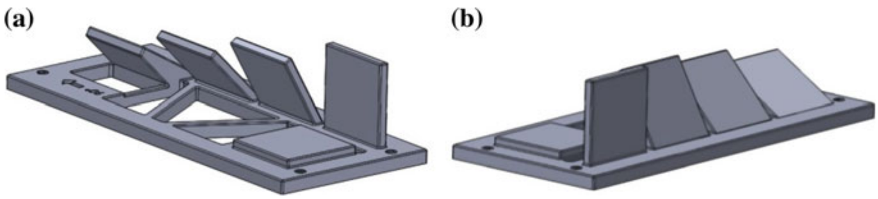

Fig. 1. Test artefact with five square elements: **a** left view; **b** right view

As post-building process, the specimen was finished using sand blasting. The artefacts were removed from the working bed and then the lower plane was milled to become the first datum for geometric metrology.

The test artefact was designed to assess the flatness of five surfaces oriented with respect the datum, in dependence to their position in the working volume. The planar elements have dimension 30 × 30 mm^2 and 3.5 mm of thickness. The elements are oriented at 0°, 30°, 45°, 60° and 90°. Generally hanging surfaces or with low angularity must be sustained by the introduction of support structures. In order to avoid inflection of the upper surface and avoid support structures, only the surface with angularity of 30° was sustained with an increasing thickness of the lower surface, towards the base. All other planar elements were built with uniform thickness. Further a set of lightening have been designed in order to reduce the effect of residual strength in the material during solidification of each layer, which tend to deform the final shape of the artefact.

In order to perform geometric measurements by means of CMM a sine bar has been designed to orient the 30°, 45°, 60° surfaces orthogonally to the tip probe. The auxiliary equipment was used to acquire the measurement by moving only one axis at a time of the CMM and not with continuously combined movements. Furthermore, the results presented below show that the use of this equipment did not introduce errors.

The artefacts were built by means of EOSINT M 280 with a working volume of 250 × 250 × 325 mm^3.

Figure 2 reports the picture of the build volume during AM session, in which can be seen both artefacts positioned along two sides of the working area, and one artefact ready to be measured.

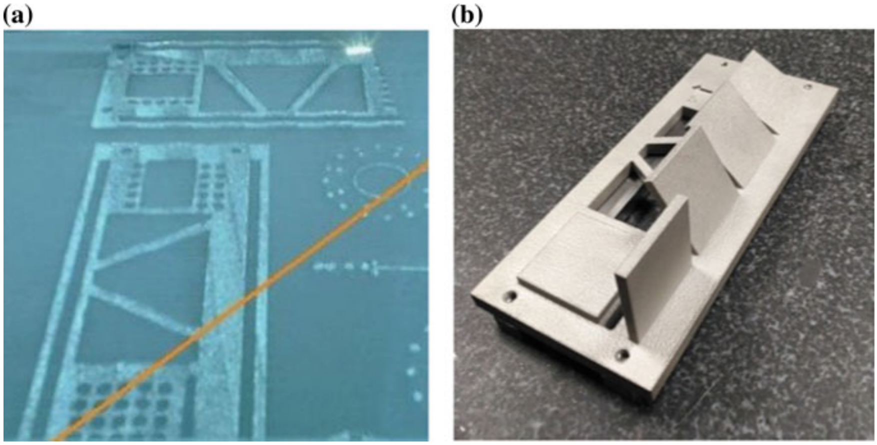

Fig. 2. **a** Both artefacts during production phase; **b** the artefact ready to be measured.

In order to check the geometric characteristics of the five planar elements, the artefacts were measured by the CMM ARES 10.7.5 of COORD3™. The touch-trigger probe PH10T of Renishaw™ was equipped with a stylus of 20 mm length and 4 mm diameter.

The first survey regarded the check if the position in the build volume induces different results. The first involved parameter has been the flatness of each square element. To this scope a pattern of 9 points, arranged as Union Jack grid (similar to the uniform rectangular) was used. Further, 13 repetitions were performed, changing the position of the pattern on the surface. Due to the nature of a surface obtained by AM, measure repetition and quantification of measure uncertainty is basic to validate AM machine performance.

A second survey, employing a pattern of 25 points, arranged as uniform rectangular grid, was used to emphasize the difference and similarity between both artefacts. In Fig. 3 both patterns of points are shown. Both extraction strategies are consistent with the ISO 12781-2011.

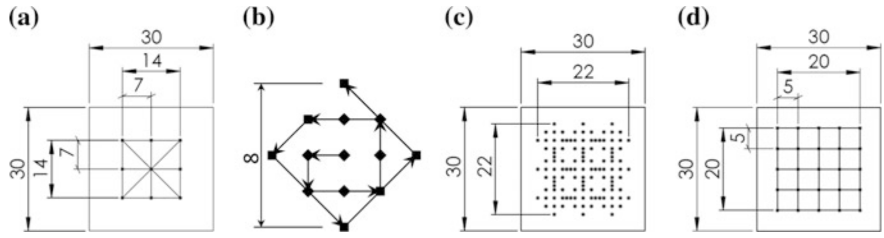

Fig. 3. **a** Union Jack pattern of 9 points for the first survey; **b** path of the Union Jack pattern origin; **c** position of all the 117 points acquired in the first survey; **d** Uniform rectangular pattern of 25 points for the second survey (Units in [mm]).

4 Results and Discussion

The measurements obtained by the first survey are presented in Fig. 4. The box plot graphs represent the statistics of the 13 repetitions, for each square element: the mean value, its variance, min and max value. As generally reported in literature, not all surfaces are suitable to be obtained by AM. Surfaces oriented with an angle lower than 40° need special attention in term of need of support elements. Also in this study, nevertheless the presence of a thicker structure, the surfaces of the square elements oriented at 30°, with respect to the datum, present a wide dispersion of measurements.

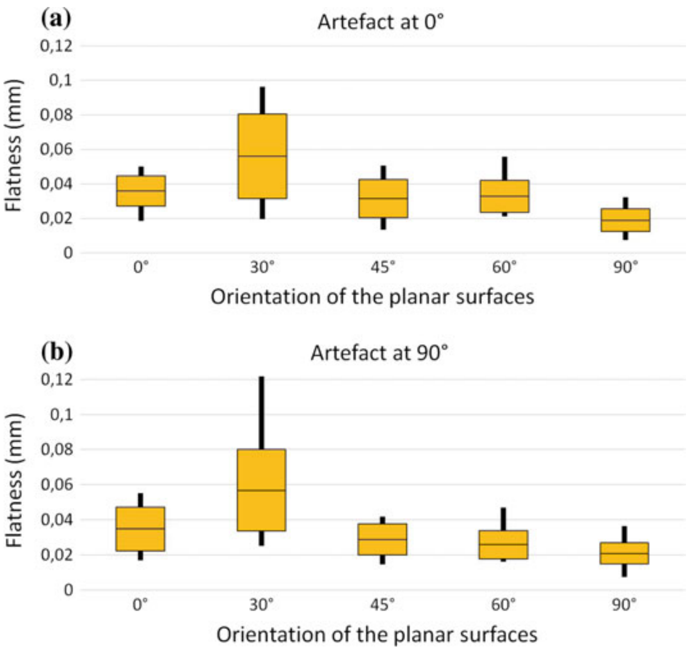

Fig. 4. Statistics of the flatness measurements: **a** relieved on the artefact oriented along the length (0°); **b** relieved on the artefact oriented along the width (90°).

On the other hand, the feature more interesting is the substantially equivalent behaviour if the squares with the same orientation are compared. This result is strictly related to the characteristic of the AM machine employed. The nature of the surface does not change if the position of the artefact changes in the AM working area.

The second survey emphasizes this similarity, comparing the natures of the surfaces corresponding to the same orientation. Figure 5 contains the interpolated surfaces obtained on the basis of the points detected on each square surface. The pattern of 25 point, reported in Fig. 3d have been used. The table is organized in two columns, comparing the surfaces put on the two artefacts positioned as described above. The five surfaces with different angularity with respect to the datum, represented by the lower plane surface of the artefact, are collected row by row.

The analysis of the surfaces takes into account three parameters: flatness, as defined in ISO 12781:2011; 3D Mean Surface Roughness - Sa, as defined in ISO 25178-2:2012 [20]; orientation tolerance, as defined both in ISO 1101:2017 or ASME Y14.5-2009. The first two parameters are computed with respect to the least square reference plane; the orientation tolerance are evaluated with respect to the datum.

It is necessary to point out the meaning of Sa and flatness in this context. Both Sa and flatness were measured by the CMM equipped with the stylus described above, on the basis of the 25 points pattern. Even if 25 points pattern is sufficient to assess flatness, this can be considered a rather coarse sample point for the computation of the 3D Mean Surface Roughness, that requires more measurement points.

Sa has been computed as

$$Sa = \frac{1}{NM} \sum_{i=1}^{N} \sum_{j=1}^{M} \left| w\left(u_i, v_j\right) \right|, \tag{1}$$

where u and v are the coordinates of the local reference system on the square element, and N = M.

Due to the nature of the surfaces obtained by AM, flatness seems not to be a parameter that completely can characterize them. This is mainly due to outliers that can be present in the domain. More attractive is the Sa parameter, being a mean value that smooths the outliers occurrence and allows to describe the behaviour of the surface, more globally. This allows to compare surfaces of the same type, built in different positions. Further Sa is straightforwardly related to the surface as a whole and its computation is not affected by the surface orientation with respect to the detection direction, as this happens with the Ra average roughness, not considered in the present analysis, because it is intrinsically associated to the detection direction.

As can be seen in the Fig. 5, Sa values of corresponding square surfaces are more similar than the associated flatness. For example, in the case of the square element with angularity of 30° Sa and flatness are really dissimilar: in the artefact oriented along the width (90°), the flatness reaches 0.1188 mm, more than double of the value obtained on the other artefact (0.0532 mm), probably due to some relevant peaks touched by the probe. On the other hand Sa values are comparable (0.0135 mm vs. 0.0152 mm).

Analysing more in deep Fig. 5, it can be seen that the global shapes of the interpolated surfaces of the square domains are really similar, considering both artefacts

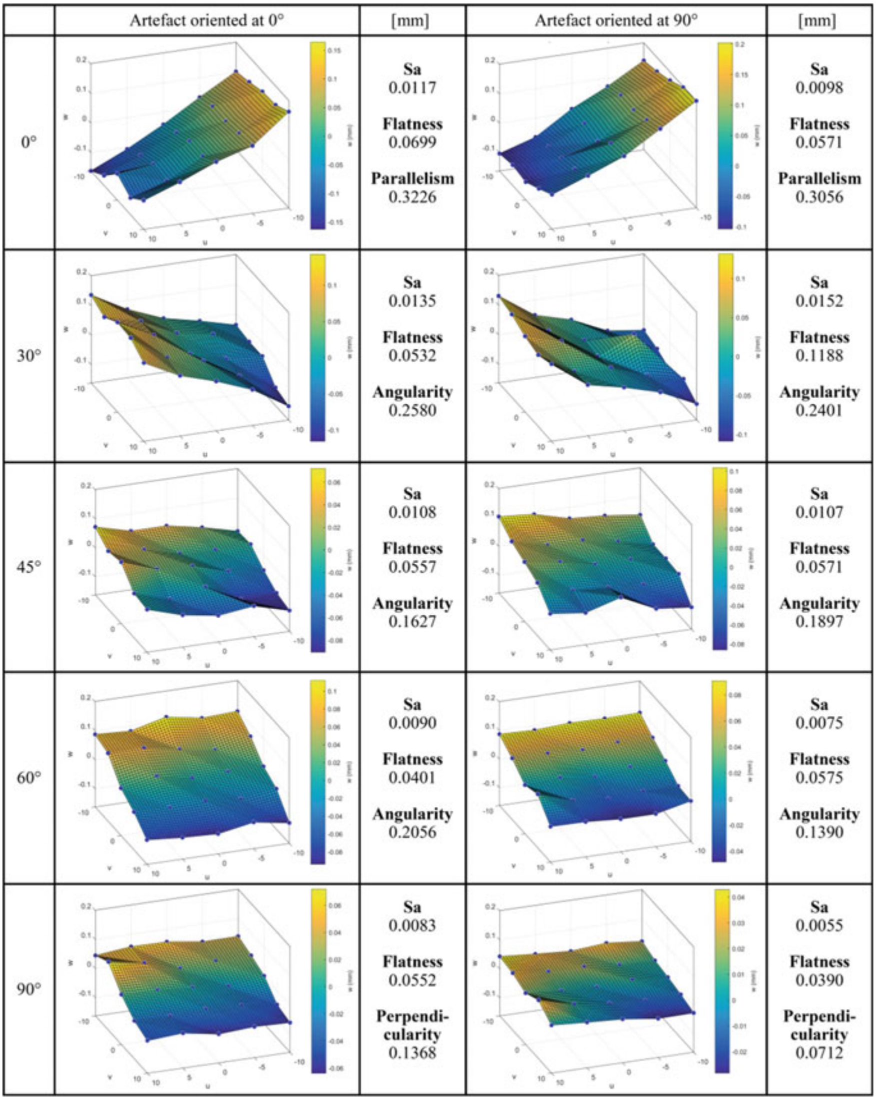

Fig. 5. Interpolated surfaces of the planar surfaces on the square domains relieved on both artefacts. Indication of Sa—3D mean surface roughness, flatness and orientation geometric tolerances.

orientation in the working area. Also the orientation tolerances are comparable. This suggest that the artefacts was not influenced by the position in the working area.

This comparison confirms how the AM machine employed and the DMLS method achieved a good level of accuracy. This consideration is valid from the technological point of view. Several issues concerning the design phase still remain open.

The nature of the geometric tolerances of orientation changes the point of view in the measurement of the geometric error, giving information on the relation between the surfaces and a datum. The geometric error of orientation is greater than Sa and flatness, of about one order of magnitude (two order of magnitude with respect some orientation tolerances).

The nature of a surface must be considered carefully not only in itself, but in relation with other surfaces, or datums, even in functional conceiving of shape, both its manufacturing process and its geometric verification.

The measurement of a geometric tolerance of orientation requires the identification of a datum, that typically coincides with the granite table of the CMM. Even in the manufacturing with AM a planar geometry may be associated to the printing tray.

If one thinks to the assembly of more components in a device, a tolerance chain must be identified as a sequence of geometric relations between features of individual parts. In this regard, the general orientation of a component in the building volume has great importance. In particular the surface that lies on the printing tray, since requires a milling operation, may be used as datum.

Taking into consideration the artefact proposed in the paper, choosing as first datum the surface lying on the working area, a special attention must be paid during manufacturing in order to reduce to a minimum the errors that can be introduced on it, mainly due to the cutting phase and milling operation, necessary to assure the first datum.

Furthermore, considering that both artefacts followed the same sequences of post machining and same positioning under the milling machine, it can be argued that the artefacts was not influenced by the position in the working area during AM process.

The amplitude of the geometric error is mainly due to the direction of detection of the width between the planes that define the tolerance range.

5 Conclusion

With respect to the results reported in the Figs. 4 and 5 some consideration confirm results present in literature. The best surfaces, either in term of Sa and flatness, and macro geometric error, are put at 90° with respect the working plane. In these specific artefacts, the working plane of the AM machine coincided with that one of the CMM.

In general, the objects built by AM process are created with the geometric relations among the surfaces, already detailed in phase of modelling. From the designer point of view, it is extremely important to enhance which are the datums with respect the geometric errors of orientation and position must be checked.

During the design phase of the solid model of a part that will be created by AM process, all the relations of dependency among the surfaces and the datums must be declared. This is essential in order to reduce to a minimum the need for further machining operation. Better if the surface put on the working plane is not functional, being not subjected to such kind of error. These consideration are more basic for laser-based powder bed fusion process, considering the possibility to employ the component made by AM “as is”, or reducing to a minimum the post processing phase.

Another final consideration can be dedicated to the geometric control of the planar surfaces obtained by DMLS process. The Sa, 3D mean surface roughness, is more appropriate with respect to flatness, avoiding to include outliers in the parameter computation. Furthermore, a strategy of measurement must be defined every time it is necessary to check all surfaces that have not to be re-machined.

In conclusion, designers are invited to identify and refine new and suitable design criteria and guidelines for Additive Manufacturing by DMLS.

Acknowledgments. The research work reported here was made possible by the financial support of DIMEG at University of Calabria.

References

1. ASTM F2792-12a (2015) Standard terminology for additive manufacturing technologies (Withdrawn 2015). ASTM International, West Conshohocken, PA, 2012, pp 1–3
2. Gao W, Zhang Y, Ramanujan D, Ramani K, Chen Y, Williams C, Wang C, Shin Y, Zhang S, Zavattieri P (2015) The status, challenges, and future of additive manufacturing in engineering. Comput Aided Des 69:65–89 (2015)
3. Huang Y, Leu MC, Mazumder J, Donmez A (2015) Additive manufacturing: current state, future potential, gaps and needs, and recommendations. ASME J Manuf Sci Eng 137 (1):014001–014001-10. https://doi.org/10.1115/1.4028725
4. Frazier WE (2014) Metal additive manufacturing: a review. J Mater Eng Perform 23 (6):1917–1928
5. Shellabear M, Nyrhilä O (2004) DMLS-Development history and state of the art. In: Proceedings of the 4th LANE, 2004 Sep 21–24, Erlangen, Germany. Meisenbach-Verlag, Bamberg (2004)
6. Monzon MD, Ortega Z, Martinez A, Ortega F (2015) Standardization in additive manufacturing: activities carried out by international organizations and projects. Int J Adv Manuf Technol 76(5–8):1111–1121
7. Seifi M, Gorelik M, Waller J, Hrabe N, Shamsaei N, Daniewicz S, Lewandowski JJ (2017) Progress towards metal additive manufacturing standardization to support qualification and certification. JOM 69(3):439–455
8. Moylan S, Slotwinski J, Cooke A, Jurrens K, Donmez MA (2014) An additive manufacturing test artifact. J Res Natl Inst Stan 119:429–459
9. Moylan S, Cooke A, Jurrens K, Slotwinski J, Donmez MA (2012) A review of test artifacts for additive manufacturing. Report No. NISTIR, 7858, National Institute of Standards and Technology (NIST), Gaithersburg, MD
10. Moylan S (2015) Progress toward standardized additive manufacturing test artifacts. In: Achieving precision tolerances in additive manufacturing, ASPE 2015 Spring Topical Meeting. ASPE, North Carolina State University, Raleigh, NC (2015)
11. Rebaioli L, Fassi I (2017) A review on benchmark artifacts for evaluating the geometrical performance of additive manufacturing processes. Int J Adv Manuf Technol 93(5–8):2571–2598
12. Berger A, Sharon Y, Ashkenazi D, Stern A (2016) Test artefact for additive manufacturing technology: FDM and SLM preliminary results. In: The Annals of "Dunarea de Jos" University of Galati. Fascicle XII: welding equipment and technology, Galati, vol 2729-37
13. ISO 1101:2017 (2017) Geometrical product specifications (GPS)—geometrical tolerancing —tolerances of form, orientation, location and run-out, ISO, Geneva, Switzerland

14. ASME Y14.5-2009 (2009) Dimensioning and tolerancing. ASME, New York
15. Ameta G, Lipman R, Moylan S, Witherell P (2015) Investigating the role of geometric dimensioning and tolerancing in additive manufacturing. J Mech Des 137:111401–111410
16. ISO 12781-1:2011 (2011) Geometrical product specifications (GPS)—Flatness—Part 1: Vocabulary and parameters of flatness, ISO, Geneva, Switzerland
17. ISO 12781-2:2011 (2011) Geometrical product specifications (GPS)—Flatness—Part 2: Specification operators, ISO, Geneva, Switzerland
18. Das P, Mhapsekar K, Chowdhury S, Samant R, Anand S (2017) Selection of build orientation for optimal support structures and minimum part errors in additive manufacturing. Comput Aided Des Appl 14:1–13. https://doi.org/10.1080/16864360.2017.1308074
19. Yap CY, Chua CK, Dong ZL, Liu ZH, Zhang DQ, Loh LE, Sing SL (2015) Review of selective laser melting: materials and applications. Appl Phys Rev 2(4), art. no. 041101
20. ISO 25178-2:2012 (2012) Geometrical product specifications (GPS)—Surface texture: areal —Part 2: Terms, definitions and surface texture parameters, ISO, Geneva, Switzerland

New Customized Elbow Orthosis Made by Additive Manufacturing

R. I. Campbell[1], T. Ingrassia[2(✉)], V. Nigrelli[2], and V. Ricotta[2]

[1] Loughborough Design School, Loughborough University, Loughborough LE11 3TU, UK
[2] Dipartimento di Ingegneria, Università degli Studi di Palermo, Viale delle Scienze, building 8, 90128 Palermo, Italy
tommaso.ingrassia@unipa.it

Abstract. Orthoses are additional devices that help people with disabilities. The focus of this work is the design and manufacture of a new customized elbow orthosis completely made by Additive Manufacturing (AM). One of the innovative characteristic of the device is the use of torsion springs that simulate the action of physiotherapists during exercises for patient rehabilitation. Parametric modeling approach based on generative algorithms was used to design the device. Finally, FEM analyses have been performed to validate the design.

Keywords: Additive manufacturing · 3D acquisition · Computer aided engineering

1 Introduction

Orthoses are external medical devices used in orthopedics in the treatment of some pathologies to correct a functional anomaly, but which don't replace missing ana-tomic parts. These devices limit the relative movements in a joint affected, for example, by trauma, arthrosis, ligament sprains or that has been subjected to surgery. For patients with disabilities that induce functional limitations, orthoses are employed to apply forces on the body for biomechanical needs by helping patients during walking and limb movement.

Orthoses can be prefabricated or customized. The prefabricated ones are less expensive and readily available on the market. Customized orthoses, instead, are better adapted to the patient's body than the prefabricated devices and ensure better performances [1, 2].

The fundamental aspects in the design of customized orthoses are functionality, ergonomics and aesthetics. Designing an orthosis by combining all three of these aspects means being able to make a prosthetic device that fully meets the needs of patients. Additive Manufacturing (AM) is a suitable technology to make customized orthoses, especially for its ability to realize complex shapes in a short time and with lower costs than manual fabrication [3–7]. Most of the orthoses on the market are prefabricated devices that can be adapted to different sizes by means of appropriate bands or other methods. Most of the commercial orthoses are only partially realized

F. Cavas-Martínez et al. (Eds.): *Advances on Mechanics, Design Engineering and Manufacturing II*, LNME, pp. 473–483, 2019.
https://doi.org/10.1007/978-3-030-12346-8_46

with AM technologies and then assembled to constitute the final device, with a consequent increase in production phases and costs depending on the particular orthosis to be made.

In the literature there are different works about wrist orthoses [8], foot orthoses [9] and hip orthoses [10], but there is not much information about the customized elbow orthosis completely manufactured using techniques of AM.

For this reason, this work focuses on the study of an elbow orthosis.

The aim of this work is the design of a new customized elbow orthosis completely manufacturable by AM and the implementation of generative algorithms for parametric modeling and creation of 3D patterns to be adapted to the CAD model.

The present work has been divided into four main steps. The first step consists of the 3D acquisition process and then the realization of the CAD model of the arm of a patient. In the second step, the CAD modeling of the customized orthosis has been performed. During this step, generative algorithms have been developed for the realization of a Voronoi tessellation and for the creation of patterns with different modules in order to better customize the device. In the third step, the prototype of the orthosis has been realized using AM techniques. In particular, the Selective Laser Sintering (SLS) process with PA 2200 material has been used. Finally, results obtained by the FEM analyses performed during the last step were used to validate the design.

2 New Model of Elbow Orthosis

The basic idea of this work is to design of a new customized elbow orthosis manufactured entirely by AM technology, able to help patients during the rehabilitation phase.

One of the fundamental exercises during the rehabilitation of the patient is the execution of flexion and extension movements of the forearm (Fig. 1) that help to slowly return to the full functionality and mobility of the arm. Starting from the neutral position (angle between arm and forearm of 90°) during the flexion and extension movements the physiotherapist opposes resistance. After, to return to the neutral position, the patient is eased by the physiotherapist.

In order to simulate this rehabilitation exercise, with no support of physiotherapists, it was decided to apply two torsion springs to the orthosis that oppose resistance during the flexion and extension movements and help the patient to move the arm until to reach the neutral position. In this way the patient can carry out itself the rehabilitation exercise.

The spring have been chosen taking into account that the patient, during the rehabilitation phase, should not lift weights more than 5 kg.

2.1 3D Acquisition and CAD Modeling of the Arm

In order to model correctly the shape of the patient's arm, and in particular the elbow area, it was decided to reproduce a copy of it using a plaster cast.

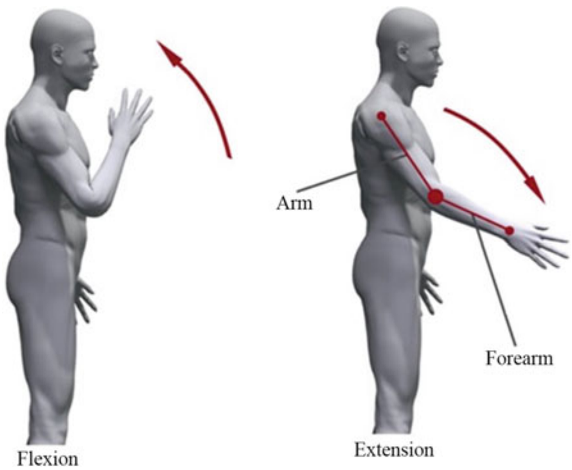

Fig. 1. Flexion and extension movements of the forearm

A direct acquisition of the patient's arm, in fact, could lead to a poor model or require very complex post-process phases due to the impossibility of keeping the patient's arm perfectly fixed during the whole scanning phase.

To avoid these drawbacks, a plaster cast of the patient's arm has been made. Once the cast has been made, it was acquired using a 3D scanner, the ZScanner 800 by ZCorporation.

This scanner has been chosen for its main features: the self-orienting and the possibility of moving the object during the scan. Thanks to the self-orienting feature, the scan system does not need a fixed position tripods, voluminous mechanical arms or external positioning devices, which make the acquisition of some hidden surfaces difficult or almost impossible.

These characteristics have facilitated greatly the acquisition and post-processing phase, reducing the time required to obtain the digital model of the arm.

The model obtained from the scan is only the part related to the elbow area. In order to model the remaining part of arm, a series of measurements of some sections of the arm have been made at different positions. Subsequently, it has been possible reconstructed the entire model of the arm by means of a loft function (Fig. 2).

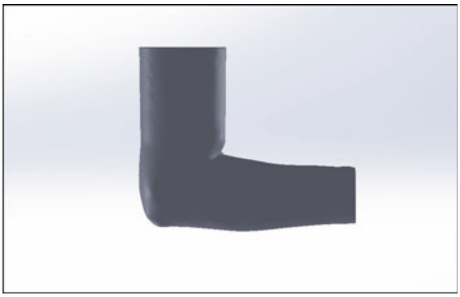

Fig. 2. CAD Model of the arm surface

3 CAD Modeling of the Orthosis

Customized orthoses, besides to adapt better to the patient, also allow optimizing their stiffness and flexibility to inhibit some movements and to integrate new morphological characteristics.

The modeling of a customized orthosis starts from the CAD model of the patient's arm. To ensure a good level of ergonomics, the orthosis should be perfectly adapted to the arm. However, it is also necessary to consider the presence of swelling of the patient's elbow and ensuring that the orthosis does not compress excessively, in order to avoid tissue inflammation or other undesired effects.

Regarding the functionality, one of the aspects to be taken into consideration is the possibility for the patient to wear and remove the orthosis easily and independently, with no discomfort at the elbow.

In order to meet the aforementioned ergonomics and wearability requirements, starting from the reconstructed surface of the arm, a 2 mm offset has been applied, ensuring a small clearance between the arm and the orthosis; moreover, two openings have been made, so to allow both to wear the orthosis without problems and to increase the adaptability.

To ensure a suitable stiffness of the orthosis, but at the same time don't add weigh to the entire device, preliminary, a thickness of 4 mm of the structure has been chosen. This value of thickness is usually adopted in commercial orthoses.

The next step was the conversion of the model into NURBS surfaces and then into a CAD model.

The relative rotation between the arm and forearm during the extension and flexion movements is ensured by a hinged mechanism.

Obtained the basic CAD model of the orthosis, all the components have been modelled and assembled into the final CAD model of the orthosis by SolidWorks software (Fig. 3).

Fig. 3. CAD model of the elbow orthosis

3.1 Generative Algorithms

Generative algorithms allow finding solutions to problems that can be encountered with the classic CAD systems when complex shapes, especially when these would be realized using AM techniques [12–16], must be modelled.

In this work, generative algorithms have been implemented for the modeling of non-structural parts of the orthosis that, in addition to lightening the structure, must make the orthosis pleasant from an aesthetic point of view.

Two different algorithms have been developed with Grasshopper [17, 18]; the first allows the creation of patterns on complex surfaces, the latter allows to realizing a Voronoi tessellation.

3.1.1 Generative Algorithm for Creating Patterns

The developed algorithm allows users to create patterns on complex surfaces, so customizing the orthosis with different decorative geometries.

The basic function generates different parallelepipeds on the surface, used as target objects, and maps on these the geometry to repeat.

The target parallelepipeds have been generated to morph the component using the "Surface Box" function [17], adapting them to a surface based on the interval indicated by the surface domain and the height of the parallelepiped.

The final result is the pattern created on the surface that is perfectly adapted to it and that follows its morphology on a regular basis.

Figure 4 shows the block diagram of the developed algorithm.

It is possible to modify the number of elements along the parameterization directions (U and V) and also to change the basic geometry.

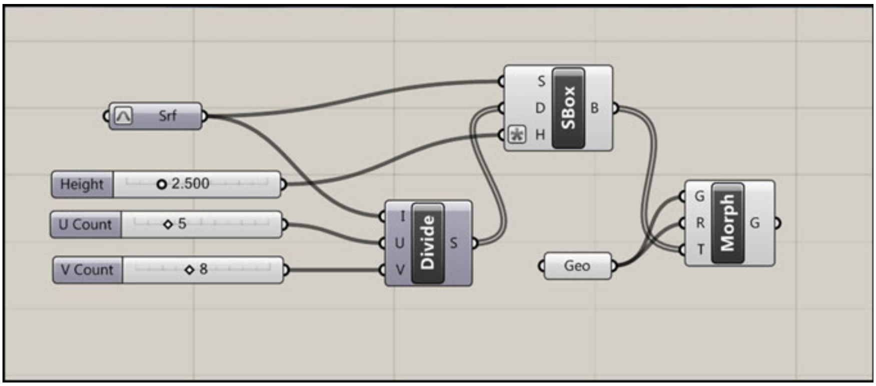

Fig. 4. Block diagram of the implemented generative algorithm

In Fig. 5 basic component to repeat (left) and pattern created with generative algorithm are shown.

In Fig. 6 some examples of patterns created with this algorithm and applied to the elbow orthosis are shown.

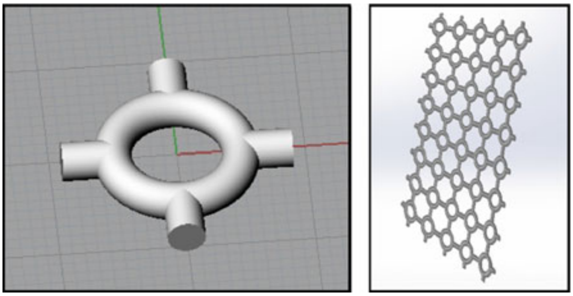

Fig. 5. Example of basic component to repeat (left) and pattern created with generative algorithm

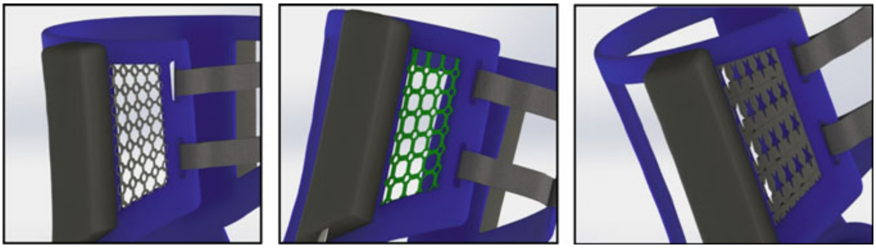

Fig. 6. Examples of patterns that can be created and applied to the orthosis

3.1.2 Voronoi Tessellation by Generative Algorithm

Because not all the commercial software allow managing independently the input parameters for the creation of Voronoi tessellations, a generative algorithm has been developed to manage these parameters (such as number of points, width of each polygon of the tessellation, etc.) and to model, parametrically, a Voronoi structure in the custom orthosis.

The Voronoi tessellation is initially created on a surface in a plane and is subsequently mapped onto the surface of the orthosis. After, with specific functions, the mesh is generated and exported.

The block diagram of the generative algorithm developed in Grasshopper for the realization of the Voronoi tessellation to be applied for the customization of the elbow orthosis is shown in Fig. 7.

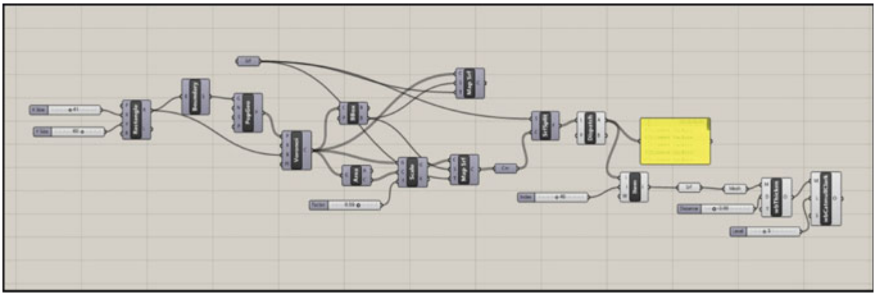

Fig. 7. Block diagram of the implemented generative algorithm for Voronoi tessellation

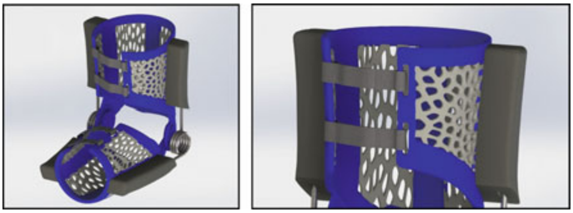

Fig. 8. CAD model of the elbow orthosis with Voronoi tessellation

The creation of the Voronoi tessellation starts from a set of points that represent the centre of the polygons of the tessellation; after, through the Voronoi function, a two-dimensional Voronoi tessellation has been created according to the set of points.

This structure is mapped onto the surface of the orthosis through the "Map to Surface" function [17], adapting itself to the morphology of the surface.

The last step of the algorithm is the creation of mesh and the smoothing of the structure so to eliminate the sharp edges.

In Fig. 8 the complete CAD model of the orthosis with the Voronoi tessellation is shown.

4 Prototype Realization by Additive Manufacturing

The designed elbow orthosis has been produced in PA 2200 by a SLS (Selective Laser Sintering) 3D printer. As case study, only the model of the orthosis with the Voronoi tessellation has been realized.

PA 2200 is a fine white powder based on polyamide, used for the manufacture of fully functional pieces with high surface quality and exposed to high thermal or mechanical stresses [11].

The EOS FORMIGA P100 printer (Fig. 9) has been used, which allows the production of small series and customized products with fully functional complex geometry.

Fig. 9. FORMIGA P100 3D printer

Figures 10 and 11 show some images of the prototype from which is possible to see the good surface finish obtained with this AM technology.

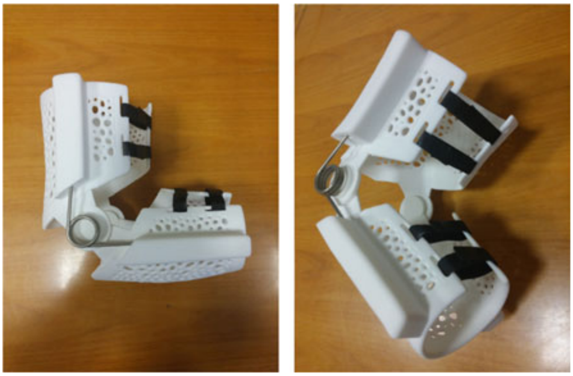

Fig. 10. Final prototype

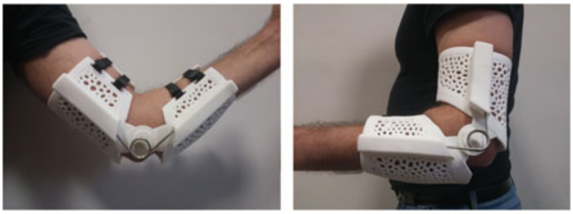

Fig. 11. Final prototype put on by patient

5 FEM Analysis

FEM analyses have been performed to verify the structural strength of the prototype [19].

Only the structural parts of the orthosis have been analysed.

The arm has been considered as a rigid body. The area near the elbow has been not considered to simplify the FEM model, always ensuring the reliability of the results.

The simulations have been performed to verify the stress state of the orthosis during flexion and extension, applying a test load of 150 N.

Although the maximum load in normal conditions of use of an elbow orthosis should be less than 50 N, a much higher test load (150 N) was chosen to test the model in very hard working conditions.

The model has been meshed with about 2,000,000 Solid 164 elements [20]. Successively the boundary conditions have been set. In particular, a frictional contact has been imposed at the orthosis and arm interface, a frictionless contact, instead, has been imposed at the torsion springs and the supports interfaces. Finally, a fixed constraint has been applied to the faces of the arm (in the upper part) which prevents them from moving or deforming. The strips have been modelled as spring elements.

Table 1. Mechanical properties of PA 2200

	Tensile strength (MPa)	Elongation at break (%)	Tensile modulus (MPa)
PA 2200	48	24	1700

Extension

Figure 12 shows Von Mises stress maps.

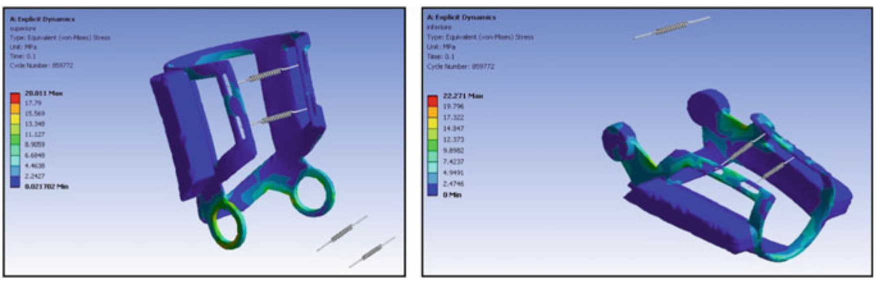

Fig. 12. Maps: Von Mises stress

It can be observed that all the maximum values of the deformation and strains are lower than the corresponding limit values (Table 1). In particular, the maximum value of the Von Mises stress is 22.27 MPa, less than half of the tensile strength of the material (48 MPa).

Flexion

Figure 13 shows Von Mises stress maps.

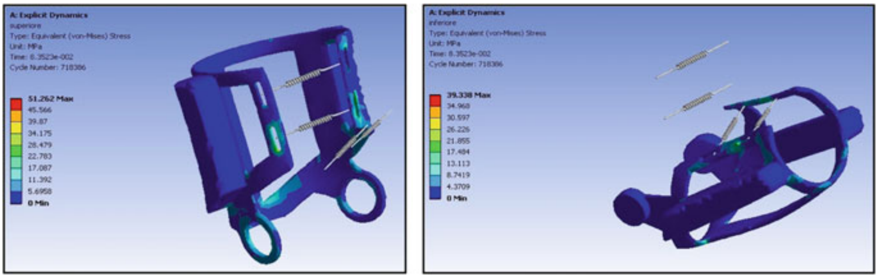

Fig. 13. Maps: Von Mises stress

Also in this case, it can be observed that all the maximum values of the deformation and strains are lower than the corresponding limit values. In particular, a maximum elongation value of 2.1% and a maximum value of the Von Mises equivalent stress of 41 MPa have been obtained.

6 Conclusions

In the work a method has been perfected for the design of a custom elbow orthosis entirely manufacturable by additive techniques. To this aim, generative algorithms for parametric modeling and creation of 3D patterns have been also developed that can solve some of typical problems of modeling for Additive Manufacturing.

The first step of the work was related to the modeling, by means of reverse engineering techniques, of the arm of a patient and the subsequent CAD modeling of the structure of the custom elbow orthosis.

Subsequently, to improve the aesthetic appearance of the orthosis, two algorithms have been implemented for the creation of 3D patterns and Voronoi tessellations for not structural parts.

Generative algorithms developed have been tested and proved to be robust, efficient and able to overcome some drawbacks of commercial software.

Subsequently, a prototype of the elbow orthosis with Voronoi tessellation has been realized by means of the SLS technology.

In the last part FEM analyses have been carried out considering the movements of flexion and extension of the arm and obtained results were used to validate the design.

References

1. Javaid M, Haleem A (2017) Additive manufacturing applications in medical cases: a review literature based. Alexandria J Med
2. Singh Sunpreet, Ramakrishna Seeram (2017) Biomedical applications of additive manufacturing: present and future. Curr Opin Biomed Eng 2:105–115
3. Chen RK, Jin Y, Wensman J, Shih A (2016) Additive manufacturing of custom orthoses and prostheses—a review. Addit Manuf 12:77–89
4. Gao W, Zhang Y, Ramanujan D, Ramania K, Chen Y, Williams CB, Wang CCL, Shin YC, Zhang S, Zavattieri P (2015) The status, challenges, and future of additive manufacturing in engineering. Comput Aided Des 69:65–89
5. Huang SH, Liu P, Mokasdar A, Hou L (2013) Additive manufacturing and its societal impact: a literature review. Int J Adv Manuf Technol 67:1191–1203. https://doi.org/10.1007/s00170-012-4558-5
6. Bikas H, Stavropoulos P, Chryssolouris G, Additive manufacturing methods and modelling approaches: a critical review. Int J Adv Manuf Technol. https://doi.org/10.1007/s00170-015-7576-2
7. Mançanares CG, de Zancul SE, da Silva JC, Miguel PAC (2015) Additive manufacturing process selection based on parts' selection criteria. Int J Adv Manuf Technol 80:1007–1014. https://doi.org/10.1007/s00170-015-7092-4
8. Paterson AM, Donnison E, Bibb RJ, Campbell RI (2014) Computer-aided design to support fabrication of wrist splints using 3D printing: a feasibility study. Hand Therapy 19(4):102–113. https://doi.org/10.1177/1758998314544802
9. Fantini M, De Crescenzio F, Brognara L, Baldini N (2017) Design and rapid manufacturing of a customized foot orthosis: a first methodological study, Design Engineering and Manufacturing, Lecture Notes in Mechanical Engineering. Springer International Publishing AG Advances on Mechanics. https://doi.org/10.1007/978-3-319-45781-9_46
10. Munhoz R, da Costa Moraes CA, Kunkel ME (2016) A digital approach for design and fabrication by rapid prototyping of orthosis for developmental dysplasia of the hip. Res Biomed Eng 32(1):63–73. https://doi.org/10.1590/2446-4740.00316
11. Singh S, Ramakrishna S, Singh R (2017) Material issues in additive manufacturing: a review. J Manuf Process 25:185–200
12. Eyers DR, Potter AT (2017) Industrial additive manufacturing: a manufacturing systems perspective. Comput Ind 92:208–218
13. Klahn Christoph, Leutenecker Bastian, Meboldt Mirko (2015) Design strategies for the process of additive manufacturing. Procedia CIRP 36:230–235
14. Hällgren S, Pejryd L, Ekengren J (2016) (Re)design for additive manufacturing. Procedia CIRP 50:246–251
15. Srinivas M, Sridhar Babu B (2017) A critical review on recent research methodologies in additive manufacturing. Mater Today Proc 4:9049–9059
16. Thompson MK, Moroni G, Vaneker T, Fadel G, Campbell RI, Gibson I, Bernard A, Schulz J, Graf P, Ahuja B, Martina F (2016) Design for additive manufacturing: trends, opportunities, considerations, and constraints. CIRP Ann Manuf Technol
17. ZUBIN KHABAZI, ALGORITMI GENERATIVI con GRASSHOPPER
18. Krish S, A practical generative design method
19. Ingrassia T, Alaimo G, Cappello F, Mancuso A, Nigrelli V (2007) A new design approach to the use of composite materials for heavy transport vehicles. Int J Veh Des 44(3–4):311–325
20. ANSYS Structural Analysis Guide

Graphical Bioengineering

Accuracy Assessment of CT-Based 3D Bone Surface Reconstruction

L. Puggelli[1], F. Uccheddu[1], Y. Volpe[1], R. Furferi[1(✉)], and D. Di Feo[2]

[1] Department of Industrial Engineering, University of Florence, Via di Santa Marta 3, 50139 Florence, Italy
rocco.furferi@unifi.it
[2] Department of Pediatric Surgery, A. Meyer Children's University Hospital, Viale Pieraccini 24, 50139 Florence, Italy

Abstract. 3D reconstruction of human anatomy from cross-sectional imaging has recently gained increasing importance in several medical fields thus designating the 3D bones reconstruction accuracy, critical for the success of the whole surgical intervention. The 3D anatomic model quality depends on the quality of the reconstructed image, on the quality of the images segmentation step and on the error introduced by the iso-surface triangulation algorithm. The influence of image processing procedures and relative parametrization has been largely studied in the scientific literature; however, the analysis of the direct impact of the quality of the reconstructed medical images is still lacking. In this paper, a comparative study on the influence of both image reconstruction algorithm (standard and iterative) and applied kernel is reported. Research was performed on the 3D reconstruction of a pig tibia, by using Philips Brilliance 64 CT scanner. At the stage of scanning and at the stage of 3D reconstruction, the same procedures were followed, while only image reconstruction algorithm and kernel were changed. The influence of such selection on the accuracy of bone geometry was assessed by comparing it against the 3D model obtained with a professional 3D scanner. Results show an average error in reconstructing the geometry of around 0.1 mm with a variance of 0.08 mm. The presented study highlights new opportunities to control the deviations on the geometry accuracy of the bones structures at the stage of cross sectional imaging generation.

Keywords: 3D model reconstruction · Kernel reconstruction · Accuracy · Computed tomography

1 Introduction

In many surgical fields (e.g. personalized cranio-maxillofacial surgery) computer-aided bone surgery requires highly accurate 3D representation of patient's bone, both for surgery planning and for implant design [1, 2].

The overall quality of a 3D anatomic model reconstruction, strictly depends on (i) the quality of the patient CT scan data, (ii) on the quality of the images processing step and (iii) on the errors introduced by the iso-surface triangulation algorithm (i.e. extract a 2D surface mesh from a 3D volume). The medical imaging quality mainly affects the spatial resolution depending on the type of computer tomography

F. Cavas-Martínez et al. (Eds.): *Advances on Mechanics, Design Engineering and Manufacturing II*, LNME, pp. 487–496, 2019.
https://doi.org/10.1007/978-3-030-12346-8_47

(CT) system and on the chosen scanning parameters. The spatial resolution depends also by the size of the voxel influenced by the slice thickness and by the matrix size. Changing the slice thickness can create a partial volume effect that needs to be considered for segmentation, and final 3D surface reconstruction [3–8]. The research community is working toward the determination of the relation between 3D model accuracy and image processing [9–13], including image enhancement and segmentation. Currently, a challenging task remains the determination of the relation between accuracy of the resulting 3D model and the medical data generation.

The quality of the resulting 3D anatomic model is, however, highly related to the quality of the reconstructed images, generally performed on board of the Computer Tomography scanner; the reconstruction chain, relies on a number of algorithms specifically designed to simultaneously optimize the imaging speed, the dose efficiency, and the general image quality. CT scans allows a number of reconstruction algorithms and relative kernels; the most appropriate combination depends on which tissues should be more or less highlighted. The Filtered back projection (FBP) method, due to its velocity and robustness, is the most common method used on-board of the clinical available CT scanners to reconstruct the cross-sectional images from raw data. However, FBP proved to be a sub-optimal algorithm choice for poorly sampled data or for cases where noise has a significant power density compared to the measured signal.

When these very high levels of noise are propagated through the reconstruction algorithm, the result is an image with significant artefacts. Way et al. [14] show that the fine tuning of the FBP parameters (i.e. the most important parameter is the reconstruction kernel), can significantly improve the quality of the resulting reconstructed images. In real clinical settings, once the images are reconstructed, the projection data is removed from the system, making further reconstruction with a different reconstruction filter parameter set impossible. Okubo et al. [15] proposed a method based on common image filtering techniques in the image space to be used instead of a reconstruction filter in the projection space for CT imaging, to achieve similar image quality.

The goal of this study is to assess the 3D accuracy of CT-based bone surface reconstruction, at varying the CT scanner internal parameters. More in detail, this study investigates into the influence of kernel selection in the image reconstruction algorithm about the accuracy of the 3D reconstruction, independently from the segmentation thresholding and from the surface reconstruction algorithms.

The study was performed in the Meyer Children's Hospital premises on a pork shank with and without soft tissues. This allows direct comparison between the CT-based reconstructions, obtained using different kernels, and the 3D model of the shank bone obtained using a professional 3D scanner.

2 From CT Scan Data to 3D Polygonal Model

According to recent literature [3], the most effective way for creating 3D models starts from the image processing of the medical image acquisition, by enhancing and segmenting some region of interest, then, converting the result into 3D models, through surface reconstruction procedures. The main steps of the pipeline are described in the following sections.

2.1 Medical Imaging Data Generation

The scan of the patient body is clinically performed by first appropriately tuning some machine parameters, which influences the final CT images.

X-rays tube potential [kV] and *current* [mAs] determine the energy of the ionizing radiation; therefore, they influence the patient adsorbed dose, i.e. the mean energy imparted to mass per unit mass by ionizing radiation. On the other hand, higher energy corresponds to more saturated images.

Scan range [mm] is the actual axial dimension of the section to be scanned. It is set to cover only the body region to investigate.

Pitch [mm/s] is the axial translation per rotation or the axial speed/the ratio between axial speed and collimation thickness.

Rotation time [s] is the time that the X-ray generators/detectors require to complete a single rotation around the axis.

Acquisition thickness [mm] is the virtual spacing between the acquired slices. A higher number of slices improve the detail in the scanning axis; on the other hand, both the time needed to complete the scan and the time to reconstruct the images increase.

These parameters directly act on the raw acquisition phase, while the *reconstruction algorithm* selection and the *reconstructed slice thickness* parameter, act on the medical image reconstruction phase. The raw data at the end of the CT acquisition is a sinogram [16] i.e. the Radon Transform of acquired data. Figuring the sinogram as an image, each one of its rows corresponds to the acquired data for each axial position, and each pixel of a selected row corresponds to the acquired datum for that axial position at a known angular position.

The *reconstructed slice thickness* [mm] is the spacing between the reconstructed slices, since it can be calculated interpolating the raw data, it does not necessarily coincides with the *acquisition thickness*: its value is usually equal or less.

Raw data must be elaborated in order to obtain the corresponding series of slices, by means of *Image reconstruction algorithms* based on Radon anti-transform e.g. the Filtered back projection (FBP) method, is commonly used on-board of the clinical available CT scanners to reconstruct the cross-sectional images from raw data [16]. Depending on the specific CT scan device, (ASIR™—GE, iDose$^{4®}$—Philips NV, IRIS®—Siemens AG, AIDR®—Toshiba Corporation, to cite some), a number of proprietary algorithms are available [17–19]. The fine-tuning of the FBP parameters (e.g. reconstruction kernels), can significantly improve the quality of the resulting reconstructed images when data are poorly sampled, or when the noise has a significant power density compared to the measured signal. Different kernels can be used optimally for different tissues, thus allowing highlighting some anatomical feature in the region of interest.

The reconstruction kernels may operate into the image domain or into the sinogram domain. Essentially, kernels are applied in order to enhance contrast resolution (low-pass or smoothing filters) or to enhance spatial resolution (high-pass or edge enhancement kernels). Each CT scan producer adopt different names for these kernels, e.g. *Detail*, *Bone* or *Edge* for edge enhancement kernels and *Standard* or *Soft* for smoothing kernels.

2.2 Image Processing and Surface Modelling

In order to further improve the classification of the different tissues on the CT scan images (i.e. bones, soft tissue or tumours), several image processing tools can be applied offline to the 2D dataset. A first image enhancement can be performed to suppress artefacts or to highlight the tissues borders. Then, a *segmentation* step is needed to identify the tissues boundaries. Segmentation is the process of dividing an image into regions with similar properties [20]. The role of segmentation on medical imaging, consists in identifying the anatomical structures in the images. As result of the segmentation task, the pixels in the image are partitioned through binary masks, in non-overlapping regions, belonging to the same tissue class. When the region of interested is naturally highlighted, as for the case of bone structures that shows high grey level pixels, an automatic thresholding can be performed to separate the bone pixels from the rest of the image.

After the segmentation phase, starting from the obtained multi slices binary masks (i.e. voxels), the 3D surface are generated by applying *Marching cubes* algorithms or other 3D contour extraction algorithms [21]. All the functions that are required to obtain a 3D polygonal model from a series of slices are included in many dedicated software, like *Mimics*® and *3D Slicer*® (Fig. 1).

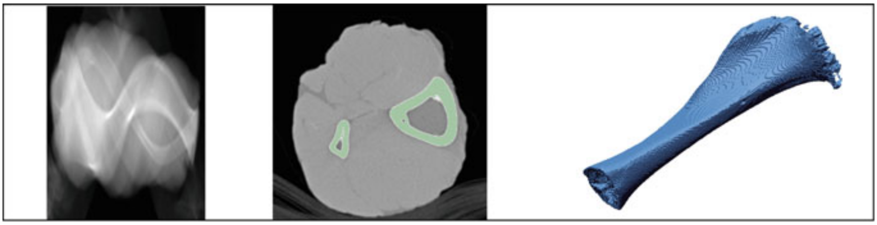

Fig. 1. From sinogram to polygonal model

3 Experimental Design

3.1 CT Scanning and Medical Images Reconstruction

CT scanning has been performed on a *Brilliance 64 CT* spiral scanner (*Philips NV*, Eindhoven, Netherland). Machine parameters (see Table 1), and in particular tube potential and tube current, have been set at standard values for children (i.e. 100 kV and 200 mAs respectively). In order to obtain a small spacing between reconstructed slices, acquisition spacing has been set at 0.8 mm. Scan range, which depends on the size of the subject to be scanned, has been adjusted at 170 mm as the size of the pig tibia.

From a single scan (i.e. from a single sinogram), six different series of images have been reconstructed by adopting both Philips image reconstruction algorithms (*Standard* and *iDose4*®) and by applying three different kernels respectively: *Smooth* (low pass filter), *Sharp* and *Bone* (high pass filters). The nomenclature adopted for the series

Table 1. CT-scan settings

Parameters	Value
Tube potential	100 kV
Tube current	200 mAs
Scan range	170 mm
Acquisition thickness	0.8 mm

makes use of the kernels DICOM acronym (A = *Smooth*, C = *Sharp*, D = *Bone*), while "S" and "I" indicates *Standard* or *iDose4*® image reconstruction algorithm [20].

3.2 3D Reconstruction from CT-images

From reconstructed medical images, the entire procedure of 3D reconstruction have been implemented by means of *3D Slicer*® software, one of the most popular free and open source software package for medical image computing and visualization [22]. In order to limit the influence of the image-processing phase, no enhancement filters have been applied to the images, and the segmentation of the bones have been performed through a thresholding operation. In this phase, a threshold value of 700 Hounsfield Unit (HU) has been used: this value corresponds to the linear attenuation coefficient associated to cortical bones [17]. As a consequence, only the diaphysis of the tibia has been opportunely reconstructed, while epiphysis and metaphysis—which have 250 · HU · 700 typical values (due to high concentration of cancellous bone)—have not been correctly detected.

Finally, the 3D polygonal model of each segment has been retrieved by means of the *Marching cubes* algorithm implemented into *3D Slicer*®, in which smoothing factor has been maintained at 0. Each reconstructed 3D polygonal model has been exported in the form of STL file. For a sake of clarity, the same nomenclature as slides series has been maintained (e.g. R_SA→R_SA.stl).

3.3 3D Laser Scanning

To obtain a high-accurate 3D virtual reconstruction of the tibia to be used as ground-truth, the dry bone (i.e. after soft tissues removal by boiling) has been acquired by means of a 3D laser scanner (*Romer Absolute Arm RA 7520 SI* with integrated *RS1* laser scanner). Such a scanner provides a volumetric accuracy in the range ± 0.058 mm within the measurement range of 2.0 m and a point repeatability lower than 0.023 mm, according to the ASME B89.4.22 certification. Both acquisition and successive 3D reconstruction operations have performed by means of *Polyworks*® software.

As soft tissues are present in the acquired CT-data, and as boiling of the pig bone may have an impact on its geometry and, consequently, on the successive accuracy assessment phase, steps 1–3 have been repeated on the dry tibia (i.e. without soft tissues), maintaining the same procedures and parameters. For this reason, 6 additional polygonal models have been used (B_XX series).

3.4 Comparison & Accuracy Assessment

CT-based reconstructions and ground truth have been imported as STL files into *Geomagic Design X*® software environment. Before performing accuracy measurements, two main operations have been carried out:

1. Invalid portions removal from each STL mesh;
2. Alignment between scan data.

As previously partially reported, CT-based polygonal models present an incomplete reconstruction of cancellous bone sections of tibia (i.e. epiphysis and metaphysis) due to segmentation at 700 HU. In addition, such models also include internal cavities of the bone, which have not been measured by means of laser scanner. In order to avoid imprecise alignment and invalid accuracy assessment, all of these portions on each mesh have been ignored.

Successively, all the polygonal models have been aligned referring to R_XX models (which are natively aligned since deriving from the same CT-scanning). To come up with this purpose, both *point-to-point* and *ICP* algorithms have been used [23].

At this point, accuracy of each CT-based STL has been assessed by comparing it against ground-truth. This operation has been carried out by means of *mesh max deviation* tool, which computes the distance between each point on a *target* and its projection on a *reference* mesh (i.e. ground-truth), along the target mesh normal. Then, for each element of the target, the maximum distance is considered.

4 Results and Analysis

Following the procedure described in Chap. 3, in Table 2 both mean (μ) and standard deviation (σ) resulting from the analysed mesh deviations are reported (see Fig. 2).

Table 2. Mesh deviation analyses

3D models	Signed dist. [mm]		Unsigned dist. [mm]		Mesh%	
	μ	σ	μ	σ	$\lvert d\rvert < 0.1$ mm	$\lvert d\rvert < 0.2$ mm
R_SA	0.141	0.128	0.162	0.101	31.7	64.2
R_SC	0.113	0.114	0.134	0.089	40.3	76.5
R_SD	0.113	0.115	0.134	0.089	40.4	76.7
R_IA	0.142	0.127	0.162	0.100	31.6	64.2
R_IC	0.113	0.114	0.134	0.089	40.3	76.5
R_ID	0.113	0.115	0.134	0.115	40.4	76.7
B_SA	–0.134	0.145	0.160	0.115	35.7	65.8
B_SC	–0.039	0.137	0.115	0.083	49.5	83.0
B_SD	–0.029	0.137	0.114	0.082	50.1	83.7
B_IA	–0.134	0.145	0.160	0.115	35.7	65.8
B_IC	–0.039	0.137	0.115	0.083	49.5	83.0
B_ID	–0.029	0.137	0.114	0.082	50.1	82.4

In all the analyzed comparisons, only little differences are visible: μ is between ± 0.13 mm (signed distance) or between 0.11 ÷ 0.16 mm (unsigned distance) and relative σ is between 0.11 ÷ 0.14 mm (signed distance) or between 0.08 ÷ 0.11 mm (unsigned distance).

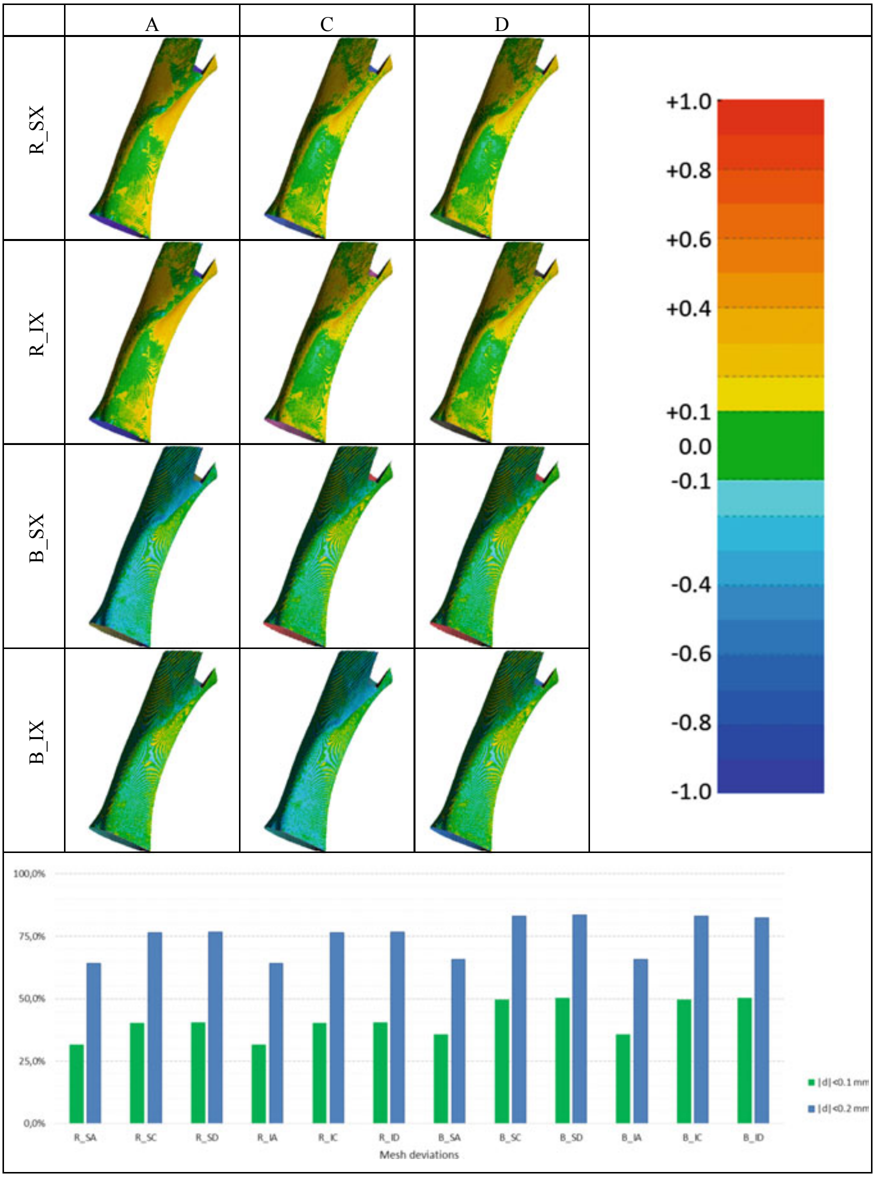

Fig. 2. Obtained mesh deviation maps

In addition, 3D reconstructions obtained by means of *Standard* and *iDose*$^{4®}$ algorithms show almost the same identical statistical values, even if slide images visibly differ. This lead to suppose that *iDose*$^{4®}$ helps in augmenting the readability of medical images without affecting bones silhouette and, on the other hand, that there is no evident reason to adopt *iDose*$^{4®}$ to 3D reconstruction purposes, since it is more time consuming with respect to *Standard* algorithm. The same observation is still valid for what concerns the kernel choice. However, in this case, some slightly differences are numerically visible between *Smooth* (*A*) kernel and both *Sharp* (*C*) and *Bone* (*D*) kernels.

Especially paying attention to the two last columns of Table 2, it emerges that in the analysed case study, the mesh percentage of R_XA beneath $|d| < 0.1$ is almost 30% lower than R_XC or R_XD, while no tangible difference appears between the latter two (31.7 vs. 40.3% and 40.4%). Similar values are reported when analysing the mesh percentage of R_XA beneath $|d| < 0.2$ (20% lower, 64.2 vs. 76.5% and 76.7%). Similar consideration are valid also for all B_XX polygonal models.

On the light of this analysis on this case study, even if difference is almost invisible and probably negligible, it seems to be suggestable the adoption of *Standard* image reconstruction algorithm with *Sharp* or *Bone* kernel.

5 Conclusion and Future Developments

In this paper, authors report a first investigation into the influence of kernel choice in the accuracy of a CT-based 3D reconstructed polygonal model. In particular, attention has been focused on *Brilliance 64 CT* spiral scanner (*Philips NV*, Eindhoven, Netherland) and relative image reconstruction algorithms (*Standard* and *iDose*$^{4®}$). The reconstruction of a pig tibia has been used as case study. Three different kernels have been selected a priori due to their relevance: *Smooth, Sharp* and *Bone*. Tube voltage, tube current and *iDose*$^{4®}$ level have been maintained constant and the same procedure to reconstruct 3D polygonal model from CT-images has been followed. Accuracy of each CT-based 3D reconstruction has been assessed by comparing the resulting polygonal model against a high-accurate 3D virtual model, considered as ground-truth, obtained by means of Romer Absolute Arm and RS1 3D laser probe. Mesh deviation analyses showed no evident difference varying image reconstruction algorithm and kernel. However, two main observations have to be made: 1. there is an almost total overlap between 3D reconstructions obtained with *Standard* and *iDose*$^{4®}$, making the first preferable due to less computational time; 2. *Sharp* and *Bone* kernels provide slightly more accurate 3D reconstruction with respect to *Smooth* one. Despite limited to a single case study, this analysis paves the way for a correct use of different kernels in TC scanning, thus allowing the choice of the best option when the main intent is to reconstruct the 3D anatomy of bones.

References

1. Fuessinger MA et al (2018) Planning of skull reconstruction based on statistical shape model combined with geometric morphometrics. Int J Comput Assist Radiol Surg 13(4):519–529
2. Marreiros FMM et al (2016) Custom implant design for large cranial defects. Int J Comput Assist Radiol Surg 11(12):2217–2230
3. Rengier F et al (2010) 3D printing based on imaging data: review of medical applications. Int J Comput Assist Radiol Surg 5(4):335–341
4. Lee Ventola C (2014) Medical applications for 3D printing: current and projected uses. P and T 39(10):704–711
5. Do A-V et al (2015) 3D printing of scaffolds for tissue regeneration applications. Adv Healthc Mater 4(12):1742–1762
6. Choi JW, Kim N (2015) Clinical application of three-dimensional printing technology in craniofacial plastic surgery. Arch Plast Surg 42(3):267–277
7. Ridwan-Pramana A et al (2016) Structural and mechanical implications of PMMA implant shape and interface geometry in cranioplasty—a finite element study. J Cranio-Maxillofac Surg 44(1):34–44
8. Park E-K et al (2016) Cranioplasty enhanced by three-dimensional printing: custom-made three-dimensional-printed titanium implants for skull defects. J Craniofac Surg 27(4): 943–949
9. Stull KE et al (2014) Accuracy and reliability of measurements obtained from computed tomography 3D volume rendered images. Forensic Sci Int 238:133–140
10. Lalone EA et al (2015) Accuracy assessment of 3D bone reconstructions using CT: an intro comparison. Med Eng Phys 37(8):729–738
11. Gelaude F, Vander Sloten J, Lauwers B (2008) Accuracy assessment of CT-based outer surface femur meshes. Comput Aided Surg 13(4):188–199
12. Tan CJ et al (2017) Influence of scan resolution, thresholding, and reconstruction algorithm on computed tomography-based kinematic measurements. J Biomech Eng 139(10):104503
13. Naddeo F et al (2017) An automatic and patient-specific algorithm to design the optimal insertion direction of pedicle screws for spine surgery templates. Med Biol Eng Comput 55(9):1549–1562
14. Way TW et al (2008) Effect of CT scanning parameters on volumetric measurements of pulmonary nodules by 3D active contour segmentation: a phantom study. Phys Med Biol 53(5):1295–1312
15. Ohkubo M et al (2011) Image filtering as an alternative to the application of a different reconstruction kernel in CT imaging: feasibility study in lung cancer screening. Med Phys 38 (7):3915–3923
16. Brooks RA, Chiro DG (1976) Principles of computer assisted tomography (CAT) in radiographic and radioisotopic imaging. Phys Med Biol 21(5):689–732
17. Li H et al (2016) A comparative study based on image quality and clinical task performance for CT reconstruction algorithms in radiotherapy. J Appl Clin Med Phys 17(4):377–390
18. Beister M, Kolditz D, Kalender WA (2012) Iterative reconstruction methods in X-ray CT. Physica Med 28(2):94–108
19. iDose^4 Technical White-paper: http://incenter.medical.philips.com/doclib/enc/fetch/2000/4504/577242/577249/586938/587315/iDose4_-_Whitepaper_-_Technical_-Low_Res.pdf%3fnodeid%3d8432599%26vernum%3d-2
20. Uccheddu F et al (2017) 3D printing of cardiac structures from medical images: an overview of methods and interactive tools. Inter J Interact Des Manuf (Article in press)

21. Lorensen WE, Cline HE (1987) Marching Cubes: a high resolution 3D surface construction algorithm. Comput Graph (ACM) 21(4):163–169
22. Fedorov A et al (2012) 3D Slicer as an image computing platform for the quantitative imaging network. Magn Reson Imaging 30(9):1323–1341
23. Besl PJ, McKay ND (1992) A method for registration of 3-D shapes. IEEE Trans Pattern Anal Mach Intell 14(2):239–256

Comparative Study of Mussel Shells Using 3D Scanning

H. Eguiraun[1,2(✉)], E. Gil-Uriarte[2], L. Barrenetxea[1], E. Lizundia[1], I. Zuazo[1], and M. Soto[2]

[1] Department of Graphic Design & Engineering Projects, Faculty of Engineering in Bilbao, University of the Basque Country UPV/EHU, 48013 Bilbao, Spain
harkaitz.eguiraun@ehu.eus

[2] Research Center for Experimental Marine Biology and Biotechnology—Plentziako Itsas Estazioa PiE, University of the Basque Country, UPV/EHU, 48620 Plentzia, Spain

Abstract. Present work examines the feasibility of using light based 3D scanning as a tool to fulfil mussel shells' morphological and dimensional analysis and establishes a scanning methodology for future studies. These analysis will serve as a first step to determine a methodology to scan, to build and to set paths for analysing the 3D objects (points clouds) in order to achieve comparative studies with large amount of individuals (>100). 2 mussels from 4 different species and locations were scanned: Blue mussel (*Mytilus edulis*) from Norway, Mediterranean mussel (*Mytilus galloprovincialis*) from the estuary of Bilbao in the north of Spain, Baltic blue mussel (*Mytilus trossulus*) from Baltic sea and Black pygmy mussel (*Xenostrobus securis*) from a different spot in the estuary of Bilbao. Different scanning methodologies were tested: (i) with/without ambient light, (ii) with/without black plasticine inside the valve and (iii) different mussels' positions. Results show that the best methodology in terms of time elapsed, post-processing cost and fidelity to reality was to scan both valves laid down with their outer part outwards filled up with black plasticine and with ambient light. These results will sever us to set a scanning methodology to use in studies that require the analysis of large amount on individuals, for example in toxicological, origin and/or species studies among others.

Keywords: 3D modelling · Mussel shell · Morphology · Biological structures · Bioindicator

1 Introduction

Molluscs in general and mussels in particular are not only a very appreciated ingredient in cuisine with high protein content, but also a wide used marine environmental monitoring tool [1, 2]. They are able to quantify the anthropogenic impact in the sea mainly due to three reasons: (i) they can be found in groups of big amount of units, (ii) they are all over the world oceans and (iii) they act as water filters. Additionally, mussel shells have been historically used with different purposes from construction, as binding material, to jewellery due to its nacre content.

F. Cavas-Martínez et al. (Eds.): *Advances on Mechanics, Design Engineering and Manufacturing II*, LNME, pp. 497–504, 2019.
https://doi.org/10.1007/978-3-030-12346-8_48

It is known that mussel growth rate depends in various factors being the most important the tide variation and the water nutrient content. Even though some works reveal that shell growth depends primarily in circatidal variation and seasonal variation in water nutrient content, it is still unclear how other factors (i.e. salinity, temperature) affect shell morphology and growth. Additionally, some studies use different bivalves' shells as bio-indicators of the environmental anthropogenic impact [3–5], due to the alterations produced in theirs shells by the presence of contaminants.

We are not aware of any study that examines the feasibility and the methodology for scans neither such bivalve's shells nor the problems therein. Accordingly, this study aims to determine: (i) if different mussel shells' morphology are able to be scanned by means of a 3D scanner in order to get a reliable and comparable 3D objects, particularly interesting should be the amount of growth rings scanned and the accuracy in order to be able to affix landmarks to perform geometric morphometric study, (ii) if the proposed scanning methodology can be performed for studies which require large amount of units in a cost effective manner.

2 Materials and Methods

2.1 Biological Material

Mussels were collected from 4 representative spots in Europe and were named as Me, Mg, Mt and Xs according to their species: Blue mussel—Me (*Mytilus edulis*) from Norway, Mediterranean mussel—Mg (*Mytilus galloprovincialis*) from the estuary of Bilbao in the north of Spain, Baltic blue mussel—Mt (*Mytilus trossulus*) from Baltic sea and Black pygmy mussel—Xs (*Xenostrobus securis*) from another different spot in the Bilbao estuary. 2 mussels from each species and both valves of each mussel were scanned (Table 1 and Fig. 1).

Table 1. Biological material used. 2 different mussels were scanned from 4 different spots from Europe and were named as Me, Mg, Mt and Xs

Code	Name	Number of mussels	Origin	Age est. (y)	Remarks
Me	*Mytilus edulis* (Blue mussel)	2	Rissa (Norway)	2–3	Farmed. Marine
Mg	*Mytilus galloprovincialis* (Mediterranean mussel)	2	Arrigunaga (Bilbao estuary)	2–4	Wild. Native to Southern Europe. Invasive in Southern Hemisphere
Mt	*Mytilus trossulus* (Baltic blue mussel)	2	Kalmar (Sweden)	1–2	Farmed. Particular variety of mussel in low salinity (=7 psu)
Xs	*Xenostrobus securis* (Black pygmy mussel)	2	San Ignacio (Bilbao estuary)	2–3	Wild. Invasive to southern Europe (Native: Australasia) Eurihaline species

2.2 3D Scanner and Software

Mussels were scanned with an Atos Compact Scan 5 M 300 with MV150 lenses equipped with Atos Professional v7.5 software. Cloud points were posteriorly aligned and processed by GOM inspect software.

Fig. 1. Species scanned are Blue mussel—Me (*Mytilus edulis*) from Norway, Mediterranean mussel—Mg (*Mytilus galloprovincialis*) from the estuary of Bilbao in the north of Spain, Baltic blue mussel—Mt (*Mytilus trossulus*) from Baltic sea and Black pygmy mussel—Xs (*Xenostrobus securis*) from another different spot in the Bilbao estuary

2.3 Experimental Conditions

The shells were externally cleaned with alcohol and sticked matter was removed very carefully without damaging the shell. Different experimental setups were tested in order to find the better scanning procedure. The best was considered to be the one with the best fidelity to reality:

1. Both valves separated and stood up heading up and down.
2. Both valves laid down with the outer part outwards.

3. Using ambient light or performing the scans in darkness.
4. With or without powder in the external part of the valves.
5. With or without plasticine inside internal part of the valves.

Finally, the best results were obtained with the following setup (Fig. 2):

- Both valves laid down with the outer part outwards and parallel to the ground support while elevated a bit to make it easier to remove the ground from the scans.
- Filled with black plasticine (we had scanning problems without the plasticine due to the translucent characteristics of the shell).
- With ambient light.
- Without external powder.

All of the scans were performed replicating the same conditions and with the same scanner setup to reduce data acquisition variability. Both valves from each mussel were scanned at the same time.

2.4 Issues

While transporting the shells to our laboratory one of the Mt1's valves broke. Furthermore, the other Mt1's valve broke while manipulating it to introduce the plasticine.

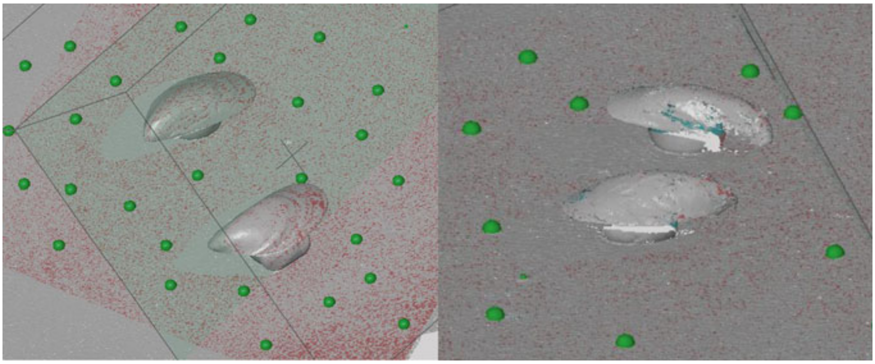

Fig. 2. Screenshot of the scanning software with two different scans running (Me1 left and Mt2 right). Scans were achieved with both valves laid down with the outer part outwards and parallel but separated to the ground support, filled with black plasticine, with ambient light and without the use of external powder. Note the "white holes" around the scans (non acquired parts) and the solid below the valves (the plasticine)

3 Results and Discussion

The resulting scanned objects are depicted in Fig. 3. Different degree of accuracy was obtained depending primarily on the colour and secondarily on the shape of the valve. The used methodology proved to be the most reliable one and all the scans were obtained in 3-approximately hours work.

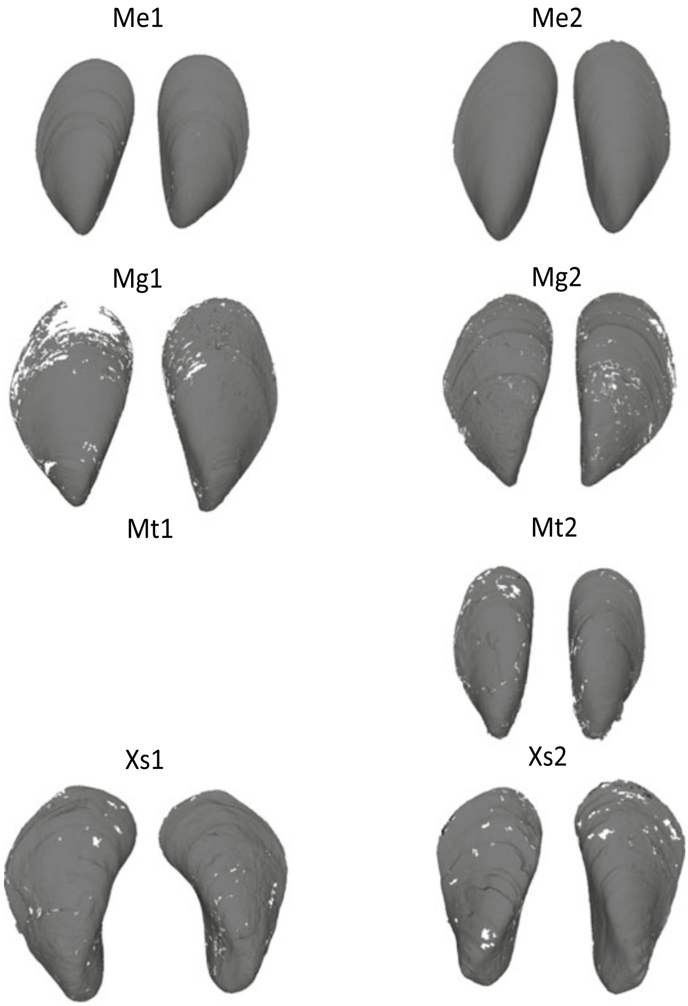

Fig. 3. Results from the scanned mussels' shells. Scans from Blue mussel—Me (*Mytilus edulis*), Mediterranean mussel—Mg (*Mytilus galloprovincialis*), Baltic blue mussel—Mt (*Mytilus trossulus*) sea and Black pygmy mussel—Xs (*Xenostrobus securis*) present different degrees of accuracy due to their colour and shape. "White holes" in the scans correspond to sections that have been impossible to digitalize

Previous attempts showed that the use of black plasticine was necessary due to the translucent nature of the valves (results not shown).

While manipulation one of the Baltic blue mussels (*Mytilus trossulus*) from Baltic Sea broke and the one scanned presented a completely different felling in terms of shell resistance compared to the other species' valves. An issue that can be explained by the low salinity of the Baltic sea or because they have been living in a spot with a high maritime traffic [6].

Best results are for Blue mussel (*Mytilus edulis*) from Norway (Me1 and Me2) due to their brown colour and smooth texture. Other mussels present calcifications in the shells, which were impossible to remove, consequently they are part of the scanned valves (Fig. 4). Surprisingly, the Black pygmy mussel—Xs (*Xenostrobus securis*) from the Bilbao estuary was the one that presented the most complicated shape but the scans showed promising results. Additionally, it has been feasible to scan the principal growth rings of the mussels despite it has been impossible to digitalize the small rings between those principal ones, probably due to the small distance between them (around 2 μm) (Fig. 4).

Although some of the scans present "white holes", parts which have been impossible to scan, we hope that they will be enough to locate the landmarks needed to study them using morphometric geometrics. The case of the Mt1 is especially disturbing because we lost it. In any case, we will proceed locating the landmarks and in case it becomes impossible, we will decide if re-scan the valve or close the "hole" by software approximation. Also, it is remarkable to appoint, that we are not aware of how other studies deal with these last issues.

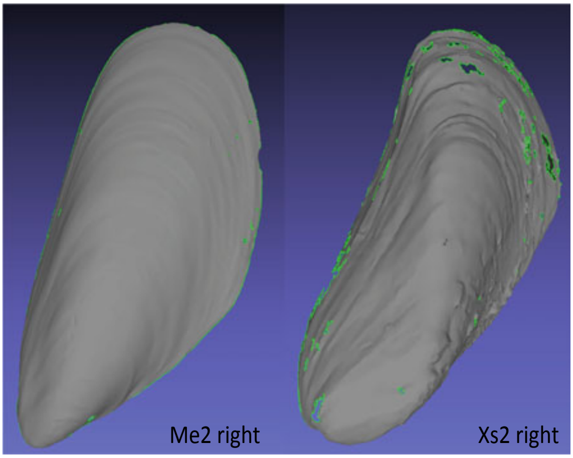

Fig. 4. Right valve of the Blue mussel—Me2 (*Mytilus edulis*) compared with the analogue valve of the Black pygmy mussel—Xs2 (*Xenostrobus securis*). The highlighted areas correspond to the non-digitalized parts. Note the differences among them in the growth rings, the texture (due to the added matter) and the form of the shell (especially rare in the Black pygmy mussel (Xs2) case)

4 Conclusions and Future Work

Present work has served as a first step to develop a methodology to scan mussel shells in order to get reliable scans to use in environmental/toxicological studies using the mussel shells shape and geometry as bioindicators.

Following other author's steps [1, 3, 6], the next phase of this study should be to analyse the obtained scans using morphometric geometry. Morphometric geometry is a tool widely used in anthropology [7, 8] which analyses the form of an object omitting its size. Thanks to the use of landmarks and semilandmarks, specific points in the objects defined by their Cartesian coordinates, it is possible to capture the different morphological shape variables, and with the subsequent use of statistics, make those "different" objects comparable.

Currently, we are working in this research line and hopefully we will be able to present and discuss some preliminary results in the conference.

Acknowledgements. We wish to thank Xabier Amezua and Unai Heras for their assistance. The work was partially supported by project: 679266-H2020-EU.3.2 *Integrated oil spill response actions and environmental effects—GRACE* from the H2020 (BG-07-2015—Response capacities to oil spills and marine pollutions). The funding sources had no involvement in the preparation of this manuscript.

References

1. Laitano MV, Nuñez JD, Cledón M (2013) Shell alterations in the limpet *Bostrycapulus odites*: a bioindicator of harbour pollution and mine residuals. Ecol Ind 34:345–351. https://doi.org/10.1016/j.ecolind.2013.05.022
2. Van der Schalie WH, Shedd TR, Knechtges PL, Widder MW (2001) Using higher organisms in biological early warning systems for real-time toxicity detection. Biosens Bioelectron 16 (7–8):457–465. https://doi.org/10.1016/S0956-5663(01)00160-9
3. Scalici M et al (2017) Shell fluctuating asymmetry in the sea-dwelling benthic bivalve *Mytilus galloprovincialis* (Lamarck, 1819) as morphological markers to detect environmental chemical contamination. Ecotoxicology 26(3):396–404. https://doi.org/10.1007/s10646-017-1772-9
4. Márquez F, Nieto Vilela RA, Lozada M, Bigatti G (2015) Morphological and behavioral differences in the gastropod *Trophon geversianus* associated to distinct environmental conditions, as revealed by a multidisciplinary approach. J Sea Res 95:239–247. https://doi.org/10.1016/j.seares.2014.05.002
5. Márquez F, Primost MA, Bigatti G (2017) Shell shape as a biomarker of marine pollution historic increase. Mar Pollut Bull 114(2):816–820. https://doi.org/10.1016/j.marpolbul.2016.11.018
6. Márquez F, González-José R, Bigatti G (2011) Combined methods to detect pollution effects on shell shape and structure in Neogastropods. Ecol Ind 11(2):248–254. https://doi.org/10.1016/j.ecolind.2010.05.001

7. Santos E, Gómez-Olivencia A, Arlegi M, Arsuaga JL (2015) Cranial morphological differences within *U. deningeri*—*U. spelaeus* lineage: a double traditional and geometric morphometrics approach. Quatern Int 433:347–362. https://doi.org/10.1016/j.quaint.2015.11.096
8. Arlegi M et al (2017) The role of allometry and posture in the evolution of the hominin subaxial cervical spine. J Hum Evol 104:80–99. https://doi.org/10.1016/j.jhevol.2017.01.002

VR Medical Treatments. A 15-Year Statistical Overview

J. M. Salmerón Núñez[1](✉), R. García Sánchez[2], and J. Ordoñez García[3]

[1] Departamento de Expresión Gráfica en la Ingeniería, Universidad Politécnica de Cartagena, C/Dr. Fleming, 2, 30202 Cartagena, Spain
juanm.salmeron@upct.es

[2] Departamento de Arquitectura y Tecnología de la Edificación, Universidad Politécnica de Cartagena, Paseo Alfonso XIII 50, 30203 Cartagena, Spain

[3] Departamento de Ingeniería de la Construcción y Proyectos de Ingeniería, Universidad de Granada, C/Dr. Severo Ochoa, 18071 Granada, Spain

Abstract. Introduction: virtual reality technology- (VRT) based rehabilitation treatments have been developed for several diseases. A previous step consists of experimental studies with methodological qualities on the efficacy of these treatments. Frequency of trials, supported by a large enough number of patients, is an index that guarantees its reliability, which is proportional to its interest and its practical application possibilities. Methods: a search of articles in the scientific literature according to pathology that present VRT-based trials. To ensure quality parameters, diseases with at least one state of the art or one study including at least 10 analyzed articles between 2002 and 2017 were selected, and the rest were eliminated. Finally, the search for more articles after those collected has been completed to date using the same criteria. Results: six scoping reviews were chosen and corresponded to five diseases: Parkinson's Disease (PD), Multiple Sclerosis (MS), Schizophrenia (SCH), Cerebrovascular Accident and Stroke (CVAS), and Post-traumatic Stress Disorder (PTSD). Finally, 107 articles, with a population of 3084 patients, were included. Authors' institutional affiliation and medical experiments were analyzed. In this way, it was possible to identify the countries that investigate VRT the most, by distinguishing all five diseases. Conclusions: VRT-based therapy thus has the potential as a useful tool for these identified diseases, while others await further investigation. Countries with less medical infrastructure can benefit from the independent community outpatient system that it involves.

Keywords: Virtual reality · Motion tracking technologies · Medical rehabilitation treatments · Cyber therapy

F. Cavas-Martínez et al. (Eds.): *Advances on Mechanics, Design Engineering and Manufacturing II*, LNME, pp. 505–516, 2019.
https://doi.org/10.1007/978-3-030-12346-8_49

1 Introduction

Investment in medical research is not only a necessity, but reports notable benefits for the subsequent treatment of the analyzed diseases. According to a British study of cardiovascular disease and mental health research [1], the yearly rate of return for health gain was 9% for cardiovascular disease, and 7% for mental health. The yearly rate of return in Gross Domestic Product (GDP) terms was 30% for all medical research in the UK. These benefits consist in cutting treatment duration, severity of symptoms, and relapse and hospitalization rates [2]. The World Health Organization in its 2013 report includes the mental health and psychosocial support as a specific topic with a priority-setting for research that focuses on humanitarian settings.

Virtual reality (VR), based on its origin to reproduce situations that pose limitations or access difficulties, first extended to the entertainment sector with video game technology and the diffusion of electronic devices. Since then, huge applications are now found in the medical field, especially in the last two decades. Audio-Visual interaction allows patients a motivating and enjoyable activity to develop of treatment [3]. Some successful rehabilitation practices focus on using a preliminary evaluation of commercial VR devices, such as customizing existing games to become more accessible and easier to use for physicians [4] or 3D glasses. Models that have recently appeared in the market allow their development in clinics and the patient's home [5].

The most widespread field of use is motor rehabilitation, which has been replacing traditional procedures [6]. In them the patient experiences the pain and physical fatigue that the VR makes patients ignore. At the same time, and if necessary, VR allows the display of mechanical aids that facilitate movements to be removed, and can even speed up or exaggerate them, by fooling the brain and stimulating neural connections. These rehabilitations are necessary in degenerative cases such as Parkinson's disease (PD), accidents with muscular or neuronal traumas, or the impact of cerebral stroke. That is the reason why medical experiments with VR on the subject have increased in recent years, many of which have been published in scientific articles.

As some recent articles [7] demonstrate, VR rehabilitation programs are more effective than traditional one as regards physical outcome development. The reason for this consists in excitement, physical and cognitive fidelity mechanisms. However, all these research works have focused on a specific disease or studying the use of VR in the general medical rehabilitation field. We herein propose an overview that identifies, compares, and characterizes VR development in five diseases, with proof of effectiveness (PD, MS, SCH, CVAS and PTSD).

2 Materials and Methods

A comprehensive scientific literature search was done, in Science Direct and Research Gate using the keywords of this article. Title and Abstract were tested and the selected articles with comparisons of more than 10 published research work on controlled trials. Diseases that matched the inclusion criteria (randomized and quasi-randomized controlled trials of VR exercises) were found. These selected articles were also used for search, in more extensive online data banks (e.g. PD selection used Cochrane, Embase, Cinahl, Scielo, Pubmed, Liliacs, Medline and PEDro, whereas SCH selection used PsycINFO, ASC, CINAHL, WSBSP). Another search was done to complete these articles with more recent ones that fulfilled their conditions (without comparisons, but including randomized trials), as underlined in Table 1. In them all of the number of patients involved in the trials was analyzed (Table 2).

In CVAS, Darekar et al. [8] is the author of a state of the art with a comparative study of 24 articles (two about the same) published between 2004 and 2013, including measurements of balance exercises results about mobility. Five more articles were found [9–13]. Botella et al. [14] did 12 research works from 2007 to 2014 that belonged to PTSD. In PD there were two scoping reviews: De Paula et al. [3] with 16 articles, whereas Dockx et al. [15] had in common two of its eight studies.

Massetti et al. [16] published about MS, and compared 11 articles between 2005 and 2015, and was added by Kalron et al. [17] to another one in 2016. Finally according to inherited and acquired components, SCH was the most widely investigated disease, as represented by a comparison of 33 articles in Marcedo et al. [18], completed by Ruse et al. [19]. Autism Spectrum Disorder (ASD) was tested and ruled out for its state of the art, as published by Bellani et al. [20], with only six articles, and because it did not meet the inclusion criteria. Only a few more articles on were found, such as Didehbani et al. [21]. Very few isolated studies on other diseases were found, like chronic pain or phobias [22, 23], which still had no state of art. All this led to the inclusion of 107 articles, which were distributed into the aforementioned five diseases with a study population of 3084 patients (Table 2).

3 Results and Discussion

From the global comparison made (Table 2), it was deduced that the VR treatment of SCH was the most practiced in terms of number of trials (34), and patients (1417), and its frequency remained from 2003 to 2014. Secondly came CVAS with 28 trials and 491 patients, with an average of 17 patients per trial, which was much lower than the 41 for SCH. PD obtained shows a slightly larger study population than the previous one, but involved fewer medical tests (approx. 21). Thus the average number of patients per trial came to 24. However, representation by years was very irregular and concentrated in 2011 with eight trials. The fourth most studied disease with VR treatments was

Table 1. Selected VR medical treatments published between 2002 and 2017

Year	PTSD	PD	CVAS	MS	SCH	n
2002		Albani et al.				1
2003					Ku et al.	1
2004			Deutsch et al., Jaffe et al.		Ku et al., Costa and Carvalho, St. Germain and Kurtz	5
2005			You et al.	Fulk	Kim et al., Jang et al., Ku et al., Sorkin et al.	6
2006		Klinger et al.	Betker et al., Fung et al.	Baram and Miller	Ku et al., Sorkin et al., Baker et al.	7
2007	Difede et al.	Messier et al.	Flynn et al.	Leocani et al.	Kim et al., Ku et al., Kurtz et al.	7
2008			Yang et al., Dunning et al.		Fornells-Ambrojo et al., Weniger and Irle	4
2009			Mirelman et al. (2), Kim et al.		Lallart et al., Park et al., Josman et al., Chan et al.	8
2010	Gamito et al., Botella et al., Ready et al., McLay et al.		Walker et al., Shin et al.	Baram and Miller	Dyck et al.	8
2011	McLay et al., Baños et al.	Wang et al., Ma et al., Synnott et al., Griffin et al., Yen et al., Park et al., Shine et al.	Yang et al., Feasel et al.		Park et al.	12
2012	De la Rosa et al., Miyahira et al.	Esculier et al., Arias et al., Loureiro et al., Pompeu et al., Mendes et al.	Cikaljo et al., Cho et al., Lewek et al., Jung et al., Kim et al.		Han et al., Gutierrez-Maldonado et al., Rus-Calafell et al., Han et al., Spieker et al.	17
2013		Pedreira et al.	Cho et al., Fritz et al., Rajaratnam et al., Singh et al., Kober et al.	Gutierrez et al., Ortiz-Gutierrez et al.	Tsang and Man, Zawadzki et al.	10

(*continued*)

Table 1. (*continued*)

Year	PTSD	PD	CVAS	MS	SCH	n
2014	Difede et al., Rothbaum et al., Roy et al.	Van den Heuvel et al., Shen et al.	Shin et al.	Lozano-Quilis et al., Mahajan et al., Turekca et al.	Rus-Calafell et al., Moritz et al., Ruse et al.	12
2015		Lee et al., Liao et al., Yang et al.		Eftekharsadat et al., Sampon et al.		5
2016			Faria et al., Mathews et al.	Kalron et al.		3
2017			Cannell et al.			1
Total	12	22	28	12	34	107

Table 2. Number (n) and size (S) of the published VR- selected treatments

	PTSD		PD		CVAS		MS		SCH		Tot. Diseases	
Year	n	S	n	S	n	S	n	S	n	S	n	S
2002			1	12							1	12
2003									1	26	1	26
2004					2	24			3	63	5	87
2005					1	10	1	1	4	135	6	146
2006			1	10	2	6	1	16	3	96	7	128
2007	1	21	1	28	1	1	1	24	3	113	7	187
2008					2	21			2	92	4	113
2009					2	42			6	272	8	314
2010	4	41			2	38	1	21	1	40	8	140
2011	2	36	7	165	2	19			1	64	13	284
2012	2	42	5	117	5	90			5	219	17	468
2013			1	44	5	111	2	100	2	147	10	402
2014	3	201	2	84	1	23	3	69	3	150	12	527
2015			3	79			2	35			5	114
2016					2	33	1	30			3	63
2017					1	73					1	73
Total	12	341	21	539	28	491	12	296	34	1417	107	3084

PTSD, which covered 12 trials, 341 patients and an average of 28 patients per trial. It presented only representatives between 2007 and 2014. Finally, MS had the same number of trials, and almost 300 studied patients, and spread more from 2005 to 2016.

During our study period (Fig. 1), the first VR-tested disease was PD, but discontinuously so therefore, it was possible to score SCH in this first place in 2003, but it was relegated to fourth position in 2006. The second one corresponded to CVAS in 2004, with trials in all the consecutive years included in this study, except for 2015.

Thirdly, MS trials started in 2005, but no such trials were run in five years within the study range. The last place corresponded to PTSD, which began to be tested in 2007, and was represented in only four other years with trials. After taking into account the evolution of the VR trials in all five diseases, we can state that it has increased constantly until 2014. After three years of very little research activity, the year 2005 exceeded 100 patients tested in six experiments, and 2009 already exceeded the 300 patients with eight published trials. A maximum was reached in 2012 with almost 500 patients and 17 trials.

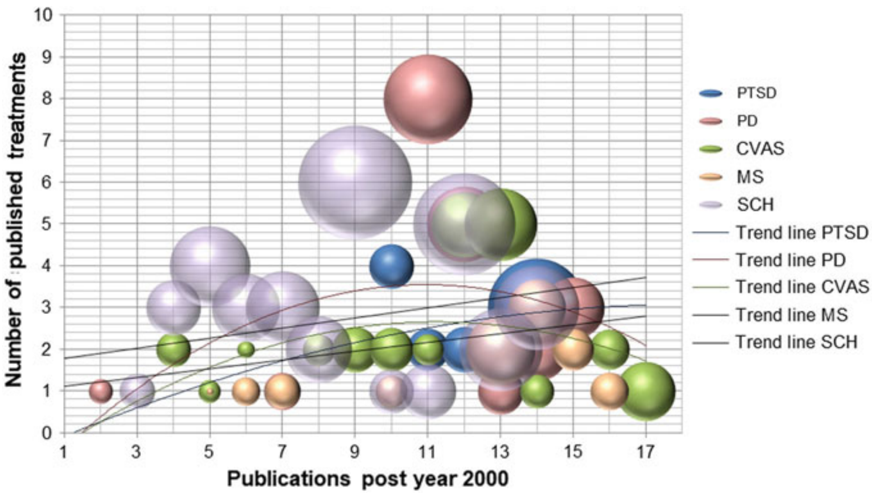

Fig. 1. Evolution of the VR- selected treatments published during 2002–2017 by size and disease

We sought the origin of each article, and assigned the authors' institutional affiliation to a country and, therefore, the number of patients who participated in trials. Table 3 reflects all this way, with a breakdown for all five studied diseases. The four final columns summarize data; e.g. the total patients involved (TPi), the number of articles/country (No. Art), population (in millions) of a country [P (m)] and the number of patients per million of the national population (P/Pi), and also for continents.

By putting this methodology into practice, 20 countries were identified with research works published on the subject. According to each country's contribution to the research of the five selected diseases, in SCH almost 40% of the patients were Koreans, followed by Americans (20%) and Israelis (12%). For PD, Taiwan obtained 35% of the total size of trials, followed by Brazil with 20%. South Korea was also a leader with 33% of the total patient population for CVAS- tested diseases, which excelled the USA and Australia with 17% and 15%, respectively. For PTSD, 83% of the research size corresponded to the USA. The last to analyze, was MS, which dominated in Spain with 37%, followed by Israel and the USA with 22% and 20%, respectively.

The country with the most published articles was the USA with 27 (Fig. 1). One in every four patients who underwent VR experimental trials was American, and the same was highlighted by the research into PTSD and SCH.

The second country on this list was South Korea with 24 articles, but practically the same number of patients as the USA, and also came in second place for relative importance given its population: 14.2 patients per million. Other remarkable countries according to number of published researches were Spain, Taiwan and Israel, whereas in population terms, and apart from South Korea, came Israel, Slovenia and Taiwan.

Table 3. Patients in the selected published VR treatments per country

Country	PTSD	PD	CVAS	MS	SCH	TPi	NºArt	P(m)	P/Pi
USA	285	29	85	59	271	729	27	325	2,2
Canada		18	6		72	96	4	36	2,6
Mexico	20					20	1	123	0,2
Brazil		109			4	113	5	207	0,5
UK		32		5	42	79	4	66	1,2
France		10			38	48	2	65	0,7
Netherlands		33				33	1	17	1,9
Germany					123	123	3	83	1,5
Austria			22			22	1	9	2,5
Italy		12		24		36	2	61	0,6
Slovenia			28			28	1	2	13,6
Portugal	10		18			28	2	10	2,7
Spain	26	34		111	43	214	9	46	4,6
S Korea		23	163		542	728	24	51	14,2
Malaysia			28			28	1	31	0,9
China		51	19		102	172	4	1382	0,1
Taiwan		188	34			222	7	23	9,4
Iran				30		30	1	80	0,4
Israel				67	180	247	6	8	28,9
New Zealand			15			15	1	5	3,2
Australia			73			73	1	24	3,0
N. America	305	47	91	59	343	845	32	485	1,7
S. America	0	109	0	0	4	113	5	511	0,2
Europe	36	121	68	140	246	611	25	738	0,8
Asia	0	262	244	97	824	1427	43	4400	0,3
Oceania	0	0	88	0	0	88	2	39	2,3
Total	341	539	491	296	1417	3084	107		

After analyzing the role of each continent, (see Fig. 2), North America specialized in PTSD research, but South America and Oceania specialized exclusively in PD and CVAS, respectively. Europe came over as being more balanced, with MS predominating the other diseases. Finally the most balanced continent of all was Asia, where SCH is emphasized with no search into PTSD. Considering the results affected by population, Oceania was the first continent with 2.3 patients per million inhabitants who underwent VR medical experiments, followed by North America (1.7) and Europe (0.8). Paradoxically, the considerable Asian activity, due to its population of 4.4 billion, came next (0.3), followed by South America (0.2) represented exclusively by Brazil.

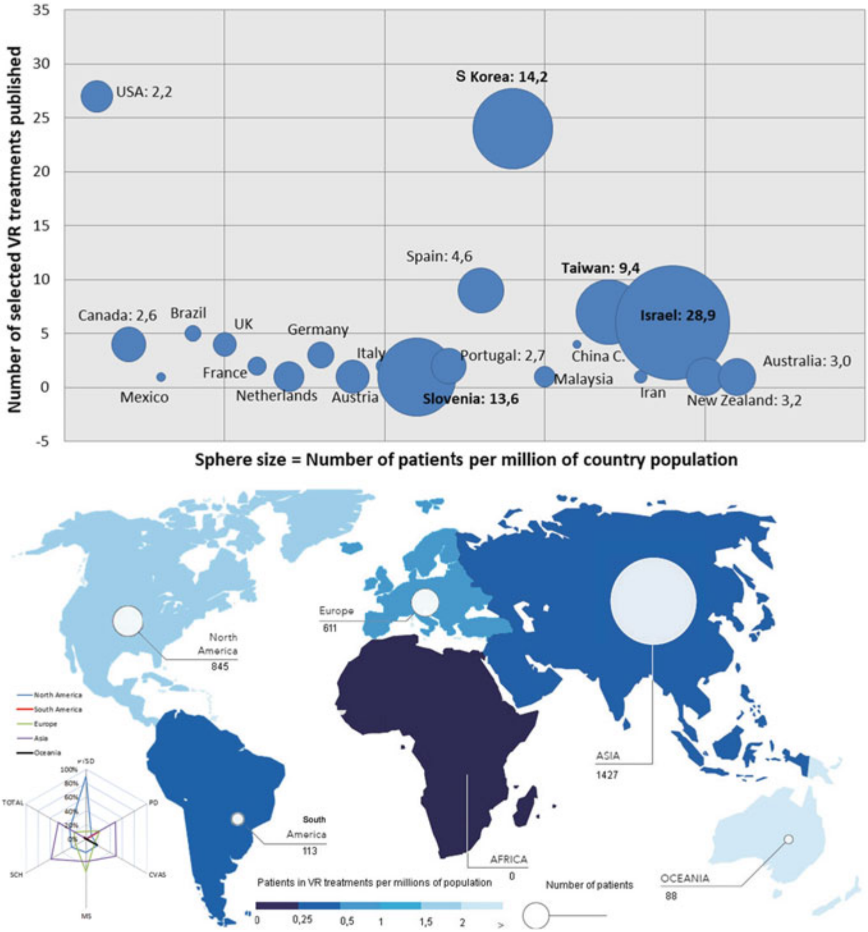

Fig. 2. Patients per millions country's population, in VR selected treatments published 2002–2017

4 Conclusions

This paper reviews the state of the art of VR treatments in selecting medical fields where trials with methodological qualities have been published more in the scientific literature in the last 15 years. This was how five diseases were found. The possibilities of VR treatment in degenerative diseases whose frequency grows with age (PD, MS), became even greater with increasing life expectancy and consequent progressive population aging. For another disease (CVAS) prevention depends on habits and healthy lifestyles which are not provided in developed countries, and whose results coincided with those where this disease treated with VR has been experienced (USA, S Korea, Australia). The large number of trials in this field, particularly in these diseases, is proof of the potential of VR treatments as an efficient alternative to traditional treatments.

Acquired pathologies and associated specific situations that their patients, (terrorism, traffic accidents, fighting in war) have lived (PTSD) is the newest addition to VR medical trials. The USA leads with the vast majority of tested patients. Its programming and methodology are not universal, but depend on emotional experience and are less effective than VR motor rehabilitation outcomes. However, the capacity of VR adaptation to the specificities of these patients is a great advantage over other treatments. The most tested disease with VR (SCH) matched that with the strongest influence of all, with about 1% of the world's population, and was more typical at the beginning of adulthood. Trials, which were studied mainly in the USA, Germany, South Korea and Israel, demonstrate its higher incidence in developed countries. Diseases with an emotional component (PTSD, SCH) also occur in young patients and youths, and they allow VR treatments to take advantage of their greater involvement and their familiarity with this technology (especially children).

Having taken into account the constant evolution of VR technology, we see that its potential will grow and access by patients will be facilitated. It is not a coincidence that technologically developed countries like Taiwan, South Korea and Israel are those highlighted in the obtained results, stressed by the extension of the VR medical experiments performed by them. Tele-rehabilitation with remote access and the possibility of accurately assessing the results are characteristics that will help its expansion and success. In the Results and Discussion section we see a country and continent specialization where these techniques are investigated and applied to specific disease types. In this way, and given the technological characteristics of treatments, it is possible to benefit communities with less sanitary infrastructure or those that lack research in this subject.

A limitation of this technology lies precisely in its flexibility and adaptation. It consists of appropriately prescribing VR treatment by evaluating the results and their correction externally. For those treatments received at home or remotely, VR supplements of medical follow-ups and controls, and their consideration and programming are necessary. For certain cases, customizing has left aside generalist VR treatments, or targets only one particular aspect of rehabilitation and leaves other objectives aside, and thus loses all the potential that can be obtained.

References

1. Health Economics Research Group, Brunel University (2008) Office of health economics, RAND Europe: medical research. What's it worth? Estimating the economic benefits from medical research in the UK. UK Evaluation Forum, London
2. Nason E, Janta B, Hastings G, Hanney S, O'Driscoll M, Wooding S (2008) Health research—making an impact. The economic and social benefits of HRB funded research. Health Research Board, Dublin. Available http://hdl.handle.net/10147/110561. Last accessed 1 Mar 2018
3. De Paula Vieira G, Freitas Guerra D, Araujo Leite MA, Correa CL (2014) Virtual reality in physical rehabilitation of patients with Parkinson's disease. J Hum Growth Devel 24(1):31–41
4. Koenig S, Ardanza A, Cortes C, De Mauro A, Lange B (2014) Introduction to low-cost motion-tracking for virtual rehabilitation. In: Pons JL, Torricelli D (eds) Emerging therapies in neurorehabilitation. Springer, Heidelberg, (Biosystems & Biorobotics, vol 4), pp 287–303. https://doi.org/10.1007/978-3-642-38556-8_15

5. Baldominos A, Sáez Y, García Del Pozo C (2015) An approach to physical rehabilitation using state-of-the art virtual reality and motion tracking technologies. Procedia Comput Sci 64:10–16. https://doi.org/10.1016/j.procs.2015.08.457
6. David L, Bouyer G, Otmane S (2017) Towards a low-cost interactive system for motor self-rehabilitation after stroke. Inter J VR 17(02):40–45
7. Howard MC (2017) A meta-analysis and systematic literature review of virtual reality rehabilitation programs. Comput Hum Behav 70:317–327. https://doi.org/10.1016/j.chb.2017.01.013
8. Darekar A, McFadyen BJ, Lamontagne A, Fung J (2015) Efficacy of virtual reality-based intervention on balance and mobility disorders post-stroke: a scoping review. J Neuroengineering Rehabil 12:46. https://doi.org/10.1186/s12984-015-0035-3
9. Kober SE, Wood G, Hofer D, Kreuzig W, Kiefer M, Neuper C (2013) Virtual reality in neurologic rehabilitation of spatial disorientation. J Neuroengineering Rehabil 10:17. https://doi.org/10.1186/1743-0003-10-17
10. Shin J, Ryu H, Jang S (2014) A task-specific interactive game-based VR rehabilitation system for patients with stroke: a usability test and two clinical experiments. J Neuroengineering Rehabil 11:32. https://doi.org/10.1186/1743-0003-11-32
11. Faria AL, Andrade A, Soares L, i Badia SB (2016) Benefits of virtual reality based cognitive rehabilitation through simulated activities of daily living: a randomized controlled trial with stroke patients. J Neuroengineering Rehabil 13:96. https://doi.org/10.1186/s12984-016-0204-z
12. Mathews M, Mitrovic A, Ohlsson S, Holland J, McKinley A (2017) A virtual reality environment for rehabilitation of prospective memory in stroke patients. Procedia Comput Sci 96:7–15. https://doi.org/10.1016/j.procs.2016.08.081
13. Cannell J, Jovic E, Rathjen A, Lane K, Tyson AT, Callisaya ML, Smith S, Ahuja K, Bird ML (2017) The efficacy of interactive, motion capture-based rehabilitation on functional outcomes in inpatient stroke population: a randomized controlled trial. Clin Rehabil 1:10. https://doi.org/10.1177/0269215517720790
14. Botella C, Serrano B, Baños RM, García-Palacio A (2015) Virtual reality exposure-based therapy for the treatment of post-traumatic stress disorder: a review of its efficacy, adequacy of the treatment protocol, and its acceptability. Neuropsychiatric Dis Treat 11:2533–2545. https://doi.org/10.2147/NDT.S89542
15. Dockx K, Bekkers E, Van den Bergh V, Ginis P, Rochester L, Hausdorff JM, Mirelman A, Nieuwboer A (2016) Virtual reality for rehabilitation in Parkinson's disease. Cochrane Database Syst Rev (12). Art. No.: CD010760. https://doi.org/10.1002/14651858.cd010760.pub2
16. Massetti T, Lopes I, Arab C, Meire F, Cardoso D, Bandeira C (2016) Virtual reality in multiple sclerosis—a systematic review. Multiple Sclerosis Relat Disord 8:107–112. https://doi.org/10.1016/j.msard.2016.05.014
17. Kalron A, Fonkatz L, Frid L, Baransi H, Achiron A (2016) The effect of balance training on postural control in people with multiple sclerosis using the CAREN virtual reality system: a pilot randomized controlled trial. J Neuroengineering Rehabil 13:13. https://doi.org/10.1186/s12984-016-0124-y
18. Marcedo M, Marques A, Queirós C (2015) Virtual reality in assessment and treatment of schizophrenia: a systematic review. Jornal brasileiro de psiquiatria:70–81. https://doi.org/10.1590/0047-2085000000059
19. Ruse S, Harvey P, Davis V, Atkins A, Fox K, Keefe R (2014) Virtual reality functional capacity assessment in schizophrenia: preliminary data regarding feasibility and correlations with cognitive and functional capacity performance. Schizophr Res: Cogn 1:e21–e26. https://doi.org/10.1016/j.scog.2014.01.004

20. Bellani M, Fornasari L, Chittaro L, Brambilla P (2011) Virtual reality in autism: state of the art. Epidemiol Psychiatr Sci 20:235–238. https://doi.org/10.1017/S2045796011000448
21. Didehbani N, Allen T, Kandalaft M, Krawczyk D, Chapman S (2016) VR social cognition training for children with high functioning autism. Comput Hum Behav 62:703–711. https://doi.org/10.1016/j.chb.2016.04.033
22. McCann RA, Armstrong CM, Skopp NA, Edwards-Stewart M, Reger GM (2014) VR exposure therapy for the treatment of anxiety disorders: an evaluation of research quality. J Anxiety Disord 28:625–631. https://doi.org/10.1016/j.janxdis.2014.05.010
23. Valmaggia LR, Latif L, Kempton MJ, Rus-Calafell M (2016) Virtual reality in the psychological treatment for mental health problems: an systematic review of recent evidence. Psychiatry Res 236:189–195. https://doi.org/10.1016/j.psychres.2016.01.015

Geometry Modelling of Regular Scaffolds for Bone Tissue Engineering: A Computational Mechanobiological Approach

A. Boccaccio(✉), M. Fiorentino, M. Gattullo, V. M. Manghisi, G. Monno, and A. E. Uva

Dipartimento di Meccanica, Matematica e Management, Politecnico di Bari, Viale Japigia 182, 70126 Bari, Italy
a.boccaccio@poliba.it

Abstract. Scaffolds are porous biomaterials that serve to replace missing portions of bone. Scaffolds must possess a proper geometry and hence have to be adequately designed to correctly undergo to the load and to favor the differentiation of the mesenchymal stem cells invading it, into osteoblasts. It is commonly known that scaffold geometry affects the quality of the regenerated bone creating within the scaffold pores. Scaffold properly designed trigger favorable values of biophysical stimuli that are responsible for the reactions cascade leading to the bone formation. In this paper an optimization algorithm is proposed that, based on mechano-regulation criteria, identifies the optimal geometry of scaffolds, i.e. the geometry that favors the formation of the largest amounts of bone in the shortest time. In detail, the algorithm, written in the Matlab environment, incorporates parametric finite element models of different scaffold types, a computational mechanobiological model and structural optimization routines. The scaffold geometry is iteratively perturbed by the algorithm until the optimal geometry is computed, i.e. the geometry that triggers the most favorable values of the biophysical stimulus which lead to the formation of mature bone. Mesenchymal stem cells were hypothesized to spread within the fracture domain and uniformly occupy the scaffold pores.

Keywords: Unit cell geometry · Hexahedron unit cell · Rhombicuboctahedron unit cell · Mechanobiology

1 Introduction

1.1 Scaffold Design

In order to preserve the physiological functionality after traumatic events, bone is subjected to continuous remodeling. However, specific diseases may alter the bone remodeling process and hence can make the bone tissue unable to maintain unaltered the original mechanical properties. In such a case, fractured bones require mandatorily surgical operations to re-establish the structural integrity. Large dimension defects in bone require the implantation of scaffolds that work as an incubator favoring the proliferation of the mesenchymal stem cells and their differentiations into specific

F. Cavas-Martínez et al. (Eds.): *Advances on Mechanics, Design Engineering and Manufacturing II*, LNME, pp. 517–526, 2019.
https://doi.org/10.1007/978-3-030-12346-8_50

phenotypes. An aspect of crucial importance that should be taken into account in the design process of scaffolds is that they have to promote and favor vascularization and production of extra-cellular matrix. Furthermore, they have to transfer the load to the adjacent tissues in the most “natural” manner.

The design process of scaffolds is a very challenging task. The large number of variables to be taken into account, the difficulty in modelling the mechanical behavior of the bone tissue, the complexity of the scaffold geometry, are aspects that the scaffold designer has to face.

Currently, in tissue engineering, the typical approach adopted to design scaffolds is the trial-and-error approach, where, a given scaffold geometry is changed based on the results of experimental studies. The recent development of bioreactors allowed more reliable in vitro experiments to be carried out thus consequently, favoring the adoption of the trial-and-error approach. However, the trial-and-error approach requires the adoption of costly protocols both in economic terms and in terms of time [1]. Furthermore, it is important to consider that the results obtained with in vivo experiments are, in general, different from those obtained in vitro. For example, while in vivo high porosity values produce large quantities of bone, on the contrary in vitro, low porosity values favor bone regeneration [2]. This must necessarily be taken into account when designing the scaffold.

1.2 The State of the Art

The computational models allow simulating the process of differentiation of the tissues that originate in scaffolds. Furthermore, the use of mechanobiological models not only allows us to predict the differentiation patterns experimentally observed but also to further deepen all the mechanisms that govern bone regeneration. In-Depth knowledge of these mechanisms leads, of course, to more reliable scaffold designs [3, 4].

In the design of the scaffolds, the integration between CAD and FEM tools is particularly useful. By combining CAD and rapid prototyping techniques it is possible to physically produce scaffolds and design structures mimicking the natural structure to be replaced [5–7]. Furthermore, conventional scaffold fabrication can be improved by controlling scaffold microstructure, regulating cell distribution and incorporating cells into scaffolds [8].

The scaffolds produced by rapid prototyping techniques show a rather low resolution and a rather smooth surface. The latter fact does not favorite initial cell adhesion. Although such an issue was properly addressed in the recent literature [9], conventional production techniques were made controllable and hence limited the use of CAD to the reconstruction of scaffold geometries [2].

The mechanical environment certainly exerts a considerable influence on the process of bone regeneration [10]. It is commonly known, in fact, that controlled quantities of motion in the vicinity of a bone fracture favor the healing process. However, when these motions become excessively large, they have a negative effect on the bone regeneration process [11].

Numerous studies have been conducted aimed at identifying the relationship that exists between the mechanical environment and the cascade of biological processes that occurs during the bone regeneration process. One of the first studies [12] of this type dates back to the 19th century that found that stem cells react to mechanical stimuli. The branch of biology that deals with studying the relationship between mechanics and biology is known as mechanobiology. Obviously, the knowledge of the relationships between mechanical stimulation and cellular response could favor the development of techniques to mechanically stimulate the bone and the development of therapeutic strategies aimed at minimizing healing times.

Mechanobiology studies how the mechanical forces produce a biophysical stimulus and how this stimulus is received by stem cells [13]. The large number of variables involved makes the experimental study of the mechano-regulation processes extremely complex. Experimentally, it is almost impossible to replicate the same experiment by changing only one variable at a time and it is therefore difficult to associate a certain effect with a specific variable. In mechanobiological computational models, instead, it is possible to study the effect of the single variable and thus acquire a wider knowledge of the phenomenon. Very often, computational models are combined with experimental models and this helps to deduce further conclusions regarding the mechanical environment and biophysical stimulus relationship [13]. Furthermore, the development of computational models suggests further experiments to be carried out aimed at deducing further conclusions.

One of the first computational models of mechano-regulation was the one developed by Pauwels [14] who hypothesized that cellular differentiation is mainly governed by two stress tensor invariants, i.e. the octahedral shear stress and the hydrostatic stress. For example, Pauwels found that high values of hydrostatic stress and low octahedral shear stress values favor cartilage formation. In contrast, high levels of octahedral shear stress and low values of hydrostatic stress lead to the formation of fibrous tissue. A number of other theories were successively developed as well as experimental studies aimed at identifying the computational model that best reproduces the process of tissue differentiation observed in vivo or in vitro. One of the most important mechano-regulation models is the one developed by Prendergast and Huiskes [15], which hypothesizes that the biophysical stimulus is a function of the deviatoric strain and of the fluid velocity.

1.3 The Theoretical Model

Prendergast et al. [15] modeled the bone as a poroelastic biphasic material and hypothesized that the biophysical stimulus S that regulates the tissue differentiation process is a function of the octahedral shear strain γ and of the interstitial fluid flow ν:

$$S = \frac{\gamma}{a} + \frac{v}{b} \tag{1}$$

being a and b empirical constants [16], with the following values $a = 0.0375$ and $b = 3\ \mu\text{m s}^{-1}$. In detail, based on the specific values that S assumes, the following tissue phenotypes create [17, 18]:

$$\text{If} \begin{cases} S > 3 \Rightarrow \textit{fibroblast and fibrous tissue formation} \\ 1 < S < m \Rightarrow \textit{chondrocyte and cartilagineous tissue formation} \\ 0.53 < S < 1 \Rightarrow \textit{osteoblast and immature bone tissue formation} \\ 0.01 < S < 0.53 \Rightarrow \textit{osteoblast and mature bone tissue formation} \\ 0 < S < 0.01 \Rightarrow \textit{bone resorbtion} \end{cases} \quad (2)$$

This mechano-regulation model was combined with finite element models simulating the anatomical region where bone regeneration takes place. The FEM provides the values of octahedral shear strain and of the interstitial fluid flow agent in the mesenchymal tissue and thus allows to know, in the fracture domain, the value assumed by S point by point. Using this approach, the algorithm has been successfully used to predict the pattern of tissue differentiation in fractured irregular bones and to simulate the bone regeneration process in time [19–23].

Other computational models have been proposed that take into account not only mechanobiological factors but also biochemical factors such as growth factors [24]. Another aspect that can also be considered is vascularization [25].

In this study we implemented the mechanobiological model of Prendergast et al. [15] to determine the optimal geometry of scaffolds with different unit cell geometries, namely: hexahedron unit cell with homogeneous porosity, hexahedron unit cell with functionally graded porosity, rhombicuboctahedron unit cell.

2 Hexahedron Unit Cell, Homogeneous Porosity

A parametric finite element model of a regular scaffold based on the hexahedron unit cell with circular holes was developed (Fig. 1). Each unit cell can be obtained starting from a cubic volume where cylindrical holes are realized along the three directions of the coordinate axes. The radius R of the holes was considered as the parameter that was optimized via the algorithm below described. The scaffold pores were hypothesized to be filled with granulation tissue [26] that was obtained with the Boolean operation of subtraction: from the cubic volume delimiting the entire scaffold, the volume of the scaffold itself. The bottom surface of the model was hypothesized to be clamped while a distributed compression load was applied on the top surface via a rigid plate that guarantees the equality of the displacements (measured in the proximity of the top surface) experienced by the granulation tissue and those experienced by the scaffold itself. Three different values of force were considered that give origin to the following values of force per unit area: 0.1 MPa, 0.5 MPa and 1.0 MPa. To simulate the free exudation, the pore pressure p_{pore} acting on the outer surface of the granulation tissue was hypothesized equal to zero: p_{pore}= 0 MPa. The same modelling strategy was adopted in a previous study [27]. The model was built and discretized with tetrahedral poroelastic finite elements (C3D4P) in Abaqus 6.12 (Dassault Systèmes, France) (Fig. 2). The scaffold was modelled with a linear elastic material with a Young's modulus of 1000 MPa, according to Byrne et al. [27]. In Table 1 the values of the material properties utilized in the model of the granulation tissue occupying the scaffold pores are listed.

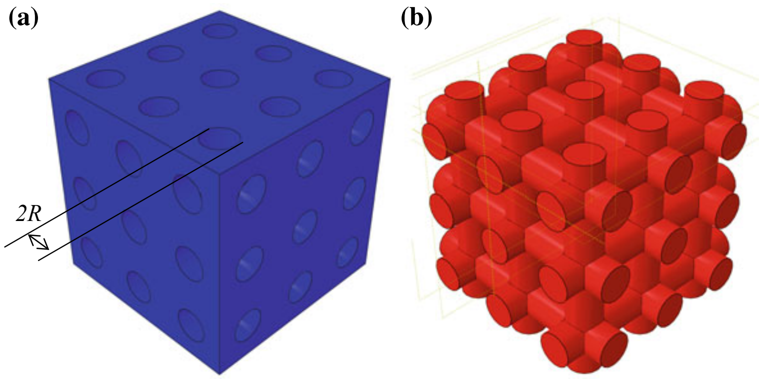

Fig. 1. **a** CAD model of scaffold (highlighted in blue) and granulation tissue (highlighted in red)

Table 1. Value of the material properties implemented for granulation tissue

Material property	Value
Young's modulus	0.2 MPa
Poisson's ratio	0.167
Bulk modulus grain	2300 MPa
Bulk modulus fluid	2300 MPa

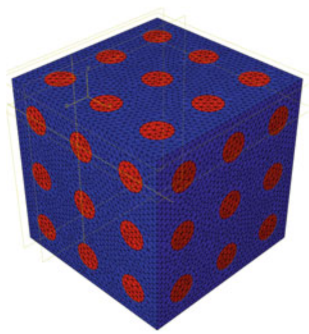

Fig. 2. Finite element mesh utilized in the model

The model included about 50000 nodes and 250,000 elements (Fig. 2). A tie constraint was fixed between the surface of the granulation tissue and the adjacent surface of the scaffold. Thanks to this strategy, no contact algorithms were implemented in the analysis thus significantly simplifying the FE computation.

By implementing the function *fmincon* available in Matlab, a mechanobiology-based optimization algorithm was developed that combines the finite element model of the scaffold, with the computational mechanobiological model by Prendergast et al.

[15]. The algorithm perturbs the scaffold geometry and computes the biophysical stimulus acting on the volume domain highlighted in red (Fig. 1). Therefore, it determines the distance between the computed stimulus and the value of an ideal stimulus that corresponds to the formation of mature bone. The algorithm stops once this distance becomes smaller than an a priori fixed value ε (Fig. 3).

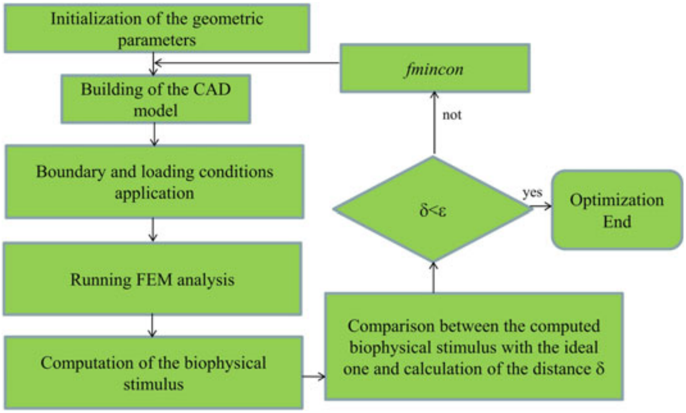

Fig. 3. Schematic of the algorithm implemented in Matlab environment to optimize the scaffold geometry

In Table 2 the values of *R* for each of the hypothesized values of the compression loading are listed. The predicted dimensions of the pores are consistent with those reported in experimental studies [28].

Table 2. Optimal values of *R* for different values of the compression load

Pressure	Radius *R*
0.1 MPa	285 μm
0.5 MPa	245 μm
1.0 MPa	215 μm

3 Hexahedron Unit Cell, Functionally Graded Porosity

The same algorithm above described was utilized to determine the function $R = R(y)$ of the pore radius R along the vertical direction y. In other words, we determine the shape of the function that describes how the porosity of functionally graded scaffolds must change in the space [29] (Fig. 4).

Table 3 list the values of R in function of y, in the case of pure compression and shear load. Interestingly, it can be seen that in the case of compression, the optimal scaffold tend to have all the pores with the same dimensions. Other boundary and loading conditions can be investigated with the proposed mechanobiological algorithm.

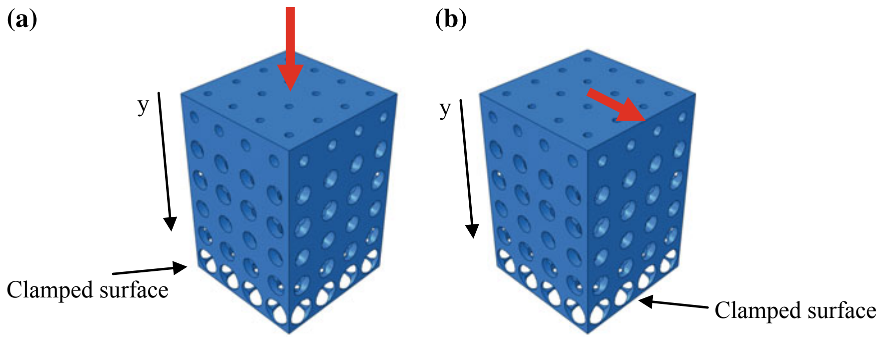

Fig. 4. CAD Model of the scaffold with functionally graded porosity subjected to compression (**a**) and shear (**b**) load

Table 3. Optimal values of *R* predicted by the algorithm and expressed in function of y (Fig. 4)

y (μm)	Radius *R* (μm) compression	Radius *R* (μm) shear load
0	194.36	217.81
318.5	196.29	211.5
637	198.22	205.19
955.5	200.15	198.88
1274	202.08	192.57
1592.5	201.08	186.26
1911	199.35	179.95
2229.5	197.63	178.77
2548	195.91	177.59
2866.5	193.25	176.42
3185	191.32	175.24
3503.5	189.38	174.06
3822	187.44	172.88

4 Rhombicuboctahedron Unit Cell

The same algorithm as that shown in Fig. 3 was implemented to determine the optimal geometry of a scaffold based on the rhombicuboctahedron unit cell [30] (Fig. 5).

In Table 4 are listed the values of the radius *R* of each beam element included in the scaffold in function of the compression load applied on the scaffold itself.

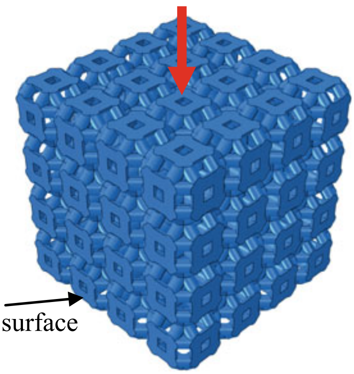

Fig. 5. CAD Model of the scaffold based on the rhombicuboctahedron unit cell

Table 4. Optimal values of *R* predicted by the algorithm in function of the compression load

Load (MPa)	0.05	0.1	0.5	1	1.5
Radius *R* (μm)	24.07	32.69	63.05	76.00	76.00

Interestingly, the patterns of the bony tissue predicted with the proposed algorithm are consistent with those observed experimentally [28]. Future research should be carried out on the mechanobiological optimization of irregular load adapted scaffolds [31].

5 Conclusions

The optimal geometry of scaffolds based on different unit cell geometries was determined via a mechanobiology-based optimization algorithm. Different boundary and loading conditions were considered. The algorithm successfully predicted the micro-architecture favoring the formation of the largest volumes of bone.

References

1. Sanz-Herrera J, Garca-Aznar J, Doblaré M (2009) A mathematical approach to bone tissue engineering. Philos Trans Roy Soc Lond A: Math Phys Eng Sci 367:2055–2078
2. Karageorgiou V, Kaplan D (2005) Porosity of 3D biomaterial scaffolds and osteogenesis. Biomaterials 26:5474–5491
3. Sun W, Lal P (2002) Recent development on computer aided tissue engineering—a review. Comput Methods Programs Biomed 67:85–103
4. Sun W, Darling A, Starly B, Nam J (2004) Computer-aided tissue engineering: overview, scope and challenges. Biotechnol Appl Biochem 39:29–47
5. Ambu R, Morabito A (2017) Design and analysis of tissue engineering scaffolds based on open porous non-stochastic cells. In: Advances on mechanics, design engineering and manufacturing. Springer, pp 777–787

6. Carofalo A, De Giorgi M, Morabito A (2013) Geometric modelling of metallic foams. Eng Comput 30:924–935
7. Ambu R, Morabito A (2018) Porous scaffold design based on minimal surfaces: development and assessment of variable architectures. Symmetry 10:361
8. Li M, Tian X, Chen X (2009) A brief review of dispensing-based rapid prototyping techniques in tissue scaffold fabrication: role of modeling on scaffold properties prediction. Biofabrication 1:032001
9. Kim GH, Ahn SH, Lee HJ, Lee S, Cho Y, Chun W (2011) A new hybrid scaffold using rapid prototyping and electrohydrodynamic direct writing for bone tissue regeneration. J Mater Chem 21:19138–19143
10. McKibbin B (1978) The biology of fracture healing in long bones. J Bone Jt Surg British volume. 60:150–162
11. Goodship A, Kenwright J (1985) The influence of induced micromovement upon the healing of experimental tibial fractures. Bone Jt J 67:650–655
12. Roux W (1895) Gesammelte abhandulgen uber entwicklungsmechanics der organismen. Wilhem Engelmann, Leipzig
13. van der Meulen MC, Huiskes R (2002) Why mechanobiology? A survey article. J Biomech 35:401–414
14. Pauwels F (1941) Grundrieb einer Biomechanik der Fracturheiling. In: 34e Kongress der Deutschen Orthopadischen Gesellschaft Stuttgart: Ferdinand Engke, pp 464–508
15. Prendergast P, Huiskes R, Søballe K (1997) Biophysical stimuli on cells during tissue differentiation at implant interfaces. J Biomech 30:539–548
16. Huiskes R, Van Driel W, Prendergast P, Søballe K (1997) A biomechanical regulatory model for periprosthetic fibrous-tissue differentiation. J Mater Sci Mater Med 8:785–788
17. Lacroix D, Prendergast P (2002) A mechano-regulation model for tissue differentiation during fracture healing: analysis of gap size and loading. J Biomech 35:1163–1171
18. Kelly D, Prendergast P (2005) Mechano-regulation of stem cell differentiation and tissue regeneration in osteochondral defects. J Biomech 38:1413–1422
19. Boccaccio A, Kelly DJ, Pappalettere C (2011) A mechano-regulation model of fracture repair in vertebral bodies. J Orthop Res 29:433–443
20. Boccaccio A, Pappalettere C, Kelly D (2007) The influence of expansion rates on mandibular distraction osteogenesis: a computational analysis. Ann Biomed Eng 35:1940–1960
21. Boccaccio A, Prendergast PJ, Pappalettere C, Kelly DJ (2008) Tissue differentiation and bone regeneration in an osteotomized mandible: a computational analysis of the latency period. Med Biol Eng Compu 46:283–298
22. Boccaccio A, Lamberti L, Pappalettere C (2008) Effects of aging on the latency period in mandibular distraction osteogenesis: a computational mechanobiological analysis. J Mech Med Biology 8:203–225
23. Boccaccio A, Kelly DJ, Pappalettere C (2012) A model of tissue differentiation and bone remodelling in fractured vertebrae treated with minimally invasive percutaneous fixation. Med Biol Eng Compu 50:947–959
24. Bailon-Plaza A, Van Der Meulen MC (2001) A mathematical framework to study the effects of growth factor influences on fracture healing. J Theor Biol 212:191–209
25. Geris L, Gerisch A, Vander Sloten J, Weiner R, Van Oosterwyck H (2008) Angiogenesis in bone fracture healing: a bioregulatory model. J Theor Biol 251:137–158
26. Boccaccio A, Uva AE, Fiorentino M, Lamberti L, Monno G (2016) A mechanobiology-based algorithm to optimize the microstructure geometry of bone tissue scaffolds. Int J Biol Sci 12:1–17

27. Byrne DP, Lacroix D, Planell JA, Kelly DJ, Prendergast PJ (2007) Simulation of tissue differentiation in a scaffold as a function of porosity, Young's modulus and dissolution rate: application of mechanobiological models in tissue engineering. Biomaterials 28:5544–5554
28. Zadpoor AA (2015) Bone tissue regeneration: the role of scaffold geometry. Biomater Sci 3:231–245
29. Boccaccio A, Uva AE, Fiorentino M, Mori G, Monno G (2016) Geometry design optimization of functionally graded scaffolds for bone tissue engineering: a mechanobiological approach. PLoS ONE 11:e0146935
30. Boccaccio A, Fiorentino M, Uva AE, Laghetti LN, Monno G (2018) Rhombicuboctahedron unit cell based scaffolds for bone regeneration: geometry optimization with a mechanobiology – driven algorithm. Mater Sci Eng, C 83:51–66
31. Naddeo F, Cappetti N, Naddeo A (2017) Novel "load adaptive algorithm based" procedure for 3D printing of cancellous bone-inspired structures. Compos Part B: Eng 115:60–69

Parenthood Perception Enhancement Through Interaction with 3D Printed Fetal Face Models

D. Speranza[1](✉), F. Padula[2], B. Motyl[3], S. Tornincasa[4], F. Marcolin[4], E. Vezzetti[4], and M. Martorelli[5]

[1] Department of Civil and Mechanical Engineering, University of Cassino and Southern Lazio, via G. Di Biasio, 43, 03043 Cassino, Italy
d.speranza@unicas.it
[2] Department of Prenatal Diagnosis, ALTAMEDICA, Fetal Maternal Medical Centre, Rome, Italy
[3] Polytechnic Department of Engineering and Architecture, University of Udine, Udine, Italy
[4] Department of Management and Production Engineering, Politecnico di Torino, Turin, Italy
[5] Department of Industrial Engineering, University of Naples Federico II, P.le Tecchio 80, 80125 Naples, Italy

Abstract. This paper deals with parenthood perception (maternal and paternal) after the visualization and interaction (touch) with a 3D printed facial fetal model. The model is created using Additive Manufacturing techniques, starting from the image elaboration of routine ultrasound data. In this study, the method used for the elaboration and construction of 3D printable models of fetal faces starting from routine ultrasound images is briefly described. In addition, we present the results of a new survey conducted with future parents at the Altamedica clinic (Rome, Italy) to verify whether there are any benefits derived from the use of 3D printing models with future parents, both regarding the improvement of the parenthood experience, and the improvement of the understanding and collaboration with the physicians in case of fetal malformations, using 3D models coupled with the data of routine ultrasound examinations.

Keywords: Additive manufacturing · Image processing · 3D ultrasound · Fetal face · Survey · Parenthood perception

1 Introduction

It has been reported [1, 2] that fetal visualization at ultrasound (US) allows future parents to start a positive emotional relationship with their newborn child. The view of the baby's first picture (2D or 3D US data) is one of the most memorable moments for future parents [3].

Also, since Additive Manufacturing (AM) technologies are widely used in different fields, and above all in medical applications, they represent promising techniques in terms of both usage and benefits, including the creation of prostheses and 3D anatomical models, and the printing of human organs [4–8].

F. Cavas-Martínez et al. (Eds.): *Advances on Mechanics, Design Engineering and Manufacturing II*, LNME, pp. 527–535, 2019.
https://doi.org/10.1007/978-3-030-12346-8_51

Recent studies [9–14] have shown that 3D modeling from US imaging can help physicians in the prenatal screening of complex fetal abnormalities [15, 16]. Therefore, 3D printing can be considered as the next step of 3D/4D US.

Under these conditions, the study of the emotional impact on parenthood (maternal and paternal) due to the use of real 3D printed models is an interesting aspect to explore.

Recently, we conducted a preliminary investigation on these topics to understand the degree of interest in this type of models and how these same models can be perceived by the parents both in terms of aesthetic utility and/or memory maintenance, and in relation to the display of possible fetal malformations [17]. In this new study, we have further improved the quality of the model printed in 3D and we would also like to investigate, in more detail, the perceptions of the future parents after the interaction with a 3D model of a fetal face, extending the sample of parents involved in the previous study.

2 Fetal Face Detection and 3D Model Reconstruction

The process to create the 3D printable model begins by acquiring the image stack generated by a 3D-US prenatal routine examination at 21 and at 34 weeks of gestation. Data volume acquisitions were conducted with the latest generation of GE Healthcare Voluson and Samsung Medison ultrasound systems (Fig. 1).

The steps of the proposed reconstruction method are the typical steps of medical imaging, namely filtering, segmentation, and extraction of the Region of Interest (ROI).

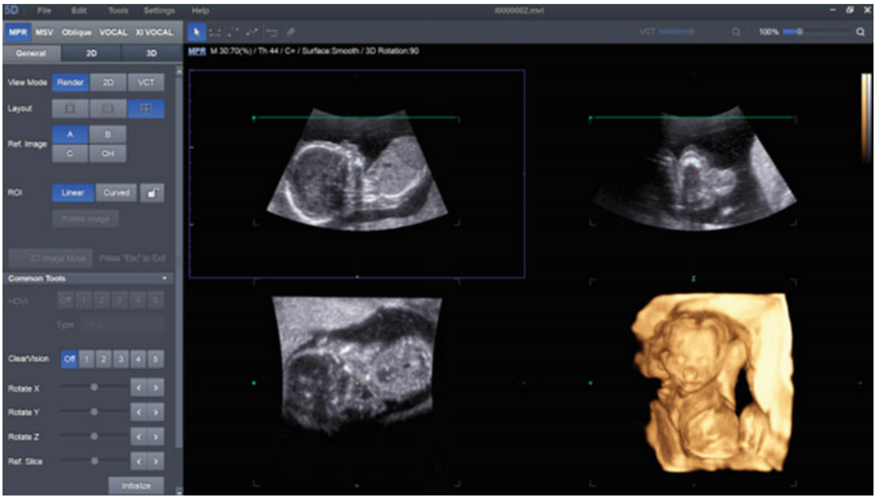

Fig. 1. Screenshot from 5D Viewer by Samsung Medison [20]

However, this procedure presents some disadvantages such as the inability to directly export the proprietary volumetric dataset, usually in a .VOO or .MVL file format, in a standard file format for 3D modeling (e.g. IGES, …).

Recently, the latest version of 4DView, the software used for processing ultrasonic data sets with GE Voluson systems [18], allows you to directly export the reconstructed 3D data volume in a .STL format. However, it is not possible to intervene manually on the reconstruction process and the used segmentation algorithms are not explicit, so the 3D reconstructed model often presents defects.

It is, therefore, more convenient to manually export the stack of 2D images through the GE Voluson 4D View or the Samsung Medison 5D Viewer applications [18, 19]. Hence, first, the stack must be exported from the US system, using an image file format (for example .jpeg, .bmp, .tiff), and second it must be reconstructed manually in another environment, using specific applications for data volumes analysis and management.

The manual reconstruction phase presents some problems. The first problem is that the resolution of the saved image depends on the US system used. The second problem is the impossibility of simultaneously saving the various images (slices) that constitute the volumetric dataset. So, to overcome these problems, it was necessary to repeat the saving operation up to 250 times, depending on the total number of slices that compose the data volume being processed. In this study, a slice consists of a 2D image that represents a section of the volume of the acquired anatomical part, with a non-null thickness between 0.3 and 0.5 mm, which corresponds to the height of the considered voxels. A Recursive Gaussian Filter (with sigma value set to 1) was used to blur the image and reduce noise.

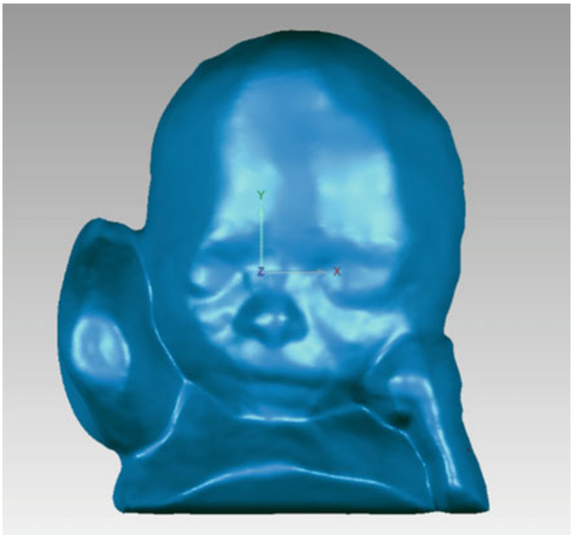

Fig. 2. Example of model elaborated with Geomagic Studio

The next phase is the segmentation of the data volumes to highlight the desired anatomic parts (in this case the face of the fetus). Medical images must then be segmented to identify regions of interest (ROI). The reconstruction phase of the 3D model is performed using an algorithm implemented in many of the most popular open-source [20, 21] and commercial [22–25] software packages for medical image elaboration.

In this case, an automatic segmentation procedure was performed, based on the selection of gray thresholds, with a gray scale ranging from 50 to 255 [26]. If necessary, morphological filters can be applied to improve the definition of the obtained contour definition.

After segmentation, the generated file may present some defects as anatomical parts and/or elements that do not belong to the face of the fetus. Therefore, it is necessary to further process the model with a CAD software before generating the .STL model and the G code for 3D printing. As a consequence, the face model is first translated into a point cloud format (for example .xyz file format), and then it is processed with Geomagic Studio software [27], to clean and eliminate possible errors (holes, separate parts, etc.). Subsequently, the polygonal mesh surface is created to obtain a 3D CAD model (Fig. 2). The resulting mesh is automatically and directly converted into an STL

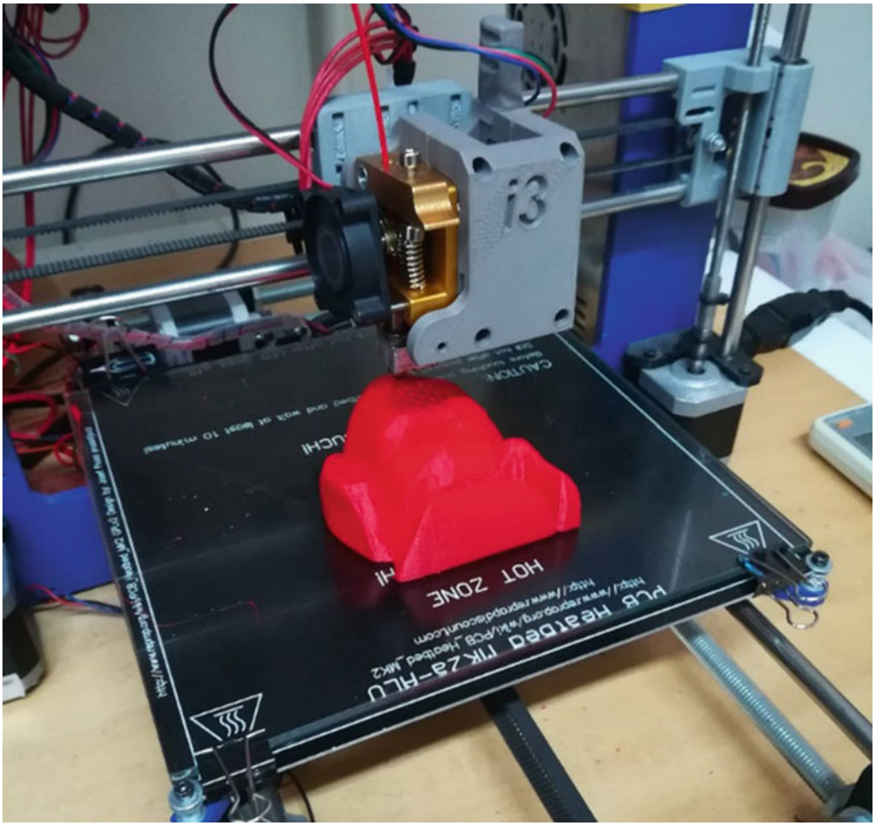

Fig. 3. Prusa I3, 3D FDM printer

file format suitable for 3D printing. Then, the G-code file for printing is obtained using Cura software [28]. Following this procedure, the total amount of time usually needed by a single operator, to process a single face model, is between 5 and 6 h.

Two kinds of 3D printers were used for printing the models (Fig. 3): a Zortrax M200 and a BQ Prusa i3 Hephestos. These printers are based on FDM building technology and use ABS and/or PLA materials. Table 1 shows the printing parameters used.

The models were printed in three colors, white, red and ancient pink (Fig. 4).

Table 1. Printing parameters

Parameters	Values/settings
Material	PLA, ABS
Quality: layer height	0.1–0.2 mm
Shell: wall thickness	1 mm
Infill	20%
Printing temperature	215 °C (PLA)–255 °C (ABS)
Diameter	1.75 mm
Flow	100%
Print speed	400 mm/s
Travel speed	120 mm/s
Build plate adhesion type	Raft Raft air gap 0.3 mm Initial layer Z overlap 0.15 mm Raft top layers 2

Fig. 4. 3D printed models in PLA material with two colors, red and ancient pink

3 Methods

From January 2018, 224 patients (mothers) and their partners (if presents) were involved in this study. These women went to the Altamedica Fetal-Maternal Medical Center (Rome, Italy) to perform a US scan at any gestational age. Each patient answered a questionnaire, after having observed, touched and interacted, for a few minutes, with a 3D facial model of a 21-week fetus (Fig. 4). The questionnaire consisted of 21 items that explored socio-demographic information of the sample, the perception of emotions and tactile sensations evoked by the model, the perception of the utility of the model itself in case of fetal malformation, and the subjective evaluation of the model.

4 Results

All the enrolled women and their partner accepted to participate in the survey without problems. The sample of 224 subjects consisted of 60% of women and the remaining 40% of men. The average age of the participants is about 34 years (Table 2).

Considering the level of education, 75% of the whole sample has a high school degree, 23% a university degree, and 2% a primary school qualification.

According to the gestational age, we had about 35% in the first trimester, 35% in the second and 30% in the third trimester.

Most of the interviewed (87.5%) had heard about 3D printing, and only a small percentage of them (14.2%) had read about baby 3D printing.

Almost all of the subjects (92.8%) enjoyed the model, in particular, they liked the shape and the tactile sensation, but they didn't appreciate the color and the material.

In general, (78.5%), when they touched the model, they felt a positive sensation (50% male vs 50% female), in particular, a 75% of them would touch the 3D model of their own baby (43% male vs 57% female).

However, only a 44.6% of them think that the model could make the presence of their baby more real (36% male vs 64% female).

The 39.2% of parents think their children could enjoy touching the 3D model of their future sibling before the birth. Comparing a 3D scan to the model, most of them (62.5%) feel differences, especially women (34.3% male vs. 65.7% female).

Table 2. Socio-demographic information of the parents' sample

Interviewed subjects	Females #	%	Males #	%
Tot: 224	136	60.8	88	39.2
Age distribution (years)	#	%	#	%
<35	76	33.9	40	17.9
>=35	60	26.8	48	21.4

Furthermore, they don't think that the model could be very useful to create a maternal bonding (median value 3, ranging from 1 not useful, to 5 very useful) or a stronger parental bonding (median value 3, ranging from 1 not useful, to 5 very useful).

A part of the interviewed (28.5%) think that they would have indifferent feelings to see the model after birth (especially women 68.7% vs men 31.3) and that it wouldn't be so useful to strengthen the positive memories of their pregnancy (60.7%).

Table 3. Answers to "would you like to own this model for?" (multiple responses were possible)

Categories of responses	% All	% Mothers	% Fathers
Memory of pregnancy	51.3	50.0	53.6
Birth announcement	9.2	6.3	14.3
Create a positive moment	17.1	14.6	21.4
Create a bond with brothers/sisters	13.2	16.7	7.1
Support in case of malformation	7.9	10.4	3.6
Not responding	1.3	2.1	–

Furthermore, in case of fetal malformation, only a 25% of them, think the model could be very useful to understand the pathology.

Globally, they think the model has a median value of 4 (ranging from 1 low to 5 high). They liked mainly the possibility to have a memory of the time they were pregnant (Table 3) and, especially the interviewed women think that the model could be useful, not only for medical purposes but also for creating a bonding with the other siblings.

Only a 32.6% of the interviewed wrote what they didn't like about the model, and they reported that the material and the color were the main characteristics (Table 4).

Table 4. Answers to "what features of this model do not you like?" (multiple responses were possible)

	N	%
Color	16	9.3
Shape	4	2.3
Material	28	16.3
Utility	8	4.7
Not responding	116	67.4

5 Discussion

As soon as 3D/4D US was introduced, its use has been appreciated not only to improve a medical diagnosis but also to positively affect maternal-fetal bonding.

Nowadays, the use of Additive Manufacturing techniques let the parents see and touch models extracted from routine US data of fetal faces.

While discussing whether these techniques can be useful in the medical field in case of fetal abnormalities, it is interesting to investigate the emotional impact they may have on parents and their expectations.

We have recently conducted a pilot study on the interest of a 3D face model of a fetus at 32 weeks. After improving the 3D extraction techniques, we decided to interview a wider population of pregnant women and their partners [17].

In both studies, the model evokes similar positive sensations (in this study 78.5% vs 72% in the pilot study). The value of the model has increased (from a median value of 3 to 4), and the interviewed may appreciate a difference between 3D US and the model (from 46 to 62.5%). However, they have not changed their mind about the role of the model in creating or strengthening a parental bonding.

This survey demonstrates a higher interest towards the 3D model that is considered mainly as a positive memory of pregnancy. It also underlines the need to improve the quality of the 3D model, choosing better materials and more realistic colors.

6 Conclusion

We have analyzed the possible benefits of 3D printing/ Additive Manufacturing in the use of 3D models in pregnancy. Also, we have investigated whether 3D printed models may contribute to enhance the parenthood perception of future parents. As observed and reported in the discussion section we believe that 3D printing is gradually becoming the next step of 3D US, but we need further research by an interdisciplinary team, to produce better 3D models that could also be suitable for medical, affective and diagnostic purposes, in clinical practice.

Acknowledgements. The research work reported here was made possible by collaboration with the Altamedica Clinic Research Group (Rome, Italy).

References

1. Menozzi F, Mazzoni S, Ammaniti M (2014) Co-parenting during pregnancy and ultrasound image of the baby, vol 35. In: 14th World Association for Infant Mental Health, World Congress. Supplement to the Infant Mental Health Journal, Scotland, pp 177
2. Ammaniti M, Trentini C, Menozzi F, Tambelli R (2014) Transition to parenthood: studies of Intersubjectivity in Mothers and Fathers. In: Emde RN, Leuzinger-Bohleber M (eds) Early parenting and prevention of disorder: psychoanalytic research at interdisciplinary Frontiers. Karnac, London, pp 129–164
3. de Jong-Pleij EAP, Ribbert LSM, Pistorius LR, Tromp E, Mulder EJH, Bilardo CM (2013) Three-dimensional ultrasound and maternal bonding, a third-trimester study and a review. Prenat Diagn 33:81–88. https://doi.org/10.1002/pd.4013
4. Thompson MK, Moroni G, Vaneker T et al (2016) Design for additive manufacturing: trends, opportunities, considerations, and constraints. CIRP Ann Manuf Technol 65(2):737–760. https://doi.org/10.1016/j.cirp.2016.05.004
5. Gibson I, Rosen D, Stucker B (2015) Additive manufacturing technologies: 3D printing, rapid prototyping, and direct digital manufacturing, 2nd edn. Springer

6. Clemente C, Esposito L, Speranza D, Bonora N Firecracker eye exposure: experimental study and simulation. Biomech Mode Mechanobiol 16(4):1401–1411. https://doi.org/10.1007/s12008-014-0244-1
7. Petzold R, Zeilhofer HF, Kalender WA (1999) Rapid prototyping technology in medicine-basics and applications. Comput Med Imaging Graphics 23(5):277–284. https://doi.org/10.1016/S0895-6111(99)00025-7
8. Jacobs CA, Lin AY (2017) A new classification of three-dimensional printing technologies: systematic review of three-dimensional printing for patient-specific craniomaxillofacial surgery. Plast Reconstr Surg 139(5):1211–1220. https://doi.org/10.1097/prs.0000000000003232
9. Marro A, Bandukwala T, Mak W (2016) Three-dimensional printing and medical imaging: a review of the methods and applications. Curr Prob Diagn Radiol 45(1):2–9. https://doi.org/10.1067/j.cpradiol.2015.07.009
10. Menezes GA, Araujo Júnior E, Lopes J, Belmonte S, Tonni G, Werner H (2016) Prenatal diagnosis and physical model reconstruction of agnathia–otocephaly with limb deformities (absent ulna, fibula, and digits) following maternal exposure to oxymetazoline in the first trimester. J Obstet Gynaecol Res 42(8):1016–1020. https://doi.org/10.1111/jog.13014
11. Werner H, Dos Santos JRL, Fontes R et al (2010) Additive manufacturing models of fetuses built from three-dimensional ultrasound, magnetic resonance imaging and computed tomography scan data. Ultrasound Obstet Gynecol 36(3):355–361. https://doi.org/10.1002/uog.7619
12. Werner H, Lopes J, Tonni G, Júnior EA (2015) Physical model from 3D ultrasound and magnetic resonance imaging scan data reconstruction of lumbosacral myelomeningocele in a fetus with Chiari II malformation. Child’s Nerv Syst 31(4):511–513. https://doi.org/10.1007/s00381-015-2641-6
13. Van Koevering KK, Morrison RJ, Prabhu SP et al (2015) Antenatal three-dimensional printing of aberrant facial anatomy. Pediatrics 136(5):e1382–e1385. https://doi.org/10.1542/peds.2015-1062
14. Lioufas PA, Qualyle MR, Leong JC, McMenamin PG (2016) 3D printed models of cleft palate pathology for surgical education. Plast Reconstru Surg Glob Open 4(9). https://doi.org/10.1097/gox.0000000000001029
15. Vezzetti E, Speranza D, Marcolin F, Fracastoro G (2015) Diagnosing cleft lip pathology in 3D ultrasound: a landmarking approach. Image Anal Stereology 35(1):53–65. ISSN:1580-3139. https://doi.org/10.5566/ias.1339
16. Moos S, Marcolin F, Tornincasa S et al (2017) Cleft lip pathology diagnosis and foetal landmark extraction via 3D geometrical analysis. Int J Interact Des Manuf. ISSN:1955-2513. https://doi.org/10.1007/s12008-014-0244-1
17. Speranza D, Citro D, Padula F et al (2017) Additive manufacturing techniques for the reconstruction of 3D fetal faces. Appl Bionics Biomech 2017:10. https://doi.org/10.1155/2017/9701762 (Article ID 9701762)
18. 4D View, GE Healthcare’s Voluson. https://voluson-sw.gehealthcare.com
19. 5D Viewer, Samsung Medison Co., LTD. www.samsunmedison.com
20. https://www.slicer.org/
21. https://www.cti.gov.br/pt-br/invesalius
22. http://www.osirix-viewer.com/
23. http://www.materialise.com/en/medical/software/mimics
24. https://www.synopsys.com/simpleware/products/software.html
25. https://www.mathworks.com/products/image.html
26. Otsu N (1979) A threshold selection method from gray-level histograms. IEEE Trans Syst Man Cybern 9(1):62–66
27. http://support1.geomagic.com
28. https://ultimaker.com/en/products/ultimaker-cura-software

System of Precision Osteotomy in Bone Reconstruction Surgery: PUVACO

C. M. Baño[1(✉)], P. Puertas[2,3], and B. Abellán Rosique[4]

[1] Diplomado en Enfermería. Ingeniero Tec. Industrial, Responsable de IngenieriaQx.com, Murcia, Spain
conrado@ingenieriaqx.com
[2] Unidad Tumores Musculoesqueléticos. Traumatología y Cirugía Ortopédica, Hospital Clínico Universitario Virgen Arrixaca, Murcia, Spain
[3] Facultad Medicina, Universidad de Murcia, Murcia, Spain
[4] Unidad de Mama, Hospital Reina Sofía, Murcia, Spain

Abstract. Within the framework of bone tumor reconstructive surgery, one of the treatment tools is the en bloc resection of the bone where the bone tumor is located. When performing this en bloc resection, a cut must be made in the bone, that is, an osteotomy, which should be precise since near the osteotomy area, in addition to the musculature, the vascular nervous structures and the injury of the same can cause serious consequences to the patient. With the aim of improving this surgical step, a system of surgical instruments has been created and patented that allows us to perform the osteotomy with precision (that is, a bone cut at 90° with respect to the major axis of bone, or with an obliquity that we can define intraoperatively).

Keywords: 3D printing · 3D anatomic models · Surgical planning

1 Introduction

In many pathologies, surgeons need to perform the osteotomy (cut perpendicular to the axis of the bone), very precisely, in addition to being very careful with the exact location of the cut, they have to protect the soft tissues, vascular and nervous packets. Until now, surgeons protected all soft parts with separators, which are very narrow and are not designed for this function. Once the saw begins to cut the bone, the soft parts are always damaged, producing a lot of necrosis in the tissues (Fig. 1).

Another problem that presented the traditional way of performing osteotomies, is that it required the presence of two very skilled surgeons, one to perform the osteotomy, and the other to separate the soft tissues.

With the Puvaco instruments (patented instruments), the osteotomy can be performed by a single surgeon, very precisely, since with one hand it holds the Puvaco instruments and with the other hand performs the osteotomy. The Puvaco instrument protects and separates the soft parts with respect to bone, and allows the surgeon to perform the osteotomy without problems.

F. Cavas-Martínez et al. (Eds.): *Advances on Mechanics, Design Engineering and Manufacturing II*, LNME, pp. 536–541, 2019.
https://doi.org/10.1007/978-3-030-12346-8_52

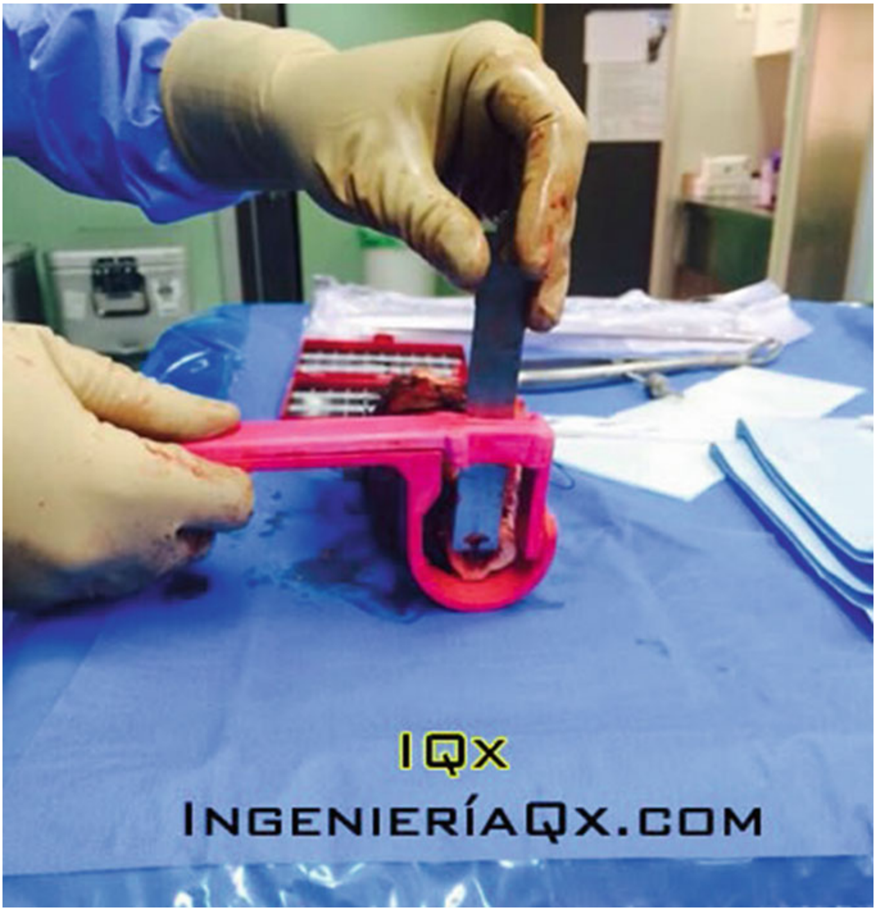

Fig. 1. Demonstration **osteotomy** with Puvaco instruments with 3D printing

2 Materials and Methods

The Puvaco instrument was designed based on the previous experience of Dr. Pablo Puertas, Dra. Beatriz Abellan Rosique and the engineer and nurse Conrado Miguel Baño Pedreño. Given the usual practice for the realization of an osteotomy was the placement of two shovel-shaped surgical displays, the idea of designing the Puvaco, to protect the soft tissues and use it in a simple way without the help of another surgeon. There were no previous instruments to perform this technique.

The Puvaco instrument design was made with CAD tools, and the first prototypes were made with 3D addition printers. The material used is polylactic acid (PLA) (Fig. 2).

The Puvaco instrument consists of a handle in the shape of a "U", which protects and separates the soft parts of the bone. It has a sharp tip so that it is very easy to introduce the separator, but at your sight, it does not damage the tissues.

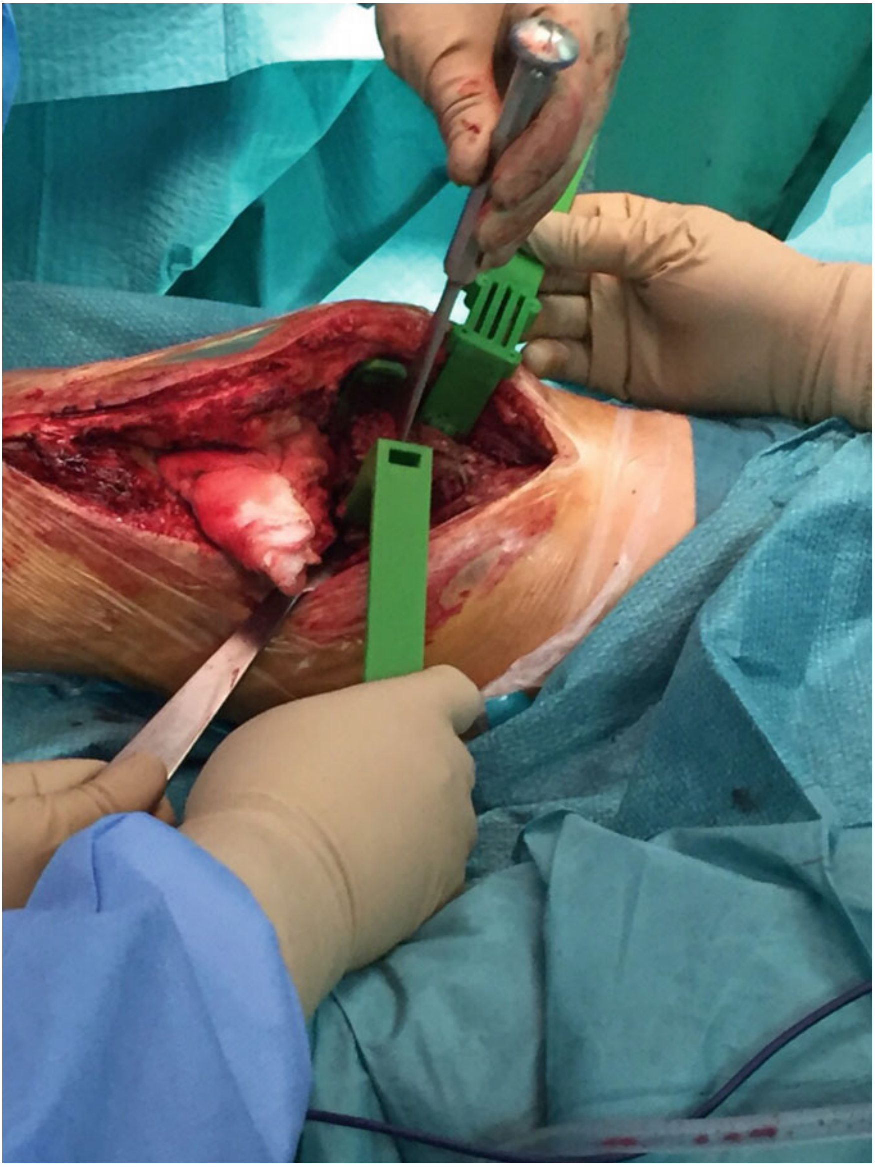

Fig. 2. Introduction of Puvaco instrument

Once it has been introduced, the cutting guide is assembled in the upper part, which provides 3 slots capable of performing the osteotomy at the height that most interests the surgeon (Fig. 3).

As you can see in the images, the “U” shape of the Puvaco instrument is perfectly designed to work with any section of the long bones of the human body.

Fig. 3. Definitive Puvaco instruments

3 Results

All the osteotomies performed to date with the Puvaco instruments have been very satisfactory, since it provides the surgeon with accuracy and reliability that they did not have to date, in addition to the speed that it offers.

The instrumental Puvaco, allows the surgeon not to depend on another assistant, with what now a lot of time and effort (Fig. 4).

4 Conclusions

Until today, all the surgeons performed the osteotomies at free height, without millimeter precision. From now on, all bone osteotomies should be performed with the Puvaco instruments, for the following reasons;

– Quick introduction and assembly.
– Does not require an assistant surgeon.
– Perfectly protects all soft parts.
– We avoid tissue damage.
– We increase the accuracy at the highest level.
– The handle is very ergonomic.
– It’s very easy to manipulate.

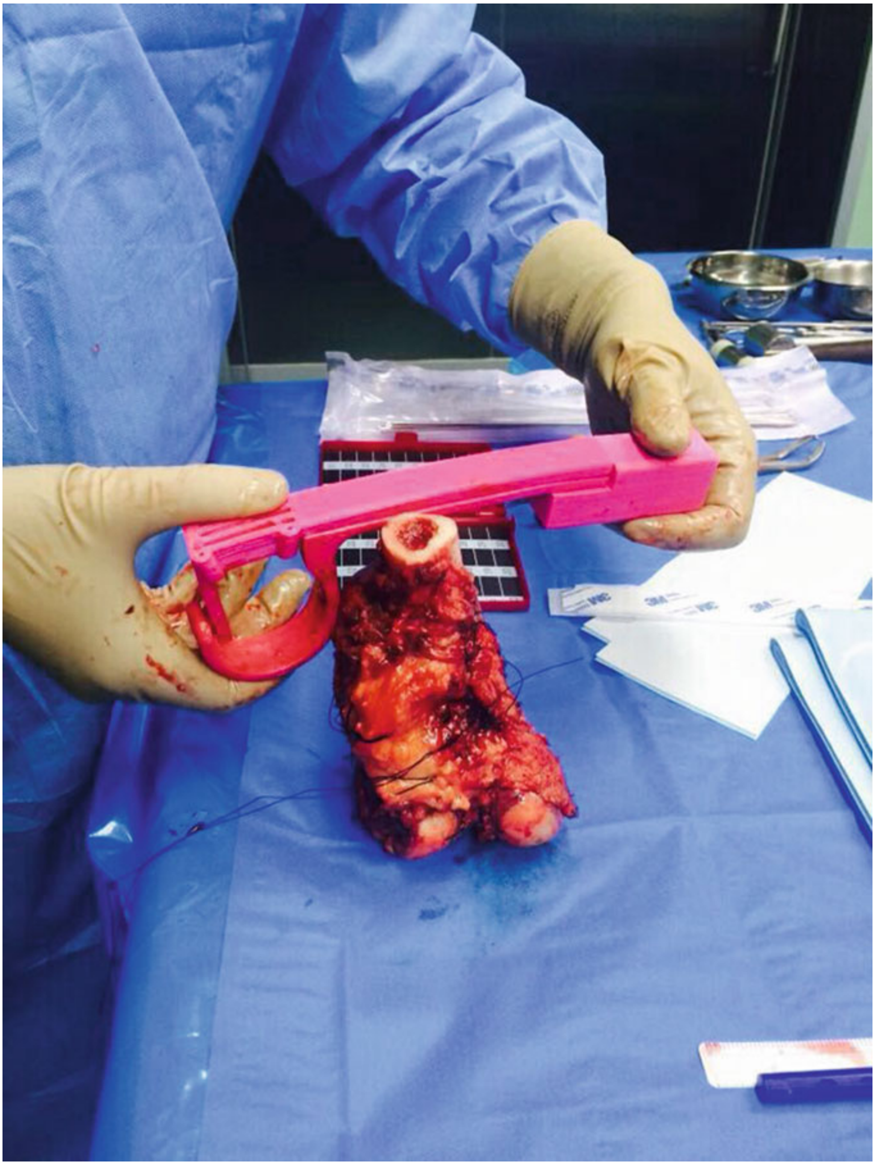

Fig. 4. Osteotomy performed with Puvaco instruments with 3D printing

The Puvaco instruments are very simple and easy to use, and provide the surgeon with the necessary tools to perform perfect osteotomies, with a very high degree of precision.

Acknowledgements. The research work reported here was made possible by IngenieríaQX.

References

1. Surgical experience at the Virgen de la Arrixaca University Hospital
2. Surgical experience of Dra. Beatriz Abellan Rosique at the Reina Sofía Hospital. Murcia. Spain
3. Surgical experience of IngenieriaQx.com

3D Simulation of Hazelnut Chopping—A Geometrical Study Compared with Experimental Results

C. Conigliaro, S. Tornincasa(✉), and V. Vicentini

Dipartimento di Ingegneria Gestionale e della Produzione- DIGEP, Politecnico di Torino, Corso Duca Abruzzi 24, 10129 Turin, Italy
stefano.tornincasa@polito.it

Abstract. The present work deals with the best method and tool design for chopping hazelnut kernels. The requested final product must have a standard appearance both in size and shape. This is not easy to be achieved. A geometrical study using 3D models—both for kernel and cutting tools—simulates the industrial process and forecasts shape and size distribution of the final product. Final comparison between 3D simulation and experimental results shows an acceptable agreement. A simplified and symmetrical geometry is discussed in the present paper. Work is in progress and further and more complete results are expected, but the method of 3D simulation proved to be very useful.

1 Chopped Hazelnuts Production

Italy is the second world producer of hazelnuts (200.000 tons/year) and Italian machines designed to process hazelnuts (husking, selection, refining, roasting, dicing, …) from harvesting in the field to final products for pastry and consumer goods are in continuous development.

Usually second-choice kernels are chopped into small parts to obtain a crisp and crunchy product which is widely used in the pastry industry and add consumer appeal. Ideally this product should be uniform in size and have a dice shape with a minimum of waste (Fig. 1).

Different machines were designed to obtain this chopped product. Usually a pair of counter-rotating rollers are used to have a crush (like in a press) or a frontal cut (like using a knife) or a milling cutting (as in a machine-tool shown in Fig. 2).

F. Cavas-Martínez et al. (Eds.): *Advances on Mechanics, Design Engineering and Manufacturing II*, LNME, pp. 542–551, 2019.
https://doi.org/10.1007/978-3-030-12346-8_53

Fig. 1. Hazelnut kernels after roasting (*left*) and final “chopped” product (*right*)

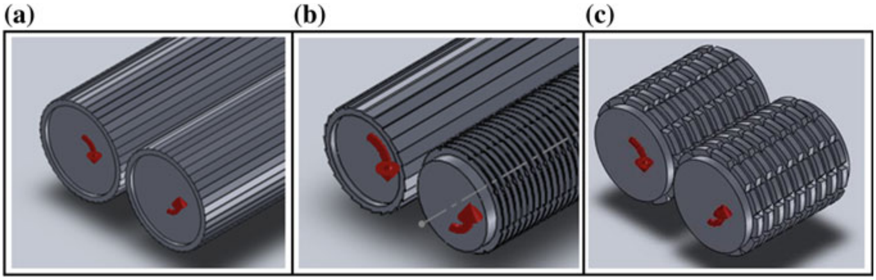

Fig. 2. Different design of counter-rotating rollers: **a** Crushing **b** Cutting **c** Milling

The ideal tool is not yet found.

In the present study we deal with a rather efficient and modern chopping unit formed by of a pair of counter-rotating rollers each consisting of a series of 6 mm thickness discs having cutting edges on their circumference. In each roller the discs are spaced 6 mm apart and axially offset with reference to the counter-rotating roller, as shown in Fig. 3.

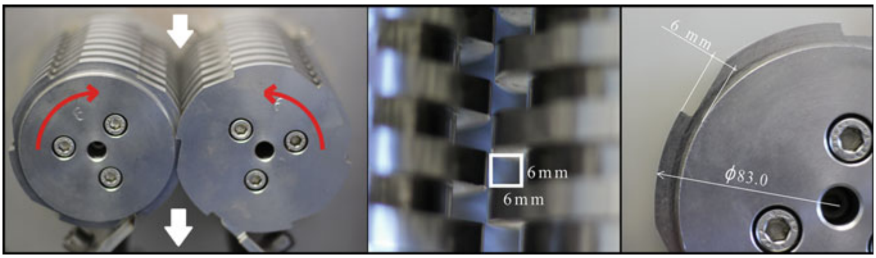

Fig. 3. The chopping unit simulated in this paper

Note that—in the facing discs—the angular orientation of the cutting edges is not in phase. Kernels fall from above and the final chopped product comes out from below. The nominal passing way through the rollers is 6 × 6 mm.

2 Hazelnut Kernel Model

The hazelnut we considered is the "Tonda Gentile Piemonte" cultivar. Actual size and shape distribution is fully discussed in references [1] and [2] in which 3D generation techniques for a parametric model are also proposed.

However in the present study the kernel was simply represented by an ellipsoid containing a cavity. The three dimensions (a, b, c) along X, Y, Z axis have a standard value of 10, 12 and 14 mm and the internal cavity is 5 × 6 × 7 mm.

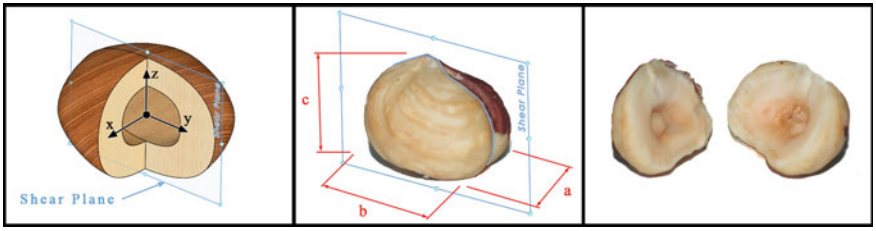

Fig. 4. Typical shape of hazelnut kernel of "Tonda Gentile Piemonte" cultivar. The kernel consists of two cotyledons

A statistical shape generation method based on ellipsoidal mapping as proposed in references [3] and [4] would represent a more refined step and should be used in future.

The orientation of XYZ axis and the position of the shear plane, which divides the two kernel cotyledons, is shown in Fig. 4.

3 Simulation of Chopping Sequence—Initial Position

To simplify and add symmetry to chopping sequence simulation we assumed that the kernel falls from above onto the counter-rotating rollers, having the Y axis horizontal and the X axis vertical and symmetrically placed with reference to the cutting edges of the discs facing each other, as shown in Fig. 5.

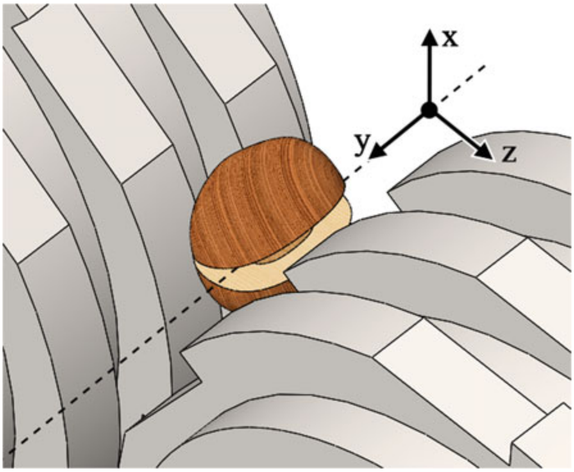

Fig. 5. Starting point of chopping sequence simulation

The 3D model of counter-rotating rollers is very useful to point out the very starting point of the process and to decide where the cutting edges and opposite points of contact (i.e. external forces) are positioned with reference to the kernel.

But to get started with geometrical analysis of chopping sequence we have to make assumptions on which way the two kernel cotyledons (which consist of a rather brittle material) can be broken into pieces.

Here two techniques come to help. On one side we made some preliminary compression tests of the kernel using a vice equipped with two jaws simulating the cutting discs (see Fig. 6. left). On the other hand we used the SolidWorks Simulation tool to have the stress and strain analysis of the kernel submitted to the applied forces and to detect the likely shearing surfaces (see Fig. 6 right).

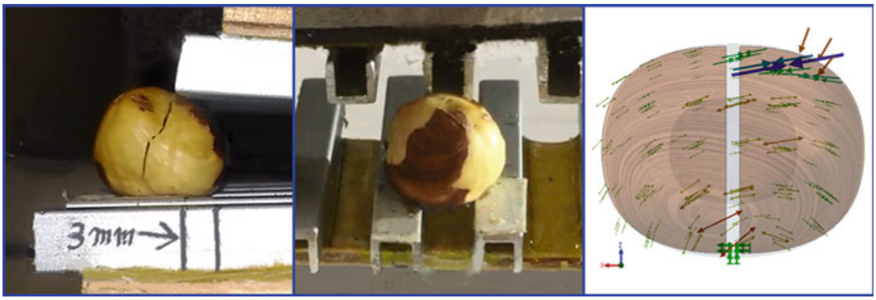

Fig. 6. Compression tests (*left*) and Stress Analysis (*right*) of the hazelnut kernel

4 Next Steps of 3D Chopping Simulation

As already said and with the assumed simplification the kernel chopping sequence first step is the separation of cotyledons (the part below is N1 and the symmetrical part above is N1res).

According to the chosen geometry this first step takes place when the left roller rotates 32 ° clockwise and the corresponding counter-rotating roller is about 2 ° anti-clockwise (see Fig. 7).

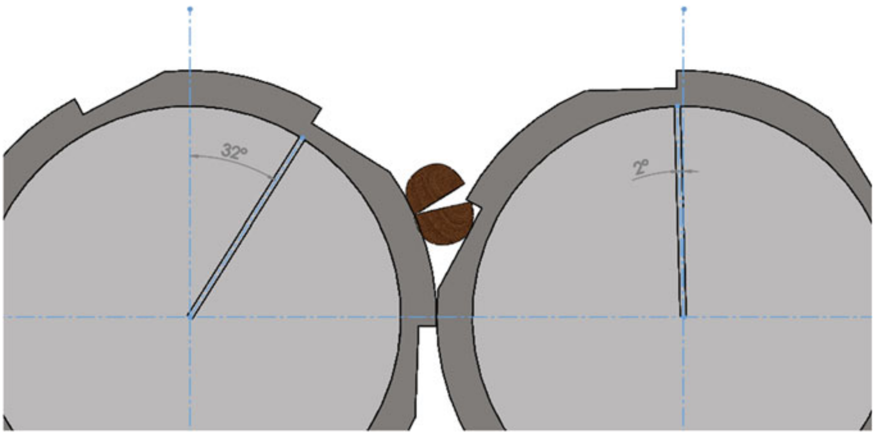

Fig. 7. Chopping sequence first step

3D Simulation will continue (second step) chopping the only cotyledon called "part N1" (the cotyledon called "part N1res" is left floating in the air for a while). As shown in Fig. 8 part N1 is initially divided into three: a central slice and twice N2 which can pass through the rollers opening without further breakage.

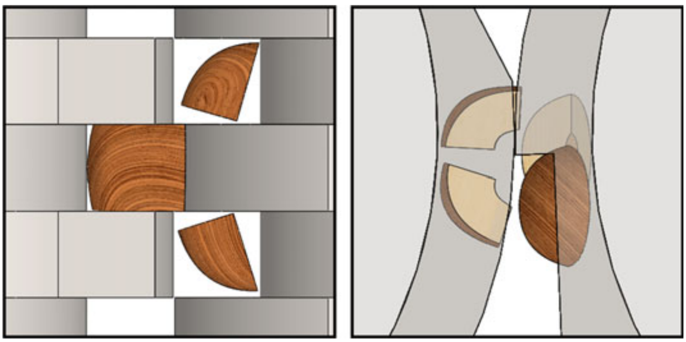

Fig. 8. Chopping sequence: *Left*: second step: N1 is divided into a central slice + (twice N2)—*Right*: third step: central slice is broken in two

As the central slice has an internal cavity, which appears to be a point of weakness, according to experimental compression tests, it breaks into N3 and N3res which both pass through the rollers openings (see Fig. 8 *right*).

Simulation continues supposing that the remaining half kernel (cotyledon) N1res—which was left floating in the air—falls into the milling rollers but in a position which is different from that initially assumed by N1 (Fig. 9). This opens to a study of other chopping scenarios.

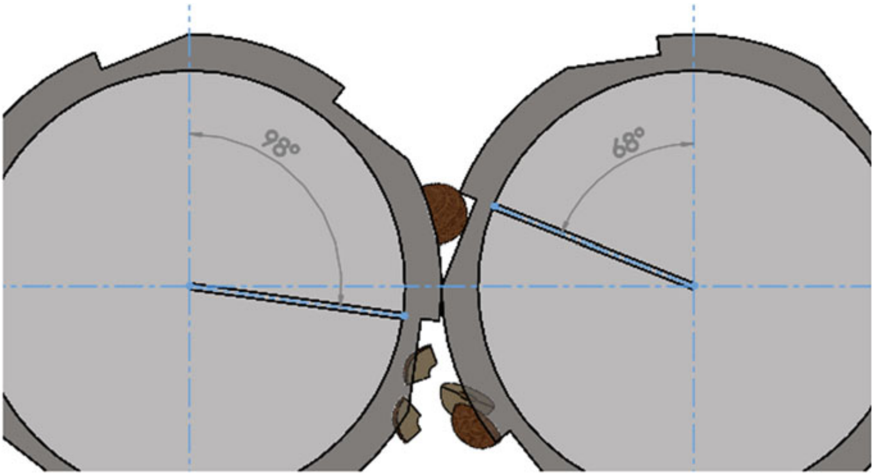

Fig. 9. Chopping sequence fourth step: chopping N1res

3D simulation get going using the same guidelines shown previously but taking into account the different orientation of the half kernel N1res.

Without entering into a detailed description the chopping simulation leads to a final result of 11 non-symmetrical kernel parts as shown in Figs. 10, 11 and Table 1.

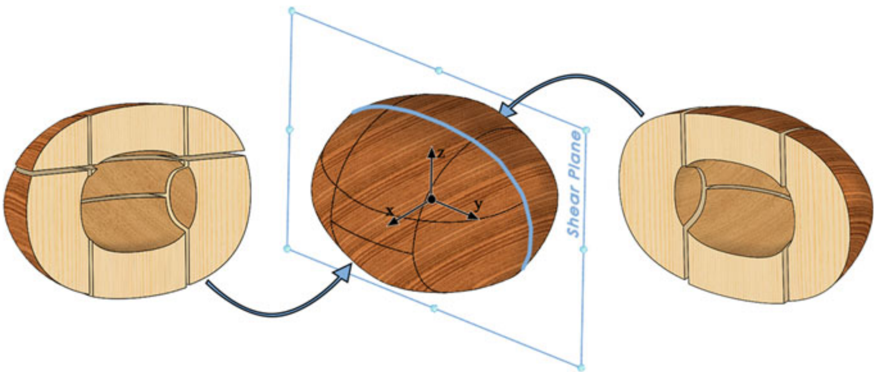

Fig. 10. Final results of chopping simulation

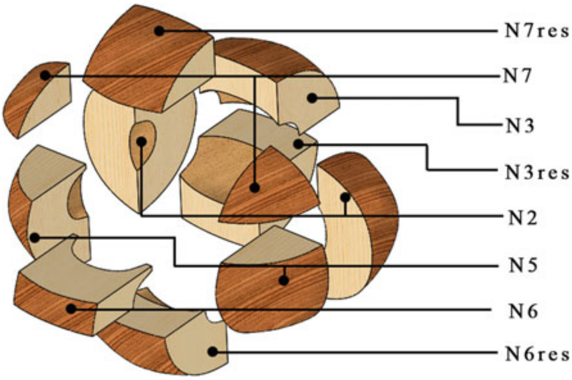

Fig. 11. Chopped hazelnut kernel exploded view

Table 1 Hazelnut kernel chopping sequence

N0	N1 res	**N2**		
		N2res	**N3**	
			N3res	
	N1	N4	**N7**	
			N7res	
		N4res	**N5**	
			N5res	**N6**
				N6res

First remark is that—with reference to the ideal dices 6 × 6 × 6 mm which were supposed to be the results of the chopping procedure—dimensions of final parts are both larger and smaller (Fig. 12). As an instinctive approach it seemed that a part exceeding 6 × 6 × 6 mm could not pass through the milling rollers, which is not true. We indeed found that 2 parts (N3 and N3 res) cannot pass through a sieving mesh of 6 mm, whatever their orientation.

The second remark is that the obtained shapes are rather different from that of a dice. And both remarks correspond to what is observed in practice during production activity.

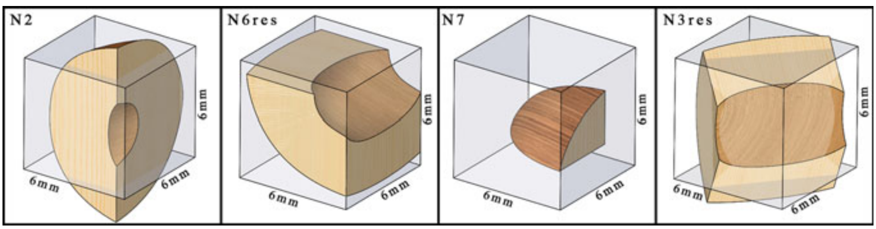

Fig. 12. Shape and size of some chopped parts obtained with Simulation

5 Comparison with Results Obtained by Industrial Production

To add more results to the 11 chopped parts obtained from the chopping simulation of the kernel positioned as in Fig. 5 we also simulated the chopping of a kernel positioned as in Fig. 13 The obtained 9 chopped parts were added to the previous 11 parts and all parts were ordered according to size classes (i.e. the sieving mesh through which they could pass).

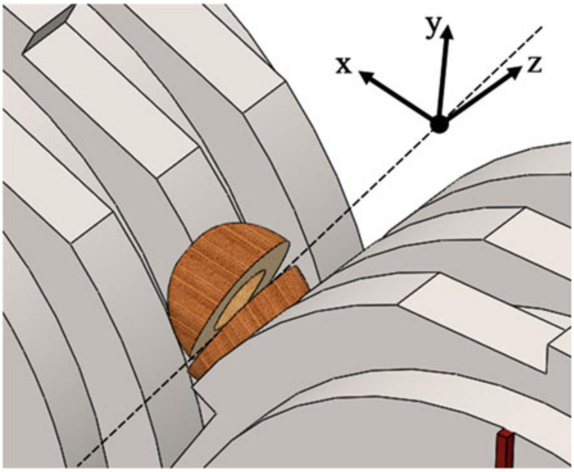

Fig. 13. Alternative orientation of the kernel

The comparison of frequency density of size classes between the actual hazelnut chopped product and results from the 3D simulation described above is shown in Fig. 14 *left*.

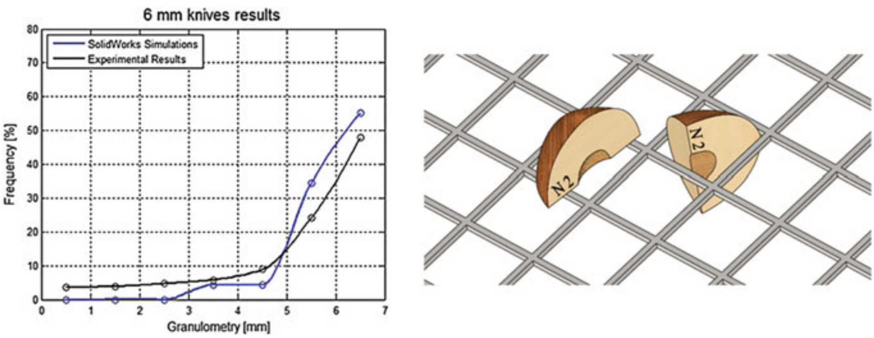

Fig. 14. *Left*: Comparison between simulation and tests—*Right*: A non-symmetrical part "passes" or "does not passes" through the sieving mesh according to its orientation

It is obvious that the 3D simulation cannot take into account the generation of small parts (like chips and crumbs, called in the jargon "flour") which come out:

- of the friction of cutting tools against the kernel.
- and the pressure to which the kernels are subjected inside the grooves of the counter-rotating rollers.

This is the reason of the difference between simulation and experimental results in the diagram of Fig. 14 *left*.

Note that—in dividing the simulated results into dimensional classes—we made a virtual "sieving" operation, taking into account the probability that a part that exceed the sieving mesh in only one or two dimension could pass or not pass through the openings. A statistical criterion is taken into consideration (see Fig. 14 *right*).

6 Conclusion

Using 3D models of cutting rollers and a simplified 3D elliptic model of hazelnut kernel a chopping process was simulated. Simplified assumptions of kernel (rather brittle material) shearing planes were made and a reasonable agreement with experimental results obtained with current production machines was obtained.

3D Simulation proved that a certain amount of chopped parts are larger than the standard dice 6 × 6 × 6 mm (which—at first—seemed rather strange) and other are somewhat smaller. A statistical distribution is given.

In the present work the study is restricted to a single kernel with standard dimensions (a, b, c) and a given position and orientation with reference to cutting tools.

The relevant research activity is in progress and should be extended both to discuss:

on one side—different position and orientation of falling kernels to better fit the actual process simulation,
on the other side—to add a statistical variation of kernel geometry,
and finally—to compare different types and geometry of existing industrial tools in order to improve efficiency and obtain the requested shape and size of chopped product.

Acknowledgements. This paper is part of a research program (Corylav) sponsored by the Italian Regione Piemonte. We thank Dr. F. Canova, CEO of the Company "La Gentile" partner of the project, who supported the research activities.

References

1. Bonisoli E (2011) Modelli virtuali 3D per le nocciole delle Langhe. Il Progettista Industriale 31(9):35–38
2. Tornincasa S, Bonisoli E, Brino M (2011) 3D models for Langhe Hazelnuts. Int J Mech Control 12(2):21–28. ISSN 1590-8844

3. Tornincasa S, Bonisoli E, Brino M (2016) Parametric, asymmetric and stochastic-based 3D CAD model of Tonda Gentile Trilobata hazelnut variety. Biosyst Eng 144:72–84
4. Danckaers F, Huysmans T, Van Dael M, Verboven P, Nicolai B, Sijbers J (2017) Building 3D statistical shape models of horticultural products. Food Bioprocess Technol. https://doi.org/10.1007/s11947-017-1979-z

Surgical Planning in Shoulder Prostheses with 3D Reconstruction and Customized 3D Guides

C. M. Baño[1](✉), J. F. Abellán[2], E. Melendreras[2], and B. Abellán Rosique[3]

[1] Diplomado en Enfermería. Ingeniero Tec. Industrial, Murcia, Spain
conrado@ingenieriaqx.com
[2] Shoulder Unit. Hospital Morales Meseguer, Murcia, Spain
[3] Unidad de Mama, Hospital Reina Sofía, Murcia, Spain

Abstract. To date, all primary shoulder prostheses, as well as any other joint, were made with standard metallic instruments for all types of patients, said instruments have great deficiencies since they were developed to cover all types of surgeries, with the great variety of bone sizes of patients, types of approaches (method to get to the bone, separating and respecting skin, muscles, vascular and nervous package, facias), etc. In addition to all this, each surgeon has specific surgical techniques, and for all of them, the standard guides of the instruments have deficiencies in terms of the complexity of their application, sizes, etc. With the current diagnostic elements, surgeons are perfectly aware of the patient's pathology, but new 3D planning techniques offer surgeons knowledge of the anatomy of each bone, as well as its disposition in space, due to the deformities that occur in joints due to osteoarthritis and different degenerative pathologies. This is of great help to be able to plan the placement of the surgical implant and in this way, the height and angulation of the osteotomy (cutting line perpendicular to the bone). With this technology we are raising the quality of prosthetic implant surgery to a higher level, since the surgeon knows in advance perfectly the state of each joint, the anatomical shape of each bone due to the deformities that it suffers, and knows in advance how the prosthesis is implanted, at your discretion. This has not happened to date, since before the existence of 3D reconstruction and surgical planning, the surgeon presented blindly to the surgeries. Another field of application very important for this technology, are the tumor prostheses. Thanks to PET-CT (positron emission tomography), which delimits the tumor three-dimensionally in space with respect to bone with different degrees of malignancy that are classified according to SUV value. Thanks to 3D reconstruction and surgical planning, we can perform more advanced tumor surgery.

Keywords: 3D printing · 3D anatomic models · Surgical planning

F. Cavas-Martínez et al. (Eds.): *Advances on Mechanics, Design Engineering and Manufacturing II*, LNME, pp. 552–563, 2019.
https://doi.org/10.1007/978-3-030-12346-8_54

1 Introduction

The surgical instruments of each prosthesis are designed in a standard way so that they can be used with all patients worldwide, and consider the standard anatomical forms of a healthy bone. Because of this, surgeons complain about the guides of all the instruments, whatever the manufacturer, since they are often difficult to apply, or they can not be applied due to a specific pathology of the patient. In addition, problems often appear when using instruments, because they do not adapt well to patients who have too small or large sizes.

Another major problem that traditional prosthetic surgery presents is the orientation of the anchoring screws of the different components of each prosthesis. The deformity of the bone, the difficulty of the approach, and above all, the difficulty of viewing through the soft parts, complicate the correct final placement of the screws or anchoring elements.

With the new technology of 3D reconstruction, surgical planning and personalized cutting guides, we solve all these problems, and we elevate the quality of surgeries to a higher level. Since we eliminate the surprise factor of surgeries, and we provide surgeons tools never seen before, since they are designed according to the criteria, tastes and needs of each surgeon.

In this way, we went from performing surgeries in series to personalized surgeries for each patient. The quality of health care increases considerably.

One of the great advances we provide in tumor surgery, since we provide new tools to the surgeon that allow you to perform a more accurate and planned surgery according to your criteria.

2 Materials and Methods

Over several years, we have developed cases of surgeries of all joints; humero, hip, knee, experimental column with pigs, tumor surgery with PET-CT and maxillofacial surgery. In all the steps of 3D reconstruction, surgical planning and development of personalized instruments and guides have been developed.

Below we detail the cases that we present in this article, all are shoulder pathologies, and we add a case of maxillofacial, because we consider that it represents the importance of this technology in the medical sector.

2.1 Study Cases

- Case 1: Primary humerus prosthesis in a 70-year-old male patient.
- Case 2: Primary humerus prosthesis in a 77-year-old female patient.
- Case 3: Fracture of the humerus with bursting of the reduced humeral head with proximal humerus osteosynthesis plate.
- Case 4: Tumor tumoral surgery with PET-CT. Surgical planning valuing value of SUV. Woman 45 years old.

– Case 5: Maxillofacial microsurgery with fibular insert in the lower jaw. Use of cutting guides in mandible, fibula and mandibular spacer. Woman 32 years old.

2.2 3D Reconstruction and Surgical Planning

Table 1. Description of clinical cases

	Joint	Diagnosis	Type of surgery	Custom guides	PET-TC
Case 1	Shoulder	Severe osteoarthritis	Shoulder prosthesis	Yes	Not
Case 2	Shoulder	Severe osteoarthritis	Shoulder prosthesis	Yes	Not
Case 3	Shoulder	Shoulder fracture	Osteosynthesis shoulder	Yes	Not
Case 4	Shoulder	Tumor	Rescue prosthesis	Yes	Yes
Case 5	Maxilo	Tumor	Microsurgery	Yes	Not

For a correct surgical planning, we have to perform the following steps: (Table 1).

2.2.1 Performing a CT or PET-CT to the Patient

The CT (Computerized Axial Tomography) and PET-CT (Positron Emission Tomography) are basic diagnostic techniques that are very necessary for the evaluation of pathologies by the medical team. This examination provides images in DICOM format that we can export to a 3D reconstruction software. This software reconstructs all the images volumetrically and allows us to export them in STL format (Figs. 1, 2 and 3).

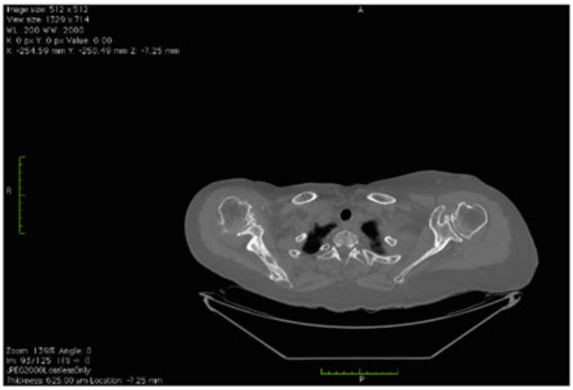

Fig. 1. Case 1

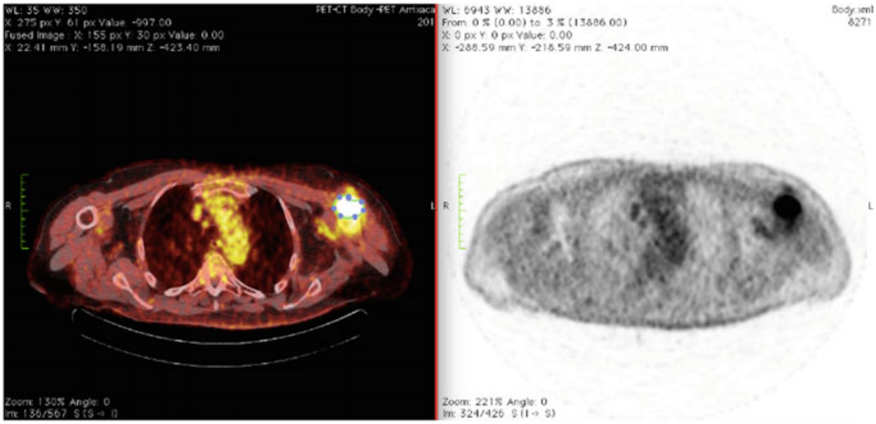

Fig. 2. Case 4. PET-TC

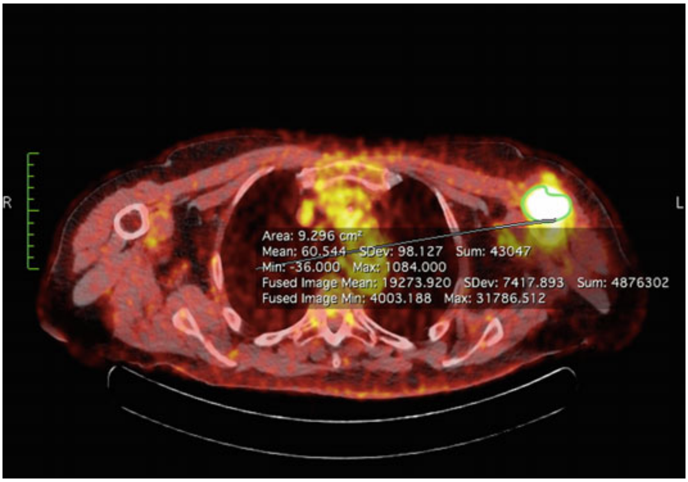

Fig. 3. Case 4. PET-TC. SUV indicator of higher degree of malignancy

2.2.2 Printing of 3D Models and Surgical Planning

We take 3D models in STL format and print them on a 3D printer. The printer based on the technology of deposition by layers, must be able to print in layers of 0.1 mm in height, to be able to provide the necessary precision to 3D models. The material that crashes is PLA (Polylactic Acid), which is a biocompatible material and easy to sterilize. It is essential that the 3D printing equipment has the exact resolution at 0.1 mm layer height, since a very high precision is required so that the customized guides adapt perfectly to the bone and have the lowest possible tolerance (Figs. 4 and 5).

Once we have the 3D reconstructions of the bony parts, soft tissues and vascular packages, we meet with the surgeon to evaluate the 3D reconstructions, plan both the surgery approach and the osteotomies and necessary personalized guides adapted to each concrete implant. Depending on each patient, a specific type of implant is required, and to implant said implant, specific cuts and guides are required (Figs. 6, 7, 8 and 9).

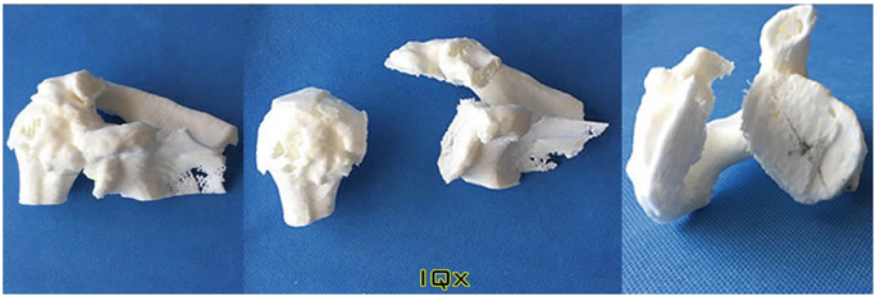

Fig. 4. Case 4. PET-TC. SUV indicator

Fig. 5. Case 1. Reconstruction 3D

2.2.3 Virtual Surgical Planning and Design of Personalized Guides

Once we have all the 3D models, we meet with the surgeon, to study them, plan the surgery, and tell us how you want the cutting guides, how you want to orient the guides of the pins and drills, etc.

With CAD design software, we developed customized cutting guides to perform the osteotomies that each specific implant requires, in addition to the guides for the screws and guide needles necessary for anchoring the implants. All this must be done taking into account the criteria of the surgeon and the technical and dimensional needs of each implant.

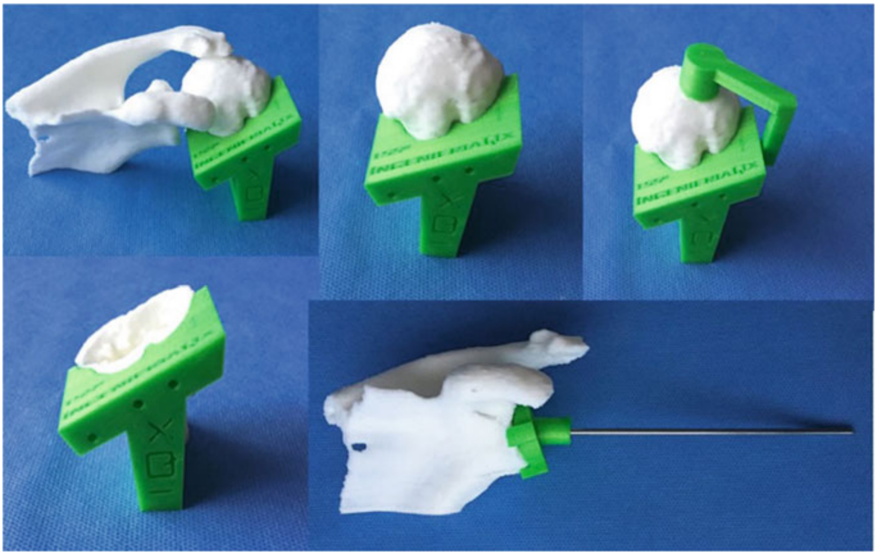

Fig. 6. Case 1. Custom cut guides

Fig. 7. Case 2. Custom cut guides

Fig. 8. Case 3. Virtual 3D reconstruction

Fig. 9. Case 5. Reconstruction 3D with customized guides and simulation of final result

2.2.4 Printing of Personalized Guides

The next step is to print the personalized guides with the same equipment that the 3D reconstructions were printed, with a striking color. It is essential to select a layer height of 0.1 mm so that the parts have the highest possible precision. These guides must be designed taking into account:

- Approach.
- Position of the patient.
- Position of soft parts with respect to bone.
- Periostization of the tissues (separate the soft tissue bone.
- Spinal axes of the joint bone.
- Osteotomy axis (bone cut).
- Angle of inclination of the implants.
- Dimensioning of implants with respect to bone.

Once the personalized guides are printed, they are presented to the surgeon for approval, and if it is affirmative, they are sterilized in the hospital's sterilization service (Figs. 10, 11 and 12).

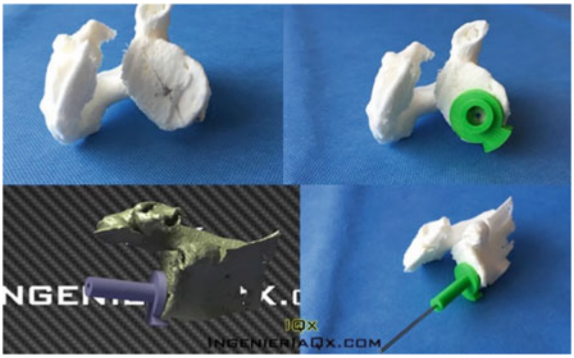

Fig. 10. Case 1. Custom cut guides

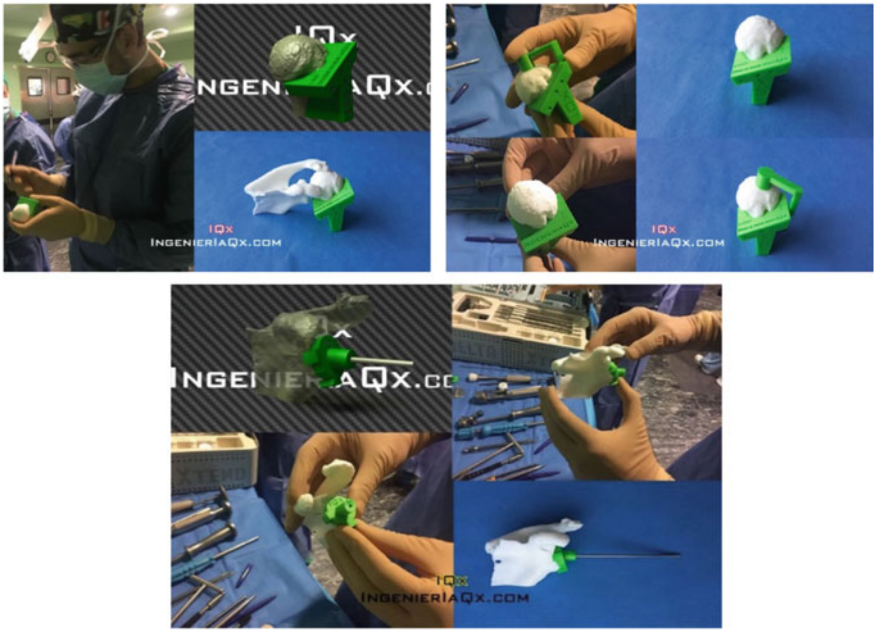

Fig. 11. Case 2. Custom cut guides

2.2.5 Surgery

In the surgical process, the surgeon checks first, both the 3D reconstructions, and the cutting guides, for what the 3D model of the printed patient uses. Once you have made the approach, use the personalized guides to perform the osteotomies and guides for the guidance of the pins, screws and implants.

The surgical instruments used by conventional prostheses are designed for all types of patients, and it is quite complicated to use for certain patients. With the personalized cutting guides, they adapt immediately, making the surgery much faster.

It is also very useful in these cases, to work with the reconstruction of PET-CT, in cases of tumor surgery. Use the 3D model of the tumor (image with a higher SUV grade), to see which soft parts and bone parts are affected by a tumor (Figs. 13, 14, 15, 16 and 17).

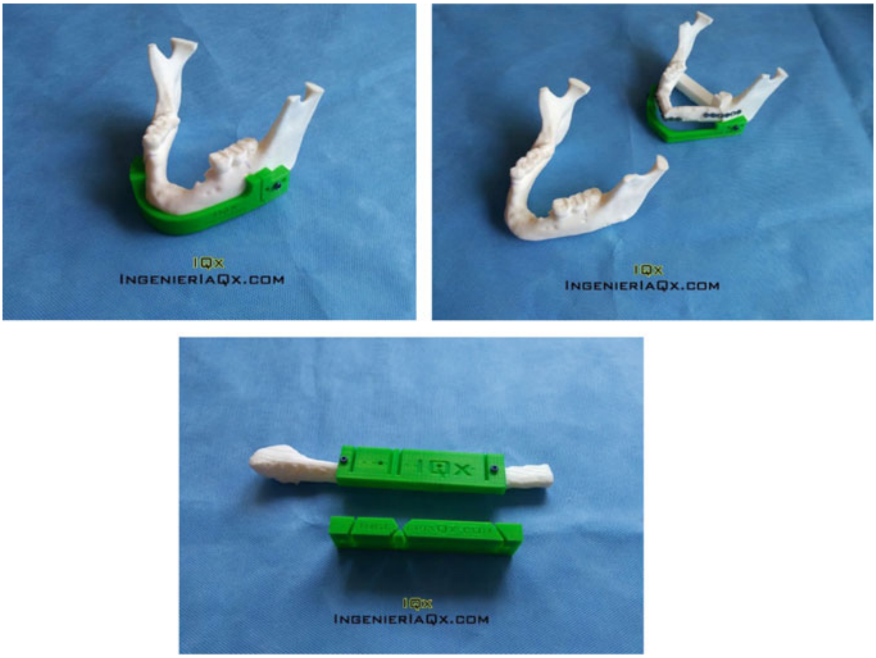

Fig. 12. Case 5. Custom cut guides

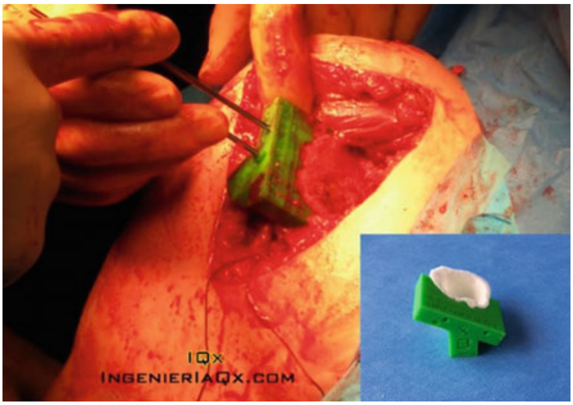

Fig. 13. Case 1. Custom humeral cutting guide

3 Results

The results of all the cases carried out to date are very satisfactory. The surgical planning prior to surgery is shown to offer a very important medical value to the surgeon, since it provides tools to have more relevant data before starting the surgery,

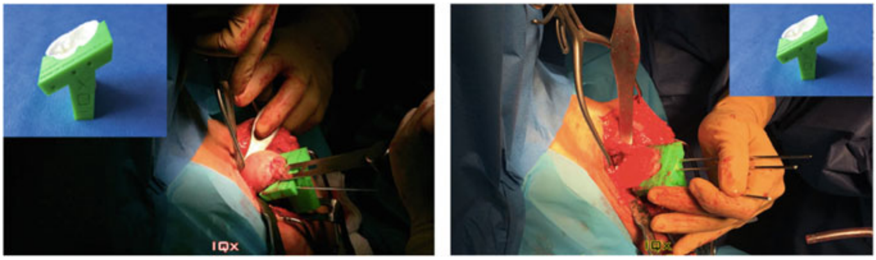

Fig. 14. Case 2. Custom humeral cutting guide

Fig. 15. Case 2. Custom cut guides. Glena

Fig. 16. Case 4. PET TC. Shoulder

such as the exact size of certain anatomical parts such as the case of surgery glenoid in scapula.

The 3D models and the cutting guides are of very good quality, since they faithfully reproduce the anatomy of the patient, and the cutting guides adapt perfectly to the bone parts.

Fig. 17. Case 5. Microsurgery

The results of all the surgeries have been very satisfactory.

4 Conclusions

It is demonstrated after a series of cases that the support offered by surgical planning with 3D models to surgeons is very valuable.

Surgical planning provides the surgeon with the support of a team of engineers who work under their criteria and guidelines. The surgeon can plan his surgery in this way in a much more comfortable manner, since the communication is carried out telematically, without the need for travel.

The quality of 3D models and cutting guides is very high, very close to 1: 1 ratio. During the surgery, the guides adapt perfectly to the patient, making it very easy to use. And they guarantee that the osteotomy of the bones and the guides that are needed for the rest of the instruments are perfectly located in the X, Y, Z axes, for a perfect placement of the implants.

For all these reasons, the use of surgical planning, 3D models and personalized cutting guides offer an aid to the surgeon of enormous medical value.

The best conclusion we can offer is that the surgical planning with personalized 3D guides facilitates the realization of the surgical technique, reducing the risk of error. And it greatly facilitates the surgical technique by avoiding using complex cutting systems that slow down surgery and offer some confusion.

References

1. Surgical experience of Drs. Abellan and Melendreras at the Morales Meseguer Hospital, Murcia, Spain
2. Surgical experience of Dra. Beatriz Abellan Rosique at the Reina Sofía Hospital, Murcia, Spain
3. Surgical experience of IngenieriaQx.com

Combined Urban Furniture Designed by a Bio-Inspired Approach

D. Parras-Burgos(✉), J. Hernández, J. S. Velázquez,
F. Cavas-Martínez, F. J. F. Cañavate, and D. G. Fernández-Pacheco

Department of Graphic Expression, Technical University of Cartagena,
C/Doctor Fleming, S/N, 30202 Cartagena (Murcia), Spain
dolores.parras@upct.es

Abstract. The design of a product is not an easy task; it must be a balanced combination of functionality, usability and aesthetics. The creative process of an industrial designer can be facilitated by the use of different sources during the search for ideas. Nature is full of geometries and movements that supply us with a great variety of forms and its use provides greater doses of empathy in the user-product relationship. This communication shows the process of designing urban furniture with bioinspired forms taken into account, in addition, other aspects such as ergonomics, sustainability, accessibility, etc., achieving an attractive, functional and ecological product.

Keywords: Bioinspiration · Product design · Sustainability · Aesthetic, creativity

1 Introduction

Industrial design is characterized by an important aesthetic component but also technological components, unlike in the past when products were adorned without taking into account their functionality. Nowadays, the unity between technology and aesthetics must be achieved in the first stage of product design, to ensure that the object, in addition to being functional, is pleasing to the eye [1].

When an industrial designer has the challenge of finding a formal solution to the design of a product, he may need resources or sources of inspiration to help him find the most suitable form, one of these sources can be Nature. Human beings assign aesthetic qualities to that which makes us feel emotions. Nature is full of optimal shapes and geometries, so biomimicry can be efficient in aesthetic terms. "*Biomimetics is an attitude, a way of thinking as creativity can be. Although the transfer of solutions between nature and technology has its limitations, the exploration and possibilities of Biomimicry are practically unlimited*" [2].

The inspiration in forms of nature for product design is not new, there are many designers who already use these resources, from a formal point of view, as a model for their designs and can be applied in a variety of elements [3–5].

In general, people are attracted to natural phenomena [6]. Nothing that is perceived acts on its own, everything acts together. The geometric and organic shapes that make up objects, produce acceptance thanks to preexisting analogous sensations in each

F. Cavas-Martínez et al. (Eds.): *Advances on Mechanics, Design Engineering and Manufacturing II*, LNME, pp. 564–572, 2019.
https://doi.org/10.1007/978-3-030-12346-8_55

person. As the psychology of perception affirms, it is precisely by this formal aspect, based on reason or not, that an object can be recognized as something natural, and that, if it were reasonably close to the natural form it might be called bionic aesthetic [7]. In this sense, the concept of "*aesthetic intelligence*" arises, which tells us that we possess it in an innate way, and sometimes, unconsciously. It is a capacity to perceive a wide range of product qualities that shape our response to them. A design process for the senses is proposed as a means to provide products with which users can feel a greater degree of empathy [8].

Bioinspired designs are widely used in product design to emphasize emotional interaction. Therefore, the understanding of the psychological effects of this type of design is becoming an important issue in the development of products with strong affective qualities. There are studies that analyze all of these types of elements whose results indicate that consumers have different degrees of emotional responses to products that present different levels of biomimetics [9].

On the other hand, the design of sustainable urban furniture that combines different aspects such as functionality, design, integration with the urban landscape and environmental quality, taking into account energy savings in each one of its elements and processes is being enhanced in the cities [10–12].

This communication presents the development of an urban furniture design that has been based on the inspiration of elements of nature for the development of its forms, in addition, other aspects have been taken into account such as ergonomics, sustainability, accessibility, etc., achieving an attractive, functional and sustainable product.

2 Materials and Methods

The Design process of a product is made up of several stages, three of which will be highlighted: (i) definition of the requirements of the new product, (ii) search for ideas and definition of the conceptual design, (iii) detailed design of each of the parts that make up the product.

The target objective of this project is an urban furniture piece that combines the concepts of a table, seating, lighting and a paper bin, that is eventually integrated into its environment resulting in a functional, pleasant and welcoming place.

2.1 Design Requirements

The objective of this project is to design, in a bioinspired way, an urban furniture product that complies with the following premises:

- Rest place.
- Social meeting place.
- Place to eat informally.
- Connection to recharge mobile devices.
- Design adapted to the environment.

- Sustainability characteristics in materials and operation.
- Modularity.
- Bioinspired aesthetics.

A search was conducted for urban furniture that fulfilled one of the aforementioned characteristics (Fig. 1) but no piece was found that fulfilled all of the premises described.

Fig. 1. Examples of urban furniture: **a** Intelligent furniture Soleo of Yupcharge, **b** Picnic table of Forestgreen, **c** ConnecTable Cafe of CarrierClass Green infrastructure, **d** Solar Tree of Ross Lovegrove, and **e** Toyota Prius Solar Flowers

Next, the characteristics that the design of this new product must meet based on the initial premises are defined below in more detail:

- The product will be designed with shapes inspired by elements of nature to favor an emotional interaction with the user.
- The seating elements and the table must have a pleasant touch so that the users feel comfortable.
- The surfaces will be smooth to facilitate cleaning.
- The materials must be resistant to aging and corrosion because their location will be outdoors.

- The temperature and conduction of materials will be taken into account, in order to avoid excessively cold or warm temperatures due to their exposure to the weather.
- The edges of the elements that are in direct contact with the user will be rounded to avoid damage and promote fluid aesthetics.
- The design will be based on a modular system that allows replacing damaged parts without having to change the entire product. This option also allows designing different configurations with the same elements.
- Concepts of ergonomics and anthropometric dimensions will be taken into account for a better adaptation to the user.
- Accessibility for people with wheelchairs will be taken into account.
- To favor the sustainability of the product, a system of solar panels will be designed to provide sufficient energy for the illumination of the whole piece and the recharging of mobile devices.
- The product will have elements to produce shade during the day and at night the lighting system will be activated, in this way, the product can be used for longer periods of time.
- This product will be located in different environments such as parks, common educational areas, etc.

2.2 Conceptual Design

Taking into account the initial premises and the requirements that the product must have, the next phase consists of a search for ideas to shape the product. This phase requires a large dose of creativity and searching for information to develop a large number of bioinspired ideas. The elements of nature that have served to define each of the elements of the product are: a snake whose sinuous shape defines the bench to sit on, the water of a puddle or a lake defines the table, and the leaves of the water lily emulate the surface that will cover the whole piece (Fig. 2). Figure 3 shows a sketch of the initial idea of the product taking into account these concepts.

Fig. 2. Elements from nature that have inspired the product (*Source* www.pixabay.com)

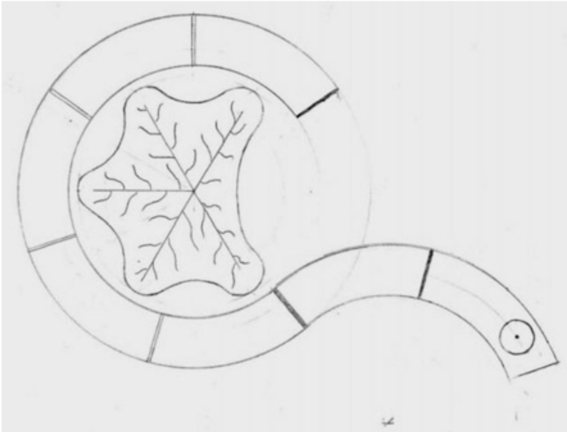

Fig. 3. Initial sketch of product

2.3 Detail Design

Once the conceptual design of the product has been defined, other aspects are studied such as ergonomics, anthropometric dimensions, safety concepts, sustainability, etc. to specify each one of the elements that compose it [13–17]:

- The depth of the seat should not be excessive, which means that the dimensions should be between 40 and 50 cm.
- The height of the seat should oscillate between 38 and 48 cm, which allows the feet to rest on the ground.
- The leading edge of the seat area must be curved so that it can accommodate the popliteal gap.
- The width of the seat per person must be between 40 and 45 cm.
- The height of the table should be between 70 and 78 cm, this allows a sufficient space between the seat and the table to sit comfortably.
- The dimension of the table is defined with a radius of 70–80 cm. to be able to reach any part of the table with comfort.
- The height of the support structure is 4 m.
- To meet environmental and sustainable criteria, the design has taken into account the use of recycled and/or recyclable materials, favoring local suppliers to reduce the environmental impact of transport.
- To increase energy efficiency, the product will be designed to use renewable energy and energy-saving lamps.
- The product will have elements for waste management.
- The expected battery would have dimensions of $278 \times 175 \times 190$ mm and approximately 90 amps. The battery size has been studied to work for several days without charge in case there is not enough sunlight.

Taking into account the conceptual design, each of the parts that make up the product have been designed with the computer-aided design software SolidWorks

2016. The three main parts of the product are the seat, the table and the awning with the light fixture. The seat (Fig. 4a) is a curved module with smooth surfaces and rounded edges. The main structure (Fig. 4b) is formed by a pole that supports a structure with the awning. This structure holds the light and the solar panels that feed the entire system. The table (Fig. 4c) has the shape of a drop of water, where the surfaces are also smooth and with rounded edges.

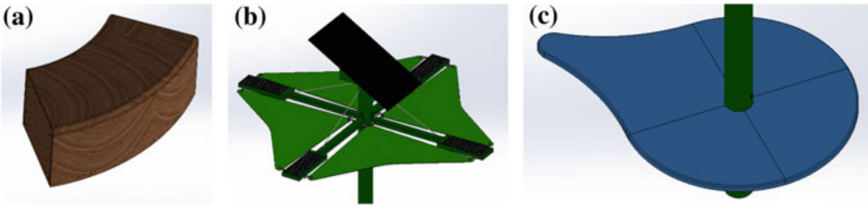

Fig. 4. Main elements of the product: **a** seat, **b** awing and light fixture, and **c** table

Figure 5a shows the USB connection that is coupled to the structure's pole. This location is very accessible and comfortable for all of the product's users. Figure 5b shows the design of the wastebasket, an element that is considered important to enhance the management of waste and raise the degree of sustainability.

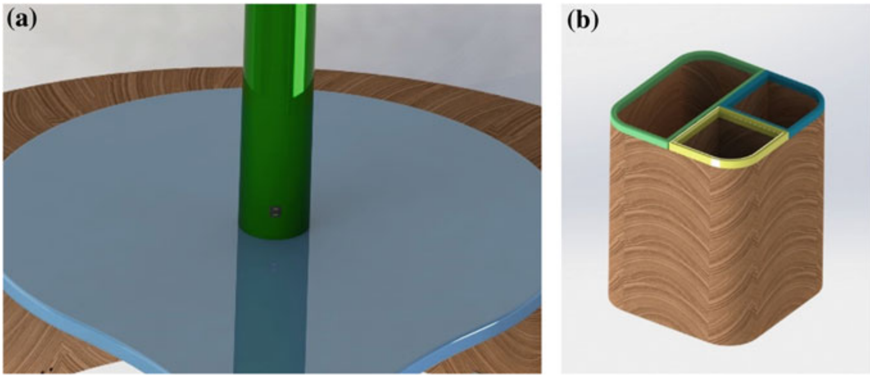

Fig. 5. **a** USB connections for recharging mobile devices, and **b** Wastebasket for waste management

2.4 Materials

The sitting bench will be made of wood, taking into account that this material does not transmit the temperature and can allow its use in midday hours. On the other hand, the use of certified forest products (FSC, Forest Stewardship Council) is recommended because it promotes responsible management of forest resources from an environmental point of view. The table will also be made of plywood with a smooth finish for easy cleaning and maintenance.

The main structure of the product, which is formed by the pole and upper structure, will be made of galvanized steel, taking into account that it must be a robust and safe element. The element responsible for producing shade is a polyester fabric with PVC coating on both sides, which will be attached to the upper structure.

3 Results

Figure 6 shows the final design of this product. The basic design concept is a snake that creeps with sinuous movement around the table that recreates a river or lake. The structure emulates a stem and the leaves of the water lily cover the whole piece.

A part of the bench, following the sinuous form that it has, lays outside of the piece to offer the possibility to the users to sit down without needing to be around the table. On the other hand, we have left an access to the set for people in wheelchairs with an amplitude greater than 80 cm, the minimum established for this type of access. The position of the wastebasket is strategic, neither near nor far, enough for users to use it for the management of their waste and to promote a clean and sustainable environment.

Nowadays, the use of electronic devices is encouraging the location of recharging points in many places. It is still difficult to find this type of service outdoors, so offering it in this type of product is an added value.

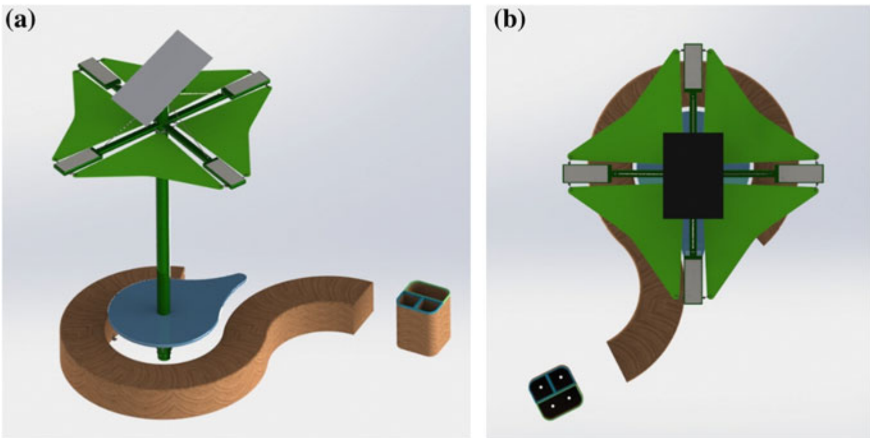

Fig. 6. Final design of the product: **a** Perspective view, **b** Top view

4 Conclusions

Nature can be an inexhaustible source of ideas, it is full of forms and movements that can serve to develop the conceptual design of any product. In this communication the most important phases of the process of designing a bioinspired urban furniture piece have been shown. This product arises from the need for a type of environment, located in common educational areas or parks, which encourage social gathering, rest or leisure for any type of user. To provide greater added value to the product, other important aspects are offered in the design, such as adequate access for people with wheelchairs, use of solar panels for self-consumption of the lighting and recharging system, and elements for the management of waste. In this way, different aspects such as social, environmental and economic have been reflected in the product, which serve to balance its global value.

References

1. Gay A, Samar L (2004) El diseño industrial en la historia. Tec
2. Soroa D (2016) Arquitectura biomimética. http://cuantics.blogspot.com.es/2008/07/arquitectura-biomimtica.html (7/01/2016)
3. Ding W, Yang L, Zhao Y (2011) The conception design of flower-shaped seat in park landscape. In: International conference on materials and products manufacturing technology, ICMPMT 2011, Chengdu, pp 111–114
4. Tavsan C, Tavsan F, Sonmez E (2015) Biomimicry in architectural design education. Procedia-Soc Behav Sci 182:489–496
5. Tavsan F, Sonmez E (2015) Biomimicry in furniture design. In: 7th world conference on educational sciences, Athens, Greece, pp 2285–2292
6. De Fusco R (1981) Historia de la arquitectura contemporánea. H. Blume Ediciones
7. López AD (2010) La naturaleza, madre del diseño. Universidad de Palermo (Buenos Aires, Argentina), Fuente de inspiración para la creación de objetos
8. Macdonald AS (2001) Aesthetic intelligence: optimizing user-centred design. J Eng Des 12:37–45
9. Wu TY, Chen HK (2015) Products with biomimetic shapes convey emotions more effectively. In: 4th international conference on design, user experience and usability, DUXU 2015 held as part of 17th international conference on human-computer interaction, HCI international 2015, vol 9186. Springer, pp 559–566
10. Calero V (2011) Biomímesis como equivalente de sostenibilidad. Universidad del País Vasco - Euskal Herriko Unibertsitatea (UPV-EHU), País Vasco, Las sociedades en emergencia energética como muestra
11. Fabra ML (2015) Sensorialidad, emotividad, reciclado y reutilización: Un diálogo sostenible con las ciudades. Departamento de Ingeniería de Sistemas Industriales y Diseño. Universitat Jaume I, Castellón
12. Iguarán NJ, Hernández OJR (2016) Biomímesis: Una propuesta ética y técnica para reorientar la ingeniería por los senderos de la sustentabilidad. Gestión y Ambiente 19:155
13. Guía de mobiliario urbano sostenible con eficiencia energética (2009) Direccion General de Industria, Energía y Minas de la Comunidad de Madrid y SIARQ (Mobiliario Urbano Sostenible): Madrid

14. AENOR (2004) Principios ergonómicos para el diseño de sistemas de trabajo. Madrid, vol UNE-EN ISO 6385
15. AENOR (2010) Definiciones de las medidas básicas del cuerpo humano para el diseño tecnológico. Parte 1: Definiciones de las medidas del cuerpo humano y referencias. Madrid, vol UNE-EN ISO 7250-1, p 30
16. Benjumea AC (2003) Aspectos antropométricos de la población española aplicados al diseño industrial. Instituto Nacional de Seguridad e Higiene en el Trabajo
17. Cabello EV (2008) Antropometría. Instituto nacional de seguridad e higiene en el trabajo. www.insht.es

Tumor Reconstructive Surgery Assisted by Scale Models Using 3D Printing

D. Parras-Burgos(✉), P. Puertas García-Sandoval, C. Baño Pedreño, F. Cavas-Martínez, F. J. F. Cañavate, and D. G. Fernández-Pacheco

Department of Graphic Expression, Technical University of Cartagena, C/Doctor Fleming, s/n, 30202 Cartagena, Murcia, Spain
dolores.parras@upct.es

Abstract. A surgical planning of tumor reconstructive surgery requires a multidisciplinary collaboration between the surgeon, the radiologist, the nuclear medicine doctor and the pathologist. Nowadays, this team has been incorporating other profiles not related to the health field, such as engineers and researchers that favor the use of new technologies such as virtual modeling or 3D printing. In this study we describe the different phases of surgical planning of four cases of musculoskeletal tumors (knee, pelvis, femur and humerus), in which the latest technology such as virtual modeling of the anatomy of patients, the design of surgical guides and 3D printing of all models have been used. With this type of planning, surgeons are helped by being able to analyze in a millimetric way the tumor, the bone, the soft tissue, the cutting areas and to foresee the possible complications that could arise during this type of surgical intervention.

Keywords: 3D printing · 3D anatomic models · Surgical planning

1 Introduction

Musculoskeletal tumors are those malignant tumors that originate in connective tissue (cartilage, muscles and bones). To determine their existence, it is necessary to carry out several medical tests from the beginning. Different studies that establish tumor stage and treatment planning should be performed before the biopsy, because radiological studies can be influenced by the surgical manipulation of the lesion and complicate interpretation [1]. Protocol indicates that different imaging tests such as XR (X-Rays), CAT (Computerized Axial Tomography) or MRI (Magnetic Resonance Imaging), as well as, PET-CAT (Positron Emission Tomography) should be performed to assess the possible extension of the lesion and the grade of the tumor locally. For a final diagnosis, a multidisciplinary collaboration among the surgeon, the radiologist, the nuclear medicine doctor and the pathologist is necessary [2].

The surgical treatment of these tumor lesions should lead to acceptable local control, a correct motor function, or acceptable consequence that allows the affected member to be autonomous. Three types of oncological surgical treatment can be differentiated [3]:

F. Cavas-Martínez et al. (Eds.): *Advances on Mechanics, Design Engineering and Manufacturing II*, LNME, pp. 573–582, 2019.
https://doi.org/10.1007/978-3-030-12346-8_56

- Intralesional excision, which consists of a type of curettage with filling of the cavity with bone graft or cement.
- Resection in block of the tumor, in which the removed segment is usually replaced by megaprosthesis or bone transplants, or a combination of both, when it is necessary from the mechanical point of view.
- Amputation, when resection is not possible due to the invasive characteristics of the tumor.

This study focuses on surgical treatment through block resection of the tumor and subsequent reconstruction of the created defect in patients affected by sarcomas in the humerus, knee, femur and pelvis. For the surgical planning of a block resection, a multidisciplinary team of professionals is necessary. Nowadays, this team has incorporated other profiles not related to the health field, such as engineers and researchers, which favor the use of new technologies such as 3D printing, enabling the translation from a virtual planning to a tangible one [4–6].

There are studies in which fetal faces have been replicated using 3D printing. Not only do these replicas diagnose possible malformations, but they also help future parents to achieve emotional and affective goals. This process is not simple; steps are already being defined to reliably and accurately transfer all the data obtained with medical images to the physical model obtained by 3D printing [7]. Additive manufacturing technologies are reaching new perspectives every day. Recent studies are testing various implantable devices in which 3D printing can achieve benefits such as personalization, optimization and the fabrication of very complex geometries [8].

In summary, this study describes the different phases of surgical planning of four cases of reconstructive tumor surgery, in which cutting edge technology has been used, such as virtual modeling of patients' anatomy, design of surgical guides and 3D printing of all models. The realization of models obtained by 3D printing, which exactly replicate the anatomical part of the patient being treated, helps surgeons to analyze in a millimetric way the tumor, the bone, the soft tissue, the cutting zones and to foresee possible complications that could arise during the surgical intervention.

2 Materials and Methods

For this work four patients affected by malignant tumors of the humerus, knee, pelvis and femur have been studied by planning reconstructive surgery with different imaging techniques, such as virtual modeling and 3D printing of scaled models of the anatomy of each patient. The study was conducted at the Musculoskeletal Tumor Unit of Traumatology of the University Hospital Virgen de la Arrixaca (HCUVA) in Murcia (Spain), and was approved by this institution. Informed consent was obtained from all subjects.

2.1 Case Studies

The four case studies dealt with in this work are of patients affected with tumors in a musculoskeletal region. More details of each patient is provided below:

- **Case study 1**: A 28-year-old male diagnosed with a primary bone tumor (osteosarcoma) of the proximal tibia. Planning with implantation of knee megaprosthesis associated with bone transplantation of the proximal tibia and extensor apparatus. Coverage with gastrocnemius flap.
- **Case study 2**: A 72-year-old male diagnosed with bone tumor metastasis in the iliac region (pelvis) secondary to thyroid cancer. Planning with previous embolization of branches of the superior gluteal artery and lumbar branches. Complete resection and reconstruction with cementation and osteosynthesis.
- **Case study 3**: A 56-year-old male diagnosed with a primary bone tumor (chondrosarcoma) located in the lower trochanter of the femur and with involvement of the adductor muscles. Planning with previous neoadjuvant radiotherapy and resection surgery.
- **Case study 4**: A 72-year-old man diagnosed with bone metastasis in the proximal humerus secondary to lung cancer. Planning with mega-prosthesis of humerus.

2.2 Surgical Planning

The surgical planning of interventions with block resection of the humerus, knee, femur and pelvis with bone tumor effects, includes the following five phases: (i) scanning phase, in which the patient has x-rays, resonances and PET-CT done to obtain medical images, (ii) virtual phase, in which a virtual model of the patient's anatomy is obtained from the medical images, (iii) 3D printing phase, in which a 3D model is printed from the virtual model, (iv) phase of study, in which the surgical intervention is planned based on the medical images and 3D printing obtained, and (v) the surgery phase, in which the surgery is performed. Each of the phases described is detailed below.

- **Scanning phase**

Medical images are a compilation of techniques and processes used to create images of the human body for clinical purposes. Imaging allows doctors to look inside the body for signs of a medical condition. There is a great variety of devices and techniques that can create images for the diagnosis of pathologies or as a preventive procedure: radiography, ecography, magnetic resonance imaging, positron emission tomography, computed axial tomography, cone beam computed tomography, etc.

In the present study, three imaging techniques have been used in the surgical planning of the four case studies. On the one hand, radiography (XR), which is considered the most important imaging method and the first to be performed in the diagnosis of bone tumors. This diagnosis method analyzes lesions by defining the location of the tumor, the opacity, the margins, the transition zone, possible periosteal reactions, mineralization, size and number of injuries, as well as the soft tissue component and the presence or absence of fractures [9]. The equipment used to obtain medical images with this technique is the Toshiba model i-Rad DR of high resolution of the HCUVA (Fig. 1).

The second technique used is magnetic resonance imaging (MRI) with the Philips MR Systems Achieva Release 2.6.3.9 2013-10-30 SRN: 32051 (1.5 Teslas). The MRI stands out for its ability to highlight the contrasts in the soft tissue, which becomes useful when identifying problems in joints, cartilage, ligaments and tendons (Fig. 2).

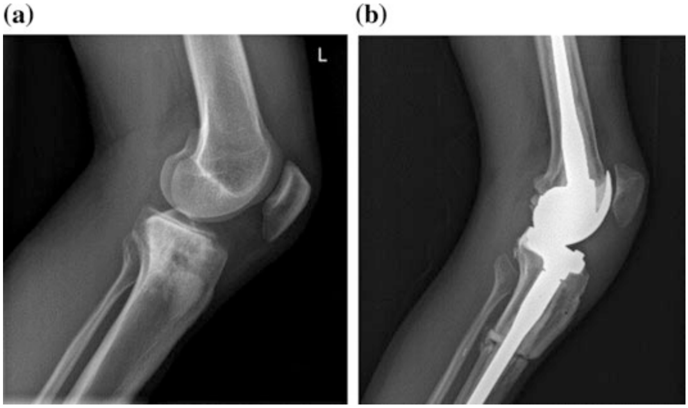

Fig. 1. Case study 1: **a** XR before surgery, and **b** XR after surgery

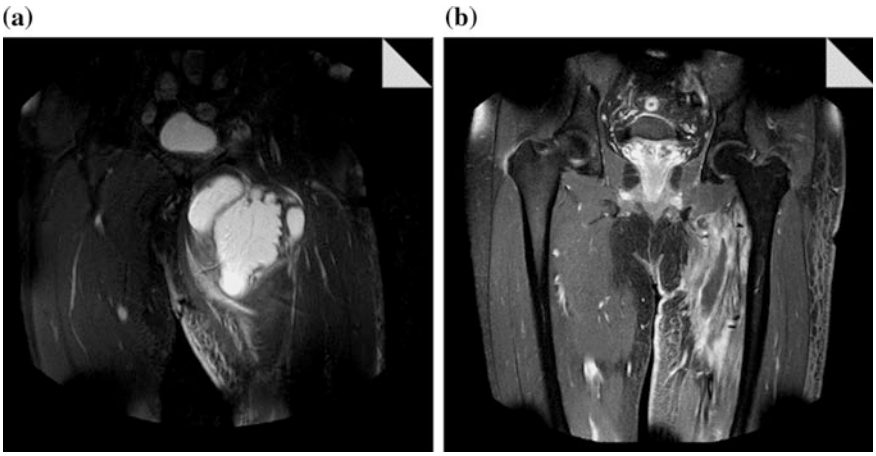

Fig. 2. Case study 3: **a** MRI before surgery, and **b** MRI after surgery

Finally, a hybrid was used between two imaging techniques, CT or CAT (Computerized Axial Tomography) and PET (Positron Emission Tomography), which represent a revolution in the diagnosis and treatment of tumor pathology. PET-CT with 18 F-flurodeoxyglucose (F18-FDG) is performed as a single test in the Nuclear Medicine Service of the HCUVA with the Philips PET/TC hybrid model Gemini GXL (origin: Amsterdam, The Netherlands) that integrates a CT of 16 cuts and a 3D high resolution PET for the realization of this type of study. The CT scan is a radiology test that studies the morphology assessing both the location of the lesion and its size. PET technology is used to obtain a metabolic image, in which the presence of lesioned areas is detected at an early stage, even when they are very small (Fig. 3).

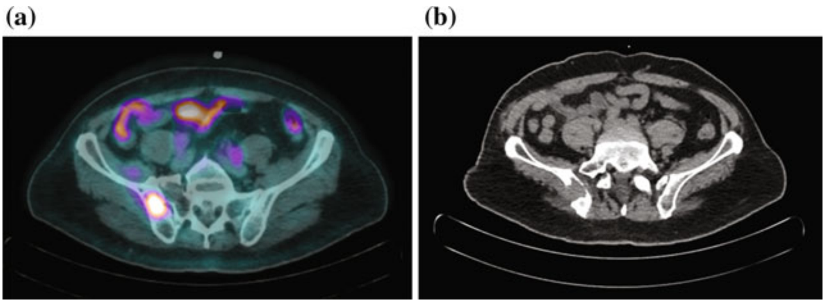

Fig. 3. Case study 2: **a** PET-TC before surgery, and **b** TC after surgery

- **Virtual phase**

The data obtained by PET-CT is stored in DICOM format (Digital Imaging and Communications in Medicine) and processed by a specific program to obtain a virtual model of the patient's anatomy. With this virtual model, surgeons can work to design cutting guides, references and other necessary elements for surgical intervention. Both the anatomical model of the patient and the designed elements are exported in STL format for use in the next phase, 3D printing (Fig. 4).

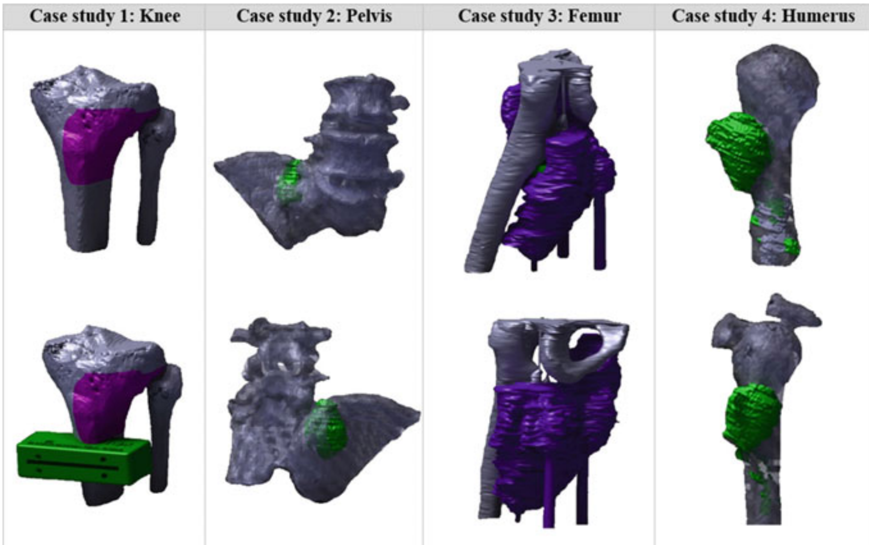

Fig. 4. Virtual models of all case studies

- **3D printing phase**

Nowadays, there are different technologies used to obtain prototype models, in which different materials can be started, deformed, melted and joined. For some time, physical models have been able to be manufactured from 3D virtual models through material deposition techniques. This type of additive technology is based on the dispersion-accumulation principle. The processes of material contribution or additives are those that solidify a material, originally in solid, liquid or powder state, by successive layers within a predetermined space and with electronic procedures. These methods are also known by the acronym MIM (Material Increase Manufacturing), and their classification can be made according to two different factors, such as the starting material and the process of obtaining the model (Table 1).

In this study, the 3D printing technique chosen for the manufacture of the anatomical models and the elements designed for the surgical intervention is Fused Deposition Modeling (FDM) due to its manufacturing characteristics and the properties of the contribution material. Thanks to this technology, reproductions on a natural scale of the patient's anatomy are obtained, helping to plan the aspects of the surgical approach that will be followed. The device used for the manufacture of the models is Ultimaker 2+ with a maximum construction volume of 223 × 223 × 205 mm. The layer thickness can vary from 20–600 μ with a speed of up to 24 mm^3/s.

The models (Fig. 5) are made with biodegradable polylactic acid (PLA) derived from lactic acid, which is a thermoplastic obtained from corn starch. This material stands out for its use in the field of medicine for its good resistance to traction, for its superficial quality and its ease to work at high printing speeds. In addition, it can be sterilized and used during surgery.

Table 1. Additive manufacturing processes

Material	Process	Tool	Name
Liquid	Solidification	Ultraviolet radiation from a laser	Stereolithography (SLA)
			Solid Object Ultraviolet Laser Printer (SOUP)
		Ultraviolet-light lamp	Solid Ground Curing (SGC)
			Inkjet Rapid Prototyping or Poly Jet
Solid	Smelting/Solidified	Extrusion head	Fused Deposition Modeling (FDM)
		Injection head	Headform Injection
	Carving and adhesion	Lamination	Laminated Object Manufacturing (LOM)—Selective Deposition Lamination (SDL)
Powder	Join	Binder	3D Printer
	Sinter	Laser	Selective Laser Sintering (SLS-DMLS)

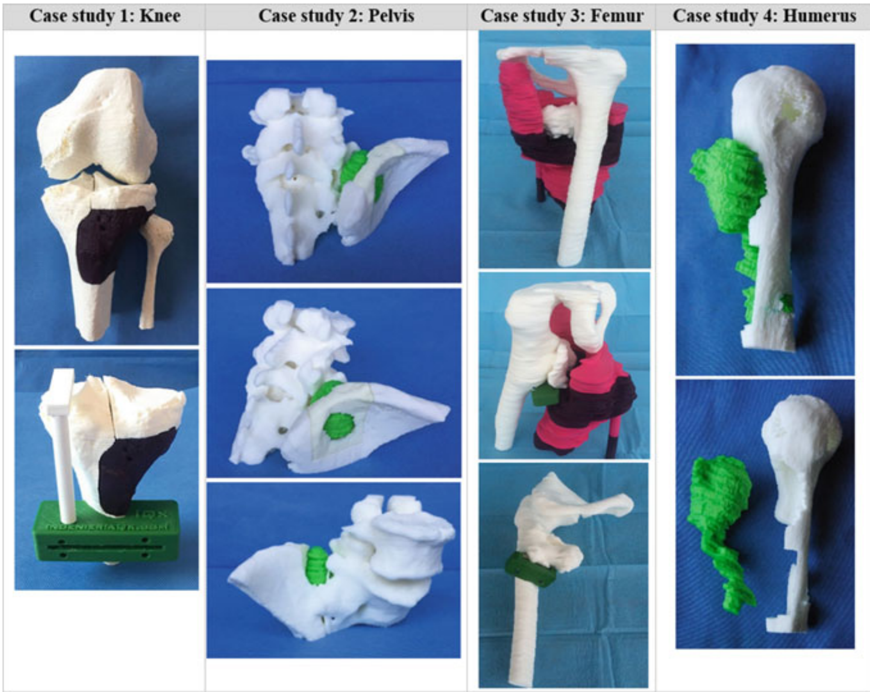

Fig. 5. Models obtained by 3D printing

- **Study phase**

A computer system called SELENE 5.3.3 is used for the creation and classification of patients' medical records at the HCUVA, as well as a medical image viewer called Siemens DRX 3.0 Viewer. With the collection of the different clinical tests, the obtained images and the 3D printed models, the medical team can study each clinical case carefully and plan out step by step the surgical intervention (Fig. 6).

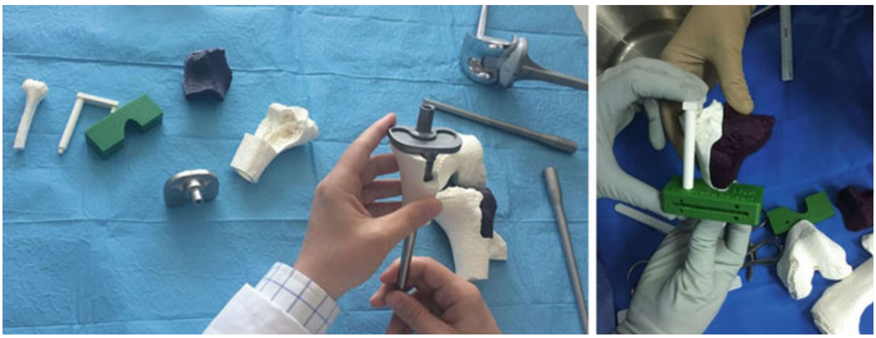

Fig. 6. Surgical planning case study 1

In the preoperative planning of each clinical case, the following information is determined: the implications of the tumor on the different adjacent structures (vessels, nerves, muscle groups, joints); the dimensions of the resection that must be performed; the implants or prostheses that will be used and their possible sizes; as well as, if necessary, the use of surgical guides to perform the most precise osteotomies (cuts of bone structures). After the tumor resection, to reconstruct the defect created and thus maintain the length of the bone and its functionality, larger than conventional prosthetic systems called megaprosthesis are used. These prosthesis are formed by modular elements that are assembled until the exact measurement of the bone defect is obtained. They are usually used in knee, shoulder and femur and its use is notable because it avoids the morbidity of the donor area, requires less surgical time and preserves mobility [2].

- **Surgical phase**

The surgical team that intervenes in this type of operation is usually composed of two orthopedic surgeons, a traumatology resident, an anesthetist and three operating room nurses. Surgical intervention can be divided into three distinct parts: (i) oncological resection of the area affected by the bone tumor, (ii) intraoperative biopsy of the healthy bone end to verify that it is free of tumor lesions, and (iii) placement of the megaprosthesis replacing the created defect. This megaprosthesis is incorporated at one end by the new prosthetic joint and, on the other, by a cemented stem attached intramedullary to the remaining bone of the patient.

3 Results

As seen in Table 2, thanks to previous planning, a considerable reduction of time is achieved, between 30 min and 1 h, in each of the surgical interventions.

For the clinical assessment of each patient the MSTS scale (Musculoskeletal Tumor Society Rating Scale) was used, which assess different aspects such as pain, function, gait, the need for support and the emotional component [10] differentiated according to whether they are superior or inferior limbs. The range goes from 0 to 30 and, as it can be seen, in all cases the values are very high, ranging between 26 and 30 points. In most cases the emotional component of patients is high, since they have been diagnosed with cancer with one possible treatment being amputation. Thanks to megaprosthesis implant systems, the tumor can be removed and the affected limb left with acceptable function, maintaining its autonomy in most cases.

After surgery, patients remain admitted for analgesic control and with intravenous antibiotics. Afterwards they are followed up on an outpatient basis by the outpatient clinics, and after the healing of the surgical wounds, a progressive mobilization protocol is initiated. The patient of the case study one had a slower healing time than the required, and was also subjected to cycles of chemotherapy after surgery. The patient began walking without external devices at 12 weeks, with a range of mobility of 0º of extension and 110º of flexion. The second case initiated ambulation at 2 weeks with an external device and from the fourth, with complete autonomy. The third case study presented a torpid evolution at the beginning due to a seroma that was resolved by

Table 2. Results of case studies

	Case study 1	Case study 2	Case study 3	Case study 4
Surgery time (h)	6	4	4	5
Approximate reduction by surgical planning (h)	−1	−1	−0.5	−1
3D printing	Yes	Yes	Yes	Yes
Cutting guides	Yes	No	Yes	No
Resection length	7 cm	–	–	11.5 cm
MSTS (0–30)	26	30	26	28
Complications	None	None	Seroma of the wound that required drainage	None
Late complications	None	None	None	None
Mobility range	0º–110º	Complete wandering without external devices	Complete wandering with adduction deficit	Abduction 90º Antepulsion 100º Retropulsion 20º

draining the seroma and began complete ambulation at 8 weeks. The fourth case study initiated pendular and abduction movements from the fourth week, which is when the healing of the reinserted musculature in the prosthesis is optimal.

4 Conclusions

Obtaining virtual models and 3D printed models of anatomical parts of patients affected by malignant tumors, helps to carry out a more exhaustive planning of the surgical intervention. Moreover, a more precise planning of the surgery permits to achieve a reduction between 30 min and 1 h in surgery time. In this way, the risks of infection or any other complication that might arise are also reduced, and the shorter postoperative period is less painful. All of this planning and surgery process makes two important things possible: the complete excision of the tumor and the maintenance of the mobility of the affected limb.

Acknowledgments. The research reported here was made possible by IngenieríaQX.

References

1. Malawer MM, Shomookler BM (1995) En: Sugarbaker, p.H. & malawer, m.M. Estadiaje, patología y radiología de tumores musculoesqueléticos. In: Cirugía del cáncer musculosquelético: Principios y técnicas. Mosby-Doyma Libros, Madrid, pp 27–30
2. Valcárcel A (2011) Experiencia del hospital universitario "virgen de la arrixaca" en el manejo del tumor óseo de células gigantes. Análisis retrospectivo. Universidad de Murcia

3. Turcotte RE, Isler M, Doyon J (2001) Tumor de células gigantes. In: Encyclopedie médico-chirurgicale. Elsevier, Ed. Paris
4. George E, Barile M, Tang A, Wiesel O, Coppolino A, Giannopoulos A, Mentzer S, Jaklitsch M, Hunsaker A, Mitsouras D (2017) Utility and reproducibility of 3-dimensional printed models in pre-operative planning of complex thoracic tumors. J Surg Oncol 116:407–415
5. Pérez-Mañanes R, Calvo-Haro J, Arnal-Burró J, Chana-Rodríguez F, Sanz-Ruiz P, Vaquero-Martín J (2016) Nuestra experiencia con impresión 3d doméstica en cirugía ortopédica y traumatología. Hazlo tú mismo. Revista Latinoamericana de Cirugía Ortopédica 1:47–53
6. Tack P, Victor J, Gemmel P, Annemans L (2016) 3d-printing techniques in a medical setting: a systematic literature review. Biomed Eng online 15:115
7. Speranza D, Citro D, Padula F, Motyl B, Marcolin F, Calì M, Martorelli M (2017) Additive manufacturing techniques for the reconstruction of 3d fetal faces. Appl Bionics Biomech, 2017
8. Zanetti EM, Aldieri A, Terzini M, Calì M, Franceschini G, Bignardi C (2017) Additively manufactured custom load-bearing implantable devices: grounds for caution. Aust Med J (Online) 10:694
9. Sánchez-Torres L, El Santos-Hernández M (2012) arte de diagnosticar tumores óseos. Acta Ortopédica Mexicana 26:57–65
10. Enneking WF, Dunham W, Gebhardt MC, Malawar M, Pritchard DJ (1993) A system for the functional evaluation of reconstructive procedures after surgical treatment of tumors of the musculoskeletal system. Clin Orthop Relat Res, 241–246

Innovation

Eco-Ideation Workshops: Definition and Requirements

I. López-Forniés[1(✉)] and J. Sierra-Pérez[2]

[1] Dpto. Ingeniería de Diseño y Fabricación, C/María de Luna s/n, Saragossa 50018, Spain
ignlopez@unizar.es

[2] CUD Centro Universitario de la Defensa, Ctra. de Huesca s/n, Saragossa 50090, Spain

Abstract. To develop creative eco-ideation workshops it is necessary to structure a series of objectives and tasks, establishing the design of the workshop itself. In our work the theoretical process is presented, its justification and an example of preparation of a workshop is shown. The design process establishes design and manufacturing requirements, plays a key role in eco-innovation, and the eco-design phase must be integrated into the generation of ideas and concepts. Only a few creativity tools have been adapted for eco-innovation, so the ideation phase of eco-innovation is limited, this fact allows the definition of a proper process for the development of creative workshops in eco-innovation projects. Specificities for eco-ideation process are the definition of objectives, the expert profile selection and environmental parameters included in the metrics. The preliminary stages of preparation define the process, but also establish the criteria for selecting participants, creative techniques, and criteria for evaluating results. There is no described methodology to apply in these processes and this work aims to define a series of basic actions and reflect the experience of a real project.

Keywords: Eco-ideation · Eco-innovation · Creative process · Creative workshop · Creative group configuration · Design process

1 Introduction

Eco-ideation [1] is part of the creative process in eco-design within eco-innovation projects [2], the success of any workshop that includes a creative process depends on the dedication and time for preparation. The better preparation and anticipation of possible events the better results and greater control in the management of the workshop itself. To develop creative eco-ideation workshops [3, 4] it is necessary to structure a series of objectives and actions, establishing the design of the workshop itself. In the paper the theoretical process is presented, its justification and an example of preparation of a workshop is shown.

The design process establishes design and manufacturing requirements, plays a key role in eco-innovation, and the eco-design phase must be integrated into the generation of ideas and concepts. In a comparative study [5] it was detected that there are very few

F. Cavas-Martínez et al. (Eds.): *Advances on Mechanics, Design Engineering and Manufacturing II*, LNME, pp. 585–595, 2019.
https://doi.org/10.1007/978-3-030-12346-8_57

eco-design tools or methods that focus on the eco-ideation process, and the current proposed tools or methods have proven to be complex, theoretical and little used [1]. A few creativity tools have been adapted for eco-innovation, so the ideation phase of eco-innovation is limited [6], this fact allows the definition of a proper process for the development of creative workshops in eco-innovation projects.

The design of the workshop implies a series of previous steps in which to define the objectives and expected results, the definition of the creative group and its participants, the techniques that will be applied, the schedule, the material and work space requirements. These preliminary stages of preparation define the process, but also establish the criteria for selecting participants, creative techniques, and criteria for evaluating results. There is no described methodology to apply in these processes and this work aims to define a series of basic actions and the experience of a real project.

In an eco-ideation process, there are two objectives to be defined. First, it is necessary to align the creative session with the objective of the eco-innovation project. This objective implies defining expected results, so that the evaluation criteria of the ideas or concepts generated. Second, the definition of the requirements of the creative sessions in terms of participant profiles, techniques, duration, and so on. To establish the needs for innovating from an environmental approach, in most cases, quantitative or semi-quantitative environmental information will be necessary to assess whether the results of the eco-design process have improved the initial state.

The selection of the group is done in two stages. The first one tries to define the participant to be selected for the creative session that are responsible for putting the ideas obtained into action. Moreover, in the second one, they look for complementary participants to cover the needs of the session defined by the described objectives. Then, the working group is formed, the group is usually interdisciplinary and this defines a particular way of work and interaction. The interdisciplinary nature consists of the integration of two profiles, the creative core profile related to creativity and design and the expert profile related to some of the subjects of the topic to be solved. In the working group, several roles are defined: facilitator, registrar and participants.

Moreover, when defining the creativity techniques to be developed, the criteria for choosing them are established. Usually, they are adaptations or transformations required by the group's own configuration. In this preparation of the techniques, it is important to highlight the warm-up phase.

Finally, the structure of the creative sessions is defined. The planning is done with time allocation to each part that defines the sequence of activities and the expected margins of time, since time is a limiting factor in creative sessions to be able to obtain results of quality. The needs in terms of the workspace, the workshop materials, way of recording information and idea registration for further processing are also defined.

2 Eco-Ideation Workshop Process

In every design process, there is a phase for idea generation and conceptualization. When the objective of the project is led towards eco-innovation, it is necessary to establish a specific phase of eco-ideation in order to achieve concepts that comply with previously established environmental goals.

The main specificities between a classic creative process and an eco-ideation process are: the definition of objectives, due to the fact that an environmental challenge is included; the selection of the group since it needs participants with an experienced LCA (Life Cycle Assessment) or environmental profile; and finally, in same occasions the creative techniques must be adapted if the participants are not used creative sessions. Also the evaluation phase could be specific, since some environmental parametres are included in the metrics.

In Table 1 a theoretical process for an eco-ideation workshop is set. Along the text, every phase is explained and detailed with the tasks and different commitments involved.

Table 1. Process for an eco-ideation workshop

Phase	Task/commitment
Objectives definition	Environmental goals/impact reduction/LCA (Life Cycle Assessment) improvement Expected outcome
Participant selection	Creative leaders and creative team Expert team
Creativity techniques selection	Warm-up activities (icebreakers) Idea generation techniques Concept generation
Programming	Schedule and temporary planning Material requirement definition Space requirement definition
Creativity sessions	Playing sessions. Warm-up/idea generation/concept generation
Results evaluation	In situ/group evaluation Subsequent expert evaluation Concept definition and selection

2.1 Objectives Definition

Initially, the environmental goals are set for the eco-ideation process. These are established by the main objective of the project, and also have to be written as a design problem in order to plan the ideation session. An environmental goal coexists with the design goals. That is, product design specifications have to be accomplished as well as the environmental goals, formal and functional requirements must be compatible with impact reduction or LCA improvement solutions.

Sometimes, the environmental goals match with a redesign process, in order to improve problems detected by environmental analysis. Therefore, the eco-ideation process is led to solve specific problems that can be well defined and measurable; the results will be easily quantifiable versus the expected. On the other hand, some others, the goals are led to a new design or even a new concept design. In those cases, the design process starts with a fuzzy front-end and the results will be compared with existing products that can have an inaccurate and subjective measure.

In order to set the environmental goals some specific information is needed, quantitative or semi-quantitative. It allows us to mark a series of expected results to assess whether the results have improved the initial state. To obtain this environmental information from the starting situation, the most common eco-design tools can be used [7, 8]; among them, the most widespread is the LCA [9].

2.2 Participant Selection

The group formation is a crucial phase to obtain the expected results, since it defines the profiles of the participants and what is expected from each one. We can classify them in two ways: first if they are participants in the project or if they are invited, and second if their contribution is the creative task or if they are an expert in some factor related to the environment. When the group is formed by people who must implant the ideas and concepts generated, and also by external people who only attend the creative session, a balance is needed. Since a lack of environmental experts can lead to unrealizable solutions and an excess can derive in an uncreative and unoriginal work in which only the environmental factors are contemplated.

The group is formed trying to cover the main factors of the design project, bearing in mind that the environmental is a key one. This interaction needs to be well manage because not all participants knows each other and are not familiar to such a particular way of work, so the participant profile is selected by its expertise and contribution as well as the personal traits. Diversity in participants' groups increase creativity by expanding the group knowledge available and introducing different perspectives that can be generate novel ideas. The integration of creative and expert profiles defines the interdisciplinary group, being the creatives the core of the group for that design phase, integrated by designers and creative facilitators or just participants. The expert plays an environmental role that will provide information and data, or may be an evaluator of the ideas and concepts in case of being in charge of setting the environmental criteria; expertise could be in engineering, architecture, materials, LCA assessment, etc.

The roles of the creativity [10] core are the facilitator, as a leader of the group that orchestrates every element of the session and make easy for every participant in achieving the particular goals. Participants, that are familiar with creative process, are capable to generate ideas shared with the expert, producing ideas according to requirements that meet the environmental goals. Finally, the registrar that plays a special role by obtaining the documentation of the session in different formats, written and audiovisual are the most common. All this documentation will serve as for an after analysis of the session to complete the work and generate the concepts.

The balance of the group, the ratio of participants' technical/creative, is determined by the objectives of the workshop. For workshops in which a great capacity for the generation of ideas is required, and without many technical requirements, it is necessary a ratio lower than 1. In workshops where the focus is to generate ideas very close to the realization is necessary a ratio greater than 1. A ratio around 2 is suitable for creative sessions, but a higher number could cause a lack in novelty during.

2.3 Creativity Techniques Selection

The creativity techniques must be chosen depending on the group configuration. If there are participants not familiar with creativity processes, then the techniques must be as simple as possible. That is techniques easy to start with and with no previous requirements, based on dialogues, conversations or answering questions methods [11].

The first part of the creativity session is planned out by warm-up activities, there are a numerous kind of icebreakers exercises to introduce participants that they do not know each other, that is the first objective [10]. These exercises will set a relaxed and friendly atmosphere, and serve as a barrier eliminator by unblocking the participants' thoughts, the second objective. The icebreaker exercises can be brain games not related to the session task or activities that will serve to ulterior part of the session.

Workshops in which all participants have experience in creative sessions can use techniques without the need for transformation. The selection is made based on the creative focus of the workshop, being able to gather methods of analysis of problems followed by generation or directly idea generation. In the case of starting with problem analysis, techniques based on questions, provide a situation of "cause finding" or "unobserved search". This allows a divergent and open process, part of the idea generation is structured into small stages to answer each of the issues raised in the analysis of problems. On the other hand, if the session goes straight to the idea generation, it starts with techniques that introduce random elements to produce a divergent and provocative effect. Then techniques of idea transformation are used, oriented to the definition of concepts, as a grouping of ideas.

If the group has not experience, then the facilitator may change the techniques and use adaptations or transformations that make the process easy and friendly. The techniques used belongs to the same creative methods, as if the group have experience, but some characteristics like time span, deferred judgment, initial requirements or idea registration are adapted. In addition, some techniques are mixed taking some traits from another technique, for example using random input in an associative method.

Some creative sessions address to generate concepts, including the definition of the ideas as solutions. Others instead, deep in the definition of an idea or how to achieve it. In that part of the session, the group have to set a list of requirements that matches with the objectives of the project, for example. If the project is assessed by technical or economic criteria, the concept generation have to give information about how to solve the technical particularities or economic needs, or how much could improve the present situation.

2.4 Programming

The process divided in stages needs a schedule and a temporary planning [10]. The schedule fixes the dates for the workshop and the timetable for each session, that can be divided in parts assigning time for each, including breaks. If the group does not have invited members, setting a date is simpler, in case of having guests or external parties it is necessary to establish a common agenda, in date and time. The duration of the workshop is set in the planning establishing whether one or two sessions are necessary and how many parts each one should have. If the workshop focuses only on idea generation, one session is enough, while if there are concept generation and even its evaluation, it is necessary to have two sessions. An evaluation session must be done separately, it is recommendable to have a differed judgment of the ideas, and it may be necessary to generate certain documentation for the evaluation. Necessary documentation may be drawings or renders of conceptual proposals, calculations of LCA, or technical and economic documentation. In addition, it is necessary to establish a metric that allows to evaluate each concept, comparing with what exists.

Planning also takes charge of the definition of the necessary, which are related to the techniques. Moreover, as well as the selection of the room, which will mainly depend on the number of participants and will be adjusted to the requirements of the session. The most usual, is to have a wide and luminous space, with movable tables and chairs, facilitating the mobility of the participants, large size blackboard/screen, note and drawing paper, self-adhesive papers and markers, registration cards and similar materials.

2.5 Creativity Sessions

Once the group has been formed and the sessions have been defined, it is time to start the workshop. The group can be divided into small groups for some activities, and working as a whole for some others. An icebreaker is a facilitation exercise intended to help a group to begin the process of forming themselves into a team. Icebreakers are commonly presented as a game to "warm up" the group by helping the members to get to know each other. The warming-up is important to do it always, if the participants are experts can be used to guide the workshop or to determine some particular aspect or clarify details. Its duration is short about 10 or 25 min, should be easygoing and must make the whole group participate and integrate.

After the warm-up the creative process continues with the techniques selected and participants follow the instructions of the facilitator. In small groups the facilitator acts as a registrar, in charge of the recording and taking notes of the important points. Some techniques ask the participants to elaborate drawings or writing texts that are collected at the end. Ending each part of the session, there is a sharing and debate with the whole group, it is time to share the ideas and discuss the novelties, opportunities or difficulties for each idea. The sharing can define the concepts in such a way that it is only necessary to make a roadmap for each one of them. In this sense, it is necessary to explain what a remarkable contribution it has regarding to what exists, how it could be achieved, what limitations has and defines the difficulties to be overcome.

2.6 Results Evaluation

Once this part is done, the metric is defined taking into account the key factors of the project. An evaluation and discussion of the results is carried out, which can lead to a revision of the concepts and even of the creative session through the revision of the registered material.

Sometimes an in-situ evaluation is done, so the same group assess the ideas. The advantage of these sessions is that the participating experts apply their knowledge and criteria, the assessment is immediate and a debate can be held. However, this type of evaluation only applies when the session is a single generation of ideas.

For the sessions in which there is a generation of concepts, there is a time to generate the documentation mentioned above and it is possible that a different group is formed. The contribution of the new group is to filter the ideas, leaving only the best concepts applying critical sense, different from the creative point of view provided by the first group.

3 Results and Discussion. Case Study

The results here presented are related to a workshop carried out to study new applications for cork as an insulation material in construction sector. The workshop was divided in two sessions, the first for idea generation and the second for concept evaluation, in the meanwhile of the two sessions the task for concept definition was developed by the facilitators.

Objectives definition. The main eco-ideation workshop objective was to diversify the market of cork material. The building and construction sector was identified as the highest potential, due to its valuable physical properties, besides of its use as insulation material. The workshop was focused in this respect. Analyze and evaluate together with the participants the technical feasibility, the economic viability and the potential demand of the concepts of new products presented is the final objective.

Participant selection. There were two facilitators, one with a background in design and LCA, and the other in creativity and design. Both were in charge of the design of the workshop. The interdisciplinary of creative groups was assured by the participation of different experts from different fields of knowledge, among them: environment, product design, creativity, energy efficiency of buildings, architecture, building construction, marketing and business.

The profile of the participants in the first session was more technical, since it required a greater expertise and the ideas should have a realistic orientation for its application in construction. There were ten guests in the first session, of which eight were technicians and two were designers, these last two belong with the facilitators to the creative core. The ratio technical/creative were 2.

The profile of the participants in the second session was linked to business and marketing, since this group was required to evaluate and criticize the concepts. There were more than 20 participants from different companies, approximately half belonged to technical departments and the rest to commercial departments, marketing or managers. Market knowledge was prioritized in this second session. The ratio technical/creative were 0.1, the facilitators only lead the evaluation.

Creativity techniques selection. A combination of different techniques were proposed in order to obtain the most innovative and creative ideas. As warm up activity the use of the technique called "forced relationship" or "random stimuli" [12] was selected. During this dynamic, each participant combined randomly two different terms: one physical property of cork and a potential application sector of cork. From each combination, participants generated some sentences or ideas. The ideas generated were used in a subsequent forum-style conversation and specified.

The next part of the workshop was focused in resolving some problems based in previous studies about environmental performance of building products. For that, the hypothesis of how cork could solve these problems was proposed. Some of the participants were no used to creative sessions, for that reason there was no specific technique, all ideas were specified using techniques based on questions introduced by facilitators in conversations. The dynamic is a reflection with direct questions to an expert for the generation of hypothesis. It is necessary to take prepared examples to start the debate, for example, recovery of cork in a demolition. A list of current problems listed as questions, "How could you …? in a more optimal way … for which it is necessary … And that's why we propose a product that … " are the initial questions to start. It is important to keep the list to deal with and take them out as they are running out and solutions are being proposed.

In the final part, the material developed is used for concept proposal. A record sheet is used, recording the idea definition, the form in which it can be reached/realized, the difficulties to obtain it and the benefits that proposes with respect to what already exists. It is not a creative technique itself, but a way to define concepts, highlighting the positive and negative aspects. It is a very basic definition but can serve to relate to other ideas and lead to a more complete concept.

For the evaluation session a modification of the PNI technique [13] is used, in which a color code is inserted, a justification related to the color and a limited number of contributions for each participant. PNI is a technique in which for each idea a series of phrases are pointed out that highlight the positive, negative and interesting aspects. In this modification each participant evaluates 4 concepts, using 9 adhesive color papers, 3 red for the negative aspects, 3 yellow for the interesting ones and 3 green for the positive ones. Once the concepts are explained, they are discussed by the whole group and after a reflection time each participant places his adhesive papers.

Programming. This first session for idea generation is divided into three parts, warm-up (25′), generation of ideas (60′) and synthesis in proto-concepts (50′), the duration is not fixed since some activities were extended in time and there are sharing activities and delays for the breaks. The second session of idea evaluation is divided into three parts, an activity for results presentation (25′), a warm-up activity (40′) and finally the concept evaluation (90′). The evaluation activity is divided in two parts a debate between all the participants and the final assessment.

For this first warm-up session, a set of cards were prepared in two colors, one for characteristics and the other for applications. For each idea generation activities, two specific record sheets were prepared. Every participant had access to these sheets and could take their notes, although the facilitators had their own register at each table. In the second session it is only necessary, some blank sheets to take notes during the warm-up activity and some adhesive papers in three colors for the assessment.

As for the place chosen in the first session was a room with enough space to have two separate large tables and avoid acoustic interferences, since debate is generated and the noise can be annoying. The room was equipped with a large screen to show the specific information and had enough natural light supported by artificial light. In the second session the room had the same characteristics, it was configured in a large circle so everyone can see everybody's faces, since the most important is the debate.

Creativity sessions. At the beginning of the session there is a small welcome from the participants and it is useful for them to get to know each other, informally a coffee is offered to establish presentations and conversations. In this particular session a few minutes were spent to present a series of data related to the cork to the participants. This information about the characteristics of the cork is used in the following warm-up activity, in which the group is divided in two, which ends in a sharing of the results.

There is a brief pause, the session should be cut and have periods of relaxation. Then a brief presentation of construction systems in which cork has a potential application is shown, this information balances the level of knowledge of the group and allows the less technical to participate from their creative point of view. The session continues with the second technique, the ideas are recorded and a sharing is made between the participants. After that, the session is paused for coffee break.

The last part of the session ends defining ideas of application. In this part the groups are mixed so that there is no fixation of the idea, that is to say that a group has detected a good idea and keeps working on it, losing the potential exploitation of others. Ideas are recorded and finally a sharing takes place, a small debate is made asking opinion to the experts in a critical way.

At the end of the workshop a short survey was carried out, inquiring for strengths and weaknesses of the process, and also about subjects of the workshop as overall satisfaction, objectives, creative methods used, work climate, schedule and programming and results satisfaction. Finally, there is a group meal, idea discussion continues and comments appears in a more relaxed venue, but still interesting. The opinions of the participants were very positive, for both the result and the personal experience of their participation.

The creative process resulted in a great quantity and variety of ideas, which fits perfectly with the significant cork characteristics, taking advantage of its good physical properties.

Results evaluation. In this case study, the evaluation of concepts resulted from the eco-ideation workshop were done using two different methods. On the one hand, a specific session was hold to evaluate the ideas. In that session, different experts from the cork sector analyzed each concept from different approaches: technical feasibility, financial viability, innovation and market impact. On the other hand, concepts were evaluated by a metric, designed for this purpose. The factors included were the novelty, usefulness, the technical feasibility and the environmental factor. The main difference between both methods is that the latter included the environmental factor in the valuation, and is a semi-qualitative method, but less subjective because follows the same guidelines for all concepts. Moreover, the former is a more qualitative method, based on the experience of participants.

The results, in terms of quality of concepts, were very satisfying. Because the proposed ideas contribute to building market not substituting other materials. Generated concepts take advantage of cork properties proposing new applications. For example, the most valuable one was a light room partition for indoor environments with high traffic of people. Its modular system and cork's lightness allows a great versatility, in addition to improve the acoustic insulation.

4 Conclusions

The objectives of the workshop should be aligned with the objectives of the eco-innovation project and determine the needs of the same, in terms of group formation, selection of creative techniques, programming and start-up. The more time is devoted to the preparation of the workshop, the better the results.

It is important to have a good definition of each element of the workshop, to define properly the expected results, to help define the techniques and profiles of the participants. Find the balance of the group is an objective of the preparation of the workshop, the ratio technical/creative has to be tuned and adjusted to the group, techniques and time requirements. The chosen techniques should not condition the performance of the group, therefore sometimes it is necessary to adapt them, so that they are easy to apply by any participant. A technical expert has a high value in a creative session but an inappropriate technique cannot frustrate his participation.

The duration of the sessions must be short, so that they are very dynamic, but time should not be a strict requirement. If the group works well and it is participative, the time can be extended, trying not to affect the rest of the programmed activities.

The criteria selected for evaluation must be clear and easy to apply; to apply qualitative criteria is easier than the quantitative criteria. The latter are difficult to define and require specific knowledge and particular information as occurs with the metrics.

References

1. Bocken N, Allwood J, Willey A, King J (2011) Development of an eco-ideation tool to identify stepwise greenhouse gas emissions reduction options for consumer goods. J Cleaner Prod 19:1279–1287
2. Andersen M (2010) On the faces and phases of eco-innovation on the dynamics of the greening of the economy. In: Summer conference opening up innovation strategy organization technology 2010, 24
3. López-Forniés I, Sierra-Pérez J, Boschmonart-Rives J, Gabarrell X (2017) Metric for measuring the effectiveness of an eco-ideation process. J Cleaner Prod 162
4. Sierra-Pérez J, López-Forniés I, Boschmonart-Rives J, Gabarrell X (2016) Introducing eco-ideation and creativity techniques to increase and diversify the applications of eco-materials: the case of cork in the building sector. J Cleaner Prod 137:606–616
5. Tyl B, Legardeur J, Millet D, Vallet F (2015) A comparative study of ideation mechanisms used in eco-innovation tools. J Eng Des 25:325–345
6. Vallet F, Eynard B, Millet D, Mahut SG, Tyl B, Bertoluci G (2013) Using eco-design tools: An overview of experts' practices. Des Stud 34:345–377
7. Finnveden G, Moberg Å (2005) Environmental systems analysis tools—an overview. J Cleaner Prod 13:1165–1173
8. Byggeth S, Hochschorner E (2006) Handling trade-offs in ecodesign tools for sustainable product development and procurement. J Cleaner Prod 14:1420–1430
9. ISO (2006) ISO 14040: Life cycle assessment—principles and framework. Environ Manage 3:28
10. Parjanen S, Harmaakorpi V, Frantsi T (2010) Collective creativity and brokerage functions in heavily cross-disciplined innovation processes. Interdisc J Inf Knowl Manag 5

11. Lévy P (2013) The creative conversation of collective intelligence. In: Delwiche AA, Henderson JJ (eds) The participatory cultures handbook. Routledge, New York, pp 99–108
12. De Bono E (2010) Lateral thinking: creativity step by step. Harper Collins 304
13. De Bono E (1994) De Bono's thinking course. Facts on File, New York

Modular Design: Product Design Opportunities and a Case Analysis

L. Asión-Suñer and I. López-Forniés(✉)

Universidad de Zaragoza, Dpto. Ingeniería de Diseño y Fabricación, C/María de Luna s/n, Saragossa 50018, Spain
ignlopez@unizar.es

Abstract. In recent decades, modular design has been fully developed due to its important role in the current industrial evolution. The numerous advantages offered by its application to product design has made companies from different sectors opt for its use to solve particular needs. Many authors have studied modular design from a theoretical viewpoint, but it is necessary to learn about its application by studying real cases that allow us to understand what the object of its application is, the different methods used to obtain modular products and the results obtained in each case. Accordingly, we can know modular design's most characteristic features and benefits, the business of its application, what its evolution has been, and what path it is currently on as part of the current industrial evolution. To do this, a case study research is carried out, which is divided into two parts. The first consists of a bibliographic review that focused on the main authors who studied modular design and documented real cases of its application, especially at the beginning of modular design in industry. The second focused on investigating the current cases that have not been previously documented, which shows how modular design is currently applied and how it evolves.

Keywords: Design methods · Modular design · Product platform · Design opportunities · Case studies

1 Introduction

Modular design began in the mid-1960s with modular production. In recent years, the competitive needs of companies in mass production sectors (e.g. automotive or industrial) have forced modular design to be implemented into companies to achieve greater competitiveness, higher supply diversity and more product portfolio options [1]. The present work is an analysis of modular design as an application in various productive sectors and as a future industrial design opportunity. Twenty-nine cases were analyzed in these sectors: industrial [2], transport [3], automotive [4], electronic [5], consumer product [6], architecture [7] and furniture [8]. The study focused on three aspects: the design phase in which modular design is applied, the purpose of its application and the particularities of each case. This study confers a poorly extended design method visibility and high potential by providing real-life examples of its characteristics and benefits [9].

F. Cavas-Martínez et al. (Eds.): *Advances on Mechanics, Design Engineering and Manufacturing II*, LNME, pp. 596–609, 2019.
https://doi.org/10.1007/978-3-030-12346-8_58

The first aspect to be studied is the phase as part of the design process, in which modular design is applied [10], where we find three different options. The first, when applied in the product life cycle, is where particular cases are identified in which companies have developed their own methodologies [11]. In this application we observe that there are links to the life cycle analysis from the environmental point of view, which has been a basic pillar in modular design for easy assembly, maintenance, replacement and disposal purposes [3]. The second option focuses on classic design process phases, such as the conceptual, design and development phases, with some conclusions about application opportunities in initial process phases. Finally, a particular case is analyzed, which is a research project applied as a previous phase to modular design [12]. Such research aims to determine which elements can make up architecture, platforms or product families in which to work on aspects such as interchangeability.

The second aspect to be studied is the objective that modular design aims by reflecting certain convergence toward module and product architecture definitions [15]. We observe that production flexibility [17], standardization [20], product platform generation [2] and model configuration [4] are the objectives found in the study. Other particular objectives tend to diverge with previous ones, and suggest decentralized production, multiple uses or mass customization.

Finally, the third aspect refers to the particularities of each case that allow a diverse definition of the modular design characteristics to be given. In both the bibliographic review and case analysis, lack of modular design characterization is observed along with specific applications, which generate particularities. However, a certain relationship is noted that can be established among the used model, the design phase and the desired characteristic to obtain a reference when applying modular design.

In the case study analysis, a reference is made to the various known methods and models [25], which are framed within methods of structural analysis [26], functional analysis [27] and matrix models [28].

Not every case has a clear reference to a model, but relationships can be established to define their theoretical framework. In this way, the study of cases also serves to reflect on current models and the need to implement new or more specific ones.

2 Method Description

The main objective of this study focuses on research through a bibliographic review, and by analyzing real cases to which modularity has been applied throughout the product's life cycle phases.

As a result, we hope to find a series of cases that show which companies and sectors are related to modular design to know in which design phase it is applied, what purpose is set and what the particularities of each case are.

To achieve this, a bibliographic review that focused on various theses and articles, whose authors studied modular design, was carried out. Many research works focus on the initial applications in which modular design is first included, and show the need for its development [2]. At present, and given the many offered advantages, it is still developing. Some studies have conducted work on the documentation of real cases of applications in products as strategies or in platforms systems [3].

However, there are currently many cases that have not been previously documented and belong to sectors other than those already documented. For this reason, a search was made of new cases in the news, science magazines and on websites of various companies. A series of key sectors in which modular design had been applied due to the number of cases found in each one was identified.

Finally, two representative cases were included for these sectors: automotive, architecture, furniture, toys and electronics. The analyzed cases show the different ways of applying modular design by each company in the market, and describes what is being developed and what is the path that modular design is taking in relation to the future.

All the collected information was summarized in two tables, which provide basic information on the case (the product it affects, the company that applies it and the sector of the industry it belongs to) and a brief description of it, which includes the design phase in which it is applied, its purpose and particularities.

With the results already obtained in the form of a table, we conclude the study with the analysis of the results in the form of discussion and conclusions that deal directly with aspects related to modular design applications.

3 Results

In the bibliographic review, we found that 19 cases had been already documented and 10 recent cases to be studied, which means 29 cases to be analyzed from various sectors and companies.

The analysis of the results is included in Table 3. This table analyzes the relationship of all the 29 cases studied with the three identified aspects:

1. Design process phase. There are three different instances: Life Cycle Analysis (LCA). Design phase (Conceptual phase, which refers to a new idea that did not previously exist; Design phase, which refers to a solution that can be achieved without having to develop something new; Development phase, which refers to progress in a specific direction, as in technology, production, parts/components/modules of a product, etc.). Research.
2. Purpose of application as for configuration and platform. This aspect refers to the objective of the modular design in each case, such as obtaining new structures or product architectures, generation of modules, improvements in manufacturing machinery, etc.
3. Particularities or specific applications of each case. These particularities define the characteristics that differentiate them from the rest, which are related to modular design characteristics.

3.1 Documented Cases

Table 1 shows a list of the 19 cases found in the bibliographic review documented in other research works with basic data and a summary of each one.

Table 1. Documented cases

Case (product, company and industrial sector)	Case summary
Sperry-Sun Drilling Services [2] (Electronic sensors, Sperry-Sun Drilling Services, Machinery)	The company developed a range of products that allowed the incorporation of new technology. At the same time they were compatible and combinable with existing products. Because of this, the company opted for a strategy based on a modular product philosophy
Crosfield Electronics [2] (Digital scanner, Crosfield Electronics, Electronics and printing)	The company created the Crosfield Product Life Cycle Process (CPLCP), a modular product development process in charge of defining modules in the conceptual phases and identifying the interactions that occurred between them
Ford Motor Company [2] (Engines, Ford Motor Company, Automotive)	Ford restructured its business process worldwide under the name Ford 2000, which included the Ford Product Development System (FPDS) that allowed easy changes in the process through flexible production
British United Shoe Machinery [2] (Shoes Machinery, British Shoe Machinery, Machinery)	Given its expansion in the global market, the BUSM company went from highly complex functional manufacturing machines to simpler cheaper ones that required less skilled operators
Modular system in truck manufacturing: The SAAB-SCANIA [4] (Scania trucks, SAAB, Automotive)	The case of Scania is one of the first modular design cases and its objective was to make modular trucks. Eight types of cabins were developed thanks to the use of standardized modules that allowed to make a new variant in a minimum time
The case of Sony Walkman [5] (Walkman, Sony, Electronics)	This case is a classic example of success thanks to the use of modular platforms. Sony managed to create more product variants by adding modules to a platform, which made it very successful in the market
Volkswagen platform strategy [11] (Automobile, Volkswagen, Automotive)	The multiple ranges of Volkswagen vehicles use product platforms to create product families. The company managed to develop a modular strategy that evolved over time, but always responded to market needs

(*continued*)

Table 1. (*continued*)

Case (product, company and industrial sector)	Case summary
Modular German submarine [13] (Submarine, German army, Transport)	German submarines case (Submarine Type XXI) in which a submarine of a standard model was divided into several modules of longitudinal assembly to carry out decentralized production
Locomotive Dash 2 Series [14] (Locomotive, General Motors, Transport)	Locomotives Dash 2 presented a new electric driving system based on separable modules that allowed defective modules to be replaced without having to take the entire locomotive to repair
Merima Ltd. [8] (Logistic organization, Merima Ltd., furniture)	Merima Ltd. applied modularity to the design and logistics of a restaurant to be installed on a ship. The restaurant was built on the facilities, dismantled, transported in modules and delivered with assembly instructions
Tunnel drilling rig [3] (Drilling rig for tunnels, Tamrock and Jumbo, Machinery)	This is a research project in which the use of platforms for different product families of the Tamrock and Jumbo drilling brands was analyze, and offered an analysis on how to apply greater modularization according to their functions
Diesel locomotive [3] (Locomotive, Valmet, Transport)	The Valmet locomotive was designed and manufactured with a modular structure, which allowed it to be modified and have multiple uses. This modularity is based on assembly and facilitated maintenance in general, with a saving of 30%
Passenger ship [3] (Passenger ship, Finnish financing agency for technology, Transport)	It is a project that seeks to improve the efficiency of ship delivery through modularity and flexible standardization to discover the division of the ship based on modules to develop modular ships
Safe-deposit box [3] (Safe box, Kaso Ltd., Machinery)	Families of safety deposit box products were examined to discover opportunities to move from the production of standard models to the production of configurable products
Machine tool [3] (Machine tool/Twin-Mill, Fastems Ltd., Machinery)	The company undertook a modular development project whose objective was to define the structure of a Twin-Mill machine by finding out where to implement a division of modules based on their functions, and creating a range of configurable products

(*continued*)

Table 1. (*continued*)

Case (product, company and industrial sector)	Case summary
Ambulance [3] (Ambulance, Profile Vehicles Ltd., Transport)	The functional structure of an ambulance was evaluated and lists of its main functions were made. Thus the opportunities to create a modular structure based on the functional structure were examined
Forestry machine [3] (Forestry machine, Ponsse Ltd., Machinery)	The Ponsse company created modules that did not only focus on assembly, but also on functionality. Several modules were sets of parts located around the machine that could not be assembled separately
Volvo trucks [15] (Configurables trucks, Volvo, Automotive)	Volvo developed a configuration system for its range of trucks as part of the CATER project (2006), whose objective was to create business networks and mass customization in the automotive industry
Micro Compact Car (MCC) [16] (SMART, Micro Compact Car (Daimler), Automotive)	MCC established diverse relationships among product family development processes, product architectures and a multi-rand modular organization to create a collaborative modular development project organization

3.2 Recent Cases

The previous section shows that more than half the previously documented cases corresponded to the transport or automotive sector, followed by the machinery development sector. At present, more industry sectors that are closely related to modular design have not yet been documented. Table 2 shows 10 recent cases that correspond to the following sectors: automotive, architecture, furniture, toys and electronics.

Table 2. Recent cases

Case (product, company and industrial sector)	Case summary
PSA (Peugeot-Citroën) [17] (Platform for several compact models, PSA Group, Automotive)	PSA seeks to manufacture most of their compact models of the four brands on the same product platform. The company has two global platforms that are compatible with the industrial resources launched in The Factory of the Future programm: the CMP (Common Modular Platform) and the EMP2 (Efficient Modular Platform)
Renault Mégane [18] (Renault Mégane, Renault, Automotive)	The latest Renault Mégane's model contains a modular interior that is one of the most spacious and adaptable models in its segment. It offers an interior with a range of options that adapt to the user's needs
BoKlok [19] (BoKlok, IKEA, Architecture)	BoKlok is a housing concept whose objective is to build blocks of flats and houses for low-economy people. IKEA developed modular houses of a few square meters by making them spacious and affordable at the same time
Blokable [7] (Blokable, Amazon, Architecture)	Blokable develops prefabricated building modules (Bloks) in a wide range of sizes and configurations to provide living spaces, common areas and services that meet the specific needs of each project type
IKEA products (BESTÅ, shelves and children's furniture) [20] (Products IKEA, IKEA, Furniture)	IKEA has several examples of applying modular design in its products: the BESTÅ furniture, a set of modules with standardized measurements; shelves of different sizes and colors; and children's storage furniture, to name but a few
Ori Systems [21] (Ori Systems, MIT, Furniture)	It is scalable modular furniture that changes shape to create more efficient spaces. Its goal is to make life more affordable, productive and enjoyable for users. This versatile piece of furniture confers different rooms space, such as a room or study
Mindstorms [6] (Mindstorms, LEGO, Toys)	It is a line of robotic toys that works with the combination of modular pieces and the programming of actions interactively. Its use is based on the construction of integrated models with computer-controlled electromechanical parts

(*continued*)

Table 2. (*continued*)

Case (product, company and industrial sector)	Case summary
Meccano [22] (Meccano, Meccano, Toys)	Meccano has upgraded its building model system by assembling modular parts, such as plates, angle beams, wheels, axles and gears, and plastic parts that are connected together by nuts, bolts and fixing screws
GoldieBlox [23] (GoldieBlox, GoldieBlox, Toys)	GoldieBlox offers toys that are sold in kits, and that incorporate modular pieces for structure construction. Thus, these toys introduce engineering concepts through storytelling and construction
Modular Smartphone [24] (Various products, various companies, electronics)	It is a smart phone manufactured with modules that can be updated to reduce electronic waste, repair costs and increase user comfort. The most important component is the main board, to which the modules are connected (processor, battery, camera, etc.). Some brands, such as Motorola, LG or Google, have already worked in this field

In Table 3 the 29 cases described in Tables 1 and 2 can be analyzed, and an analysis is done by taking the three initially described aspects, and observing in the summary column what particularities are more remarkable in each aspect, and the details of each aspect in the corresponding column for each case. The results of Table 3 are discussed in Sect. 4.

Table 3. Case analysis

		1	2	3	4	5	6	7	8	9	10	11	12	13	14	15	16	17	18	19	20	21	22	23	24	25	26	27	28	29	∑
1st aspect	LCA		x																											x	2
	Concept	x	x	x	x	x	x	x	x	x	x	x		x	x		x						x	x							15
	Design	x		x	x	x	x	x	x	x	x	x	x	x		x		x	x	x	x	x	x	x	x	x	x	x	x	x	25
	Development	x		x	x	x	x	x	x	x	x	x		x		x				x	x						x			x	15
	Research											x																			1
2nd aspect	Configuration					x																									1
	Platform	x		x								x									x										4
	Family											x			x																2
	Architecture/structure						x	x								x	x	x	x	x											7
	Block/module								x	x	x			x									x	x	x	x	x	x	x	x	12
	Own method		x	x																											2
3rd aspect	Interface/interaction		x																								x	x			3
	Maintenance									x			x																	x	3
	Compatible	x																													1
	Combinable	x																													1
	Repair									x																				x	2
	Product flexibility			x										x																	2
	Production flexibility			x																	x										2
	Decentralized product								x		x																				2
	Simplicity				x																										1
	Assembly												x																		1
	Economy				x																		x	x							3
	Functionality						x	x				x	x			x	x	x													7
	Standardization					x																			x						2

(*continued*)

Table 3. *(continued)*

	1	2	3	4	5	6	7	8	9	10	11	12	13	14	15	16	17	18	19	20	21	22	23	24	25	26	27	28	29	∑
Logistics																														0
Variability																														0
Time economy					x																									1
Configurable						x								x							x		x							4
Personalization																					x			x						2
Market																			x											1
Integration																										x	x			2
User narrative																												x		1

4 Discussion

In a globalized and competitive market, modular design has proven a useful design tool to face this competitiveness through higher supply diversity and a better response to changing market demands, while making the manufacturing process more adaptive to change. The analyzed cases prove the usefulness of modular design and the advantages of its application to industrial development in last decades. Nowadays its main objective is the application of methodologies in which the design phase prevails, the definition of modules to seek functionality and the possibility of generating configurations. Therefore, modular design offers a development opportunity due to the context in which it is found with the variables directly related to its objectives; e.g., a competitive market, fewer resources, more demands and the latent need for product customization. In economics and business, the modularity of products, services and processes is a key factor in technological, economic and social development.

The analysis of the most recent cases reflects the importance of modularity as a future industrial design opportunity in the current industrial evolution. These cases use modular design as a tool to face current challenges, such as the needs of customers and companies, new technologies like Industry 4.0, the standardization of design entities and agile manufacturing. In addition, the growing demand for customized products is pushing companies to adopt the principle of modularization in their product design and development phases, which offers them the advantage of creating customized products or services easily and economically. As shown in Table 3, no registered case's objective was product personalization, while there are two recent cases that did [18, 20]. This is why modular design development can be established as a milestone in the history of industrial production, where modularity can become a great future challenge.

By analyzing the studied cases, three design process points were detected in which modular design was applied. The first is its application in the product life cycle, where modularity allows it to be extended by adapting it to new requirements and its evolution by incorporating new features. This means that modular design fits an environmental context with a strong link to the circular economy, and modular design can bring major improvements by allowing the development of reusable, repairable and updatable characteristics. At this point, an opportunity is detected to develop a line of modular design that addresses the environment given the scarcity of cases that focus on this aspect (only two cases). The second point refers to classic design process phases. In this case, an opportunity is identified to apply modular design to the initial conceptualization phases with new design methodologies as cases are scarce. The third point is the opportunity to introduce research into modular design methods. This situation may vary the aim of modular design by introducing the search for new requirements before the process starts.

The second aspect is related to the blocks or modules that can shape a product's architecture, which are determined to create a platform that gives rise to a family of products by bearing in mind the interchangeability of components. In line with this, it is observed that while the documented cases focus on product architecture, most recent cases center on the module (Table 3).

The characteristics of the modular design and the third aspect are closely linked to its benefits. These characteristics are specific and particular to each case, and modular design application to the product design and development increases the final product's level of modularity by providing traits that offer significant advantages during its life cycle. Differences in the use of these characteristics exist between documented cases and recent cases. While documented cases opt for functionality, product decentralization or product flexibility, the most recent cases opt for those such as interaction, economy, personalization or integration (Table 3). By connecting independent modules on a single product platform, modular design makes the product variable and configurable. Many companies use this fact to lead to characteristics such as adaptability, and the ability to mutate according to the needs of users and the environment; personalization both before manufacturing the product (automotive) and during its life cycle (modular smartphone); multifunctionality, integrating multiple functionalities through modules; and flexibility, especially regarding the manufacture of the product. These characteristics arise thanks to the standardization and connectivity of modules, which render them interchangeable, reusable and updatable which, in turn, improves the economy of scale.

5 Conclusions

The study of documented cases of modular design applications allowed us to know the reasons why it was first used in industry to thus understand the bases that established it and its subsequent development in industries of various sectors. Otherwise, the study of recent cases shows the diverse forms and purposes of applying modular design to the current economy, and the place it occupies in the present industrial evolution. At the same time, the results of this study reveal that there are numerous sectors in which modular design is not currently used, but where a potential application will possibly exist if it continues to develop. Table 3 shows the need to increase the efforts being made in many aspects, such as configuration, compatibility, simplicity or variability, as part of the current industrial evolution.

As shown in the results, some sectors whose development and evolution from the past to the present are greater include: automotive, with companies such as Ford or Volkswagen; architecture, BoKlok of IKEA; furniture, Ori Systems developed by the MIT; electronic, Sony Walkman; toy maker, Mind Storms of LEGO; computers, with hardware and software development; mechanics, especially as regards machinery design. The use of modular design in some of these sectors has been so influential that it has given rise to new design concepts such as *kit car*, *kit house* or *modular smartphone*. However, there are several sectors in which modularity has not yet been incorporated into product design, such us the food, textile or sanitary sectors. This means that there is a large niche market where modular design can be incorporated into if it continues to develop in the near future.

Our results show that there are numerous methodologies and models, some theoretical and some particular to each company, that allow modularity to be applied to product design. As shown in the case summary in Table 1, the effectiveness and reiteration of its application results in a series of models that have already been consolidated and validated for decades, and are classified into: methods of structural analysis, functional analysis and models based on matrices. Some of these models are more recent and offer a more limited application in real cases, which means they are currently in an experimentation and development state. However, it has been detected that its use in conceptual development phases is lacking in most methods, which represents an excellent opportunity to develop a new method.

References

1. Baldwin CY, Clark KB (2000) Design rules: the power of modularity. The MIT Press, Cambridge, Massachusetts
2. Marshall, R. Design modularisation: a systems engineering based methodology for enhanced product realisation. Doctoral Thesis, Loughborough University, UK (1998)
3. Lehtonen T (2005) Designing modular product architecture in the new product development. Doctoral Thesis, Tampere University of Technology, Tampere, Finland
4. Sjöström S (1990) The modular system in truck manufacturing. The SAAB-SCANIA Griffin, 2–12
5. Sanderson S, Uzumeri M (1995) Managing product families: the case of Sony Walkman. Res Policy 24:761–782
6. LEGO MindStorms, https://www.lego.com/es-es/mindstorms. Last accessed 7 Feb 2018
7. Amazon Homepage, http://www.blokable.com/. Last accessed 7 Feb 2018
8. Taneli H (2007) Laivan matkustajatilojen suunnittelun uudelleenkäytön hyödyntäminen vakioinnin ja moduloinnin keinoin. MSc-thesis, Tampere University of Technology
9. Gershenson JK, Prasad GJ, Allamneni S (1999) Modular product design: a life-cycle view. J Integr Des Process Sci 3(4):1–9
10. Ulrich K, Tung K (1991) Fundamentals of product modularity. Manag Des, 219–231
11. Rendell J (2001) VW top, but others are catching up fast. Automot World, 26–34
12. Dahmus JB, Gonzalez-Zugasti JP, Otto KN (2000) Modular product architecture. In: ASME design engineering technical conferences and computers and Information in engineering conference
13. Williamson G (2005) Wolf Pack—the story of the U-Boat in World War II. Osprey Publishing, Wellingborough (UK)
14. Kerr JW (2004) Phenomenical SD40 diesel-electric locomotives. Delta Publications
15. Shamsuzzoha AHM (2010) Modular product development for mass customization (Selection of Articles). University of Vaasa, Vaasa, Finland
16. Stephan M, Pfaffmann E, Sanchez R (2008) Modularity in cooperative product development: the case of the MCC 'smart' car. Int J Technol Manage 42(4):439–458
17. García F (2016) Los eléctricos del Grupo PSA tendrán 450 km de autonomía. El Mundo
18. Fernández A (2016) Renault Mégane Estate 2016, la opción más dinámica. Motor
19. Boklok Homepage, https://www.boklok.com/. Last accessed 7 Feb 2018
20. IKEA Homepage, http://www.ikea.com/es/es/. Last accessed 7 Feb 2018
21. Ori Systems Homepage, https://www.orisystems.com/. Last accessed 7 Feb 2018
22. Meccano Wikipedia, https://en.wikipedia.org/wiki/Meccano. Last accessed 7 Feb 2018
23. Goldie Blox Homepage, https://www.goldieblox.com/. Last accessed 7 Feb 2018
24. Modular smartphone Wikipedia's page, https://en.wikipedia.org/wiki/Modular_smartphone. Last accessed 7 Feb 2018
25. Gershenson JK, Prasad GJ, Zhang Y (2003) Product modularity: definitions and benefits. J Eng Des 14(3):295–313

26. Dori D (2011) Object-process methodology: a holistic systems paradigm. Springer Science & Business Media
27. Stone RB, Wood KL, Crawford RH (2000) A heuristic method for identifying modules for product architectures. Des Stud 21(1):5–31
28. Eppinger SD, Browning TR (2012) Design structure matrix methods and applications. MIT press

Is the Design a Vector to be Considered in the Agri-food Industry? An Interprofessional Analysis in Andalusia (Spain)

Ó. González-Yebra(✉), M. A. Aguilar, and F. J. Aguilar

Department of Engineering, University of Almeria, Ctra. de Sacramento s/n, La Cañada de San Urbano, 04120 Almeria, Spain
oglezyebra@ual.es

Abstract. We currently live in a globalized world where the imperative need to both generate added value and new products and services has been strengthened. Some of the problems pending to solve can be properly faced from the field of "Design". However, and up to now, there is no design science serving as a knowledge pivot for developing and building the solutions required. On the other hand, design is cross-cuttingly present in the different activities of a country like Spain, where one of the most important sectors is agriculture. Starting from this context, a survey about the role of design in the agri-food industry has been developed through the well-known Delphi method, constituting a panel of experts from the private sector of Andalusia. To the best of our knowledge, this is the first study in which a forum of these characteristics has aimed to involve both CEOs and managers of agri-food businesses and design professionals to work together around this topic. The results obtained suggest that design component in the agri-food industry is mainly present in activities related to graphic design, showing less presence in the industrial-product design or, specially, in the environment design. They also point out that design is an important tool to explore in the agri-food sector since it might provide both tangible and intangible benefits. The findings of this work seem to be very valuable as a diagnostic to characterize the design component, also contributing to uncover and develop the design as an important factor of dynamization.

Keywords: Design · Agri-food industry · Innovation · Interdisciplinary research · Delphi method

1 Introduction

Agriculture is one of the main Spanish strategic sectors for the development of the country [1], being the agri-food industry one of its main business areas according to the high added value it brings to raw agricultural products. In southern Spain, the agri-food industry presents a high-level of innovation focused on food quality and safety, sustainability and, more recently, due to the generation of new products with the implementation of the organic production [2]. Nowadays it is needed to generate added value in agri-food products, considering that most socio-economic activities are evaluated in

F. Cavas-Martínez et al. (Eds.): *Advances on Mechanics, Design Engineering and Manufacturing II*, LNME, pp. 610–621, 2019.
https://doi.org/10.1007/978-3-030-12346-8_59

terms of innovation and the capacity to create (or recreate) new products and services. It is worth noting that most of these aspects are directly related to the field of design. In this sense, it is relevant to define the concept of Design, accepting that there are endless definitions for the word “Design”. These definitions vary depending on the focus and final goals, comprising terms such as industrial design, graphic design, package design, production design, service design, etc. Although a common denominator can be identified, the term “Design” can refer to the process of the creating something mostly tangible [3]. Design becomes a key variable in the culture of innovation, being very important that organizations integrate innovation through its different applications [4]. There are many authors [5–7] that point out that more and more companies in developed countries identify design as not only an activity which refers to the aesthetics of goods or services, but it is a multidisciplinary and holistic process involving economic, sociocultural, technological and environmental factors, constituting an important source for the generation of innovation in any of the activities of companies and organizations.

From the scientific-academic point of view, “Design” could be currently considered as a postmodern discipline that, in practice, is essentially linked to graphic expression/communication, architecture and product engineering, although it is not considered a fully developed scientific discipline, still being in a growth phase [8]. This aspect was evident in a previous stage 0 of this research line consisting of a bibliometric study focused on the main bibliographic data bases for the search of scientific literature. “Scopus” (Elsevier) and “Web of Science” (Thomson Reuters) were the platforms used to search for best references of peer-reviewed publications and conferences. This previous work turned out to be a difficult task, since there was no specific category in “Design” and thus a very extensive search had to be undertaken in a wide range of categories (e.g., Arts, Engineering Multidisciplinary, Architecture, Management and so on). Another fact that denotes the difficulty of gathering information in this field is that there is no “Design” descriptor among the UNESCO codes. All these difficulties were sharped when relating “Design” with the “Agri-Food Sector”.

In this second phase, and after including Google Scholar as an additional search engine delimited to the last 5 years (period 2012–17), some conclusions could be extracted: (i) Most of the reported documents were about design in the sense of agricultural holdings. On the other hand, (ii) those works directly related to design were focused on packaging, product brand and denomination of origin, in line with the conclusions obtained in the first phase of this research line [9]. Note that only two works were found with respect to design in the agri-food sector of Andalusia. One of them was related to the subject of consumption of agri-food products, making up a classification in different cases and trends, and identifying the most useful tools for improving design (i.e. materials, textures, shapes, styles of illustration, photography or type of messages that allow to connect with the values and taste of consumers) [10]. The other work was focused on the history of the graphic design in the companies of the horticultural sector of Almería, proving that the functional aspect of the communication of design was not developed as it should [11].

During the first phase of this work [9] was constituted a panel of experts from the public arena to explore new research lines in which “Design” is related to “Agri-food

Industry". An example of the design component in the agri-food sector can be seen in Fig. 1. Since the preliminary bibliometric analysis concluded that the information about the role of design in agri-food sector was scarce, this research line started from scratch by characterizing the design component in the agri-food industry through the application of the Delphi method. This method is based on a systematic and iterative process aimed at obtaining answers to specific objectives from a panel of experts [12].

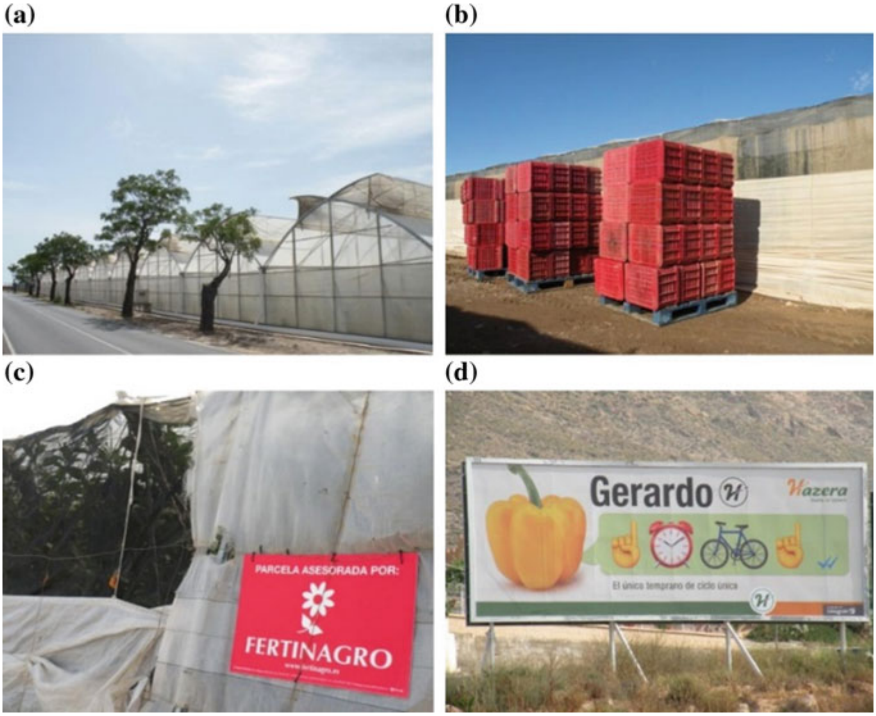

Fig. 1. Examples of the design component in the agri-food sector in the province of Almeria (southeast of Spain): environment design (**a**), industrial/product design (**b**) and graphic design (**c–d**)

The research questions were focused on uncovering the perception about the role of design in the agri-food industry. As a basic reference, the experience of a group of experts linked to the agri-food sector is taken to answer to the following questions: *What is the presence of the design component in the Andalusian agri-food cluster? Is design an interesting tool to explore in the agri-food sector?* For the selection of the main items to be assessed, the previous work carried out in this line of study has been used [9]. The final goals of this work would be the following ones: (i) To identify the main design areas within the agribusiness and agri-food sector. (ii) To know the importance of the design component by areas as well as the tangible and intangible benefits that it can provide to the agri-food industry. (iii) To go further in the search of the main design-sector lines of action.

2 Materials and Methods

This section will describe the methodological differences with respect to the first phase of this research line divided into three sub-sections: (i) panel of experts, (ii) instrument of measurement, and (iii) analysis of data. An in-depth description of the general methodology applied can be found in Authors [9]. In this preliminary stage, two working groups were constituted, that is, the coordinating group and the group of experts. As in the previous phase, the coordinating group was composed of the members of the research group RNM-368 of the Andalusian Plan for Research, Development and Innovation and the Campus of International Excellence in Agri-Food (ceiA3; further information can be retrieved from http://www.ceia3.es/en).

2.1 Characterization of the Expert Panel

The final panel of experts consisted of 22 participants, although a higher number was contacted, so that the final sample was the same as in the previous phase [9]. The final distribution by professional areas was the following: 68% were professionals of the Andalusian agri-food industry belonging to representative corporations such as, e.g., "*ANECOOP, Empresa Cooperativa Hortofrutícola de Segundo Grado*" [cooperative fruit and vegetable enterprise of the second degree] or "*COEXPHAL-APROA, Asociación de Organizaciones de Productores de Frutas y Hortalizas de Almería y Andalucía*" [association of fruit and vegetable producers' organizations of Almeria and Andalusia]. 32% of panel members corresponded to design professionals in Andalusia associated to most representative corporations such as "*AAD, Asociación Andaluza de Diseñadores*" [Andalusian association of designers] or "SURGENIA, *Centro Tecnológico Andaluz de Diseño*" [Andalusian design technology center].

Regarding genre, 27% were women and 73% were men. Note that in the preliminary phase of the profiles selection, an attempt was made to find an equitable percentage of men and women, so that in the exploratory phase there would be a significant participation of expert women. But in most cases it was not possible, due in part to the low number of women who hold management positions. These participants were mostly presenting (91%) higher education (see Fig. 2) in very diverse areas of knowledge. This is required to ensure the interdisciplinarity of the panel (e.g., marketing, social and agrarian economy, agri-food cooperativism, engineering projects, industrial design, graphic design, etc.). The 50% of panel member counted on a professional experience of more than 20 years, while 23% of them had between 15 and 20 years of experience. Finally, 59% of the participants knew or had worked with the Delphi method. To the question "What do you mean by design?", 95% responded that design is a structured work process. 91% of them claimed that design should be a fundamental line of study regardless of the sector involved (industrial, social, academic…). None of the experts considered that design is a punctual activity (a style or fashion) nor a synonym for advertising. All these answers denote the degree of expertise and knowledge of the panel members with respect to this topic.

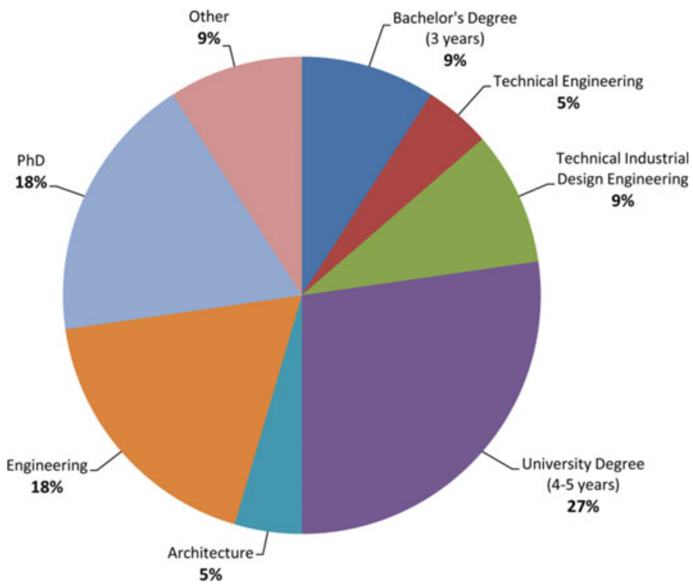

Fig. 2. Professional qualification of the Delphi panel members

2.2 Measuring Instrument

From a methodological point of view, significant modifications have been introduced in the measurement and procedure instrument with respect to the first phase (further information in [9]). Following the recommendations of different authors [13, 14] indicating that increasing the number of points on a scale can increase reliability, the Likert scale of response was increased up to 9 points to achieve a more precise assessment (e.g., Nothing Present: 1/Very Present: 9). In addition, new variables related to tangible and intangible benefits have been added (two subsections to the second question, 2.1 and 2.2) following the recommendations of [15]. Table 1 shows a summary of the items of the first two questions (30 items). The exploratory phase was developed throughout 2016, lasting several months and requiring between 1 to 3 months to complete each of the consultation rounds and incorporate the corresponding feedback.

2.3 Analysis of Results

In relation to the quantitative analysis through descriptive statistics, the median (m) has been calculated as a central measure for detecting trends. The arithmetic mean (μ) and the standard deviation (σ) were computed as complementary indicators to establish the relative order between items with the same median.

In this second phase we have incorporated a new metric based on the coefficient of variation (CV) as a panel agreement estimate, since literature does not provide a single guideline to follow [16]. In fact, Shah and Kalaian [17] suggest that CV is the most appropriate test for studies of this type. Simultaneously, it is necessary to determine a

Table 1. Items raised in the Delphi questionnaire

No. Item	Description
Fields of action/areas of design (first question)	
1	Development of agro-industrial buildings and secondary industries. Landscape integration (industrial and environment design)
2	Facilities and equipment (industrial design)
3	Development of agricultural machinery (industrial design)
4	Agri-food packaging, manufacturing of packaging (graphic and product design)
5	Design of new packaging[a] (product design)
6	Graphic application to existing packaging[a] (graphic design)
7	Trade fair stands and materials (graphic and spaces design)
8	Corporate identity of agri-food companies and sector associations (graphic design)
9	Product System[a] (graphic design)
10	Product communication (graphic design)
11	Conception of products and trademarks (graphic design)
Importance by area (Second question)	
12	Training centers (Study plans)
13	R&D&I centers
14	Government authorities
15	Small and medium enterprise
16	Large companies
17	Large distribution chains[a]
18	Consumers
Tangible Benefits[a] *(2.1 question)*	
19	Increase in competitiveness
20	Improvement of the product development process
21	Increase in exports
22	Development of industrial and intellectual property
23	Reduction of environmental impact
24	Market-Sale Quotas
25	Profit-Profitability
Intangible Benefits[a] *(2.2 question)*	
26	Differentiation and positioning
27	Quality improvement
28	Entry into new markets
29	Customer satisfaction and loyalty
30	Improvement of the corporate image

[a]New items added in this second phase (not present at the first phase of this research line [9])

threshold value that indicates the degree of consensus of the panel experts. There is no single criterion. For instance, Keeney [18] used a 75% consensus level, while Loughlin and Moore [19] suggested a value of 51%. This work has followed the recommendations published in [16] and [20] to build up five consensus categories: (i) CV $\leq$ 25%; very high agreement. (ii) CV > 25% and $\leq$50%; high agreement. (iii) CV > 50% and $\leq$75%; average agreement. (iv) CV > 75% and $\leq$100%; low agreement. (v) CV > 100%; very low agreement.

3 Results and Discussion

To the best of our knowledge, this is the first study in which a forum of these characteristics has been constituted, allowing to group different agents of the private sector for trying to define what is the role of design in agri-food industry. It is necessary to highlight that in 27 out of the 30 consulted items a high or very high degree of agreement has been reached, what is relevant considering the participation of two well differentiated areas: CEOs and managers of agri-food business and design professionals. The results obtained in this second phase are presented below, also providing a comparison between the trends detected in both studies (i.e. public and private sectors).

3.1 Presence of the Design Component in the Agri-Food Industry

In this second phase the trend with respect to the study carried out in the first phase has been maintained [9].

If we conduct the comparison taking as reference the order of presence of the design component in the agri-food industry, design lacks presence in the projection of agricultural constructions both for the private and public sectors panel members (see Table 2, item 1), although the degree of agreement around this issue was greater in the first phase. With respect to corporate identity (item 8), the trend has not been maintained for the private sector, occupying position 5 in the design presence ranking. Note that in the case of the public sector it was ranked the first place. Furthermore, the private sector has given more importance to the item related to "Trade fair stands and materials" (item 7), followed by two new items introduced in this phase such as "Graphic application to existing packaging" (2nd position), and "Design of new packaging" (3rd position). In the main, the trend related to the degree of perception of the design component is maintained in the first positions in both sectors.

3.2 Importance of Design Ranked by Area and Its Benefits

Regarding the public sector, the Delphi experts agreed that design is quite or very important for large agri-food companies. This trend remains in this second phase for the private sector, also showing a high degree of agreement as can be seen in Table 3 (item 16–17). Table 3 is also depicting that consumers positioning is situated in the first place (item 18), while most experts pointed out that both Training Centers (undergraduate and postgraduate curricula) (item 12) and Government Authorities (item 14) considered that design is not a fundamental element for the innovation and improvement of the competitiveness of the agri-food sector. It can be added that these two issues aroused especially the interest of some participants.

Table 2. Presence of the design component in the agri-food industry

Order	Item	m	μ	σ	CV	Agreement
1	7	6.5	6.05	2.03	33.7	High
2	5	6.5	5.59	2.38	42.6	High
3	6	6.0	6.00	1.75	29.1	High
4	4	6.0	5.45	2.15	39.5	High
5	8	5.0	5.45	2.04	37.4	High
6	3	5.0	5.23	1.85	35.4	High
7	2	5.0	5.18	2.08	40.2	High
8	10	5.5	5.14	2.10	40.9	High
9	9	5.0	4.82	2.42	50.3	High
10	11	4.0	4.77	2.31	48.4	High
11	1	3.0	3.59	1.89	52.7	Medium

μ = Arithmetic Mean; σ = Standard Deviation; m = Median; CV = Coefficient of Variation (expressed in %). Reference qualifiers: (1) Nothing Present–(9) Very Present

Table 3. Importance of design by area

Order	Item	m	μ	σ	CV	Agreement
1	18	7.0	6.68	1.64	24.6	Very High
2	17	7.0	6.23	1.72	27.6	High
3	16	6.5	6.18	1.56	25.3	High
4	13	5.0	4.73	1.78	37.6	High
5	15	4.0	4.45	1.74	39.0	High
6	12	4.0	3.77	1.95	51.7	Medium
7	14	3.5	3.64	1.97	54.0	Medium

In this phase a series of items have been included around the tangible and intangible benefits that could be obtained from the incorporation of the design component in the agri-food industry. For each of the benefits two different items were drawn up trying to reflect the same approach, subsequently obtaining the mean between both items to obtain the most reliable valuations possible. For example, for the item "Increase in competitiveness" (item 19) the panel members claimed: (i) The position of the Andalusian agri-food sector should be improved with respect to its competitors; (ii) the products of the Andalusian agri-food companies should gain competitiveness. Regarding the tangible benefits, the increase in competitiveness was the most valued with a high degree of agreement as can be seen in Table 4 (item 19). The item perceived as the least important turned out to be the reduction of the environmental impact (item 23), although good scores were obtained for all. Regarding the intangible benefits, the one that obtained the best evaluation was the improvement of the corporate image of the agri-food companies and organizations, as it is shown in Table 5 (item

Table 4. Tangible benefits obtained from the application of design in the agri-food industry

Order	Item	m	μ	σ	CV	Agreement
1	19	7.5	7.55	1.07	14.1	Very High
2	25	7.3	7.02	1.67	23.7	Very High
3	21	7.0	7.00	1.64	23.4	Very High
4	24	7.0	6.89	1.91	27.8	High
5	22	7.0	6.68	1.51	22.6	Very High
6	20	6.5	6.34	1.56	24.6	Very High
7	23	6.0	6.05	1.54	25.5	High

Table 5. Intangible benefits obtained from the application of design in the agri-food industry

Order	Item	m	μ	σ	CV	Agreement
1	30	8.0	7.82	1.05	13.5	Very High
2	26	7.5	7.57	1.07	14.2	Very High
3	29	7.3	7.57	1.00	13.3	Very High
4	28	7.0	7.09	1.43	20.1	Very High
5	27	7.0	6.93	1.09	15.8	Very High

μ = Arithmetic Mean; σ = Standard Deviation; m = Median; CV = Coefficient of Variation (expressed in %). Reference qualifiers Table 3: (1) Nothing Important–(9) Very Important; Table 4 and 5: (1) I totally disagree–(9) I totally agree

30). Although very similar assessments were obtained in all cases, the improvement of quality (item 27) was placed in last position.

From the results obtained it can be deduced that, in all the cases raised, the panel of experts attaches great importance to design as an element of non-technological innovation within the agri-food sector. Aspect that was not reflected in a study conducted in 2012 on innovation in Andalusian companies [21]. In this work was looking for sought to answer the question: how do companies innovate?, from a sample of 100 companies for the specific case of the agricultural sector. The results that were obtained were quite surprising, since only one variable was identified that favored clearly the level of innovation. Specifically, reference was made only to patents and other industrial properties. At this point it is important to mention that although everything points out that design in general is not incorporated in the sector, there are transversal aspects that have begun to be incorporated in recent years. For example, in a special edition of a multidisciplinary agriculture journal, it was very clear that Computational Fluid Dynamics (CFD) related to Computer-Aided Design is now close to maturity in the eyes of agricultural engineers [22]. Finally, it should be emphasized that the set of benefits studied in this work can help overcome one of the main limitations of agri-food products, the non-differentiation of the product in relation to the products of other agricultural holdings, i.e. the lack of a brand. Limiting very notably the application of other strategies related to marketing, as is the case of advertising [23].

3.3 What Lines of Design-Sector Action Do You Think Are Necessary?

In this second phase, the 7 design-sector action lines already raised in the first phase from the public sector were also included at this second stage [9]. The Delphi panel of the private sector determined that the most relevant line was the one related to eco-design as a tool for the development of new packaging in the agri-food industry ($\mu = 7.32$; $\sigma = 1.46$). The action line related to design as an analysis instrument for landscape planning and integration of agricultural facilities took the second place ($\mu = 7.05$; $\sigma = 1.70$). In both cases a high degree of consensus was obtained. As a result of this second phase, new lines of action have emerged such as: (i) Design of a tourism-agrarian strategy. (ii) Promote knowledge of design as a function of companies. (iii) Design as a dynamic element in the new paradigm of the "Bio-economy". (iv) Explore alternative methodological tools for design training from the teaching-learning point of view.

Regarding packaging, it would be very interesting to incorporate environmental variables in the design process by exploring the growing wave of the so-called emotional design [24]. For example, Tassina and Cacioppo [25] studied how the emotions of consumers were affected by the product (i.e. design results). Regarding the design line of developing tools and analysis instruments for planning and landscape integration, a very consistent coherence in the results was observed. In fact, it was the component to which less presence was assigned (item 1), and subsequently stands out as a necessary line to be developed in the agri-food sector. This proposal would be framed in the context of what is commonly called "Landscape Architecture", a research line started in Spain by mainly focusing on agricultural constructions with an important technical component [26–28]. However, the applications of this promising research line on the specific case of plastic covered greenhouses areas and issues related to land planning is practically nonexistent. This is the reason why we have recently started a new research line in which widely known tools such as "Remote Sensing Techniques" and "Landscape Metrics (spatial)" are applied to develop a methodological proposal headed up to facilitate rural landscape evolution studies, land planning and monitoring, and policy management in areas of intensive agriculture.

Finally, and from an academic perspective, we propose the introduction of the "Design Process" as a topic to be incorporated in the subjects of the "Graphic Expression" module at degree or master level. This approach could allow the development of innovation and creative empowerment skills.

4 Conclusions and Future Research Lines

Regarding the first question, the experts panel from the private sector considered that the design activities mostly present in the agri-food sector have to do with graphic design. It should be noted that in this case, unlike the Delphi panel from the public sector, they considered that the design component is more present in trade fair stands and materials where, in addition to the graphic design, the design of products and space plays a relevant role. With regards to the incorporation of design into organizations and companies in the agri-food sector, the group of experts considered that it is an interesting tool to be explored, an idea that is based on the good scores granted to tangible and intangible benefits which could be obtained from this approach.

Finally, the findings obtained in this work (putting together both public and private agri-food sectors) represent an indispensable preamble to get insight about the current situation regarding the presence of the design component in the agri-food industry. In this sense, an important background is already available so that further works will try to get a detailed picture of specific agri-food clusters to allow understand how design is present in the companies of the agri-food sector. This could favor the transfer of R & D & I results to the agents of the sector to increase the social impact of this work and the development of the design culture. In summary, the milestone provided by this new line of research seems to be very valuable as a diagnostic tool to characterize the design component in the agricultural sector. That in turn can help to discover and develop design as a tool of non-technological innovation and a factor of dynamization for the creation of environmental, social and economic value in the agri-food sector.

Acknowledgments. This work has been supported and financed by an FPI predoctoral fellowship (first author) granted in the framework of University of Almeria Research Programme. It also takes part of the general research lines promoted by the Agri-food Campus of International Excellence ceiA3. Thanks for the advice regarding the preparation of the exploratory phase of this study are due to the professors and researchers Emilio Galdeano and Laura Piedra, members of the research group "Economic Development and Agrifood Economy (SEJ-529)" of the Andalusian Plan for Research, Development and Innovation, thanks. Finally, the authors wish to sincerely thank the experts of the agri-food and design industry in Andalusia who made up the Delphi panel for their very valuable contribution to the results obtained in this work.

References

1. Ministerio de Agricultura, Alimentación y Medio Ambiente (2016) La contribución del sistema agroalimentario a la economía española. (Actualización ejercicio 2014). Análisis y Prospectiva - Serie AgrInfo 27. Available online: http://goo.gl/kL61Yg
2. Galdeano-Gómez E, Azanar-Sánchez JA, Pérez-Mesa JC (2013) Sustainability dimensions related to agricultural-based development: the experience of 50 years of intensive farming in Almería (Spain). Int J Agric Sustain 11(2):125–143
3. Hertenstein JH, Platt MB, Veryzer RW (2013) What is "good design"?: an investigation of the complexity and structure of design. Des Manag J 8(1):8–21
4. Johnson MP, McHattie L-S (2014) Making design explicit in organisational change: Detour o Latour. In: 19th DMI: academic design management conference, London, 2–4 Sept 2014. Available online: https://goo.gl/U5LzPH
5. Lecuona M (2005) Conceptos básicos de la gestión del diseño en las pymes. Edición Servicio de Publicaciones Universidad Politécnica de Valencia, Valencia
6. Perks H, Cooper R, Jones C (2005) Characterizing the role of design in new product development: an empirically derived taxonomy. J Prod Innov Manag 22:11–127
7. Costa J (2010) Diseño global en la empresa. In: Jarauta, F. Cuadernos de diseño: Diseño, innovación, empresa, 3, 150–165. Instituto Europeo di Design, Madrid
8. Gemser G, de Bont C, Hekkert P, Friedman K (2012) Quality perceptions of design journals: the design scholars' perspective. Des Stud 33:4–23

9. González-Yebra Ó, Aguilar MA, Aguilar FJ (in press) A first approach to the Design Component in the agri-food industry of southern Spain. Revista de la Facultad de Ciencias Agrarias UNCuyo
10. Sarmiento F, Muñoz RM, González J, García-Moreno MB (2012) Una nueva metodología para la investigación de tendencias en diseño. I+Diseño 7(7):28–42
11. Luque EM, Blázquez EB, Ladrón de Guevara MC, Castillo F (2013) Agrodiseño. El diseño gráfico en el poniente almeriense. I + Diseño 8(8):120–134
12. Dalkey N, Helmer O (1963) An experimental application of the Delphi method to the use of experts. Manage Sci 9(3):458–467
13. Matell MS, Jacoby J (1971) Is there an optimal number of alternatives for Likert scale items? Study 1: reliability and validity. Educ Psychol Measur 31(3):657–674
14. Lozano LM, García-Cueto E, Muñiz J (2008) Effect of the number of response categories on the reliability and validity of rating scales. Methodology 4(2):73–79
15. Buil I, Martínez E, Montaner T (2005) Importancia del diseño industrial en la gestión estratégica de la empresa. Universia Bus Rev 8:52–67
16. Keeney S, Hasson F, McKenna HP (2006) Consulting the oracle: ten lessons from using the Delphi technique in nursing research. J Adv Nurs 53(2):505–512
17. Shah H, Kalaian SA (2009) Which parametric statistical method to use for analyzing Delphi data? J Mod Appl Stat Method 8(1):226–232
18. McKenna HP, Bradley M, Keeney S (2000) Primary care nursing: a study exploring key issues for future developments. University of Ulster, Ulster
19. Loughlin KG, Moore LF (1979) Using Delphi to achieve congruent objectives and activities in a pediatrics department. J Med Educ 54(2):101–106
20. Muñoz Fernández S, Lázaro de Mercado P, Alegre López J, Almodóvar González R, Alonso Ruiz A, Ballina García FJ et al (2013) Quality of care standards for nursing clinics in rheumatology. Reumatol Clin 9:206–215
21. Martínez Román JA, Gamero Rojas FJ, Tamayo Gallego JA, Romero García JE (2012) Modelización, análisis y medición de innovación en las empresas andaluzas. Documentos de trabajo (Centro de Estudios Andaluces), Serie 1, 8, 1–41
22. Norton T (2013) CFD in the agri-food industry: a maturing engineering design tool. Comput Electron Agric 93:149–150
23. Martínez Navarro G, López-Rua MG (2012) Marketing Agroalimentario: Una aproximación al uso de las nuevas tecnologías en el sector. Revista Internacional de Economía y Gestión de las Organizaciones 1(1):73–94 (2012)
24. Norman DA (2004) Emotional design: why we love (or hate) everyday things. Basic Books, New York
25. Tassinary LG, Cacioppo JT (1992) Unobservable facial actions and emotion. Psychol Sci 3:28–33
26. García L, Hernández J, Ayuga F (2003) Analysis of the exterior colour of agroindustrial buildings: a computer aided approach to landscape integration. J Environ Manage 69(1):93–104
27. Hernández J, García L, Ayuga F (2004) Integration methodologies for visual impact assessment of rural buildings by geographic information systems. Biosys Eng 88(2):255–263
28. Hernández J, García L, Ayuga F (2006) Assessment of the visual impact made on the landscape by new buildings: a methodology for site selection. Landscape Urban Plan 68:15–28

Description of Moisture Thermal Patterns in Concrete for the Thermal Inspection Method by Infrared Thermography

P. Cárdenas-Del Campo[1(✉)], F. Soto-Lara[2], and M. Marín-Granados[1,2]

[1] Escuela de Ingenierías Industriales, Calle Doctor Ortiz Ramos, 29010 Málaga, Spain
pcardenasdelca@gmail.com
[2] INTERMAL, Calle Giacomo Puccini, Alhaurín de la Torre, 29130 Málaga, Spain

Abstract. The aim of this paper is to collect graphical information (with thermal images) on how moistures can appear in building materials such as concrete, and to develop a method that detects moisture using infrared thermography. This research work was prompted by the fact that moisture is one of the greatest building pathologies, along with the fact that there are insufficient standards and documentation for using this technology in specific applications such as moisture detection. Real specimens of concrete were built with the specific purpose of generating moisture. Infrared images (thermograms) were then taken to show their development, and were analysed with FLIR Tools+ and FLIR ThermaCAM Researcher software. The results of the experiments revealed important information for defining the thermal patterns to be detected. Using this information, the graphic characteristics of a typical qualitative (without measurement of temperatures) thermal pattern in a wet material are described, as well as the qualitative thermal pattern of the rise in capillarity, which is suffered by a part of the material. In addition, the humidity levels were checked with a thermo hygrometer to confirm the different areas shown by thermography in the previous thermal patterns. This research will be useful for professionals who have the suitable equipment for moisture detection and treatment, because once the visible moisture marks have been produced, they endure regardless of whether or not the material is damp.

Keywords: Infrared thermography · Inspection method · Graphic analysis · Moisture

1 Introduction

Thermography is a technique that detects infrared energy emitted from objects, upon which this is converted into temperature, finally displaying an image of its temperature distribution [1]. By definition, this technology operates at infrared frequencies and is sensitive to both temperature and emissivity variations. The possibility of taking

F. Cavas-Martínez et al. (Eds.): *Advances on Mechanics, Design Engineering and Manufacturing II*, LNME, pp. 622–631, 2019.
https://doi.org/10.1007/978-3-030-12346-8_60

pictures and their later analysis offers a considerable number of potential applications within the engineering field [2, 3].

Even though thermography portable cameras aimed at engineers, construction, or maintenance technicians have been on the market for more than 50 years, there is a lack of documentation and standards for their use in specific applications. In addition, the equipment is widely used without any methodology or tests that can confirm whether the detection has been carried out in the optimal way.

In this research, thermography was applied to moisture detection in concrete, one of the most widely used and readily available construction materials on the market. It is widely accepted that moisture problems in construction are responsible for a considerable amount of building damage. In fact, according to the *Análisis Estadístico Nacional de Patologías en la Edificación* developed by the MUSAAT Foundation in 2013 [4], moisture is the direct cause of 40% of building failures. Therefore, the different types of moistures that can appear in materials have been distinguished by their origin, condensation, filtration, and capillarity [5, 6].

However, thermography is able to predict this pathology, and allows for a qualitative evaluation of the real state of the moisture and its dimensions within a wall. For this reason the objective of this research was to exploit this technology in an attempt to establish a method that ensures easier detection, focusing on the capillarity of the moisture. Thus, the aim was to find a common thermal pattern that helps to identify if moisture exists, and whether or not the material is completely wet.

A wall that is in perfect condition, without moisture problems, will show a homogenous picture when taken with an infrared camera. However, if it is affected by water, the thermogram will change and it will display different areas where the thermal pattern is characterized according to the type of moisture. This information will be more accurate prior to analysis with the corresponding software.

2 Materials and Methods

The experiment began with the manufacture of two concrete blocks (left side of Fig. 1), which were constructed with the same dimensions of 21.5 × 16 × 9 cm. One of the blocks was kept dry, to serve as a comparison. The other block was subjected to numerous tests in which the specimen was placed in a bucket with water with the aim of inducing moisture. The right side of Fig. 1 shows the finished specimens ready to start the analysis.

The procedure consisted of placing one of the concrete blocks in water, and

Fig. 1. Concrete blocks studied

monitoring its development by taking infrared images every 10–15 min. Different tests provided a total of 65 images on different days where the development of moisture was observed. These images were then analysed using the corresponding software, choosing the four most representative images, all of which were produced by the final test (It should be noted that several tests were carried out to confirm the repetitive behavior of the thermal patterns observed, as well as the influence of the time of day and the thermal conditions at the time of testing).

This choice of images was made taking into account the fact that the experiment is conducted several times and therefore the wetting and capillarity processes are repeated. Thus images are taken of the various phases of the process, with those most common and repetitive being regarded as the most representative, providing a good sample of the phases of the wetting process of the models.

In general, the methodology followed in thermography inspections consists firstly of recognizing and/or measuring in situ the object of study with the camera, which is equipped with a screen and the basic tools needed to make an initial interpretation of the image. Later, a more in-depth analysis can be carried out using the corresponding software.

When using both the camera and software, the image has to be corrected. This means that certain parameters must be introduced such as emissivity or reflected apparent temperature. Emissivity refers to how efficiently an object radiates heat. It is defined as the ratio of infrared energy emitted by the object, compared to that emitted by an ideal blackbody, if both are at the same temperature. It is represented by either a percent or a decimal, and in the current experiments it takes the value 0.95. The second parameter, reflected temperature, is any thermal radiation originating from other objects that reflect off the target being measured [7], which is calculated by the ISO 18434-1 and takes the value 21.3 °C.

In spite of taking these parameters into account, it is very common to regard the measures obtained as qualitative in many thermography studies where measuring an exact temperature is not strictly necessary. In these cases only thermal patterns should be identified, comparing the different level of radiation obtained between the specimen tested and its normal conditions. Nevertheless, these parameters are considered to be more rigorous.

Following this, the color palette was chosen, which is a useful tool for thermal image interpretation. There is no such thing as the optimal palette since the one that shows the best thermal patterns is selected in each case [8]. The criterion followed in this research was to select the palette that gives a high thermal contrast, since temperature gradients are not so large and it is necessary to choose a palette where the different temperatures in the specimen stand out.

Finally, straight lines were drawn using other software tools with the aim of observing the temperature distribution on the block surface (see Fig. 2).

The images were taken by a FLIR T-355 thermography camera and were analysed with FLIR Tools+ and FLIR ThermaCAM Researcher software. A thermo hygrometer was used to verify relative humidity levels (Extech Instruments model MO297).

3 Results and Discussion

3.1 Thermal Image nº41, 11:00 h (Time Zero). Dry Specimen

The following image in Fig. 2 shows a screenshot of the analysis software, the ThermaCAM Researcher. In the thermal image both concrete blocks can be seen, the one used for testing, which is in contact with water on the left, and the comparison block, which is displayed on the right. With the aim of studying temperature distribution throughout the piece/object, two straight lines were drawn (L01 and L02). A graphic is obtained from those lines showing how the temperature on the surface changes, on the y-axis, along the image pixels, placed on the x-axis. The exact temperature value in each pixel is known by means of a cursor that can be moved over the lines. This information is indicated in the Position tab.

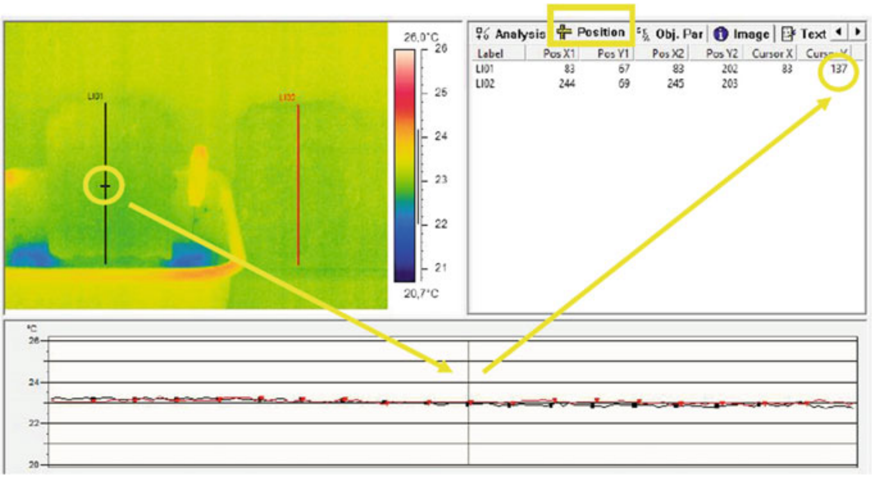

Fig. 2. Screenshot of ThermaCAM Researcher Software with the first thermal image analysed

This image belongs to the beginning of the experiment (using the last specimen put in water). The specimen had just been put into water, and therefore we were yet to observe an increase in moisture by capillarity. In this case, the thermal patterns that the image reveals are homogeneous and equal, and the graphic of the temperature distribution is constant. Figure 3 shows the previous image analysed in the visible range.

Fig. 3. Visible image of Fig. 2

3.2 Thermal Image nº44, 11:30 h (Time 30′). Specimen with no Capillarity Area

Half an hour later, the porosity of the material causes water to rise rapidly through the specimen. The thermal pattern is no longer homogeneous and two areas can be distinguished (Fig. 4), which are discernible and coincident in both the infrared and visible ranges The lower area, in blue, represents the completely wet side that has the lowest temperature distribution, while the other has a higher temperature corresponding to the dry side of the block.

The temperature distribution declines on the side that is completely wet, but it rapidly becomes stable, without any transition area between the wet and dry side. In other words, there is no point on the graph in which the temperature descends gradually, as will be seen in the following section.

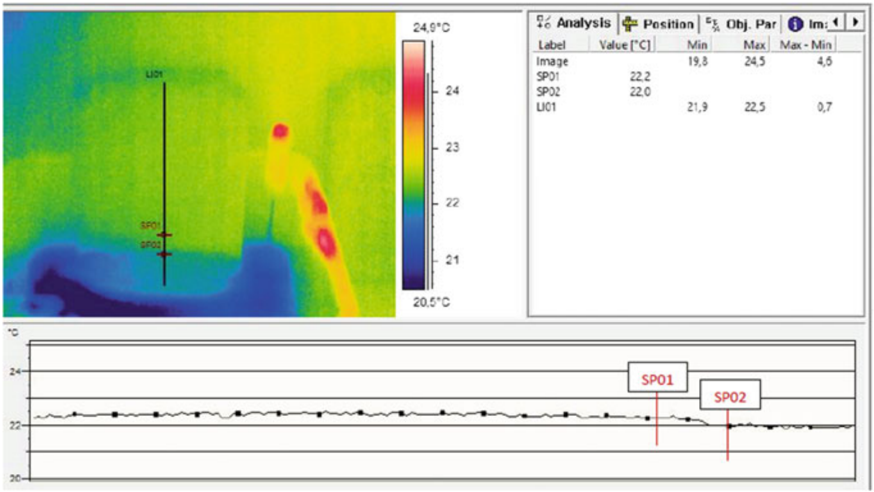

Fig. 4. Screenshot of ThermaCAM Researcher Software with image nº44 analysed

3.3 Thermal Image nº50, 12:34 h (Time 94′). Specimen with Capillarity Area

This image, shown in Fig. 5, with its corresponding visible range image in Fig. 6, is the most representative image of the entire experiment since a significant change was found in the thermal pattern. There is a band beyond the visible range, with a temperature that is different from the other sides studied previously. This means that if the thermogram is compared with the visible range image, this area is not perceptible to the human eye, thus showing that thermography provides a level of analysis that goes beyond what people are able to see. This thermal pattern was monitored from that point in order to verify that it is not a coincidence.

The temperature profile is directly related to that previously analysed, showing similar behaviour on both the wet and dry sides. In both cases the highest temperature is constant (this being on the dry side) and in the wet area it does not fall rapidly to become stable again with a constant lower temperature. However, in this case there is a transition band between the two areas already identified, defined by the P01 and P02 points, where the temperature declines gently, and which coincides exactly with the new thermal pattern discovered, represented in light blue. This band represents the partly wet material, which is the area suffering from capillarity and the one which will become completely wet over the passage of time. Thus, thermography acts as a warning sign.

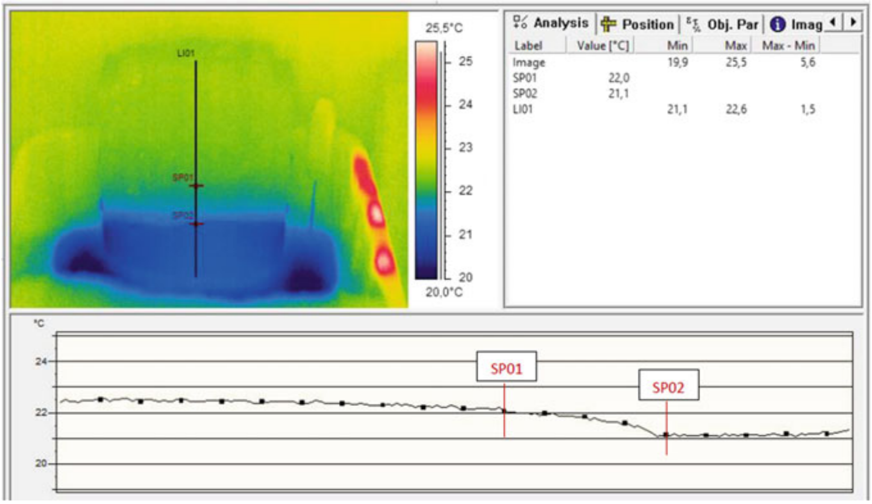

Fig. 5. Screenshot of ThermaCAM Researcher Software with image nº50 analysed

Fig. 6. Visible image of Fig. 5

3.4 Thermal Image nº59, 14:00 h (Time 180′). Verification of the Capillarity Area

The final image analysis, presented in Fig. 7, verifies the thermal pattern that was revealed in the previous section. This confirms the presence of the partly wet area that is not perceptible in the visible range. Moreover, with thermography the three bands are now more readily distinguishable than before. Regarding temperature distribution, a transition area again appears, defined by P01 and P02, coincident with the band only visible in the infrared range, and this area is even larger than that observed previously.

To provide more information, the thermogram and visible image are conjointly presented in the same figure (Fig. 8), option that is available when sing the FLIR Tools + software. Both images are the same, with the exception that the temperature scale that overlaps them is different, thereby showing the desired temperature intervals. This again indicates that the partially wet thermal pattern is not perceptible to the human eye.

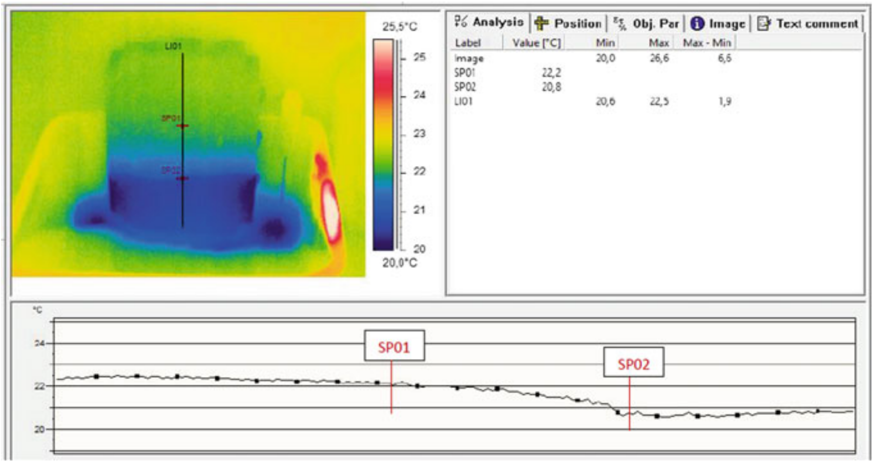

Fig. 7. Screenshot of ThermaCAM Researcher Software with image nº59 analysed

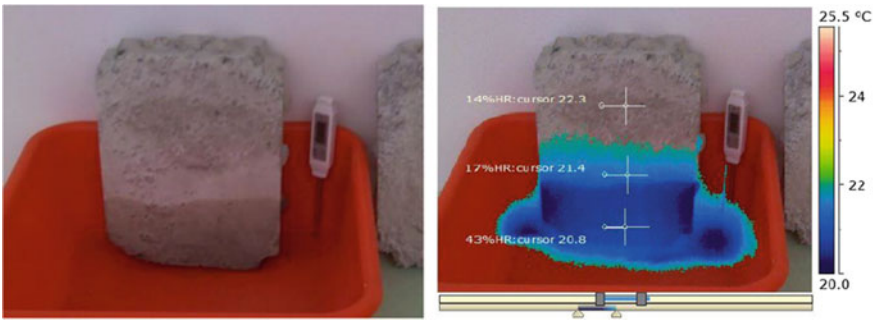

Fig. 8. Overlapped infrared and visible image

3.5 Moisture Levels

The humidity levels measured with the thermo hygrometer were obtained to verify the different areas previously found. This action shows that humidity levels change in each part of the block, but these are merely illustrative. In the wet area there is always 40–43% relative humidity, in the partially wet band there is 17% RH, and in the dry area this value is 14%.

4 Conclusions

Repeated thermal patterns were obtained throughout the experiment, which have given rise to a way of defining how capillarity moisture is represented with thermography. Using this technique, the following instructions are of potential use for professionals who need to carry out a moisture inspection.

Using thermography, three perfectly distinguishable bands are shown in Fig. 9.

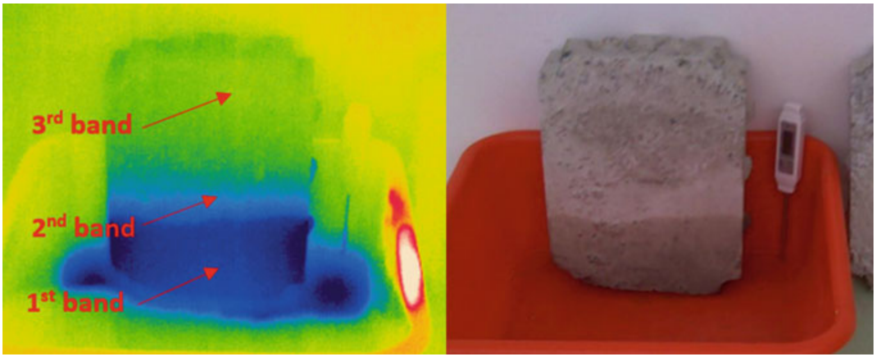

Fig. 9. Three infrared bands of moisture

The first of these is defined as a "completely wet" area, with a thermal pattern accessible with little thermal *adjustment* and taking the lowest (but stable) temperature of the distribution. This band is between the bottom of the specimen, which is in direct contact with the water, and the water mark that is visible to the human eye. The border where this band ends is shown as a well-defined and distinguishable line.

A second band then appears with an intermediate temperature in relation to the other two bands, but in this case it is variable in each pixel. This is the transition area previously defined. In addition, whilst this is not distinguishable in the visible range, it is detectable in the infrared range. This area is suffering from a rise in water by capillarity, and it is known as the "partly wet" area because insufficient time has yet passed for it to be completely wet. The thermal pattern associated with this area requires a color palette with higher thermal contrast in order to be identified, which was not the case in the previous band. Now, the border of this pattern is not well defined and it appears as a cluster of dots. In this case thermography has an advantage, since it predicts the appearance of future moistures.

Finally, the third band is shown, where the specimen is already dry. The temperature is again stable, reaching the highest value. The thermal pattern is homogeneous and it resembles the pattern present at beginning of the experiment and the comparison specimen.

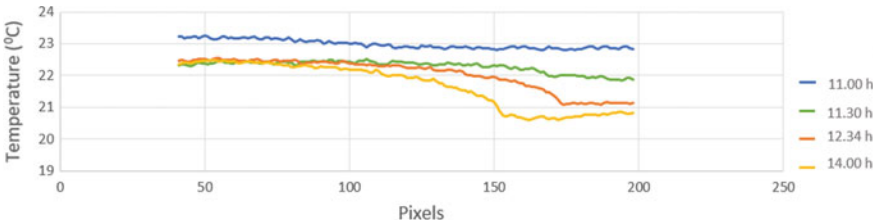

Fig. 10. All temperature distributions in the same graphic

Temperature values in each pixel can be exported from software to an Excel spreadsheet, which allows for combining all the previous temperature distributions into a single distribution. This is shown in Fig. 10, where it is easier to see that the transition area becomes larger with the passage of time.

References

1. Çengel Y (2007) Transferencia de Calor y Masa, 3rd edn. McGraw-Hill, Mexico
2. Grupo Álava Ingenieros, http://www.grupoalava.com/ingenieros/actualidad/guias-educativas-de-termografia/. Last accessed on 18 April 2017
3. Melgosa Revilla S, https://www.fenercom.com/pdf/publicaciones/Guia-de-la-Termografia-Infrarroja-fenercom-2011.pdf. Last accessed on 18 April 2017
4. Carretero Ayuso MJ, Moreno Cansado A (2016) Análisis estadístico nacional sobre patologías en edificación 2008–2013. Fundación MUSAAT
5. Jiménez López L (2011) Humedades en la construcción, 1st edn. Planeta DeAgostini Profesional y Formación, Barcelona, pp 25–69
6. García Morales S (1995) Metodología de diagnóstico de humedades de capilaridad ascendente y condensación higroscópica en edificios históricos. Ph.D. thesis, Escuela Técnica Superior de Arquitectura, Madrid
7. Infrared Training Center, http://irinformir.blogspot.com.es/2012/02/thermographic-measurement-techniques.html. Last accessed 10 May 2017
8. The Snell Group, https://www.thesnellgroup.com/blog/cual-es-la-mejor-paleta-de-color. Last accessed 5 Sept 2017

Joint Development of Video Mapping Contents on the Industrial and Cultural Heritage of Zaragoza (Spain)

F. J. Galán-Pérez(✉) and A. Biedermann

Department of Design and Manufacturing Engineering, Observatorio Aragonés de Arte en la Esfera Pública, María Luna 3, 50018 Saragossa, Spain
jgalan@unizar.es

Abstract. Within the framework of the joint-project MIE (Mediation, Innovation and Entrepreneurship) led by the Zaragoza City Council and the University of Zaragoza, it has been carried out during the year 2017 a project of joint development of videomapping contents at the industrial & cultural heritage of Zaragoza (Spain) in order to rediscover the paths to strengthen the production and dissemination of artistic work related to technology, engineering and innovative development. Formative pills of Adobe Premiere, Adobe After Effects, Adobe Photoshop, Madmapper and the TacTool interface system were made in the content workshop. With the sufficient number of hours to grant autonomy to the creators of contents that later would project on the façade of building of the neighborhood of Rabal de Zaragoza known as "Casa del Director", a house that was inside the industrial facilities of the Sugar Mill of Rabal. With this procedure it was possible to establish an exit route to disseminate digital content for videomapping, enhance local industrial heritage, generate means of production that maximize budgets and democratize an art and engineering environment normally reserved for those who can afford it.

Keywords: Open workshops · Social engineering · Collaborative contents design · Free engineering

1 Introduction

Public investment in art, technology and design usually imposes very restricted spending patterns, which negatively (and sometimes decisively) impact the work of artists and professionals [1], sealing a circle that hinders or even makes it impossible to achieve artistic works with a periodicity greater than a year as well as its subsequent output to international markets.

This is normally happening given the normal legal restrictions imposed by the public function, where the control of expenditure prevails [2] as well as the investment for the local use of such investments in the form of exhibitions in one of the city's galleries. It defines in practice how much the correct management of public spending matters, and also indicates the *hamster wheel* where most of the artists-living in the city of Zaragoza- are located [3].

F. Cavas-Martínez et al. (Eds.): *Advances on Mechanics, Design Engineering and Manufacturing II*, LNME, pp. 632–638, 2019.
https://doi.org/10.1007/978-3-030-12346-8_61

Therefore, initiatives for progressively moving away the two most critical items of the artistic process (production and dissemination) from the administrative paradoxes are intended for multiplying the possibilities for local artists to be able to rise to sustained rhythms of work, in order to acquire market competences in a more agile way: works cv, logistics knowledge, contact agenda or continuous training among many others.

In recent times serious movements have been emerging from academic and institutional instances [4, 5] showing that the time to take certain distances and renew this contract of administrative use and enjoyment of the cultural and artistic has arrived, where both parties are conveniently treated, something that does not happen nor has it happened in the time we have of democracy.

Video mapping is just one of the techniques used in this project to integrate the administrative, academic and artistic stakeholders. It is also technique interesting from the engineering [6, 7] as well as artistic [8, 9] and urbanistic [10, 11] point of view.

2 Program Where the Action Is Framed

The MIE [12] program (Mediation–Innovation–Entrepreneurship) consists of a public initiative promoted by the University of Zaragoza and Zaragoza Activa (institution belonging to the Zaragoza City Council), inspired by actions of participation, social entrepreneurship and public innovation of the Nordic countries and the methodology of Medialab Prado in Madrid, which are a paradigm of public, private and social collaboration.

2.1 Mediation

Within the framework of mediation, each of the selected projects works on the creation of a community of Open Innovation for all citizens, which involves different agents of the entrepreneurial and innovative ecosystem of Zaragoza related to the theme of the projects, helping identify new problems, as well as propose, create and experiment with solutions from a shared, open and collaborative approach.

2.2 Innovation

All projects have an innovative perspective that consists in the development of their project in a framework of constant learning, generation of knowledge and documentation, sharing and opening the contents of the same to the community, through publications and various activities such as open workshops, events or work groups.

2.3 Entrepreneurship

Mediators seek, while developing their projects, to transform society from economic and social sustainability, becoming agents of change and social entrepreneurs.

3 Objetives

In this way, the “Rocketz” proposal is, as a MIE project [13], an innovative way of supporting local artistic creation, with a view to the global, and with the healthy intention of talking about funding. No more money, of course, but about the way in which public funds are enabled and used for local art, without forgetting that, by the way, Zaragoza has first-class facilities that could serve to increase them. In short, the question -we will see later how it is answered- of the Rocketz project is: Would we accept a redesign of the existing relationship between artists, curators and other art and culture professionals with local institutions, in this case with the Zaragoza City Council Rocketz, as a proactive project, designs an exchange of goods and services that attends to sustainable production over time and economically sustainable, as well as its dissemination and promotion in dynamic market niches.

For this reason, within the framework of the joint-project MIE led by the Zaragoza City Council and the University of Zaragoza, it has been carried out during the year 2017 a project of joint development of videomapping contents at the industrial & cultural heritage of Zaragoza (Spain) to rediscover paths that strengthen the production and dissemination of artistic work related to technology, engineering and innovative development.

The objectives have been:

- To carry out a mediation project among the agents involved in the dissemination of current art, with a view to the protection of the production and artistic promotion phases, which promotes the international projection of artists and their works.
- To carry out a mapping of local resources, as well as artists of international projection, which will lay the foundations for the project, as well as research on an artistic export methodology that culminates in a real prototype, as an example of good practices that can be replicated in the future.

4 Development of the Project

After a period of consultations and interviews with the cultural and design agents of the city (agents developing their activity in a professional mannert with an income based on their artistic, design or engineering activity) an new plant activity was designed combining both the possibility of teaching the technique of videomapping to a wide range of individuals and, in addition and in a definitely way, to draw attention to the industrial and cultural heritage of the Rabal district of Zaragoza.

To achieve the project, it was decided to hold a collaborative content workshop [14, 15] (including the necessary software and hardware) to subsequently project them in a disused industrial heritage building in the city of Zaragoza, and its subsequent repetition in another location outside of Spain in collaboration with another institution to minimize expenses and promote the dissemination of content realized by artists specializing in new media at the local level. Being in this case the City of Mexico, and the UNAM, through the C3 Institute, the collaborating entity.

Formative pills of Adobe Premiere [16], Adobe After Effects [17], Adobe Photoshop [18], Madmapper [19], and the TagTool [20], interface system were made in the content workshop. With a number of hours to grant autonomy to the creators of contents that later would project on the façade of building of the neighborhood of Rabal de Zaragoza known as "Casa del Director", a house that was inside the industrial facilities of the Sugar Mill of Rabal, built in 1903, consists of 515 m^2 distributed on two floors and a small basement and is surrounded by a garden of 300 m^2 (Fig. 1). It is currently in process of rehabilitation.

With this procedure it was possible to establish an exit route to disseminate digital content for videomapping, enhance local industrial heritage, generate means of production that maximize budgets and democratize an art and engineering environment normally reserved for those who can afford it.

The results were highly satisfactory (Figs. 2, 3 and 4), opening the possibility of converting this way of working in a future festival of lights in Zaragoza, whose aims will be inter-institutional collaboration, training in art and engineering, the democratization of an expensive technological medium and the most important of everything: to encourage investment in production and diffusion in digital graphic artistic work.

Fig. 1. House of the Director in the District of Rabal in Zaragoza. Industrial heritage that survived the closing of the Sugar Factory closure back in the 80s

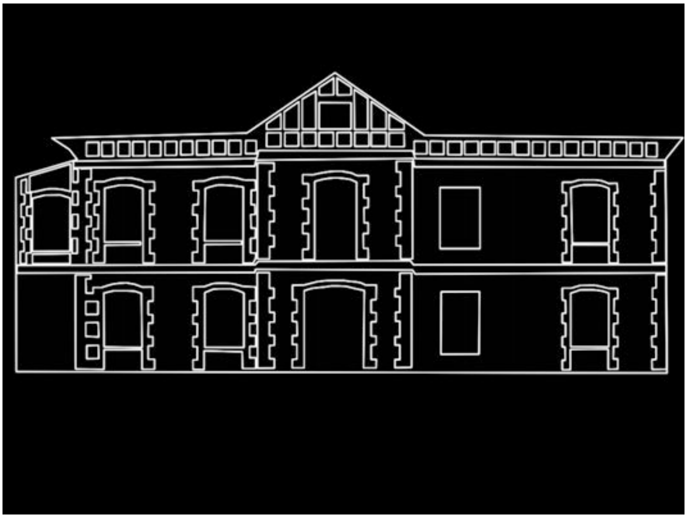

Fig. 2. RGB template of the main façade of the House of the Director in the District of Rabal

Fig. 3. Night in which the contents of the workshop were issued with a duration of 45 min. The works of Zaragoza artists Edu Cortina, Fermín Serrano, Yanguar Art and Flores were also shown

Fig. 4. Setting of the blue screen, previous step towards template adaptation to the real façade

5 Conclusions

This methodology of open production and shared diffusion -through international collaboration with other institutions- is not only an example of how to use public budgets in very important items of the life of the designer and the artist of new media, but also allow that many more people interested in knowing the videomapping technique can do it at zero cost. The number of people attending the Rocketz workshops was fifteen people.

In addition, knowing that it was a collaborative videomapping project, that is, where all the participants could pour their entire artistic projection into the screening, there were well-established artists from the city who wanted to participate.

References

1. El Diario. https://www.eldiario.es/cultura/arte/Arte-precario-artistas-comisarios-jovenes_0_612438962.html. Last accessed 21 Mar 2018
2. Heraldo de Aragón. https://www.heraldo.es/noticias/aragon/zaragoza-provincia/zaragoza/2016/04/08/edificios-publicos-vacios-contenido-espera-nuevos-usos-841516-301.html. Last accessed 21 Mar 2018
3. Blog Zac. http://blogzac.es/rocketz-del-arte-hacia-lo-publico/. Last accessed 21 Mar 2018
4. Boletín official de cortes generales. http://www.congreso.es/public_oficiales/L12/CONG/BOCG/D/BOCG-12-D-37.PDF#page=38. Last accessed 21 Mar 2018
5. Boletín official de cortes generales. http://www.congreso.es/public_oficiales/L12/CONG/BOCG/D/BOCG-12-D-48.PDF#page=3. Last accessed 21 Mar 2018
6. Wechsler R, Weiß F, Dowling P (2004) EyeCon—A motion sensing tool for creating interactive dance, music, and video projections. In: Proceedings of the SSAISB convention

7. Wechsler R, Weiss F (2004) Motion sensing for interactive dance. In: IEEE-pervasive computing, mobile and ubiquitous systems. IEEE Computer Society Publications
8. Berna EKİM (2011) A video projection mapping conceptual design and application: Yekpare. Turk Online J Des Art Commun 1(1)
9. Quniz E, Lovell R (2002) "Digital performance" Anomalie digirtal_arts. ATI Press, Rome, pp 124–130
10. Struppek M (2006) Urban screens—The urbane potential of public screens for interaction. In: Intelligent agent, vol. 6, no 2, Special issue: papers presented at the ISEA2006 symposium
11. Pop S, Stalder U, Struppek M, Tscherteu G (eds) (2012) Urban media cultures. Avedition
12. http://blogzac.es/programa-mie-mediacion-innovacion-emprendimiento/. Last accessed 21 Mar 2018
13. http://blogzac.es/rocketz-del-arte-hacia-lo-publico/. Last accessed 21 Mar 2018
14. https://www.zaragoza.es/zac/events/41863. Last accessed 21 Mar 2018; 16 May 2018
15. http://www.unizar.es/actualidad/vernoticia_ng.php?id=37492. Last accessed 16 May 2018
16. Adobe Premiere https://www.adobe.com/es/products/premiere.html. Last accessed 16 May 2018
17. Adobe After Effects. https://www.adobe.com/es/products/aftereffects.html. Last accessed 16 May 2018
18. Adobe Photoshop. https://www.adobe.com/es/products/photoshop.html. Last accessed 16 May 2018
19. Madmapper. https://madmapper.com/. Last accessed 16 May 2018
20. Tagtool. https://www.omai.at/tagtool/. Last accessed 16 May 2018

Service Design and Sound: A Chance for Exploration in Oncological Treatment Rooms

R. Sanz-Segura[1(✉)], C. Romero-Piqueras[1], E. Manchado-Pérez[1], and E. Özcan[2]

[1] Departamento de Ingeniería de Diseño y Fabricación, Escuela de Ingeniería y Arquitectura de la Universidad de Zaragoza, c/María de Luna 3, 50018 Saragossa, Spain
rsanz@unizar.es

[2] Department of Intensive Care Erasmus Medical Centre Rotterdam, Faculty of Industrial Design Engineering, Delft University of Technology, The Netherlands

Abstract. The value of sound design is increasing in the field of product development, and even more so in critical contexts such as healthcare. A well-designed sound can have an impact over job satisfaction, efficiency in work environment, user experience and well-being of healthcare staff and users as a whole. On the other hand, service design is a particular domain within design engineering focused on how the relationship between service providers and users can be improved. An emerging community highlights the utility of the tools and techniques to effectively include system stakeholders in the design and implementation of health technology and healthcare service design. Service design has been applied successfully in several projects to improve patient experience as well as in other areas of public sector. This paper states the potential contribution of service design to sound design, as another methodological approach in order to improve audible alarm design for product development in healthcare environment. Likewise, the paper offers designers and engineers possibilities to implement together both the tools and methods of service design and product sound design deriving from the review of existing literature and empirical conclusions compiled from observation and analysis of oncological treatment rooms at different hospitals.

Keywords: Sound design · Service design · Design methods · Healthcare · Alarm fatigue

1 Introduction

The value of sound design is increasing in the field of product development, and even more so in sensitive sectors such as healthcare. A well-designed sound can have an impact over job satisfaction, efficiency in work environment, user experience and well-being of healthcare staff and users as a whole. From the perspective of nurses, inadequate audible alarms interfere with communication, create distractions, and affect cognitive ability and ease of concentration, which all together increase stress and

F. Cavas-Martínez et al. (Eds.): *Advances on Mechanics, Design Engineering and Manufacturing II*, LNME, pp. 639–648, 2019.
https://doi.org/10.1007/978-3-030-12346-8_62

fatigue and therefore an overload in mental activities linked to their workflow. From the point of view of patients and their relatives, alarms have an adverse effect on comfort and recovery, interrupt sleep and disturbs daily routines, and reduce the overall perceived satisfaction of the patient, especially in critical care [1].

The need to adjust sound levels, reduce noise and environmental stress associated with it, is a recurrent aspect in the literature, and multiple authors and organizations have shown the need to reduce noise level and alarm fatigue [2–4] from the exorbitant number of false or non-actionable alarms, unnecessary, not standardized or without an efficient hierarchy [5]. However, there are studies that highlight the potential of sound as an essential element in transferring information from the product to the user, which on the other hand, significantly affects the experience that one offers to the other. This refers to the use of sound as an essential parameter to be taken into account throughout the design process. This way, through the characterization of a certain sound, the listener (nurse, patient or family members) can perceive in great complexity and full of nuances, the message conveyed through sound fulfilling the requirement of clinical critical contexts.

Therefore, the optimization of sounds allocation in the design of a digital interface offers enormous potential, especially in the case of interaction with complex products, such as clinical equipment or critical care settings. Thus, existing studies in the literature serve as a reference for the implementation of these approaches, however, they have their complications when applied to practice that concerns us, due to their own idiosyncrasies, requirements and limitations.

This paper states the potential contribution of service design to product sound design, as another methodological approach in order to improve audible alarms and alerts design in healthcare environment. The paper offers designers and engineers possibilities to implement together both the tools and methods of service design and product sound design deriving from the review of existing literature and empirical conclusions compiled from observation and analysis of oncological treatment rooms at different hospitals.

Service design is a specific domain within design engineering focused on how the relationship between service providers and users can be improved [6]. An emerging community highlights the utility of the tools and techniques to effectively include system stakeholders in the design and implementation of health technology and healthcare service design [7]. Service design has been applied successfully in several projects to improve patient experience [8, 9] as well as in other areas of public sector [10, 11]. Following the experience demonstrated in previous studies with service design techniques based on the in situ observation of the work environment and visualization methods and focus group interviews, a proposal for a first phase of study is stated.

2 Service Design and Patient Experience in Healthcare

In the field of research in design, there is an ever wider field for the application of working methods and capabilities of design professionals in non-industrial contexts, and which have not traditionally been addressed from a design perspective. Similarly, the knowledge and good practices from the fields of Design Thinking and Service Design together can help improve services and even innovate new ones based on the analysis of people's experiences in certain contexts or situation [12].

There is also an emerging field of application in the area of healthcare linked to the development and analysis of services. Within the design for health services foreground, projects such as the mourning room for family members of The Vall d'Hebron University Hospital (VHUH), or the Philips Healthcare project that revolutionizes the body scanner experience for children through a playful process in which children learn to scan stuffed animals and understand the process that they will experience later [13]. Another relevant project is the set of services included in Sant Joan de Déu (SJD) Barcelona Hospital, such as the therapy with animals [14], the volunteer service to maintain the school year, or the spaces for internal consultations. All of them are results of projects in which the various design methodologies have been applied to the development of specific cases.

Patient Experience is a complex set of experiences, sensations, emotions, assessments and satisfaction in terms of health care services; it results of the phenomenon of interaction with people and touch points (spaces, equipment, information, among others) that make up this service. Offering experiences patient-centered is considered by various authors [15–17] as a synonym for quality in patient care, problem-solving and a holistic approach based on the set of human values. The American Medical Association proposes the assessment of patient experience as one of the best indicators of the quality of health care. Based on the statements of several authors [18], the working principles of Service Design in health care context could be summarized as follows:

1. People, patients, family members and workers are part of the development of new care solutions and at the center of the design process. Their needs are studied from a mainly qualitative approach through ethnographic techniques, interviews and participatory processes.
2. Projects are addressed in multidisciplinary working groups in which the different agents related to the services identify problems and co-create solutions.
3. Services are studied as a sequence of events, identifying moments of truth and points of improvement.
4. Solutions are prototyped and evaluated constantly during the design process in order to learn from mistakes and improve.
5. A holistic approach is considered that allows a global view of the service in its context and on a larger scale.

This is the conceptual framework of service design; a proposal to address and improve the patient experience.

2.1 Applying Service Design in the Area of Healthcare. Methodology

The service design approach exposed in this communication can be considered as a part of a larger focus oriented in previous experiences carried out in different hospitals that aimed to improve the experience of any oncological patient at different stages of the service, from its diagnosis to the subsequent treatment at the end of the disease. This approach is developed from an action-research methodology already tested [19], in which the medical oncology service acts as a client that has a problem, being the research team through the best design of services who brings the solutions. This proposal is strictly focused on the treatment stage and the main objective is to map and represent the patients' experience in relation to the service. For this, it is necessary to know first-hand the different processes and experiences carried out by the different agents involved (patients, relatives, nurses, oncologists).

The action-research methodology is structured into two groups of actions:

– Actions oriented to know the different views of the stakeholders: in-depth interviews, context observation and focus group interviews. The use of these techniques allows obtaining a series of initial qualitative information for the next actions.
– The following action represents the patient's experience in the oncological treatment room using a customer journey. Customer journey is one of the essential tools in service design; a visualization of the path of a patient through the different touch points of the service [20]. For example, the main stages of a customer journey detected in existing literature related to healthcare services could be the following: consultation of first impact; analytical; request for consultation appointment; consultation of treatment; request of drug treatments; request for treatment appointment; and treatment.

Table 1. Action-research methodology

Action-research methodology		
Action	Stakeholders	Purpose
In-depth interview	Research team, patients and relatives	Patients and relatives insights
Context observations	Research team	Environment and products insights
Focus group interviews	Research team, nurses and medical team	Nurses and medical team insights
Customer journey	Research team	Patient's experience visualization

Within these stages, patients and staff perform different actions that affect the service experience. In addition to these actions, the patient has other interactions with products, spaces and diverse stimuli (sounds, images, etc.) that also have an impact on the perceived quality of care. In this paper, the stated focus is at some point of the treatment stage, and more specifically, on analyze how the sounds of the treatment equipment affect to the patient's experience in particular, and staff work processes in general. Table 1 shows the list of the actions carried out, the stakeholders involved in the action and its purpose:

3 Clinical Approaches to Audible Alarms

Alarm management has been investigated in complex nature environments such as aircrafts piloting, power plants monitoring or autonomous car driving where decision-making processes require very often time-critical responses. Studying these critical scenarios we can conclude several common aspects that are especially relevant to take into account: the differentiation of the alerts according to their urgency level; the criticality of the system events; and the influence in the response time to the stimuli to take the appropriate action (operator response) [21–23].

Clinical alarm management is a subject of study especially in those units that require special care services such as intensive care (ICU) or neonatal intensive care units (NICU), in which several cases of studies and evidences can be found that make it relevant and a real safety concern [24]. Alarms that do not require actions influence on hospital resources, contribute to the alarm fatigue and can affect the quality of patient care. Desensitization can even become a matter of life or death. Alarm fatigue was identified as the main technology hazard for health organizations, and is the focus of the National Patient Safety Goal (NPSG) about the alarm system management of the Joint Commission [25]. "*The Joint Commission now requires that its accredited hospitals to improve their alarm systems, aiming to alleviate the constant barrage of bells and whistles that are often the hallmark of a hospital stay for patients and that contribute to alarm fatigue of healthcare workers*" [26]. Since alarms ranked first in the Emergency Care Research Institute (ECRI) list of Top 10 Health Technology Hazards in 2014 [27], the issue of alarm management is an essential part of patient safety for healthcare organizations.

Usually, these studies are carried out from the perspective of clinicians and more specifically nurses as they are the main operators of clinical equipment, responsible for setting up and responding to device alarms. In this proposal, the patient has been placed at the center of the research, in application of the user-centered-design and service design principles. An unheard, silenced or unattended alarm can have unpleasant consequences for the patient. This situation justifies including a more detailed view of the patient, complementary to the previous ones; observing the perception of the patient, the space that surrounds him/her, the understanding of the monitoring equipment and also his/her concerns and expectations. Since a human centered approach is set as the starting point, service design tools and methods can be very helpful for the team to set up a first observation stage that would be scalable to other studies in the future.

3.1 Sound Experience by Oncological Treatment Rooms (OTR) Users

An oncological treatment room (OTR) is a complex environment with nurses (operators) monitoring different circumstances that can take place simultaneously from different beds (range of events). In the case considered, the treatment is provided by an infusion pump system analogue to the one showed in Fig. 1. The system monitor shows a series of visual indicators and sound warnings about the operation device. This kind of process is carried out based on standards as the Chemotherapy Administration Safety Standards [28].

Fig. 1. Infusion pump system

The observation of patients at the treatment rooms stated that there is a strong emotional implication to them and their relatives at the point of receiving a treatment expected to be very aggressive and full of secondary effects to treat a serious disease. Patients feel sometimes scared and insecure, and lack information about the functioning of a system that automatically delivers the treatment, and that seems extremely complex for them. Such clinical systems are normally provided with a set of audible or visual alarms to inform the nurses of a range of information and malfunctions that, nevertheless, can be observed by the patient, other patients, and their relatives (Fig. 2).

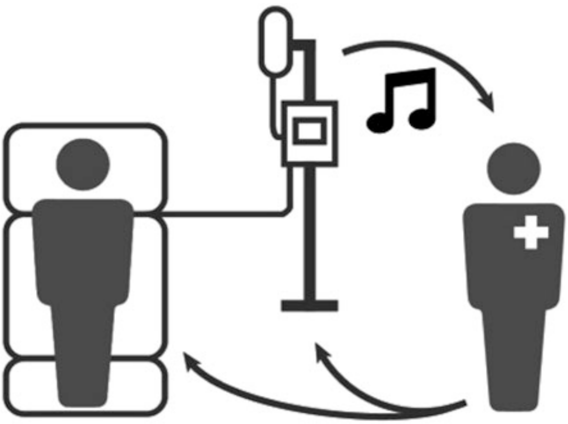

Fig. 2. Oncological treatment system

The set of alarms that surround the patient and operators are summarized in malfunctions and/or operational stage of the device such as the drug programming has been completed (volume to be infused completed or dose end); low battery; and occlusion due to different causes (movement of the patient, tube bent or plugged).

These alarms are medically actionable and represent events for which the nurse has to attend, in order of importance. The nurse needs to do not hear these alarms to understand and be sure that everything is working correctly and by this is getting an overall feedback of the patient's status, being the visual stimulus coming from the monitor insufficient, since she/he is not always in the bedside and is responsible of several patients at the same time, some of them very often located in different rooms with different layouts and occupations, reaching up to seven seats per room in some of the cases observed (Fig. 3).

Every nurse is responsible of several patients at the same time, being very often some of them located in different rooms with different layouts and level of occupation (reaching up to seven beds per room in some of the cases observed, Fig. 3). Since the nurse is not always in the bedside, the visual stimulus coming from the monitor is insufficient, and so these alarms are dedicated to provide an overall feedback of the patient's status, so if none alarm is perceived, the nurse understands that everything is running correctly.

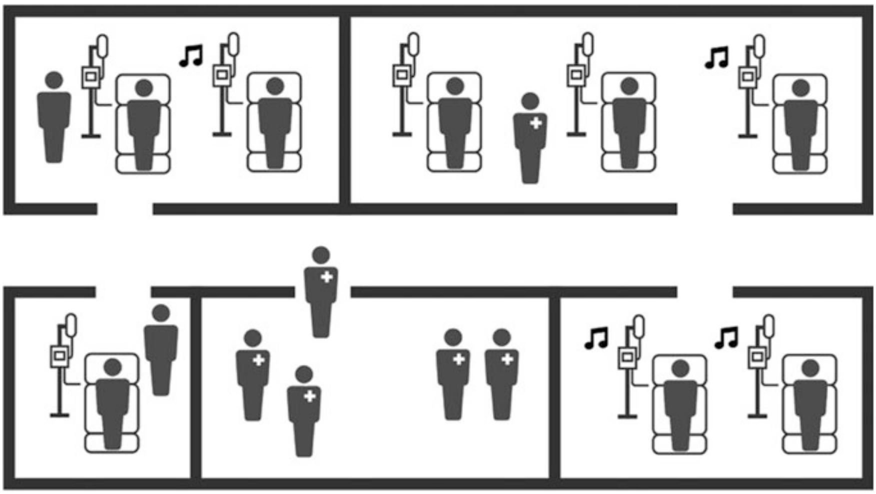

Fig. 3. Oncological treatment room layout

These alarms can refer to different events caused by system failures or monitor disconnection, due for example to the movement of the patient. However, auditory alarms are not hierarchical to communicate a series of system events (malfunction vs the drug is over), but a generic alarming sound is used for all messages, without any difference. That is, the alarm does not represent different circumstances that are really happening to the patient. Another problem is caused because all units, assigned to different patients even on different rooms are identical, and so are their alarms, so the nurses need to identify the origin of the alarm just by ear. While the patients are receiving their treatment at certain rooms, the nurses are located normally at a different facilities, and the current systems do not count on any remote alarm or warning system, so nurses need to hear the alarm from a point located apart. Several patients are treated at the same time so several alarms can happen at any time, causing alarm fatigue on nurses, while anyway can expect some colleague to respond to any alarm, causing also at certain moments some lack of perceptual concentration.

As a result, patients and their relatives are the first to listen to the alarm informing that some unidentified problem occurs, but it can take a while until the alarm is attended by nurses. This causes an unnecessary stress on patients that can affect somehow to the success of the treatment and that has a negative influence on the experience of the service provided. Also affects to their relationship with nurses and can produce some conflicts such as relatives demanding attention to nurses that did not noticed that some event required their attention.

Thus, a systematic service design approach is proposed to identify potential improvements for the design of auditory information provided by this units, bearing in mind a closer approach to the context of OTRs, that requires it to be tailored to suit both the needs of the operators and users (health staff, patients and in some cases family) identified at the service design research and analysis stages. [29–31]. This proposed project to be developed can take into account more experiences and service design analysis at some other hospitals in order to make it universal, and/or take into consideration some analogue experiences coming from the field of service design and/or sound design at different areas. A promising example of this is the project CareTunes, a concept that challenges the clinical utilization of audible alarms (beeps) of monitoring devices found in Intensive Care Units (ICUs) and developed it as a musical streaming of patient vital signs in critical care [32].

4 Conclusions

From a first phase of observation at different hospitals, the potential of improvement in the design of the auditory signals provided by oncological treatment systems is detected. Existing literature evidences the high potential of these procedures in the improvement of critical context such as (but not only) healthcare units and at different stages. By means of service design tools application a qualitative study could be carried out to identify chances for reviewing alarms functioning, in order to improve the overall experience of the system by the patients.

In the proposal presented, the aim of service design is to provide specific insights, design specifications and recommendations for product sound designers and engineers. Qualitative observation sessions, focus group interviews and in-depth interviews seem to be especially useful to highlight insights about the routines and key activities of a nurse day work but also and more important, about the experience of patients during their 5 h treatment. The proposal exposed illustrates how some easy-to-carry service design tools can provide high valuable knowledge able to produce technical engineering and design specifications, obtaining high potential results at low project costs.

Because the work sequence proposed is based on the analysis of certain aspects common to other hospital services, the project to be developed in an oncology service is easily replicable and scalable to other areas, and further experiences can provide future lines of study and learning.

References

1. Joseph A, Ulrich R (2007) Sound control for improved outcomes in healthcare settings. Center for Health Design, Concord, CA
2. Excellence BP (2013) The Joint Commission announces 2014 national patient safety goal. Joint Commission Perspectives
3. ECRI Institute (2014) The alarm safety handbook: strategies, tools, and guidance. ISBN: 0981924174. https://www.ecri.org/components/Pages/Alarm_Safety_Handbook.aspx. Last accessed 10 Jan 2018
4. AAMI Horizons (2011) Alarms pose challenges to healthcare facilities. Horizons. https://s3.amazonaws.com/rdcms-aami/files/production/public/FileDownloads/Horizons/Alarms_Pose_Challenges_5.pdf. Last accessed 10 Jan 2018
5. Johnson KR, Hagadorn JI, Sink DW (2017) Alarm safety and alarm fatigue. Clin Perinatol 44(3):713–728
6. Griffioen I, Melles M, Stiggelbout A, Snelders D (2017) The potential of service design for improving the implementation of shared decision-making. Des Health 1(2):194–209
7. Williams I (2016) Travelling an unfamiliar road: implications for the entry of design practitioners into healthcare. Queensland University of Technology, Diss
8. Tsianakas V, Robert G, Maben J, Richardson A, Dale C, Wiseman T (2012) Implementing patient-centred cancer care: using experience-based co-design to improve patient experience in breast and lung cancer services. Support Care Cancer 20(11):2639–2647
9. Stacey PK, Tether BS (2015) Designing emotion-centred product service systems: the case of a cancer care facility. Des Stud 40:85–118
10. Service Design Impact Report (2016) Public sector. ISSN 1868–6052. https://www.service-design-network.org/uploads/sdn-impact-report_public-sector.pdf. Last accessed 10 Jan 2018
11. Service Design Impact Report (2018) Health sector. https://www.service-design-network.org/headlines/service-design-impact-report-health-sector. Last accessed 10 Jan 2018
12. Brown T (2009) Change by design
13. KittenScanner (2018) Involving kids in their own care. https://www.90yearsofdesign.philips.com/article/30. Last accessed 28 Jan 2018
14. SJD Barcelona Hospital (2018) Pet-assisted interventions. https://www.sjdhospitalbarcelona.org/en/pet-assisted-interventions. Last accessed 28 Jan 2018
15. Edvardsson D, Winblad B, Sandman PO (2008) Person-centred care of people with severe Alzheimer's disease: current status and ways forward. Lancet Neurol 7(4):362–367
16. McCormack B (2004) Person-centredness in gerontological nursing: an overview of the literature. J Clin Nurs 13(s1):31–38
17. Mead N, Bower P (2000) Patient-centredness: a conceptual framework and review of the empirical literature. Soc Sci Med 51(7):1087–1110
18. Stickdorn M, Schneider J, Andrews K, Lawrence A (2011) This is service design thinking: Basics, tools, cases (vol 1). Wiley, Hoboken
19. Coghlan D, Brannick T (2014) Doing action research in your own organization. Sage
20. Koivisto M (2009) Frameworks for structuring services and customer experiences. Designing services with innovative methods, pp 136–149

21. Sousa B, Donati A, Özcan E, van Egmond R, Jansen R, Edworthy J, Voumard Y (2017) Designing and deploying meaningful auditory alarms for control systems. In: Space operations: contributions from the global community (pp 255–270). Springer International Publishing
22. Kristensen M, Edworthy J, Özcan E (2017) Alarm fatigue in the ward
23. Baldwin CL, Lewis BA (2014) Perceived urgency mapping across modalities within a driving context. Appl Ergon 45(5):1270–1277
24. Freudenthal A, Van Stuijvenberg M, Van Goudoever JB (2013) A quiet NICU for improved infants' health, development and well-being: a systems approach to reducing noise and auditory alarms. Cogn Technol Work 15(3):329–345
25. Joint Comission (2017) National patient safety goals effective. Hospital Accreditation Program. https://www.jointcommission.org/assets/1/6/NPSG_Chapter_HAP_Jan2017.pdf. Last accessed 28 Jan 2018
26. Philips Healthcare (2018) Hospital alarm fatigue. Alarm management strategies to achieve national patient safety goal compliance. https://www.usa.philips.com/healthcare/articles/alarm-system-management/alarm-management-strategies. Last accessed 28 Jan 2018
27. ECRI (2014) ECRI institute top 10 health technology hazards report for 2014. http://www.ormanager.com/wp-content/uploads/2015/01/0215_ORM_15_ECRI-Institute-Perspectives.pdf. Last accessed 27 Jan 2018
28. Marcela DFE, Sylvia GNE, Carlos LCEJ, Aracely TME (2013) Enfermería oncológica: estándares de seguridad en el manejo del paciente oncológico. Revista Médica Clínica Las Condes 24(4):694–704
29. Sowan AK, Tarriela AF, Gomez TM, Reed CC, Rapp KM (2015) Nurses' perceptions and practices toward clinical alarms in a transplant cardiac intensive care unit: exploring key issues leading to alarm fatigue. JMIR Human Factors 2(1)
30. Kitzinger J (1995) The methodology of focus groups: The importance of interaction between research participants. Sociol Health Illn 16:103121
31. Kitzinger J (1995) Qualitative research: Introducing focus groups. BMJ: Br Med J 311:299302
32. Bogers K (2018) CareTunes: music as a nurses' monitoring tool. Master thesis. Delft University of Technology

Form and Function: Functional Optimization and Additive Manufacturing

L. Barbieri(✉), F. Calzone, and M. Muzzupappa

Department of Mechanical, Energy and Management Engineering (DIMEG), Università della Calabria, Rende, (CS) 87036, Italy
loris.barbieri@unical.it

Abstract. In these last years, with the advent of Additive Manufacturing, a deep review of the design methodologies has occurred. This is mainly due to two reasons: the technological progress and the new manufacturing capabilities that offer designers much greater freedom for the creation of complex geometries; the modern engineering optimization tools that are spreading widely in the industrial design field, and offer new opportunities for searching a compromise between form and function. On the basis of these two reasons, the paper presents some reflections and exemplifications on the changes that new AM technologies, together with the optimization tools, are bringing in the design process.

Keywords: Additive manufacturing · Design theory and methodology · Topology optimization

1 Introduction

In the product design, the antinomy between form and function has always existed, a long-running diatribe that has been over-simplified and polarized into the atavistic quarrel between architects and engineers.

This antinomy arises from the fact that the form belongs to the perceptible unmeasurable world, whereas the function to the rational measurable one. While the form addresses the aesthetic, perceptive and emotional expressions, on the contrary, the function refers to the rationality, technique, and performance.

In the industrial design field, this dichotomy never existed: form and function have always been of equal relevance and importance, and from antithetical become complementary terms. In the development of design products, in fact, form and function are tightly related and closely interlinked to each other. This is demonstrated by the fact that successful industrial products on the international market feature both high aesthetic and functional qualities.

Although the ultimate goal of designers is to achieve an optimal balance between form and function, the design process is affected by the instruments and tools that support designers' work and by their experience and consolidated knowledge. In fact, the tools and systems, traditionally adopted in the design process, on the one hand, support and simplify the designer work, but, on the other hand, could influence the design process and put some limits to the designers' creativity. This is quite evident in the traditional design process, which starts with the definition and modeling of the

F. Cavas-Martínez et al. (Eds.): *Advances on Mechanics, Design Engineering and Manufacturing II*, LNME, pp. 649–658, 2019.
https://doi.org/10.1007/978-3-030-12346-8_63

geometry of the product, and follows with its functional analysis and technical feasibility. Then, as far as form and function have the same importance, in the practice, products are developed with function as a primary consideration but according to a form-to-function approach. As above mentioned, this is essentially due to the tools and systems that support designers' work which require a geometric model to proceed with the functional simulation and analysis.

On basis of the abovementioned considerations, it is quite evident how Additive Manufacturing (AM) represents a radical change not only from a technological point of view but also because it enables designers to rethink the overall product development process and revolutionize their approach to design.

Although AM was originally referred to a novel class of manufacturing processes for rapid prototyping applications, it has rapidly evolved in flexible and reliable technologies for end-use part production and tooling a variety of materials, including metals. This has been an industrial breakthrough in manufacturing technology thanks to its capabilities to overcome the technological limitations and constraints imposed by conventional manufacturing techniques.

In the last few years, in response to the development of AM techniques, a variety of design theories and methodologies (DTM) based on AM has emerged, therefore entailing and supporting a smooth transition from Design for Manufacturing (DfM) to Design for Additive Manufacturing (DfAM). The AM revolution, in fact, on the one hand, has led to a greater freedom and a higher number of solutions in the product design. But, on the other hand, it required both a radical re-think of the current best practices for product design and the development of new design paradigms [1].

On this subject, the paper presents some reflections and exemplifications on the changes and implications that the new AM technologies, coupled with the engineering optimization tools, are bringing in the product development process. In fact, its huge capabilities open up a multitude of potential design approaches, ranging from traditional ones to completely new methods and techniques. In this regard, starting from the current DfAM concept and definitions, two radically different design approaches are discussed. The first one focuses on designers' creativity and their greater freedom for the creation of complex geometries that were unimaginable before the advent of AM. The AM technologies, in fact, encourage designers and engineers to go beyond the conventional thinking tailored to the capabilities of traditional manufacturing methods and push them toward a "*form-driven design*" approach that unlocks their imagination for creating innovative designs. On the other hand, the second one exacerbates the "*function-driven design*" approach by focusing on the functional properties of the product and postponing a detailed and accurate definition of the geometry in the last stages of the design process.

2 Traditional Method

Design methodologies and tools provide an effective way to rationalize the design and production processes, foster and guide the abilities of designers, encourage creativity, and at the same time drive home the need for objective evaluation of the results. Thanks to these methods it is then possible to structure the design activities in a purposeful way that forms a clear sequence of main phases and individual working steps so that the flow of work can be planned and controlled. According to a traditional design approach, the design process consists of three main phases: concept design, embodiment design, and detail design.

As above mentioned, designers then start a design process by defining design goals and planning a sequence of activities and tasks that, in practical terms, are influenced by the tools and instruments that they use. In fact, the tools and systems, that are traditionally adopted in the design process, on the one hand, support and simplify the designer work, but, on the other hand, prioritize some activities and goals that drive design creativity.

The following Fig. 1 shows the traditional design method as it evolves from the concept to the physical prototyping stage. In order to verify the functionality and feasibility of the product, the CAx tools require a geometry as input. This entails that the design process starts in the conceptual stage by developing the functional specification, over the user needs, that are then immediately translated into geometric shapes by means of a CAD system.

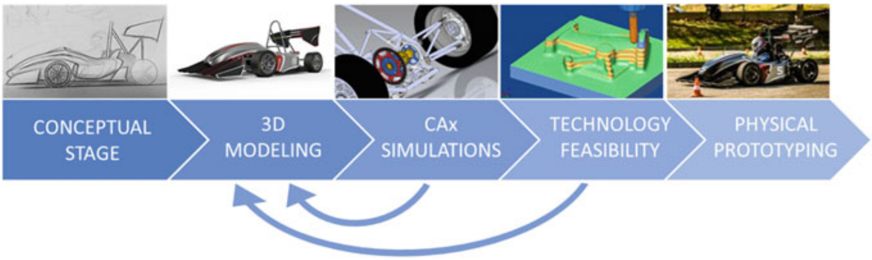

Fig. 1. Traditional design approach

On the basis of these considerations, it is possible to agree on two points. Firstly, the traditional approach starts by working on the geometry in order to give form to a function. Secondly, the iterative process that occurs between the modeling stage and the simulation analysis is crucial for the development of a successful product that puts the emphasis both on the aesthetical and functional aspects.

3 Design for AM

Because of the technical and economic properties of a product, and the commercial importance of timely and efficient product development, it is of fundamental importance to have a well-defined design procedure that guides and supports designers to find optimum design solutions by addressing the given design requirements and manufacturing constraints.

The AM revolution has led to a rethinking of the current design best practices and the development of new design paradigms [1]. Furthermore, in order to get the maximum benefit from the potentials offered by AM technologies, a natural paradigm shift has occurred from DfM to DfAM.

The purpose of DfAM is a "synthesis of shapes, sizes, geometric mesostructures, and material compositions and microstructures to best utilize manufacturing process capabilities to achieve desired performance and other life-cycle objectives" [2]. DfAM is the set of methodologies and tools that help designers to take into account the specificities of additive manufacturing (technological, geometrical, pre/post-processing, etc.) during the design stage [3].

Graziosi et al. [4] highlight (through the description of the re-design activity performed using the software tools currently available on the market) the number of heterogeneous aspects that need to be taken into account when designing for AM in order to fulfill all the functional, technical and manufacturing requirements. The aim is to use the acquired experience to reflect on the possible strategies to put in place for a better synthesis of the functional and process-based aspects.

In [5], the authors propose a complex DfAM framework for designing end-use components and products. The proposed framework has been developed on the basis of information collected by means of personal interviews occurred with designers and AM professionals that have great experience in product design oriented to AM.

Particularly significant are the works that show topology optimization (TO) applications in the AM field. In [6] the authors present two customer cases with the goal of redesigning existing products for manufacture with SLM. In [7], a benchmark design framework for assembly level DfAM that utilizes functional integration, part consolidation, and design optimization is also proposed. Doutre et al. [8] compare different possible approaches to generate a CAD model from topological optimization analysis results. An exhaustive bibliography of AM-related structure design optimization methods is presented in [9]. In this paper, the authors classify DfAM research studies in two categories: the first one focuses on DfAM methodologies that define comprehensive and systematic design frameworks oriented to the concept of combining functional requirements and manufacturing constraints in an AM-related design; the second one sticks to the scope of AM-enabled structure optimization design methods in terms of shape optimization, size optimization, and topology optimization.

4 Some Considerations About DfAM

In [9], the authors affirm that "manage design and represent design knowledge is affected by the no-tooling and sustainable manufacturing way", in other words, the new CAx systems, introduced by AM, enable designers to rethink the overall design process and revolutionize the traditional approach.

Starting from the classification proposed by Yang and Zhao [9], it is possible to reprocess the design methodology elaborated by Pahl and Beitz [10] on the basis of two completely different design approaches. The first one focuses on the greater freedom offered by AM technologies to designers for the creation of more complex geometries when compared to with traditional manufacturing processes (milling cutting, forming, casting process). The main difference resides in the fact that in traditional manufacturing processes shaping of materials takes place across the entire physical domain of the desired part whereas in AM processes the shaping of material primarily takes place in the formation of elementary elements (voxels, filaments, and layers) [11]. In this case, the impact of AM in the design process is reflected in the design considerations for aesthetic, manufacturing, assembly, and performance.

The second design approach focuses on the functional optimization. In this regards, the traditional design approach undergoes a substantial modification because the definition of the geometry is demanded primarily to the optimization tools and no longer to the designers.

4.1 Technological Optimization

The difficulty of defining, with simplicity and unambiguity, a DfAM approach related to the optimization of the technological process is mainly due to the large number of AM technologies currently available on the market, each of which requires to satisfy specific geometric and technological constraints.

Even if AM techniques allow high degrees of customization of the geometry with little impact on manufacturing constraints, complexity and cost [11], evidence dispelling the myth that everything is possible with AM.

In any case, whichever shall be the AM technology adopted, the designer will conceive the product in a new and different manner. In fact, there is no more an initial volume from which removes material, but a void to fill with creativity.

Ponche et al. [12] proposed a global approach aiming at defining part shapes subjected to the manufacturing process and functional requirements. In their research, functional specifications and AM process characteristics were directly combined at the early stage. This is because the choice of manufacturing direction and manufacturing trajectories, as well as manufacturing volume, microstructure, geometry, and manufacturing time, are the keys for a good DfAM [9].

In practice, in a design approach oriented to the AM, the designer has to learn to think about the product differently than he/she is used to with the traditional approach because he/she must take proper account of the 3D printing technology to adopt and its related technological and manufacturing constraints.

If compared to the traditional design method, a DfAM approach oriented to the optimization of the technological process entails two peculiarities:

1. it gives value to the designer’s creativity and imagination. In fact, AM enables the building of highly complex shapes, multiple parts in one piece and functionally integrated objects. It allows also to improve product’s performances by designing complex shapes for the inner geometries.
2. There is a change of position between technology and functional feasibility stages (Fig. 2). This is mainly due to the lack of knowledge of the designers on the potentials and limits of the 3D printing processes, and, at the same time, to the freedom left to them in conceiving the shape of the product.

These two aspects, strongly correlated with each other, entail the necessity for a continuous checking of the feasibility of the product by means of AM, with the consequence that the technical feasibility appears earlier in the design method.

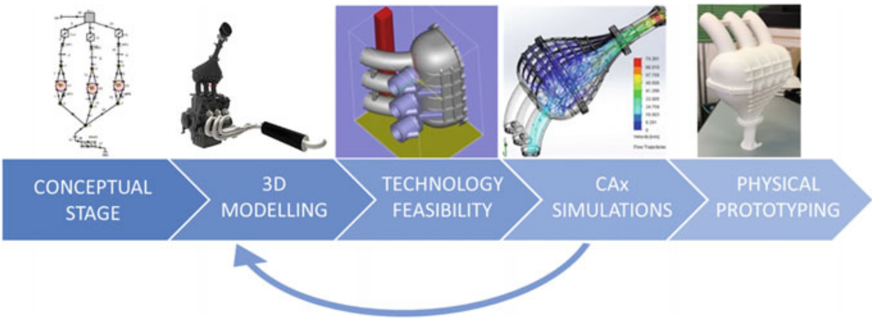

Fig. 2. Technological optimization approach

4.2 Functional Optimization

The optimization methods can be classified into two groups based on the predictability of the inner topology. If it is unpredictable, this type of optimization method is defined as a passive optimization; otherwise, it is called positive optimization [9]. Passive optimization methods include shape optimization, size optimization, and topology optimization. For a positively optimized part, its topology is usually in hierarchical patterns, such as lattice structure.

In literature, there is an extensive bibliography that proposes AM-enabled structure optimization design methods in which the functional optimization of the part is entirely focused on the function, carrying to the extreme the function-driven design approach. In fact, by adopting a functional optimization approach (Fig. 3), the optimization tools are the only responsible for defining the geometry that is determined on the basis of the functional requirements defined in the conceptual stage. Then, according to this approach, the form of the part is not the result of the designers' creativity, that requires simulation analysis in order to be approved for the production, but is the direct result of the functional optimization that may not require subsequent modifications because of the manufacturing capabilities provided by the AM technologies.

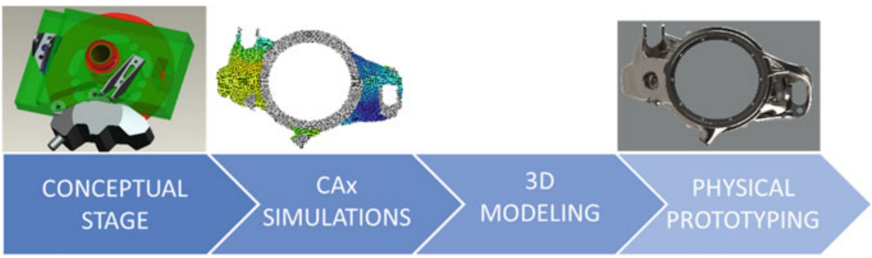

Fig. 3. Functional optimization approach

This is made possible thanks to two main reasons. First, 3D printing processes do not require binding manufacturing constraints. The second reason is related to an aesthetical evaluation of the geometries obtained as result of optimization analysis. In this regard, the literature presents many studies in which the geometries, outcomes of functional optimizations, are characterized by very particular shapes that could easily meet the aesthetic canons that leads to the definition of "beauty".

To sum up, according to a functional design approach, in the first conceptual stage designers define the functional requirements on the basis of which the functional surfaces of the product are established. These data are then elaborated by means of CAx tools that provide the optimal shape in terms of the goals and constraints imposed in the simulation. If on one side this approach would seem to exclude the contribution of the designer about the aesthetics of the product, on the other side it offers a new perspective on the development of new design forms.

4.2.1 Topology Optimization Analysis

Before the effective introduction and spread of the AM technologies in the industrial field, topology optimization analysis required an intensive and significant intervention of designers and engineers both for interpreting the analysis results and for managing the optimized geometry data used as input for the redesign of the product. To this end, some studies [13–15] have investigated these issues, due to the poor integration between topology optimization tools and CAD systems, by proposing methods and guidelines that facilitate the interpretation and extraction of useful geometrical information from the results of the topology optimization analysis, and support and simplify the geometric model redesign.

The necessity to redesign the optimized geometries, in order to obtain a feature based manufacturable product model, has been overcome thanks to the AM technologies. In fact, as above mentioned, AM offers the unique ability to fabricate incredibly complex geometries with organic shapes. Then the optimized geometries could be manufactured immediately without the necessity to import these geometries in the CAD system for further refinements. In this regard, the following Fig. 4 depicts some case studies in which topology optimization results have been fabricated by means AM technology as they are, without any intervention of the designers on the geometry of the parts.

It is worth to notice that in the examples depicted in Fig. 4, the designers have decided to print the results of the optimization analysis on purpose, in order to emphasize the "functional aesthetics" of the parts. In this way, the 3D modeling stage, usually adopted for the redesign of the optimized geometry, is then entirely skipped to switch directly on the prototyping stage.

Therefore, the re-design of the optimized model is at the discretion of the designer that may import the results of the optimization analysis into the CAD system in order to refine the geometry for an efficient fabrication via AM or simply to enhance its aesthetics. But, in any case, the geometry of the part is highly dependent on the function it has to fulfill.

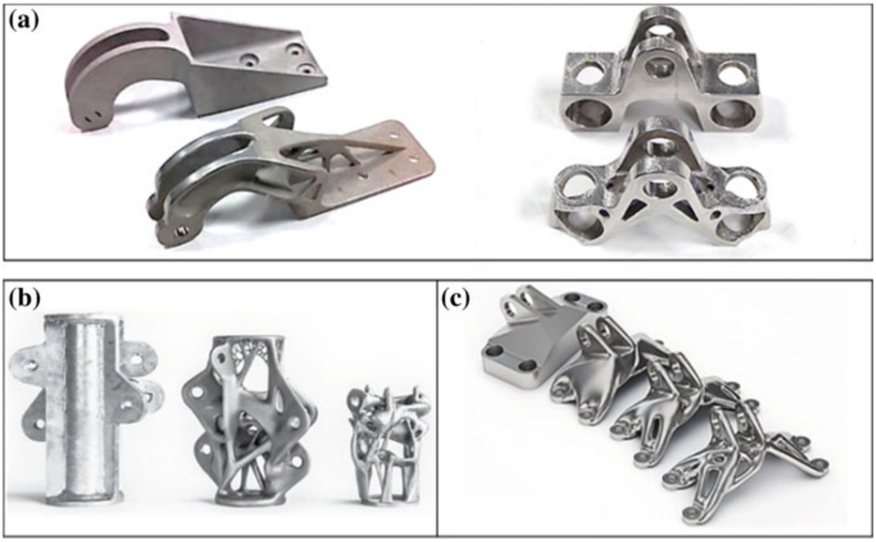

Fig. 4. Traditional design compared to optimized parts manufactured with to 3d printing technologies: **a** metal parts for aerospace field [16]; **b** element optimized with generative design [17]; **c** design topology optimization [18]

4.2.2 CFD Analysis

An interesting alternative to the function-driven approach based on topology optimization tools has been studied in a thesis work [19] carried out in collaboration between the University of Calabria and the Bochum University of Applied Sciences. The research focused on the functional optimization of a valve manifold block for hydraulic actuator (Fig. 5a) performed by means of CFD (Computational Fluid Dynamics) analysis. In particular, the CFD analysis has been carried out for calculating the optimal flow path with least pressure drop and highest average velocity (Fig. 5b). These results have been used as guidelines for the modeling of the geometry of the manifold, and for defining the loading conditions of the structural simulation processed on this geometry. Subsequently, the design has been refined for efficient production via AM in order to use the least material possible while avoiding building support structures in non-machinable features of the manifold (Fig. 5c).

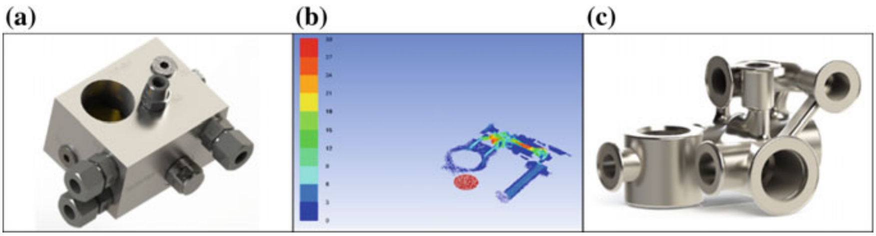

Fig. 5. **a** Initial design of the manifold block; **b** CFD analysis; **c** final design of the manifold block manufactured by means SLS technology [19]

Also, in this case, the tool adopted for the functional optimization, i.e. CFD analysis, defines the final geometry of the component that is then manufactured by means of AM technology without the need for designer interventions.

5 Conclusions

After many years of using consolidated methodologies and tools, the advent of AM has revolutionized the way of thinking about the product resulting in a reinvention of the design process. The paper has presented two different design approaches oriented to the AM fabrication of the product. The first approach focuses on the much greater freedom for the creation of complex geometries. The second one concerns with the optimization tools that allow designers to focus on the product's function thus relegating a detailed and accurate definition of the geometry in the last stages of the design process.

The two different design approaches discussed in the paper invites the reader to reflect on the tight relation that occurs between design methods and instruments and how it could evolve. If on one hand CAx instruments are traditionally conceived as tools that support and facilitate the practical implementation of design methods, on the other hand, we are assisting to the introduction and improvement of design tools, specifically developed to make more efficient AM technologies, that could influence and stimulate engineers to rethink and change the design process and then bring to the emergence of new design methods.

References

1. Sossou G, Sossou G, Demoly F, Montavon G, Gomes S (2018) An additive manufacturing oriented design approach to mechanical assemblies. J Comput Des Eng 5:3–18
2. Rosen DW (2007) Computer-Aided Design for Additive Manufacturing of Cellular Structures. Comput-Aided Des Appl 4(5):585–594
3. Laverne F, Segonds F, Anwer N, Le Coq M (2014) Dfam in the design process: a proposal of classification to foster early design stages. In: Proceedings of the Conference 2014, Croatie
4. Graziosi S, Rosa F, Casati R, Solarino P, Vedani M, Bordegoni M (2017) Designing for metal additive manufacturing: a case study in the professional sports equipment field. In: Proceedings of the 27th international conference on flexible automation and intelligent manufacturing, pp 27–30, Italy (2017)
5. Zhu Z, Pradel P, Bibb R, Moultrie J (2017) A framework for designing end use products for direct manufacturing using additive manufacturing technologies. In: Proceedings of the 21st international conference on engineering design (ICED17), Vol 5, pp 327–336, Canada
6. Komi E (2014) Design for additive manufacturing. Research report, VTT-R-03159–16
7. Yang S, Tang Y, Zhao YF (2016) Assembly-level design for additive manufacturing: issues and benchmark. In: Proceedings of ASME 2016 international design engineering technical conference and computers and information in engineering conference
8. Doutre PT, Morretton E, Vo TH, Marin P, Pourroy F, Prudhomme G, Vignat F (2017) Comparison of some approaches to define a CAD model from topological optimization in design for additive manufacturing. Adv Mech Des Eng Manuf 233–240. (Springer, Cham)

9. Yang S, Zhao YF (2015) Additive manufacturing-enabled design theory and methodology: a critical review. Int J Adv Manuf Technol 80:327–342
10. Pahl G, Beitz W (2013) Engineering design: a systematic approach. Springer Science & Business Media
11. Yang L, Hsu K, Baughman B, Godfrey D, Medina F, Menon M, Wiener S (2017) Additive manufacturing of metals: the technology, materials, design and production. Springer, Schwitzerland
12. Ponche R, Hascoet JY, Kerbrat O, Mognol P (2012) A new global approach to design for additive manufacturing. Virtual Phys Prototyp 7(2):93–105
13. Barbieri L, Bruno F, Cugini U, Muzzupappa M (2008) Design Automation tools as a support for knowledge management in topology optimization. In: Proceedings of the ASME 2008 international design engineering technical conferences & computers and information in engineering conference, New York
14. Muzzupappa M, Barbieri L, Bruno F (2011) Integration of topology optimisation tools and knowledge management into the virtual Product Development Process of automotive components. Int J Prod Dev (IJPD) 14(1–4):14–33
15. Barbieri L, Bruno F, Muzzupappa M, Cugini U (2010) Methodology and tools to support knowledge management in topology optimization. J Comput Inf Sci Eng (JCISE). ASME publications 10(4), Art. n. 044503
16. https://www.3ders.org/articles/20150606-northwestern-university-study-confirms-3d-printed-metal-parts-help-reduce-aircraft-weight.html. Last accessed 01 May 2018
17. https://www.protocam.com/learningcenter/blog/generative-design. Last accessed 01 May 2018
18. https://3dprint.com/169436/a-few-questions-for-frustum. Last accessed 01 May 2018
19. Alshare AA, Calzone F, Muzzupappa M (2018) Hydraulic manifold design via additive manufacturing optimized with CFD and fluid-structure interaction simulations. Rapid Prototyp J

New Bottling Machine for Different Glass Jar Geometries in Continuous Processes

F. Cateura, J. S. Velázquez-Blázquez(✉), F. Cavas-Martínez, D. Parras-Burgos, F. J. F. Cañavate, and J. Nieto

Department of Graphical Expression, Technical University of Cartagena, C/Doctor Flemming s/n, 30202 Cartagena, Spain
jose.velazquez@upct.es

Abstract. One of the main problems that exist nowadays in agri-food industries, is making more flexible production lines in continuous bottling processes, regarding different geometries and sizes of glass receptacles (cap/bottle). Present communication analyses different commercial solutions that exist nowadays in the market, and basing on one of them, proposes a bottling machine that allows modifying its electro-mechanical bottling capacity in continuous processes for different glass container formats. This innovative machine concept will allow working continuously with three types of glass jars, depending on customers' demands, reducing delay ratio derived from this kind of machines, associated with manual accessory change needed to adapt machine to the size of the container.

Keywords: Innovation design · CAD/CAM · Process automation · Flexible manufacturing · Bottle capping

1 Introduction

There is a great variety of machines in industries that are used in lines for processing and bottling of products that show flexibilization shortcomings when integrated in continuous bottling process lines [1]. This is why innovation at conceptualizing a new machine must be based in adaptability and versatility towards new productive demands parameters, without leaving apart its efficiency and lifespan [2–5]. In this regard, some authors [6] highlight the necessity of proposing design strategies in which manufacturers increasingly consider client needs during use phase in their design process, as a way of getting new customers.

And it is right there where this work focuses; more precisely in agri-food industry, where preserves closing machines play an important role when it comes to slowing down and/or speeding up bottling process depending on geometries and sizes of bottles. In these cases, one of the most efficient solutions is using a flexible machine, in which different formats can be fitted whilst maintaining or augmenting the number of closed bottles per minute.

Some of the machines available nowadays in the market, show a series of problems that affect their performance, such as having the tap feeder box located at a high height (see Fig. 1), or problems of contact with relief-less caps that lead to defective closings [7].

F. Cavas-Martínez et al. (Eds.): *Advances on Mechanics, Design Engineering and Manufacturing II*, LNME, pp. 659–669, 2019.
https://doi.org/10.1007/978-3-030-12346-8_64

Other commercial models suffer from functional rigidness that prevent them of adapting to different receptacle sizes, showing also a small sized cap feeder box.

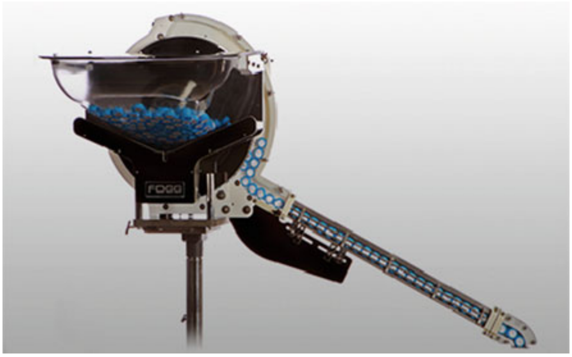

Fig. 1. Rotational cap filler [7]. Refilling is uncomfortable due to its height

There are other machines that allow adaptation to container format, perform a controlled close by torque limiter, and count with a cap feeder with hopper at a certain level, that improves filling comfort. However, these designs present two problems: firstly, they suffer from important wear of torque limiter, which reduces its precision progressively and shortens its service life, and secondly, their higher cost compared with other machines.

2 Objectives

In this communication, the design and modelling of a new concept of glass jar bottling machine is proposed. To do so, starting from a real machine and under its manufacturers demand, redesign has been made aiming to:

- Augment its production from fifteen closed jars per minute to 30 closed jars per minute.
- Improve precision of hermetic closing of receptacles.
- Improve machine's flexibility and reduce closing and adjusting times when using different geometries of caps and bottles.

Furthermore, the following secondary objectives has been stablished:

- Improving elevator's functionality, making it more rigid and modifying its design concept to use just one motor instead of the three used now.
- Modifying bottle-fixing clamp's geometry so it fits any kind of bottle.
- Implementing an auxiliary table at the end of the transport line so bottles can be picked up by user.
- Implementing a new double rod pneumatic cylinder to avoid possible turns of fixing clamp, hitting or damaging bottles.

- Implementing a ball detent torque limiter to adjust closing with precision and thus limiting wear by friction and progressive imprecision.
- Stiffening caps line and improving alignment system up to actuator.
- Implementing a fast fixing and easy access mandrel for new actuator.

3 Materials and Methods

From agri-food productive sector and very different technological areas, innovation has been made by means of several working methods in the field of development of new products with a common objective: stablishing them according to a repeatable and traceable scheme, with the aim of obtaining better finished products for final users [5]. Many of these development methods have generated tools that hold a great potential in aiding design professionals when planning their activities, catching their clients wishes and needs, searching for information, detecting problems or finding solutions [3]. In this scenario, two stages have been defined [8].

Strategic Definition: in this stage, a thorough analysis of existing problems of a commercial model in a real factory environment has been done, jointly with machine manufacturer.

Concept Design: in this stage, technical solutions that improve design have been proposed, and later modelled using CAD/CAM design software. Furthermore, due to machine vast size, it has been split into sub-assemblies to allow focusing attention in each of its components' details, and later making an overall analysis of the whole machine collecting all relevant descriptions of each sub-assembly. Considered sub-assemblies has been: elevator, cap feeder line, actuator, table-chassis, protection frame and transport line.

3.1 Software Used, and Rules, Regulations and Standards Followed

For the design, modelling and later calculation of every component of the machine, SolidWorks 2017 software has been used, while CES EduPack 2010 has been the software chosen for selecting the machine's materials.

In addition, during design and later fabrication processes, European Union standards [9–11], national standards [12] and UNE-EN-ISO standards [13–15] were followed.

4 Results and Discussion

As it has been mentioned before, machine design has been considered in several sub-assemblies.

4.1 Elevator

Main problems detected during Strategic Definition stage and adopted solutions in Design Stage have been described in Table 1.

Table 1. Elevator problems summary

Concept	Problem description	Adopted solution
Cap stirring motor	A motor is required to stir up caps and push them towards magnetized conveyor belt	Using a magnetized conveyor belt with its segments forming a 30° angle with horizon line, that allows avoiding the use of two motors, and problems of cups stuck in cap selector duct
Motor for removing stuck caps	A motor linked with two pulleys through a plastic rope is needed to remove stuck cup with friction	
Entrapment/jamming of cap selector	Several times, when cap selector diverts the cap to the duct that leads to the hopper, it gets stuck in the borders of the metal plate	
Hopper	Hopper dimensions are limited	Increase in hopper dimensions
Mounting and calibration of elevator	Mounting and calibration of return duct for caps and vertical guides	Removal of vertical guides and return duct for caps
Stiffening of the machine	Swinging problems in elevator due to its great height, causing misalignment in actuator	Elevator chassis improvement by adding a stand at middle height with its base on the protection framework

Figure 2 shows original design of cap elevator versus the refined design one.

4.2 Cap Feeder Line

In Strategic Definition stage, the main problem detected has been the motor that feeds caps towards actuator, provided that its size is excessive, and it surpasses line width, colliding with the protective framework. Also, protective carcass of this motor, due to its great volume, usually collides with the bottles of greater height.

As a solution to this problem in Concept Design stage, it has been proposed to replace original motor by a reduced size and lower energy consumption one. To do so, a step-by-step direct current motor has been selected, with a consumption of one Ampere instead of two. Figure 3 shows the result of final refined design for the cap feeder line.

4.3 Actuator

Main problems detected during Strategic Definition stage and adopted solutions in Design Stage have been described in Table 2.

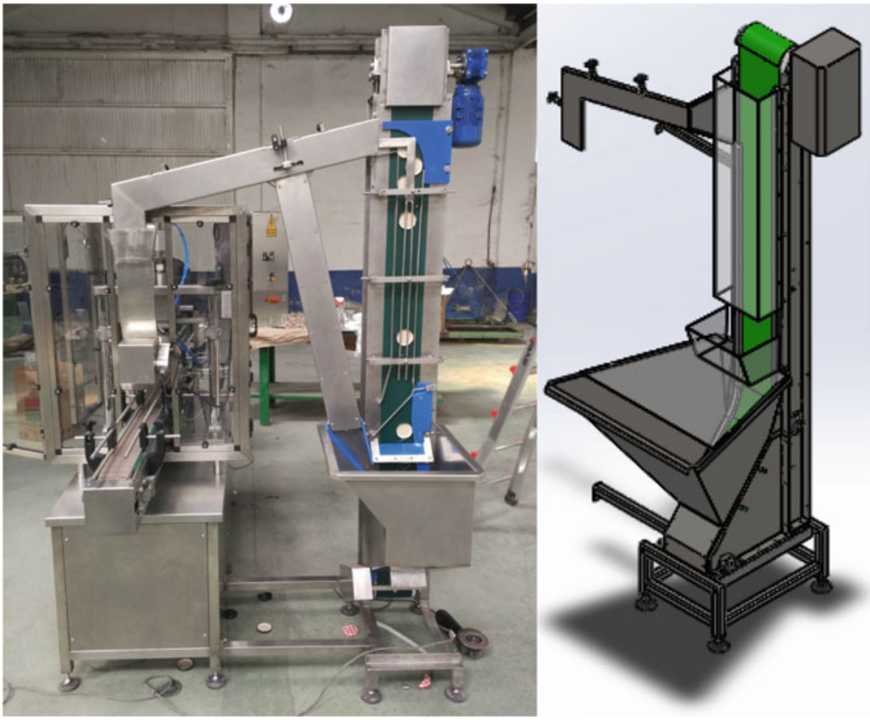

Fig. 2. Original tap elevator versus refined design one

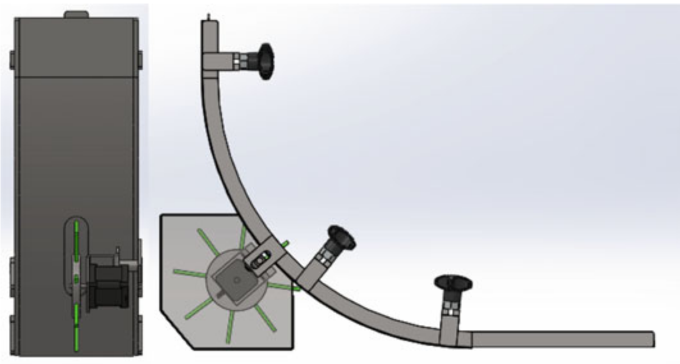

Fig. 3. Tap line front and side perspectives

Table 2. Actuator problems summary

Concept	Problem description	Adopted solution
Fixing clamp	Manufacture of three fixing clamps with different dimensions, when bottle format changes, a fixing clamp change is required with an associated cost in time and money	Possibility of manufacturing a single and adjustable fixing clamp that fits all types of bottles that customer may demand
Fixing piston	Undesired turning of the bottle due to the existence of a single rod in piston, and problems of corrosion in it as it was not manufactured with stainless steel	Implementing a double rod stainless steel piston, removing undesired turning and improving corrosion resistance
Fixing system adjustment	System allowed only an axial adjustment of piston. In addition, it was guided by an embedding, which made probable that it could be bended, causing a misalignment cap-bottle	Allowing a guided adjustment by means of a 4 mm. embedding in the direction of piston axis and perpendicularly to it
Mandrel formats	Recipient change requires a mandrel modification, in which, due to is geometric structure, is difficult to insert an adequate tool, taking more time than desired	Finding a fixing way that requires less time to perform change and allows a more comfortable way to do it
Chain location	Chain location forces to install motor in an unfavourable position, since it generates unbalance due to its own weight	Chain location change to make a more compact, more balanced and stiffer structure. Also, pulley has been located on the table for a better height grading of the actuator
Caps platform stiffness	Cantilever structure with stand welded to plate, which favours vibrations that disarrange caps with regard to glass jar	Increase in plate thickness and implementation of a new symmetric stand for higher system stiffness
Torque limiter	Friction plate torque limiter, gets worn easily causing adjustment problems and defective closings in several containers	Selection of a ball detent torque limiter, with higher precision when closing bottles and when adjusting it, minimum possible wear and acceptable price

Final improved design results for fixing clamp, piston and centring device versus original ones can be seen in Fig. 4. Also, original mandrel design is compared with renewed one in Fig. 5.

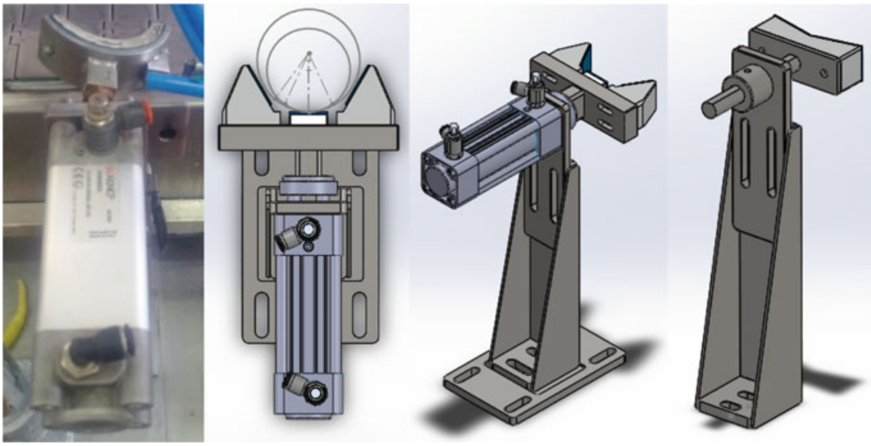

Fig. 4. Left to right, original fixing system versus redesigned clamp, piston and centring device

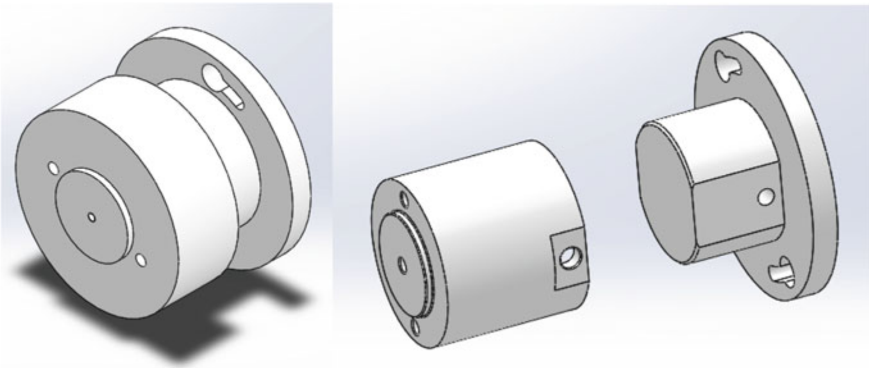

Fig. 5. Original mandrel versus redesigned one. New design allows easier access with a screwdriver

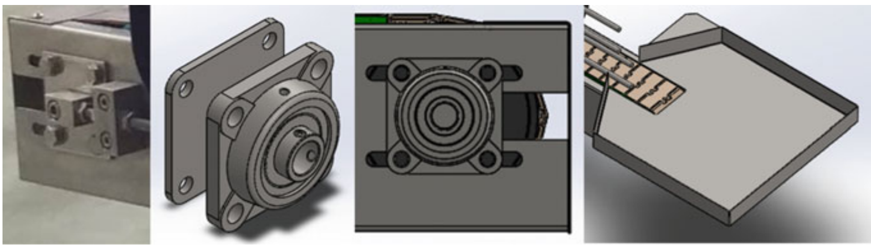

Fig. 6. Original transport line tensor versus redesigned one, and reception table

4.4 Transport Line

Main problems detected in transport line have been the impossibility of storing bottles in the line itself until their pick up, due to the lack of a reception table, and the high complexity of line tensor, as a consequence of the high number of pieces that composed it. Proposed solutions in Concept Design stage were adding to the final design a reception table at the end of the transport line, and simplifying tensor system, by using a lubricated bearing to reduce friction (see Fig. 6).

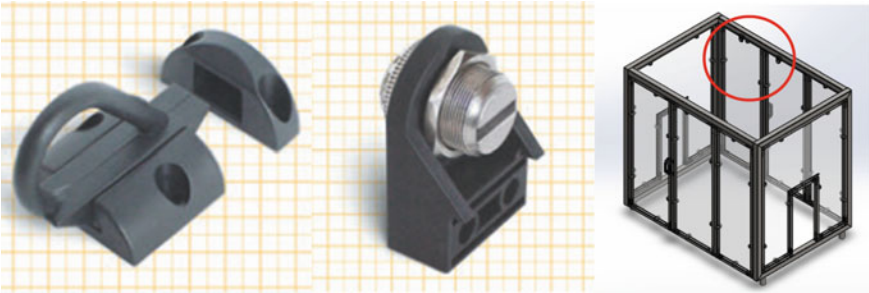

Fig. 7. Original door catching device versus new one [16], and its placing

4.5 Protective Framework

During Strategic Design stage, the main problem that existed in this sub-assembly was that mechanical catching device used for door opening did not count with a lock. This system does not guarantee a reliable closing and any hooking with it caused an accidental door opening and thus a complete stop of the machine. To eliminate this problem, in Concept Design stage a magnetic door catching device was selected and placed in the inner part of the framework instead of externally and visible as it was before, taking advantage of the circumstance that door profiles are metallic (see Fig. 7). Cap filler line was also included inside protective framework to meet security standards.

4.6 Table-Chassis

In Concept Design stage several problems showed up during assembly process, motivated by the different modifications made in the frame and in the actuator, mainly because of the change of location of the actuator's chain, since to be able to generate ascent as well as descent of actuator it is necessary that chain is located in a way that it eases machine's adjustment. Therefore, pulley and conduit where electric wiring is inserted forced to increase protective frameworks' width, as well as the one of the table-chassis that supports them. All this integration has implied that new design of table-chassis increases its dimensions compared to reference machine in 160 mm. (see Fig. 8).

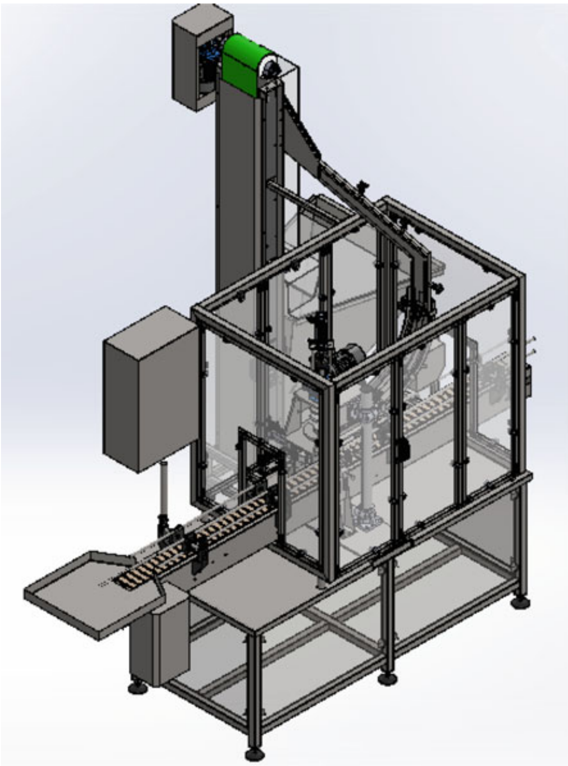

Fig. 8. Isometric view of final refined design

4.7 Materials Selection

Once finished Concept Design stage, materials for new model were selected using software CES EduPack 2010. Most used material in agri-food sector is stainless steel [17, 18], hence stablished selection parameters were density-yield stress ratio, price-resistance to strong alkalis relation, carbon percentage <0.05% and nickel percentage 9–11%, and AISI 304L was selected for metallic parts of the machine.

Equally, for transmission rollers, elevator canvas guides, mandrel and pieces of fixing system in contact with the recipient, it was searched a material with low friction coefficient and low density to avoid elevating load values in plate and transmission stands. In this case, selection parameters were tensile strength-impact strength, price under 2 €/kg, density between 100 and 1000 kg/m^3 and excellent behaviour in salty water and alkaline ambiences, concluding that optimal material would be polypropylene.

5 Conclusions

The process of development and cooperation carried out between a private company and researchers of Technical University of Cartagena succeeded in designing first bottling machine for different geometries of glass jars in a continuous bottling process, representing and injection of innovation and modernization without precedents in the traditional agri-food industry of Region of Murcia.

In a first stage of this new development, the one that comprises Strategic Definition stage, all problems of a bottling machine in a continuous manufacturing environment were identified, by means of a work developed jointly between company's engineers and university's engineers, to later on, in a second stage named Concept Design stage, proposing a new design using computational geometry tools. Data provided by the simulation of the new model in a virtual environment, shows that it allows to improve bottling process from 15 to 30 closed jars per minute, improves precision of hermetic closing of receptacles, and to sum up, improve flexibility of the machine in terms of closing and adjusting times when used with receptacles of different caps and geometries. At the moment, first prototype which will allow us to validate theoretical model developed in present work, is in mechanical fabrication stage.

References

1. Casani S, Rouhany M, Knøchel S (2005) A discussion paper on challenges and limitations to water reuse and hygiene in the food industry. Water Res 39:1134–1146
2. Charterina J, Basterretxea I, Landeta J (2017) Collaborative relationships with customers: generation and protection of innovations. J Bus Indus Mark 32:733–741
3. Kurilova-Palisaitiene J, Sundin E, Poksinska B (2018) Remanufacturing challenges and possible lean improvements. J Clean Prod 172:3225–3236
4. Sakao T, Lindahl M (2014) In: Pcp (provider—customer—product) triangle: how can manufacturing intelligence be maintained? Procedia CIRP, 2014, pp 362–367
5. Walker DHT (2016) Reflecting on 10 years of focus on innovation, organisational learning and knowledge management literature in a construction project management context. Constr Innov 16:114–126
6. Lindahl M, Sundin E (2013) Product design considerations for improved integrated product/service offerings. In: Handbook of sustainable engineering, pp 669–689
7. FOGGFILLER website. http://www.foggfiller.com/espanol/sorters/. Last accessed 19 Jan 2018
8. Khadilkar DV, Stauffer LA (1996) An experimental evaluation of design information reuse during conceptual design. J Eng Des 7:331–339
9. Parliament European (2006) Directive 2006/42/EC of the European Parliament and of the Council of 17 May 2006 on machinery and amending Directive 95/16/EC (recast). Official J Eur Union 157:24–86
10. Parliament European (2014) Directive 2014/35/EU of the European Parliament and of the Council of 26 February 2014 on the harmonisation of the laws of the Member States relating to the making available on the market of electrical equipment designed for use within certain voltage limits. Official J Eur Union 96:357–374

11. Parliament European (2008) Decision No 768/2008/EC of the European Parliament and of the Council of 9 July 2008 on a common framework for the marketing of products and repealing Council Decision 93/465/EEC. Official J Eur Union 13:82–128
12. Spain (2008) Real Decreto 1644/2008, por el que se establecen las normas para la comercialización y puesta en servicio de las máquinas. Official State Gazette 246:40995–41030
13. UNE (2012) Safety of machinery—general principles for design—risk assessment and risk reduction (ISO 12100:2010). AENOR, Madrid
14. UNE (2016) Safety of machinery—Emergency stop function—Principles for design (ISO 13850:2015). AENOR, Madrid
15. UNE (2007) Safety of machinery—Electrical equipment of machines—Part 1: general requirements (IEC 60204-1:2005, modified). AENOR, Madrid
16. AVE website. http://www.avetm.com/Articulos/. Last accessed 19 Jan 2018
17. Brody AL, Bugusu B, Han JH, Sand CK, McHugh TH (2008) Innovative food packaging solutions. J Food Sci 73:107–116
18. Marsh K, Bugusu B (2007) Food packaging—roles, materials, and environmental issues: scientific status summary. J Food Sci 72:39–55

Moving Away from the Basic, Adopting a New Approach to the Creative Process

J. C. Quiñones-Gómez(✉)

Department of Mechanic Engineering and Fluid Mechanics,
University of Málaga, C/Dr. Ortiz Ramos s/n, 29071 Málaga, Spain
juancarlosq02@gmail.com

Abstract. The role of creativity in Industrial Design Engineering's design process is fundamental and indispensable. Without it, design loses its potential for innovation – the process through which ideas generated by the creative process may be implemented attaining commercial value. The impact a product has can often be attributed to creativity in the engineering design process. Design in the arts is often considered to be the creative process per se, whereas in engineering, it refers to a concise record or encapsulation of appropriate concepts and experiences. For this reason, creativity is now a key skill in the practice of engineering and an essential part of its training. The present article discusses theories of the creative process which have been proposed in the last century. The stage based model of the creative process is discussed and the evolution of these models is mapped out. Further perspectives are identified for upcoming research; bringing data science and creativity together in such a way will necessitate development in both design and models of creativity.

Keywords: Creativity · Design · Creative process · Design methodology

1 Introduction

Creativity is a complex concept and is mysterious to many people. It has been suggested that, while they may have difficulty precisely defining product creativity itself, the majority of people is able to identify it [1]. This approach to creativity drives an ongoing interest in further researching the relationship between product creativity and science during the creative process in industrial design engineering product development. According to this research, the design process and the creative process do not represent the same reality, however creativity is considered an essential component of design [2], aided by data and using an adaptive, integrated model.

The present study's underlying hypothesis leads us to believe that the formulation of an advanced methodology to generate new insights will allow us to better understand creativity.

This research demonstrates the different perspectives that must be analysed in the development of a new methodology. The professional sectors of design have changed radically in the last twenty years, design methods and creative processes must mature to become a real alternative to conventional problem-solving strategies. With this in mind, existing literature in the fields of creativity and the creative process was examined to

F. Cavas-Martínez et al. (Eds.): *Advances on Mechanics, Design Engineering and Manufacturing II*, LNME, pp. 670–679, 2019.
https://doi.org/10.1007/978-3-030-12346-8_65

determine which are the key factors in creative production. Additionally, the designer's changing role is studied in relation to advances in emerging design methodologies related to big data.

As such, a general overview of relevant theories of the creative and design processes is presented, followed by an analysis of different types of data. This leads us to the data-driven design model as an instrument to stimulate creativity and promote innovation.

2 Theoretical Background

Creativity has become an important topic for discussion, analysis, controversy and, potentially, even revolution. It speaks of an economic [3], sociological [4, 5], or psychological perspective [6, 7], and has also become part of debates on social class, urbanization, industry and education among other topics. There has been confusion over the concept of creativity as a valuable entity in terms of product design and innovation; however, organizations and individuals have typically been unaware of its importance [8]. The term has not only been studied from the psychological perspective, but there have been several advocates from different disciplines who have attempted to define it in recent decades. These include pedagogues, scientists, artists, communicators, politicians, business-people, publicists, teachers, etc., who have suggested as many different definitions of creativity as there are authors who have researched the subject. A total of more than 100 different creative and design processes have been analysed and considered. The results presented in this paper are based on a comparison of about half of these. Common features found in the definitions include: (1) Creativity is an ability to adapt to the needs of reality. (2) It is novel or original. (3) Responses show wide variability as it covers a wide range of potential actions. (4) The result is a structural, qualitative leap forward. (5) The result is so unpredictable that it surprises even the person who generates it. Mayer [9] attempted to compile the historical and widely shared drivers used to shape creativity from the abundance of proposed definitions. The conclusion was that the terms "original and useful" were the most common denominators, although often presented in the form of synonyms such as "novel and appropriate", "new and valuable", etc. In addition to the aforementioned criteria, it may be considered that a solution or product is only seen to be creative as far as it is widely accepted to be such [1]. However, as Runco and Jaeger [10] concluded, Stein [11] was the first to conceptualize what is considered the standard definition of creativity, choosing to define creativity as something new and useful (Fig. 1).

Fig. 1. Definition of creativity

In addition, the evaluation of creativity within the field of computational creativity has been studied and researchers (e.g. Brown [12]) have proposed that computing can contribute to it because of greater accuracy through the use of computable constraints. Computer science can also support studying design creativity through the creation of support tools that enable collaboration, manage difficulty, maintain history and rationale, and underpin the exploration process [13, 14]. The intersection between creativity, computer science through big data and product development is the core area of exploration for this research (Fig. 2).

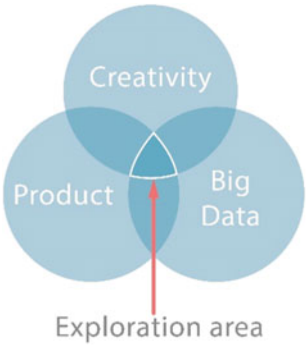

Fig. 2. Exploration area as a result of the intersection of creativity, product development and big data

3 The Evolution of the Creative Process

Guilford [15] noted that there was "considerable consensus on the four phases comprising the creative process", which are traditionally recognized as preparation, incubation, illumination and verification. However, Guilford, not being satisfied with the above description wrote: "that such an analysis is very superficial from the psychological point of view". It does not reveal anything about the mental operations that really happen. Therefore, he was able to determine a number of skills that affect creativity, such as problem sensitivity, the capacity to generate a large number of ideas, the potential to transform one's own mind-set, the capability to reorganize, the capacity to deal with complexity and the capacity to evaluate. After more than 50 years, our vision and understanding of the abilities and cognitive processes involved in creativity have evolved so considerably, introducing innovations as radical as they are ultra-fast, that the next 40 years would lead to more changes in society than in the preceding four thousand. A large number of researchers have based and continue to base their studies on the four-phase model or its variants to better understand the creative process [16–23]. One of the most recent updates of this model corresponds to Amabile [24], who incorporated a new vision, describing a creative process with several phases: (a) identification of the problem, (b) preparation (collection and reactivation of information), (c) generation of responses and (d) validation and communication of responses. An important aspect of Amabile's contribution is the proposal for a later final decision-making phase, based on the result obtained. It is possible to stop the process because a successful outcome has been achieved, to suspend it due to an unwanted outcome or to return to any of the previous phases and continue working. Amabile's contribution is considered an important aspect of this study. The creative process is therefore considered a process in continuous development. Thus, according to Guilford [15], and other some studies, the creative process can be studied or replaced.

4 The Design Process in Engineering

In this research, however, the approach focusses on creativity as an essential element of the industrial design engineering process. The presence of creativity is often the greatest influence on a product's impact. Design in the arts is usually considered to be the creative process per se, whereas in engineering, it may mean a concise record of embodiment of appropriate concepts and experiences. Creativity has therefore become a requisite skill for engineers and a part of their basic training. While creativity and design are defined in different ways and are subject to differing use in research, based on the reviewed literature, the following definitions are proposed: (1) Creative Process: A cognitive process resulting in the formulation of an idea. (2) Design Process: A work process resulting in a proposal for a product or process. A philosophical perspective would posit that different movements conceptualise engineering's design process differently. Positivism assumes a structured, scientific method which aims to identify causal factors and guide outcomes. This approach is analytical and problem-focused; investing in innovation, it employs a sequential cascade process centring on creativity. The sequential engineering process was shaped by Herbert Simon's research [25], which proposes three steps: problem setting, problem solving (creative) and solution evaluation. Constructivism, on the other hand is linked to postmodernism, rejecting absolute truth. This approach conceives of reality as a social construct dependent on context: It is solution-focused and co-constructs problem and solution together through iteration [26]. The design process brought about by this approach is circular, not sequential and creativity is present throughout the entire project. Many design trends of recent times are evidence of this approach. These include: information technology [27], user-centred design [28], agile software development [29], design thinking [30] and lean start-up [31]. This paper proposes that the creative processes of design result from the integration of the creative process (as understood through cognitive psychology) and the engineering design process. Although it is recognized that the design processes observed in practice are more inaccurate than most representative scenarios suggested, it is argued that understanding the connections in the overall process will help engineers make better use of creative tools, methods and techniques. This deeper understanding will enable more effective tools to be created and utilized, helping the engineering designer to produce more ideas that are original or to generate them more quickly. The 'creative' processes could be linked into the engineering design processes with which the engineering design research community is familiar, with potentially considerable benefit. However, cross-disciplinary research and agreement of terminology and process boundaries will be essential in developing effective prescriptive processes to aid creativity throughout the design process. The different methodologies applied to the discipline of industrial design engineering and the evolution of its methods highlight cultural and scientific background knowledge as a starting point of thought as a response to needs; everything coming through the instrument of creativity to achieve of the proper and necessary balance between intuition and reason, design and science.

5 Comparison of the Processes

The two processes referred to have some common characteristics, especially the way in which the models are developed. The literature on creative and design processes consists mainly of linear models. In addition, the bibliography concerning both processes outlines two other main types of process models, one which involves divergent-convergent processes, and another which describes information spaces (design) and problem and solution spaces (creativity). These processes also share the similarity of requiring data collection, analysis and comprehension at the outset of the process (preparation or task phase analysis). The design and creative processes primarily differ in the dimension and scope of their sub-processes. In the design process, the sub-processes will consist of logical assumptions, evaluation, decisions and rejected solutions en route to the final recommendation. The creative process is limited to the generation and validation of individual ideas.

6 Moving Towards Data

With their history of employing creative empirical data collection methods, designers' role in using quantitative and qualitative data in the user-centric design of products and services is significant. However, the discipline is now faced with new and more sophisticated forms of data, which are being used differently due to the prevalence of mobile and ubiquitous computing. The way that designers interact with and design around data has therefore changed. While data have always had the potential to provide an analysis or prior events, big data now makes it possible to, in essence, predict future behaviour and events. Big data belongs to the field of computing known as machine learning, part of the more general area of artificial intelligence (AI). Despite its name, machine learning does not involve teaching a computer, nor is it expected to think as humans do; it does, however, refer to the inference of probabilities through the application of mathematics to huge data sets. This permits the identification of approximations of phenomena, allowing the present to be accurately described and the future predicted. With the invention of computers during the 20th century, previously theoretical concepts of artificial intelligence were able to be put into practice. Now with the advent of the Internet of Things, we assume the all devices are connected and able to collect data about their use and functioning and share it. With access to this information, everything can be measured through machine learning toots and other analytical tools. Furthermore, data analysis methods such as predictive analytics allow phenomena to be predicted and issues solved before they become problematic. One application of this is the prediction of structural or mechanical faults in infrastructure or machines: sensors which collect and transmit data can be fitted to track changes which have potential to become problems if left unchecked. AI systems allow the more effective exploitation of large data sets so that they may be a more productive tool and facilitate the decision-making process [32].

7 Gathering Data

The initial stages of the design process are usually characterised by the processing of information and the generation of ideas (often called “conceptualisation”). During these stages, designers utilise several kinds of information to reduce abstraction through the integration of an increasing number of conditioning factors. In this sense the designer’s cognitive activity can considered a form of information processing (data processing). This information handling process can be described as an information cycle: a fundamental part of initial phase of the design process, including informative, generative and decision making (evaluation-selection) phases, and whose result is an intermediate and evolutionarily iterative concept.

Given that the majority of research into design is derived from the results of empirical studies, its primary interest tends to lie in specific activities, such as “where” designers find inspiration. Results regarding the use of implicit information and its processing may be able to bridge the informative and generative phases of the design process. The central mechanism of this process is to broaden then possibility space as much as possible through “divergence”, before, at a given moment of an exhaustive procedure, converging: taking decisions about what may be a viable solution and what is not.

The exploration phase generates a huge quantity of information, the majority of which is qualitative (and frequently is not digital) and through the integration of big data in the process, it is possible to begin to make sense it. Based on the decisions made in the first convergence phase, ideas are generated. By taking advantage of deep learning, the designer’s capacity to widen areas of study, interpret a large amount of data and convert it into insight is drastically increased without additional effort.

8 Stimulating Creativity Through Data

The preceding analysis highlights creativity’s crucial role in the design process and the importance of data collection and analysis to stimulate the creative process at its outset; a trait shared with the design process. Deliberate creativity in the initial phases of the design process has been the basis of several models of the creative process. Maiden et al. [33] based their work on models and structures suggested by Osborn [20], Wallis [34] and Borden [35]. These models are summarized in [36]. A common feature of all models of creativity is their inclusion of an initial idea generation phase and it is this phase that has been the focus of efforts in supporting creativity. A preparatory stage is another feature often shared by various models of creativity. At this stage, we are interested in how idea generation later in the process can be stimulated by supporting the earlier preparatory stages of the creative process, optimizing the industrial design engineering process. Between 2005 and 2010, the amount of data generated grew from 150 exabytes to 1200 exabytes [37]: an increased availability of data which presents great opportunities if utilized effectively. This may be possible through the use of human visual cognition and perceptual abilities to visualize the data, gaining insight and exploring it more deeply. Due to the influence that data exert over the design process, we must clarify which data should be used and when. Speed and Oberlander [38] describe three classes of data use in the design process (Fig. 3): (1) Design from data: systems are modelled on measurable qualities of humans, computers, their conditions and contexts. (2) Data Design: Systems designed by humans which account for the flow of data through them. (3) Data Design: Systems designed largely autonomously by another system.

Fig. 3. Data within the design process

According to Yu and Zhu [39], in accordance with the data's existing form, data are composed of "abstract data" and "concrete data". Abstract data are conceptual data and do not exist in reality. Concrete data already exist in reality and can be collected and processed. This study centres on the more specific model of data suggested by author [40], with the aim of presenting a more focused approach. In this model data may be present in the design process in one of two distinct classes (Fig. 1): (1) Concrete data: based on the processing of pre-existing data sets. (2) Abstract data: existing information processed in new ways with predictive analytics to predict future situations and gain deeper insight into the data. Abstract data can be employed by the designer in the design process to generate new insights and concepts in the same way that concrete data may support or define design. Based on this assessment, it is understood that while large data sets may improve design, design can provide further understanding of data. This statement is the basis of the hypothesis on which this study is based. Having access to large sets of data during the design process is assumed to aid creativity and as such allow a greater number of potential solutions. Abundance of data grants the designer freedom to explore more concepts and new perspectives or analyses while paying closer attention to certain facets of the process without losing the central focus.

The design process is potentiated by the data collected from the thousands of connected devices in use today; transmitting information about their use and functioning. Through the integration of concrete and abstract data, as seen in the Data

Driven Design process [40] (Fig. 2), we are able to perform analyses to identify trends; this in turn generates abstract data which may be used in predictive analytics, helping identify future performance scenarios or support a product's continued development. This model's integration into the engineering design process can be considered a breakthrough in the discipline's evolution, increasing the efficiency and effectiveness of the innovation process. In this model, Wilford's considerations are represented, as well as the Amabile's contribution to allow a model in permanent progress. This integration into the proposed model provides an evolved, flexible and transversal model. In-depth practical studies will be necessary to verify its impact. Using data, it is possible to predict consequential behaviours or use an experimentation framework to define opportunities; formulate hypotheses, and test different options stimulating designers' creativity and inspiring a new way of thinking. While data may describe a problem, creativity is necessary to generate a solution. Despite data's growing prevalence and importance, the crucial role of creativity can not be understated and its focus should be on strengthening design. The careful use of big data is a boon to the decision-making process, facilitating the designer's work. This integration of creativity and data science, as in the Data Driven Design model, is a step forward for the engineering design process.

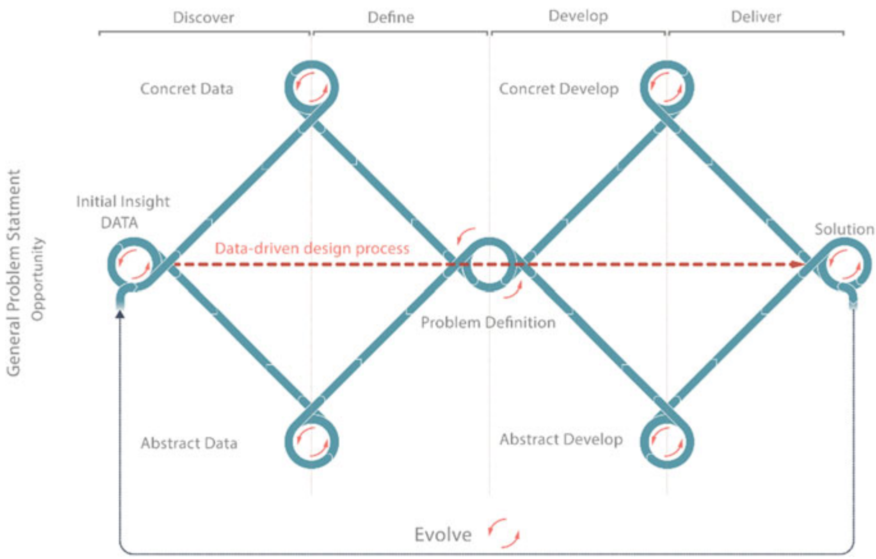

Fig. 4. Data-driven design model

9 Conclusion

New opportunities are available to designers thanks to big data and this is especially true in the field of industrial design engineering. The framework presented in this study (Fig. 4) allows a faster design process and outlines the influence of data over this process. It was found that data correlations used in the initial phase of the process stimulate creativity by increasing efficiency and effectiveness on, introducing new patterns of innovation. In this context, the designer's expertise would shift from creativity itself to facilitating creativity. Just as design engineers have extensive knowledge of product development and iterative processes related to design, the creative class has a much deeper understanding of the cognitive processes involved in creativity and the generation of ideas. However, the data-driven design model makes it possible to integrate these processes, both of which have their origin in the double diamond model supplemented with data in its initial phase. Although systems which are supported by big data or artificial intelligence devices may not yet be possible, systems can assist the creative design process by making them even more creative. While this is a challenging approach that requires more research, making use of the assets provided by recent technological developments to support processes and track their progress holds great potential value. In this way, this study contributes to improving our understanding of the use of big data, defining future research objectives. The most remarkable result that emerges from this research is that deep learning and big data are a step forward in the creative process compared to traditional models, stimulating creativity, improving the process and results.

References

1. Amabile T, Kidd R (1983) Social psychology of creativity. Springer, US, New York
2. Chakrabarti A (2006) Defining and supporting design. In: 9th international design conference DESIGN 06, pp 479–486, Dubrovnik
3. Hawkins J (2005) The creative economy. How people make Money from ideas. Penguin Books, London
4. Joas H (1996) The creative of action. University of Chicago Press, Chicago
5. Joas H (2002) Creatividad, acción y valores. Hacia una sociología de la contingencia. Biblioteca de Signos, México
6. De Bono E (2006) El pensamiento lateral. Paidós, Barcelona
7. Csikszentmihalyi M (1996) Creativity: flow and the psychology of discovery and invention. Harper Collins, New York
8. Sternberg RJ (1988) The nature of creativity: contemporary psychological perspectives. University Press, Cambridge
9. Mayer R (1999) Problem solving. Encyclopedia of creativity, vol 2, pp 437–447. Runco & S. R. Pritzker Academic, San Diego (1999)
10. Runco MA, Jaeger GJ (2012) The standard definition of creativity. Creat Res J 24(1):92–96
11. Stein MI (1974) Stimulating creativity: individual procedures. Academic, New York
12. Brown DC (2008) Guiding computational design creativity research. In: Proceedings of the international workshop on studying design creativity. University of Provence, Aix-en-Provence (2008)
13. Lubert T (2005) How can computers be partners in the creative process? Int J Hum Comput Stud 63:365–369
14. Shneiderman B (2007) Creativity support tools: accelerating discovery and innovation. Commun ACM 50:20–32
15. Guilford JP (1950) Creativity. AmericanPsychologist 5:444–454

16. Busse TV, Mansfield RS (1980) Theories of the creative process: a review and a perspective. J Creat Behav 14:91–103, 132
17. Cagle M (1985) A general abstract–concrete model of creative thinking. J Creat Behav 19:104–109
18. Goswami A (1996) Creativity and the quantum: a unified theory of creativity. Creat Res J 9:47–61
19. Ochse R (1990) Before the gates of excellence: the determinants of creative genius. Cambridge University Press, New York
20. Osborn AF (1953) Applied imagination. Scribners, New York
21. Stein MI (1953) Creativity and culture. J Psychol 36:31–322
22. Taylor IA (1959) The nature of the creative process. In: Smith P (ed) Creativity: an examination of the creative process. Hastings House, New York, pp 51–82
23. Taylor IA, Austin GA, Sutton DF (1974) A note on "instant creativity" at CPSI. J Creat Behav 8:208–210
24. Amabile T (1996) Creativity in context. Westview Press, Colorado
25. Simon HA (1973) The structure of ill-structured problems. Artif Intell 4:181–201
26. Visser W (2009) La conception: de la résolution de problèmes à la construction de représentations. Le Travail Humain 72:61–78
27. Boehm BW (1988) A spiral model of software development and enhancement. J Comput 21 (5):61–72
28. ISO13407 (1999) Human-centred design processes for interactive systems. International Organization for Standardization, Genève
29. Beck K, Beedle M, van Bennekum A, Cockburn A, Cunningham W, Fowler M, Grenning J, Highsmith J, Hunt A, Jeffries R, Kern J, Marick B, Martin RC, Mellor S, Schwaber K, Sutherland J, Thomas D (2001) Manifesto for agile software development
30. Cross N (2011) Design thinking: understanding how designers think and work. Bloomsbury, Berg
31. Ries E (2011) The lean startup: how today's entrepreneurs use continuous innovation to create radically successful businesses. Crown Business, New York
32. Solares C (2017) iLifebelt™. Evolución del Big Data a Inteligencia Artificial. Available: http://ilifebelt.com/evolucion-del-big-data-a-inteligencia-artificial/2017/04/. Last accessed 06 Feb 2018
33. Maiden N, Gizikis A, Robertson S (2004) Provoking creativity: Imagine what your requirements could be like. IEEE Softw 21(5):68–75
34. Wallas G (1926) The art of thought. Harcourt Brace, New York
35. Boden MA (2004) The creative mind: myths and mechanism. Psychology Press, New York
36. Lubart TI (2001) Models of the creative process: past, present and future. Creat Res J 13(3–4):295–308
37. Helbing D, Balietti S (2011) From social data mining to forecasting socio-economic crises. Eur Phys J Special Topics 195(1):3–68
38. Speed C, Oberlander J (2016) Designing from, with and by Data: introducing the ablative framework. In: Proceedings of DRS 2016, design research society 50th anniversary conference, pp 2991–3004, Brighton
39. Yu C, Zhu L (2016) Product design pattern based on big data-driven scenario. Adv Mech Eng 8:1–9
40. Quiñones Gómez JC (2017) The growing influence of design data in the design process through a methodological development. In: Proceedings of international conference 4D designing development developing design, pp 178–187, Kaunas

Teaching—Learning

Proposal About the Introduction of the Soft Skills in the Teaching of Product Development

E. Rovida[1(✉)] and G. Zafferri[2]

[1] Politecnico di Milano, via La Masa 1, 20156 Milan, Italy
edoardo.rovida@polimi.it
[2] Officina della conoscenza, Piazza Velasca 5, 20122 Milan, Italy

Abstract. Particularly in technical professions, many competences are greatly needed: those specific of the profession (Hard Skills) and transversal (Soft Skills), which are particularly important for Engineer 4.0. Soft Skills are relative to, e.g., behavior, interpersonal relationships, communication, deontology. One important aim of Soft Skills is to reach the "Personal Acumen". In this way, someone can accomplish the role of "difference maker": i.e., (s)he can confer his/her life a new very important aspect for the subject, for all other persons, and in all professional and personal fields. The aim of the present paper is to investigate the link between Soft Skills and the teaching process of product development. The link between Soft Skills and product development phases, with a specific reference made to design process teaching, is considered. Finally, some proposals about contents regarding Soft Skills in Engineering Design Education are made. Some examples of the considered Soft Skills from the bibliography are: Communication, Courtesy, Flexibility, Integrity, Relationship development, Positive attitude, Professionalism, Responsibility, Teamwork, Work ethics, etc. The authors propose, in line with their studies and experience, the following Soft Skills: Creativity, Awareness, Human aspects of technology, Talent development, IQ + EQ = IF, which means Intellectual Quotient plus Emotional Quotient results in Intellectual Fusion (a complete personality requires not only intellectual, but also emotional components). The conclusions of the paper are some proposals of including Soft Skills in teaching.

Keywords: Soft skills · Teaching · Learning · Product development

1 Introduction

The present paper aims to investigate how Soft Skills can play an important role in the teaching process of industrial product development. After finding individual Soft Skills from the bibliography [1], the authors proposed upgrading. A link between Soft Skills and product development phases, with a specific reference made to teaching, is considered. Finally, some proposals about contents regarding Soft Skills in Engineering Design Education are made.

By way of introduction, some definitions can be useful [1]. Hard Skills comprise the technical knowledge required to do a job. Soft Skills, however, are interpersonal qualities and personal attributes that can be considered transversal in all stages of the learning process and in the engineering field.

F. Cavas-Martínez et al. (Eds.): *Advances on Mechanics, Design Engineering and Manufacturing II*, LNME, pp. 683–695, 2019.
https://doi.org/10.1007/978-3-030-12346-8_66

2 Soft Skills

The starting point is to consider the product development activity steps (Table 1).

Table 1. Product development activity steps

No.	Steps	Time periods	Notes
1	Experiences	Until the 15th century	
2	First systematic observations	15–16th centuries	
3	First theories	17–18th centuries	
4	Developing theories	19th century	Engineering 1.0
5	Designing science	1900–1950	Engineering 2.0
6	Designing globalization	1950–2020	Engineering 3.0 & 4.0

The Engineering 4.0 step, which is very important today, plays an important role. Soft Skills are a significant complement, generally of engineering education, and particularly of design education.

In the proposed paper, and after performing a bibliographic research about the definition and list of types of Soft Skills, the authors propose upgrading the above-mentioned list by including some other Soft Skills that derive from their studies and experience.

The authors consider these Soft Skills acknowledged in the bibliography [1].

(a) Communication capability: speaking, writing, presenting, listening.
(b) Courtesy: manners, etiquette, business etiquette, graciousness, saying please and thank you, being respectful.
(c) Flexibility: adaptability, willing to change, lifelong learning, accepting new things, inclined to settle.
(d) Integrity: honest, ethical, high morale, has personal values, does what is right
(e) Interpersonal relationship: nice, look, sense of humor, friendly, polite, empathetic, self-control, patient, social skills.
(f) Positive attitude: optimistic, enthusiastic, encouraging, happy, confident.
(g) Professionalism: businesslike, formal-dress, appearance, poised.
(h) Responsibility: accountable, reliable, gets the job done well, resourceful, self-disciplined, conscientious, common sense.
(i) Teamwork: cooperative, gets along with others, agreeable, supportive, helpful.
(j) Work ethics: hard working, willing to work, loyal, initiative, attentive, self-motivated, on time.

In addition, and in line with their studies and experience, the authors suggest the following:

(l.1) Creativity: ability to find innovative solutions
(l.2) Awareness: equilibrium between opposite moods
(l.3) Human aspects of technology

(1.4) IQ + EQ = IF talent development, which means: Intellectual Quotient plus Emotional Quotient equal Intellectual Fusion (i.e., a complete personality requires not only intellectual, but also emotional components).

By considering the above-mentioned list, the authors propose a link between this list and the industrial product's life cycle (Fig. 1) [2, 3].

The above-mentioned links are the source of the proposal to upgrade Engineering Design Education by considering Soft Skills.

3 Product Development

The industrial product is a creation made by human beings, whose aim is to perform a useful function. The logical schema of an industrial product design could be considered to be constituted by the following steps.

Objective; i.e. the function to be performed by the product and the functional requirements that characterize the function;

Concept; i.e. the issue utilized to perform the function, expressed by a schematic representation;

Binding; i.e. covering the schema with surfaces made with materials manufactured by technological processes; i.e. embodiment is expressed by assembly drawings;

Constructive definition; i.e. individually selecting all the constructive information that needs reading: dimensions, tolerances, materials, defining standard components.

Figure 1 represents an example of steps (b) and (c) of an industrial product that performs the function "allow rotations of a rigid body around a fixed axis" (hinge). In the above-mentioned figure, it is possible to observe the concept of a hinge to the link while, on the right, we can see two possible embodiments: these embodiments are represented by assembly drawings, with different constructive solutions in relation to all the component functions.

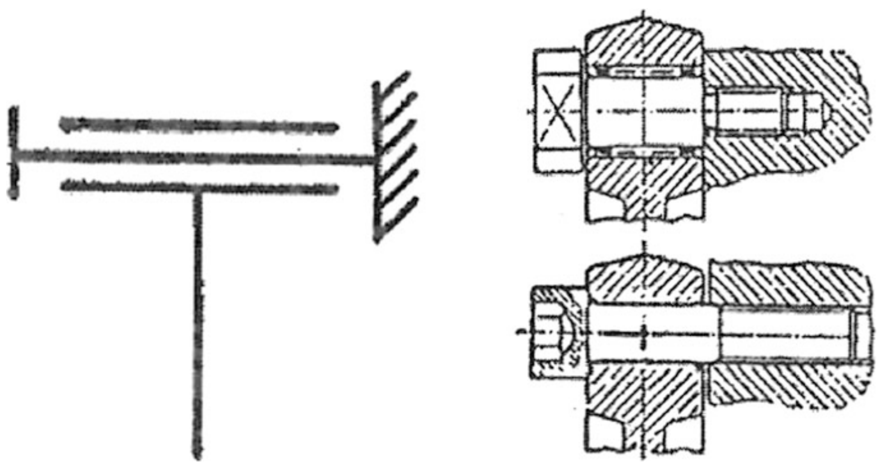

Fig. 1. Example of the concept (links) and embodiments (right) of a hinge

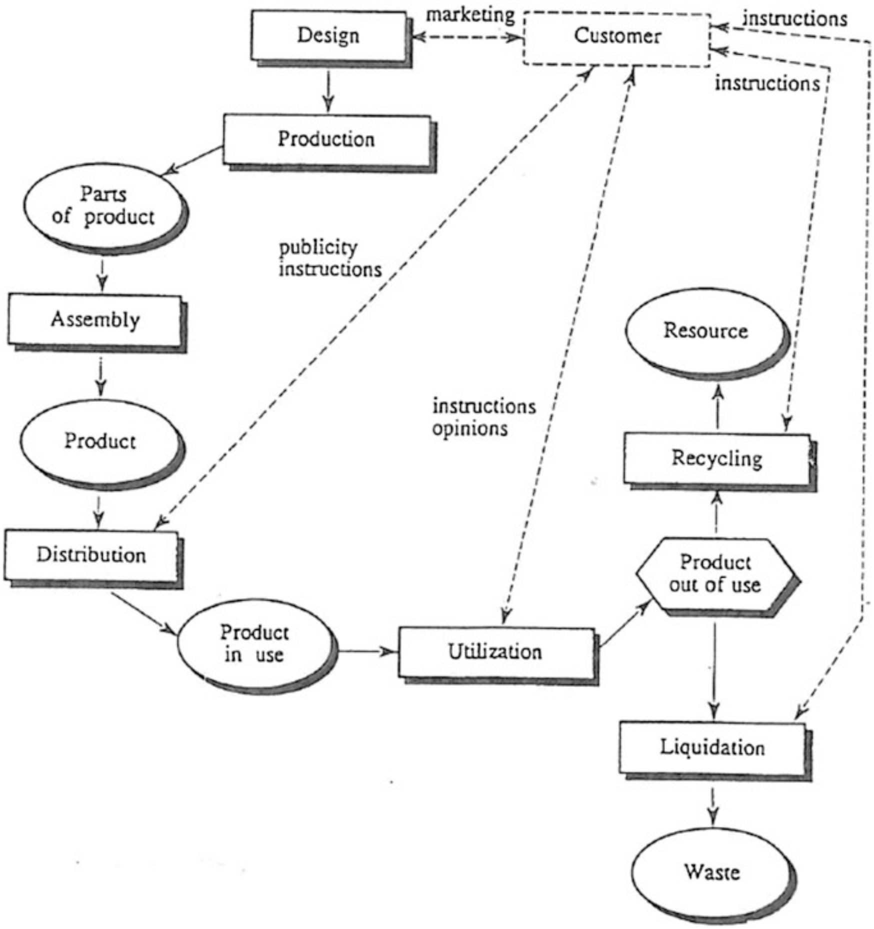

Fig. 2. Life cycle of the industrial product [2, 3]

Figure 2 represents the life cycle of the industrial product. After the design phase (and particularly after defining all the constructive information) the design (i.e. an information complex) is the starting point of the production phase, which can be considered to be constituted by two steps: production of components and their assembly. The production phase objective is to manufacture the product. This product, after distribution, becomes a used product, which is when its utilization phase begins. The end of utilization corresponds to product use phase out, and successive phases can include removal (the product becomes waste) or recycling (the product becomes a resource).

Obviously, product acceptance is necessary in all its life cycle phases, which is no easy task for designers.

4 Soft Skills in Product Development

After some information about a general product development schema, we now examine how Soft Skills are linked to a product's life cycle. Table 2 shows the connection between the above-mentioned Soft Skills and product development.

Table 2. Links between soft skills and product development

Soft skills	Examples related to the life cycle
(a) Communication capability	(a.1) Instruction of the industrial product's assembly, use and maintenance (a.2) Information from users to the producer (e.g. through questionnaires) (a.3) Transforming users from customers into prosumers (a.4) Updating engineers (a.5) Study mode and criteria (a.6) Matrix of Eisenhower
(b) Courtesy	(b.1) Ability to respect all people contacted
(c) Flexibility	(c.1) Ability to adapt to variations in the market, the enterprise and the working environment
(d) Integrity	(d.1) Ability to follow engineering deontology (d.2) Ability to consider that technical products can harm users
(e) Interpersonal relationship	(e.1) Ability to create a pleasant working environment (e.2) Ability to establish good relationships with people from upper and lower levels
(f) Positive attitude	(f.1) Ability to be optimistic and to transmit optimism to colleagues
(g) Professionalism	(g.1) Ability to have a look and display behavior that are congruent to the specific work environment's requirements
(h) Responsibility	(h.1) Self-discipline and awareness
(i) Work ethics	(i.1) Ability to work hard
(j) Creativity	(j.1) Ability to find new solutions, to overcome negative and frequent situations, i.e. repetition and plagiarism (j.2) Ability to evaluate technical products' performance
(k) Awareness	(k.1) Ability to takey a balanced position between two opposite situations, feelings or mental states
(l) Human aspects of technology	(l.1) Clear idea that technology is for humans and humans are not for technology (m.2) Ability to evaluate positive and negative effects that technical products may have on users
(m) Talent development	(n.1) Ability to acquire a complete personality by striking a balance between the intellectual quotient and the emotional quotient: the result is intellectual fusion

Some considerations about the most significant and the most related skills with product development are made. The following examples result from the authors' experience.

Instructions for use and maintenance

Instructions for use and maintenance are an important part of scientific-technical communication. Instructions play an important role, and one that is linked to the industrial product's safety [3] (Table 3).

Table 3. General index of a manual for use and maintenance

1	Index
2	General data
3	Manual for use and maintenance
4	Product description
5	Forecasted use
6	Transport, assembly and fitting
7	Access
8	Carrying out
9	Verifying and regulating
10	Maintenance
11	Disassembling
12	Normal repairs
13	Dangers and emergencies
14	Training operators
15	Liquidation and recycling
16	Spare parts

Information from the user to the producer, i.e. approach to the transformation from consumers into prosumers.

Information from the user to the producer is significant and can be important feedback for the producer. By using the above-mentioned information, the producer can enhance a product's performance. Thus the consumer can play the role of prosumer (Table 4).

Table 4. General index of a questionnaire from the consumer to the producer

Customer's general data	– Name – Age – Studies – Profession
General product data	– Data about the consumer who uses the product – Type of product – How long the product has been used – How long similar products have been used
General evaluation	– General correspondence of the product to customer requirements – The product's most satisfying aspects – The product's least satisfying aspects
Specific evaluation	– Degree of satisfaction with the various aspects and/or part of the product – Observed problems – Proposal and suggestions

Updating engineers

Updating designers is very important: Continuing Education allows a designer's knowledge to be maintained over time. From this point of view, the preparation phase of a Continuing Education course is very important [4].

Eisenhower—Box

Eisenhower, the 34th President of the United States from 1953 to 1961, reaches a very high level of productivity, and by also applying the Eisenhower—Box [5]. This box (Fig. 3) allows the most rational decisions by classifying the things to do as being more or less "important" and "urgent".

Creativity

Creativity in the design education field can be defined as the ability to propose new concepts and embodiments of industrial products. Some criteria are used to develop creativity, and these criteria can be a teaching subject in Design Schools.

By way of example, we find the critical analysis of historical heritage. Historical solutions can, in some cases, be a source of new ideas. Old ideas can be proposed again today, e.g. with new materials and new technologies.

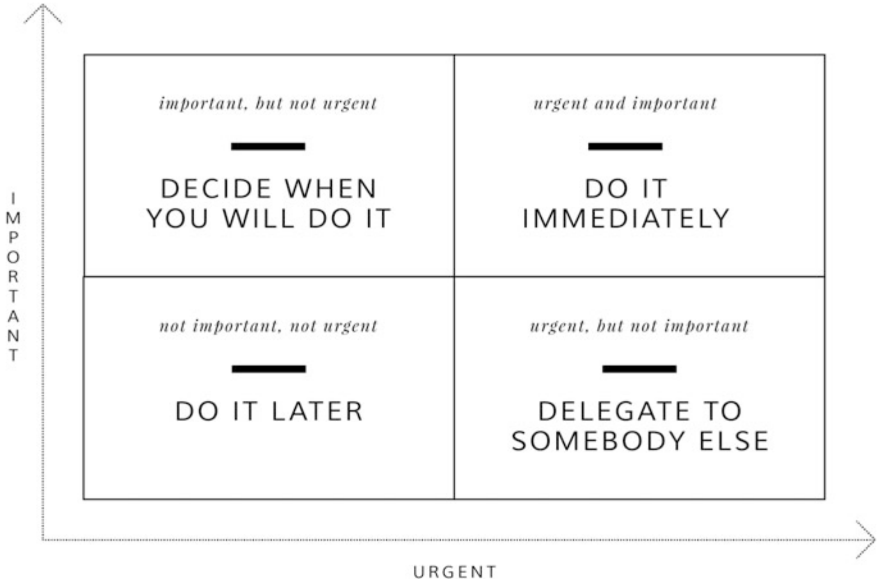

Fig. 3. Eisenhower—Box

Figure 4 represents the links to a historical German patent (1940) for car suspension which allows a car body to be leveled. To the right, we find a proposal of modern suspension made by abstracting the historical concept: variation of the height of the fixed point of the spring to the car body [6].

Figure 5 represents many concepts of a steamroller by changing the relative position of wheels, the engine and the driver.

Figure 6 illustrates a proposal of some different concepts of a glyph mechanism by changing the relative position of the fixed point and the point in motion.

Other important tools toward innovation are TRIZ [7–9] and biomimetics, i.e. the development of technical products by observing natural phenomena [10].

Awareness

The designer should very carefully consider the balanced position with no excess (Table 5).

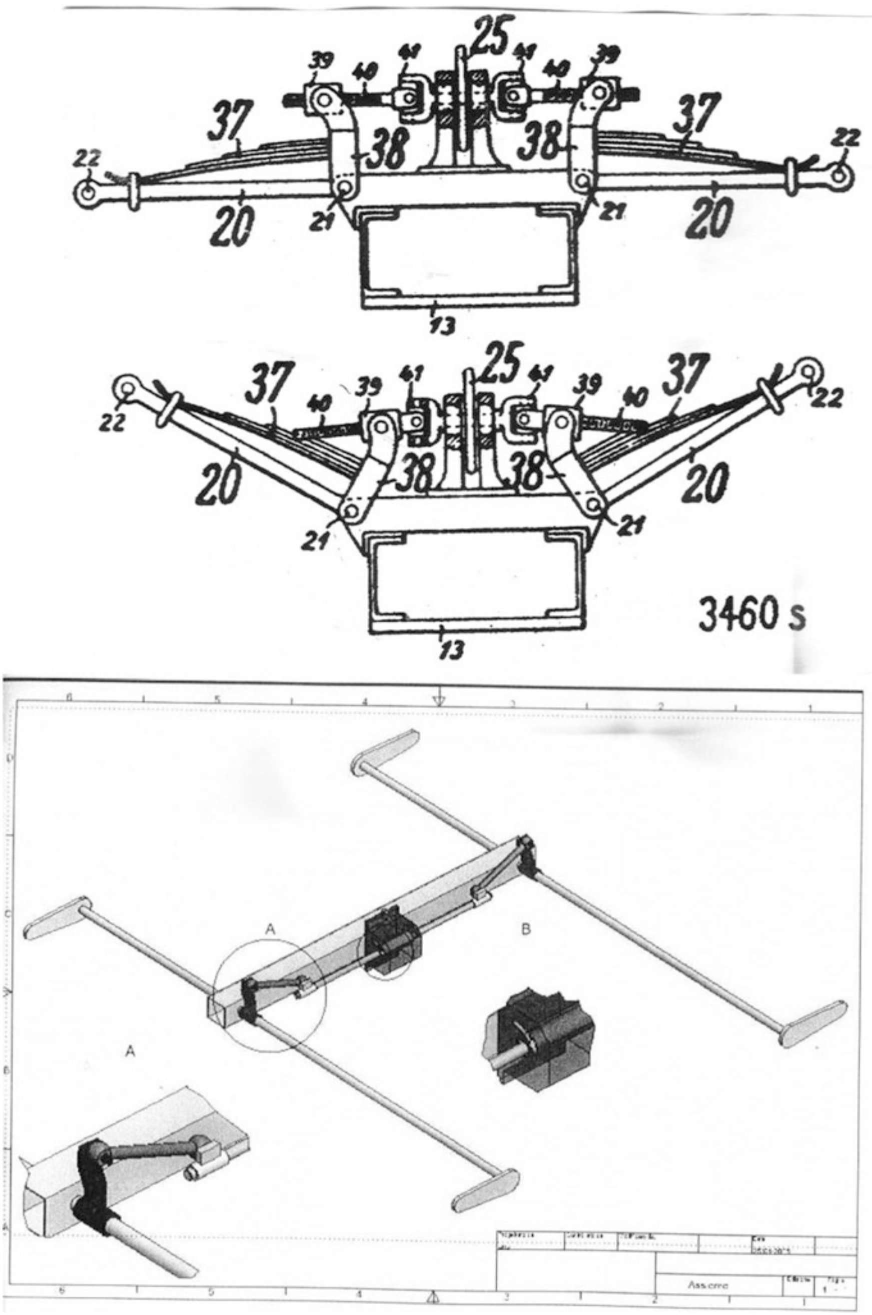

Fig. 4. Historical solution (over) and a modern proposal based on the same concept (under)

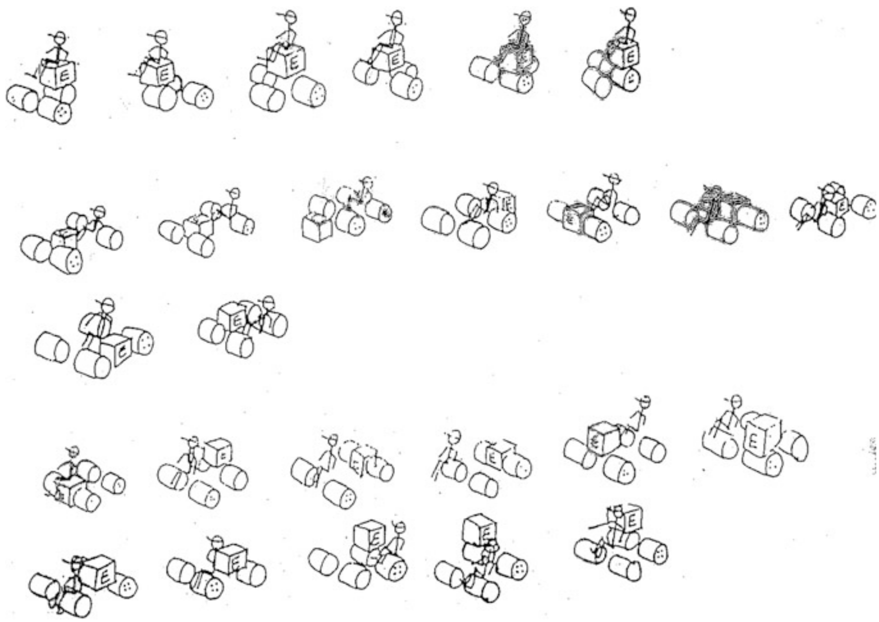

Fig. 5. Concepts of a steamroller by changing the relative position of wheels, the engine and the driver

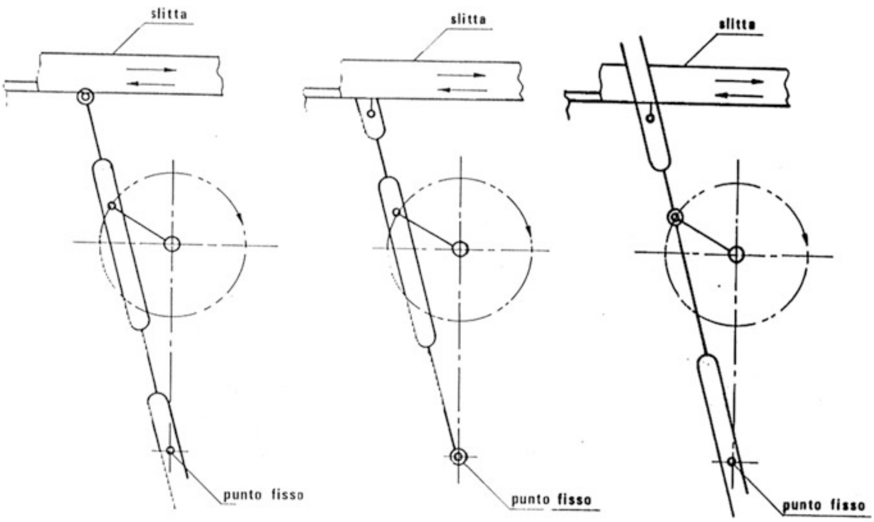

Fig. 6. Different concepts of a glyph mechanism by changing the relative position of the fixed point and the point in motion (*slitta* means *point in motion*, *punto fisso* means fixed point)

Table 5. Correct and excessive behavior (super ego)

Confidence	A sense of infallibility
Quickness	Overhastiness
Sharp wit	Abrasiveness
Alertness	Narrow focus
Dedication	Workaholism
Control	Inflexibility
Courage	Foolhardiness
Perseverance	Resistance to change
Charm	Manipulation
Ambition	Coercion
Power	Autocracy
Flexibility	Ambivalence

Human aspects of technology

Development of technology can be for or against humanity. Figure 7 is about sustainability, but can also be valid for human aspects. To gain human technology, it is necessary to upgrade technological development and culture, where culture is intended to act as an integration of knowledge and deontology.

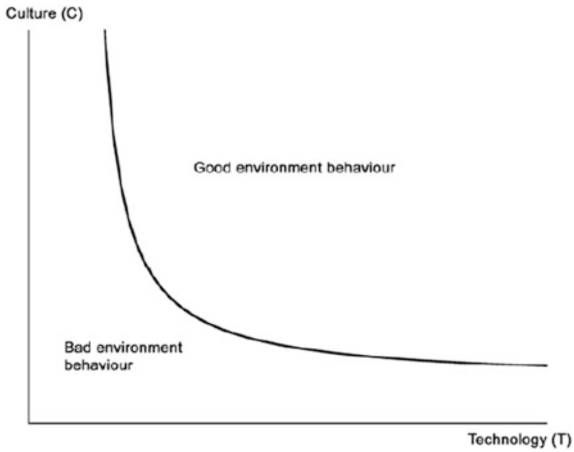

Fig. 7. To have good (environmental, human, etc.) technology, it is necessary to upgrade technology and culture (knowledge and deontology)

5 Proposal

The highlighted important role of Soft Skills in Design Education can be the inspiration to introduce some relative contents into Design Education courses. Table 6 shows some proposals made.

Table 6. Proposal of soft skill contents in design education courses

Phase	Examples of soft skills
Orientation (before university)	Acquisition of a method to study Information about different faculties Role of Soft Skills in Design Education
Bachelor	Introducing Soft Skills into Design Education Engineering Design Deontology Elements Human aspects of technology The designer's responsibility Flexibility in design activity
Master	Courtesy in the relationship with colleagues Interpersonal things: contributing to create a Positive attitude to conduct good environmental work Professionalism in the way to face different situations of design activity Awareness of the need to balance a psychological situation between two opposite and both negative situations Creativity, i.e. the ability to create and to evaluate new ideas
Continuing education	More in-depth study about some of the above-mentioned arguments

6 Conclusions

The authors believe that Soft Skills play an important role in all engineering activity fields and, consequently, in Engineering Education. The present paper analyzes some aspects of Soft Skills in an important part of Engineering Education, i.e. Design Education. Some years ago, one of the authors (Edoardo Rovida) applied some of the above-mentioned knowledge to the course "Methods of Mechanical Design" at the Politecnico di Milano.

For more in-depth information about Soft Skills, see also [11–16].

The authors are members of an Italian organization called "Officina della Conoscenza" (Workshop of Knowledge). Giulio Zafferri is a founder member: this organization and, of course the authors, are involved in many educational aspects (e.g. the course "Development of Personal Acumen through Soft Skills" at the Order of Engineers in Milan) and are willing to cooperate with interested colleagues and institutions.

The authors are currently preparing a book whose temporary title is "Think If".

References

1. Robles MM (2012) Executive perceptions of the top 10 soft skills needed in today's workplace. Bus Commun Q 75(4) 453–446
2. Asimow M (1962) Introduction to design. Prentice Hall
3. Rovida E (1997) Customer involvement as contribution to the "Design for Costs". In: International conference on engineering design ICED 97 Tampere August 19–21
4. Rovida E (1996) Alcune riflessioni sulla progettazione di un corso di aggiornamento Direzione del personale 2/3
5. http://jamesclear.com/eisenhower-box. Last visit 19.03.2018
6. Biggioggero GF, Calabrò S, Menzio G, Rovida E (2003) Il progetto e la memoria Politecnico di Milano Dipartimento di meccanica
7. Altshuller G (1996) And suddenly the inventor appeared Technical innovation Center Worchester
8. Michelewicz Z, Fogel DB (2000) How to solve it: modern heuristic. Springer, Berlin
9. Orloff A (2002) Grundlagen der klassischen TRIZ. Springer, Berlin
10. Chakrabarti A, Sarkar P, Leelavathamma B, Nataraju BS (2005) A functional representation for aiding biomimetic and artificial inspiration of new ideas Ai Edam 19 (02)
11. https://www.kobo.com/it/it/ebook/the-strategy-pathfinder. Last visit 21.03.2018
12. Bennıs W (1989) The habits of highly effective people. Simon and Schuster
13. Negroponte N (1996) Being digital Vintage book, New York
14. Goleman D (2004) Primal ledership. Learning to lead with emotional intelligence. Harvard business Review Press
15. Robinson K (2009) The element. How finding your passion changes everything. Penguin Group
16. Covey SR (2006) The speed of trust. Simon and schuster

Which Didactic Methodology Is the Most Appropriate for My Subject?

J. López(✉), I. Herrero, P. Jimbert, M. Iturrondobeitia, and N. Toledo

Faculty of Engineering in Bilbao, University of the Basque Country (UPV/EHU), Paseo Rafael Moreno "Pitxitxi" nº 3, 48013 Bilbao, Bizkaia, Spain
jaime.lopez@ehu.eus

Abstract. Which didactic methodology is the most appropriate considering the contents of my subject? What are the activities that suit my possibilities? What evaluation method is fair and formative for the competences of my subject? The teaching team of the subject of Graphic Expression in the Engineering of the Engineering School of Bilbao (UPV/EHU) decided to act in order to improve the teaching-learning process. For this purpose a restructuring of the entire subject that would be carried out by making a disruptive approach to redesign the subjetc was thought. The main objective was to capture the students' interest in the subject and, as a result, improve the success rate. For this purpose, a restructuring of the whole subject was sought by applying educational methodologies and updated technologies according to the new requirements by the students and the teachers. The main idea is to give importance to the knowledge and ability of extracting the necessary data to represent graphically the reality, identifying the real problem posed with a method of theoretical resolution. At the same time, to minimize the importance of memorizing steps, data can be consulted in the bibliography. With the objective of implementing the main ideas above, the teaching team inquired about pedagogic models, and found that the Flipped Classroom suited the necessary characteristics, mainly the effective use of time in the classroom. Finally, it is important to notice that the creative process followed has allowed the teaching team to unify criteria and agree on results. This way, all members have felt involved in the project.

Keywords: Graphic expression in engineering · Didactic methodology · Teamwork · Creativity · Flipped classroom

1 Introduction

Flipped Classroom, Project Based Learning (PBL), Cooperative Learning, Gamification, Problem Based Learning, Design Thinking (DT), Thinking Based Learning (TBL), Competency Based Learning, Multiple Intelligences, Proactive Tutoring, Kolb's Learning Cycle, Just-in-time Teaching (JiTT), etc.

Which didactic methodology is the most appropriate considering the contents of my subject? What are the activities that suit my possibilities? What evaluation method is fair and formative considering the competences of my subject?

F. Cavas-Martínez et al. (Eds.): *Advances on Mechanics, Design Engineering and Manufacturing II*, LNME, pp. 696–704, 2019.
https://doi.org/10.1007/978-3-030-12346-8_67

The teaching team of the subject of Graphic Expression in the Engineering of the School of Engineering of Bilbao (UPV/EHU) decided to act to improve the teaching-learning process. The approach was a full restructuring of the entire signature, with the mentality of making a disruptive approach to the design of the subject was pursued. At the same time, the team considered the application of educational methodologies and updated technologies according to the new requirements by the students and the teaching staff [1, 2].

The process of this action was addressed using creativity techniques such as Brainstorming, Cause-Effect Diagram or Method 6-3-5 [3, 4].

The expected result of this action was to obtain a more participatory teaching methodology that would motivate the students and the teaching staff, and consequently, improve the success rate of the subject.

It was also expected to minimize the impact of external agents, such as teacher changes, changes in class lists, calendar, etc.

The context of this annual subject is the following: 9 credits in first course, it is common for the Degrees in: Electrical Engineering, Industrial Electronics and Automation Engineering, and Mechanical Engineering. It has bilingual character, is taught in Spanish and in Basque to more than 600 enrolled students. The teaching team consists of 5 teachers who dedicate most of the teaching to this subject and another 2–4 teachers that only partially lecture this subject.

2 Motivation

The results of the examinations show that students are not able to apply the same concepts to different situations, hence, it is clear that the students do not understand the basics of the subject. Using the usual type of exercises from previous calls, two exercises with the same geometry were proposed (Fig. 1).

The exercise on the left deals with the basic management of the system of representation. The theory of technical drawing can be directly applied in this exercise. In this exercise, real data related with the geometry shown in Fig. 1 is requested.

The exercise shown on the right side of Fig. 1 is an exercise of practice application. The exercise describes a molding machine to manufacture the geometry described in the geometry of the exercise on the left. The description of the geometry of the matrix was requested: views and dimensions.

The solution in both exercises was the same, but many students who solved the first exercise were not able to solve the second exercise.

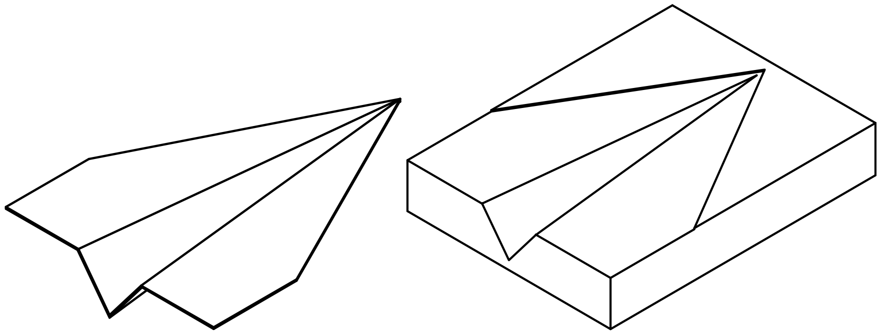

Fig. 1. Geometry of the exercises

There is also a lack of motivation of the students, evidenced by the attendance to the classes and the lack of rigor in carrying out the tasks that are scheduled weekly.

The students are 1st year in school and come from different centers and studies. In some cases with low expectations, little previous motivation and no vocation to the profession.

The result is that, in this subject, we have a very low success rate compared to the rest of the subjects of the same course and same grades.

3 Methodologies

The tasks to be carried out to develop the project were:

- T1. Team training in creativity techniques. The process was made using creativity techniques, therefore, it was necessary that the entire team had knowledge of this way of working.
- T2. Analysis of the detected problem. The causes of the detected problems in the subject were analyzed exhaustively to clearly determine their origin.
- T3. Search for ideas in the different fields of action that allowed solutions to the detected problems.
- T4. Identification of the priority areas and selection of the actions to be implemented considering their relevance and impact in achieving the objective.
- T5. Study of success cases in active methodologies that adjust to the selected actions and that are from areas related to the subject.
- T6. Design of the subject. Definition of the different aspects that comprise the subject: methodology, contents, documentation, evaluation, etc.

The scope of actions is the factors on which the team has the capacity to act and modify, covering the design, development and evaluation of the subject. The factors that can not be intervened, such as financing, student selection, material resources, etc., were eliminated from the improvement process.

Specifically, improvements will focus on the syllabus of the subject, the teaching methodology, documentation and evaluation.

The syllabus is given in the accreditation card of the degree, but you can modify the time dedicated to each of the topics depending on the chosen methodology.

It is intended to progressively implement the teaching methodology based on active methodologies, currently used in computer practices, to the whole subject.

The documentation is to be unified among the different groups and languages, and to update the supports of the information (videos, web, etc.).

Two of its members leaded the formation of the team in creativity techniques. These two members have extensive experience imparting this type of training and facilitate the development of different creativity techniques [5].

Ideas on how to guide the previous objectives were obtained through a Brainstorming. This group creativity technique was developed by Alex Osborn in the 30s and published in 1963 in the book "Applied Imagination". Brainstorming is the foundation on which most creativity techniques are based [3, 4].

Many ideas where related with the need of identifying the causes of the failure of the students, and therefore the teaching staff. With these results, the performance framework of the improvements was established.

The possible causes of the problem were searched by means of a Cause-Effect Diagram, proposing as effect the central idea obtained in the previous Brainstorming, and as causes the four areas of action: subject's syllabus, teaching methodology, documentation and evaluation. Developed in 1943 by Kaoru Ishikawa, it is an effective tool to study processes and situations, and to develop a data collection plan [3, 4].

Once the possible causes of the problem were defined, solutions were sought using the 6-3-5 method, a group creativity technique elaborated by Warflied (Bernd Rohrbach en 1968) that is characterized by being reflexive [3, 4].

At the same time, the very first day of class an anonymous test of previous knowledge was passed to all 1st year students.

In addition, an opinion poll on the teaching of the graphic expression subject was prepared to ask the students about the documentation preferences and teaching methodology for the development of the classes. This poll was made through online survey software on the last days of the course, outside of class, also to all students in 1st grade.

The selection of ideas to be implemented was done through a multi-criteria matrix to be as objective as possible. This is a support tool for the decision-making process developed in the 60s, and from the second half of the 1970s began to experience an important development, becoming a scientific tool [3, 4].

The identification and the definition of the criteria to evaluate the ideas and their relative weighting was a subject of long discussion. Finally, the most decisive criterion would be the motivation of the students and of the teaching staff (Table 1).

Table 1. Criteria

Nº	Criterion	Weighing
CR1	How important is it for you that students acquire the knowledge of the subject?	9.0
CR2	How important is it for you that the students are motivated with the subject?	8.8
CR3	How important is it for you that the teacher is motivated with the subject?	8.2
CR4	How important is it for you that the actions can be applied in the short term?	5.0
CR5	How important is it for you that actions need few material resources?	1.6
CR6	How important is it for you that the actions need little dedication from the teaching staff?	3.4

In view of this evaluation, the most valued ideas were taken, incorporating also those ideas that completed them with little added effort. All of them gave rise to the innovation to be implemented.

4 Results

As previously explained, ideas on how to guide the previous objectives were obtained through a Brainstorming. Many ideas where related with the need of identifying the causes of the failure of the students, and therefore the teaching staff. The ideas on how to guide the previous objective were:

- How to analyze the spatial capacity of Engineering students and what minimum requirements of spatial capacity are necessary to study Graphic Expression in Engineering.
- Analysis of the "native computer" student body in the understanding and realization of Graphic Expression documents in Engineering.
- The reason for the failure in the teaching of Graphic Expression in Engineering.
- Deficiencies that the students present in the Graphic Expression in Engineering. Especially in the realization and interpretation of plans.
- Criticism and evaluation of the teaching methodology by the teaching staff.
- Assessment of the previous works implemented on research in teaching methodologies.
- Contact students to detect difficulties: surveys of students from previous courses, periodic meetings, brainstorming with students, etc.
- Compilation of all information and analysis. Design of future steps.

The possible causes of the problem were searched by means of a Cause-Effect Diagram proposing, as effect the central idea obtained in the previous Brainstorming, and as causes the four areas of action: subject's syllabus, teaching methodology, documentation and evaluation.

In a summarized way (Table 2), several causes were related with little work on basic concepts and scarce continuous work.

Table 2. Result of the cause-effect diagram

Causes of failure in graphic expression	
Exams	*Methodology*
Level too high: – Excessively complicated assemblies. Scarce time Statements: – Statements without descriptive memory	Waste of time delineating No description of assemblies is made: – Students are not asked – It is not given to the students Abuse of the slides: – The reference of the level of demand is lost The students do not do the weekly tasks Lack of motivation: – Little attendance to class
Syllabus	*Documentation*
Very extensive agenda: – The axonometric system seems stuffed It goes too deep in some topics	The students do not bring documentation to class: – No notes are taken The student does not complete the documentation after class The consultation documentation is very scattered: – The slides are mute – Very varied books

The conclusion obtained from the Cause-Effect Diagram confirms that a complete restructuring of the subject is necessary, and that the fields of action covered cannot be treated independently if one wants to be free to propose something novel.

Once the possible causes of the problem were defined, solutions were sought using Method 6-3-5. Once analyzed and grouped similar ideas, 40 ideas were obtained:

- 2 Ideas on the agenda
- 24 Ideas on methodology
- 10 Ideas on documentation
- 4 Ideas on the exam

At the same time, an anonymous test of previous knowledge was pass to all 1st year students, with 397 responses. One of the most striking conclusions is that a high percentage of students have previous drawing training (91.4%), however, few consider to be well prepared (29.2%).

In addition, an opinion poll about the teaching of the graphic expression subject was also passed, asking the students about the documentation and methodology preferences for the development of the classes, obtaining 125 responses. The most striking conclusion was that they preferred classical methods, that is, that teachers explain and make examples in class (72%) and paper documentation (60%).

The selection of ideas that would be implemented was made through a multi-criteria matrix. The criteria for evaluating the ideas and their relative weighting are shown in Table 1. The five best valued ideas were about teaching methodology and are shown in Table 3. In addition to the most valued ideas, other related ideas are incorporated, and they only entailed a small added effort.

Table 3. Results of the selection of ideas

Assessment	Ideas
Best valued ideas	
324	Make sheets of drawings and exercises in pairs or teams and correct them by pairs following some correction guidelines. To motivate, raise it as "contest or game" and/or value it with a note
320	Explain with practical examples in class
310	That the students generate tutorials of Solid Edge (CAD software), so that they use it of consultation in the works and in the examination
301	Photo Safari. That the students look for examples of surfaces, sets, etc. and take pictures
298	Draw pieces or sets based on real physical models that can see and touch
Related ideas	
293	Work on the visualization of objects using computer generated models
288	Take every four months a complex problem that serves as the common thread of the whole agenda
282	CAD Documentation: find each course a set (better if it is physical) to work on in the classes. The faculty would present the documentation that will guide all the steps for the elaboration of the whole project. Making of assembly and cutting plans, and assembly plans, as well as the explanatory documentation
275	Visiting companies where CAD tools are used to motivate students and see the usefulness of the subject. Select students through work related to the visit
257	Raising "all" the subject, or a high percentage, as a resolution of a complete project, covering the minimum knowledge of the subject
252	Write the statements of the exercises and sheets of drawing with more enthusiasm, so that they seem more real and that the students have the feeling that they are useful for something
248	Go from big to small. Begin watching sets and their operation, to go down to the details, unions, tolerances, etc.

5 Discussion

The statement of the innovation to be implemented would be: take a real complex situation that serves as a thread to address various issues.

The starting point would be an image of a real situation (photo or virtual), and then make the graphic representation of a specific part. This graphic representation poses some problems as representation of surfaces, views, intersections, etc. Data such as distances and angles can also be request. As well as propose redesigns, add new elements, etc. [6]

This starting situation raises the need to apply the theoretical knowledge that would be the contents of the subject's syllabus.

In order to see various applications and to include all the sections of the agenda, several different starting situations will be proposed.

The main idea is to give importance to the knowledge and ability of extracting the necessary data to represent graphically the reality, and identifying the real problem posed with a method of theoretical resolution. At the same time, to minimize the importance of memorizing steps and data that can be consulted in the bibliography.

> "The teacher guides and trains the student to" link "information. Learning is deeper when it connects, when it knows the genealogy of the specific content and, not only that, but when it is able to put it in contact with other content, different and also specific." [7]

With the objective of implementing the main ideas above, the teaching team inquired about pedagogic models, and found that the Flipped Classroom suited the necessary characteristics, mainly the effective use of time in the classroom. As it is known, the Flipped Classroom transfers certain aspects of learning outside the classroom, in order to use class time for the development of cognitive processes of greater complexity than favor meaningful learning [7, 8].

This practice enhances the practice of knowledge and the development of other processes of acquisition, analysis, etc., as well as the teachers' own experience, enriching the interaction between teachers and students.

6 Conclusions

The work dynamics put in place, as a consequence of the creative process carried out, minimizes the impact of external agents such as shared faculty, changes in class lists, calendar, etc. It also favors the incorporation of new faculty to the methodologies proposed.

The subject is restructured to obtain a teaching methodology that motivates the students and the teaching staff. As a consequence, the success rate of the subject may improve, based on a more participatory methodology.

The main idea is to give importance to the knowledge and ability of extracting the necessary data to represent graphically the reality, and identifying the real problem posed with a method of theoretical resolution. At the same time, to minimize the importance of memorizing steps and data that can be consulted in the bibliography.

In short, the restructuring of the subject is focused in making the students independent to seek information and solve arising problems.

The changes in society alter the educational dynamic and the synergy of learning. The current faculty must renew, strengthen or modify their competences not to be left behind. The teaching-learning process is no longer reduced to a mere unidirectional transmission of data, but to a purely creative mission. Information has multiplied and, therefore, access to knowledge has been facilitated. Currently it is more about an analysis of the content, of teaching and training to connect, rather than to accumulate. The faculty ceases to be a transmitter to become a guide, guiding the students to the relevant contents.

The student survey on teaching revealed that the vision of the students is not the same as that of the teaching staff. All the contributions that come from the students through different media are really valuable to achieve improvements.

A pedagogical model like Flipped Classroom is needed in order to use class time for the development of cognitive processes of greater complexity that favors meaningful learning.

Finally, it is important to notice that the creative process followed has allowed the teaching team to unify criteria and agree on results. In this way, all members have felt involved in the project.

References

1. Biggs J, Tang C (2011) Teaching for quality learning at university. What the student does (4th edn). McGraw-Hill, Maidenhead, England. ISBN: 978-0-33-524275-7
2. Beesley A, Apthorp H (eds) (2010) Classroom instruction that works, second edition: Research report. McRel International, Denver, CO
3. Tanner D (2009) Igniting innovation: through the power of creative thinking. Myers House, LLC., Editorial. ISBN 9780972190015
4. Betancourt Morejón J (2008) Atmósferas creativas 2: Rompiendo candados mentales. Editorial El Manual Moderno. ISBN: 9786074481556
5. Caro JL, López J (2010) (eds) (2010) Manual - Guía del curso de Diseño Industrial y Desarrollo de Producto. Bilbao. ISBN: 978-84-693-9063-4
6. Toledo N, López J, Jimbert P, Herrero I (2016) A multidisciplinary PBL-based learning environment for training non-technical skills in the CAD subject. In: Fischer X, Daidie A, Eynard B, Paredes M (eds) Book research in interactive design. Mechanics, design engineering and advanced manufacturing, vol 4. Springer, Berlin, pp. 607–612. ISBN: 978-3-319-26121-8. https://doi.org/10.1007/978-3-319-26121-8
7. Santiago R, Díez A, Andía LA (2017) Flipped classroom. 33 experiencias que ponen patas arriba el aprendizaje. Editorial UOC, Barcelona, Spain. ISBN 978-84-9116-975-8
8. Anderson LW, Krathwohl DR (eds) (2001) A taxonomy for learning, teaching and assessing: a revision of Bloom's taxonomy of educational objectives. Allyn & Bacon. Boston, MA (Pearson Education Group)

Integrated Approach to the Innovation of Technical Drawing Teaching Methods

G. Baronio[1], I. Bodini[1], A. Copeta[1], L. Dassa[1], B. Grassi[1], R. Metraglia[1], B. Motyl[2], D. Paderno[1], S. Uberti[1], and V. Villa[1(✉)]

[1] Università degli Studi di Brescia, Via Branze 38, 25123 Brescia, Italy
valerio.villa@unibs.it
[2] Università degli Studi di Udine, Via delle Scienze 206, 33100 Udine, Italy

Abstract. Motivations for the research activity on teaching methods could be listed as: institutional duty; reduction of evaluation costs; establishing convenient relationships between teaching, research and publications; developing educational programs for non-academic learners; consolidating learning outcomes. Teaching is the most commonly recognized mission of university, and evaluation has a cost in terms of time and resources, both precious: at least a portion of the exam, the one concerning factual knowledge, may be done in economies of scale. The most of basic technical drawing teachers works with very large classes and faces the dilemma of choosing what to sacrifice among teaching quality, research projects, earning opportunities, personal interests, etc. A possible partial solution to such a dilemma is to work on projects aimed at teaching innovation, so to create convenient relationships between teaching, research and publications. A further consequence of lowering the cost of evaluation would be to make cost effective a more tests and, consequently, to achieve less temporary learning. Not just simple notions but also skills and abilities. In this paper the authors presents a structured synthesis of teaching innovation experiences of a ten-year span. Over time, they were divided into four integrated directions: definition of prerequisites, expected outcome evaluation grids; authentic assessment methods; teaching and learning tools.

Keywords: Technical drawing · Design methods · Engineering education · Learning techniques

1 Introduction

Motivations for the research activity on teaching methods are several. They could be listed as: institutional duty; reduction of evaluation costs; establishing convenient relationships between teaching, research and publications; developing educational programs for non-academic learners; consolidating learning outcomes.

Teaching is the most commonly recognized mission of university: we cannot escape trying to do more and better.

Moreover, new budget cuts will come and, at the same time, new unexpected competitors will appear. Evaluation has a cost in terms of time and resources, both precious. The traditional exam setup follows diseconomies of scale: examining twice

F. Cavas-Martínez et al. (Eds.): *Advances on Mechanics, Design Engineering and Manufacturing II*, LNME, pp. 705–713, 2019.
https://doi.org/10.1007/978-3-030-12346-8_68

the candidates takes more than twice the time. This is a crucial aspect, often underestimated. Simply enough, evaluators need to coordinate, replicate structures, reiterate checks, etc. We got used to this and we accept it as inevitable. However, at least a portion of the exam, the one concerning factual knowledge, may be done in economies of scale [1].

The most of basic technical drawing teachers works with very large classes and faces the dilemma of choosing what to sacrifice among teaching quality, research projects, earning opportunities, personal interests, etc. Extraordinary people who can balance all these things exist, but they are indeed extraordinary exceptions [2]. A possible partial solution to such a dilemma is to work on projects aimed at teaching innovation, so to create convenient relationships between teaching, research and publications [3].

Moreover, the increasingly pervasive globalization of industrial production has also reached the supply chain level of the subsystems and consequently the small and medium-sized enterprises that made the typical Italian industrial base, with a delay of about ten years compared to large industry. The staffs of technical areas are realizing that they are drawing "in local dialect", finding problems to carry out the supply of products and their components. In the search for junior engineers, the request for skills in the GPS/GD&T field is increasing. As a consequence, "profit" opportunity in company training for technical drawing opens up. However, it is important to note, that the type of corporate learner has many characteristics opposed to the academic learner; those who pay for their training are not interested in a final grade, while they often ask the initial and final levels of specific competences to be assessed objectively. With regard to what has just been said, it follows that an essential element of this approach is the development of objective evaluation tools. In some cases, the objective evaluation tools favour the reduction of the evaluation cost.

If we gather our thoughts to when we were under examination, we realize that we remember better notion and concepts that we had to use to overcome those exams (there are studies according to which the 80% of the concepts learned are forgotten about 15 months after the exam [4]). Furthermore, each teacher has the experience to observe how much attention students have during exam than during traditional lessons or lab activities. A further consequence of lowering the evaluation cost would therefore be to make cost effective a more number of test and, consequently, to achieve less temporary learning. Not just simple notions but also skills and abilities.

In this paper the authors presents a structured synthesis of teaching innovation experiences of a ten-year span. Over time, they were divided into four integrated directions: definition of prerequisites [5, 6], expected outcome evaluation grids [7, 8]; authentic assessment methods [9]; teaching and learning tools [10–15].

2 Available Tools

In the last ten year, in Brescia, we have developed different tools for an integrated approach to innovate the methods to teach technical drawing.

2.1 Exercise Book to Fulfill Pre-requisites

In the period between 2003 and 2007 students was given the possibility to attend revision classes to fulfill the general gaps in technical drawing, especially for those students coming from non-technical schools enrolled in degree courses of the industrial engineering area.

The workbook [5] published in 2007 with the ADM is a collection of tutorial exercises that can be carried out with minimal teacher intervention. The experience has been positive and currently, even if it is no longer possible to conduct those classes, the workbook is strongly recommended during the introductory lesson of the basic courses.

After ten years the tool should be revised and, in this case, it would be interesting to rigorously evaluate the effectiveness of this tool in order to publish the results.

2.2 The Adventures of Mr. Clumsey, The Engineer

"The adventures of Mr. Clumsey, the engineer" is a comic story in 12 episodes in which a clumsy junior engineer is facing the typical problems of a technical office, as shown in Fig. 1.

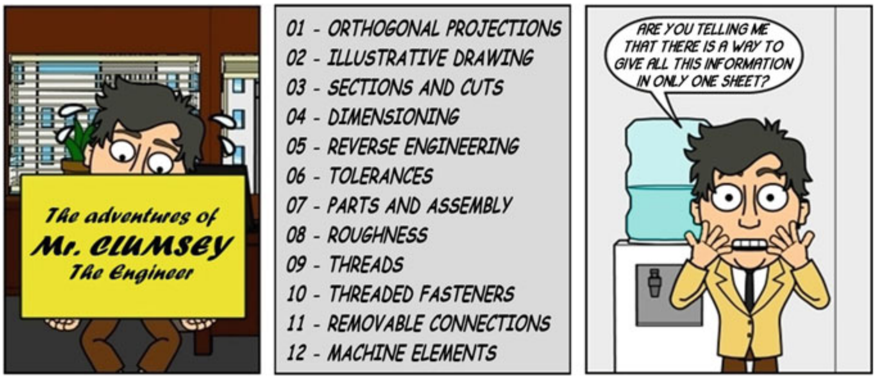

Fig. 1. Mr. Clumsey, the engineer

The strips were developed with "Bitstrips" which allowed to develop rather long stories and to export them in image format, before being incorporated into Facebook. Some students of the Industrial Design Degree Course were involved as trainee.

All the strips are available at: https://goo.gl/PmcgUk. The purpose of the project is to support students' motivation by introducing in an entertaining way twelve topics of technical drawing.

The experience, from the chair point of view, is that, after having made the students chuckle, even the teacher plays a better lesson.

The effectiveness of this tool has been demonstrated with some experiments reported in [6].

2.3 Technical Drawing Test

To carry out closed-questions tests is not something new, but to implement this type of test means to face the following problems: (i) if there are few questions, it is easier to memorize the answers than to learn the matter; (ii) three types of inconveniences are possible if students are requested to propose new questions, in order to produce a lot of queries: (a) pedestrian implementation of trivial questions, (b) excessively specific questions, (c) more or less sophisticated self-responding questions; (iii) it is necessary to be able to identify and manage questions with errors or low performance; (iv) it is necessary to be able to evaluate the performance of every single question, in fact, to propose effective questions is less easy than you think; (v) if the questionnaire is in paper form, it is completed quickly but the cost of correction is high; (vi) if the questionnaire is on-line, there are computer security problems and problems with the number of workstations.

After about 6 years of paper questionnaires in which a few hundred of industrial technical design questions were developed, four years ago we implemented an on-line questionnaire, shown in Fig. 2, within the MOODLE (Modular Object-Oriented Dynamic Learning Environment) platform. This questionnaire is carried out in asynchronous mode: there are twenty workstations and a group of one hundred candidates fill out a questionnaire of thirty questions in two hours. Doubling the number of queries, the required time is much less than the double.

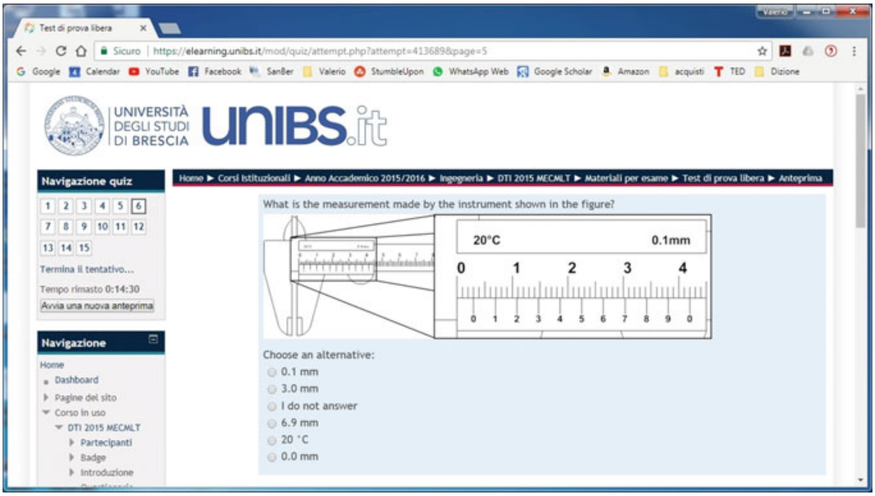

Fig. 2. On-line questionnaire implemented in the Moodle platform

Among all the developed instruments, this has had the greatest impact on the reduction of the evaluation cost. In particular, from the very first developments, it was clear that a transition from diseconomy to economy of scale has happened.

2.4 Technical Drawing Learning Tools (TDLT)

Around two years ago, we developed an interactive presentation for the self-study of technical drawing and mechanical machining fundamentals. The application, developed for Windows, Mac OS X and Android, is shown in Fig. 3. It is based on the assumption that apparently dogmatic rules can be made clearer, almost obvious, by highlighting the close relationship between dimensioning and machining process. The underlying concept is to understand how the machine works in order to understand how to communicate the morphological desiderata.

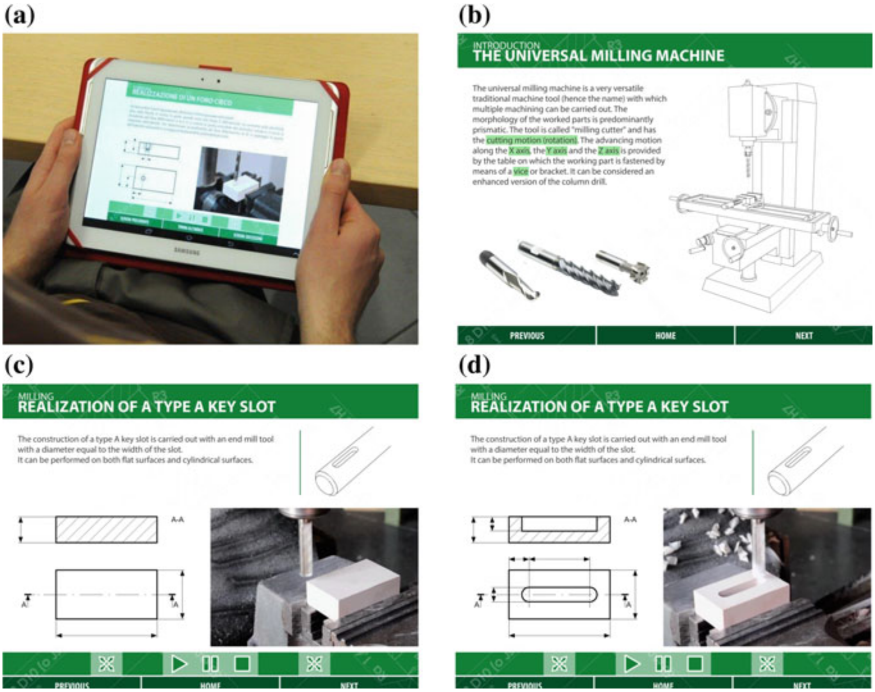

Fig. 3. Interactive application for self-study of technical drawing and mechanical machining fundamentals. **a** The application. **b** The general description of the milling machine. **c** The initial phase of a milling. **d** The final phase of a milling

Each machining is presented through an interactive sheet, where the schematic drawing of the machine tool gets animated when the mouse hovers over prescribed keywords in the description (parts of the machine, rotation or translation axes).

Then, for each machining a sheet with two synchronized videos is displayed: on one side, the video shows the machining process, and on the other side an animated technical drawing shows the piece dimensions only as soon as the machine requires them. The dimensions are also animated so to “guide” the tool motion.

Some tests to evaluate the effectiveness of the tool on the students have already been carried out, and the results have been published in [10, 11].

At the moment we are negotiating with an editor to publish the tool in connection with textbooks.

2.5 Essay Questions

The drawing of a part extracted from the drawing of an assembly is a widespread examination method, but it has the big limit of correctly evaluating only those examined that obtain a good or an excellent evaluation. In fact: (i) it is only possible to correctly represent the morphology of the part with the minimum number of views and sections when its morphology is perfectly understood; (ii) you can correctly dimension a drawing only after perfectly representing views and sections; (iii) tolerances can only be correctly indicated after a perfect dimensioning.

To overcome these limitations, we decided to restructure the examination procedure so that individual skills can be assessed independently through open questions. An example is shown in Fig. 4: Fig. 4a shows one question of the test, in which students have to complete the draw, marking the theoretically exact dimensions and indications; Fig. 4b shows one correct answer, available on-line.

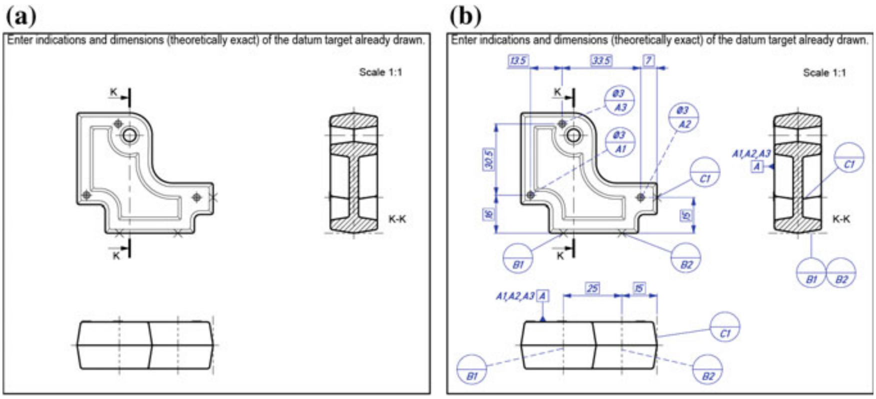

Fig. 4. Example of an open answer test

3 Implemented Methods and Results

The research activities have been structured in four coordinated directions: (i) definition of pre-requisites; (ii) definition of expected proficiency grids; (iii) tools and methods for objective evaluation; (iv) tools to support teaching and learning.

3.1 Definition of Pre-requisites

The definition of prerequisites is often overlooked: the ministerial programs for the middle school are more than enough to start an engineering or architectural path, but the new entrants completely lack of the most elementary notions [8, 9]. However, it is not possible to start teaching from the very beginning and, at the same time, it is necessary to enable the most lacking students to make up their gaps, therefore a tutorial exercise for the recovery of prerequisites has been developed [5].

3.2 Definition of Expected Proficiency Grids

Once the minimum level of competence have been defined for each course, it is possible to define and articulate the levels of expected competences at the end of each training activity.

In our experience, in order to properly develop assessment systems with closed questions and open-answer questions, we thought necessary to develop a multi-layered grid of expected skills to ensure consistent and repeatable evaluations [7].

The type of grid adopted is the one provided for the EQF (European Qualifications Framework). This instrument considers three aspects: knowledge, skills, and competences.

In elaborating the grid we thought about drawing in its double nature: instrument and language, as it happens also for writing.

The EQF was recommended in 2008 by the European Union and theoretically should be developed by 2010 for each of the subject taught. Now, in the light of the latest regulations, the grid should be thoroughly revised: it is on the agenda but we would like to share the work with a larger group.

3.3 Tools and Methods for Objective Evaluation

Once the expected articulation and levels of competence have been defined, it is possible to choose and define the most suitable objective evaluation methods and tools, as presented in Paragraph 2.

In a nutshell, objective evaluation requires that we first define: who, what, how, where, when and why to evaluate.

The application of the Bloom Taxonomy (a fundamental instrument in Education Science [14, 16]) is useful in this context. In summary it says that: (i) to understand a concept, you must first know it; (ii) to apply a concept, you must first understand it; (iii) to analyze a concept, you must first be able to apply it; (iv) in order to judge the value of knowledge, it is first necessary to analyze it; (v) to create something new you first need to have judged the values at stake.

In fact, regarding Bloom's taxonomy: (i) you can correctly represent the morphology of the part with the minimum number of views and sections only when you understand the morphology perfectly. (ii) It is only possible to dimension correctly after perfectly representing views and sections. (iii) Tolerances can only be correctly indicated after a perfect dimensioning, as already said in Paragraph 2.5.

Possible applications are as follows: (i) closed answer questions for the verification of prerequisites and basics; (ii) open questions for the assessment of individual competences; (iii) carrying out an internship or thesis for the assessment of the independent integration capabilities of several competences.

3.4 Results

Since the introduction of a closed-questions test and an open-answers test, a decrease in the number of students late with their studies has been observed. This happened even if enrolments slightly increased.

4 Conclusions

We believe that the most logical structure to analyze the problem of an integrated approach to the innovation of technical drawing teaching methods is the following: (i) pre-requisites; (ii) expected proficiency grids; (iii) evaluation tools; (iv) teaching tools.

It is important that this structure is agreed upon to the largest extent possible. We are discussing and updating it on the basis of meetings with colleagues in the sector, trying to understand how important it is to harmonize contents and expected levels in technical drawing teaching between the different universities, and who has the authority to promote this activity, and to what extent the four aspects of the proposed integrated approach should be harmonized or standardized.

References

1. Ben-Peretz M, Flores MA (2018) Tension and paradoxes in teaching: implications for teacher education. Eur J Teach Educ 41(2):202–213
2. Hubbard JK, Couch BA (2018) The positive effect of in-class clicker questions on later exams depends on initial student performance level but not question format. Comput Educ 120:1–12
3. Duckworth E (1986) Teaching as a research. Harvard Educ Rev 56(4):481–496
4. Thalheimer V (2010) How much do people forget? Retrieved 26 Feb 2018, from http://www.work-learning.com/catalog.html
5. Baronio G, Villa V (2007) Precorso di Disegno Tecnico Industriale; ADM website (http://adm.ing.unibo.it); Italy. ISBN 88-902096-0-7
6. Metraglia R, Villa V, Baronio G, Adamini R (2015) High school graphics experience influencing the self-efficacy of first-year engineering students in an introductory engineering graphics course. Eng Des Graph J 79(3):16–30
7. Metraglia R, Baronio G, Villa V (2011) Learning levels in technical drawing education: Proposal for an assessment grid based on the European qualifications framework (EQF). In: ICED 11–18th international conference on engineering design—impacting society through engineering design, vol 8, pp. 161–172

8. Metraglia R, Baronio G, Villa V (2015) Issues in learning engineering graphics fundamentals: Shall we blame cad? In: Proceedings of the international conference on engineering design, ICED, 10 (DS 80–10), pp 31–40
9. Scouller K (1998) The influence of assessment method on students' learning approaches: multiple choice question examination versus assignment essay. Higher Educ 4(35):453–472. https://doi.org/10.1023/A:1003196224280
10. Metraglia R, Villa V (2014) Engineering graphics education: webcomics as a tool to improve weaker students' motivation. Res J Appl Sci Eng Technol 7(19):4106–4114
11. Baronio G, Motyl B, Paderno D (2016) Technical drawing learning tool-level 2: an interactive self-learning tool for teaching manufacturing dimensioning. Comput Appl Eng Educ 24:519–528. https://doi.org/10.1002/cae.21728
12. Speranza D, Baronio G, Motyl B, Filippi S, Villa V (2017) Best practices in teaching technical drawing: experiences of collaboration in three Italian Universities. In: Lecture notes in mechanical engineering—advances on mechanics, design engineering and manufacturing (pp 903–913)
13. Fredricks JA, Blumenfeld PC, Paris AH (2004) School engagement. Potential of the concept, state of the evidence. Rev Educ Res 1(74):59–109. https://doi.org/10.3102/00346543074001059
14. Kahu ER (2013) Framing student engagement in higher education. Stud High Educ 5(38):758–773. https://doi.org/10.1080/03075079.2011.598505
15. Violante MG, Vezzetti E (2016) Guidelines to design engineering education in the twenty-first century for supporting innovative product development. Eur J Eng Educ 6(42):1344–1364. https://doi.org/10.1080/03043797.2017.1293616
16. Airasian PW, Cruikshank KA, Mayer RE, Pintrich PR, Raths J, Wittrock MC (2000) A taxonomy for learning, teaching, and assessing: A revision of Bloom's taxonomy of educational objectives, by Lorin W. Anderson e David R. Krathwohl, Allyn and Bacon. ISBN 978-0-8013-1903-7

Are We Training Our Novices Towards Quality 2D Profiles for 3D Models?

C. González-Lluch(✉) and R. Plumed

Department of Mechanical Engineering and Construction, Universitat Jaume I, Castellón 12071, Spain
mlluch@uji.es

Abstract. In the history-based, feature-based, parametric CAD approach, 2D profile sketches are the basis for 3D models. Fully-constraining profiles is mandatory to create robust profiles. At present, neither CAD applications nor Model Quality Testing Tools usually check whether 2D profiles contain redundant constraints. Besides, our experience shows that novices tend to introduce redundant constraints. We hypothesize that 2D profiles over-constrained with redundant relations are more difficult to edit than those that avoid redundancies. In the present work—and as a first step to demonstrate this hypothesis—an experiment was conducted. Students of the subject "Graphics engineering" were taught on the creation of constrained 2D profiles. Then, they were asked two questions. On the one hand, novices had to identify and reason whether a simple given profile was fully-constrained, over-constrained or under-constrained. On the other hand, they had to identify and point out the types of the constraints. The results showed that in spite that novices received a specific training, roughly half of them failed to say if the 2D profile sketch was fully-constrained and which type of constraints it contained. Furthermore, the results of the second question revealed that more than the half of students did not recognize perpendicularity as a geometric constraint. As future work, we will try to demonstrate whether a reinforced training through simple exercises and a quick and effective feedback, will allow novices to improve the identification and removal of redundant 2D constraints when drawing 2D profile sketches (thus helping to produce robust profiles).

Keywords: CAD model quality · 2D profile sketch · Fully-constrained profile · Over-constrained profile · Under-constrained profile

1 Introduction

Currently, 3D CAD models are an important issue in New Product Development (NPD) process. This fact has influenced the development of the CAD data quality field. "Product data" includes CAD (computer aided design) data, CAM (computer aided manufacturing), CAE (computer aided engineering) and PDM (product data management) among others. Poor data quality management compromises the benefits of history-based parametric feature based on mechanical CAD systems (MCAD), and specifically with the CAD model reuse.

F. Cavas-Martínez et al. (Eds.): *Advances on Mechanics, Design Engineering and Manufacturing II*, LNME, pp. 714–721, 2019.
https://doi.org/10.1007/978-3-030-12346-8_69

High quality models are essential [1]. Contero et al. [1] proposed three levels of quality to classify CAD models: Morphologic, Syntactic and Semantic/pragmatic. The third level (Semantic/pragmatic), considers the CAD model capability for reusing and modification. Reusability and interoperability of a CAD model are the most typical tasks carried out during the product design process. Reusability of CAD models is an important issue to create high quality models. A model is reusable when it allows modifications while it maintains its design intent [2], and if it is simultaneously flexible (facilitate design alterations) and robust [3, 4]. A robust model must allow for changes while must not produce unexpected failures. According to Jackson, et al. [5] up to 48% of CAD models fail after a change is performed. A model is ineffective if its design intent is not maintained when the model is altered [2]. Generally understood, design intent is a CAD model's anticipated behavior when it is altered. Attending to ISO definition, design intent is the, "intentions of the designer of a model with regard to how it may be instantiated or modified" [6]. Models with high quality must reliable allow for modifications while maintaining their original design intent. In terms of training in CAD systems, very few studies have pay attention to students and how to create models which can be easily understood, altered and reused by others [7]. A recent study [8], addresses the reuse of 3D CAD models from the point of view of CAD learning and it takes into account the use of design intent during this learning.

A feature and history-based parametric CAD model builds models on top of 2D profiles—where geometric, dimensional and position constraints are introduced—using modeling operations, and through a model sequence (model tree). Otey et al. [9] present that sketch constraints join to "relationships between modeling operations" and "modeling operations" to embed the design intent in 3D CAD models. However, redundant restrictions don't provide additional information to the intent design. Quality of 2D profile is tightly related to its constraints. Ault et al. [10] showed that constraints can be applied to obtain flexible geometric models avoiding undesirable geometry or topology changes. According to González-Lluch et al. [2], the model is efficient if among other conditions, the design decisions are traceable within the model tree. As non-functional constraints, redundant constraints are inefficient and a type of "missing design intent" error in procedural models [2]. To obtain a robust and quality 2D profile, this must be necessary fully-constrained [11]. A common way to identify the quality of 2D profiles is to quantify their degrees of freedom. A profile which is not fully-constrained has at least one degree of freedom.

While editing the profile, some 3D CAD applications provides some useful training information to students. For example, in case of the CAD 3D SolidWorks® software, it is possible to detect whether a profile is fully constrained since it is been created by observing its line color, which can be configured from the program's configuration menu. Furthermore, a minus sign (−) preceding the profile name appears when the sketch is under constrained. Therefore, this history-based parametric CAD application provides information to user about under and over-constrained profile sketches. However, it should be pointed out that in case of over constrained profile with redundant relations, i.e. repetitive but not incompatible, the application does not provide any warning.

We classify constraints as: dimensional, constraints that associate geometric entities to each other (coincident, concentric, collinear, parallel, perpendicular, tangent, smooth, symmetric, equal, etc.…), position and orientation constraints.

Our experience in teaching novices is that students tend to introduce redundant constraints when 2D profile sketches are created in a 3D model. Users can receive help from user's manuals and Model Quality Testing tools (MQT). Although, as it was shown in a recent study [12]—which examined a representative commercial MQT—these tools provide limited testing and tutoring capabilities. Therefore, we strongly believe that a correct training of novices and a quick feedback are essential for learning. As some researches of the literature show, educators have worked in the incorporation of activities which introduce product data quality concepts like the assessment of CAD models through the development of rubrics [11, 13], and the increase of students' awareness of methodological aspects of CAD model construction using activities or specific exercises [8, 14–16]. Some studies have shown that an early feedback is essential to improve their modeling strategies [17]. In addition, this feedback should be continuous in a formative sense [18].

Our hypothesis is that 2D profiles over-constrained with redundant relations are more difficult to edit than those that avoid redundancies. In a related study, González-Lluch et al. [19] demonstrated that the use of fix constraints (a typical case of a low semantic level constraints) compromises the reusability of the 3D model. Our experience like CAD instructors is that students tend to use redundant relations while creating 2D profiles. We consider that this type of relation prevents easy reuse of CAD models.

To demonstrate the hypothesis that "2D profiles (in 3D models) that contain over-constrained with redundant relations are more difficult to edit than those that are fully constrained, even if they use low semantic constraints", it is necessary to follow several steps. In this work, we present the first step, which consists in conducting an experiment to know if students are capable of: (1) identifying fully-constrained profiles by an example, and (2) if they are able to detect (on the same example) dimensional, geometric, position and orientation constraints. Results show (in spite of students' training) that more than half of the polled students did not give a correct answer.

2 Experiment

One of the learning outcomes of the subject "Graphics engineering" (third course of "Bachelor's Degree in Mechanical Engineering" at Jaume I University) is that students have to apply computer-aided three-dimensional modeling (3D CAD) for the resolution of graphic engineering problems. Throughout the course, students attend both theory and practical classes.

In the beginning of the course, students are introduced to the creation of 2D profiles following the first chapter of [20]. On the one hand, during theory classes, students receive knowledge about constraints. In addition, they learn to distinguish the differences between over-constrained and under-constrained profiles. On the other hand, during lab hours, students are introduced to the use of a 3D CAD application

(SolidWorks®) and specific rubrics to convey quality criteria in Mechanical CAD Systems (assertions maps can be consulted in [11]).

Students are trained to create robust and flexible profiles through easy and simple examples (Fig. 1). To this end, profiles are defined using geometric, dimensional, position and orientation constraints. In order to check the correctness of the constraining process, some changes are proposed on the profiles by editing the figures. The objective is to detect if these changes are allowed and if they result in the new expected profiles, or on the contrary, profiles fail to be recalculated by the CAD application.

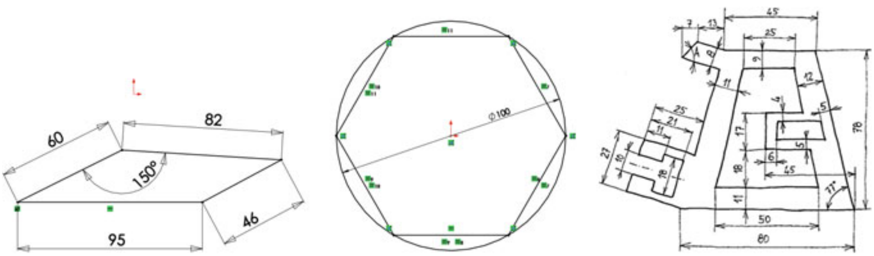

Fig. 1. Profiles created during the first two sessions by students following teachers' guide

In the first midterm exam of the 2017/2018 course, students who coursed this subject had to solve two questions related with constraints. In the first question, students were asked if the profile showed in Fig. 2 was fully-constrained, over-constrained or under-constrained. The answer had to be reasoned.

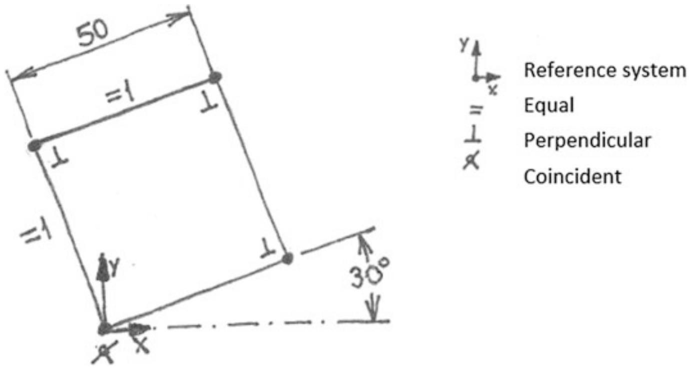

Fig. 2. First question of midterm of "Graphics engineering"

The correct answer, to this first question, is that this 2D profile is fully-constrained. This answer is easily testable to a 3D CAD application (for example Solidworks®).

In the second question, the same Fig. 3 was presented. In this case, students had to identify and point out each type of the constraint. The types of constraints that they were asked to distinguish were: dimensional or geometric (F), position and orientation (P) and the rest (B). In addition, they had to argue their answer.

Considering the discretionary margin of the solution, we consider that this 2D profile includes the constraints of Fig. 3.

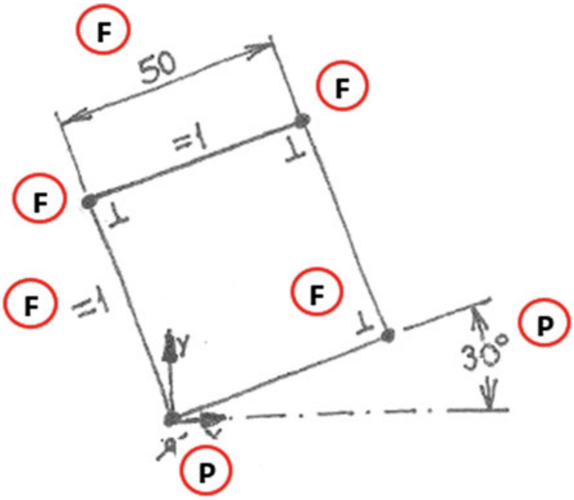

Fig. 3. Considered constraints of the 2D profile proposed in the first question

In the case of the angular restriction (30°), another alternative could be to consider it as dimensional or geometric (F). Instead, we consider this angular restriction as an orientation constraint, because it associates the geometry of the profile with the reference system.

3 Results of the Experiment

A total of 34 answers were collected from the students and considered to the study. All the students answered both questions.

The percentage of students that successfully answered question 1 (fully constrained profile) is shown in Table 1.

Table 1. Data summary from the A question

Question A:	"Fully constrained"	"Over constrained"	"Under constrained"
(%) students	47.1	50	2.9
Total of students	16	17	1

Table 2, shows the percentage of students that successfully answered question 2. In case of incorrect answer, detailed information/failure description is showed in Table 3.

Table 2. Data summary from the B question

Question B:	Correct answer	Incorrect answer
%	47.1	52.9
Total of students	16	18

Table 3. Additional information from incorrect answers from B question

Student answer	% students	Total of students	Additional information
All perpendicular constraints	87.4	14	From this result: 11 students, pointed that perpendicular constraints are of type P 3 students pointed that perpendicular constraints are of type B
2 incorrect perpendicular constraints	6.25	1	The student pointed that 2 perpendicular constraints are of type B
1 incorrect perpendicular constraints	6.25	1	The student pointed that 1 perpendicular constraint is of type B
Equal constraints	18.75	3	The students pointed that the equal constraints are of type B
Dimension constraints	12.5	2	The students don't point one of the dimensions

The results showed that despite students had received specific training with theoretical and practical classes, more than a half of them (52.9%) did not distinguish if the simple 2D profile was fully constrained.

In reference to the results from the second questions, the results show that more than half of participants failed to differentiate between dimensional/geometric and position/orientation constraints. Results from question B (Table 3) show that most of students who had failed the question (87.4%), did not recognized the perpendicular constraints as a geometric restriction, as the majority of students considered these constraints as type P (position and orientation) and B (the rest).

4 Conclusions

In current work, we present a study to prove if we are training our novices towards quality 2D profiles for 3D models. At this end, we have conducted a pilot experiment which shows that students fail to recognize the different types of constraints in the examples proposed. This fact, suggests that students are unlikely to use constraints in a robust and efficient way to avoid redundant constraints. They are also unlikely to choose the more representative constraints to convey the design intent. Our experience shows us that novices tend to introduce redundant constraints even in simple profile sketches, although they have received a specific training and a limited assistance by CAD 3D system.

The results of the experiment showed that half of students could not identify a fully-constrained profile neither the type of constraints that contained. Therefore, we conclude that an improvement of the knowledge of novices is necessary as a previous step to obtain profiles with less redundant constraints. Hence, our natural next step is the preparation of a tool that provides knowledge and early feedback to obtain profiles with less redundant constraints to facilitate the edition of 2D profiles, in 3D CAD models.

Acknowledgements. The research work reported here was made possible by the "Universitat Jaume I" through project UJI-A2017-15 and DPI2017-84526-R (MINECO/AEI/FEDER, UE), project CAL-MBE. The work has been carried out within the framework of an innovative education projects of the UJI.

The authors would like to thank Pedro Company for his support during the experiment.

References

1. Contero M, Company P, Vila C, Aleixos N (2002) Product data quality and collaborative engineering. IEEE Comput Graph Appl 22(3):32–42
2. González-Lluch C, Company P, Contero M, Camba JD, Plumed R (2017) A survey on 3D CAD model quality assurance and testing tools. Comput Aided Des 83:64–79
3. Camba JD, Contero M, Company P (2016) Parametric CAD modeling: An analysis of strategies for design reusability. Comput Aided Des 74:18–31
4. Cheng Z, Ma Y (2017) A functional feature modeling method. Adv Eng Inf 33:1–15
5. Jackson C, Buxton M (2017) The design reuse benchmark report, pp 1–20
6. ISO 10303-55:2005 Industrial automation systems and integration—Product data representation and exchange—Part 55: integrated generic resource: procedural and hybrid representation. https://www.iso.org/obp/ui/#iso:std:iso:10303:-55:ed-1:v1:en. Last accessed 22 Feb 2018
7. Peng X, Mcgary P, Johnson M, Yalvac B, Ozturk E (2012) Assessing novice CAD model creation and alteration. Comput-Aided Des Appl 2:9–19
8. Barbero BR, Pedrosa CM, Samperio RZ (2017) Learning CAD at university through summaries of the rules of design intent. Int J Technol Des Educ 27(3):481–498
9. Otey J, Company P, Contero M, Camba JD (2018) Revisiting the design intent concept in the context of mechanical CAD education. Comput-Aided Des Appl 15(1):47–60
10. Ault HK (1999) Using geometric constraints to capture design intent. J Geom Graph 3 (1):39–45
11. Company P, Contero M, Otey J, Plumed R (2015) Approach for developing coordinated rubrics to convey quality criteria in MCAD training. Comput Aided Des 63:101–117
12. González-Lluch C, Company P, Contero M, Camba JD, Colom J (2017) A case study on the use of model quality testing tools for the assessment of MCAD models and drawings. Int J Eng Educ 33(5):1643–1653

13. Ault HK, Linjun B (2014) Solid modeling strategies—analyzing student choices. Proceedings of the 121ST ASEE annual conference and exposition. Indianapolis, June 15–18, Paper ID #9242
14. Branoff TJ (2004) Constraint-based modeling in the engineering graphics curriculum: laboratory activities and evaluation strategies. Proceedings conference of the engineering design graphics division of the American Society for Engineering Education, Williamsburg, VA, p 132–138
15. Devine KL, Laingen MA (2013) Assessing design intent in an introductory-level engineering graphics course. In: 68TH mid-year conference. ASEE engineering design graphics division, Worcester, pp 59–63
16. Branoff T, Wiebe E, Hartman N (2003) Integrating constraint-based CAD into an introductory engineering graphics course: activities and grading strategies. In: Proceedings of the 2003 american society for engineering education annual conference & exposition, American Society for Engineering Education, Session 1338, pp 1–10
17. Kirstukas SJ (2016) Development and evaluation of a computer program to assess student CAD models. ASEE annual conference & exposition, paper ID 15834, New Orleans, Lousiana, pp 26–29
18. Race P (2015) The lecturer's toolkit: a practical guide to assessment, learning and teaching. Routledge-Falmer, Glasgow, Great Britain
19. González-Lluch C, Company P, Contero M, Pérez-López D, Camba JD (under review) On the effects of the fix geometric constraint in 2D profiles on the reusability of parametric 3D CAD models
20. Company P, González-Lluch C (2013) CAD 3D con SolidWorks® Tomo I: Diseño básico. Publicacions Universitat Jaume I, Castellón

An Analysis of Supervised Practical Work as a Didactic Methodology in the Subject of Graphic Expression in Engineering

L. Diago Ferrer(✉)

Departamento de Ingeniería de Diseño Y Fabricación, EINA, Universidad de Zaragoza, C/María de Luna 3, 50018 Saragossa, Spain
lauradf@unizar.es

Abstract. The following text outlines 9 years of teaching experience in the use of a learning methodology based upon supervised practical work. This practical work formed part of a degree in Product Design and Engineering at the University of Zaragoza, concretely within the subject of Graphic Expression. The teaching methodologies used and the results obtained are described below, as well as the roles played by different participants within the process and the methodological strengths and weaknesses which were identified. The text concludes with proposals for an ongoing debate on how to improve the process.

Keywords: Practice · PBL · Supervised learning · Teaching · Engineering

1 Introduction

With the introduction of the Bologna Process, and the creation of the European Higher Education Area, a strategy was initiated in order to adapt the subject matter of university studies to social demands. Its main objective was to improve student performance and stimulation, placing the learner at the heart of the didactic process [1, 2].

Supervised Practical Work could therefore be defined as a case in point for Project Based Learning, since students are presented with a single set of common problems to resolve. However, whilst students continue to work in groups, the presentation and grading of results is individual [3, 4].

This learning strategy represents an active methodology, in which students learn by doing [5]. This promotes research and allows us to move from a traditional teaching approach (based on lectures and individual study), towards the encouragement of teamwork, thus increasing critical learning capacity and greater interaction between teacher and student [6]. This kind of methodology fits very well within the Bologna strategy as well as in the European Higher Education Area.

As started in the abstract, all teaching experience pertained to a course in Graphic Expression, a constituent subject within an undergraduate degree in Product Design and Engineering at the University of Zaragoza. This is a core subject, comprising 9 ECTS (4.5 theory, 1.5 problem-solving and 3 computer-based practical work), which is taught in the second semester of the first course (1 credit = 10 h). According to figures from recent years, this subject has an average enrollment of 50 students.

F. Cavas-Martínez et al. (Eds.): *Advances on Mechanics, Design Engineering and Manufacturing II*, LNME, pp. 722–731, 2019.
https://doi.org/10.1007/978-3-030-12346-8_70

2 Graphic Expression in Product Design and Engineering

The course of Graphic Expression in Engineering aims to train students to design and graphically represent geometric figures, industrial parts and objects. The universal language employed facilitates understanding by third parties and subsequently the ensuing manufacturing process.

To this end, the subject is taught over a semester and is divided into three parts, with the following hours and percentages of the total of the subject:

– **Theory and problems** (**60 h**). Here, students receive instruction on the main systems of geometric representation (dihedral, axonometric and conical). Class time is divided into four hours per week, three of which correspond to theory (3 h × 15 weeks = 45 h). The remaining hour is dedicated to the resolution of geometrical problems in theory classes (1 h × 15 weeks = 15 h). This accounts for 60% of the overall score and is assessed by way of an exam at the end of the semester.
– **Standardization** (**30 h of personal attention**). Here, the evolution of each student is assessed via closely supervised practical work. This work focusses on the realization of plans through the necessary dihedral views, cuts and sections, which must be properly delimitted, as well as the correct application of current industrial drawing regulations. Similarly, axonometric, cavalier or conical perspectives are employed for the correct interpretation of represented objects. Students must receive guidance and authorization from their professor throughout the practical process, which itself accounts for 30% of the overall mark (via Supervised Practical work or formal examination).
– **Computer Aided Design** (**30 h**). This comprises fifteen two-hour sessions, in which the student is introduced to the management of a 2D and 3D graphic design program. Evaluation is by way of continuous assessment and accounts for 10% of the final grade.

It is intended that students will assess the possibilities of technical drawing as a research tool, as well as the potential scope for standardization as an appropriate convention in order to simplify both production and communication. This leads to a greater appreciation of universal target language in the clear transmission of graphic information.

The course and its expected outcomes reflect the following approach and general objectives:

– Acquisition of basic professional knowledge.
– Ability to learn.
– Capacity for analysis and synthesis.
– Ability to generate new ideas.
– Ability to solve problems.
– Ability to apply knowledge to practice.
– Oral and written communication skills.
– Responsibility at work.
– Motivation for work.
– Ability to work independently.

- Interpersonal skills.
- Concern for quality and improvement.
- Precise, clear and objective expression of graphic solutions.
- Visualization of objects from different positions in space.
- Use of computers for the graphical representation of project plans.

3 Subject Teaching Experience Before 2009/2010

Prior to the Bologna process, the course of Graphic Expression in Engineering consisted of 120 h per year, divided into two parts:

- **Theory and problems** (**90 h**) in which the student learned the dihedral system of geometric representation during the first four months of the course, followed by a further four months dedicated to the study of standardization. Teaching hours were divided into three per week, two of which corresponded to theory (2 h × 30 weeks = 60 h). A further hour served to resolve geometry problems and standardization exercises related to knowledge provided in the theory classes (1 h × 30 weeks = 30 h).
- **Computer Aided Design** (**30 h**). Consisting of fifteen two-hour sessions. Continuous assessment of Standardization was carried out over the course of the second quarter, by commissioning a series of works that the student would carry out based on the explanations received in theory class. Students had the opportunity to develop their work in class, presenting completed projects on a predetermined date. However, as class attendance was not required, most students chose not to attend lectures, instead preferring to carry out the work on their own.

This coursework did not absolve students from the final exam, in which they had to solve a standardization exercise similar to that which they had done during the course, as well as an additional two geometry exercises. The coursework could potentially change the exam grade.

Students, who showed particular interest could attend tutoring sessions for clarification. However, it became clear that few students made use of this opportunity, and those that did waited until the eleventh hour in order to do so. Tutoring consultations, poorly attended during the course, were subsequently inundated in the run-up to the final deadline, leaving teachers too little time to address queries properly.

4 Subject Teaching Experience Since 2009/2010. Supervised Practices

With the launch of the Bologna process in the 2009–10 academic year, a new teaching method was proposed in order to assess the degree of learning in the Standardization aspects of the Graphic Expression course. This method involved a system of Supervised Practical Work.

4.1 Participants

From 2009 to 2010, all students enrolled in the subject participated in the experiment. The average number of students per course was 90, and these were evenly distributed between groups 11 and 12, studying in the morning and the afternoon respectively.

4.2 Supervised Practical Work

The students had to do 6 exercises in A4 format, which were taken from a book of problems on the subject, and whose instructions were given to the students at the beginning of the course. These were then executed over a period of two months. The proposed work consisted of six industrial pieces represented from dihedral or axonometric views, which then had to be resolved from other views, that is, by the cutting, marking, dimensioning, projecting and handling of scales. The main objective was to increase the spatial capacity of the student.

From 2009 to 2010, the structure of the proposed exercises was maintained, although the practical work was different every year. Thus, Exercise 1 was always a simple auxiliary view, and Exercise 3 a double auxiliary view. Exercises 2 and 5 differed from each other in the spatial complexity of their respective pieces, but both of them consisted of the realization of the proposed cuts. Exercises 3 and 6 involved representing the pieces given form an axonometric perspective by means of the dihedral views and cuts that the students had estimated and subsequently in dimensioning of the views.

4.3 Methodology

Exercises were handed in groups of three, so that there were two installments of work, with a timeframe of one month between them. Two weeks after being presented with the first three exercises, during which time students could work through them, appointments were assigned with the corresponding teacher. Students had to go to the office of the teacher in groups of three or four in order to correct what had been done.

In these sessions, the tutor, focused primarily on the correct representation of views, cuts and dimensions, as well as adherence to UNE standards and the correct delineation of the whole plan, correcting individually the observed errors.

The group corrections allowed each student to learn from the mistakes of their peers and also encourage a critical attitude in order to evaluate the different projects. On the one hand, mistakes due to learning problems or difficulties were corrected by the tutor in a personal and individualized manner. This therefore complemented the work of the theory professor. On the other hand, if the teacher responsible for tracking the progress of the work noticed that the same mistake was made by a large number of students, one might suspect a fault in the transmission of concepts, therefore alerting the theory professor of the need for possible correction or reinforcement in class.

After this correction, the student had two further weeks to amend their exercises, taking all the guidelines of team correction into consideration. The submission of the first three papers was about a month after its start date.

Once this first batch of exercises was submitted, students were immediately presented with the next three. The methodology was the same: two weeks for individual work and research, and again a new detailed correction in groups of three or four in the tutor's office. Later, after two weeks of individual work the final delivery was made.

4.4 Evaluation

Throughout the course, students' work was evaluated through regulated and individualized monitoring. Each piece of work was evaluated out of a total of 10 points, establishing correction criteria that are common to all teachers.

The evaluation was carried out using a Likert scale, where 0% of the score for each section was "very deficient" and 100% was "very good". From each exercise, between 5 and 8 indicators were evaluated that reflected the correct or incorrect application of UNE standards seen in the theory classes. Each indicator had a different score, depending on its relevance and the work phase in which we were currently working (Fig. 1).

After the first installment, the teacher assessed the first three jobs and produced a provisional list of notes, so that the student, in the case of an unfavorable result, could see their errors and corresponding corrections in tutoring sessions. This would consequently

>1 important failure	VERY DEFICIENT (0% NOTE)
1 important failure or >5 unimportant failures	DEFICIENT (25% NOTE)
between 3 and 5 unimportant failures	REGULAR (50% NOTE)
< 3 unimportant failures	GOOD (75% NOTE)
without failures	VERY GOOD (100% NOTE)

EXERCISE	AIM	INDICATOR	SCORES	% TOTAL
E1 VIEWS	To solve the given axonometry piece with the plan view, the elevation view and the simple auxiliary view.	1. Have they filled the data box correctly?		5%
		2. Have they used technical writing?		15%
		3. Is the disposition of the views correct?		10%
		4. Have they been able to solve the plant view and the elevation view?		15%
		5. Have they been able to solve the simple auxiliary view?		25%
		6. Have they been able to interpret the axes lines in the views?		10%
		7. Have they been able to interpret the hidden lines in the views correctly ?		10%
		8. Have they been able to interpret the thicknesses according to regulations?		10%
				100%
E2 CUT VIEW 1	To solve the proposed cuts and to apply UNE standards	1. Have they filled the data box correctly?		5%
		2. Have they used technical writing?		10%
		3. Is the disposition of the views correct?		10%
		4. Is the solution of the cut correct?		30%
		5. Have they been able to interpret the axes lines in the views?		15%
		6. Have they been able to interpret the hidden lines in the views correctly ?		15%
		7. Have they been able to interpret the thicknesses according to regulations?		15%
				100%
E3 y E6 VIEWS_CUTS and DIMENSION 1 and 2	To solve the given piece with the necessary views and cuts and to dimension according to UNE standards	1. Have they been able to solve the exercise with the right number of views?		10%
		2. Have they been able to solve the plant view?		10%
		3. Have they been able to solve the elevation view?		10%
		4. Have they been able to solve the cut views?		10%
		5.Have they been able to interpret the axes lines and the hidden lines in the views correctly ?		10%
		6.Have they been able to interpret the thicknesses according to regulations?		10%
		7. Have they solved the dimensioning of the piece correctly?		40%
				100%
E4 DOUBLE AUXILIARY VIEW	To solve floor, elevation view, profile view and double auxiliary view	1. Is the layout of the views correct according to the projection directions?		10%
		2. Have they been able to solve the plant view, the elevation view and the profile view?		30%
		3. Have they been able to solve the view of the first plane change?		20%
		4. Have they been able to solve the double auxiliary view?		20%
		5. Have they been able to interpret the thicknesses according to regulations?		20%
				100%
E5 CUT VIEWS 2	To solve the proposed cuts views and to apply UNE standards	1. Have they been able to solve the proposed AA cut?		20%
		2. Have they been able to solve the proposed BB cut?		20%
		3. Have they been able to solve the proposed CC cut?		20%
		4. Have they been able to interpret the axes lines and the hidden lines in the views correctly ?		30%
		5. Have they been able to interpret the thicknesses according to regulations?		10%
				100%

Fig. 1. Evaluation indicators

improve results in the face of the second installment. This review was not mandatory, but improved the final outcome among those students who took advantage of it.

After the second submission, a definitive list of grades with the arithmetic average of the six papers per student was produced. A student gaining above four points in this part of the subject was considered to have acquired sufficient knowledge to pass, so that the grade could be added to their average score for the remainder of the course, assuming that the student had passed this via continuous evaluation.

In the case of a student failing to produce satisfactory practical work throughout the course, there existed the legal possibility of a standardization exercise in the final assessment test. However, this opportunity was rarely taken up by students, given the evident difficulty of passing such an important test in one single session and with very limited time.

5 Analysis of Results

Figure 2 analyzes course results in the 2008–2009 academic year—prior to the implementation of Supervised Practical Work—and compares them with those of 2009–2010 and 2016–2017—in which practical work had already been implemented. We can see that in 2008–2009 the percentage of students passing standardizing assignments was 18%, whereas in the following year the average pass rate was 81%. However, the difference in pass rate is not so extreme at the end of the course, which in 2008–2009 was 62% and in subsequent courses was 54%.

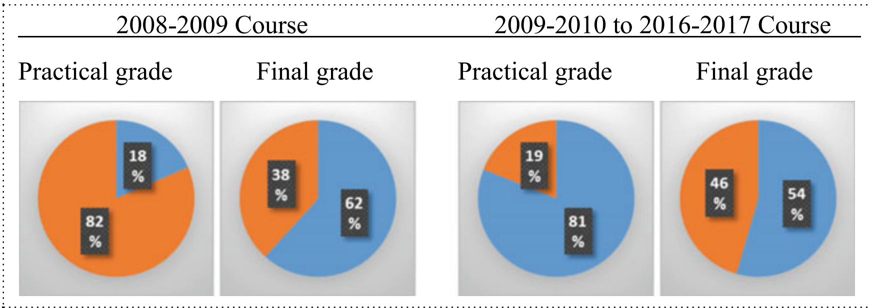

Fig. 2. Pass (Blue)/Fail (Orange). Comparison of results before and after the Bologna Plan

We had two groups per course, one of then in mornings (group 11) and the other one in afternoons (group 12).

A course by course results analysis shows that students' grades for tutor-supervised practical work were consistently higher than their overall final grades. This means that students could compensate for weaker results in other areas of the subject by obtaining stronger ones in their practical work. This was not apparent in courses prior to 2009–2010 (Figs. 3, 4, 5, 6, 7 and 8).

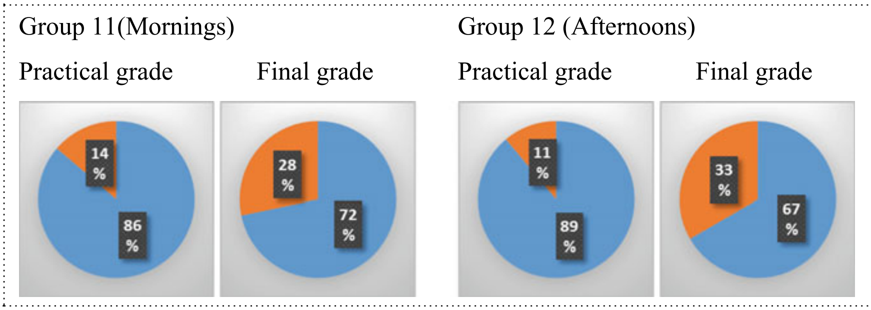

Fig. 3. Results of 2009–2010 Course. Pass (Blue)/Fail (Orange)

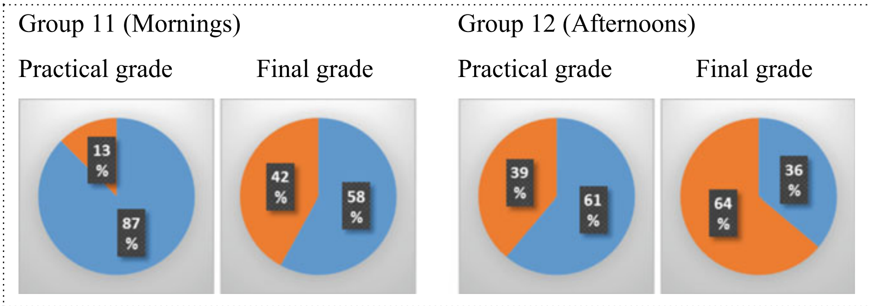

Fig. 4. Results of 2010–2011 Course. Pass (Blue)/Fail (Orange)

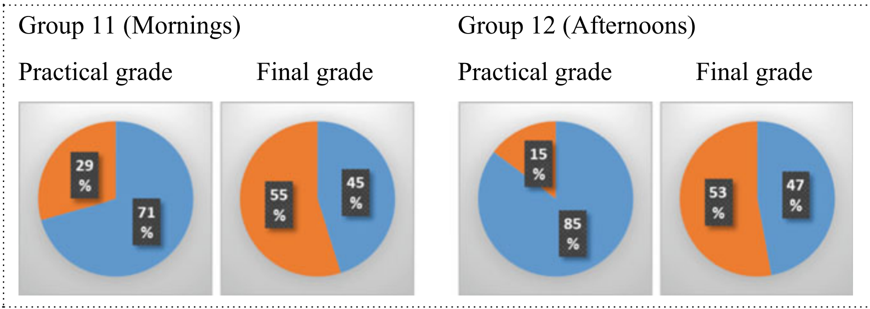

Fig. 5. Results of 2011–2012 Course. Pass (Blue)/Fail (Orange)

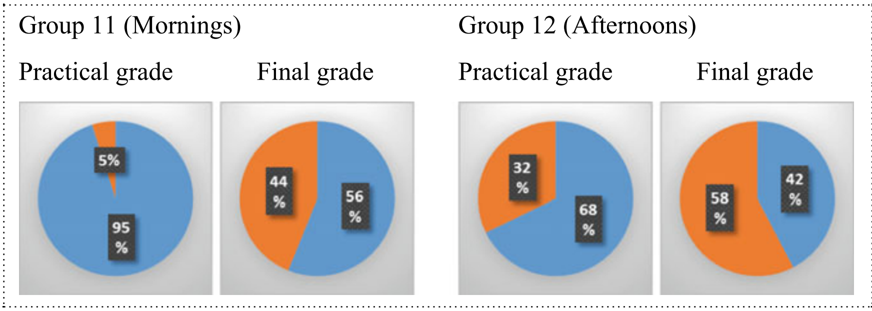

Fig. 6. Results of 2012–2013 Course. Pass (Blue)/Fail (Orange)

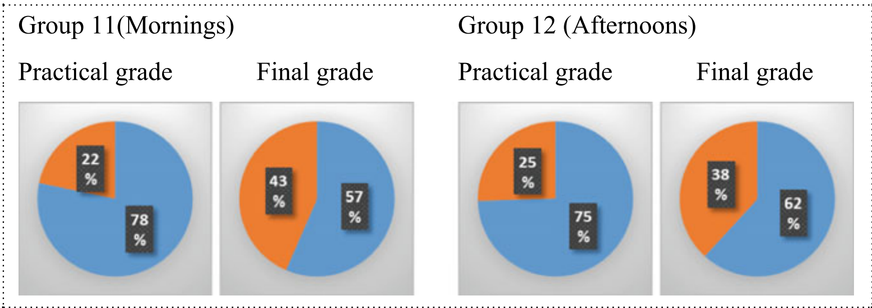

Fig. 7. Results of 2013–2014 Course. Pass (Blue)/Fail (Orange)

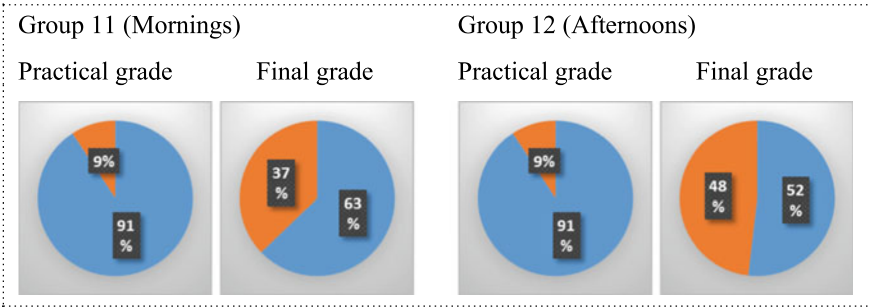

Fig. 8. Results from 2014–2015 to 2016-2017 Course. Pass (Blue)/Fail (Orange)

Eighty percent of students who reviewed exercises with their tutors on receiving results from the first assessment round improved their results in the second submission.

It was observed that around 50% of students had more problems solving exercises 1 and 3, which focused on auxiliary views, than the exercises on cuts or plan and elevation views.

Furthermore, more than 85% of students solved the exercises we proposed to them in groups, helping each other to interpret the exercises three-dimensionally.

6 Strengths, Weaknesses and Possible Improvements

Through nine years of experience in Supervised Practical Work, we have been able to identify a number of strengths and weaknesses, which offer us the possibility of making improvements each course.

Strengths (Positive points)

- By correcting exercises in small groups and offering close individualized tuition, the learning process and subsequent results in this part of the course are greatly improved.
- The methodology encourages research and problem solving by students. Although they are given research guidelines and instructed at all times on how to solve the work, the tutor does not intervene in the actual solution of problems. Thus, the student is who ultimately must decide what solution to adopt.
- Group work is encouraged. This is possible because all students have the same task instructions to follow, and, although submission is individual, it is possible that students can help one another to resolve the exercises in groups, thus sharing knowledge.
- The methodology helps to foster critical thinking amongst students. As the tutor does not intervene in the solution of exercises, and instead simply guides them through the process, students must develop a critical awareness of the correct or incorrect execution of tasks.

Weak points (Negative points)

- One of the biggest problems we face as teachers is the excessive number of students per class, amounting to an average of 50.
- The work of the tutor is too repetitive, because students tend to make similar mistakes.
- Students lack consistency, and tend to wait for the tutor to guide them in tutorials, especially in the first submission of work.

Improvement actions

- The creation of a rubric or evaluation system that would serve as a reference so that students could be made aware of the evaluation points and criteria expected of them by teachers. This would provide motivation and focus.
- The adjustment of deadlines, in order to ensure that students genuinely work and acquire knowledge, rather than copying from each other.

7 Conclusions

The intention of this analysis has been to present the methodology used since 2009/2010 in practical elements of a Graphic Expression course, which forms part of the degree in Product Design Engineering at the University of Zaragoza. This methodology bases itself upon on a more permanent and personalized monitoring of work done throughout the course.

It is not intended that this paper should statistically analyze the new system of practical work, but rather, that it should present a new methodology which, if more extensively implemented (and in light of its strengths and weaknesses), might serve to improve and complement current procedures.

From the current analysis and from hands-on experience, we can affirm that the implementation of Supervise Practical Work as a teaching methodology within the Graphic Expression Course improves the results of practical elements of the course substantially.

Furthermore, this methodology improves students' aptitude for teamwork, spatial vision and analysis, as well as fomenting self-awareness in critical research. Whilst we cannot ensure that all students will respond homogeneously, it would certainly be interesting to carry out a more scientific study of results in a wider context in order to validate this new methodology.

References

1. Orta Cuevas MM, García Asuero A, Alarcón de la Lastra C, Jos Gallego A, Mencia García E (2008) Adaptación de la asignatura Practicas Tuteladas al espacio Europeo de Enseñanza Superior mediante el empleo de tecnologías de la información y comunicación. Colección: "Innovación y Desarrollo de la Calidad de la Enseñanza Universitaria, (17):275–282
2. Gorbaneff Y (2006) Aprendizaje basado en problemas. Innovar 16(28):244–246
3. Martí Gòdia E, Gil Resina D, Vivet M, Julià C (2008) Balance de cuatro años de experiencia en la implantación de la metodología de Aprendizaje Basado en Proyectos en la asignatura de Gráficos por Computador en Ingeniería Informática
4. Morales P, Landa V (2004) Aprendizaje basado en problemas. Theoria 13(1):145–157
5. Navarro LP (2006) Aprendizaje activo en el aula universitaria: el caso del aprendizaje basado en problemas. Miscelánea Comillas. Revista de Ciencias Humanas y Sociales 64(124): 173–196
6. Molina XM, Tamayo MDB (2006) Aprendizaje basado en problemas. Innovación Educativa 6(35):1–12

Content Management System for the Dissemination of Research Results on Agustín de Betancourt's Historical Inventions

J. I. Rojas-Sola[1](✉) and A. I. Aguilera-García[2]

[1] Department of Engineering Graphics, Design and Projects, University of Jaén, Campus de las Lagunillas, s/n, Jaén 23071, Spain
jirojas@ujaen.es

[2] Department of Computer Science, University of Jaén, Campus de las Lagunillas, s/n, 23071 Jaén, Spain

Abstract. In this paper, a Content Management System (CMS) developed in WordPress for the teaching-learning process of the historical inventions by Agustín de Betancourt is shown. The exhibition is made from the point of view of engineering graphics, and also pursues the educational objective of disseminating the results obtained in a research project of excellence which focuses on the figure of this outstanding Spanish engineer. The contents of this CMS are structured on the basis of 3 fundamental pillars: historical, technological and graphical, and we aim to show them depending on the profile of user access. From the historical point of view, we seek to show all his work in pdf format, including all the information available in each file, i.e. the descriptive or functioning memories of the historical inventions, as well as his scarce planimetry; from a graphical point of view, we aim to show the 3D models, as well as the assembly plans with all their elements and exploded views, the virtual recreations of their operation, as well as the applications of virtual and augmented reality; finally, from the technological point of view derivative publications related to the study of computer-aided engineering (CAE) that have been generated from the 3D models of the analyzed inventions are shown. Finally, the developed CMS presents a very intuitive interface and easy navigation for the user, which facilitates its understanding, and therefore its dissemination and valorization. The self-assessment tests carried out reflect a high degree of satisfaction.

Keywords: Agustín de Betancourt · Historical technical heritage · Content management system · WordPress

F. Cavas-Martínez et al. (Eds.): *Advances on Mechanics, Design Engineering and Manufacturing II*, LNME, pp. 732–741, 2019.
https://doi.org/10.1007/978-3-030-12346-8_71

1 Introduction

This paper presents the development of a Content Management System (CMS) for the teaching-learning process of the historical inventions of Agustín de Betancourt, available online thanks to the compilation efforts of the Canary Orotava Foundation of History of Science, and named the Betancourt Project [1]. Other similar experiences of Content Management Systems have been developed by the authors in other area of research [2], which have revealed the convenience of their development for the dissemination of research results.

The exhibition is presented from the point of view of engineering graphics, and also pursues the educational objective of disseminating the results obtained in the research project of excellence, which focuses on the figure of this outstanding Spanish engineer from the mid-eighteenth century and the early nineteenth century (1758–1824).

After an introduction, and presenting the objectives of the research project of excellence, the contents of this Content Management System (CMS) are structured on the basis of 3 fundamental pillars: historical, technological and graphic, and we aim to show these depending on the profile of user access.

From the historical point of view, it is sought to show all his work in pdf format including all the information available in each file, i.e. the descriptive or functioning memories of the historical inventions, as well as his scarce planimetry; from a graphic point of view, we aim to show the 3D models, as well as the assembly plans that include all their elements and exploded views, and the virtual recreations of their operation, as well as the applications of virtual and augmented reality; finally, from the technological point of view, all the derivative publications related to the study of computer-aided engineering (CAE) that have been generated from the 3D CAD models of each of the inventions analyzed are shown.

Specifically, five historical inventions were analyzed: the wind machine for draining marshy ground (1789) [3], the machine for cutting cane and other aquatic plants in navigable waterways (1795) [4], the mill for grinding flint (1796) [5], the plunger lock (1801) [6], and the mechanical dredger in the port of Kronstadt (1810) [7].

2 Election of the CMS and Hosting

One of the objectives of the research project that frames this communication focuses on promoting the educational use of research results, that is to say pursuing a new approach in the teaching-learning process.

For this reason, a CMS has been designed and developed, consisting in a software that allows users to create, edit and publish content such as text or multimedia files through a graphical user interface, making the work much easier and allowing the realization of more attractive websites with less effort.

Nowadays, there are more than 250 programs on the market for developing a CMS, so choosing the best is not easy, since some stand out in certain characteristics and others in others. These can be classified into 3 groups:

- Those which manage web content, allowing users to create and manage content online. This would be the case with our investigation.
- Those which publish blogs/news for the creation and management of blogs.
- Those which develop social publication/communities for the creation and management of communities. The communities are similar to blogs, but more complex, since they are designed to communicate to a group of active people, differently from blogs which are usually designed to communicate to passive groups.

For the selection of the CMS that best suits the type of research results developed, a study of the most popular CMS was carried out (Table 1). In 2017 there were already 1,800 million websites [8], and of all these sites almost 60% of the market for them had been created in WordPress [9], followed by Joomla [10] and Drupal [11] with 6.6 and 4.6% respectively.

Table 1. Most popular CMS

CMS	Market share (%)	Active websites	Websites (millions)
WordPress	59.9	26.701,222	239,139
Joomla	6.6	2.009,717	13,480
Drupal	4.6	964,820	23,330
Magento	2.4	372,915	12,095
Blogger	1.9	758,571	15,779
Shopify	1.8	605,506	11,587
Bitrix	1.5	200,210	3925
TYPO3	1.5	582,629	3568
Squarespace	1.5	1.390,307	9799
PrestaShop	1.3	262,342	2099

Source BuiltWith, SimilarTech, and Google Trends

Thus, a comparative study of the three most used CMS (WordPress, Joomla and Drupal) was undertaken, assessing the following characteristics: Easy installation and configuration, administration, management and creation of content, incorporation of modules for user management, incorporation of modules that manage security and service, web creation that includes optimization in search engines (SEO, Search Engine Optimization), and use of receptive typography [12, 13].

Finally, as a global assessment it was decided to use WordPress, an open source software under the GPL (General Public License), and developed in PHP (Hypertext Preprocessor). As well as being the most used, it has many additional advantages: it has more than 18,000 free extensions and more than 14,000 templates, its installation is very simple and can be operational in a few minutes, the URLs generated can be accessed by the search engines, allowing optimal indexing, and it also contains a large number of manuals and tutorials, as well as numerous forums where anyone can consult any doubts or problems that may arise when the project is created. However, the main problem with WordPress is that being the most used means it also suffers the most security attacks, with most of the security breaches coming from the add-ons that are installed on it. In addition, another problem is that it usually has low performance when the server is overloaded.

Once the program for developing the CMS is chosen, the next step is to choose a hosting provider to host it. In the case of this research it was installed on a local server on which all the tests were performed, and once all the contents of the CMS had been organized a hosting was sought for public access.

The local server that was used to test our CMS was a package of the AMP family since it includes an Apache web server, a MySQL database and an FTP client. Specifically, the package used was XAMPP.

Afterwards, the different options were analyzed in order to find a free hosting provider to host the CMS (x10Hosting, Byethost, AwardSpace, WebFreeHosting or Free Web Hosting), evaluating the following characteristics: storage space, transfer rate, technical support, possibility to administer several websites from the same panel, use of SSL certificate, registration of domain by the provider, time that the web will remain online (free of falls), incorporation of auto-installer, and automatic and programmable backup copies.

3 Working Inside the CMS

3.1 Architecture

Before starting with the design of the CMS, it must be clear how the navigation and the content of the website will be structured. Therefore, the architecture of the website is the basis for building simple websites, where the user can find the information they are looking for quickly; that is to say that they are very functional sites that are easily adaptable to different mobile devices.

Fig. 1. Diagram of the architecture of the website

Thus, in the architecture of a website the information on how the different web pages that make up the site are connected is shown. Figure 1 shows the architecture of the website used to show the results obtained in the research project.

3.2 Structure

On the other hand, the structure of the website that is marked by the theme chosen in WordPress must be designed. As previously indicated, the software chosen to develop the CMS is WordPress, and for its appearance the Twenty Sixteen theme was chosen (Fig. 2).

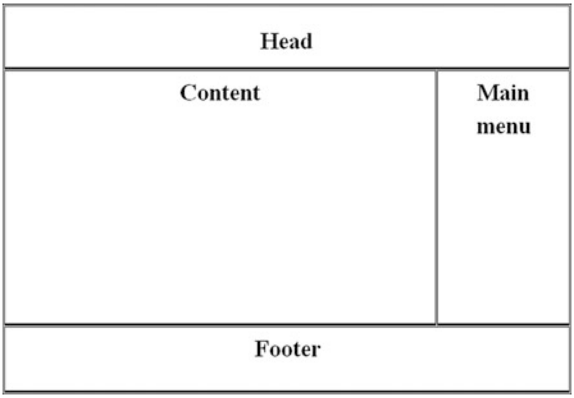

Fig. 2. Diagram of the structure of the website (according to the Twenty Sixteen theme)

Figure 3 shows the main page (interface) of the website following the structure indicated in Fig. 2.

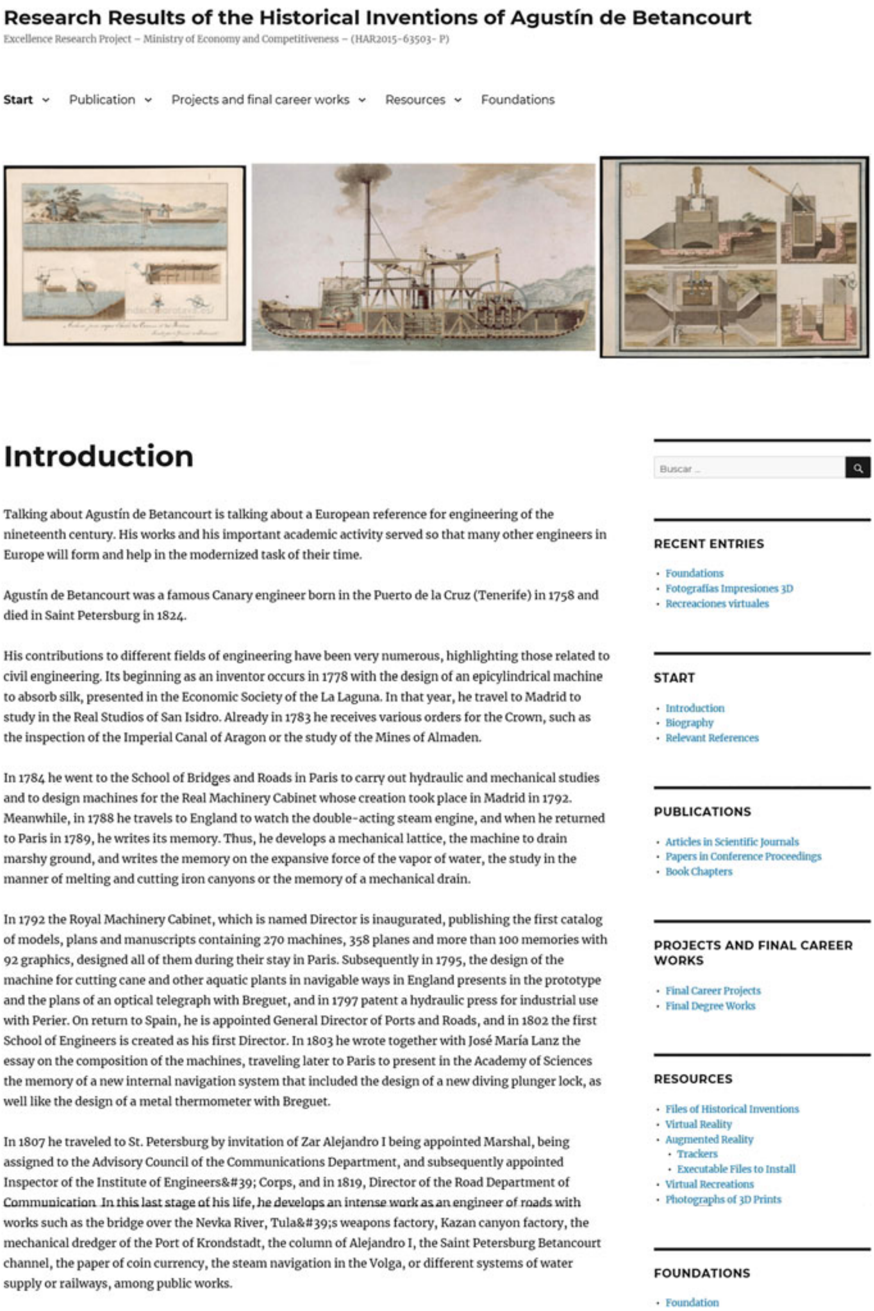

Fig. 3. Website interface

3.3 Categories and Contents

The contents shown on the project website are structured into logically related categories and subcategories (Table 2).

Table 2. Categories and contents of the website

Start	Publications	Career projects and Degree works	Resources	Foundations	User access
• Introduction • Biography • Relevant references	• Articles in Scientific Journals • Papers in International Conference Proceedings •Book Chapter	• Final Career Projects • Final Degree Works	• Files of historical inventions • Virtual reality • Augmented reality • Trackers • Executable files • Virtual • Recreations • Photographs of 3D printings	• Fundación Canaria Orotava de Historia de la Ciencia • Fundación Agustín de Betancourt	Create an account Forgot your login? Forgot your password?

3.4 Menus

In order to make the information more accessible, two menus were incorporated into the structure of the web, one in the header and one on the right side. The menus were structured following the distribution of the contents among previously-shown categories. Thus, the menu that appears in the header of the website only shows the main categories, and once one of these is selected its subcategories are displayed. For its part, the right side menu directly shows all categories and subcategories. In Fig. 3 the two types of menus are shown.

3.5 Extensions

After analyzing all the different project results they were classified into four different types: text, pdf documents, photos and videos. Similarly, in order to show these results in WordPress for the different types of documents it was only necessary to install a plug-in (PDF Viewer) for the visualization of the PDF documents within the website (Fig. 4), and for the visualization of photos and videos, we used the media library installed in WordPress by default (Fig. 5).

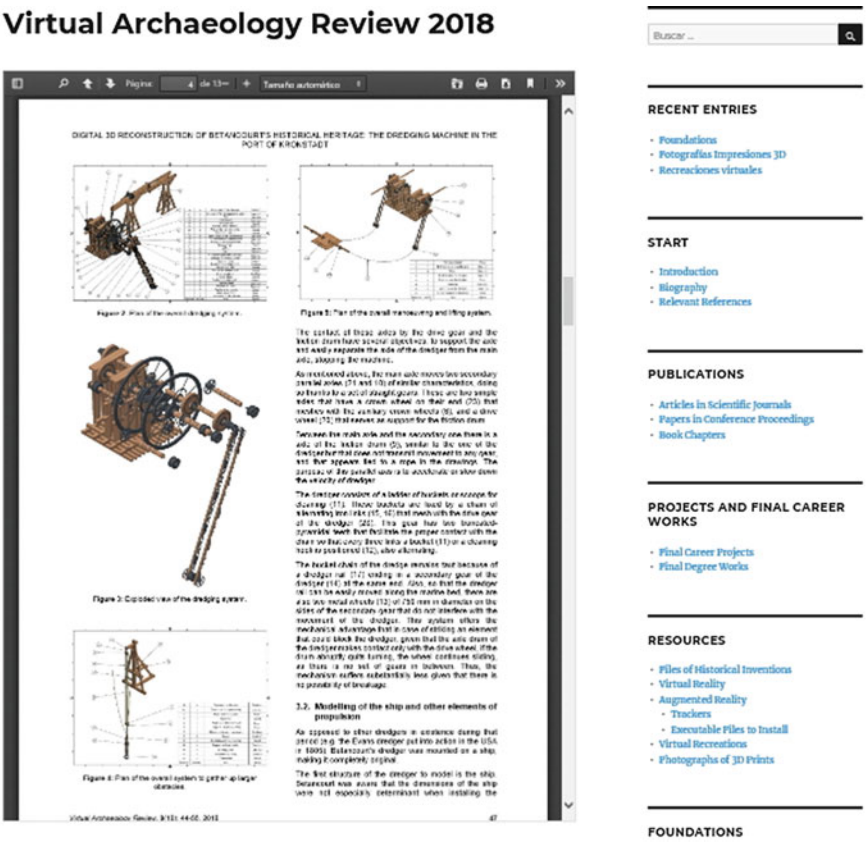

Fig. 4. Website where the document of a publication is displayed in PDF format

4 Conclusions

In the present communication a CMS has been designed for the historical inventions of Agustín de Betancourt related to civil engineering, the results of a research project of excellence for its value and diffusion, implemented with WordPress and structuring the contents into 6 categories and subcategories.

The CMS obtained stands out because the interface used is very intuitive and easy to navigate, which facilitates user assimilation of contents in the teaching-learning process, as evidenced by the self-assessment tests carried out that reflect a high degree of user satisfaction. The CMS developed have been self-assessed using a 5-question questionnaire with a scale of 1–5 (1: very unsatisfactory; 2: unsatisfactory; 3: indifferent; 4: satisfactory; 5: very satisfactory). The issues used and the results are: user friendliness (mean = 4.8), easy browse (mean = 4.7), and overall assessment (mean = 4.6).

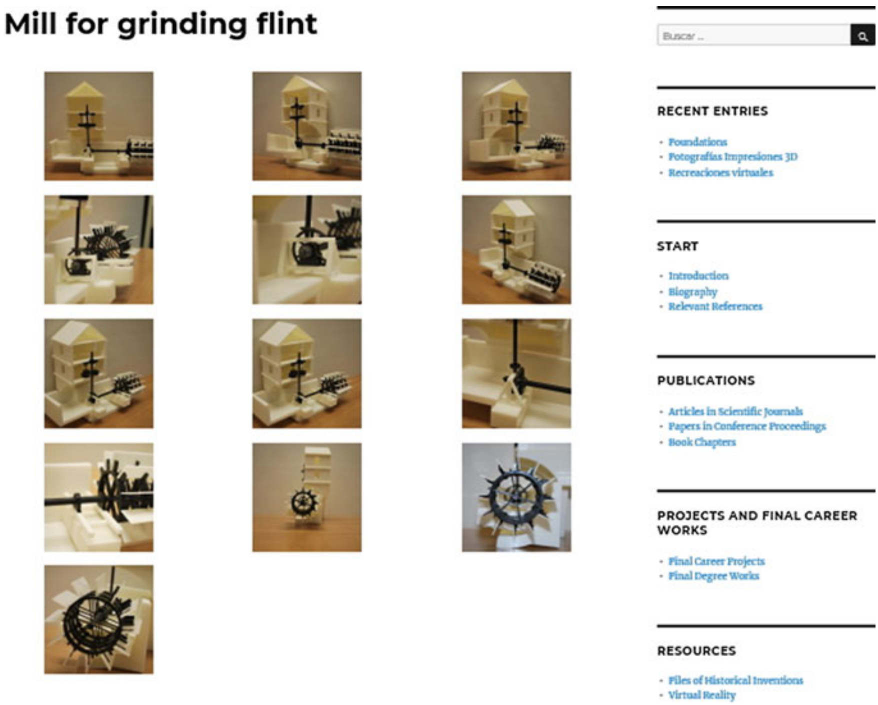

Fig. 5. Website where the photo gallery of the 3D printing of an invention is shown

Acknowledgements. This research has been developed within the research project entitled "Agustín de Betancourt's historical heritage: a comprehensive study of contributions to civil engineering from the perspective of engineering graphics for its valuation and dissemination" (HAR2015-63503-P), funded by the Spanish Ministry of Economic Affairs and Competitiveness, under the Spanish Plan of Scientific and Technical Research and Innovation (2013–2016), and European Fund Regional Development (EFRD). Also, we are very grateful to the Fundación Canaria Orotava de Historia de la Ciencia for permission to use the material of the Betancourt Project available on their website.

References

1. Betancourt Project. http://fundacionorotava.es/betancourt. Last accessed 02 May 2018
2. Rojas-Sola JI, Castro-García M, Carranza-Cañadas MP (2011) Content management system incorporated in a virtual museum hosting. J Cult Heritage 12(1):74–81. https://doi.org/10.1016/j.culher.2010.10.004
3. Betancourt y Molina, A. Sur le nouveau moulin à vent. http://fundacionorotava.es/pynakes/lise/betan_mouli_fr_01_18XX/2. Last accessed 02 May 2018
4. Betancourt y Molina, A. Description d'une machine à couper les roseaux et les autres plantes aquatiques qui obstruent beaucoup de Canaux et de rivières navigables, http://fundacionorotava.es/pynakes/lise/betan_coupe_fr_01_1800. Last accessed 02 May 2018

5. Betancourt y Molina, A. Explication des principales parties du moulin pour moudre le sílex. http://fundacionorotava.es/pynakes/lise/betan_silex_fr_01_1796. Last accessed 02 May 2018
6. Betancourt y Molina, A. Mémoire sur un nouveau système de navigation intérieure. http://fundacionorotava.es/pynakes/lise/betan_memoi_fr_01_1807. Last accessed 02 May 2018
7. Betancourt y Molina, A. Explication d'une machine destinée à curer les ports de mer. http://fundacionorotava.es/pynakes/lise/betan_expli_fr_01_1808. Last accessed 02 May 2018
8. Netcraft website. https://news.netcraft.com/archives/2017/01/12/january-2017-web-server-survey.html. Last accessed 02 May 2018
9. WordPress website. https://es.wordpress.com. Last accessed 02 May 2018
10. Joomla website. https://www.joomla.org. Last accessed 02 May 2018
11. Drupal website. https://www.drupal.org/. Last accessed 02 May 2018
12. Batalla de CMS: WordPress vs. Joomla vs. Drupal. https://www.lancetalent.com/blog/batalla-cms-wordpress-vs-joomla-vs-drupal-cw/. Last accessed 02 May 2018
13. Comparativa WordPress, Drupal y Joomla. http://mangusoft.com/2016/10/05/comparativa-wordpress-drupal-joomla/. Last accessed 02 May 2018

WebGL for the Dissemination of Research Results on Agustín de Betancourt's Historical Inventions

J. I. Rojas-Sola[1(✉)] and A. I. Aguilera-García[2]

[1] Department of Engineering Graphics, Design and Projects, University of Jaén, Campus de las Lagunillas, s/n, 23071 Jaén, Spain
jirojas@ujaen.es

[2] Department of Computer Science, University of Jaén, Campus de las Lagunillas, s/n, 23071 Jaén, Spain

Abstract. This paper shows the process undertaken to publish and disseminate in WebGL format 3D models that recreate the operation of historical inventions designed by Agustín de Betancourt. The main objective is the creation of a website with different inventions, on which the user can interact through the mouse or keyboard, being able to observe them animated and from different points of view and better understand their operation. The methodology allows 3D models created with Autodesk Inventor Professional (in.ipt single piece format) to be exported to Unreal Engine to be assembled correctly by applying materials and textures with topological mapping (Bump Mapping), and where the scenes for each historical invention have been created, including an animated 3D model. In a similar manner, in order to establish the user's interaction with the 3D model from HTML5, a program has been developed using the Visual Blueprint script system, which makes possible to rotate the model when the left mouse button is pressed, to move the pointer across the screen, zooming in and out the camera using the central mouse's wheel or use a series of keys that allow to move, rotate or zoom on the model. The results obtained have been very good according to the user experience, since from the educational point of view interaction with the model has allowed an optimal understanding of its operation, improving the teaching-learning process.

Keywords: Agustín de Betancourt · Historical technical heritage · WebGL · HTML5 · Unreal Engine

1 Introduction

The main objective of this research is the creation of a website that includes a series of historical inventions designed by Agustín de Betancourt, on which the user can interact through the mouse or keyboard, being able to observe them from different points of view, and in this way, understanding better their operation. 3D graphics, well used, can be a good tool for teaching and understanding the functioning of 3D models that recreate the behavior of different machines and devices, and they enable access to a greater number of users.

F. Cavas-Martínez et al. (Eds.): *Advances on Mechanics, Design Engineering and Manufacturing II*, LNME, pp. 742–750, 2019.
https://doi.org/10.1007/978-3-030-12346-8_72

The Web has been evolving since its origins, when it allowed only the inclusion of text, until today, when a web page cannot be conceived without multimedia contents included (images, videos and sounds). With the appearance of 3D models, the need to incorporate them into web pages has been created, and for this purpose different proprietary and open technologies capable of showing 3D graphics (3DXML, VRML, X3D, Flash, Silverlight, Java, etc.) have appeared. The drawback of all these technologies is that they have not come to be supported by all browsers, forcing users to install a series of specific plugins for each one of them. This made the use of this 3D technology by ordinary users quite uncomfortable, since they were asked to work with the 3D graphics before installing the corresponding plug-in, depending on which format the graphics were recorded, causing many users to leave the web page without being able to see the 3D graphics that were displayed on it.

HTML5 is the fifth revision of the basic HTML language of the World Wide Web. The most striking contributions of HTML5 to the web are its tags as Canvas, Audio and Video, which replace the Flash plugin since it consumes many resources. In general terms, no browser is 100% compatible with all the features of HTML5 and CSS3, although HTML5 is fully compatible with all modern browsers. The HTML5 Test [1] is an appropriate tool to know the level of HTML5 support, since it offers a total score that indicates, item by item, the HTML5 support of the browser used.

Fortunately, this changed a few years ago with the appearance of Windows 8.1, since this software had installed Internet Explorer 11 browser that allows use of a 3D technology called WebGL. With this implementation, Internet Explorer was no longer the only desktop browser that did not incorporate this open standard for the management of 3D graphics. WebGL makes it possible to use the hardware features of the graphics card, allowing the display of high quality 3D graphics and their interactivity within the Canvas element of HTML5. When using an environment that does not recognize the WebGL technology, either because the browser does not support it or because the graphics card drivers do not work correctly by not using the OpenGL technology that comes with WebGL, it only shows the static images of 3D models, without the possibility of interacting with them. Therefore, after analyzing all the possible formats we have chosen to develop the web page in WebGL.

A WebGL program consists of a JavaScript control code and a shader code. The shader code runs on the computer graphics card (GPU) and the results that are obtained are displayed in the browser. It is a code that includes the necessary instructions to specify how to render the surface of objects, and how light and shadow interact with 3D objects [2]. In WebGL the shaders are written in GLSL (OpenGL Shading Language) [3]. Of the different types of shader codes with which we can work, WebGL only uses Vertex Shader (3D) and Fragment Shader (2D) [4]. The JavaScript control code is responsible for initializing the WebGL context and selecting which Canvas element to run, managing the logic of the program, the inclusion of interface controls in the Canvas element, and user event handling. WebGL can be used to make 3D designs in the browser. Also, there are graphic engines specially created for the development of 3D environments compatible with WebGL such as Unreal Engine [5] or Unity [6]. In addition, WebGL has been incorporated into the latest desktop and mobile browsers that must support HTML5. Table 1 shows the compatibility of WebGL with the most commonly used browsers.

Table 1. Compatibility of browser versions in WebGL [7]

WebGL—3D canvas graphics									
Method of generating dynamic 3D graphics using JavaScript, accelerated through hardware									
IE	Edge	Firefox	Chrome	Safari	IOS Safari	Opera Mini	Chrome for android	UC Browser for android	Samsung internet
			49		10.2				
			63		10.3				4
11	16	58	64	11	11.2	Not support	64	11.8	6.2
	17	59	65	11.1	11.3				
		60	66	TP					
		61	67						

2 Materials and Methods

2.1 Material

The starting material has been the information available in the files of the historical inventions of Agustín de Betancourt, accessible thanks to the Betancourt Digital Project of the Orotava Canary Foundation for the History of Science [8], from which the digital restitution of their 3D models has been performed.

2.2 Software Used

The software used to edit and process the 3D model for inclusion in a WebGL project has been:

- Unreal Engine as multiplatform video game engine programmed in C and C++ with free and proprietary license, available for Microsoft, OS X and Linux.
- Visual Studio [9] for programming scripts (Dreamspark).
- Blender [10] primarily to convert .stl (stereolithography) files into .fbx files (open structure file developed by AutoDesk for 3D data transfer that creates a high level of interoperability), which is the type of file chosen for working with Unreal Engine.
- CrazyBump [11] for creating textures with Bump Mapping.

2.3 Methodology. Limitations

First, each piece (.ipt) of a set or assembly (.iam) made with Autodesk Inventor Professional was converted to the.stl format and the pieces were imported from Blender in order to export them in.fbx format, which is the type of file chosen for working with Unreal Engine.

One limitation found was that the complete assembly (.iam), once exported to graphic engine Unreal Engine, could not be animated conveniently, this causing that the pieces equipped with movement had to be exported one by one, assembling them correctly to obtain the set, and establishing for each of them the triangle mesh and the limits of their movements.

On the other hand, textures were applied with a UV mapping with Blender, since the 3D model did not allow export when not adding a position reference. Finally, materials and textures were created in the Unreal Engine environment using the topological mapping technique (Bump Mapping) with CrazyBump.

Similarly, a series of programmed animations were designed for each of the models. For example, for the model of the machine for cutting cane and other aquatic plants in navigable waterways (Fig. 1), the horizontal rotation system (crank, crank shaft, T-power and bevel gear), the vertical rotation system (vertical axis, double blade), and the movement of the vertical frame in order to adapt the double blade to the slope of the channel.

3 Working with WebGL

Specifically, the objective of this research has been to develop, from an educational point of view, a project in WebGL in order to study a historical invention by Agustín de Betancourt: the machine for cutting cane and other aquatic plants in navigable waterways (1795) [12].

Thus, a scene was created in which an animated 3D model is included that simulates the functioning of the same. Figure 2 shows the final result obtained in WebGL with the 64 bit Google Chrome browser version 66.0.3359.181.

Also, each of the scenes has a control over the 3D models that allows interacting with these by rotating them, thus allowing us to better observe their operation. This is done by pressing the left mouse button on the model and moving the cursor through the window. Six keys have also been added that allow the camera to approach the model (key W), move away from the model (key S), and to move the model horizontally (keys A and D) or vertically (keys Q and E).

Fig. 1. Axonometric view of the 3D model

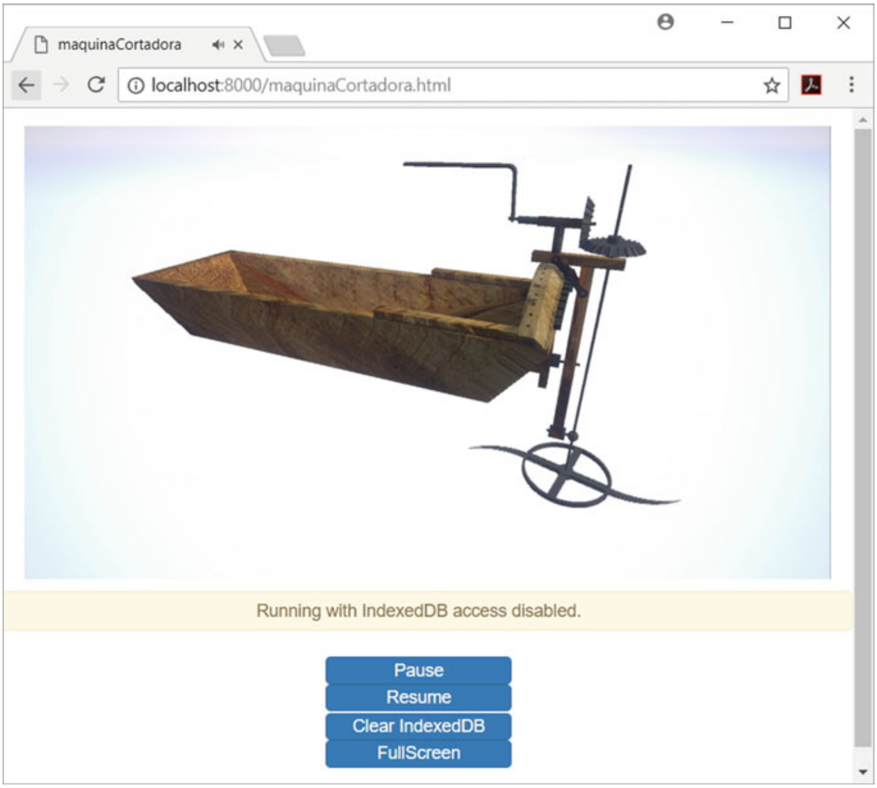

Fig. 2. Google Chrome browser window with the WebGL project open

3.1 Animation of the 3D Model

As indicated previously, in order to achieve the animation of the historical invention, it was divided into separate pieces. For example, in Fig. 3 these different pieces can be seen that make up the assembly of the machine for cutting cane and other aquatic plants in navigable waterways.

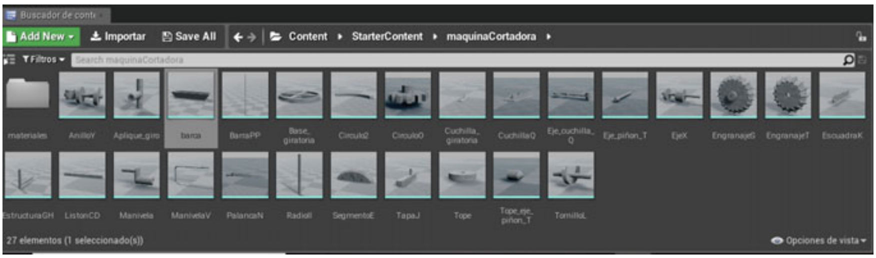

Fig. 3. Individual pieces that make up the 3D model of the assembly

Therefore, each of those pieces was grouped by elements with equal movement and some of these groups were associated with an animation. Figure 4 shows the different groups of elements created for this 3D model.

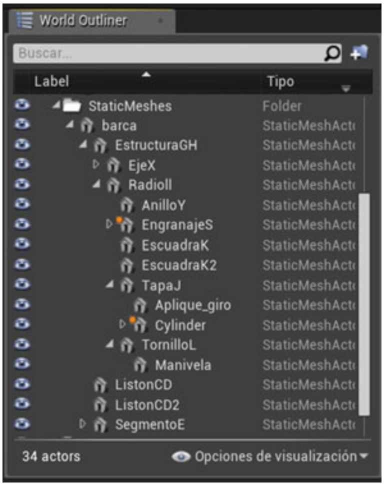

Fig. 4. Grouping of elements created for the 3D model

On the other hand, for an element to be animated, all the pieces that form it must be marked as movable. To do this, in the 'Details' tab, it is necessary to mark the property of Mobility as 'Movable', so that the elements selected as 'Movable' change their icon inside the 'World OutLiner' tab (Fig. 5).

The animation of the 3D model of an assembly is formed by the animations of each one of the mobile elements into which it has been divided. Unreal Engine allows to program the animation using the C++ programming language or using the Visual Blueprint script system, on which the order and sequence of execution of the different animations can be programmed. Figure 6 shows the graph to control the animation of the assembly.

3.2 Interaction with the 3D Model

In order to be able to interact with the 3D model of the invention, once the HTML 5 project has been generated, and opened from the browser, a program of script type using the graphic editor BluePrint was incorporated into the model. This program allows the model to be rotated when the left mouse button is pressed, moving the mouse pointer across the screen, zooming in and out of the camera model with the mouse's central wheel, or using two keys (W and S, respectively), and to move the 3D model horizontally (keys A and D) or vertically (keys Q and E).

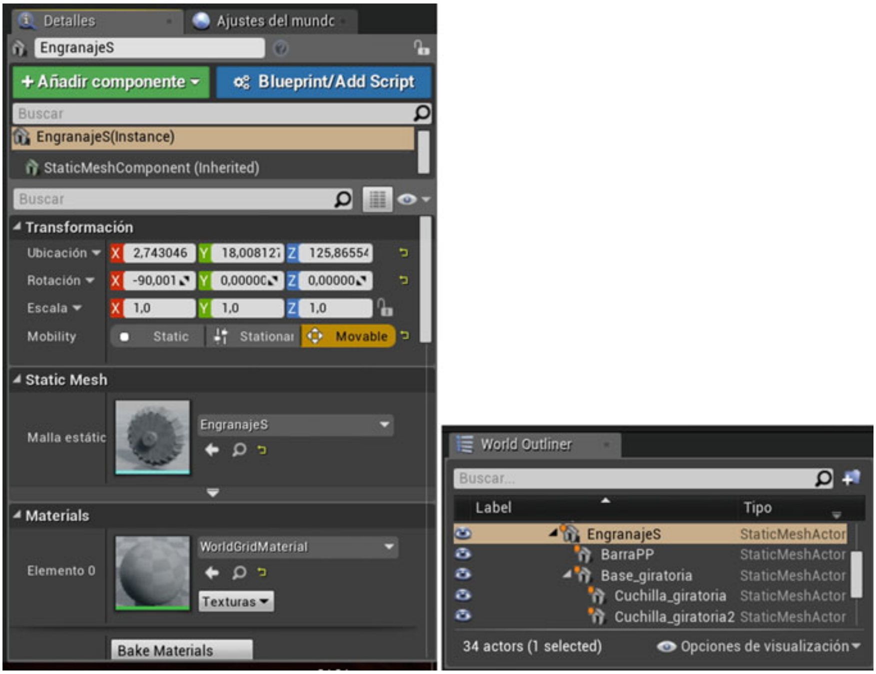

Fig. 5. Pieces with the property 'Movable' activated and its visualization in the icon

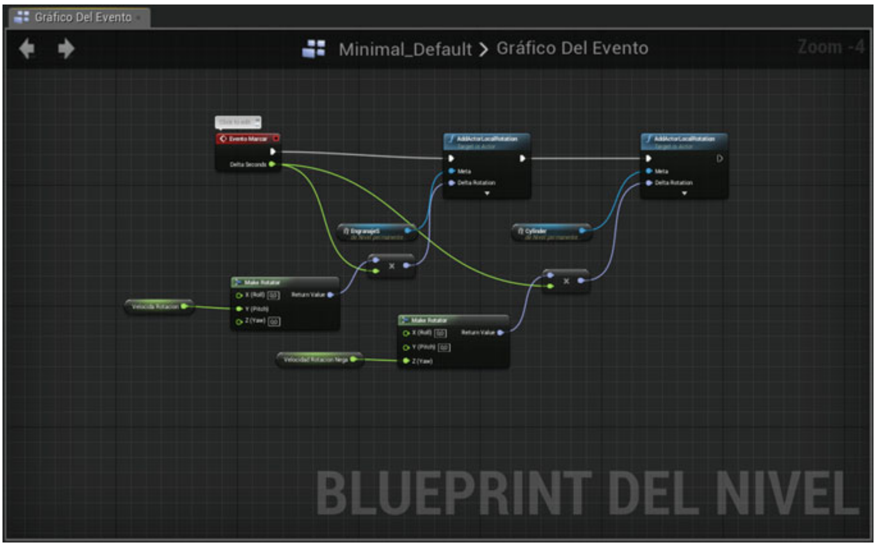

Fig. 6. Graph to control the animation of the assembly

3.3 Assignment of the Materials

A material for each one of the created pieces was assigned. For this, Unreal Engine incorporates a graphic editor for the creation of materials. In addition, three images were used to create the most realistic materials: real, normal and specular. Figure 7 shows an example of the graph for generating a wooden material.

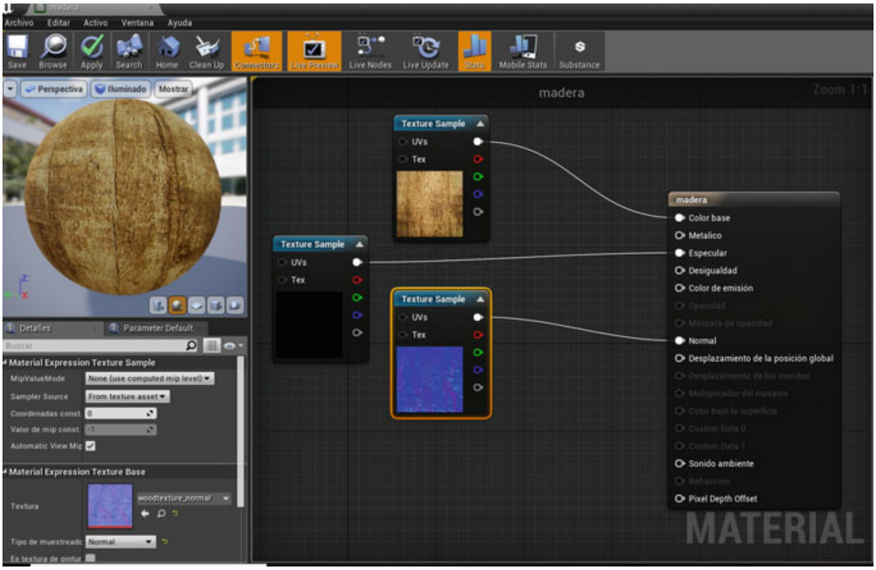

Fig. 7. Graphic to generate a wooden material

4 Conclusions

In this paper, the procedure employed to generate 3D models for a HTML5 project in WebGL based on the digital restitution of 3D CAD models has been presented.

The importance of this research lies in the establishment of a work methodology for the development of HTML5 projects with Unreal Engine applied to the learning of historical technical heritage, which improves the user experience.

The advantages of the applications developed are three: firstly, they do not suppose an expensive investment, since educational and free licenses of the software used are available; secondly, they are easily installable in any browser that allows the execution of WebGL projects, enabling standard access through the Internet, and thirdly, they present a friendly environment, easy to use with a clear and comprehensible interaction, and with a quick response.

Finally, and from the educational point of view, interaction with the model allows an optimal understanding of its functioning, improving the teaching-learning process, so it becomes an ideal tool in the educational process.

Acknowledgements. This research has been developed within the research project entitled "Agustín de Betancourt's historical heritage: a comprehensive study of contributions to civil engineering from the perspective of engineering graphics for its valuation and dissemination" (HAR2015-63503-P), funded by the Spanish Ministry of Economic Affairs and Competitiveness, under the Spanish Plan of Scientific and Technical Research and Innovation (2013–2016), and European Fund Regional Development (EFRD). Also, we are very grateful to the Fundación Canaria Orotava de Historia de la Ciencia for permission to use the material of Project Betancourt available on their website. In addition, we sincerely thank José Luis López Ruiz for his collaboration.

References

1. HTML5 test. http://html5test.com. Last accessed 22 May 2018
2. Shader. https://en.wikipedia.org/wiki/Shader. Last accessed 22 May 2018
3. OpenGL Shading Language. https://en.wikipedia.org/wiki/OpenGL_Shading_Language. Last accessed 22 May 2018
4. WebGL Shaders and GLSL. http://webglfundamentals.org/webgl/lessons/webgl-shaders-and-glsl.html. Last accessed 22 May 2018
5. Unreal Engine. https://www.unrealengine.com/what-is-unreal-engine-4. Last accessed 22 May 2018
6. Unity 3D. https://unity3d.com/es. Last accessed 22 May 2018
7. Can I use WebGL? http://caniuse.com/#feat=webgl. Last accessed 22 May 2018
8. Betancourt Digital Project. http://fundacionorotava.es/betancourt. Last accessed 22 May 2018
9. Visual Studio. https://visualstudio.microsoft.com/. Last accessed 22 May 2018
10. Blender. https://www.blender.org. Last accessed 22 May 2018
11. Crazybump. http://www.crazybump.com. Last accessed 22 May 2018
12. Betancourt y Molina, A. Description d'une machine à couper les roseaux et les autres plantes aquatiques qui obstruent beaucoup de canaux et de rivières navigables. http://fundacionorotava.es/pynakes/lise/betan_coupe_fr_01_1800. Last accessed 22 May 2018

Free Software Usage in Subjects of the Industrial Design and Product Development Engineering Degree

N. Muñoz-López(✉), A. Biedermann, A. Serrano-Tierz, and F. J. Galán-Pérez

Department of Design and Manufacturing Engineering, María Luna 3, Saragossa 50018, Spain
nataliam@unizar.es

Abstract. In recent years, the availability of funding for acquiring licenses for the different computer tools used by students, that are so common in scientific and technical careers, has been reduced. Learning in the use of technological tools of information and communication by students is considered essential for its application in daily life and in their work. These facts, together with the current rise of free software, is generating a migration towards free tools, both in teaching and in the industrial world. The increase in its use entails the reduction in expenses by institutions, as well as it encourages the scientific curiosity of the student outside the classroom. In detecting this need, free substitutes to the commercial software previously used in the subjects of Artistic Expression II and Graphic Design Applied to Product of the Industrial Design and Product Development Engineering Degree have been introduced. It was done in order to, on the one hand facilitate the access of students to the programs, and on the other hand, share the philosophy of using free media, working with the communities where the source code of the program is developed in response to the problems of the users. This experience has served to verify the benefits of teaching with free software versus commercial.

Keywords: Free software · Graphic design · Artistic expression

1 Introduction

"Free software" [1] means software that respects users' freedom and community. Roughly, it means that the users have the freedom to run, copy, distribute, study, change and improve the software.

Thus, it is considered that the software is free if it guarantees the following four freedoms [2]:

- Freedom 1, to run the program for any purpose (private, educational, public, commercial, etc.).
- Freedom 2, to study and modify the program (for which it is necessary to be able to access the source code).
- Freedom 3, to copy the program so that you can help the neighbor or to anyone.

F. Cavas-Martínez et al. (Eds.): *Advances on Mechanics, Design Engineering and Manufacturing II*, LNME, pp. 751–760, 2019.
https://doi.org/10.1007/978-3-030-12346-8_73

- Freedom 4, to improve the program, and make improvements public, so that the whole community benefits.

Its origin is related to the activity developed by the first computer programmers, the "hacker" culture, emerged in laboratories of American universities and research centers at the beginning of the computer age, such as the Artificial Intelligence Laboratory of the Massachusetts Institute of Technology (MIT) [3]. In that time, it was considered that sharing knowledge (and the code) freely was usual and even beneficial for the advancement of knowledge. Based on these premises, the ideological foundations of the free software movement were established in the 1980s thanks to the vision of Richard Stallman [4].

From other point of view, the use of free software in higher education, is a practice that extends itself both nationally and internationally. Spanish universities such as the University of Oviedo [5], the Carlos III University in Madrid [6], or the Polytechnic University of Valencia [7], University of Rioja [8], are using free software in their teaching methodologies. In Italy University of L'Aquila and University of Modena and Reggio Emilia [9], University of Bologna [10–12] University of Messina [13]. Also, American universities are joining this initiative [1, 2, 14–18]. However, the bet for the use of free software in Asian universities is not very widespread, but there are initiatives to implement its use in the educational system of Central Asia [19] (Fig. 1).

Fig. 1. Spanish universities best committed to the use of free software in 2016 [20]

It is worth mentioning the role of the RuSL (ranking de universidades en software libre/universities and free software ranking) Free Software Universities Network when it comes to providing a standardized methodology that allows to know in detail the impact of the actions carried out by educational institutions regarding the use of free software, as well as in which areas they stand out and how they disseminate their use in relation to other universities. Its analysis is based upon the analysis of 65 indicators, assessing 11 dimensions of the university: production, external collaboration, research, help, teaching, culture in free software, technological, disclosure, webmetry, institution and administration.

2 Context

This communication describes the experience of introducing free software: Gimp [21], Inkscape [22] and Scribus [23] in the subjects of Artistic Expression II and Graphic Design Applied to Product in the realization of graphic projects in both subjects. Inside this experience, students from the 2nd year of Industrial Design and Product Development Engineering Degree at the University of Zaragoza (IDPDE) participated.

The use of free software in these subjects supports and contributes to promote the values of the University of Zaragoza and its Office of Free Software (OSLUZ) [24].

3 Methodology

3.1 Description of the Experience

To carry out the experience, the main utilities of the free software programs are explained in class to do the exercises, leaving the student to choose whether working with free or with commercial software. In order to compare the benefits offered by free and commercial software, no changes have been made in terms of the teaching methodology or the content included in the teaching guides. The same calendar of activities planned for the two subjects has also been applied. Regardless of their choice, students must mainly perform the following tasks corresponding to the subjects:

- In Artistic Expression II, they perform 2D graphic representation tasks, starting from the digital drawing, chiaroscuro treatment, representation of highlight backgrounds, color ranges and image filters. These tasks can be solved both with the use of commercial software Adobe Photoshop, and with free software Gimp. Both programs allow the manipulation of images, they have numerous tools for digital retouching, color editing and composition. The learning process is developed through practical and theoretical classes, computer practices, workshop practices, tutored works and autonomous student work. These actions are framed in a collaborative work environment. The evaluation process is developed continuously in which the supervised works weigh up to 80% and the global test of contents of the subject up to 20%.
- In Graphic Design Applied to Product the tasks include typographies, branding, packaging, surface and interface graphics, composition and layout. For creating and

editing vector graphics students can use Adobe Illustrator or Inkscape (free software). The Adobe Indesign layout software or Scribus, free software, allow the management of image frames and blocks of text organized through a structure of pages, guides and grids for obtaining printed and digital documents. The learning process is developed through practical and theoretical classes, computer practices, supervised works and autonomous student work. These actions are framed in a collaborative work environment with an important presence of the service learning model. The evaluation process is developed continuously in which the supervised works weigh up to 70% and the global test of contents of the subject up to 30%.

The teachers solve the doubts arising from the use of the programs that the students have chosen to work.

The objectives of the implementation of the free software have been as follows:

- To use and evaluate free software in the subject.
- To contrast the quality of free tools with respect to those commonly used.
- To avoid costs to both students and the university for the licenses of the software used.
- To support the philosophy of the Free Software of the CRUE Spanish Universities group and to increase the degree of involvement and implementation of the use of free software at the University of Zaragoza.
- To prevent students from working with tools without an official license.

As this project is part of the strategy of the University of Zaragoza, it has had the participation of OSLUZ (Free Software Office of the University of Zaragoza), which made the presentation of a talk for knowledge of philosophy, possibilities and benefits of the free software.

3.2 Experience Evaluation

In order to analyze this experience, two ways of collecting information have been established: on the one hand, the perception of students through the survey carried out on Google Forms and distributed to students by email, and on the other hand, the comparison made by the teaching team between the commercial programs used in previous courses and the free software, through the use of a rubric.

The survey proposed to the students has been structured as follows: previous use of software and choice of software with which to carry out the projects of the subject. The answer to this last question conditioned the rest of the survey.

The survey addressed to students who used free software consisted of 8 questions, 5 were assessed by means of a Likert scale of 5 points (1—totally disagree and 5—totally agree) and 3 questions were open. Students were asked about accessibility (download, installation, versions), usability (intuitive interface, easy handling), their expectations and the satisfaction of the results obtained.

On the other hand, the survey aimed at students who used commercial software consisted of 4 questions, of which 2 were qualitative regarding the use of official license and their willingness to continue using this type of software or not and 2 open questions regarding considerations and motivations when deciding the software.

It has only been possible for students of the subject of Artistic Expression II to respond by referring to the Gimp and Photoshop programs, since the subject of Graphic Design applied to Product is still being studied at this time.

For the evaluation of teachers, a rubric has been designed that compares key aspects regarding accessibility, usability, structure, formats and exit modes. The items of this rubric have been incorporated after the previous evaluation process between four professors following the model of the Delphi method proposed by Williams, Boone and Kingsley (2004) [25].

4 Results and Discussion

A total of 58 out of the 83 students (69.8%) enrolled have completed the survey about the use of Photoshop and Gimp.

Regarding the knowledge of image treatment programs, the results indicate that all students know some of these programs. 51.7% of students knew Photoshop (30 students), 12.1% Gimp (7 students) and 36, 2% handled both programs (21 students). For the work of the subject 60.3% decided to use Gimp (35 students).

4.1 Results of Surveys of Students Who Have Used Gimp

These students have evaluated the following aspects of the program:

Accessibility: Students rated the accessibility of the software positively (48.6% agree that the accessibility is satisfactory −4 points on the Likert scale and 22.9% evaluate this aspect as completely satisfactory –5 points on the Likert scale) (Fig. 2).

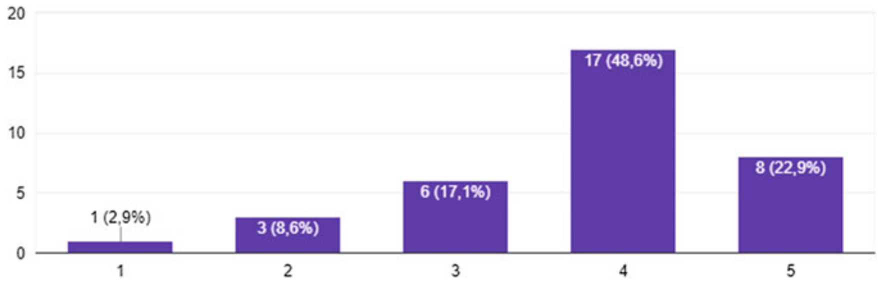

Fig. 2. Students' perception of Gimp's accessibility (download, installation and versions)

Usability: The surveys reveal some lack of satisfaction, being clear that none of the students was fully satisfied (Fig. 3).

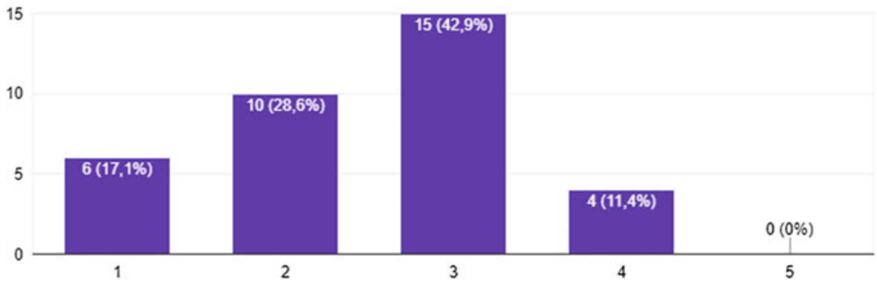

Fig. 3. Students' perception of the usability of Gimp (intuitive interface, tools and easy handling)

Software recommendation: 34.3% of students indicate some indecision about the possible recommendation of the software, however there is a group of 54.3% that would not recommend it, so only 11.5% would recommend the use of Gimp (Fig. 4).

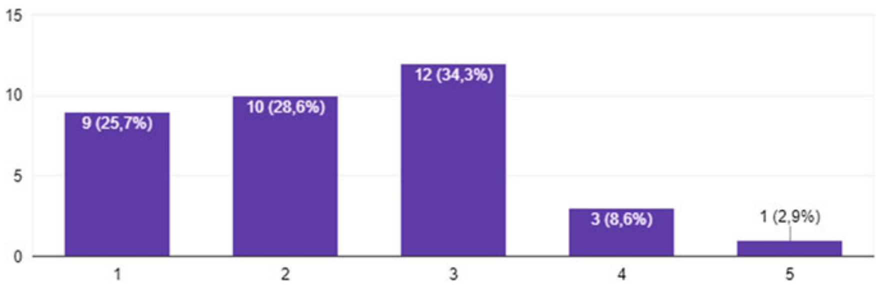

Fig. 4. Recommendation of the use of Gimp

In the open questions the students stand out as an advantage the free access and easy download, however they do not see other advantages and they are convinced that it will not be the program that is demanded in the labor market.

4.2 Results of the Surveys of Students Who Have Used Photoshop

Of the students who have decided to use the pay-per-use software (39.7% of the total, 23 students), 91.3% have used the program without the official license (21 students). And the vast majority of them (82.6%, 19 students) intend to continue using it in the future.

In the open questions students highlight the extended use of Photoshop in the professional world, and the previous knowledge of it as reasons for not using the free software proposed in class.

4.3 Results of the Comparison Made by the Teaching Team

The perception of the teaching team (four teachers) is summarized in the following tables that compares the aspects of accessibility, usability of tools, structure, formats and exit modes in the free software proposed in class and commercial software (Tables 1, 2 and 3).

Table 1. Comparison made by teaching team between free software (Gimp) and commercial software (Photoshop) for bitmap image edition

Parameters	Gimp	Photoshop
Accessibility		
– Download – Installation – Compatibility platforms	– Free – Quick – Windows, Mac and GNU/Linux	– Payment – Slow – Windows and Mac
Usability of tools		
– Vector traces – Bitmaps work – Filters	– Ease of creation and edition of vector outline – Multiple bitmap treatment options with some difficulty in their use – Wide variety of filters for free download	– Ease of creation and edition of vector outline – Multiple bitmap treatment options with intuitive use – Gallery of sufficient filters included in the license with possibility of extension by payment
Formats and output modes	– Saves as xcf – Possibility to save in different formats (jpg, tiff, png, etc.) – Difficulty saving files in CMYK – Low possibility of visualization of the change results in color mode	– Saves as psd – Possibility to save in different formats (jpg, tiff, png, etc.) – Easy and direct change of color mode
Structure and interface	– Intuitive structure – Customizable interface	– Clear structure, although overwhelming for novice users

Table 2. Comparison made by teaching team between free software (Inkscape) and commercial software (Illustrator) for vector image edition

Parameters	Inkscape	Illustrator
Accessibility		
– Download – Installation – Compatibility platforms	– Free – Quick – Windows, Mac and GNU/Linux	– Payment – Slow – Windows and Mac
Usability of tools		
– Vector traces – Bitmaps work	– The tools meet expectations, some interesting options in form modification – Free and downloadable filters	– Good functionality of the tools – Gallery of sufficient filters included in the license with possibility of extension by payment
Formats and output modes	– Saves as svg. – Does not support spot colors, does not allow export in CMYK directly – Crop marks, limit and color bars must be done with extensions and have to appear in the workspace itself (impractical)	– Saves as ai. – It allows outputs for virtual environment and for printing – It incorporates pallets of spot color – Option to add crop marks, limit and color bars when exporting to pdf
Structure and interface	– There are options that are not located where it would be logical to look for them	– Clear structure, although overwhelming for novice users

Table 3. Comparison made by teaching team between free software (Scribus) and commercial software (In Design) for publishing

Parameters	Scribus	InDesign
Accessibility		
– Download – Installation – Compatibility platforms	– Free – Quick – Windows, Mac and GNU/Linux	– Payment – Slow – Windows and Mac
Usability of tools		
– Blocks of text – Images	– Good functionality, especially in the loading of the text and its edition	– Good functionality
Formats and output modes	– Save as sla, export to pdf, eps, svg, tiff, jpg, png. – Supports CMYK and spot colors	– Save as.indd, export to pdf, eps, jpg, png. – Supports CMYK and spot colors
Structure and interface	– There are certain structure failures that make it not intuitive, however, the properties menu that allows you to modify almost every aspect is very useful	– Clear structure, although overwhelming for novice users

Although the Adobe interface can be overwhelming for novice users, the 3 programs share similar structure and interface, so if the user knows one of them, learning the other two is much easier. On contrary no relation between the structure and interface of Gimp, Inkscape and Scribus has been observed.

5 Conclusions

The experience presented shows the perception of teaching staff and students enrolled in the subjects of Artistic Expression II and Graphic Design Applied to Product of the Industrial Design and Product Development Engineering Degree, at the time of introducing free software in the works carried out so far by students with commercial software.

The introduction of free software in the two subjects has been an additional effort, however it has shown that free software designed to work with images, vector graphics and layout represents an alternative to commercial software, although there are aspects of structure and intuitiveness of interface that could be improved.

Although there are certain difficulties observed in the use of free software related to the use of some tools, modes and output formats, the teaching team considers that free software has allowed a satisfactory performance in all the tasks that address relevant issues in the graphic communication processes that are closer to the profile of Graphic Expression in Engineering.

Since the research in Graphic Expression focused on 3D open source software has been broadly developed, the authors consider that the 2D graphic design, based on the visual communication codes and esthetics requirements represents the potential to develop new educational research. The detection of the limitations of free software, can provide a starting point to introduce possible improvements in a software design more suitable for higher education that takes into account the market requirements.

With the use of free software, access to the software has been facilitated both in the classroom and outside of it, preventing illegal downloads of commercial software.

The students' prior knowledge of commercial software has led to a preference for this one, so it is considered important that in previous educational stages the use of free software must be disclosed.

The students emphasize the importance of the use of commercial software since this is the one that is mainly used and is currently demanded in the business environment. However, the teaching team considers free software as a good alternative for entrepreneurs.

The experience has gathered the conviction of the students of the dominant position of the commercial software in the labor market, however from the teaching point of view we are convinced that the students can be the carriers of change by offering the companies in which they are going to work free software, stable and in constant development, while the management of free software can facilitate their impulse in actions/entrepreneurship situation.

Acknowledgements. The experience has been supported by the 17_152_PIIDUZ–Innovation Teaching Project promoted by of Vice-rector of Academic Policy at the University of Zaragoza.

References

1. El sistema operativo GNU homepage. https://www.gnu.org/philosophy/free-sw.en.html. Last accessed 5 Mar 2018
2. Celaya CL, Martínez SLD (2007) Uso de software libre y de Internet como herramientas de apoyo para el aprendizaje. RIED. Revista iberoamericana de educación a distancia, 10 (1):83–100
3. Rodríguez WR (2014) Software libre para educación e investigación en Ingeniería. Revista Educación en Ingeniería 9(18):12–22
4. Williams S (2002) Free as in Freedom (2.0): Richard Stallman and the Free Software Revolution, published by the Free Software Foundation. Available online: https://sagitter.fedorapeople.org/faif-2.0.pdf. Last accessed 5 Mar 2018
5. Gayo JEL, Lanvin DF, Salvador JC, del Río AC (2006) Una experiencia de aprendizaje basado en proyectos utilizando herramientas colaborativas de desarrollo de software libre. Dpto. de Informática Universidad de Oviedo C/Calvo Sotelo S/N CP, 33007
6. Moreiro González JA, Sánchez Cuadrado S, Palacios V, Barra E (2011) Evaluación de software libre para la gestión de archivos administrativos
7. Moreno P, Cerverón V (2006) Plataforma tecnológica para potenciar los procesos de enseñanza-aprendizaje: desarrollo en la Universitat de València basado en software libre y colaborativo. In Proc: SIIE 06. VIII Simposio Internacional de informática aplicada a la enseñanza

8. Santamaría-Peña J, Benito-Martín M, Sanz-Adán F, Arancón D, Martinez-Calvo M (2017) Reliable low-cost alternative for modeling and rendering 3D objects in engineering graphics education. In: Eynard B, Nigrelli V, Oliveri S, Peris-Fajarnes G, Rizzuti S (eds) Advances on mechanics, design engineering and manufacturing. Lecture notes in mechanical engineering. Springer
9. Di Angelo L, Leali F, Di Stefano P (2016) Can open-source 3D mechanical CAD systems effectively support university courses? Int Journal Eng Educ 32(3):1313–1324
10. Fantini M, Curto M, De Crescenzio F (2017) TPMS for interactive modelling of trabecular scaffolds for bone tissue engineering. In: Eynard B, Nigrelli V, Oliveri S, Peris-Fajarnes G, Rizzuti S (eds) Advances on mechanics, design engineering and manufacturing. Lecture notes in mechanical engineering. Springer
11. Fantini M, De Crescenzio F, Brognara L, Baldini N (2017) Design and rapid manufacturing of a customized foot orthosis: a first methodological study. In: Eynard B, Nigrelli V, Oliveri S, Peris-Fajarnes G, Rizzuti S (eds) Advances on mechanics, design engineering and manufacturing. Lecture notes in mechanical engineering. Springer
12. Caligiana G, Francia D, Liverani A (2017) CAD-CAM integration for 3D hybrid manufacturing. In: Eynard B, Nigrelli V, Oliveri S, Peris-Fajarnes G, Rizzuti S (eds) Advances on mechanics, design engineering and manufacturing. Lecture notes in mechanical engineering. Springer
13. Cella U, Cucinotta F, Sfravara F (2017) Sail plan parametric CAD model for an A-class catamaran numerical optimization procedure using open source tools. In: Eynard B, Nigrelli V, Oliveri S, Peris-Fajarnes G, Rizzuti S (eds) Advances on mechanics, design engineering and manufacturing. Lecture notes in mechanical engineering. Springer
14. Cuervo MC, Delgado Becerra J (2005) El software libre como herramienta para el desarrollo de sistemas de información (Experiencia de una práctica empresarial en Caracol S.A.). Revista Ventana Informática, (12) Ed. Universidad de Manizales
15. Cuervo MC (2005) La Ingeniería de Software Libre y sus herramientas aplicadas a proyectos informáticos. Reportes Técnicos en Ingeniería del Software 7(2):30–35
16. Pagola L, Nomade P (2006) Software libre: caja abierta y transparente. Instalando, Arte y cultura digital
17. Marzocchi VA et al (2010) Las TICs en la enseñanza de la química: una experiencia con software libre de visualización y modelado molecular. FABICIB 14(2):40–45
18. Serrano JE, Narváez PS (2010) Uso de Software libre para el desarrollo de contenidos educativos. Formación universitaria 3(6):41–50
19. United Nations Educational, Scientific and Cultural Organization homepage. http://en.unesco.kz/development-and-implementation-of-free-and-open-source-software-in-educational-systems-of. Last accessed 5 Mar 2018
20. Universia España homepage, Ranking de universidades que usan Software Libre. http://noticias.universia.es/educacion/noticia/2016/04/28/1138733/ranking-universidades-usan-software-libre.html. Last accessed 5 Mar 2018
21. Gimp homepage. www.gimp.org. Last accessed 5 Mar 2018
22. Inkscape homepage. www.inkscape.org/es/. Last accessed 5 Mar 2018
23. Scribus homepage. www.scribus.net/. Last accessed 5 Mar 2018
24. Oficina Software Libre Universidad de Zaragoza homepage. https://osluz.unizar.es/. Last accessed 5 Mar 2018
25. Williams DL, Boone R, Kingsley KV (2004) Teacher beliefs about educational software: a Delphi study. J Res Technol Educ 36(3):213–229

Education for the Industry of the Future (IoF) with the 3D Experience Platform

V. Gomez-Jauregui[1(✉)], F. Cue-Palencia[2], C. Manchado[1], and C. Otero[1]

[1] EGICAD Research Group, School of Civil Engineering, Universidad de Cantabria, Avda. Los Castros s/n, 39005 Santander, Spain
valen.gomez.jauregui@unican.es

[2] School of Industrial and Telecommunicatins Engineering, Universidad de Cantabria, Avda. Los Castros s/n, 39005 Santander, Spain

Abstract. The role of universities is essential for the divulgation of the competences of the Industry of the Future (IoF) in students around the world. Therefore, the existence of different CAD software for Industrial Engineering, developed by several computer software companies (e.g. Autodesk, Siemens, Dassault Systèmes or Bentley Systems among many others), together with its possibility of working in a shared environment have vital importance. In this way, Dassault Systèmes, one of the most recognized software modeling company in the world, created 3D Experience Platform. This platform jointly includes some of the programs of the Dassault Systèmes package such as Catia, Delmia or Enovia. Moreover, it is available on the premises and in a public or private cloud environment, where there is the Peer Learning Experience Platform, which offers teaching material, mainly based on Project-Based Learning (PBL). These characteristics make it an important tool for the future of the engineering world, in accordance to Industry 4.0, in which some Spanish universities currently have a key role.

Keywords: Industry of the Future · 3D Experience · Peer Learning · Education · Design

1 Introduction

Since the second half of the 18th century to the present, the industry has undergone profound changes to adapt to the demand and to take advantage of the technology of the moment (Fig. 1 shows schematically this evolution). It all started with one of the most important changes in the history of mankind: The First Industrial Revolution. It began in the 18th century in United Kingdom (UK) with appearance of the steam engine, which was applied to new means of transport such as rail and steamboat. This meant a great social, economic and technological change throughout the world. In the 19th century, The Second Industrial Revolution emerged with new sources of gas, oil or electricity, as well as other major appearances like automobile, telephone or radio. In the middle of the 20th century, The Third Industrial Revolution (also called "the digital revolution") arose, more focused on renewable energies, process automation and the

F. Cavas-Martínez et al. (Eds.): *Advances on Mechanics, Design Engineering and Manufacturing II*, LNME, pp. 761–769, 2019.
https://doi.org/10.1007/978-3-030-12346-8_74

use of the Internet [1]. The current industrial revolution is called Industry 4.0 or Industry of the Future (IoF). It was originated in 2011 by the German government to describe the intelligent factory, a vision of computerized information with all processes interconnected by Internet of Things (IoT). IoF consists of the digitalization of the productive processes of the factories through sensors and information systems to transform and make them more efficient. For this purpose, it is necessary the incorporation of new technologies to the industry such as artificial intelligence, cloud computing, Big Data, IoT, augmented reality, cybersecurity or robotics (Fig. 1).

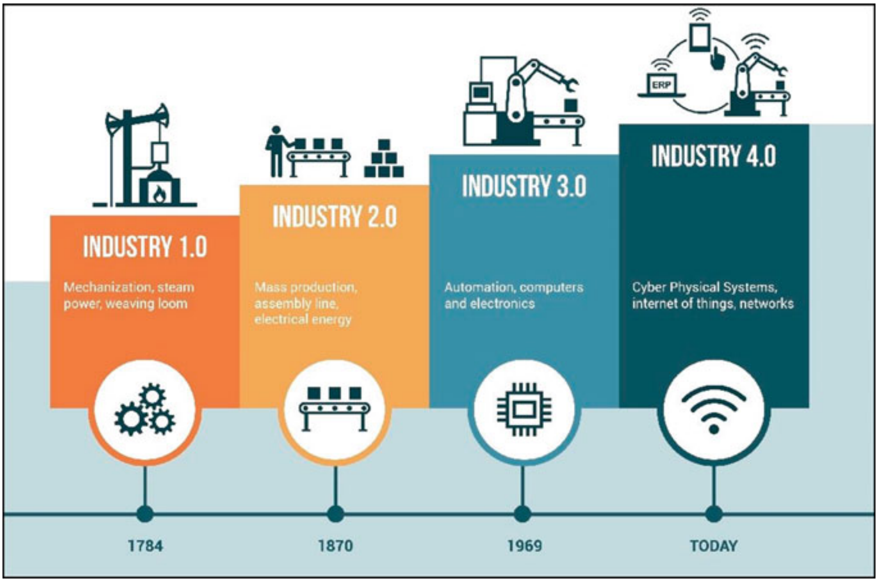

Fig. 1. Evolution of the industry at world level (*Source* http://www.aberdeenessentials.com/opspro-essentials/industry-4-0-industrial-iot-manufacturing-sneak-peek)

In Spain, IoF is also being implemented little by little. One of the most interesting ways of establishing all the competences and skills of this revolutionary industrial movement in the whole society is through education. For this reason, the role of the universities is vital because, nowadays, some engineering students finalize their academic degrees without receiving the adequate training in the face of a highly technological society [2]. Specially, in the industrial and engineering sector there are some specific aspects that should be disseminated in the education world: (i) knowledge and competences on computational technologies (mainly programming), (ii) understanding and competences in planning and management of project, and (iii) competences in teamwork [3]. Moreover, engineering students must be trained in technical knowledge, practical tasks, skills in CAx (Computer-Aided Applications, which refers to the use of computer technologies associated with the lifecycle of a product such as CAD, CAM, CAE, CAID, among others) and collaborative work skills, that is, Project-Based Learning (PBL).

In particular, the role of teachers and teaching staff is essential because current engineering students will be a fundamental part of human evolution and they will have to work in a context of Industry 4.0 (maybe even version 5.0 to come). The Universidad de Cantabria, with eleven other Spanish universities—Cádiz, Jaén, Jaume I Castellón, León, Mondragon, Basque Country, Politècnica de Catalunya, Politécnica de Madrid, Sevilla, Vigo and Zaragoza-, three French universities—ENI Metz, EC Nantes and U. Versailles S-Q-Y—and one Italian university—Politecnico di Milano—have participated in different workshops, seminars, webinar, etc. for the coordination of the project named "Accelerating the adoption of Industry of Future (IoF) supporting technologies by Spanish Universities" [3]. This project was partially organized by La Fondation Dassault Systèmes, establishing as the main topic the great importance that universities have for dissemination of the competences of IoF. This project is focused on three main objectives:

- Accelerate the adoption of learning practices and competences in IoF technologies, in particular, related to CAX-PLM in the manufacturing area.
- Harmonize the lecturing practices and educational material to contribute actively to an international community of educators with similar motivation in the field.
- Improve the students' learning experience, their digital competences in IoF and, consequently, their employment perspectives.

There also exist some other similar projects, such as "Project-based collaborative engineering learning to develop Industry 4.0 skills within a PLM framework" [4]. This project is about the importance that some applications like Computer-Aided Applications (CAx) or Product Lifecycle Management (PLM) can have in the development of Industry 4.0.

This communication does not intend to show an experimental research project or a study case, but to show the capabilities of the teaching methodology supported by a certain software. Therefore, the next stage will be to design an experiment for researching about the efficiency of the method based on the teachers' opinion, the academic results and the students' feedback.

2 Present About CAD Model and 3D Design Software

Currently, there are multiple modelling CAD software [5] for Industrial Engineering developed by several computer software companies, such as Autodesk (e.g. AutoCAD, Inventor), Siemens PLM Software (e.g. Solid Edge, NX Unigraphics), Dassault Systèmes (e.g. Catia, Solid Works), Bentley Systems (e.g. Microstation, ProjectWise), etc. These CAD solutions have many applications for the real engineering products, which are used by leading companies. One of the main characteristics of some of these types of software is the possibility of working in a shared environment, which allows to users to save, manage and share models and files directly online [6]. Among many others, an example of working collaboratively is Vault, by Autodesk, that allows each member of the team to work without changing the data of the other co-workers and sharing the projects with people outside the design group. Other example is PLM, by Siemens, that offers the management and administration of information throughout the lifecycle of a product, which allows to design, produce and control all features of the product with a single software. We can also mention Creo, by PTC, which is a software that offers the possibility of working in a multi-CAD environment in order to avoid inefficiencies and redundancies. Finally, any Bentley software offers a collaborative environment that allows to share content and products in a more controlled and managed environment.

One of the most competitive organizations recognized worldwide in modelling software and 3D design is Dassault Systèmes. This company provides virtual universes to business and people in order to imagine sustainable innovations. All of this is achieved with the help of its sophisticated software as Catia-software [7] of 3D design, product development and analysis-, Delmia-software for the engineering of the manufacturing processes that allows to plan, manage and take better advantage of the time-, Simulia -software that provides realistic simulation and Finite Element Analysis (FEM)- or Enovia -software that allows to manage and store all the information related to materials, geometries, modifications or projects in general.

3 3D Experience Platform on the Cloud

In accordance with the Industry 4.0 or IoF, Dassault Systèmes created the 3D Experience Platform [8], a collaborative platform that integrates some of their software in a unique working interspace. This online platform provides industry-leading applications for each of the company's departments, from sales marketing to engineering: Design & Engineering, Manufacturing & Production, Simulation, Governance & Lifecycle, 3D Design Experience for Professionals, as well as a broad catalog of services that were also included in the original packages of Catia, Simulia and Delmia.

Thanks to a single user-friendly interface, it encourages industry solution experiences, based on 3D design software, analysis, simulation and intelligence in an interactive collaborative environment. It is available on the premises and in a public or private cloud environment, which will transform the way companies do business due to it brings value on the innovation side. So, this possibility offers cost effective and seamless experience, adaptability and flexibility, improve collaboration globally and, security and efficiency.

The platform allows the user to register in the different roles or profiles depending on their position in the company or entity. This platform is divided mainly into four sections, corresponding to the four parts of its characteristic logo. These are: 3D Modelling Apps, Content and Simulation Apps, Information Intelligence Apps and Social & Collaborative Apps. In the section of 3D Modelling, the users have access to the most powerful mechanical design software of Dassault Systèmes -Catia- along with all its characteristic modules such as Part Design, Drafting, Generative Wireframe & Surface, etc. In the simulation section users have access to the Delmia and Simulia software, very useful tools to emulate and simulate different mechanisms and designs. In Information Intelligence Apps, there are basic tools like calculator, mail or web notes. Finally, the collaborative section is one of the most interesting parts of 3D Experience Platform, allowing the users to relate their work environment through the cloud in a simple way and to contact colleagues immediately via chat.

3D Experience Platform has access to the cloud environment (Fig. 2). This technology is not new, and some other trending applications work also on the cloud. Applications based on cloud computing (like Google Drive, iCloud, Dropbox, Office 365 or Autodesk 360 among many others) have numerous advantages, such as efficient use of the energy, possibility of working in a common environment with other companions or that the client can dispense with installing any kind of software. However, it also has some disadvantages like the availability of applications depends on the Internet connection, the security issues or the software size, which means that for some applications it is needed to have a powerful computer.

Fig. 2. Graphical user interface on the 3D experience on the cloud platform

It must be taken into account that 3D Experience Platform is still under development. This implies that some features of the platform should be improved. One of the main aspects to enhance is the speed of the software, since it usually takes some time to execute the commands. In this context, other typical problem of 3D Experience Platform is that it is often not possible to access it, sometimes due to maintenance periods or simply due to systems crashes. Moreover, it could be interesting to include some other solution modules like Geovia for modelling and simulating the natural environment of the infrastructures.

4 Peer Learning Experience and Companion Learning Space

Nowadays, we are immersed in a process of change that involves a qualitative leap in the educational model of the European Union. It is derived from the different agreements reached by the European Union to build a European Higher Education Area (EHEA). For this reason, the skills and abilities that society demands of its future professionals is a fundamental aspect that must be considered in the design of any educational strategy [9]. In this context, 3D Experience Platform provides a web portal that offers on-cloud teaching material of engineering, design, project management, etc., which are shared by some experts and universities, so the quality of the teaching material is continuously improving. The name of this web portal is Peer Learning Experience (PL'EXP) [10], in which the users have access to tutorials of all modules of 3D Experience Platform posted on the web portal through the users themselves (Fig. 3).

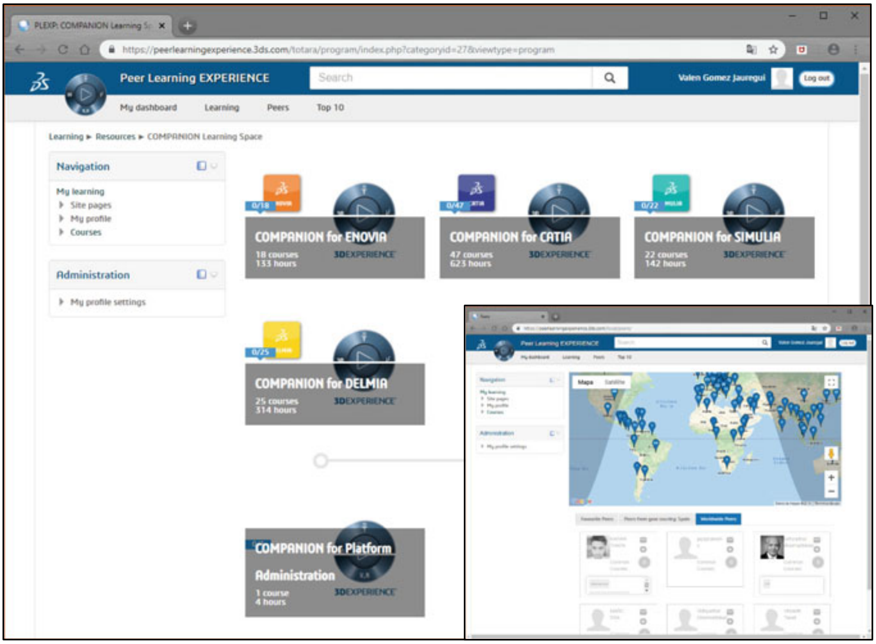

Fig. 3. Peer learning experience platform: learning and peers sections (lower right corner)

The teaching material is organized by themes and sections, letting the users to learn at their own pace. In addition, there is a customizable dashboard where it is possible to monitor the learning activities, the learning community, etc. One of the main keys of the portal web is the Peers (Fig. 3), which refers to the innovative method of learning between people with the same interests and objectives within the field of engineering, allowing to connect with other colleagues or personal teachers from anywhere in the world.

Apart from PL'EXP, Dassault Systèmes provides another web portal to start or reinforce knowledge about 3D Experience Platform. This cybernetic resource is Companion Learning Space [11], where experts and apprentices can navigate in search of information about science or engineering. Furthermore, the users can filter their searches by level of difficulty, engineering sector in which you are interested or specific software of Dassault Systèmes you wish to use it (e.g. Catia, Delmia, Enovia, etc.) (Fig. 4).

PL'EXP and Companion Learning Space are mainly based in Project-Based Learning (PBL), which is a very important concept for education. It is a pedagogical method based on students as protagonists of their own learning in which the acquisition

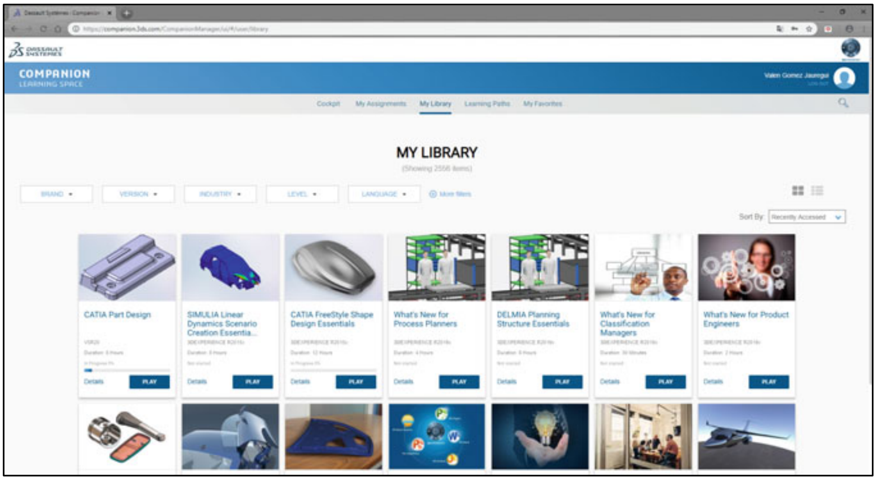

Fig. 4. Companion learning space

of knowledge takes a fundamental factor. It is based on the need to change the concept of the current learning in which, sadly, the students acquire concepts without knowing their usefulness or what sense it has in practical life. In this way, collaborative work is essential since students can share information in which they are specialists as well as

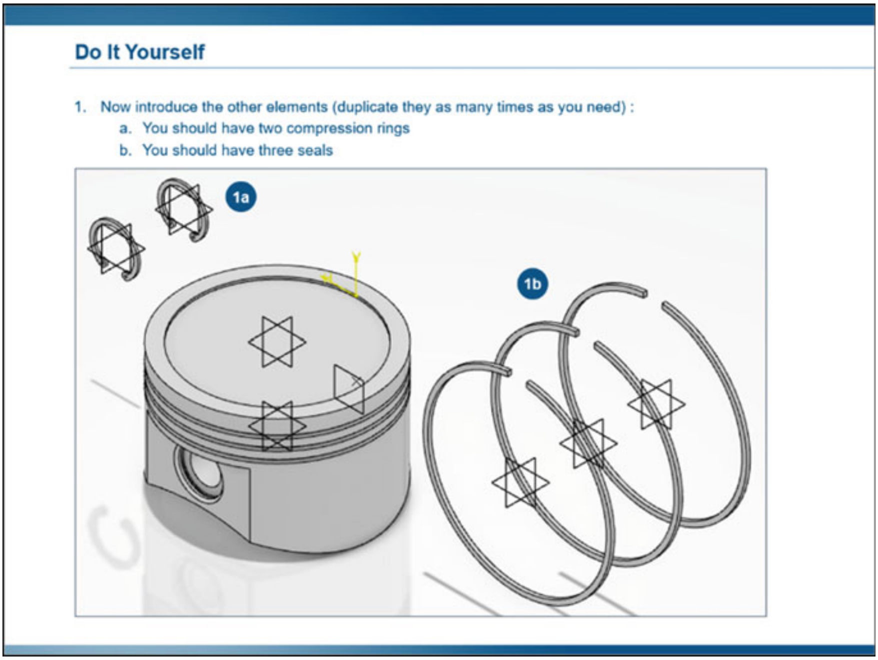

Fig. 5. Example of teaching material (Assembling tutorial) created by Universidad de Cantabria

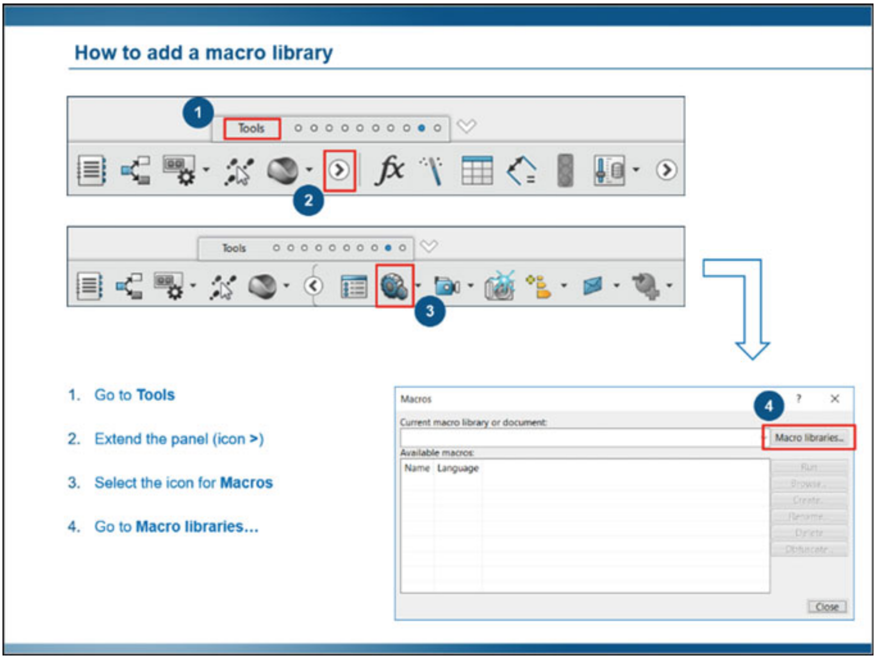

Fig. 6. Example of teaching material (Programming tutorial) created by Universidad de Cantabria

expand information by observing the projects and work of other people [12]. In this context, the Universidad de Cantabria supplies teaching material (e.g. tutorials about designing, assembling, drafting, programming, etc.), which provides added value for both educators and apprentices because, at the same time, it is an innovative and efficient way to learn and teach (Figs. 5 and 6).

In addition, PBL method offers an essential role to students, avoiding their passive character and, therefore, facilitating them to work actively and critically in their tasks. This learning method is in the vein of Industry 4.0 and it has several advantages:

- Developing skills and competences like collaboration, project planning, communication, decision making and time management by students.
- Increasing motivation.
- Preparing students better to face real problems.
- Increasing students' self-esteem and self-confidence.
- Learning in a practical way the use of science and technology.

5 Conclusions

In all probability, software applications like the 3D Experience Platform will be useful tools for the future of the engineering, improving the life of the whole society, in accordance with the IoF. For this, the role of the universities will be of vital importance, since they will have the possibility of providing and disseminating all the skills and competences for a highly technological society. Therefore, self-learning platforms, like Peer Learning Platform, are based on the students as the protagonists of their own learning process. This can be very positive, being their skills able to improve progressively through the material uploaded to the platform by their peers, in accordance with the Project-Based Learning (PBL) pedagogical system. Moreover, both 3D Experience and Peer Learning Platforms will be accessible to all engineering companies, providing a connection to the whole planet through the cloud, simply by accessing to Internet.

Further stages will consider the design of an experiment for researching about the efficiency of the method based on the teachers' opinion, the academic results and the students' feedback.

References

1. Mario H, Tobias P, Boris O (2016) Design principles for industrie 4.0 scenarios. In: System sciences, Hawaii international conference. Print ISSN 1530-1605. https://doi.org/10.1109/hicss.2016.488
2. Dolchinkov R Teaching methods in process system computer design. In: International conference of Education, Research and Innovation, Seville, 18–20 Nov 2013, pp 5785–5795
3. Ríos J, Mas F, Marcos-Bárcena M, Chevrot T (2016) Accelerating the adoption of industry of the future (IoF) supporting technologies by Spanish universities. Unpublished. Available online: https://www.researchgate.net/project/Accelerating-the-adoption-of-Industry-of-the-Future-IoF-supporting-technologies-by-Spanish-Universities. Accessed on Feb 2018
4. Vila C, Ugarte D, Ríos J, Abellán JV (2017) Project-based collaborative engineering learning to develop Industry 4.0 skills within a PLM framework. https://doi.org/10.1016/j.promfg.2017.09.050
5. Narayan KL (2008) Computer-aided design & manufacturing. PHI learning Pvt. Ltd., New Delhi, India, p 3. ISBN 812033342X
6. Fuh JYH, Li WD (2005) Advances in collaborative CAD: the-state-of-the art. Comput Aided Des 37(5):571–581, ISSN 0010-4485. https://doi.org/10.1016/j.cad.2004.08.005
7. Catia Software. Available online: https://www.3ds.com/products-services/catia/. Last accessed on Feb 2018
8. 3D Experience Platform. Available online: https://www.3ds.com/. Last accessed on Feb 2018
9. de los Ríos I, Cazorla A, Díaz-Puente JM, Yagüe JL, (2010) Project-based learning in engineering higher education: two decades of teaching competences in real environments. Procedia- Soc Behav Sci 2(2): 1368–1378. https://doi.org/10.1016/j.sbspro.2010.03.202
10. Peer Learning Platform. Available online: https://academy.3ds.com/plexp. Last accessed on Feb 2018
11. Companion Learning Space. Available online: https://companion.3ds.com/CompanionManager/ui/#/user/. Last accessed on May 2018
12. Maldonado M (2008) Aprendizaje basado en proyectos colaborativos. Una experiencia en educación superior 14(28):158–180

A Guide for Learning Design Practice

R. Sanz-Segura(✉), A. Fernández-Vázquez, E. Manchado-Pérez, and I. López-Forniés

Departamento de Ingeniería de Diseño y Fabricación, Escuela de Ingeniería y Arquitectura de la Universidad de Zaragoza, c/María de Luna 3, 50018 Saragossa, Spain
rsanz@unizar.es

Abstract. The learning and acquisition of industrial design skills and, in particular, methods and design process, are implemented in the scope of Bachelor's Degree in Industrial Design and Product Development Engineering at the University of Zaragoza, Spain. This publication presents contents related to the methodological control of the design process, included in the subject "Design workshop II: methods and design process", conducted during the first semester of the 2nd year of the degree. From this experience, this contribution shows the tools used in the subject to ensure that students are given the necessary knowledge to be able to apply a methodology and propose a clear and structured design process. The experience is based on the use of detailed scripts that structure practice sessions, showing and exemplifying their application through the projects developed during the course. This material can serve as a guide for its use and implementation in future teaching activities and academic projects in the field of engineering, in which a methodological basis and control of the design process is required, linking these aspects with the development of different analyses focused on the provision of essential information for the project. The result of these teaching practices is to facilitate a meaningful learning for the student, the interdisciplinary integration of knowledge for its application to the design process, the improvement of academic goals as well as an efficient coordination among teachers that improves communication among all the members of the university community involved in the degree.

Keywords: Design process · Design methods · Design methodology · Teaching · Learning design

1 Introduction

Industrial design engineering is a technical activity with a twofold objective: to improve people's lives through the development of new products, and to enhance the economic growth of companies that launch these products to the market by increasing user satisfaction. To reach this goal, various tasks are carried out, some of them specific to the discipline and others shared with another fields such as the study of the characteristics of users, their needs and expectations, the proposal of new technological developments because of their potential use at the service of people, the analysis of the market; or the prospective approach of future scenarios, among others.

F. Cavas-Martínez et al. (Eds.): *Advances on Mechanics, Design Engineering and Manufacturing II*, LNME, pp. 770–779, 2019.
https://doi.org/10.1007/978-3-030-12346-8_75

The results could be: (a) the generation of ideas for new products or services that improve existing ones or provide skills that increase the quality of people's life, generating in either case new market opportunities; (b) the development of ideas from the evaluation and prototyping stage to serial production; or (c) the execution of communication elements based on corporate identity, such as packaging.

With regard to industrial design, another important issue is the control and monitoring of project activity to ensure, as far as possible, the achievement of the described objectives and the generation of documentation to strengthen existing knowledge in the field of the project. The learning and acquisition of these skills and, in particular, methods and design process, is implemented in the scope of Bachelor's Design and Product Development Engineering at the University of Zaragoza, through a series of modules where the studied concepts are put into practice, following a vertical structure in which the different learning goals are gradually integrated [1]. Thus, it is possible to build up from the knowledge of some basic elements of the project activity, continue working on the development of the communicative capacity of the products and then, in order to deepen the methodological control skill over the whole process, integrate the most diverse technical and humanistic knowledge and, finally, develop cross-cutting skills that facilitate teamwork in the context of the business world.

This publication presents contents related to the methodological control of the design process, included in the subject "Design workshop II: methods and design process" [2]. The subject is conducted during the first semester of the 2nd year of the degree, as part of the 2nd module of subjects. Its overall goal is to provide students with the tools and knowledge necessary to perform analysis, obtain conclusions and propose improvements of one product, so that it can be materialized through a final representation.

The result of these teaching practices is to facilitate a meaningful learning for the student, the interdisciplinary integration of knowledge for its application to the design process [3], the improvement of academic goals as well as an efficient coordination among teachers that improves communication within all the members of the university community involved in the degree.

2 Methodology for Learning Design Practice

The general aim of the degree is to provide the student with the skills to address the management of knowledge and design capacity necessary for the planning and development of the entire conception, manufacturing process and life management of a product [4]. In this sense, the subject has a project-based learning approach [5, 6], as the implementation and development of these skills are pretended to be acquired by the student through experimentation in the context of a real product design experience [7, 8].

Learning design practice is based on a theoretical understanding of content, explained in lectures to the entire group, which are supplemented by case studies while applied simultaneously in projects. Projects development is supervised and reviewed during a series of practical sessions or design workshops within smaller groups in which the theoretical contents are put into practice. This practical and experimental learning allows the setting of the contents, and allows the implementation of various tools and techniques of analysis previously shown during the theoretical lectures.

A product design project is important and complex enough as to entrust its success just to intuition, luck or chance [9]. Therefore, in the development of the design activity, it is necessary to apply a methodology, for the available work methods must be known in advance. It is also necessary to work following a pre-established and controlled approach throughout the process, especially considering the difficulty of effective teamwork learning. Method and control are necessary for ensuring that students acquire the essential knowledge about the environment in which the project is going to be developed and applied, and control the technique and deadlines for its execution.

A method is defined when a set of actions, processes and tools are theoretically considered [10]. This approach is subsequently tested and validated empirically. In the academic field presented, the actions to be carried out are:

- Market study and segmentation, product positioning maps.
- Structural and functional-formal analysis of the product.
- Semiotics and communication structure analysis of the product.
- Study of users both from ergonomics and use sequence of the product.
- Project briefing.
- Applied creativity to innovative product conceptualization.
- Definition of manufacturing processes, and value/costs analysis.
- Documentation of the Project, including 2D and 3D rendering, and models and prototyping production.
- Packaging development.
- Presentation of results.

3 Design Process

The design process starts from the analysis of the internal characteristics of a product, analyzing the solutions adopted for its realization, questioning them, proposing possible improvements, and providing the necessary technical and formal evolution to achieve the materialization of the new product, also through an exterior shape. It is therefore a process of construction from inside to outside.

Sometimes, decisions are taken in the very early stages of the design process, and are maintained throughout the project without having been the result of a profound reflexion of the various existing possibilities. This is a very serious but unfortunately too frequent mistake. Those first determinations condition the whole developing of the project, as inadequate decisions taken too soon are very difficult, or too expensive, for being changed in later stages.

For this reason, the subject emphasizes the importance of these first phases, helping and encouraging students to reserve a significant amount of time for the analysis and evaluation of the alternatives and, if necessary, for modifying, but never totally rejecting, the various options considered.

The second consideration is that the process serves to manage with at least a minimum guarantees relevant aspects such as the symbolic load of the shape. As well as for the development of the function is necessary the methodological control, it is required the adequate handling of the expressive tools associated with the precise development of the aesthetics of the product, so as to avoid interpretations or subjective approaches that can lead to confusion or, at worst of the cases, mistakes in the interpretation of the product.

Experience has shown that for fixing knowledge definitively, it must be exposed repeatedly, and with an approach that combines theory and practice. In this way it is evident to the student, without any doubt, the practical potential of the taught subject, while generating the necessary practice in the tools associated with said theoretical base. The order and the rigor in the exposition of the subject has been demonstrated fundamental to reach the formative objectives sought.

Different methodologies have been developed for the process of product design and development [11–13], but all of them involve or essentially propose three basic actions: planning, development and realization. This sequence is repeated on a different scale, both globally within the project, and in detail within each of the tasks necessary for the resolution of the intermediate phases and the final details.

This methodology is very similar to the Deming circle [14], which establishes the steps of planning, doing, checking and acting, and varies only the verification phase, which in the case of the design processes developed within the subject is done automatically at the end of each phase through meetings with presentations to project managers.

Sometimes phases overlap, so that when one has not yet finished, the next one begins, thus continuity exists between the different phases or parts of the project, always depending on the type of project. And sometimes they are developed jointly, as in the case of the first two (previous phase and information phase). But these circumstances do not alter the basic scheme of the process, which is structured in the manner described in the following section.

Firstly, students perform a generic approach of a design process, to structure it in stages, apply a methodology and select the design strategy. Additionally, students define product design specifications in order to develop relatively complex products up to a satisfactory technical grade, which includes the way and needs to develop the project.

As already stated, this is a typical methodological process. Broadly speaking, it refers to a sequence of work commonly accepted and extended among professionals, based on analysis, a controlled creativity, and the control of phases and project decisions. Thus, the methodology is proposed in different ways by the different professionals, in a search of the greatest possible effectiveness and each professional adapts the method based on their own experience. As a summary, the following scheme is proposed corresponding to the product design process followed by students (Fig. 1).

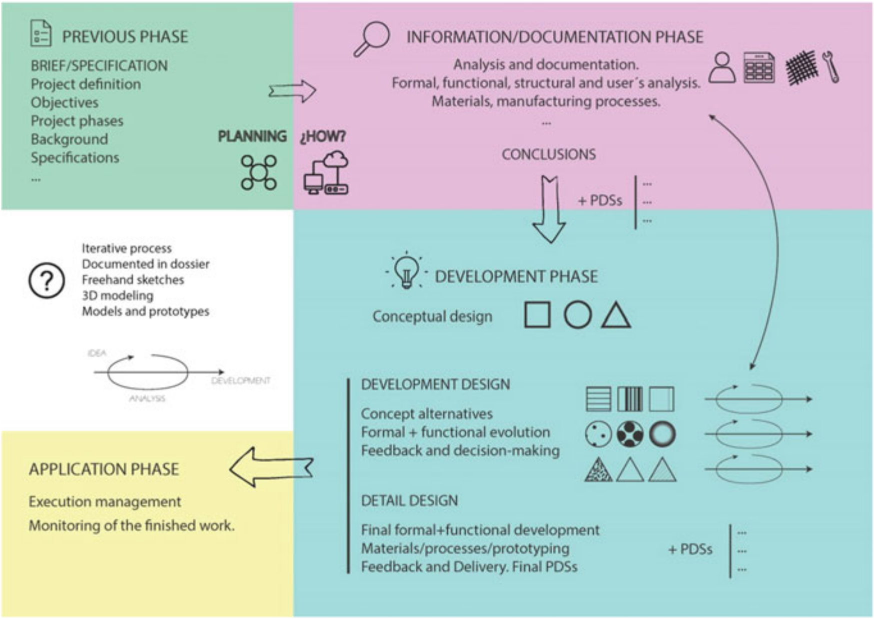

Fig. 1. Design process. Adapted from "Métodos y proceso de diseño. Taller de diseño" [2]

4 Guide for Design Workshops Schedule

Based on this previous academic experience, Table 1 shows one of the tools used in the subject during practical sessions to ensure that, during its development, students are given the necessary knowledge to be able to apply a methodology and propose a clear and structured design process. This is intended to provide students with a base that enable them to integrate and relate, in a vertical manner, the rest of the subjects that will be taught throughout the degree.

The experience is based on the use of detailed scripts that structure practice sessions, showing and exemplifying their application through the projects developed during the course. This material can serve as a guide for its use and implementation in future teaching activities and academic projects in the field of engineering, in which a methodological basis and control of the design process is required, linking these aspects with the development of different analyses focused on the provision of essential information for the project.

Design workshops are presented in 2-hour practical sessions. The schedule of the workshops is divided into four sections: board explanation; teamwork; discussion; and next session "to do". The duration of each activity is not mandatory, and can vary depending on the needs or circumstances of each group of students, but all of the activities must be developed, as the training objectives of each session must be accomplished.

The use of detailed scripts with the necessary steps to translate the theory into practice has had one of its best results in *methods and tools description* section "design

Table 1. Design workshop description

Tasks	Objectives	Work description	Recommendations	Timing
Board explanation	Description of session objetives Relate theory to practice Revision of calendar and global objectives	Theory introductory speech Methods and tools description Design requirements	Key points Timing Process-based approach Assessment Engagement	30′
Teamwork	Student teamwork planning Teamwork coordination Tasks definition Decision-making	Definition and sources searching Research Methods implementation Analysis Conclusions Teacher review	Collaboration Critical thinking Communication Team coordination Divergent/convergent thinking Iterative process	70′
Discussion	Sharing information Feedback collecting Problem solving	Support the students to achieve their goals	Collaboration Critical thinking	15′
Next session "to-do" list	Summary and conclusions	List and review tools, methods and documentation to be delivered Workshop conclusions	Board work summary Screenshot	5′

factors" corresponding to one of the main *theory introductory speechs*: "Analysis and techniques applied to the design process. Market and product". Students, frequently and recurrently year after year, find difficulties in understanding the difference between design factors and design specifications. Once the student collects the information of the product to be developed and coming from different sources (*definition and sources searching/research*), he has the ability to create homogeneous sets of consumers within a specific market (segmentation). Under a series of common criteria and design factors, as many as necessary, analyze products of the same category (or segment) with each other in order to obtain relevant conclusions (*methods implementation*).

The design factors are specific aspects of each product and allow us to analyze similar products based on the same criteria (or design factors) to eliminate uncertainty and, on the other hand, to start the design with the necessary information and a series of conclusions that allow generating concepts of design that can be further developed.

An example of this type of analysis based on common design factors is shown in Fig. 2, corresponding to the *teamwork* done by a group of students. It does not compare objects that are different but those that have a common base (they belong to the same market segment and are analyzed according to common factors); this is the precondition for perceiving differences. The analyzes and design tools used give meaning to the different variables and allow to discriminate the most important ones. Thus, it is able to identify the points of improvement, weaknesses or strengths of the analyzed products.

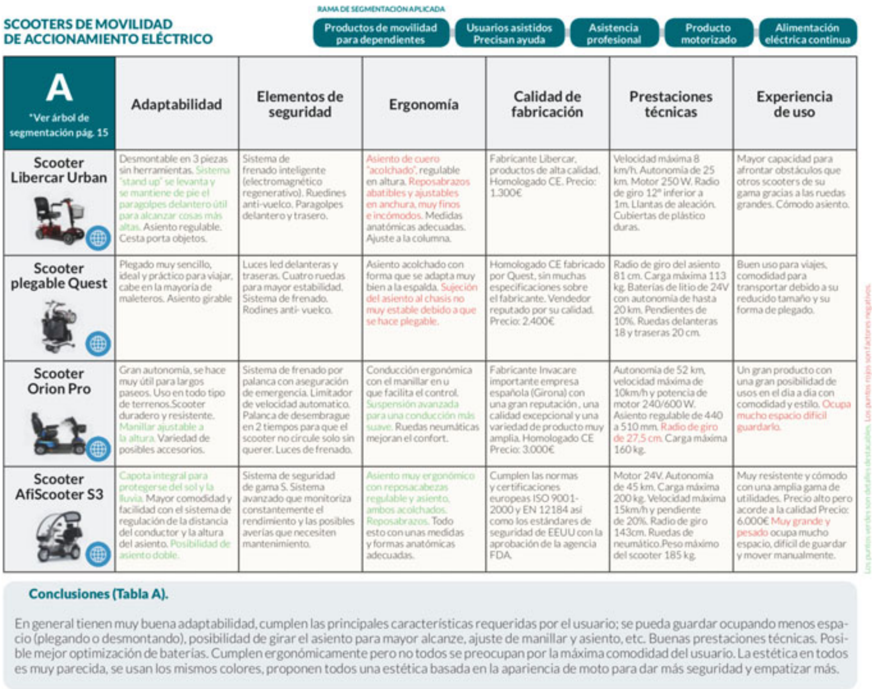

SCOOTERS DE MOVILIDAD DE ACCIONAMIENTO ELÉCTRICO

RAMA DE SEGMENTACIÓN APLICADA: Productos de movilidad para dependientes | Usuarios asistidos Precisan ayuda | Asistencia profesional | Producto motorizado | Alimentación eléctrica continua

A *Ver árbol de segmentación pág. 15	Adaptabilidad	Elementos de seguridad	Ergonomía	Calidad de fabricación	Prestaciones técnicas	Experiencia de uso
Scooter Libercar Urban	Desmontable en 3 piezas sin herramientas. Sistema "stand up" se levanta y se mantiene de pie el paragolpes delantero útil para alcanzar cosas más altas. Asiento regulable. Cesta porta objetos.	Sistema de frenado inteligente (electromagnético regenerativo). Ruedines anti-vuelco. Paragolpes delantero y trasero.	Asiento de cuero "acolchado", regulable en altura. Reposabrazos abatibles y ajustables en anchura, muy finos e incómodos. Medidas anatómicas adecuadas. Ajuste a la columna.	Fabricante Libercar, productos de alta calidad. Homologado CE. Precio: 1.300€	Velocidad máxima 8 km/h. Autonomía de 25 km. Motor 250 W. Radio de giro 12° inferior a 1m. Llantas de aleación. Cubiertas de plástico duras.	Mayor capacidad para afrontar obstáculos que otros scooters de su gama gracias a las ruedas grandes. Cómodo asiento.
Scooter plegable Quest	Plegado muy sencillo, ideal y práctico para viajar, cabe en la mayoría de maleteros. Asiento girable	Luces led delanteras y traseras. Cuatro ruedas para mayor estabilidad. Sistema de frenado. Rodines anti- vuelco.	Asiento acolchado con forma que se adapta muy bien a la espalda. Sujeción del asiento al chasis no muy estable debido a que se hace plegable.	Homologado CE fabricado por Quest, sin muchas especificaciones sobre el fabricante. Vendedor reputado por su calidad. Precio: 2.400€	Radio de giro del asiento 81 cm. Carga máxima 113 kg. Baterías de litio de 24V con autonomía de hasta 20 km. Pendientes de 10%. Ruedas delanteras 18 y traseras 20 cm.	Buen uso para viajes, comodidad para transportar debido a su reducido tamaño y su forma de plegado.
Scooter Orion Pro	Gran autonomía, se hace muy útil para largos paseos. Uso en todo tipo de terrenos.Scooter duradero y resistente. Manillar ajustable a la altura. Variedad de posibles accesorios.	Sistema de frenado por palanca con aseguración de emergencia. Limitador de velocidad automatico. Palanca de desembrague en 2 tiempos para que el scooter no circule solo sin querer. Luces de frenado.	Conducción ergonómica con el manillar en u que facilita el control. Suspensión avanzada para una conducción más suave. Ruedas neumáticas mejoran el confort.	Fabricante Invacare importante empresa española (Girona) con una gran reputación , una calidad excepcional y una variedad de producto muy amplia. Homologado CE Precio: 3.000€	Autonomía de 52 km, velocidad máxima de 10km/h y potencia de motor 240/600 W. Asiento regulable de 440 a 510 mm. Radio de giro de 27,5 cm. Carga máxima 160 kg.	Un gran producto con una gran posibilidad de usos en el día a día con comodidad y estilo. Ocupa mucho espacio difícil guardarlo.
Scooter AfiScooter S3	Capota integral para protegerse del sol y la lluvia. Mayor comodidad y facilidad con el sistema de regulación de la distancia del conductor y la altura del asiento. Posibilidad de asiento doble.	Sistema de seguridad de gama S. Sistema avanzado que monitoriza constantemente el rendimiento y las posibles averías que necesiten mantenimiento.	Asiento muy ergonómico con reposacabezas regulable y asiento, ambos acolchados. Reposabrazos. Todo esto con unas medidas y formas anatómicas adecuadas.	Cumplen las normas y certificaciones europeas ISO 9001-2000 y EN 12184 asi como los estándares de seguridad de EEUU con la aprobación de la agencia FDA.	Motor 24V. Autonomía de 45 km. Carga máxima 200 kg. Velocidad máxima 15km/h y pendiente de 20%. Radio de giro 143cm. Ruedas de neumático.Peso máximo del scooter 185 kg.	Muy resistente y cómodo con una amplia gama de utilidades. Precio alto pero acorde a la calidad Precio: 6.000€ Muy grande y pesado ocupa mucho espacio, difícil de guardar y mover manualmente.

Los puntos verdes son detalles destacables. Los puntos rojos son factores negativos.

Conclusiones (Tabla A).

En general tienen muy buena adaptabilidad, cumplen las principales características requeridas por el usuario; se pueda guardar ocupando menos espacio (plegando o desmontando), posibilidad de girar el asiento para mayor alcanze, ajuste de manillar y asiento, etc. Buenas prestaciones técnicas. Posible mejor optimización de baterías. Cumplen ergonómicamente pero no todos se preocupan por la máxima comodidad del usuario. La estética en todos es muy parecida, se usan los mismos colores, proponen todos una estética basada en la apariencia de moto para dar más seguridad y empatizar más.

Fig. 2. Analysis of design factors. Screen capture of teamwork developed by second-year students (2017–2018) corresponding to the project "design to improve the mobility of dependent users"

5 Primary Results of the Experience Developed

The experience with the scripts of practices, which have been used for the first time in the subject during the year 2017–18, has materialized in a significant improvement of the achievements of the work developed by the students in the first phases of the projects.

The combination of the information provided in the theoretical classes with the reinforcement of the knowledge that was realized in the practical sessions has allowed, in addition, that the work that was developed during the practical classes served as a base for complementary work which the students had to develop outside the classroom. The final sharing of the results achieved has allowed, in each of the sessions, to detect errors from the most initial phases of the project, avoiding that these were maintained throughout the entire project.

Finally, a better coordination has been achieved in the development of practical sessions that not only facilitated the work of teachers, clarifying the tasks to be developed in each session, but also providing the students with a sense of homogeneity and rigor in the subject that has avoided both misunderstandings and differences in the pace of development of the work among different class groups.

This improvement has been measured by comparing the appraisal of the evaluation surveys fulfilled by the students at the end of the courses 2016–2017 and 2017–2018. The analysis has focused in the valuation of questions regarding coordination. The response rate in the academic year 2017–18 was 65.91% (58 responses from a total of 88 students), considerably higher than the response rate in the academic year 2016–17, whose participation was 33.75% (27 responses from a total of 80 students). As it is shown in Fig. 3, the theoretical and practical classes have been better coordinated, and it has improved the evaluation of the way the subjects have been explained by teachers, avoiding repetitions between them. But the real improvement can be seen in the rising up to a 20% increase of the evaluation of the coordination between teachers.

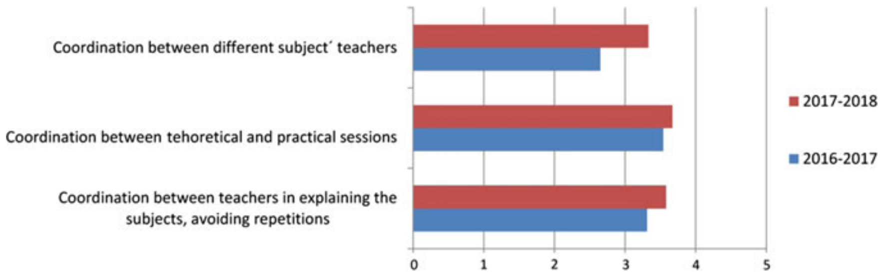

Fig. 3. Comparison of the evaluation of students, between consecutive years, of coordination problems within the subject

In any case, the experience developed has only been a first test that should be continued and improved in future years. Some aspects that may be susceptible to improvement have been detected, such as the degree of participation and involvement of students in the activities, which should be analyzed in future experiences. These will allow, in addition, to evaluate in a more quantifiable way the improvement that this methodologies entails in the acquisition of knowledge by the students.

6 Conclusions

It is important to state that the academic project should not be confused with the professional assignment. The academic project aims firstly to show a way of working and provide its experimentation to achieve a learning through the project, more than to achieve project results themselves.

Methodology must be differentiated from process. Knowing the process establishes the method or methods to follow (sometimes, vice versa). All methodologies have a common base; the flexibility in applying one method or another is the key to success in different environments, which is another goal to reach in a learning experience. No method is infallible in absolute terms. The same method can be correct in some situations and incorrect in others. The projects are different. The methods experienced in other projects can be reused provided they are evaluated positively in terms of this new situation.

There are different methods of projecting according to the designer and type of project. Any method can be enriched with new methods. A new method can always be developed before a new project. It can be improved by modifications or reviews of existing old methods.

In a creative environment, creativity is applicable to the process and to the methodologies themselves. Creating new methods is a necessary task itself to develop stimulation techniques of creativity workshops, since sometimes saturation or lack of references can block the student's generation of ideas. To be able to do this work requires creative ability, have technical knowledge and also strive to know well how are the people who will use the product, where they will use it, what their needs are and what will be the best way to manufacture the product, among others aspects. So the multidisciplinary identity of the design process is something that the students must bear in mind at every moment while experimenting with specific tools.

Though the process exposed in this paper the design student:

– Will be able to know, to experience, and to understand different methods of industrial design approaches, their potential evolution and their application possibilities depending on the kind of project to be carried on.
– Will learn to particularize the design process, making it applicable to any project design, and adapting it to any particular case.
– Will understand the need and relevance of structuring design processes in phases to keep a control of the project environment, an adequate scheduling and a proper management of the overall frame of work.
– Will gain confidence on their training to find solution to different problems of increasing complexity, based on the development of conceptual proposals within a design process.
– Will able to reach a technically viable product proposal from a conceptual proposition.

References

1. Manchado Pérez E, López-Forniés I (2012) Coordinación por módulos de asignaturas en el Grado de Ingeniería de Diseño Industrial y Desarrollo de Producto de la Universidad de Zaragoza. REDU. Revista de Docencia Universitaria, [S.l.]; vol 10, 3, pp 195–207. https://doi.org/10.4995/redu.2012.6020
2. López-Forniés, Ignacio, Manchado, Eduardo, Sanz, Rosana (2016) Métodos y proceso de diseño. Taller de diseño. Prensas de la Universidad de Zaragoza, Zaragoza. ISBN 978-84-16515-77-6
3. Tempelman E, Pilot A (2011) Int J Technol Des Educ 21:261. https://doi.org/10.1007/s10798-010-9118-4
4. Christiaans H, Venselaar K (2005) Creativity in design engineering and the role of knowledge: modelling the expert. Int J Tech Des Educ 15(3):217–236
5. Blumenfeld PC, Soloway E, Marx RW, Krajcik JS, Guzdial M, Palincsar A (1991) Motivating project-based learning: sustaining the doing, supporting the learning. Educ Psychol 26(3–4):369–398
6. Eger AO, Lutters D, van Houten FJ (2004) Create the future: an environment for excellence in teaching future-oriented Industrial Design Engineering. In DS 33: Proceedings of E&PDE 2004, the 7th international conference on engineering and product design education, Delft, The Netherlands, 02.-03.09
7. Dym CL, Little L (2003) Engineering design: a project-based introduction, 2nd edn. Wiley, New York
8. Dym CL (1994) Teaching design to freshmen: style and content. J Eng Educ 83(4):303–310
9. Thackara J (2006) In the bubble: designing in a complex world. MIT press
10. Blessing LT, Chakrabarti A (2009) DRM: a design reseach methodology. Springer London, pp 13–42
11. Munari B, Rodriguez CA (1983) ¿Cómo nacen los objetos? GG
12. Dym CL, Agogino AM, Eris O, Frey DD, Leifer LJ (2005) Engineering design thinking, teaching, and learning. J Eng Educ 94(1):103–120
13. Hubka V, Eder WE (2012) Theory of technical systems: a total concept theory for engineering design. Springer Science & Business Media
14. Deming WE (1989) Calidad, productividad y competitividad: la salida de la crisis. Ediciones Díaz de Santos

Improving Spatial Abilities and Comprehension in Technical Drawing Students Through the Use of Innovative Activities and Augmented Reality

E. Olvera-García, M. D. Marín-Granados(✉), and F. J. Ortíz-Zamora

Department of Graphic Expression, Design and Projects, Doctor Ortiz Ramos St, 29071 Málaga, Spain
951 9 52276mdmarin@uma.es

Abstract. Spatial abilities are essential not only for engineers but for those in many other professions such as medicine, archaeology and architecture. It has proven possible to improve these skills using sports or video games. An engineer must be capable of expressing ideas and understanding drawings, and for this, technical drawing and these abilities are an essential part of the learning process at the university. Courses such as Graphic Expression aim to help the student to have better spatial skills. However, this is not always an easy task. Many engineering students do not have the experience and knowledge when they begin their studies, and so they face a number of difficulties in understanding lessons that are of a higher level. The study we are presenting proposes a series of innovative exercises that include augmented reality to help students develop their skills and improve their understanding. These exercises could be applied in the future to other age ranges and subjects such as mechanics.

Keywords: Graphic expression · Engineering · Teaching · Augmented reality

1 Introduction

The importance of spatial skills is not only limited to the communication of concepts or ideas, but helps to create relationships between the real and the abstract to improve the understanding of certain problems or calculations. It has been demonstrated that it is not only study that increases our spatial abilities. Other activities such as sports [1] have also been related to a person's skills, since they involve analysing positions, space, and objects among others. Other authors such as Subrahmanyam [2] and Feng [3] have found evidence of the relationship between video game usage and an improvement in spatial abilities.

Innovative teaching methods are now being tested and used in many universities. As evidenced in articles such as [4], online tests for self-assessment on Technical Drawing are being offered to the students to help them identify their level of understanding of certain subjects in technical drawing courses. Moreover, Interactive self-learning tools for teaching manufacturing dimensioning are being used in the classroom "to teach dimensioning criteria of mechanical features concerned with elementary

F. Cavas-Martínez et al. (Eds.): *Advances on Mechanics, Design Engineering and Manufacturing II*, LNME, pp. 780–788, 2019.
https://doi.org/10.1007/978-3-030-12346-8_76

machining processes". These consist of video and drawing animations "that link real machining processes with the dimensioning of the correspondent work piece" [4].

With respect to teaching techniques that include AR, there are relatively few previous studies such as [5], which involved a short and intensive course of 16 h of work for two weeks. It was offered to freshman engineering students that were enrolled in the "Graphical Expression" course of the Bachelor's Degree in Industrial Technologies Engineering. This experience was divided into two blocks: the first consisted of some classic paper and pencil exercises about metric geometry, the foundations of graphical representation and multi-view and axonometric representation systems. In this phase, the students were given some wooden models to help understand the exercises. During the second part of the experiment, the students used an AR book with an augmented reality application that uses virtual 3D models. The exercises were of increasing difficulty and the student could use YouTube tutorials for help with each type of exercise.

As we can see, augmented reality has been used to help the visualisation of spatial vision exercises, but in this experience, we went a step further. In the case presented here, augmented reality is not only a way to help the student see the exercise. The simulations created for the purpose of this experience allow for an understanding of what the activity is about, along with the steps required to reach the answer, thus improving comprehension.

In previous experiences augmented reality has been used merely to show models in space without any programming in them and without presenting changes during the lesson [6]. The presented simulators, however, allow for a continuous interaction between the student and the exercise (including all of its elements). The simulators are entertaining and capture the student's attention because they allow the student to navigate through them unaided, allowing each of the parties to take the time needed.

2 Context

2.1 Location and Academic Setting

This experience took place in Málaga, Spain. We focused on Graphic Expression students in their first year of university, from which data that included their individual profiles, skills, and influences, among others, were collected.

These same students were those that participated in the whole experimental process, and included those that were not part of the experimental group, due to their evaluations throughout the semester. The hypotheses and analysis of this experience are part of an Educational Innovation Project of the University.

2.2 Student Profile

It is well known that many students in Spain start their technical studies at university with little or no prior knowledge of subjects such as technical drawing. With regard to Graphic Expression, the curriculum in both Primary and high school is established by the Spanish Ministry of Education, Culture, and Sport.

Relatively few are given the opportunity to learn about graphic expression because it is not mandatory for the schools to offer this during high school, and during the Baccalaureate only a few students choose to do so. In any case, the students are able to select any undergraduate program of their choosing, provided that they achieve the required grade

This, in fact, is a large part of the problem, since many students that decide to enrol on an engineering undergraduate course come from a range of backgrounds, and so not all of them will have the level required to deal with the difficulties associated with many of the courses.

This research focuses on the Graphic Expression class for mechanical engineering students. Thanks to the data obtained we can see that the percentage of students without pre-university experience in technical design is 34%, which is considerably high, given that there are specific prerequisites of prior knowledge for participating in this class. Whilst this percentage does not reach half of the population of the students surveyed, it still represents a substantial number of people with no prior experience.

In this same group, it was also observed that 42% of the students who formed our initial sample are repeaters of this same course. Thus, they are likely to be unmotivated by the same type of exercises and could lack the confidence required to succeed.

Therefore, it is clear that students need motivation and support that is sometimes difficult to give due to a large number of students and the shortage of available hours of teaching. This aim of the present research was to contribute towards reaching this goal.

2.3 Description of the Research

As mentioned at the beginning of this article, it has been shown that certain activities such as traditional games and video games can help to improve spatial skills. Further, on the basis of the data collected before the experiment, we observed that students that usually play 3D simulation video games at home have better spatial abilities than the others.

Thus, in order to exploit these games as a tool for enhancing these skills and to make the learning process somewhat easier, we created a series of seven simulators for Android (Fig. 1).

Fig. 1. Augmented reality app used

The activities or games simulated in these android games complement each other and support the mandatory exercises of the course. This gives the students satisfaction since they can see their progress, which facilitate the learning process.

For the teaching process, we then used theoretical classes, practical classes with the proposed exercises, appointments to interact with augmented reality problems, and interactive online and bibliographic resources.

At the start of the experience, we used DAT tests: SR v01 [7], MRT test [8] and a questionnaire to determine the students' profiles. Tests were also employed at the end of the experiment, these being the DAT test: SR v02 [7] and the PSVT test [9], to determine the final skills and to measure the progress of the students.

Using the data collected on spatial vision and spatial relation skills, the participants were divided into two groups: Group A1, the control group, which has superior abilities, and Group A2, the experimental group. Although this subdivision presents a bias regarding the skills of each subgroup, A1 and A2, this distinction was made in order to have homogeneous subgroups at the beginning of the experience. Within the Educational Innovation Project, more hypotheses are discussed than those presented here, for which this distinction is ideally suited.

Moreover, as indicated in the results, this division was not an obstacle to testing one of the hypotheses (rate of improvement among subgroups) in the results section. Once the students had been assigned to their groups, they attended the practical classes separately, so that Group A1 followed the routine procedure. In the case of Group A2, of the five classroom sessions (one per week), in four of these they followed the same procedure as Group A1.

In the first of the practical classes, a tutor provided Group A2 with an explanation regarding the details of how the experience would be developed. Each week the students were given the opportunity to attend appointments (arranged by themselves) on the virtual campus platform to use the simulators prepared for the practical assignments for each week.

In this first practical class, Soma Cubes were also presented to the students so that they could work with them as an innovative way of learning with games. The Soma Cube is a three-dimensional puzzle designed in 1936 by PietHein and in this case, the 3D pieces were pre-printed in order to be used to create figures that emerge from the students' own imagination, so that later they could practice the creation of views (Fig. 2).

Fig. 2. Example of Soma Cube used

The subsequent practical classes were identical to those of the control group with the exception that, on each week, the student will not only have prepared the corresponding exercise on paper but will have experienced it thanks to the simulators.

Each week the students participated in pairs in these augmented reality sessions lasting for ten minutes. For these sessions, the necessary materials were a Tablet or any Android device to which the student could only have access in this ten-minute period, an "ImageTarget" that served as the activator of the game, and a tripod or similar object to make the handling and interaction more natural.

Fig. 3. Students using one of the apps

The mandatory exercises that were used for the present work deal with distances, angles, and the dihedral angle. These games were also used to obtain a better understanding of the axonometric and knight perspectives with the main views of objects.

Following each of the simulator sessions, the students were required to answer a question regarding both their initial comprehension of the exercise before having worked on the video game and their understanding after working on this game.

After the whole experience had been completed and all the exercises were handed into the professor, the students from both subgroups took several tests. To measure these skills at the end of the experience, the DAT: SR v02 was used for measuring spatial vision and the PSVT test was used for measuring spatial relations skills. The student also completed the CIS test [10], which was modified to fit the experience.

3 Results

3.1 Influence of the Experience with Video Games on the Student's Spatial Abilities

Data regarding the use of video games at home among the group studied were recorded at the beginning of the experience. We focused on video games that recreate three-dimensional environments such as Simcity, Minecraft, Call of Duty, or similar. We observe that 51% of students use them between two and five hours a week.

After collecting data on initial spatial abilities, no significant differences were found between the spatial visualization skills of the group that often uses video games at home. However, such differences were found on the MRT test that measures spatial relations applied in 165 subjects.

A Mann-Whitney U statistical test was conducted (adopting a p-value of 0.001), which revealed statistically significant differences between the students that experiment with video games and those who do not, with the former having a better spatial relations ability. This test was used due to the small sample and continuous quantitative variables.

In the group of students without experience of simulation video games, the average score is 3.64, the median 3.5, the variance 4.033, and the standard deviation 2. In the case of students with experience in video games, the average was 4.84; the median 4.5, with a variance of 5.1 and a standard deviation of 2.25.

Therefore, spatial relations skills are superior in students who often use this type of video game.

3.2 Comprehension of the Practical Exercises of the Subject with the Help of Augmented Reality Simulators

The students were asked to rate their understanding of the exercise presented before and after experience with augmented reality. In addition to asking the students to try to understand the activity before the AR appointment, they were asked to sketch perspective with the data of the statement and the possible results in space. This helps the professor or the student to see the starting point.

With regard to the specific simulators created to improve spatial comprehension, the data related to comprehension of the exercise before and after the experience with augmented reality are displayed in Fig. 3. In this, C0 will refer to the initial comprehension and Cf the final comprehension.

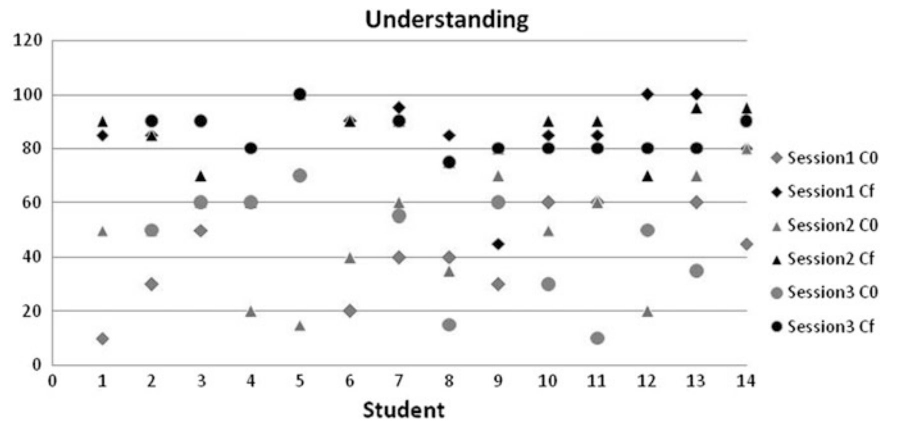

Fig. 4. Comprehension results

It is clear from Fig. 4 that there is a significant increase in the student's understanding, demonstrating a substantial improvement in confidence at the time of performing the exercise.

During the practical classes, this confidence is marked when participating in class.

3.3 Effects of Training with RA Simulations in Evaluations

During the course, different continuous evaluations were conducted, similar to the exercises carried out in the different parts of the course. These exercises were identical for both groups and corrected by the same teacher using the same criteria.

As discussed above, our starting point was to use two groups, where Group A1 had a higher level of spatial vision than Group A2. In the continuous evaluation of axonometric perspective, however, the following results were obtained: The group that does not use AR and that demonstrated better spatial abilities at the beginning of the course (A1) showed an average score of 0.54 (out of 1), with a median of 0.54, variance of 0.059 and a standard deviation of 0.24. The group that uses AR (A2) had an average score of 0.53, a median of 0.6, a variance of 0.073, and a standard deviation of 0.27 (Fig. 5).

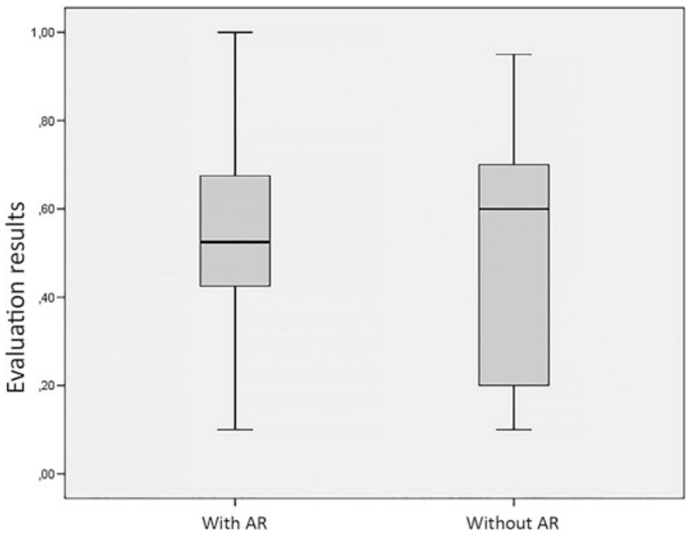

Fig. 5. Evaluation results with students using AR and students not using it

A non-parametric Mann-Whitney U test (adopting a p-value of 0.01) revealed no differences between these two groups, suggesting that they now show equivalent skill levels. This test was used due to the small sample and continuous quantitative variables.

We can see, therefore, how the two groups that began with very different spatial vision skills showed almost identical results when tested post-experience.

3.4 Effects of RA Training on Spatial Skills

As would be expected, and because the groups were divided according to their scores on the initial tests, there is a significant difference between the groups with and without AR in terms of the scores on the DAT test: SR 01. The mean in the group of students who did not use AR is 9.18 with a median of 9.4, variance of 0.178, asymmetry of −1.126, kurtosis of 1.63 and minimum and maximum of 8.20 and 9.8 respectively. In the group of students who participated in AR, the mean is 6.96, the median 7.4, variance is 3.465, asymmetry is −0.974, kurtosis is −0.229, and minimum and maximum are 3.4 and 8.8 respectively.

DAT: SR 02 was the test used at the end of the experiment, and it is of a higher level of difficulty than the initial test. Nonetheless, we still observed differences between the experimental and control groups. However, it is possible to argue that the rate of improvement or development in the group that experienced AR was considerably higher. The group that had not experienced the AR, showed a mean score of 9.1667, median of 9.1, variance of 0.253, asymmetry of 0.061, kurtosis of −1.518 and maximum and minimum scores of 9.8 and 8.4 respectively. In the case of those who had experienced AR, the mean score is 7.18, the median 7.4, variance 3.088, asymmetry −0.864, kurtosis 0.413 and maximum and minimum scores were 9.2 and 3.6 respectively.

In order to compare the results between the different groups concerning the continuous variables, the non-parametric Mann-Whitney U test was used with a p-value of 0.002, which revealed differences between the group that used augmented reality and the group that did not. This test was used due to the small sample and continuous quantitative variables.

Although there is still a difference between the two groups in terms of the scores on the second DAT: SR test, the difference between means and the deviations presented by the samples clearly indicates that the difference between groups has decreased even though the level has increased. While the group that did not experience AR has maintained its mean score, the group with AR showed a considerable improvement.

4 Conclusions

We found significant differences in the scores on the initial MRT test between those who often use 3D simulation video games at home and those who do not, suggesting that spatial relationship skills are higher in students who use these types of video games.

Based on this notion of a link between spatial skills and the use of video games, a series of AR exercises were prepared and used to enhance knowledge. In this sample, we observed that there is a significant improvement in the abilities if we include these tools in the traditional systems of teaching technical drawing at university.

It is also observed that the use of these types of AR simulators in the classroom improves the academic results in certain areas of learning related to Graphic Expression.

All the exercises used in this experience were created in the Department of Graphic Expression, Design, and Projects of the University of Malaga with Unity and Vuforia as free tools in the academic field. As these games are usable on any Android device, they can be used repeatedly in successive courses for the teaching of perspectives and dihedral. Further, with specific knowledge and use of modelling tools, other environments can be created for new exercises.

This material can be used in a large number of subjects related to technical professions similar to that of Graphic Expression. Moreover, AR could be used in many other fields to help the student understand and visualise complicated concepts such as biology or mechanics.

Within the School of Industrial Engineering, these new techniques could be applied in ten subjects with a target population of 1172 students. These methodologies and exercises could not only be used in university education, but also in baccalaureate technical drawing subjects that, although of a more fundamental level, present difficulties for the student.

Acknowledgements. The work reported here was made possible by all the students that participated and all the professors that gave their time to collect the information used in this research.

References

1. Cherney I, London K (2006) Gender-linked differences in the toys, television shows, computer games, and outdoor activities of 5- to 13-year-old Children. Sex Roles 54:717–726
2. Subrahmanyam K, Greenfield P (1994) Effect of video game practice on spatial skills in girls and boys. Effect of video game practice on spatial skills in girls and boys. J Appl Dev Psychol 15:13–32
3. Feng J, Spence I, Pratt J (2007) Playing an action video game reduces gender differences in spatial cognition. Psychol Sci 18(10):850–855
4. Speranza D, Baronio G, Motyl B, Filippi S, Villa V (2017) Best practices in teaching technical drawing: experiences of collaboration in three Italian Universities. In: Advances on mechanics, design engineering and manufacturing: proceedings of the international joint conference on mechanics, design engineering & advanced manufacturing. Springer International Publishing, pp 903–913
5. Contero M, Gomis J, Ferran N (2012) Development of an augmented reality based remedial course to improve the spatial ability of engineering students. Front Educ Conf Proc 1–5
6. Ayala Alvarez F, Blazquez Parra E, Montes Tubio F (2017) Improving graphic expression training with 3D models. J Visual
7. Bennett G, Seashore H, Wesman A (2000) DAT 5, Test de Aptitudes Diferenciales. TEA ediciones
8. Vandenberg SG, Kuse AR (1978) Mental rotations, a group test of three-dimensional spatial visualization. Percept Mot Skills 47(2):599–604
9. Bodner GM, Guay RB (1997) The Purdue visualization of rotations test. Chem Educ 2(4): 1–18
10. Keller M (2010) Course interest survey

Implementation of Learning by Doing Method in the Graphical Engineering Field

M. D. Marín-Granados(✉), E. B. Bláquez-Parra, P. Mora-Segado, L. Miravet-Garret, F. J. Ortiz-Zamora, F. Gómez-Hermosa, and E. Olvera-García

University of Málaga, C/Doctor Ortiz Ramos s/n, 29018 Málaga, Spain
+34-952-951-276mdmarin@uma.es

Abstract. Regarding the different alternatives to teaching approaches with excessively theoretical contents, there are several innovative learning strategies for active students' involvement. According to most demanded professional profiles in the field of business [1], applicants not only should have a prominent academic background but also good personal skills, such as initiative, entrepreneurship, communication skills, and commercial vision, among others. This paper presents a experiment that aims to achieve the objectives and catching the skills by the Learning by doing technique, through a contextualization of the subject "Container and Packaging" in the Industrial Design Degree. Moreover, a close relation between university and business is achieved. In this way, students can acquire the requirements demanded by the companies. A particularization of an industrial design methodology proposed by the Technological Institute of Packaging, Transport and Logistics (ITENE, Valencia) has been implemented for the packaging's design and packaging itself. Besides using this method, students take on a project-based learning (PBL) work under the role of a company. Then, they carry out the redesign of the container of a manufactured product close to their province of residence. This practice will not only look for improving the student's ability to research and solve problems, but also to manage the professional and personal relationships that occur within each work group. These situations are necessary in the training process since they will be faced daily in their future professional life.

Keywords: PBL · Methodology · Packaging · Learning by doing

1 Introduction

The main purpose of the methodological proposal is to promote the talent of the students beyond the university pathway. There is great talent among university students that, in many cases, does not rise above the academic field.

In order to achieve the required competences, an industrial design methodology has been carried out within the theoretical-practical program of the last-year course, being implemented into the technological institute ITENE for packaging design [2]. Students were highly motivated to participate since, thanks to the strategy of 'learning by doing' [3], they were able to materialize their own ideas, designs and prototypes. Another

F. Cavas-Martínez et al. (Eds.): *Advances on Mechanics, Design Engineering and Manufacturing II*, LNME, pp. 789–797, 2019.
https://doi.org/10.1007/978-3-030-12346-8_77

advantage is that the introduction of Project Based Learning (PBL) in this methodology, allows them to simulate actual conditions in the life cycle of their designs.

The starting point for the promotion of graduates among the contacted companies was precisely the possibility of taking advantage of these digital technologies and being able to manufacture the designed prototypes by means of 3D printing [4].

The outcomes obtained from the research study included eleven prototypes of original packaging designs and their respective posters, as shown in Fig. 1. All processes were supervised, and the students received training in ArtiosCAD (a specific software for packaging). They also had to create groups under established criteria, determining roles and collaborating with local companies. Additionally, the different members of the same group had the chance to evaluate each other. Hence, teachers and supervisors could know the internal problems because they had to tackle and solve their assignment tasks. Another evaluation was carried out by a self-assessment of each group. The first one under an aesthetic, practical and symbolic criteria and the second one related to technical requirements suggested by the analyzed company.

Fig. 1. Two prototypes of original packaging design

From the results, it could be seen that all students had exceeded the initial expectations. Moreover, the satisfaction level was higher than in previous years. Finally, according to the companies' point of view, their interest as designers in the training received in our faculty and in this educational project was considered satisfactory.

2 Objectives

Learning by designing digital prototypes is the most important objective. These prototypes are manufactured with 3D printers [5]. Also, other purposes have been considered from different perspectives. For example, from the teaching perspective [6] it has been considered to accomplish technical and practical competences using suitable equipment, tools and methods. From the learning perspective, it has been considered to promote individual and team work through PBL, initiative, communication skill and commercial practices. Finally, from learning management perspective, it has been considered essential to design online follow-up tools (forums, tasks …) and to design practices from a sustainable point of view [7], as well as to publish the work achieved as a professional projection.

3 Methodology

In 4th year, students of Industrial Design and Projects Development Engineering degree in the subject ‘Containers and Packaging Design’ used the Project Based Learning (PBL). They had the opportunity to contact local companies and carrying several interviews with technical representatives along the different stages of the project. They based their work on the market-and-commercialization surveys for the product they had chosen.

In the academic context, this part of the work was considered as part of the course practices with a 40% score of the final grade, the group analyzed a daily consumption production which was preferably manufactured in their place of residence, and that reflected their packaging redesign, both primary and secondary.

3.1 Groups Formation

Regarding the group formation, teaming up according to the student place of origin was tested the previous year. Low performance and diverse conflicts were detected in one third of the groups. The following year, students were asked about how to organize the teams and 95% of them agreed to organize themselves. At the end of the year, it was found that hardly any conflicts among the groups had arisen.

3.2 Student Roles

In each group, three roles were established: two of the roles were assigned to two pairs of students and the last role was assigned to the group coordinator. All students with the same role shared discussion online in the forums of The ‘Moodle Virtual Campus’ to promote discussions with the teacher and also to share technical information on markets, processes, logistics, etc. This cross-group coordination helped the groups in making decision (Fig. 2).

Fig. 2. Questionnaires in Moodle Virtual Campus to record the demand of each project

Thanks to the different roles, the students can specialize themselves in different tasks. This allows them to distribute the work between the different students in the group in this stage of the project. The coordinator of the group had to assume the role that was unattended by the members in the group. It also allowed him to supervise the progress of each student, and thereby rate the personal work of all members of the group.

These roles were changing in every stage: each student assumed certain task, based on their expertise and knowledge field. For example, the student with the best expertise in SolidWorks was in charge of creating the 3D model, the ones who had studied the subject of "Photography and digital treatment of the image" were in charge of taking pictures, prototype reports and creating samples.

3.3 Collaboration with Local Companies

To promote the final works, it was important to take into account the group of local companies. Through a cover letter, the teacher presented his students to the companies. As a consequence, the companies allowed the students to know their industrial processes and facilitated technical information of their products.

Sometimes, it was not easy to contact the necessary technical staff, for that reason, it took a long time to find the right information.

The companies were invited to check the results on the web page www.packaging.uma.es, and thanks to that fact, they could know the projects made by the students, which allowed the possibility of catching their interest for a future collaborative project.

3.4 Moodle Virtual Campus

To organize the work of almost 100 students, the use of Moodle Virtual Campus has been essential. The questionnaire tool helped to coordinate the work of each group. Each student with his own role had his questionnaires and specific forums. In case that anyone in the group did not attend the questionnaires ordered, the group coordinator would answer for him (Table 1).

Table 1. Moodle and workshop

Site	Stages
Moodle	Preliminary questionnaire
Moodle	Technical requirements questionnaire
Moodle	Competitor analysis
Moodle	Technical assessment of conceptual designs
Workshop	Manufacturing of prototypes
Moodle	Self-assessment of each group

Through the preliminary questionnaire the teacher knew the professional environment of each student, as well as their skills, and the academic and professional career of every student. As a consequence, it could be evidenced if, for any particular reason, it was easier for any of the students to contact with an specific enterprise, for instance.

Students were given the freedom to choose their role. The work made by the coordinator was essential, as it helped the normal development of the rest of the tasks. The rest of the students in each group specialized in the most technical part of these phases: market analysis, product studies, manufacturing processes and regulations.

This search for information on design requirements was shared among students of the same role. In this way, similar projects helped each other. Students decided to fix 85 requirements for each Project. These requirements were taken into account to evaluate the designs that were manufactured (Table 2).

Table 2. Role and analyzed requirements

Role	Requirements	Quantity	Percentage
Market and logistics	Market	14	16
	Consumer	17	20
	Storage	6	7
	Transport and distribution	5	6
Processes and regulations	Production	6	7
	Printing	7	8
	Standard	10	12
	Environmental	6	7
Coordinator	Product	6	7
	Total	85	100

Each student was asked to search a container from other different manufacturer for similar products on the Internet. With these designs, they made a visual report with photographs of marketed products with similar packaging. This compilation was used as an inspiration for all the designs of each group [8] (Fig. 3).

Fig. 3. Competitor packaging

After the stage of design, a technical assessment of conceptual design was performed. This evaluation was done taking into account the preset requirements. Therefore, the teamwork had the prototype specifications to accomplish the product [9] (Fig. 4).

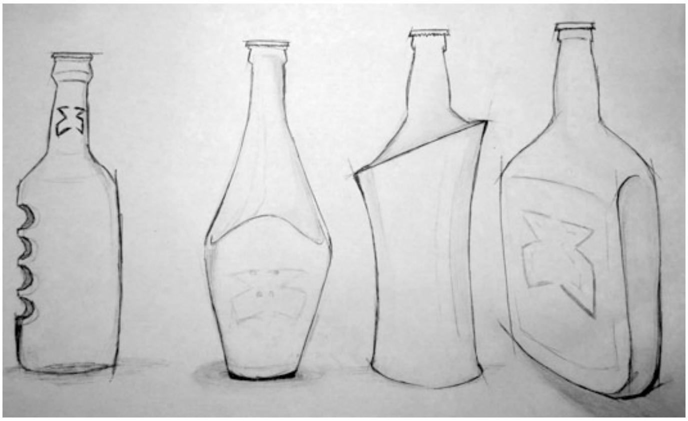

Fig. 4. Example of a conceptual design

The next step consisted in manufacturing prototypes. This stage is carried out after the CAD design and virtual simulation. Here, students test the design errors and try to solve them [10]. An appointment system had been implemented in Moodle Virtual Campus for the use of the laboratories, tools, 3D printer and numerical control cutting machine by the supervision of a qualified technician.

After the design phase, each group evaluated the total or partial fulfillment of the initial requirements. From an aesthetic, practical and design point of view, each student rated the designs of their classmates and their own designs too. This questionnaire allowed them to be critical with the work of their classmates, and also participating actively in the choice of the design to be manufactured.

There were 550 technical and commercial evaluations in total. Another questionnaire that the students had to do was the self-evaluation of the group. With this questionnaire each student rated the work of his classmates for each of the tasks that were assigned.

4 Results

The high interest of the students is a consequence of the eminently practical approach of the subject. At the end of the curse, a bivariate analysis of the answers obtained in an anonymous survey was carried out. This analysis had been made from the 46 surveys answered with SPSS version 22 program.

Table 3. Interest level in practical and theoretical teaching

			Perception		Total
			Practical	Theoretical	
Interest level	*High*	*N*	19	2	21
		%	46.3	40.0	45.7
	Medium	*N*	20	3	23
		%	48.8	60.0	50.0
	Low	*N*	2	0	2
		%	4.9	0.0	4.3
Total		*N*	41	5	46
		%	100.0	100.0	100.0

Table 3 shows that 45% of survey respondents found the subject very interesting. This percentage is higher in students who considered that practical teaching had been more relevant than theoretical teaching. This consideration is in terms of skills and competence acquisition. The 23 students that show an average interest in the course, mainly thought that practical teaching is more relevant than theoretical teaching.

Without a doubt, the motivation of the student raises the expectation, thanks to that fact they invested many hours of work in the prototyping workshop. At the time of giving the marks to the personal work of each student, it was very useful the satisfaction surveys that were conducted within each group. In this regard, there was no reclaim from any students.

Eleven prototypes were manufactured using machines of digital prototyping (3D scanner, 3D printer and cutting machine/recorder printer scanner). These designs were also documented with a poster exhibited at the Faculty of Industrial Engineering of the University of Málaga, and an oral presentation in class (Fig. 5).

Fig. 5. Bottle "3Monos"

5 Conclusions

The "Learning-by-doing" strategy has been without doubt motivational for the students and a challenge to monitor the participation of each student in the experience [11]. Students motivation during this experience has been very high, which has led to multiple hours at the prototyping workshop.

Working in groups has not been easy but with a correct task distribution via Moodle Virtual Campus, it has been possible. Currently, synergies between related subjects are being produced at the University of Málaga. For this reason, this project could be perfectly extrapolated to other degrees.

Acknowledgements. This project has been supported by the University of Málaga, as a Teaching Innovation Project (code PIE15-179).

References

1. Fundación Everis: III Ranking Universidad-Empresa (2017)
2. Navarro P (2017) Homepage: Guía práctica de diseño de envases y embalajes para la distribución de producto. ITENE. Last accesed 10 Jan 2018
3. DuFour R, DuFour R, Eaker R, Many T (2006) Learning by doing. A handbook for Professional Learning Communities at Work. Solution Tree Bloomington. ISBN 978-1-932127-93-5
4. Martín N, Saorín JL, de la Torre J (2014) Prototipado digital, fabricación e impresión 3D. Universidad de la Laguna
5. Bonet A, Meier C, Saorín JL, de la Torre J, Carbonell C (2017) Tecnologías de diseño y fabricación digital de bajo coste para el fomento de la competencia creativa. Arte, Individuo y Sociedad 29(1):89–104. ISSN 1131-5598
6. Blikstein P (2013) Digital fabrication and 'Making' in education: the democratization of invention. In: Walter-Herrmann J, Büching C (eds) FabLabs: of machines, makers and inventors. Transcript Publishers, Bielefeld
7. Hortal M (2016) Desarrollo básico de una metodología de evaluación técnico-ambiental de envases y embalajes mediante la combinación de instrumentos legales, normativos y medioambientales. X Congreso Internacional de Ingeniería de Proyectos, Valencia
8. Rodríguez D (2013) Prácticas Disruptivas e Intervenciones de Diseño en Estampación Digital, Imagen de Marca y Prototipado SIGraDi
9. Hallgrimsson B (2013) Diseño de producto. Maquetas y prototipos, Promopess
10. Bortolato M, Lenti C, Morelli R, Verger G (2009) EL PROTOTIPADO RÁPIDO EN PLÁSTICO ABS COMO HERRAMIENTA DIDÁCTICA. 2º Jornada de Experiencias Innovadoras en Educación en la FCEIA
11. Lorenzo C (2011) MMOL platforms: open 3D learning technologies in educational practices. Arte y Humanidades. Technological innovation in the teaching and processing of LSPs: Proceedings of TISLID'10 (2):235–242 UNED ISBN: 978-84-362-6217-9

Project-Based Learning of CAD/CAE Tools for the Integrated Design of Automatic Machines

G. Berselli(✉), P. Bilancia, and R. Razzoli

Department of Mechanics, Energetics, Management and Transportation,
University of Genova, Via all'Opera Pia 15/A, 16145 Genoa, Italy
+39335809236giovanni.berselli@unige.it

Abstract. This paper reports about project-based learning activities carried out within the course of *Design of Automatic Machines* at the *University of Genova*. This didactic experience, provided to the students enrolled in the second-level degree in Mechanical Engineering, aims at providing the knowledge of those methods and tools required to optimally design functional parts of automatic machines, here including the mechanical architecture and the actuation sub-system. Lecture hours are equally devoted to the introduction of theoretical concepts and to lab exercises, which leverage on the extensive and advanced use of dedicated CAD/CAE software tools (i.e. *PTC Creo*). In particular, the projects are related to the in-depth study of automated packaging systems, initial (sub-optimal) design solutions being provided by an industrial partner with years of practice in the sector. After a description of the educational goals, the presentation discusses the phases of the activity and the main methodological aspects. In addition, the adopted tools for the design and simulation of the developed systems are discussed in detail.

Keywords: CAD/CAE tools · Design parametrization · CAD-based shape optimization

1 Introduction

Nowadays, Computer-Aided Design (CAD) and Computer-Aided Engineering (CAE) software have unquestionably become indispensable tools on a world basis, whose advanced knowledge is necessary for young engineers taking their first steps into the competitive industrial scenario. CAD/CAE environments are indeed extensively used in several fields, including aerospace, automotive, earth-moving machines and automated plants (such as automatic machines for packaging) [1]. At the current state-of-the-art, these virtual prototyping technologies allow to simulate mechanical and mechatronic systems, starting from the geometrical and parametric representation of parts, the study of complex devices during their motion (i.e. multibody analysis), the verification and, possibly, optimization of their structural behavior (stresses and deformations). In the current literature [2, 3], it is claimed that modern CAD/CAE may soon become so advanced to simulate mechanical systems with a degree of reliability comparable to physical testing, although with the obvious advantage in terms of cost

F. Cavas-Martínez et al. (Eds.): *Advances on Mechanics, Design Engineering and Manufacturing II*, LNME, pp. 798–809, 2019.
https://doi.org/10.1007/978-3-030-12346-8_78

saving and capability to virtually test the performance of several design variants in a time efficient manner. In addition, most of the commercial CAD software available on the market (such as *SolidWorks*, *Catia*, *SolidEdge*, *Siemens NX*, *PTC Creo*, etc.), can provide this set of capabilities in a single, integrated environment.

Within this framework, the objective of the present paper is to provide an overview of the CAD/CAE teaching activities carried out at the *University of Genova*. Basically, two design tools are widely employed in the engineering curricula:

- *Bentley Microstation*, taught during the first level degree in Engineering. Despite its capabilities, the practical use of this tool is currently narrowed to the generation of 2D drafting for simple mechanical parts and schemes;
- *PTC Creo*, which is employed as the first 3D CAD tool introduced to students and it is presented during the last year of the first-level degree and, more in depth, during the second-level degree. *PTC Creo* enables an integrated approach in the design of a machine subsystem, and comprises a standard parametric CAD interface, a basic but effective multibody suite (*Creo Mechanism*), a suite for finite element analysis (*Creo Simulate*), and a built-in optimizer (*Creo Behavioral*), that can seamlessly operate on all the virtual prototype parameters (e.g. shape of parts, material properties, dynamic/kinematic variables, information about part structural behavior).

For what concerns the specific course named *Design of Automatic Machines* (i.e. the main topic of the present paper) advanced skills in the use of *Creo* are taught by means of a Project-Based Learning (PjBL) activities [4–7].

As for basic terminology, Problem-Based Learning (PBL) can be defined as an approach managing the learning process in such a way that students are stimulated to autonomously achieve solutions. Teachers and pedagogues have always reckoned the effectiveness of this method. Today, many authors differentiate between PBL and PjBL [8, 9]: the distinction is mainly based on the acknowledgment that PBL is defined by open-ended and not-well-structured problems that provide a context for learning. On the opposite, PjBL may be interpreted as an assignment or a set of tasks that the students have to perform.

PjBL is often seen a synonymous of PBL as both are student-centered methods for learning. Some experts [10] suggest indeed that PBL can only be faced in small groups and nobodies believe that PjBL can be undertaken individually. An important difference between the two approaches is that in PjBL students must generate a result in form of a report or design. In PBL, the focus is not on this kind of outcome: the tutor supervises the project and students are required to produce a solution or strategy to solve the problem. In PBL, solving the problem is part of the process, but the attention is on the problem-management, not on a clear and fixed solution. The focus in PBL is on students working out their own learning requirements so PjBL often occurs at the end of a degree program after a proper set of knowledge has been given the students the skill to face the project. PjBL can be considered as an effective mechanism for tying together several subjects under one bigger activity at the end of a course. Summing up, PjBL is a growing area of interest within engineering education, as also shown in recent literature. For instance, a description of active education methodologies can be found in [11]: in this case, engineering students have to deal with the requests of a real customer, an important aspect being the constant maintenance of a proper and professional relationship with the company itself. Another actual example of multidisciplinary didactic project is described in [12], where students and professors from different departments combine skills in the design process of new products, eventually fabricated with 3D printing FDM technology. In both cases, the possibility to interact with real problems, after an established theoretical background, shows positive results and very encouraging feedbacks from students. However, there are some barriers that inhibit the PjBL wider integration within the engineering curriculum, in fact:

- PjBL is identified as one of the most resource-intensive elements of the current engineering curriculum, often demanding tailored learning spaces, materials, tools and equipment as well as requiring significant time from faculty and support staff.
- Many engineering faculty teachers have got little confidence and knowledge in the design and application of student assessment processes in PjBL. For this reason, perhaps, many PjBL experiences are highly structured and employ a wide range of different cumulative assessment processes within a single activity, with high workload for both staff and students.

In the specific case of the course *Design of Automatic Machines*, activated since the academic year 2015–2016, the required resources are limited, as for all the practical activities are computer-based. Furthermore, the absence of heavy simulations from a computational point of view (e.g. non-linear FEM, CFD, etc.), allows to deal with all calculations in the University computer labs. The course provides 6 credits (i.e. ECTS —European Credit Transfer System), that are equally divided into hours of theoretical lessons about architectures and design aspects of automatic machines, and hours of CAE exercises. During the exercise sessions, the teachers show to the class different types of CAE-based simulations and design approaches (as described in the following). In particular, the practical part starts with a seminar given by a well-trained engineer from industry, whose role is to present a design problem related to the fascinating world of automatic machines. An initial design solution (i.e. the mechanical architecture of a machine subsystem) is shown to the students at the very beginning of the course. The students, divided in small groups of 2–4 people, are then required to go through the overall design process (here including possible design improvements achieved by the use of Creo Behavioral). The educational goals of the PjBL activities may be outlined as follows:

- To understand the chain of virtual prototyping activities ideally required before physical testing (identification of the mechanical systems architecture, motion analysis, structural analysis, actuator selection, design optimization);
- To provide methodological indications on how to go through the development process of a mechanical/mechatronic system;
- To achieve advanced specific skills in the use of modern, industrially relevant, design and simulation tools, namely: (i) parametric CAD, (ii) integrated multibody environment for motion analysis; (iii) integrated FEM environment for the structural verification of parts in the worst load-case scenario; (iv) integrated optimization routines for design improvement.

- To train the capability for analyzing/describing an engineering problem, to work in a group (and not individually), to generate and evaluate solutions under a concurrent set of design constraints, to present the results of the work (via written report and oral exposition), not neglecting a critical review of the achieved results.
- To stimulate students' creativity, practically involved, for the first time in their career, in the solution of a design problem of real interest for industry. Within the problem solving activity, emphasis is put on the comparative evaluation of design variants, which are (in most cases) directly available thanks to system parametrization.

At the end of the PjBL activity the students have potentially gained an insight of the problem, along with the knowledge of the capabilities and potentiality of the CAD/CAE integrated environment. Only at this stage, each group is required to propose a novel machine architecture and to write a detailed report about the previously assigned project activity. At the end of the course, all the design steps, comprising the new architecture and the proposed improvements, are critically discussed in an oral presentation, which represents the 50% of the final exam. The remaining part of the exam includes a written and oral test, based on the theoretical topics presented during the course.

2 Activity Organization—Problem Overview

A PjBL case study, carried out in the past year, is depicted in Fig. 1, which provides a schematic of an Automatic Machine for packaging of paper rolls with different formats.[1] The paper rolls are piled up and, subsequently, conveyed to a couple of elevators. The motion of the elevator plates is achieved by means of two slider-crank mechanisms, each driven by a brushless servomotor (not shown in the picture), which allows a very precise position control of the plates. These elevators transfer the paper rolls to the upper part of the machine, where the paper rolls envelope (a plastic film) is applied. In the current embodiment design, one elevator starts the returning (downward) stroke before the other (as clearly shown in Fig. 2), in order to allow the application of the plastic film also underneath the paper rolls. Given this case study, the PjBL activity is divided into several steps, also underlined in Fig. 1.

As previously introduced, the course starts with a seminar, in which an engineer from industry presents the design problem and provides the main specs and requirements of the automatic machine, in particular of each sub-system (e.g. elevator mechanism in Fig. 1).

Then, starting from an initial configuration presented during the seminar, the design process is organized with a sequential approach. In particular, the main steps and related CAD/CAE tools are as follows:

[1] A video showing the motion of the machine sub-systems can be found at: https://www.youtube.com/watch?v=UhUeZ3cv0DQ.

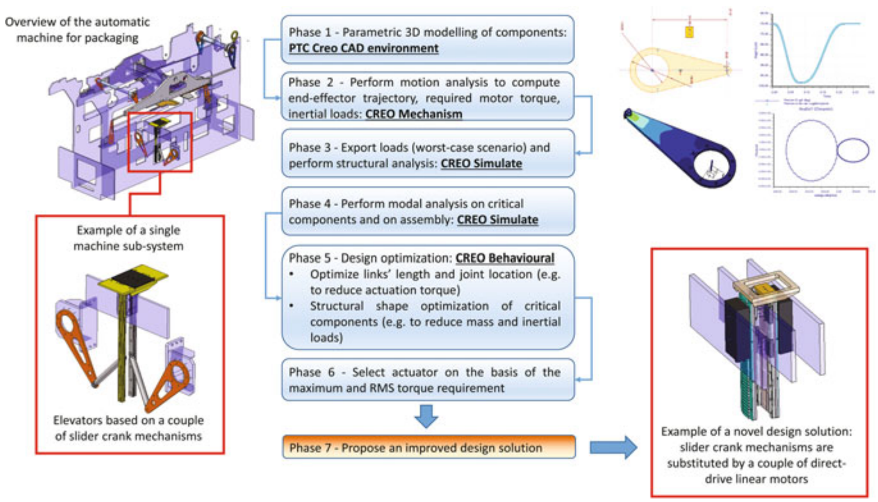

Fig. 1. Case study and design phases employed in the PjBL activity

- **Phase 1—PTC Creo CAD**: Parametric 3D modelling of (some) parts of the mechanical system.
- **Phase 2—PTC Creo Mechanism**: Motion analysis based on the end-effector's requirements, evaluation of the motor torque and of the inertial loads acting on a specific member (e.g. crank in Fig. 1).
- **Phase 3—PTC Creo Simulate**: Structural analysis for evaluating stress-strain condition on the members (e.g. crank in Fig. 1).
- **Phase 4—PTC Creo Simulate:** Modal analysis on each component and on the complete assembly in order to verify/avoid resonance during the machine working cycle.
- **Phase 5—PTC Creo Behavioural**: Shape optimization of a member based on a single objective function (e.g. stress condition).
- **Phase 6—PTC Creo Mechanism + Excel**: Selection of the actuator based on *rms* and *maximum* required torque [13].
- **Phase 7**: proposal and critical evaluation of novel design solutions.

Naturally, the design process is not completely sequential and several iterations are always necessary due to the presence of critical aspects (e.g. unacceptable stress-strain condition evaluated in Phase 3, different shapes evaluated in Phase 5, etc.), that could request the review of previous phases. As said, the last part of the learning experience requires the student to propose a novel, possibly improved, machine architecture complying with the project requirements. A possible design solution, depicted in the rightmost part of Fig. 1, is based on the use of direct-drive brushless linear motors (with obvious simplification of the system, despite increased installation cost).

3 Embodiment of the Mechanical Model and First Simulations

The initial industrial seminar ends up with the assignment of the mechanism's geometry and its detailed description, in terms of functionality of each member and related dimensions. Then, after these necessary indications, all the work-groups can deal with the case-study under the supervision of the professors. As previously said, the Phase 1 is totally dedicated at the 3D modelling of the sub-system within the PTC Creo Parametric environment. In particular, the CAD exercise is limited to the components directly involved in the simulations (Phase 2–6), since the secondary components (e.g. external structure, etc.) are provided in order to save time. Particular attention is paid to the assembly process, in order to avoid problems during all the next simulations in the *PTC Creo* integrated environment. Once the parametric mechanical model is obtained, an inverse kinematic analysis is needed to extrapolate the desired motion law at the motor shafts.

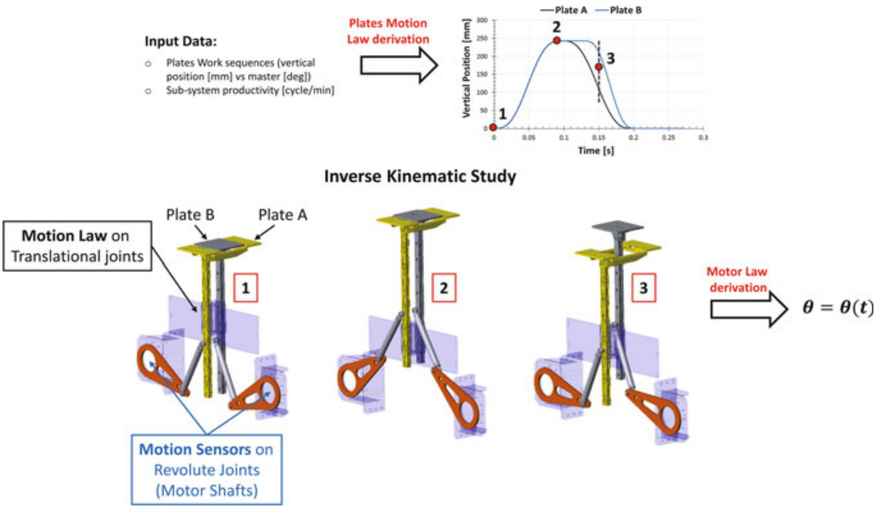

Fig. 2. Inverse kinematic: evaluation of the motion laws

The procedure (depicted in Fig. 2) starts from the motion requirements (position $[mm]$ vs master $[deg]$) assigned to the sub-system end-effectors (in this case, the two plates, Plate A and B, represented in Fig. 2). The translational motion laws, that have to be assigned in the multi-body environment (*Creo Mechanism*) in order to perform an inverse kinematic study, are evaluated on the basis of the machine's productivity ($[cycles/min]$).

Then, the final rotational motion laws ($\theta_i = \theta(t), i = 1, 2$) are evaluated through "motion sensors" on the motor shafts. The Phase 2 closes with a kineto-dynamic analysis, in which the $\theta_i = \theta(t), i = 1, 2$ laws are applied at the motor axis, while different "force sensors" are exploited for recording the inertial loads on the mechanism's components. In particular, for the reported example, the subject of the study is the crank member.

4 Structural and Modal Simulations

During the post-processing step of the previous kineto-dynamic simulation, the worst load case is automatically transferred from the multi-body environment (*Creo Mechanism*) to the structural environment (*Creo Simulate*). The integrated PTC Creo architecture allows the user to easily export all necessary information (e.g. position and module of load's vector) and to change the nature of the analysis. In the specific case depicted in Fig. 3, the crank is simulated with the FEM method in order to verify the stress-strain condition in the worst inertial load-case scenario. This approach is conservative since only the worst condition, that is a combination of single loads registered at different time-steps in the previous analysis, is tested. However, the application of the load condition in static analysis, instead of dynamic conditions, represents an important limit of the procedure. This is due to the nature of the software, that includes different simulation environments and a useful connection for data-exchange between them, even if it does not allow to perform Multi-Flexible-Body-Dynamic simulations, which is only manageable in specific CAE tools (e.g. RecurDyn [14] or Adams [15]). Once verified the correct location and direction of the load condition on the crank member, the students have to deal with the meshing step and the imposition of the boundary condition. In particular, while respecting the software's limits in terms of mesher-options, a great part of the study is focused on mesh-convergence analysis and, if necessary, on local mesh-refinement. Furthermore, the need to exclude a precise number of degree-of-freedom for the static analysis convergence represents another important issue for the boundary condition setting. The didactical purpose, at this step of the exercise, is totally concentrated in the selection of the correct constraints-set, in order to maintain coherence between the multi-body mechanism and the FEM structure from the functional point of view. The complete procedure is depicted in Fig. 3.

As it may be self-evident, Phase 3 represents the first critical point of the design process, since a re-design of the mechanical part may be necessary if the stress-strain results highlight local (unacceptable) stress concentrations or global (unacceptable) part deformations. Then, Phase 4 introduces another important aspect of the mechanism's analysis/design, proposed only from a theoretical point of view in the most part of engineering programs. The modal analyses, carried out in *Creo Simulate*, are firstly performed on each single component involved in the motion and, subsequently, on the complete assembly. Exactly like the structural analysis, also in Phase 4, the selection and discussion of the constraints-set becomes an essential step. In fact, even if the FEM solver provides feasible results for different boundary conditions, the students have to recognize the correct configuration in order to extrapolate important data in the post-processing and conclude the study.

Concerning the mechanism considered in this paper, a qualitative example of modal analysis on a single component is reported in Fig. 4, in which the crank model is initially tested in free-free configuration.

From the practical point of view, all the simulation results (natural frequencies and related modes) have to be compared to the dynamic loads acting on the component, in

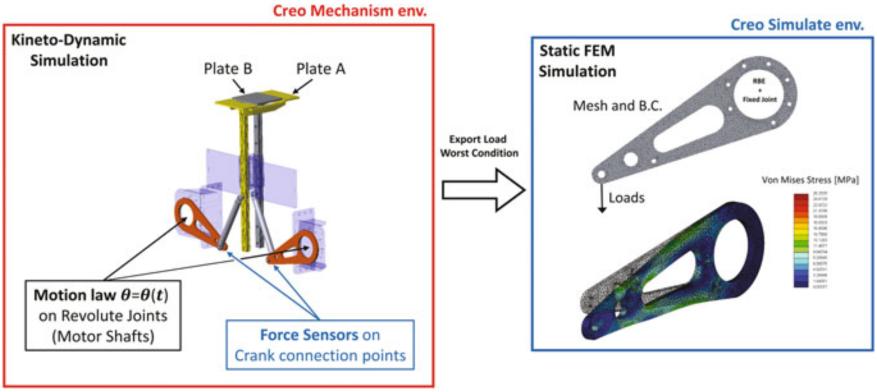

Fig. 3. FEM simulation on crank member with worst load condition

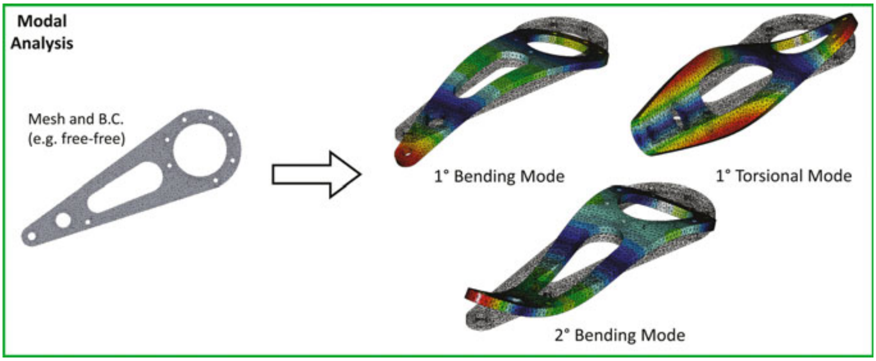

Fig. 4. Modal analysis on crank: qualitative example

order to verify the possible presence of resonances during machine's work. In most cases, after the analysis performed during Phase 3–4, the students suggest some adjustment to the CAD model, in order to correct all the detected critical issues.

5 Design Improvements and Actuator Selection

The last part of the analysis/design process, composed of Phase 5–6, exploits *Creo Behavioural* for possible performance improvements (e.g. shape optimization) and *Creo Mechanism* for what concerns the motor selection. In particular, after the previous simulation steps (Phase 1–4), the students are invited to find feasible solutions for any critical issue (e.g. Von Mises stress or motor torque exceeding acceptable limits, collisions and/or incorrect phasing due to badly designed initial trajectories, dangerous natural frequencies, etc.). Even if these problems are usually described by simple monotonic objective functions and their solution can be achieved with only basic-theoretical approach, the internal optimization toolkit is exploited in order to give to the students a complete overview of the PTC Creo environment. Considering the case study reported in this paper, a simple optimization study on the crank member can be formulated as follow:

$$\begin{aligned} &\textbf{Minimize}\, \tau_R = \tau_R(l_c) \\ &\textbf{Subject to}\, l_c \in [l_{c_{\min}}, l_{c_{\max}}] \end{aligned} \tag{1}$$

where τ_R is the reaction torque at the motor shaft and l_c is the crank's length. The results of this study, for both crank modules, are easily predictable, since τ_R increases linearly with l_c and, as a consequence, the optimal solution is the lower bound adopted.

However, this simple example allows to explain in an easy way the advantages of using a parametric CAD-CAE tool for sensitivity analysis.

Once defined the final design of the sub-system, in other words after the last geometry update as result of the iterative design process (Phase 1–5), a fast CAD-CAE based approach is applied for the servomotors selection [16]. The procedure, which exploits also Excel (or Matlab) for numerical integration during post-processing, is divided in two steps:

- Derivation of Speed-Torque curve at the motor shaft;
- Computation of the reduced moment of inertia, J_{red}, at the motor shaft.

Since the example reported in the paper is characterized by two modules (named A and B in Fig. 5), also this procedure selection has to be repeated twice. This first step can be achieved with a single kineto-dynamic simulation, where the kinematic input is a cycloidal law, that allows to investigate both negative and positive velocities. A torque sensor is placed on the same actuated rotational joint (as shown in Fig. 5), in order to record the reaction torque at each time-step.

Concerning the second step, the procedure requires two kineto-dynamic simulations (for each module), followed by a numerical integration process, which provides J_{red}, defined with Lagrange formulation:

$$J_{red} = \int_{\theta_{min}}^{\theta_{max}} J'_{red} d\theta + J(0) \tag{2}$$

where θ_{min} and θ_{max} are the lower and upper limit of the module's operative range (different for A and B), J'_{red} is the derivative of J_{red} with respect to θ and $J(0)$ is the integration constant. Once concluded the data post-processing, students have to compare different industrial manuals for the selection of the brushless actuators. The basic theory related to possible strategies for numerically computing the reduced moment of inertia, whose discussion goes beyond the purpose of the present paper, can be found in [17].

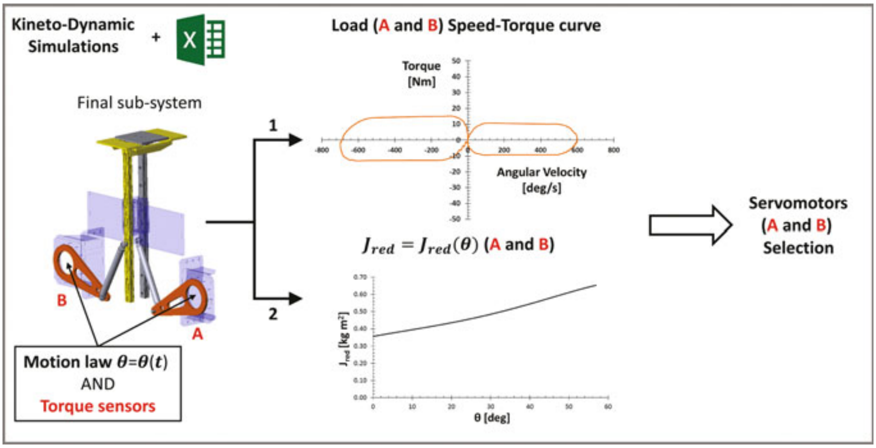

Fig. 5. CAD-CAE procedures for servomotors selection

6 Discussion and Statistics

As reported in [5], the effective development of PjBL activity in the Mechanical Engineering curriculum is outcome of several interacting factors, namely:

- The level of interest shown by the students that, on the basis of the authors' experience, is strongly stimulated by the initial industrial seminar, which underlines the real interest of industrial companies in the overall activity outcomes.
- An adequate choice of the project to be developed, that should balance between a sufficient level of difficulty and time constraints to be faced by students (due to other curricula activities carried out in parallel with the course described in the paper).
- A solid background in the most important disciplines of mechanical engineering (e.g. Industrial Technical Drawing and basic 3D CAD knowledge, Machine Design, Mechanics of Machines). In fact, the proposed PjBL activity can be hardly proposed to students at the early stages of their technical education.

The opinions of the students about the PjBL activity, collected at the end of both academic years, are summarized in Fig. 6. In particular, the statistics refers to a number of students equal, respectively, to 10 for the academic year 2015–2016 and to 16 for the academic year 2016–2017. The positive trend of the collected feedbacks stimulates to continue this kind of didactic approach.

Topic	Year	Absolutely NO [%]	More NO than YES [%]	More YES than NO [%]	Absolutely YES [%]	No response [%]
PjBL's efficacy for didactical purpose	2015-2016	0	11.11	0	66.67	22.22
	2016-2017	0	0	12.5	62.5	25
Quality of teaching and acquired skills	2015-2016	0	0	0	77.78	22.22
	2016-2017	0	0	0	100	0
Consistency with theoretical background	2015-2016	0	0	22.22	55.56	22.22
	2016-2017	0	0	25	75	0

Fig. 6. PjBL activity students' opinion

7 Conclusion

In conclusion, the PjBL activities recently introduced within the course of *Design of Automatic Machines* (Master degree in Mechanical Engineering) at the University of Genova have been here shortly presented. The first outcomes from this experience are showing a strong enthusiasm of the involved students that, for the first time in their academic career, play an active role in devising new design solutions and their optimization through well-known standard methods and advanced software tools (e.g. PTC Creo).

Considering the question “does problem-based learning work in engineering?”, it is clear that there are obstacles to its implementation across a whole engineering program.

This issue is related to the nature of engineering knowledge and practice compared to other disciplines (e.g. medicine), where PBL has been widely adopted. Professional problem-solving skills in engineering require the ability to reach a solution using data that are usually incomplete, while trying to poise demands that are usually in conflict (e.g. customer requirements in terms of productivity/reliability and cost minimization). Therefore, it seems that PjBL is likely to be an effective way to introduce students to the actual issues to be faced in their future working careers and the use of PjBL as a key component of engineering programs should be promulgated as widely as possible, since any improvement to the existing lecture-centric programs that dominate engineering would be strongly welcomed by students and industry.

References

1. Leondes CT (1998) Computer-Aided Design/Engineering (CAD/CAE) techniques and their applications, vol. 58. Academic Press
2. Um D (2017) Solid modeling and applications rapid prototyping, CAD and CAE Theory. Springer
3. Pratt MJ (1995) Virtual prototypes and product models in mechanical engineering. Virtual Prototyping 113–128
4. Chua KJ (2014) A comparative study on first-time and experienced project-based learning students in an engineering design module. Eur J Eng Educ 39(5):556–572
5. Vassura G, Macchelli A (2008) Multi-disciplinary tutoring for project-based mechatronics learning. IFAC Proceedings Volumes 41(2)
6. Hall W, Palmer S, Bennett M (2012) A longitudinal evaluation of a project-based learning initiative in an engineering undergraduate programme. Eur J Eng Educ 37(2):155–165
7. Rudtsch V, Bauer F, Gausemeier J (2013) Approach for the conceptual design validation of production systems using automated simulation-model generation. Procedia Comput Sci 16:69–78
8. Prince JM, Felder MR (2006) Inductive teaching and learning methods definitions, comparisons, and research bases. J Eng Educ 95(2):123–138
9. Savin-Baden M (2000) Problem-based learning in higher education: untold stories
10. Barrows HS, Tamblyn RM (1980) Problem-based learning: an approach to medical education. Springer Publishing Company

11. Biedermann A, Lopez NM, Tierz AS (2017) Developing students' skills through real projects and service learning methodology. In: Advances on mechanics, design engineering and manufacturing. Springer, pp 951–960
12. Thomnn G, Morais F, Werba C (2017) How to teach interdisciplinary: case study for Product Design in Assistive Technology. In: Advances on Mechanics, Design Engineering and Manufacturing. Springer, pp 931–939
13. Isermann R (2005) Mechatronic systems fundamentals. Springer, London
14. www.functionbay.org. Accessed: 25 Feb 2018
15. www.mscsoftware.com/product/adams-maxflex. Accessed: 25 Feb 2018
16. Giberti H, Cinquemani S, Legnani G (2011) A practical approach to the selection of the motor-reducer unit in electric drive systems. Mech Based Des Struct Mach 39(3):303–319
17. Berselli G, Balugani F, Pellicciari M, Gadaleta M (2016) Energy-optimal motions for servo-systems: a comparison of spline interpolants and performance indexes using a CAD-based approach. Robot Comput-Integr Manuf 40:55–65

Fostering Non-technical Skills for Future Engineers: Labour Reality in the Graphic Expression Subject

N. Toledo(✉), J. Lopez, P. Jimbert, M. Iturrondobeitia, and I. Herrero

Graphic Design and Project Engineering Department, School of Engineering of Bilbao, University of the Basque Country UPV/EHU, Leioa, Spain
nerea.toledo@ehu.eus

Abstract. 21st century engineers have to confront global society's competitiveness, so technical and technological competences have to be enriched with critical thinking, problem solving, collaboration, communication and creativity skills. To this end, teaching methodologies like Project-Based Learning (PBL) together with cooperative work, to cover the educational needs of future engineering graduates, should be promoted in class. This paper presents the SimABP project, an action where we simulate a work experience in the CAD subject presenting a real challenge to the students, tightly linking academy to real labour reality. In addition, we also define specific rubrics for evaluating the competences and we show the most significant results obtained. Our action has increased the satisfaction and motivation of the students, and the marks obtained in technical skills have been higher.

Keywords: PBL · CAD · 4C skills · Rubrics

1 Introduction

With the global society and the current trends in competitiveness, engineers are expected to master a combination of skills embracing not only technical and technological know-how for efficient problem-solving and innovation of technology, but also interdisciplinary competences like communication, cooperation and creativity. This issue passes the buck to the court of education, where new teaching methodologies that cover the demanding skills have to be implemented.

PBL is an active student-centred learning-teaching methodology where students go through an extended process of inquiry in response to a question, problem or challenge [6]. In PBL methodology, students follow the "learning by doing" concept working on a cooperative and collaborative environment in order to gain not only specific knowledge, but also the 21st century skills, which are also known as the 4Cs: critical thinking and problem solving, collaboration, communication, and creativity and innovation [9].

F. Cavas-Martínez et al. (Eds.): *Advances on Mechanics, Design Engineering and Manufacturing II*, LNME, pp. 810–824, 2019.
https://doi.org/10.1007/978-3-030-12346-8_79

In this paper, we present the approach of our action, the SimABP project (Simulating the company in the University), which aim is to bring the real labour reality closer to the students in the Graphic Expression subject using the PBL methodology and cooperative work, in order to cover the required software skills and the 4Cs. In the same way, in this paper, we propose specific rubrics that have been designed to evaluate the mentioned competences as well as other aspects of the proposed SimABP project. In addition, with the goal to compare our initiative with the traditional teaching methodology and to evaluate how students perform in both methodologies, we have conducted an analysis by means of the defined rubrics.

2 Motivation and Goals

PBL is a long tested methodology which has cooperative work in its roots. This methodology has been particularly promoted in engineering teaching [4] since it is expected that it will provide graduates with the required skills for confronting the challenges that current and future society presents.

In engineering education, the Graphic Expression subject constitutes a pillar for providing graduates with the basic knowledge of graphical representation, dimensioning and standards. Hand-drawing and paper blueprints have been replaced with CAD tools that have revolutionized engineering and industrial design and so, these have been introduced in the Graphic Expression subject. Owing to this fact, knowledge on CAD has turned into an essential part of the Graphic Expression subject. The introduction of PBL in the CAD subject may aid in providing students with the demanded skills. In this regard, there are different experiences that have demonstrated that PBL outperforms traditional teaching methodology [3, 6, 7] when teaching CAD.

Initiatives like the one presented in [2] also reinforce our SimABP project since it determines that case studies have the potential to provide authentic learning experiences. Nevertheless, the case studies used in [2] are issues found in huge projects of organizations like the NASA, and hence, are presented as examples but do not provide a context to discuss its needs with the client. Therefore, they are far for providing students with a real, tangible and actual problem-solving scenario.

Up to now, the goal of the CAD subject has been to teach students to gain software skills. First the potential of CAD and of specific software (Solid Edge in our case) is presented to the students, to afterwards conduct exercises where the presented functionalities are applied. Complex mechanical assemblies are also represented by the students to learn advanced operations of the tool. Due to the complexity of the assemblies these are solved in teams, which helps the students to gain teamwork competence. Teachers provide a number of assemblies to solve, from which students select one. Recently, we have included the option to select an assembly out of the ones specified by the teacher in order to motivate the students with their projects. Some of the projects selected by the students are shown in Fig. 1:

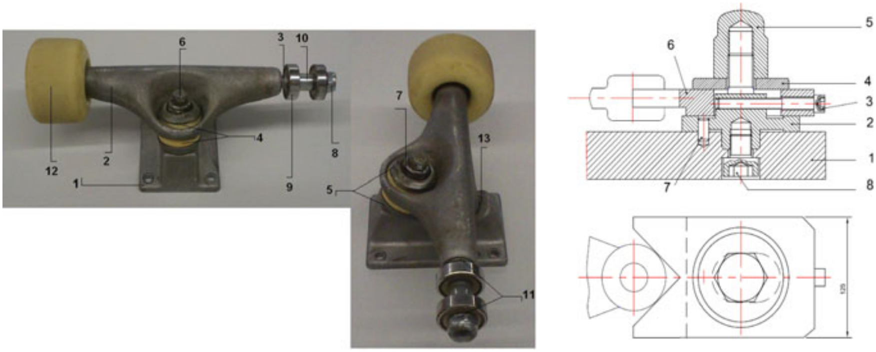

Fig. 1. Selected assembly projects by the students

Since the assemblies are completely defined and the students are requested to represent them in the CAD tool, the non technical skills such as critical thinking and problem solving, that a competitive engineer should master are not covered.

Considering the limitations of the followed methodology and the previous actions introducing PBL in the CAD subject or in related ones, we have defined a strategy based on PBL to bring closer the work experience to students in our CAD subject and provide students a context to train the 4C skills, named SimABP project. To this aim, we present to the students a real problem that the members of the Applied Photonics Research Group [1] are facing in their laboratory instead of using formulations like those shown in Fig. 1. This way, in our approach, we simulate a work experience that students will confront in their future lives when working as engineers. In addition, it is worth mentioning that the SimABP project is introduced in the first teaching year, which adds complexity to its implementation due to the change university implies in students life. Therefore, the SimABP project has the following goal:

> *Provide the students an environment that simulates a working experience to train technical knowledge together with the 4C skills. Specifically, students will gain software skills, critical thinking and problem solving by addressing the challenge proposed and creativity and innovation thanks to the openness of the solution. Moreover, collaboration and communication skills will also be covered by teamwork and meetings with the teacher and the potential client*

3 The SimABP Project: An Introduction of a Work Experience in the CAD Subject

As previously pointed out, our PBL implementation starts with the presentation to the students of a real problem the researchers, which will act as the potential clients, are facing in their laboratory. Specifically, students have to design a mechanical assembly to make easier the reproducibility of experiments in their laboratory related to Raman spectrometry-based biomolecule sensing using plastic optical fibre. The goals that the assemblies have to cover are the following:

(1) The light coupling between the optical fibre and the microscope has to be perfect, and thus, the section of the fibre has to remain completely perpendicular to the source of light.
(2) The coupling between the optical fibre and the source of liquid has to be perfect, and easily removable to use it with other fibres.

Figure 2 shows the used optical fibre and Raman microscope, that is, the working context of the assemblies that students have to design.

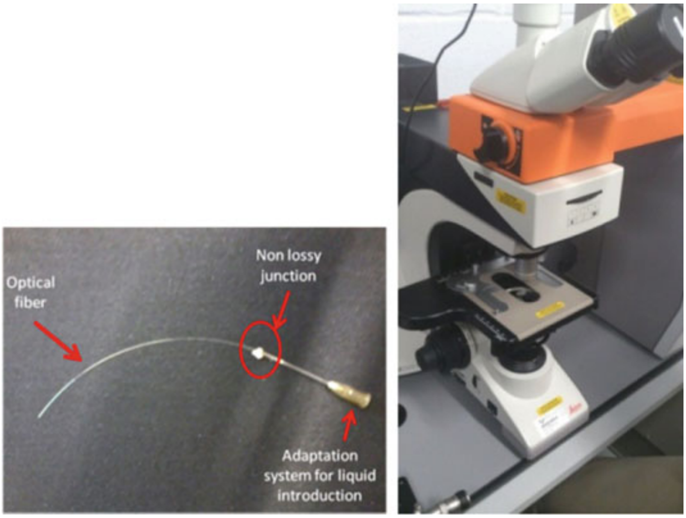

Fig. 2. Elements involved in the real problem

Once presented the challenge they have to solve, students have to follow an industrial design methodology to solve it in teams. The outcome of the project will be a mechanical assembly that covers the needs of the clients. Using the software skills learnt in the first part of the subject where the basic functionalities of the CAD tool are introduced, students have to represent the designed solution considering the graphic expression standards and dimensioning correctness.

3.1 Methodology

In order to gain the essential skills to develop the initiative presented in this paper, the potential and the features of the CAD subject are first introduced in class. Then, students worked out individual exercises to train the introduced software operations. This way, we guarantee that students gain the required knowledge to be able to address the challenge proposed. Individual exercises represent the 50% of the classroom hours, but they are intended to be the 30% of the working hours of each student of the CAD subject, while project hours are expected to be 70%.

During the development of the project, students work in teams of three in order to ensure positive interdependence and collaboration among them. With the goal of guaranteeing proper communication between students, teachers and the potential client, a forum has been developed in the Moodle platform to post queries, comments and exchange information. Additionally, meetings are established to visit the client's laboratory, in order to observe in situ the problem and let students exchange conceptual ideas of their design with the potential client. This way, discussion as well as collaboration and communication skills will be promoted.

The approach undertaken by the SimABP project follows the common industrial design process, where intermediate steps are specified. A more detailed description of this approach can be found in [5]. In order to monitor continuously students work, a planning has been defined with specific milestones that allow teachers to supervise the development of each project. That is, the teacher interviews each team in class to know the level of fulfilment of their scheduling and to be aware of the problems they might be facing. Apart from active monitoring in class by the teacher, students are requested to store all the drafts, notes, etc. they develop during the project to analyse not only the work in class, but also the work outside the classroom.

3.2 Evaluation System

Having modified the approach of the subject, the evaluation system has also been modified accordingly. Specifically, the goal of the evaluation system is to assess software skills, along with the non-technical 4C skills our initiative seeks. The evaluation system then, consists on the following aspects:

- *Software skills*: We evaluate this aspect by the individual work performed by each student through the exercises and with the team work conducted to produce the assembly in the project.
- *Critical thinking and problem solving*: We evaluate this aspect by assessing the design of the assembly produced, which will be evaluated by the client.
- *Creativity and innovation*: Thanks to the openness of the challenge, each team will work out different ideas. We evaluate the creativity and innovation of the students by evaluating the ideas and solutions students conceive in the development of the project, which will also be evaluated by the client.
- *Collaboration and communication skills*: We assess this skill by supervising classroom teamwork, along with the oral presentation of the solution in the end of the teaching year. In addition, the client is also queried about the communication skills of the students in the meetings.

Regarding software skill evaluation, it should be noted that since the aforementioned individual exercises are part of the evaluation system, each student is given an individual mark, which makes certain that the overall score will be weighted with the mentioned individual work, and not shaded with the overall work of the team. By doing so, we guarantee that the evaluation of each student is directly related to his/her work, as well as ensuring that the required knowledge is gained by each student. The evaluation system consists in the aforementioned aspects and the presentation of the project, with the following weights Table 1.

Table 1. Weights assigned to the evaluation aspects

Aspect under evaluation	Weight (%)
Software skills	65
Critical thinking and problem solving	15
Creativity and innovation	10
Collaboration and communication skills	10

3.3 Evaluation Rubrics

Apart from the described evaluation system, we defined specific rubrics to evaluate on the one hand the software skills gained in the subject, and on the other hand the non-technical skills that we seek in this project.

With respect to the evaluation of the technical skills, we have defined a specific rubric that gathers the aspects related to software skills that are demanded in the subject. In addition, it is important to notice that since the CAD subject is a critical part of the Graphic Expression subject where the drawing standards and regulations are taught, in the CAD subject the correctness of the blueprints with respect to the mentioned drawing regulations is also evaluated. This way, apart from the operations to construct 3D objects and assemblies, specific parts of the software used to appropriately complete the blueprints (measurements, notation of the surface quality, etc.) are also assessed. To this end, Table 2 presents the defined rubric for evaluating the software skills and drawing related aspects.

In the same way, the satisfaction of the client is measured in order to evaluate the functionality of the designed solutions, as well as the collaboration and communication skills of the students during the execution of the project. That is, this rubric allows evaluating the critical thinking and problem solving, and the creativity and innovation competences. To this end, we have defined the following rubric (Table 3).

In order to poll students that have undergone the project and evaluate their satisfaction level with the methodology, to enhance it in future teaching years, we have defined a rubric that assesses these issues. Next, we show the rubric defined for testing the satisfaction level of the students with respect to the methodology followed (Table 4).

The defined rubrics seek to cover the technical and the non-technical aspects defined in the evaluation system of the CAD subject. More specifically, we have defined specific aspects to consider in the different topics under evaluation that are matched with the evaluation aspects. Next, this matching is clarified, where we include the technical skills expected in this subject, the non-technical skills represented by the 4C skills and the rubrics defined (Table 5).

Table 2. The rubric defined to evaluate technical competences

Topics under evaluation	Aspects to consider	1 (Not at all)	2 (A lillte)	3 (Enough)	4 (Quite a lot)	5 (A lot)
SW operations	The selection of the used operations is appropriate					
	Used operations and their order correspond with the manufacturing process					
	The nº of operations is not unnecessarily exceeded					
Drawing standards	Minimum views and the representative ones					
	The sections are adequate, and the scratching follows the standards					
	Measurements are clear and complete					
	The tolerances and adjustments are correct and clearly indicated					
	The surface qualities are correct and clearly indicated					
	The selection of the material is correct and corresponds to the operation of the object					
	The thickness of the lines is correct					
	The scale is normalized and it is appropriate for the used format					
	All used scales are present in the drawing, next to the views and in the writing box					
Writing box and text	The information in the box is complete and correct					
Presentation	The use of the space in the drawing is correct					

Table 3. The rubric defined to evaluate the satisfaction level of the client

Topics under evaluation	Aspects to consider	1 (Not at all)	2 (A lillte)	3 (Enough)	4 (Quite a lot)	5 (A lot)
Functionality of the assembly and goal fulfilment	The assembly allows the light to perpendicularly couple the section of the fibre, maintaining it completely vertical					
	The system allows to perfectly couple the source of liquid and the fibre, which is removable and usable with other fibres					
Ease and effectiveness in handling	The assembly perfectly fits in the microscope					
	The assembly is portable					
	The manipulation of the assembly is intuitive					
Communication with the students	The communication has been fluid					
	The students have been proactive					
	The moodle platform has been useful					
	Students have visited the laboratory for a better understanding of the problem					
General	The solution proposed is useful and simple					
	The solution proposed is creative					

Table 4. The rubric defined for evaluating the satisfaction level of the students with respect to the methodology

Topics under evaluation	Aspects to consider	1 (Not at all)	2 (A lillte)	3 (Enough)	4 (Quite a lot)	5 (A lot)
Pros and cons of the methodology	Evaluate in which grade you consider this methodology has helped you to learn comparing to traditional teaching methodologies					
	Evaluate the level in which the methodology has helped you to learn the concepts					
Relation between the theory and the practice	Understand theoretical concepts					
	Establish relations between theory and practice					
	Relate the concepts of the subjects and gain an integrated view					
	Increase the interest and motivation in the subject					
Relation with the professional activity	Analyse professional activity situations					
	Take decisions with respect to a real situation					
	Solve problems or propose solutions to real situations					
	Develop your communication skills (spoken and written)					
	Enhance your teamwork skills					
	Develop needed competences for your professional activity					
Learning process	Develop your personal autonomy to learn					
	Investigate on your own about the topic proposed					
	Actively participate in your own learning process					
General view of the methodology	Considering all the aspects of the methodology, your overall assessment of the approach and the development is	Absolutely unsatisfactory	Regular	Satisfactory	Quite satisfactory	Very satisfactory

Table 5. Matching between the evaluation aspects and the defined rubrics

Technical skills and 4C	Related topic under evaluation	Specific aspect to consider
Technical skills	Software operations	The selection of the used operations is appropriate
		Used operations and their order correspond with the manufacturing process
		The nº of operations does not exceed unnecessarily
	Drawing standards	Minimum views and the representative ones.
		The sections are adequate, and the scratching follows the standards
		Measurements are clear and complete
		The tolerances and adjustments are correct and clearly indicated
		The surface qualities are correct and clearly indicated
		The selection of the material is correct and corresponds to the operation of the object
		The thickness of the lines is correct
		The scale is normalized and it is appropriate for the used format
		All used scales are present in the drawing, next to the views and in the writing box
	Presentation	The use of the space in the drawing is correct
Critical thinking and problem solving	Relation with the professional activity	Analyse professional activity situations
		Investigate on your own about the topic proposed
		Solve problems or propose solutions to real situations
Collaboration and communication skills	Communication with the students	Enhance your teamwork skills
		The communication has been fluid
		The students have been proactive
		The moodle platform has been useful
Creativity and innovation Critical thinking and problem solving	Functionality of the assembly and goal fulfilment	The assembly allows the light to perpendicularly couple the section of the fibre, maintaining it completely vertical
		The system allows to perfectly couple the source of liquid and the fibre, which is removable and usable with other fibres
	Ease and effectiveness in handling	The assembly perfectly fits in the microscope
		The assembly is portable
		The manipulation of the assembly is intuitive
	General	The solution proposed is useful and simple
		The solution proposed is creative

4 Obtained Results and Discussion

With the aim of having a rigorous evaluation system where the presence of interferences is minimized, we have considered a control group conformed by all the students that have not undergone the SimABP project but have completed the subject in the traditional teaching methodology. In this point, it is important to notice that during the teaching year in the CAD subject there have been five groups, which have been taught by four different teachers. In all the groups the project has been presented, and due to its optional nature, there have been three groups where the project has not been implemented. Consequently, we have considered the control group as the summation of the students that have not performed the project, while the group under test is comprised by the total number of students that have implemented the project regardless their teaching group where they belong to (47 out of 189). More precisely, the 24.8% of the students have selected to implement the SimABP project when studying the CAD subject.

We have used the rubric presented in Table 2 and applied it to the students from the control group and to the students that have performed the SimABP project. Note that as presented in the rubric, marks vary from 1 (not at all) to 5 (a lot). Precisely, 4 teachers of the subject teaching in all the groups have evaluated the works of the students. Evaluating the work by different teachers, we wanted to introduce variability and avoid having biased results.

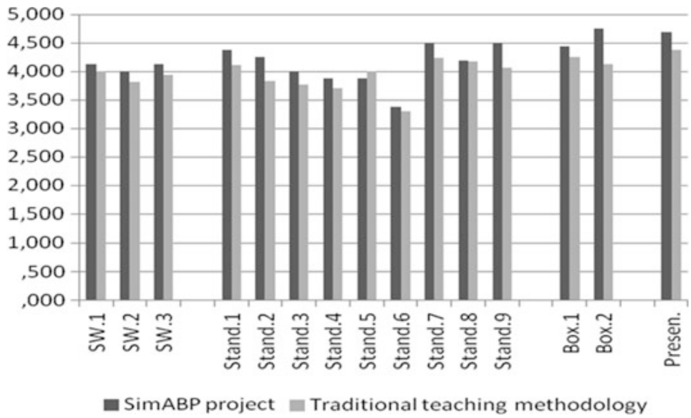

Fig. 3. Results obtained in the evaluation of the technical skills of the students

It is significant that in almost all of the aspects evaluated the students that have conducted the SimABP project obtained better marks as can be seen in Fig. 3. In the case of the software operations used, the biggest difference resides in the aspect related to the number of operations used, where the students from the SimABP project obtain better results. Thus, we can conclude that the SimABP project has improved the understanding of the SW. With respect to the accomplishment of the drawing standards, the students that conducted the SimABP project outperformed the students from the control group. This difference is especially significant in the use of adequate sections, in the following of the scratching standards, and in the introduction of all the scales in the drawing, which are critical aspects in drawing regulations. Consequently, this innovation project has also supplied a perfect framework to the students to learn specific drawing aspects. Related to this, one may think that owing to the fact that the project has been optional, best students have undergone it. Nevertheless, it is necessary to point out that a significant amount of those students have failed the writing exam, and thus, it cannot be argued that best students have developed the innovation project.

Since one of the main goals of the SimABP project is to introduce labour reality, we have also polled the client, which will be the user of the assembly that students have designed, to evaluate its satisfaction level. In order to do so, we have used the rubric defined in Table 3. Note that the client has only assessed using the rubric the most remarkable works proposed by the students, discarding the non functional ones in a first round. In this case, three projects have been evaluated. The client has evaluated each issue giving a score from 1 (not at all) to 5 (a lot). Figure 4 shows the assessment of the assemblies completed by the client.

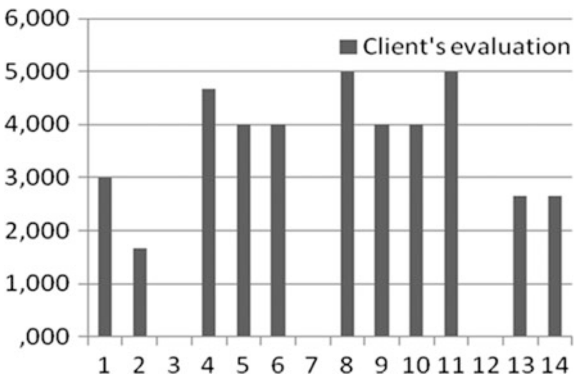

Fig. 4. Client's evaluation using the specific rubric

In the x axes, the ordinal numbers correspond to the following aspects:

1 The assembly allows the light to perpendicularly couple the section of the fibre, maintaining it completely vertical.
2 The system allows to perfectly couple the source of liquid and the fibre, which is removable and usable with other fibres.
3 The assembly perfectly fits in the microscope.
4 The assembly is portable.
5 The manipulation of the assembly is intuitive.
6 The communication has been fluid.
7 The students have been proactive.
8 The moodle platform has been valid.
9 Students have visited the laboratory.
10 The solution proposed is useful and simple.
11 The solution proposed is creative.

In the results it can be observed that the topic Functionality of the assembly and goal fulfilment (1 and 2 values of the x axis) may at a first not be satisfactory for the client. Nevertheless, and as pointed out by the client itself, addressing the missing issues is straightforward. The same reasoning can be applied for simplicity and creativity topics (13 and 14 values of the x axis). From the methodological and skill reach point of view, we can conclude that first year students do not address design necessities as expected. The reason for this could be the lack of training in critical thinking and problem solving throughout their entire academic training together with scarce maturity, and little technological knowledge.

On the other hand, the results obtained in the topic Manipulation easiness and effectiveness (4–6 values of the x axis) show that students have correctly understood the usability requirements of the client. The visit to the laboratory to analyse the working conditions of the researchers that will use the assembly have also helped in this aspect. With respect to communication skills (8–11 values of the x axis), we can observe that the contact with the students has been satisfactory for the client, who at the same time has also encouraged them to deal with the challenge proposed.

Figure 5 shows obtained results of the satisfaction level of both types of students: those that have conducted the SimABP project, and those that have completed the subject following the traditional methodology. As previously mentioned, the rubrics are given scores from 1 (not at all) to 5 (a lot).

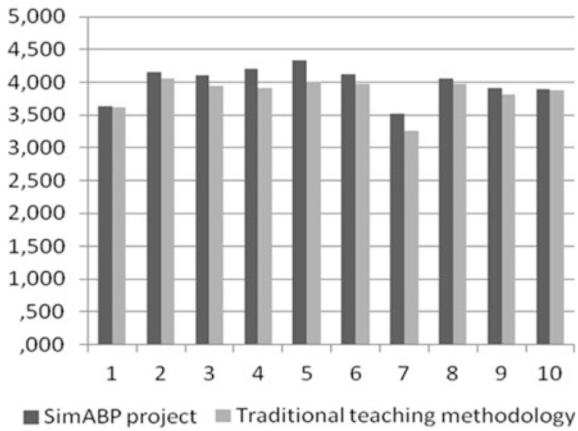

Fig. 5. Results obtained in the satisfaction level of the students

In the x axes, the ordinal numbers correspond to the following aspects:

1 Improve the understanding of theory contents
2 Better understand the relations between theory and practice
3 Increase the interest and motivation in the subject
4 Analyse professional activity situations
5 Solve problems or propose solutions to real situations
6 Take decisions with respect to a real situation

7 Develop your communication skills (spoken and written)
8 Develop your personal autonomy to learn
9 Enhance your teamwork skills
10 Develop needed competences for your professional activity.

As can be observed, in all of the aspects the responses given by those students that have conducted the SimABP project are higher compared to the responses of those students that have conducted the traditional teaching methodology.

It is interesting to mention that the highest satisfaction level perceived by the students with respect to the teaching methodology is related to the capacity to solve problems or propose solutions to real situations (4.34/5). In the same way, the strength of the project is positively assessed by the students (4.15/5) with regards to the better understanding of the relation between theoretical contents and practical contents.

As expected, problem solving and solution proposing of real situations is the fact where the difference between the SimABP project and the traditional teaching methodologies are the highest.

In general, the overall perception of both methodologies is higher than the average. It is worth pointing out that in the traditional teaching methodology the results of those students that have selected to reproduce a real object (see left figure of Fig. 1) are also included, which in a certain way could blur the benefits of the proposed SimABP project. We consider that this issue is one of the reasons for having a satisfaction level higher than the average for both methodologies.

When asked students whether they would choose a SimABP project-alike methodology in other subjects, the 92.2% of the students have responded positively. Furthermore, they have underlined the following aspects as the most beneficial of the methodology: a good approach to labour reality; promotes thinking; enjoyable; satisfactory; understandable and simple; an interesting challenge; useful for the future.

In the same way, the lack of time has been one of the negative aspects of the proposed project.

5 Conclusions

With the goal of providing future engineer graduates with the skills current global society demands, and to prepare them to be able to cope with the competitiveness the labour market presents, we have defined an action that simulates a work experience in the CAD subject named SimABP project. To this end, we propose an environment where a client requests to address a real problem they are facing in their lab. Starting with this challenge, students follow the PBL methodology to provide a solution, which is guided and supervised not only by the teacher-facilitator but also by the client.

In order to evaluate how students gain the technical and non-technical skills, we have defined specific rubrics and have make use of them to evaluate their knowledge as well as 4Cs. Results show that the students that have conducted the innovative SimABP project obtain better marks with respect to SW skills and correctness of drawing standards. More precisely, the students that have conducted the innovative project have used adequate sections, properly applied scratching standards and accurately introduced the scale, which are critical aspects in drawing regulation. Consequently, we can conclude that the SimABP project has supplied a perfect framework to the students to learn specific drawing aspects.

In the same way, and following the idea of simulating a work experience in the classroom, a rubric fulfilled by the client of the project has been defined and used to evaluate how students make progress in creativity and innovation and critical thinking and problem solving, as well as in communication issues. Obtained results show that communication skills are fully satisfied by the students while more work should be done on training critical thinking and problem solving. As part of the integration of this project, we have defined and used rubrics to poll students with respect to their satisfaction level with the methodology. Results show that the satisfaction of the students is higher than in the traditional methodology and we have seen that their motivation has significantly increased.

Consequently, our SimABP project demonstrates that proposing a real challenging problem results in an excellent framework for training technical and non-technical skills.

References

1. APRG. Applied Photonics Research Group. University of The Basque Country (UPV/EHU). http://appliedphotonicsbilbao.org/
2. Balamuralikrishna R, Raju PK, Sankar CS (2005) Established industry partnered engineering case studies to enhance engineering graphics education. In: 60th annual engineering design graphics division mid-year meeting
3. Garikano X, Osinaga M, Garmendia Mujika M, Perez Manso A. Problem-based learning, implementation and qualitative study in computer aided design subject. In: International technology education and development conference, INTED2011 proceedings, pp 1305–1314
4. Lehmann M, Christensen P, Du X, Thrane M (2008) Problem-oriented and project-based learning (POPBL) as an innovative learning strategy for sustainable development in engineering education. Eur J Eng Educ 33(3):283–29
5. Lopez J, Toledo N, Jimbert P, Herrero I, Caro JL. CAD con Solid Edge. Resolución de conjuntos basada en PBL. Open Course Ware, ISSN: 2255–2316
6. Markham T, Larner J, Ravitz J (2003) Project based learning handbook: a guide to standards-focused project based learning for middle and high school teachers. Buck Institute for Education, ISBN-13: 978-0974034300
7. Marquez JJ, Martinez ML, Romero G, Perez M (2011) New methodology for integrating teams into multidisciplinary project based learning. Int J Engineering Educ 27(4):746–756
8. Pucha RV, Utschig TT (2012) Learning-centered instruction of engineering graphics for freshman engineering students. J STEM Educ 13(4):24
9. P 21. The Partnership for 21st Century Skills. P21 Mission. http://www.p21.org/